# Willamette River Basin Temperature TMDL Model: Boundary Conditions and Model Setup


By

Robert Annear,

Mike McKillip,

Sher Jamal Khan,

Chris Berger,

And

Scott Wells

Technical Report EWR-01-04

School of Engineering and Applied Science
Department of Civil and Environmental Engineering
Portland State University
Portland, Oregon 97201-0751

January, 2004

# Table of Contents

## List of Figures

## List of Tables

# Acknowledgments

The Willamette River Temperature TMDL modeling coordinator Jim Bloom and others at the Oregon Department of Environmental Quality provided essential support that was crucial in acquiring the detailed information on the Willamette River system that was necessary for this project. Their efforts are greatly appreciated and were essential to the project's success.

There were many other individuals who were instrumental in providing data compilation and insight into understanding the Willamette River system. They include (not in order of importance): Jim Bloom, Beth Woodward, Dennis Ades, Steve Mrazik, Greg Aldrich, Agnes Lut, and Allen Hamel, all of the Oregon Department of Environmental Quality; Arthur D. Armour, Jim Britton, and Michael Knutson of the U.S. Army Corps of Engineers, Portland District; Jo (Suzanne) Miller, Stewart Rounds, and Annett Sullivan of the U.S. Geological Survey; Antonius Laenen (retired from the USGS) for his work on conducting the Willamette River dye studies in 2002; and Sam Fernald of New Mexico State University for his work on some historical dye studies on the Willamette River.

# Abbreviations

**Table 1. Report Abbreviations**

| Abbreviation | Description |
|---|---|
| AGRIMET | AgriMet, a conjunction of the words "agricultural" and "meteorology", is a satellite-based network of automated agricultural weather stations operated and maintained by the U.S. Bureau of Reclamation. |
| DEM | Digital Elevation Model |
| DMR | Discharge Monitoring Reports |
| DOGAMI | Oregon Department of Geology and Mineral Industries |
| EWEB | Eugene Water and Electric Board |
| FEMA | Federal Emergency Management Agency |
| GIS | Geographic Information System |
| GUI | Graphical user interface, usually in the context of the CE-QUAL-W2 preprocessor |
| HUC | Hydraulic unit code |
| LASAR | Laboratory Analytical Storage and Retrieval Database |
| METAR | Traditional weather reporting by the National Weather Service and the Federal Aviation Administration |
| NOAA | National Oceanic and Atmospheric Administration |
| NPDES | National Pollution Discharge Elimination System |
| ODEQ | Oregon Department of Environmental Quality |
| ODF | Oregon Department of Forestry |
| OMSI | Oregon Museum of Science and Industry |
| PGE | Portland General Electric |
| RM | River mile |
| RAWS | Remote Automated Weather Stations |
| SRML | Solar Radiation Monitoring Lab, University of Oregon |
| USACOE | U.S. Army Corps of Engineers |
| USGS | U.S. Geological Survey |
| WADOE | Washington State Department of Ecology |

**Table 2. Computer software and program abbreviations**

| Computer Software/ Programs | Description |
|---|---|
| SURFER | Bathymetric and Topographic Contour plotting software |
| QUAL2E | One-dimensional steady state flow and water quality model |
| CE-QUAL-W2 | Two-dimensional hydrodynamic and water quality model |
| UNET | One-dimensional hydrologic routing model |
| HEC | U.S. Army Corps of Engineers, Hydrologic Engineering Center one-dimensional steady and unsteady flow model |
| FORTRAN | Computer language used for CE-QUAL-W2 and post-processing of model results. |

**Table 3. CE-QUAL-W2 model geometry variable names**

| CE-QUAL-W2 terms | Description |
|---|---|
| IMP | Number of longitudinal segments in model grid |
| KMP | Number of vertical layers in model grid |
| ELBOT | Bottom of elevation of grid for specific water body |

# Introduction

The State of Oregon Department of Environmental Quality (DEQ) is developing a TMDL for temperature in the Willamette River basin shown in Figure 1. The study area included the Willamette River and all major tributaries (except the Tualatin River where a TMDL process was already concluded). A large section of the Columbia River was also modeled to provide adequate boundary representation of tidal flows in the lower Willamette River. The Willamette River below the Oregon City Falls in the Portland metropolitan area has a typical diurnal tidal range of 1 m. The development of a dynamic model of temperature and hydrodynamics of the entire river basin incorporating shading were primary requirements of this modeling study. The model would be used by DEQ to set temperature limits on point source dischargers and to evaluate the impact of management strategies on river temperatures to improve fish habitat. Some of these strategies included modifications of the dam at the Willamette River Falls south of Portland and channel reconfigurations.

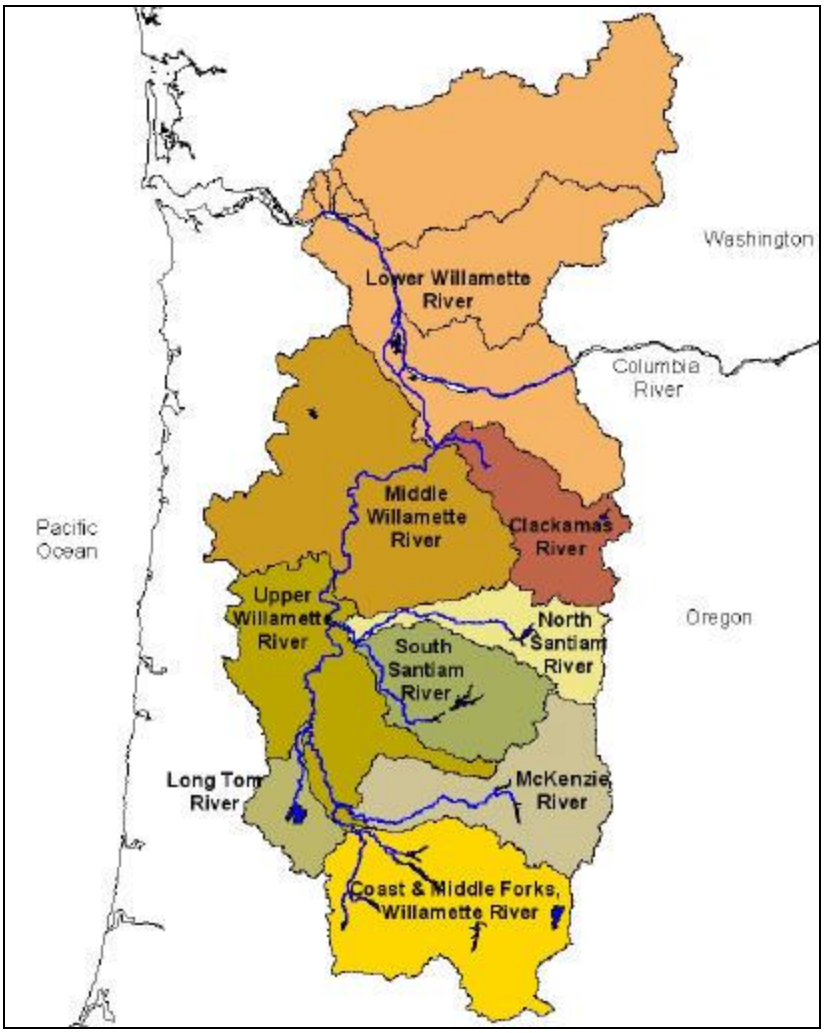


**Figure 1 TMDL study area - the Willamette River basin with drainage basins delineated.**

CE-QUAL-W2 Version 3.1 (Cole and Wells, 2002), a two dimensional (longitudinal-vertical), laterally averaged, hydrodynamic and water quality model developed by the U.S. Army Corps of Engineers

(USACOE) Waterways Experiments Station, was chosen as the appropriate model tool for this system for the following reasons:

- Dynamic temperature predictive capability
- Dynamic shading prediction based on detailed topographic and vegetative shading information
- Ability of the model to be used for water quality after the temperature study where parameters of interest are algae, periphyton, pH, dissolved oxygen
- Ability to model complex hydraulic flow paths with multiple interconnected branches using hydraulic elements (weirs, pumps, spillways) between branches
- Ability to evaluate the stratification potential of deep pools in the Willamette River where water quality and temperature data have shown significant stratification
- Ability to model estuary hydrodynamics
- Ability to model an entire river basin including upstream deep-density stratified reservoirs
- Public domain executable and source code for quality-assurance and testing

The river basin model was originally divided into several reaches. Individual models were developed for each reach. These reaches were (see also Figure 2):

- **Columbia River** - from Beaver Army Terminal (Columbia River Mile 53.8) to Bonneville Dam (RM 144.5) (Willamette River enters the Columbia River at Columbia River Miles 87 and 101);
- **Tidal Willamette River** – Lower Willamette River from mouth to Willamette Falls (RM 26.5), including the Willamette Channel and the Multnomah Channel;
- **Non-tidal Willamette River** – Willamette Falls (RM 26.5) to confluence of Coast and Middle Forks (RM 187); this section was divided further into the following reaches: Middle Willamette from the Willamette Falls (RM 26.5) to the city of Salem (RM 85); Upper Willamette from the City of Salem (RM 85) to the confluence of Coast and Middle Forks (RM 187)
- **Clackamas River** up to River Mill Dam/Estacada Lake (RM 26);
- **Santiam River** (all 12 miles), North Santiam River up to Detroit Dam (RM 49), South Santiam River up to Foster Dam (RM 38);
- **Long Tom River** to Fern Ridge Dam (RM 26);
- **McKenzie River** to RM 56, and South Fork McKenzie River to Cougar Dam (RM 4);
- **Middle Fork Willamette** to Dexter Dam (RM 17), Fall Creek to Fall Creek Dam (RM 7);
- **Coast Fork Willamette** to Cottage Grove Dam (RM 30), Row River to Dorena Dam (RM 7.5);
- **Columbia Slough** in the tidal portion of the Willamette River (about 9 miles in length)

Once the models were set-up for each section of the Willamette basin, the model was calibrated to field data and management strategies were evaluated. These are the subjects of two other reports: Annear et al. (2004b) and Berger et al. (2004).

This report outlines the model development of each of these model sections or elements for both the calibration time periods and the management scenario time periods. The calibration period for each model section differs due to the availability of boundary condition data. The model simulation periods used to investigate management scenarios (Annear et al, 2004b) also required boundary condition data that extended past the calibration periods.

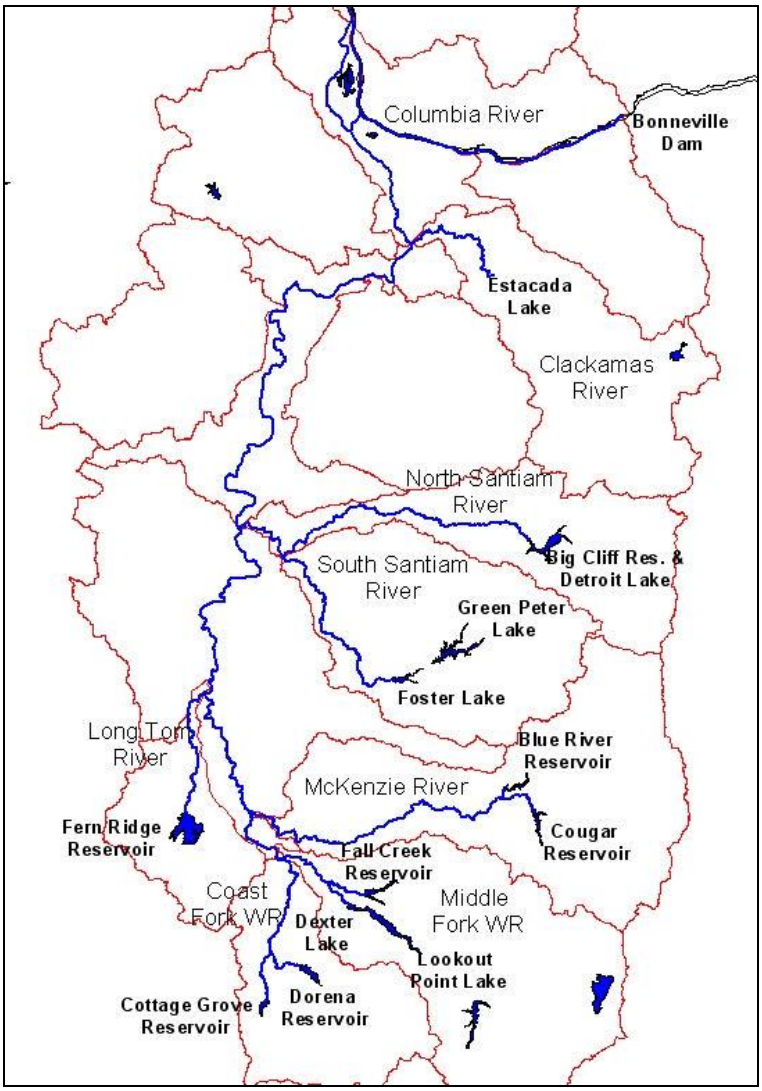


**Figure 2. Willamette River and modeled tributaries.**

This report is divided into model reaches. Within each reach the following items are discussed:

- Model bathymetry and grid
- Boundary conditions – upstream and downstream
- Tributaries
- Distributed tributaries
- Point sources
- Shading
- Meteorological conditions

## Lower Willamette River / Columbia River

The Willamette River system is a 30,800 $km^2$ watershed that drains through the Lower Willamette River from RM 0 to RM 26.8 (Willamette Falls), Figure 3. The river passes through the Portland metropolitan area before its confluence with the Columbia River at Columbia RM 106. The Columbia River is tidally influenced from the Pacific Ocean to the tailrace of the Bonneville Dam at RM 145. The Lower

Willamette River is also tidally influenced below Willamette Falls at RM 26.8. The model calibration periods are from July 26, 2001 to September 28, 2001, and from April 1, 2002 to October 1, 2002.

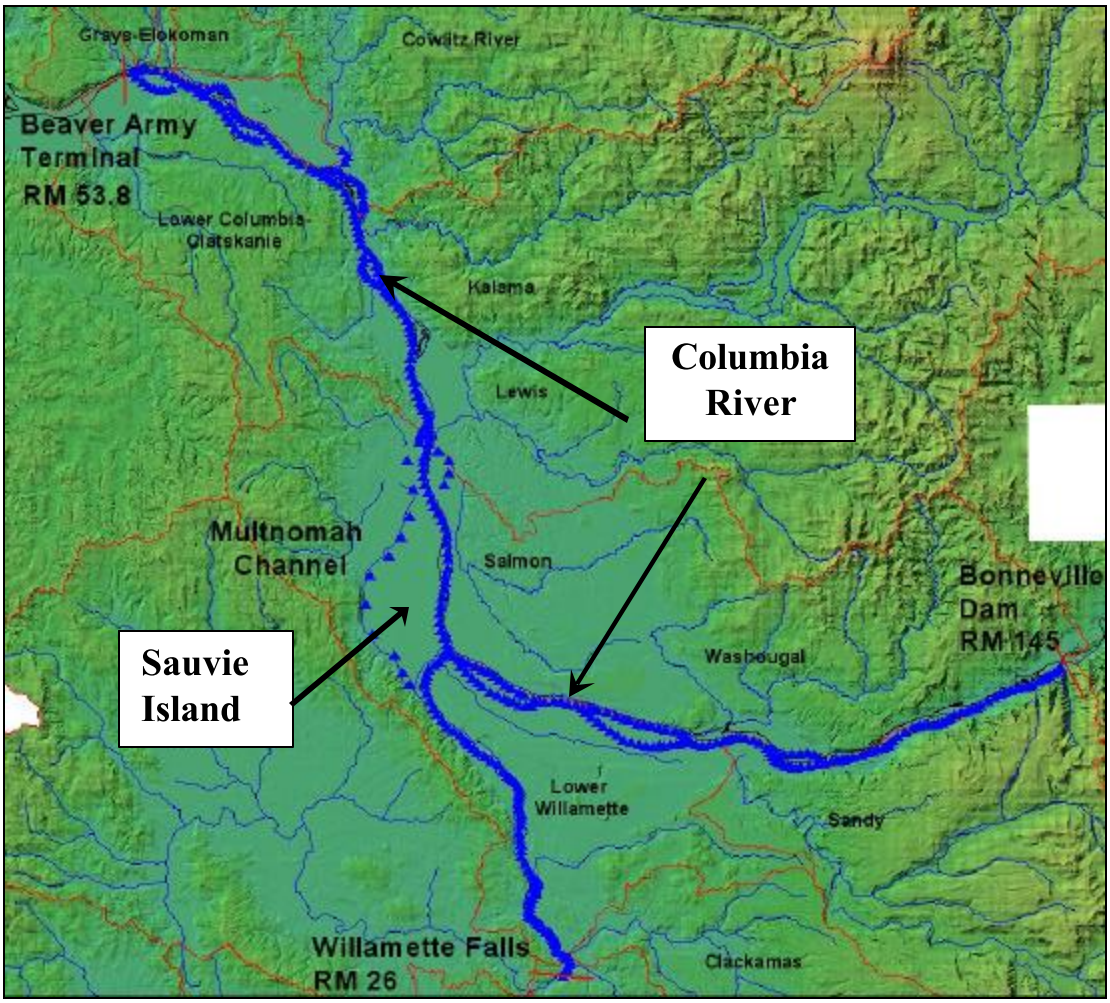


**Figure 3. Lower Willamette River basin region**

## *Model Geometry*

### Bathymetry Data

The model grid was developed from detailed cross sections for the Columbia River and the Willamette River provided by the U.S. Army Corps of Engineers (USACOE) (Knutson, 2000). The model grid was developed using cross sections from RM 145 (Bonneville Dam) to RM 53.8 (Beaver Army Terminal) in the Columbia River and from RM 0 to RM 26.8 (Willamette Falls) in the Willamette River, as shown in Figure 4. Figure 5 shows two example cross sections in the Willamette River provided by USACOE.

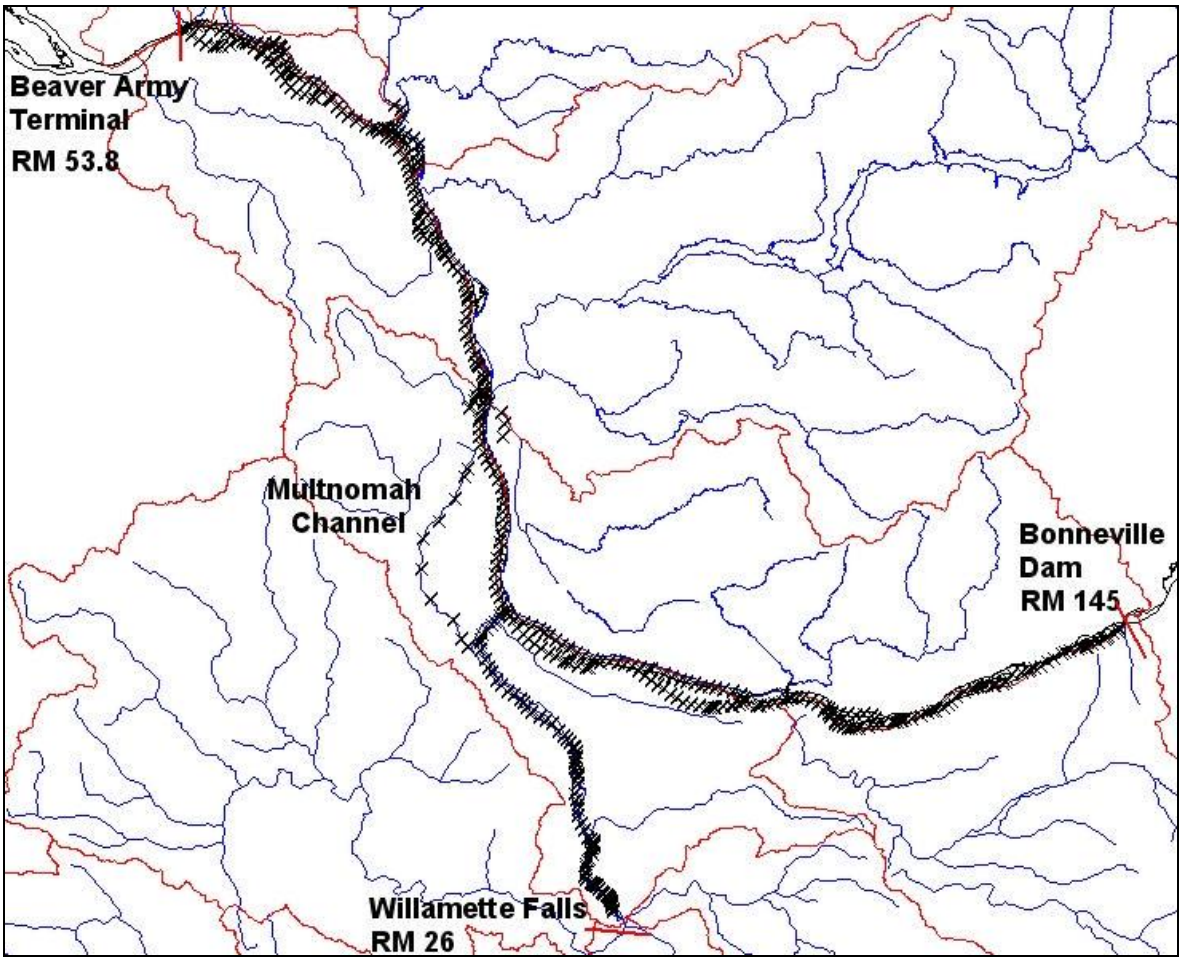


**Figure 4. Columbia River and Lower Willamette River cross section locations**

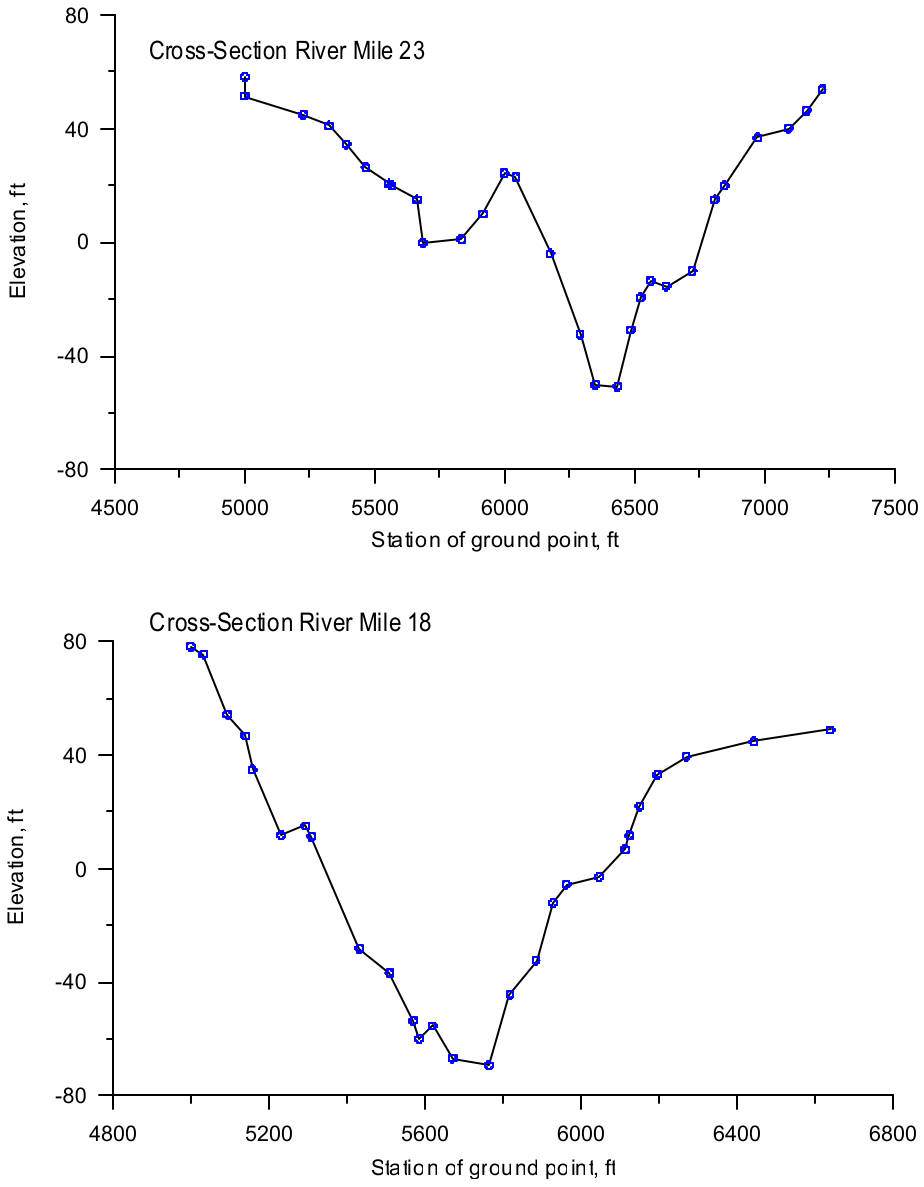


**Figure 5. Lower Willamette River cross sections at RM 18 and RM 23**

Bathymetry data in the Willamette River between RM 24 and just below Willamette Falls (RM 26.8) were obtained from a survey work done in 1999 by the USACOE using a sound transponder and Global Positioning System (GPS) (Ryel, 2002). The bathymetry data for the last 0.3 miles between the USACOE data set and the Oregon City Falls were obtained by digitizing bathymetric estimates on the USGS quadrangle map. The data sets provided x, y, and z coordinates that were combined and used in SURFER, a 3-D mapping program, to develop the model grid between RM 24 and the Willamette Falls. Figure 6 shows the location of the data provided by the USACOE and the U.S. Geological Survey (USGS) map.

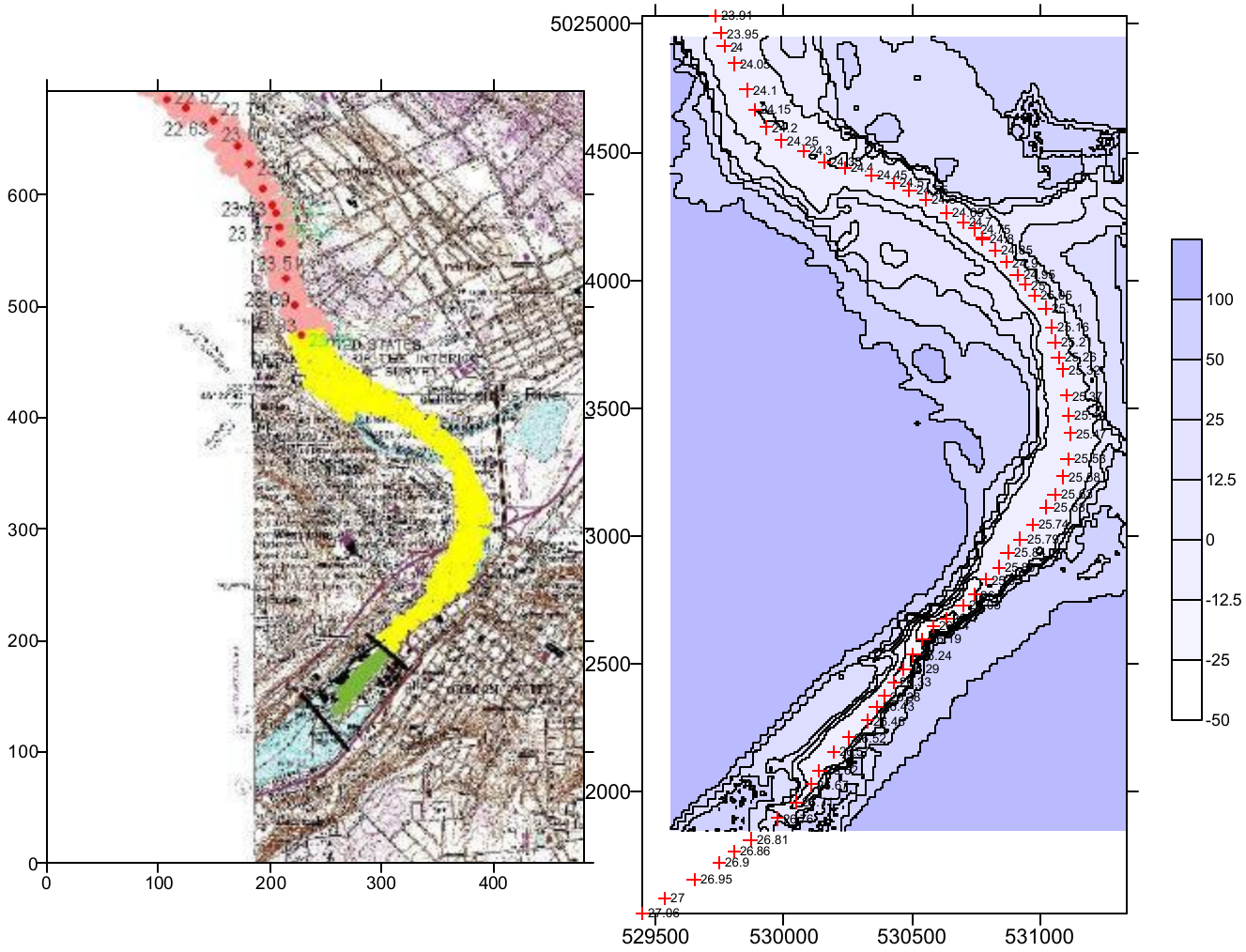


**Figure 6. Lower Willamette River bathymetry from RM 24 to 26.8**

## Model Grid Development

Using the river cross sections and the bathymetric contour plots discussed above, the model grid was developed for 2 water bodies. Figure 7 shows a layout of the model grid. A total of 13 branches make up the 2 water bodies in the model. The first water body consists of two branches; the first is the main stem of the Willamette River and the second is Multnomah Channel. The Columbia River represents the second water body with 11 branches. The first branch in water body two is the main channel of the Columbia River and the remaining 10 branches are tributary inflow reaches or side channels around islands. Segment size was based on the spacing of the bathymetry data cross sections. The model's vertical grid resolution is 2 meters throughout.

Table 4 provides the model grid specifications and boundary conditions for each branch. Figure 8 to Figure 10 show a detailed layout of the model segments for the Willamette River. Figure 11 to Figure 16 show a detailed layout of the model segments for the Columbia River. The model vertical resolution is shown in Figure 17 and Figure 18 for the Willamette River model branches and for the Columbia River branch, respectively.

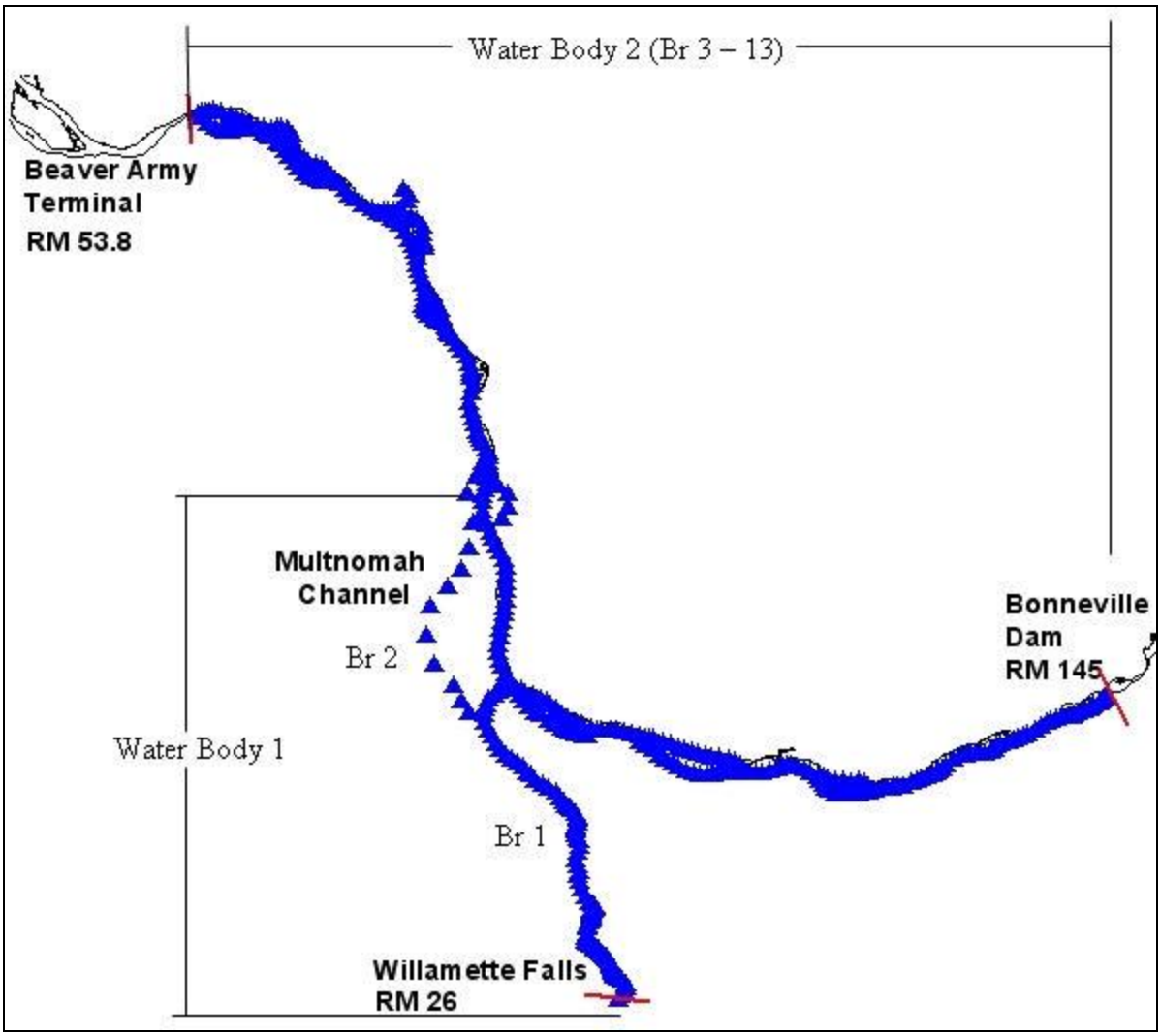


**Figure 7. Lower Willamette River model grid layout**

**Table 4. Lower Willamette River model grid layout specifications**

| Water Body | Branch | Description | Starting Segment | Ending Segment | Starting RM | Ending RM | Segment Length, m | Slope | Upstream BC | Down-stream BC |
|---|---|---|---|---|---|---|---|---|---|---|
| 1 | 1 | Falls to Columbia River | 2 | 98 | 26.5[w] | 0.0 | 80 to 925 | 0.0 | flow | internal |
| | 2 | Multnomah Channel | 101 | 115 | 22.0[m] | 0.0 | 370 to 4361 | 0.0 | internal | internal |
| 2 | 3 | Columbia River, Bonneville Dam to Beaver Army Terminal | 118 | 347 | 145.0 | 53.5 | 169 to 805 | 0.0 | flow | water level |
| | 4 | Reed Island Channel | 350 | 358 | 127.5 | 123.2 | 241 to 805 | 0.0 | internal | internal |
| | 5 | Government Island | 361 | 379 | 118.0 | 110.5 | 201 to 805 | 0.0 | internal | internal |
| | 6 | Oregon Slough | 382 | 394 | 108.3 | 102.3 | 394 to 805 | 0.0 | internal | internal |
| | 7 | Bachelor Island | 397 | 400 | 91.5 | 87.4 | 1287 to 1609 | 0.0 | internal | internal |
| | 8 | Sandy Island | 403 | 410 | 82.1 | 79.9 | 370 to 708 | 0.0 | internal | internal |
| | 9 | Carrols Channel | 413 | 425 | 74.3 | 69.8 | 306 to 805 | 0.0 | internal | internal |
| | 10 | Cowlitz River | 428 | 430 | 1.8[c] | 0.0 | 644 to 805 | 0.0 | flow | internal |
| | 11 | Lord Island | 433 | 441 | 63.7 | 59.8 | 499 to 805 | 0.0 | internal | internal |
| | 12 | Fisher Island | 444 | 451 | 52.3 | 49.8 | 402 to 805 | 0.0 | internal | internal |
| | 13 | Bradbury Slough | 454 | 461 | 42.8 | 39.7 | 402 to 805 | 0.0 | internal | internal |
| Default RM is for the Columbia River; w: Willamette RM; m: Multnomah Channel RM; c: Cowlitz RM | | | | | | | | | | |

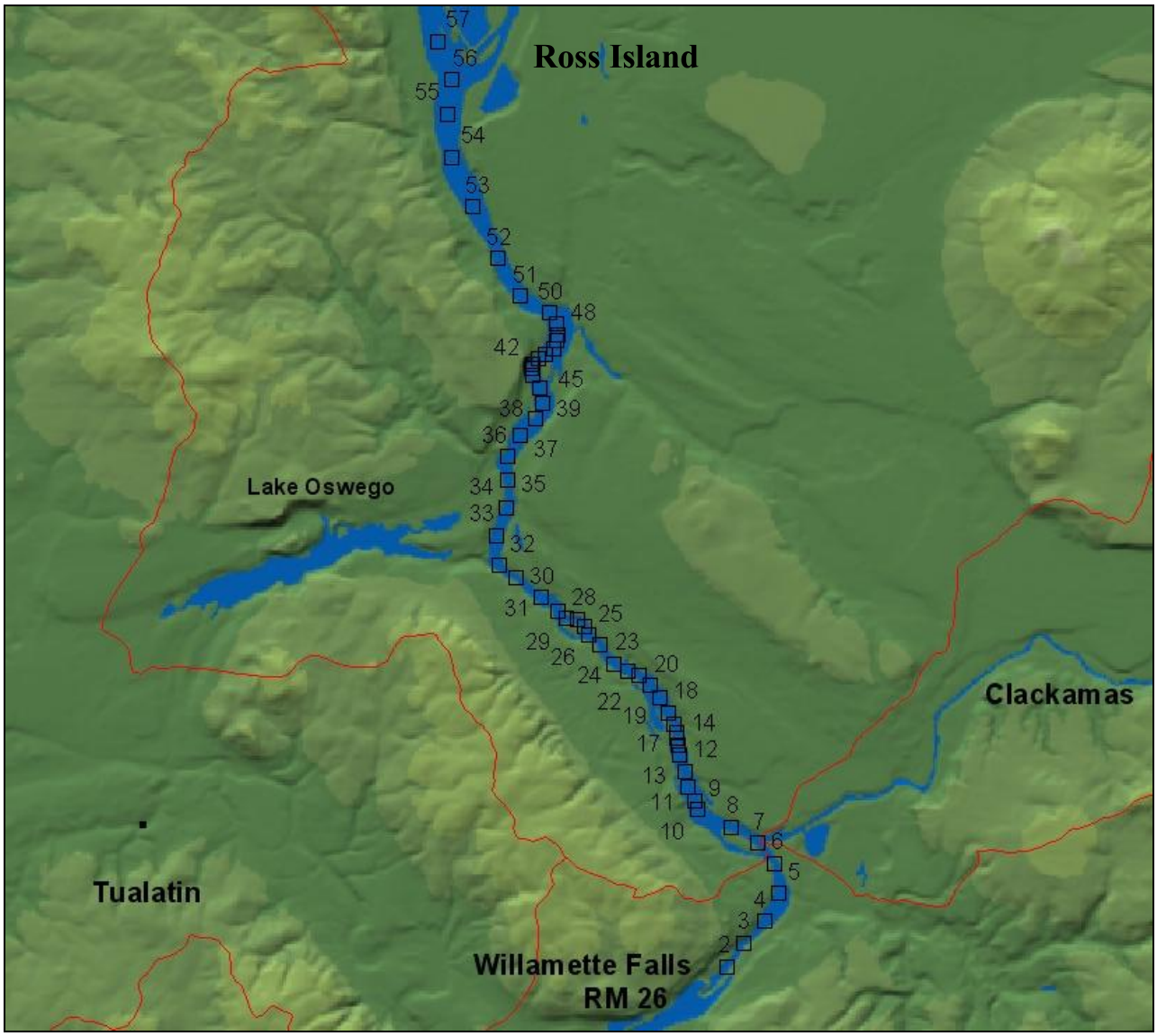


**Figure 8. Willamette Falls and Lower Willamette model segments to Ross Island**


**Figure 9. Lower Willamette River model segments near downtown Portland and Swan Island**

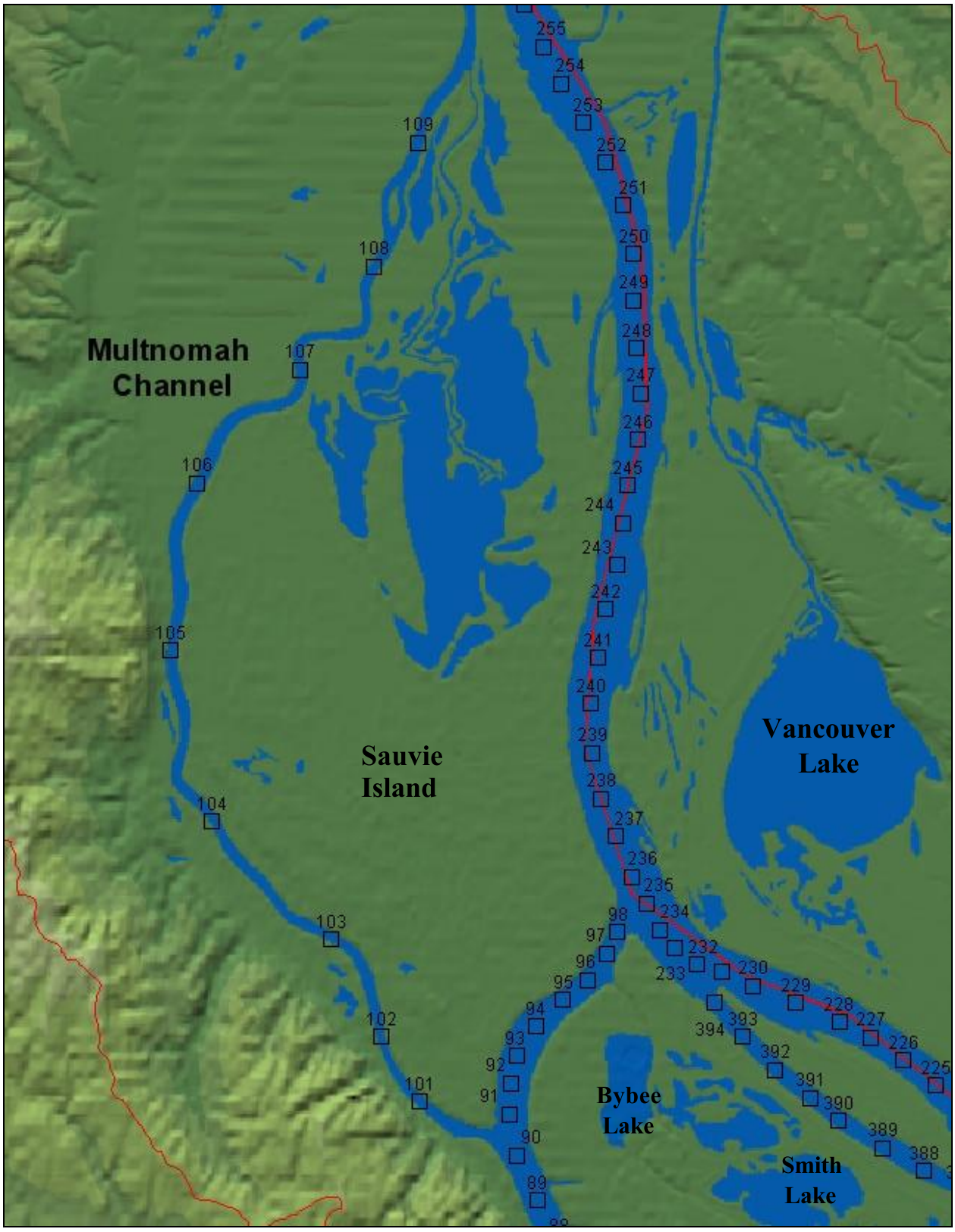


**Figure 10. Lower Willamette River model segments at confluence of Willamette River and Columbia River**

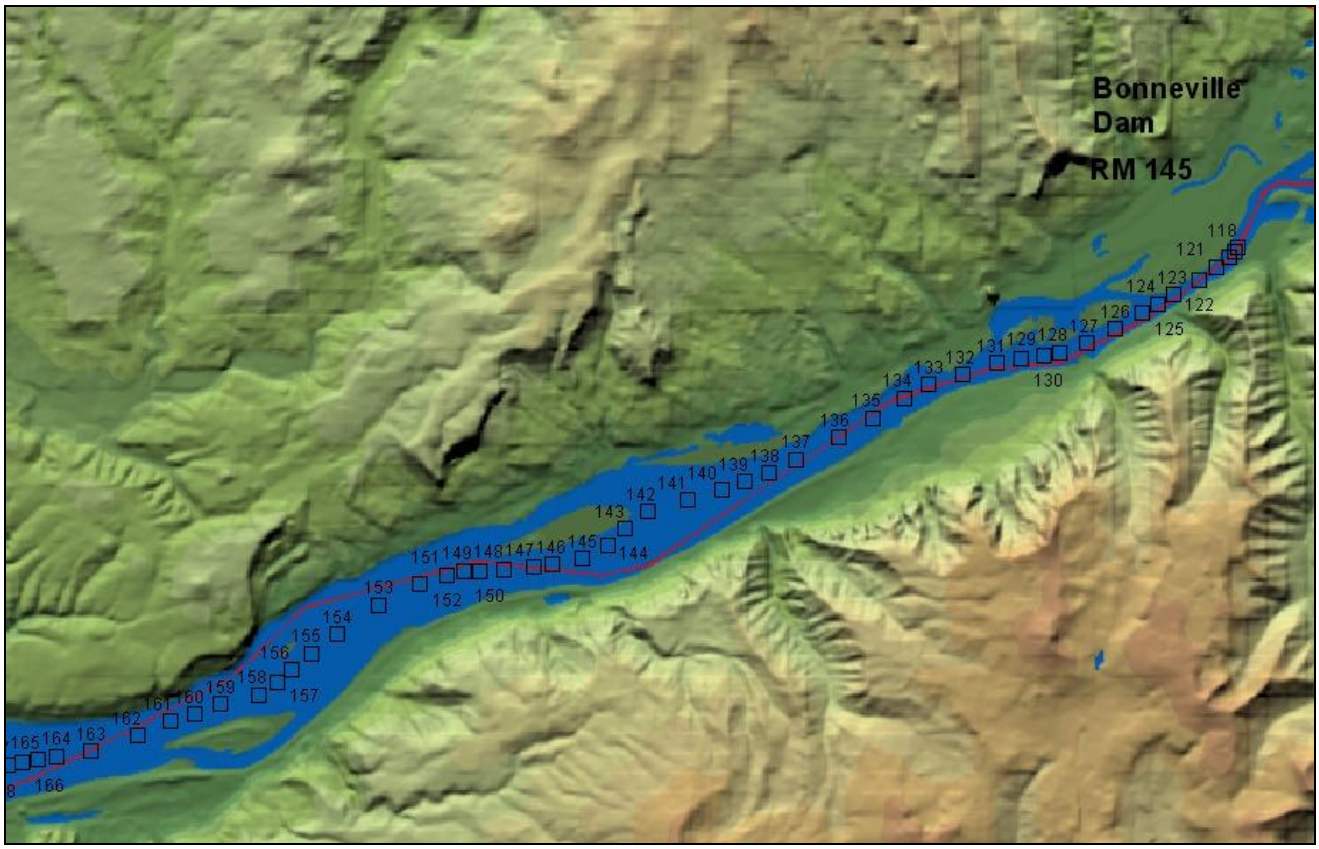


**Figure 11. Columbia River model segments near Bonneville Dam**

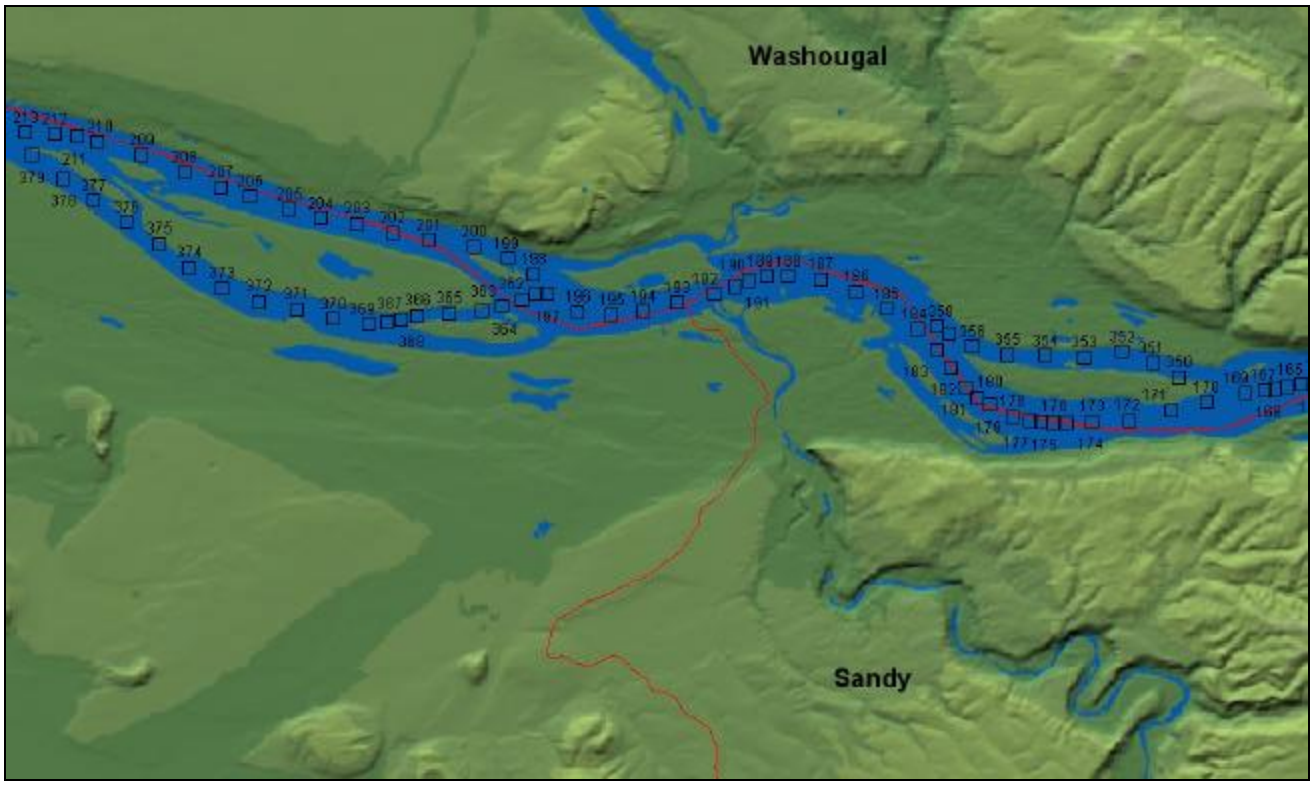


**Figure 12. Columbia River model segments near the Sandy River**

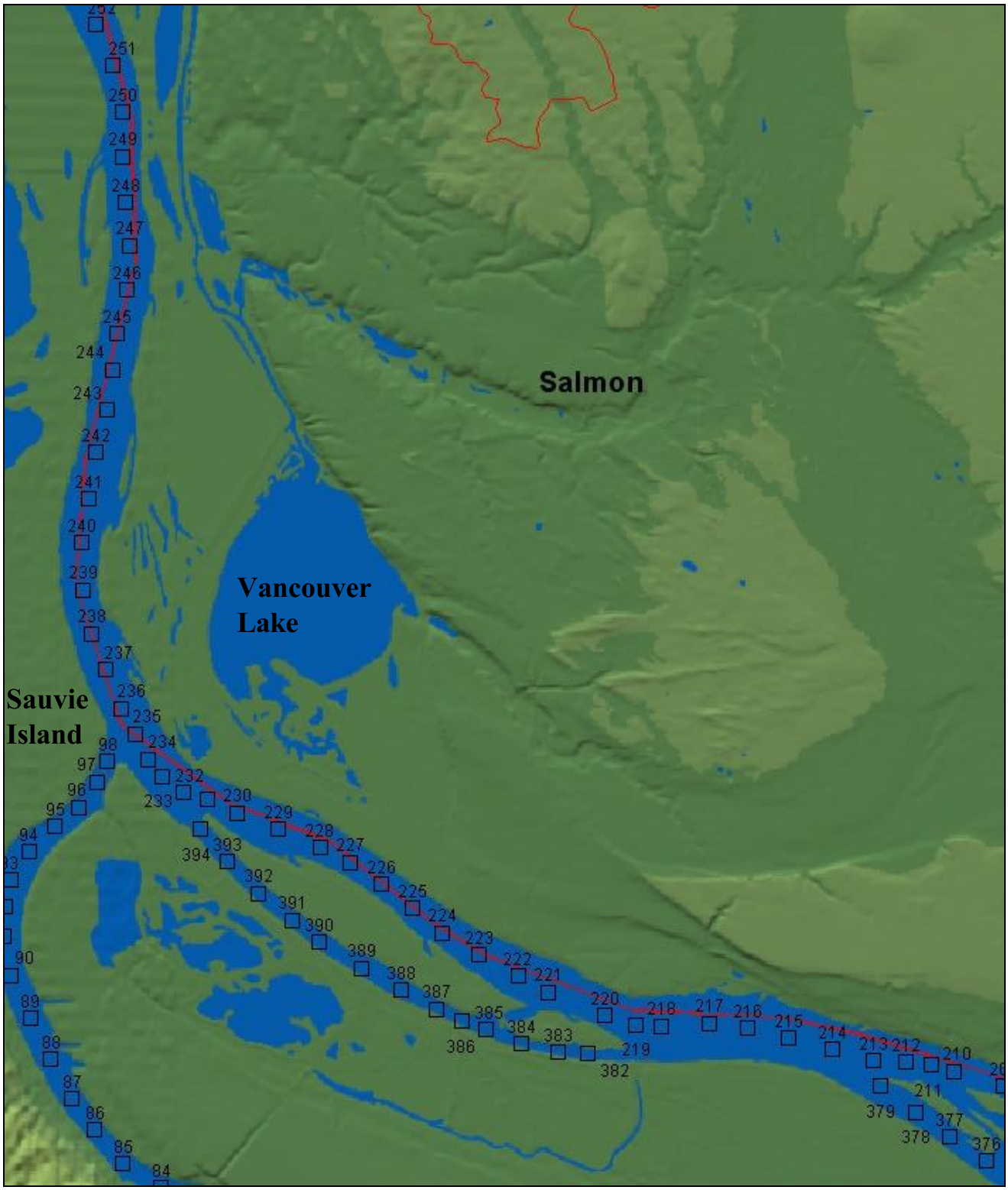


**Figure 13. Columbia model segments numbers near Sauvie Island and Vancouver Lake**

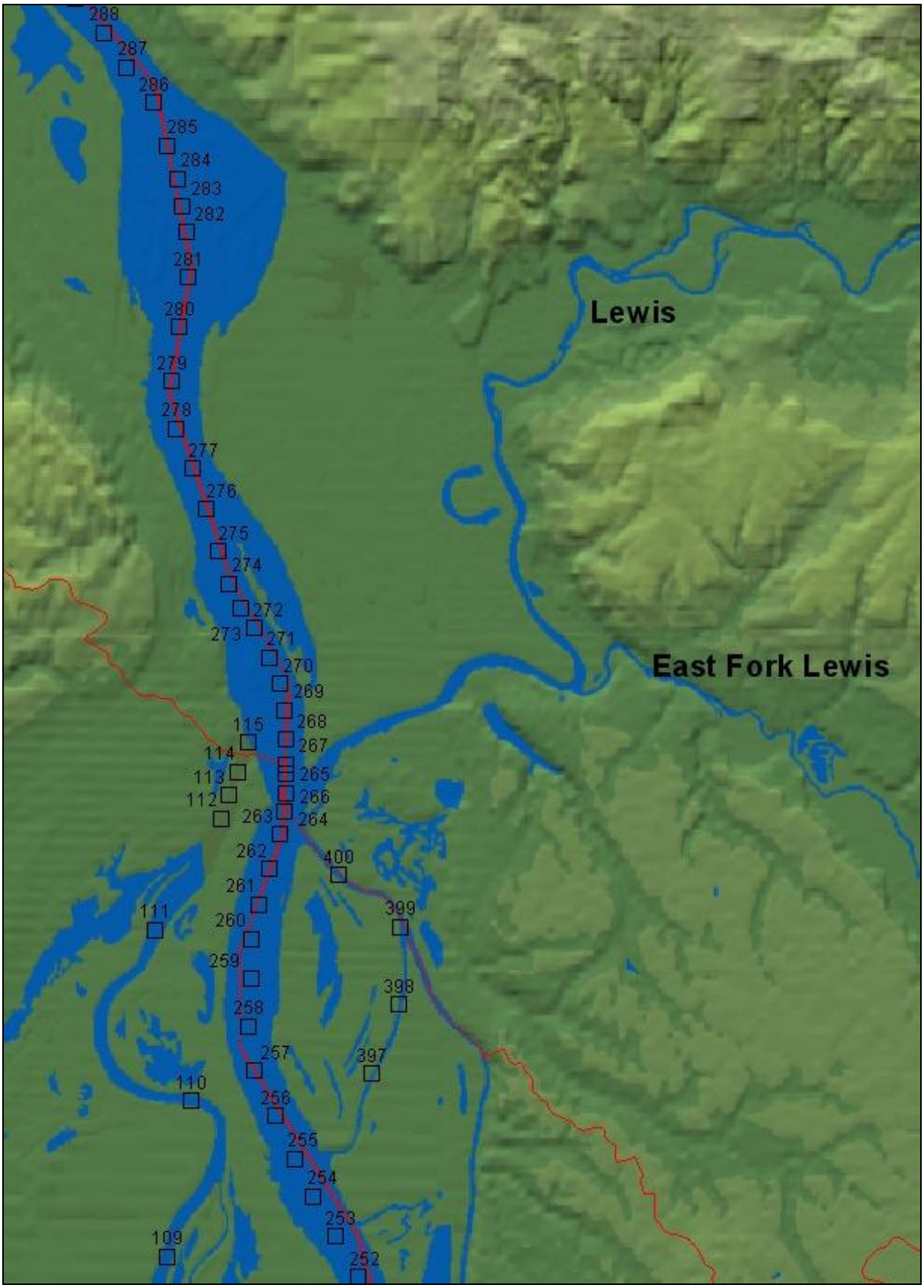


**Figure 14. Columbia River model segments near the Lewis River**

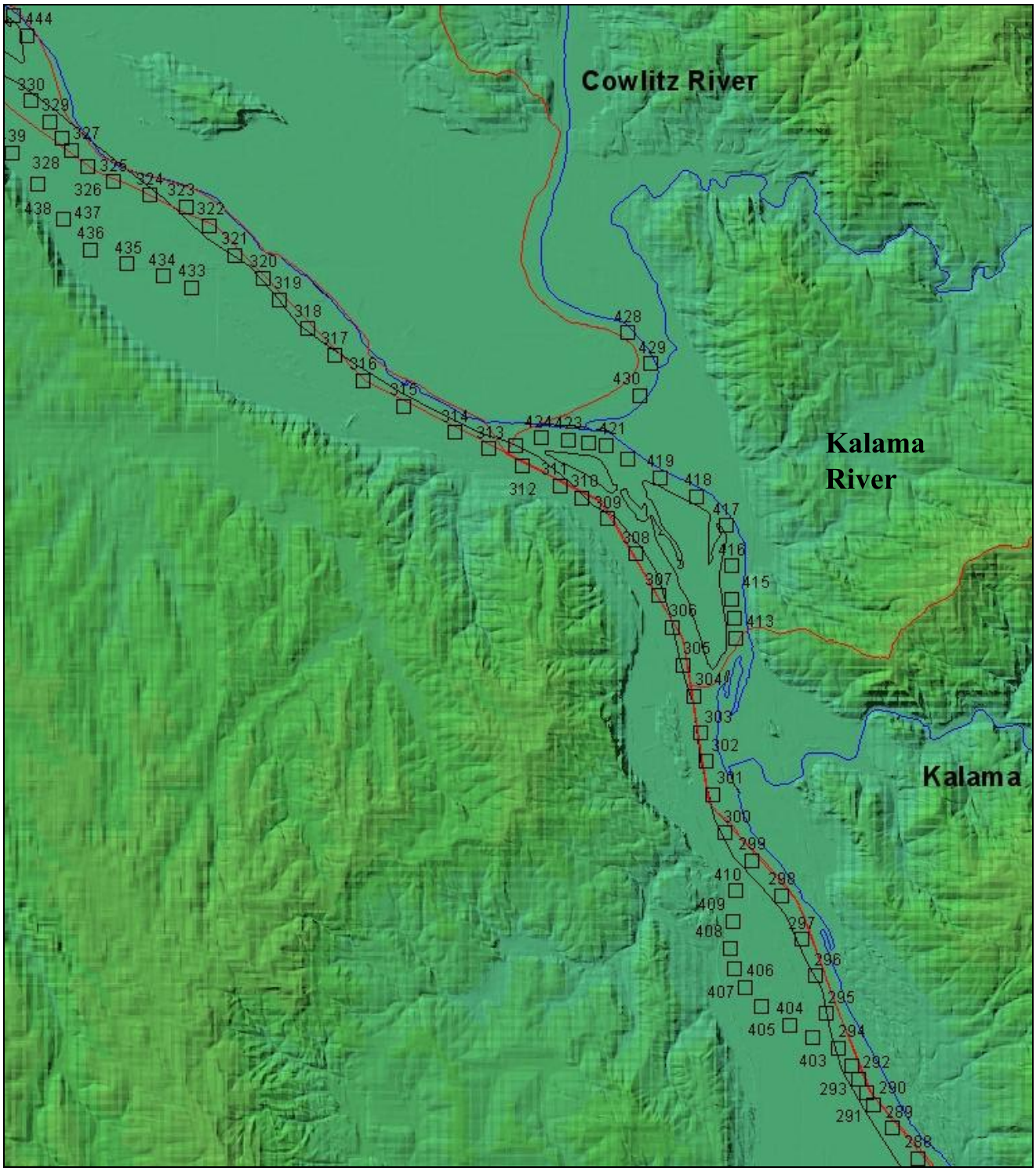


**Figure 15. Columbia River model segments near the Kalama River**

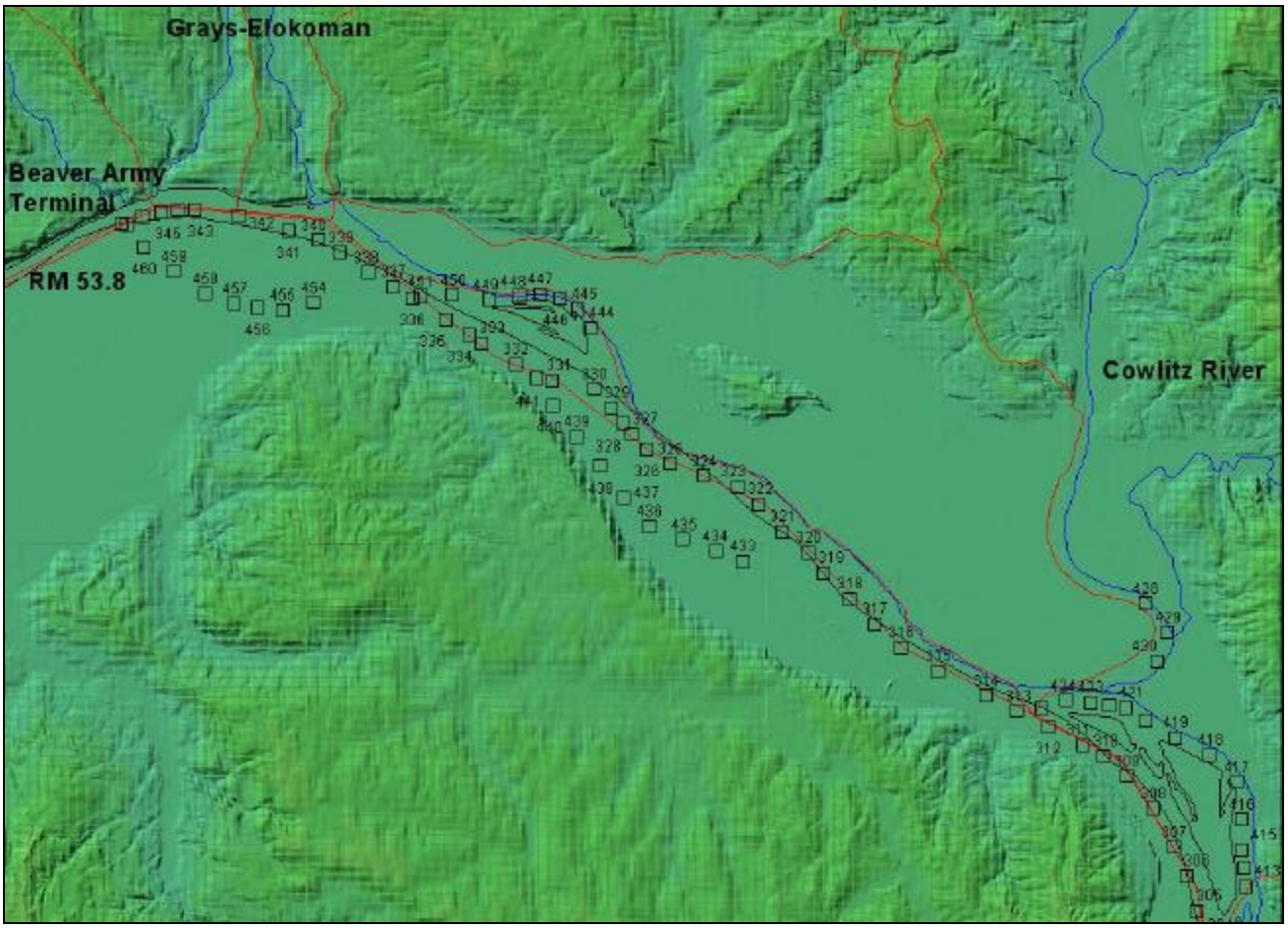


**Figure 16. Columbia River model segments near the Cowlitz River and Beaver Army Terminal**

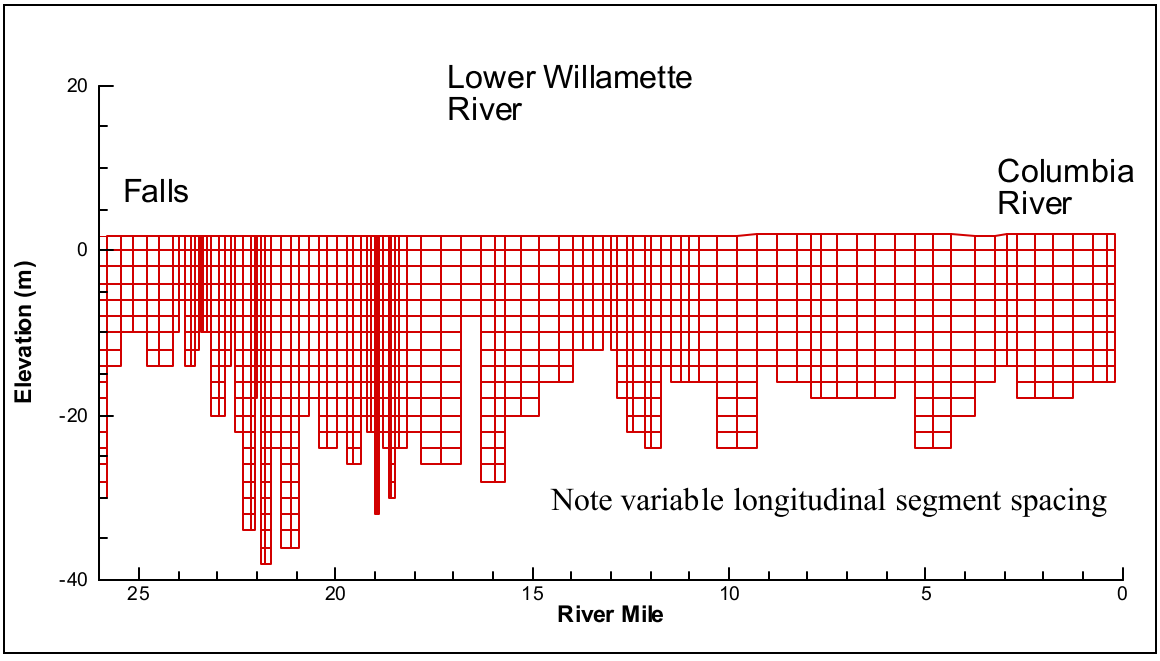


**Figure 17. Lower Willamette River vertical grid resolution**

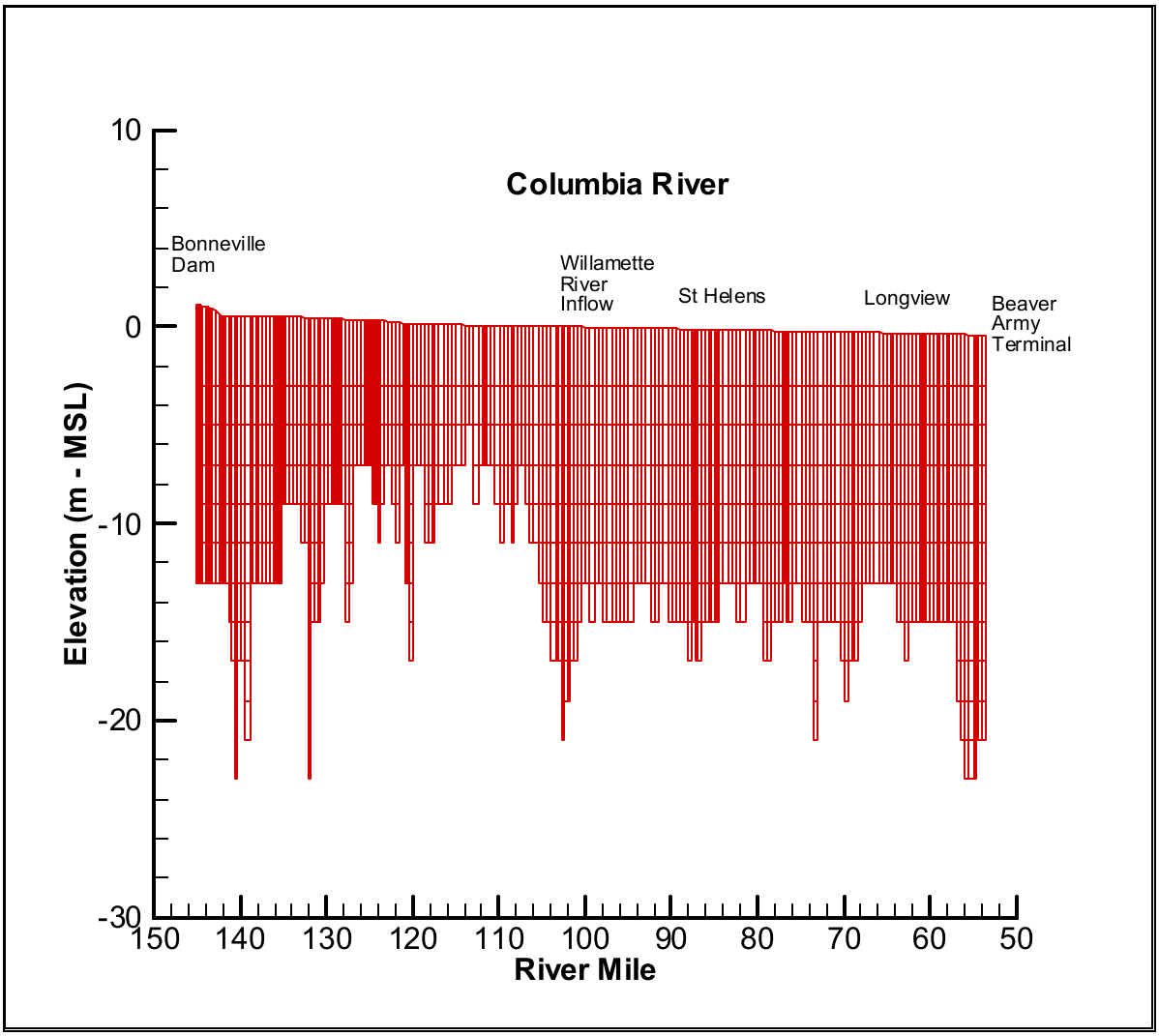


**Figure 18. Columbia River vertical grid resolution.**

## *Model Upstream & Downstream Boundary Conditions*

### Hydrodynamic Data

The boundaries for the Lower Willamette River model are Bonneville Dam (RM 145) and Beaver Army Terminal (RM 54) on the Columbia River and Willamette Falls (RM 26.8) on the Willamette River. Figure 19 shows the location of the boundaries and some large scale basins in the model region. Table 5 list the gages used in developing the hydrodynamic boundary conditions for the Lower Willamette River model.

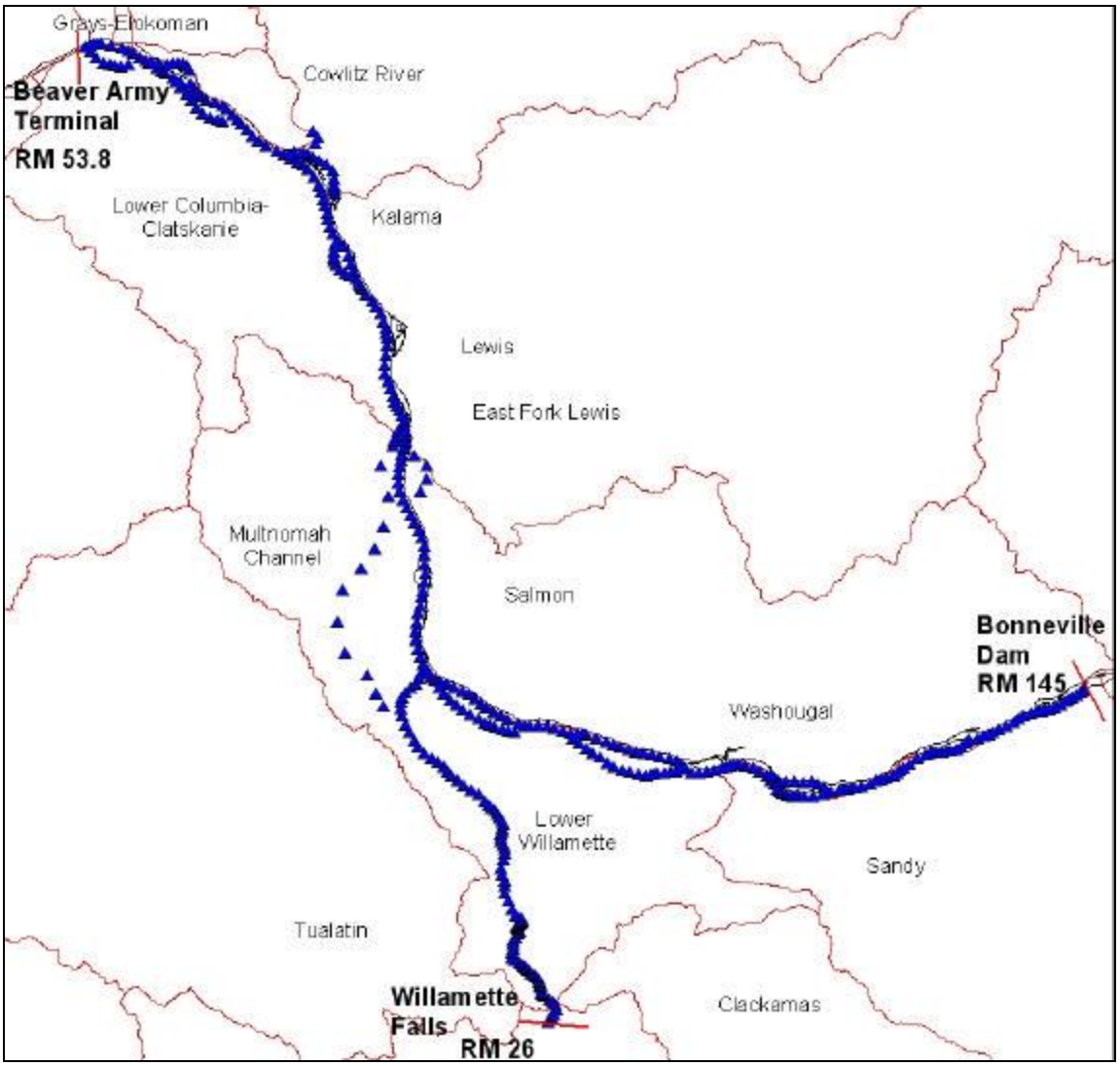


**Figure 19. Model Boundaries for the Lower Willamette River and the Columbia River**

**Table 5. Lower Willamette River model hydrodynamic boundary condition gage stations**

| Site ID | Description | RM | Model Segment |
|---|---|---|---|
| USGS14246900 | Columbia River at Beaver Army Terminal | 53.8 | 347 |
| USGS14128870 | Columbia River below Bonneville Dam | 144.5 | 118 |
| USGS14207740 | Willamette River below Willamette Falls | 26.8 | 2 |
| USGS14207770 | Willamette River above Willamette Falls | 26.8 | NA |

## Year 2001

The Beaver Army Terminal station (USGS 14246900) records water level data in 15 minute intervals. The model calibration period is from July 26, 2001 to September 28, 2001, due to other limitations in the model boundary conditions. There is a data gap from April 6 to May 2. The correlation developed by Rodriquez, et al. (2001) was used to fill the gap.

The correlation was between the Beaver Army Terminal site, the Vancouver, WA site (USGS 14144700), the Longview, WA site (USACOE LOP), the site below the Bonneville Dam (USGS 14128870) and the tidal influences on the Columbia River ($R^2$=0.8301). The tidal influence on the Columbia River represents the sinusoidal frequency of the tidal peaks that are a function of hourly, daily, monthly and annual cycles.

$$BeaverArmyTer\min alWLElev\_m = 0.0143(Hourly) + 0.0109(Daily) - 0.0062(Monthly) + 0.0054(Annually) - 0.2922(VancouverWLElev\_m) + 1.1156(LongviewWLElev\_m) + 0.0389(BonnevilleWLElev\_m) - 0.1942$$

Where:

Hourly is the tidal influence from 12.4 hour tidal cycle as: $Hourly = \sin\left(\frac{2\pi(JulianDay)}{12.4hours/24hours}\right)$

Daily is the daily tidal cycle estimated as: $Daily = \sin(2\pi(JulianDay))$

Monthly is the monthly tidal cycle estimated as: $Monthly = \sin\left(\frac{2\pi(JulianDay)}{30days}\right)$

Annually is the influence of any annual tidal fluctuations as: $Annually = \sin\left(\frac{2\pi(JulianDay)}{365days}\right)$

Figure 20 shows the water level elevation data at Beaver Army Terminal. Figure 21 shows the Columbia River flow below Bonneville Dam which were obtained from the USACOE. Although there are USGS gages station monitoring stage above (USGS 14207740) and below (USGS 14207770) the Willamette Falls, the gage above the falls is not always accurate. The upstream boundary condition for the Lower Willamette River was characterized by the outflow from the Middle Willamette River model.

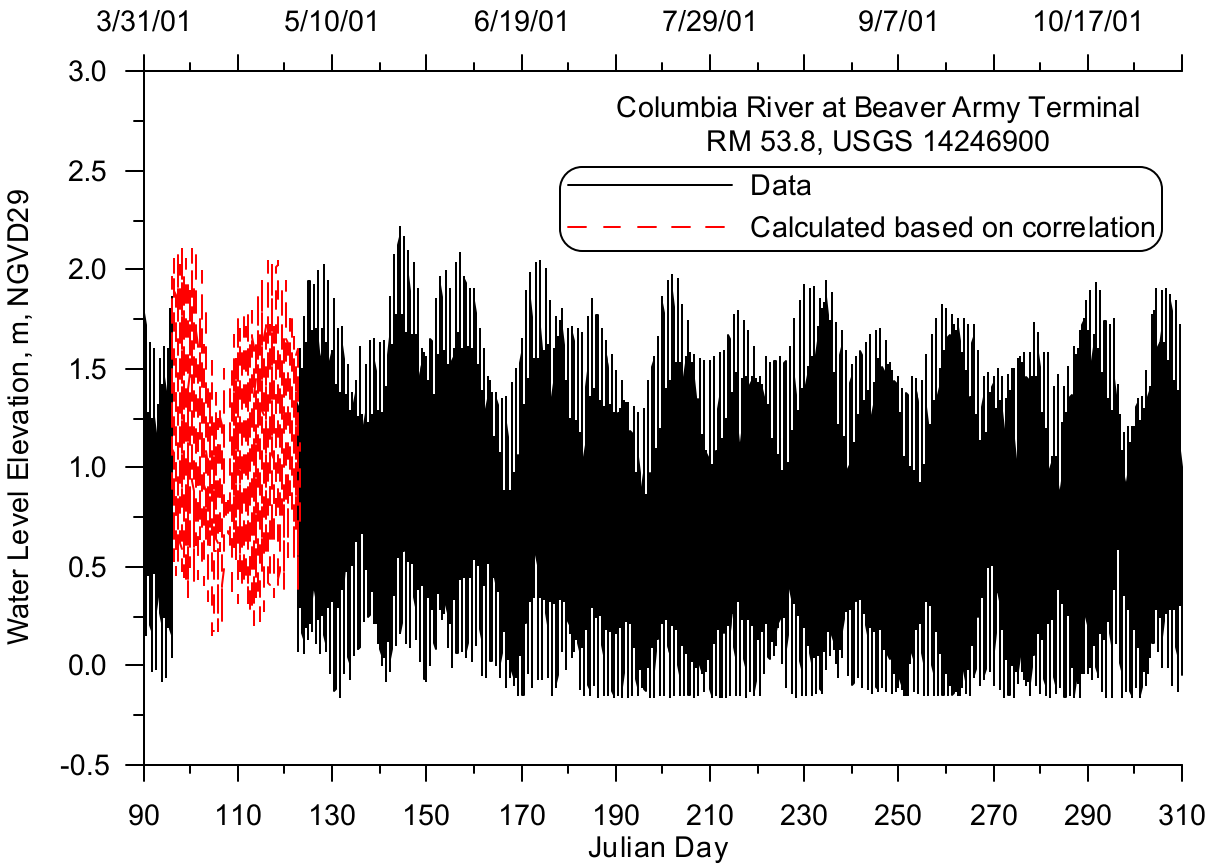


**Figure 20. Columbia River Water Level Elevation at Beaver Army Terminal, RM 53.8, 2001**

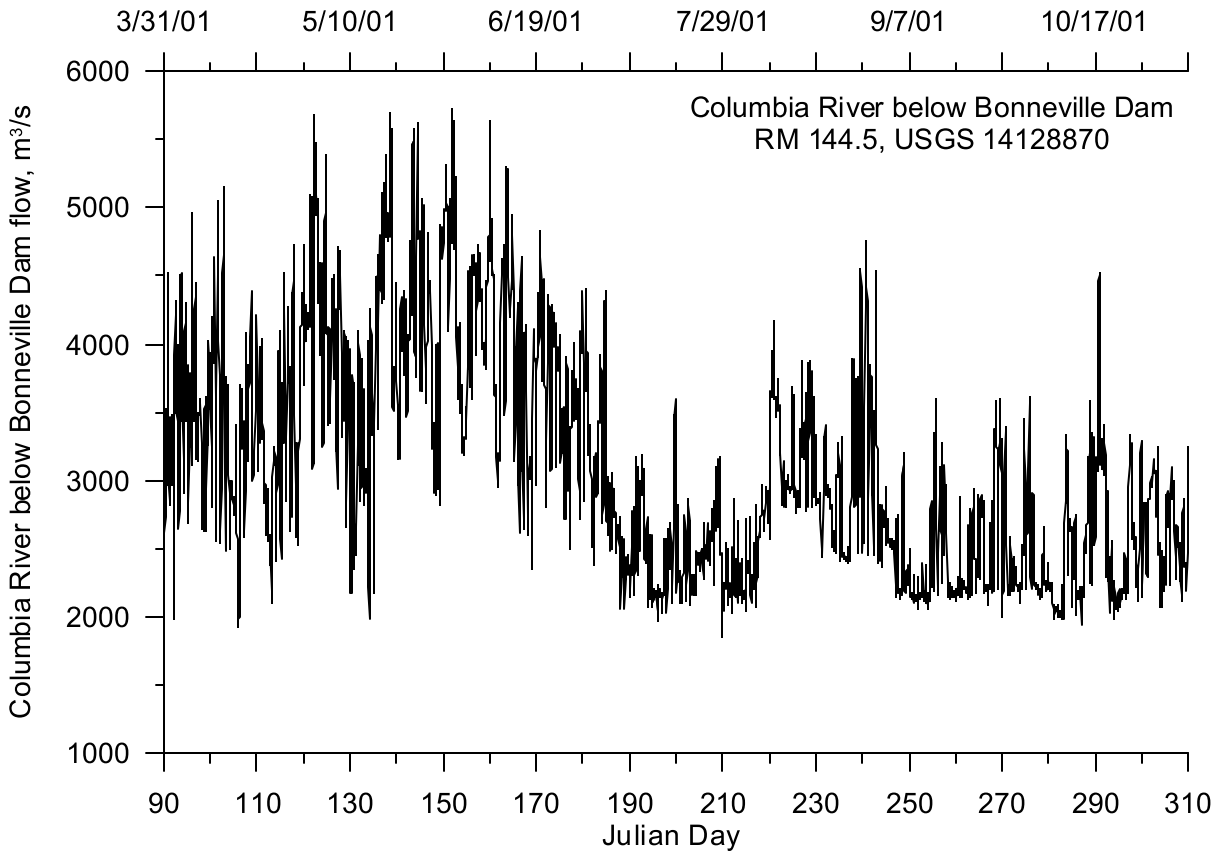


**Figure 21. Columbia River flow below Bonneville Dam, RM 144.5, 2001**

## Year 2002

The Beaver Army Terminal station (USGS 14246900) records water level data in 15 minute intervals. The model calibration period is from April 1, 2002 to October 1, 2002, and is limited by data availability in the model boundary conditions. Figure 22 shows the water level elevation data at Beaver Army Terminal with no gaps in the data. Figure 23 shows the Columbia River flow below Bonneville Dam obtained from the USACOE on an hourly basis. The upstream boundary condition for the Lower Willamette River was characterized by the outflow from the Middle Willamette River model.

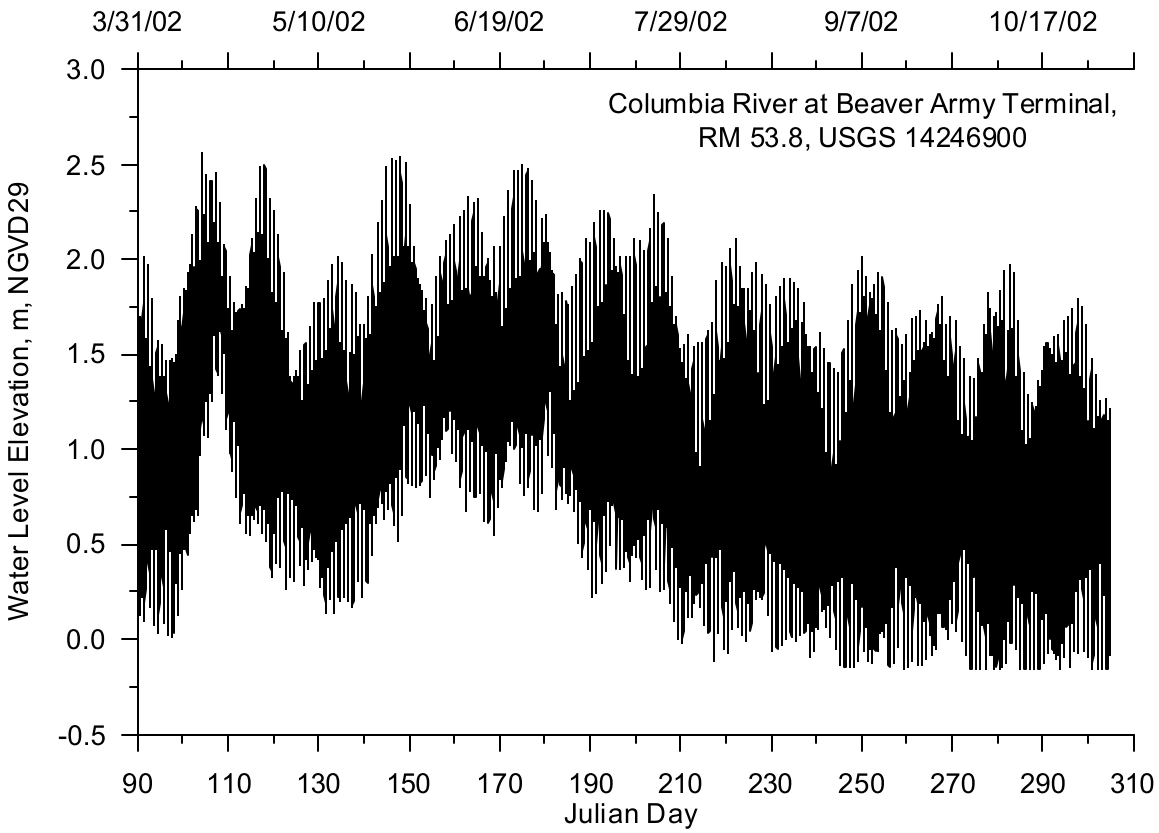


**Figure 22. Columbia River Water Level Elevation at Beaver Army Terminal, RM 53.8, 2002**

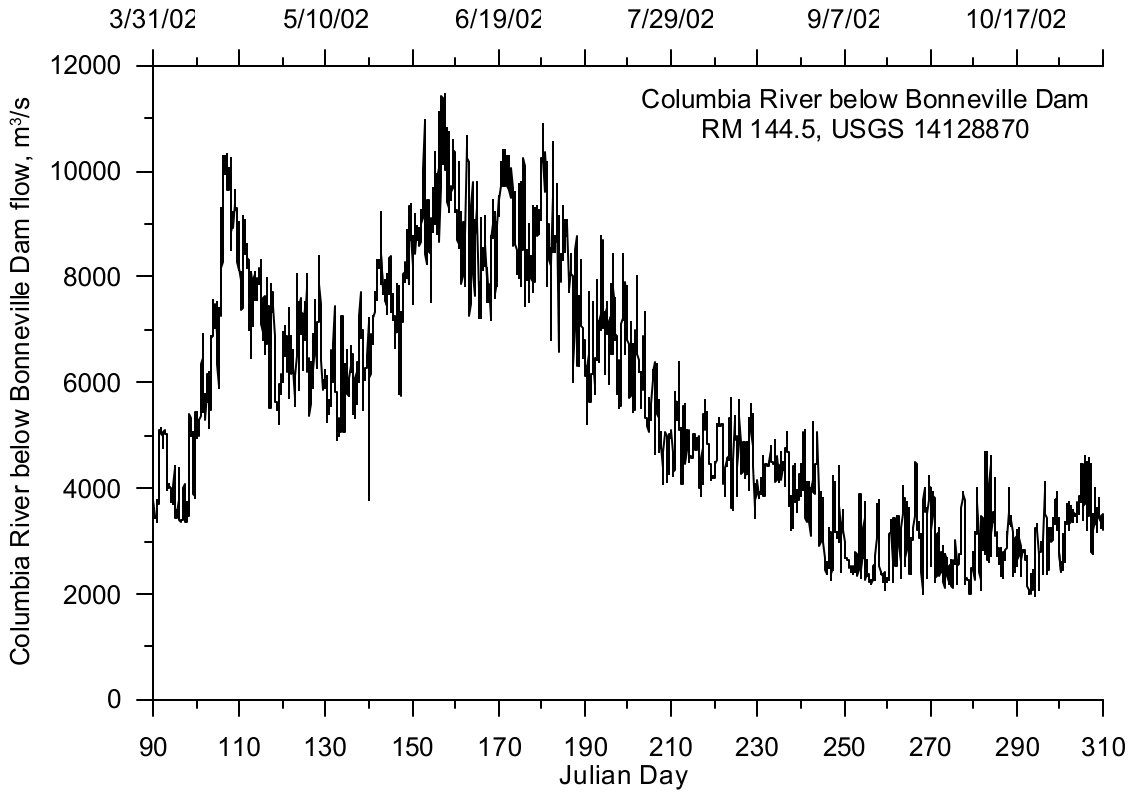


**Figure 23. Columbia River flow below Bonneville Dam, RM 144.5, 2002**

## Temperature Data

Temperature boundary conditions for the Lower Willamette River model were developed using some of the same gage stations used to develop the hydrodynamic boundary conditions. Figure 24 shows the temperature monitoring sites used for developing the temperature boundary conditions. Table 6 lists the gage stations shown in the figure and their corresponding river mile and model segment number.

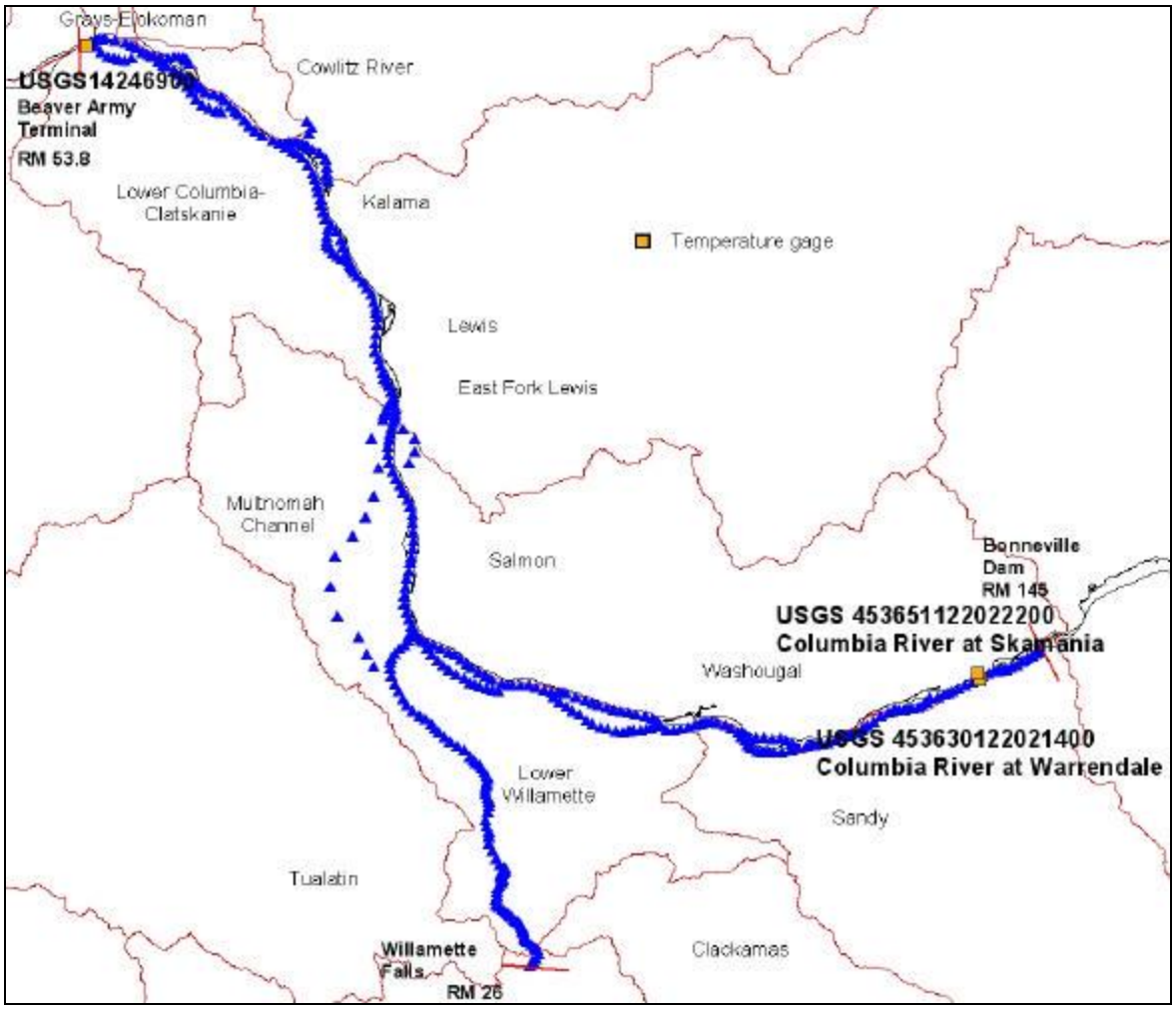


**Figure 24. Lower Willamette River model temperature boundary condition sites**

**Table 6. Lower Willamette River model temperature boundary condition gage stations**

| Site ID | Description | RM | Model Segment |
|---|---|---|---|
| USGS14246900 | Columbia River at Beaver Army Terminal | 53.8 | 347 |
| USGS453630122021400 | Columbia River at Warrendale | 141 | 118 |
| USGS453651122022200 | Columbia River at Skamania | 141 | 118 |

### Year 2001

The downstream boundary condition of the Columbia River utilized temperature data from the USACOE Beaver Army Terminal gage station. Figure 25 shows the hourly temperature data recorded at

the site. These data illustrate a general seasonal warming trend and several smaller warming and cooling patterns which may correspond to synoptic two week weather patterns. The upstream boundary on the Columbia River, just below the Bonneville Dam, has temperature data recorded near Skamania, WA, at the USGS gage 453651122022200. The gage has hourly data from April 1 to September 19, 2001. In order to fill in the data gap after September 19, a correlation was developed relating temperature data recorded at the Skamania gage with temperature data recorded at Warrendale, OR, (USGS 453630122021400). Figure 26 shows the temperature correlation developed between the two data sets and the correlation equation. Figure 27 shows the temperature record at the upstream boundary on the Columbia River with both data and calculated values from the correlation.

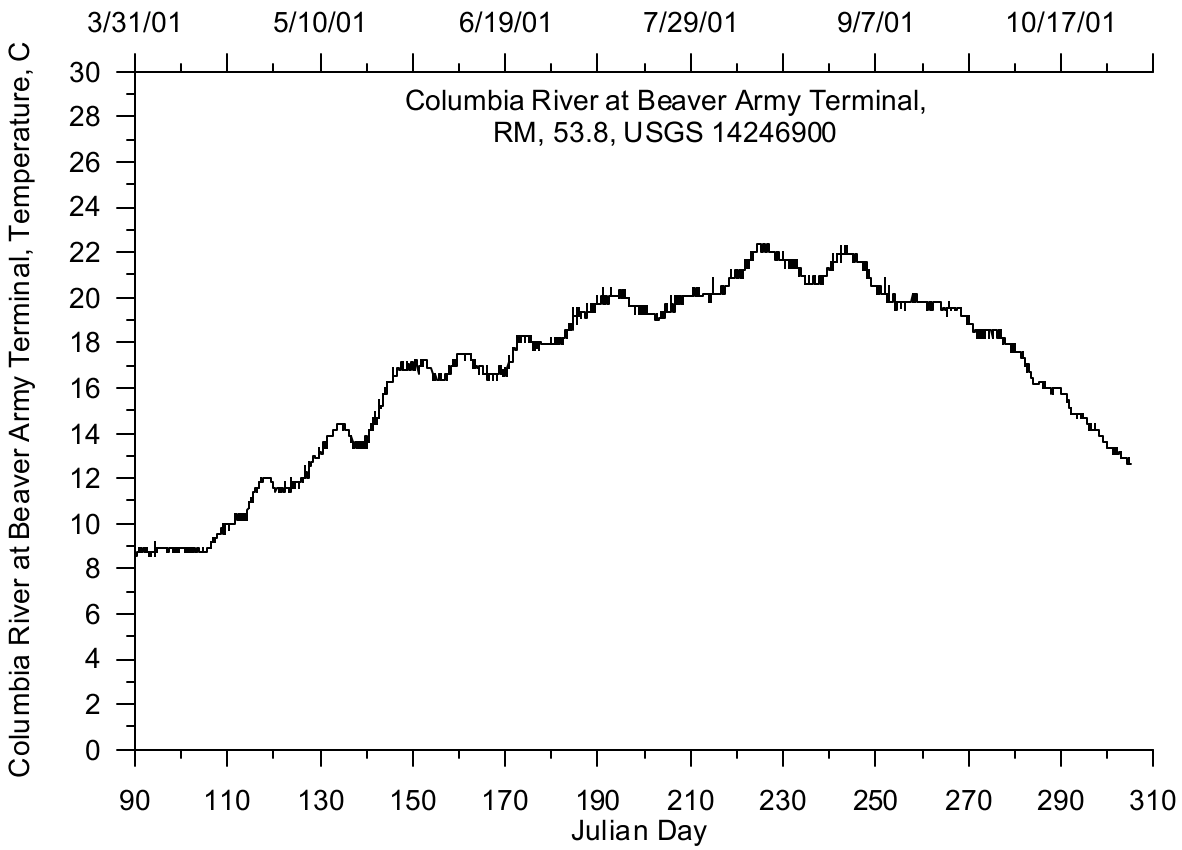


**Figure 25. Columbia River at Beaver Army Terminal Temperature, RM 53.8, 2001**

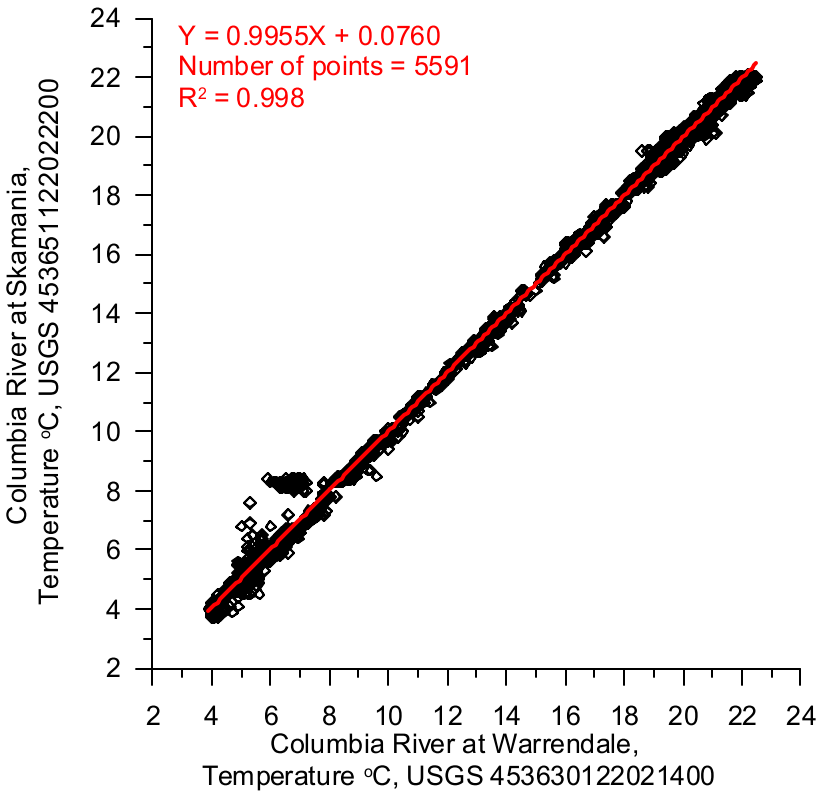


**Figure 26. Columbia River Temperature Correlation, 2001**

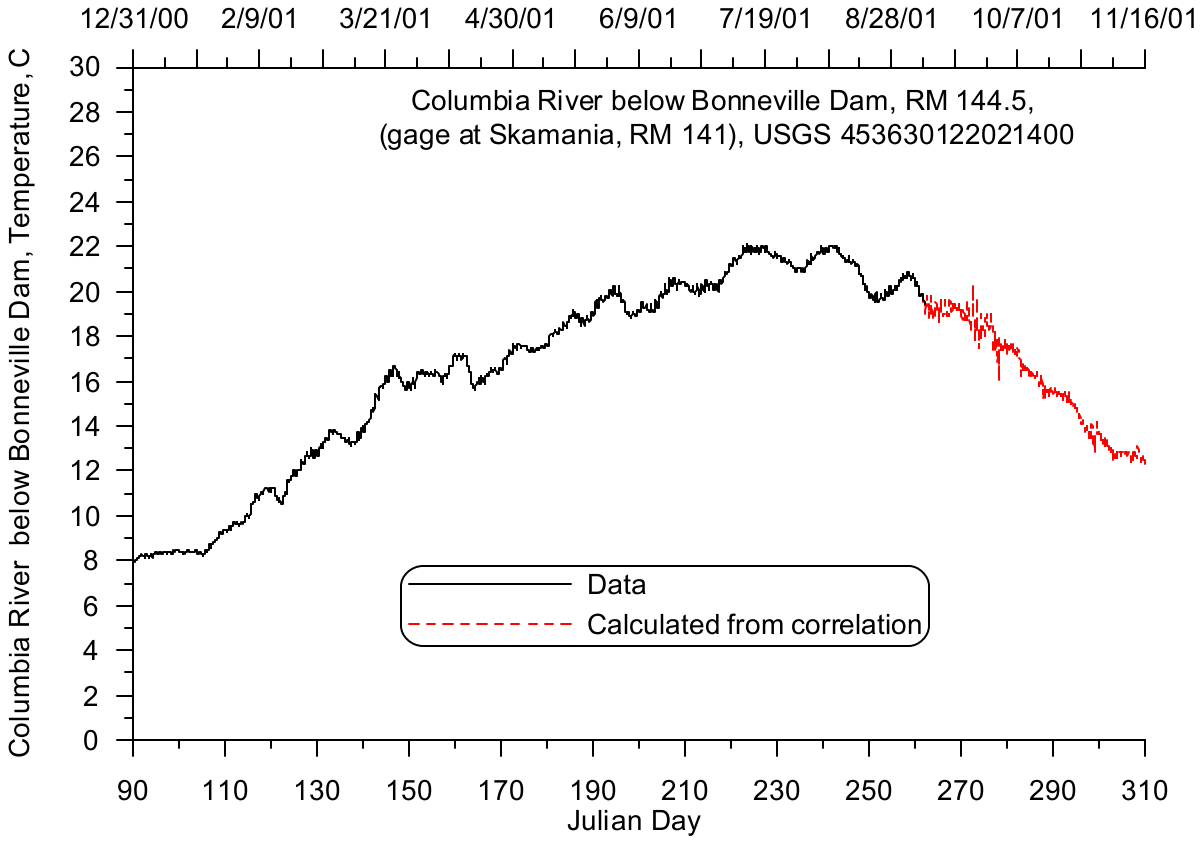


**Figure 27. Columbia River below Bonneville Dam Temperature, RM 144.5, 2001**

Year 2002

The downstream boundary condition of the Columbia River utilized temperature data from the USACOE Beaver Army Terminal gage station. Figure 28 shows the hourly temperature data recorded at the site. These data show a general seasonal warming trend over the summer. Unlike in 2001, there were very little temperature data recorded at the gage site near Skamania. Therefore, the upstream boundary on the Columbia River utilized temperature data directly from the gage station site at Warrendale, OR (USGS 453630122021400). Figure 29 shows the temperature data record at the upstream boundary on the Columbia River.

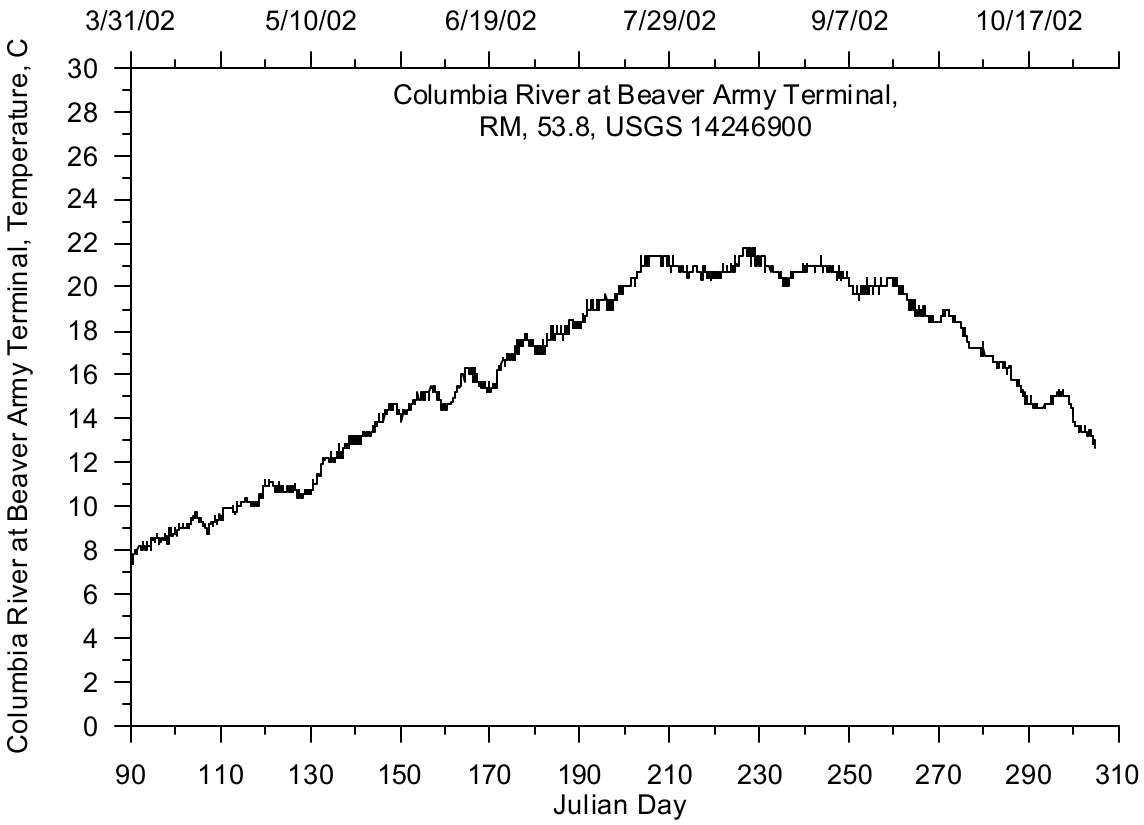


**Figure 28. Columbia River at Beaver Army Terminal Temperature, RM 53.8, 2002**

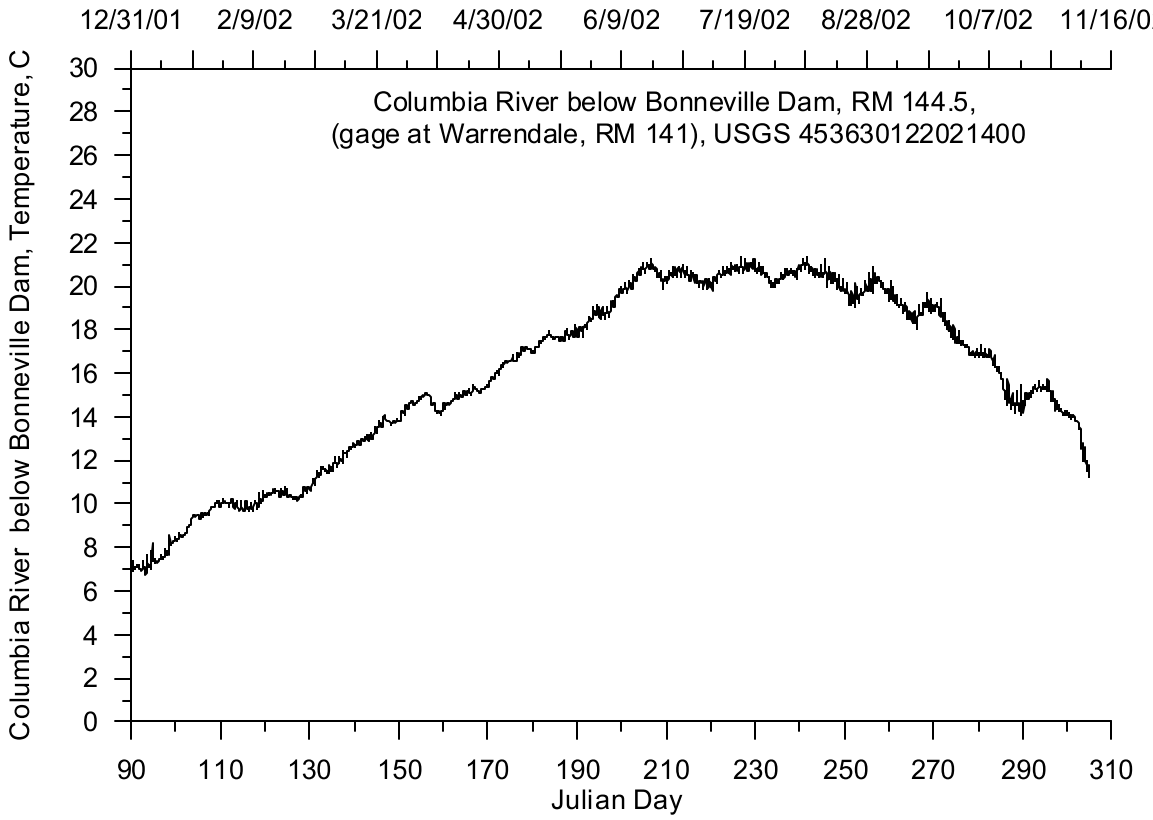


**Figure 29. Columbia River below Bonneville Dam Temperature, RM 144.5, 2002**

## *Tributaries*

The Lower Willamette River model covers 26.8 miles of the Willamette River and 90.7 miles of the Columbia River with nine tributaries directly entering the two rivers. The tributary inflows were characterized by both flow and temperature. There are some smaller basins along the Columbia and Willamette Rivers where no flow data were recorded, nor were historical values available. Flow contributions from the smaller basins were not determined individually and were incorporated as distributed tributaries.

### Hydrodynamic Data

Figure 30 shows a map of the Lower Willamette River model region along with its basins and the gage stations that were used to create the hydrodynamic inputs of the model. The model simulation period is from July 26, 2001 to September 28, 2001. Table 7 lists the gage stations used to develop the tributary inflows to the model for both 2001 and 2002.

Flow data for these tributaries were obtained from USGS gage stations and from a Washington State Department of Ecology (WADOE) study of discontinued USGS gage stations. Figure 30 shows the locations of the active and discontinued USGS stations used to develop the input files for CE-QUAL-W2. Figure 30 also shows the watersheds included in the model, which were identified by the Water Quality Research Group at Portland State University.

The Washington State Department of Ecology conducted a study to characterize base flows for rivers and streams in Washington (Sinclair and Pitz, 1999). Table 7 has six stations where recent flow measurements were not available but the State of Washington estimated monthly base flows. These stations were used to develop input flows for the model.

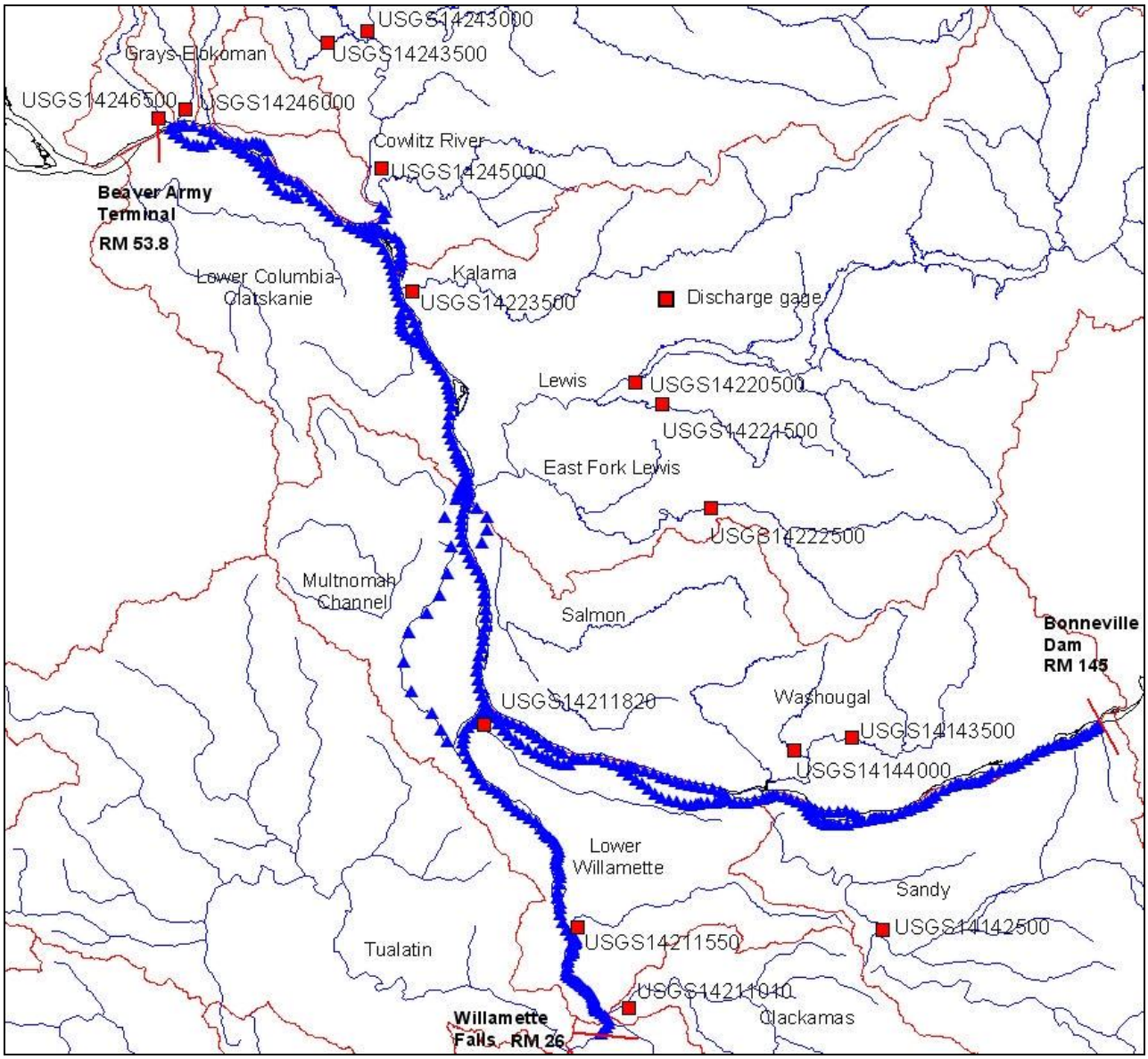


**Figure 30. Lower Willamette River model tributary gage station locations**

**Table 7. Lower Willamette River model tributary gage stations**

| Site ID | WADOE base flow study | Tributary | RM | Model Segment |
|---|---|---|---|---|
| USGS14211820 | No | Columbia Slough, OR | 1.00 | 96 |
| USGS14211550 | No | Johnson Creek At Milwaukie, OR | 18.50 | 49 |
| USGS14210000 | No | Clackamas River at Estacada, OR | NA | NA |
| USGS14211010 | No | Clackamas River at Oregon City, OR | 24.85 | 7 |

| Site ID | WADOE base flow study | Tributary | RM | Model Segment |
|---|---|---|---|---|
| USGS14142500 | No | Sandy River Below Bull Run River, OR | 120.25 | 192 |
| USGS14143500 | No | Washougal River Near Washougal, WA | 120.75 | 191 |
| USGS14144000 | No | Little Washougal River Near Washougal, WA | NA | NA |
| USGS14220500 | No | Lewis River at Ariel, WA | 87.20 | 265 |
| USGS14222500 | No | East Fork of the Lewis River Near Heisson, WA | NA | NA |
| USGS14243000 | No | Cowlitz River at Castle Rock, WA. | 67.33 | 428 |
| USGS14246000 | Yes | Abernathy Creek near Longview, WA | NA | NA |
| USGS14246500 | Yes | Mill Creek near Cathlamet, WA | NA | NA |
| USGS14243500 | Yes | Delameter Creek near Castle Rock, WA | NA | NA |
| USGS14245000 | Yes | Coweman River near Kelso, WA | NA | NA |
| USGS14223500 | Ye | Kalama River below Italian Creek near Kalama, WA | 73.00 | 301 |
| USGS14221500 | Yes | Cedar Creek near Ariel, WA | NA | NA |

Year 2001

Tributary data were used to created model input files for with period between April 1, 2001 to October 31, 2001, even though the model calibration was from July 26 to September 28. Input files for the model were developed using continuous and daily data; however, correlations were also developed using nearby stations to fill data gaps when they existed.

Columbia Slough flow data were obtained from the USGS gage station at the Lombard St Bridge (USGS 14211820). The data frequency was 15 minutes, but there were data gaps from June 6 to June 19, June 23 to July 11, and July 19 to July 27. It was not possible to fill the data gaps because there were no nearby gage stations that resulted in good flow correlations. In addition, the data gaps were short ranging from 8 to 18 days so the gaps should have little impact on the overall flows from the Columbia Slough. The average flow from the Columbia Slough to the Lower Willamette River from April 1, 2001 to October 31, 2001 was 4.3 $m^3/s$ and the average flow for the Lower Willamette River for the same period was approximately 238.3 $m^3/s$. CE-QUAL-W2 will linearly interpolate between the closest two data points in time before and after the data gaps. Figure 31 shows the Columbia Slough flow for the summer and shows large negative flows which reflect the tidal influence in the Lower Willamette River.

The Johnson Creek flow data were from the USGS gage at Milwaukie, OR, (USGS 14211820). In 2001 there were no data gaps in the record from April 1 to October 31. Figure 32 shows the flow data for Johnson Creek and shows there was a typical seasonal pattern with lower stream flows in the summer than the spring and fall. Overall, Johnson Creek flows were much lower than other tributaries in the system.

The Clackamas River flow data for 2001 has a data gap from April 1 to June 8 at the USGS gage station at Oregon City (USGS 14211010). A flow correlation was developed with the USGS gage station on the Clackamas River at Estacada (USGS 14210000). Figure 33 shows the flow correlation between the two sites and the correlation equation. The correlation equation and the flow data from Estacada were then used to calculate the flow downstream at Oregon City. Figure 34 shows both the flow data and the calculated flow values for the Clackamas River.

The Kalama River flows were characterized using monthly base flows estimated at the Kalama River near Kalama (Sinclair and Pitz, 1999) since the basin was lacking flow data. Figure 30 and Figure 70 show the relative size of the Kalama River basin compared to the Lewis River basin. Figure 35 shows the flow for the Kalama River.

Grays-Elokoman basin flow to the Columbia River was characterized by adding base flows for the Abernathy Creek near Longview and Mill Creek near Cathlamet as shown in Table 7 and Figure 30. Figure 70 also shows the fraction of the Grays-Elokoman basin included in the model. The input file for the model was created using monthly averaged base flows (Sinclair and Pitz, 1999) for the summer months modeled since no other data were available. Figure 36 shows the base flow estimated for the Grays-Elokoman basin for 2001.

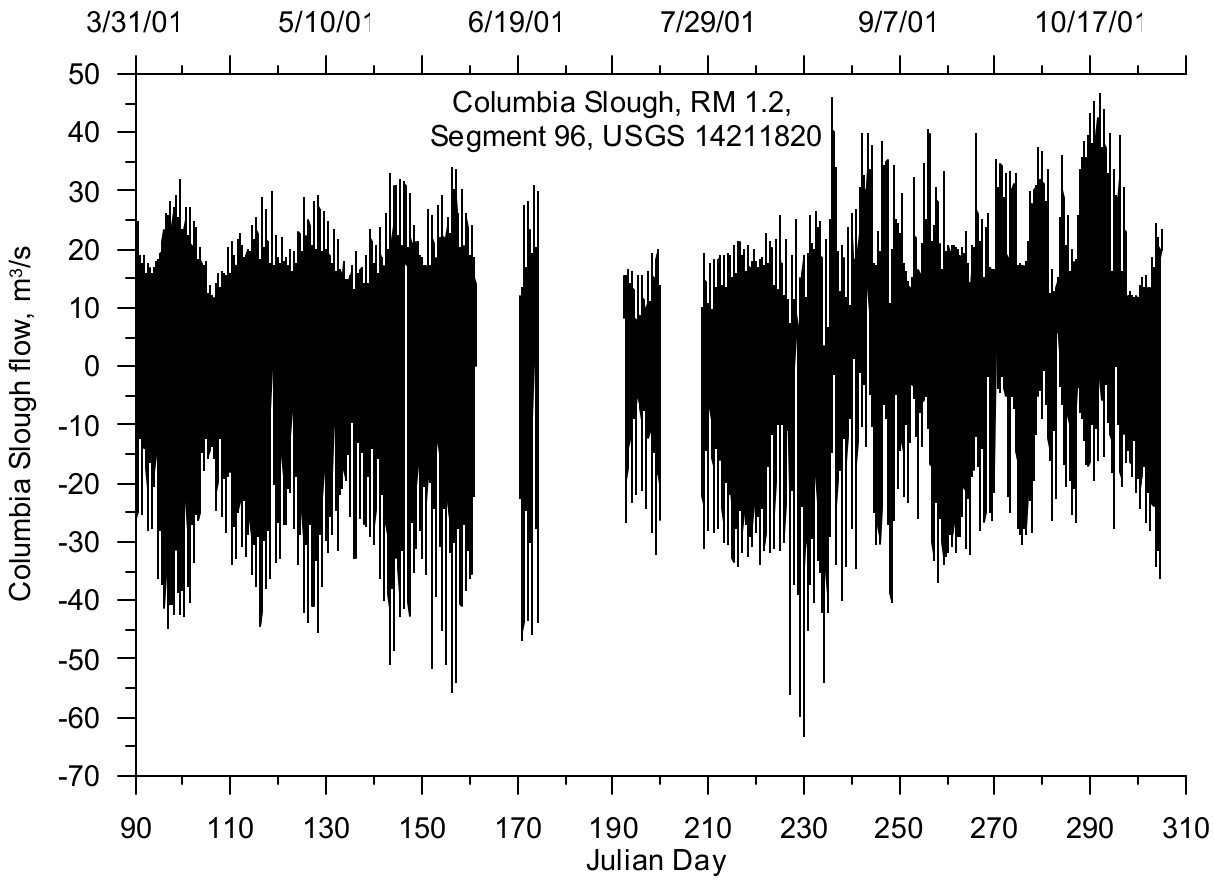


**Figure 31. Columbi a Slough flow, 2001**

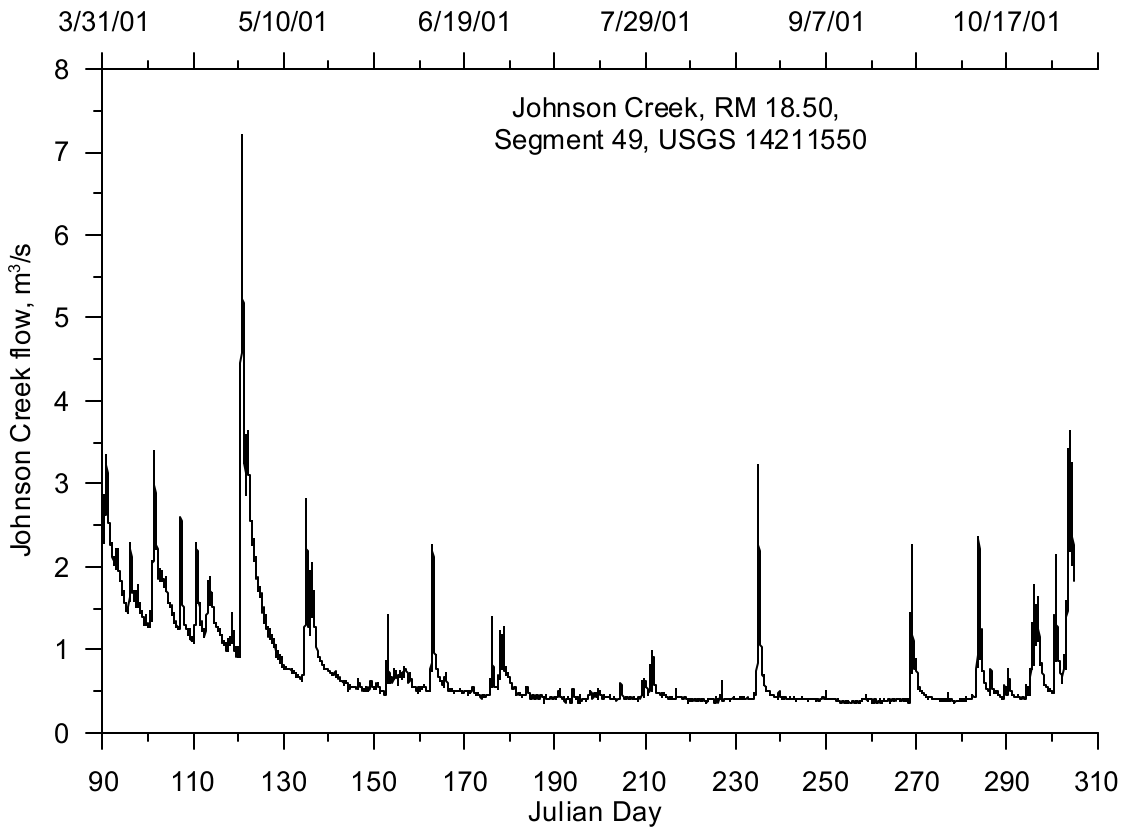


**Figure 32. Johnson Creek flow, 2001**

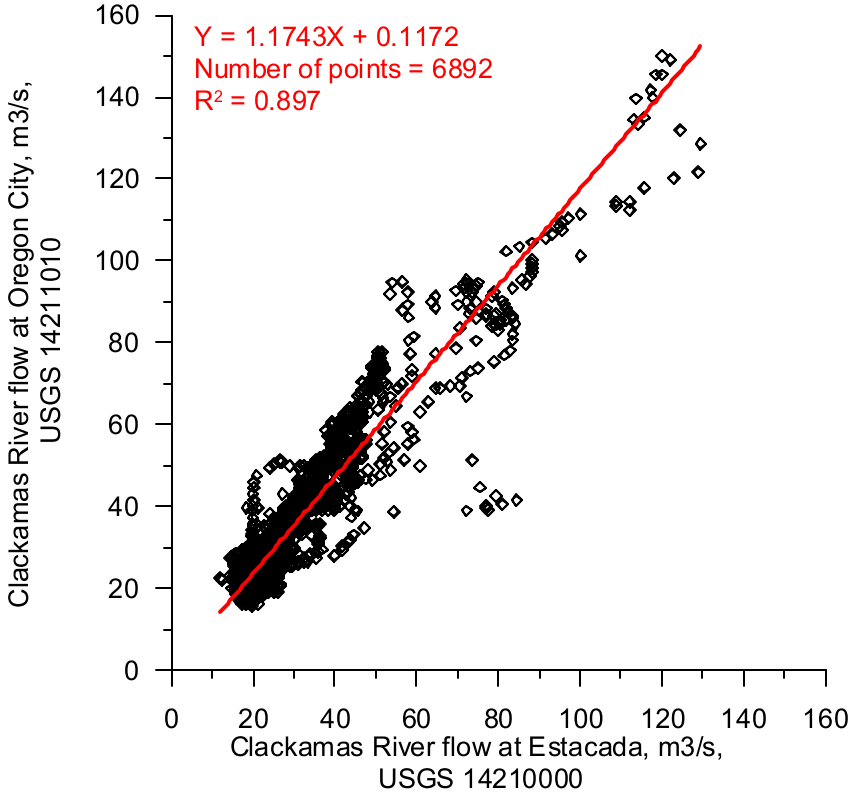


**Figure 33. Clackamas River flow correlation using flow at Estacada and at Oregon City**

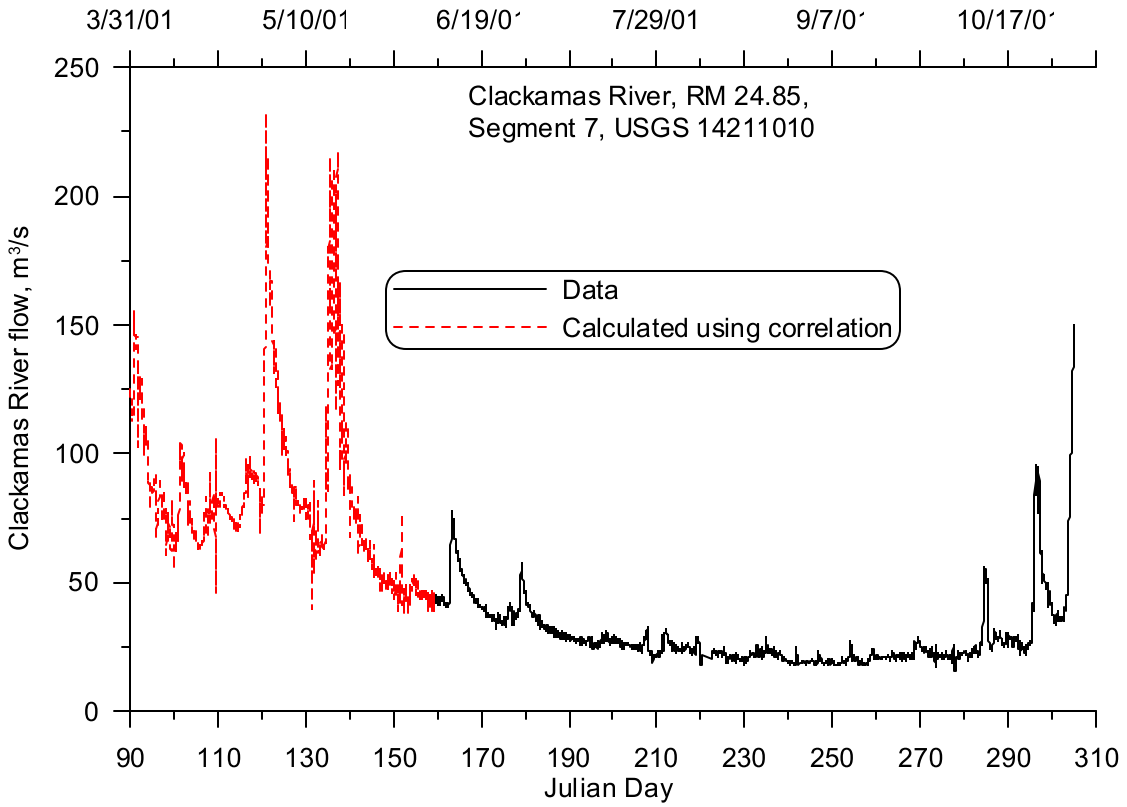


**Figure 34. Clackamas River flow, 2001**

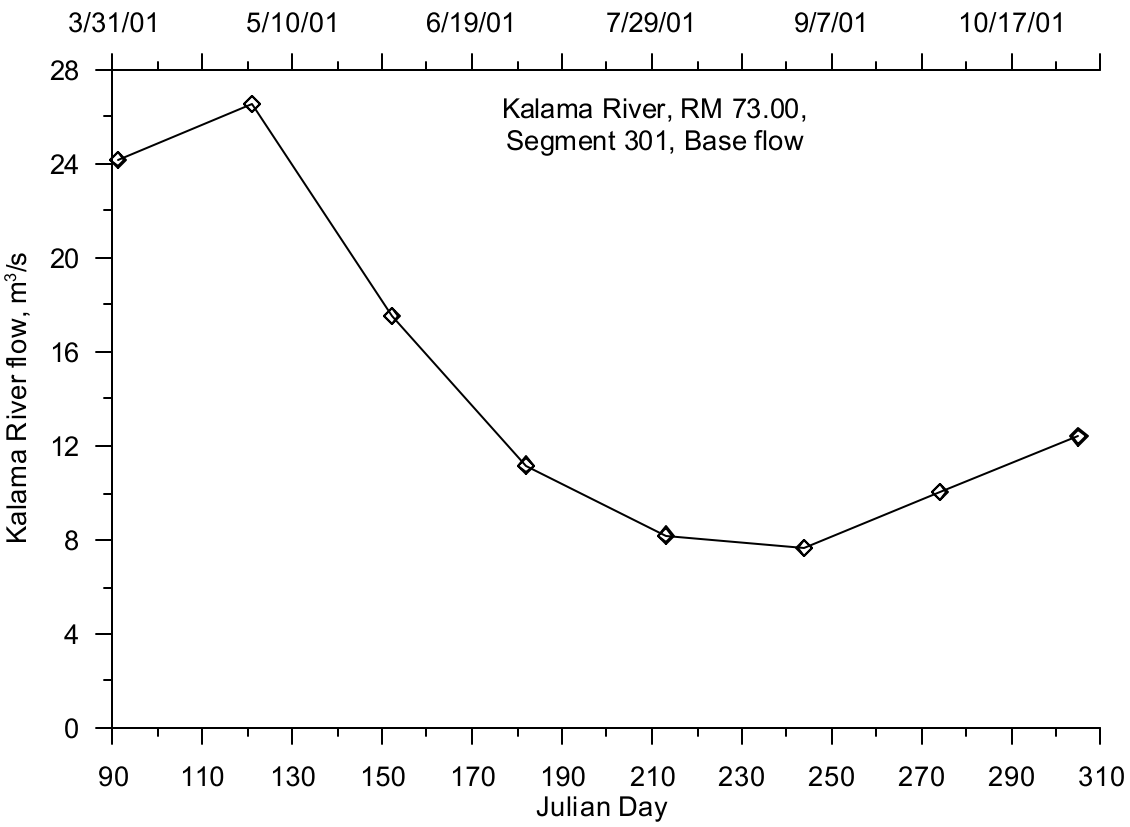


**Figure 35. Kalama River flow, 2001**

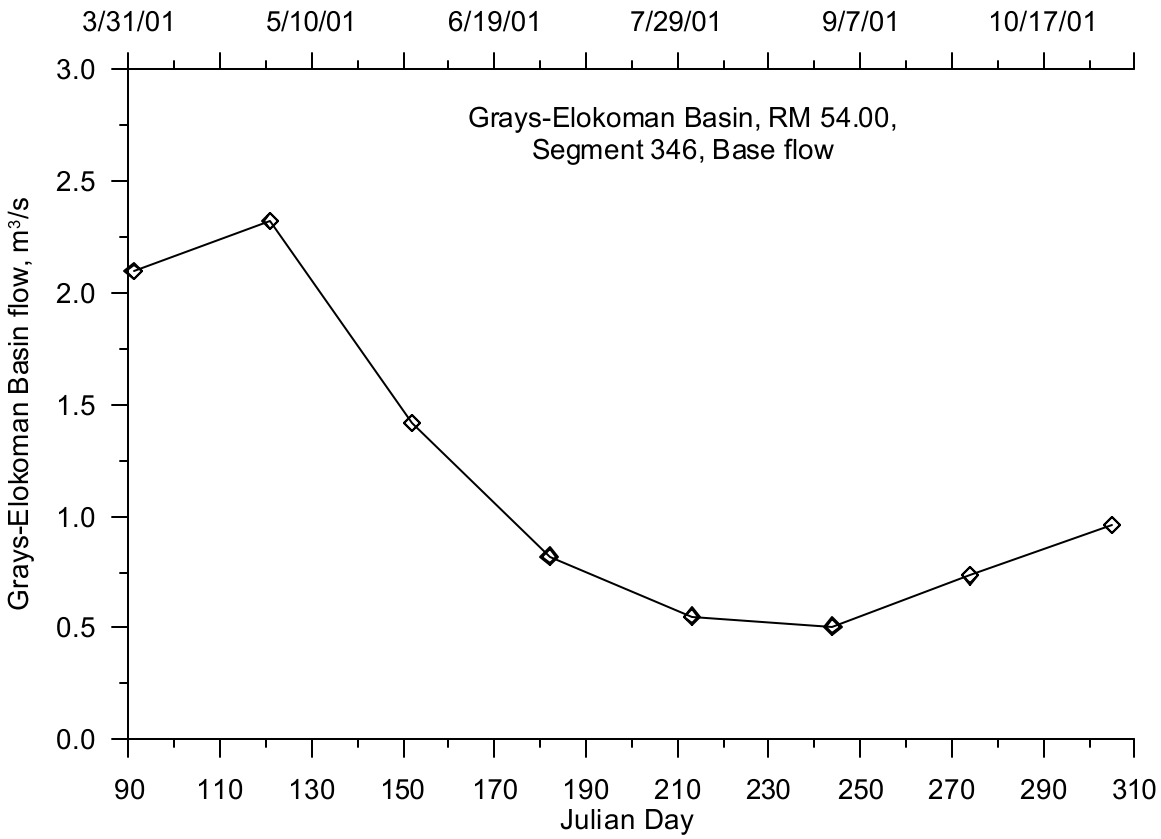


**Figure 36. Gray-Elokoman basin flow, 2001**

The Cowlitz River was characterized using continuous data for the Cowlitz River station at Castle Rock (USGS 14243000). Figure 30 shows the Cowlitz basin and its tributaries. The data from this station were added to the base flows estimated at the Delameter Creek station near Castle Rock (USGS 14243500) and the Coweman River station near Kelso (USGS 14245000) to obtain the total Cowlitz basin flow. Figure 37 shows flows for the Cowlitz River for 2001.

The Lewis River flow was calculated by adding daily average flows for the Lewis River station (USGS 14220500) and the East Fork of the Lewis River (USGS 14222500). Figure 38 shows the total flow from the Lewis River to the Columbia River. Figure 39 shows the Lewis River Basin and its tributaries. Additionally, the base flow from Cedar Creek was incorporated to generate the total flow from the Lewis River Basin.

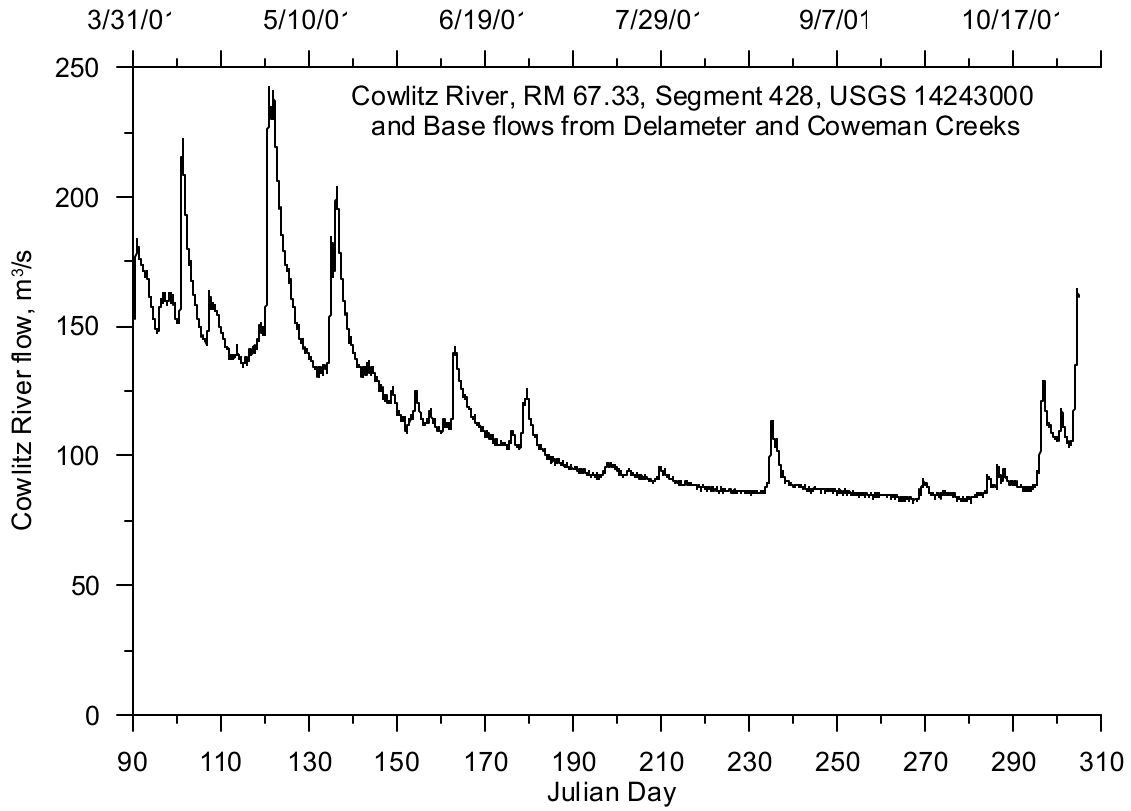


**Figure 37. Cowlitz River flow, 2001**

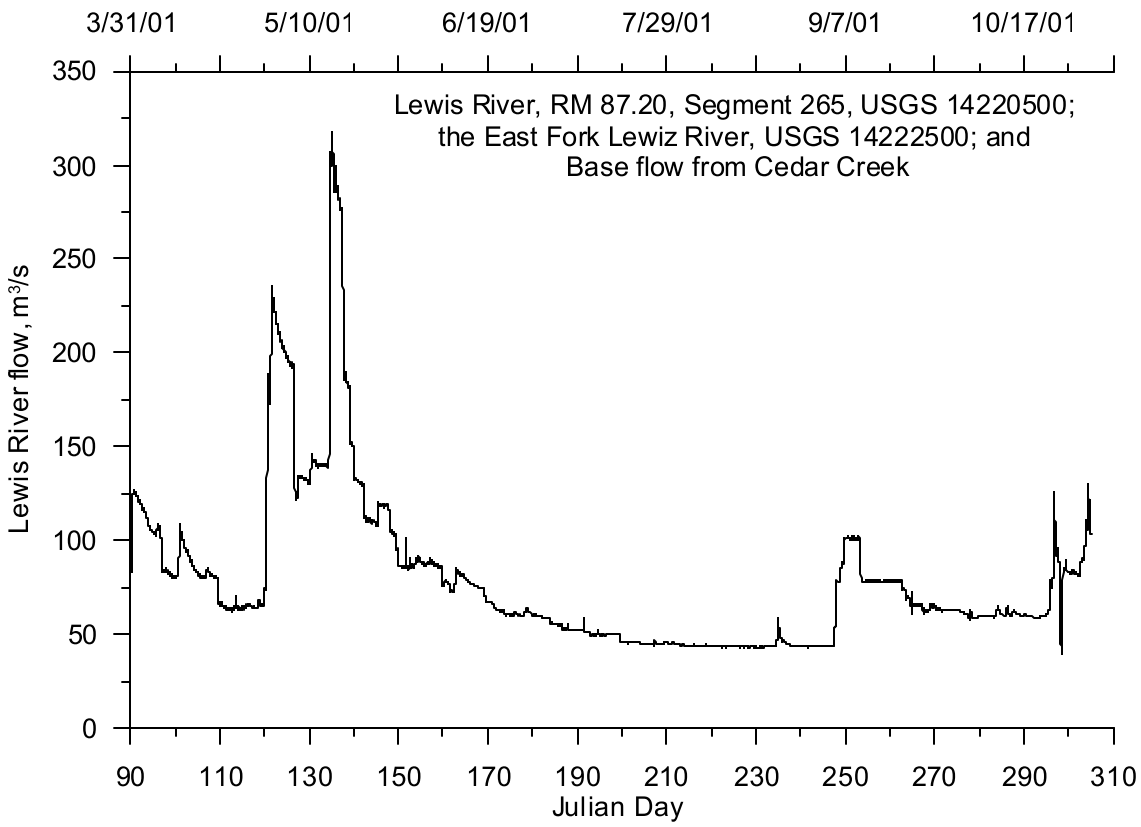


**Figure 38. Lewis River flow, 2001**

The Washougal River flow was estimated based on correlations between the East Fork of the Lewis River and the Washougal River and the Little Washougal River. Figure 39 shows a map illustrating the proximity of the Lewis River basin to the Washougal River basin. The East Fork of the Lewis River was selected for the correlation because it is an adjacent basin to the Washougal River. A correlation relating daily flows in the East Fork of the Lewis River with daily flows in the Washougal River was developed from the data record of October 1, 1944 to September 30, 1981. Figure 40 shows the flow correlation between the two sites.

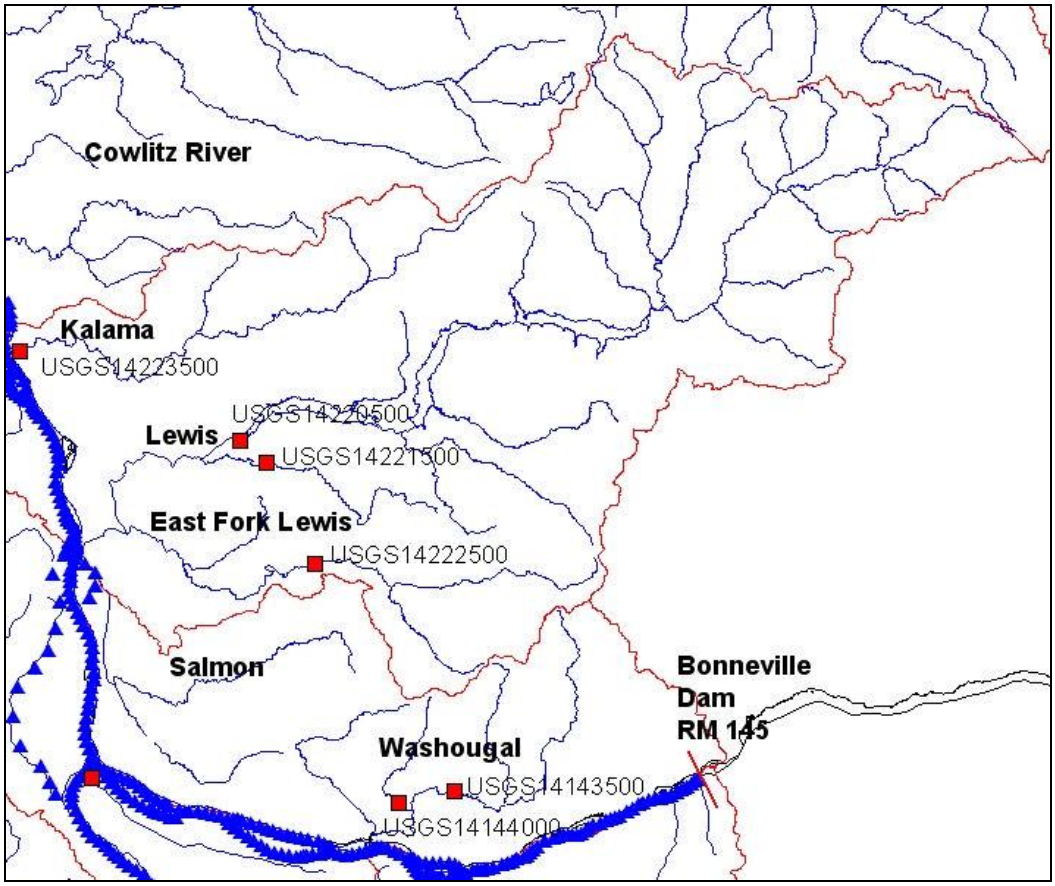


**Figure 39. Lewis River and Washougal River Basins**

Another correlation relating the daily flows in the East Fork of the Lewis River with the Little Washougal River was developed using data from the period July 1, 1951 to November 10, 1955. Figure 41 shows the flow correlation and the correlation equation. Daily flows for the Washougal River and the Little Washougal were calculated based on these two correlations. The resultant flows were then added together to create the tributary flow for the model. Figure 42 shows the calculated Washougal River flow for 2001.

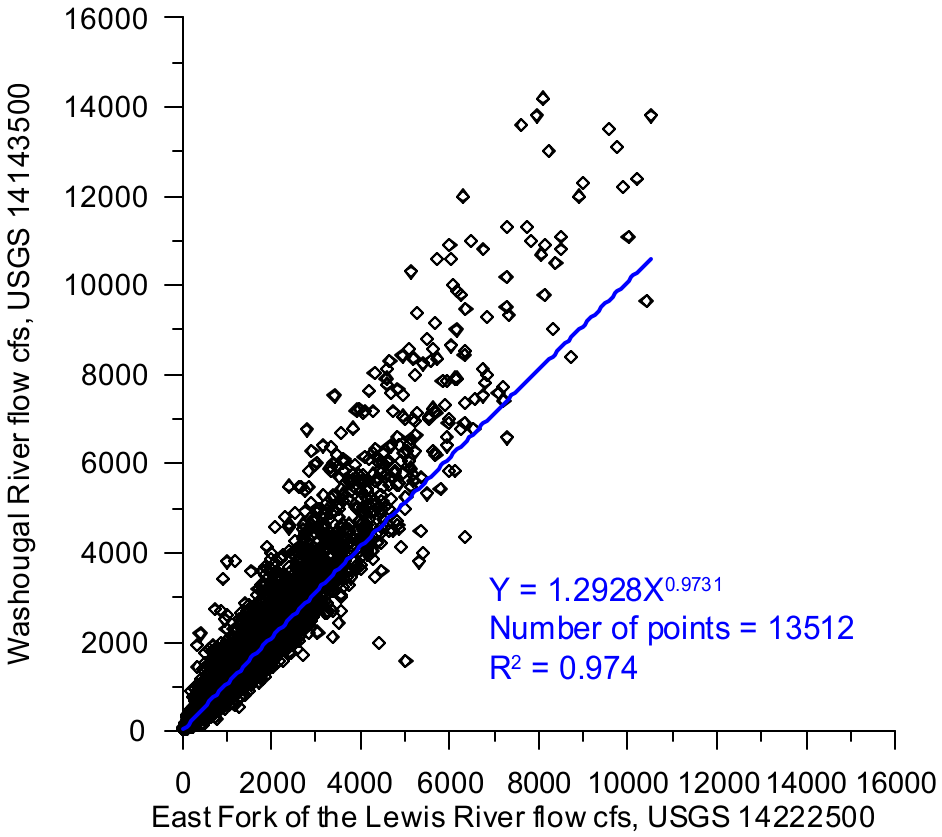


**Figure 40. Washougal River flow correlation with the East Fork of Lewis River**

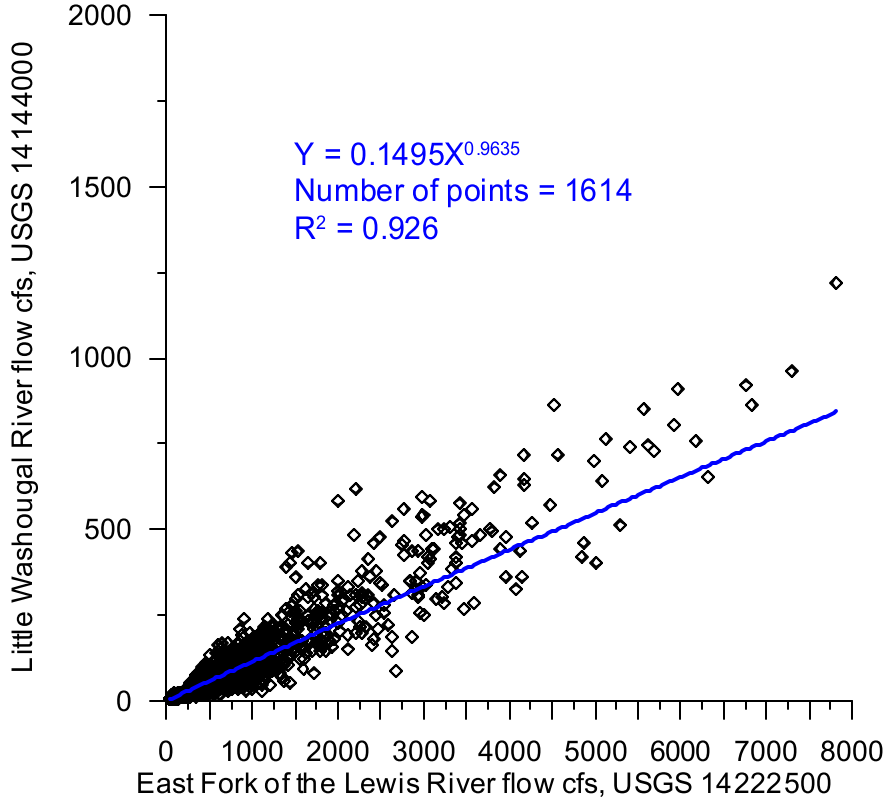


**Figure 41. Little Washougal River flow correlation with the East Fork of Lewis River**

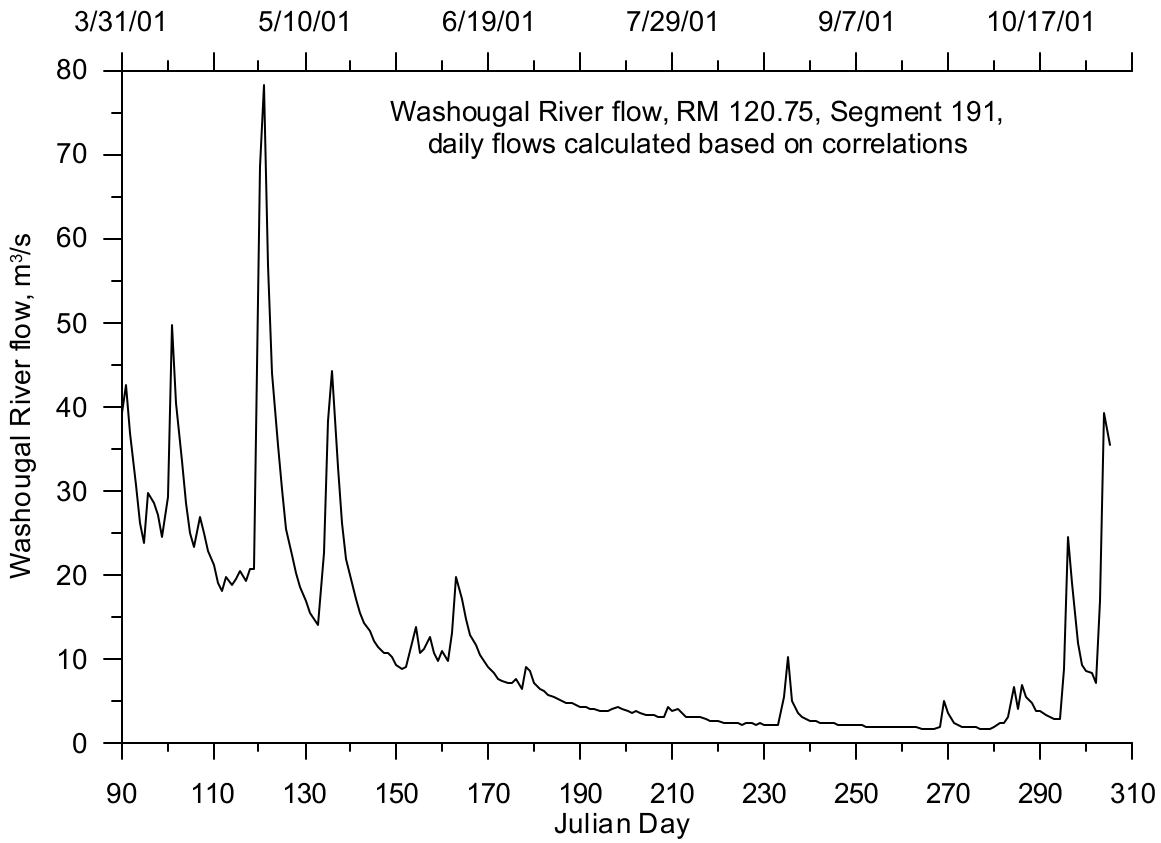


**Figure 42. Washougal River flow, 2001**

The Sandy River flow was characterized by the USGS gage station located below the confluence with the Bull Run River (USGS 14142500). Flow measurements were recorded every half-hour and there were no data gaps in the 2001 data record. Figure 43 shows the Sandy flow for the summer of 2001 indicating a sharp decline in flow from spring to summer.

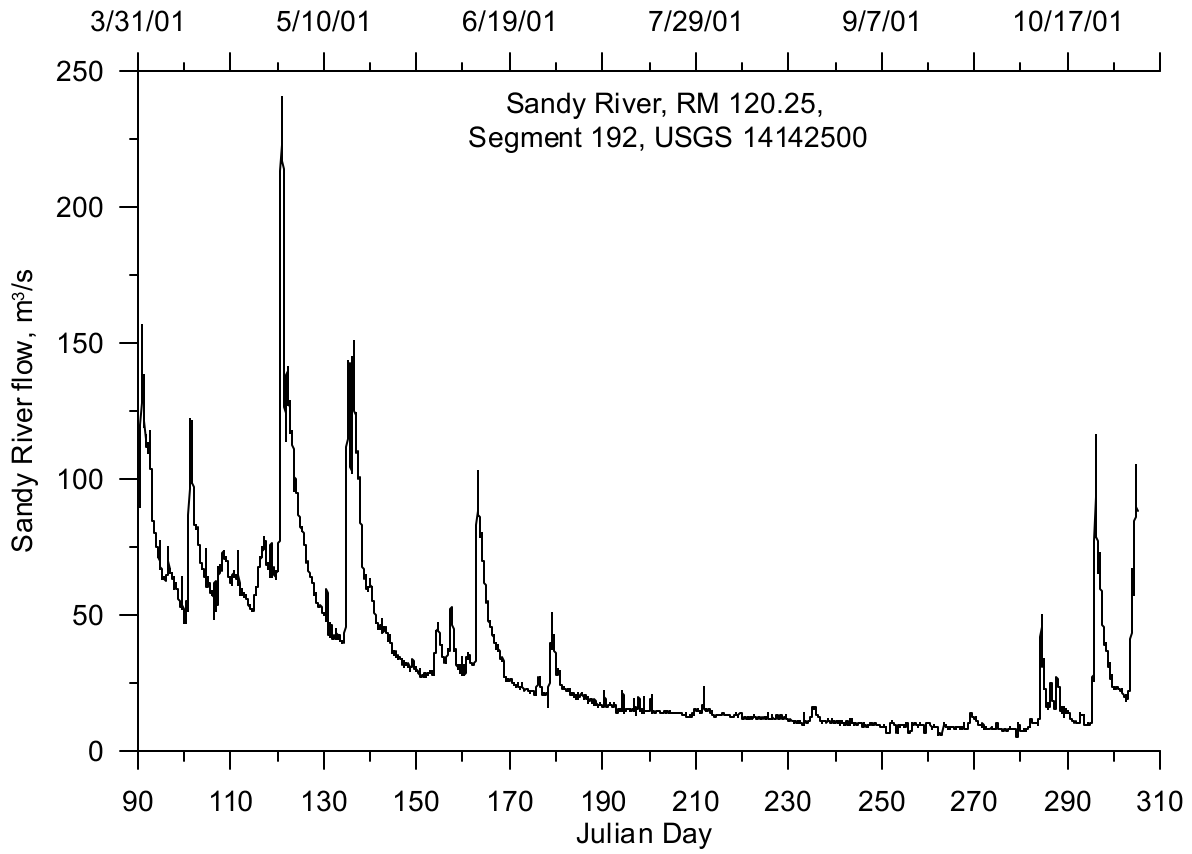


**Figure 43. Sandy River flow, 2001**

## Year 2002

Tributary data were used to create model input files from April 1 to October 31, 2002, even though the model calibration was from April 1 to October 1. Input files for the model were developed using continuous and daily data; however, correlation equations were also developed using nearby stations to fill data gaps when they existed.

Columbia Slough flow rate data were obtained from the USGS gage station at the Lombard St Bridge (USGS 14211820) where data were monitored at a frequency of 15 minutes. Figure 44 shows the Columbia Slough flow rate for the summer and shows large negative flows which reflect the tidal influence in the Lower Willamette River.

The Johnson Creek flow data were from the USGS gage at Milwaukie, OR (USGS 14211820). Figure 45 shows the Johnson Creek flow rate indicating that there was a typical seasonal pattern with lower stream flows in the summer than the spring and fall. Similarly to 2001, the Johnson Creek flows were much lower than other tributaries in the system.

The Clackamas River flow rate data for 2002 were obtained from the USGS gage station at Oregon City (USGS 14211010). A flow rate correlation equation was developed with the USGS gage station on the Clackamas River at Estacada (USGS 14210000). Figure 46 shows the Clackamas River flow rate data indicating a large spring freshet and low summer flows. The Clackamas River flow was highly regulated by a series of dam facilities along the river.

Similarly to 2001, since the basin was lacking flow rate data the Kalama River flows were characterized using monthly base flows estimated at the Kalama River near Kalama (Sinclair and Pitz, 1999). Figure 47 shows the Kalama River flow for 2002 which was the same as 2001.

Grays-Elokoman basin flow was characterized by adding base flows for the Abernathy Creek near Longview and Mill Creek near Cathlamet. The flow record was created using monthly averaged base flows (Sinclair and Pitz, 1999) since no other data were available. Figure 48 shows the base flow rates estimated for the Grays-Elokoman basin for 2002. These flow rates were the same as for 2001.

The Cowlitz River was characterized using continuous data for the Cowlitz River station at Castle Rock (USGS 14243000). The data from this station were added to the base flows estimated at the Delameter Creek station near Castle Rock and the Coweman River station near Kelso to obtain the total Cowlitz basin flow. Figure 49 shows flows for the Cowlitz River and indicates there were peaking operations on the upstream reservoir resulting in multiple sharp changes in flows downstream.

The Lewis River flow was calculated by adding daily average flows for the Lewis River station (USGS 14220500) and the East Fork of the Lewis River (USGS 14222500). Base flow from Cedar Creek was also incorporated in the total flow from the Lewis River Basin. Figure 50 shows the Lewis River flow with a general inflow decrease from early summer into early fall.

Similar to 2001, the Washougal River flow was estimated based on daily flow correlations between the East Fork of the Lewis River and the Washougal River and the Little Washougal River. The East Fork of the Lewis River flow was used with the correlations to calculate the daily flow for the Washougal and Little Washougal rivers. Figure 51 shows the calculated Washougal River flow rates for 2002.

The Sandy River flow was characterized by the USGS gage station 14142500. Figure 52 shows the Sandy River flow rate with a general reduction of flow in the middle to late June period and flow remaining low through the end of October.

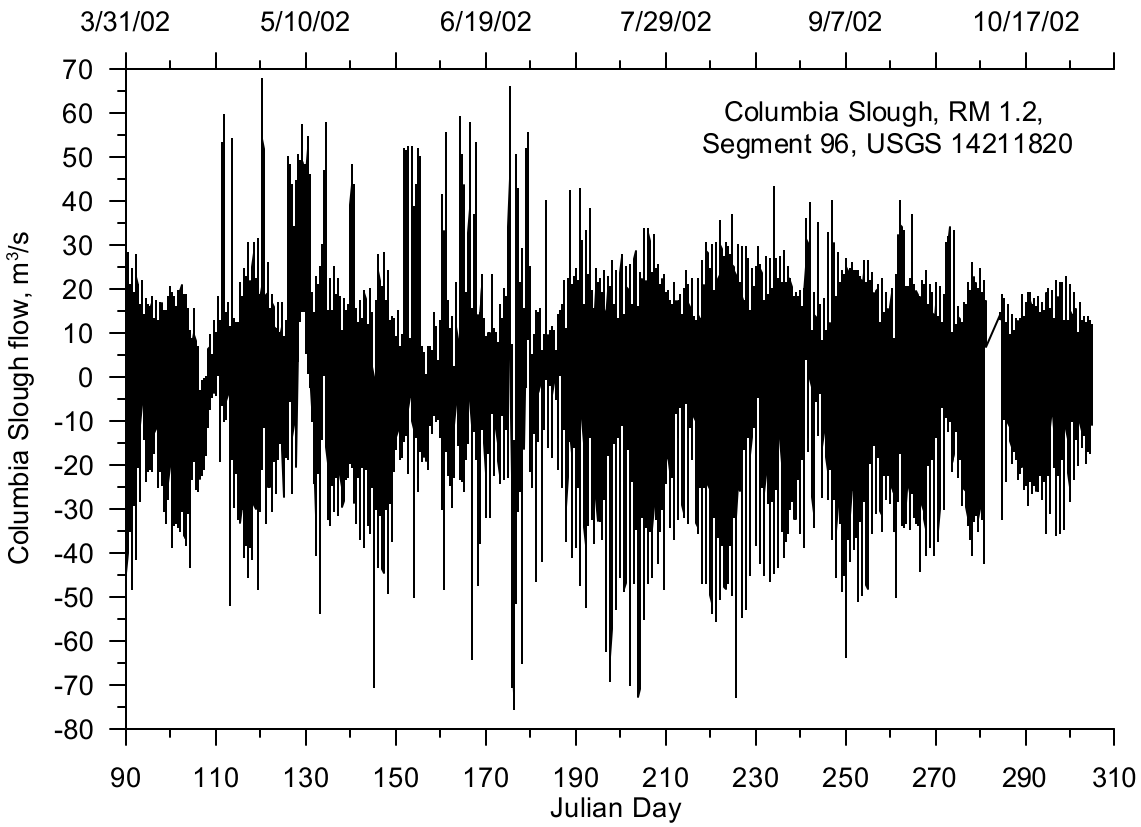


**Figure 44. Columbia Slough flow, 2002**

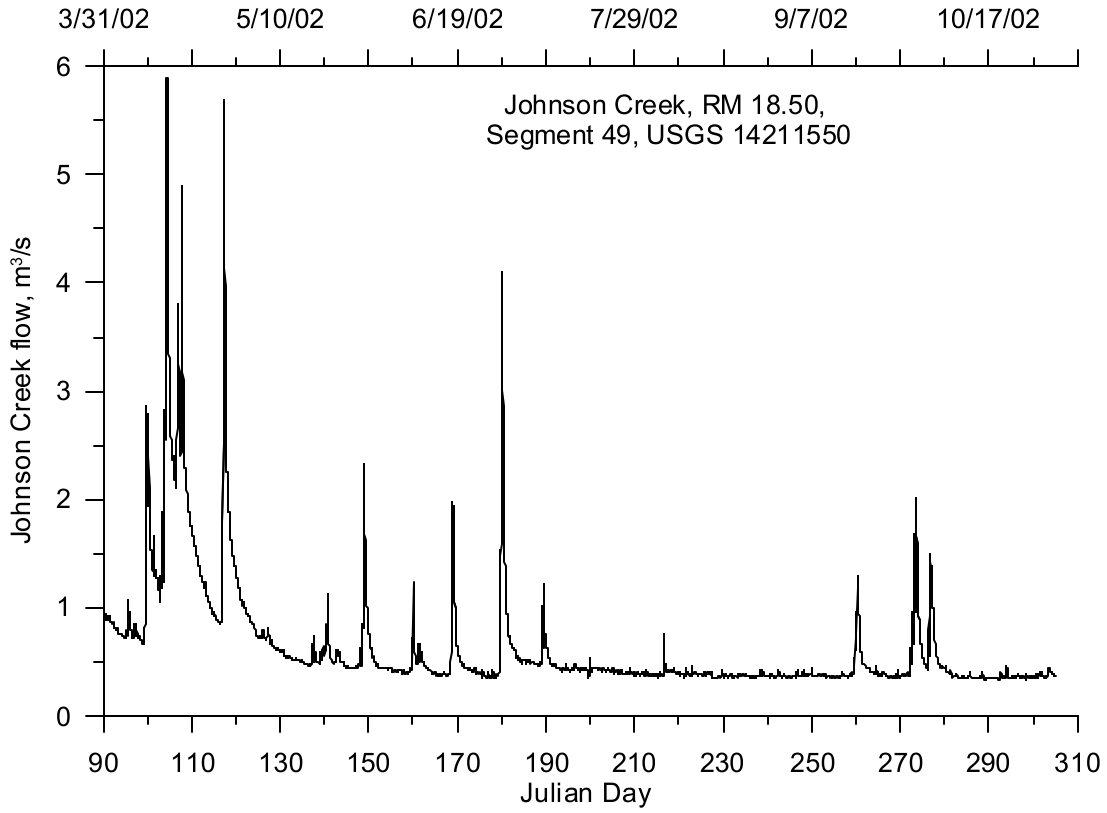


**Figure 45. Johnson Creek flow, 2002**

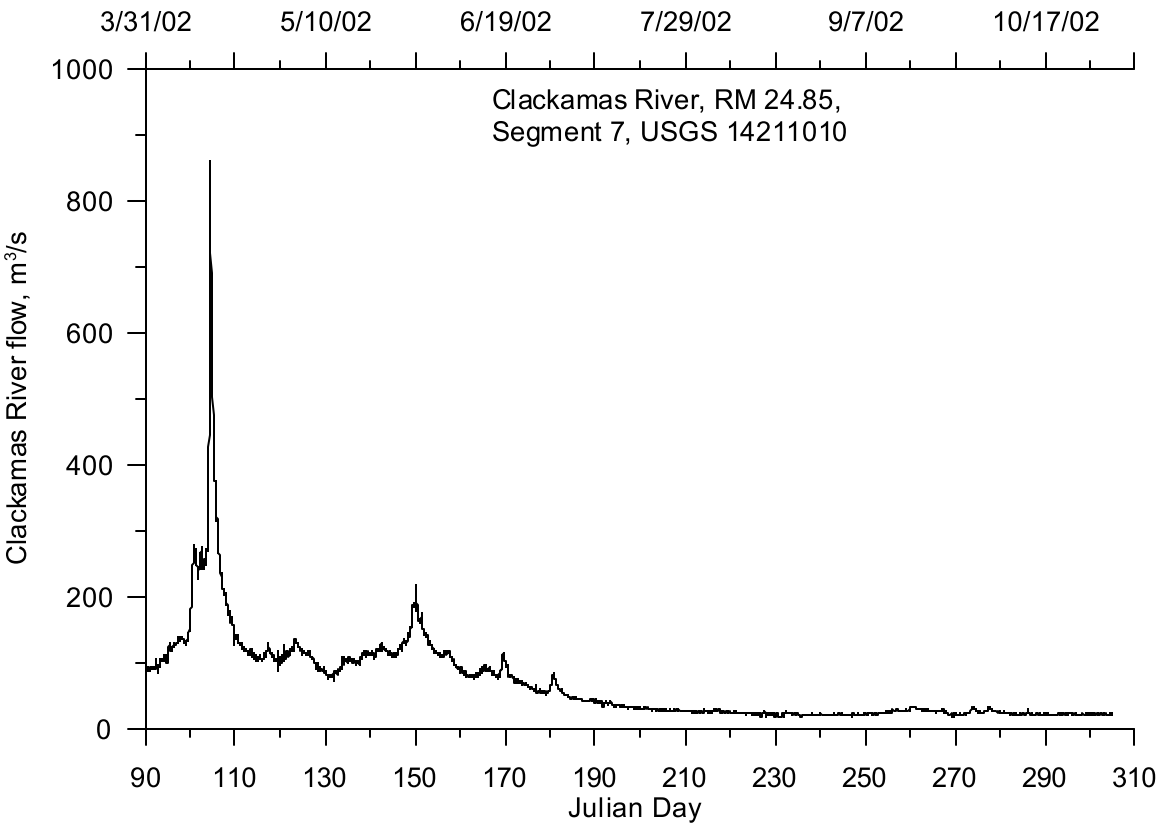


**Figure 46. Clackamas River flow, 2002**

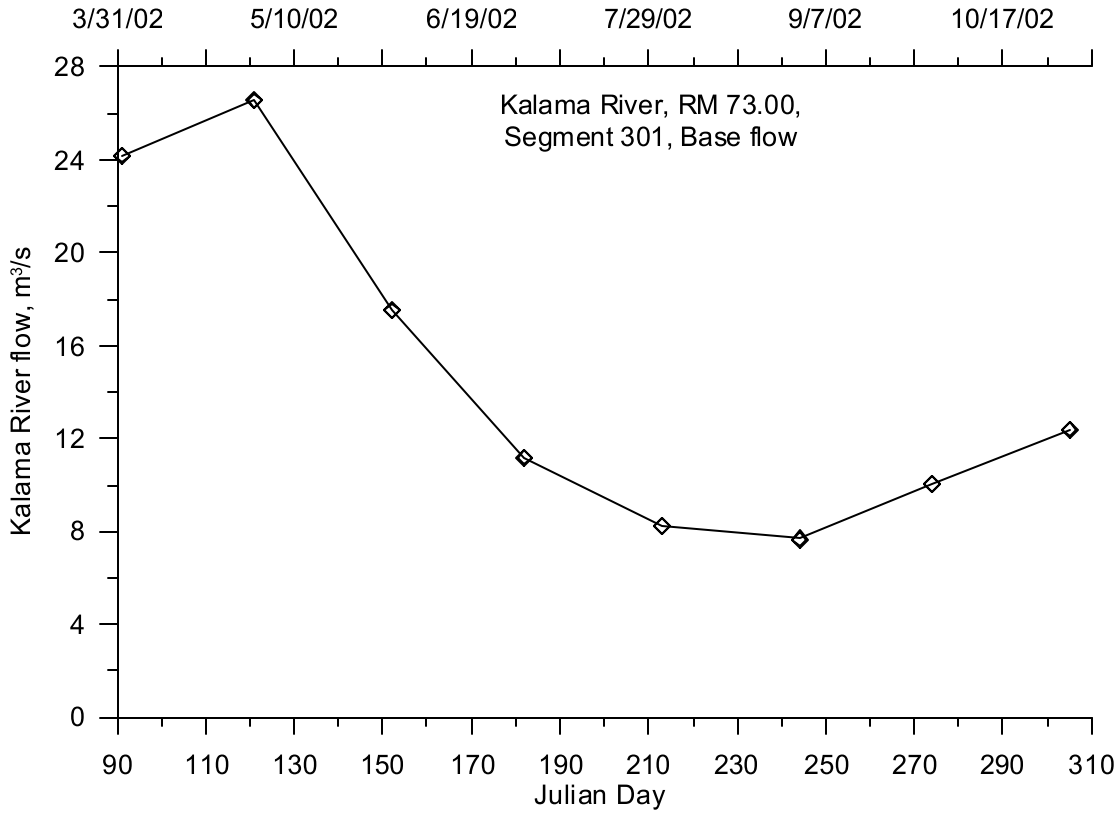


**Figure 47. Kalama River flow, 2002**

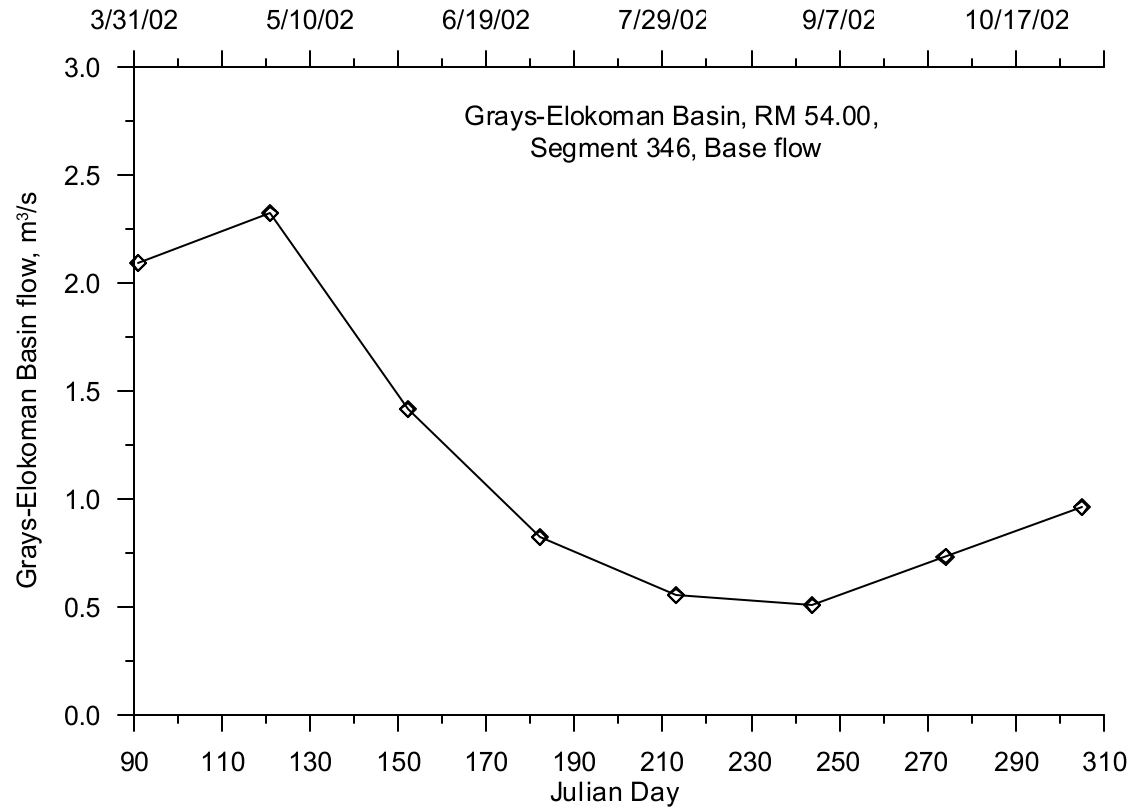


**Figure 48. Grays-Elokoman Basin flow, 2002**

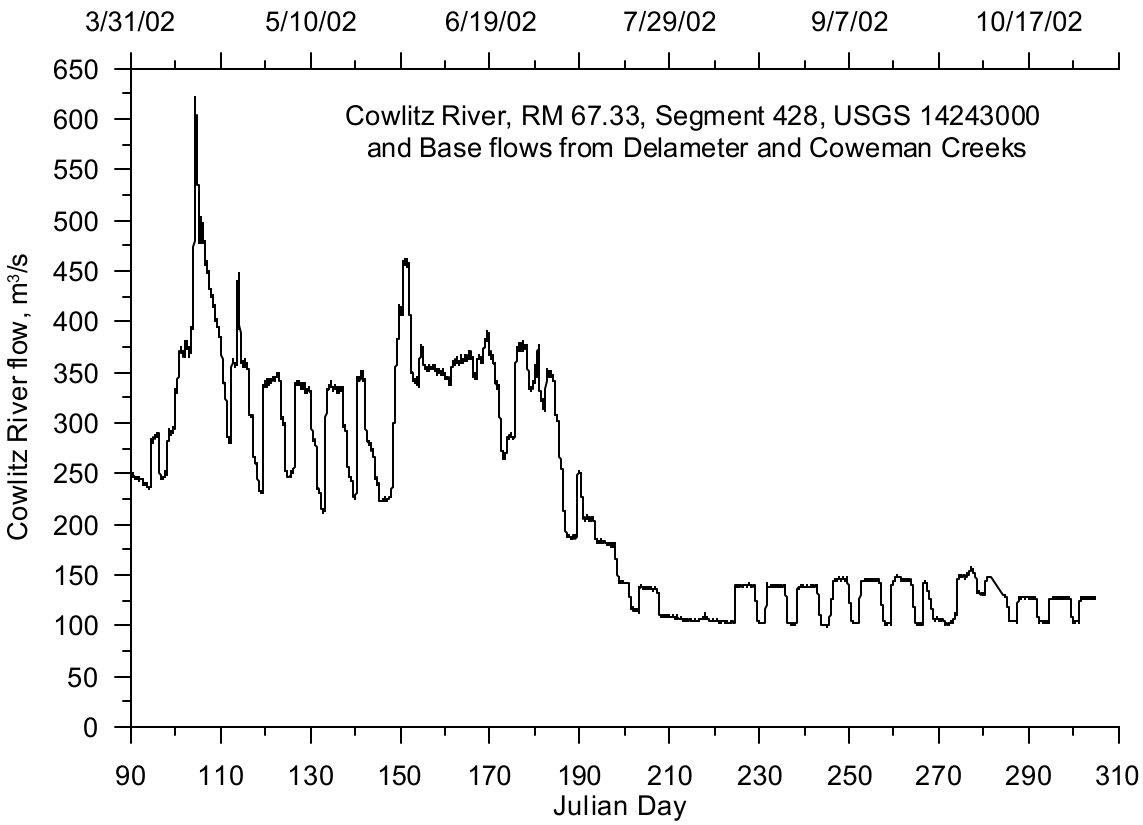


**Figure 49. Cowlitz River flow, 2002**

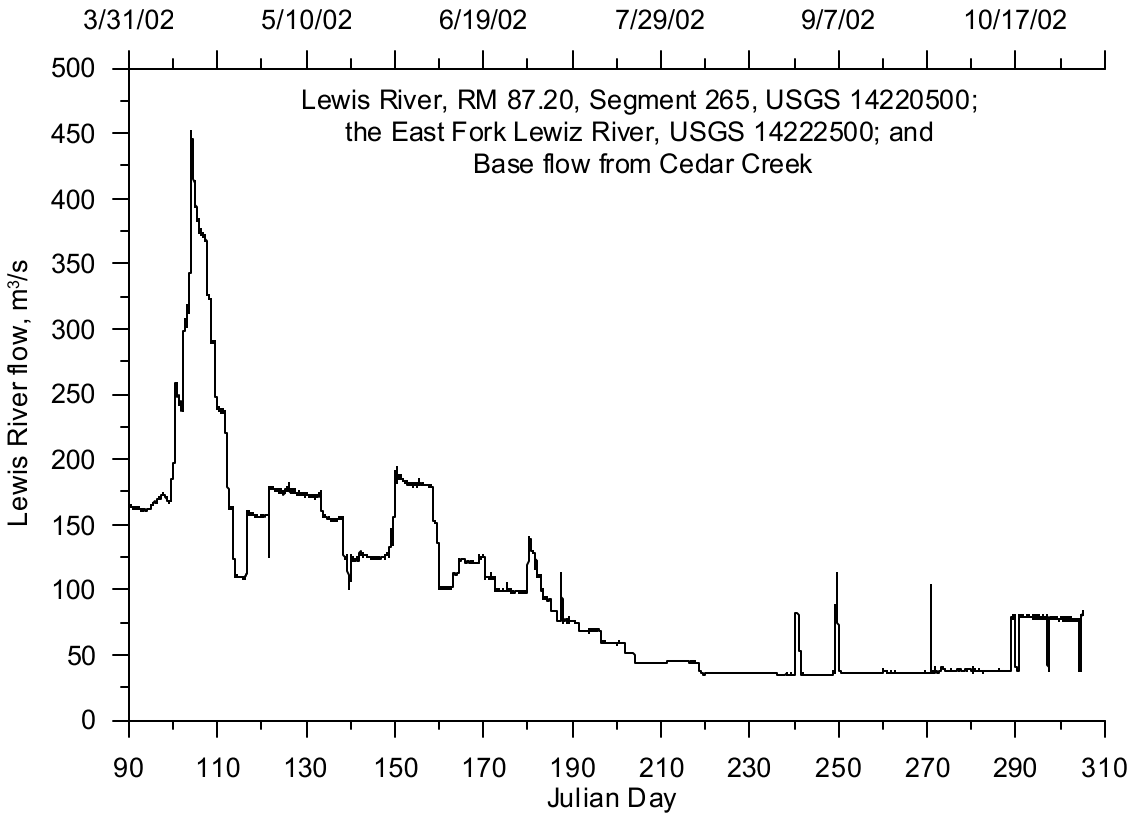


**Figure 50. Lewis River flow, 2002**

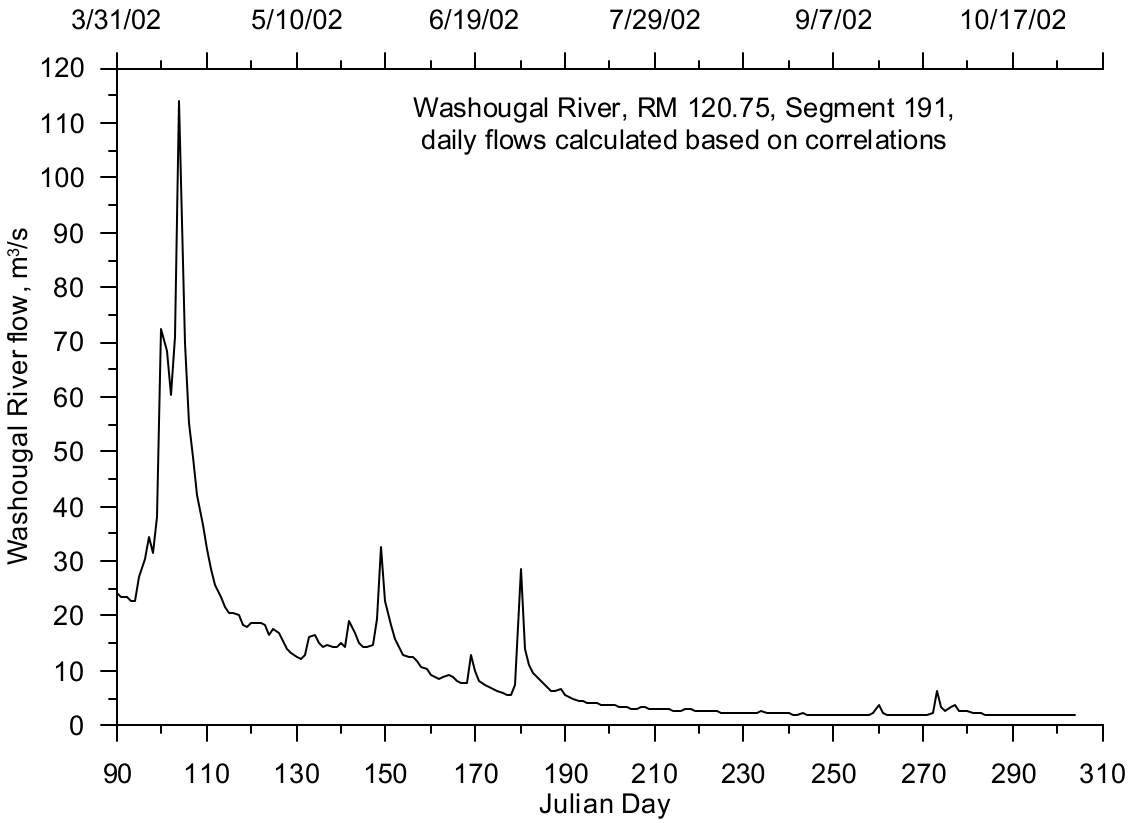


**Figure 51. Washougal River flow, 2002**

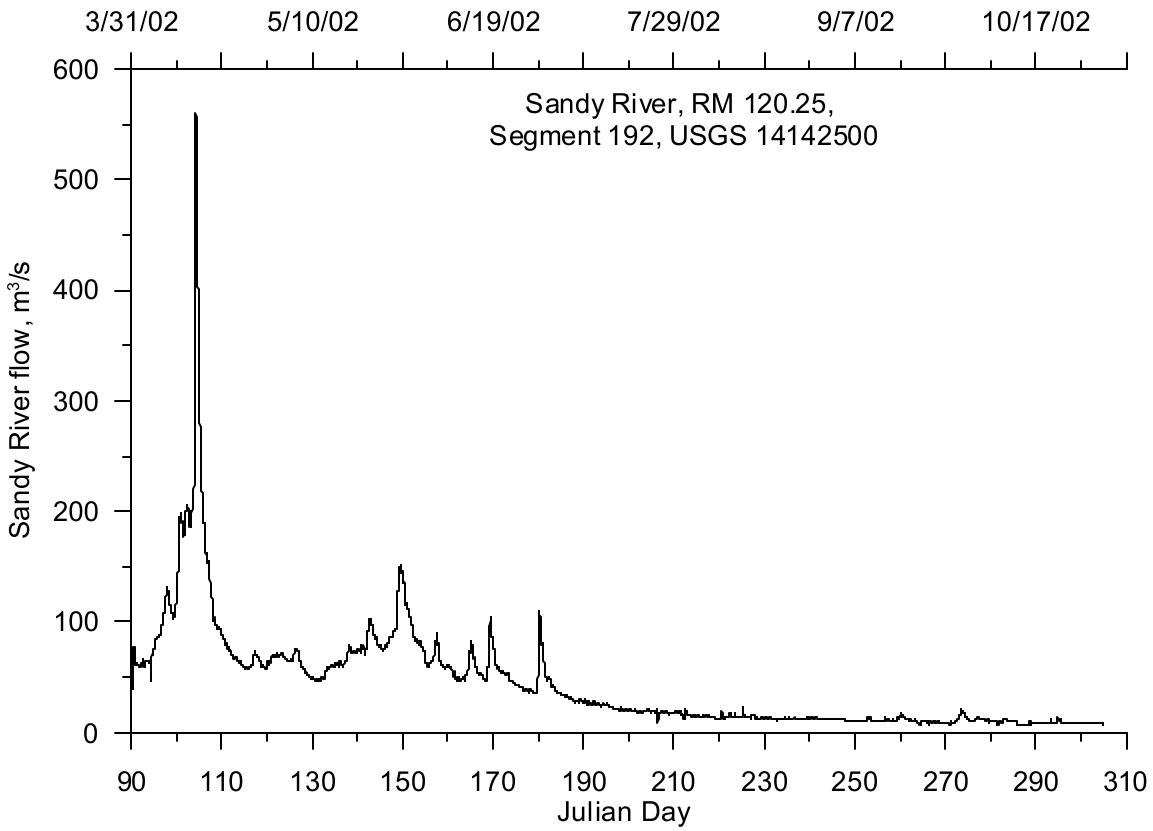


**Figure 52. Sandy River flow, 2002**

## Temperature Data

Figure 53 shows the location of the temperature monitoring stations in the Lower Willamette River model region. Many temperature records were compiled to encompass the time period from April 1 to October 31 of each year to handle possible management scenarios. Table 8 lists the gage stations used to develop the tributary inflows to the model for both 2001 and 2002. Temperature data were obtained from the U.S. Geological Survey for several gage stations. The site identification names begin with "USGS." Additional data were obtained from the Oregon Department of Environmental Quality (ODEQ) as part of their monitoring program with site names denoted with "LASAR" (Laboratory Analytical Storage and Retrieval Database). There were also additional data collected by Portland General Electric (PGE) in 2001, and these site names were denoted by "PGE".

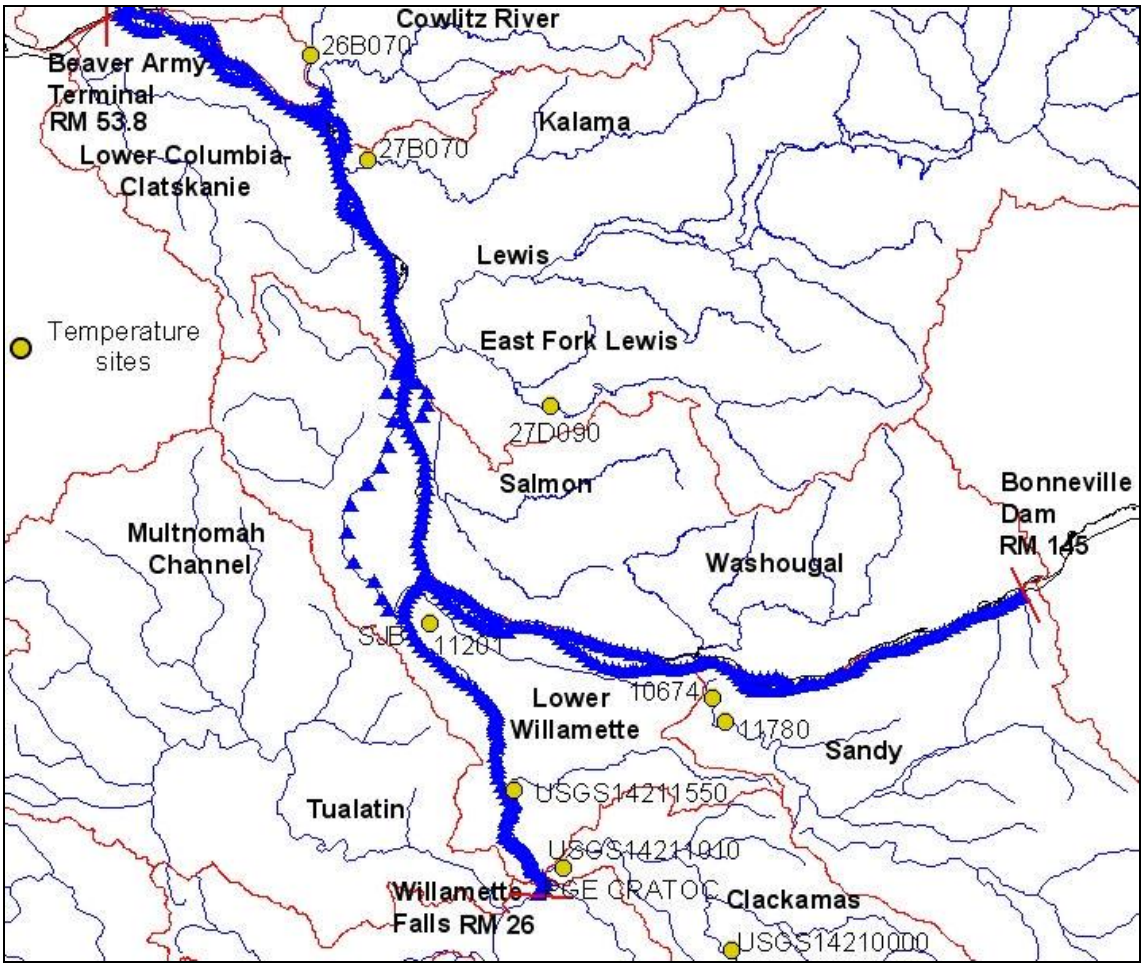


**Figure 53. Lower Willamette River model tributary temperature monitoring site locations**

**Table 8. Lower Willamette River model tributary temperature monitoring stations**

| Site ID | Tributary | RM | Model Segment |
|---|---|---|---|
| LASAR 11201 | Columbia Slough at Saint John's Landfill Bridge | 1.00 | 96 |
| Metro: SJB | Columbia Slough at Saint John's Landfill Bridge | 1.00 | 96 |
| USGS14211550 | Johnson Creek At Milwaukie, OR | 18.50 | 49 |
| USGS14210000 | Clackamas River at Estacada, OR | NA | NA |
| USGS14211010 | Clackamas River at Oregon City, OR | 24.85 | 7 |
| PGE CRATOC | Clackamas River at Oregon City, OR | 24.85 | 7 |
| LASAR 11780 | Sandy River at Dabney Bridge | 120.25 | 192 |
| LASAR 10674 | Sandy River at Troutdale Bridge | 120.25 | 192 |
| WADOE 27D090 | East Fork of the Lewis River near Dollar Corner | 87.20 | 265 |
| WADOE 26B070 | Cowlitz River at Kelso, WA. | 67.33 | 428 |
| WADOE 27B070 | Kalama River near Kalama, WA. | 73.00 | 301 |

Year 2001

The Columbia Slough temperatures were characterized by data from two monitoring instruments at the same location. The Columbia Slough was monitored by ODEQ (LASAR 11201) at the Saint John's

Landfill Bridge starting on June 21. The Metro regional government also monitors water temperature at Saint John's Landfill Bridge in the slough from April 1 to June 13. This resulted in a data gap from June 13 to 21, 2001. Since there was no other temperature data available, the model linearly interpolated the water temperature over this period. Given the relatively small Columbia Slough flow relative to the Lower Willamette River, the resulting error, from linearly interpolating temperatures, in the main stem will occur in the daily temperature extrema, and can be estimated to be less than 0.2 ºC. This error will only affect downstream model results. Figure 54 shows the combined data sets for the Columbia Slough.

Johnson Creek stream temperature was monitored at the same USGS gage that monitored flow (USGS 14211550). Figure 55 shows a time series plot of the temperatures monitored at the USGS gage station. The figure shows three patterns in the data: diurnal temperature swings, two week weather patterns of warming and cooler temperatures, and seasonal warming and cooling trends.

PGE monitored the Clackamas River at Oregon City (CRATOC) in 2001 but this data set was not complete to October 31, 2001. There was a data gap from October 26 to 31. A temperature correlation was developed between data at the USGS gage station upstream at Estacada (14210000) and the data set collected by PGE (CRATOC). Figure 56 shows the temperature correlation and the correlation equation. Figure 57 shows a time series of the both the temperature data and the calculated values based on the correlation.

The Kalama River had half-hourly temperature data recorded from July 25 to October 1 in 2001. Before July 25 and after October 1 there were only grab sample data at the same monitoring site (27B070). Figure 58 shows a time series plot of the Kalama River temperature which clearly shows when the grab sample data were replaced by the more continuous temperature data. The Kalama River summer flow was less than 1% of the Columbia main stem flow.

Similar to the Kalama River the Cowlitz River temperature monitoring site (26B070) had half-hourly temperature data from July 25 to October 1 and grab sample data outside this range. Figure 59 shows the Cowlitz River temperature data for 2001. There were no temperature data available for the Washougal River or the Grays-Elokoman basin river, so the Cowlitz River temperature data was used for both tributaries due to their close proximity. The Washougal and Grays-Elokoman Rivers summer flow was approximately 2% and 1% of the main stem flow, respectively.

The East Fork of the Lewis River had stream temperatures (27D090) recorded every half-hour from July 25 to October 1 and grab sample data outside this time period. Although the monitoring site was located on the East Fork of the Lewis River, it was used to represent the temperature for the whole Lewis River basin. The Lewis River is a minor tributary to the Columbia River at around 2% of the summer flow. Figure 60 shows the temperature time series data for the Lewis River.

The Sandy River was monitored at two sites in 2001. One site (LASAR 10674) was monitored on a monthly basis with grab samples. The other site (LASAR 11780) was monitored hourly from June 1 to August 29 in 2001. The two data sets were combined to generate a more complete temperature record of the Sandy River. Figure 61 shows the Sandy River temperature and indicates there is a general seasonal warming trend during the summer and cooling in the fall. The data also show there were fluctuations in the temperatures over the course of synoptic weather patterns of 10 to 14 days.

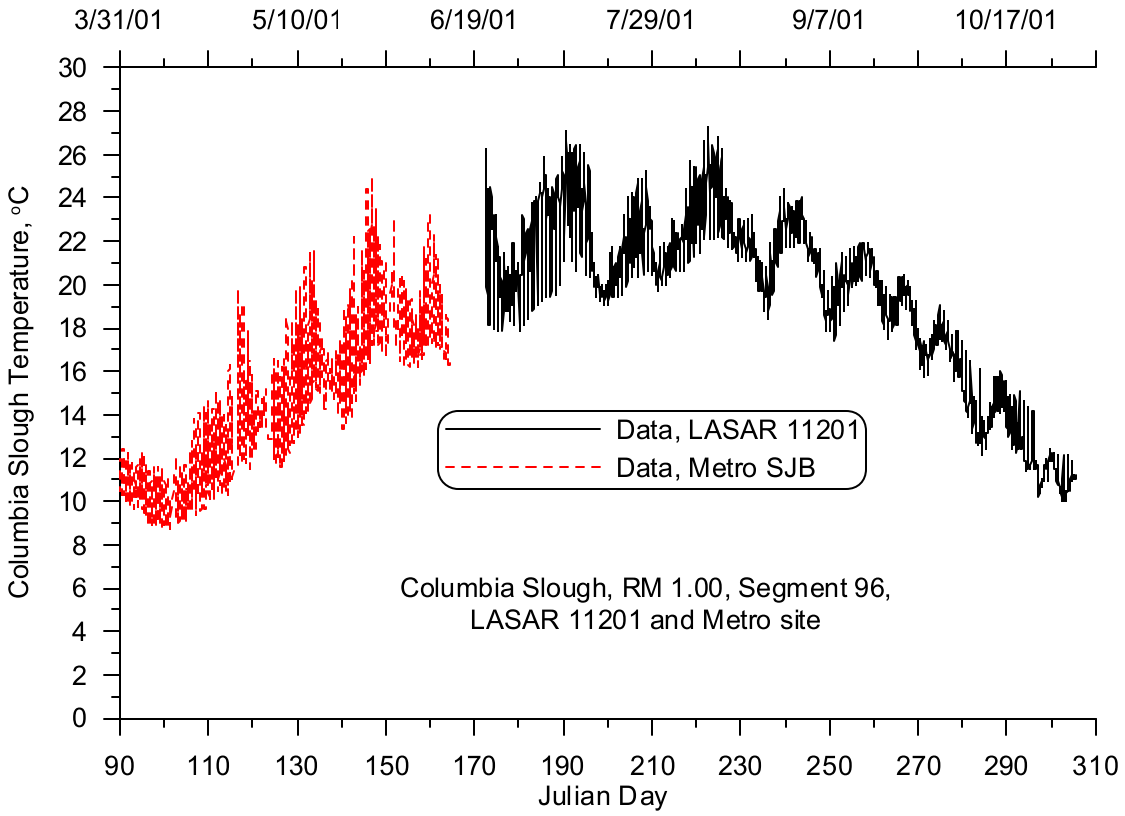


**Figure 54. Columbia Slough temperature, 2001**

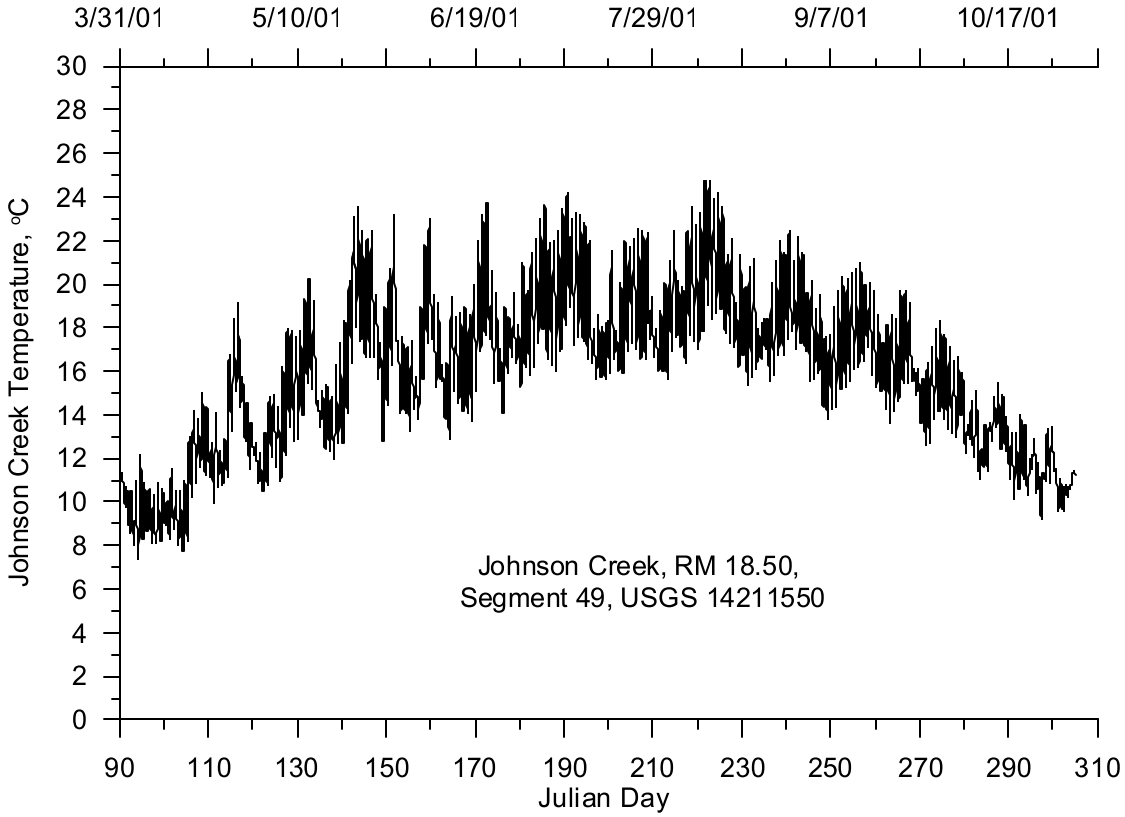


**Figure 55. Johnson Creek temperature, 2001**

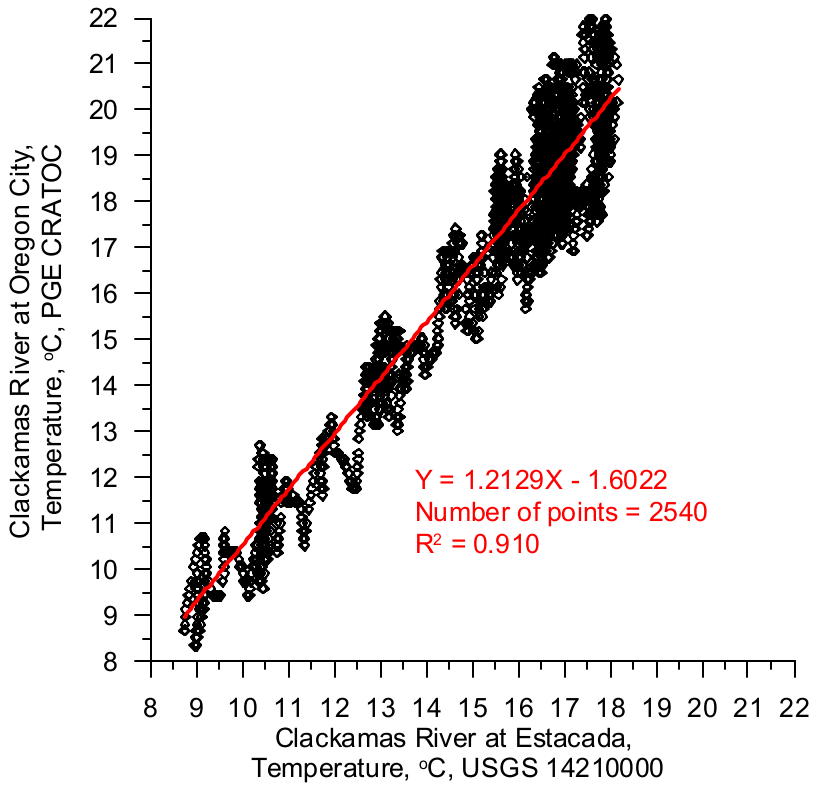


**Figure 56. Clackamas River temperature correlation, 2001**

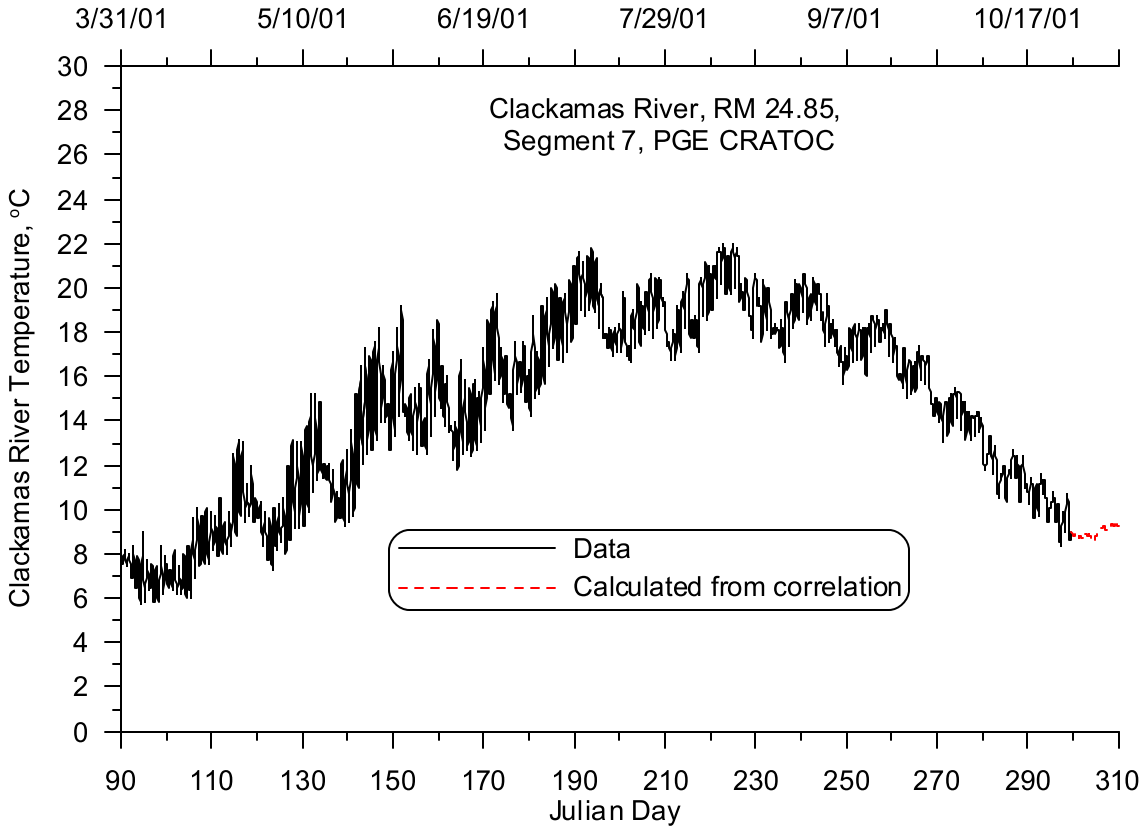


**Figure 57. Clackamas River temperature, 2001**

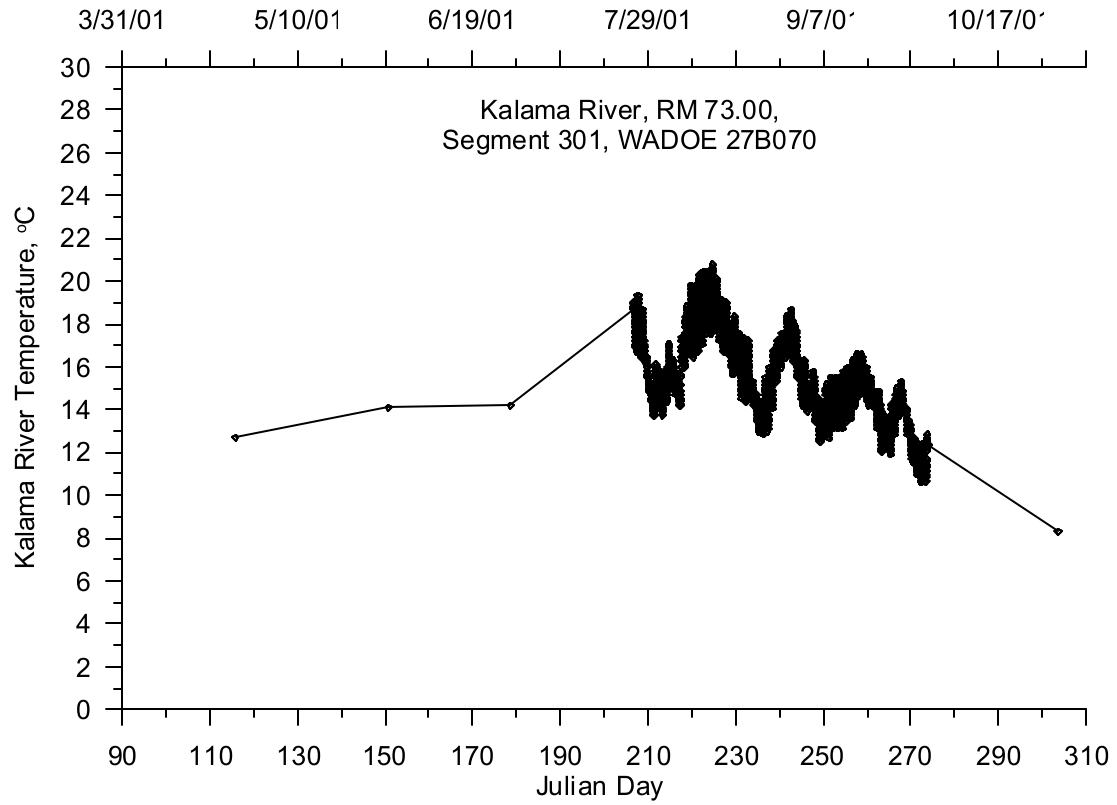


**Figure 58. Kalama River temperature, 2001**

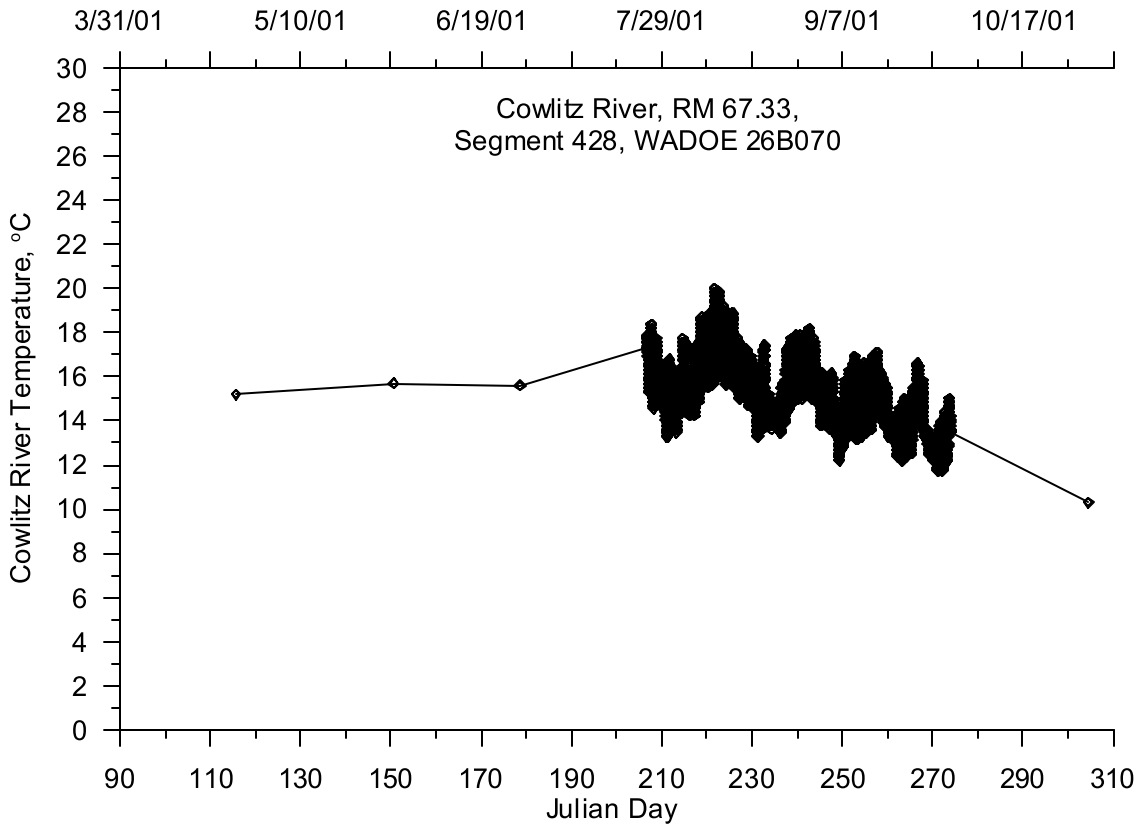


**Figure 59. Cowlitz River temperature, 2001**

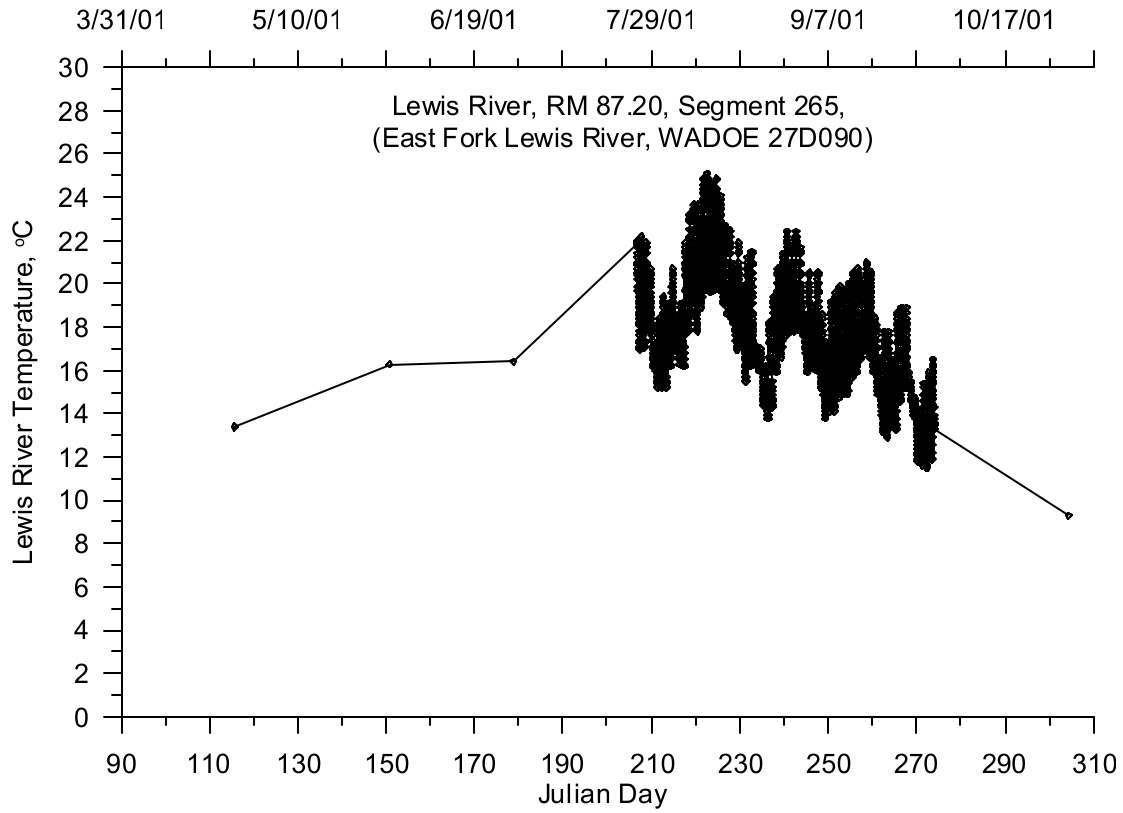


**Figure 60. Lewis River temperature, 2001**

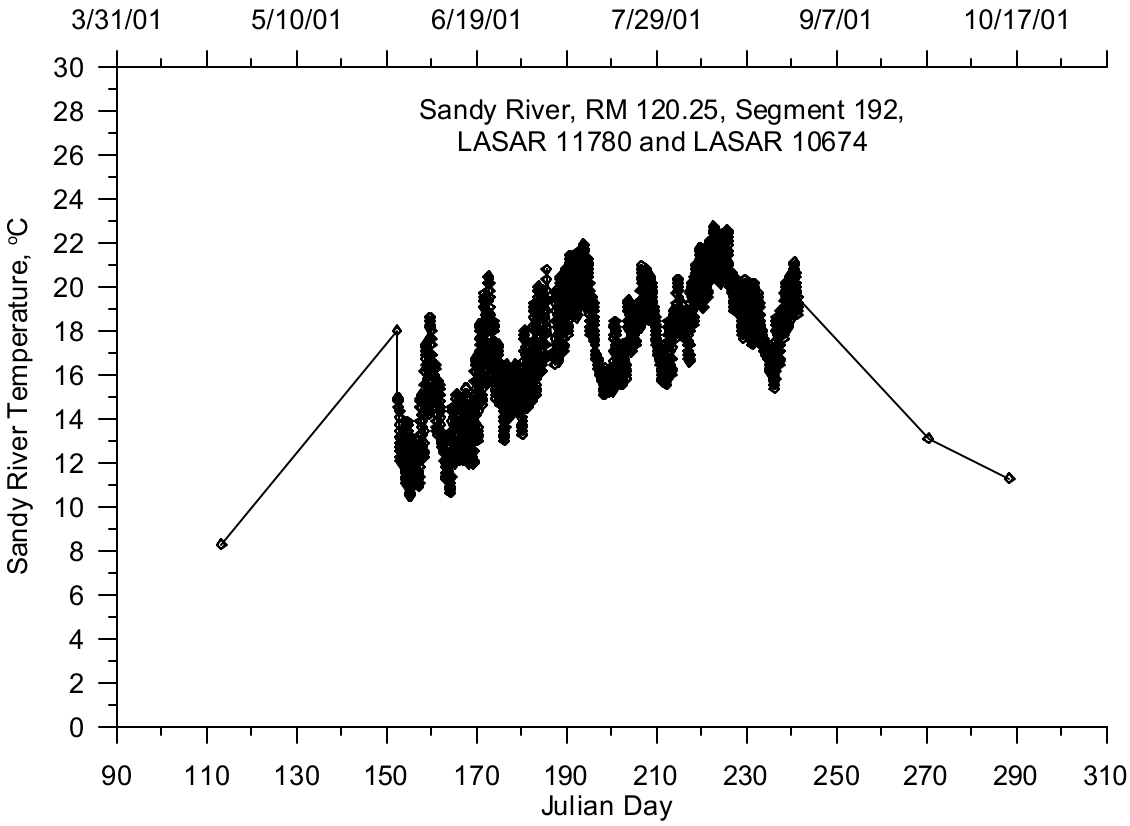


**Figure 61. Sandy River temperature, 2001**

## Year 2002

The Columbia Slough temperature was characterized by data from two monitoring sites. The Columbia Slough was monitored by ODEQ (LASAR 11201) but the data acquisition did not start until May 13. The Metro regional government also monitored water temperature at the same Saint John's Landfill Bridge (SJB) and their data filled in the period of April 1 to April 24. Neither instrument monitored stream temperature between April 24 and May 13 resulting in a data gap. This gap was filled by allowing the model to linearly interpolate between the two dates when data existed. The effect on the model predictions should be small since the Columbia Slough inflow was less than 1% of the Lower Willamette River flow. Figure 62 shows the combined data sets for the Columbia Slough.

Johnson Creek stream temperature was monitored by the USGS gage monitoring flow (14211550). Figure 63 shows a time series plot of the stream temperature. The figure shows diurnal temperature swings, 2 week weather patterns of warming and cooler temperatures, and a seasonal warming over the summer and cooling in the fall.

The Clackamas River was monitored by a new USGS gage station on the river at Oregon City (14211010) but this data collection started on June 20, 2002, creating a data gap from April 1 to June 20. A temperature correlation was developed between data at the USGS gage station upstream at Estacada (14210000) and the downstream gage at Oregon City (USGS 14211010). Figure 64 shows the resulting correlation equation. Figure 65 shows a time series of both the 2002 temperature data and the calculated values based on the correlation.

The Kalama River had half-hourly temperature data recorded from July 16 to September 25 in 2002 and was monitored with monthly grab samples at the same monitoring site (27B070) outside this time period. Figure 66 shows a time series plot of the Kalama River temperature which indicates when the grab sample data was replaced by the more continuous temperature data.

The Cowlitz River temperature monitoring site (26B070) had half-hourly temperature data from July 16 to September 24 and grab sample data outside this range. Figure 67 shows the Cowlitz River temperature data for 2002. There were no temperature data available for the Washougal River or the Grays-Elokoman basin river so the Cowlitz River temperature data were used for both tributaries.

The East Fork of the Lewis River was monitored for temperature every half-hour from July 16 to September 24 with grab sample data outside this time period. Although the monitoring site (27D090) was located on the East Fork of the Lewis River it was used to represent the temperature for the whole Lewis River basin. Figure 68 shows the temperature time series data for the Lewis River.

There was no continuous temperature monitoring on the Sandy River in 2002 which could be used for developing the tributary temperature record. There was one site (LASAR 10674) which monitored temperature on a monthly basis with grab samples. Figure 69 shows the Sandy River temperature using the monthly grab sample data.

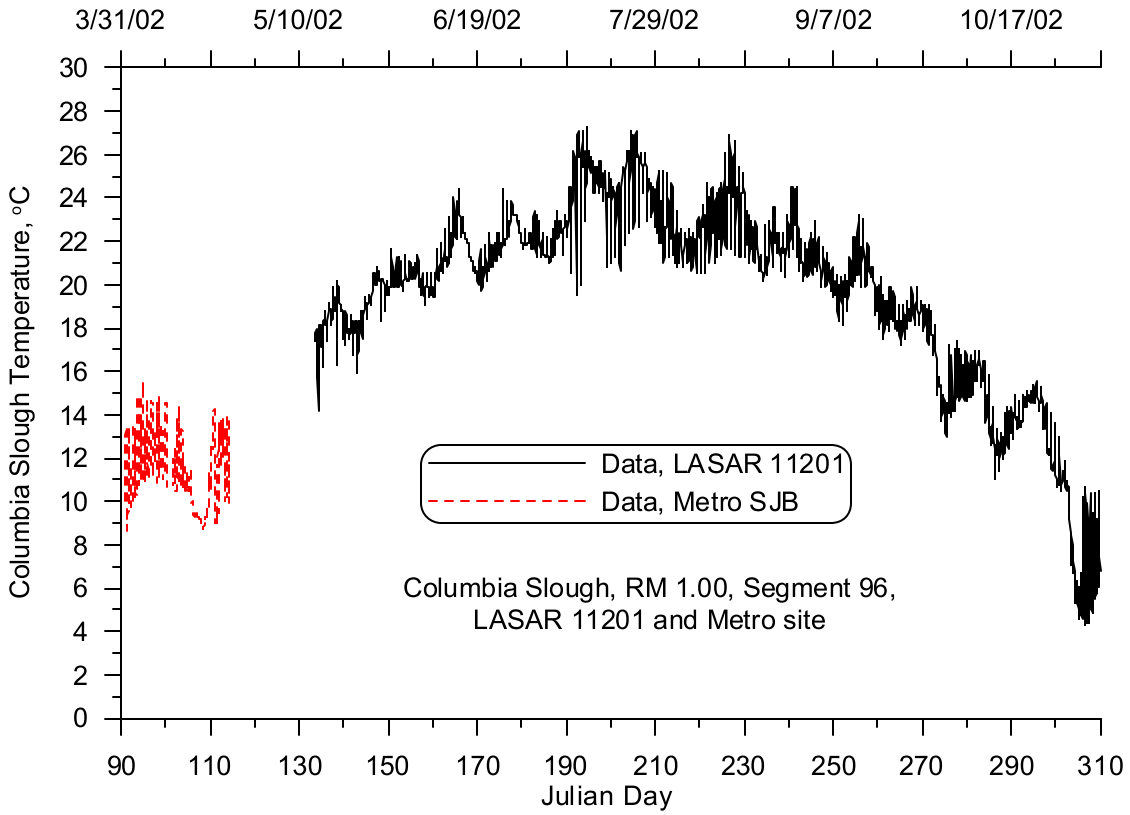


**Figure 62. Columbia Slough temperature, 2002**

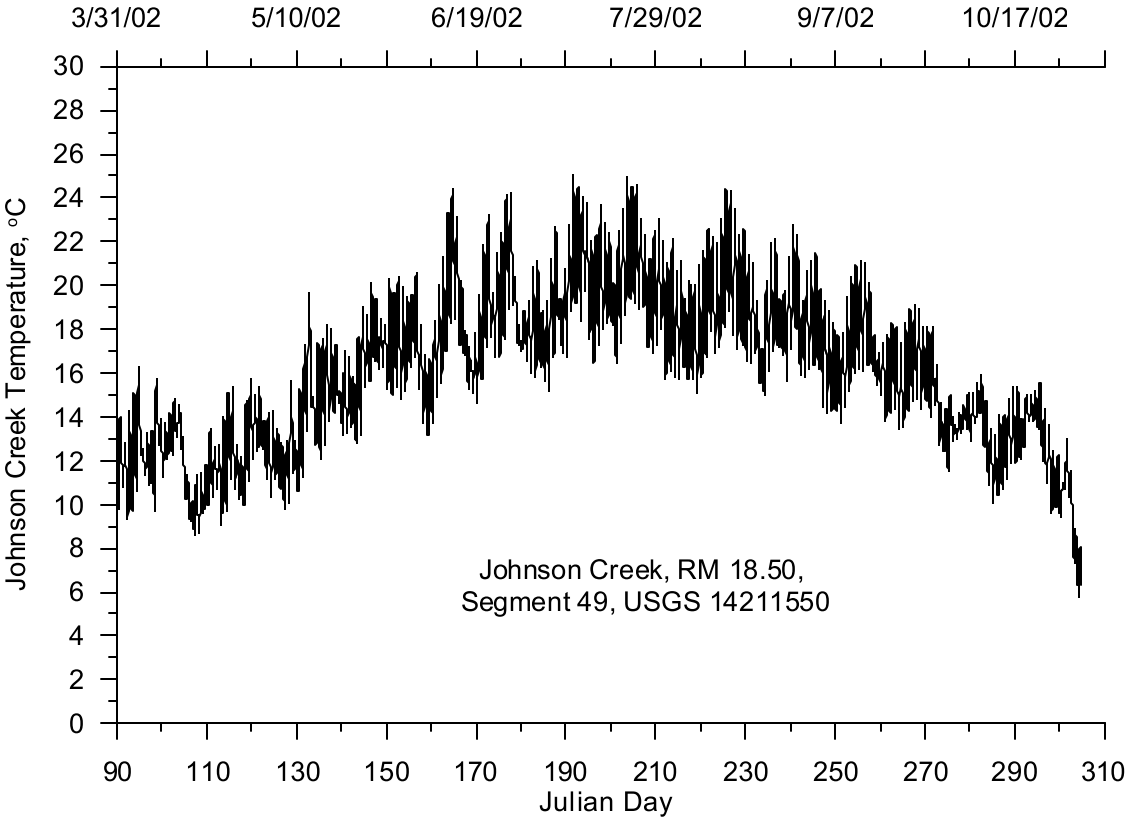


**Figure 63. Johnson Creek temperature, 2002**

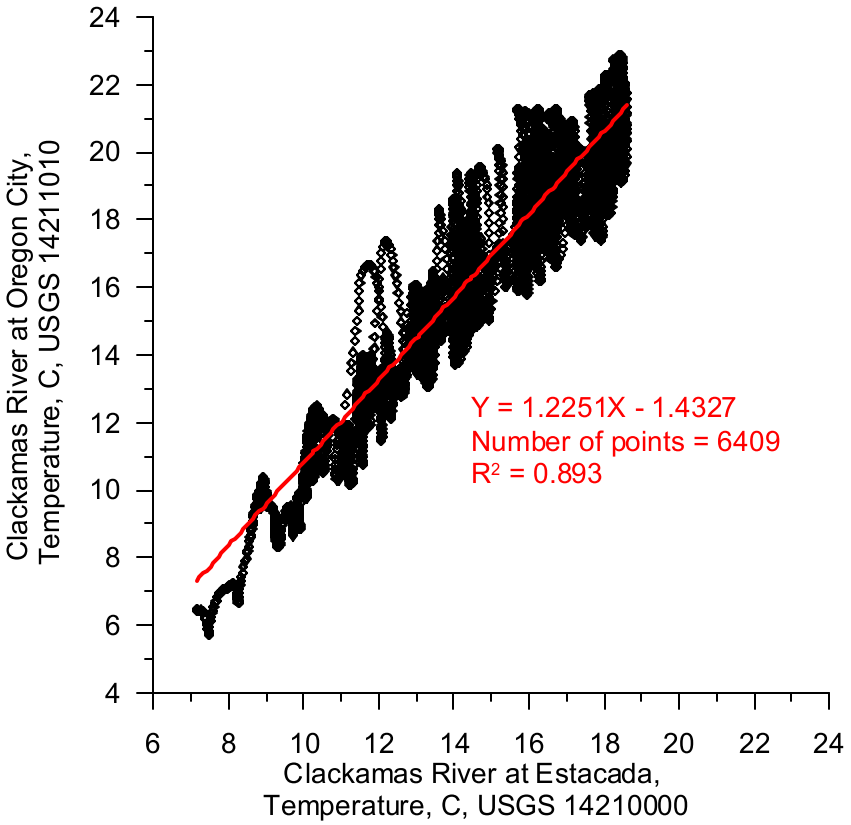


**Figure 64. Clackamas River temperature correlation, 2002**

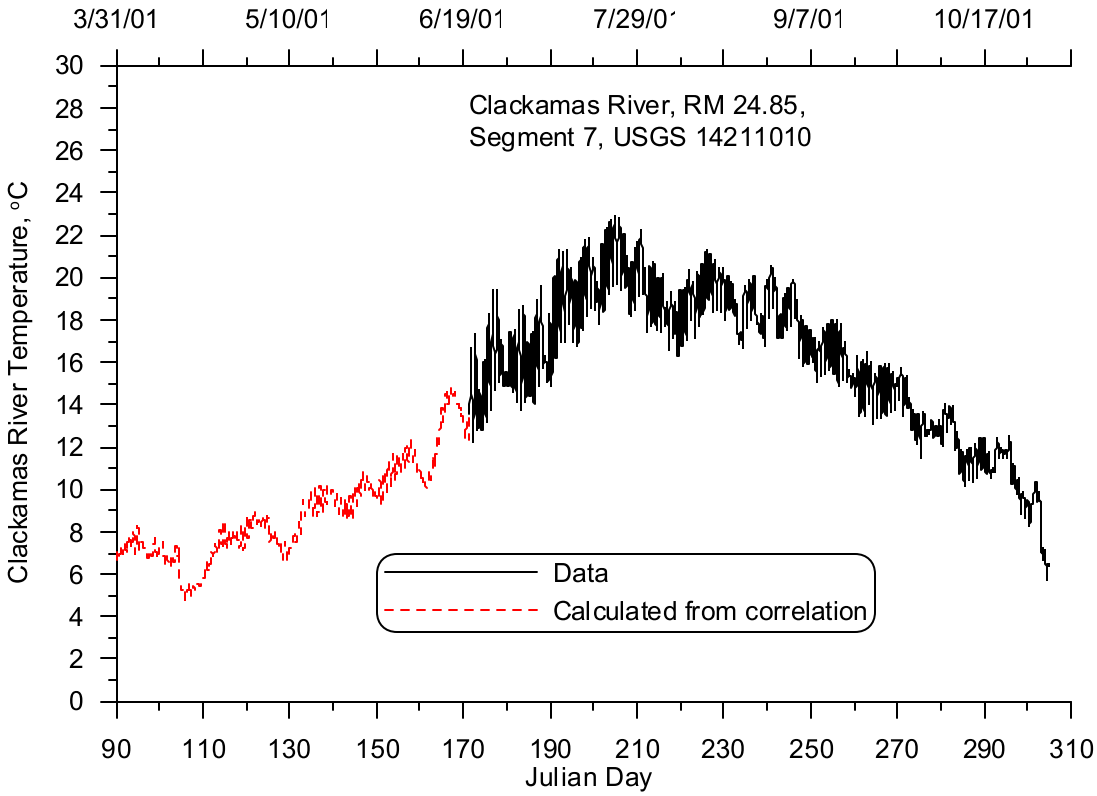


**Figure 65. Clackamas River temperature, 2002**

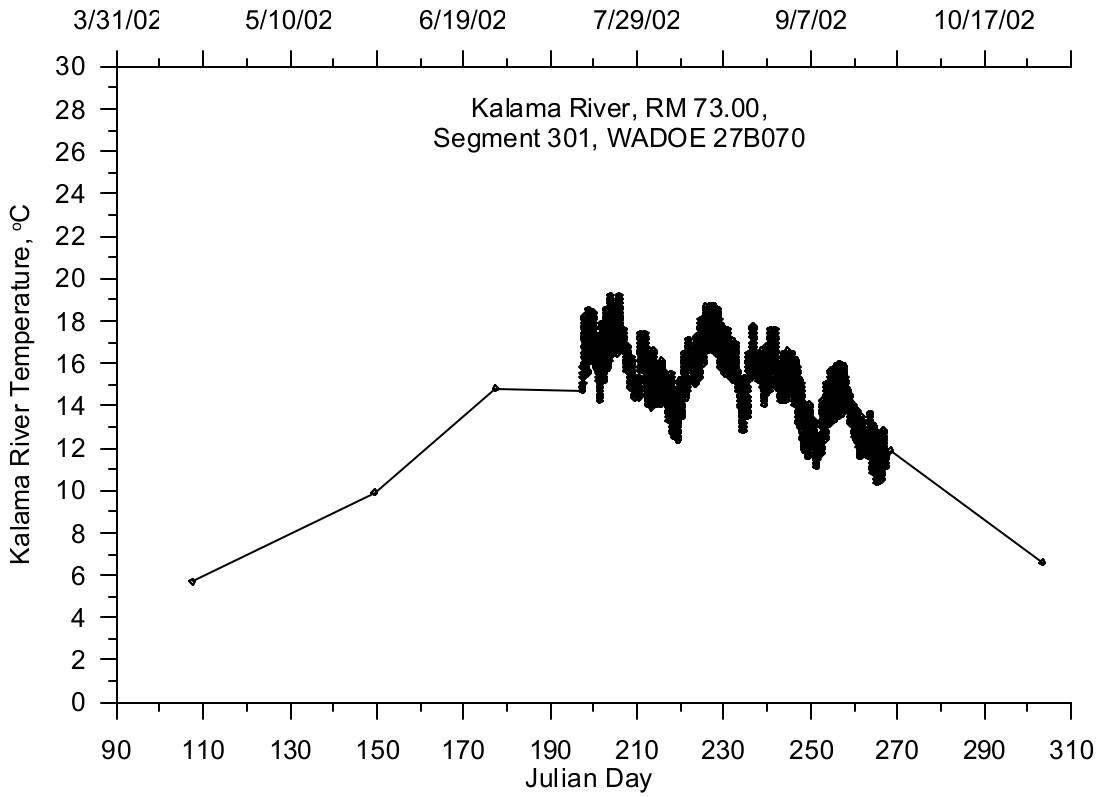


**Figure 66. Kalama River temperature, 2002**

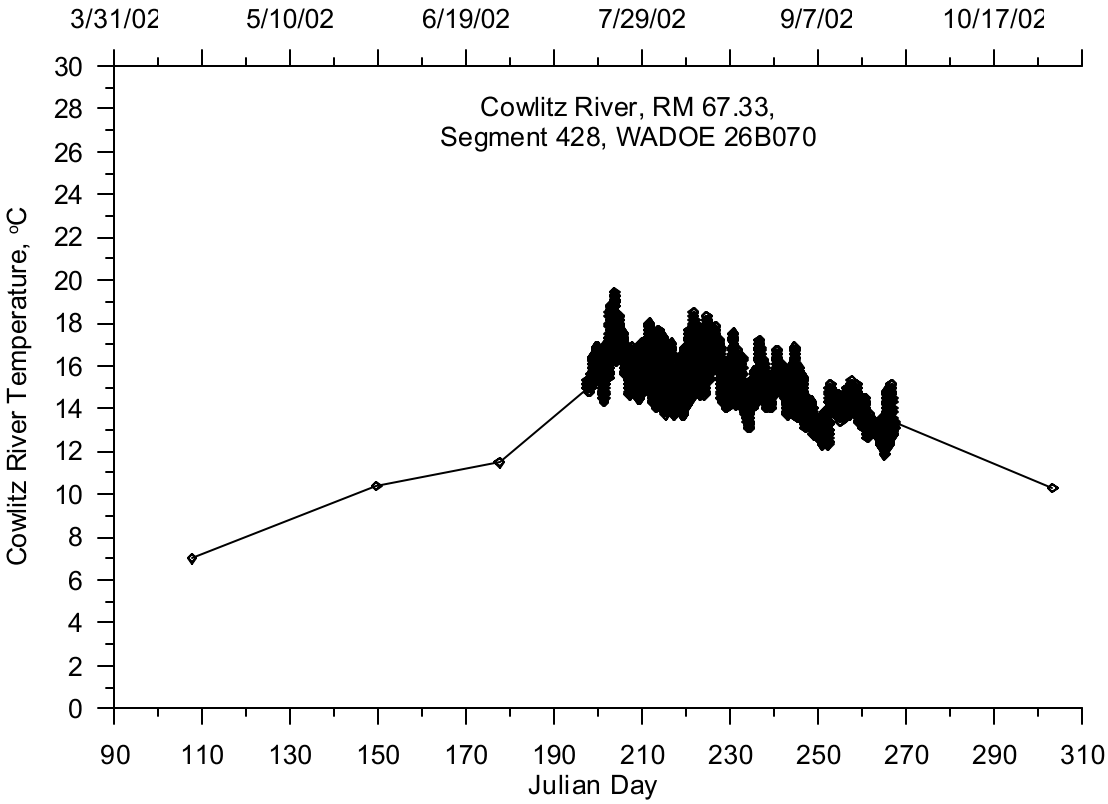


**Figure 67. Cowlitz River temperature, 2002**

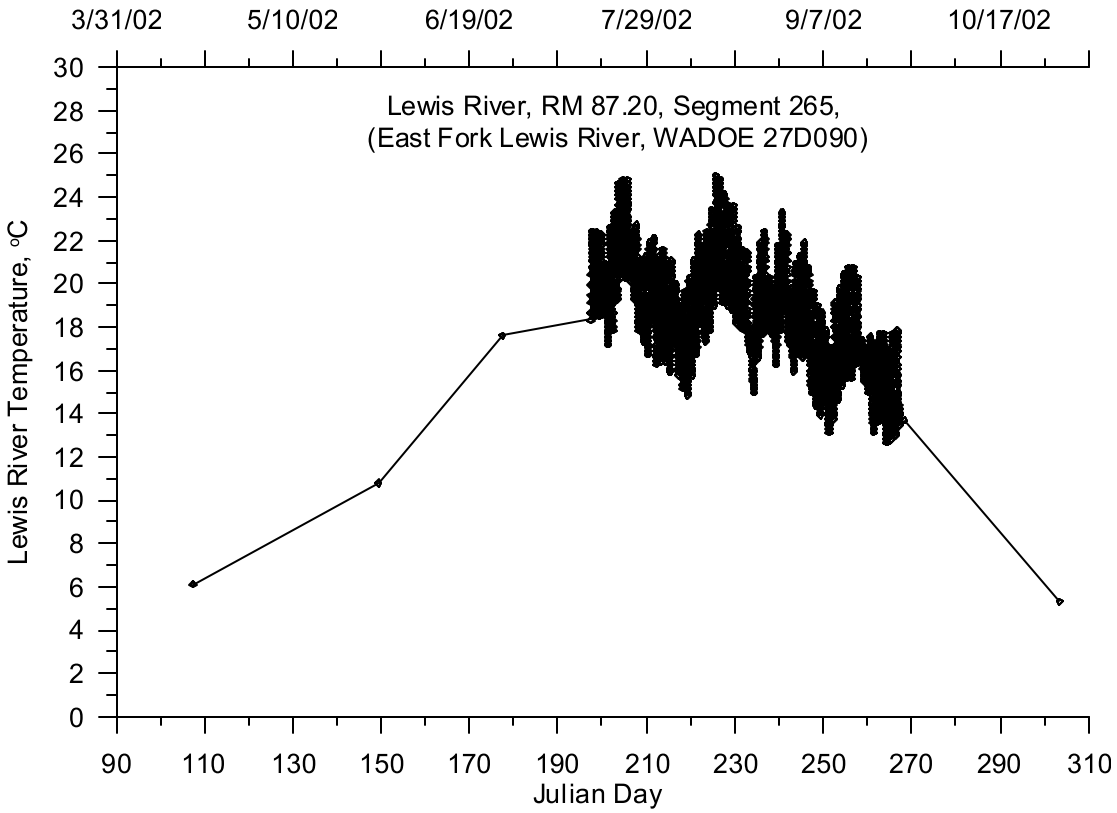


**Figure 68. Lewis River temperature, 2002**

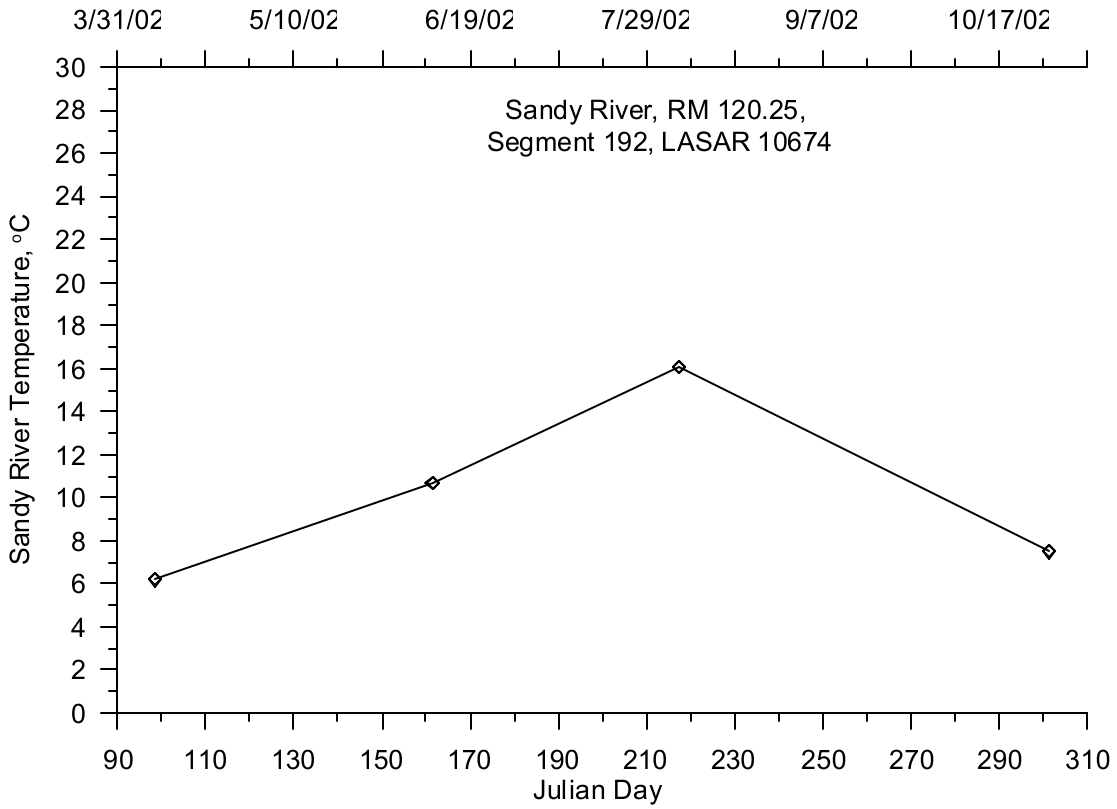


**Figure 69. Sandy River temperature, 2002**

## *Distributed Tributaries*

The majority of the tributary inflows to the Columbia and Willamette River were considered in the model. Nevertheless, a small number of these tributaries were not characterized because flow information was not available. Figure 70 shows the shaded basins where the tributary inflows were not considered explicitly in the model. An analysis conducted using a Geographic Information System determined that the total drainage area not considered in the model was about 0.34% of the entire watershed drainage. This analysis included the Columbia River basin above Bonneville Dam and the entire Willamette Basin above Willamette Falls, neither of which were shown in Figure 70.

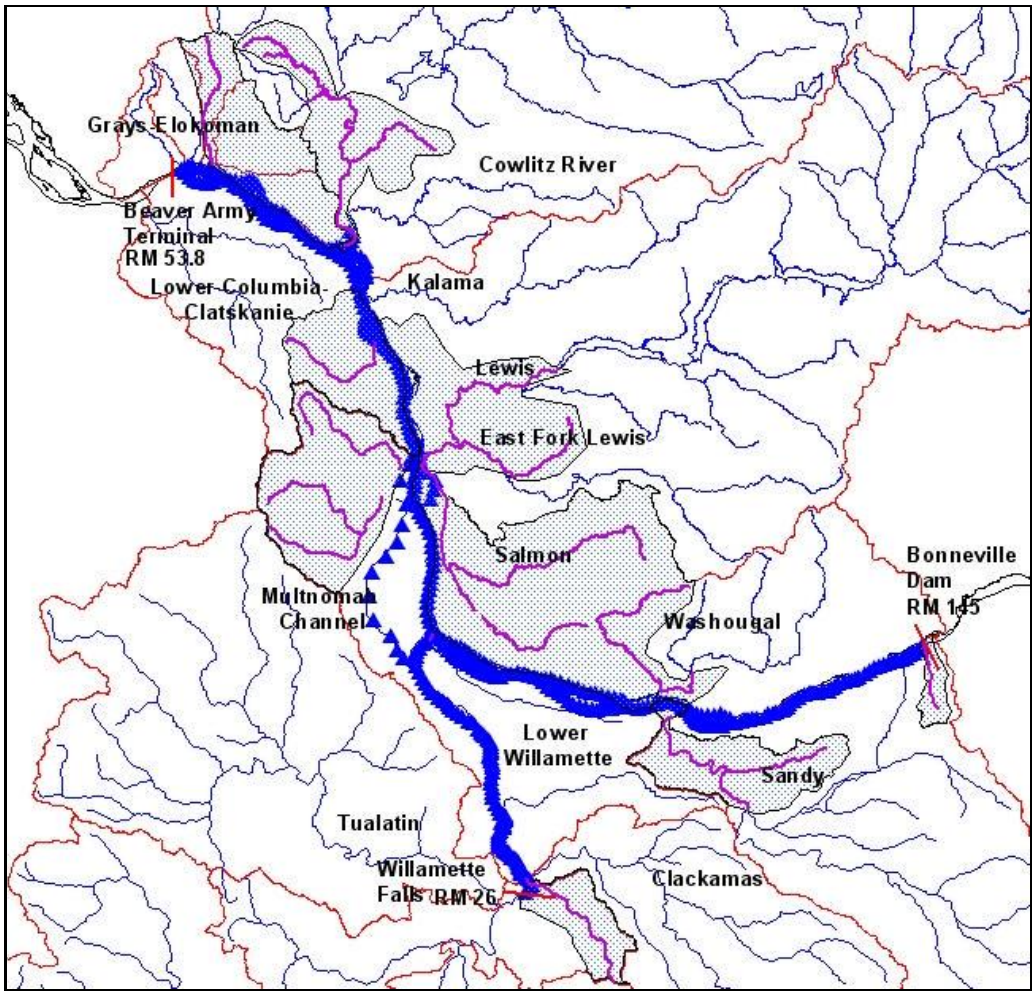


**Figure 70. Lower Willamette River model ungaged basin areas**

## *Point Sources*

Point source data for the Lower Willamette River were collected from the Discharge Monitoring Reports (DMR) provided by Oregon Department of Environmental Quality (ODEQ). The Clean Water Act requires that any discharge "pollutants" through a point source into a water body in the United States should have a National Pollution Discharge Elimination System (NPDES) permit. The NPDES permit may define minimum or maximum limits of discharge constituents and may require periodic monitoring and reporting of the discharge. This reporting is submitted to the local branches of the EPA (Permit

Compliance System) and ODEQ through a Discharge Monitoring Report (DMR). There were no point sources included in the model from Washington since it was believed these would have little influence on the temperature regime in the Lower Willamette River.

## Hydrodynamic Data

ODEQ identified the point sources to be included in the model based on their discharge flow. There were eight "major" point sources identified in the Lower Willamette River as shown in Figure 71. Table 9 lists the point sources, their river mile and their model segment locations. Flow and temperature were monitored on either a daily or in some cases on an hourly basis.

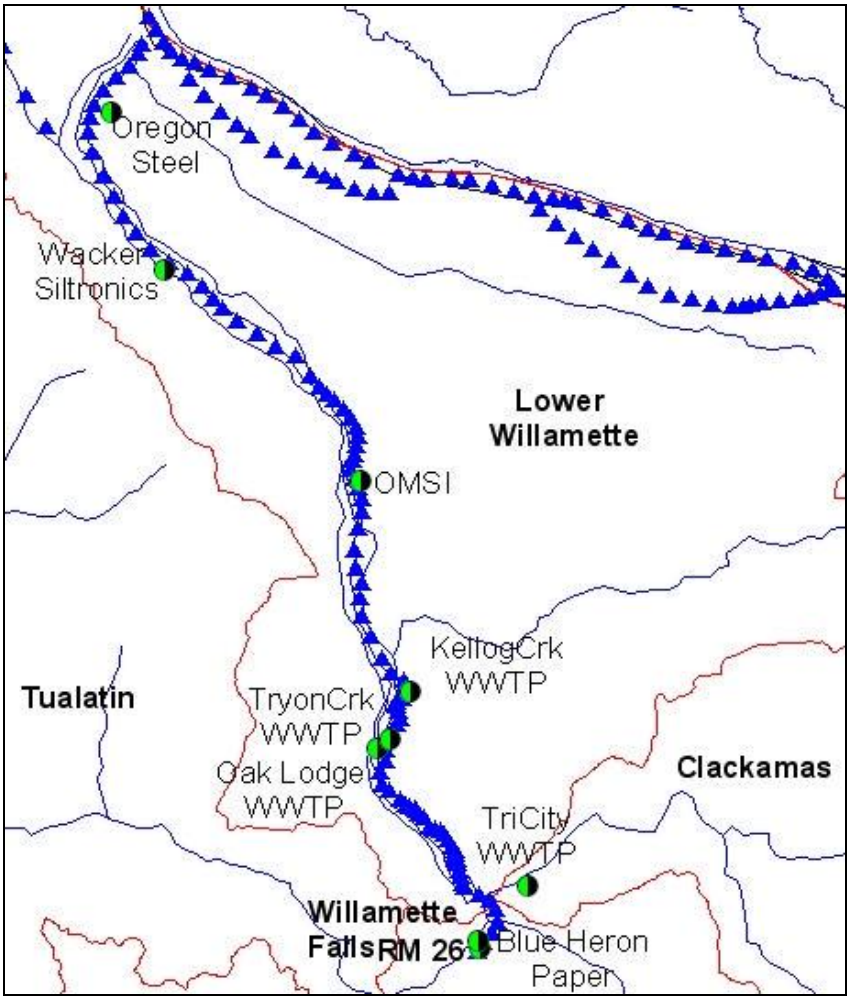


**Figure 71. Lower Willamette River model point source locations**

**Table 9. Lower Willamette River model point sources**

| Model Segment | Facility Name | Willamette River Mile |
|---|---|---|
| 2 | Blue Heron Paper Mill | 26.4 |
| 6 | Tri-City WWTP | 25.5 |
| 35 | Tryon Creek WWTP | 20.4 |
| 36 | Oak Lodge WWTP | 20.1 |

| Model Segment | Facility Name | Willamette River Mile |
|---|---|---|
| 47 | Kellogg Creek WWTP | 18.7 |
| 62 | Oregon Museum of Science and Industry | 13.5 |
| 84 | Wacker Siltronics | 6.6 |
| 92 | Oregon Steel | 2.8 |

## Year 2001

Figure 72 shows the daily discharge flows for the Blue Heron Paper Mill in 2001. Figure 73 shows the Tri-City wastewater treatment plant with daily flow values. Figure 74 shows the times series of the Tryon Creek wastewater treatment plant (City of Portland) discharge. Figure 75 shows the daily discharge for the Oak Lodge wastewater treatment plant. Figure 76 shows the daily effluent rate for the Kellogg Creek wastewater treatment plant which with the Tri-City plant is part of the Clackamas County treatment facilities. Figure 77 shows monthly discharge rates to the Willamette River from the Oregon Museum of Science and Industry (OMSI). Figure 78 shows the monthly discharge rates from Wacker Siltronics to the river. Figure 79 shows the times series effluent flow from Oregon Steel mill based on their permitted maximum amount since there was no data available. The combined point source flow is less than 1% of the main stem Willamette River flow.

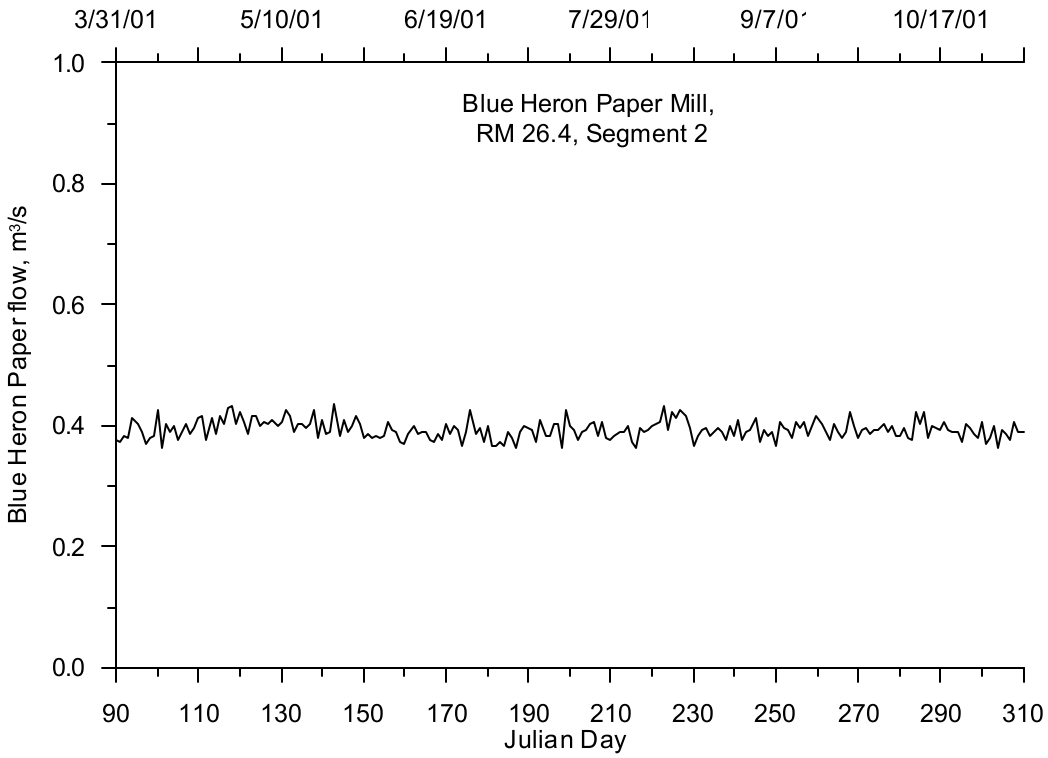


**Figure 72. Blue Heron Paper Mill flow, 2001**

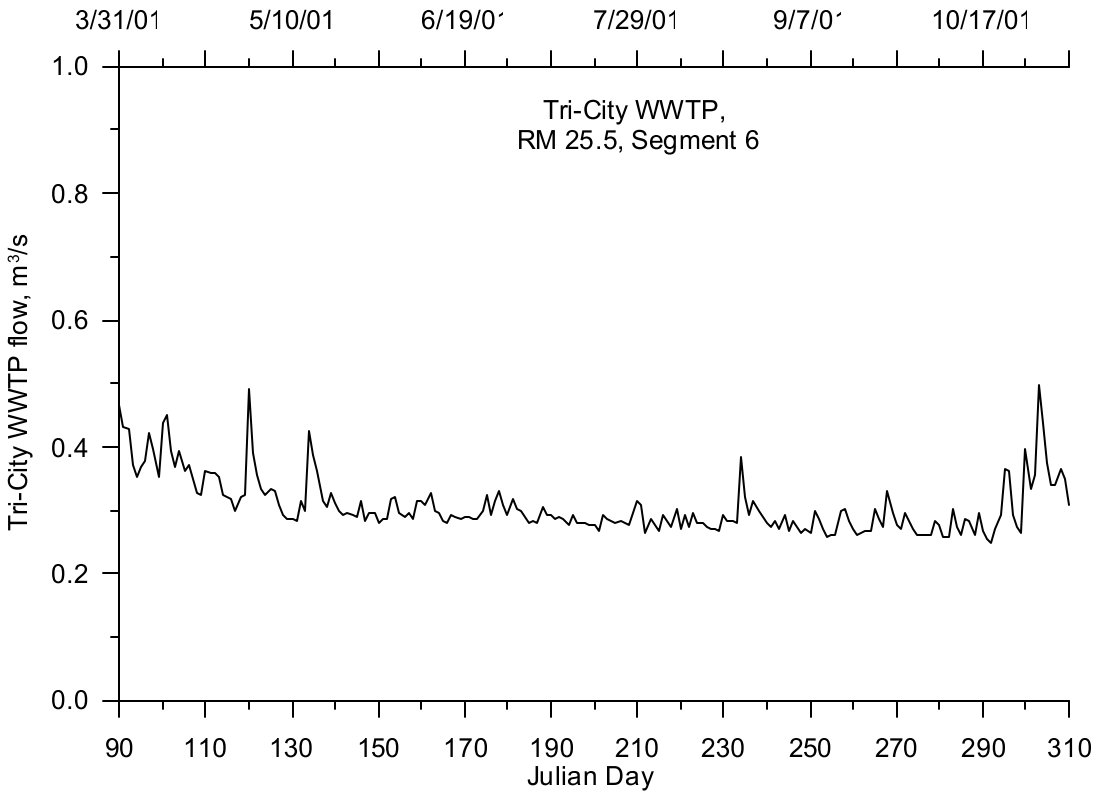


**Figure 73. Tri-City WWTP flow, 2001**

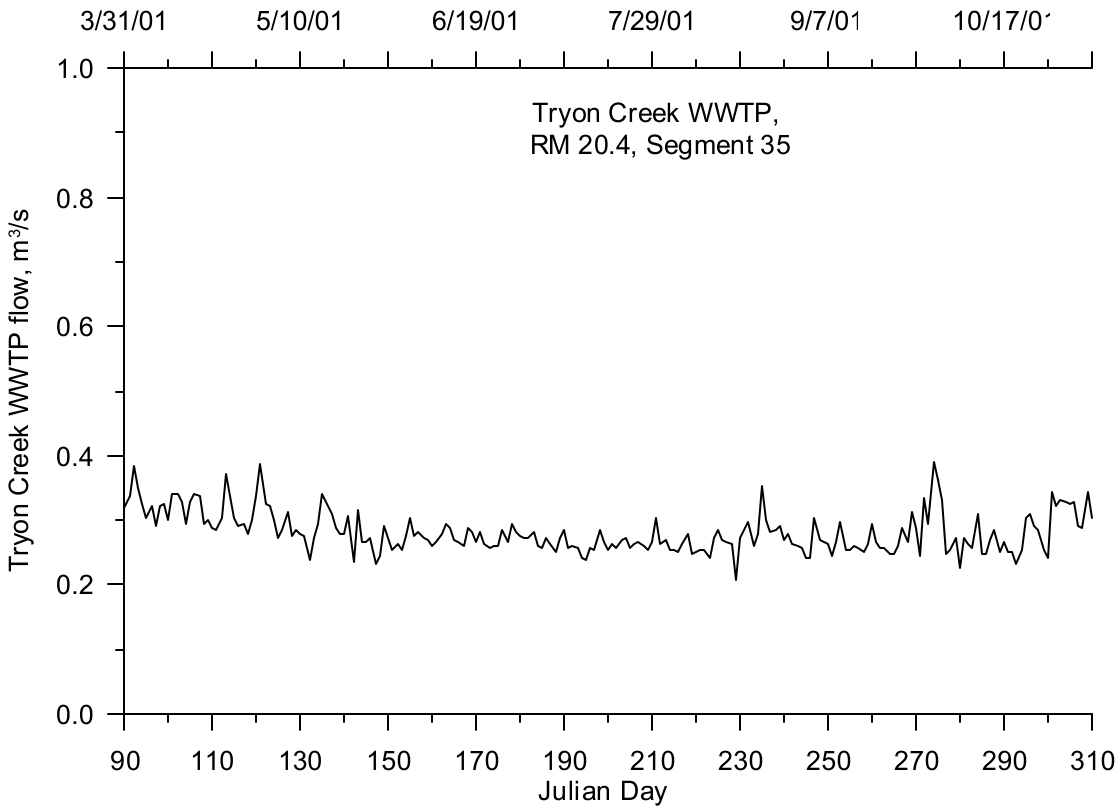


**Figure 74. Tryon Creek WWTP flow, 2001**

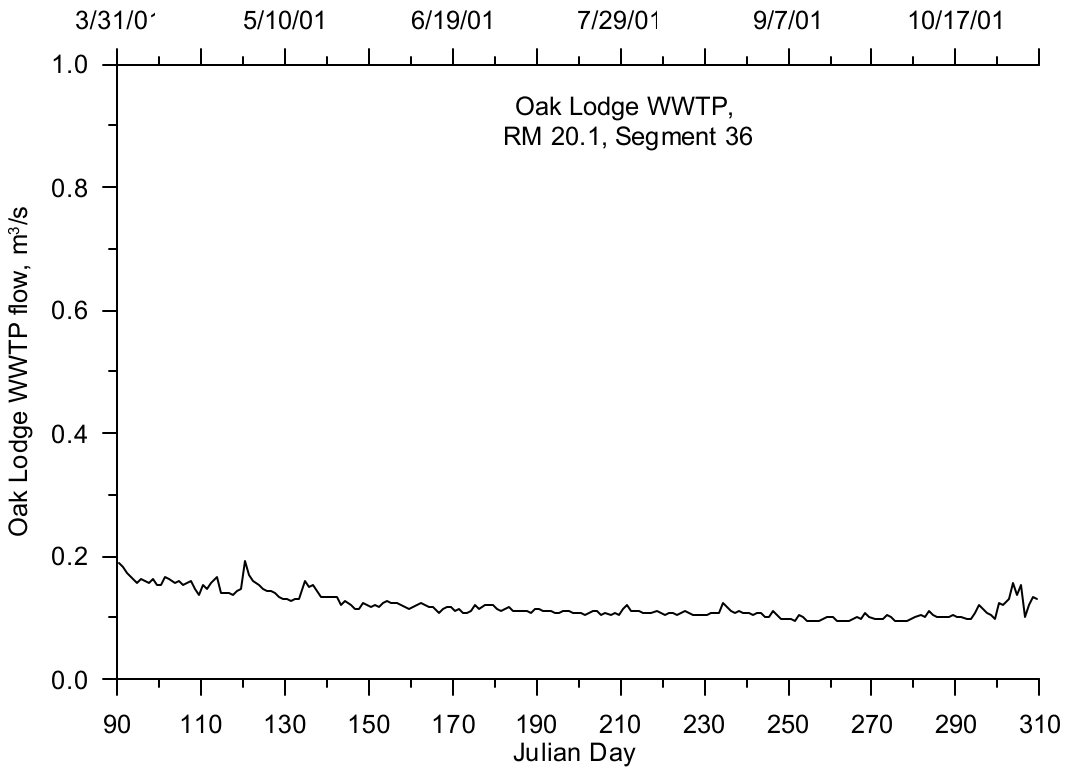


**Figure 75. Oak Lodge WWTP flow, 2001**

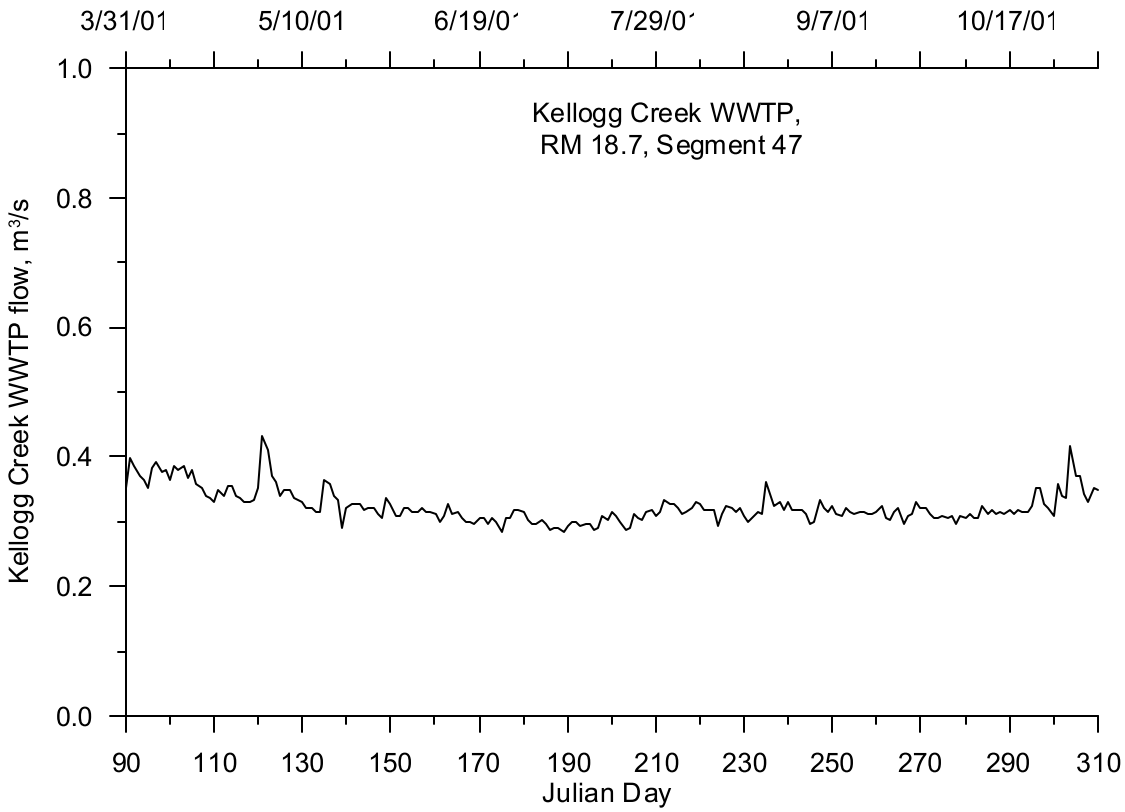


**Figure 76. Kellogg Creek WWTP flow, 2001**

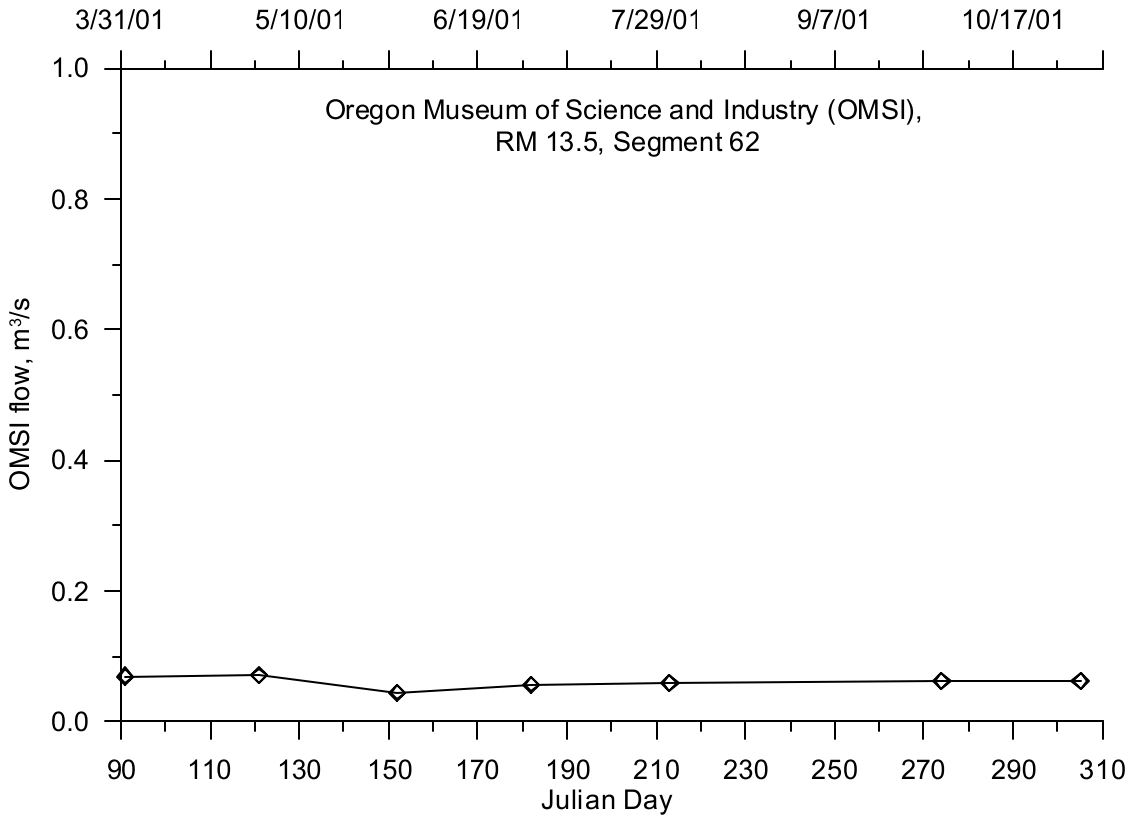


**Figure 77. Oregon Museum of Science and Industry flow, 2001**

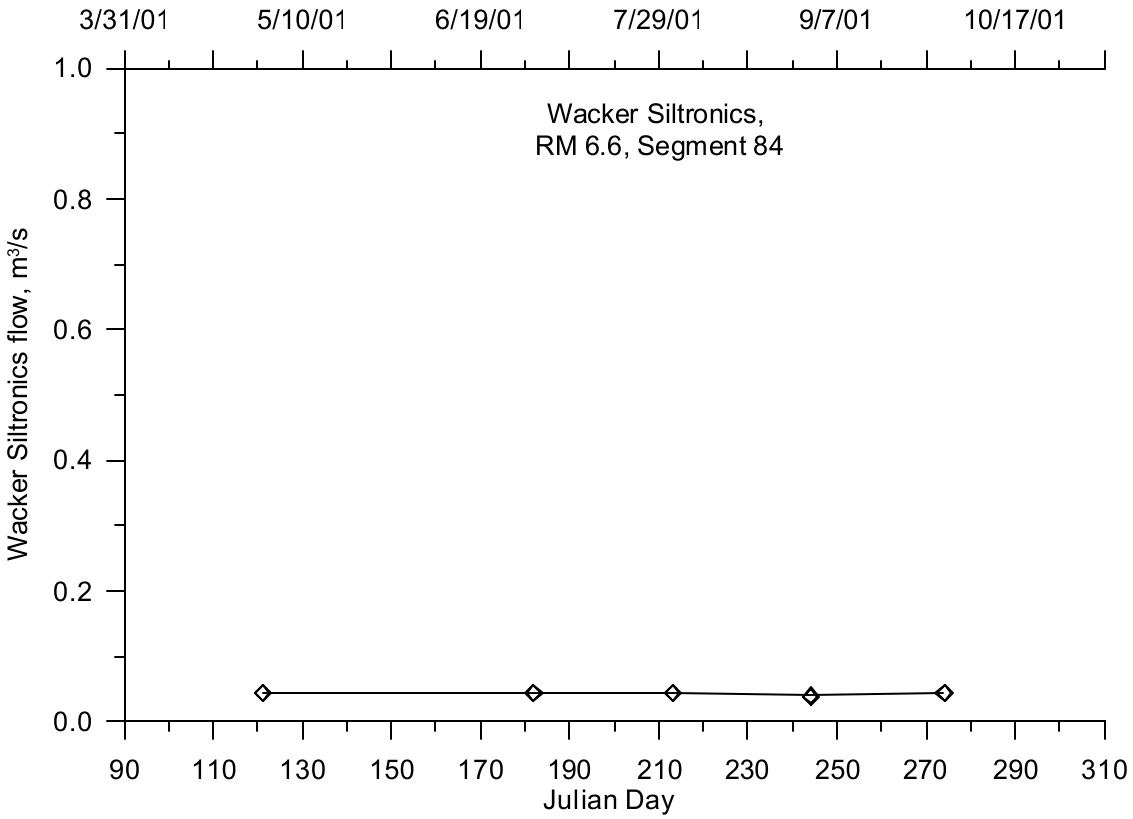


**Figure 78. Wacker Siltronics flow, 2001**

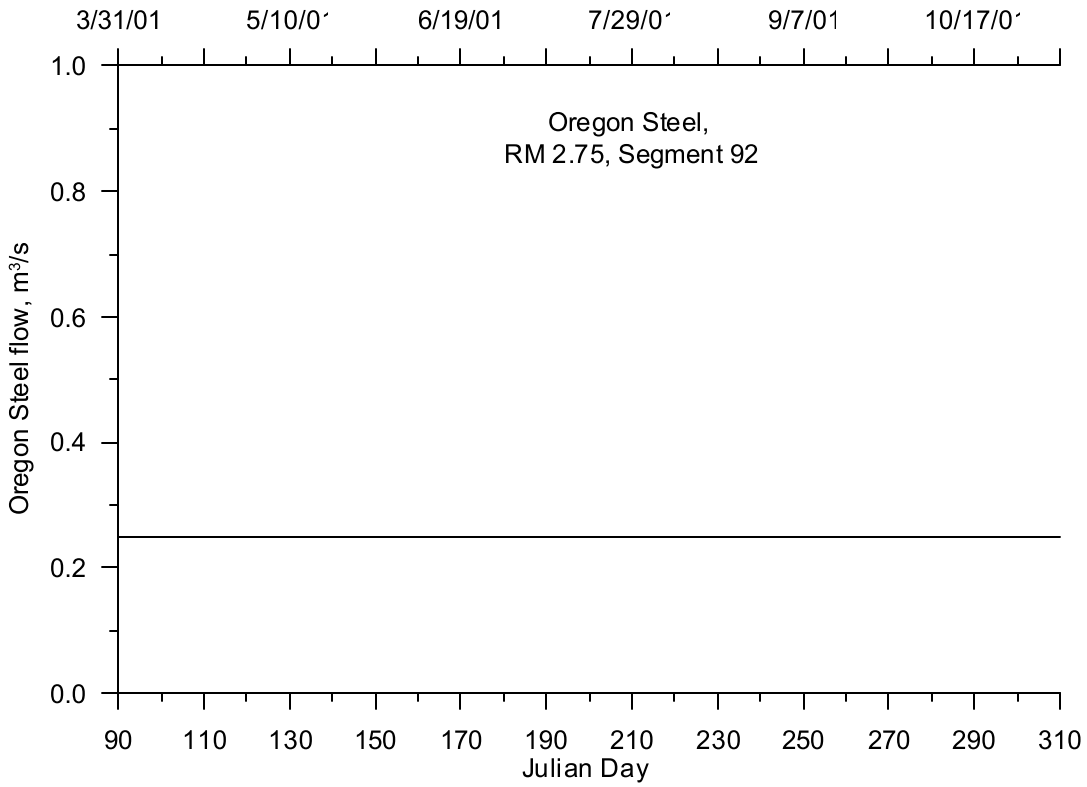


**Figure 79. Oregon Steel flow, 2001**

## Year 2002

Figure 80 shows the daily discharge for the Blue Heron Paper Mill in 2002. Figure 81 shows the Tri-City wastewater treatment plant with daily flow. Figure 82 shows the times series of the Tryon Creek wastewater treatment plant discharge for 2002. Figure 83 shows the daily discharge for the Oak Lodge wastewater treatment plant. Figure 84 shows the daily effluent rate for the Kellogg Creek wastewater treatment plant. Figure 85 shows the monthly discharge rates from Wacker Siltronics to the river. There were no new discharge data available for OMSI and the Oregon Steel Mill so 2001 data were used instead, which are represented in Figure 77 and Figure 79, respectively.

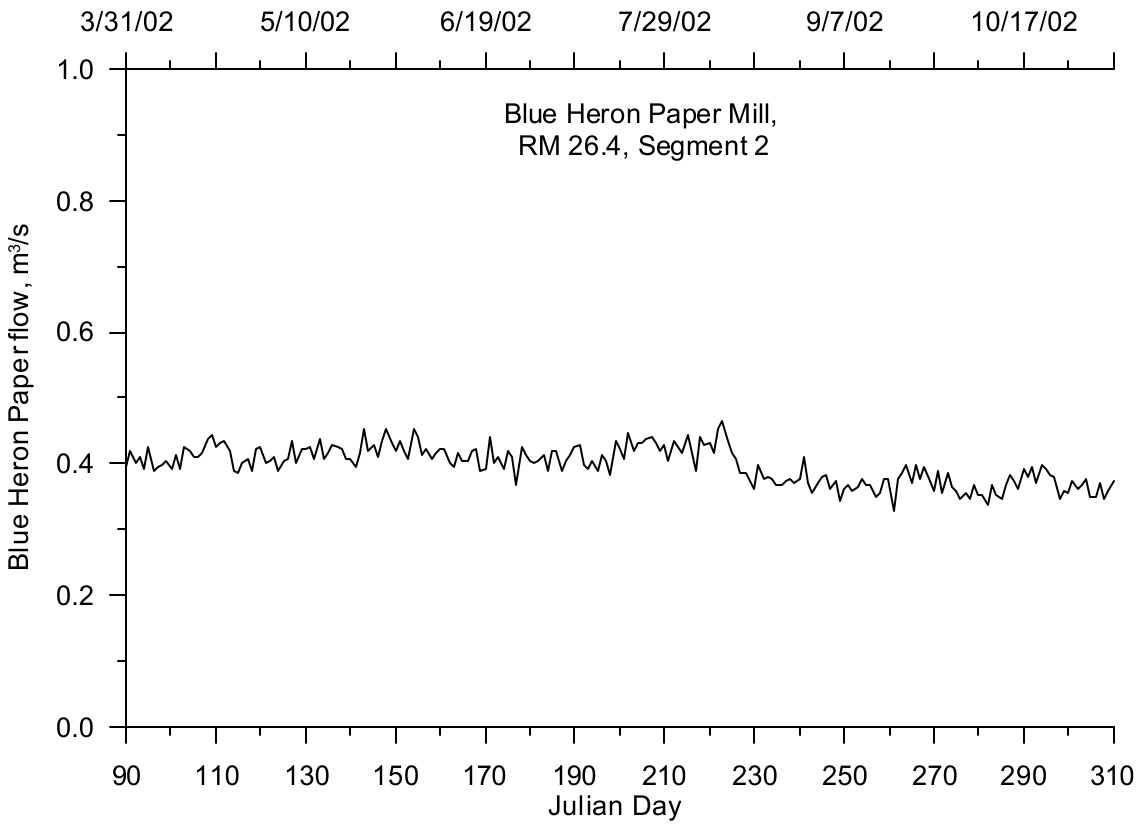


**Figure 80. Blue Heron Paper Mill flow, 2002**

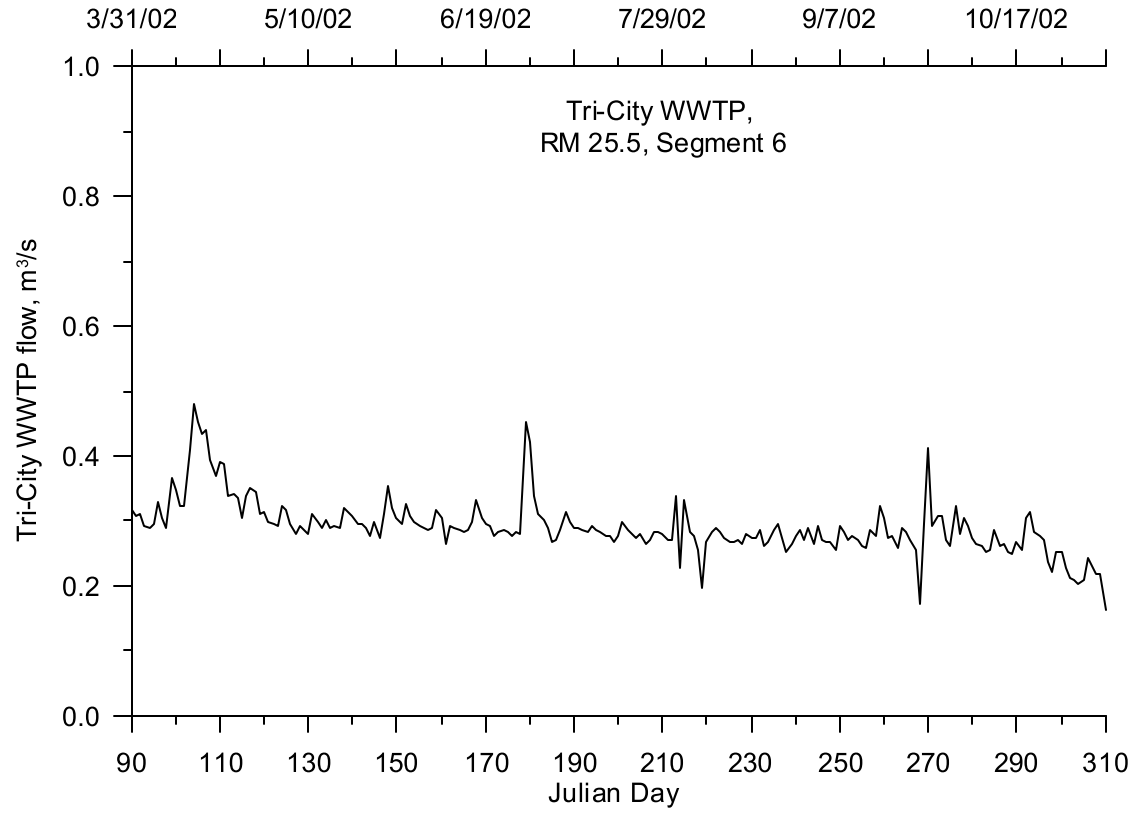


**Figure 81. Tri-City WWTP flow, 2002**

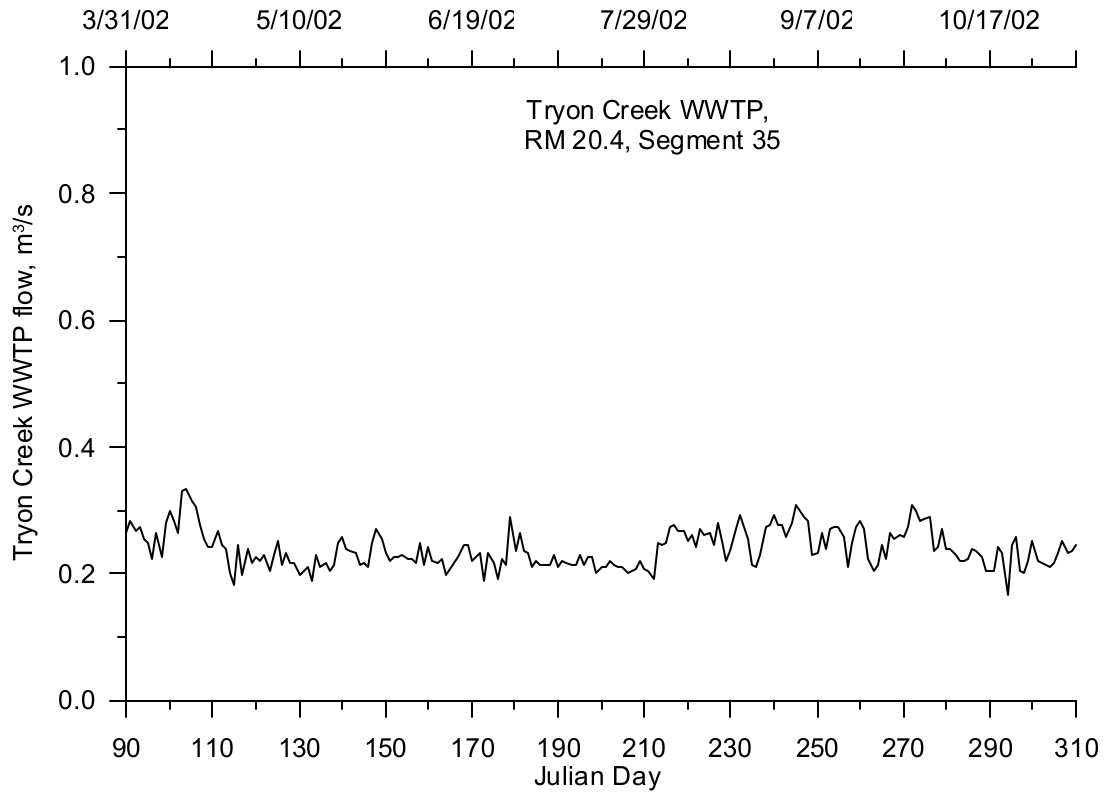


**Figure 82. Tryon Creek WWTP flow, 2002**

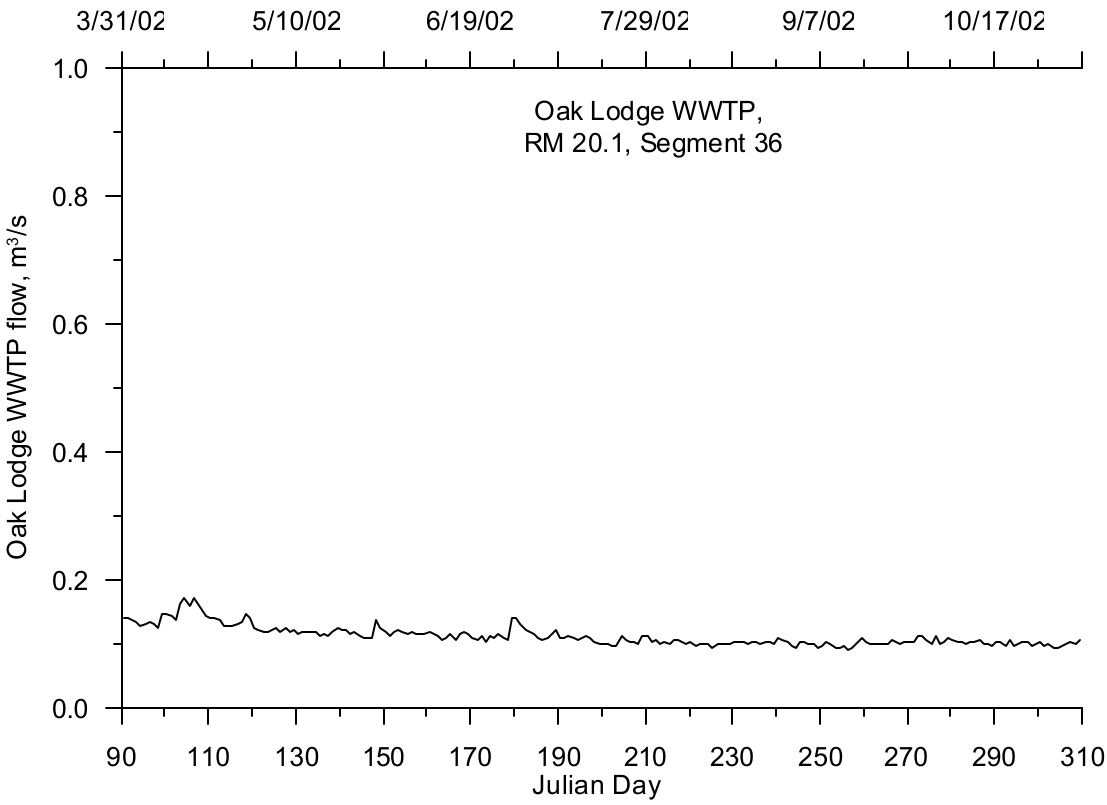


**Figure 83. Oak Lodge WWTP flow, 2002**

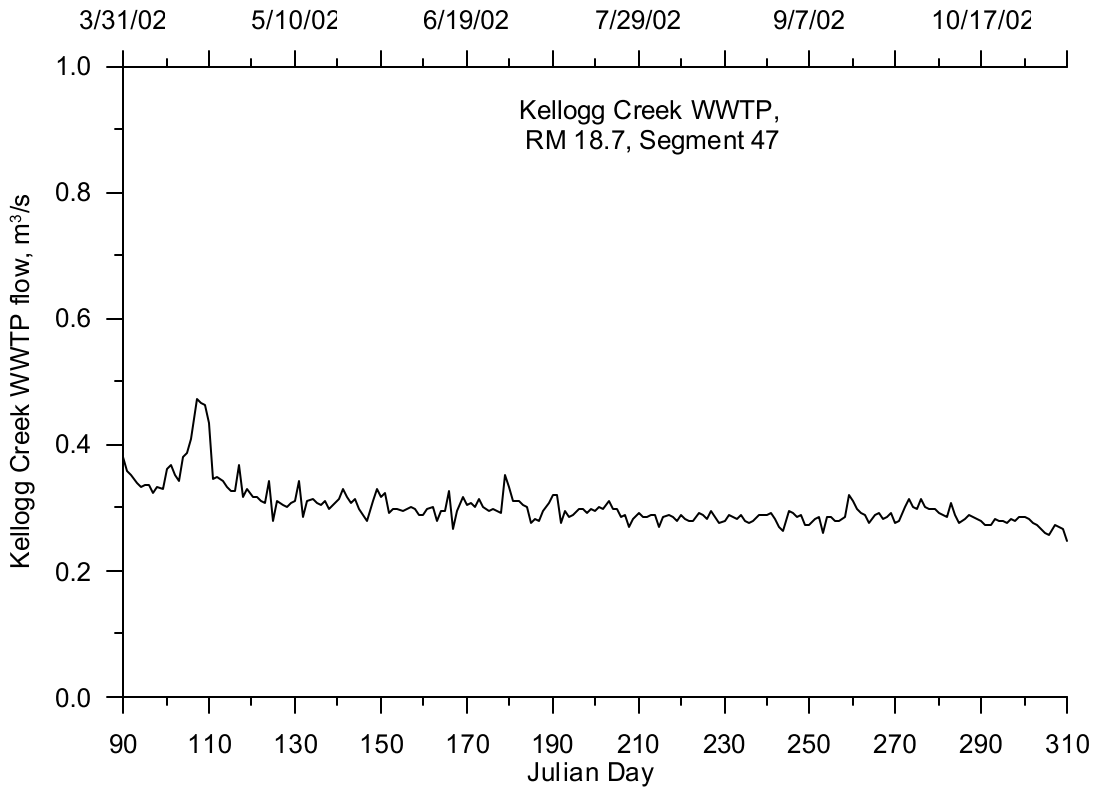


**Figure 84. Kellogg Creek WWTP flow, 2002**

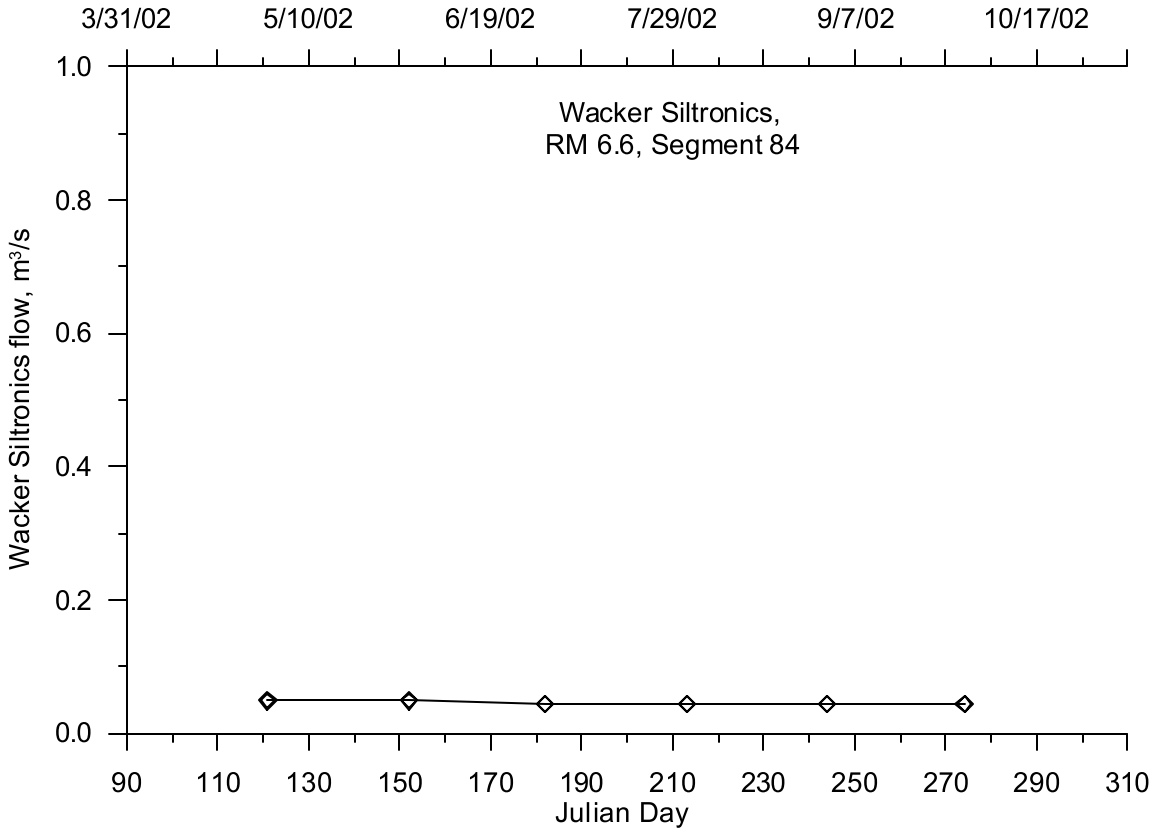


**Figure 85. Wacker Siltronics flow, 2002**

## Temperature Data

The temperature sites for each of the point sources to the Lower Willamette River were the same as those sites used for discharge rates. Figure 71 shows a map of the point source locations along the Lower Willamette, and Table 9 lists the sites in the figure along with the river mile and model segment location.

### Year 2001

Figure 86 shows the daily temperature data monitored from the Blue Heron Paper Mill effluent. There were no temperature data available for the Tri-City waste water treatment plant for 2001 so 2002 data were used instead. Figure 87 shows the time series temperature data for the plant. The figure shows there were sharp temperature decreases in the data, which corresponded primarily to weekly operation changes on Sunday mornings from 8 am to 11 am. Based on the daily flow data there was no indication of a decrease in effluent flow rates. The decrease in temperature could be due to the temperature sensor monitoring air temperature for a few hours each Sunday morning. The data were not removed from the record since there was no evidence that the effluent flow rate was zero during this weekly time window. The figure also shows there were temperature data missing from April 1 to June 7. Since there were no other data available to fill the gap a temperature value was set for April 1, and the model was allowed to linearly interpolate between two temperature values in April and June.

Figure 88 shows the Tryon Creek WWTP daily discharge temperature data for 2001. Figure 89 shows the daily temperature data for the Oak Lodge wastewater treatment plant for 2001. There were no 2001 temperature data available for the Kellogg Creek wastewater treatment plant so 2002 data were used instead. Figure 90 shows the Kellogg Creek temperature data used for 2001 and 2002. The figure also shows there was a gap in the data from April 1 to June 13. Since there were no other data to fill this gap, two values were used between April and June 13 and the model was allowed to linearly interpolate between the values.

Figure 91 shows monthly grab sample temperature data from the OMSI discharge to the Willamette River in 2001. Figure 92 shows the monthly grab sample temperature data from the Wacker Siltronics discharge to the Willamette River. Figure 93 shows the effluent temperature for Oregon Steel Mill for 2001, which was based on their maximum permitted discharge temperature since there were no temperature data.

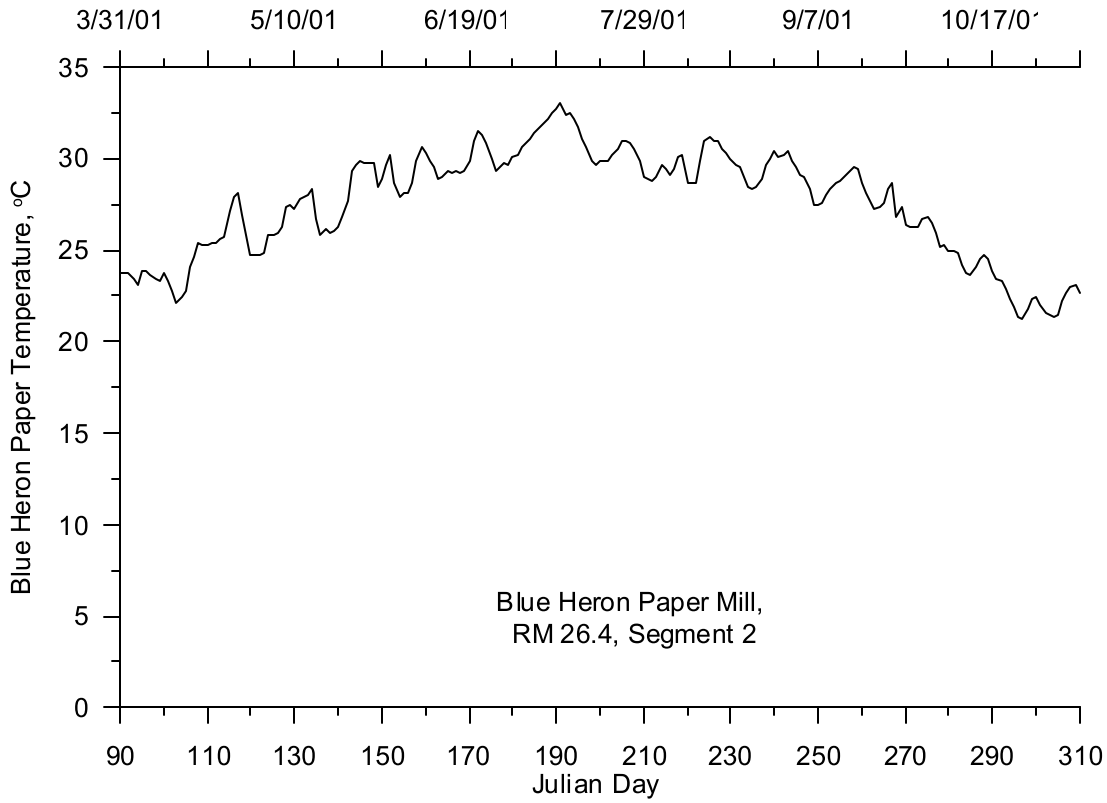


**Figure 86. Blue Heron Paper Mill temperature, 2001**

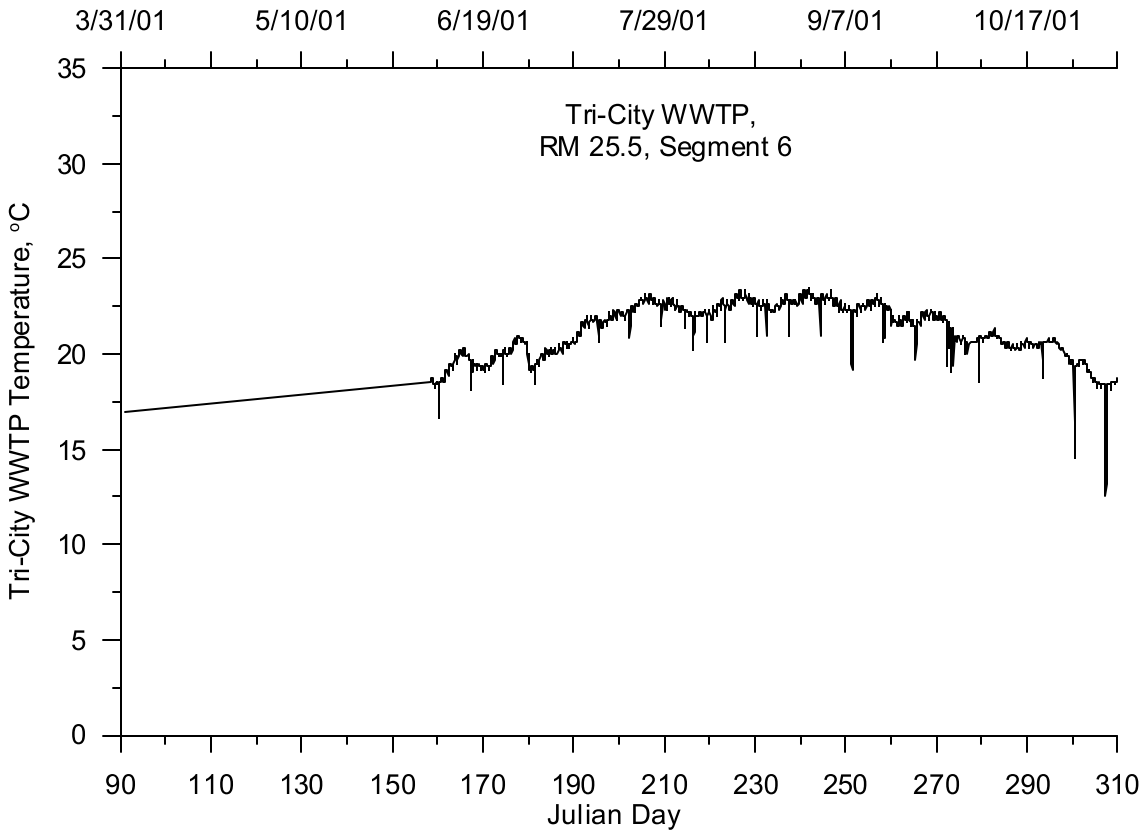


**Figure 87. Tri-City WWTP temperature, 2001**

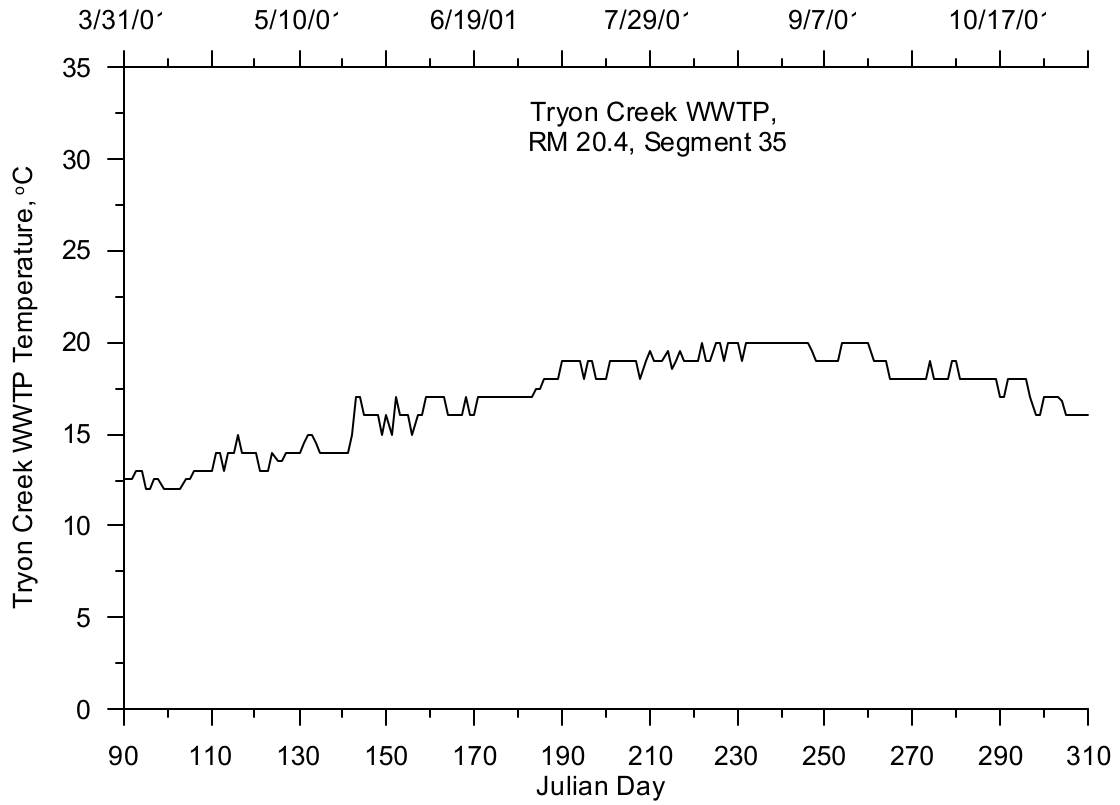


**Figure 88. Tryon Creek WWTP temperature, 2001**

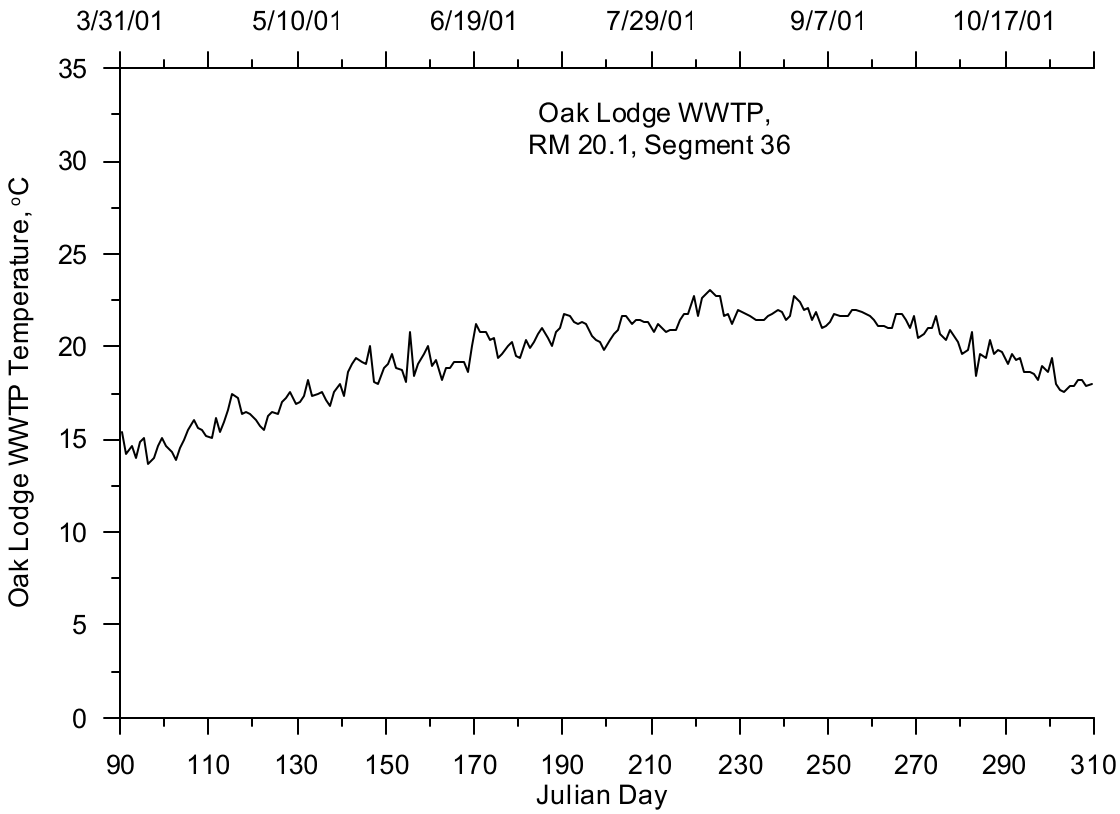


**Figure 89. Oak Lodge WWTP temperature, 2001**

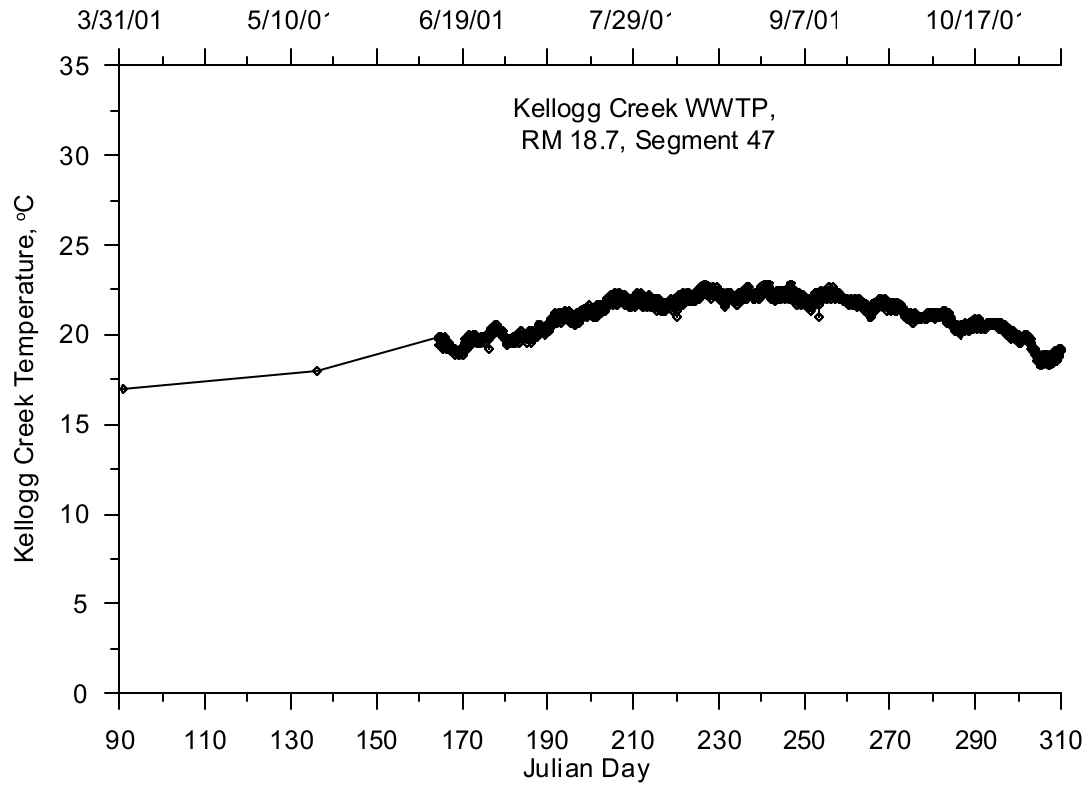


**Figure 90. Kellogg Creek WWTP temperature, 2001**

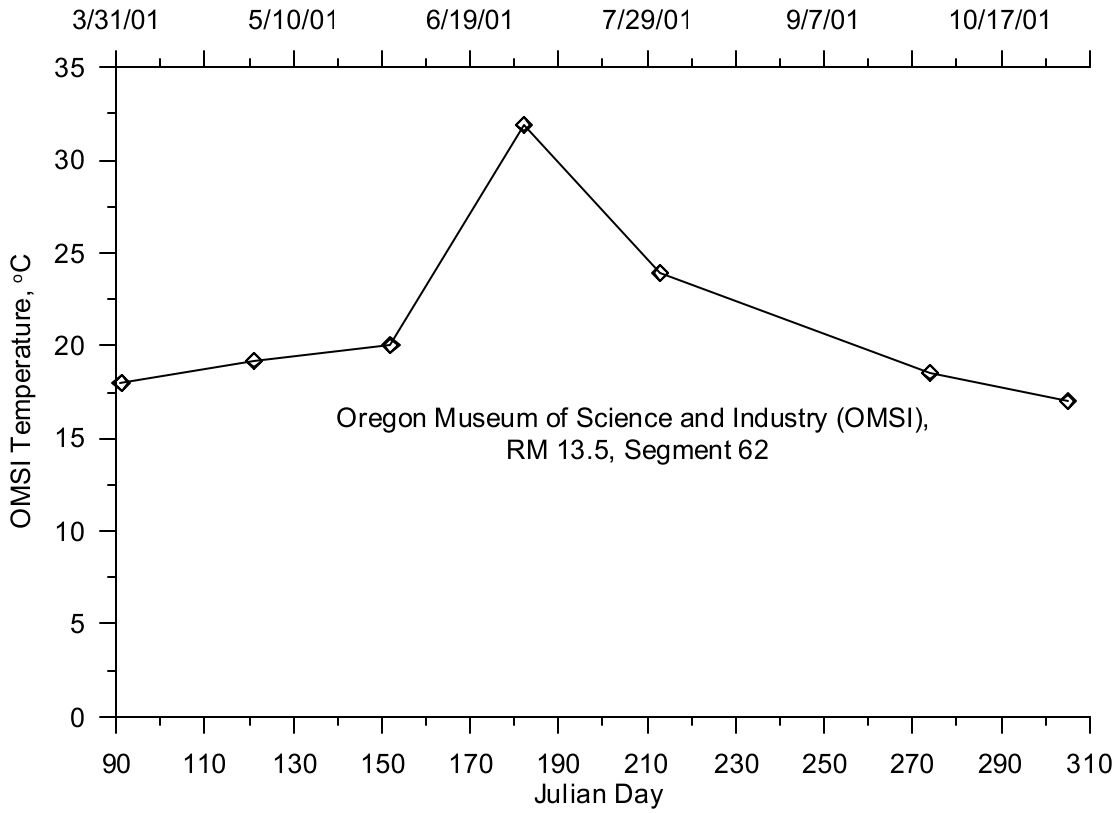


**Figure 91. Oregon Museum of Science and Industry temperature, 2001**

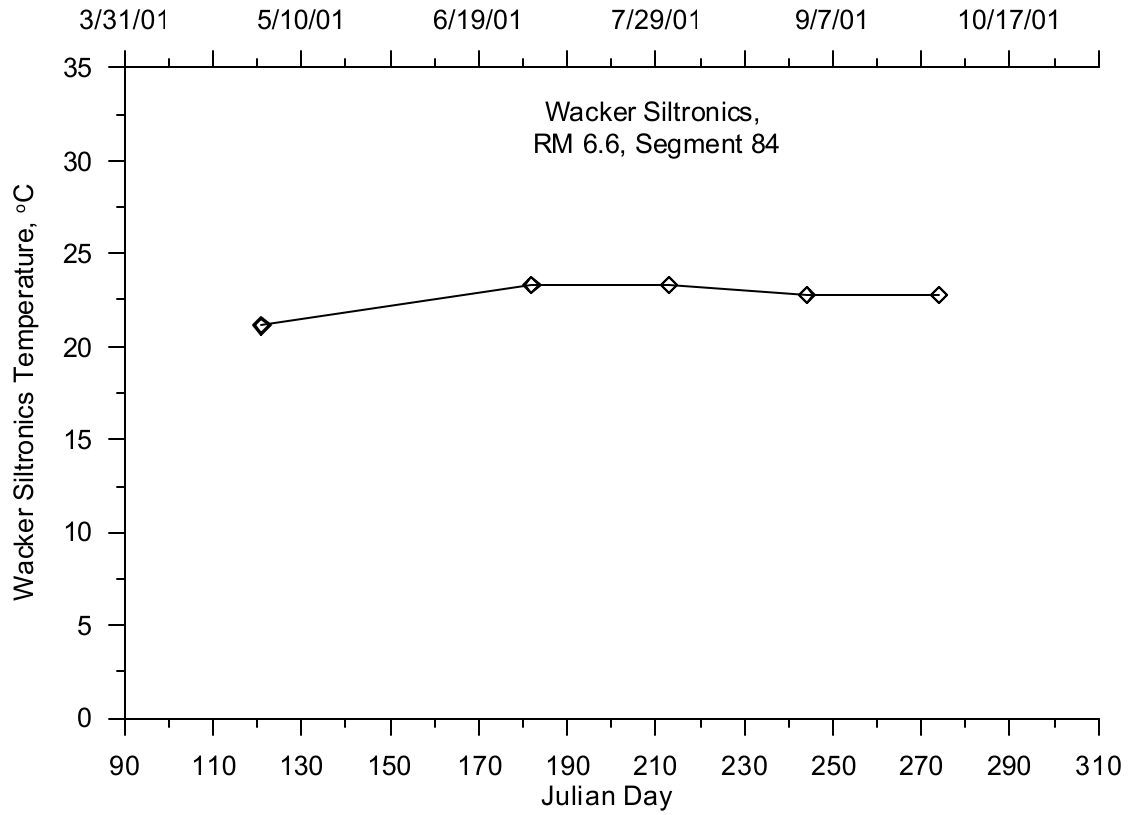


**Figure 92. Wacker Siltronics temperature, 2001**

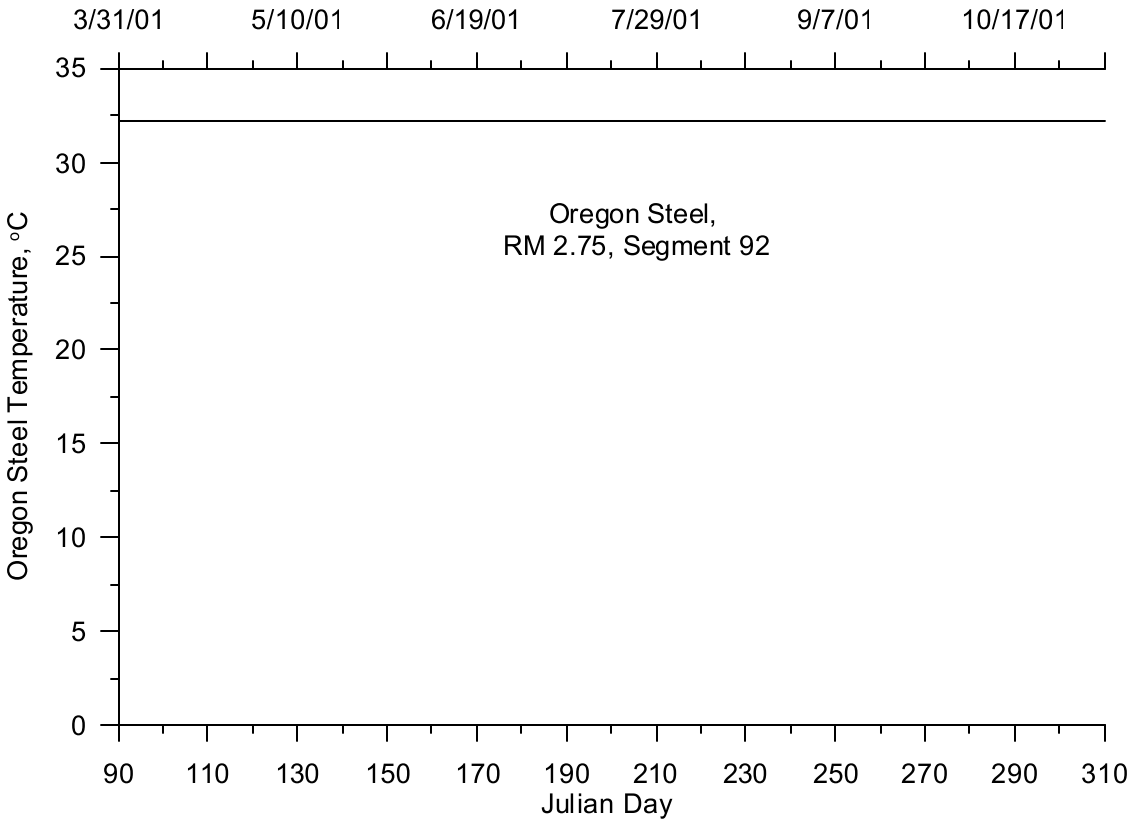


**Figure 93. Oregon Steel temperature, 2001**

Year 2002

Figure 94 shows the daily temperature data for the Blue Heron Paper Mill discharge in 2002. The Tri-City wastewater treatment plant had no temperature data for 2001 so 2002 temperature data were used for both 2001 and 2002 as shown in Figure 87. Figure 95 shows the daily temperature data for the Tryon Creek WWTP for 2002. Figure 96 shows the Oak Lodge WWTP daily discharge temperature and the figure shows there was a general seasonal warming trend as seen in some of the tributaries. Since there were no temperature data for the Kellogg Creek WWTP flow for 2001 the 2002 data were used for both years. The temperature data for 2002 are shown in Figure 90. There were no temperature data for the effluent for OMSI and Oregon Steel Mills for 2002 so the grab samples from 2001 were used for 2002 for OMSI and the maximum permitted temperature used in 2001 for the Oregon Steel Mills were also used for 2002. Figure 97 shows the monthly grab samples of temperature data from the Wacker Siltronics effluent.

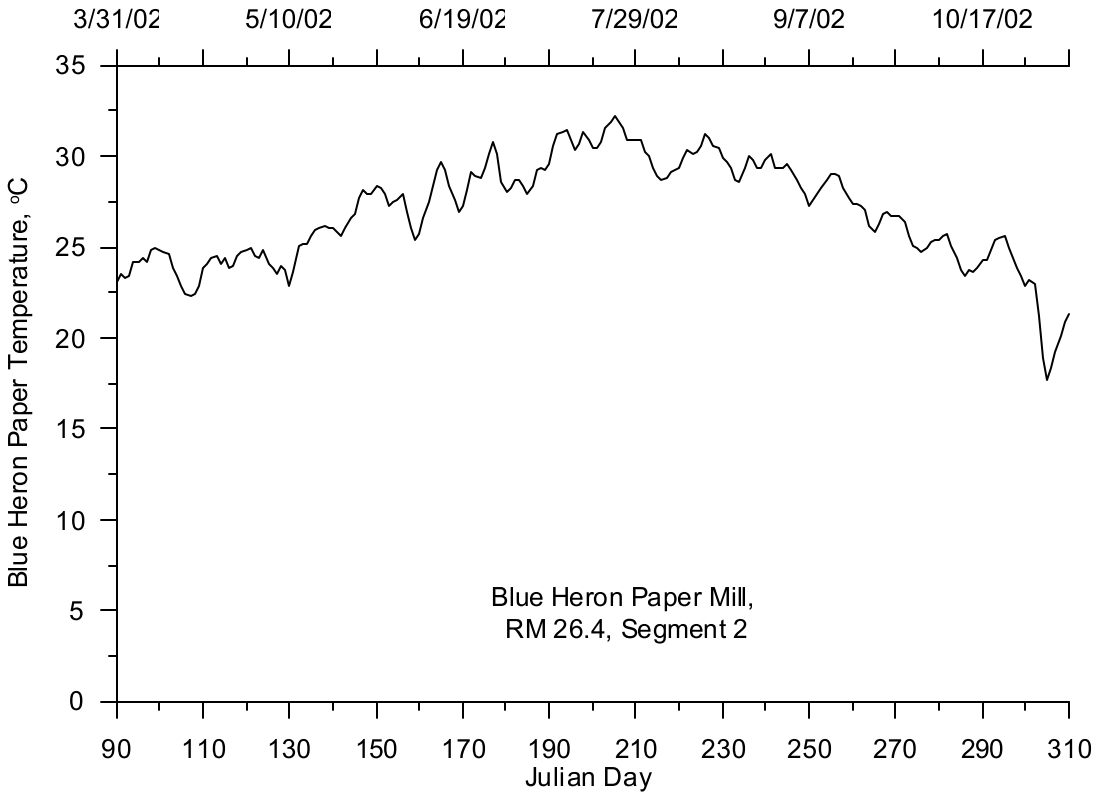


**Figure 94. Blue Heron Paper Mill temperature, 2002**

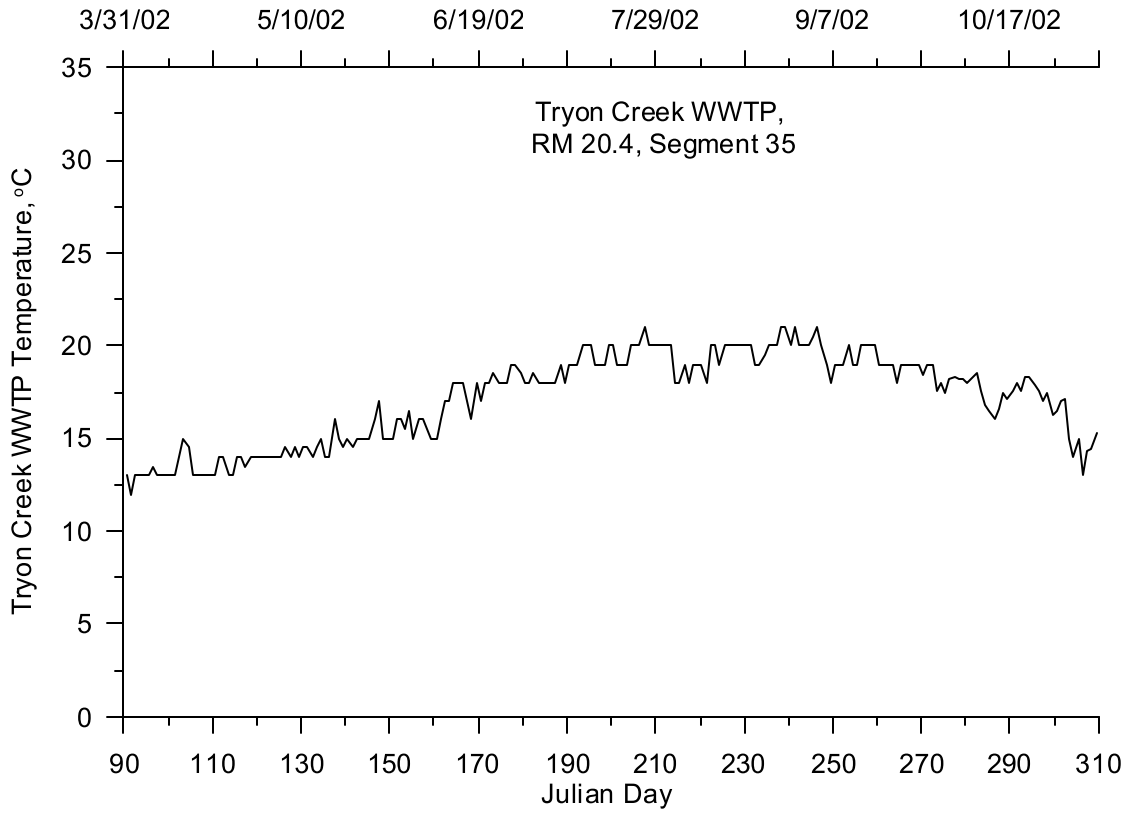


**Figure 95. Tryon Creek WWTP temperature, 2002**

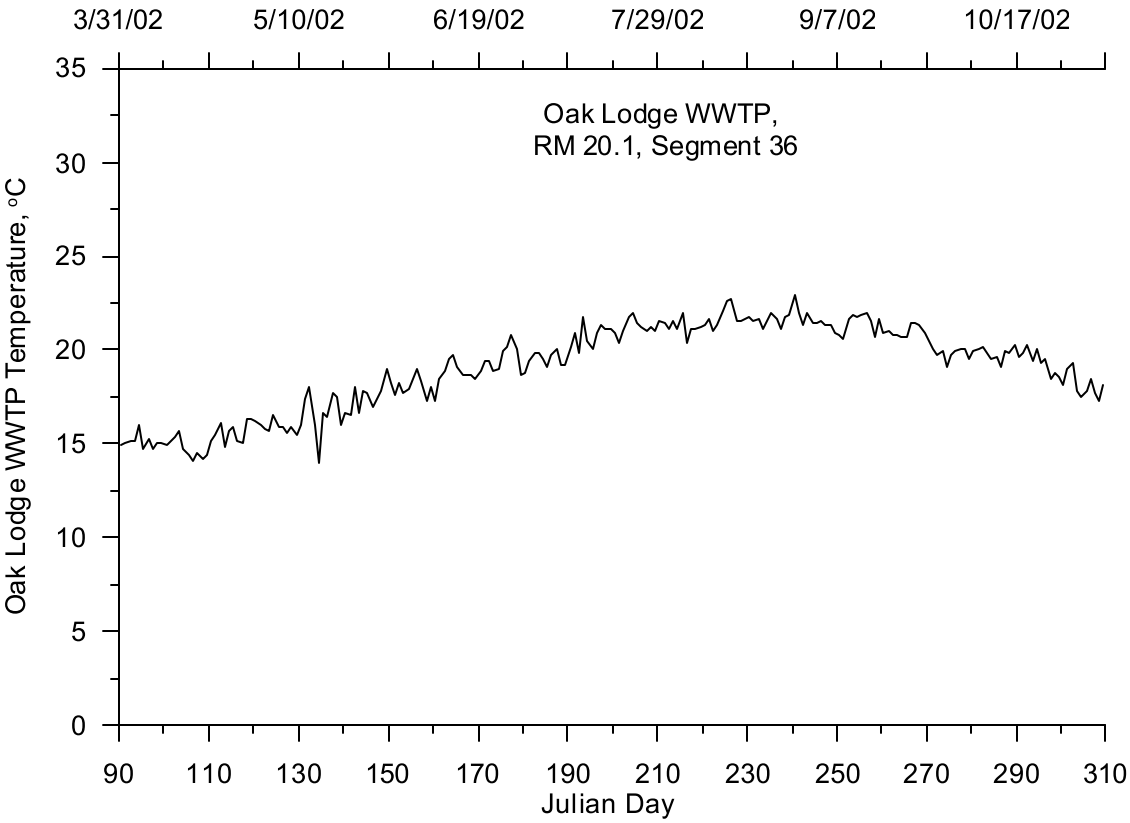


**Figure 96. Oak Lodge WWTP temperature, 2002**

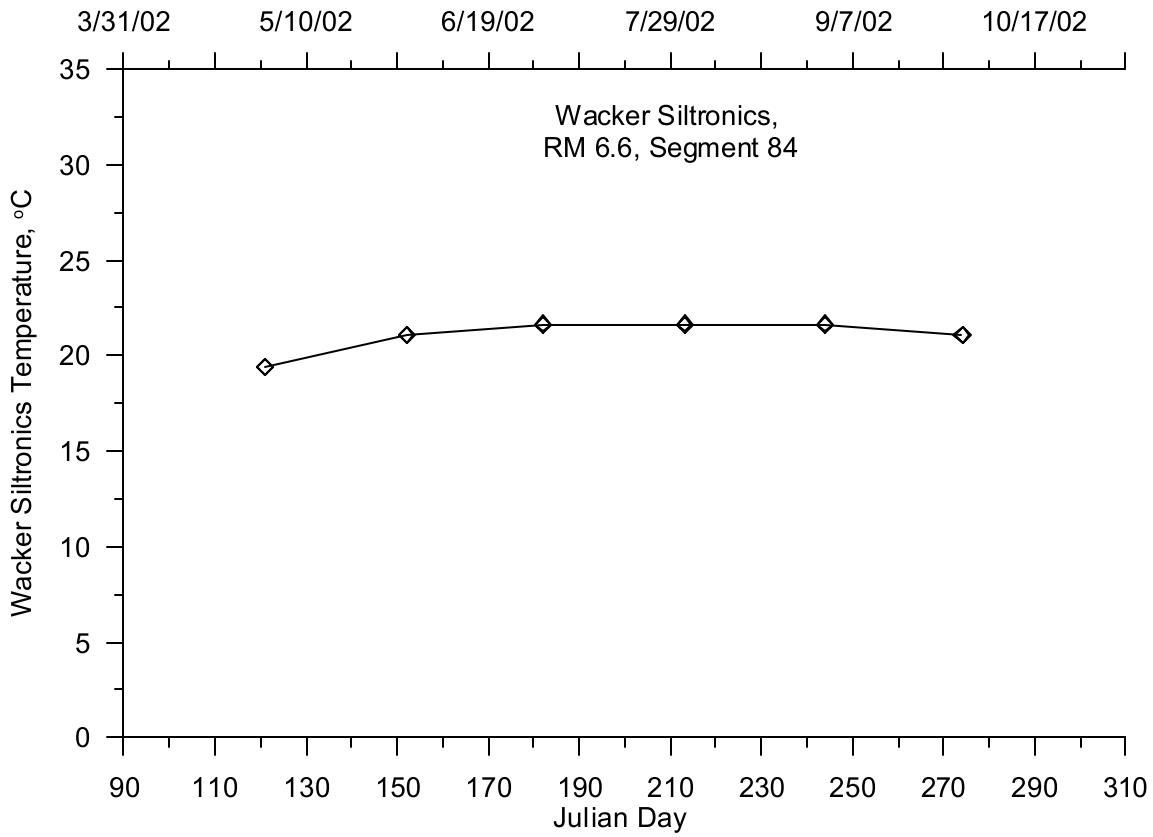


**Figure 97. Wacker Siltronics temperature, 2002**

## *Shading*

The Lower Willamette River (and Columbia River) did not have dynamic vegetation and topographic shade incorporated because the Lower Willamette River is highly developed on both sides of the channel. The urban development results in limited vegetation to provide shade. Although there may be some topography which shades the river, such as the West Hills, the Lower Willamette River is sufficiently wide and the volume large enough that shading will have little influence on the river temperature.

## *Meteorology*

Meteorological data were collected at Portland International Airport and include air temperature, wind speed, wind direction, dew point, and cloud cover. Figure 98 shows the location of the Portland International Airport and several other meteorological stations in the model region. Table 10 lists the meteorological stations in the model region and the type of data recorded. METAR meteorological data were collected by the National Weather Service and the Federal Aviation Administration. The AGRIMET network is a series of Agricultural Meteorological stations maintained by the U.S. Bureau of Reclamation. The Portland International Airport was selected because it contained the longest historical record of data and fairly represents the meteorological conditions in the model domain.

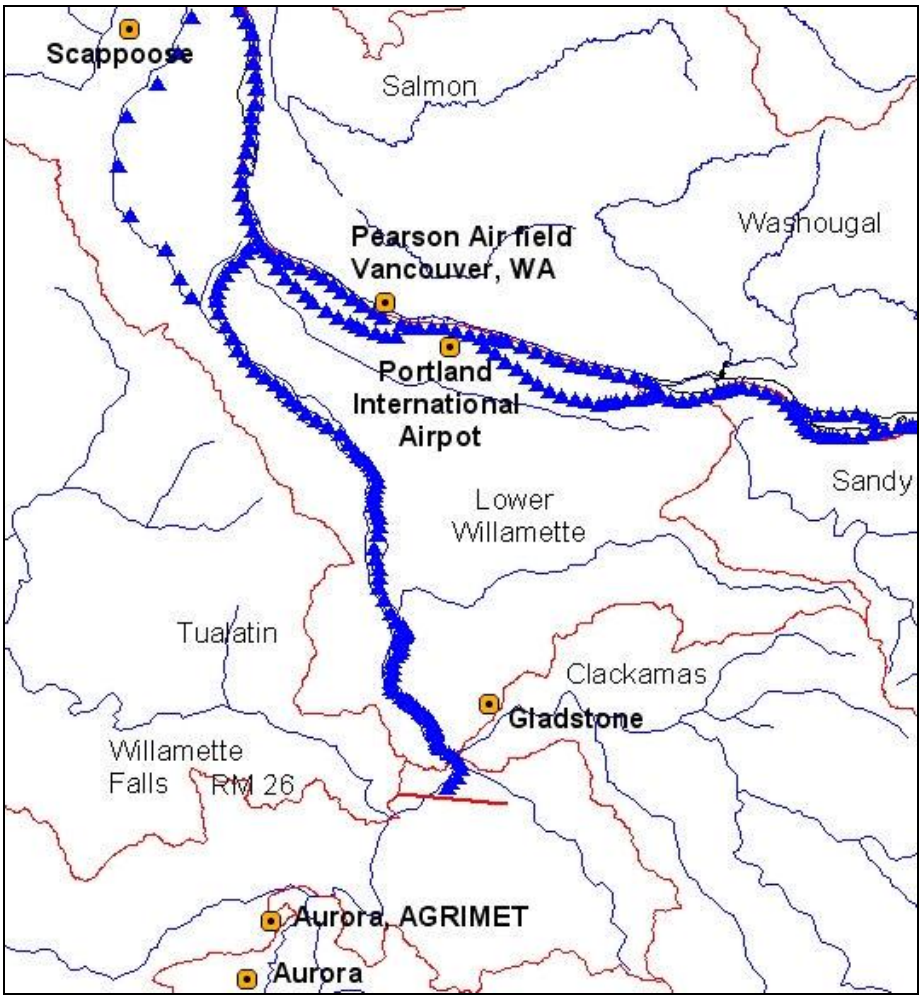


**Figure 98. Lower Willamette River model meteorological monitoring site locations**

**Table 10. Lower Willamette River model meteorological monitoring sites**

| Site | Agency (Program) | Meteorological Parameters |
|---|---|---|
| Scappoose, OR | National Weather Service (METAR) | Air Temperature, Dew Point Temperature, Relative Humidity, Wind Speed, Wind Direction, Cloud Cover |
| Vancouver, WA | National Weather Service (METAR) | Air Temperature, Dew Point Temperature, Relative Humidity, Wind Speed, Wind Direction, Cloud Cover |
| Portland International Airport | National Weather Service (METAR) | Air Temperature, Dew Point Temperature, Relative Humidity, Wind Speed, Wind Direction, Cloud Cover |
| Aurora Municipal Airport | National Weather Service (METAR) | Air Temperature, Dew Point Temperature, Relative Humidity, Wind Speed, Wind Direction, Cloud Cover |

| Site | Agency (Program) | Meteorological Parameters |
|---|---|---|
| Gladstone | University of Oregon, Solar Radiation Monitoring Lab | Solar Radiation |
| Aurora, OR | Bureau of Reclamation, (AGRIMET) | Solar Radiation |

## Portland International Airport

### Year 2001

Figure 99 through Figure 103 show the meteorological data at the Portland International Airport from April 1 to October 31, 2001. Figure 99 shows the air temperature, and Figure 100 shows the dew point temperature measured at the airport. Figure 101 shows the wind speed data measured at the airport and illustrates that the wind speeds below 1.74 m/s fall below the instruments minimum wind speed and were therefore recorded as zero. Figure 102 shows a rose diagram plot of the wind direction data recorded in the summer of 2001. The figure shows the wind direction was predominantly from the northwest. Although there was a large spike in winds from the north this result was also the due to the wind direction falling to zero (north) when the wind speed falls below the minimum wind speed. Figure 103 shows the cloud cover varying on a scale of 0 to 10 with zero representing no cloud cover and ten representing full cloud cover. In July 1996 the method for measuring cloud was changed to a scale of 1 to 4 resulting in less approximate conditions. The scale was converted to a 1 to 10 scale to be compatible with historical data. Figure 104 shows the solar radiation (global) measured in Gladstone, Oregon.

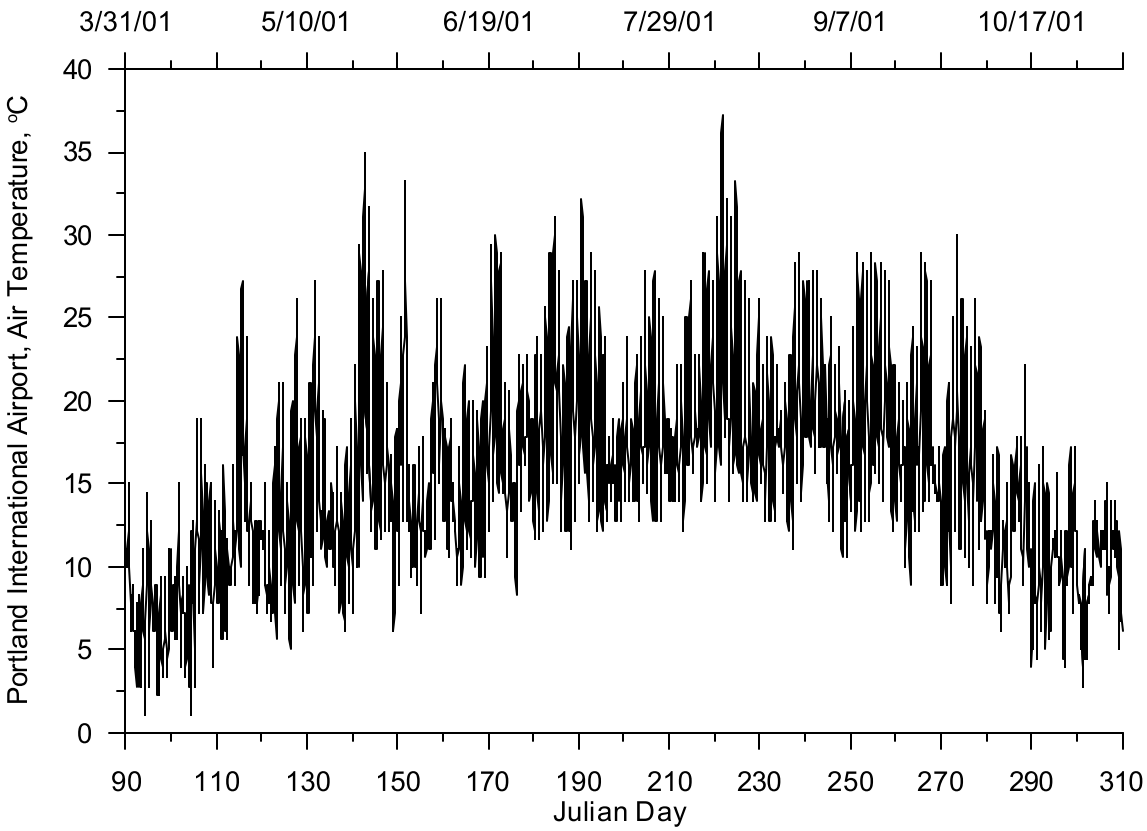


**Figure 99. Air temperature at Portland International Airport, 2001**

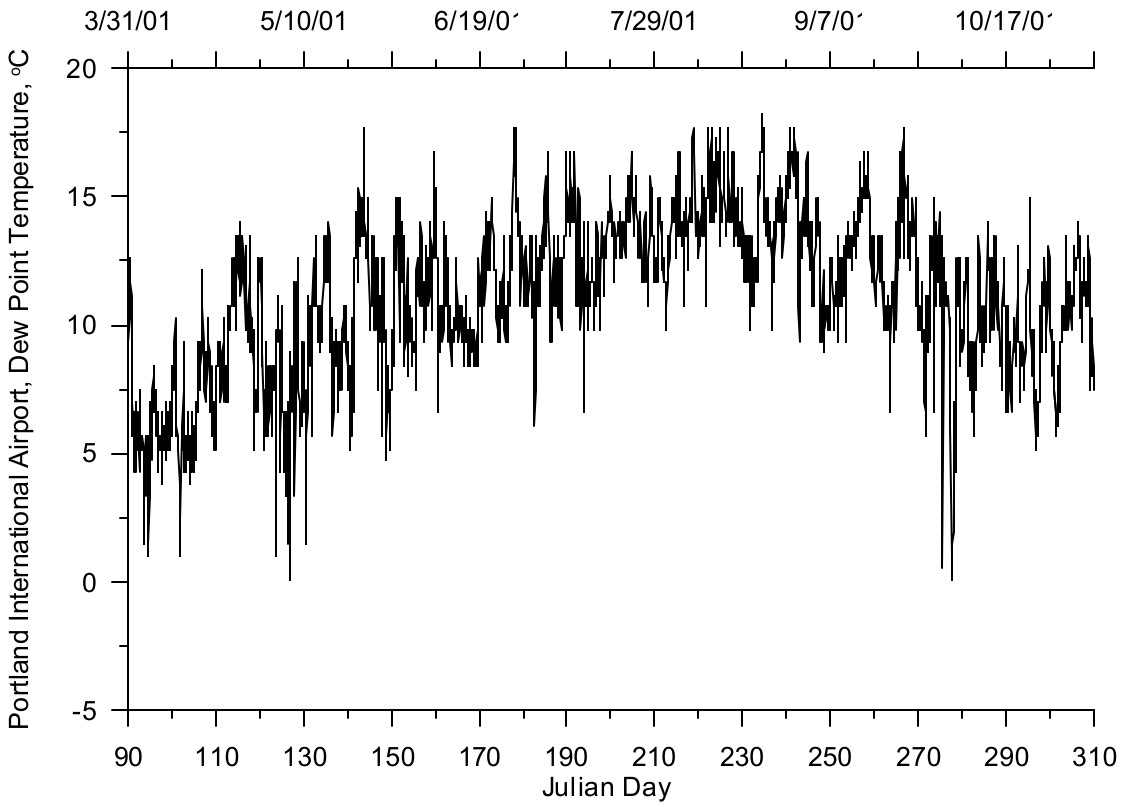


**Figure 100. Dew point temperature at Portland International Airport, 2001**

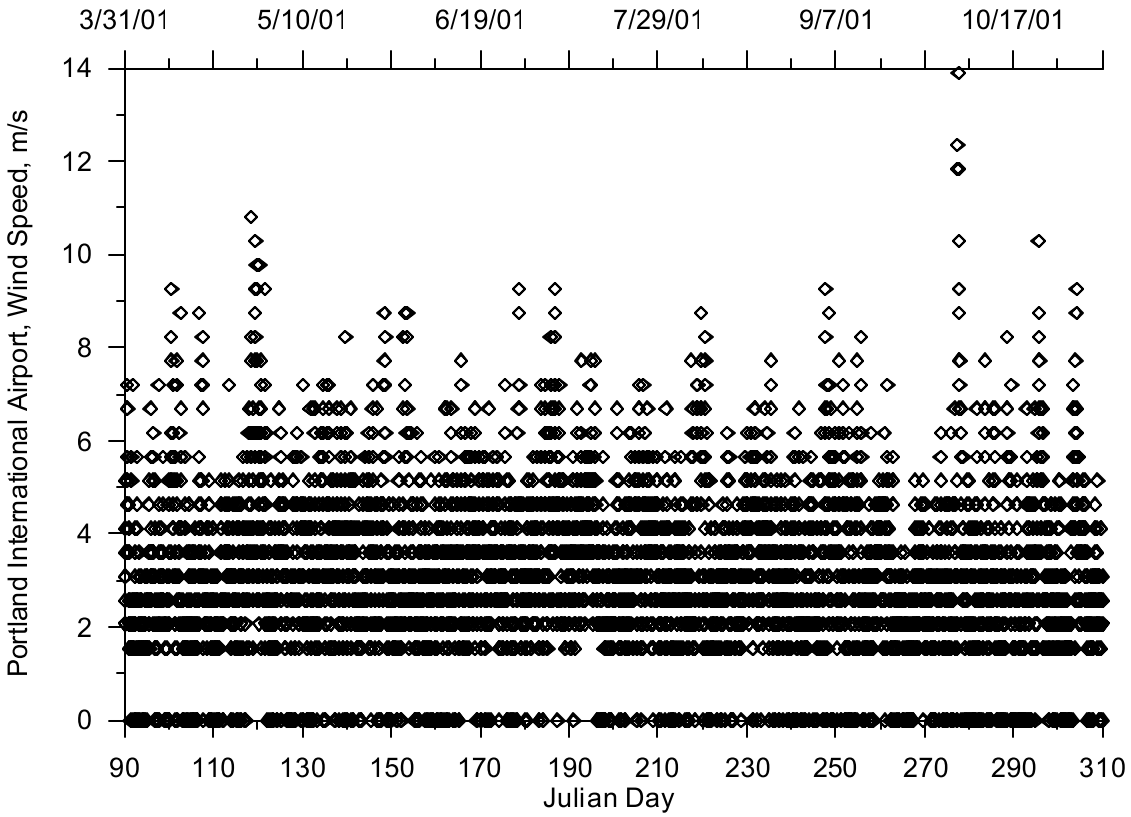


**Figure 101. Wind speed at Portland International Airport, 2001**

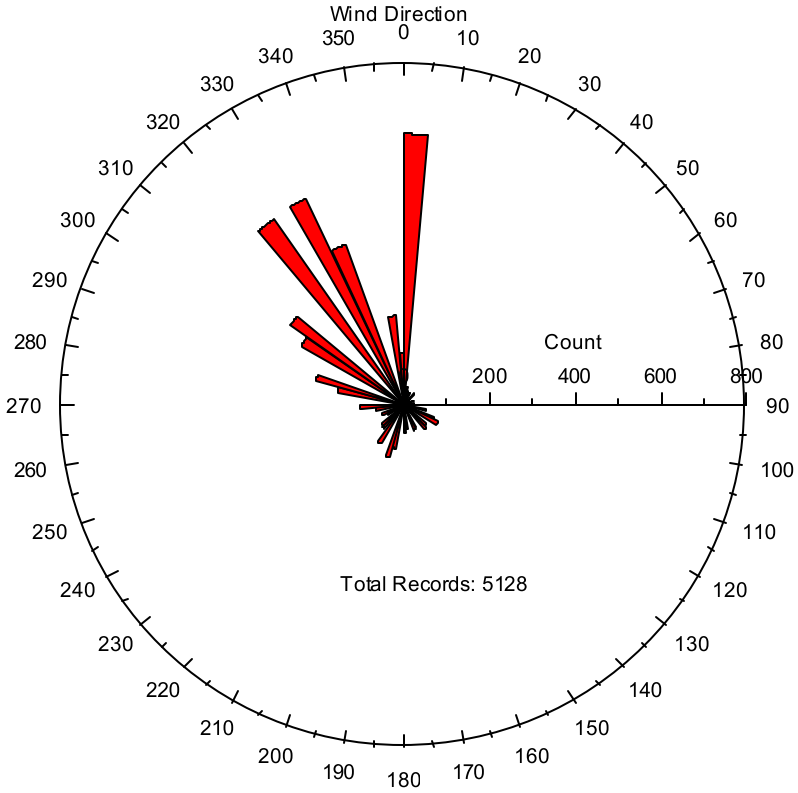


**Figure 102. Wind direction at Portland International Airport, 2001**

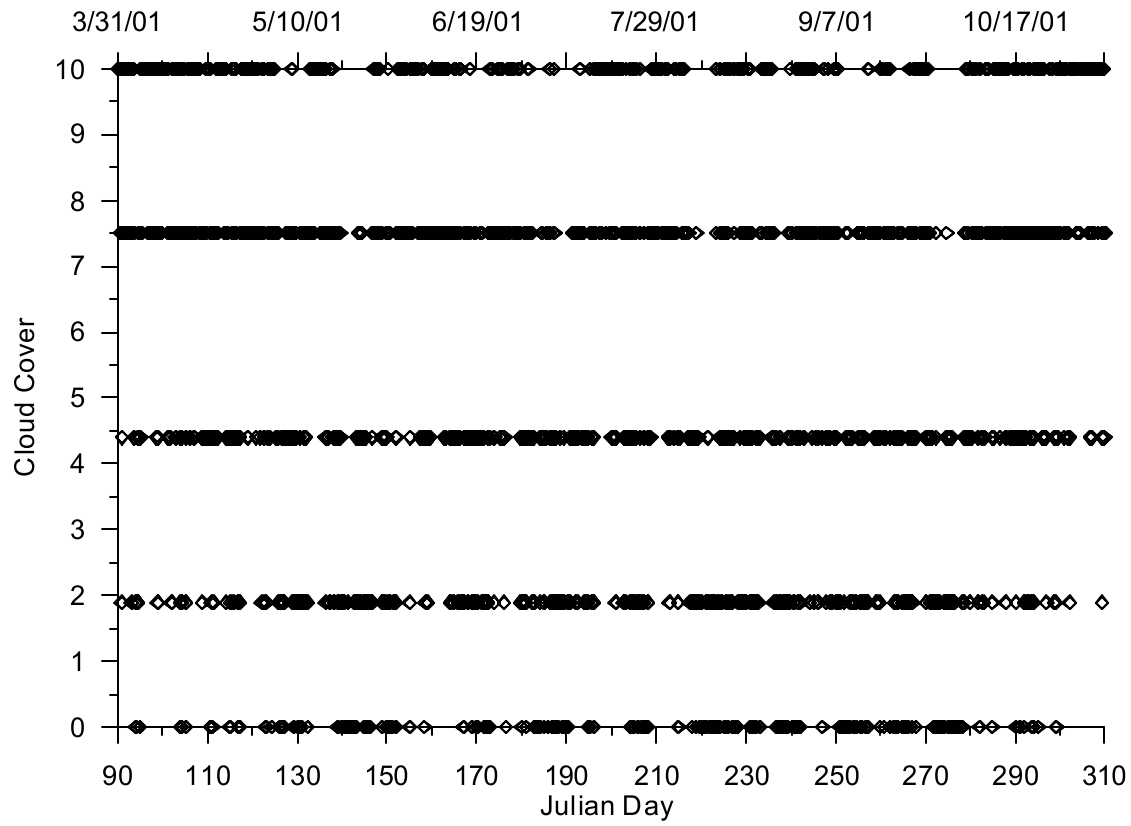


**Figure 103. Cloud cover at Portland International Airport, 2001**

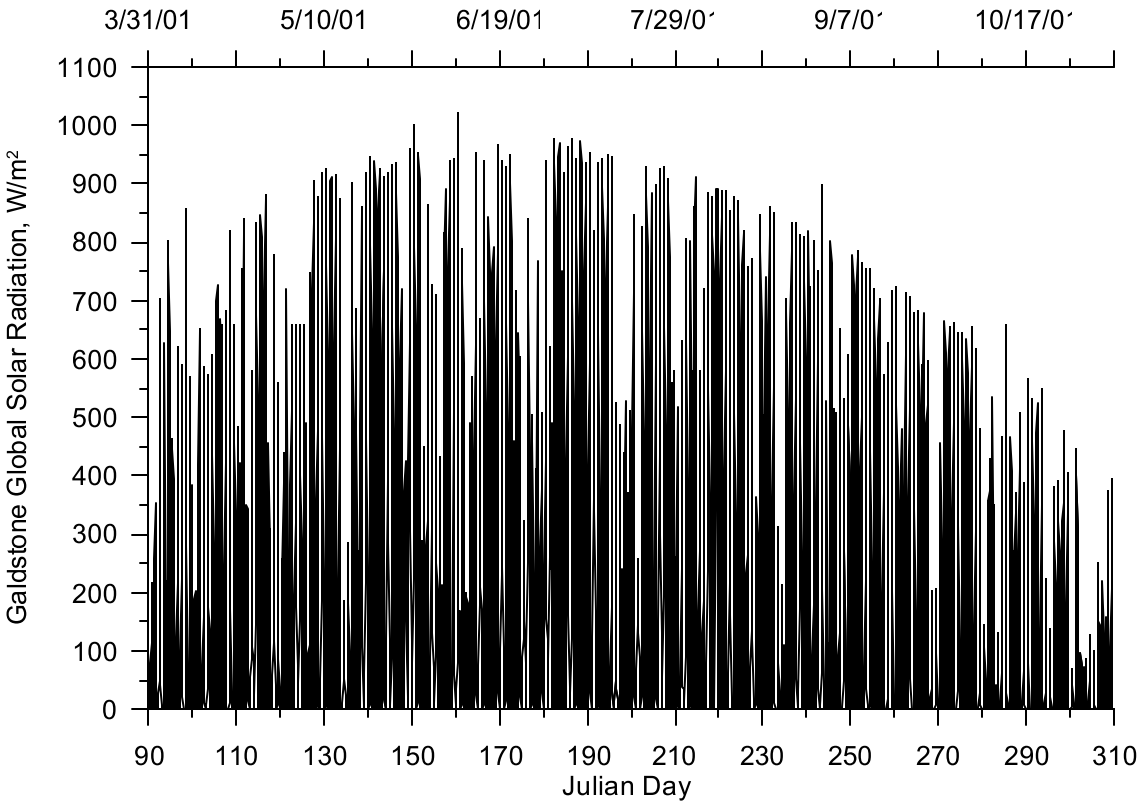


**Figure 104. Global solar radiation at Gladstone, OR, 2001**

Year 2002

Figure 105 through Figure 110 show the meteorological data measured at the Portland International Airport from April 1 to October 31, 2002. Figure 105 shows the air temperature, and Figure 106 shows the dew point temperature measured at the airport. Figure 107 shows wind speed data and illustrates that wind speeds less than 1.75 m/s fall below the instrument's minimum wind speed and are recorded as zero. Figure 108 shows a rose diagram plot of the wind direction data recorded in the summer of 2001. The figure shows the wind direction was predominantly from the northwest. Although there was a large spike in winds from the north, this was due to the wind direction being recorded as zero (north) when the wind speed fell below the minimum wind speed. Figure 109 shows the cloud cover varying on a scale of 0 to 10 with zero representing no cloud cover and ten representing full cloud cover. Figure 110 shows the solar radiation (global) measured in Gladstone, Oregon.

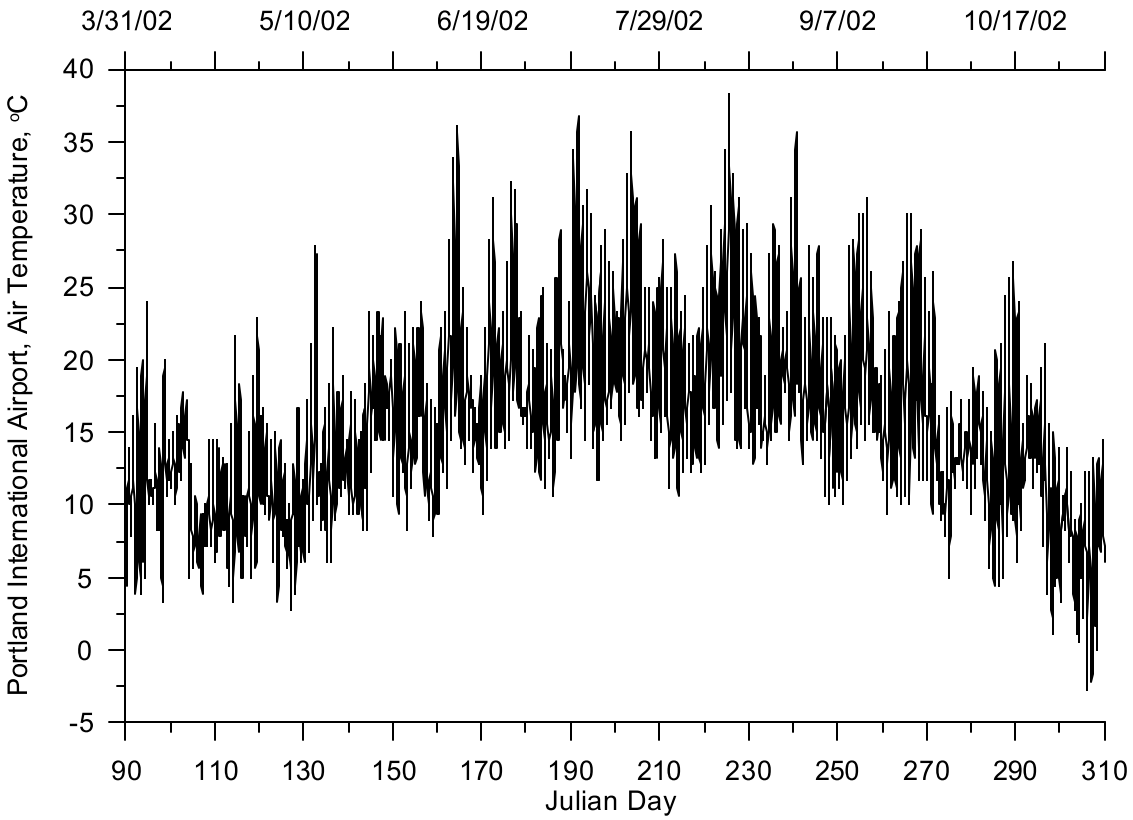


**Figure 105. Air temperature at Portland International Airport, 2002**

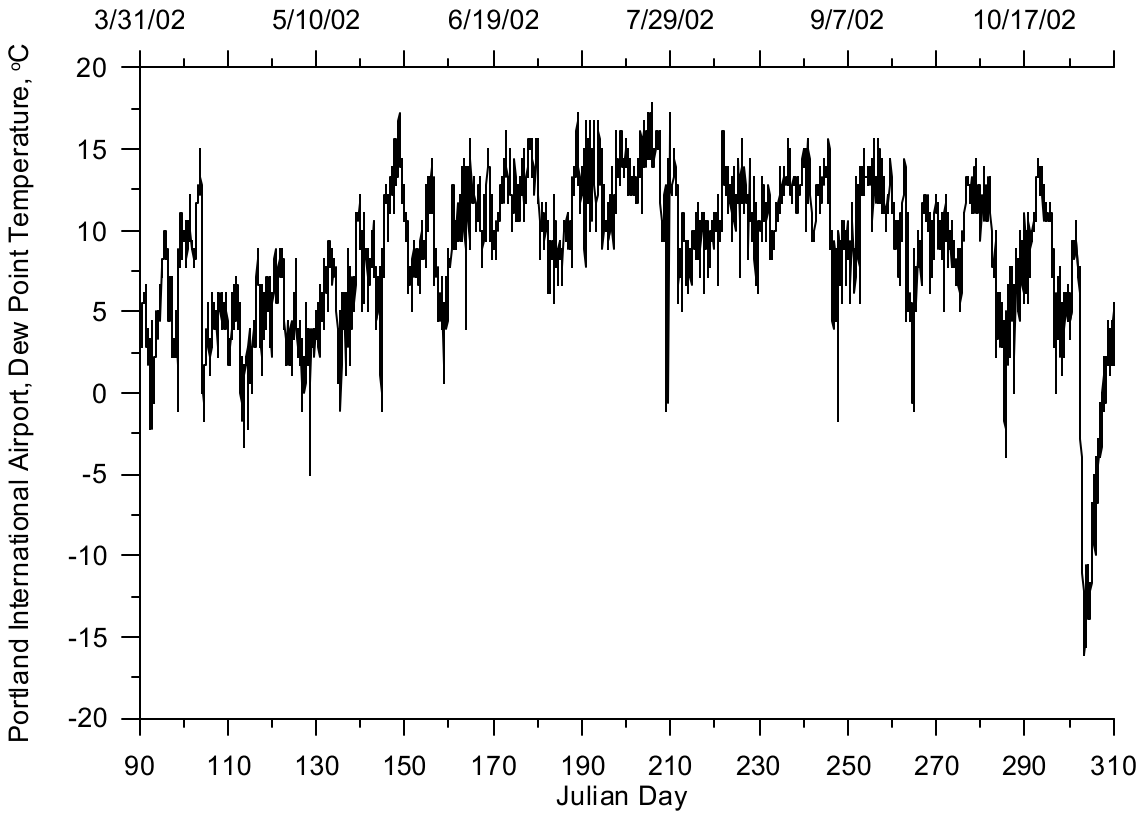


**Figure 106. Dew point temperature Portland International Airport, 2002**

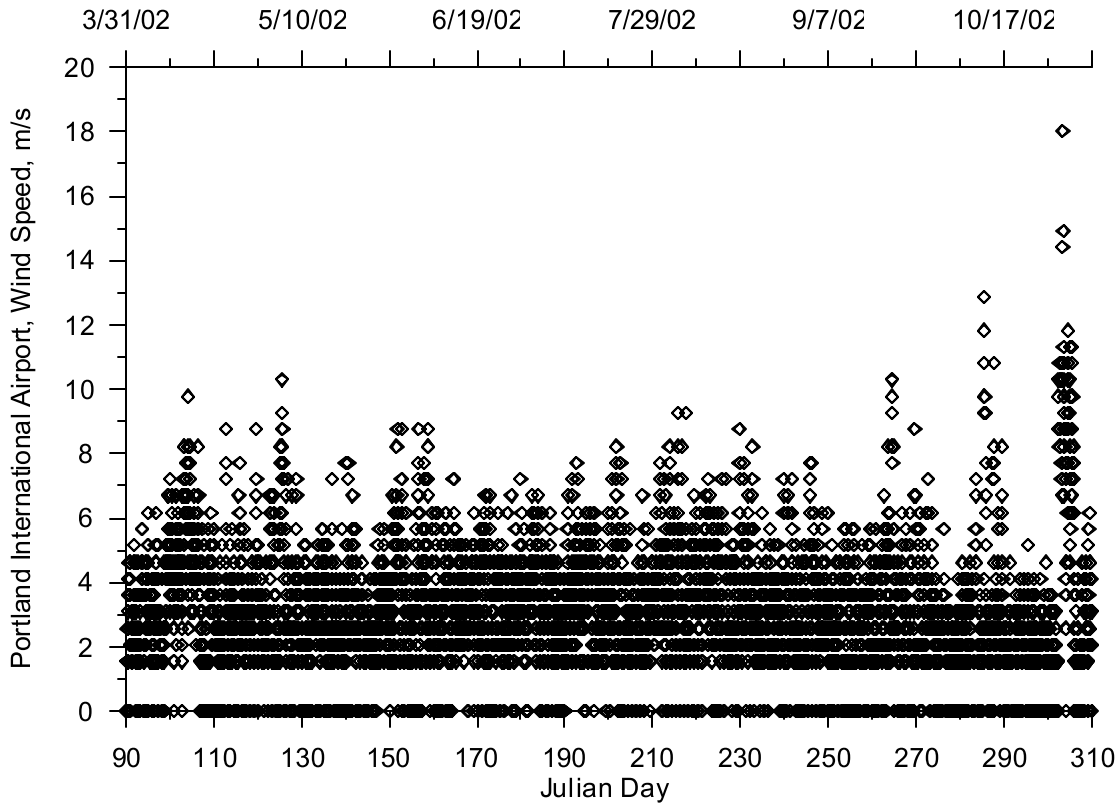


**Figure 107. Wind speed at Portland International Airport, 2002**

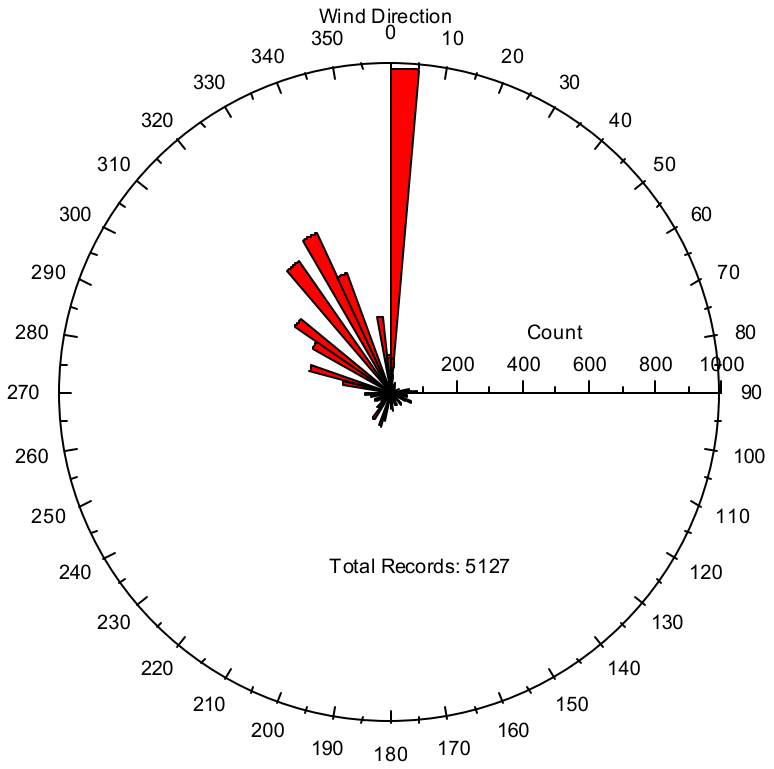


**Figure 108. Wind direction at Portland International Airport, 2002**

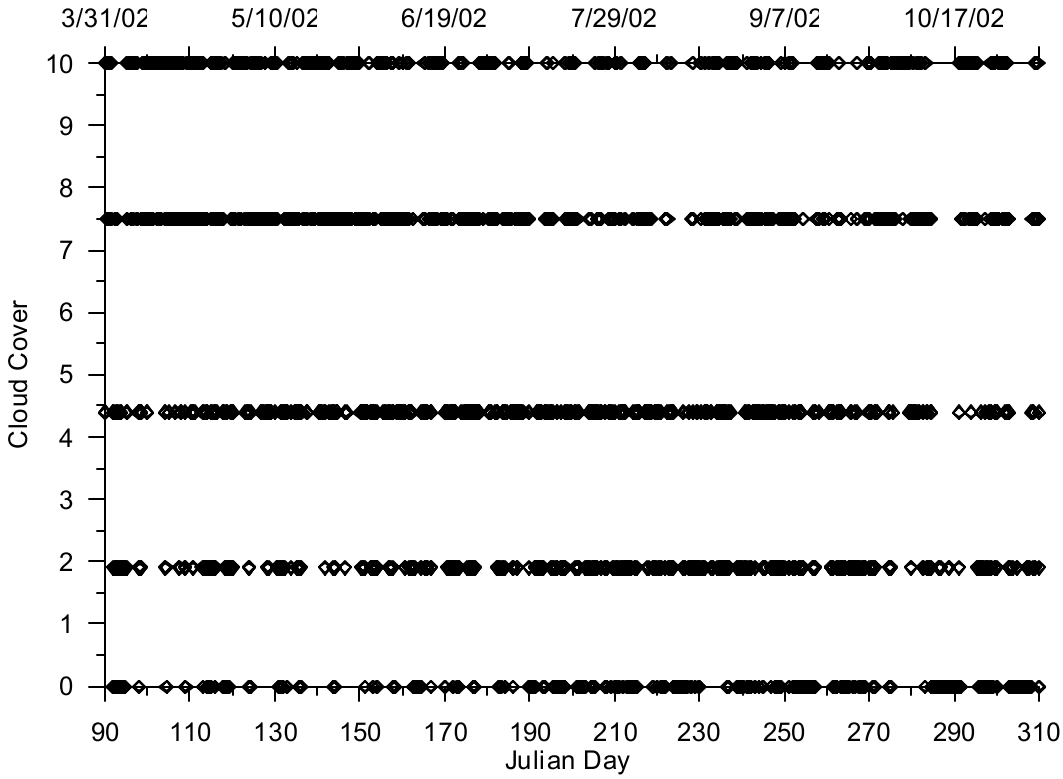


**Figure 109. Cloud cover at Portland International Airport, 2002**

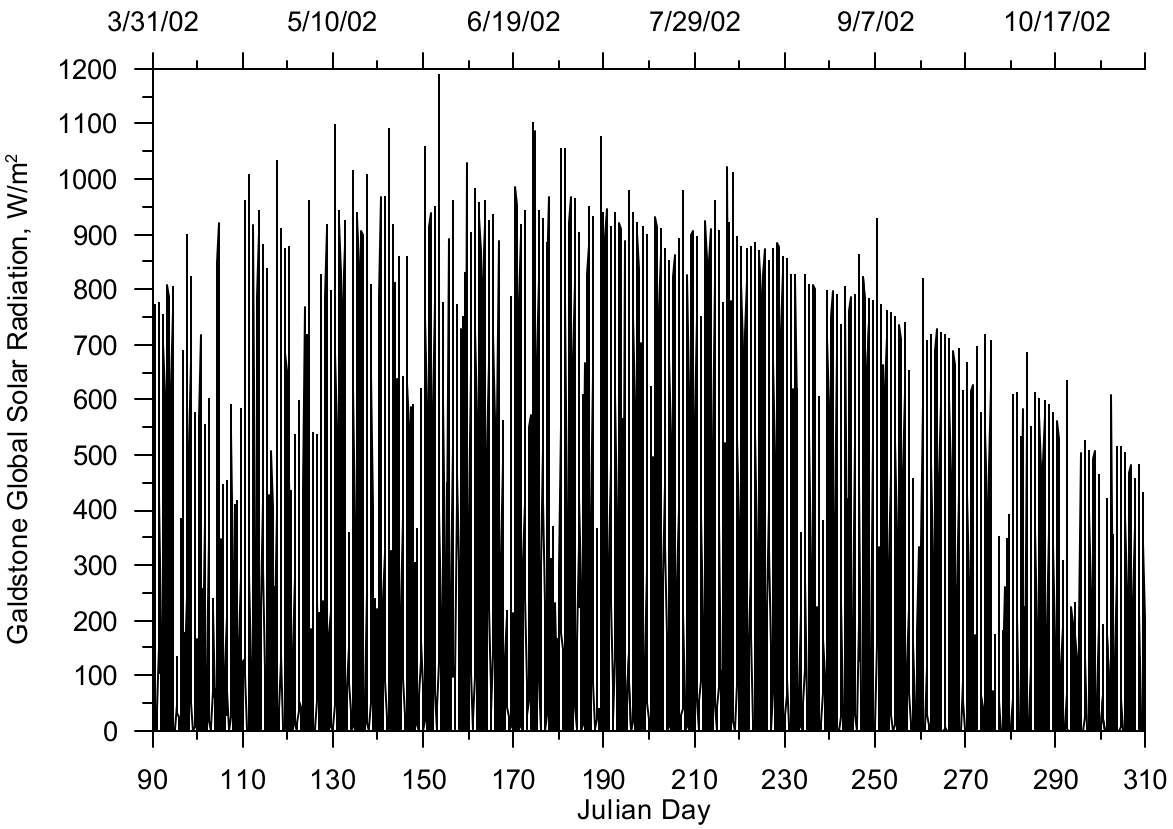


**Figure 110. Global solar radiation at Gladstone, OR, 2002**

## Middle Willamette River

The Middle Willamette River model was developed for the Willamette River from the Salem, Oregon, (RM 85.4) downstream to Willamette Falls in Oregon City (RM 26.8). Figure 111 shows the model region along with several cities and drainage areas within the model region. The model drains approximately 25,600 $km^2$ of the Willamette River Basin.

The model calibration period was from July 26 to September 30, 2001, and from April 1 to October 1, 2002. The data needed to support the model consisted of three components: the river channel bathymetry, the meteorological conditions and the boundary condition inflows and temperatures.

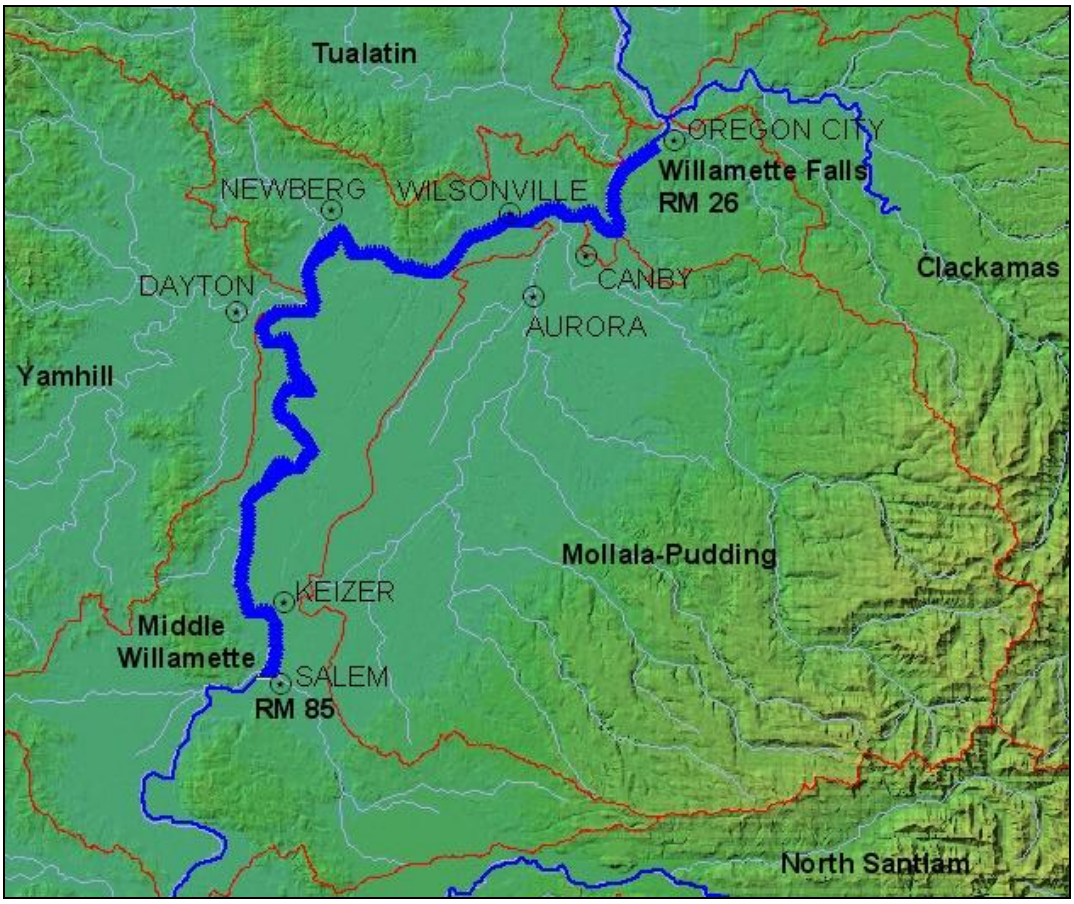


**Figure 111. Middle Willamette River model region**

## *Model Geometry*

### Bathymetry Data

Bathymetric data for the Middle Willamette River were developed from multiple sources as shown in Figure 112. Portland General Electric (PGE) collected detailed bathymetric data just upstream and downstream of the Willamette Falls (RM 26.8) as shown in Figure 113. The PGE data set extends upstream above the confluence with the Tualatin River. The National Oceanic and Atmospheric Administration (NOAA) maintain a navigation chart of the Willamette River from the Willamette Falls to Ash Island (RM 53). Figure 114 shows a sample navigation chart for the Tualatin River confluence with the Willamette River. Upstream of the NOAA navigation chart data from RM 53 to RM 85.4 (Salem), bathymetric data consisted of cross sections and thalweg data measured by the USGS (Rounds, 2002, and QUAL2E model trapezoidal cross sections provided by ODEQ (Figure 115). The stream banks and floodplain were developed from a USGS digital elevation model (DEM) data.

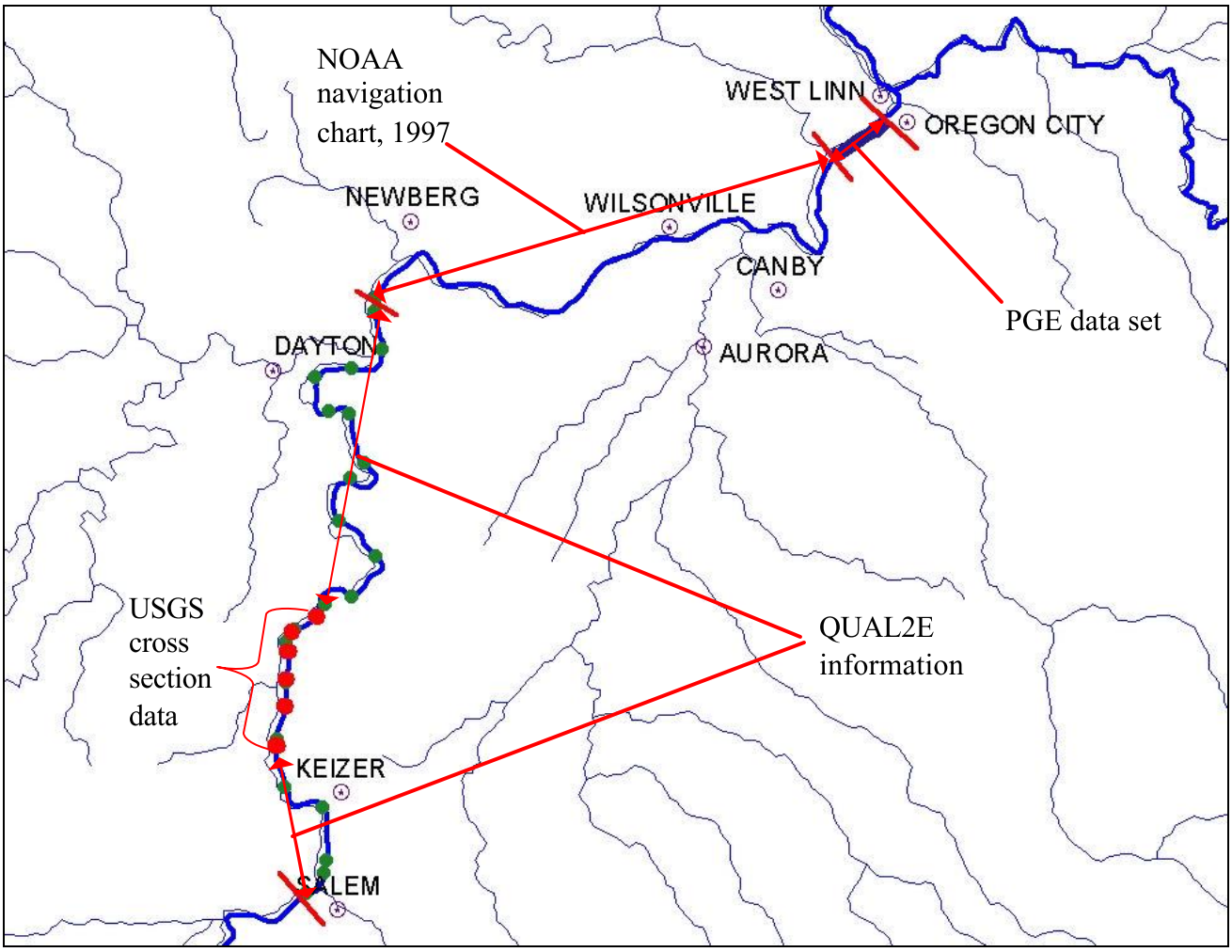


**Figure 112. Sources and extent of bathymetric data**

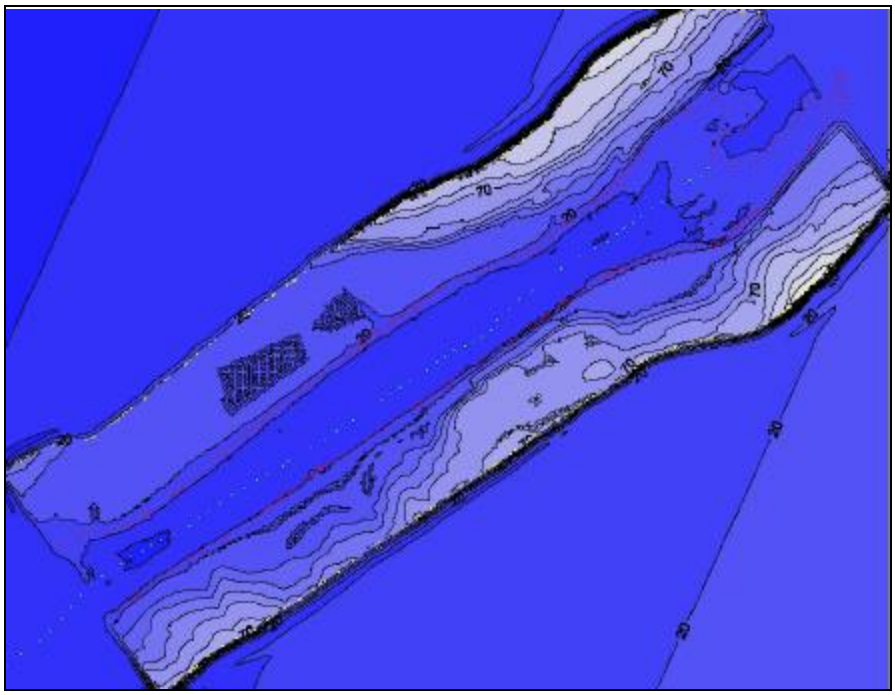

**Figure 113. Contour plot of Willamette River bathymetry just upstream of the Willamette Falls, PGE 2002**

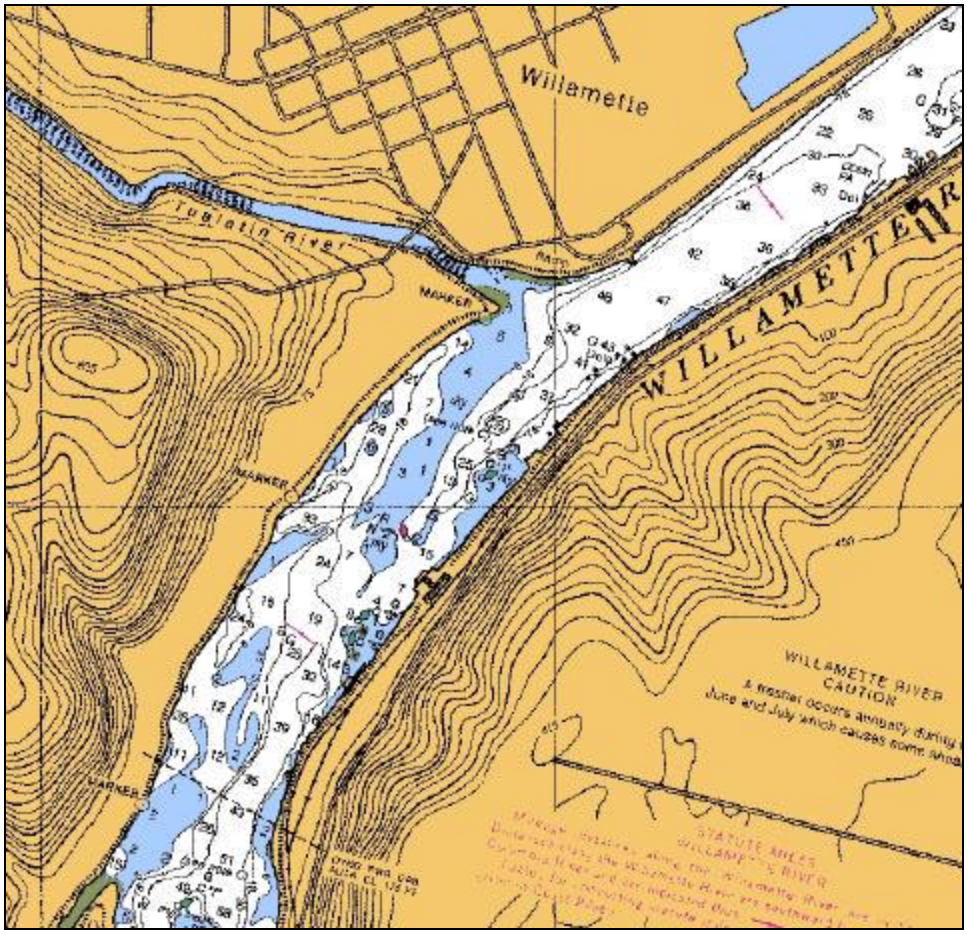


**Figure 114. NOAA navigation chart of the Willamette River from the Willamette Falls to Ash Island, RM 53**

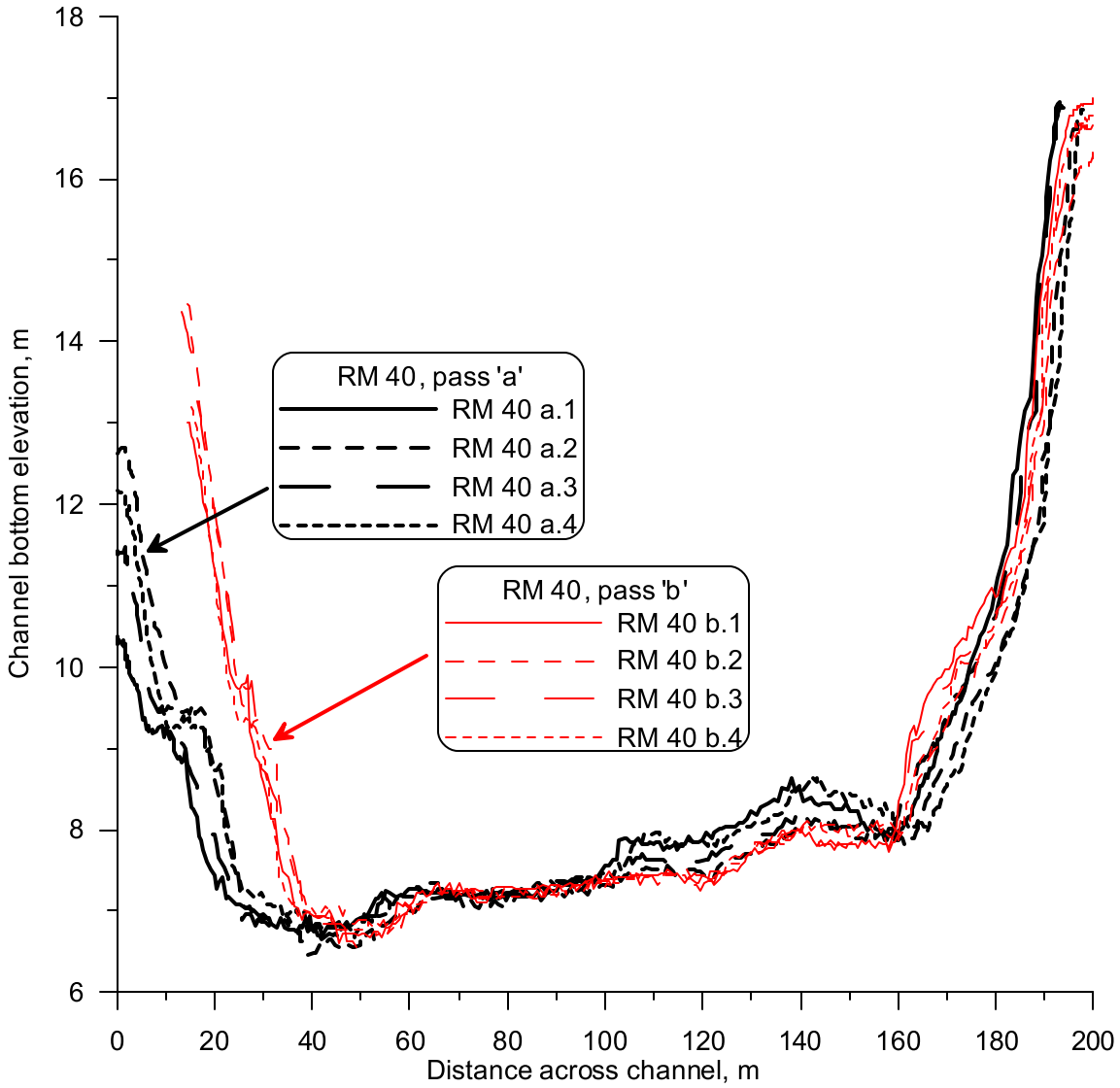


**Figure 115. Sample USGS bathymetric cross section**

## Model Grid Development

The data were combined and the plotting program SURFER was used to create a contour plot of the stream channel. The contour plot was then used to generate the model grid. The model grid consists of three water bodies and six branches. Table 11 lists the grid characteristics, and Figure 116 shows the model grid layout.

**Table 11. Middle Willamette River model grid characteristics**

| Water Body | Branch | Description | Starting Segment | Ending Segment | Starting RM | Ending RM | Segment Length, m | Slope | Upstream BC | Down-stream BC |
|---|---|---|---|---|---|---|---|---|---|---|
| 1 | 1 | Salem to Wheatland | 2 | 84 | 85.50 | 72.59 | 250.2 | 0.00052 | flow | internal |
| 2 | 2 | Wheatland to Dayton | 87 | 178 | 72.59 | 58.29 | 250.2 | 0.00006 | internal | internal |
| | 3 | Dayton to upstream end of Ash Island | 181 | 212 | 58.29 | 53.24 | 254.1 | 0.00089 | internal | internal |
| | 4 | Side channel around Wheatland Bar | 215 | 225 | 72.4 | 70.8 | 257.3 | 0.00133 | internal | internal |
| 3 | 5 | Upstream end of Ashland Island to Willamette Falls | 228 | 396 | 53.24 | 26.76 | 251.0 | 0.00000 | internal | internal |
| | 6 | Side channel around Ash Island | 399 | 406 | 52.5 | 50.9 | 268.2 | 0.00000 | internal | internal |

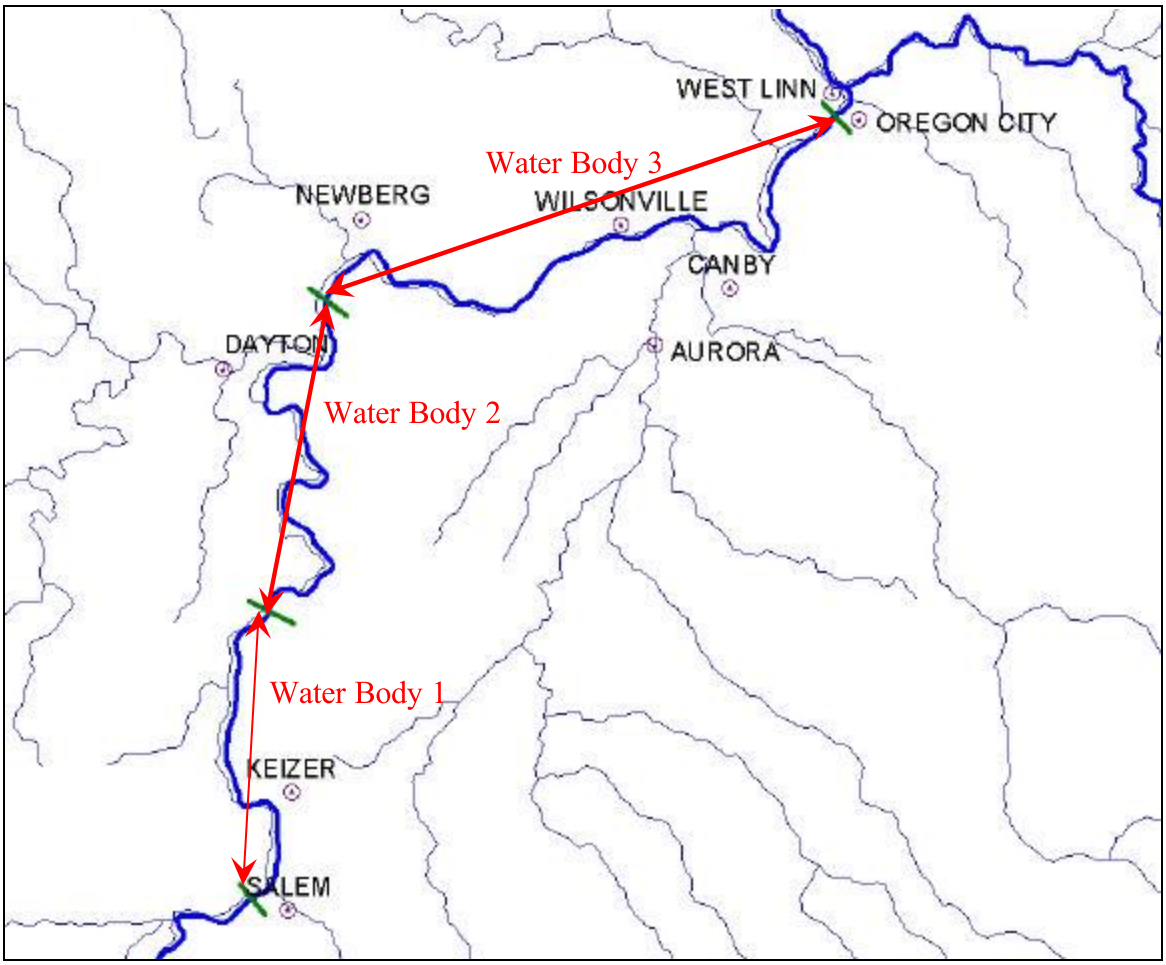


**Figure 116. CE-QUAL-W2 model grid layout showing the breaks between model water bodies**

Figure 117 shows the whole model grid but was developed in smaller sections. For each section a detailed map of the system was made and a grid constructed. In the end, the grids for each section were merged together. This report section shows the details of each piece of the bathymetric grid starting from the Willamette Falls (RM 26.8) to Salem (RM 85.4).

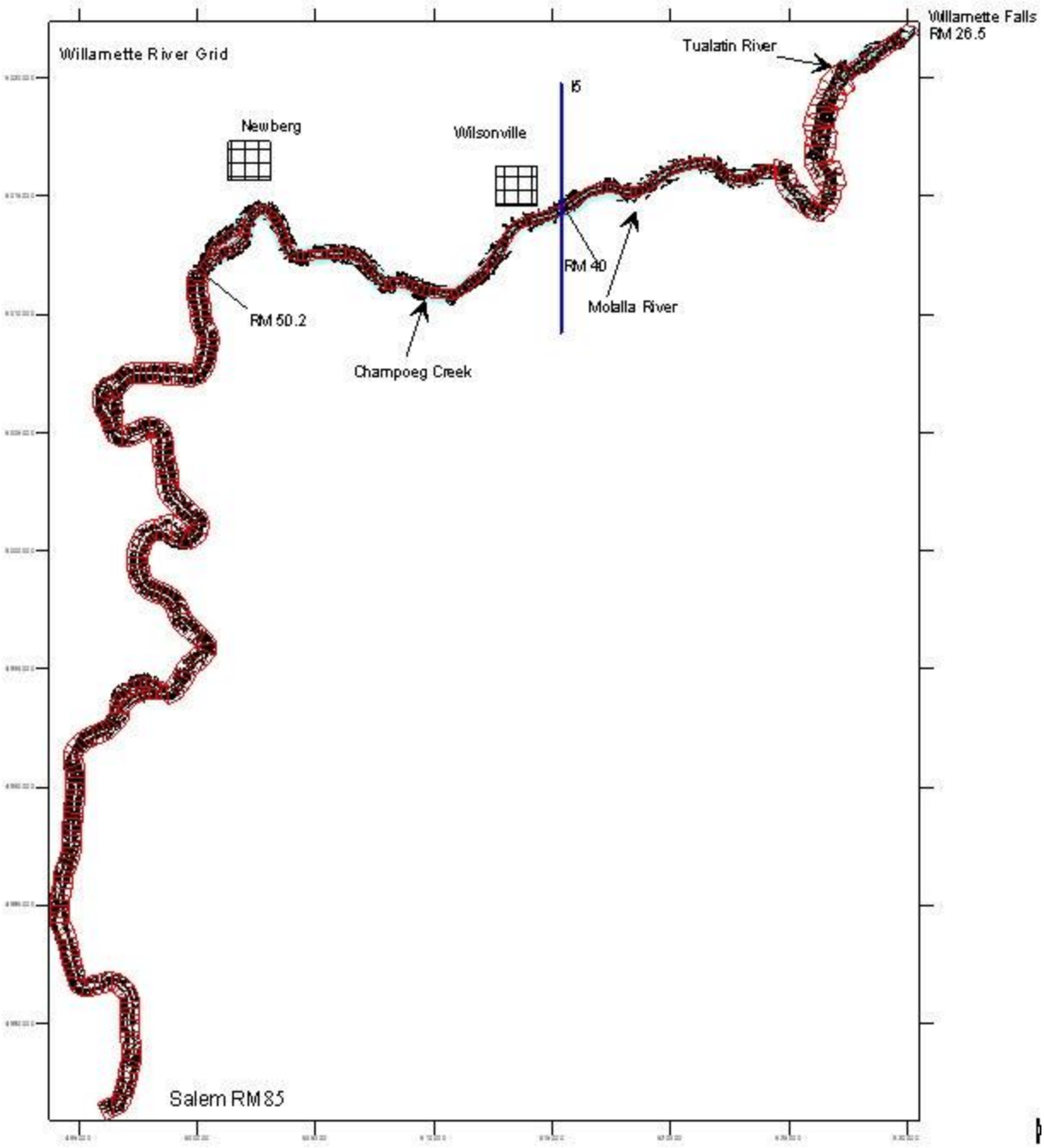


**Figure 117. Willamette River grid from the Willamette Falls to Salem.**

## Grid Section 1

The first part of the grid was developed at the Willamette Falls using detailed x, y, and z soundings from PGE in conjunction with detailed bathymetric maps from NOAA. These bathymetric contours were digitized and all the data were imported into SURFER for mapping and grid development. The first section is shown in Figure 118 with details of the grid itemized in Table 12.

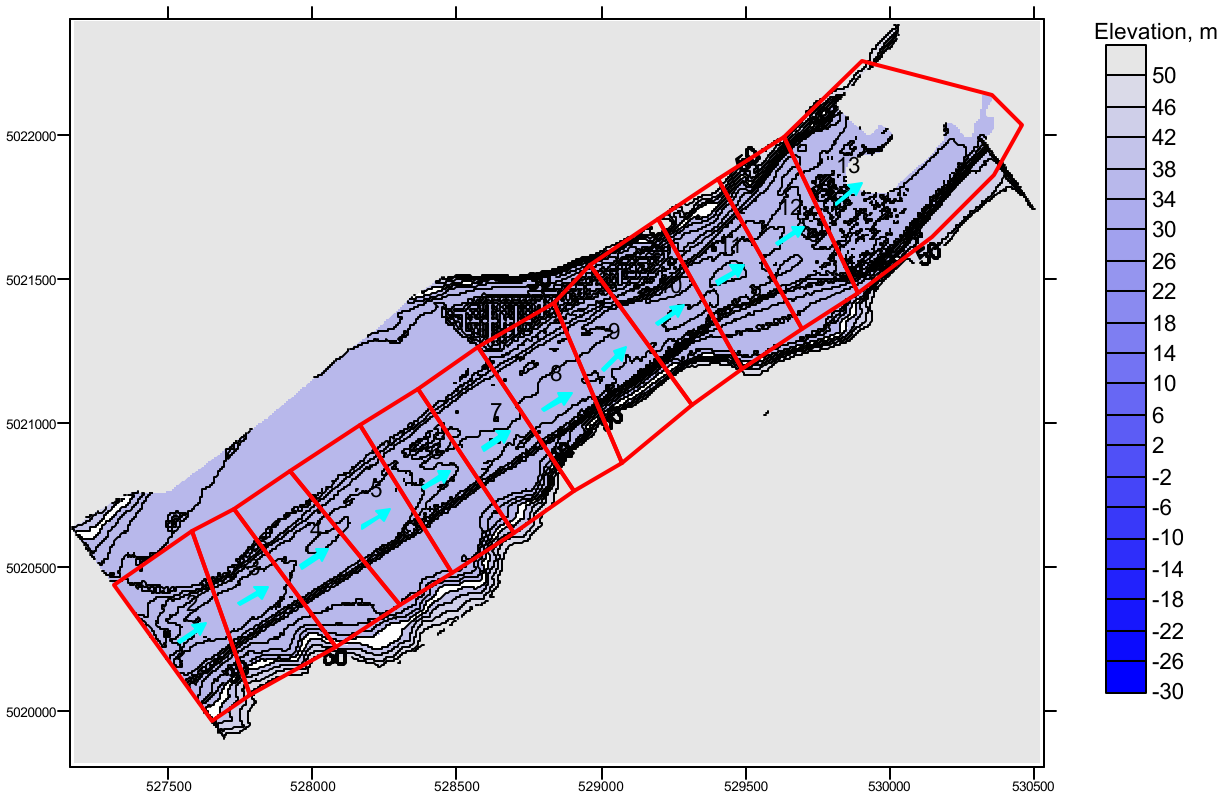


**Figure 118. Middle Willamette River grid section 1 near the Willamette Falls.**

**Table 12. Middle Willamette River grid section 1 specifications**

| Grid Parameter | Value |
|---|---|
| Number of model segments | 12 |
| Segment spacing | 250.76 m |
| IMP, model longitudinal segments | 14 |
| Reach distance | 3259.9 m |
| Reach slope | 0.0000 |
| KMP, model vertical layers | 45 |
| Vertical spacing | 1 m |
| ELBOT, elevation of bottom at downstream end | -8.0 m |

The channel bottom (the deepest point in the cross section) along the thalweg is shown in Figure 119 and was based on the SURFER elevation contour plot shown in Figure 118. The right side of the figure shows the downstream end closest to the Willamette Falls and indicates the channel becomes much more shallow just upstream of the falls.

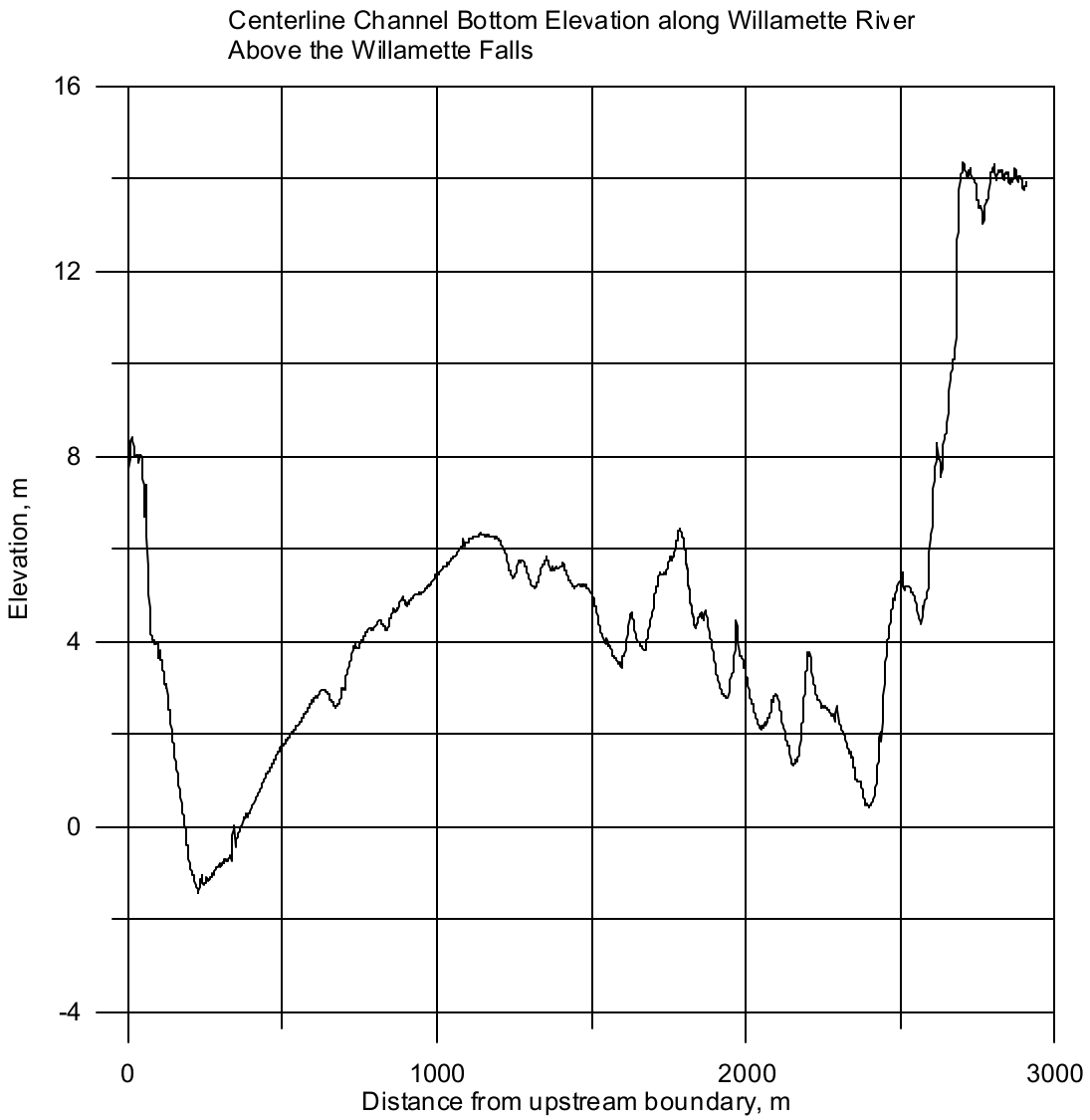


**Figure 119. Elevation along channel in section above the Willamette Falls.**

## Grid Section 2

The layout of the second grid section (NOAA nautical map: 18528A) in the Middle Willamette River is shown in Figure 120. This section as with the other grid sections used NOAA bathymetric data and new, updated bathymetric data from USGS obtained in 2001 and 2002.

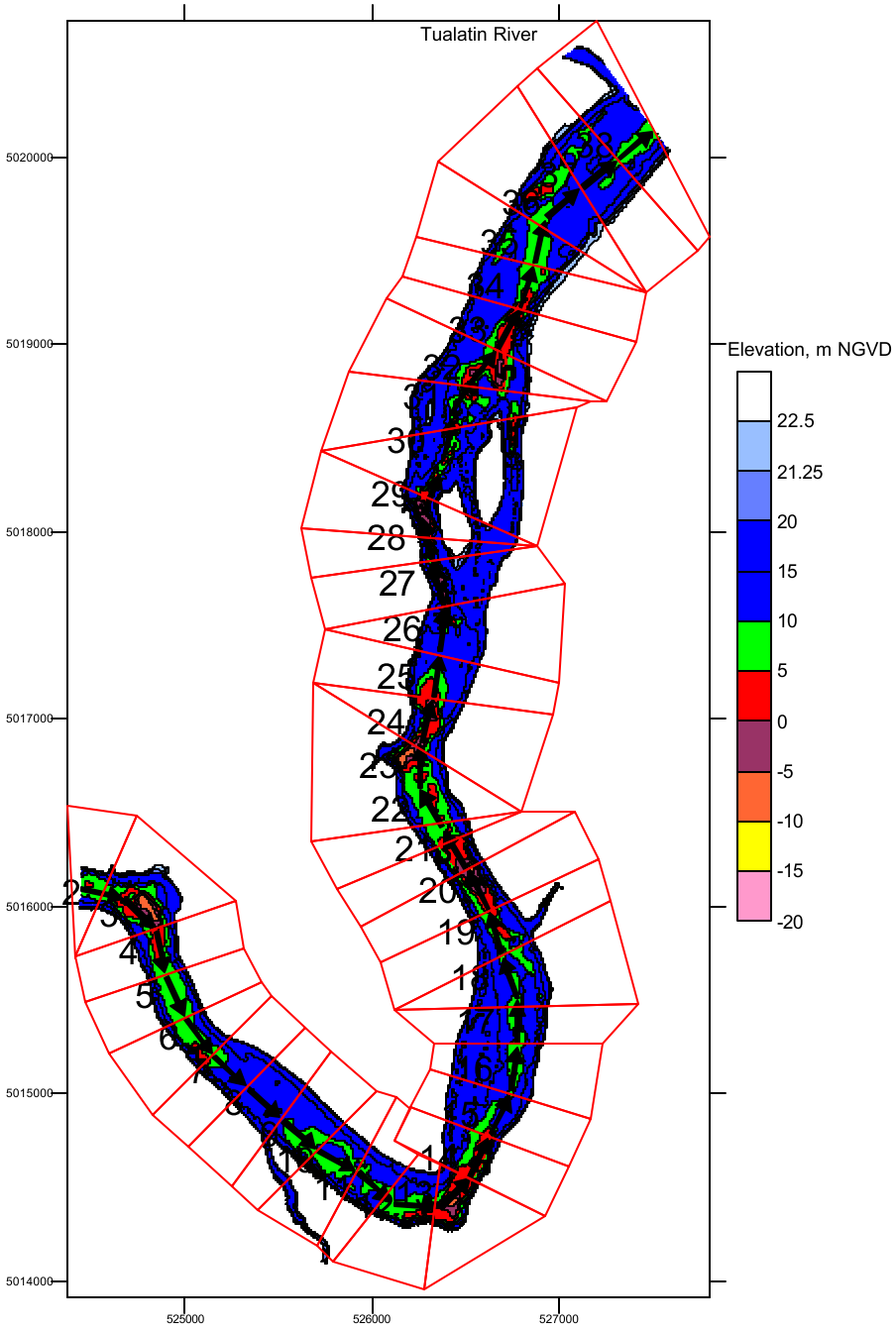


**Figure 120. Middle Willamette River grid section 2 highlighting the shallow and deeper channel areas and model segments**

Characteristics of the model grid are shown in Table 13. In all cases, comparisons were made between the W2 model grid and the SURFER area-volume-elevation curves. An example of these is shown in Figure 121 and Figure 122 for volume-elevation and surface area-elevation, respectively. The figures were used to ensure there were no mistakes in the grid construction. If errors were found, the process was debugged to determine the cause of the errors. It should be noted that the model grid was constructed to preserve volume rather than surface area (Cole and Wells, 2002).

**Table 13. Middle Willamette River grid section 2 specifications**

| Grid Parameter | Value |
|---|---|
| Number of model segments | 37 |
| Segment spacing | 253.22 m |
| IMP, model longitudinal segments | 39 |
| Reach distance | 9369.0 m |
| Reach slope | 0.0000 |
| KMP, model vertical layers | 45 |
| Layer spacing | 253.22 m |
| Vertical spacing | 1 m |
| ELBOT, elevation of bottom at downstream end | -8.0 m |

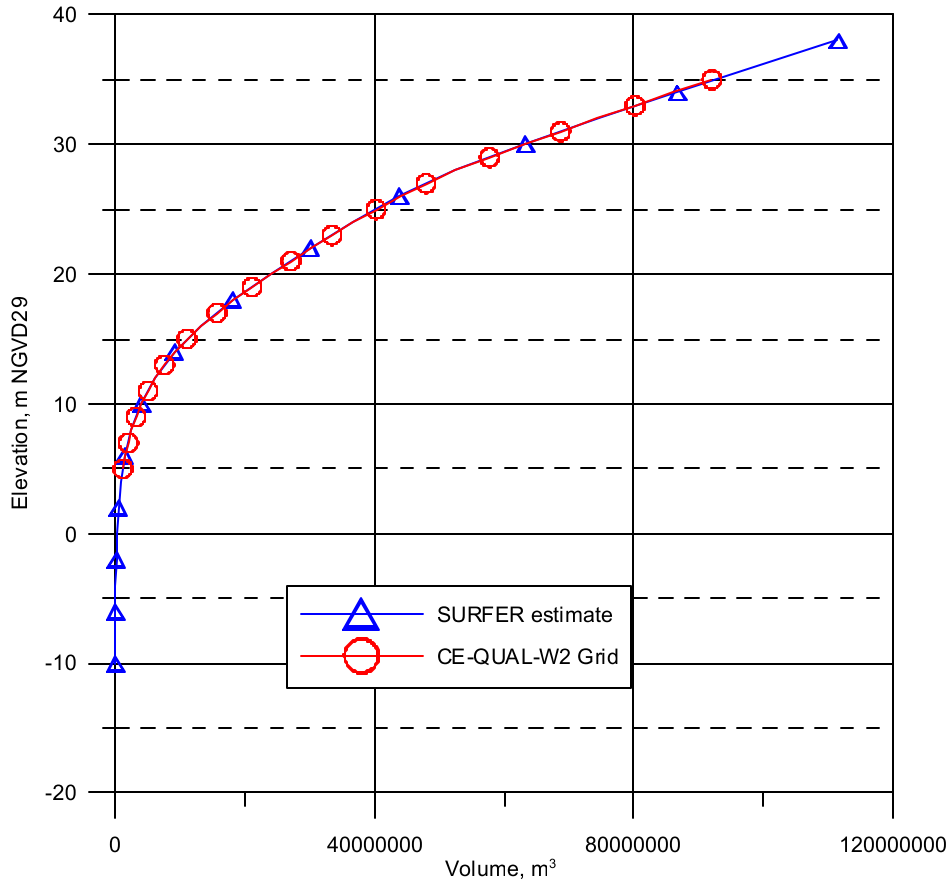


**Figure 121. Comparison of SURFER and W2 model grid for elevation vs. volume for the Middle Willamette River grid section 2**

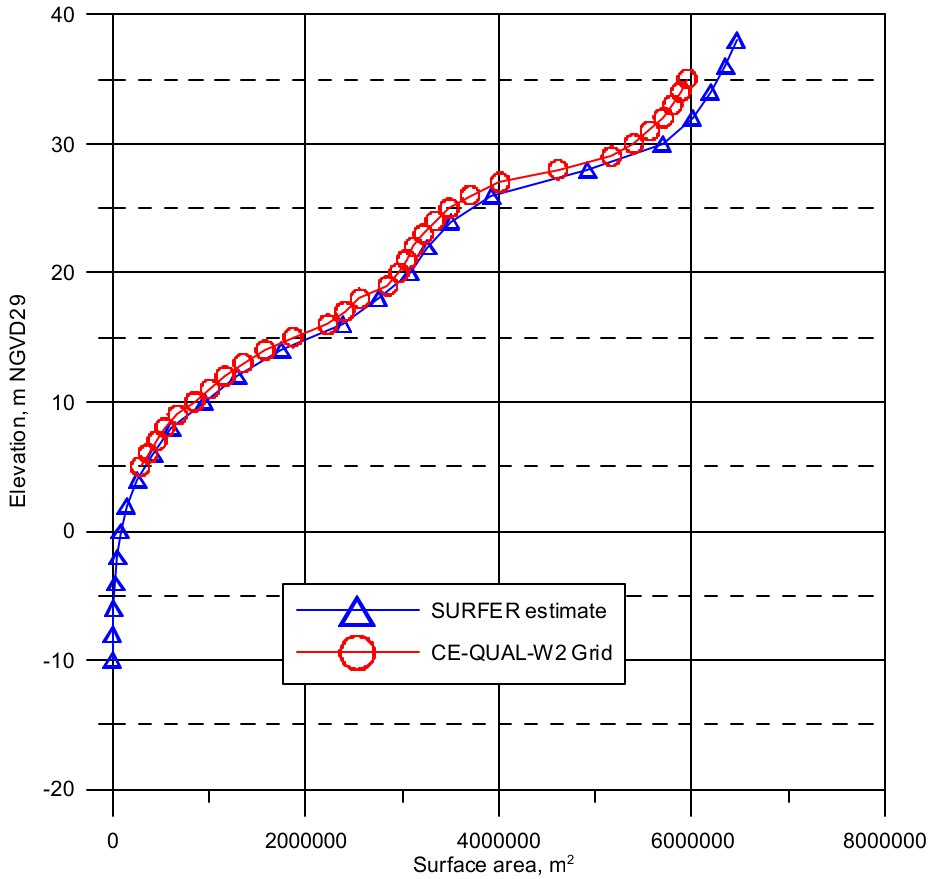


**Figure 122. Comparison of SURFER and W2 model grids for surface area – elevation for the Middle Willamette River grid section 2**

In order to illustrate how the grid was constructed, information from the CE-QUAL-W2 GUI interface was used. The GUI software produced a plan view of the grid using the surface widths (Figure 123), a representative width vs. layer schematic for two model segments (Figure 124 for Segment 3 in Grid Section 2 and Figure 125 for Segment 30 in Grid Section 2), and a side view of the grid for Section 2 (Figure 126). The elevation of the deepest part of the channel along the thalweg is shown in Figure 127.

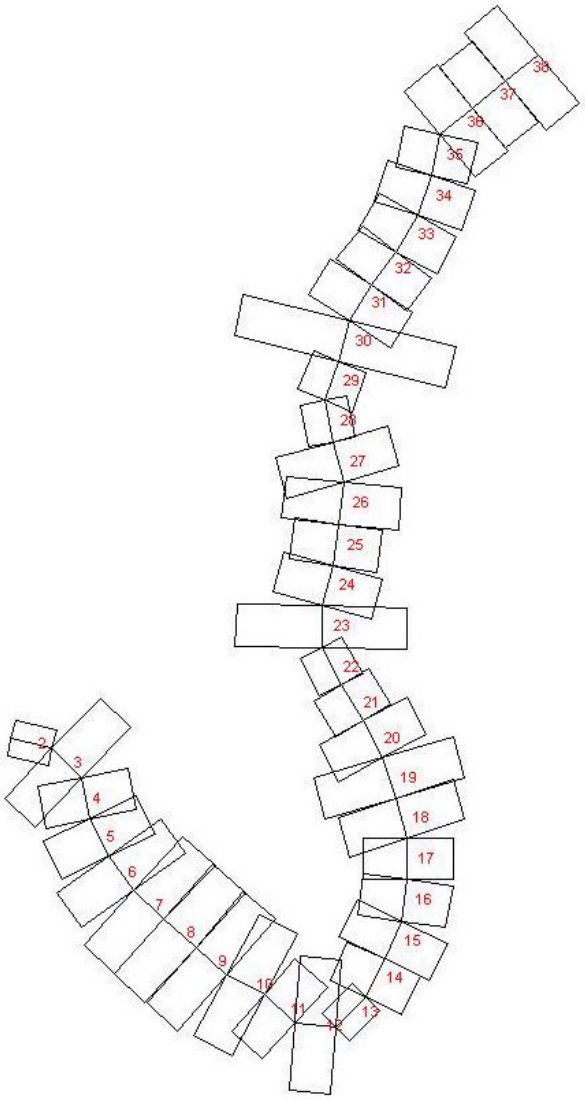


**Figure 123. Middle Willamette River grid section 2 plan view of model grid showing surface widths**

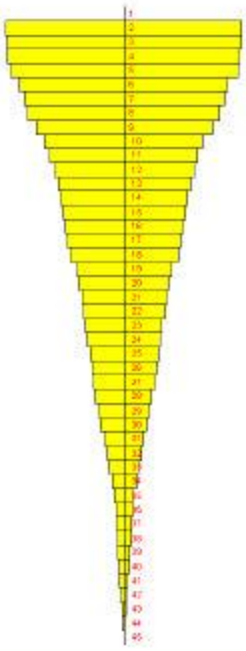

**Figure 124. Middle Willamette River grid section 2 Segment 3 layer widths**

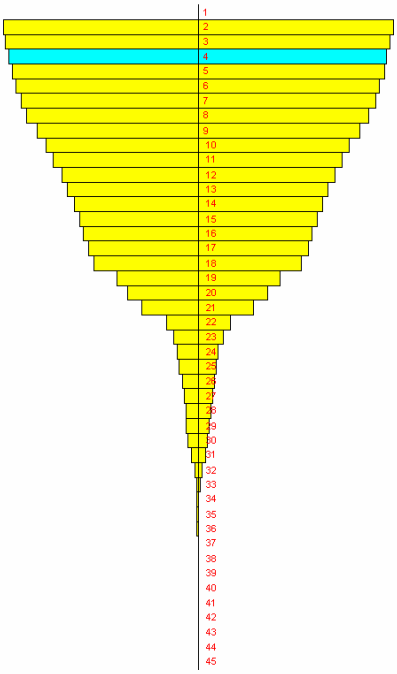


**Figure 125. Middle Willamette River grid section 2 Segment 30 layer widths**

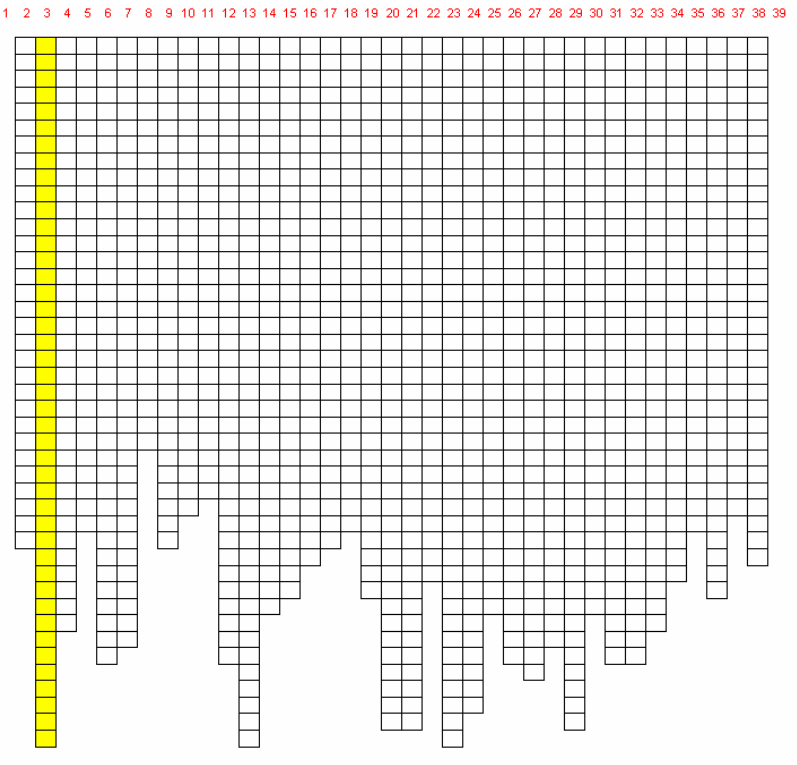


**Figure 126. W2 Grid - side view of segments for the Middle Willamette River grid section 2**

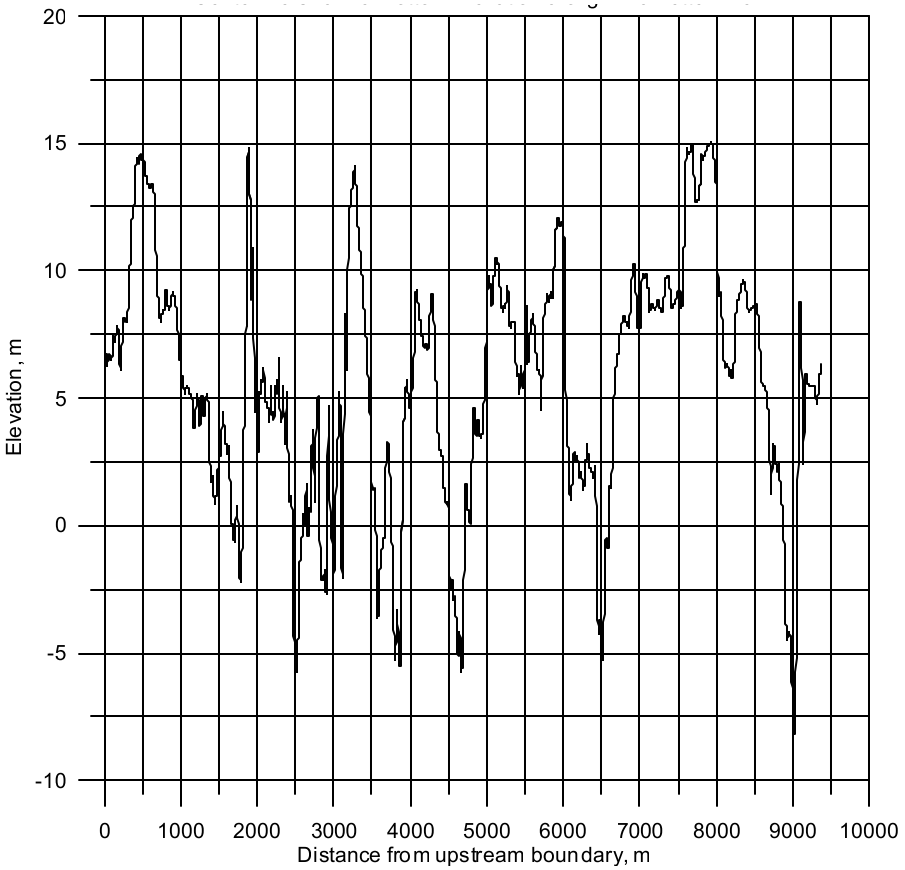


**Figure 127. Channel bottom elevation of thalweg in the Middle Willamette River grid section 2.**

## Grid Section 3

The layout of the third grid section (NOAA nautical map: 18528B) in the Middle Willamette River is shown in Figure 128. This section along with other grid sections used NOAA bathymetric data and new, updated bathymetric data obtained from the USGS in 2001 and 2002. Characteristics of the grid are shown in Table 14.

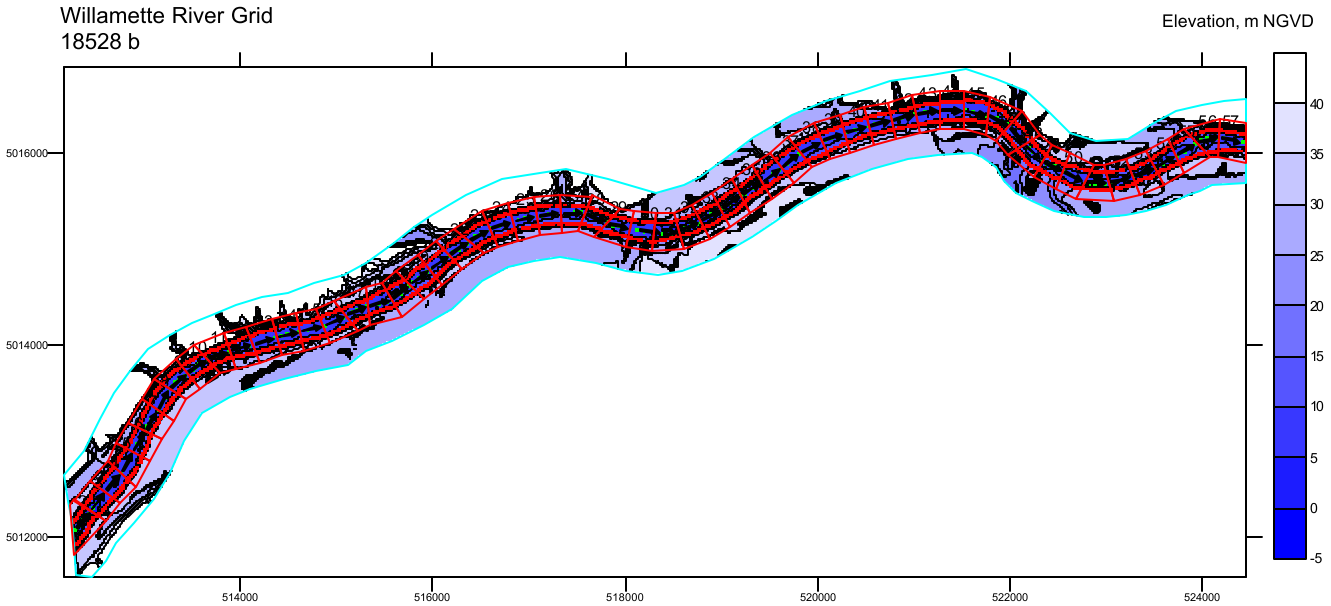


**Figure 128. Model grid for the Middle Willamette River grid section 3.**

**Table 14. Middle Willamette River grid section 3 specifications.**

| Grid Parameter | Value |
|---|---|
| Number of model segments | 56 |
| Segment spacing | 253.65 m |
| IMP, model longitudinal segments | 58 |
| Reach distance | 14204.24 m |
| Reach slope | 0.0000 |
| KMP, model vertical layers | 45 |
| Vertical spacing | 1 m |
| ELBOT, elevation of bottom at downstream end | -8.0 m |

Figure 129 and Figure 130 show layer widths for segment 57 and segment 2 for grid section 3. Figure 131 shows the side view and Figure 132 shows the plan view for the section 3 grid. Figure 133 shows the channel bottom elevation along this grid section.

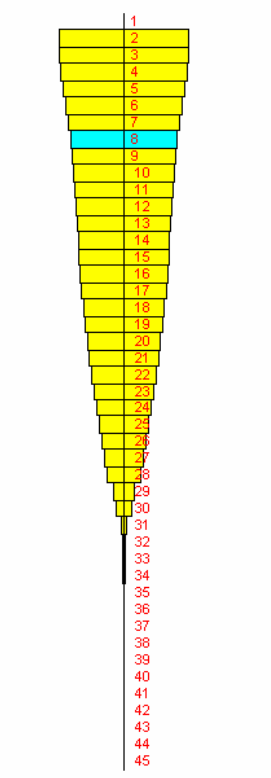


**Figure 129. Segment 57 in Middle Willamette River grid section 3 (18528b).**

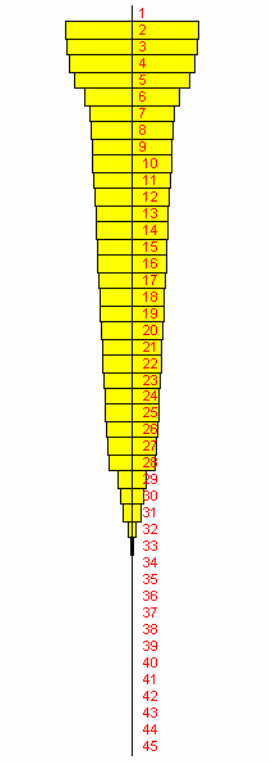


**Figure 130. Segment 2 in Middle Willamette River grid section 3 (18528b).**

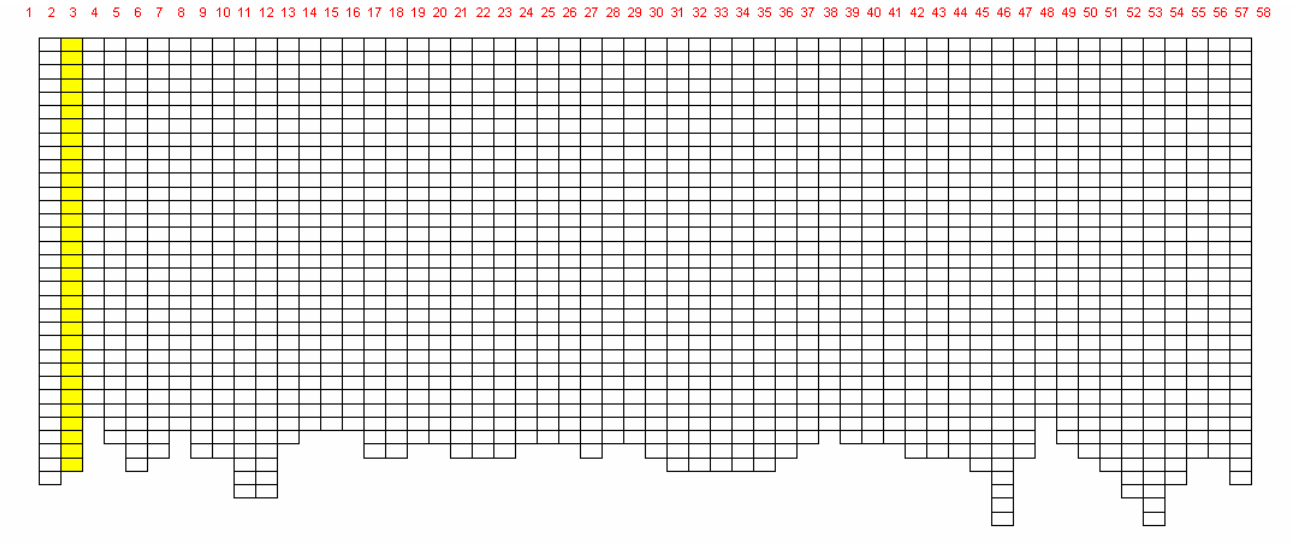


**Figure 131. Side view of Middle Willamette River grid section 3 (18528b).**

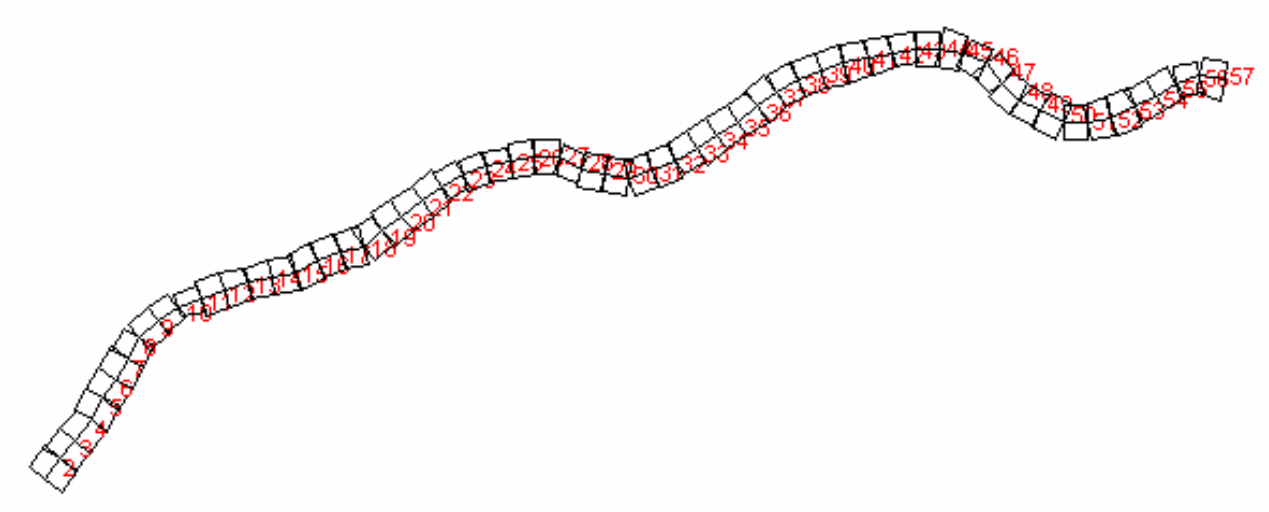

**Figure 132. Plan view of Middle Willamette River grid section 3 (18528b).**

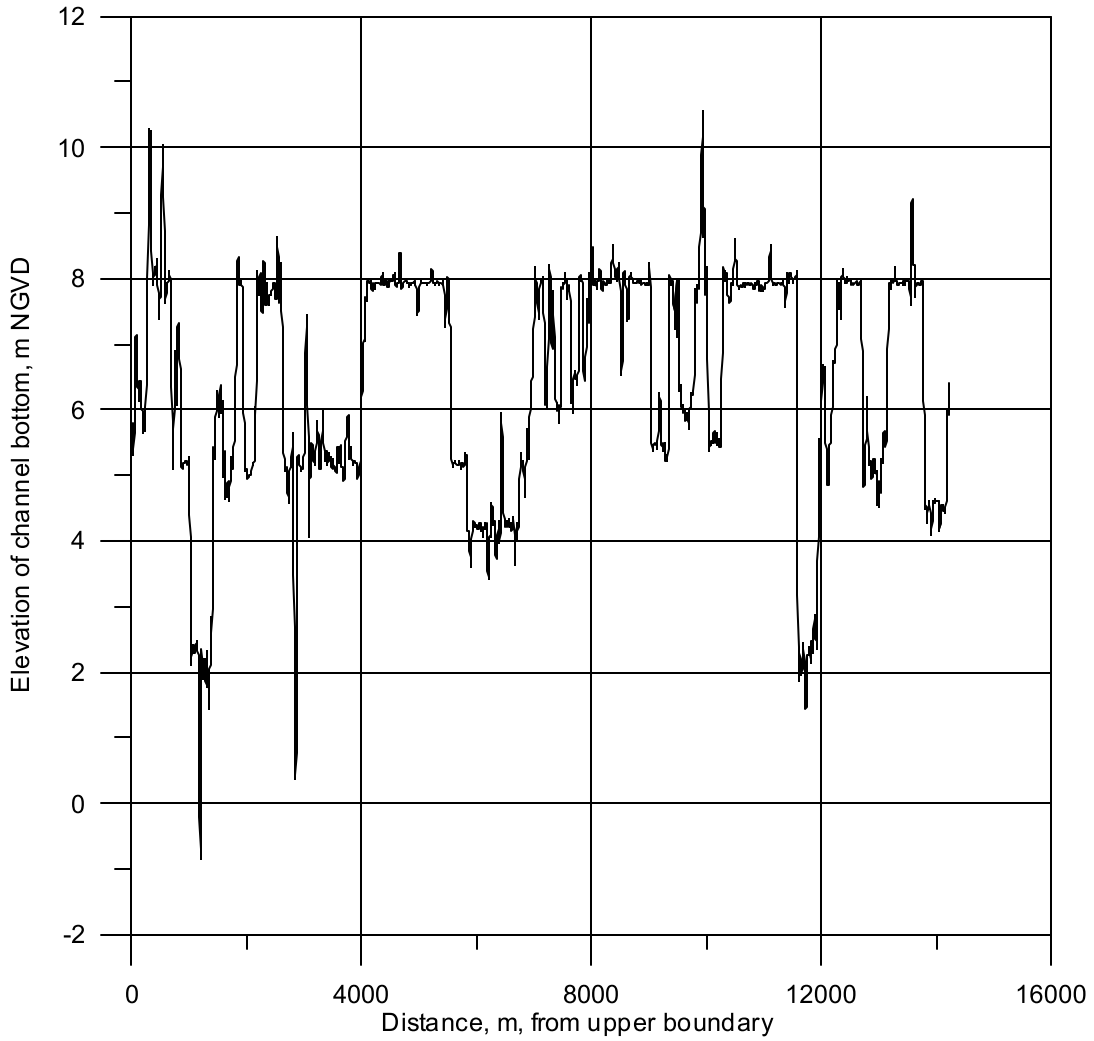


**Figure 133. Bottom channel elevation along thalweg for the Middle Willamette River grid section 3**

## Grid Section 4

The layout of the fourth grid section (NOAA nautical map: 18528c) in the Middle Willamette River is shown in Figure 134. This section, as with the other grid sections, used NOAA bathymetric data and new, updated bathymetric data from the USGS obtained in 2001 and 2002. Grid characteristics are shown in Table 15.

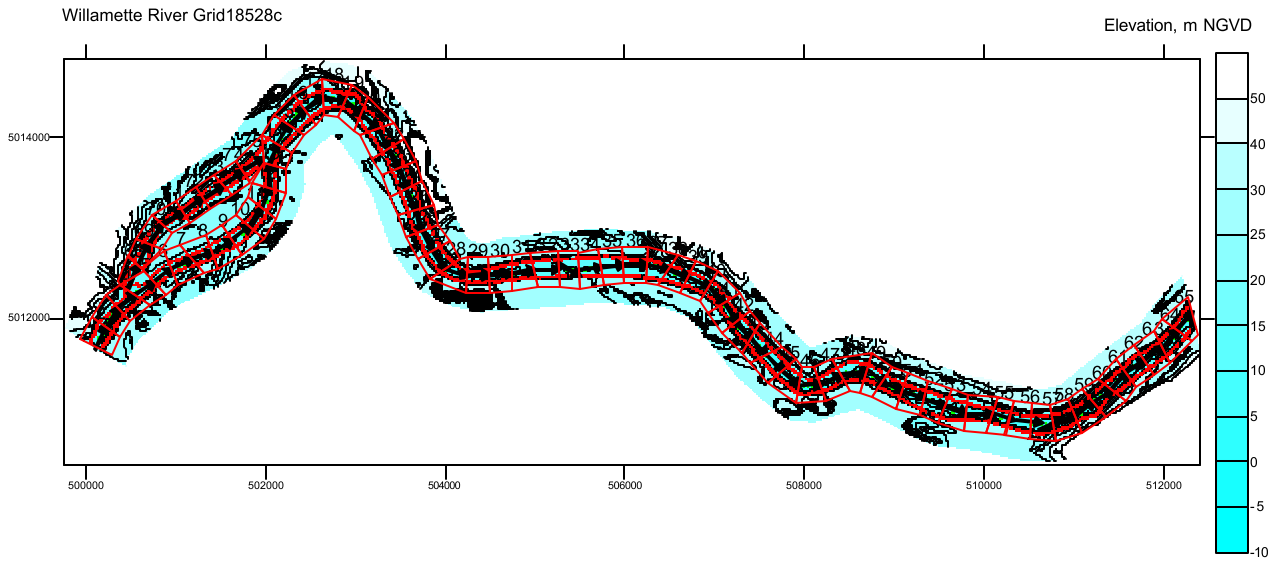


**Figure 134. Middle Willamette River grid section 4 (18528c).**

**Table 15. Middle Willamette River grid section 4 (18528c) specifications**

| Grid Parameter | Value |
|---|---|
| Number of model segments | 76 |
| Segment spacing BR1 | 250.48 m |
| Segment spacing BR2 | 268.20 m |
| IMP, model longitudinal segments | 76 |
| Reach distance BR1 | 16030.6 m |
| Reach distance BR2 | 2145.6 m |
| Reach slope BR1 and BR2 | 0.0000 |
| KMP, model vertical layers | 45 |
| Vertical spacing | 1 m |
| ELBOT, elevation of bottom at downstream end | -8.0 m |
| Branches | 2 |
| Branch 1 | Segments 2 to 65 |
| Branch 2 | Segments 68 to 75 |

Figure 135 shows the layer widths for segment 3 in section 4. Figure 135 shows the side view of the grid in section 4, and Figure 137 shows the plan view. Figure 138 shows the bottom channel elevation for this grid.

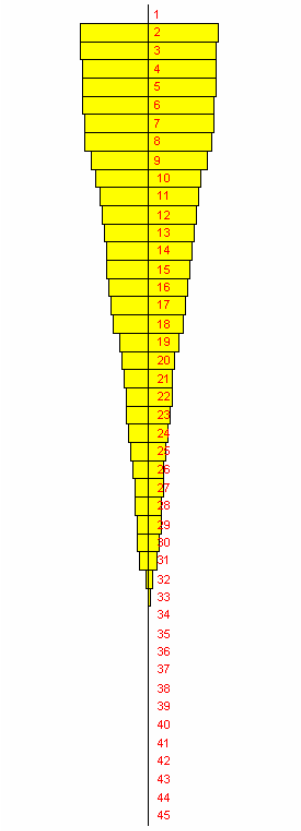

**Figure 135. Segment 3 in the Middle Willamette River grid section 4 18528c.**

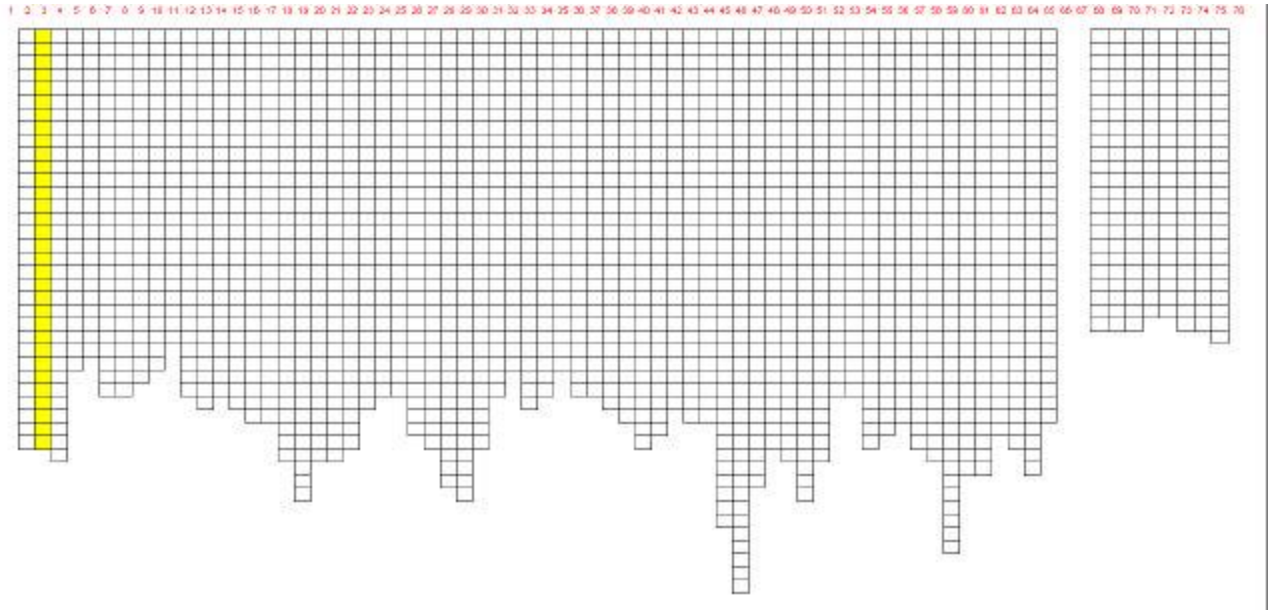

**Figure 136. Side view of the Middle Willamette River grid section 4 18528c.**

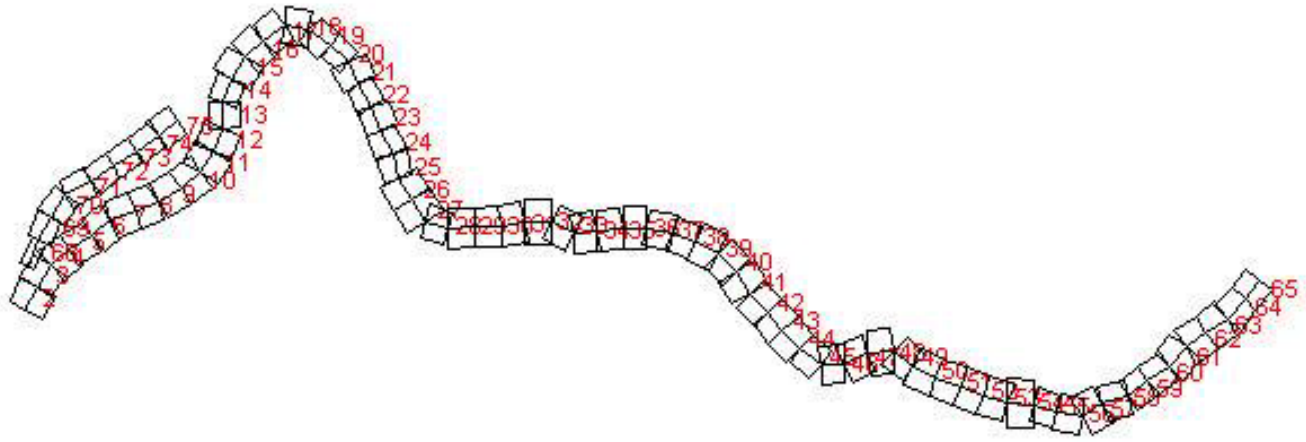

**Figure 137. Plan view of the Middle Willamette River grid section 4 18528c.**

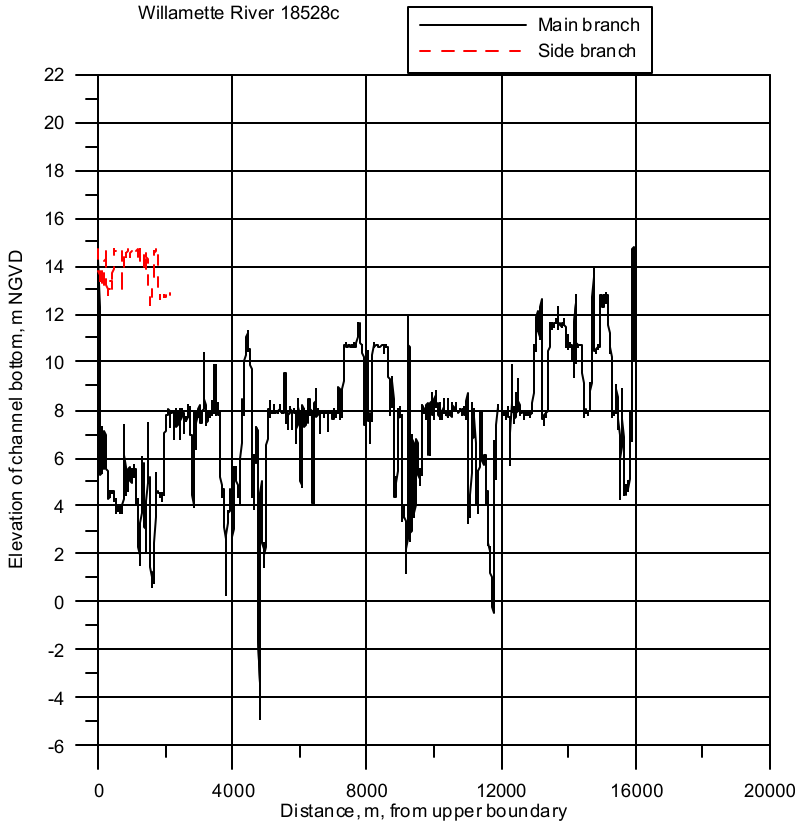


**Figure 138. Bottom channel elevation along channel thalweg for the Middle Willamette River grid section 4**

## Grid section 5 (RM 50.2 to 72)

The layout of the fifth grid section in the Middle Willamette River is shown in Figure 139. This section did not use NOAA bathymetric data since it does not extend this far upstream. Updated cross section data from USGS were used with the Digital Elevation Model data to obtain the channel shape and elevation at the banks. Details of the grid are shown in Table 16. This was the first of the several grid sections that with a channel slope. The channel bottom elevations, shown in Figure 140, illustrate the various slopes for the 3 branches in this section (as can be seen from this graph, the location of actua1 data was extremely sparse).

**Table 16. Middle Willamette River grid section 5 specifications**

| Grid Parameter | Branch 1 | Branch 2 | Branch 3 |
|---|---|---|---|
| Number of model segments | 92 | 32 | 11 |
| Segment spacing | 250.2 m | 254.1 m | 257. 3 m |
| Slope | 0.00089 | 0.00006 | 0.00133 |
| Reach distance | 23018.6 m | 8131.1 m | 2830.7 m |
| Vertical spacing | 1 m | 1 m | 1 m |
| Branch segments | 2 to 93 | 96 to 127 | 130 to 140 |

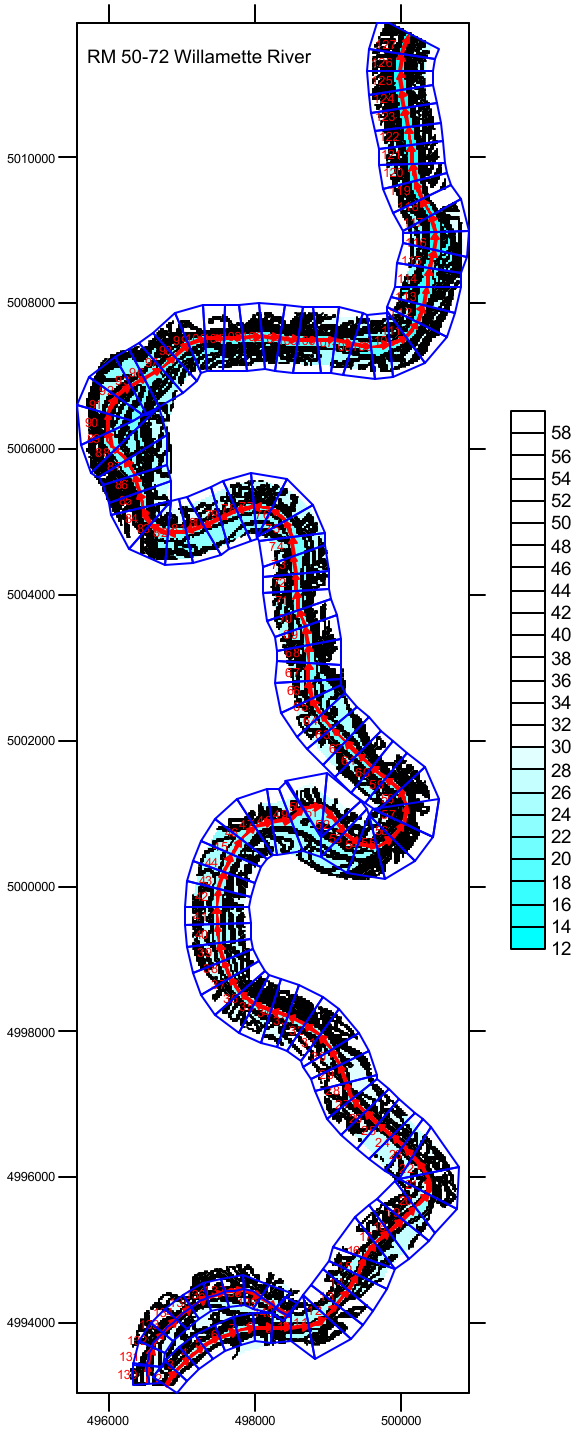


**Figure 139. Middle Willamette River grid section 5**

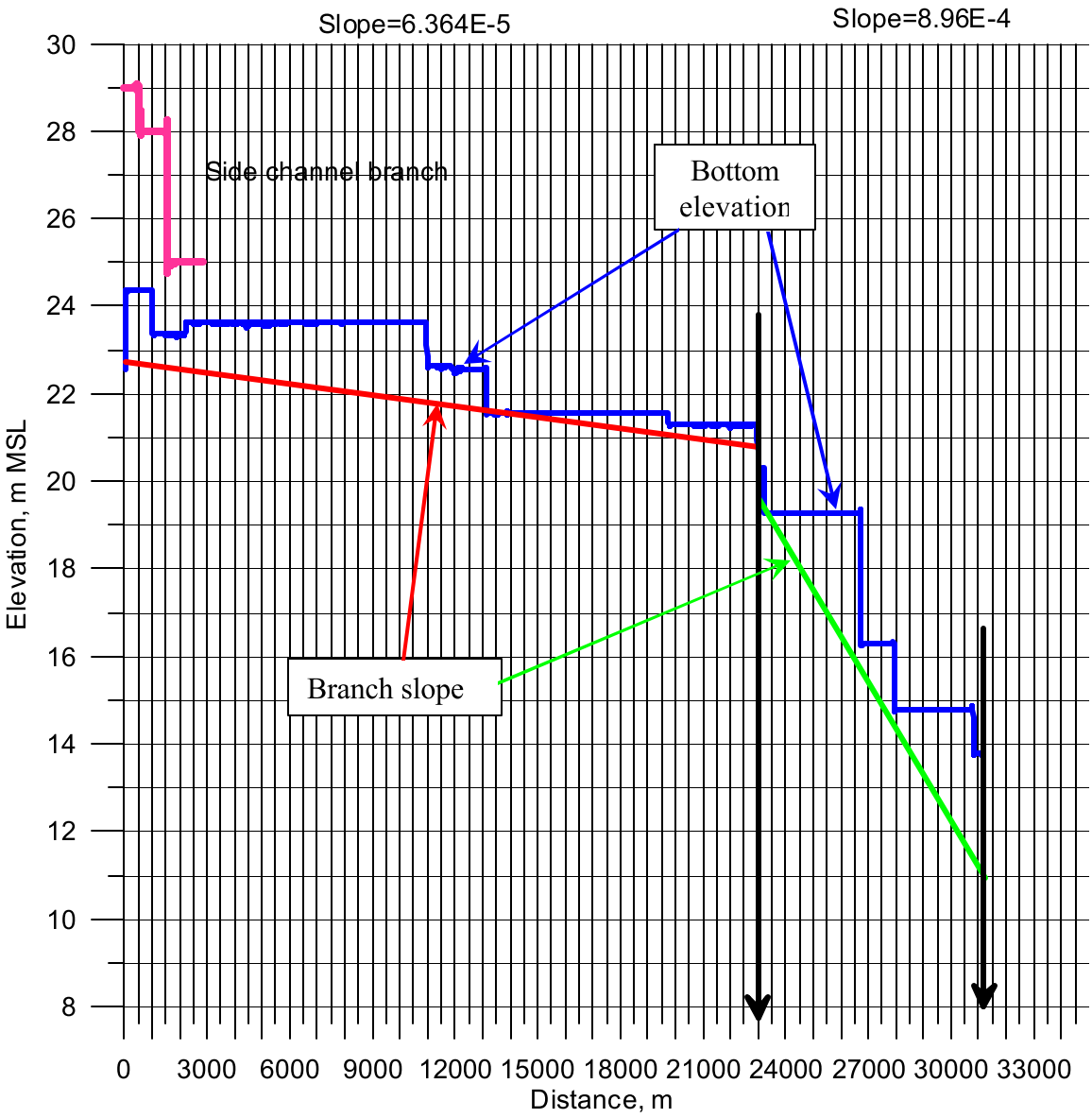


**Figure 140. Bottom elevation for thalweg of the channel for Middle Willamette River grid section 5**

## Grid section 6 (RM 72 to RM 85.4)

The layout of grid section 6 of the Middle Willamette River is shown in Figure 142. This section did not use NOAA bathymetric data because it does not extend this far upstream. Any updated data from USGS were used as well as the Digital Elevation Model data to determine the channel shape and elevation at the banks. Details of the grid are shown in Table 17. This was the second of several grid sections that had a channel slope. The channel bottom elevations, shown in Figure 141, illustrate the various slopes for the three branches in this section of the grid. As can be seen from this graph, the location of actual data was extremely sparse.

**Table 17. Middle Willamette River grid section 6 specifications**

| Grid Parameter | Branch 1 |
|---|---|
| IMP, model longitudinal segments | 83 |

| Grid Parameter | Branch 1 |
|---|---|
| Segment spacing | 250.2 |
| Slope | 0.00052 |
| Reach distance | 20766.3 |
| KMP, Model vertical layer spacing | 1 m |
| Branch segments | 2 to 84 |

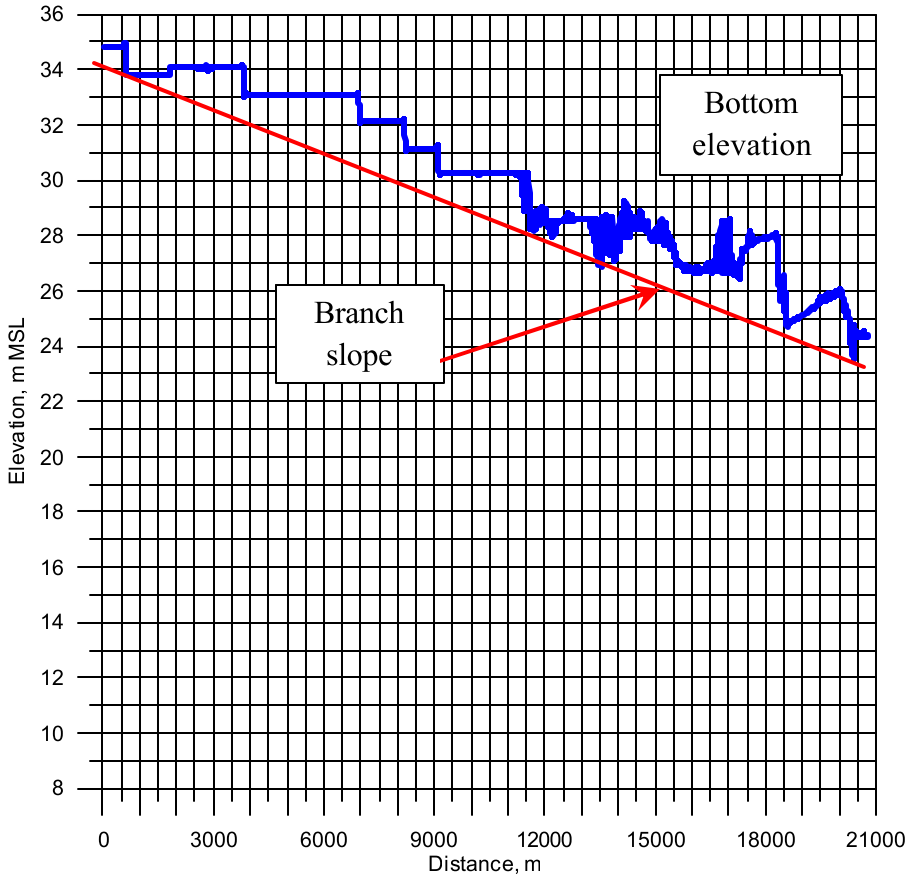


**Figure 141. Channel bottom elevation along channel thalweg for the Middle Willamette River grid section 6**

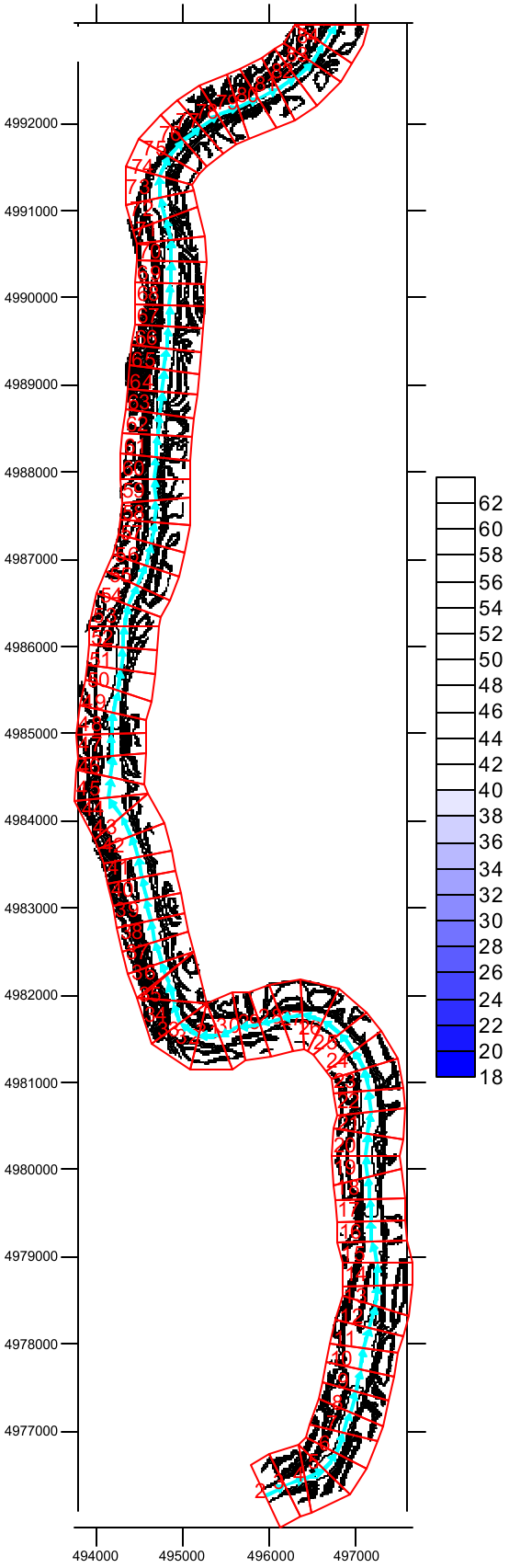


**Figure 142. Middle Willamette River grid section 6 from RM 72 to RM 85.4**

## *Model Upstream & Downstream Boundary Conditions*

The upstream boundary conditions for the model consisted of flows from the USGS gage station at Salem, OR. There was continuous record of flow, stage, and temperature data at the site in 2001 and 2002. The downstream boundary condition was developed as flow over a spillway representing the Willamette Falls that passed water downstream to the Lower Willamette River model.

### Hydrodynamic Data

Figure 143 shows the upstream and downstream boundary locations for the Middle Willamette River model. The Willamette River at Salem was used as the upstream boundary condition. The USGS maintains a gage station (14191000) at RM 85.4 on the Willamette. Table 18 lists the gage station and river mile locations for the gage shown in Figure 143.

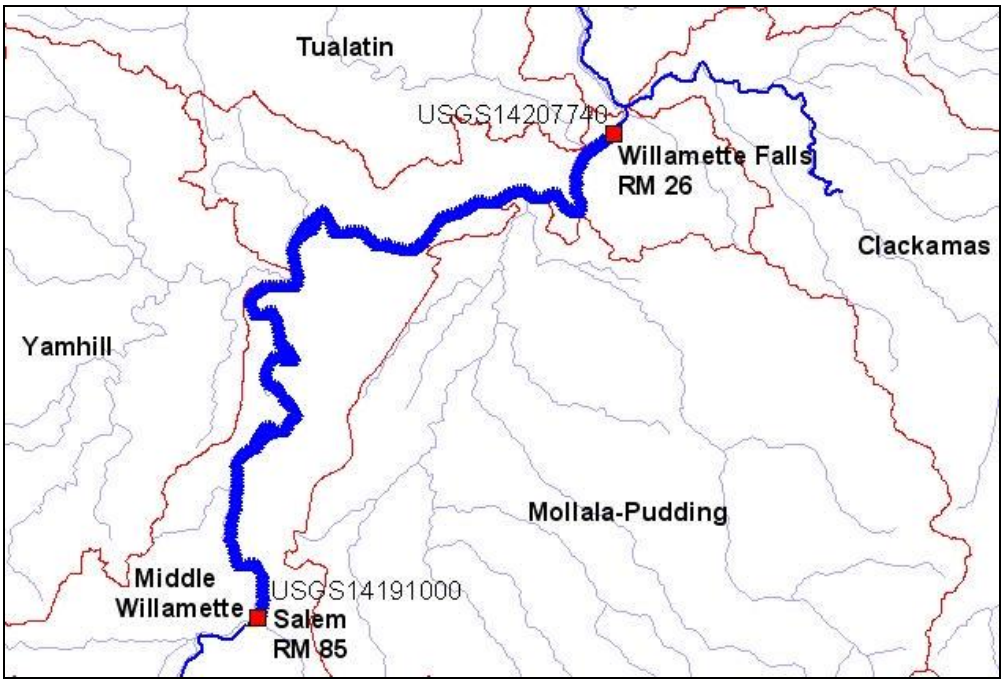


**Figure 143. Middle Willamette River upstream and downstream boundary condition flow gage stations**

**Table 18. Middle Willamette River boundary condition gage stations**

| Site ID | Tributary | RM | Model Segment |
|---|---|---|---|
| USGS14191000 | Willamette River at Salem | 85.2 | 2 |
| USGS14207740 | Willamette River above Willamette Falls | 26.8 | 396 |

#### Year 2001

Figure 144 shows the half-hourly Willamette River flow data recorded at the Salem gage station from April 1 to October 31, 2001. The figure shows a clear seasonal trend with higher flows in the spring and fall and much lower flows in the summer.

The downstream boundary for the Middle Willamette River model was handled as a spillway to represent the Willamette Falls. Since there is a weir structure and flashboards on the Willamette Falls, model output will be compared to the water level elevation data at the USGS gage station above the Willamette Falls (14207740). Figure 145 shows the water surface elevation measured above Willamette Falls for the summer of 2001.

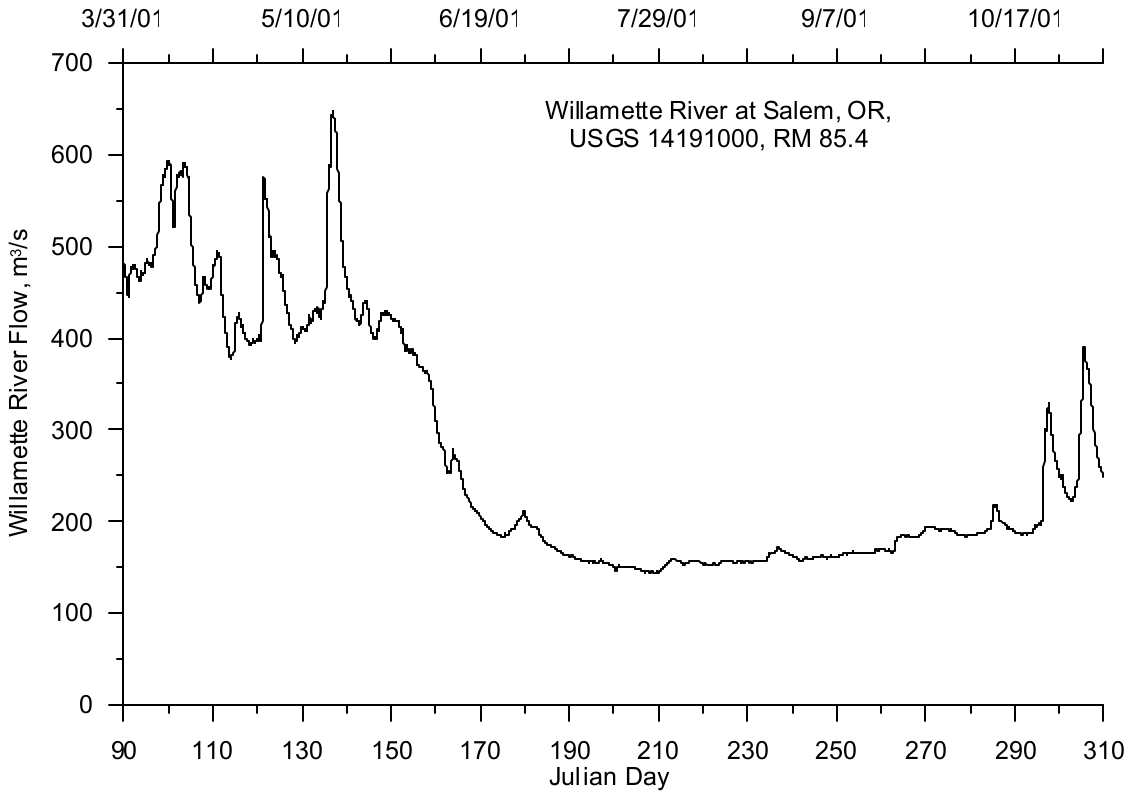


**Figure 144. Willamette River flow at Salem, OR, 2001**

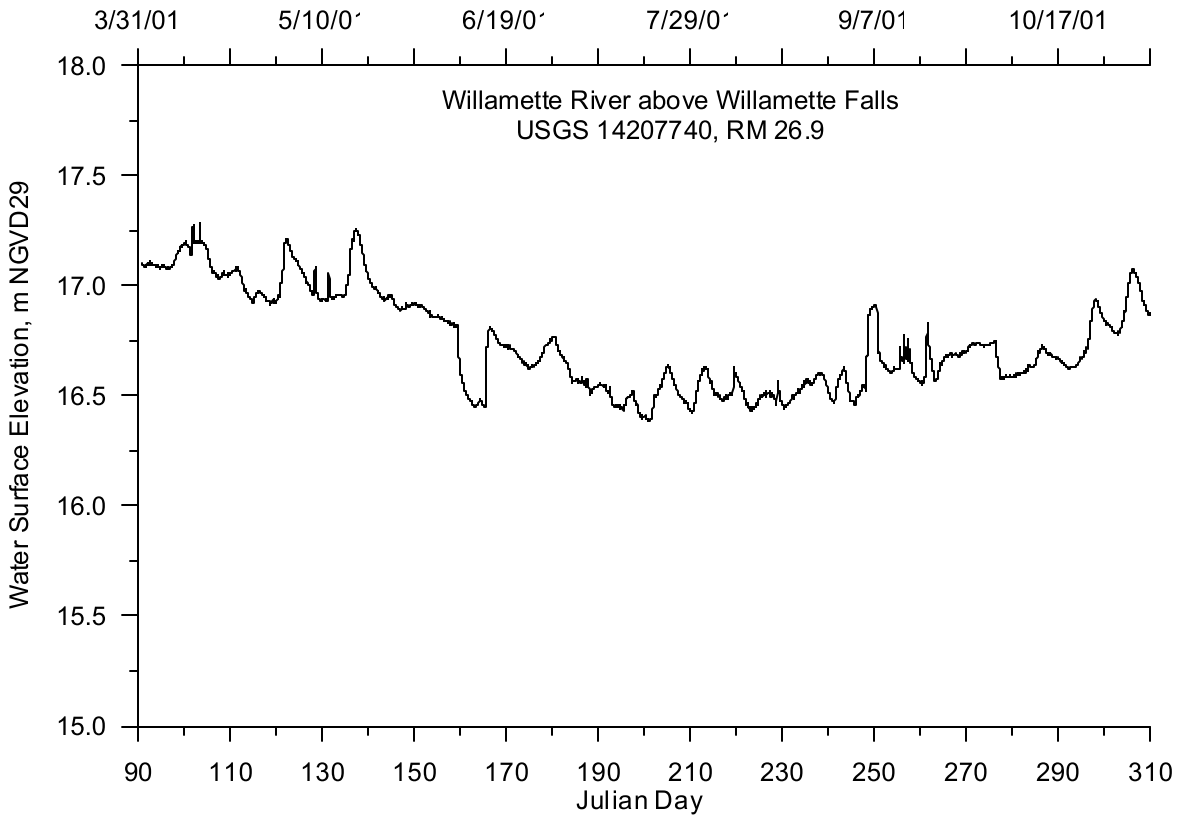


**Figure 145. Willamette River above Willamette Falls water surface elevation, 2001**

## Year 2002

Figure 146 shows the half-hourly Willamette River flow data recorded at the gage station at Salem (USGS 14191000) from April 1 to October 31, 2002. The figure shows higher flows in the spring tapering off to lower flows in the summer.

Similarly to 2001, the downstream boundary for the Middle Willamette River model was handled as a spillway to represent the Willamette Falls and its structures. Figure 147 shows the water surface elevation data (USGS 14207740) measured on the Willamette River above Willamette Falls which was used for calibrating the downstream boundary condition.

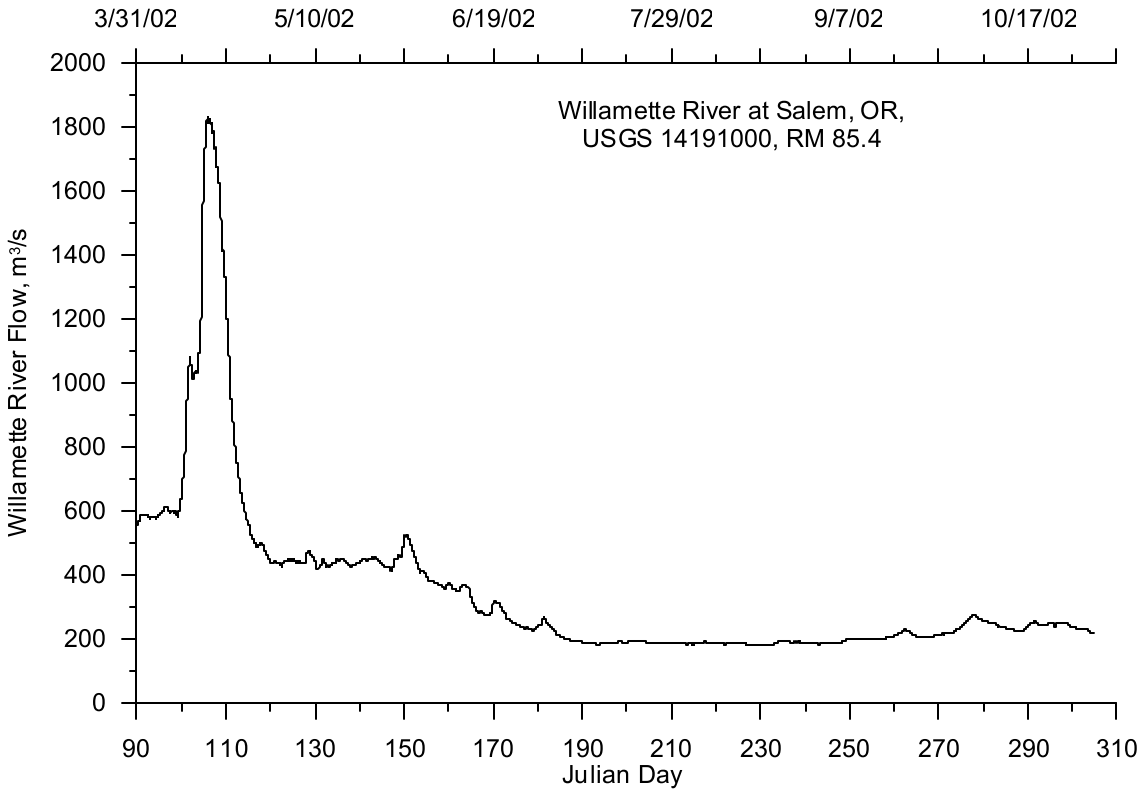


**Figure 146. Willamette River at Salem, OR, 2002**

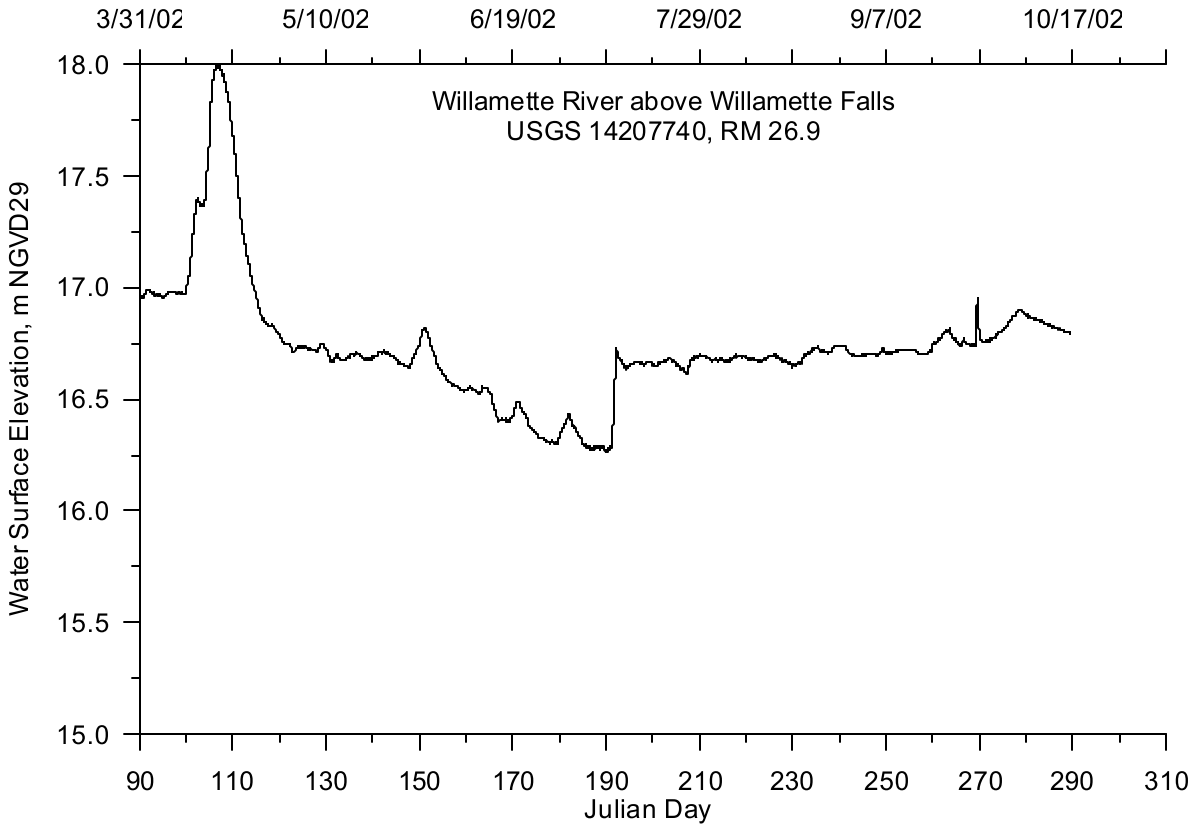


**Figure 147. Willamette River above Willamette Falls water surface elevation, 2002**

## Temperature Data

The temperature upstream boundary condition for the Middle Willamette River was developed using temperature data from three nearby monitoring sites. Figure 148 shows the temperature monitoring site locations. Table 19 lists the monitoring sites and river mile locations.

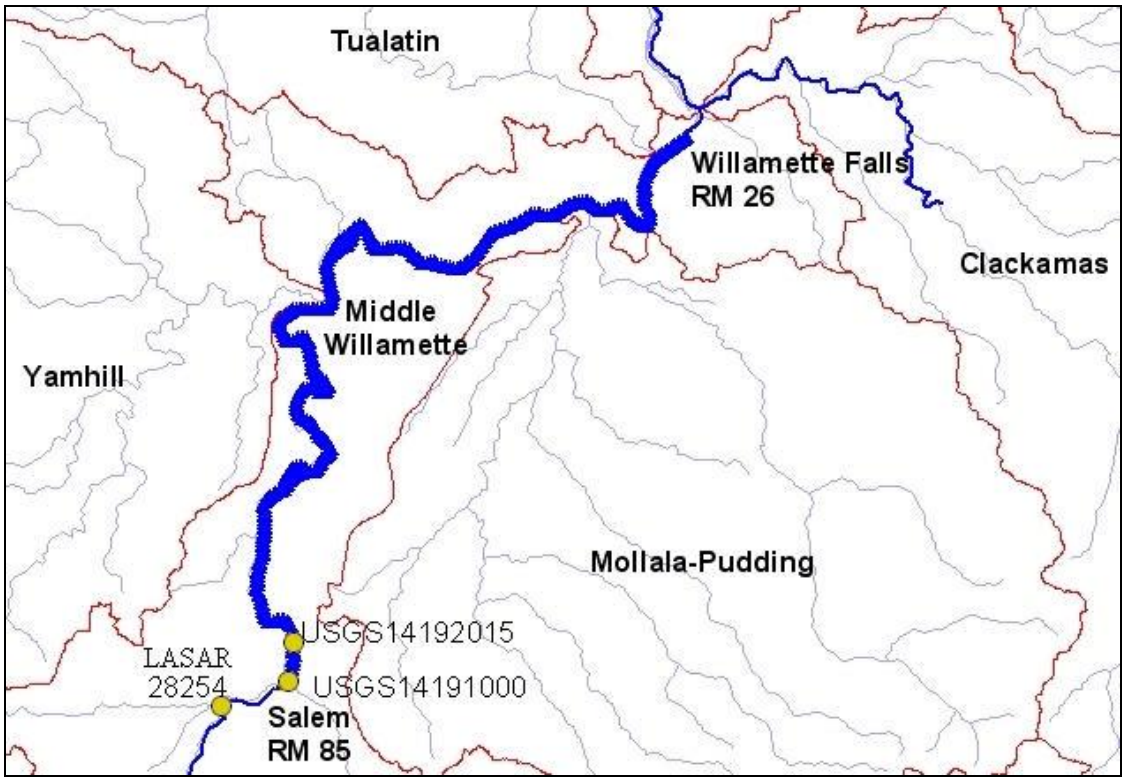


**Figure 148. Middle Willamette River model boundary condition temperature monitoring site locations**

**Table 19. Middle Willamette River model boundary condition temperature monitoring sites**

| Site Description | Site ID | RM |
|---|---|---|
| Willamette River at Salem | USGS14191000 | 85.4 |
| Willamette River at Keizer | USGS14192015 | 81.9 |
| Willamette River above Rickreall Creek | LASAR 28254 | 88.2 |

### Year 2001

Water temperature was recorded at the Salem gage station during 2001 but there was a large gap in the data from July to September. The USGS also recorded water temperature data at Keizer on the Willamette (RM 82) and at a site just upstream of the confluence of Rickreall Creek and the Willamette River (RM 88). Two temperature correlation equations were developed. The temperature correlation relationship and equation between the site at Salem and above Rickreall Creek is shown in Figure 149. The second temperature correlation, between the Salem and Keizer sites, is shown in Figure 150. Using the correlations, the Salem water temperature time series data gaps were filled. The completed time series record was plotted in Figure 151.

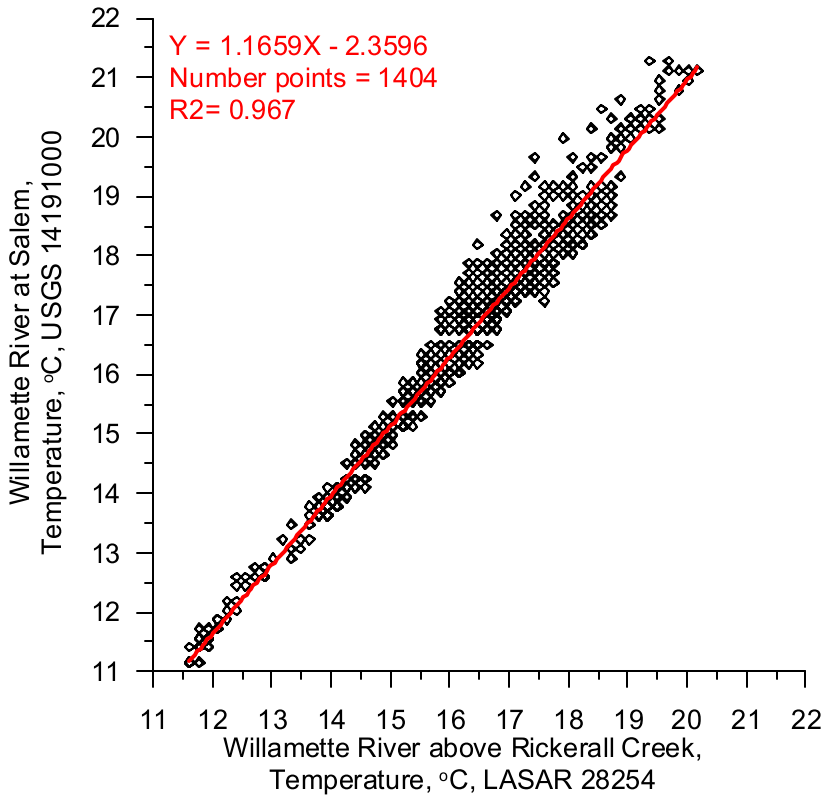


**Figure 149. Temperature correlation between the Willamette River above Rickreall Creek and at Salem**

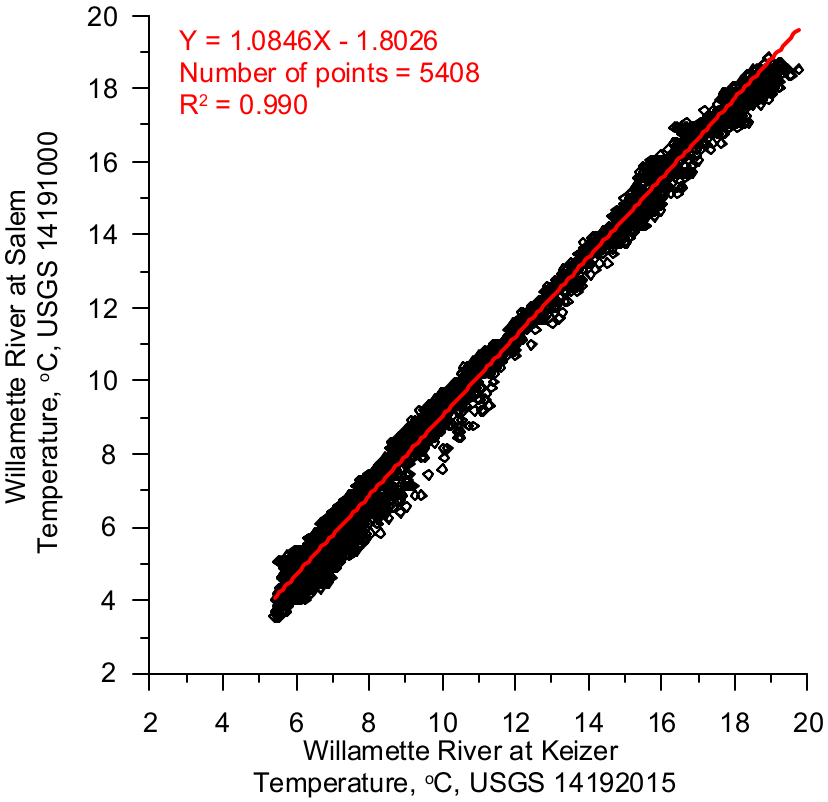


**Figure 150. Temperature correlation between the Willamette River at Keizer and at Salem**

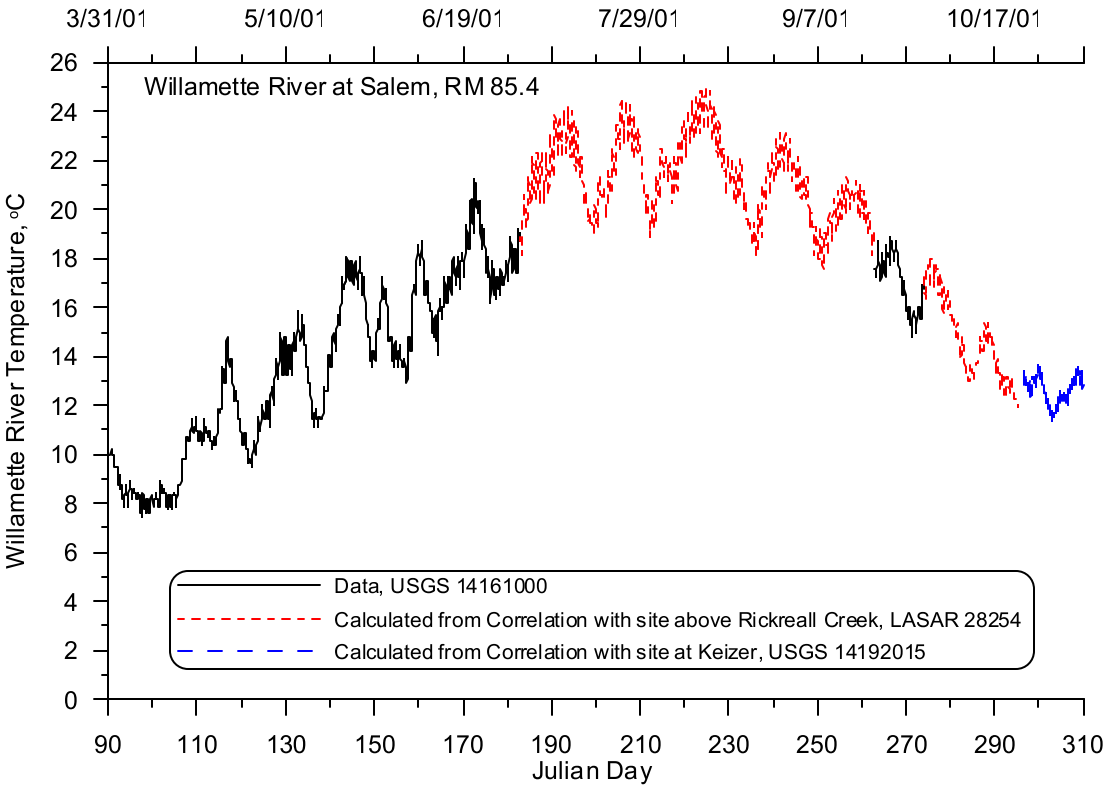


**Figure 151. Willamette River temperature at Salem, OR, 2001**

## Year 2002

In 2002 there were no temperature data measured in the Willamette River at Salem, but a continuous temperature record did exist for the USGS gage station at Keizer (14192015). The correlation developed in Figure 150 was used to estimate temperature values for the upstream boundary at Salem. Figure 152 shows the calculated temperatures values for Salem in 2002.

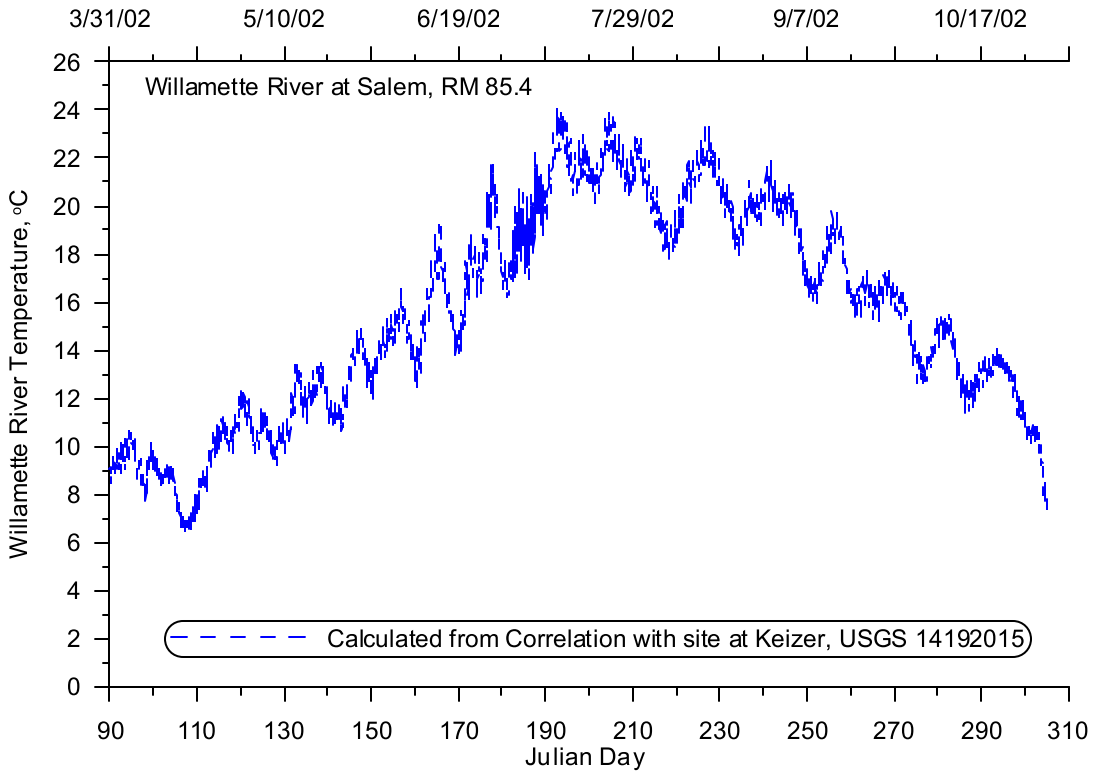


**Figure 152. Willamette River temperature at Salem, OR, 2002**

## *Tributaries*

There were three main tributaries and one small tributary included in the Middle Willamette River model. Figure 153 shows the location of the tributaries, and Table 20 shows the RM location for each tributary.

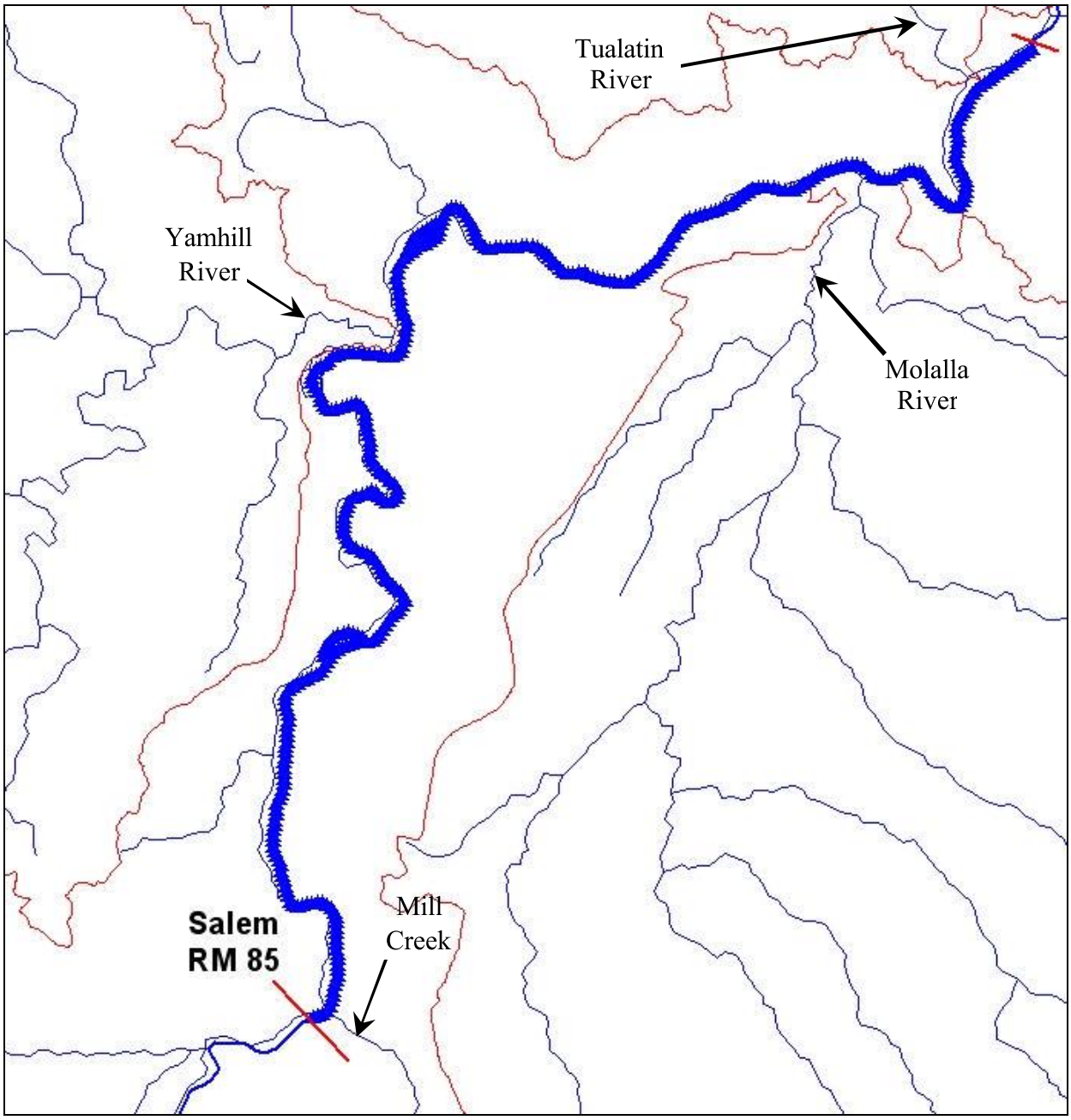


**Figure 153. Middle Willamette River model tributary locations**

**Table 20. Middle Willamette River tributary model segments and river miles**

| Tributary | RM | Model Segment |
|---|---|---|
| Mill Creek | 84.5 | 8 |
| Yamhill River | 55.1 | 199 |
| Molalla River | 35.6 | 338 |
| Tualatin River | 28.4 | 385 |

## Hydrodynamic Data

There were four tributaries contributing flow to the Middle Willamette River model. To complete the flow records, gage station data from six stations were needed. The gage stations used to develop the tributary flows are shown in Figure 154. Table 21 lists the gage stations and their locations along the river.

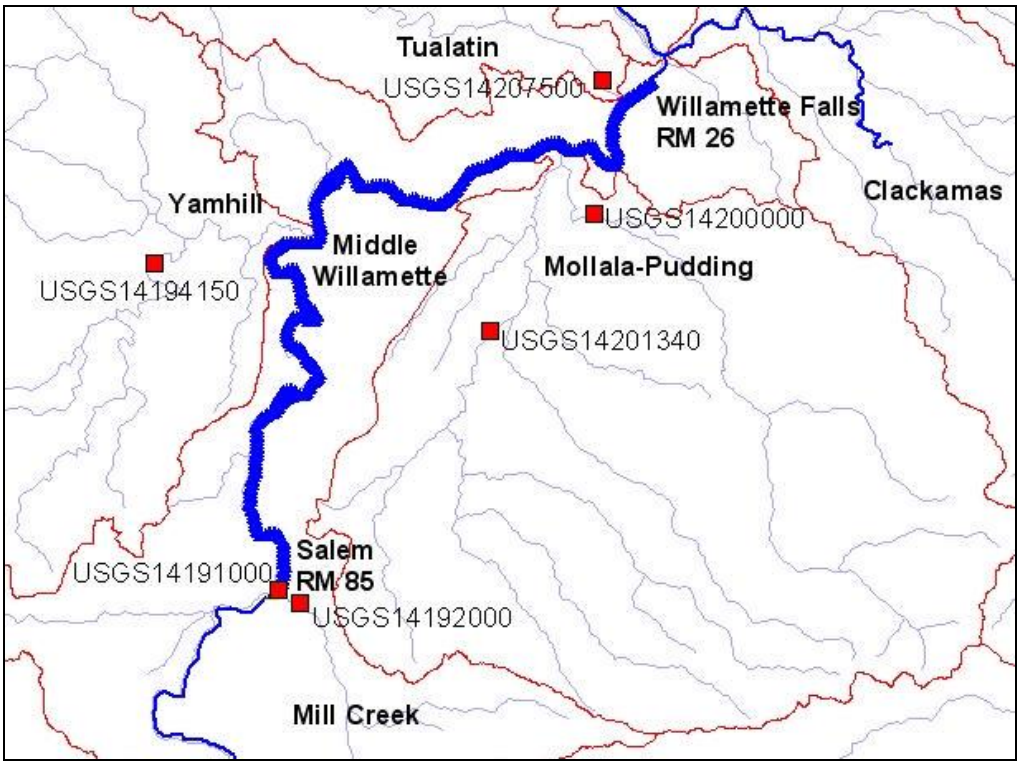


**Figure 154. Middle Willamette River model tributary flow gages**

**Table 21. Middle Willamette River model tributary flow gage stations**

| Site ID | Tributary | RM | Model Segment |
|---|---|---|---|
| USGS14194150 | South Yamhill River | 55.1 | 199 |
| USGS14201340 | Pudding River at Woodburn, OR | 35.6 | 338 |
| USGS14200000 | Molalla River near Canby, OR | 35.6 | 338 |
| USGS14207500 | Tualatin River at West Linn, OR | 28.4 | 385 |
| USGS14192000 | Mill Creek at Salem, OR | 84.5 | 8 |
| USGS14191000 | Willamette River at Salem, OR | 85.4 | NA |

### Year 2001

No gage station existed on the lower end of the Yamhill River. The Yamhill River basin flow record was developed by using the gage station on the South Yamhill River (USGS 14194150) with the drainage basin ratio between the south basin and the total Yamhill basin in the following equation:

$$TotalYamhillQ = SouthYamhillQ\left(\frac{TotalYamhillArea,772\_mi^2}{SouthYamhillArea,528\_mi^2}\right)$$

Figure 155 shows the Yamhill River flow from April to October 2001.

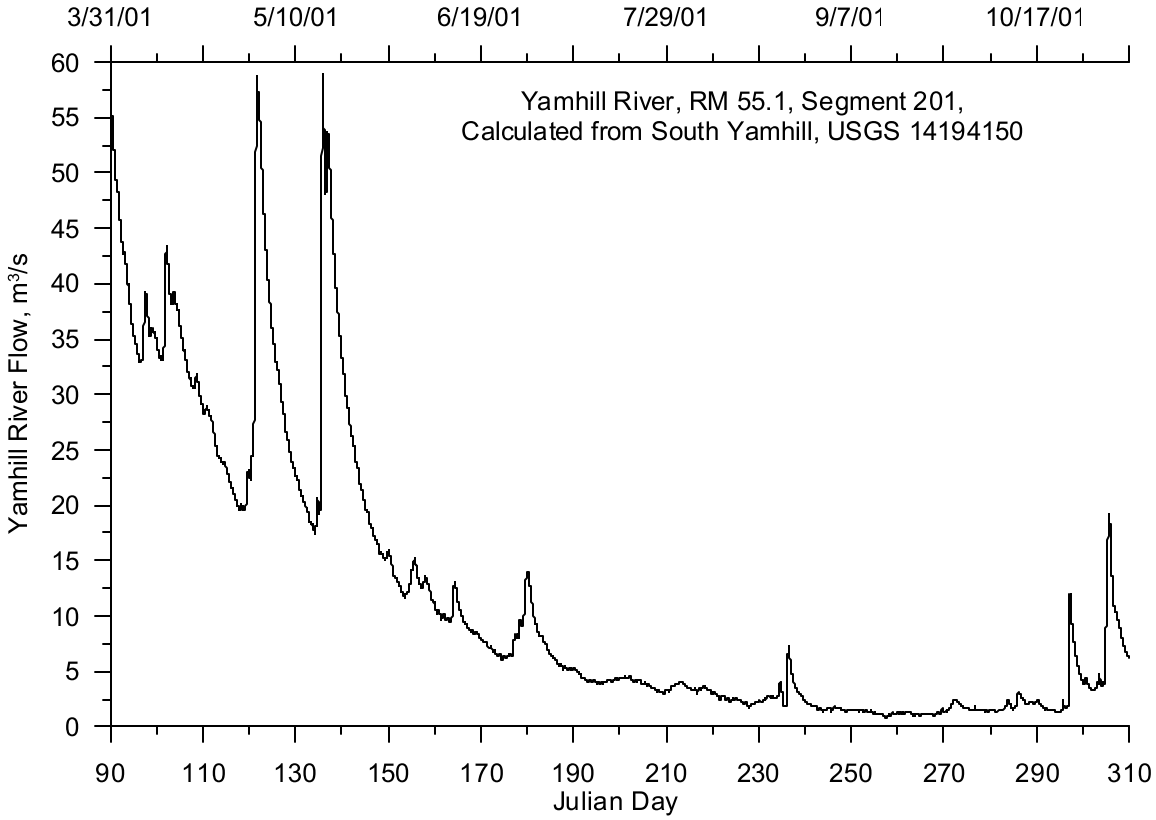


**Figure 155. Yamhill River flow, 2001**

The Molalla River basin consisted primarily of the Molalla and Pudding river basins. Flow on the Pudding River was monitored at Aurora, which is near the confluence with the Molalla River. Since 1997, the Pudding River has been monitored further upstream at Woodburn (USGS 14201340). Flows at Aurora were estimated using the same relationship shown above for the Yamhill basin.

$$Pudding\_AuroraQ = Pudding\_WoodburnQ\left(\frac{\text{PuddingAur oraBasin}\_Area,479\_mi^2}{\text{PuddingWoo dburnBasin}\_Area,314\_mi^2}\right)$$

The Pudding River flows calculated with this method were then added to flows from a gage station on the Molalla River near Canby (USGS 14200000). The combined flows, representing the Molalla-Pudding basin, are shown in Figure 156.

Tualatin River flows were obtained from the USGS gage station in West Linn (USGS 14207500). Figure 157 shows the flows from April to October 2001.

Although Mill Creek has a small inflow contribution, due to the basin's size continuous temperature data were recorded on the creek. From the 1940s to 1978, flows were monitored on Mill Creek. Using daily flow values for Mill Creek (USGS 14192000) and the Willamette River at Salem (USGS 14191000), the

correlation in Figure 158 was developed. The correlation equation was then used to estimate flows for 2001 as shown in Figure 159.

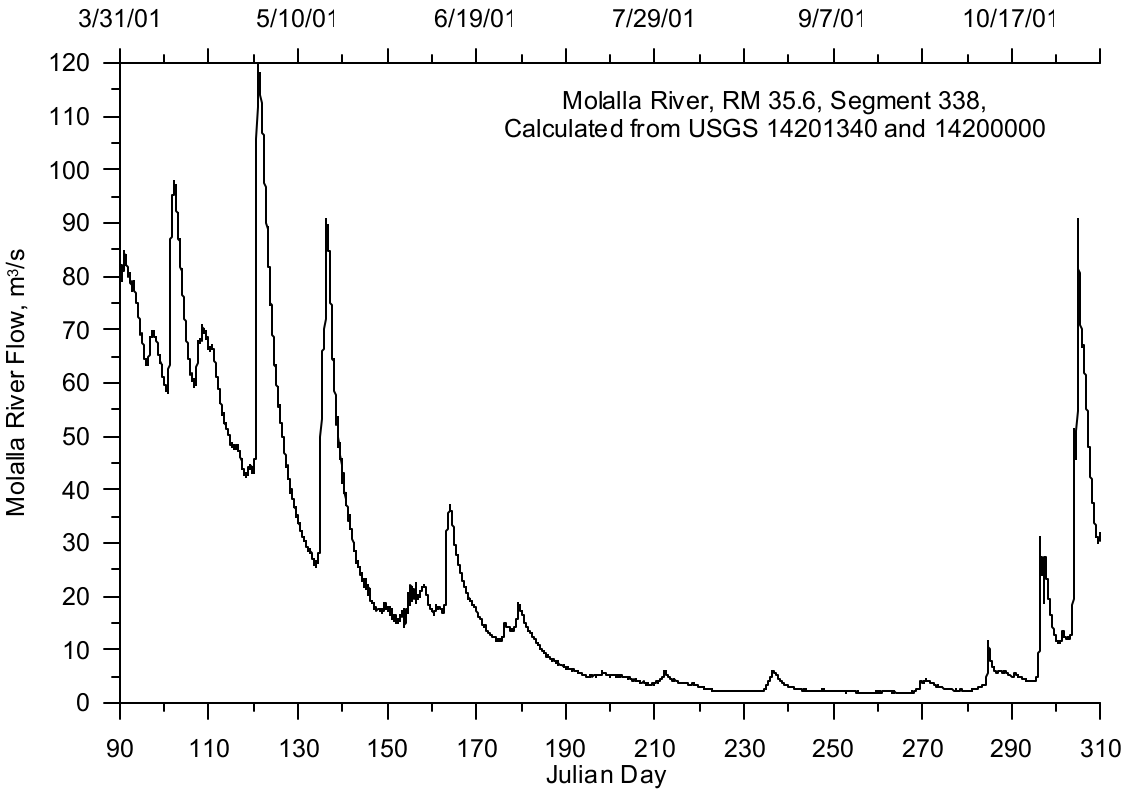


**Figure 156. Molalla River flow, 2001**

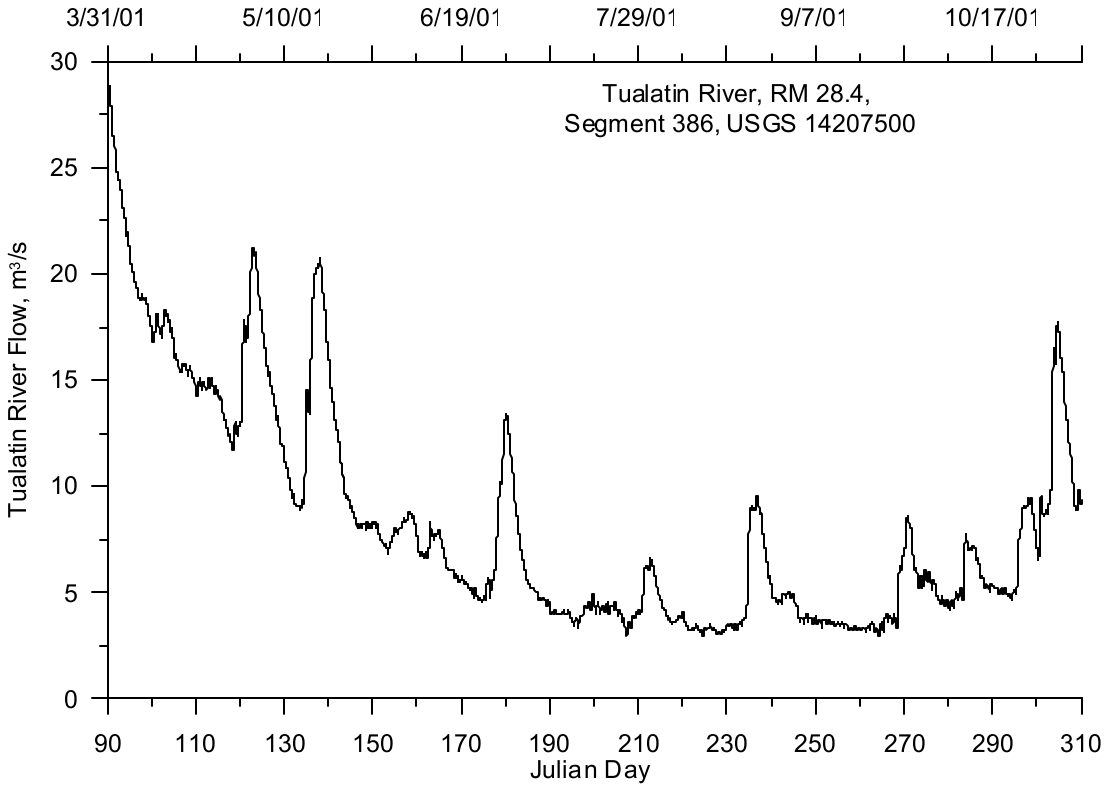


**Figure 157. Tualatin River flow, 2001**

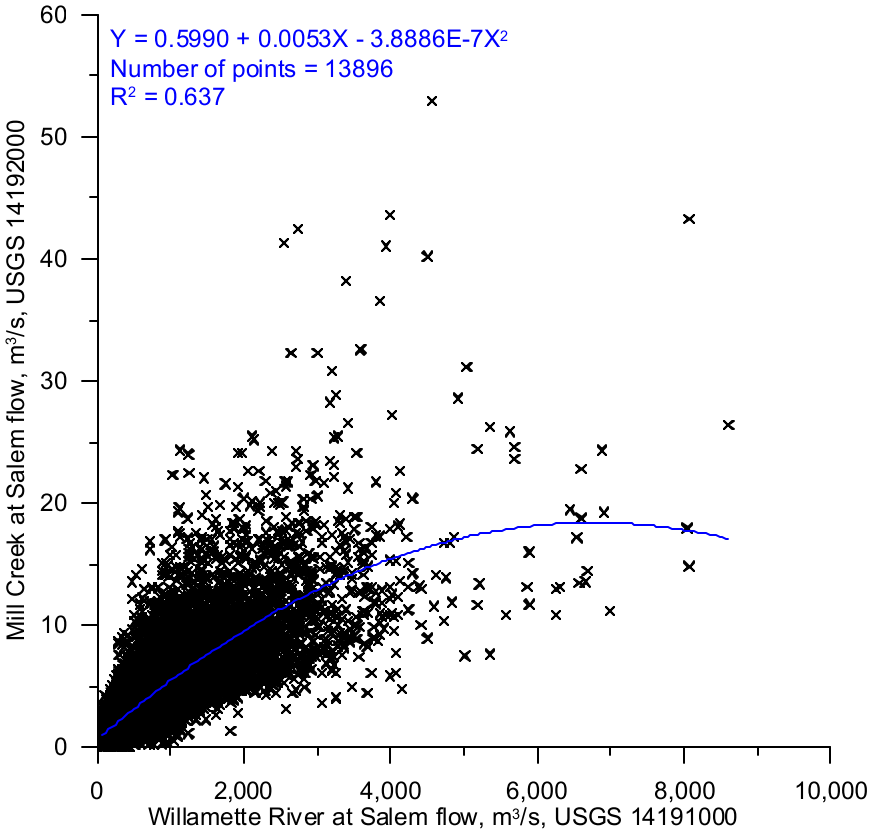


**Figure 158. Daily flow correlation between the Willamette River and Mill Creek**

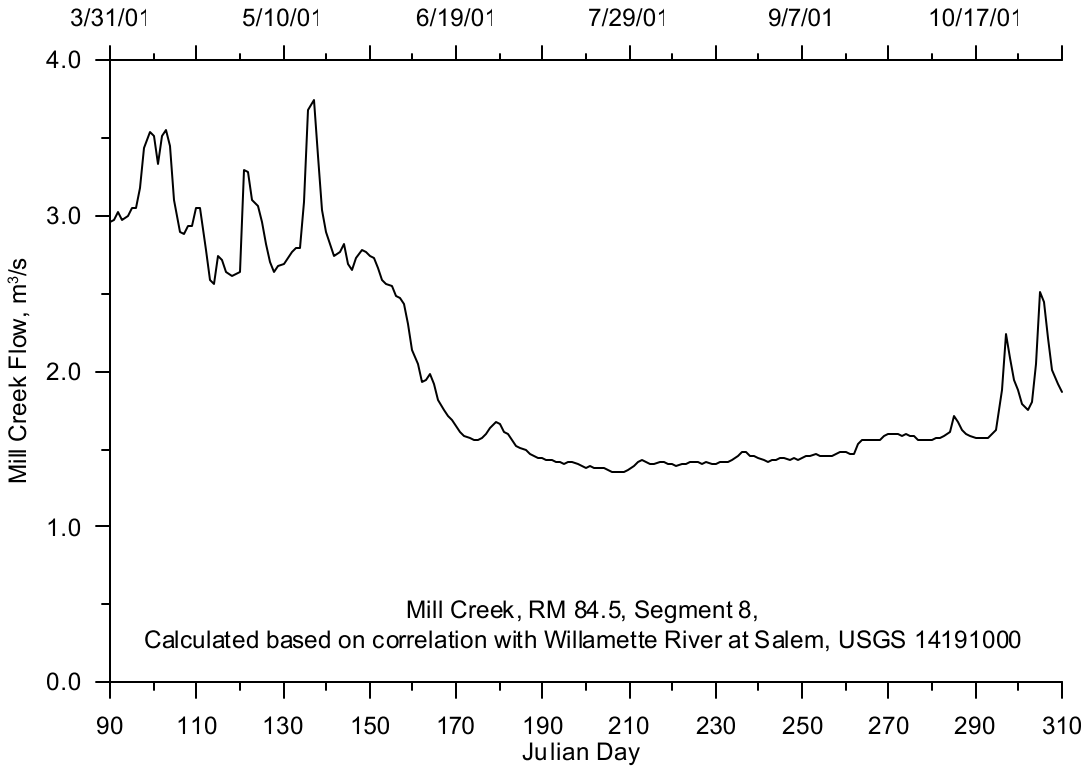


**Figure 159. Mill Creek flow, 2001**

## Year 2002

As in 2001, no gage station existed on the lower end of the Yamhill River. The Yamhill River basin flow record was developed using data collected at the gage station on the South Yamhill River (USGS 14194150). To calculate flow rates the South Yamhill River flow rates were divided by the drainage basin ratio between the south basin and the total Yamhill basin. Figure 160 shows the Yamhill River flow during the summer for 2002.

The flows for the Molalla River basin were developed for 2002 using the same methodology used for 2001. The total flow, representing the Molalla-Pudding basins, is shown in Figure 161. The Tualatin River flow for 2002 was obtained from the USGS gage station, (14207500) and is shown in Figure 162. The flow correlation developed between the Mill Creek flow and the Willamette River flow at Salem used for the 2001 model file development was also applied for the 2002 model file development.

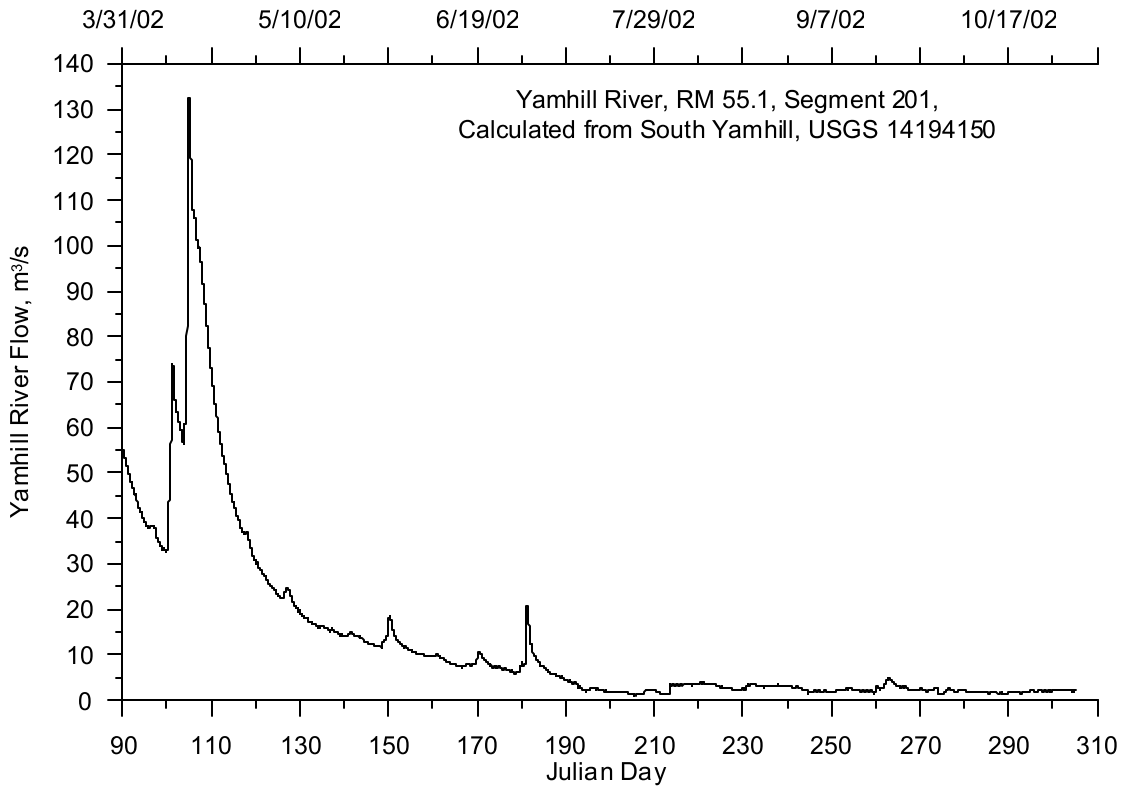


**Figure 160. Yamhill River flow, 2002**

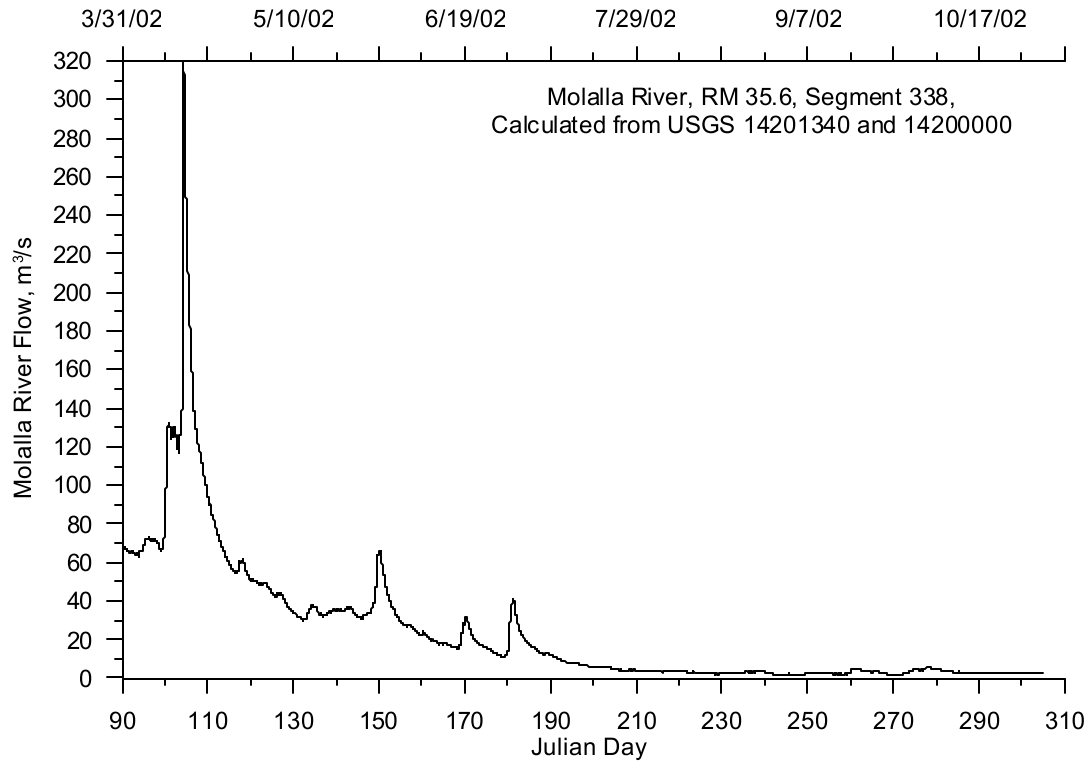


**Figure 161. Molalla River flow, 2002**

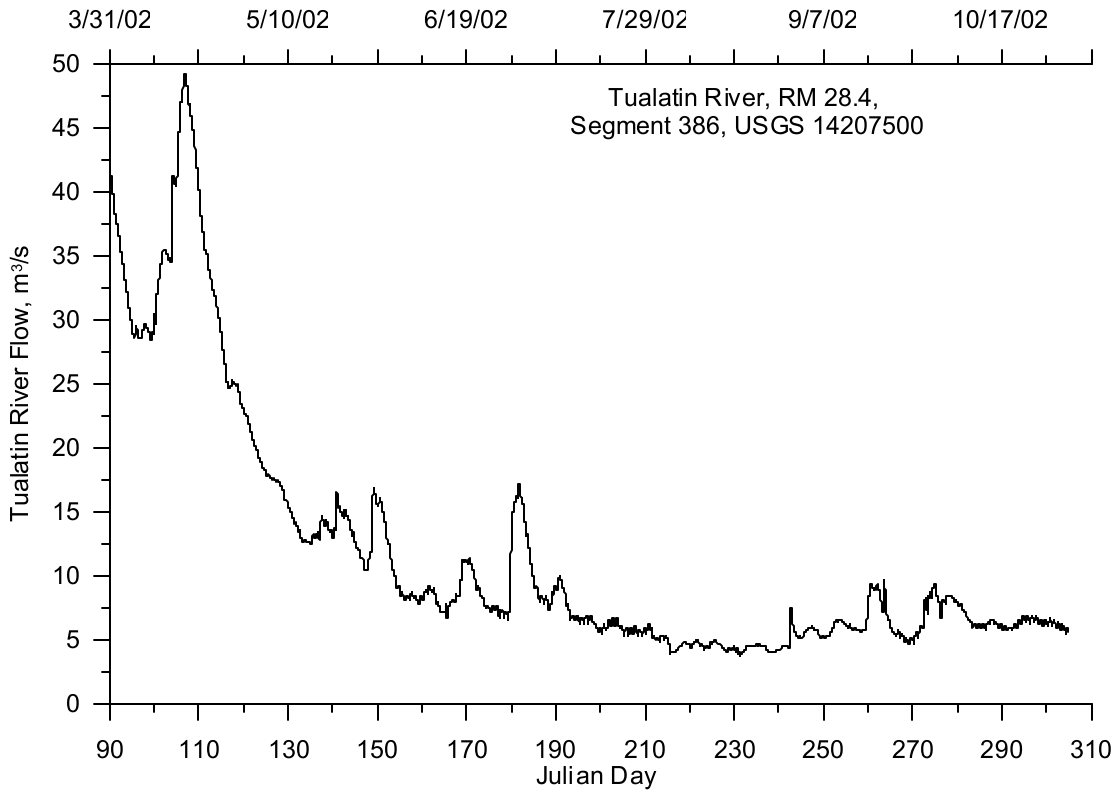


**Figure 162. Tualatin River flow, 2002**

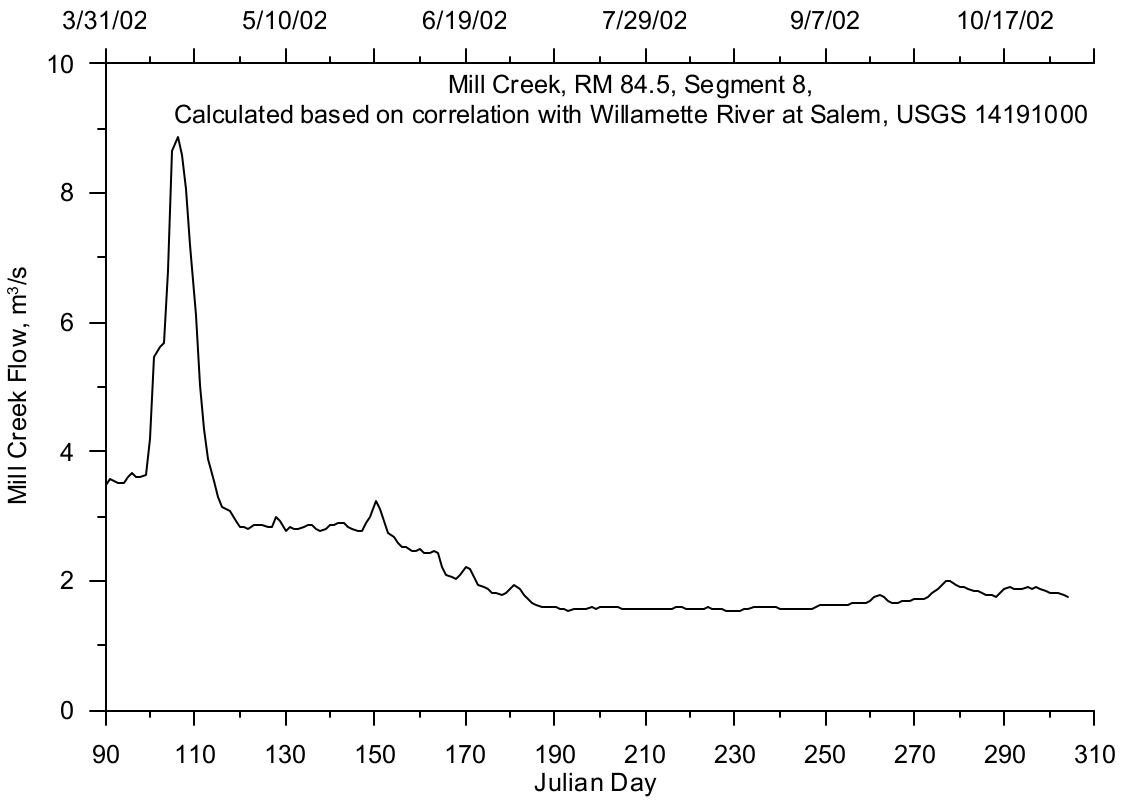


**Figure 163. Mill Creek flow, 2002**

## Temperature Data

Several temperature monitoring sites were used to develop the tributary temperature records. Figure 164 shows the temperature monitoring sites for the tributaries. Table 21 lists the temperature monitoring sites and their river mile and model segment locations.

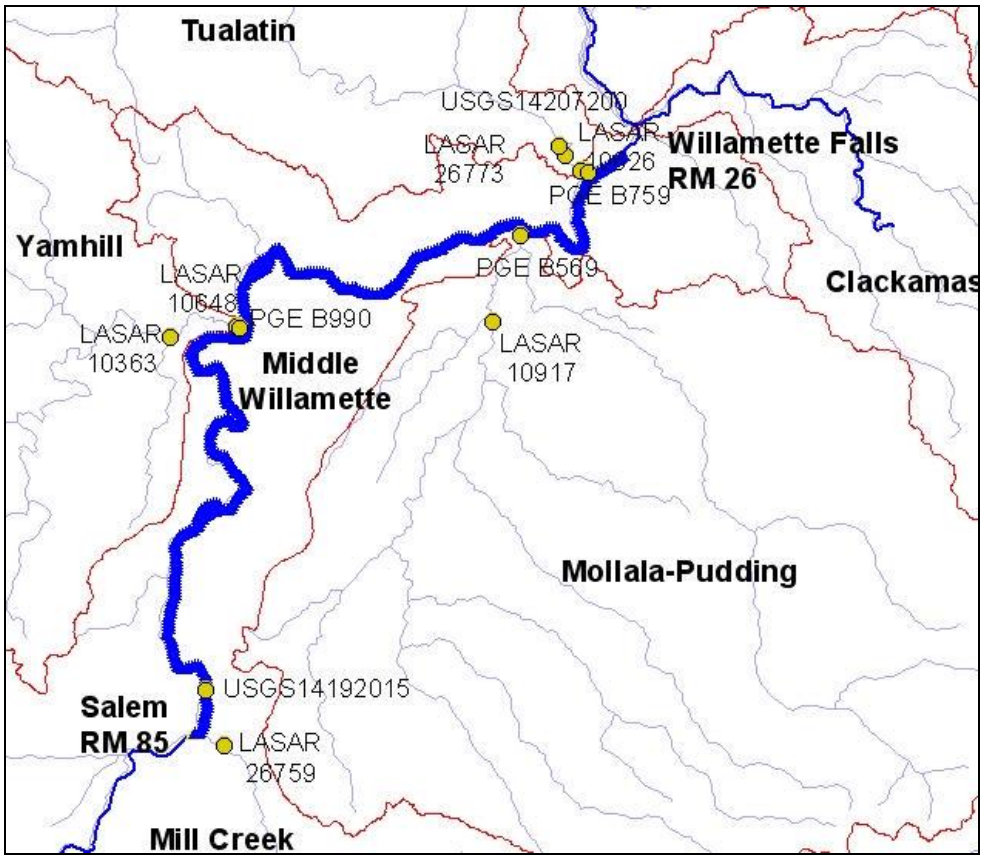


**Figure 164. Middle Willamette River model tributary temperature monitoring site locations**

**Table 22. Middle Willamette River model tributary temperature monitoring sites**

| Site ID | Tributary | Willamette RM | Model Segment |
|---|---|---|---|
| LASAR 10648 | Yamhill River mouth | | |
| PGE B759 | Yamhill River mouth | 55.1 | 199 |
| LASAR 10363 | Yamhill River at Dayton OR, RM 5 | | |
| USGS14192015 | Willamette River at Keizer, OR | | |
| LASAR 10917 | Pudding River at HWY99E, Aurora, OR | | |
| PGE B569 | Molalla River mouth | 35.6 | 338 |
| USGS14207200 | Tualatin River at Oswego Dam | | |
| LASAR 26773 | Tualatin River at West Linn, OR | | |
| PGE B990 | Tualatin River at mouth | 28.4 | 385 |
| LASAR 10626 | Tualatin River at mouth | 28.4 | 385 |
| LASAR 26759 | Mill Creek at Salem, OR | 84.5 | 8 |

Year 2001

The Yamhill River water temperatures were based on data collected for PGE by Normandeau and Associates, Inc. The temperature data were from the monitoring site "Site Key 5500" (Thermistor: B759). There were data gaps from April 1 to April 25, 2001, and from July 6 to July 25, 2001, which needed to be filled. Temperature correlations were developed between the monitoring site at the mouth from PGE and a site at Dayton, OR, which was recorded by ODEQ (LASAR 10363). The correlation

and resulting equation are shown in Figure 165. This correlation equation was used for calculating the temperature of the Yamhill River in July. Since the ODEQ data were limited in time, another correlation was developed to fill the data gap in April. A temperature correlation was developed between the mouth of the Yamhill River and the Willamette River at Keizer as shown in Figure 166. Although there was some distance between these two sites, the correlation was still good, and had a coefficient of determination of 0.9. The completed temperature time series for the Yamhill River is shown in Figure 167 with the data and the two sets of calculated values.

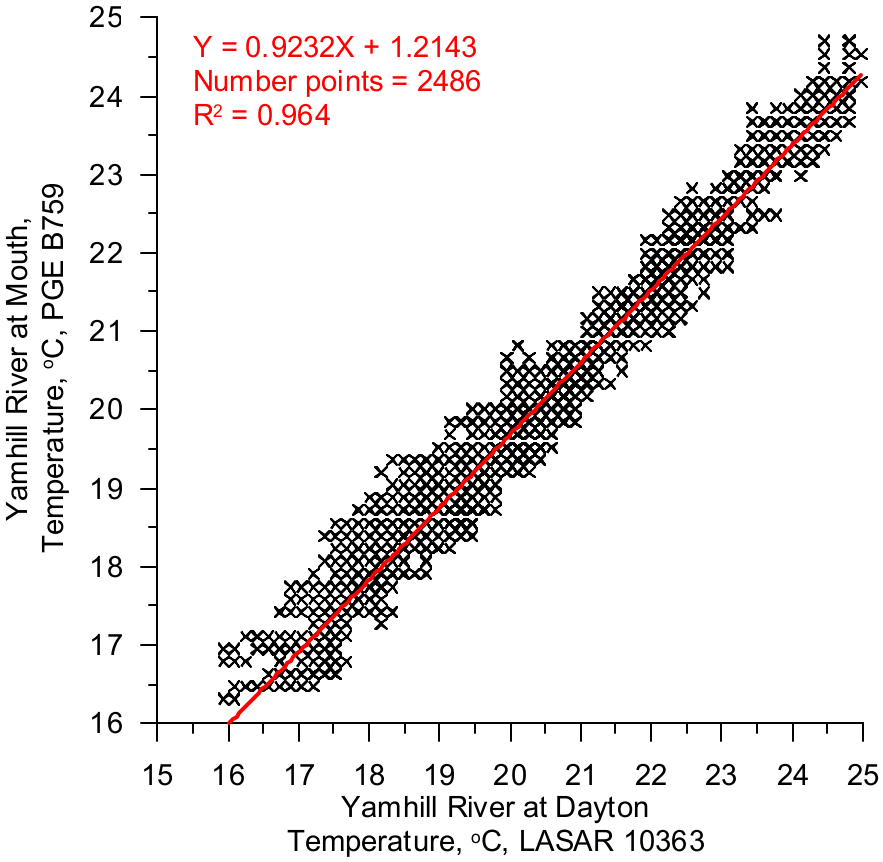


**Figure 165. Temperature correlation between the Yamhill River at Dayton and at the mouth**

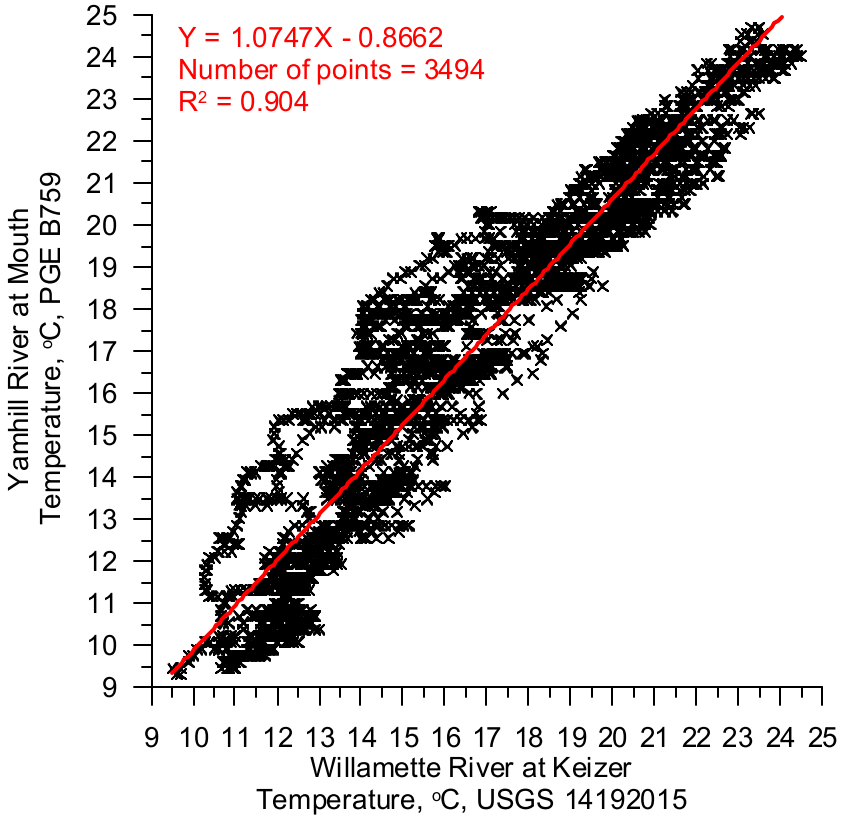


**Figure 166. Temperature correlation between the Yamhill River and the Willamette River**

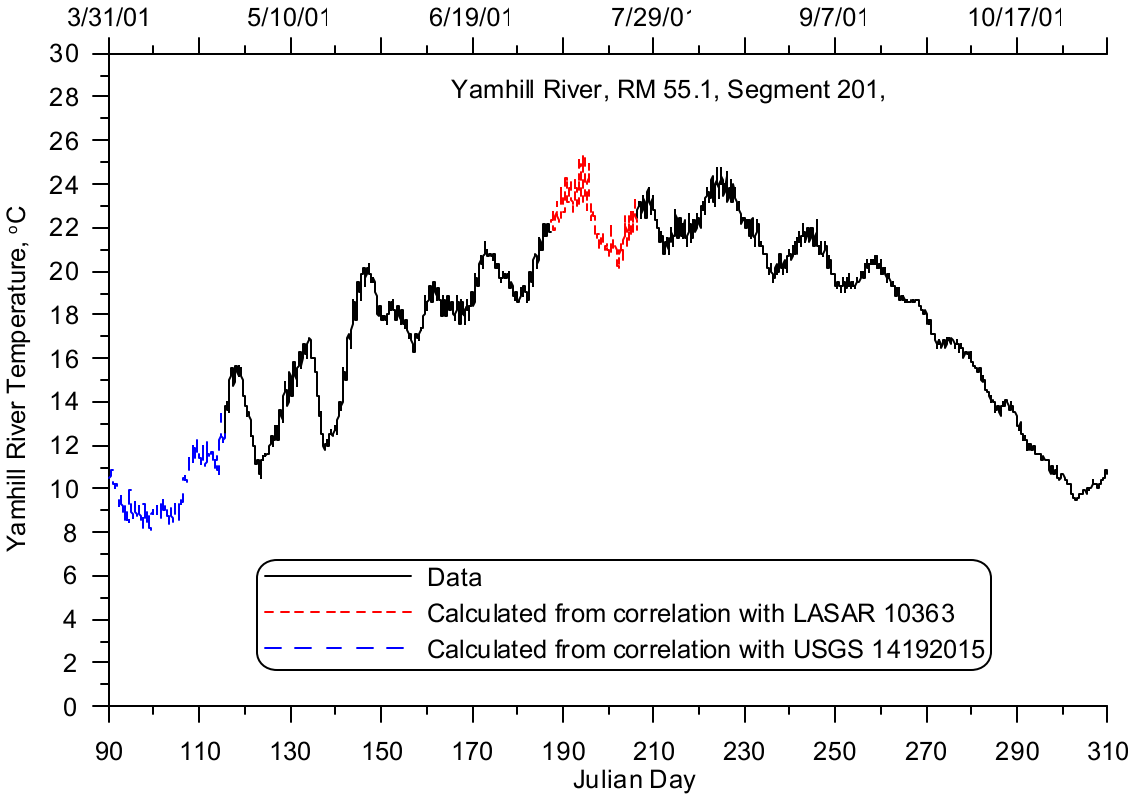


**Figure 167. Yamhill River temperature, 2001**

The Molalla River water temperatures were based on data collected for PGE by Normandeau and Associates, Inc. The temperature data were from the monitoring site with the Site Key 3590 (Thermistor: B569). The temperature time series data were recorded from April 26 to October 1, 2001.

The data gap in October (October 2 to October 31) was filled by developing a temperature correlation relating the temperature at the mouth of the Molalla River (PGE B569) with temperature data recorded on the Pudding River (LASAR 10917). The temperature correlation and the correlation equation are shown in Figure 168.

The data gap in April was filled by developing a temperature correlation with the Willamette River temperatures recorded at Keizer (USGS 14192015). The temperature data recorded on the Pudding River were not available during this time period. The temperature correlation and the correlation equation are shown in Figure 169. Figure 170 shows the complete Molalla River temperature time series including both the data and the calculated values for 2001.

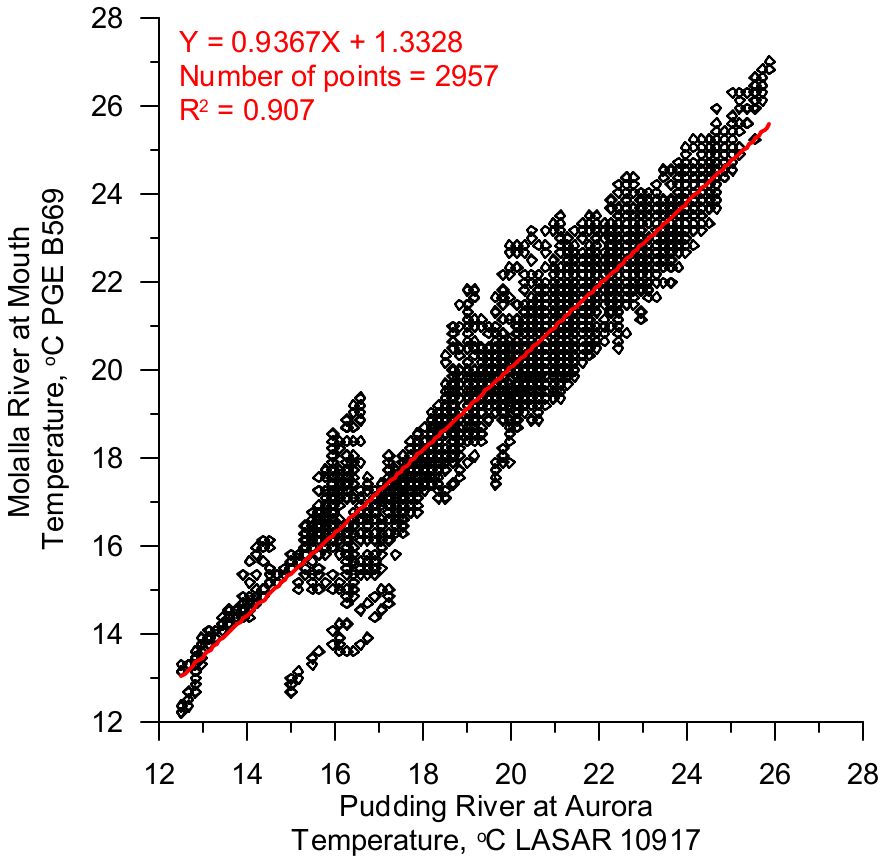


**Figure 168. Temperature correlation between the Pudding River and the Molalla River**

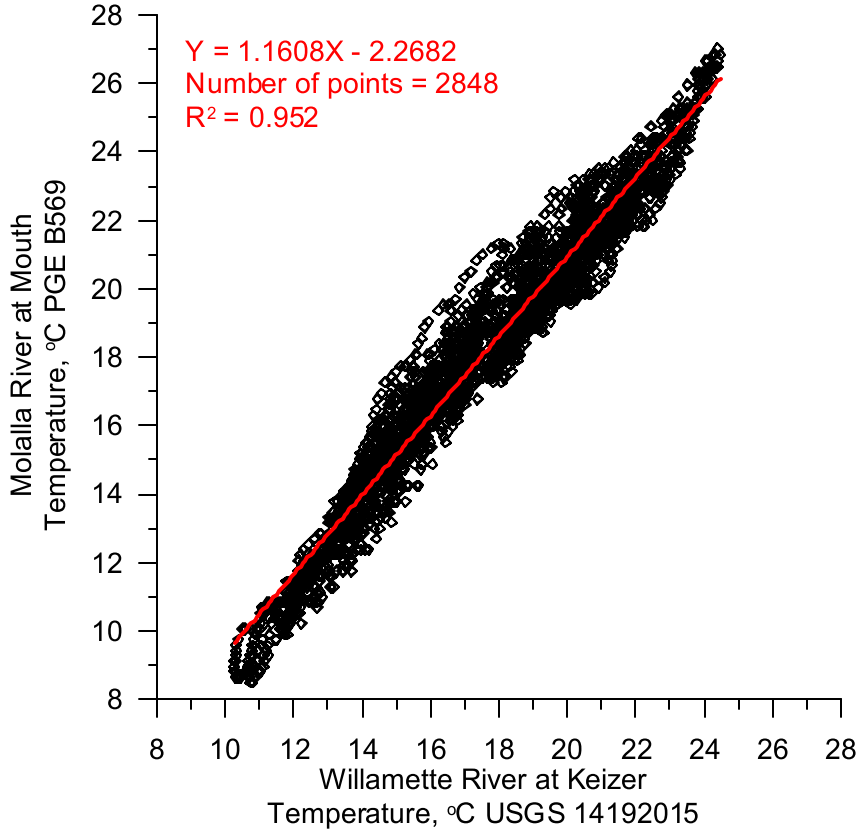


**Figure 169. Temperature correlation between the Willamette River and the Molalla River**

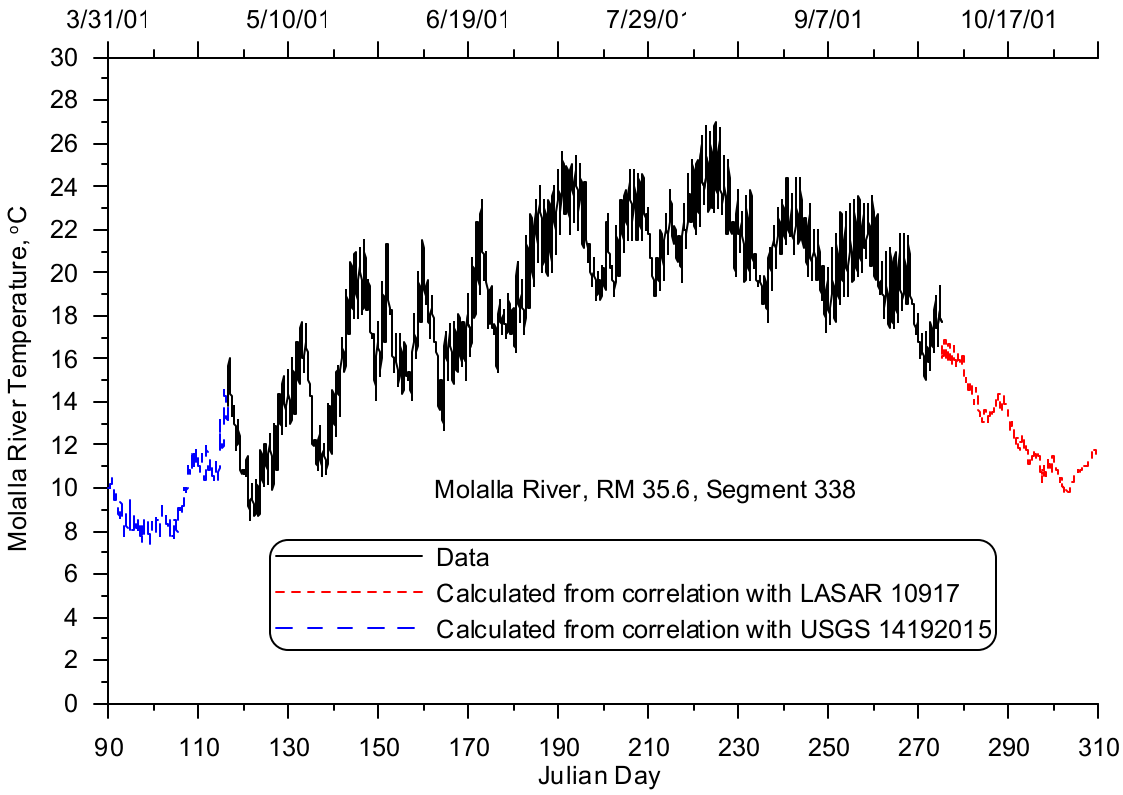


**Figure 170. Molalla River temperature, 2001**

The water temperature data for the Tualatin River primarily came from a site monitored for PGE by Normandeau and Associates, Inc. at Site Key: 2850 (Thermistor: B990), but there were data gaps from April 1 to 26 and from August 29 to October 31. The first temperature correlation developed was between the USGS gage station at RM 3.4 (14207200) and the monitoring site at RM 1.8 (LASAR 26773). The correlation and correlation equation are shown in Figure 171. The next correlation developed was between the site at the mouth of the river (PGE B990) and the site at RM 1.8, LASAR 26773. The correlation equation and correlation relationship are shown in Figure 172. The first temperature correlation was used to calculate a more comprehensive data set at RM 1.8 based on data from RM 3.4. The second correlation was then used to calculate the river temperature at the mouth. The resulting calculated temperature was then used to fill in the data gaps at the beginning and ending of summer. Figure 173 shows the river temperature data and calculated values for the Tualatin River for 2001.

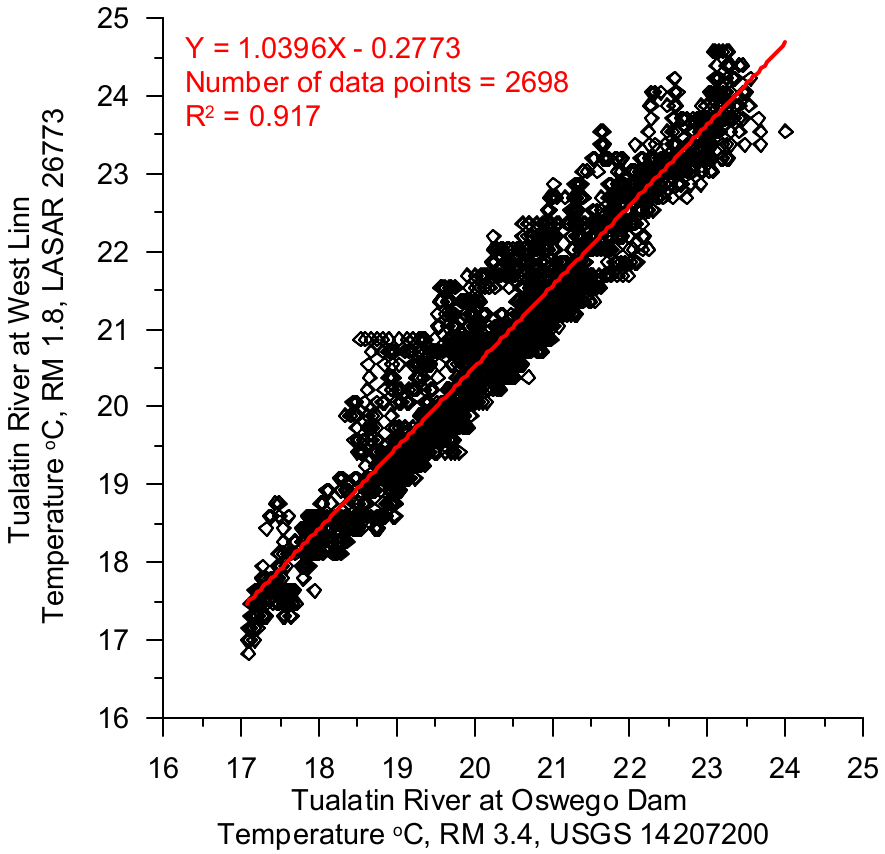


**Figure 171. Temperature correlation between the Tualatin River at Oswego Dam and at West Linn**

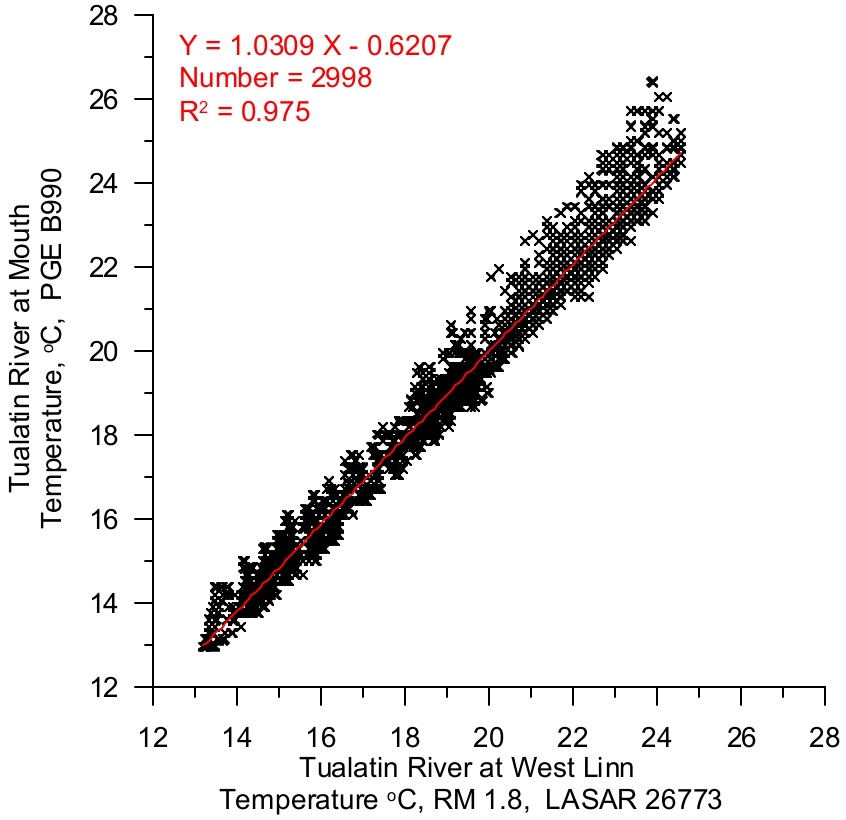


**Figure 172. Temperature correlation between the Tualatin River at West Linn and the mouth**

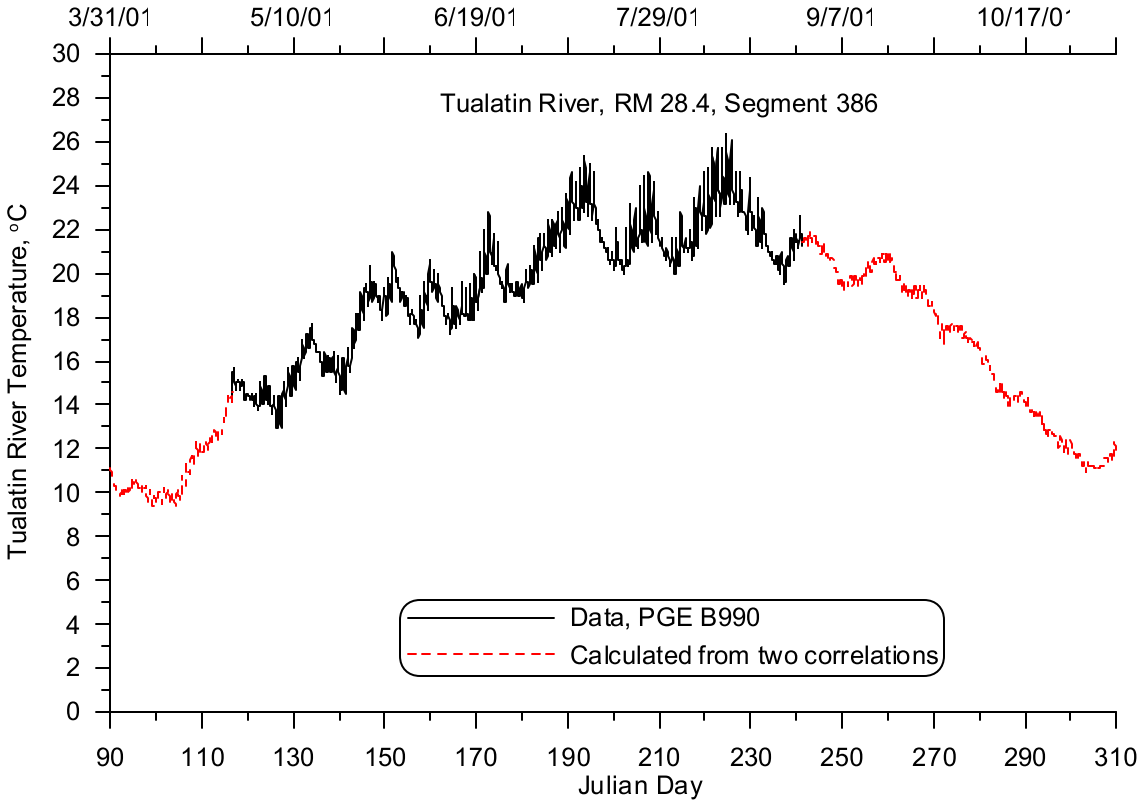


**Figure 173. Tualatin River temperature, 2001**

Temperature data for Mill Creek were monitored on a continuous basis during 2001 by ODEQ (LASAR 26759). The data set began on June 7, 2001, so to fill the data gap from April 1 to June 7 a temperature correlation was developed between the Mill Creek monitoring site and the Willamette River at Keizer site (USGS 14192015) as shown in Figure 174. Figure 175 shows the temperature time series data and calculated values for the model input.

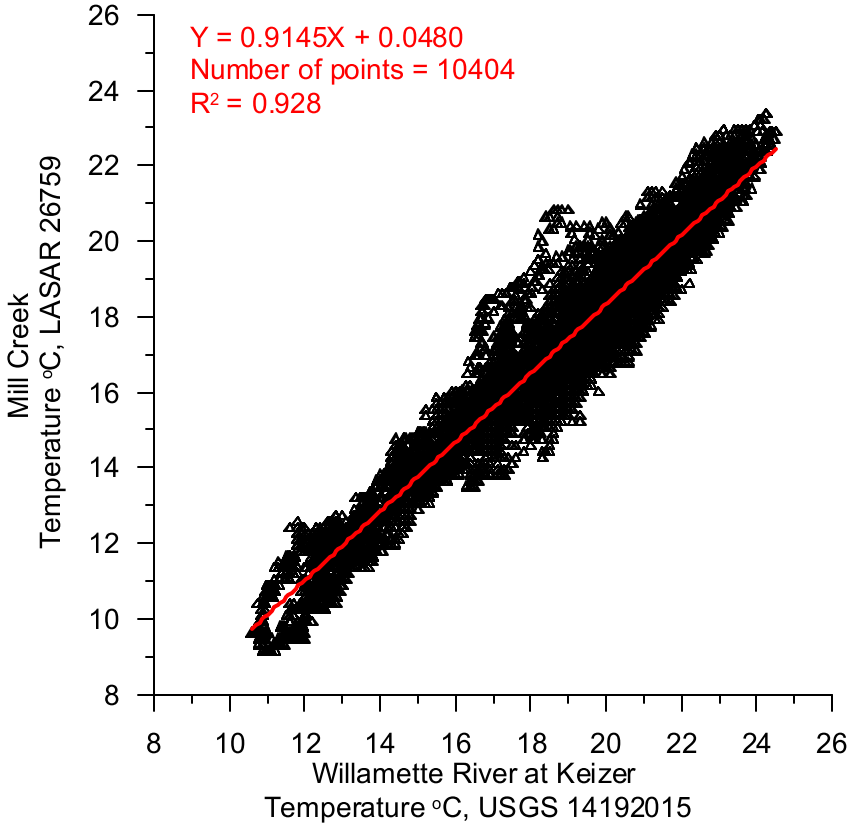


**Figure 174. Temperature correlation between the Willamette River and Mill Creek**

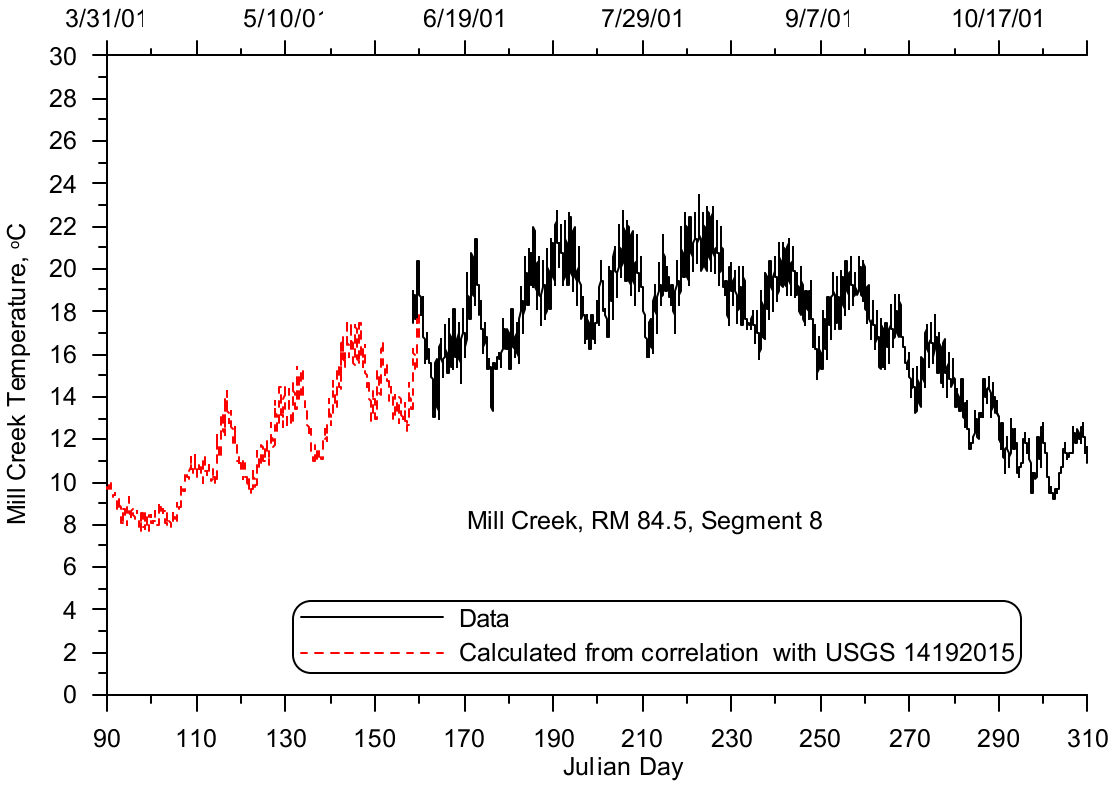


**Figure 175. Mill Creek temperature, 2001**

## Year 2002

The Yamhill River water temperatures were monitored by ODEQ in 2002. Monitoring started on May 24 and ended on October 23 which left gaps in the data from April 1 to May 24 and from October 23 to October 31. A temperature correlation was developed between this monitoring site and the monitoring site on the Willamette River at Keizer. Figure 176 shows the temperature correlation and the correlation equation used. Figure 177 shows the temperature series data and calculated values used to fill the data gaps for 2002.

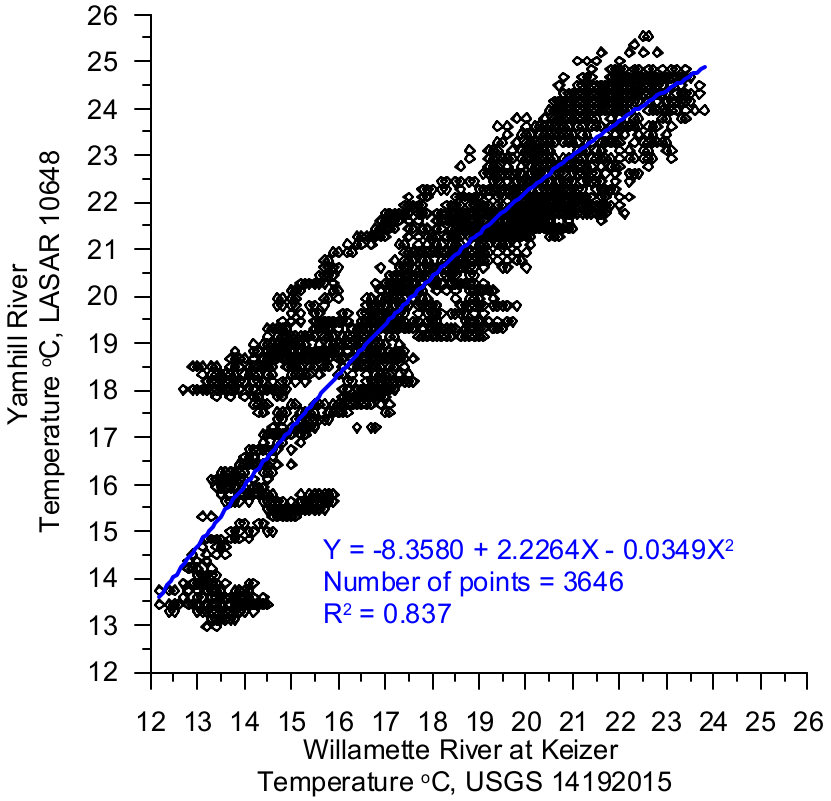


**Figure 176. Temperature correlation between the Willamette River and the Yamhill River**

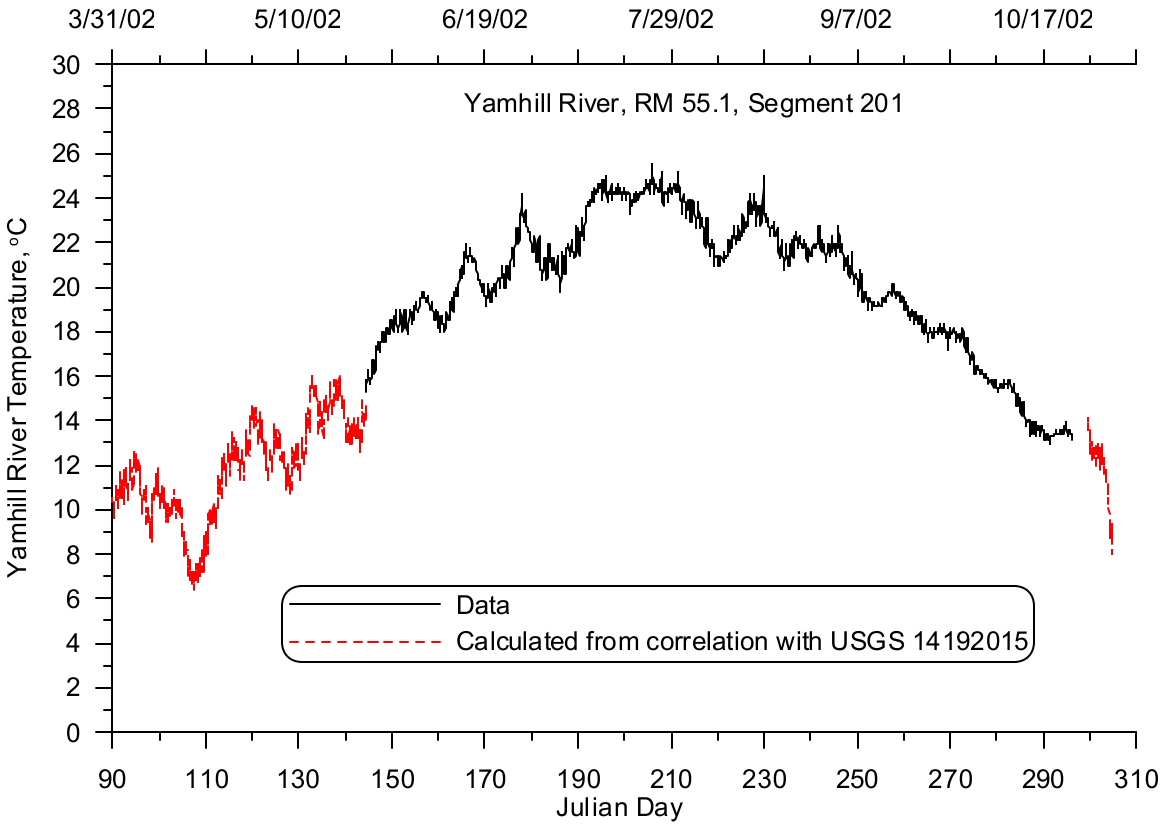


**Figure 177. Yamhill River temperature, 2002**

The two temperature monitoring sites in the Molalla River basin were on the Molalla River and the Pudding River above their confluence. The temperature records for each tributary were completed and a volume weighted temperature was calculated for the basin.

The Pudding River was monitored from June 10 to October 4 (LASAR 10917). The data gaps were filled by using a correlation with the gage on the Willamette River at Keizer (USGS 14192015) as shown in Figure 178. The flow for the Pudding River was computed based on the USGS gage station (14201340) and on applying the fraction of drainage basin above the gage to the whole basin. The same method was used in developing the Molalla basin inflow record. Figure 179 shows the temperature data, calculated temperature values, and the flow for Pudding River.

The Molalla River was limited to the same time period as the gage on the Molalla River (LASAR 10637). A temperature correlation was developed with the monitoring site on the Willamette River at Keizer (USGS 14192015) as shown in Figure 180. The flow for the Molalla River was based on the USGS gage: 14200000. Figure 181 shows the temperature data and calculated temperature values and the flow for Molalla River.

The completed temperature records were then used with flow from each tributary to calculate a volume temperature for the combined flows of the pudding and Molalla Rivers. Figure 182 shows the volume weighted temperature for the basin for 2002.

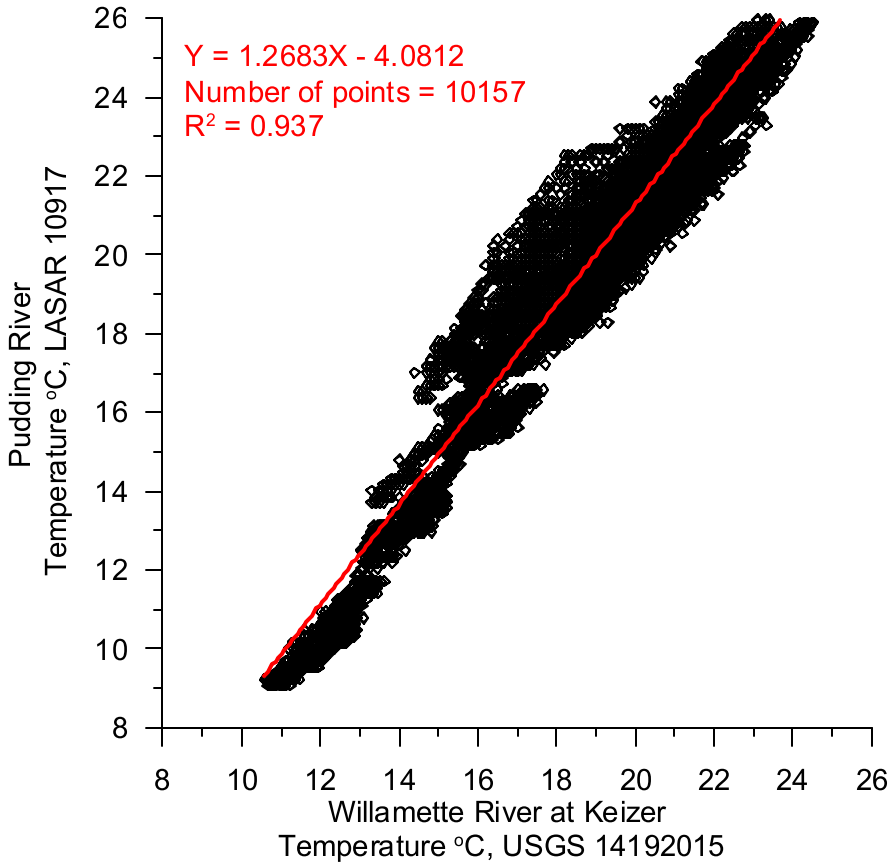


**Figure 178. Temperature correlation between the Willamette River and the Pudding River**

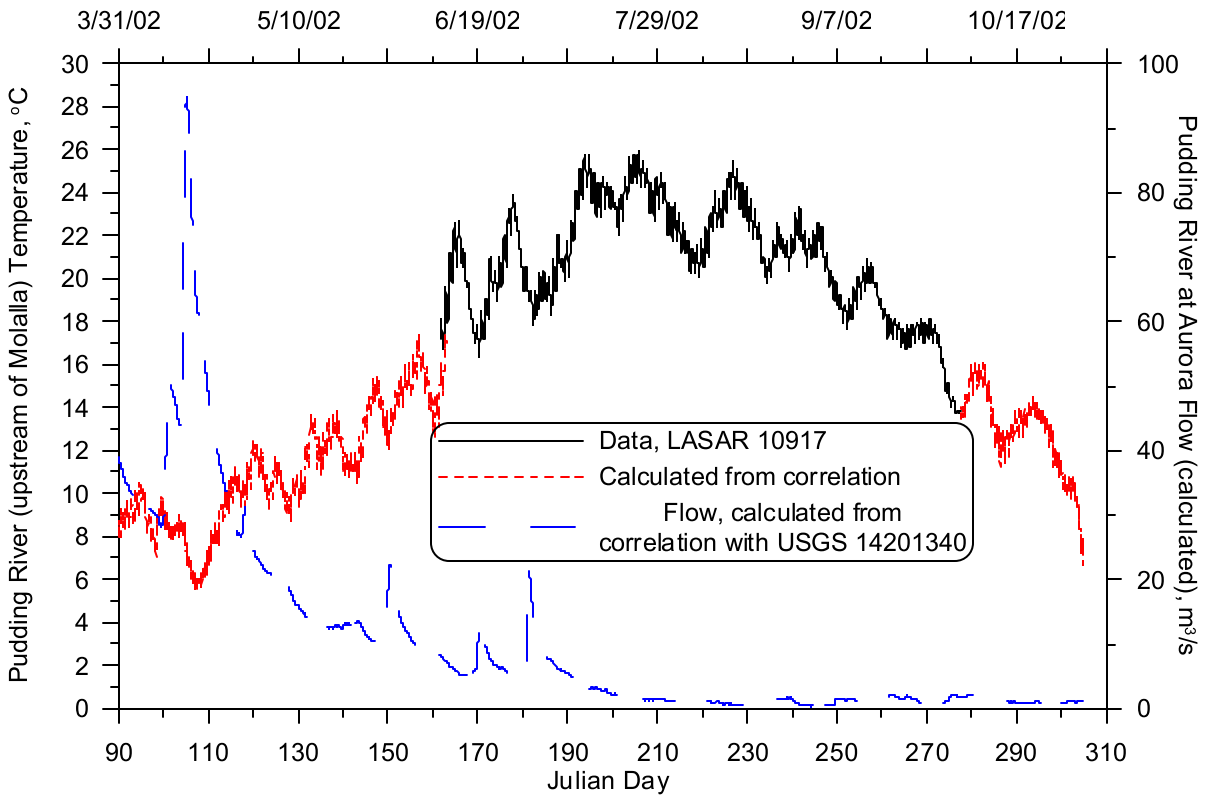


**Figure 179. Flow and temperature for the Pudding River upstream of the confluence with the Molalla River**

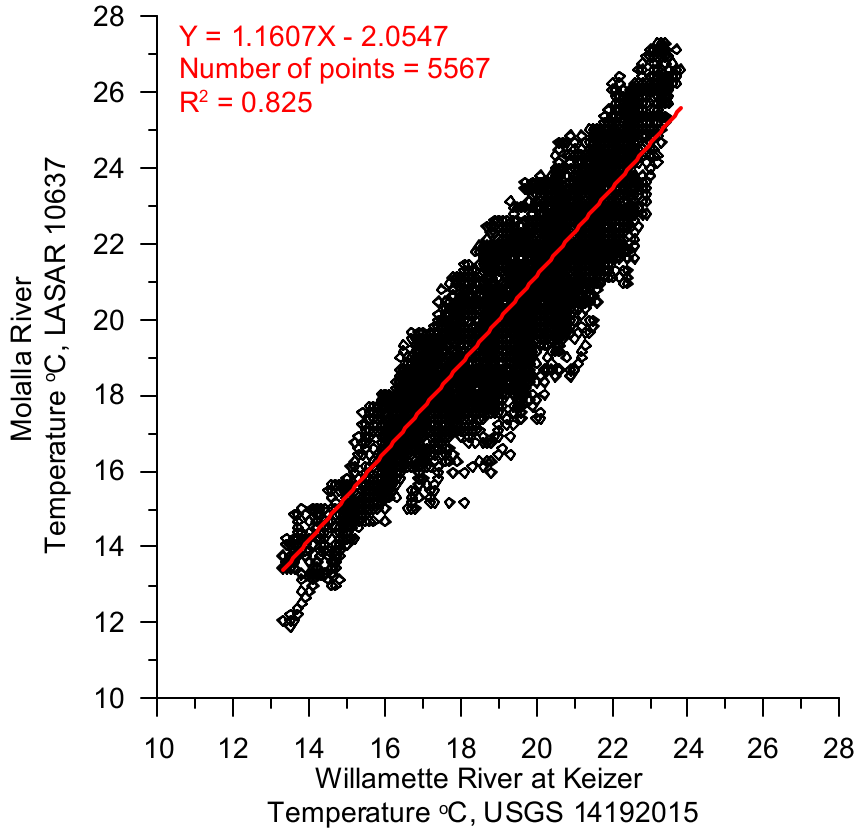


**Figure 180. Temperature correlation with data from the Molalla River and the Willamette River at Keizer**

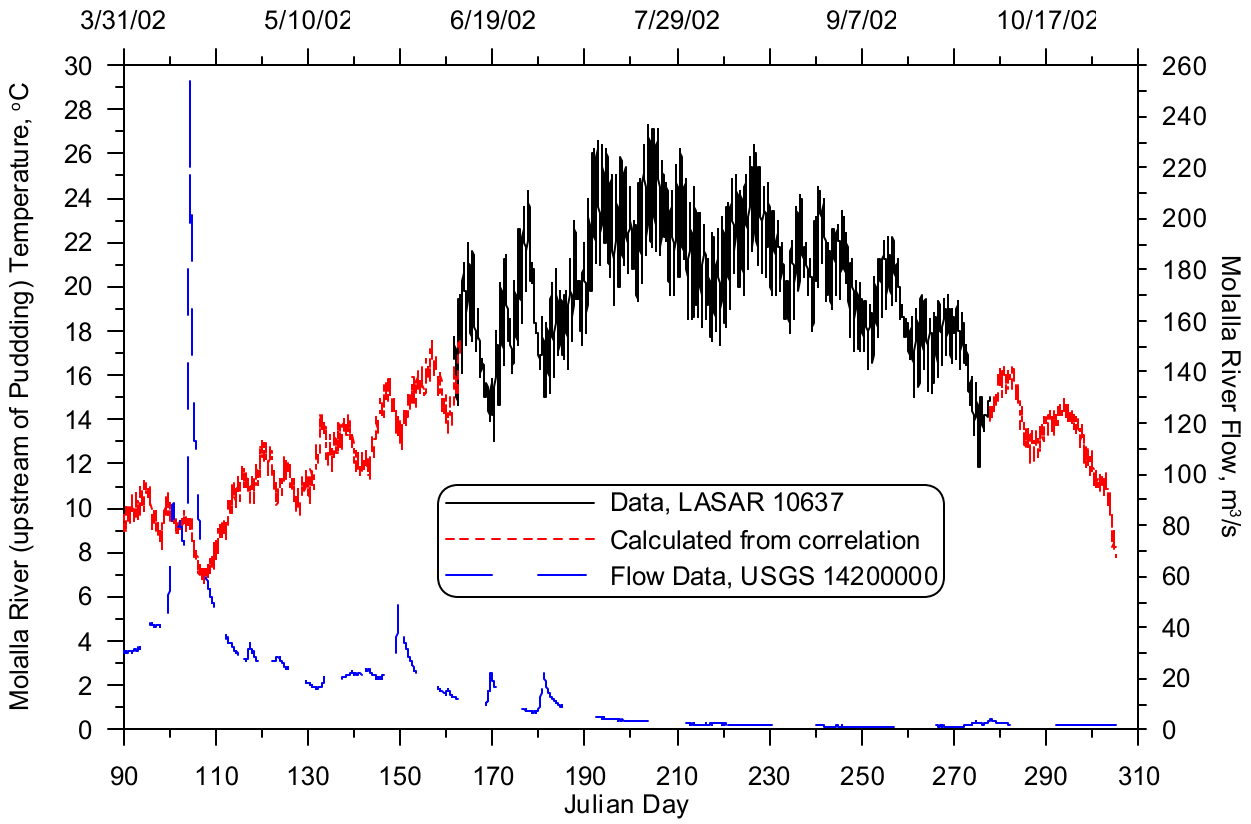


**Figure 181. Flow and temperature for the Molalla River upstream of the confluence with the Pudding River**

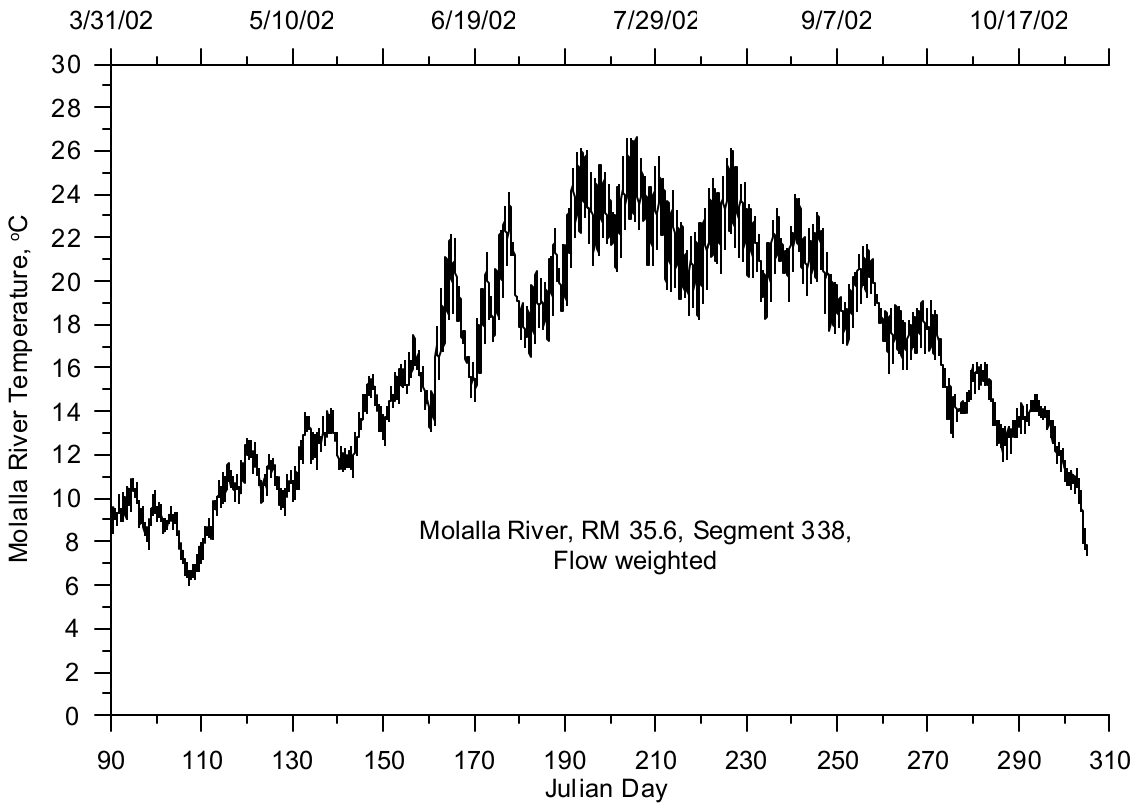


**Figure 182. Molalla River basin temperature, 2002**

In 2002 the mouth of the Tualatin River was monitored from May 23 to October 23 (LASAR 10626). The data gaps in the time series record were filled by developing a temperature correlation with data monitored at the Oswego Dam, RM 3.4 (USGS 14207200). Figure 183 shows the temperature correlation between the two sites. Figure 184 shows the completed temperature record with data and calculated values.

Temperature was monitored in Mill Creek from June 13 to October 23. The data gaps were filled using the same temperature correlation developed for 2001. The correlation and equation can be found in Figure 174. Figure 185 shows the Mill creek temperature data and the calculated temperature for 2002.

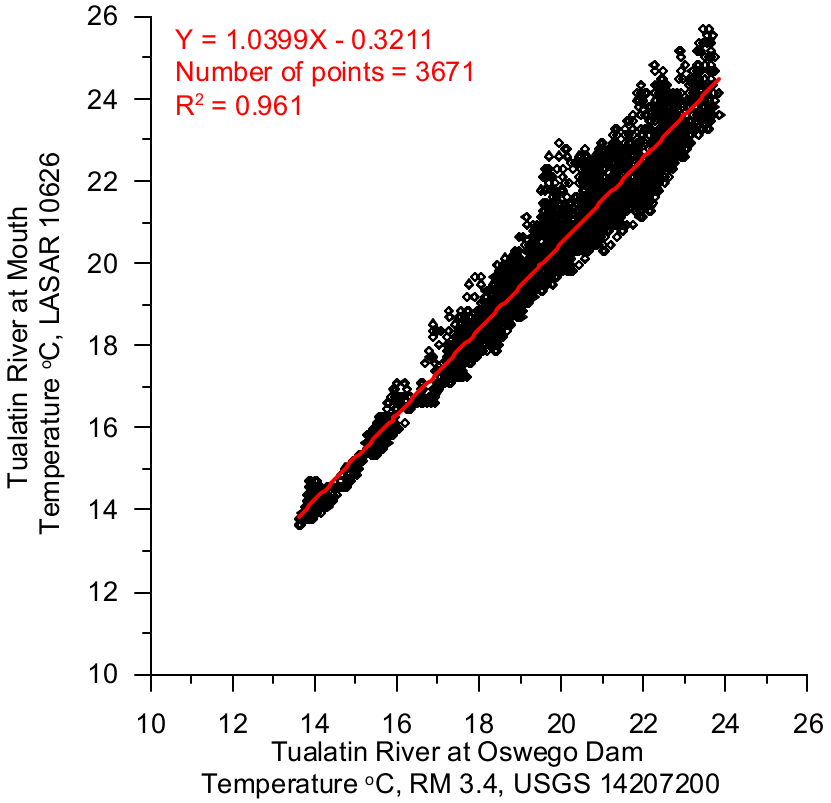


**Figure 183. Temperature correlation between the Tualatin River at Oswego Dam and the mouth**

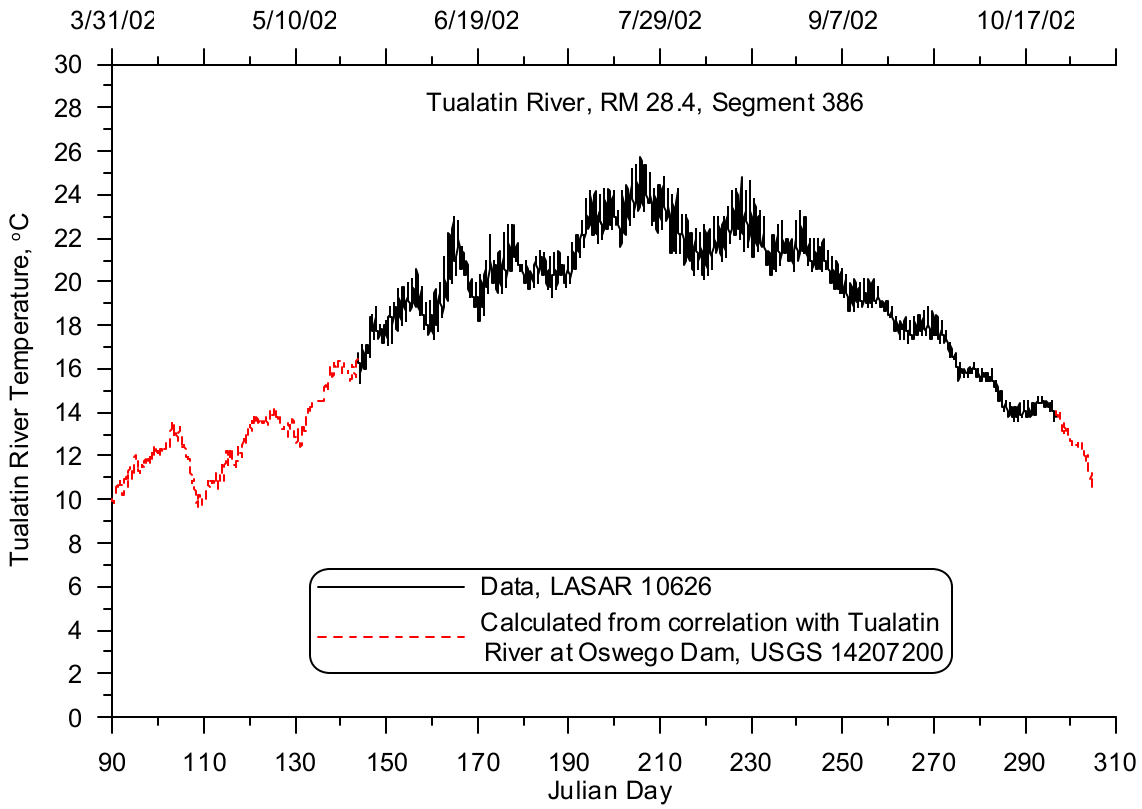


**Figure 184. Tualatin River temperature, 2002**

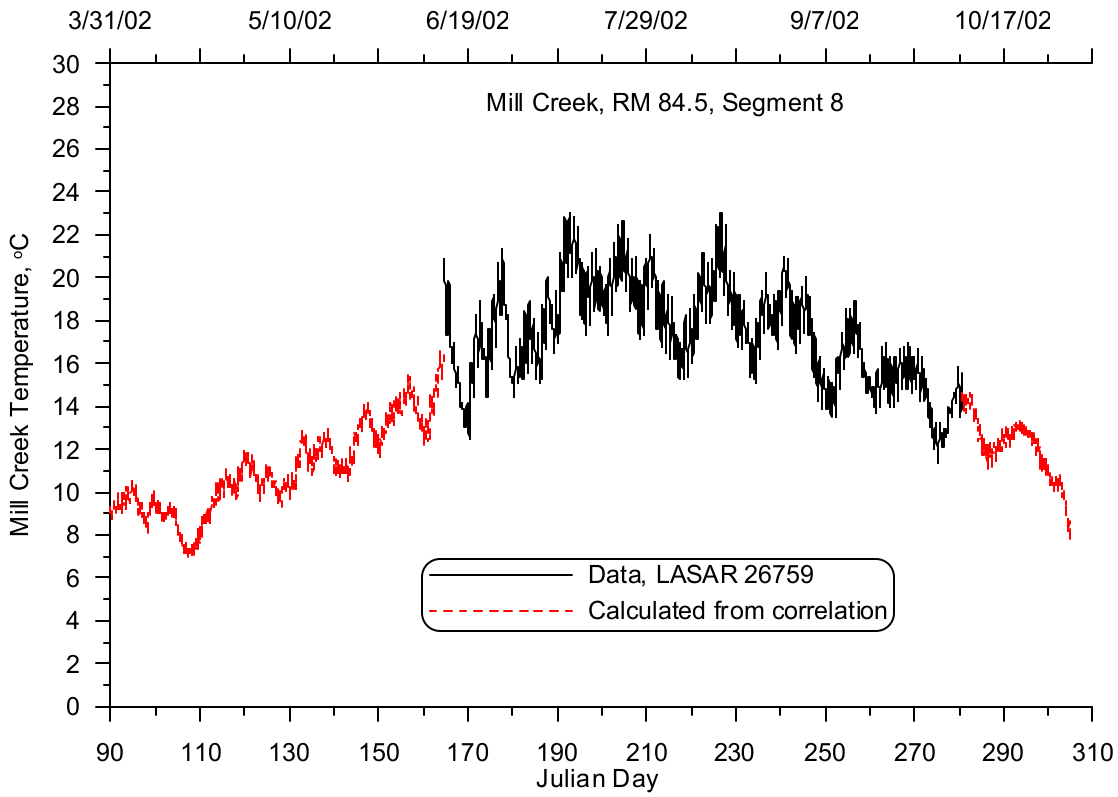


**Figure 185. Mill Creek temperature, 2002**

## *Distributed Tributaries*

In addition to the four main tributaries contributing flow to the Middle Willamette River model, there is also an ungaged drainage area adjacent to the river channel from Salem to the Willamette Falls (RM 85.4 -26.8). Figure 186 shows a map of the Middle Willamette River with the ungaged drainage area identified next to the river. This area represents approximately 976.4 $km^2$ or 3.8 % of the drainage area to the Middle Willamette River.

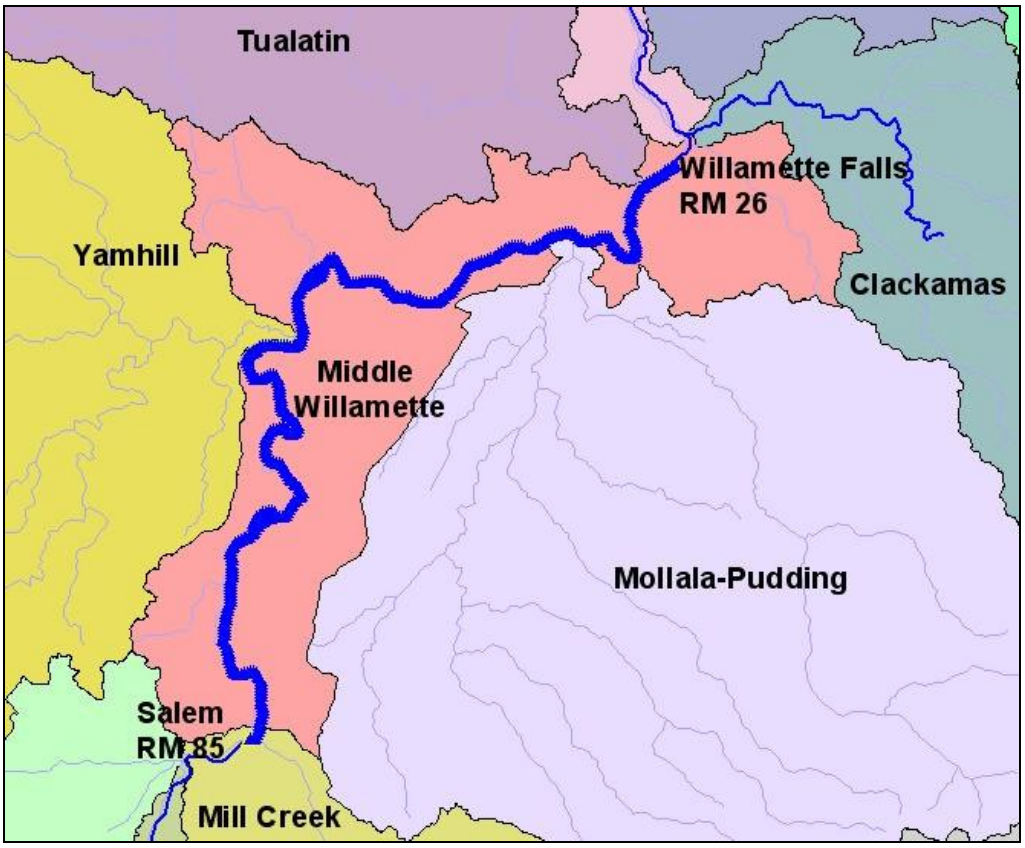


**Figure 186. Middle Willamette River ungaged drainage area adjacent to the river**

### Hydrodynamic Data

#### Year 2001

The majority of the inflows to the Middle Willamette River came from the tributaries described above, but there may be some inflows from distributed sources, such as ungaged areas like Chehalem Creek.

The U.S. Army Corps of Engineers developed a UNET Model for the Lower Columbia (Knutson, 2000). The modeling effort included developing a routing method to estimate the daily flows in the Willamette River at Portland. The flow routing model incorporated a correlation for estimating the ungaged flow between Salem and the Willamette Falls (i.e. the Middle Willamette). The equation from Knutson, 2000 was:

$$UngagedQ = PuddingRiver\_AuroraQ\left(\frac{Ungaged\_drainage\_area,\_377\_mi^2}{PuddingRiveratAurora\_drainage\_area,\_479\_mi^2}\right)$$

Daily flows were used from the gage station on the Pudding River at Woodburn to estimate flows on the Pudding River at Aurora. The calculated flows at Aurora were then used with equation above to estimate the total distributed inflows.

Since the drainage area in question is adjacent to the river from Salem to the Willamette Falls and crossed three model water bodies, the flows were divided between four branches along the river by using the fractional lineal distance along the river. For example, Branch 5 represented 45% of the total lineal distance from Salem to the Willamette Falls so 45% of the distributed inflow was allocated to Branch 5. Figure 187 shows the total and allocated -distributed inflows for each model branch.

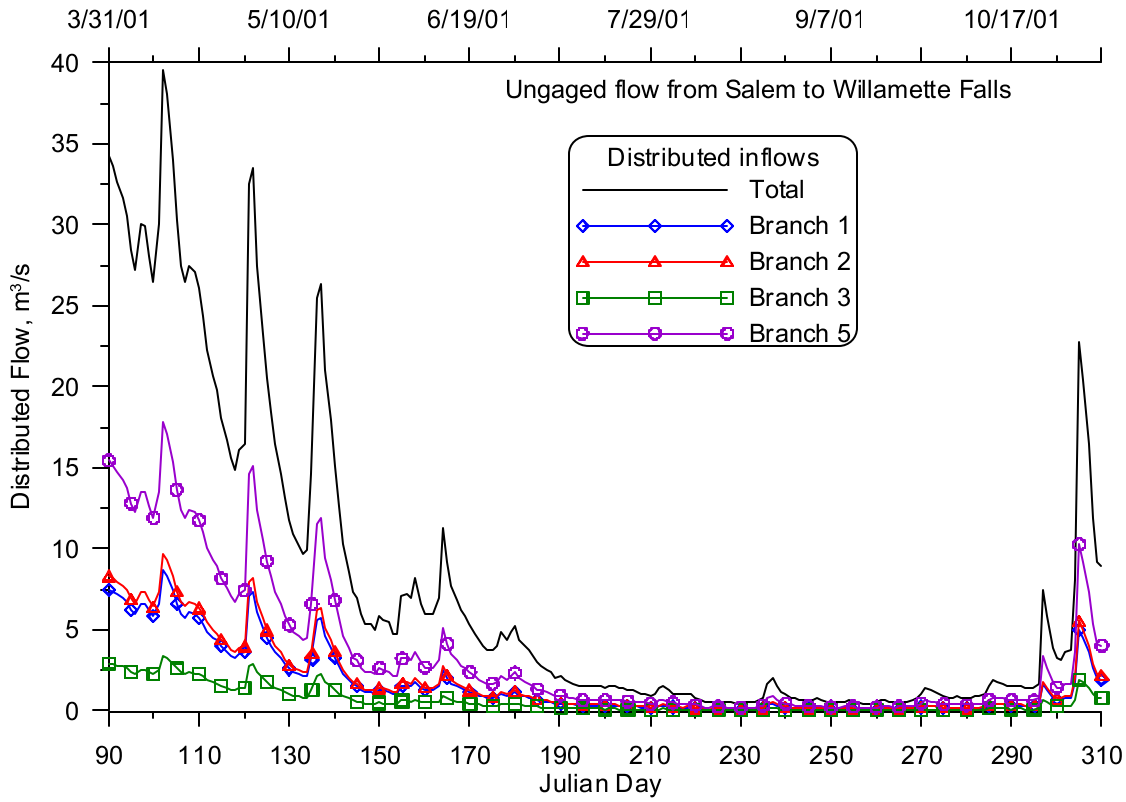


**Figure 187. Middle Willamette River model distributed tributary inflows, 2001**

## Year 2002

Distributed tributary flows for each model branch developed for 2002 were based on the work of Knutson, 2000 and the lineal distances of the model branches along the river. The same procedure used for 2001 was also used for 2002. Figure 188 shows the total and fraction of distributed inflows for each model branch between Salem and the Willamette Falls.

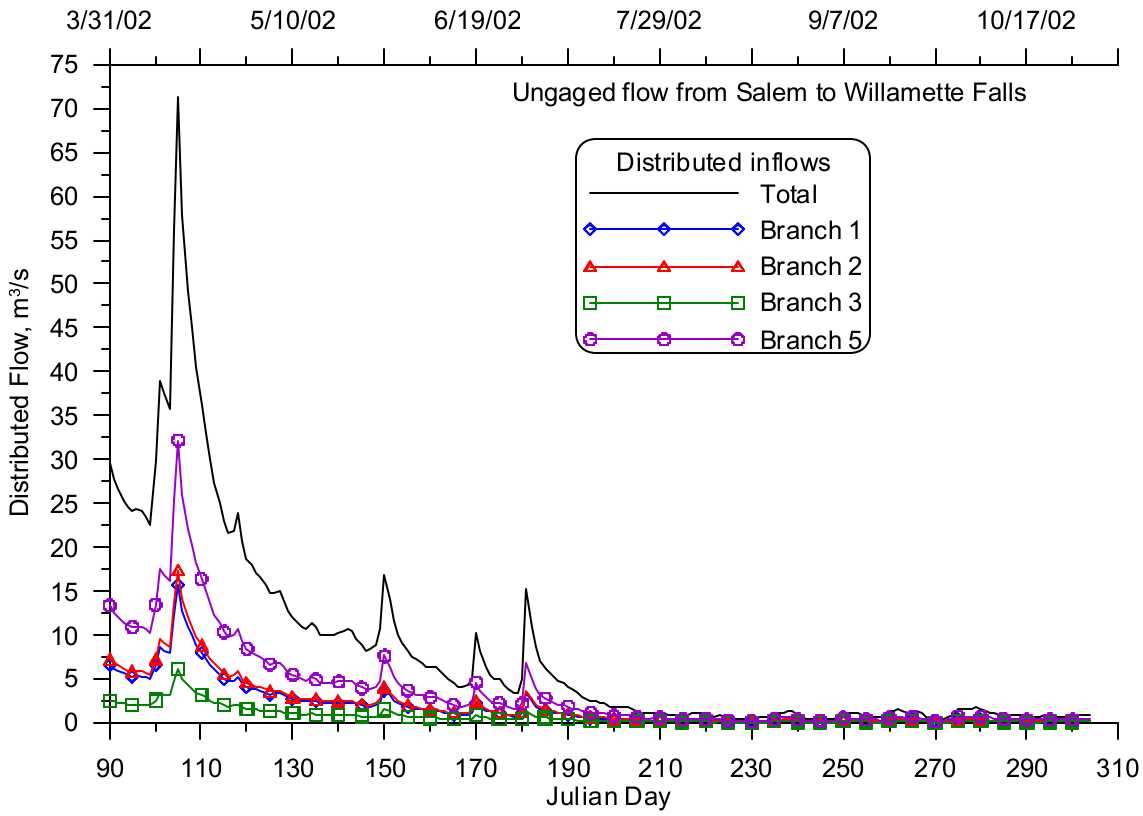


**Figure 188. Middle Willamette River model distributed tributary inflows, 2002**

## Temperature Data

### Year 2001

There are four distributed tributaries to the Middle Willamette River. Since there were no monitored temperature data for the ungaged tributaries, nearby river temperature records were used. The first model branch used the temperature time series record developed for Mill Creek for 2001. Branches 2, 3 and 5 used the inflow temperature for the Yamhill River. Figure 189 shows the temperature time series for all four of the distributed inflows.

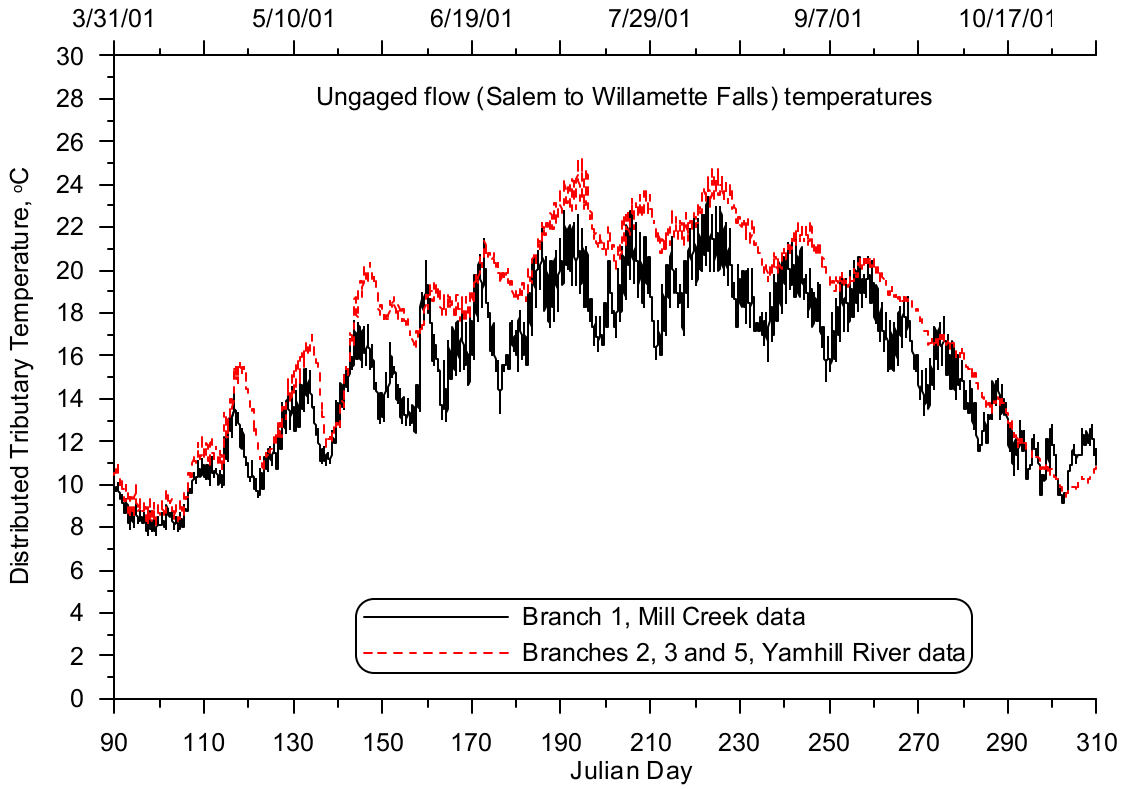


**Figure 189. Middle Willamette River model distributed tributary temperature, 2001**

## Year 2002

The four distributed tributaries to the Middle Willamette River developed for the 2001 model were also included in the 2002 model. The same methodology used for 2001 was used for 2002. The first model branch used the temperature time series record developed for Mill Creek and branches 2, 3 and 5 used the inflow temperature for the Yamhill River. Figure 190 shows the temperature time series for the four distributed inflows in 2002.

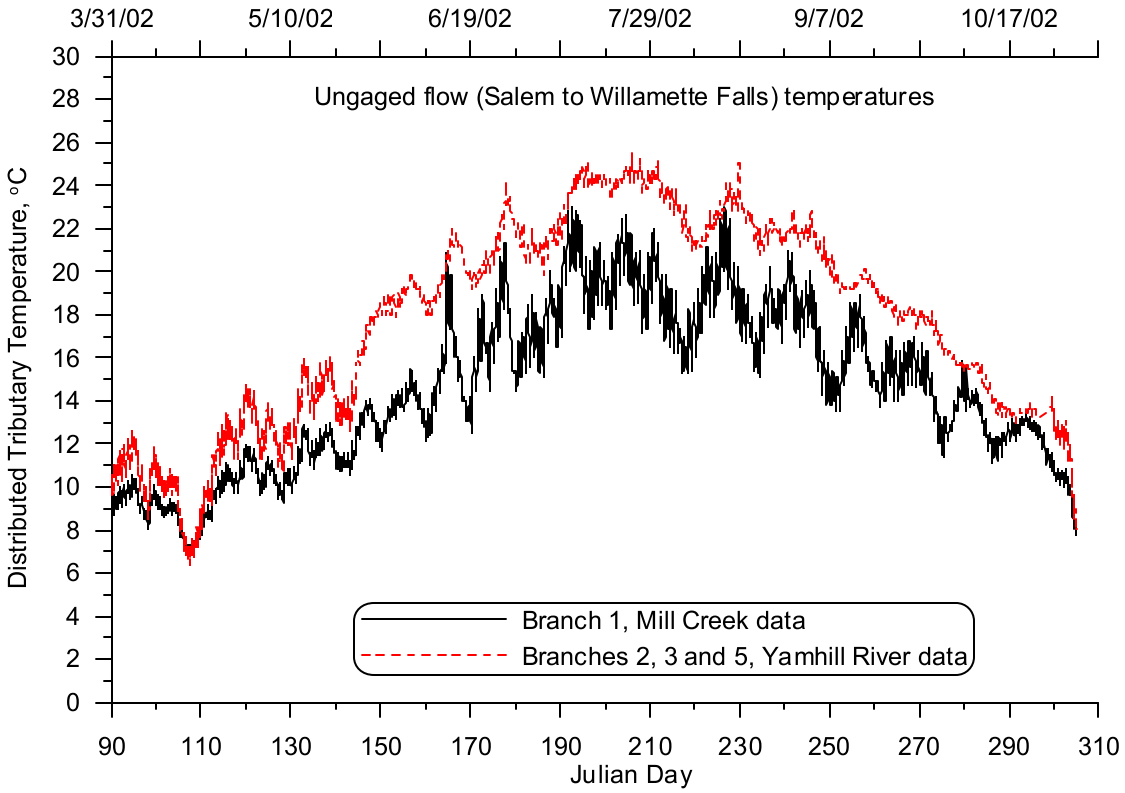


**Figure 190. Middle Willamette River model distributed tributary temperature, 2002**

## *Point Sources*

The Middle Willamette River extends from Salem, Oregon, RM 85.4, to the Willamette Falls at RM 26.8. ODEQ identified six major point source discharges along the Middle Willamette River model area on the basis of permitted discharges. Figure 191 shows the location of the point sources for the Middle Willamette River, and Table 23 lists the point source names and their respective river mile and model segment number.

The total discharge from the six point sources was generally less than 3 $m^3/s$, which was approximately 1.0 to 1.5% of the summer main stem Willamette River flow.

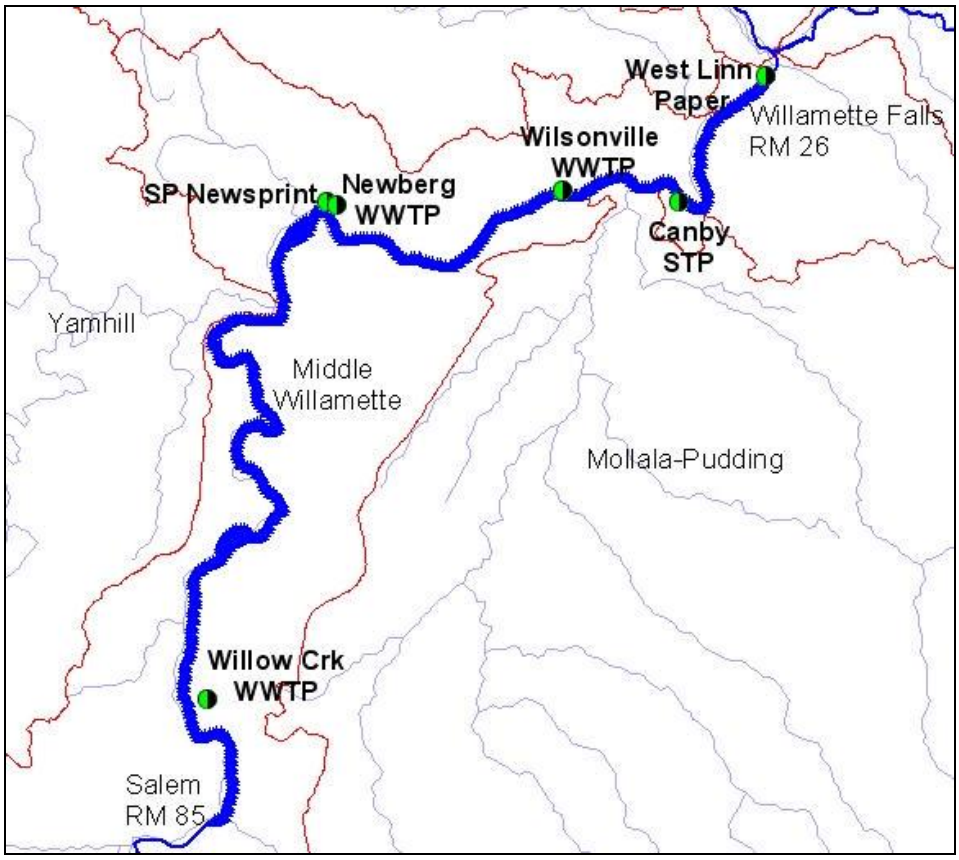


**Figure 191. Middle Willamette River model Point Source locations**

**Table 23. Middle Willamette River model points sources**

| Model Segment | Facility Name | Willamette River Mile |
|---|---|---|
| 42 | Willow Creek WWTP (City of Salem) | 78.9 |
| 245 | SPNewsprint | 50.2 |
| 246 | City of Newberg WWTP | 50.0 |
| 318 | City of Wilsonville WWTP | 38.9 |
| 353 | City of Canby STP | 33.4 |
| 396 | West Linn Paper Company | 26.2 |

## Hydrodynamic Data

### Year 2001

Flow data for the City of Salem wastewater treatment plant discharge (Willow Creek treatment plant) were provided by the City of Salem and ODEQ. The data represent hourly flows records from May 10 to October 24 and daily recorded data from April 1 to May 10 and from October 24 to October 31. Figure 192 shows the discharge flow recorded over 2001.

The SP Newsprint discharge rate for 2001 consisted of daily flow rates provided by ODEQ. Flows range from 0.3 to 0.7 $m^3/s$. Figure 193 shows the SP Newsprint flow for 2001. The City of Newberg

treatment plant discharges to the Willamette just downstream of the SP Newsprint plant. Daily flows were provided by ODEQ and are shown in Figure 194.

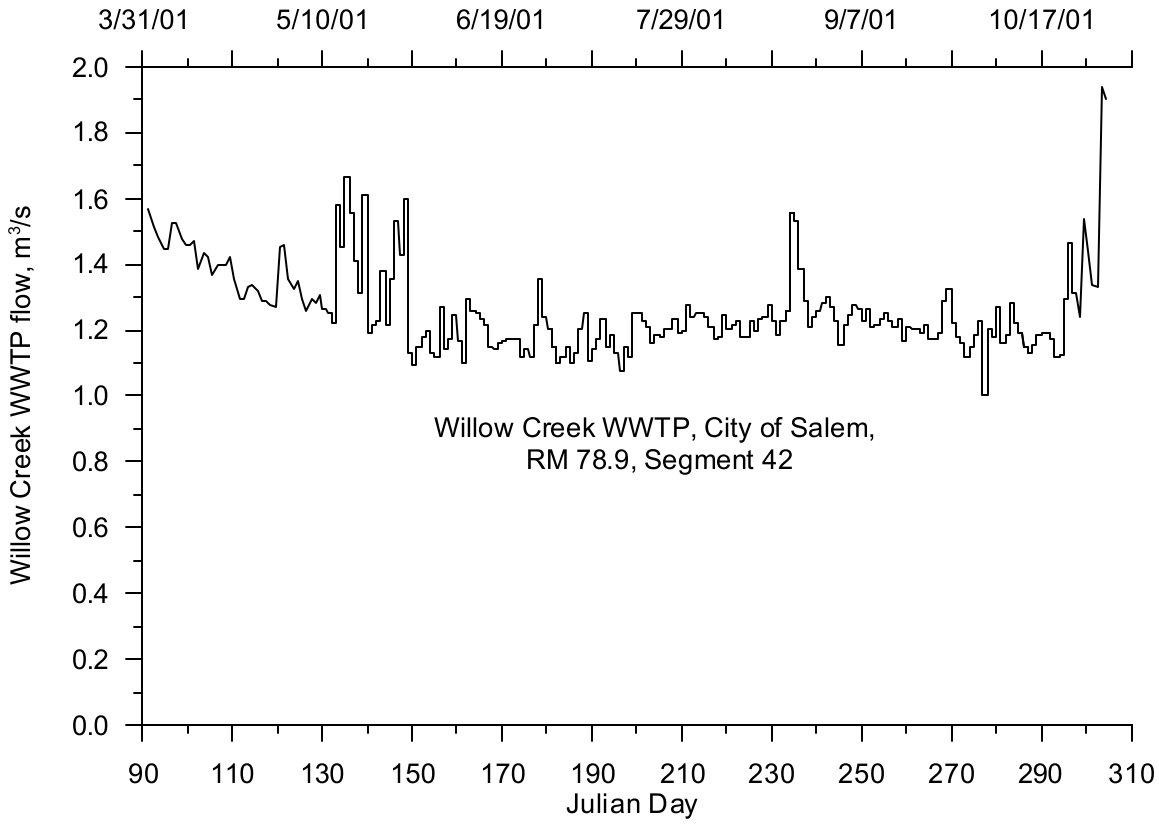


**Figure 192. City of Salem, Willow Creek Treatment Plant flow, 2001**

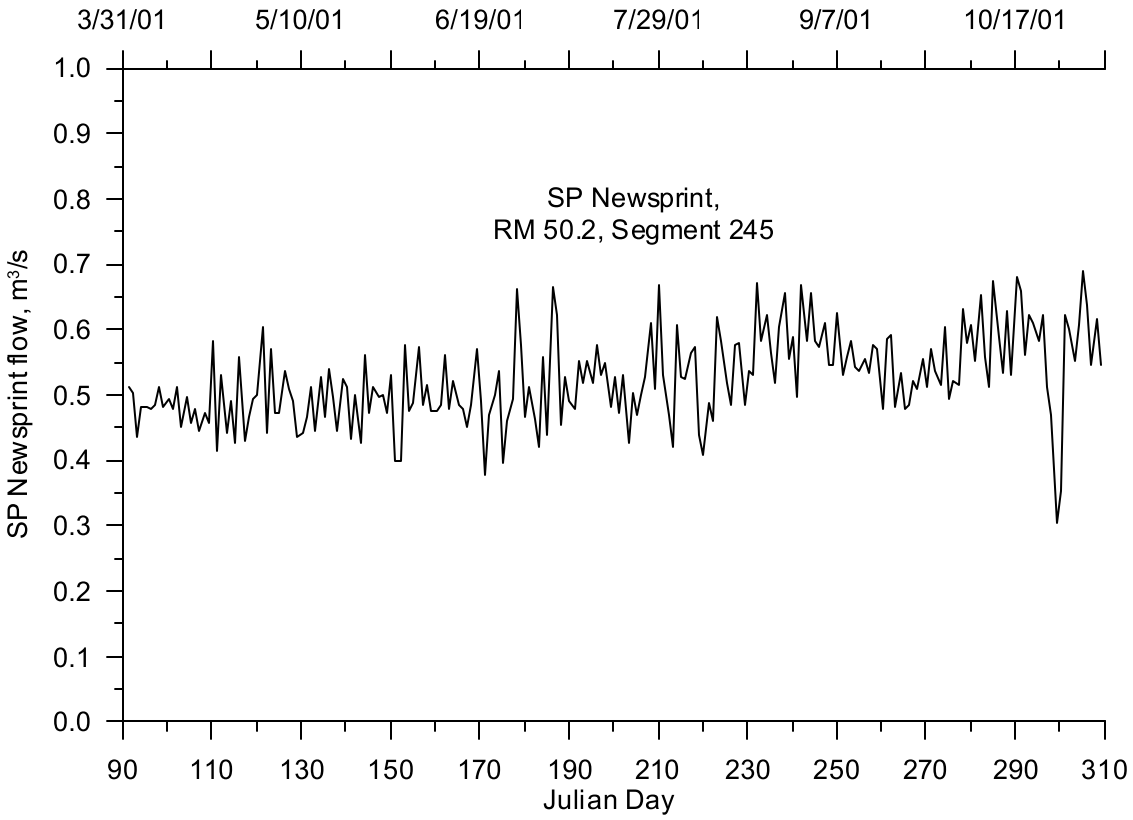


**Figure 193. SP Newsprint flow, 2001**

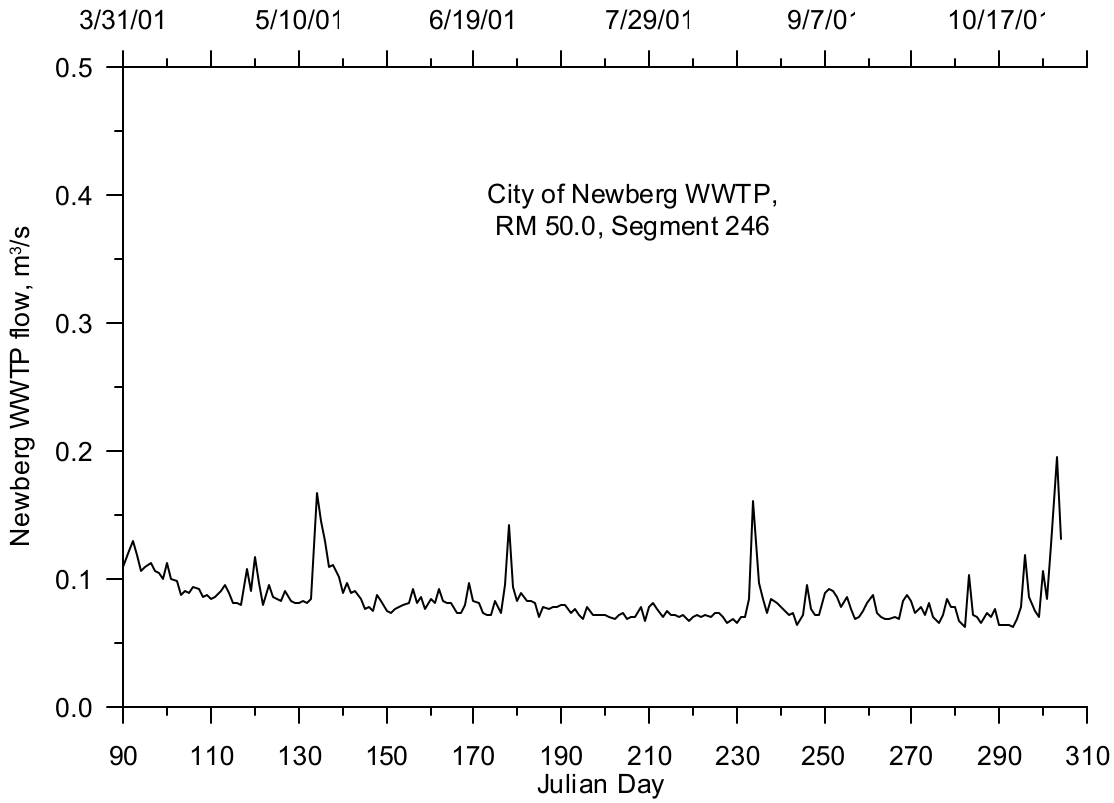


**Figure 194. City of Newberg, WWTP flow, 2001**

Flow data for the City of Wilsonville wastewater treatment plant discharge were obtained from the Daily Monitoring Reports (DMRs) submitted to the ODEQ. Figure 195 shows the discharge flow recorded over 2001. Discharge flow rates for the City of Canby treatment plant were provided on a monthly basis as shown in Figure 196. Discharge flow from the West Linn Paper Mill for 2001 consisted of daily flows from August 10 to October 31. There were no flow data available before August 10 so a constant flow rate of 0.18 $m^3/s$ was selected that was based on the flow rate after August 10. Figure 197 shows the paper mill flow for 2001.

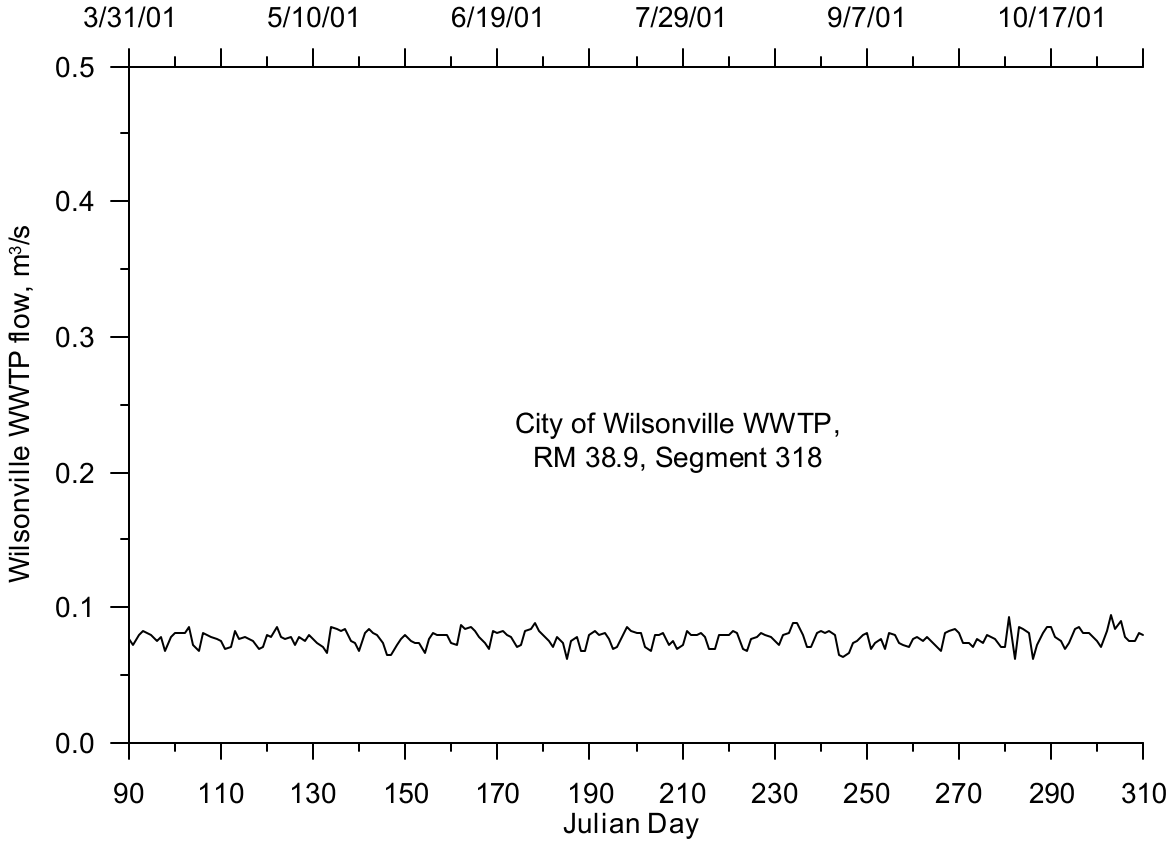


**Figure 195. City of Wilsonville Treatment Plant flow, 2001**

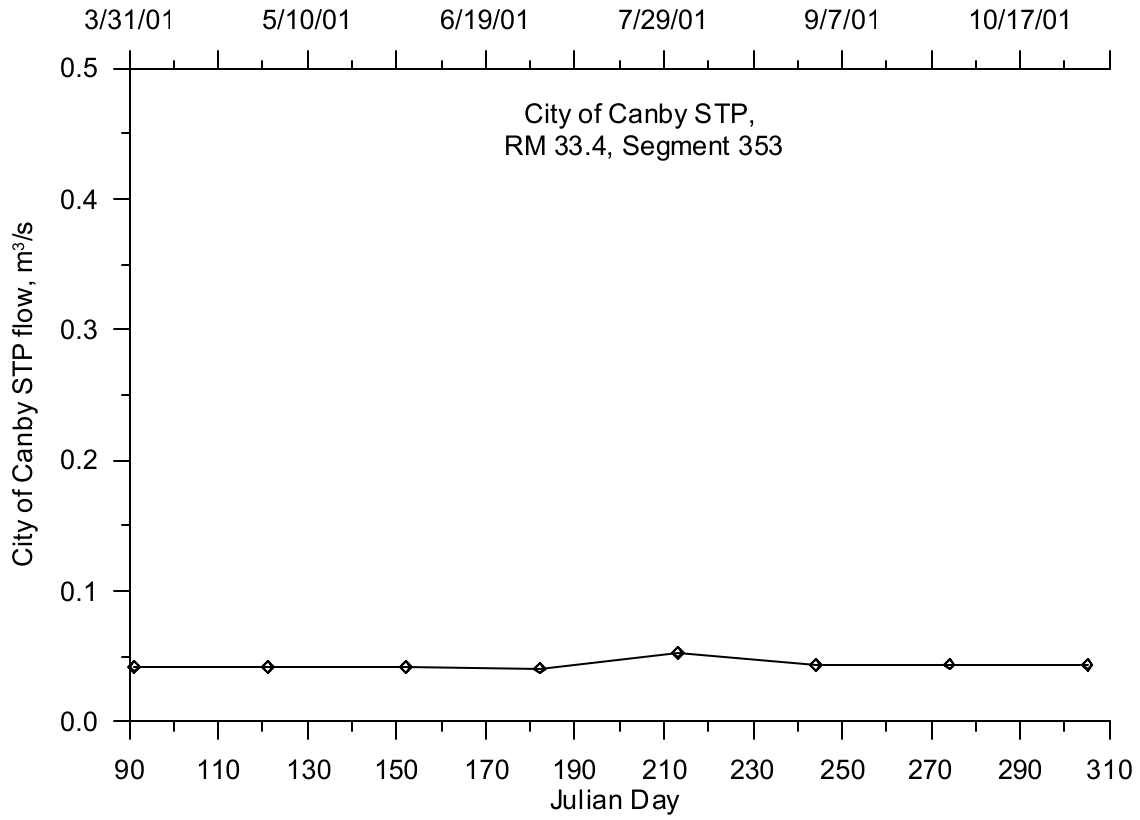


**Figure 196. City of Canby Treatment Plant flow, 2001**

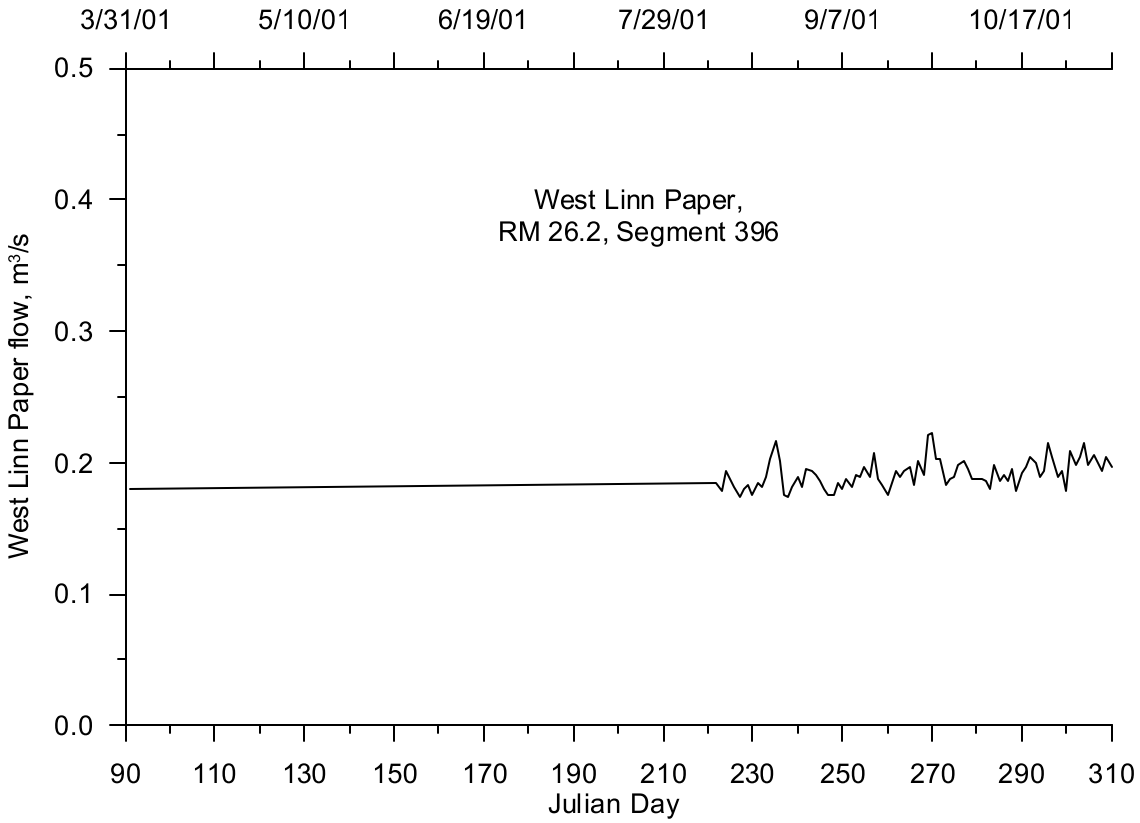


**Figure 197. West Linn Paper flow, 2001**

Year 2002

Flows for the City of Salem wastewater treatment plant discharge (Willow Creek treatment plant) were recorded daily from May 20 to October 31 in 2002. Since there were no data before May 20, a constant value was set between April 1 and May 20 based on the May 20 flow. Figure 198 shows the discharge flow recorded.

SP Newsprint discharge rate for 2002 consisted of daily flow rates provided by ODEQ as shown in Figure 199. The City of Newberg treatment plant discharge flow data were provided on a daily basis and are shown in Figure 200.

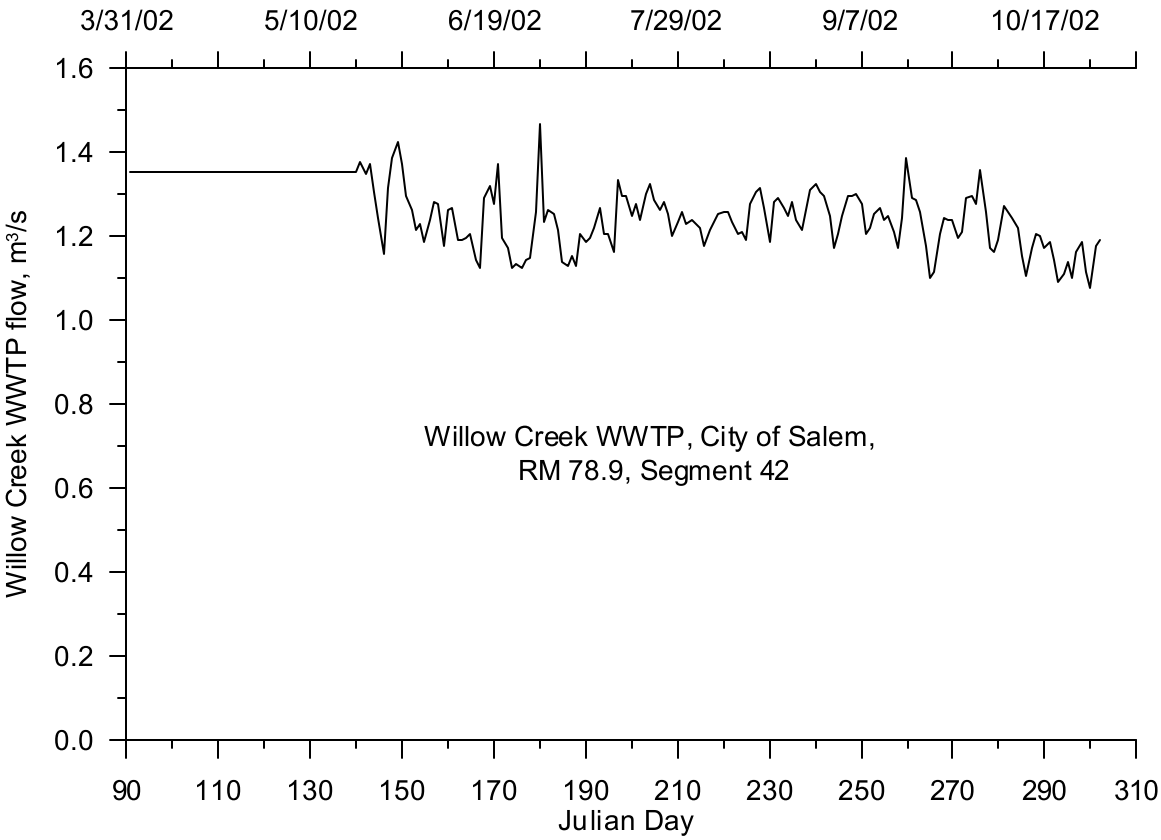


**Figure 198. City of Salem, Willow Creek Treatment Plant flow, 2002**

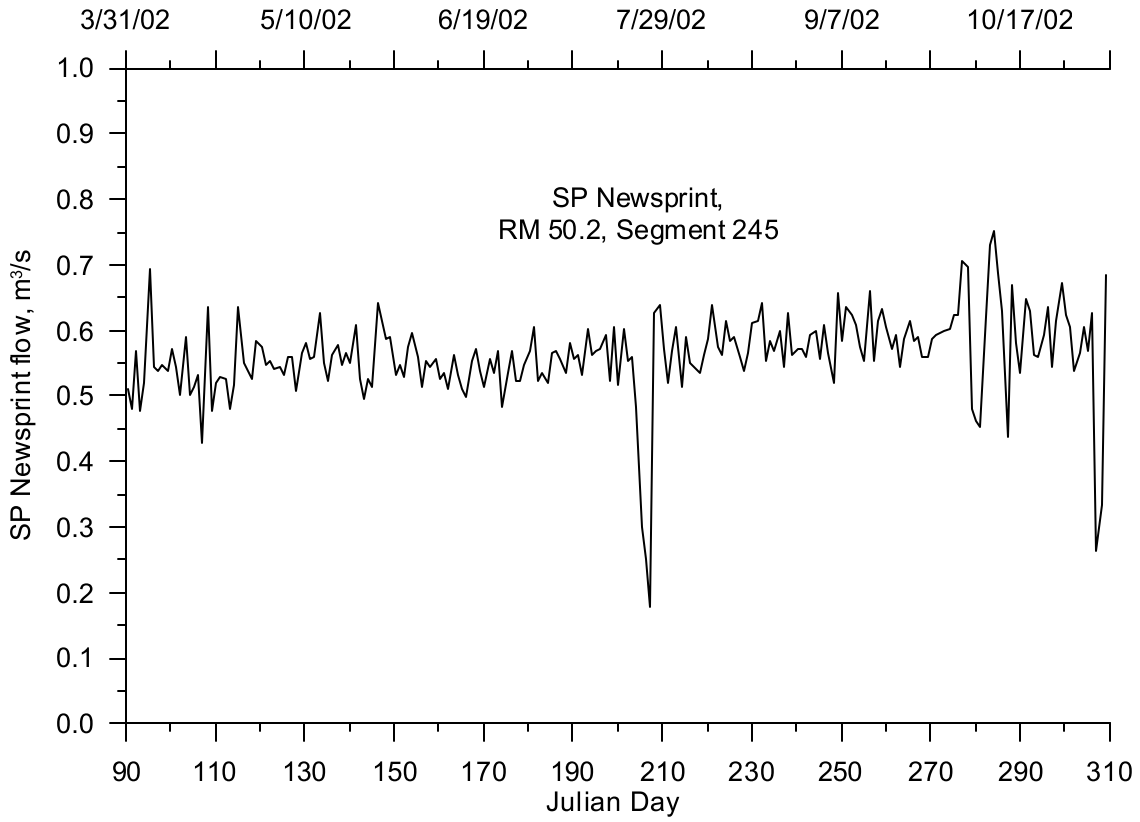


**Figure 199. SP Newsprint flow, 2002**

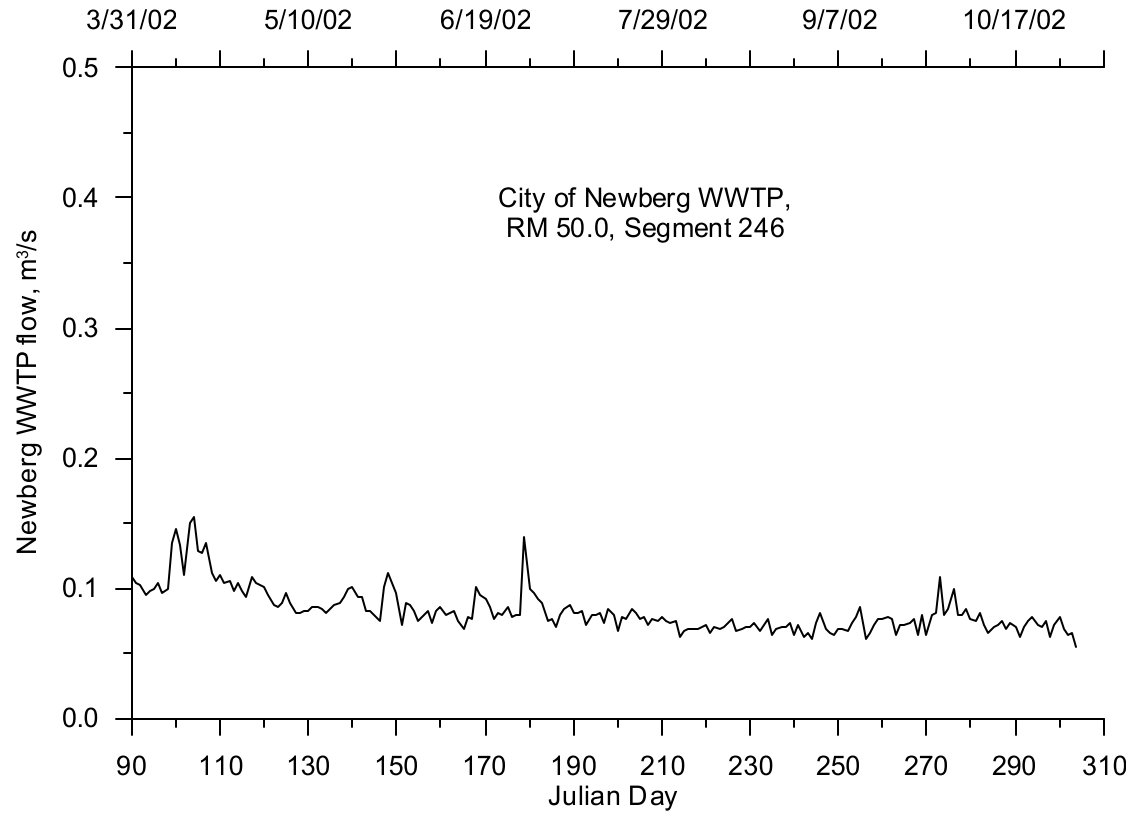


**Figure 200. City of Newberg, WWTP flow, 2002**

The City of Wilsonville wastewater treatment plant discharge flows were recorded daily and are shown in Figure 201. Discharge flow rates for the City of Canby treatment plant were provided on a monthly basis as shown in Figure 202. Discharge flow from the West Linn Paper Mill for 2002 consisted of daily flows, which are shown in Figure 203.

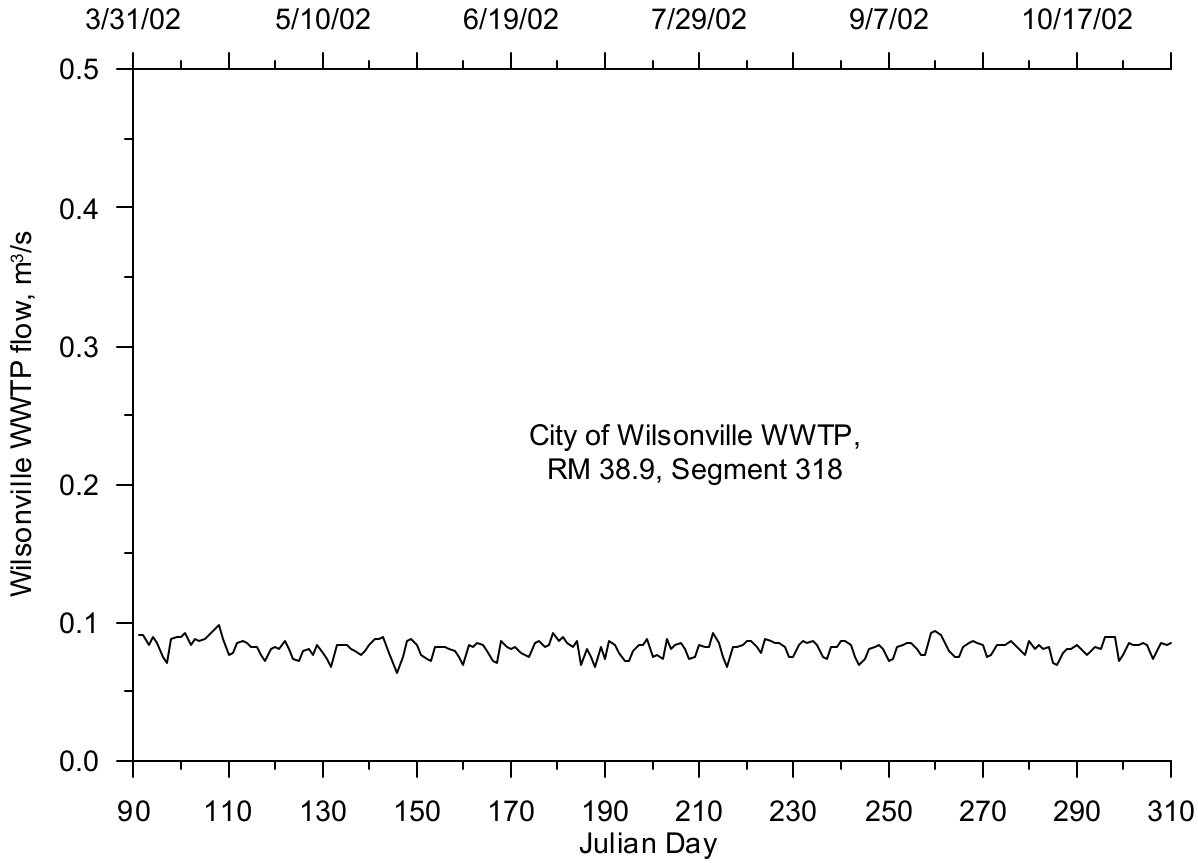


**Figure 201. City of Wilsonville Treatment Plant flow, 2002**

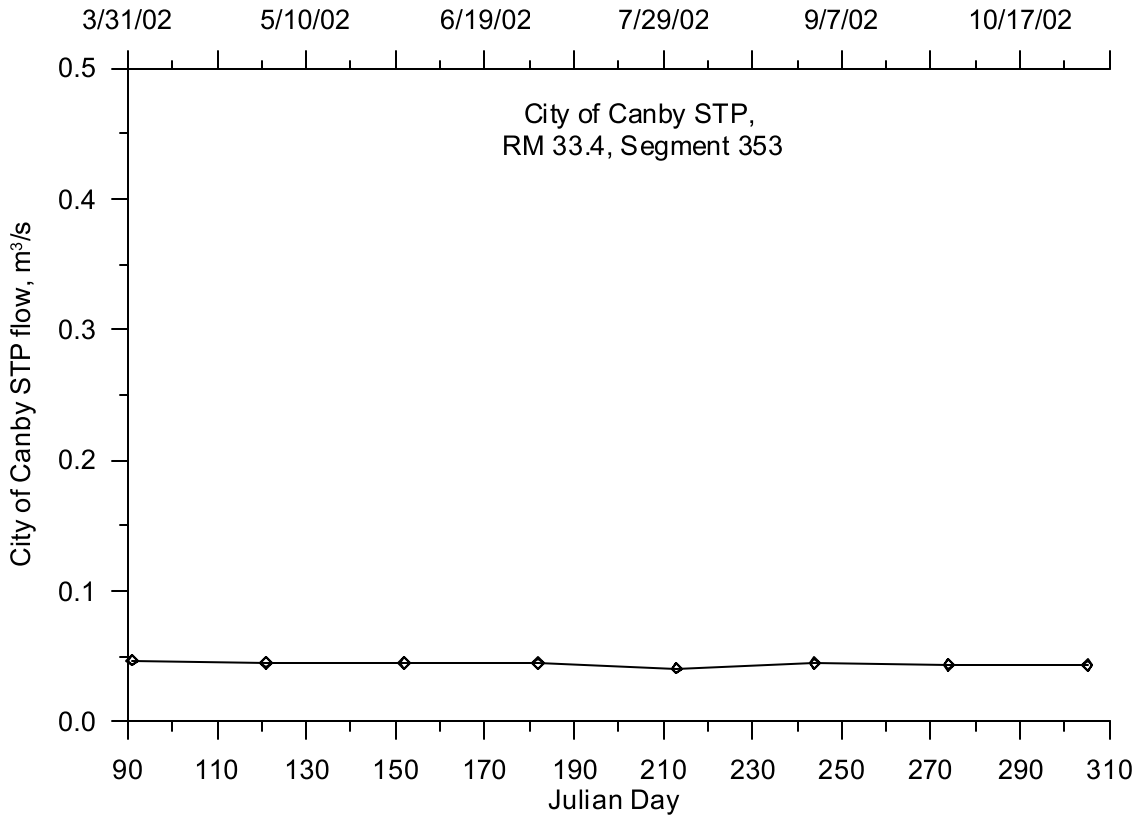


**Figure 202. City of Canby Treatment Plant flow, 2002**

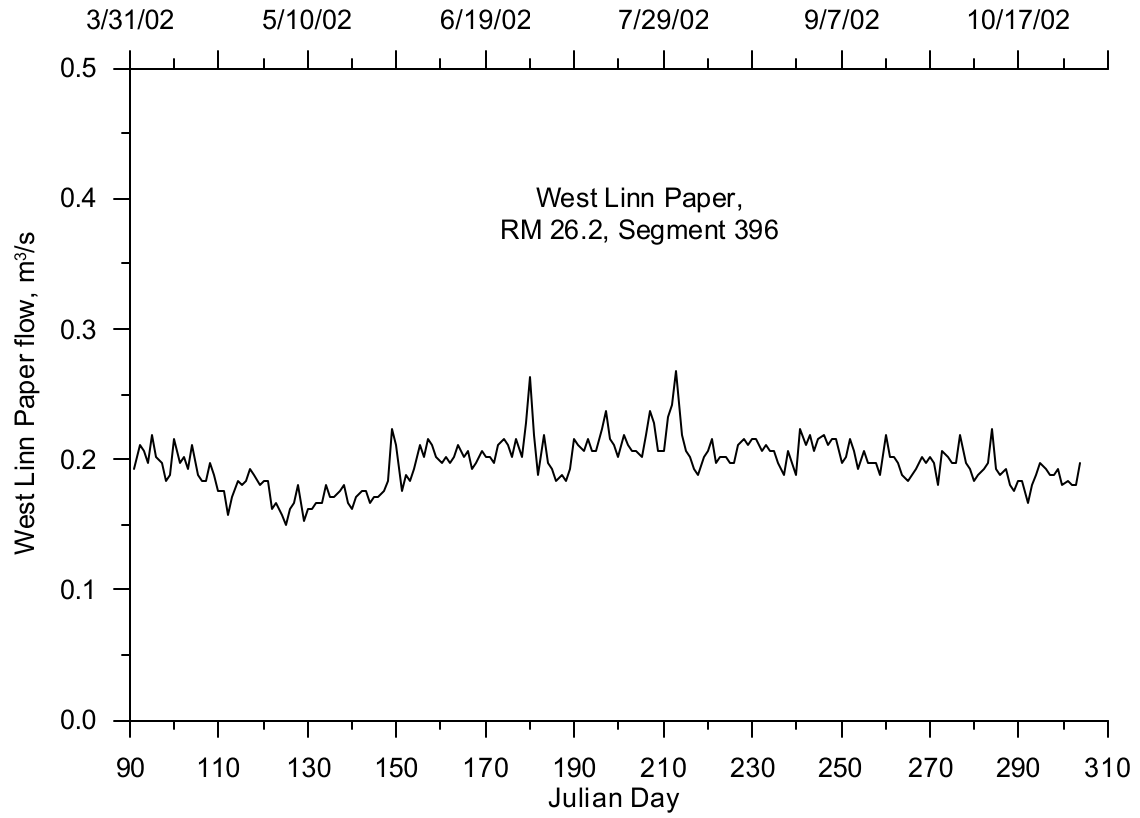


**Figure 203. West Linn Paper flow, 2002**

## Temperature Data

### Year 2001

Temperature data for the City of Salem wastewater treatment plant discharge (Willow Creek treatment plant) were provided by the City of Salem and ODEQ. Hourly data were used from May 10 to October 24 and daily data were used from April 1 to May 10 and from October 24 to October 31. Figure 204 shows the treatment plant discharge temperature.

Because there were no data available in 2001 or 2002, the discharge temperature data set for the SP Newsprint consisted of only monthly sampling data collected in 1996 and 1997. Figure 205 shows the SP Newsprint temperature for 2001. There were no temperature data available for 2001 for the City of Newberg treatment plant, so hourly data from June 5 to October 31, 2002 were used. Between April 1 and June 5 there were only two grab samples. Figure 206 shows the City of Newberg treatment plant discharge temperature for 2001.

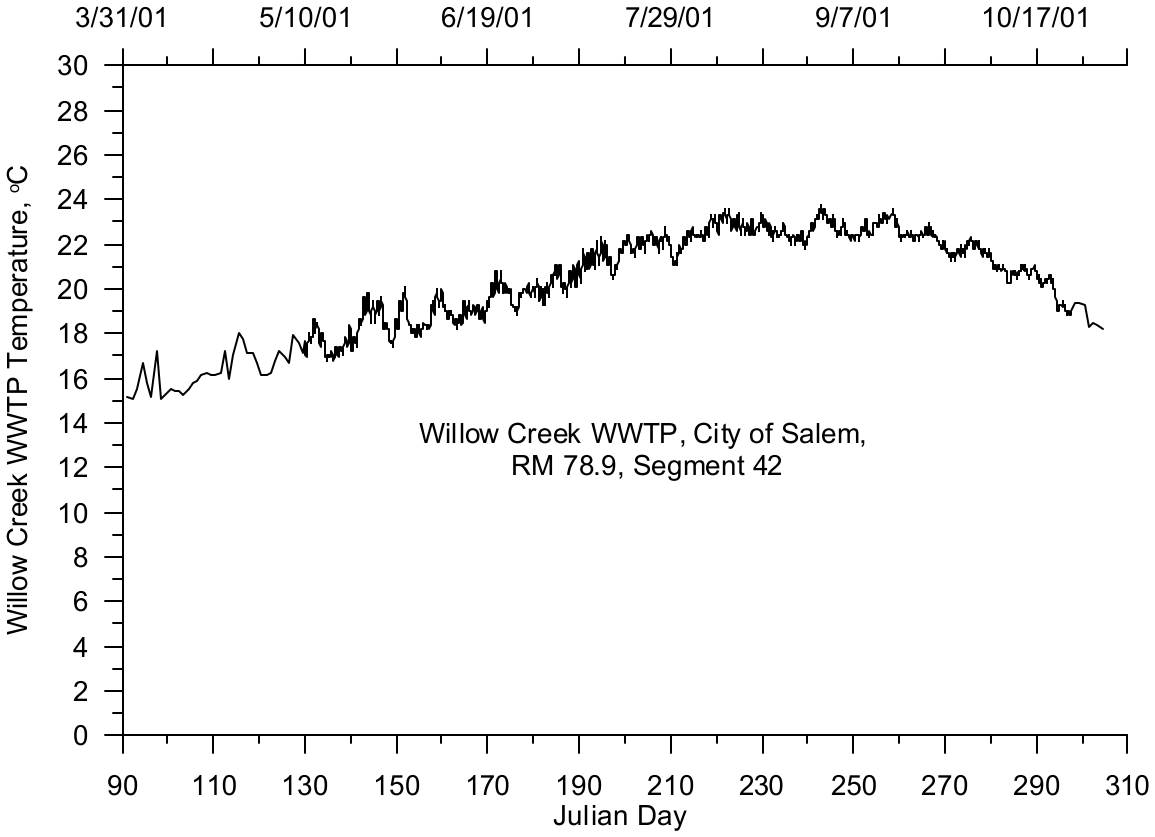


**Figure 204. City of Salem, Willow Creek Treatment Plant temperature, 2001**

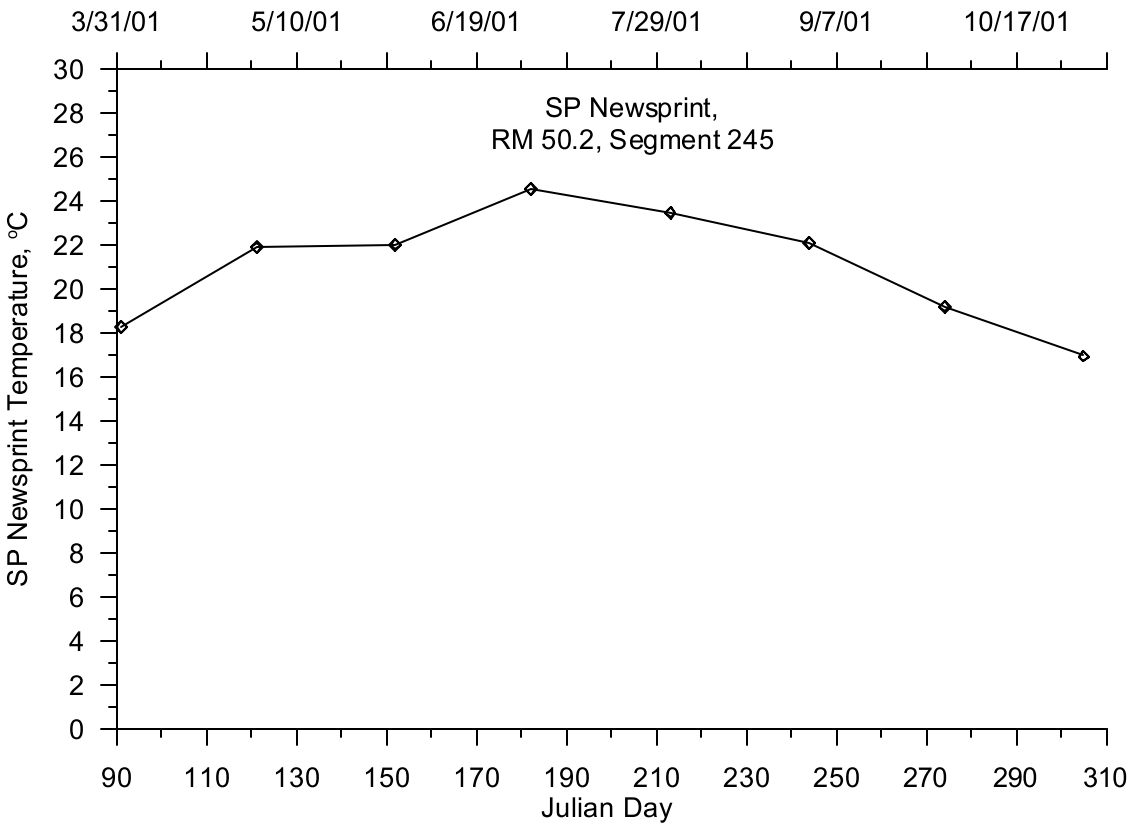


**Figure 205. SP Newsprint temperature, 2001**

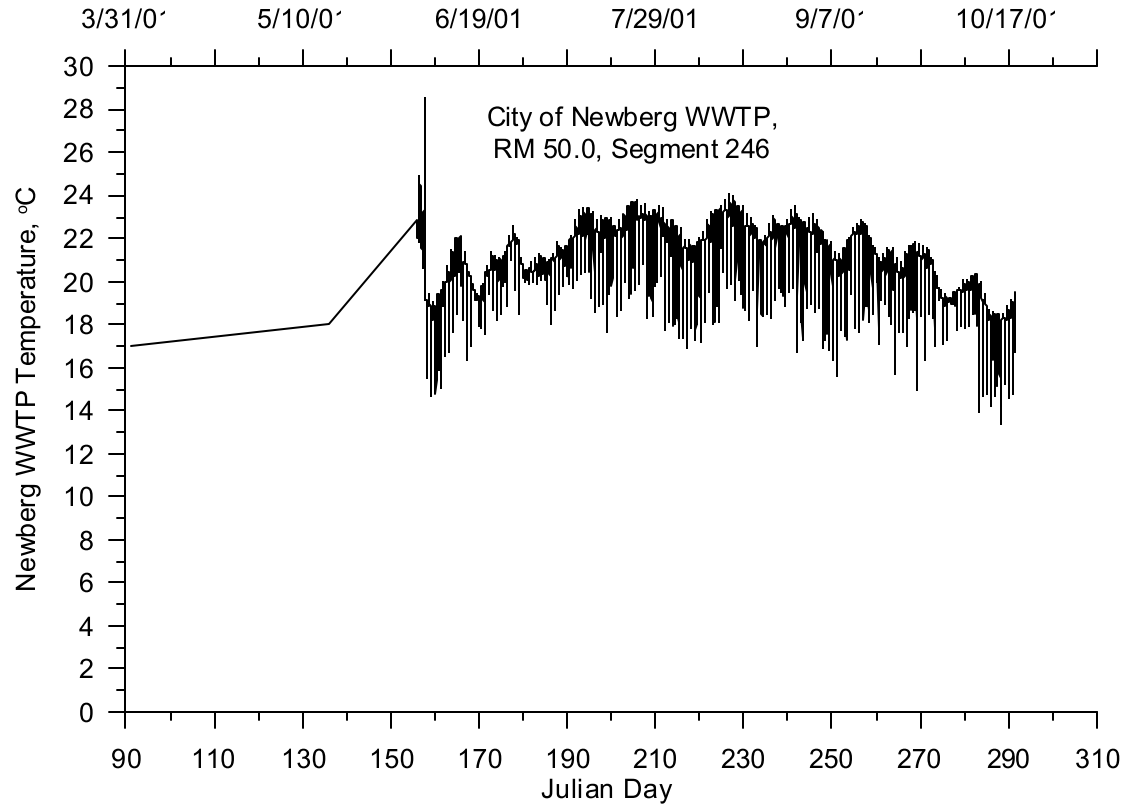


**Figure 206. City of Newberg, WWTP temperature, 2001**

Temperature data for the City of Wilsonville wastewater treatment plant discharge were obtained from ODEQ. Hourly temperatures were used from May 1 to October 31, and daily temperatures were used from April 1 to May 1. Figure 207 shows the discharge temperature. There were no City of Canby discharge temperature data for 2001, so monthly grab sample data from 2002 were used. Temperatures were assigned to April 1, 2001 and November 1, 2001 based on grab samples before April 1 and after November 1 to allow the CE-QUAL-W2 model to linearly interpolate temperatures over the whole model period. Figure 208 shows the temperature recorded in 2001. The West Linn Paper mill temperature data consisted of daily values from August 10 to October 31, but there were no data between April 1 and August 10. The data gap was filled by assigning a temperature to April 1 and allowing the model to interpolate between April 1 and August 10.

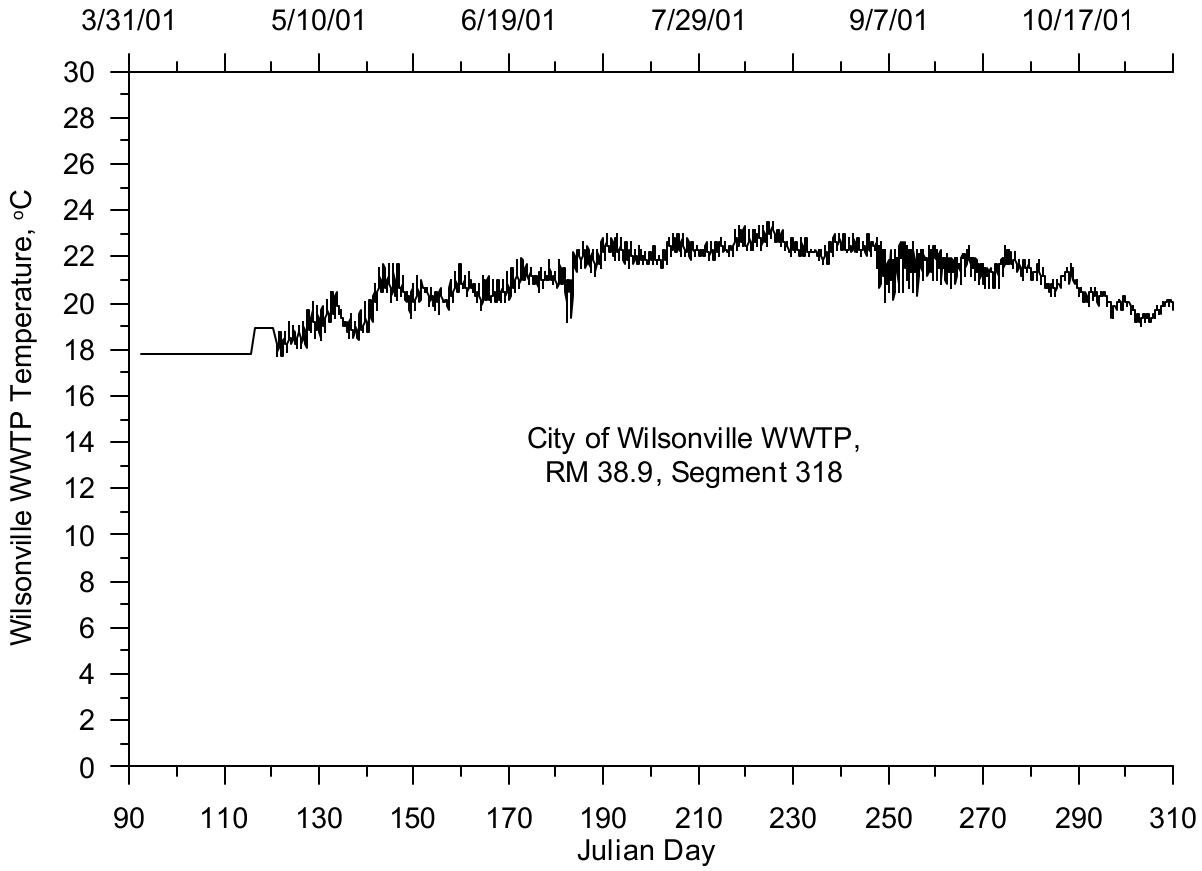


**Figure 207. City of Wilsonville Treatment Plant temperature, 2001**

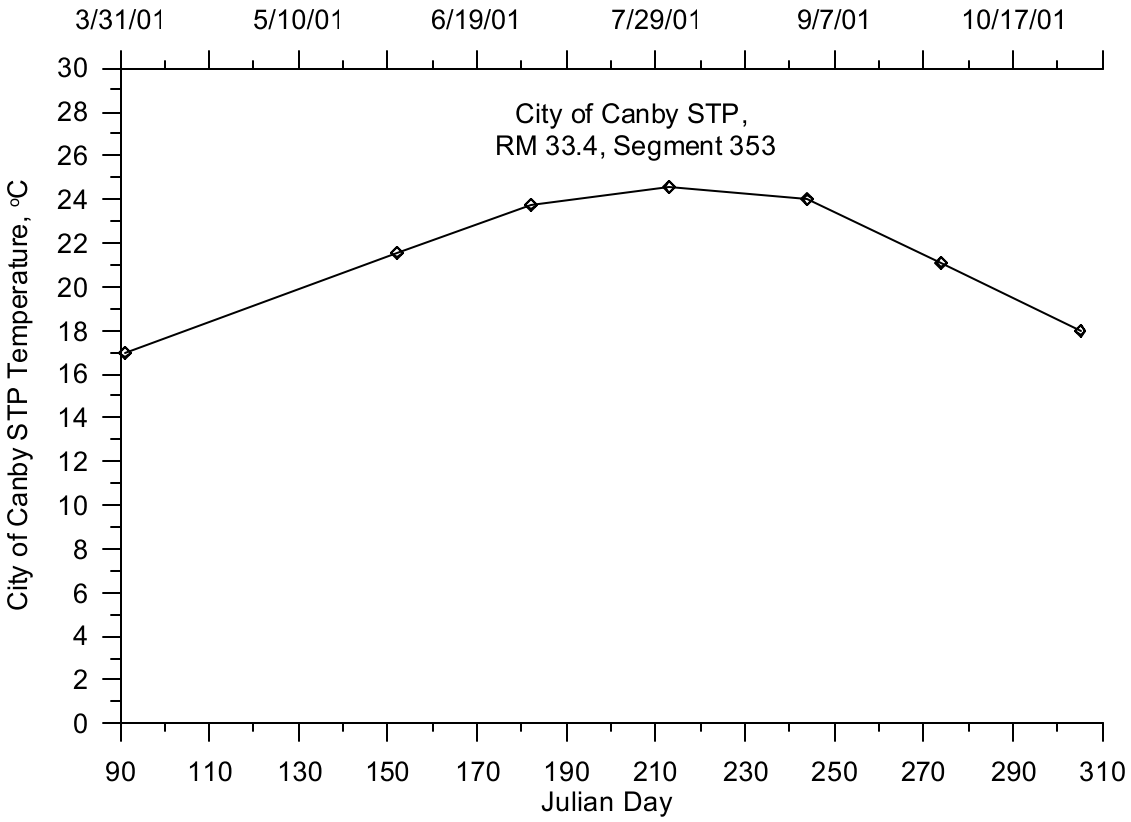


**Figure 208. City of Canby Treatment Plant temperature, 2001**

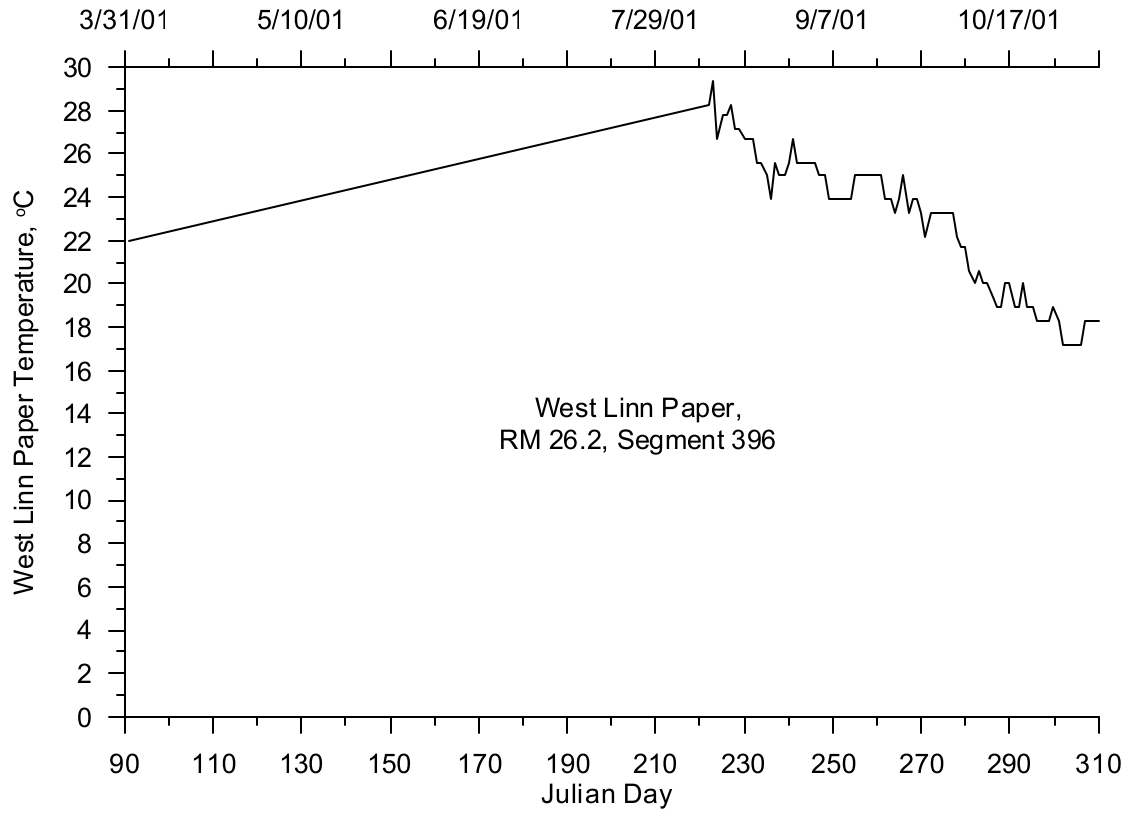


**Figure 209. West Linn Paper temperature, 2001**

Year 2002

Temperature data for the City of Salem wastewater treatment plant discharge consisted of hourly data from May 20 to October 29. Since there were no other data available, temperatures were set for April 1 and November 1, and the model was used to linearly interpolate between April 1 and May 20 and October 29 and October 31. Figure 210 shows the discharge temperature for the City of Salem treatment plant. The SP Newsprint discharge temperatures were based on grab sample data collected in 1996 and 1997 because there were no data available in 2001 and 2002. Figure 211 shows the discharge temperatures for 2002. The same temperatures were used for 2001. Since there were no data available in 2001 for the City of Newberg treatment plant, hourly data from June 5 to October 31, 2002, were used. Between April 1 and June 5, there were only two grab samples. Figure 206 shows the City of Newberg treatment plant discharge temperature used for both 2001 and 2002.

In 2002 the City of Wilsonville treatment plant discharge temperature data consisted of daily values from April 1 to October 31. Figure 212 shows the discharge temperature for 2002. The City of Canby discharge temperature data for 2002 were also used for 2001. Figure 208 shows the temperature record for the treatment in 2002. Daily discharge temperatures for the West Linn Paper Mill were provided by ODEQ. Figure 213 shows the discharge temperature for the mill during 2002.

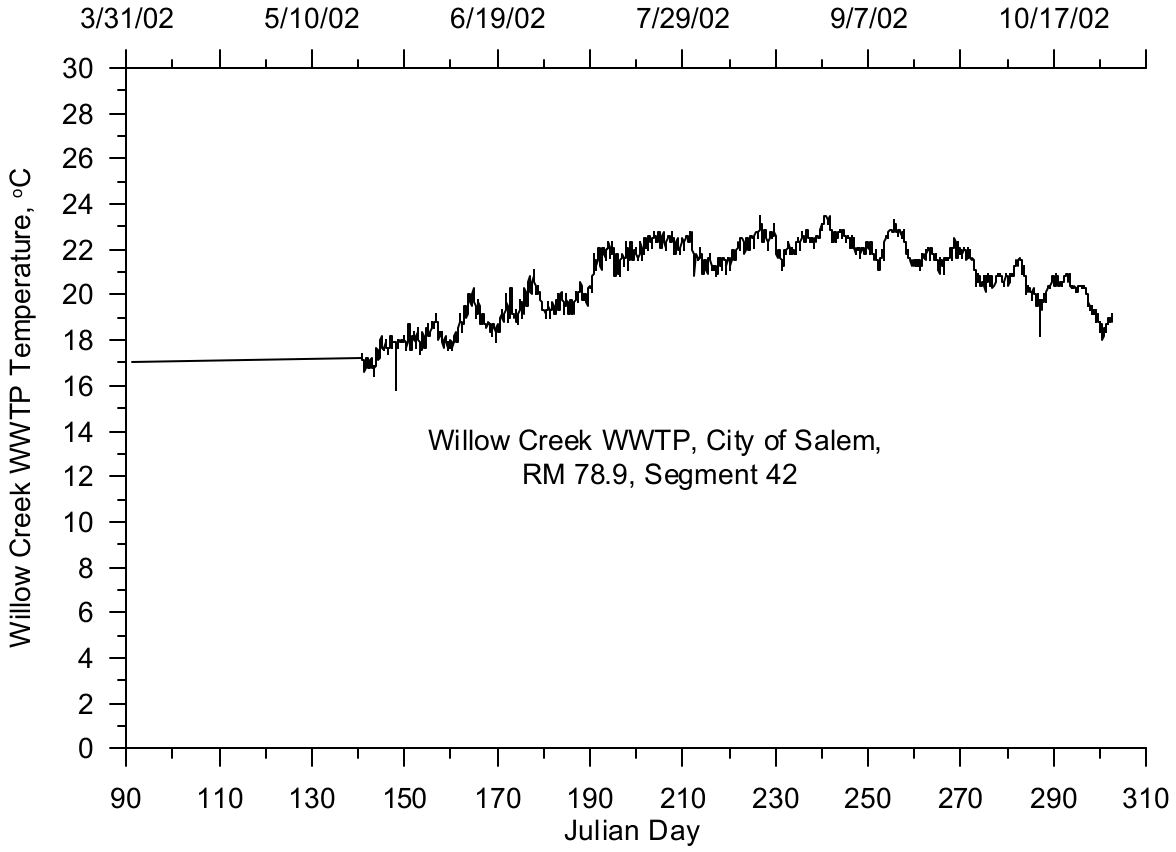


**Figure 210. City of Salem, Willow Creek Treatment Plant temperature, 2002**

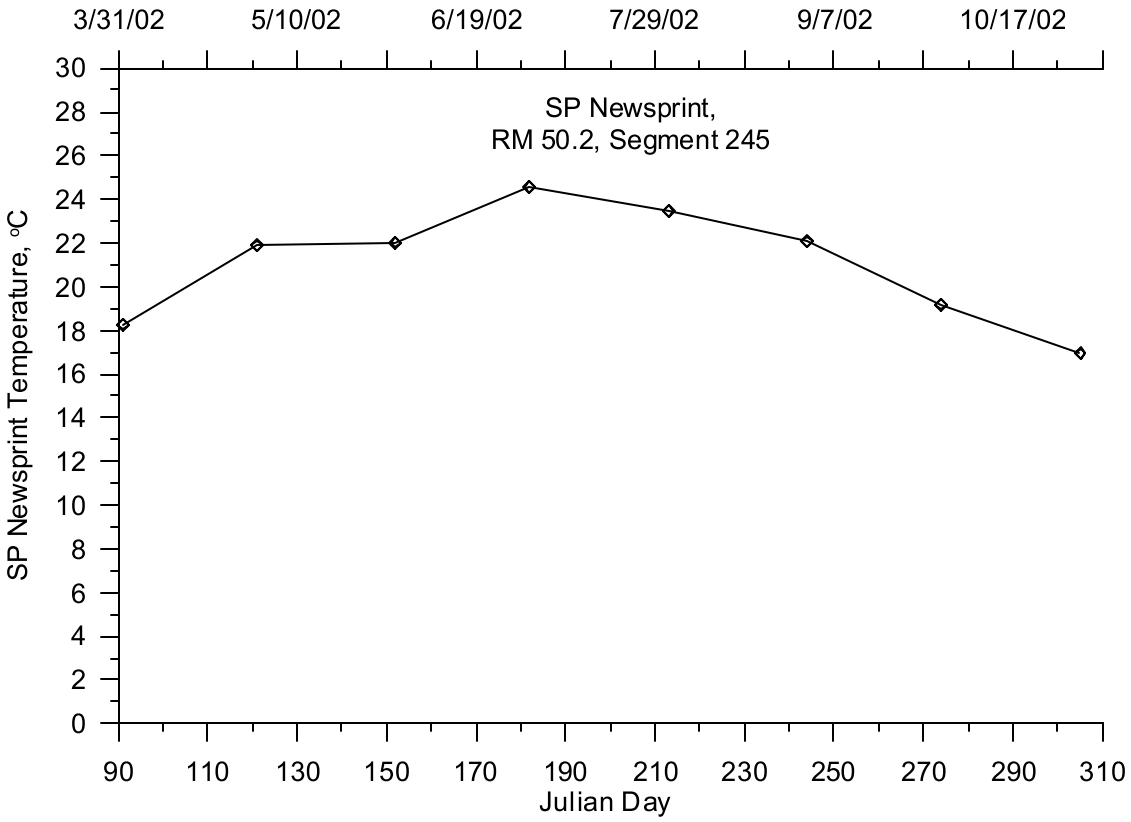


**Figure 211. SP Newsprint temperature, 2002**

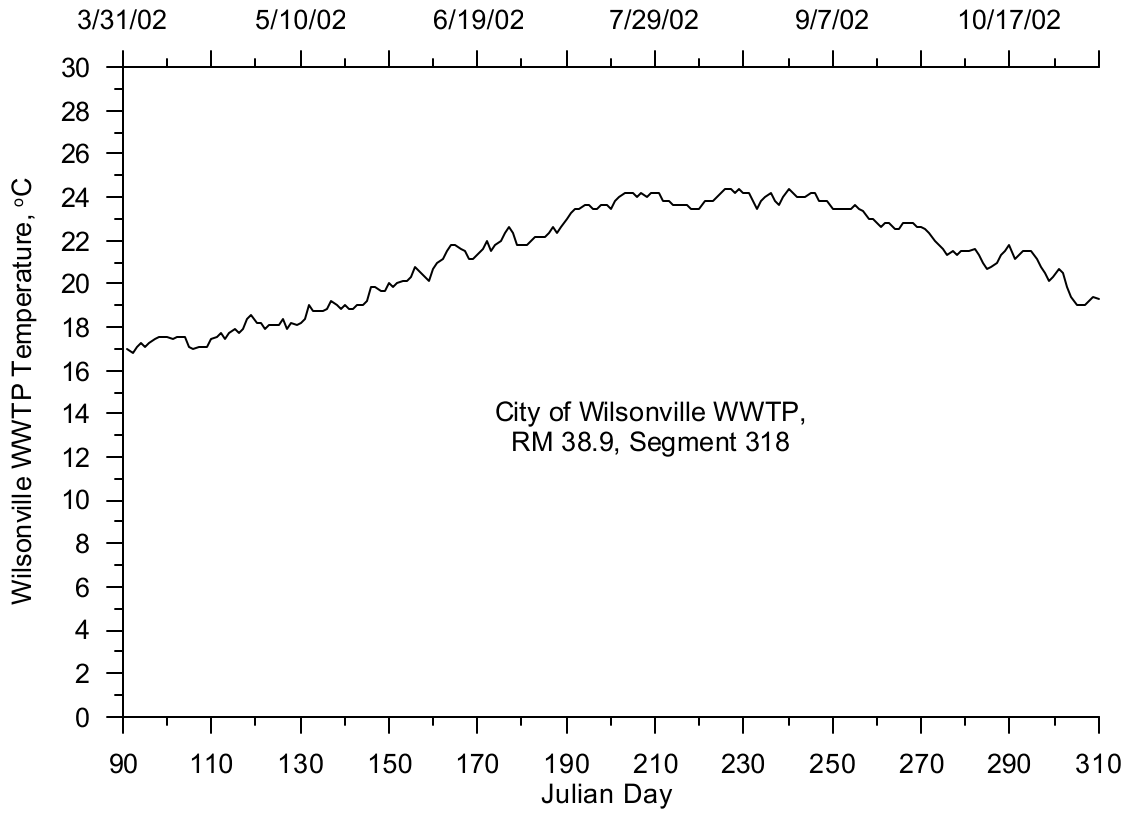


**Figure 212. City of Wilsonville Treatment Plant temperature, 2002**

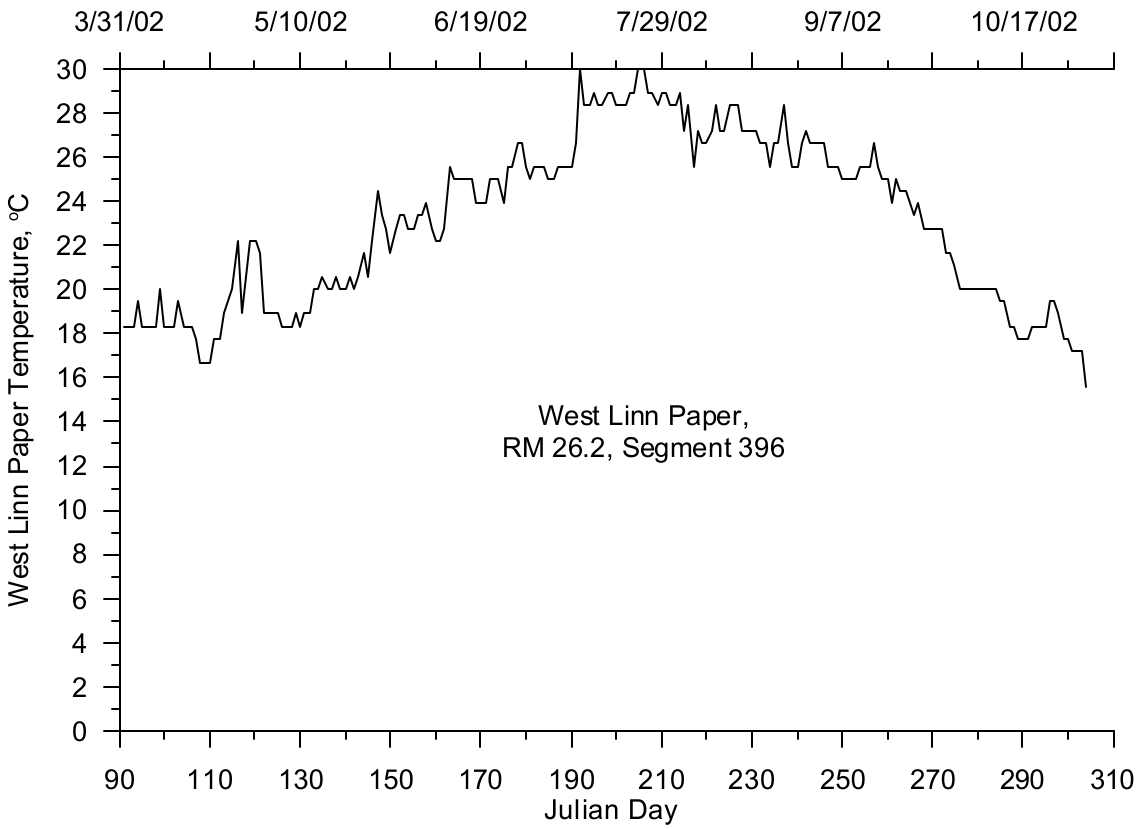


**Figure 213. West Linn Paper temperature, 2002**

## *Shading*

CE-QUAL-W2 incorporated both topographic and vegetative shade in the model. Topographic characteristics included the steepest inclination angle in eighteen directions around a model segment. The vegetative characteristics consisted of tree top elevation, distance between the river channel centerline and the controlling vegetation, and the vegetation density in summer and winter. The vegetation characteristics were provided for both banks of the river.

The vegetation and topographic characteristics for the Middle Willamette River model were developed using GIS data supplied by the Oregon Department of Environmental Quality (ODEQ). The data consisted of points every 100 ft along the thalweg of the river. For each thalweg point, additional associated data included: channel width, elevation, three topographic inclination angles, and nine vegetation compartments for each bank. Each vegetation compartment consisted of vegetation height, distance from stream bank, and density. A detailed analysis was conducted to convert the ODEQ data into the shade variables for the CE-QUAL-W2 model. A detailed description of the shade analysis is provided in Appendix A.

Figure 214 and Figure 215 show the tree top elevation for the left and right banks of the Middle Willamette River. Both banks show the tree top elevation decreasing going downstream with a few reaches with vegetation heights lower than the trend line. All plots reflect the shading characteristics along the main river channel and do not show shading characteristics on the side channels. Figure 216 and Figure 217 show the distance from the river centerline to the controlling vegetation on the left and right banks, respectively, moving downstream. These figures show that the distance to the vegetation for

both banks was relatively constant until the end reach just above Willamette Falls where the distance increased (RM 34 to RM 26.8). Figure 218 and Figure 219 show the vegetation density for the left and right banks, respectively. These plots reveal that the vegetation density for the left and right banks was relatively high with short reaches where the density decreased considerably.

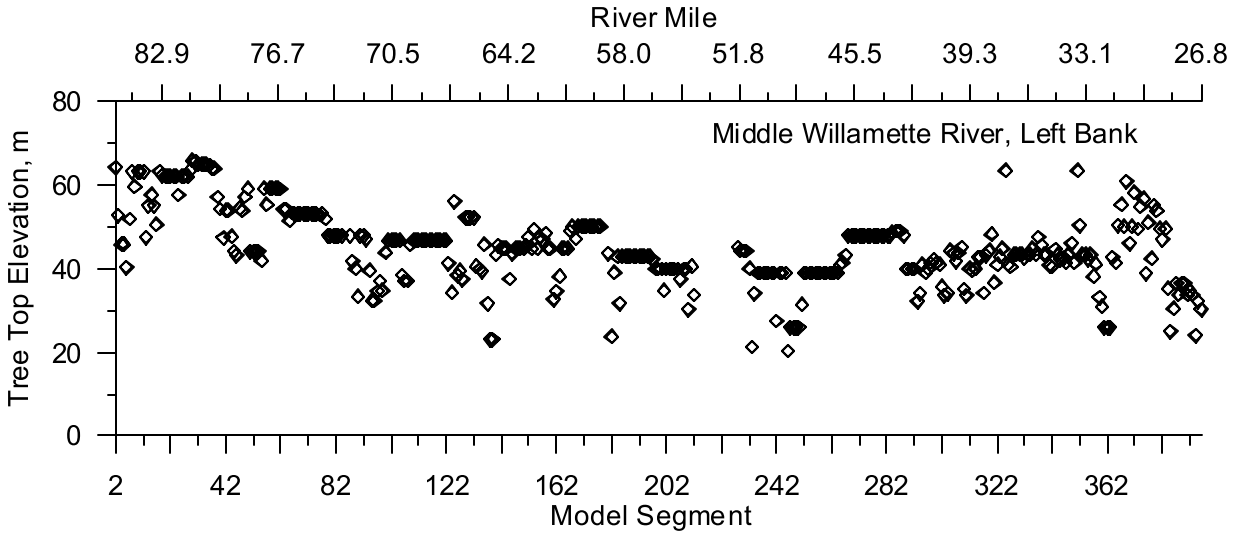


**Figure 214. Middle Willamette River Left Bank Tree Top Elevation**

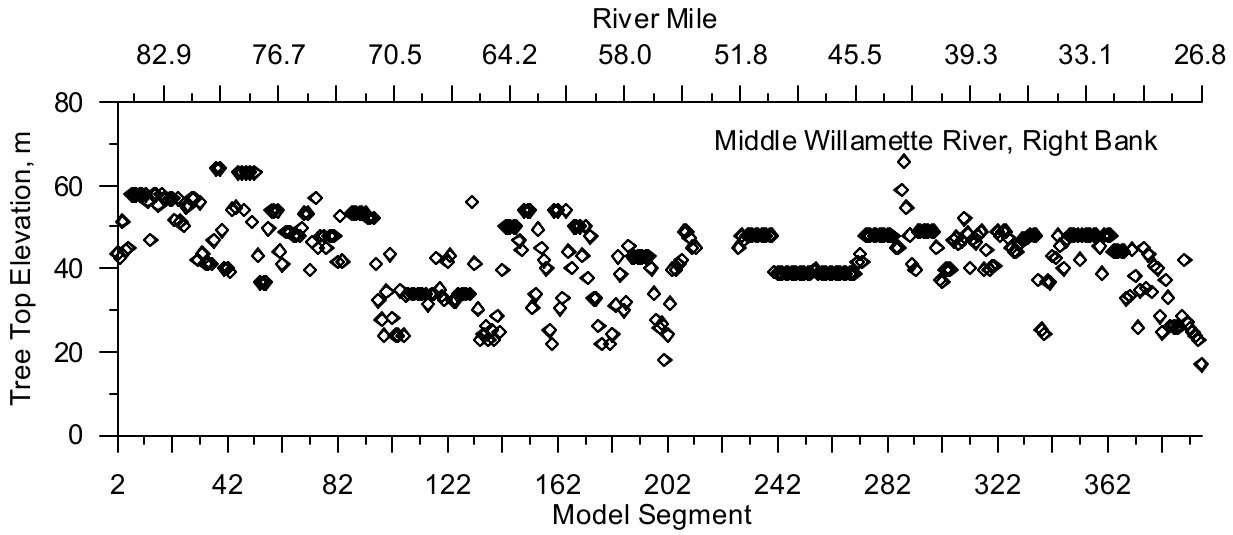


**Figure 215. Middle Willamette River Right Bank Tree Top Elevation**

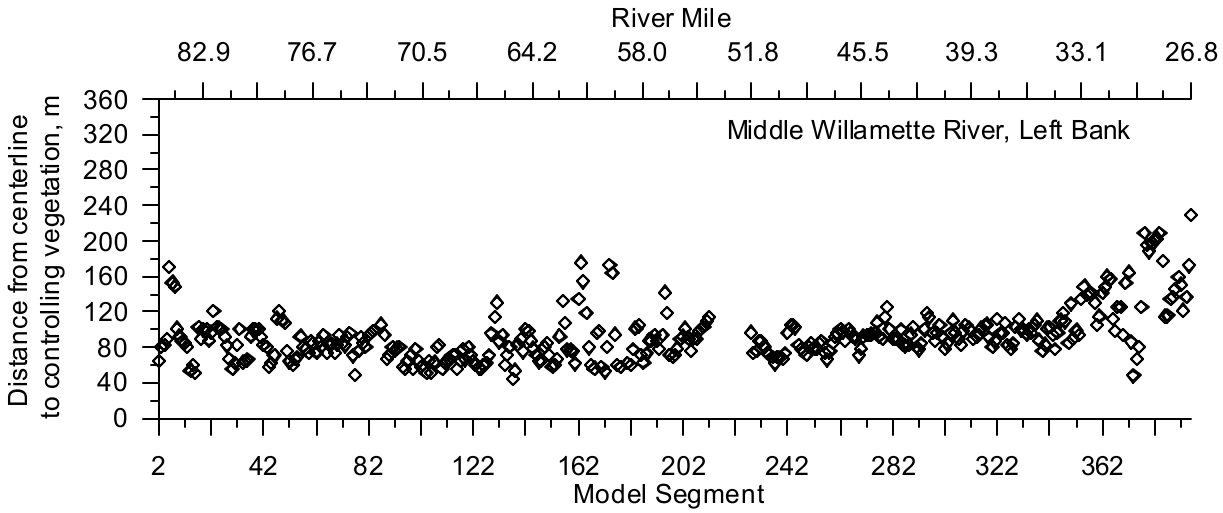


**Figure 216. Middle Willamette River Left Bank Distance from Centerline to Controlling Vegetation**

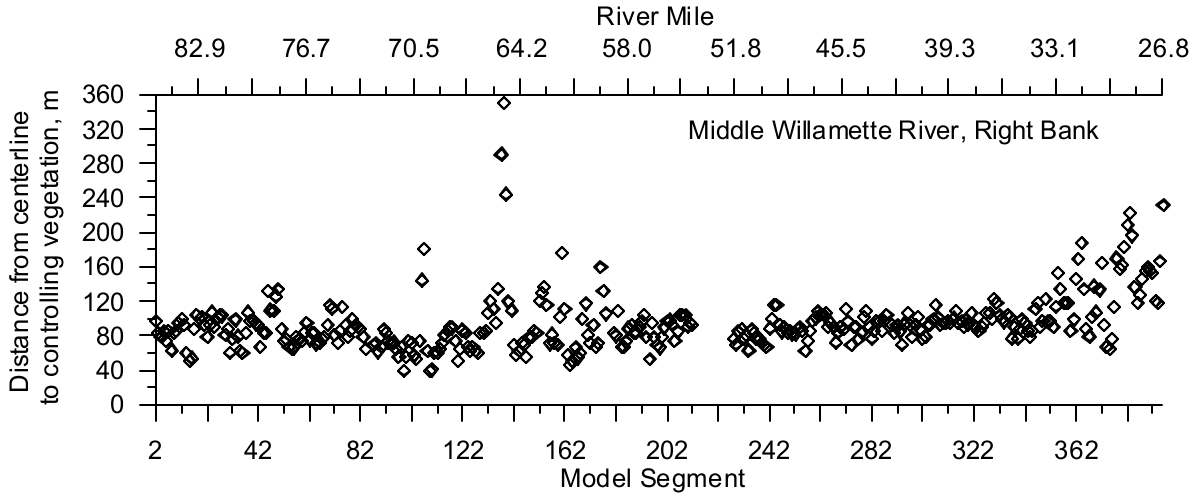


**Figure 217. Middle Willamette River Right Bank Distance from Centerline to Controlling Vegetation**

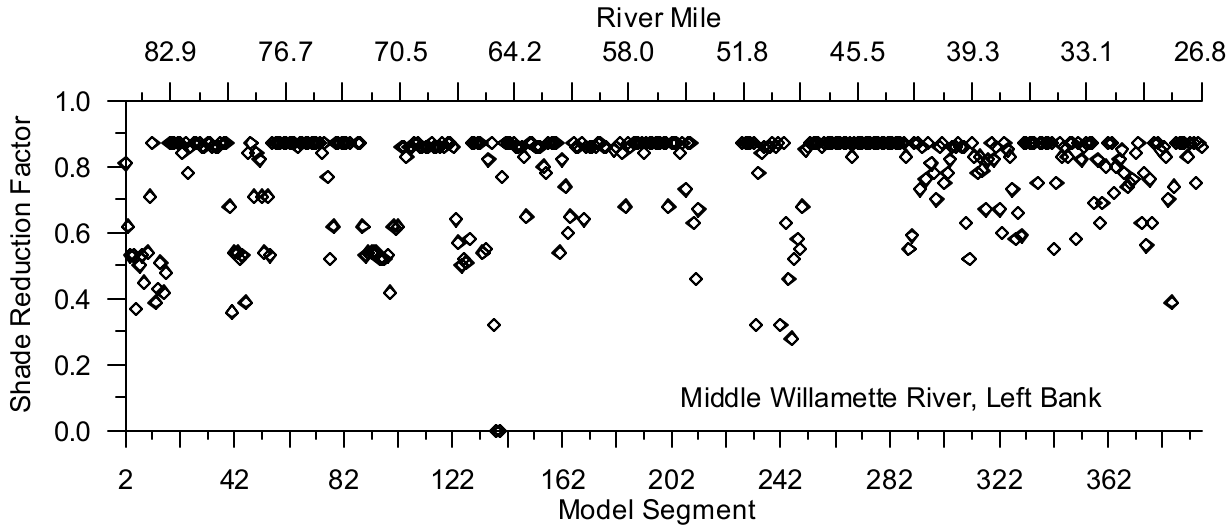


**Figure 218. Middle Willamette River Left Bank Shade Reduction Factor**

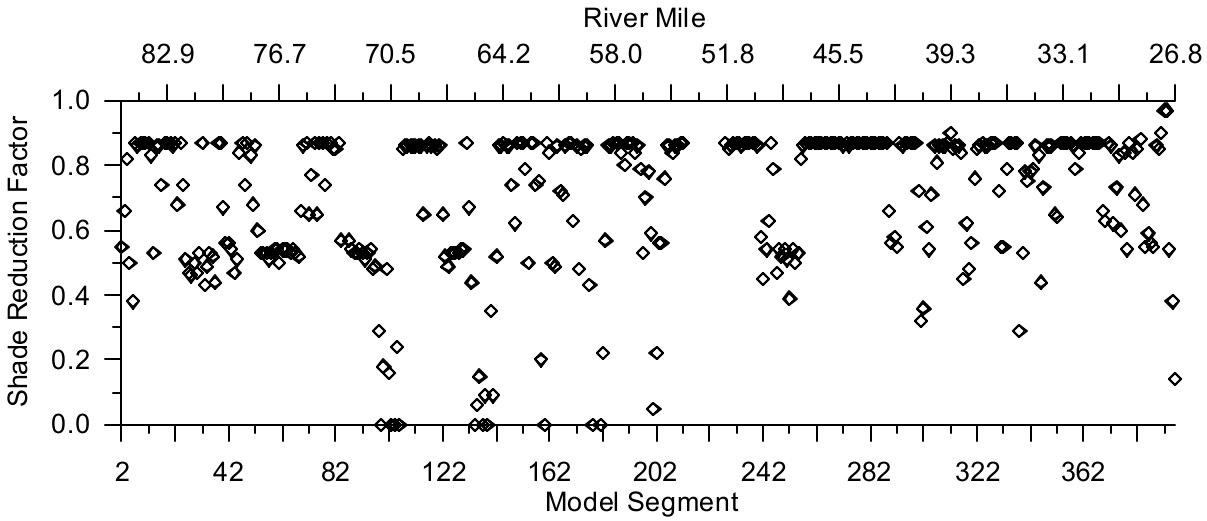


**Figure 219. Middle Willamette River Right Bank Shade Reduction Factor**

## *Meteorology*

CE-QUAL-W2 uses air and dew point temperature, wind speed and direction, and cloud cover or solar radiation. Since the Middle Willamette River system is large, covering from RM 84 to RM 26.5, several meteorological data sets were utilized as shown in Figure 220. Each model water body can have a separate meteorological data set. Water body 1 used meteorological data from the Salem airport, water body 2 used meteorological data collected at the McMinnville airport, and water body 3 used data collected at the Aurora airport.

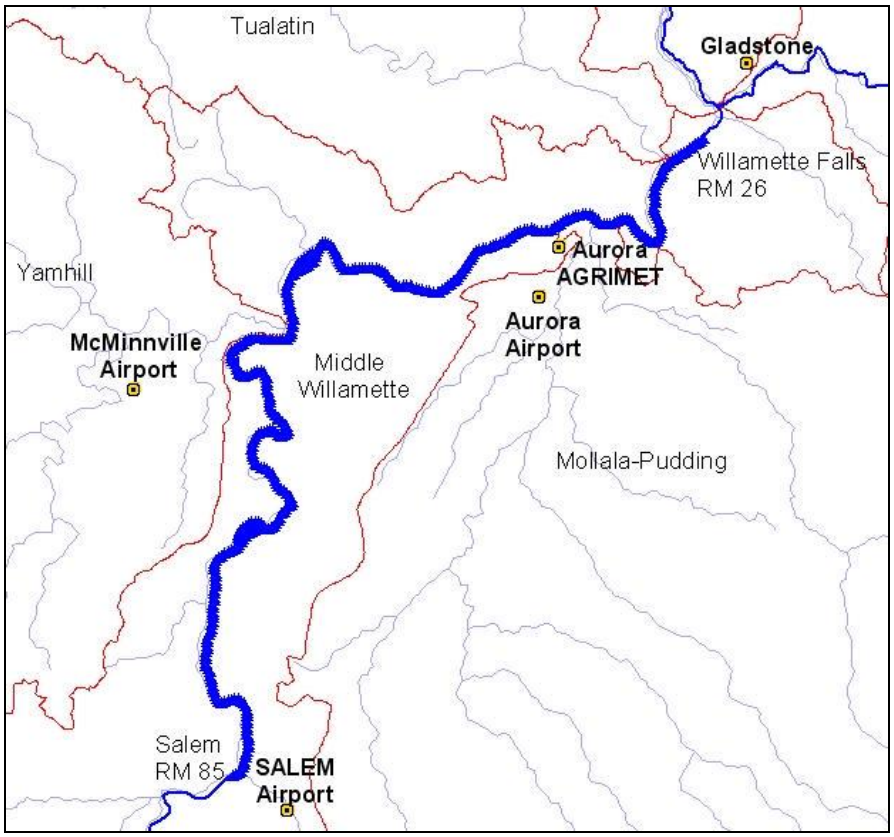


**Figure 220. Middle Willamette River model meteorological site locations**

**Table 24. Middle Willamette River model meteorological monitoring sites**

| Site | Agency (Program) | Meteorological Parameters |
|---|---|---|
| Salem Municipal Airport | National Weather Service (METAR) | Air Temperature, Dew Point Temperature, Relative Humidity, Wind Speed, Wind Direction, Cloud Cover |
| McMinnville Municipal Airport | National Weather Service (METAR) | Air Temperature, Dew Point Temperature, Relative Humidity, Wind Speed, Wind Direction, Cloud Cover |
| Aurora Municipal Airport | National Weather Service (METAR) | Air Temperature, Dew Point Temperature, Relative Humidity, Wind Speed, Wind Direction, Cloud Cover |
| Aurora, OR | Bureau of Reclamation, (AGRIMET) | Solar Radiation |
| Gladstone | University of Oregon, Solar Radiation Monitoring Lab | Solar Radiation |

## Salem Municipal Airport

Year 2001

The Salem Municipal Airport recorded air and dew point temperature, wind speed and direction, and cloud cover data, but not solar radiation data. Figure 221 and Figure 222 show the air and dew point temperature, respectively. Figure 223 and Figure 224 show the wind speed and direction, respectively. Figure 223 showed that the minimum wind speed-recording threshold was about 1.5 m/s. The rose diagram in Figure 224 indicated that the predominant wind direction was from the North with some periodic winds coming from other directions. When wind speeds fell below the minimum recording threshold, the wind speed and direction were both set to zero resulting in wind direction from the North being over represented. Figure 225 shows the cloud cover data recorded at the airport with five different cloud cover designations. Global solar radiation data was utilized from Gladstone, OR, as shown in Figure 246.

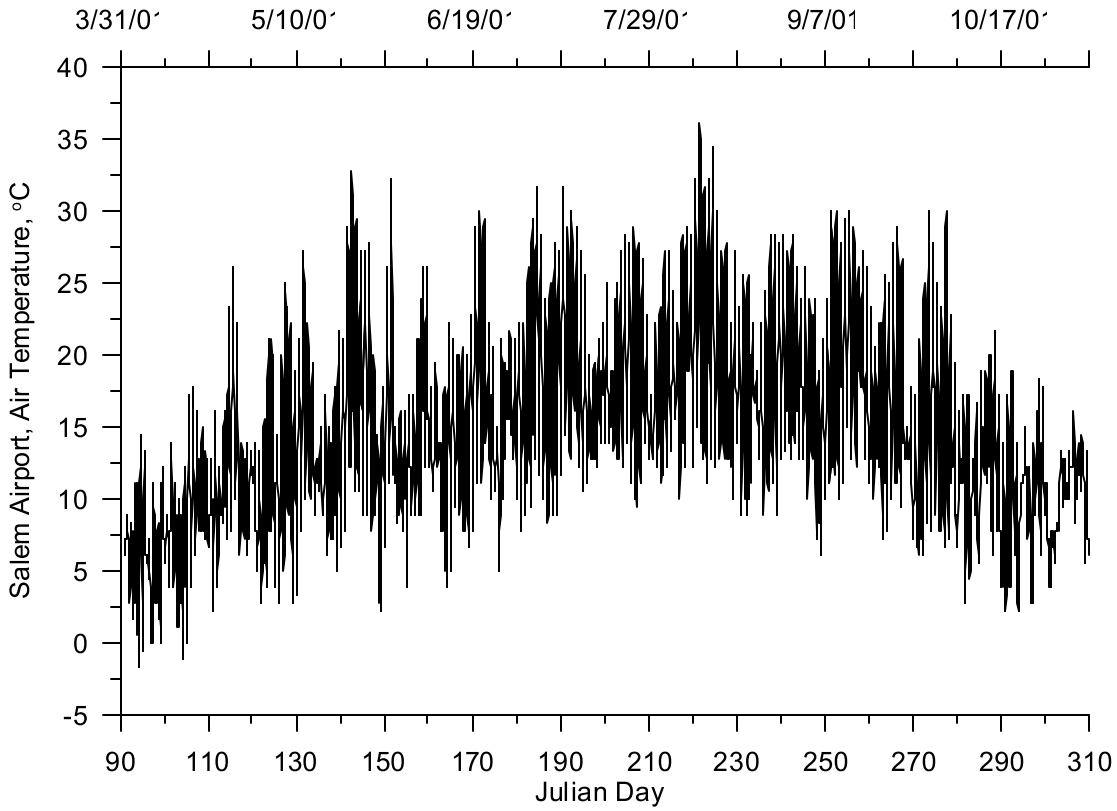


**Figure 221. Air temperature at Salem Municipal Airport, 2001**

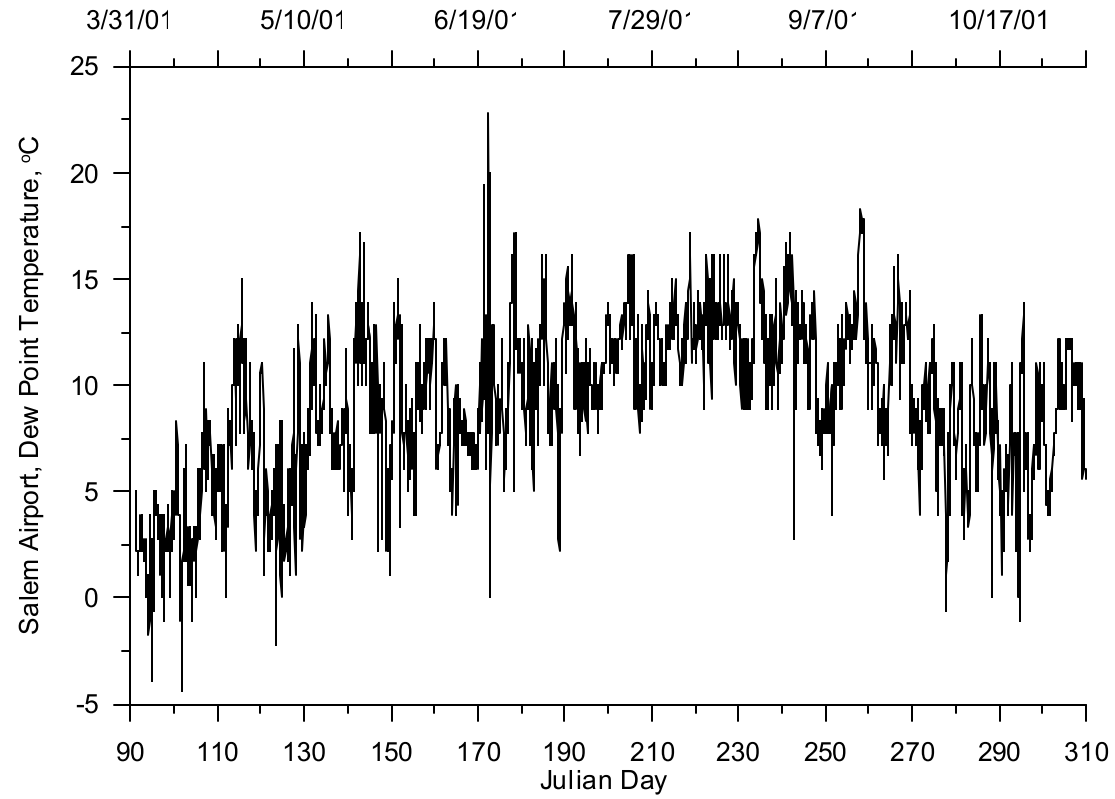


**Figure 222. Dew point temperature at Salem Municipal Airport, 2001**

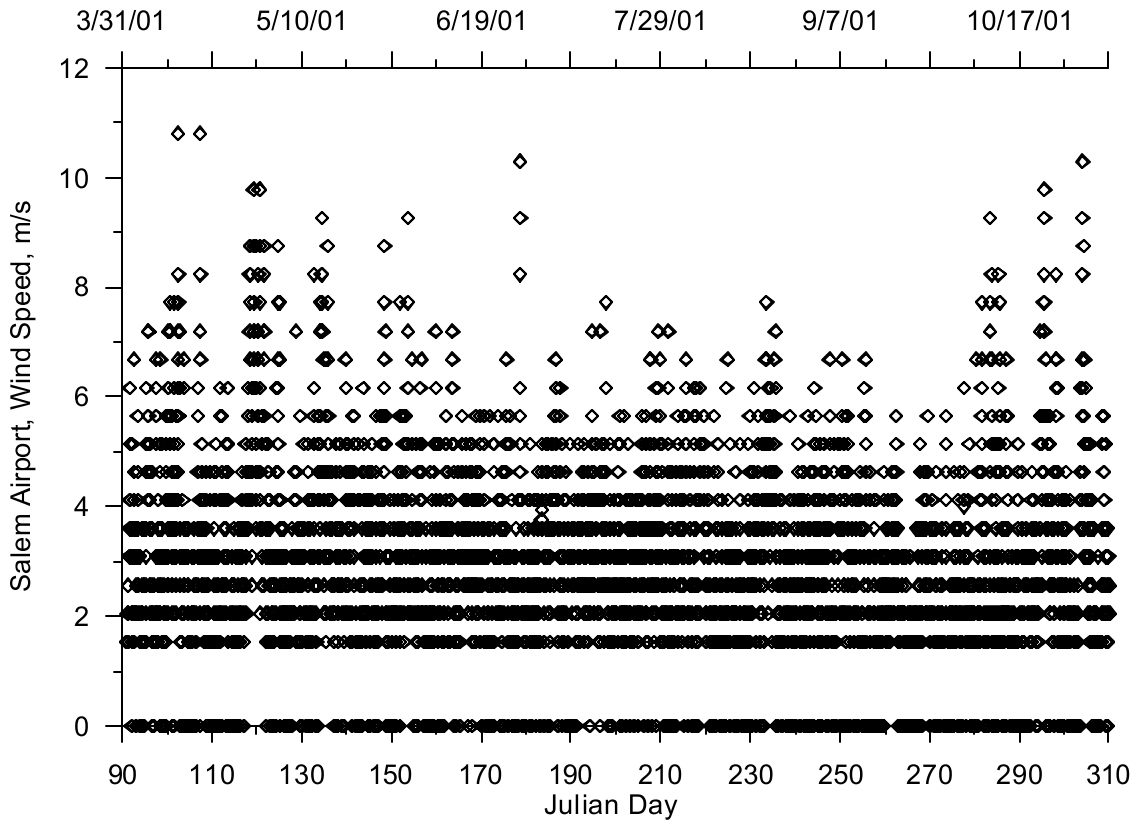


**Figure 223. Wind speed at Salem Municipal Airport, 2001**

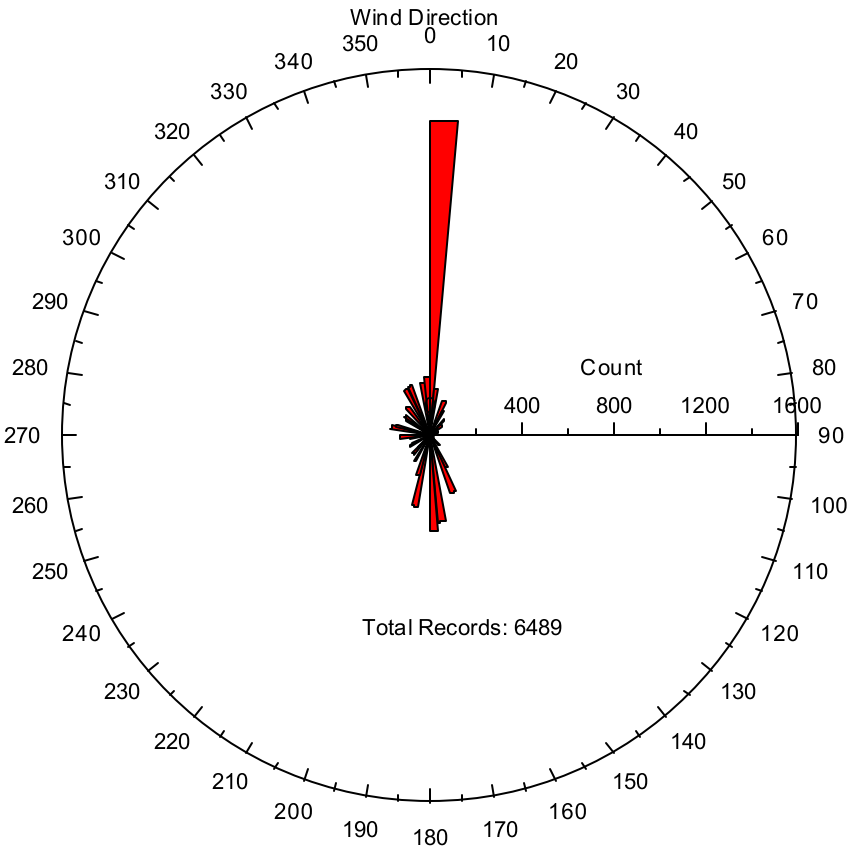


**Figure 224. Wind direction at Salem Municipal Airport, 2001**

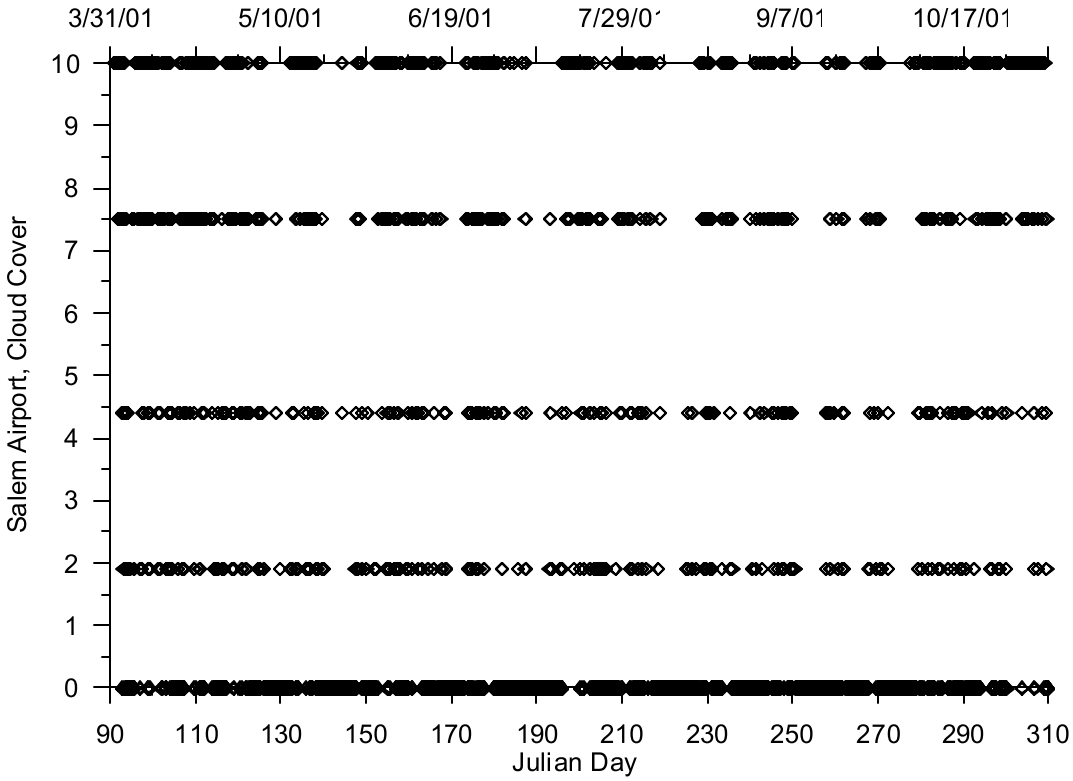


**Figure 225. Cloud cover at Salem Municipal Airport, 2001**

Year 2002

The Salem Municipal Airport records air and dew point temperature, wind speed and direction, and cloud cover data, but not solar radiation data. Figure 226 and Figure 227 show the air and dew point temperature, respectively. Figure 228 and Figure 229 show the wind speed and direction, respectively. Figure 228 indicated that the minimum wind speed-recording threshold was about 1.5 m/s. The rose diagram in Figure 229 indicated that the predominant wind direction was from the North. When wind speed fell below the minimum recording threshold, the wind speed and direction are both set to zero resulting in wind direction from the North being over represented. Figure 230 shows the cloud cover data recorded at the airport with five different cloud cover designations. Global solar radiation data were utilized from Gladstone, OR, as shown in Figure 252

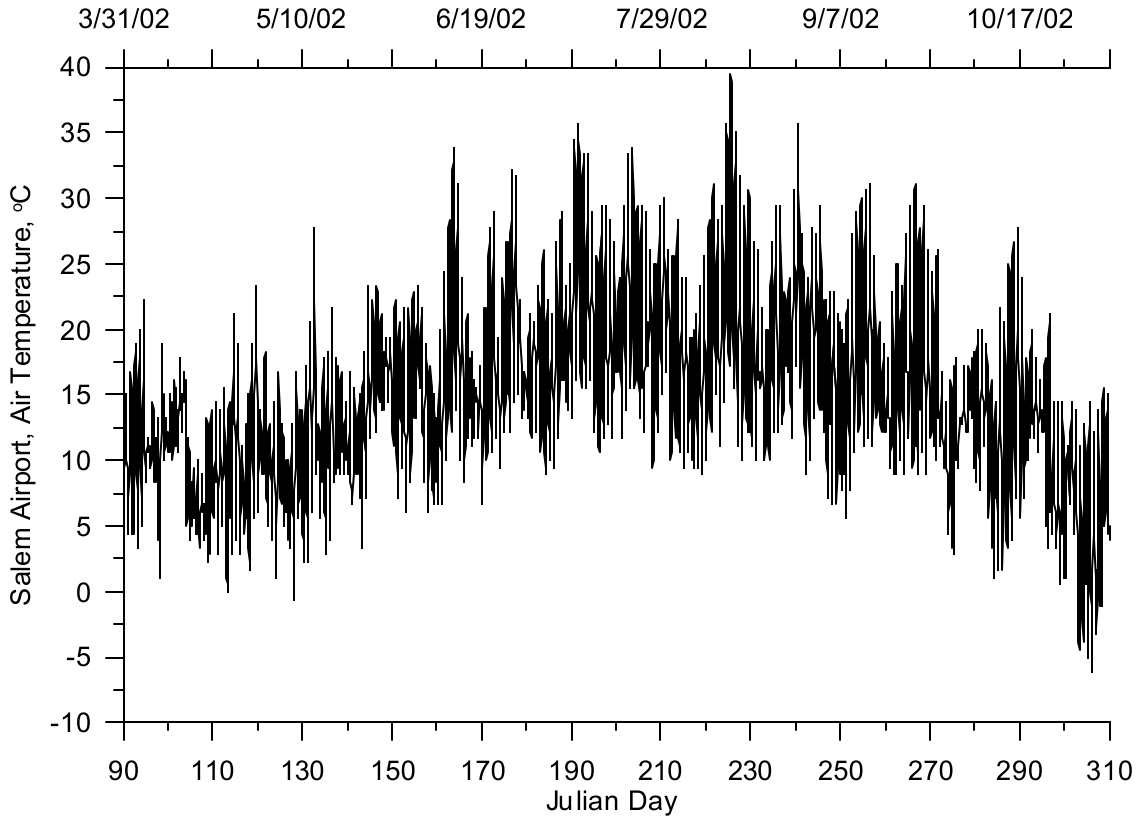


**Figure 226. Air temperature at Salem Municipal Airport, 2002**

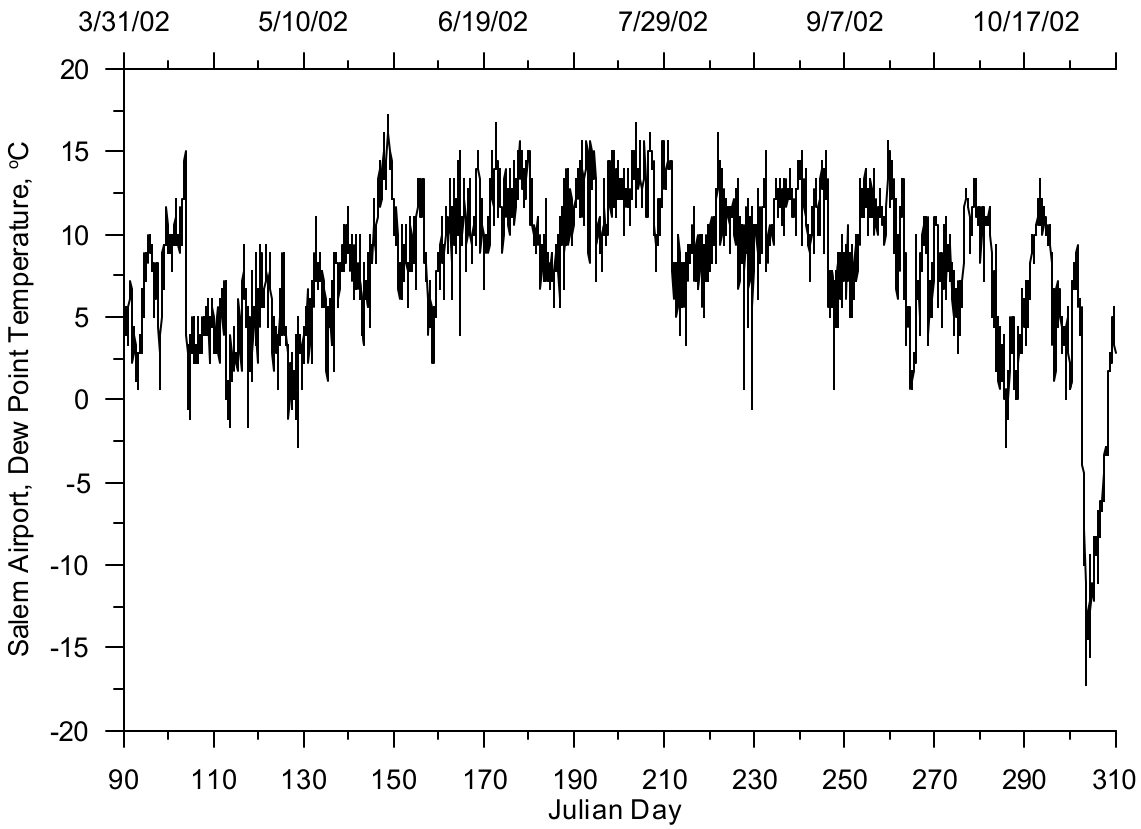


**Figure 227. Dew point temperature at Salem Municipal Airport, 2002**

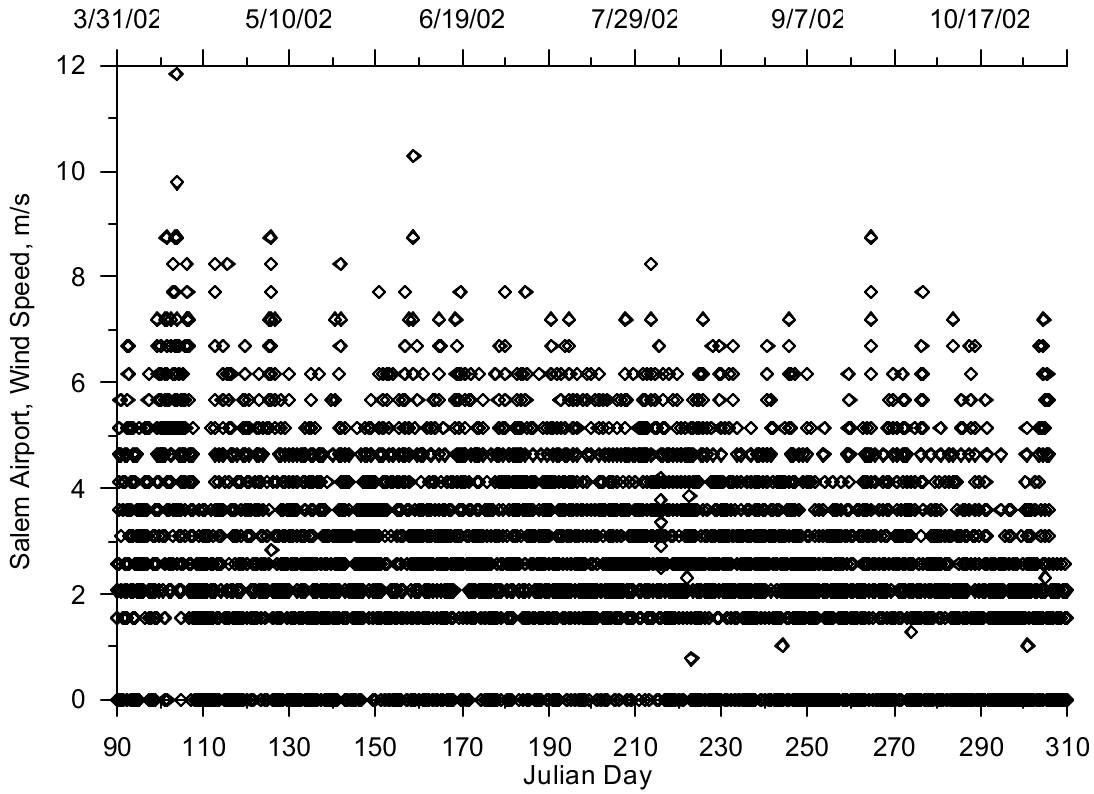


**Figure 228. Wind speed at Salem Municipal Airport, 2002**

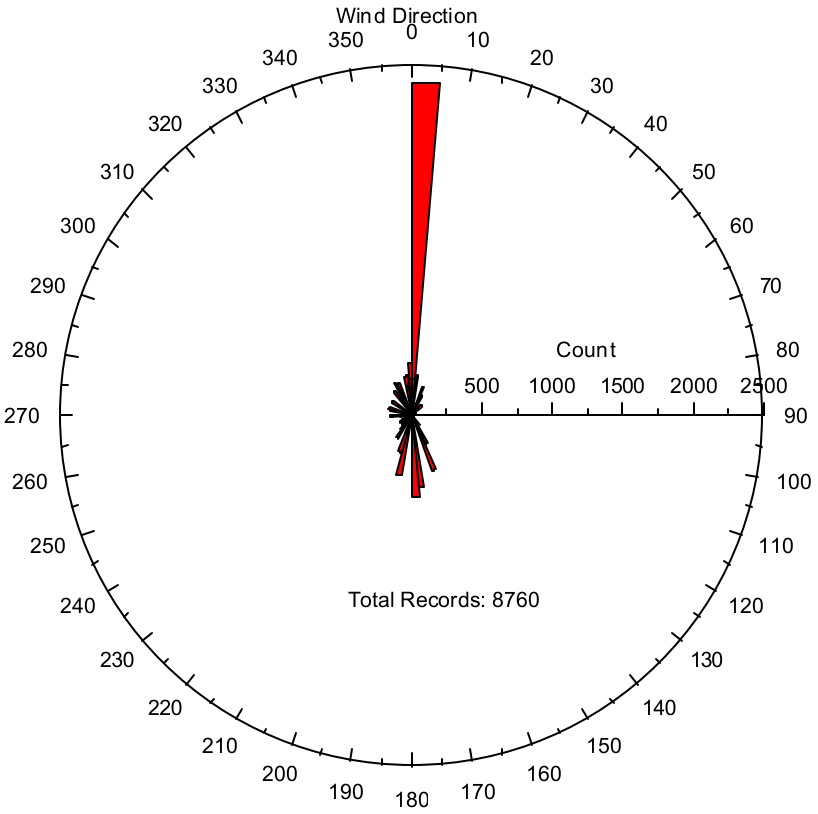


**Figure 229. Wind direction at Salem Municipal Airport, 2002**

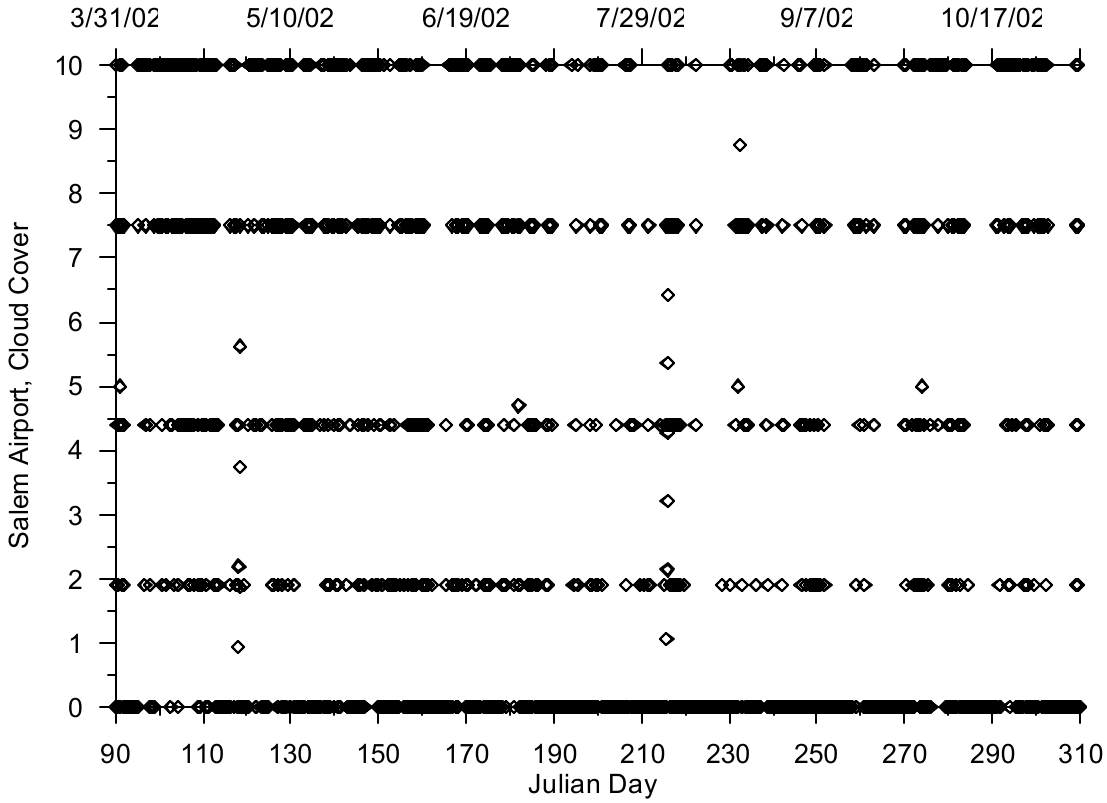


**Figure 230. Cloud cover at Salem Municipal Airport, 2002**

## McMinnville Municipal Airport

Year 2001

The McMinnville Municipal Airport recoded similar meteorological data as at the Aurora Municipal Airport with the exception of solar radiation data. Figure 231 and Figure 232 show the air and dew point temperature, respectively. Figure 233 and Figure 234 show the wind speed and direction, respectively. Figure 233 indicated that the minimum wind speed-recording threshold was 1.5 m/s. The rose diagram in Figure 234 showed that the predominant wind direction was from the North but with some periodic winds coming from the Southwest. The dominant North winds were partly due to the wind direction being set to zero when the wind speed was below the threshold velocity. Figure 235 shows the cloud cover data recorded at the airport with five designations. There were no solar radiation data available at the McMinnville Municipal Airport.

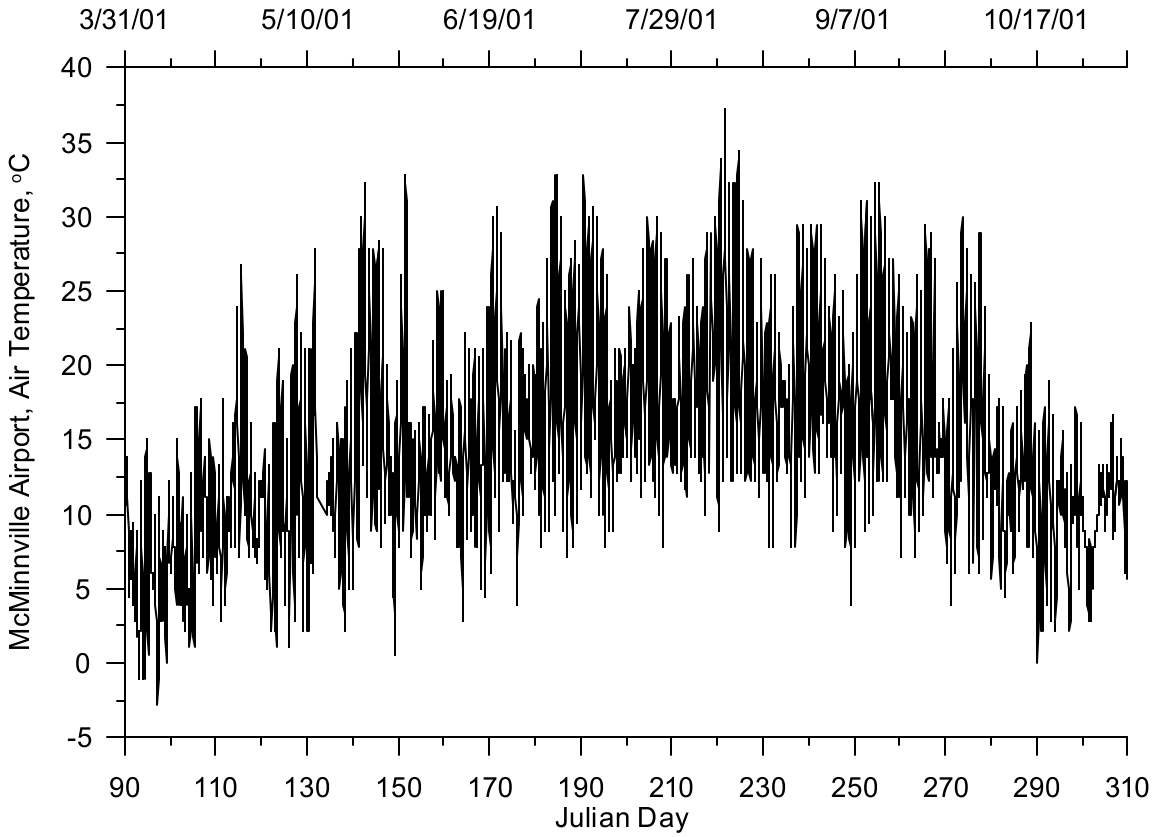


**Figure 231. Air temperature at McMinnville Municipal Airport, 2001**

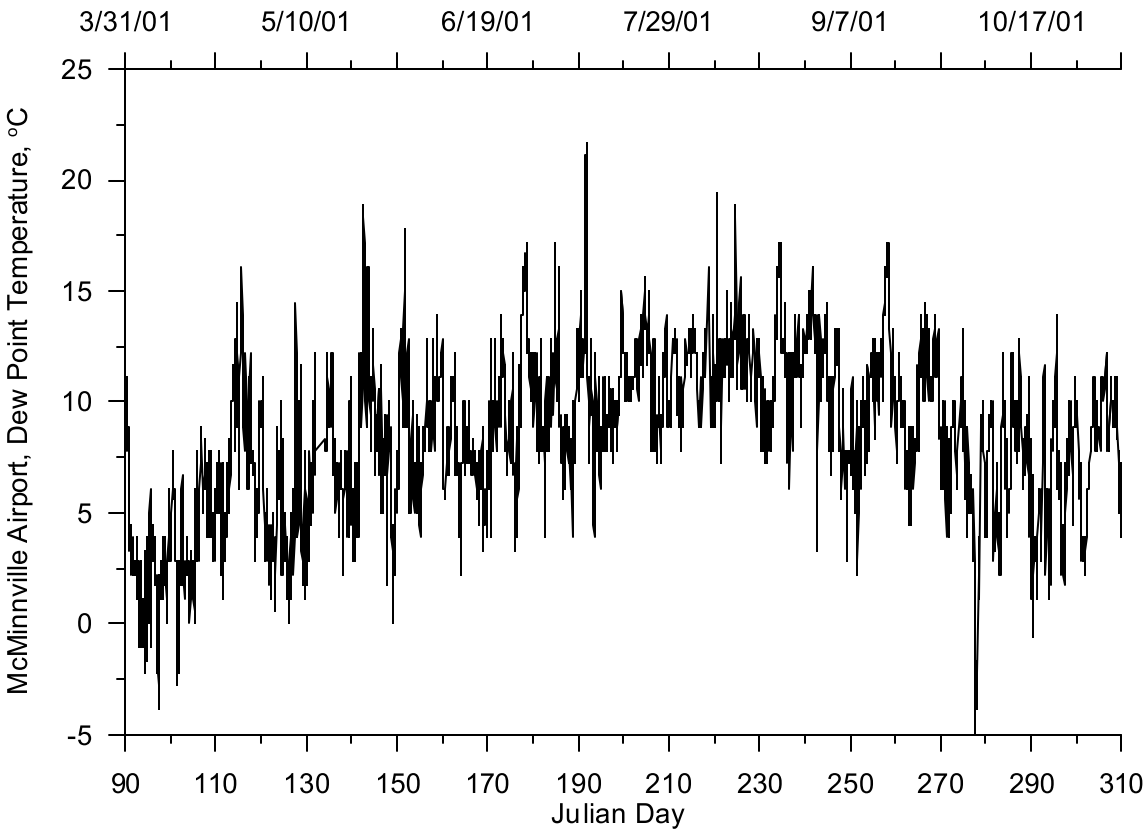


**Figure 232. Dew point temperature at McMinnville Municipal Airport, 2001**

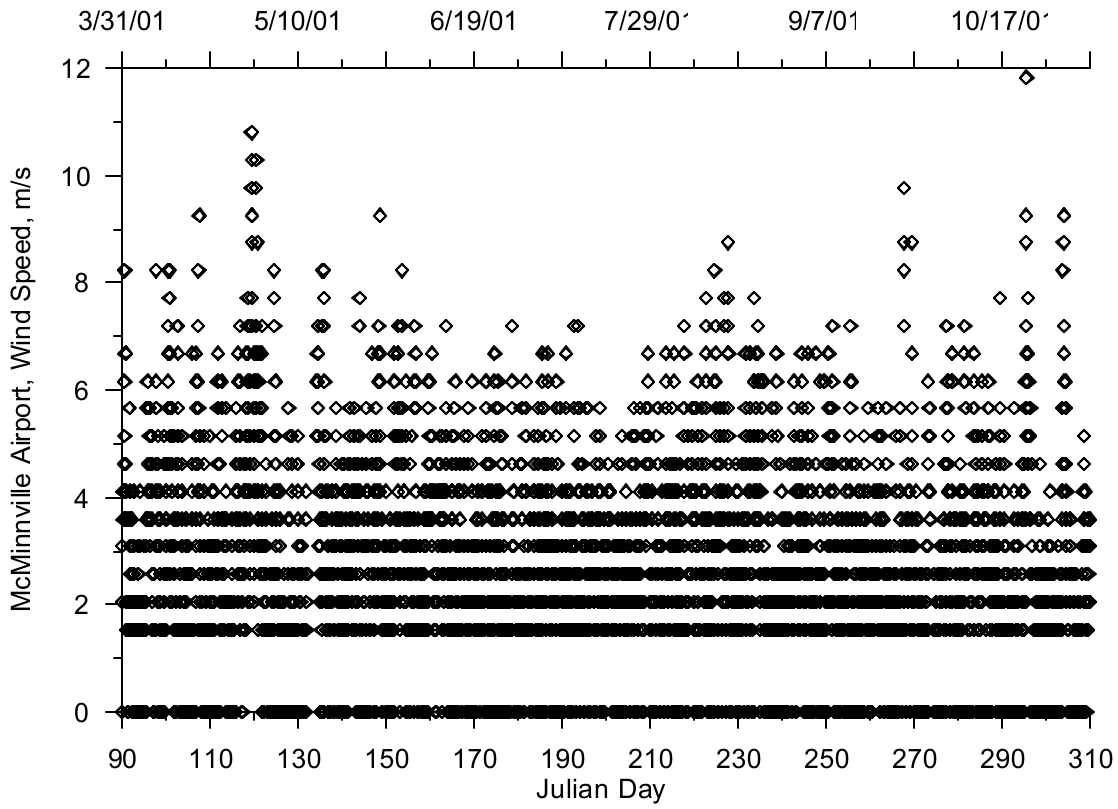


**Figure 233. Wind speed at McMinnville Municipal Airport, 2001**

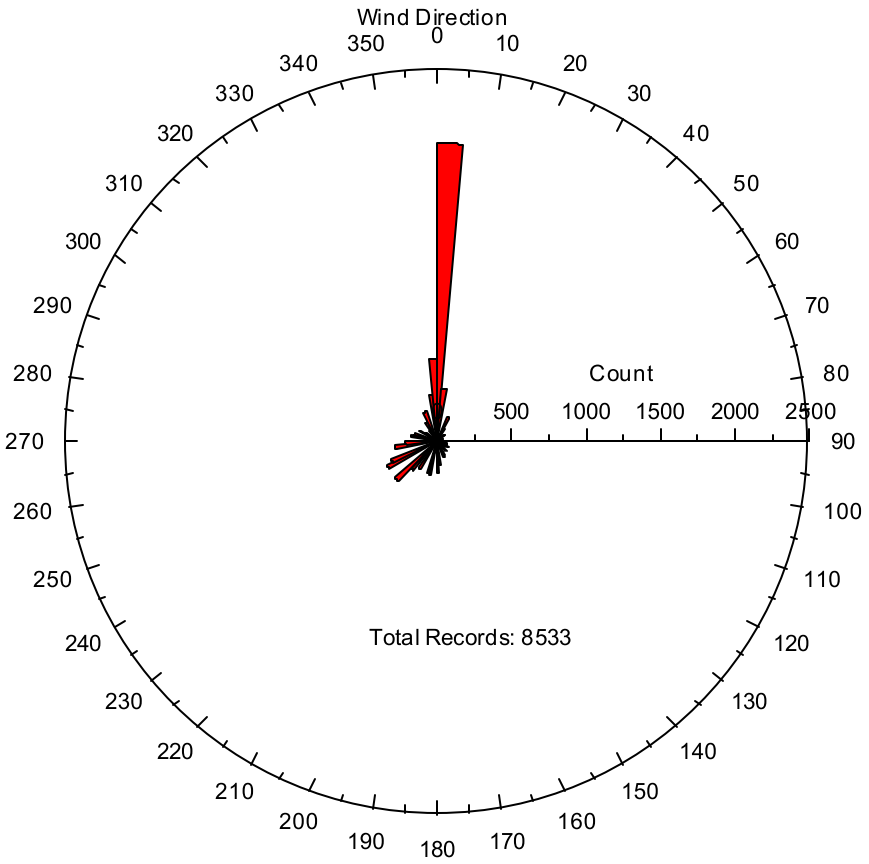


**Figure 234. Wind direction at McMinnville Municipal Airport, 2001**

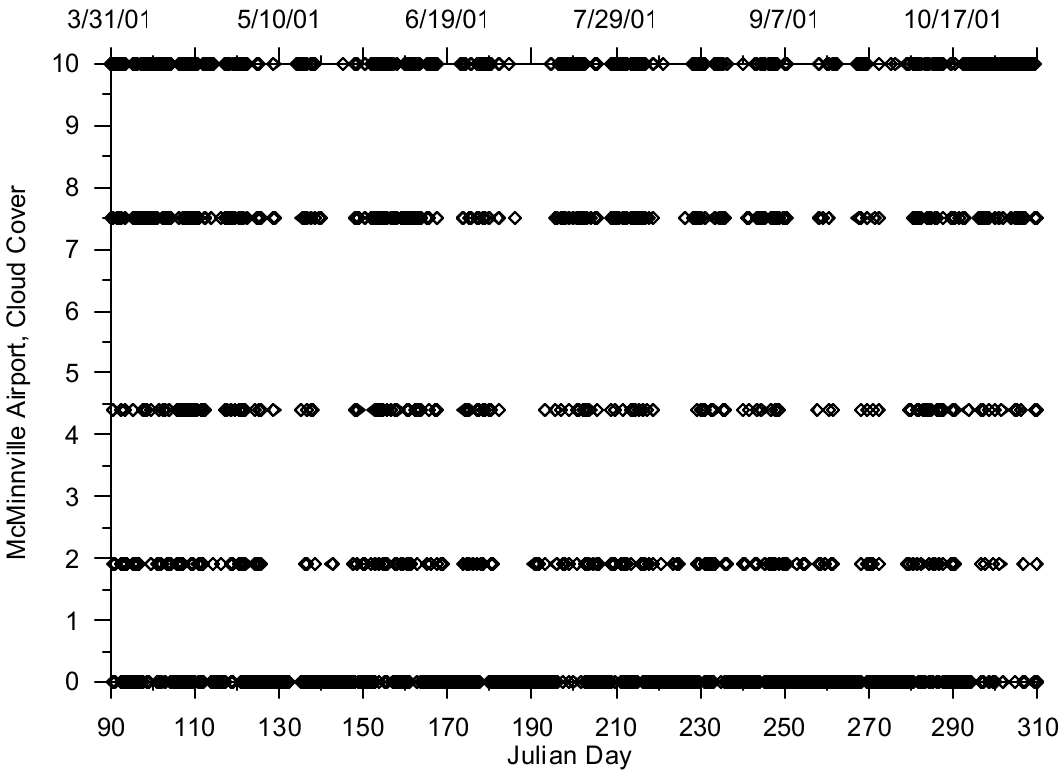


**Figure 235. Cloud cover at McMinnville Municipal Airport, 2001**

Year 2002

The McMinnville Municipal Airport recoded similar meteorological data as that at the Aurora Municipal Airport with the exception of solar radiation data. Figure 236 and Figure 237 show the air and dew point temperature, respectively. Figure 238 and Figure 239 show the wind speed and direction, respectively. Figure 238 indicated that the minimum wind speed-recording threshold was 1.5 m/s. The rose diagram in Figure 239 showed that the predominant wind direction was from the North but with some periodic winds coming from the Southwest as in 2001. The North wind predominance is partly due to wind speeds falling below the threshold velocity which sets both the direction and speed to zero. Figure 240 shows the cloud cover data recorded at the airport with five designations. There were no solar radiation data available at the McMinnville airport.

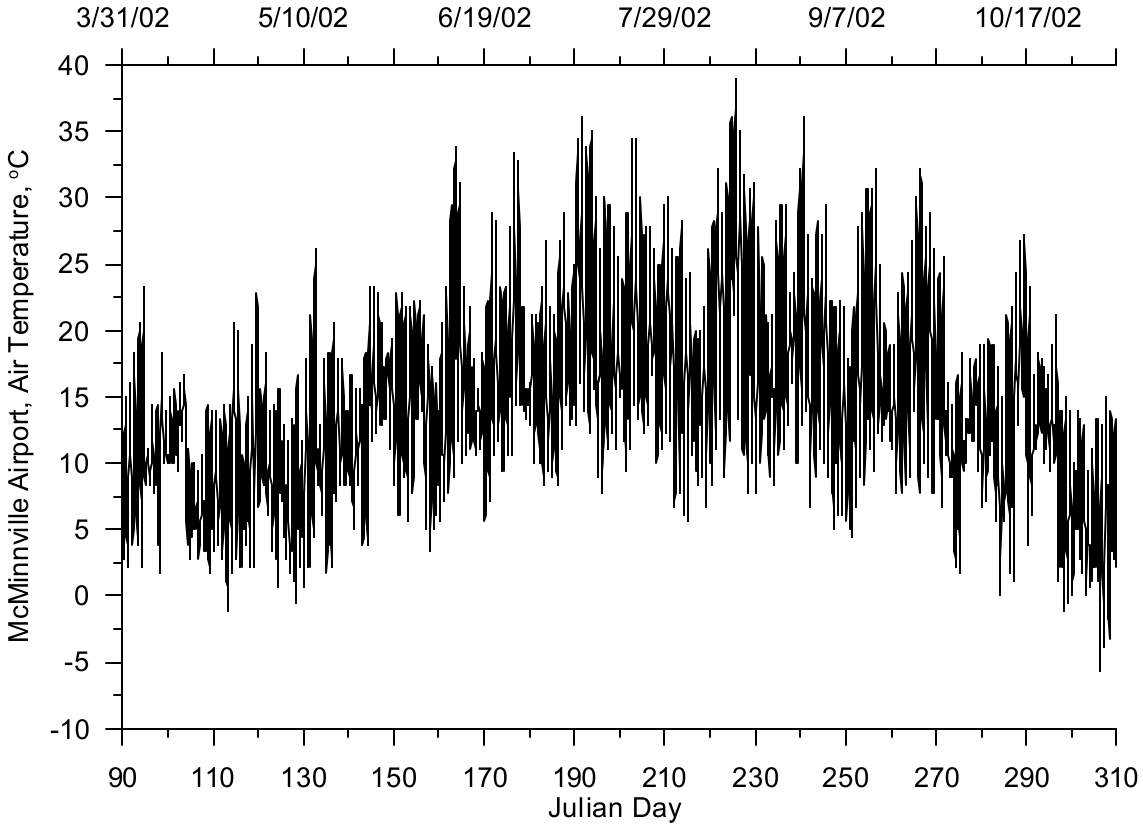


**Figure 236. Air temperature at McMinnville Municipal Airport, 2002**

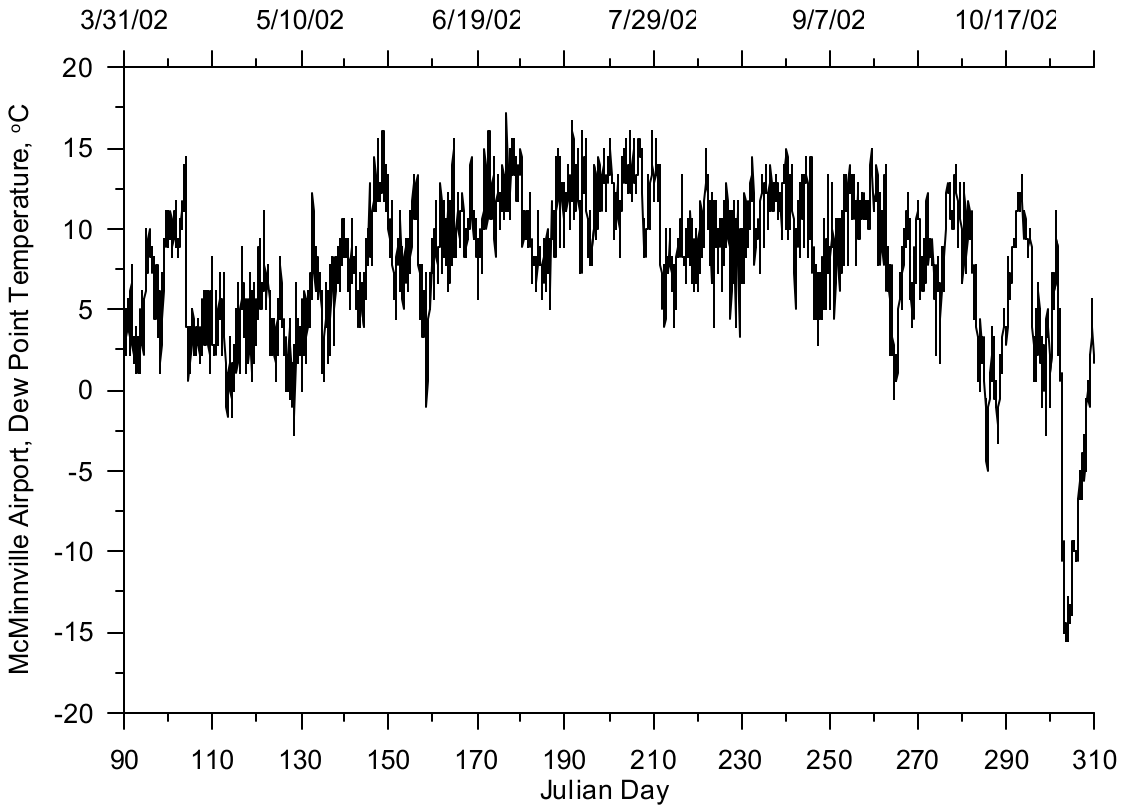


**Figure 237. Dew point temperature at McMinnville Municipal Airport, 2002**

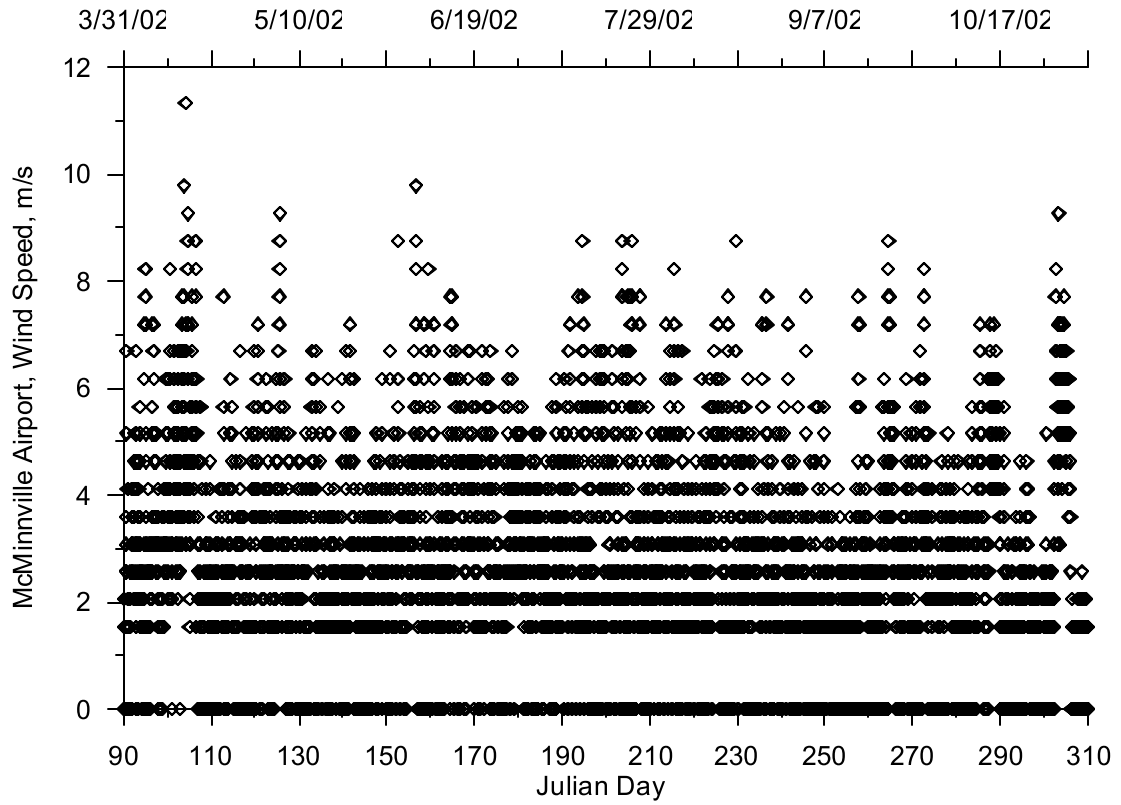


**Figure 238. Wind speed at McMinnville Municipal Airport, 2002**

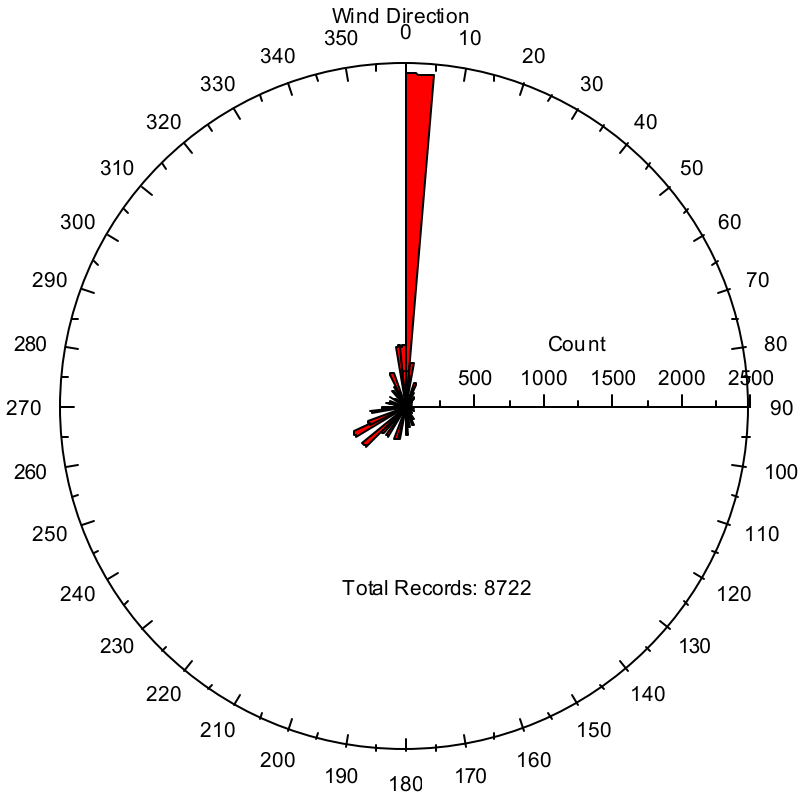


**Figure 239. Wind direction at McMinnville Municipal Airport, 2002**

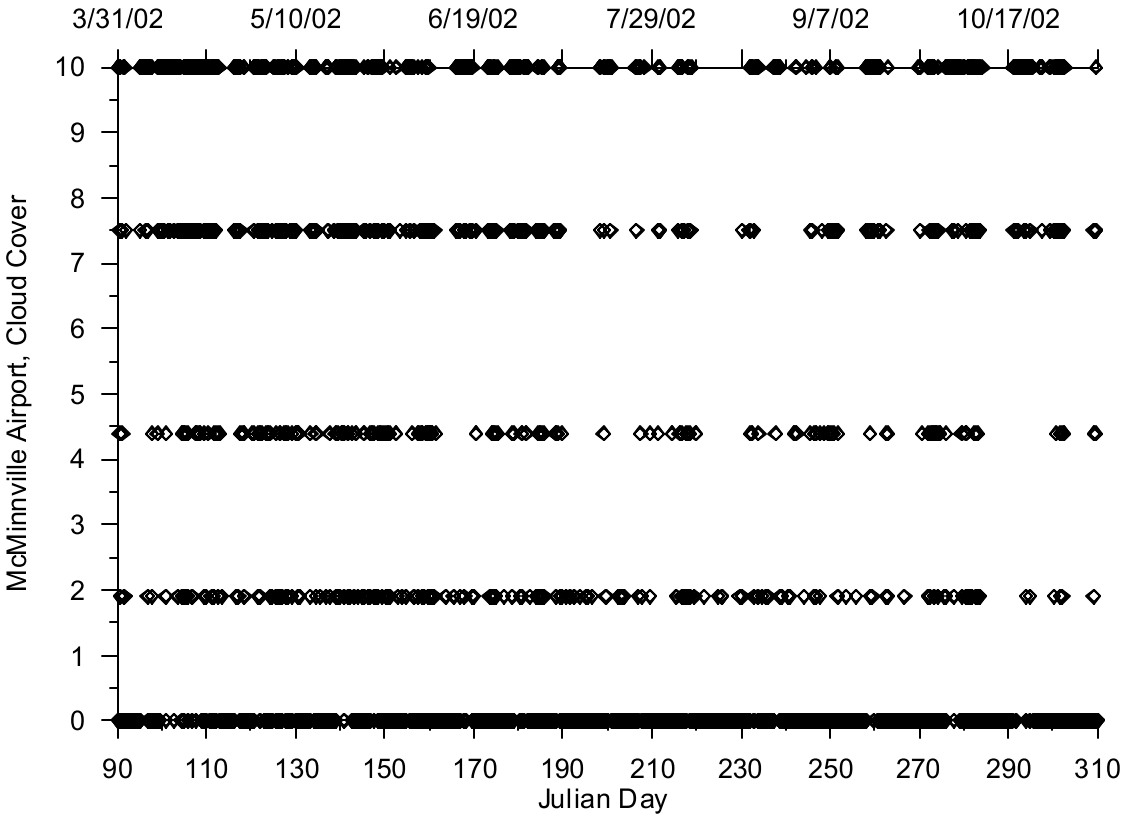


**Figure 240. Cloud Cover at McMinnville Municipal Airport, 2002**

## Aurora Municipal Airport

Year 2001

Aurora Municipal Airport provided hourly data for air and dew point temperature, wind speed and direction, and cloud cover for 2001. Figure 241 and Figure 242 show the air and dew point temperature respectively. Figure 243 and Figure 244 show the wind speed and direction, respectively. Figure 243 showed that the minimum wind speed-recording threshold was about 1.5 m/s. The value between the instrument recording values was an interpolated value. The rose diagram in Figure 244 indicated that the predominant wind direction was from the North which was partly due to the wind direction being set to zero when the wind speed was below the threshold velocity. Figure 245 shows the coarseness of the cloud cover data recorded at the airport with five different cloud cover designations. Figure 246 shows the global solar radiation recorded nearby in Gladstone, OR.

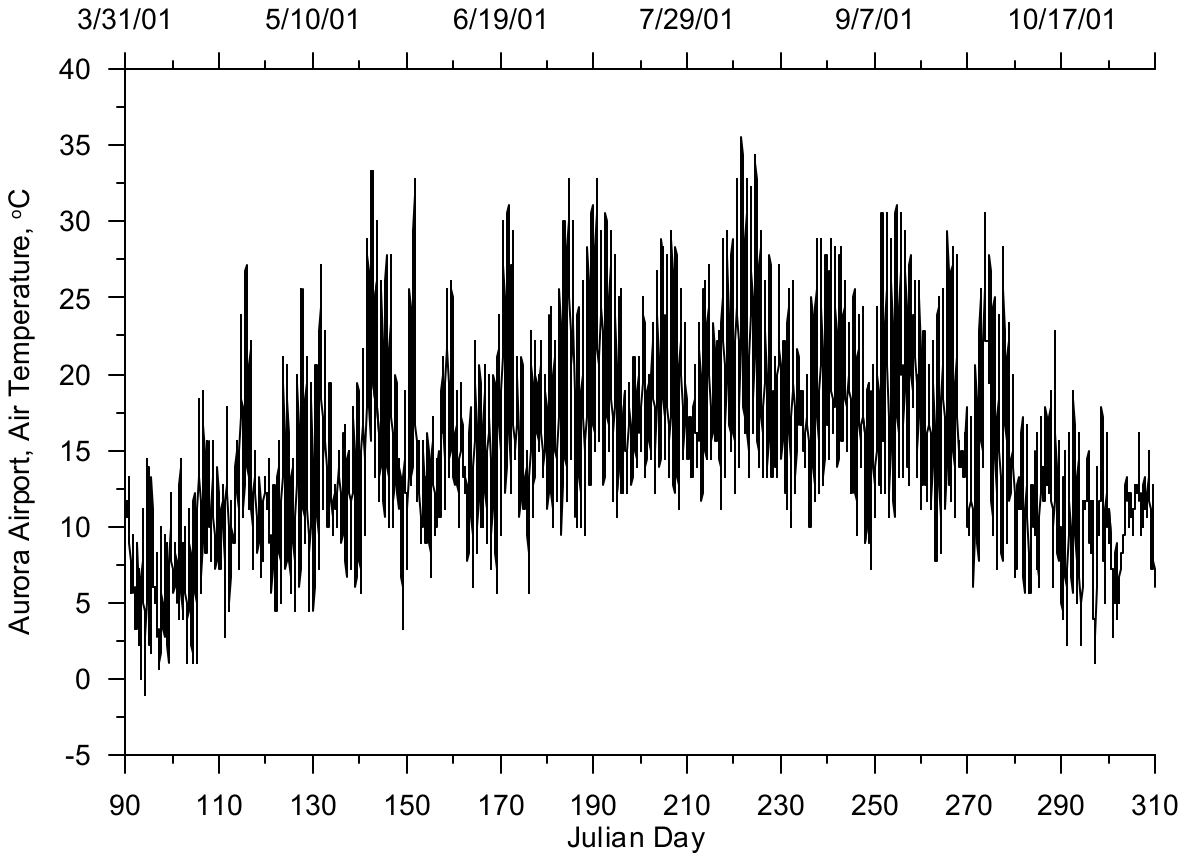


**Figure 241. Air temperature at Aurora Municipal Airport, 2001**

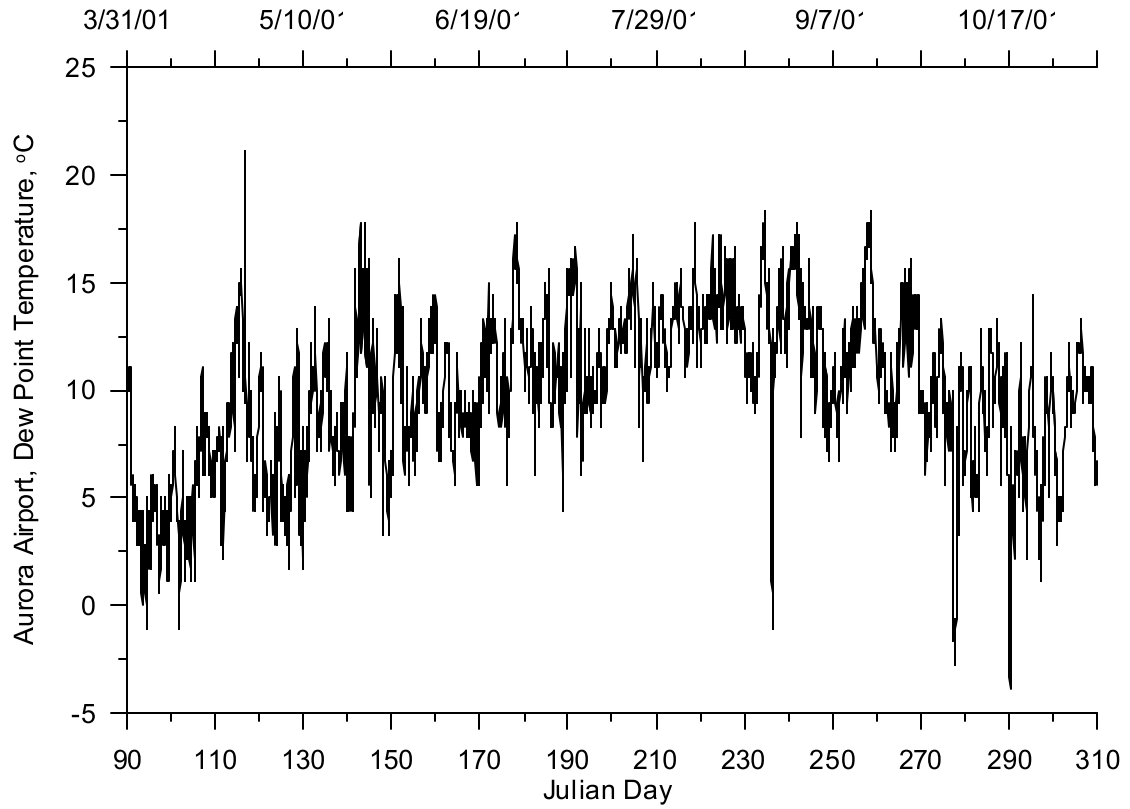


**Figure 242. Dew point temperature at Aurora Municipal Airport, 2001**

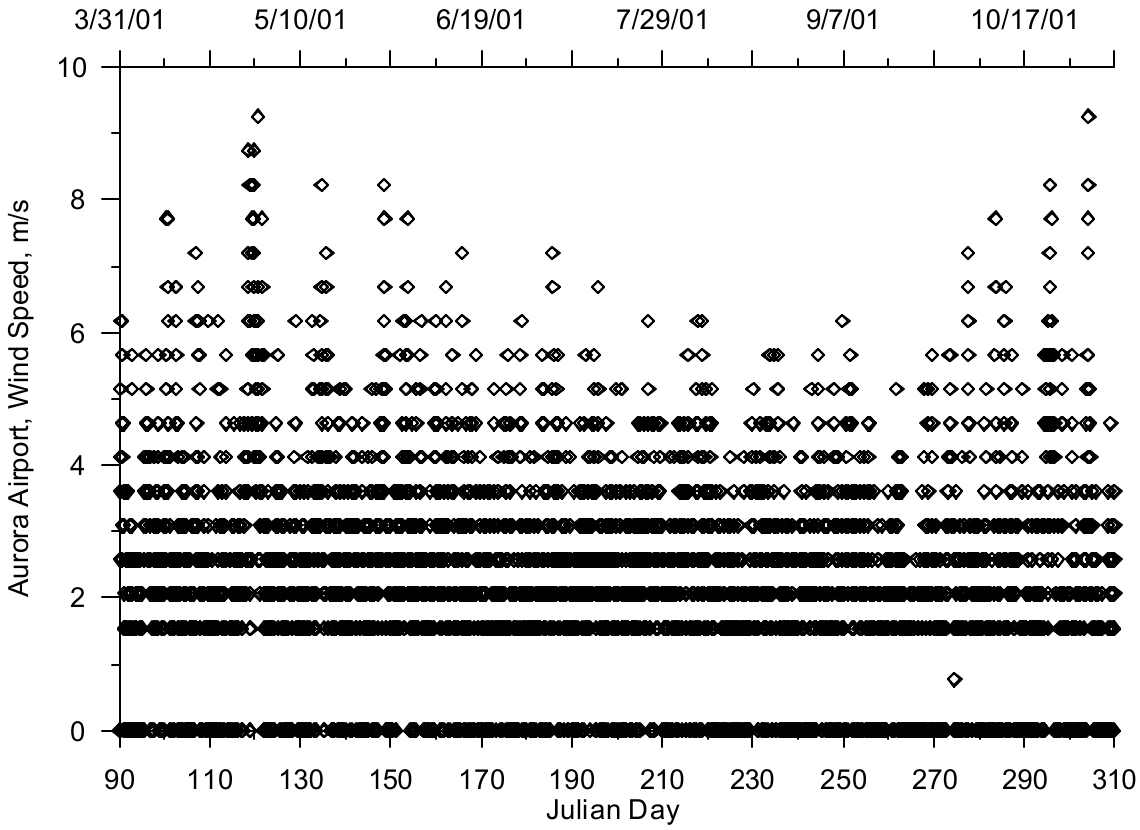


**Figure 243. Wind speed at Aurora Municipal Airport, 2001**

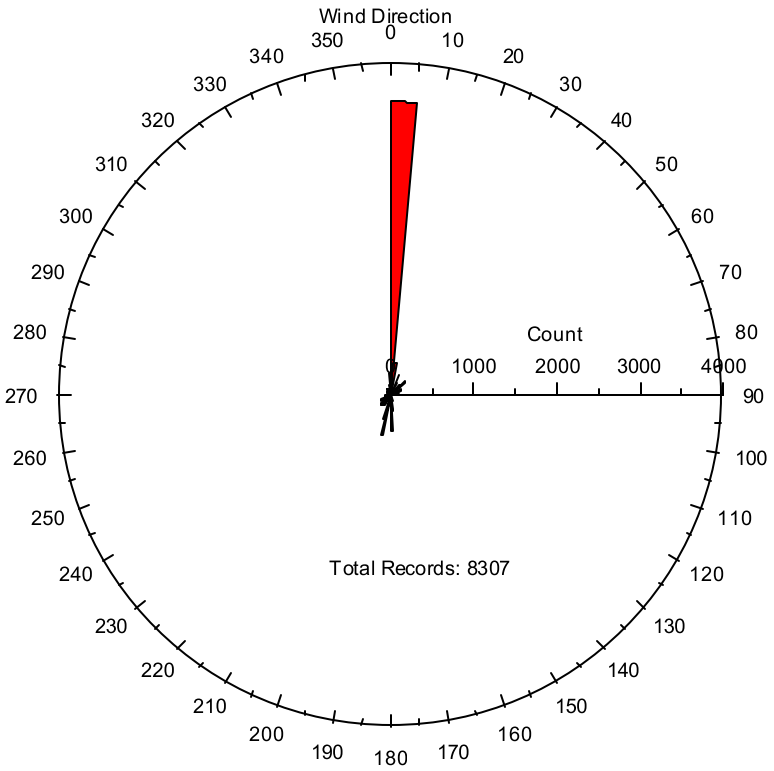


**Figure 244. Wind direction at Aurora Municipal Airport, 2001**

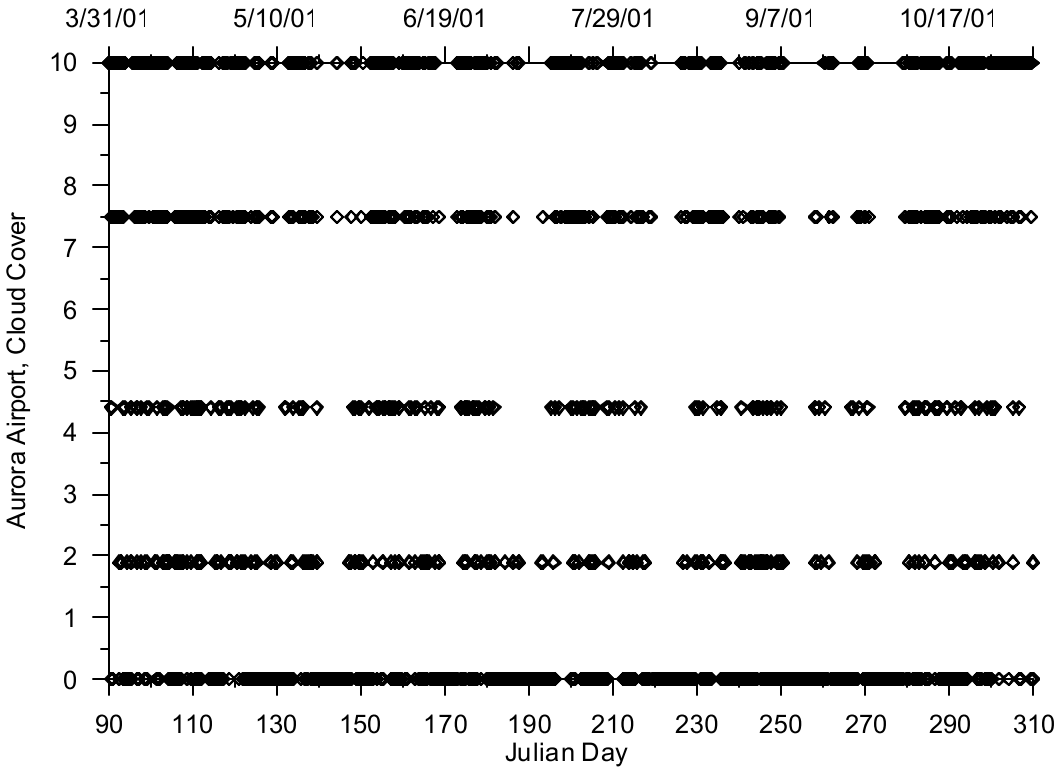


**Figure 245. Cloud cover at Aurora Municipal Airport, 2001**

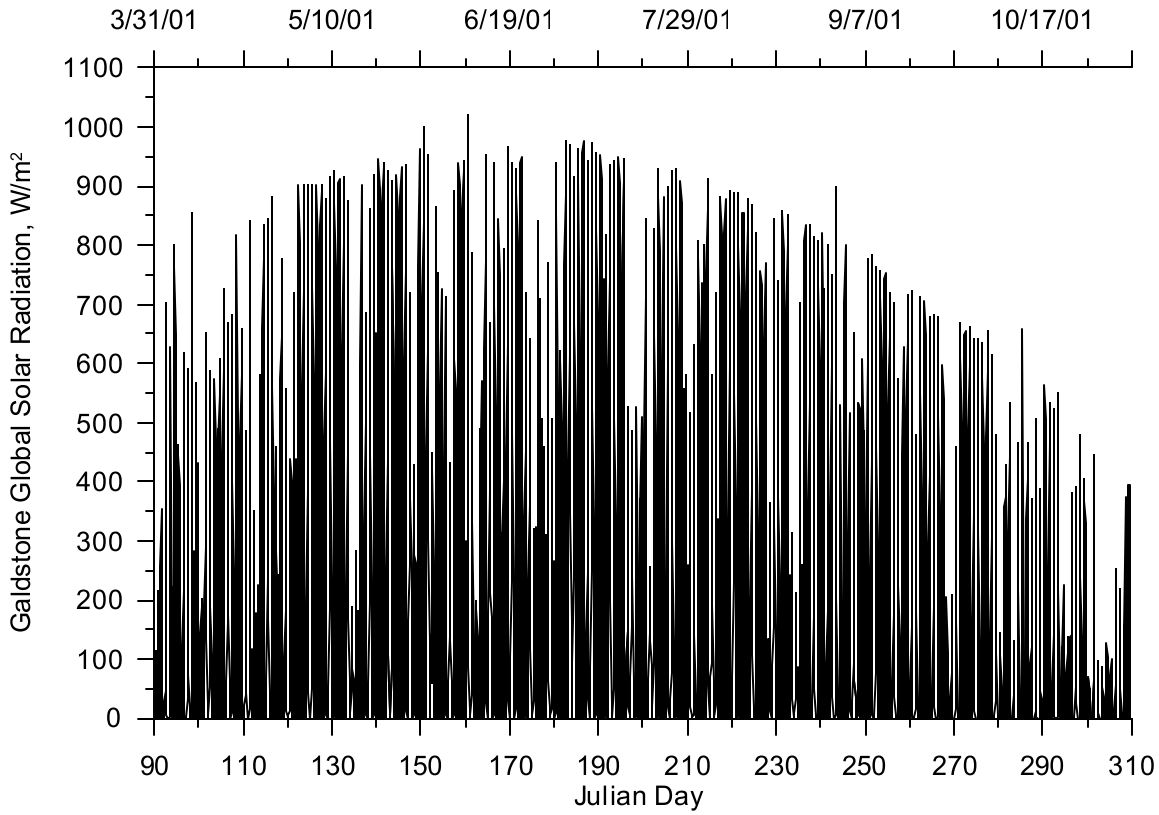


**Figure 246. Global Solar radiation at Gladstone, OR, 2001**

## Year 2002

Aurora Municipal Airport provided hourly data for air and dew point temperature, wind speed and direction, cloud cover and solar radiation for 2002. Figure 247 and Figure 248 show the air and dew point temperature respectively. Figure 249 and Figure 250 show the wind speed and direction, respectively. Figure 249 showed that the minimum wind speed-recording threshold was about 1.5 m/s. This figure also showed that some wind speeds were below this minimum recording threshold, which represented interpolated values used to fill data gaps in the times series record. The rose diagram in Figure 250 indicated that the predominant wind direction is from the North which is partly due to the wind direction being set to zero when the wind speed is below the threshold velocity. Figure 251 shows the coarseness of the cloud cover data recorded at the airport with five different cloud cover designations with some values in-between due to interpolating values to fill data gaps. Figure 252 shows the global solar radiation recorded at the Aurora Municipal Airport.

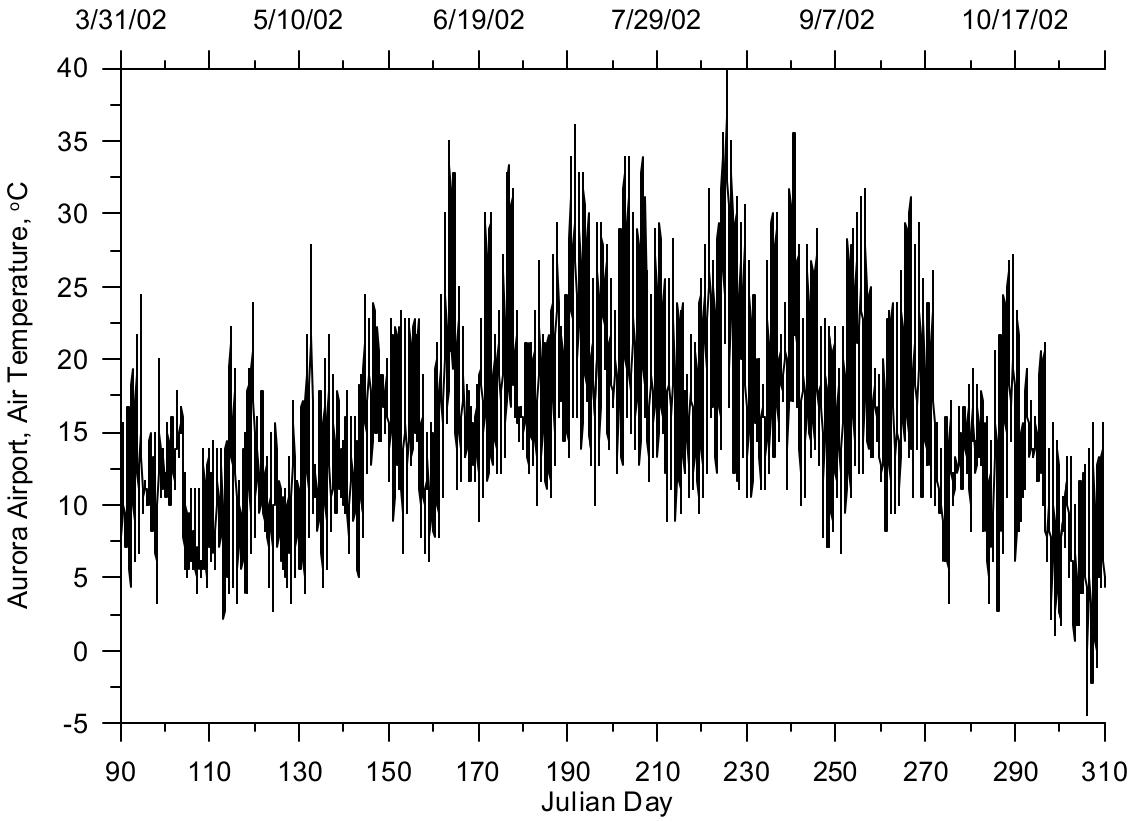


**Figure 247. Air temperature at Aurora Municipal Airport, 2002**

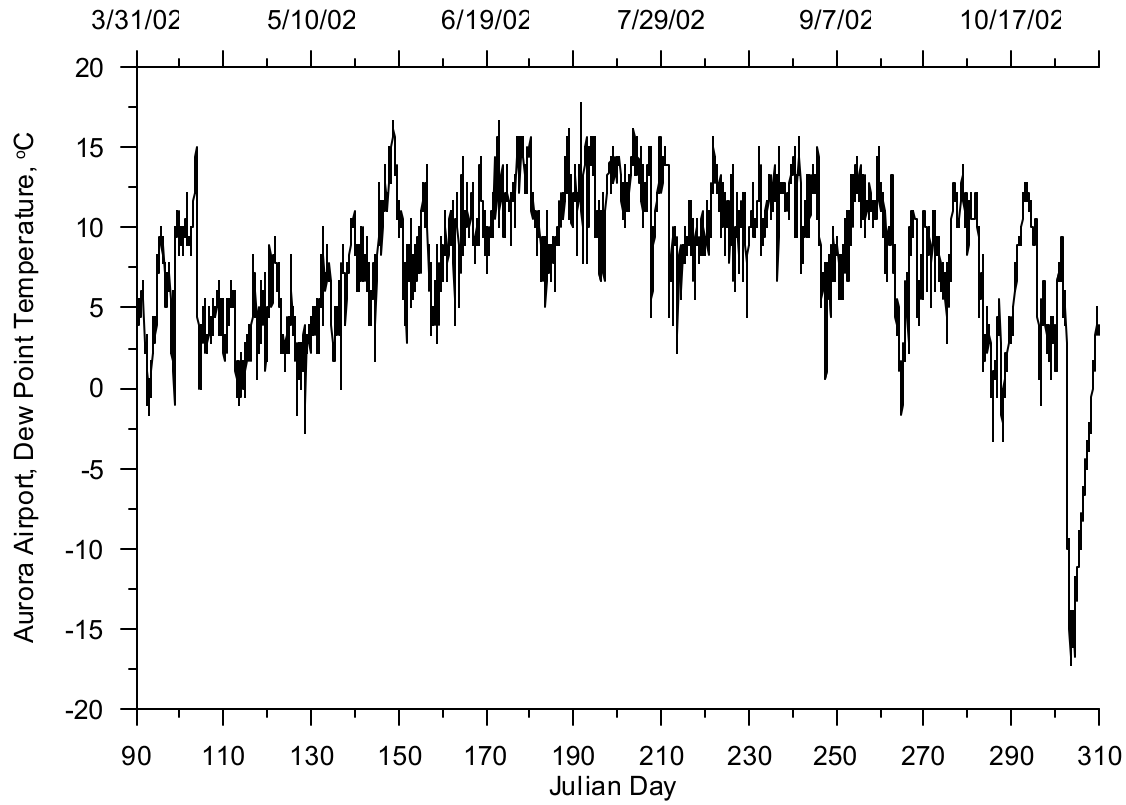


**Figure 248. Dew point temperature at Aurora Municipal Airport, 2002**

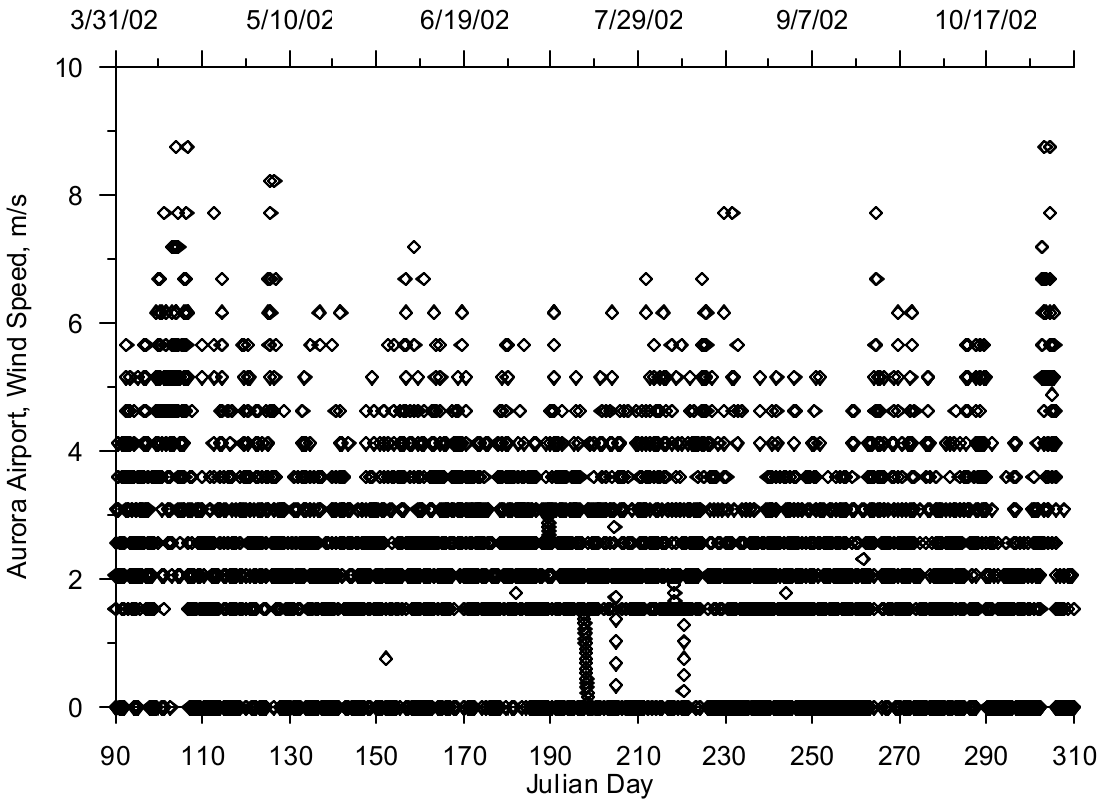


**Figure 249. Wind speed at Aurora Municipal Airport, 2002**

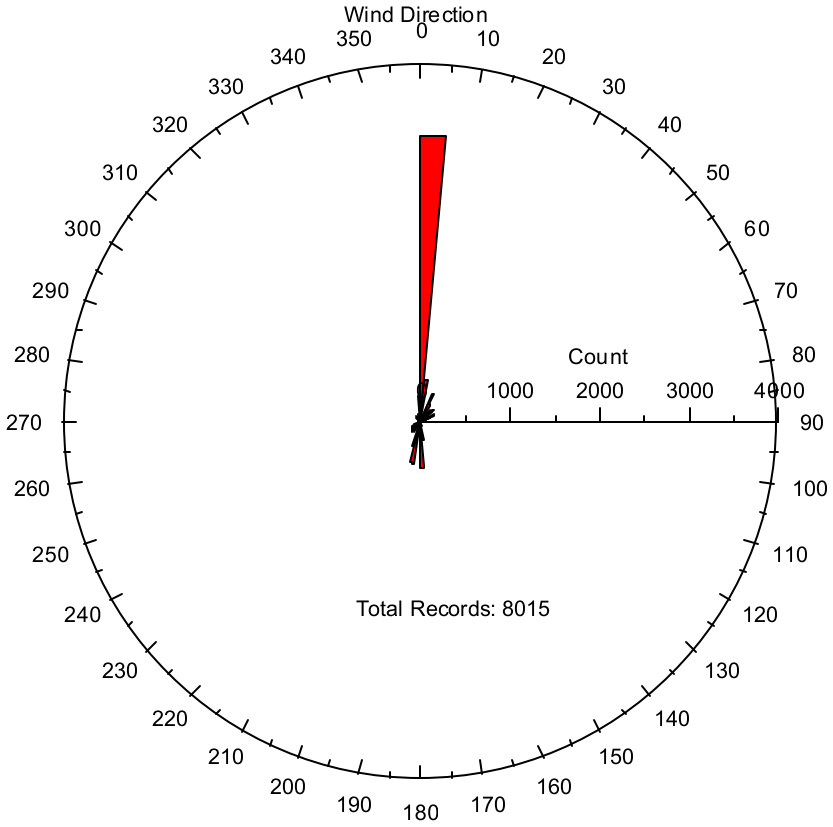


**Figure 250. Wind direction at Aurora Municipal Airport, 2002**

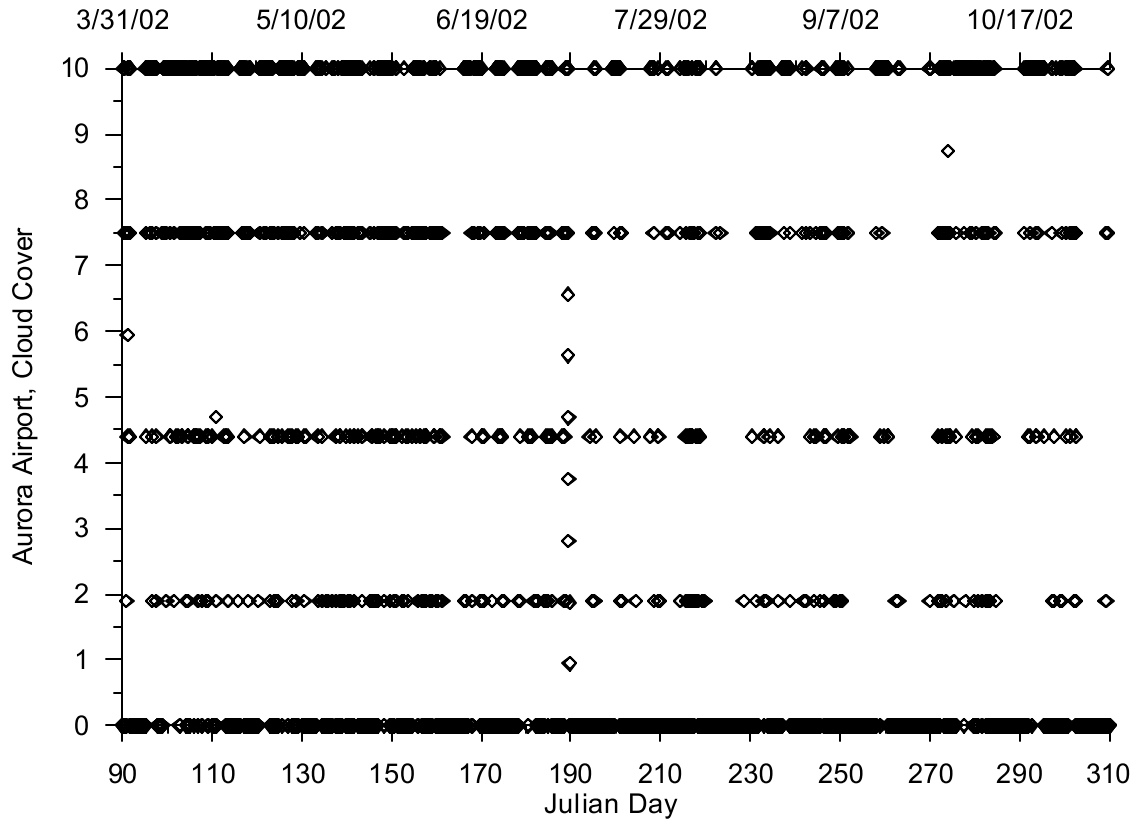


**Figure 251. Cloud cover at Aurora Municipal Airport, 2002**

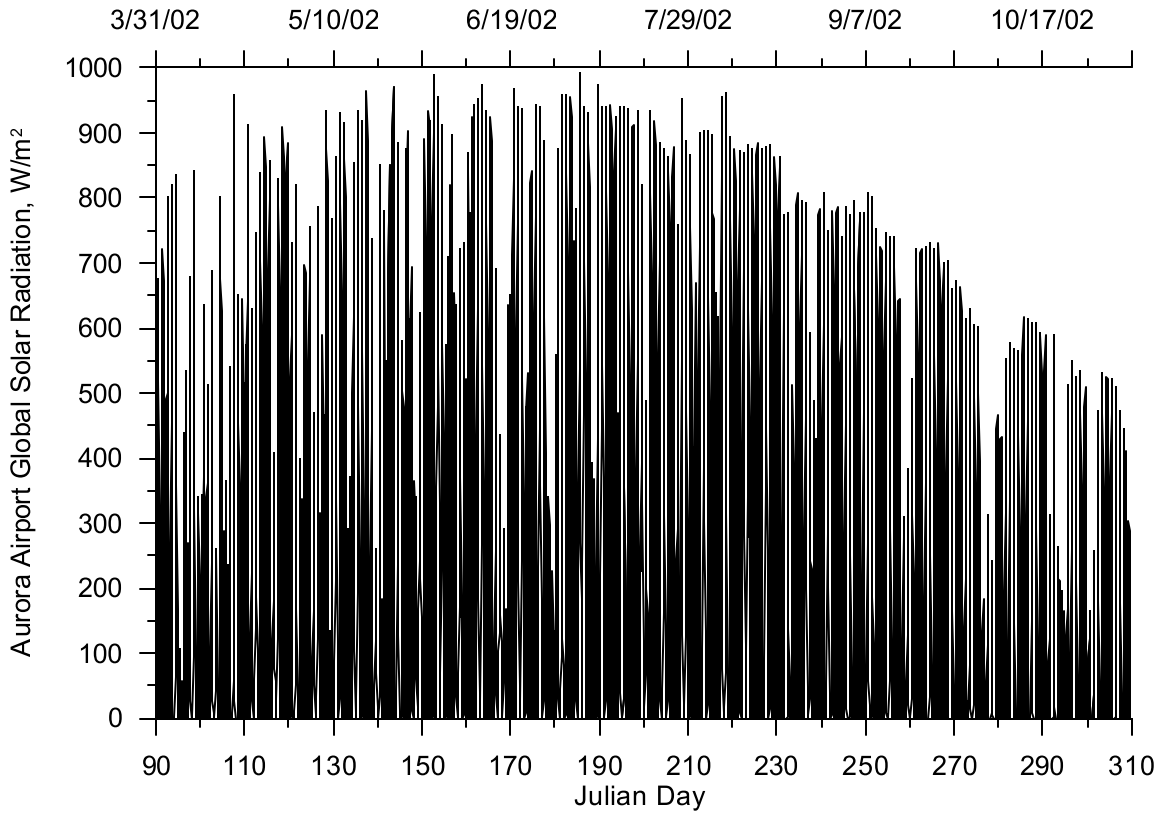


**Figure 252. Global solar radiation at Aurora Municipal Airport, 2002**

## *Willamette Falls Structures*

The primary structures the Willamette Falls are the dam and flashboards operated to hold water for power generation. Figure 253 shows a plan view of the Willamette Falls and the dam sections. In order to accurately model water surface elevations at these facilities it was important to understand the size of the dam and the operations of the flashboards. Table 25 shows a list of the dam heights with and without flashboards. Flashboards are put in place in the spring of each year and left in place until they washed out during the following winter. Figure 254 shows an aerial photograph of the Willamette Falls and the dam structures at the falls.

Since detailed bathymetric data were collected by PGE just upstream of the Willamette Falls, these data were utilized to examine the size and length of the natural "dam" if the constructed dam and flashboards were removed. Figure 255 shows a contour plot of the river bathymetry upstream of the falls, and Figure 256 shows a series of three-dimensional surface plots of the river bathymetry to illustrate flow paths through the Willamette Falls.

The natural "dam" at the Willamette Falls consisted of a low elevation weir with a crest elevation of 13.75 m above (45.11 ft) above mean sea level based on Transect 2 shown in Figure 257 and Figure 258. The flow equation applied for the low elevation weir was developed from the broad crested weir equation (Gupta, 1989):

$$Q = 0.385 C_d \sqrt{2g} L H^{\frac{3}{2}}$$

Where,

$C_d$ - broad crested weir coefficient, typical values 0.85 to 1.1;

$g$ - acceleration of gravity (m/s$^2$);

$L$ - weir length (m);

$H$ - depth of water above weir crest (m)

This single weir equation was used assuming $L$=625 m and with $C_d$ =1.0, resulting in the following equation:

$$Q = 1066 H^{\frac{3}{2}}$$

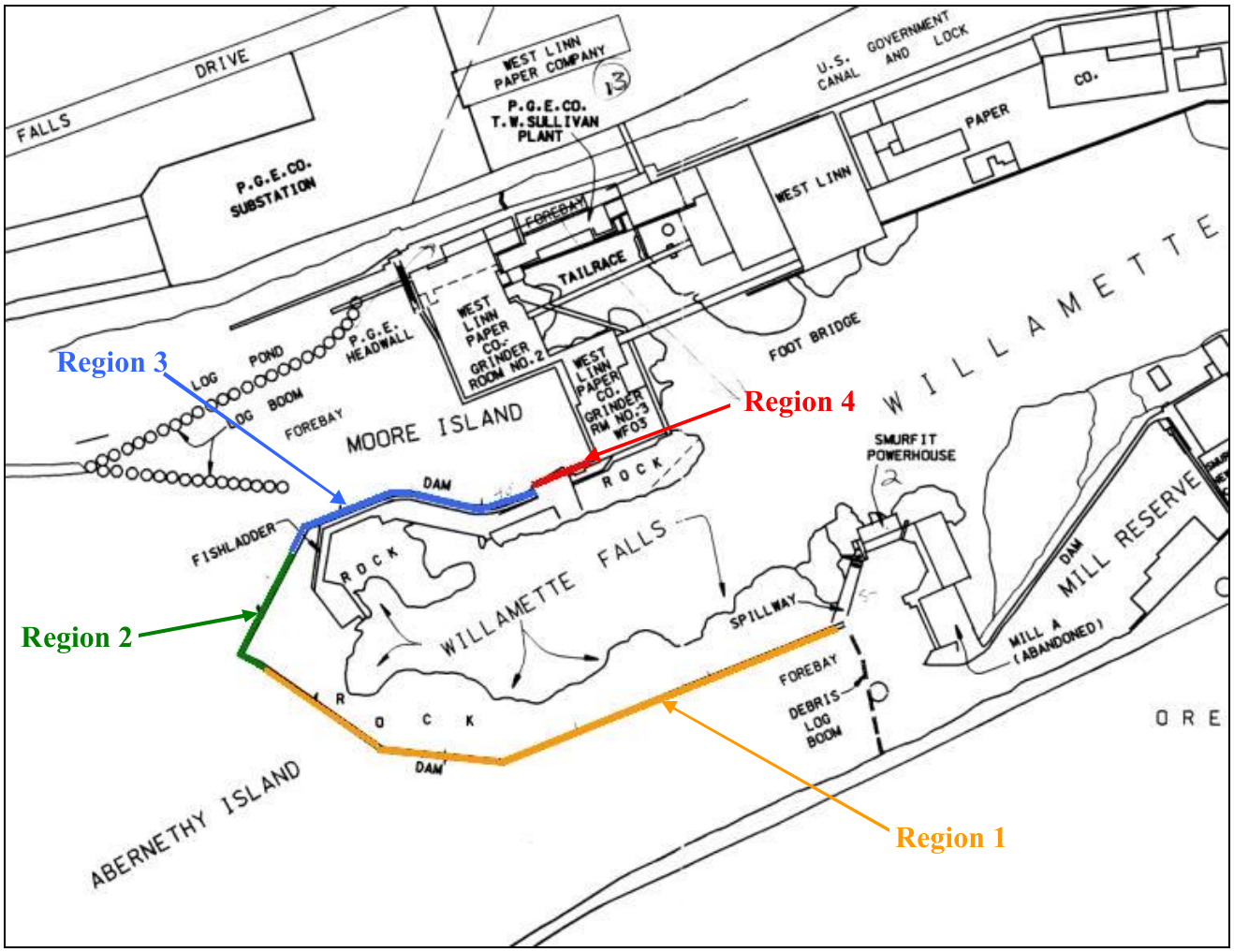


**Figure 253. Plan view of the Willamette Falls (PGE)**

**Table 25. Dam and flashboard specifications at the Willamette Falls**

| Region | Dam Section Length, ft | Dam Height, ft | Height with flashboards |
|---|---|---|---|
| 1 | 1450 | 52.0 | 54.0 |
| 2 | 350 | 54.7 | N/A |
| 3 | 375 | 52.5 | 55.5 |
| 4 | 175 | 56.9 | N/A |


**Figure 254. Aerial view of Willamette Falls and dam structures (compliments of PGE)**

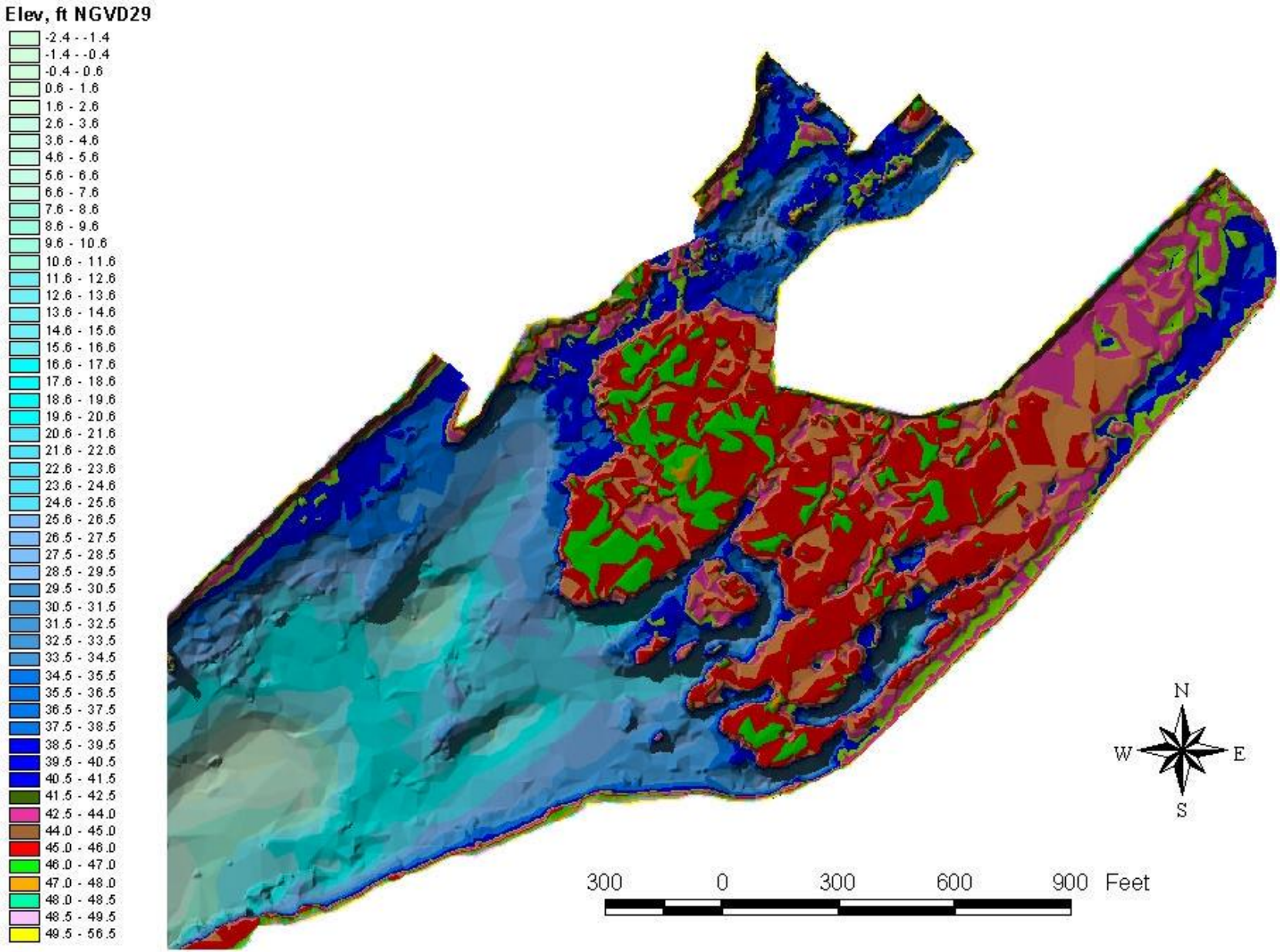


**Figure 255. Channel bathymetry surface plot upstream of Willamette Falls**

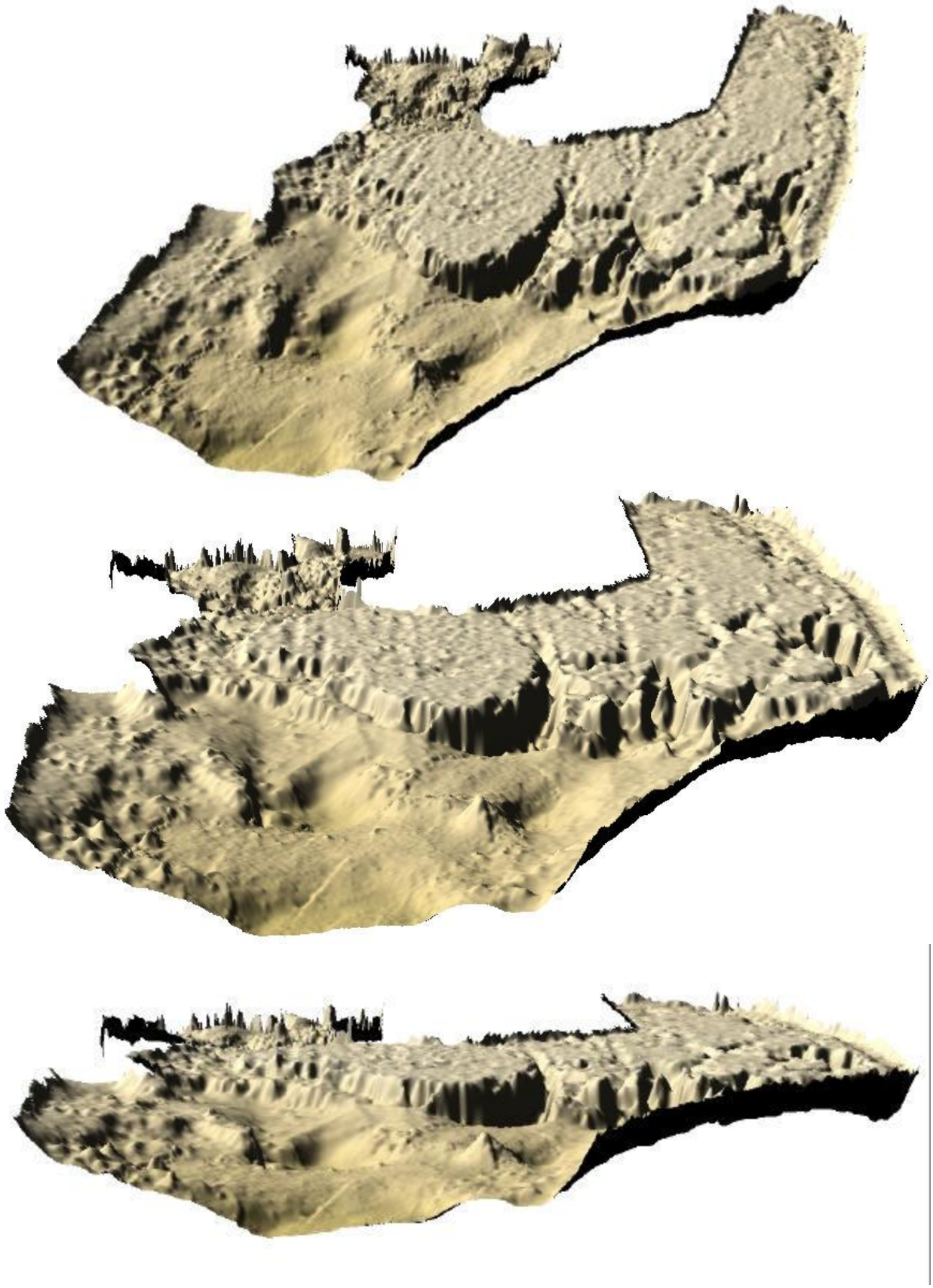

**Figure 256. 3-D view of the Willamette River bathymetry upstream of the Willamette Falls**

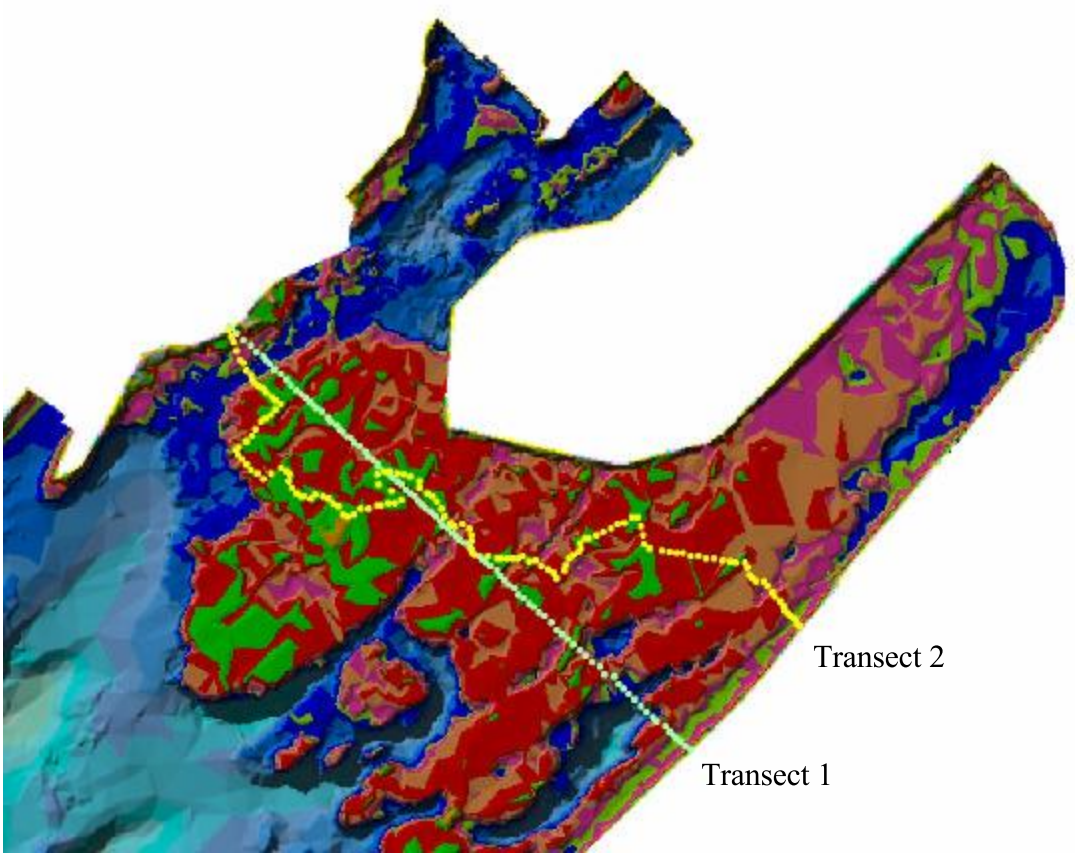


**Figure 257. Topography at the Willamette Falls. The lines indicate transects that were made to evaluate critical elevations of the Falls for modeling the system without the PGE dam.**

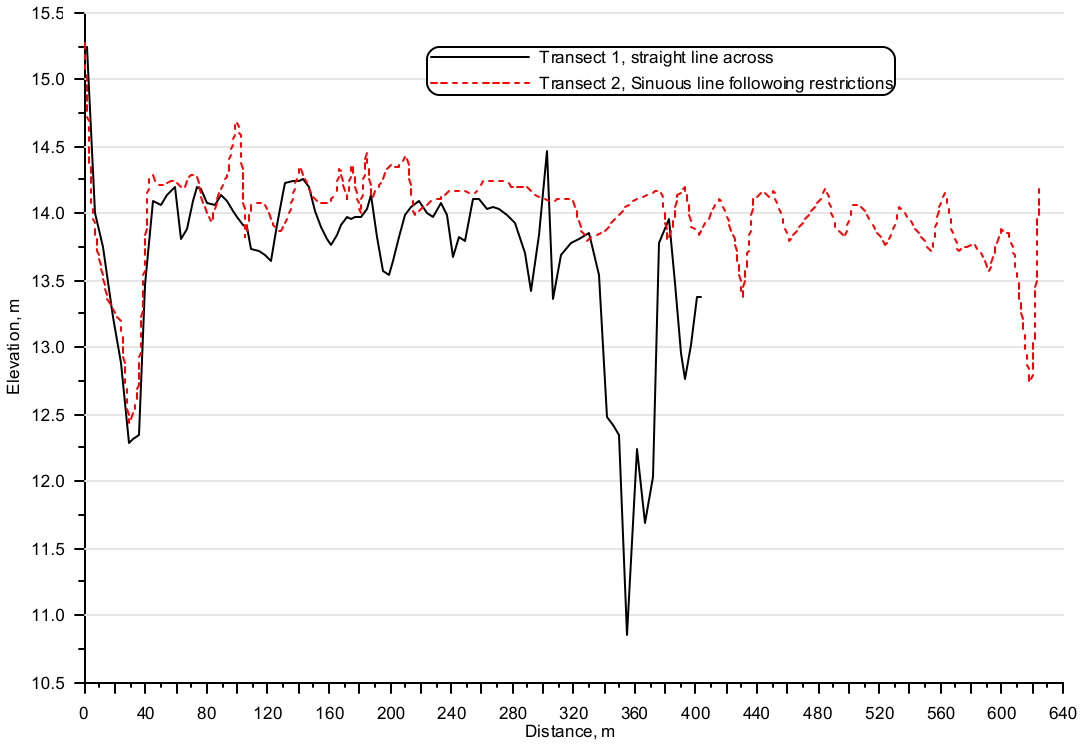


**Figure 258. Transects taken across the rock ledge at Willamette Falls.**

## Upper Willamette River

The Upper Willamette River model extended from RM 185.2 to RM 85.4, which is approximately from the City of Springfield to the City of Salem. The upstream end was below the confluence of the Coast Fork and Middle Fork Willamette Rivers. The major tributaries to the model were the McKenzie River, the Long Tom River, Mary's River, the Calapooia River, the Luckiamute River, the Santiam River, and Rickreall Creek. Figure 259 shows the model extent, tributaries, and selected cities of interest. The Willamette River at Salem has a drainage area of approximately 18,700 $km^2$ (including tributaries); The Upper Willamette River model incorporates 4,100 $km^2$ of drainage area to the model output from the Coast & Middle Fork Willamette, McKenzie River, Long Tom River, and Santiam River model areas. The calibration period for 2001 was June 12 to September 25. The calibration period for 2002 was June 4 to October 1.

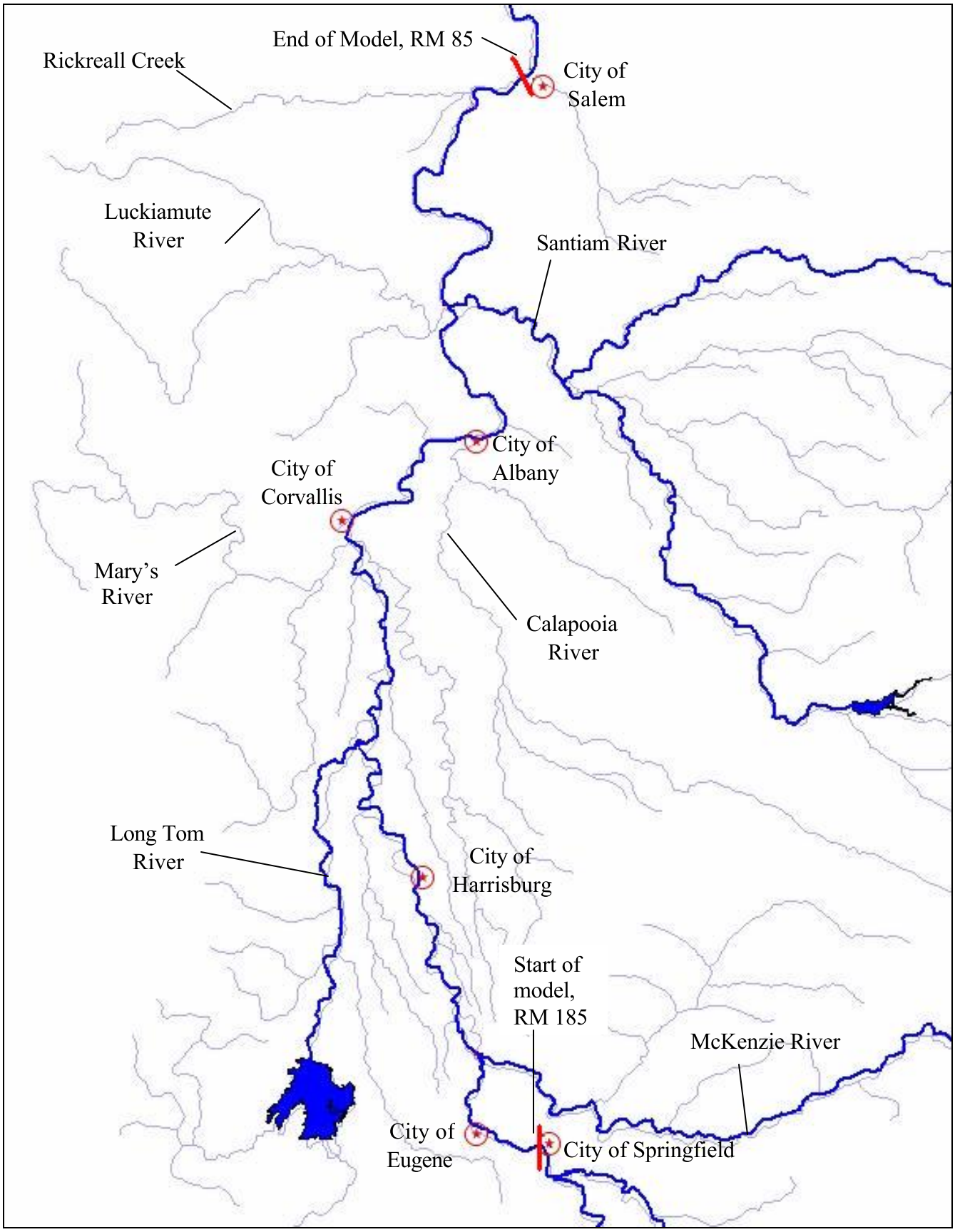


**Figure 259. Upper Willamette River model region**

## Bathymetry Data

The data used to generate the model bathymetry were obtained from a USGS bathymetric survey (Rounds, 2002) and Digital Elevation Maps (DEM). Using a boat equipped with acoustic Doppler sonar, transverse channel profiles were generated approximately once a mile. Assuming a linear water surface elevation profile between points of known water surface elevation along the river (survey benchmarks), the depth measurements were converted to elevations. The locations of the USGS bathymetric cross sections are shown in Figure 260 and extended from approximately South Salem, OR, (RM 89) to the confluence with the McKenzie River (RM 175). No cross sections were available upstream of the McKenzie River.

The DEMs had a vertical resolution of 1 m and a horizontal resolution of 10 m. Using linear interpolation, additional cross sections were generated at a spacing/frequency of 100 feet using the river thalweg point generated from a GIS analysis conducted by ODEQ. The calculated cross sections were combined with DEM data and the surveyed cross sections into the contour mapping program, SURFER. An average volume-elevation relationship was calculated over the length of each model segment using a one meter vertical resolution.

Due to the size of the area, the data could not be processed at once, so this process was repeated for the four model reaches. Table 26 lists reach descriptions. The USGS bathymetric survey cross section data started at RM 89, and the model downstream boundary was set at RM 85.4. Additional bathymetric cross sections were calculated by extending the first cross section at RM 89 downstream and adjusting the channel width based on the ODEQ GIS data set (channel widths at 30.48 m intervals along the river) and adjusting the elevation based on river slope from the ODEQ GIS data set.

The upstream end of the fourth reach originally terminated at the confluence of the Coast and Middle Fork Willamette Rivers. Although processed with the Upper Willamette River model bathymetry, approximately 2.5 miles of the Upper Willamette model bathymetry were transferred to the Coast Fork and Middle Fork Willamette River model. This allowed the temperature monitoring site (LASAR 10359) at Springfield (RM 184.4) to serve as a good temperature upstream boundary condition for the Upper Willamette River Model and a good downstream temperature boundary location for the Coast Fork and Middle Fork Willamette River model.

There were no cross-sectional data above the McKenzie River in the fourth reach. Additional cross sections were estimated in the fourth reach by extending the last river cross section upstream at RM 175 upstream and adjusting the width of the cross section based on the channel width from the GIS data obtained from ODEQ. The cross section elevations were based on the slope of the river from the same GIS data.

After the four reaches were processed, they were recombined into a single model. Seventeen cross sections were graphically spot checked. Examples are shown in Figure 261. Comparisons of the USGS thalweg and the model channel bottom are shown in Figure 262 and Figure 263.

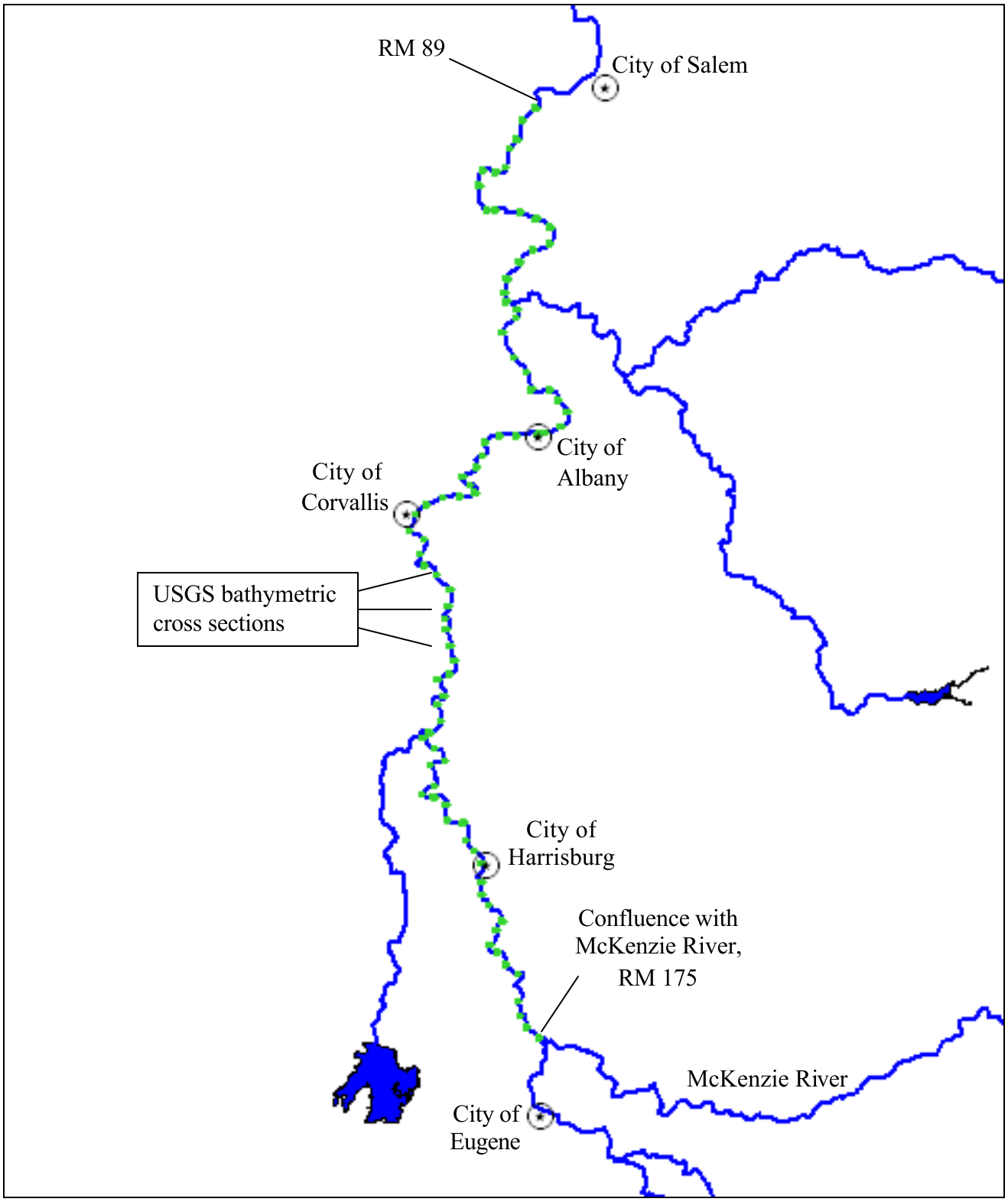


**Figure 260. 2002 USGS bathymetric cross section locations**

**Table 26. Model Grid Processing Reaches**

| Reach | Downstream RM | Upstream RM | Downstream geographical feature | Upstream geographical feature |
|---|---|---|---|---|

| Reach | Downstream RM | Upstream RM | Downstream geographical feature | Upstream geographical feature |
|---|---|---|---|---|
| 1 | 85.4 | 108.2 | City of Salem | Santiam River |
| 2 | 108.2 | 149.1 | Santiam River | Long Tom River |
| 3 | 149.1 | 175.1 | Long Tom River | McKenzie River |
| 4 | 175.1 | 186.9 | McKenzie River | Coast/Middle Fork Willamette Confluence |

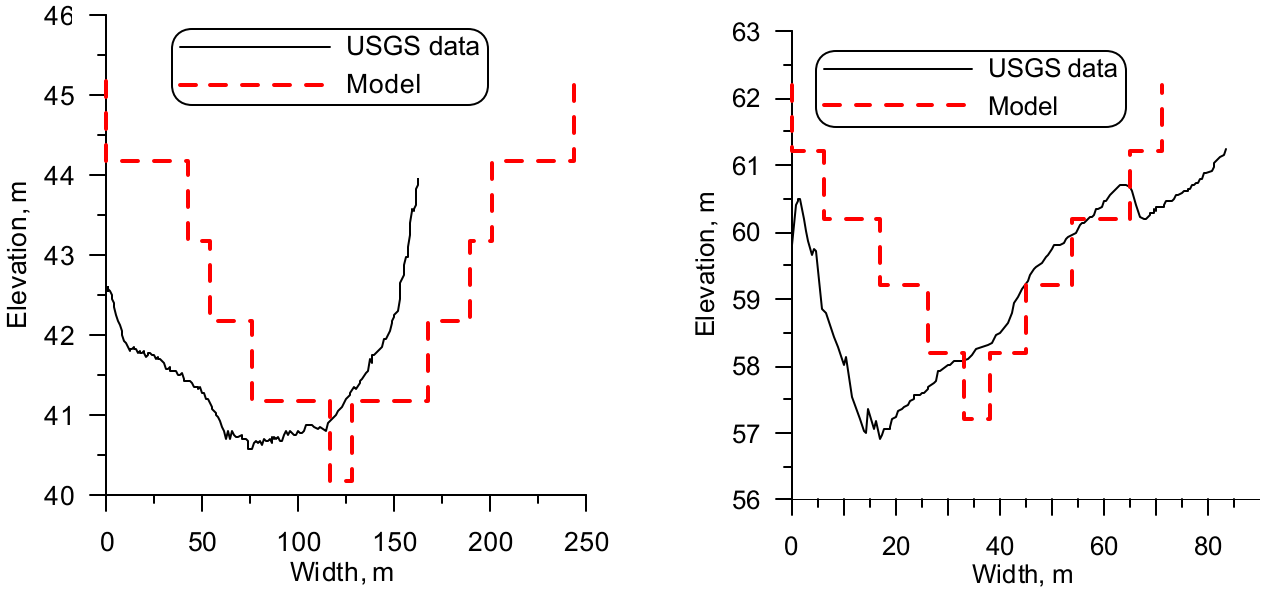


(a) RM 136.2, segment 327.

(b) RM 101.5, segment 560.

**Figure 261. Sample USGS bathymetric cross sections compared to schematized model cross sections**

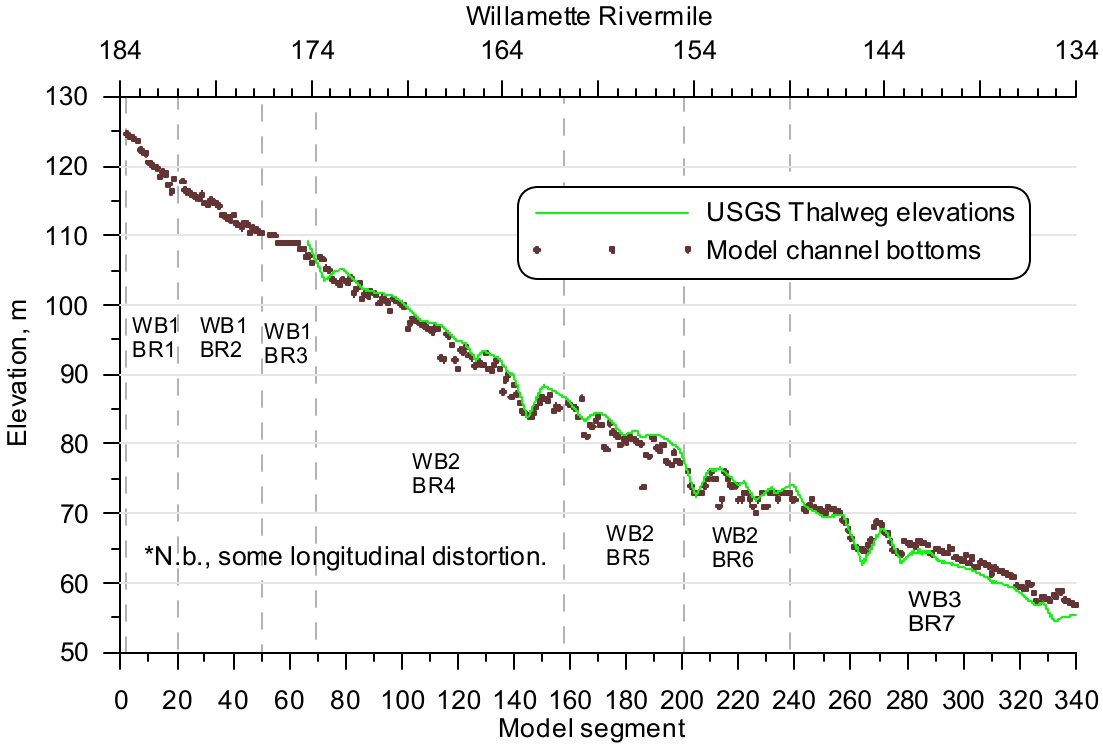


**Figure 262. Upper Willamette model channel bottom compared to USGS thalweg data, RM 184 to 134**

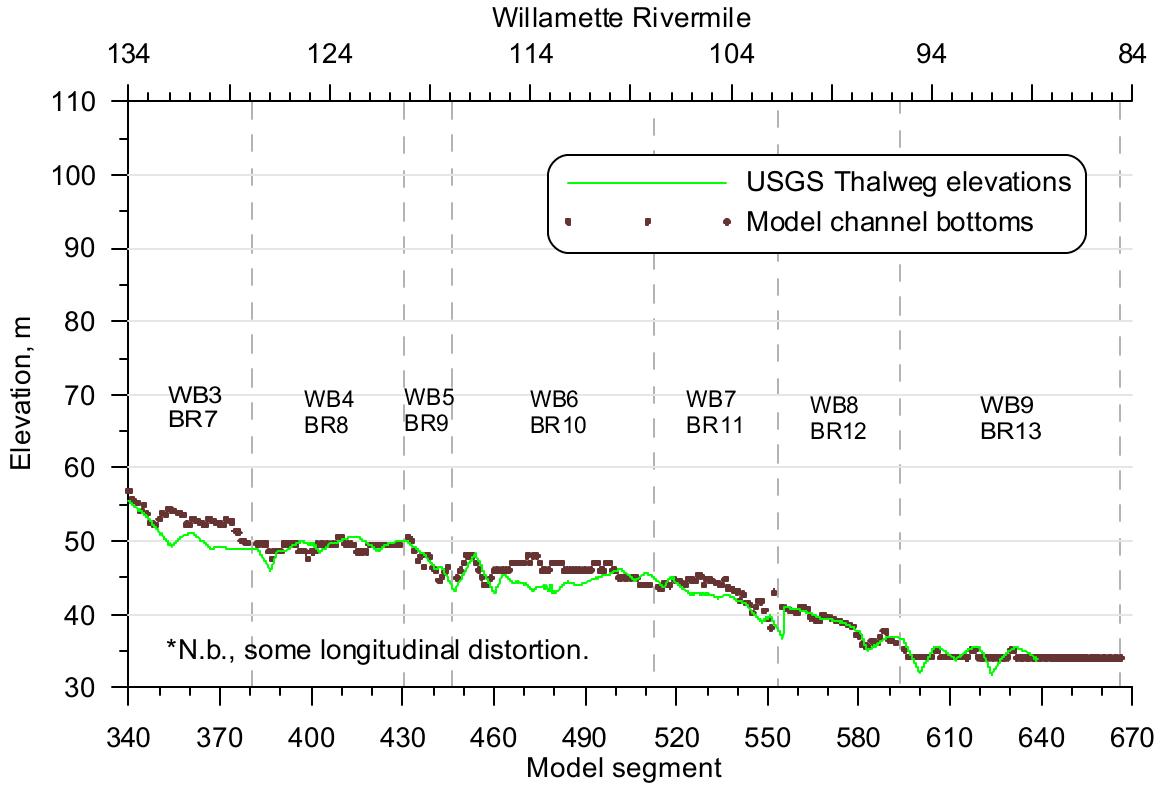


**Figure 263. Upper Willamette model channel bottom compared to USGS thalweg data, RM 134 to 85**

## Model Grid Development

The data were combined and the plotting program SURFER was used to create a contour plot of the stream channel. The contour plot was then used to generate the model grid. The model grid consists of nine water bodies and thirteen branches with grid layout specifications provided in Table 27. The grid layout for RM 85 to 108, for RM 108 to RM 149, for RM 149 to RM 175, and for RM 175 to RM 186 are shown in Figure 264, Figure 265, Figure 266, Figure 267, respectively.

**Table 27. Upper Willamette River Model Grid Layout**

| Water Body | Branch | Description | Starting Segment | Ending Segment | Starting RM | Ending RM | Segment Length, m | Slope | Upstream BC | Down-stream BC |
|---|---|---|---|---|---|---|---|---|---|---|
| 1 | 1 | Springfield to Eugene | 2 | 19 | 185.1 | 181.7 | 250.22 | 0.001070 | flow | internal |
| | 2 | Eugene to RM 177 | 22 | 50 | 181.7 | 177.2 | 250.22 | 0.001100 | internal | internal |
| | 3 | RM 177 to McKenzie River | 53 | 68 | 177.2 | 175.0 | 250.22 | 0.000020 | internal | internal |
| 2 | 4 | McKenzie River to Harrisburg | 81 | 156 | 175.0 | 161.5 | 250.51 | 0.001063 | internal | internal |
| | 5 | Harrisburg to RM 155 | 159 | 199 | 161.5 | 155.1 | 250.51 | 0.001070 | internal | internal |
| | 6 | RM 155 to Long Tom River | 202 | 240 | 155.1 | 149.3 | 250.51 | 0.000020 | internal | internal |
| 3 | 7 | Long Tom River to RM 128 | 243 | 379 | 149.3 | 127.7 | 250.56 | 0.000708 | internal | internal |
| 4 | 8 | RM 128 to Calapooia River | 382 | 429 | 127.7 | 120.2 | 250.56 | 0.000010 | internal | internal |
| 5 | 9 | Calapooia River to RM 118 | 432 | 445 | 120.2 | 118.0 | 250.56 | 0.001570 | internal | internal |
| 6 | 10 | RM 118 to Santiam River | 448 | 511 | 118.0 | 108.2 | 250.56 | 0.000010 | internal | internal |
| 7 | 11 | Santiam River to RM 102 | 514 | 552 | 108.2 | 102.1 | 250.12 | 0.000600 | internal | internal |
| 8 | 12 | RM 102 to RM 96 | 555 | 592 | 102.1 | 96.2 | 250.12 | 0.000630 | internal | internal |
| 9 | 13 | RM 96 to Salem | 595 | 666 | 96.2 | 85.2 | 250.12 | 0.000060 | internal | internal |

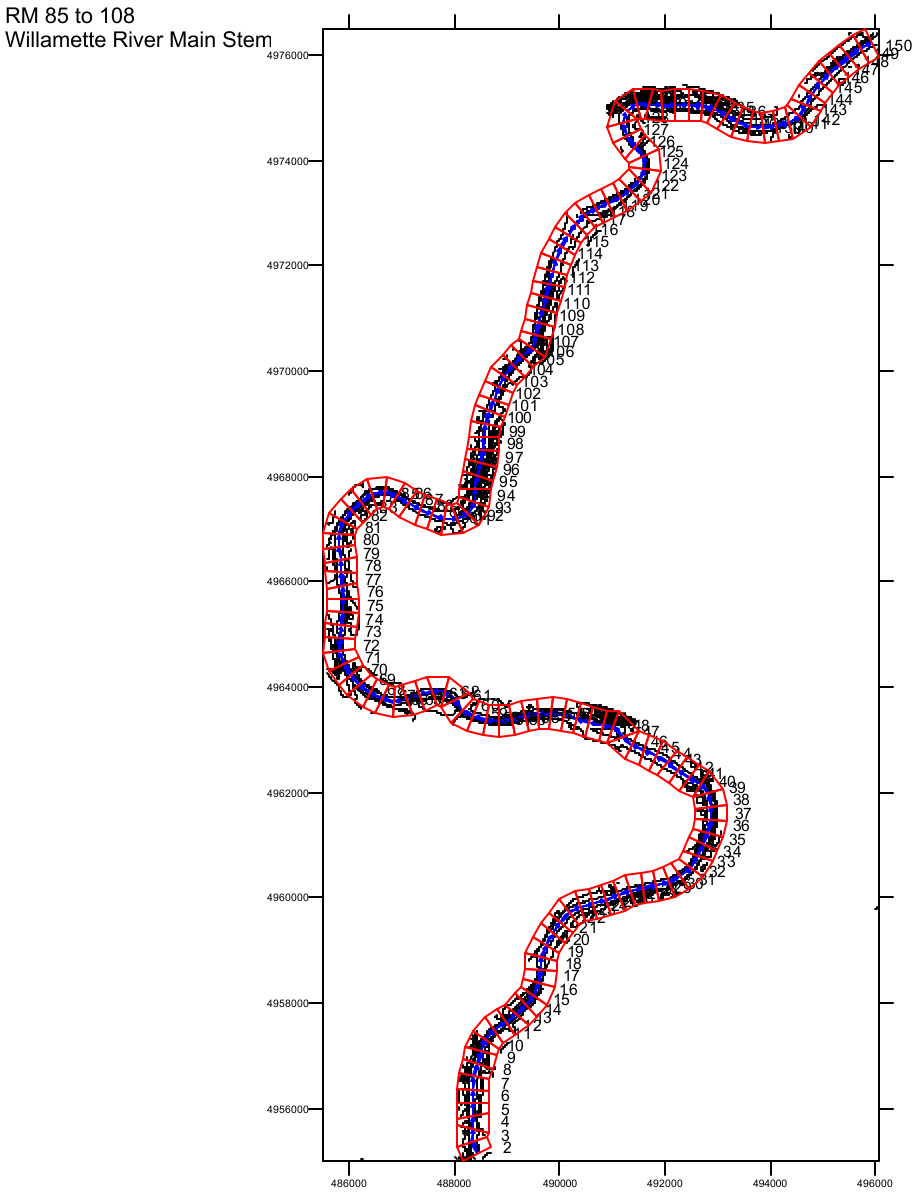


**Figure 264. Grid layout for RM 85 to RM 108.**

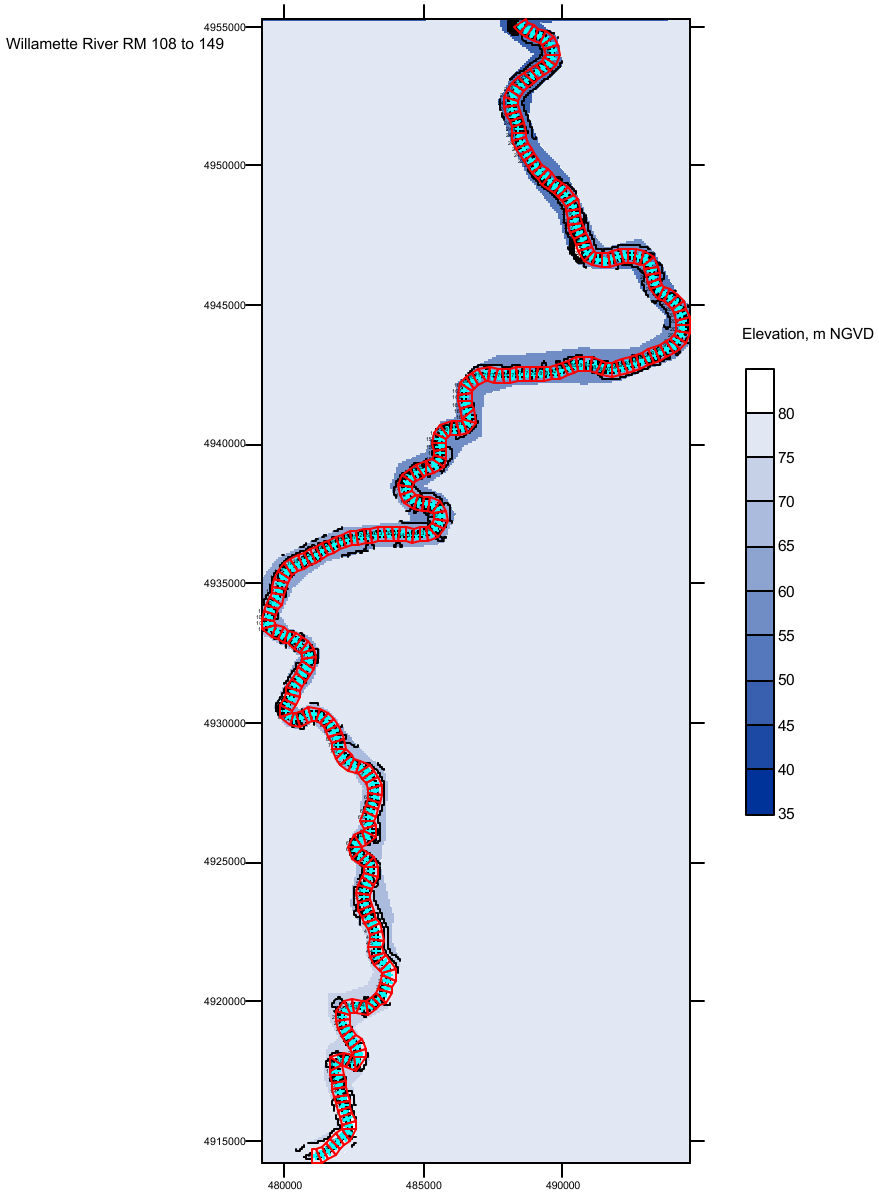


**Figure 265. Grid layout between RM 108 and RM 149.**

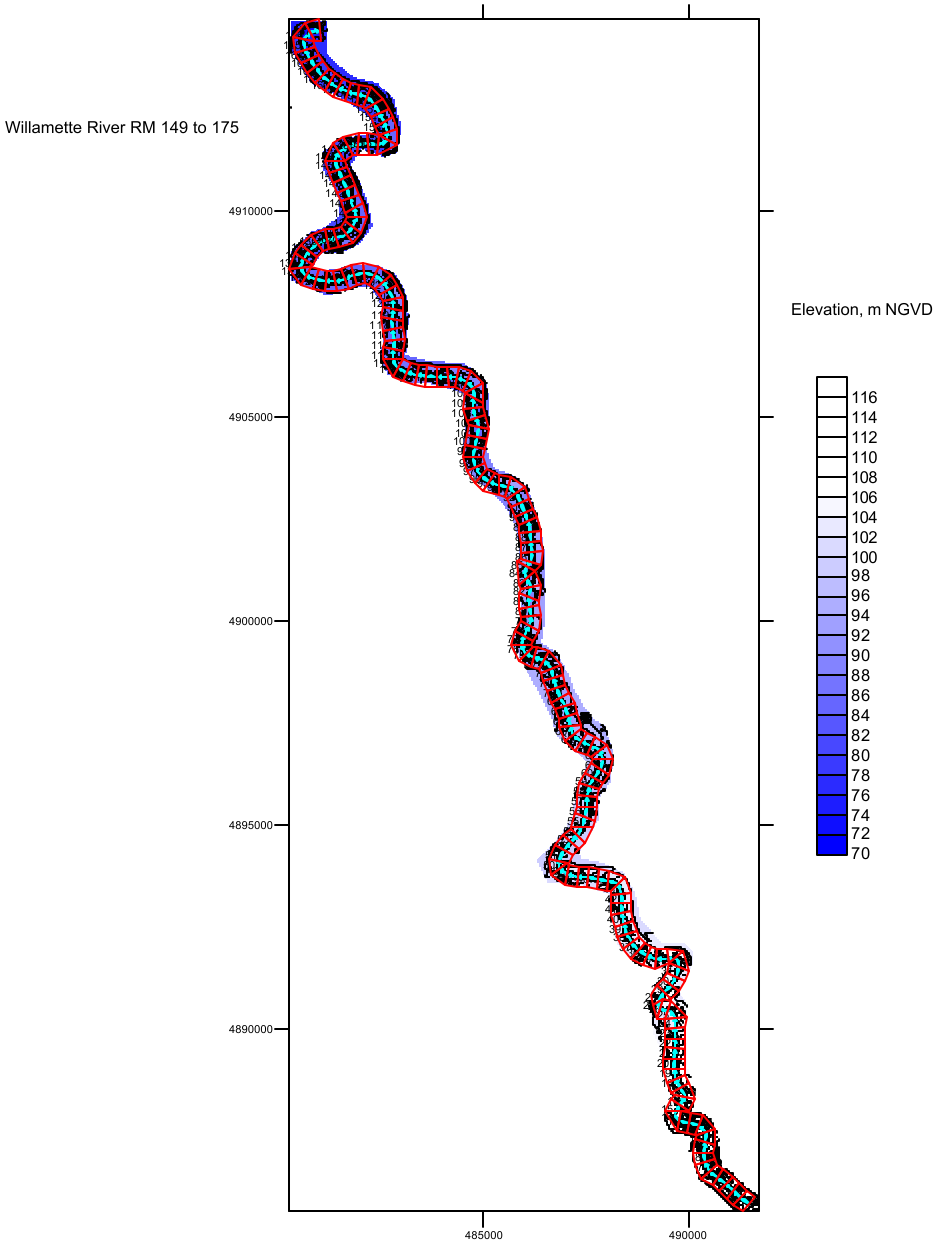


**Figure 266. Grid layout for RM 149 to RM 175.**

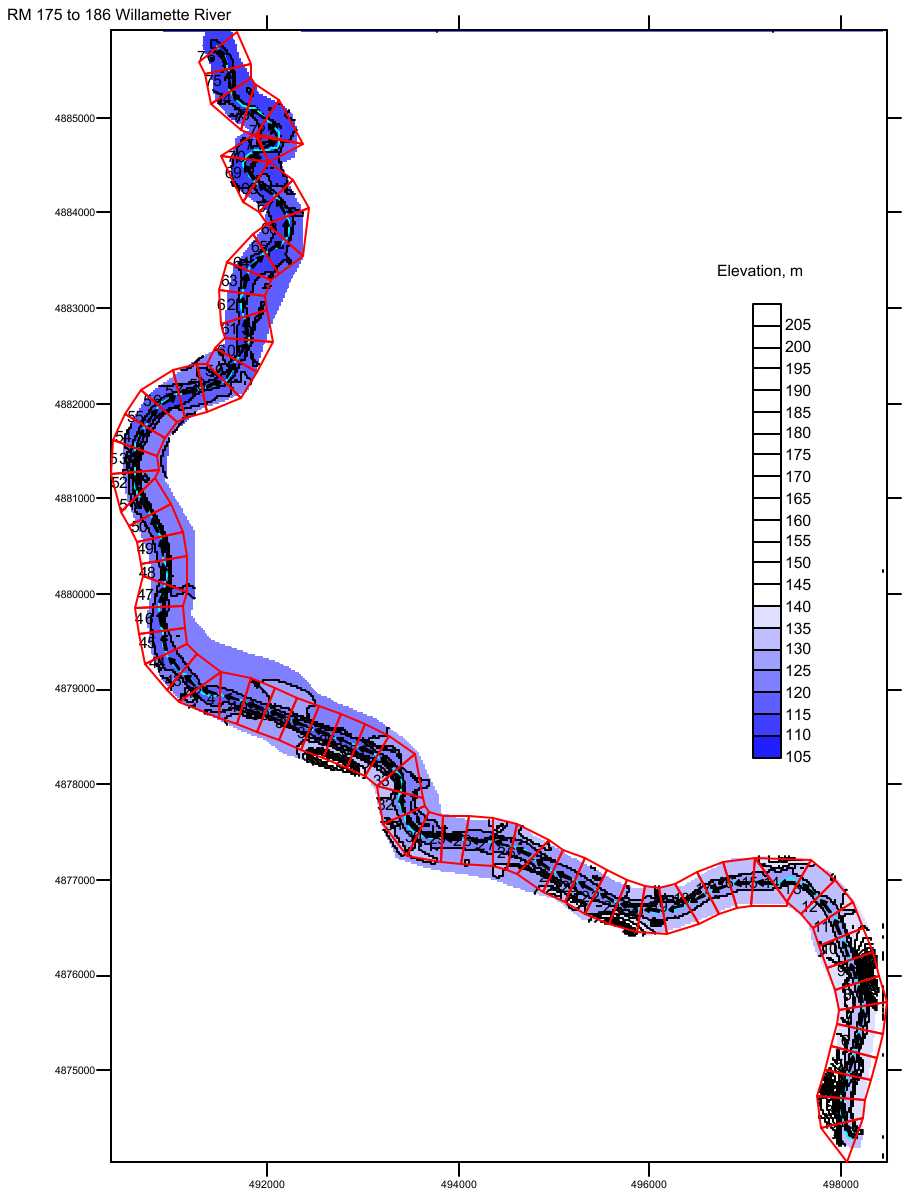


**Figure 267. Grid layout RM 175 to RM 186.**

## *Model Upstream & Downstream Boundary Conditions*

The model required upstream boundary conditions for flow and temperature. Continuous flow and temperature data were used. The downstream condition was a spillway which was used to regulate outflow from the model. The rating curve of the downstream spillway and the spillway elevation were set to minimize the upstream effects on the water surface.

### Hydrodynamic Data

The Willamette River flow at Eugene was the upstream boundary condition. The USACOE gage at Eugene (EUGO3), RM 181, was the closest flow gage to the upstream end of the model at RM 185. The data were shifted 30 minutes earlier to account for the travel time between the start of the model and the observation point. Flow data were available for January to December of 2001 and 2002 and the data were recorded at a frequency of 30 minutes.

#### Year 2001

The 2001 Willamette River flow at Eugene was calculated from stage data (USACOE EUGO3) and the rating curve shown in Figure 268. The rating curve was obtained from the NW River Forecast Center (NWRFC) website (http: //www.nwrfc.noaa.gov.) in February 2003. The 2001 flow at Eugene is shown in Figure 269. The flows during the spring months reflect storm events with peak flows up to 160 $m^3/s$. The summer flows were influenced by upstream dam operations which create the step increase in flow. Summer flow ranges from 40 to 60 $m^3/s$.

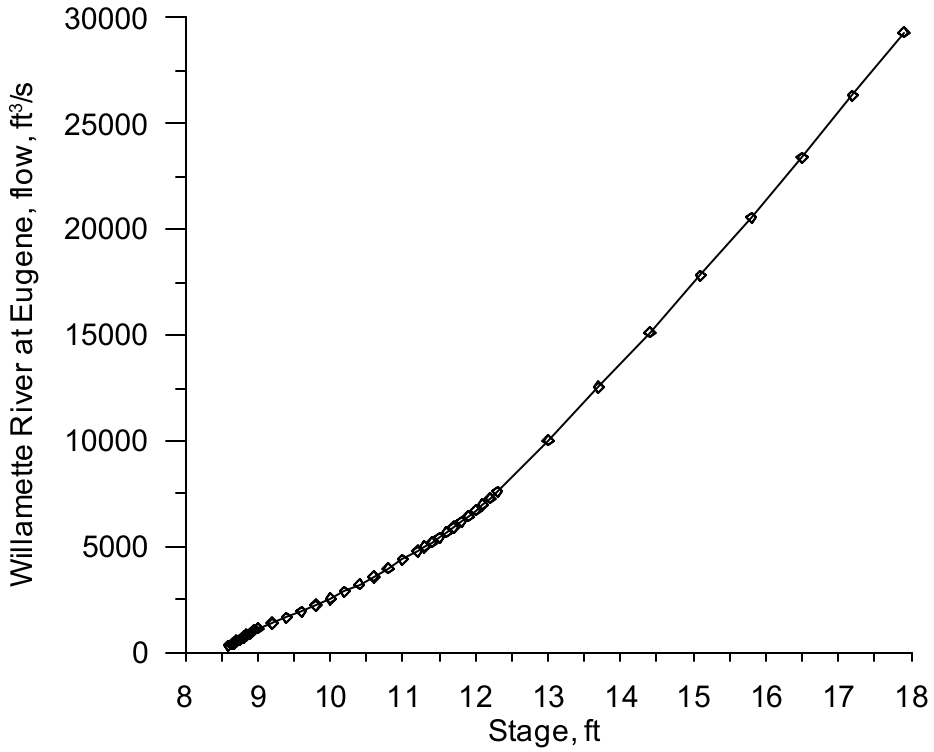


**Figure 268. Willamette River at Eugene flow-stage rating curve**

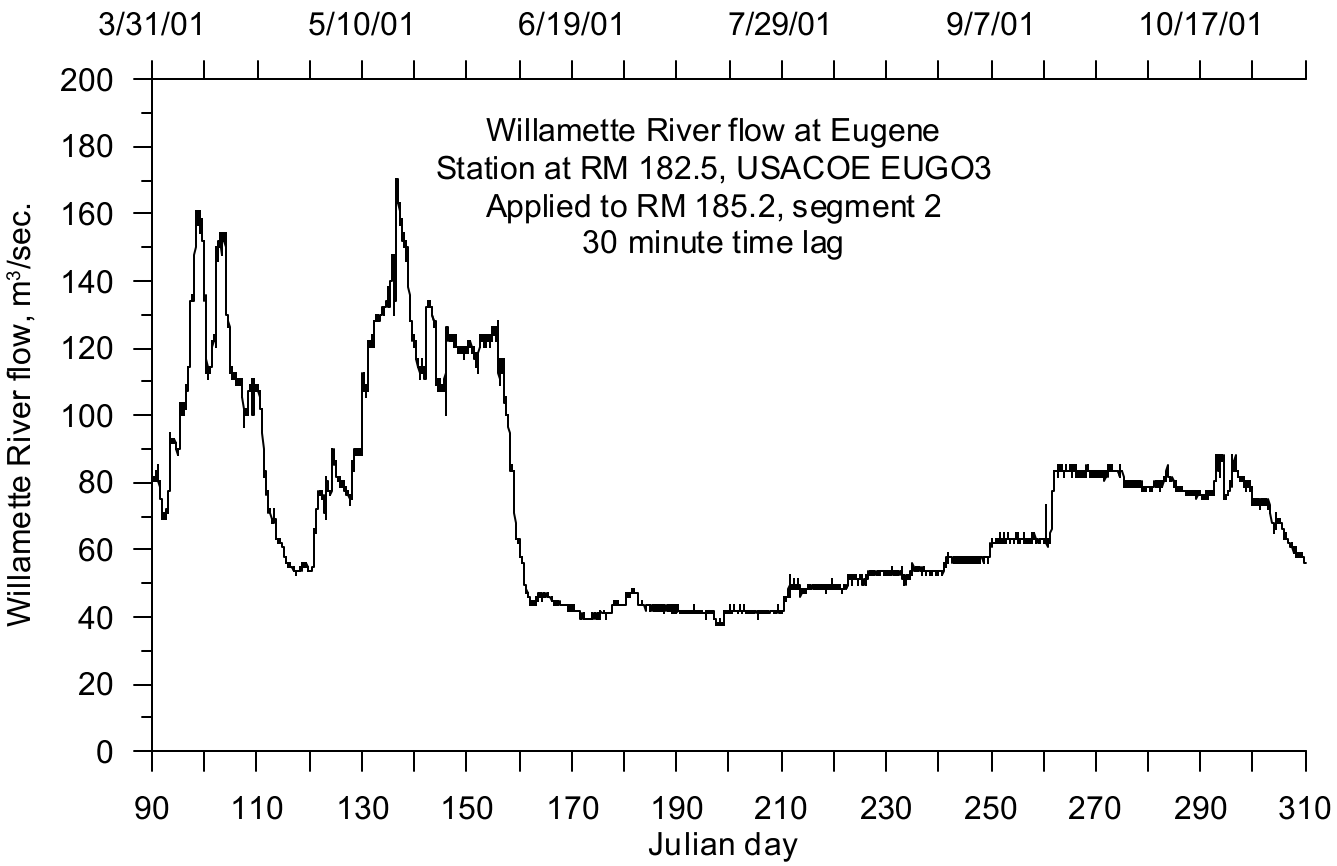


**Figure 269. Willamette River flow at Eugene, 2001**

Year 2002

The 2002 Willamette River flow at Eugene was calculated from stage data (USACOE EUGO3) and the rating curve shown in Figure 268. The rating curve was obtained from the NW River Forecast Center website (http: //www.nwrfc.noaa.gov.) in February 2003. The 2001 flow at Eugene is shown in Figure 270. The flows during the spring months reflect storm events with a peak storm flow approaching 350 $m^3/s$. The summer flows were influenced by upstream dam operations which create the step increases in flow. Summer flow ranged from 60 to 90 $m^3/s$.

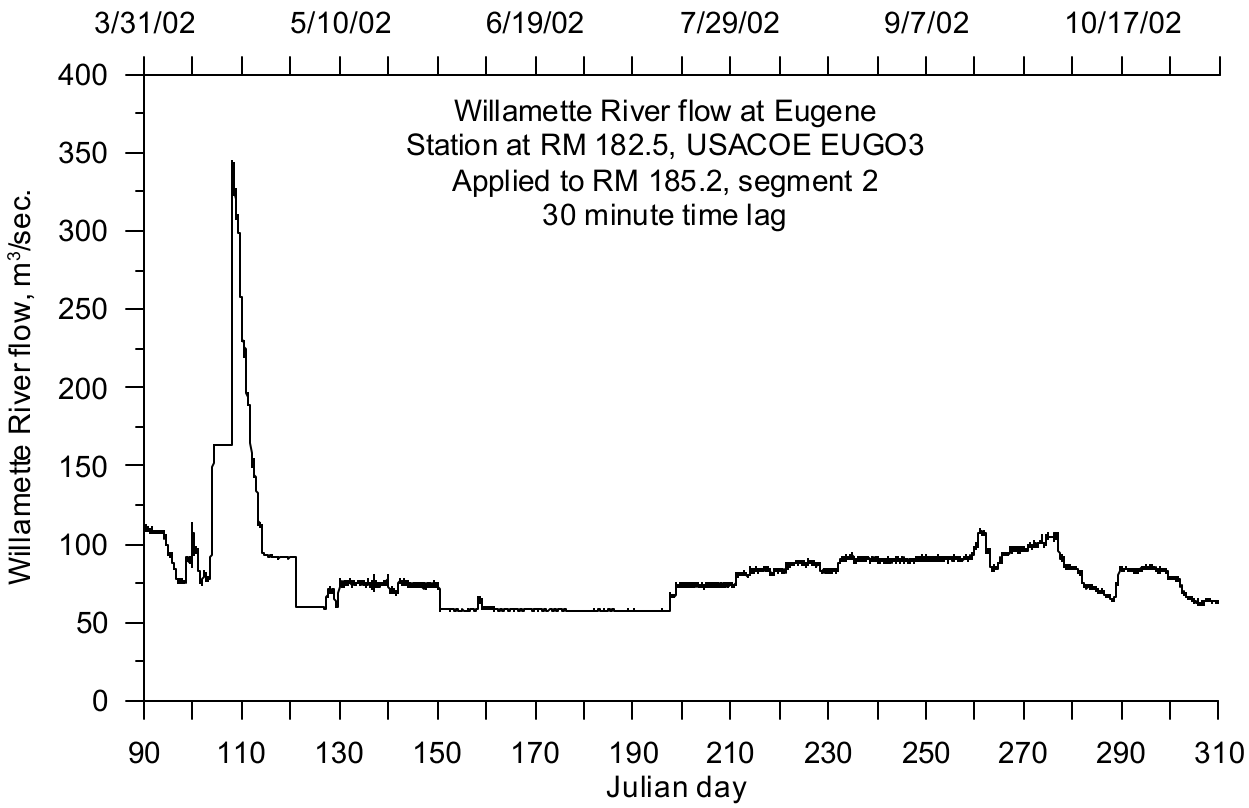


**Figure 270. Willamette River flow at Eugene, 2002**

## Temperature Data

The Upper Willamette River model originally started at the confluence of the Middle and Coast Fork Willamette Rivers. To reduce the uncertainty in the upstream temperature boundary condition, the start of the model was moved to be coincident with the Willamette River temperature station at Springfield, OR (LASAR 10359).

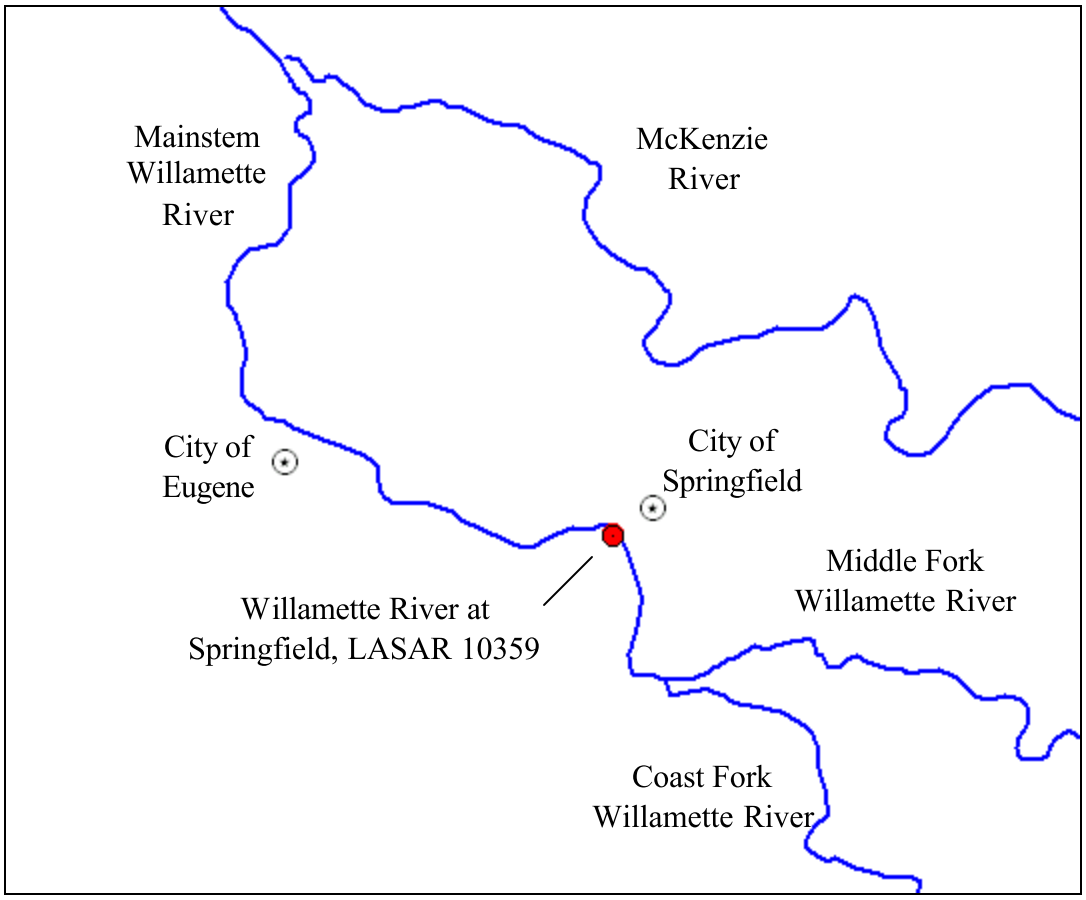


**Figure 271. Willamette River at Springfield temperature gage location**

## Year 2001

There were temperature data at LASAR 10359 from May 30 to November 2, 2001, which covers the range of the model simulation period. The data were recorded at a frequency of 30 minutes. Figure 272 shows a time series plot of the temperature data.

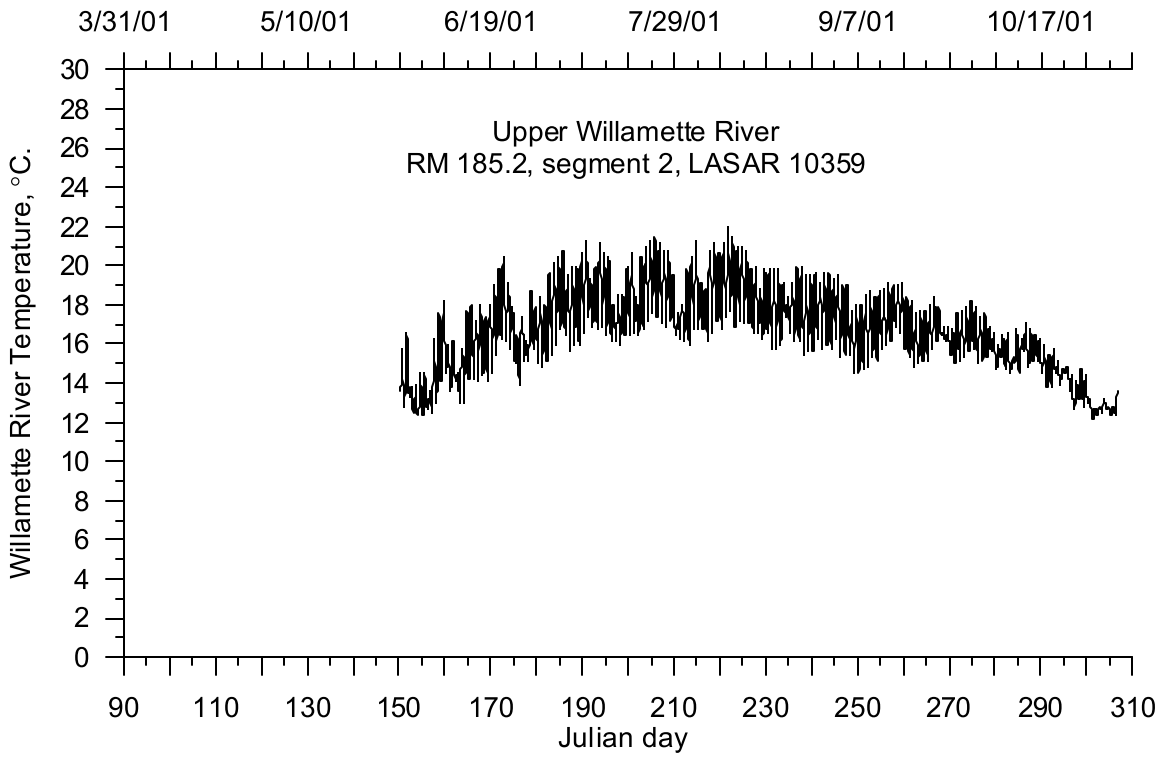


**Figure 272. Willamette River temperature at Springfield, 2001**

## Year 2002

Temperature data were available from June 3 to October 1, 2002, which does not cover the range of the model simulation period of April 1 to October 31. A correlation equation between LASAR 10359, the Willamette River at Springfield, and LASAR 28723, the Willamette River upstream of the confluence with the McKenzie River, was used to supplement the data. Data from June 18, 2001, and November 2, 2001 and from June 3, 2002, and October 1, 2002, were used to generate the correlation equation shown in Figure 273. The temperature data are shown in Figure 274.

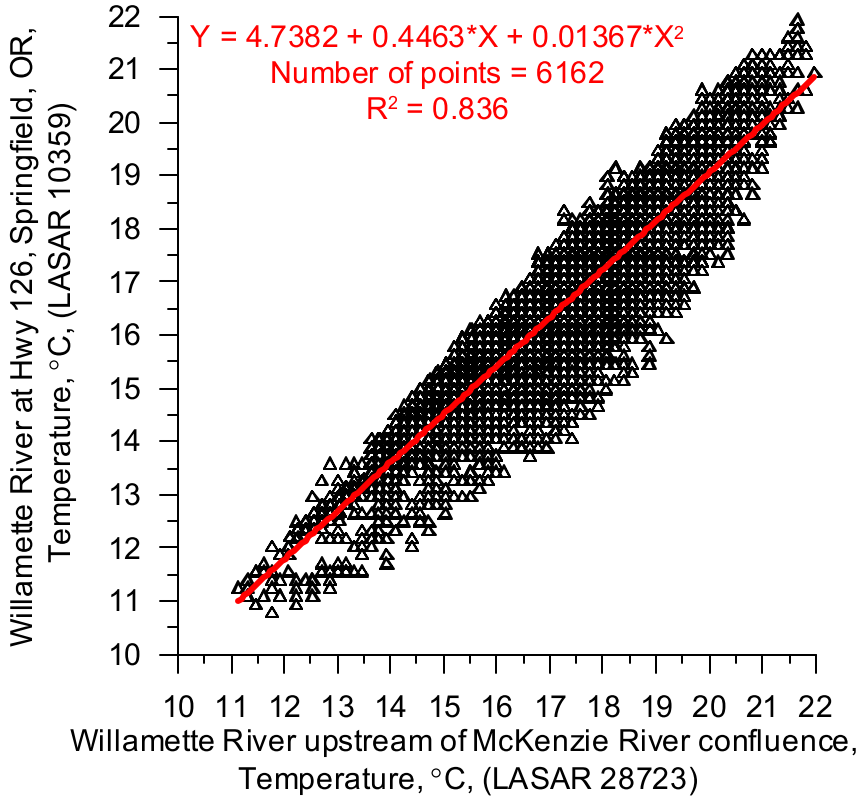


**Figure 273. Willamette River at Springfield temperature correlation, 2002**

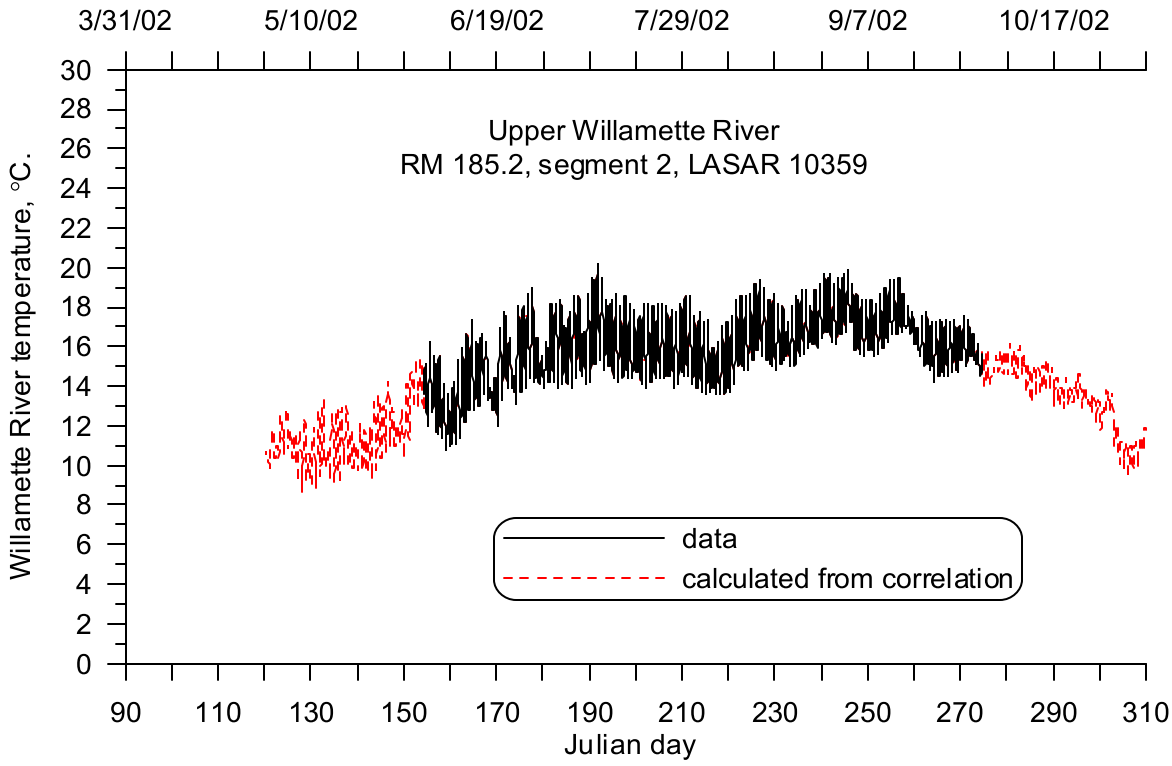


**Figure 274. Willamette River temperature at Springfield, 2002**

## *Tributaries*

There are three main tributaries and four smaller tributaries included in the model. Figure 275 shows the model tributary locations. Table 28 lists the tributaries and their river mile and model segment locations.

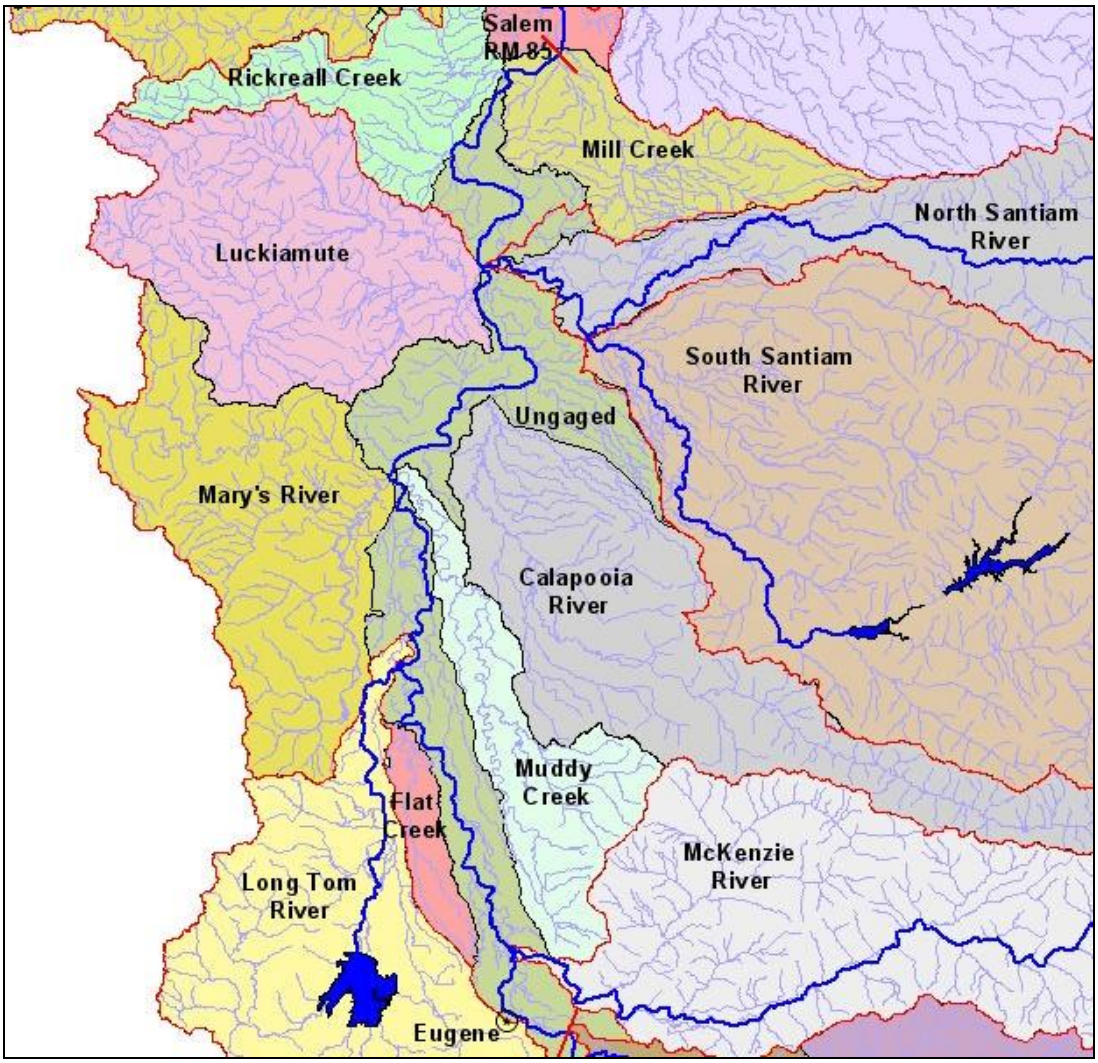


**Figure 275. Upper Willamette River model tributary basins**

**Table 28. Upper Willamette River model tributaries**

| Tributary | Willamette RM | Model Segment |
|---|---|---|
| McKenzie River | 175.3 | 68 |
| Long Tom River | 149.4 | 240 |
| Mary's River | 133.4 | 343 |
| Calapooia River | 120.2 | 432 |
| Luckiamute River | 108.7 | 508 |
| Santiam River | 108.5 | 509 |
| Rickreall Creek | 88.8 | 644 |

## Hydrodynamic Data

Flow data for the model tributaries were collected at several USGS gage stations. The McKenzie River lacked accurate flow data for 2001. No flow data exists for Rickreall Creek for both 2001 and 2002. The locations of the flow gages used for the 2001 and 2002 model inputs are shown in Figure 276. The sources for the 2001 and 2002 tributary flow data are shown in Table 29.

**Table 29. Upper Willamette River tributary hydrodynamic data sources**

| Tributary | Input Source | Willamette RM | Gage RM | Model Segment |
|---|---|---|---|---|
| McKenzie River | McKenzie River model | 175.3 | -- | 68 |
| Long Tom River | USGS 14170000 | 149.4 | 6.8 | 240 |
| Mary's River | USGS 14171000 | 133.4 | 0.5 | 343 |
| Calapooia River | USGS 14172000 | 120.2 | ~34 | 432 |
| Luckiamute River | USGS 14190500 | 108.7 | 9.2 | 508 |
| Santiam River | USGS 14189000 | 108.5 | 9.9 | 509 |
| Rickreall Cr. | fractional flow | 88.8 | -- | 644 |

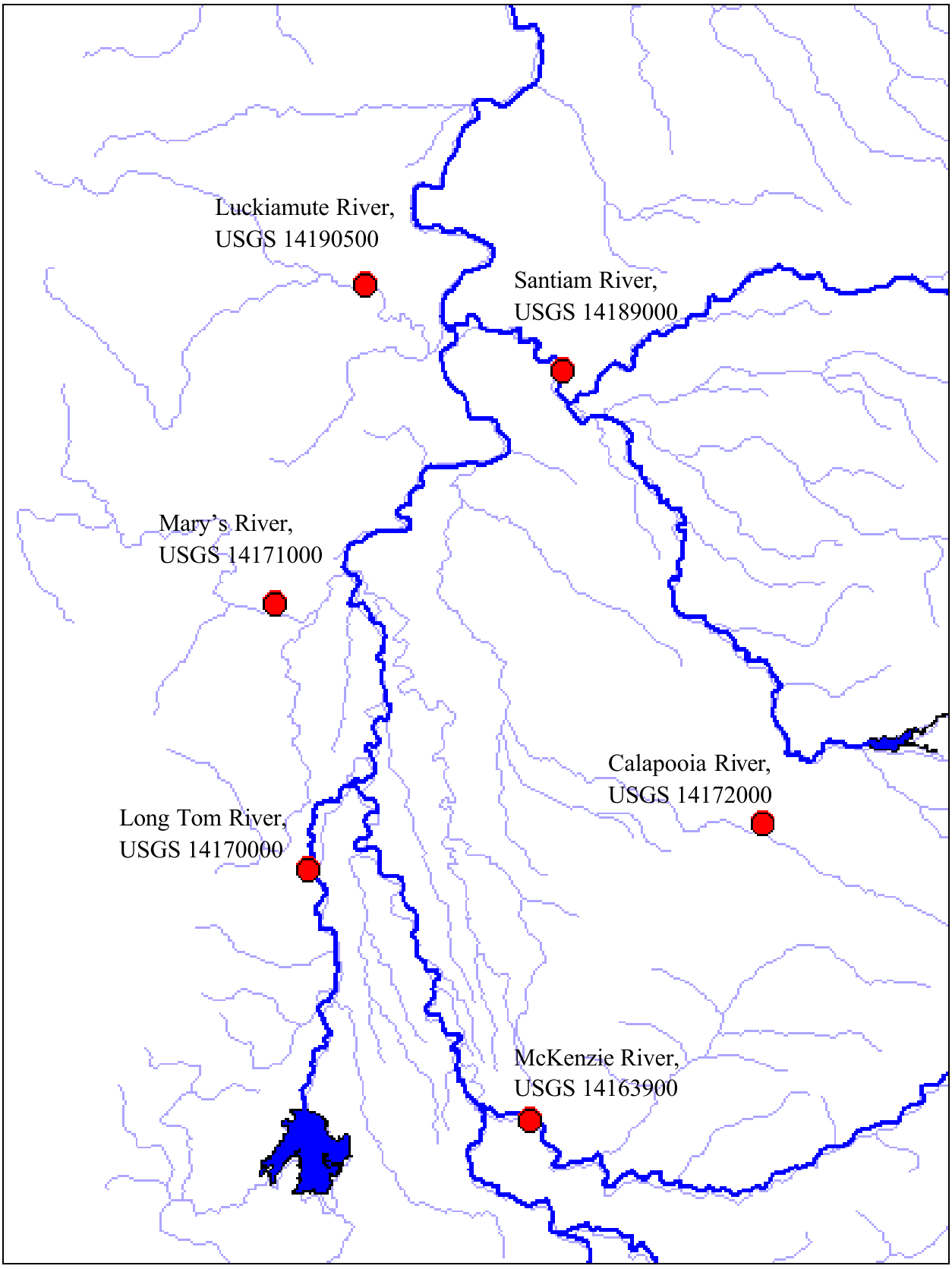


**Figure 276. Upper Willamette River model tributary flow gaging station locations**

## Year 2001

The McKenzie River flow is shown in Figure 277. The furthest downstream flow gage on the McKenzie in 2001 was at Walterville (USGS 14163900), RM 25. McKenzie River flow rates were heavily influenced by dam operations and diversion canal operations. Consequently upstream flow regimes do not correlate strongly with downstream flow regimes. Flow was added after the furthest downstream gage prior to the confluence with the Willamette River. Flow output from the McKenzie River model was used in lieu of flow calculated from correlations. The summer flow ranged from 60 to 70 $m^3/s$, which was approximately the magnitude of the Willamette River flow.

The Long Tom River flow is shown in Figure 278. Complete flow data were available from April 1 to October 31, 2001. The summer flow was less than 2 $m^3/s$ and was approximately 1% of the Willamette River flow.

The Mary's River flow is shown in Figure 279. Complete flow data were available from January 1 to November 31, 2001. The flow patterns show a strong response to storm events. Spring flow ranged from 5 to 10 $m^3/s$. The summer flows were less than 1 $m^3/s$ and were approximately 0.5% of the Willamette River flow.

2001 flow data for the Calapooia River were not available. The flow for 2001 was estimated using the daily mean of the historical daily average flows from 1935 to 1990. This data were obtained from the USGS for gage 14172000. Figure 280 shows the estimated flows, which ranged from 15 $m^3/s$ in the wet season to less than 5 $m^3/s$ during the summer. The estimated summer Calapooia flow was approximately 2 to 4% of the Willamette River flow.

The Luckiamute River flow is shown in Figure 281. Complete flow data were available from April 1 to October 31, 2001. Spring flow range from 5 to 15 $m^3/s$ and show strong response to rain events. The summer flow was less than 2 $m^3/s$ and was approximately 1% of the Willamette River flow.

The Santiam River flow is shown in Figure 282. Complete flow data were available from April 1 to October 31, 2001. Spring flow range from 125 to 200 $m^3/s$ with storm flows approaching 300 $m^3/s$. The summer flow was approximately 40 $m^3/s$ and increased the Willamette River flow by 35%.

The Rickreall Creek flow is shown in Figure 283. The flows were calculated using a fractional flow technique. The Luckiamute basin was selected due to its proximity and similarity of topography. Using a GIS coverage of four-field Hydraulic Unit Code (HUC) sub-basins, the area of the Luckiamute basin was determined to be 815.2 $km^2$, and the area of the Rickreall Creek basin was determined to be 434.4 $km^2$. Using the ratio of the basin areas, the flow at Rickreall is estimated to be 53.3% of the 2001 flow at the Luckiamute River gage, USGS 14190500.

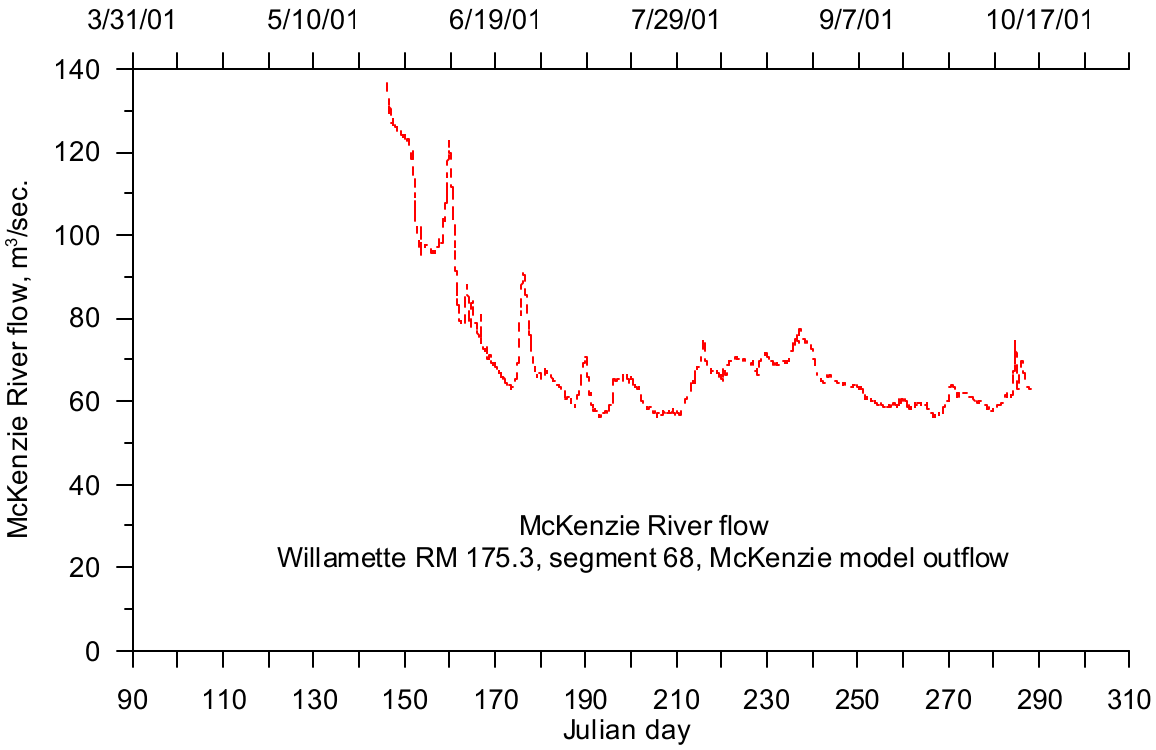


**Figure 277. McKenzie River flow, 2001**

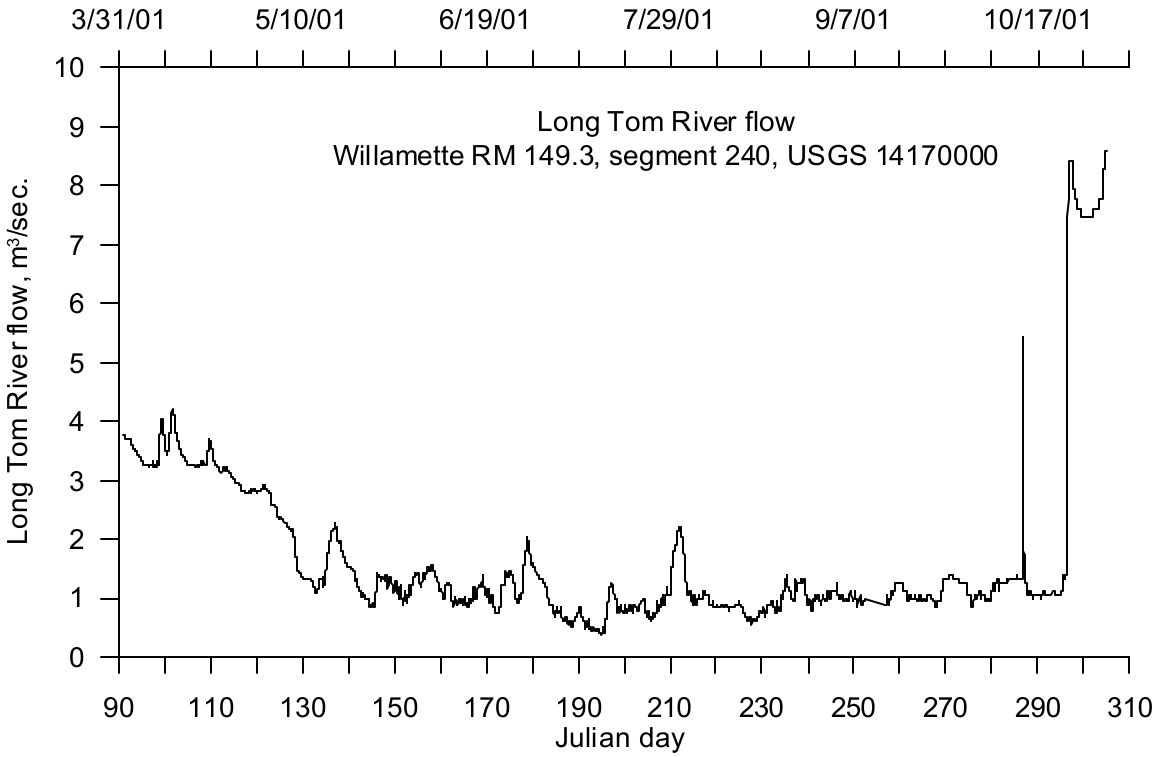


**Figure 278. Long Tom River flow, 2001**

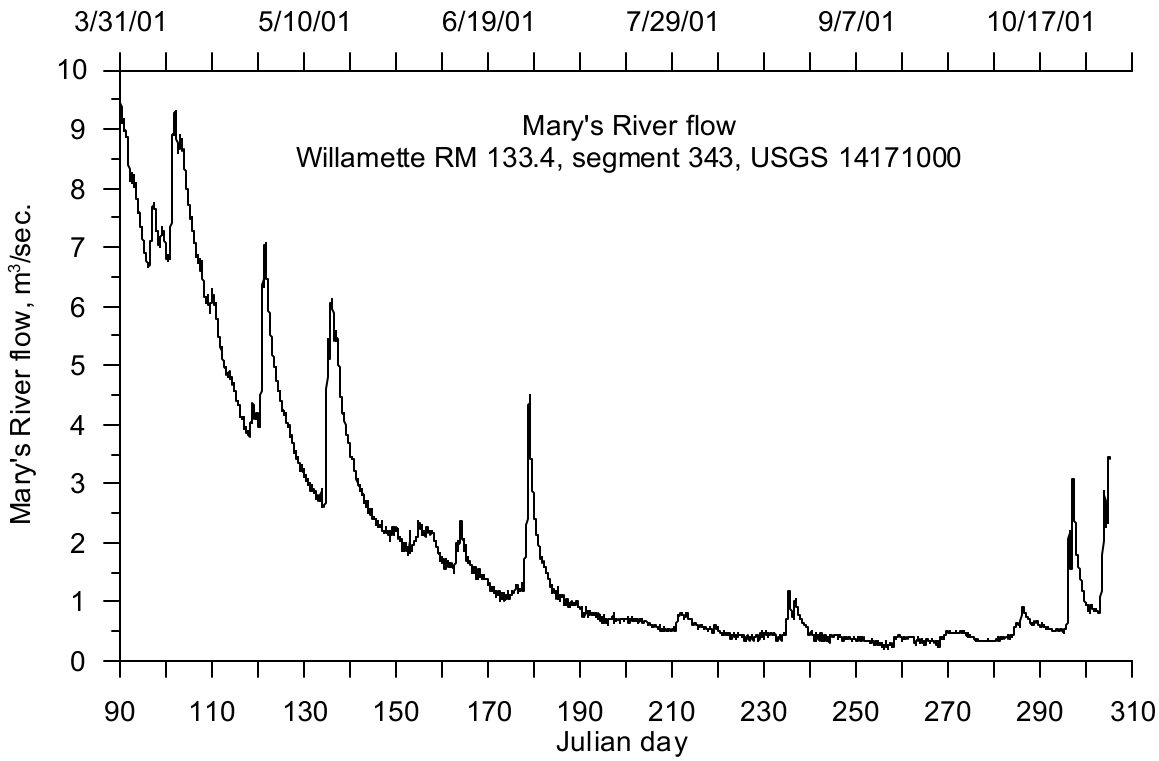


**Figure 279. Mary's River discharge, 2001**

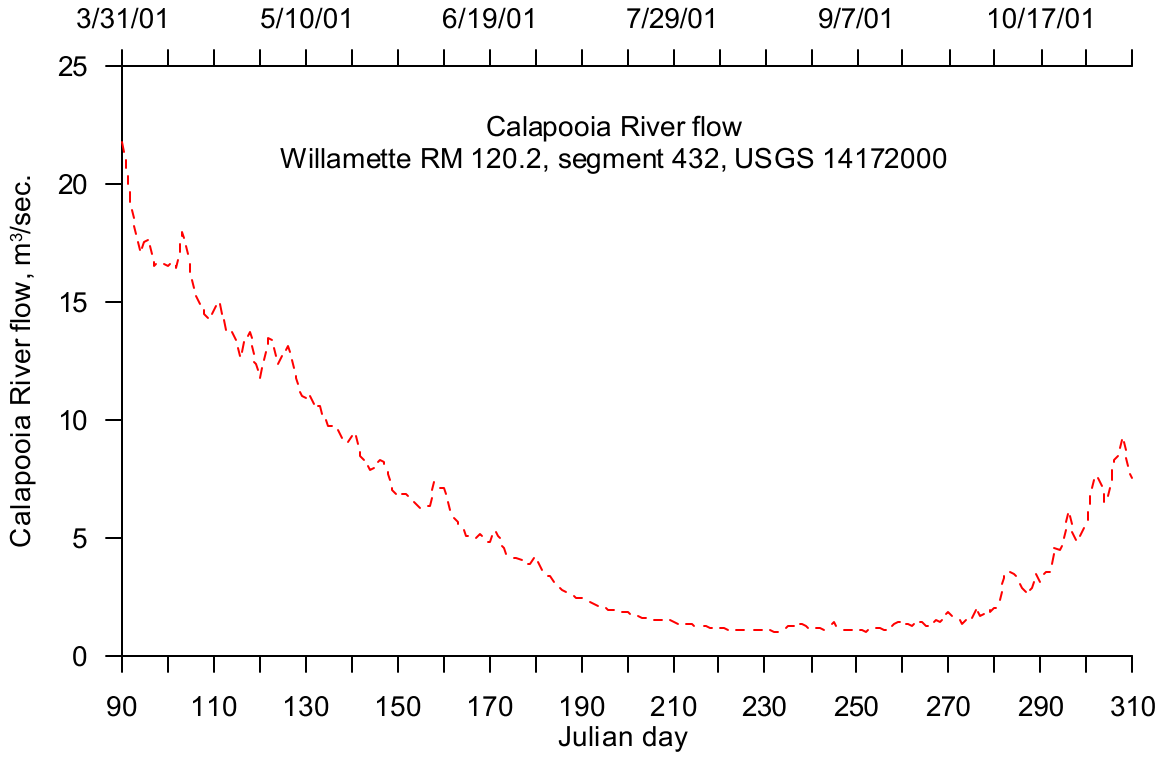


**Figure 280. Calapooia River flow, 2001**

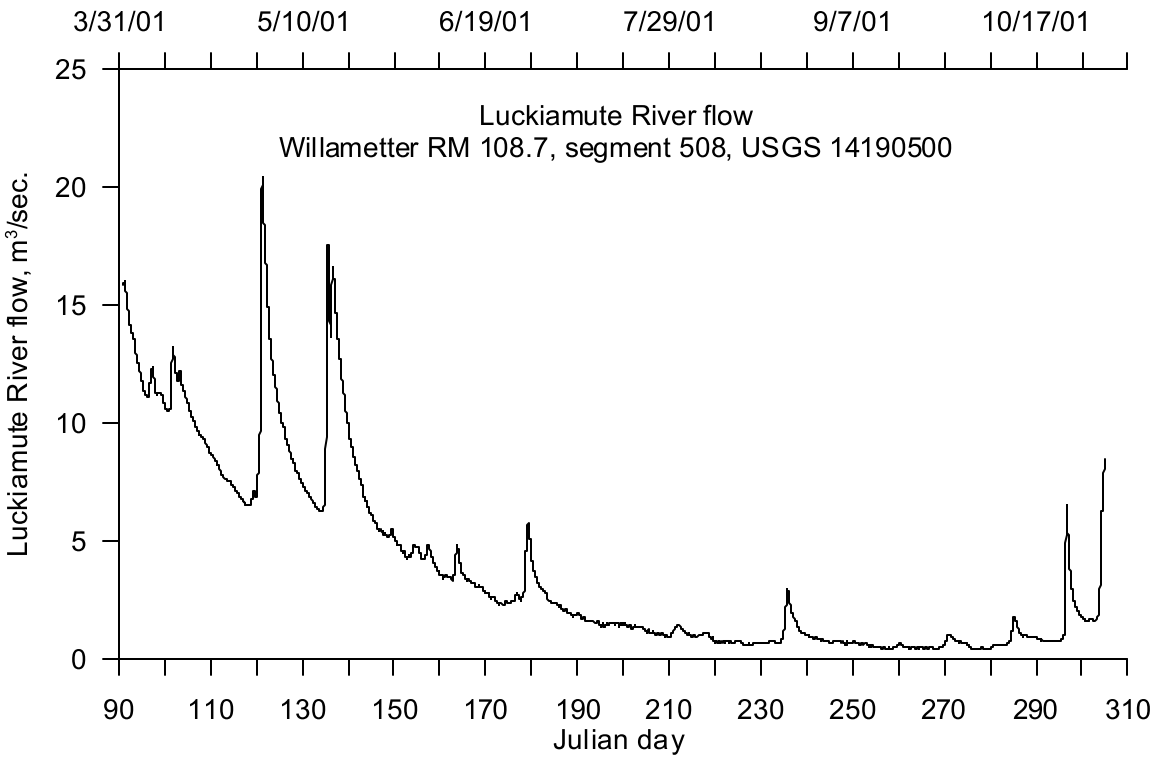


**Figure 281. Luckiamute River flow, 2001**

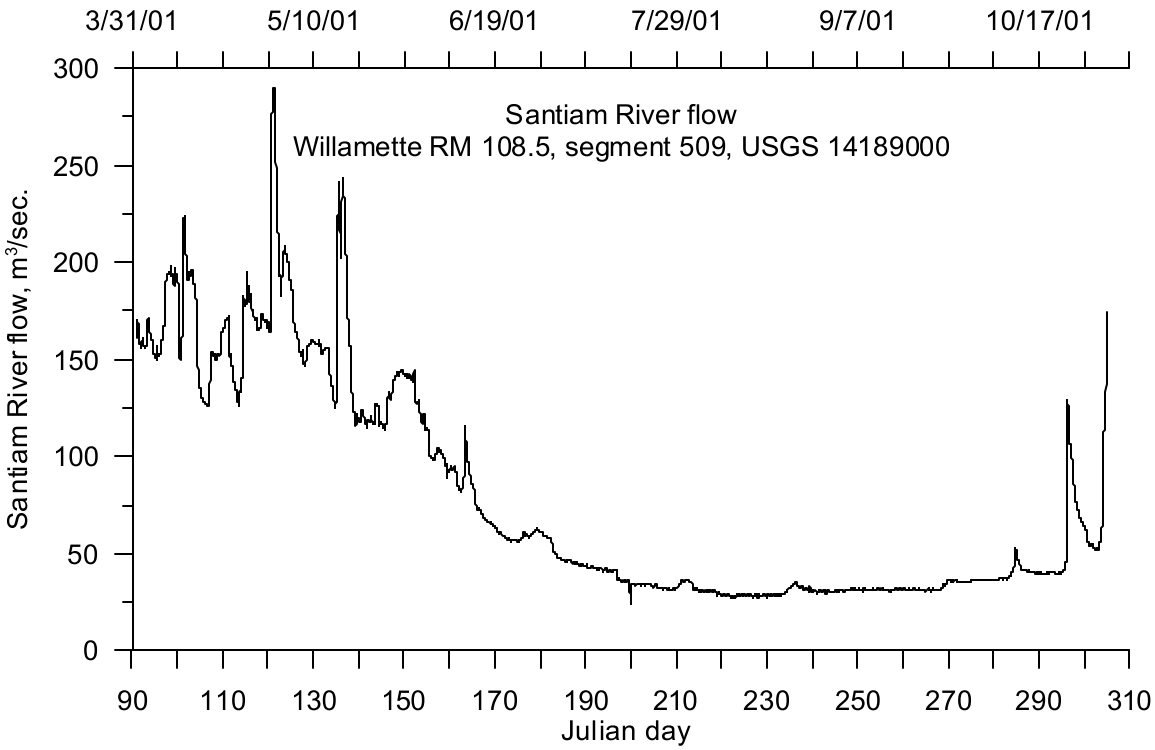


**Figure 282. Santiam River flow, 2001**

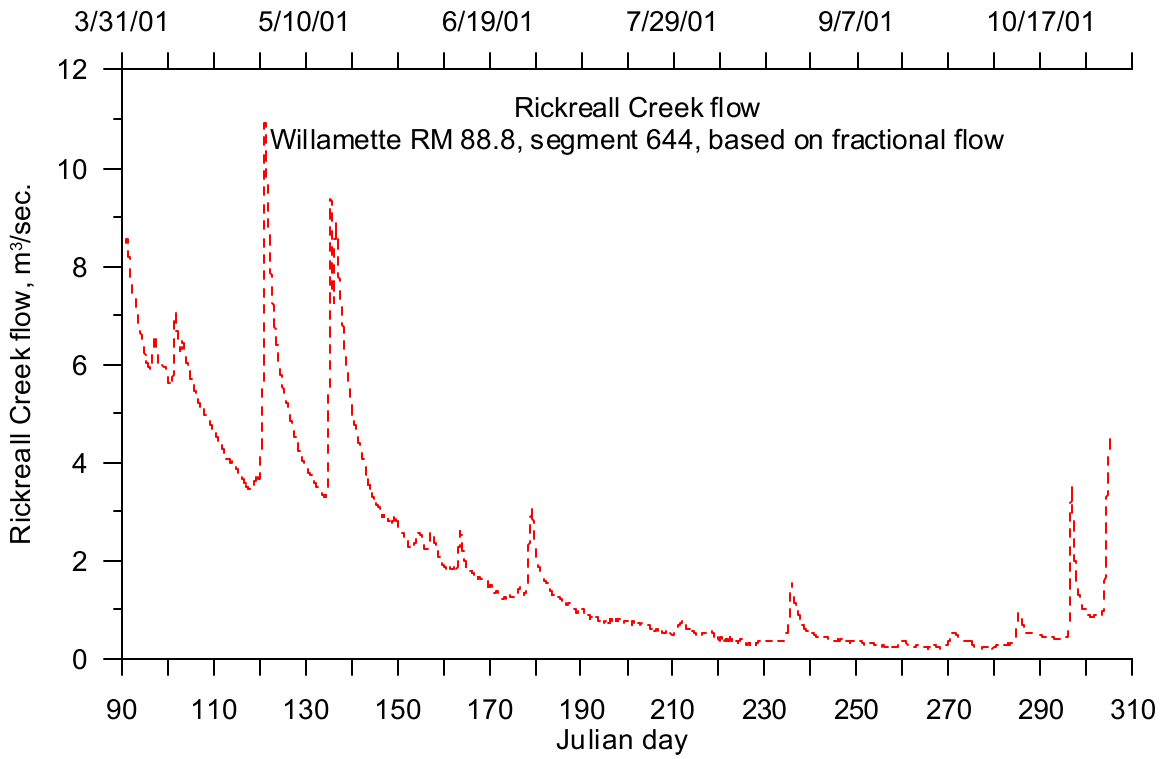


**Figure 283. Rickreall Creek flow, 2001**

## Year 2002

The McKenzie River flow is shown in Figure 284. The furthest downstream flow gage on the McKenzie in 2002 was at Walterville (USGS 14163900), RM 25. McKenzie River flow was heavily influenced by dam operations and diversion canal operations. As a consequence, upstream flow regimes do not correlate strongly with downstream flow regimes. Substantial flow was added after the furthest downstream gage prior to the confluence with the Willamette River. Flow output from the McKenzie River model was used in lieu of flow calculated from correlations. The summer flow ranged from 60 to 70 $m^3/s$, which was approximately the magnitude of the Willamette River flow.

The Long Tom River flow is shown in Figure 285. Complete flow data were available from January 1 to October 31, 2002. The summer flow was less than 2 $m^3/s$ and was approximately 1% of the Willamette River flow. Changes in dam releases results in the increase in flow around October 1 to 20 to 25 $m^3/s$.

The Mary's River flow is shown in Figure 286. Complete flow data were available from January 1 to November 31, 2002. The flow patterns show a strong response to storm events. Spring flow ranged from 5 to 10 $m^3/s$. The summer flow was less than 1 $m^3/s$ and was approximately 0.5% of the Willamette River flow.

The Calapooia River flow is shown in Figure 288. 2002 flow data were not available. The daily average flows for the Calapooia River at Albany (USGS 14163500) and the daily average flows for the Santiam River at Jefferson (USGS 14189000) from 1940 to 1982 were used to generate the correlation shown in Figure 287. The summer flow ranges from 5 to 10 $m^3/s$ and was approximately 5 to 10% of the Willamette River flow.

The Luckiamute River flow is shown in Figure 289. Complete flow data were available from January 1 to October 31, 2002. Spring flow range from 10 to 20 $m^3/s$ and show strong response to rain events with a single storm flow approaching 60 $m^3/s$. The summer flow was less than 2 $m^3/s$ and was approximately 1% of the Willamette River flow.

The Santiam River flow is shown in Figure 290. Complete flow data were available from January 1 to October 31, 2002. Spring flow ranged from 150 to 225 $m^3/s$ with a single storm flow ranging from 300 to 1100 $m^3/s$. The summer flows were approximately 50 to 90 $m^3/s$ and increased the Willamette River flow by 45 to 80%.

The Rickreall Creek flow is shown in Figure 291. The flows were calculated using a fractional flow technique. The Luckiamute basin was selected due to its proximity and similarity of topography. Using a GIS coverage of four-field HUC sub-basins, the area of the Luckiamute basin was determined to be 815.2 $km^2$, and the area of the Rickreall Creek basin was determined to be 434.4 $km^2$. Using the ratio of the basin areas, the flow at Rickreall was estimated to be 53.3% of the 2002 flow at the Luckiamute River gage, USGS 14190500.

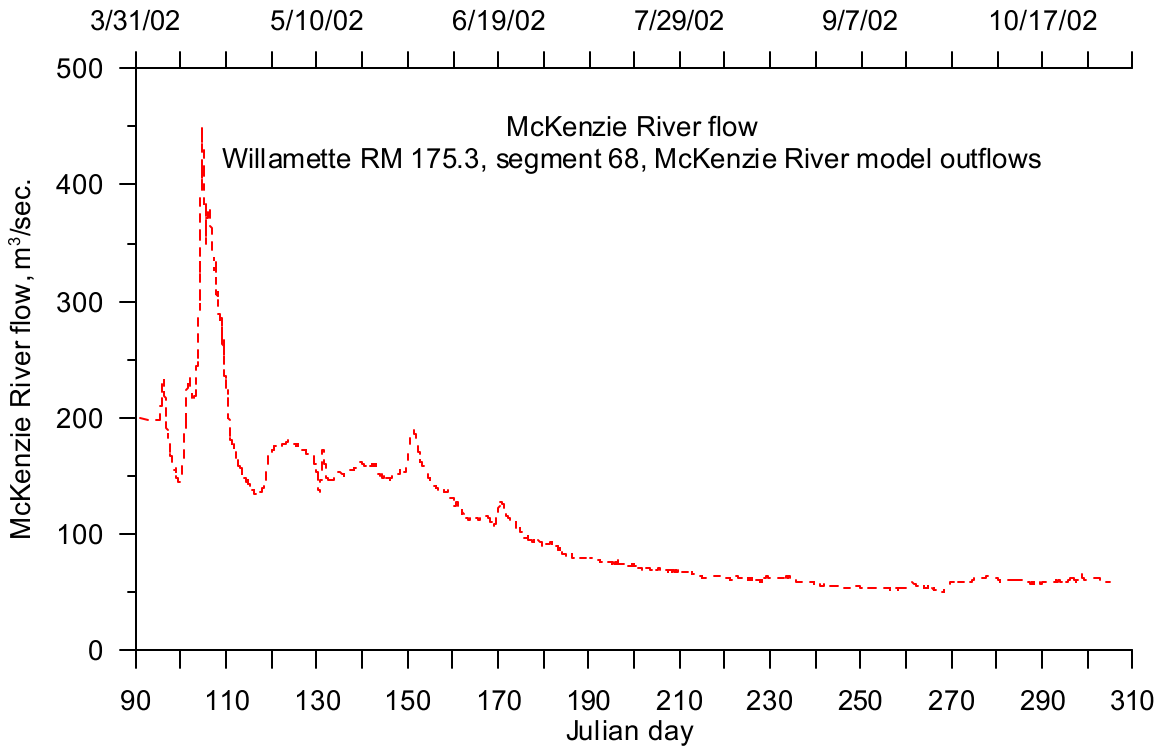


**Figure 284. McKenzie River flow, 2002**

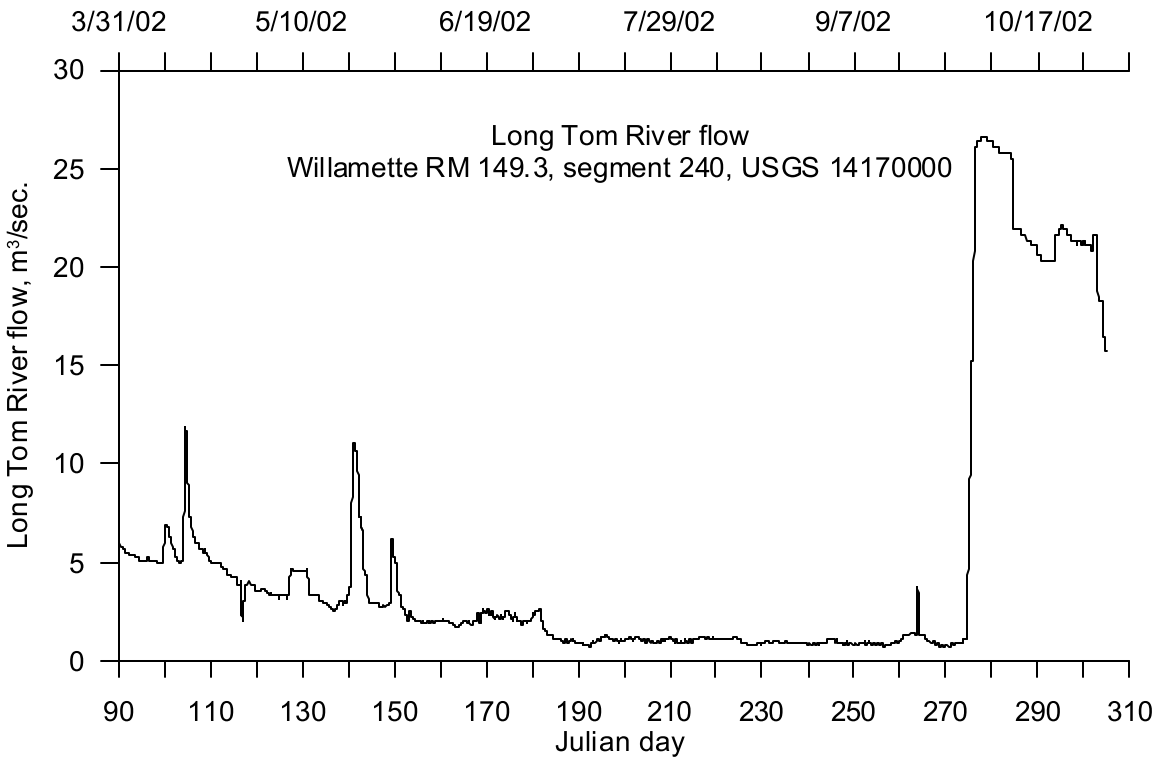


**Figure 285. Long Tom River flow, 2002**

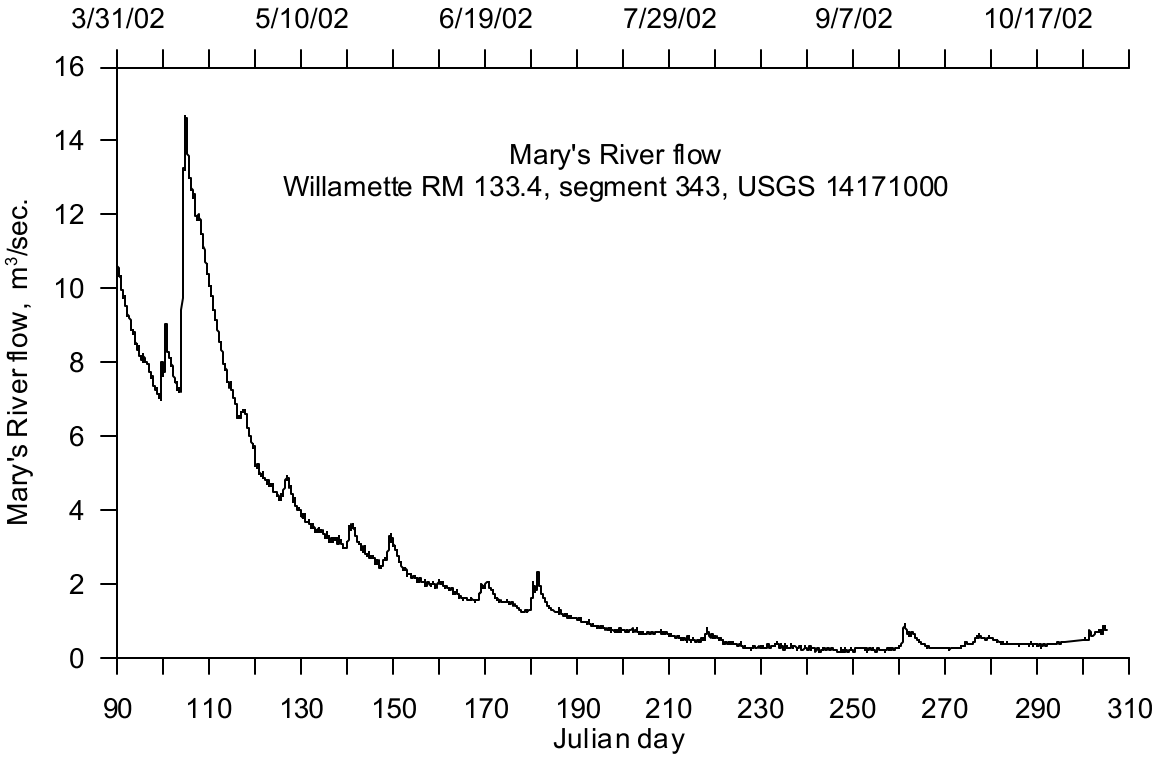


**Figure 286. Mary's River flow, 2002**

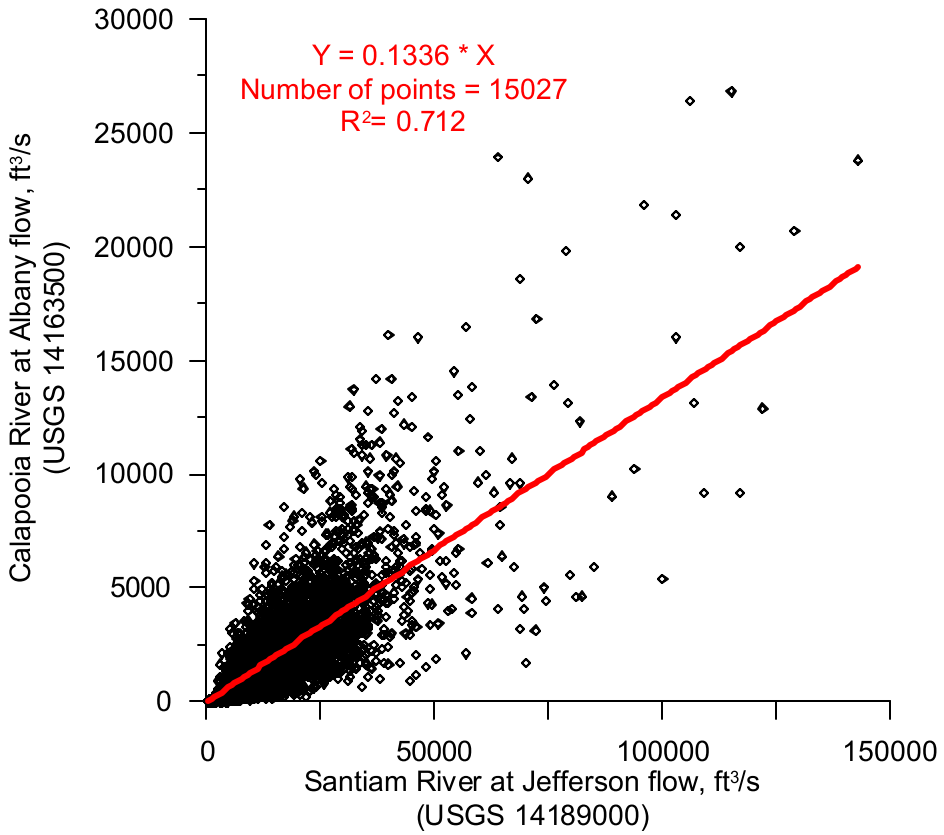


**Figure 287. Calapooia River flow correlation, 2002**

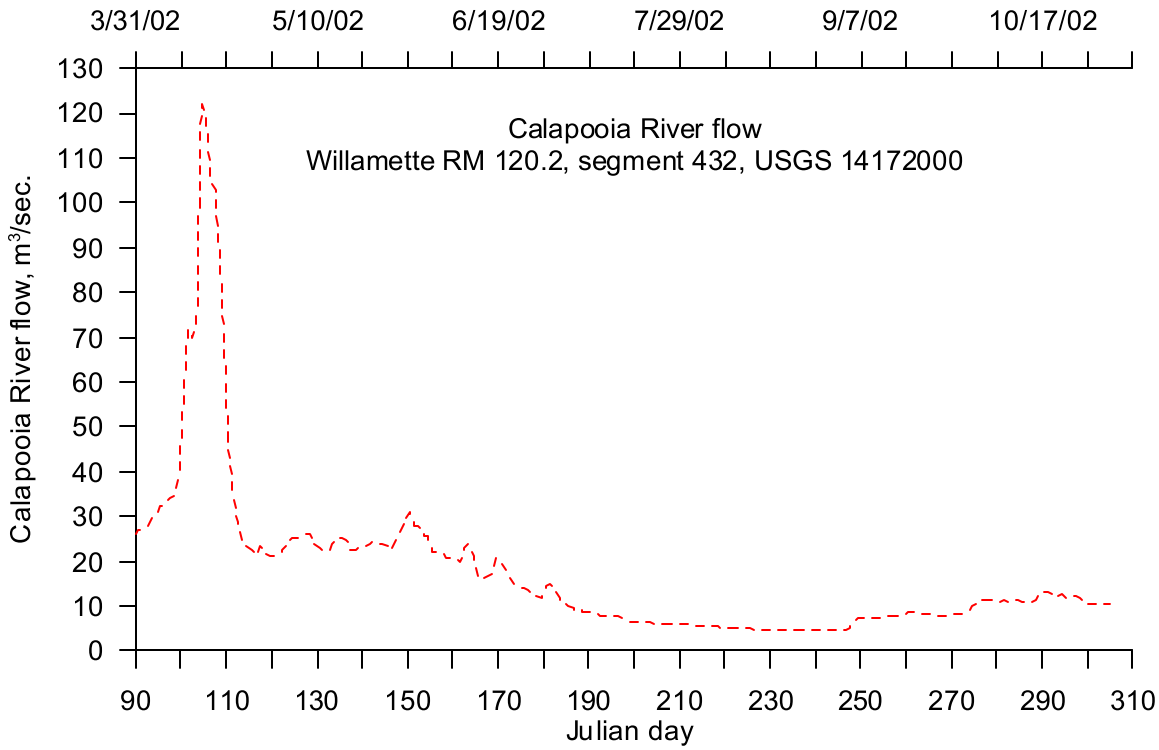


**Figure 288. Calapooia River flow, 2002**

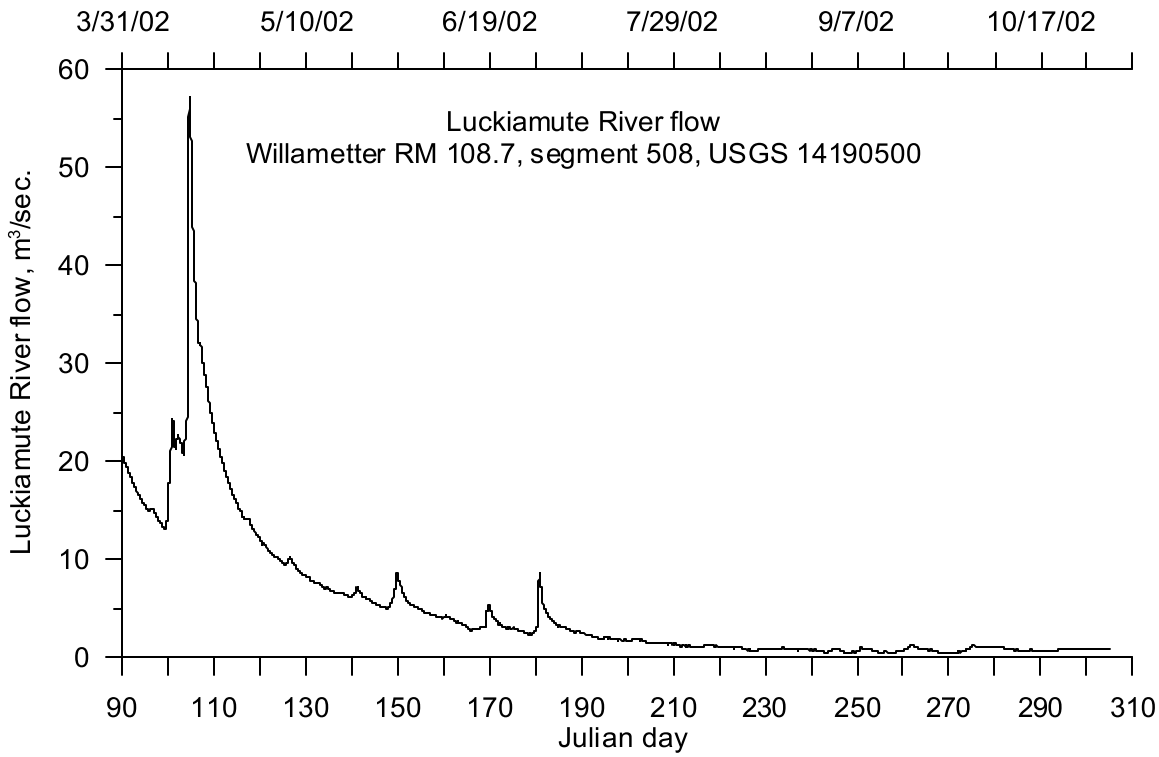


**Figure 289. Luckiamute River flow, 2002**

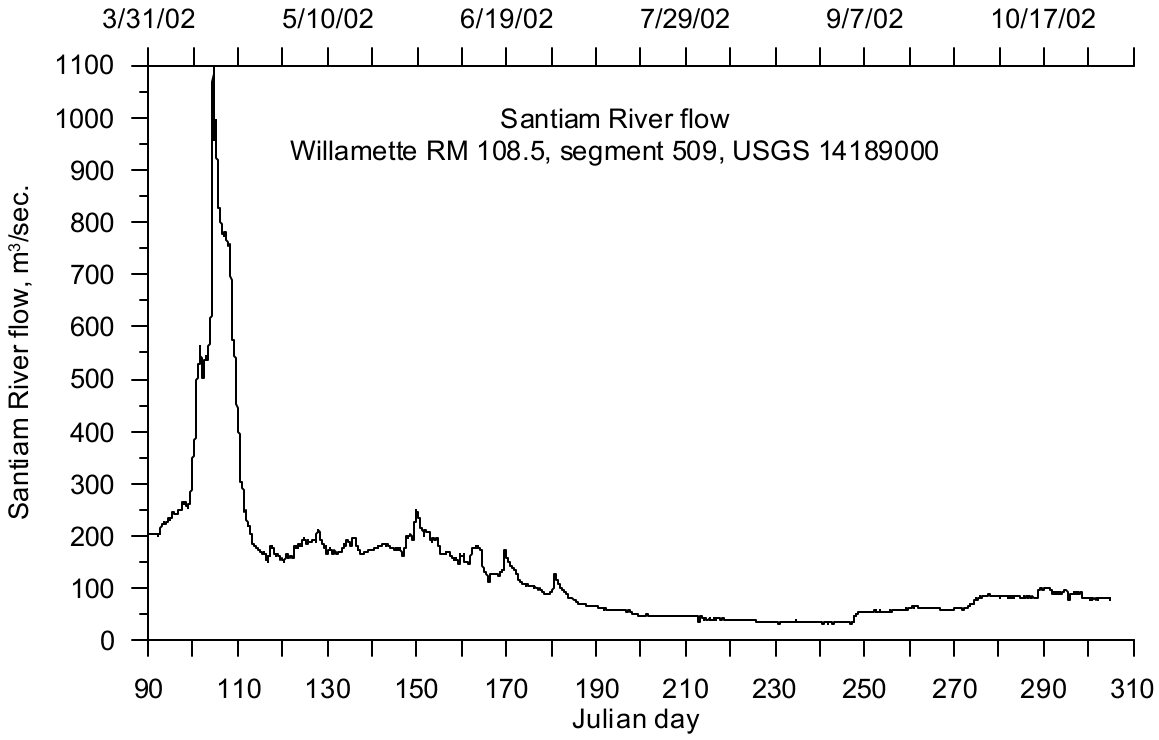


**Figure 290. Santiam River flow, 2002**

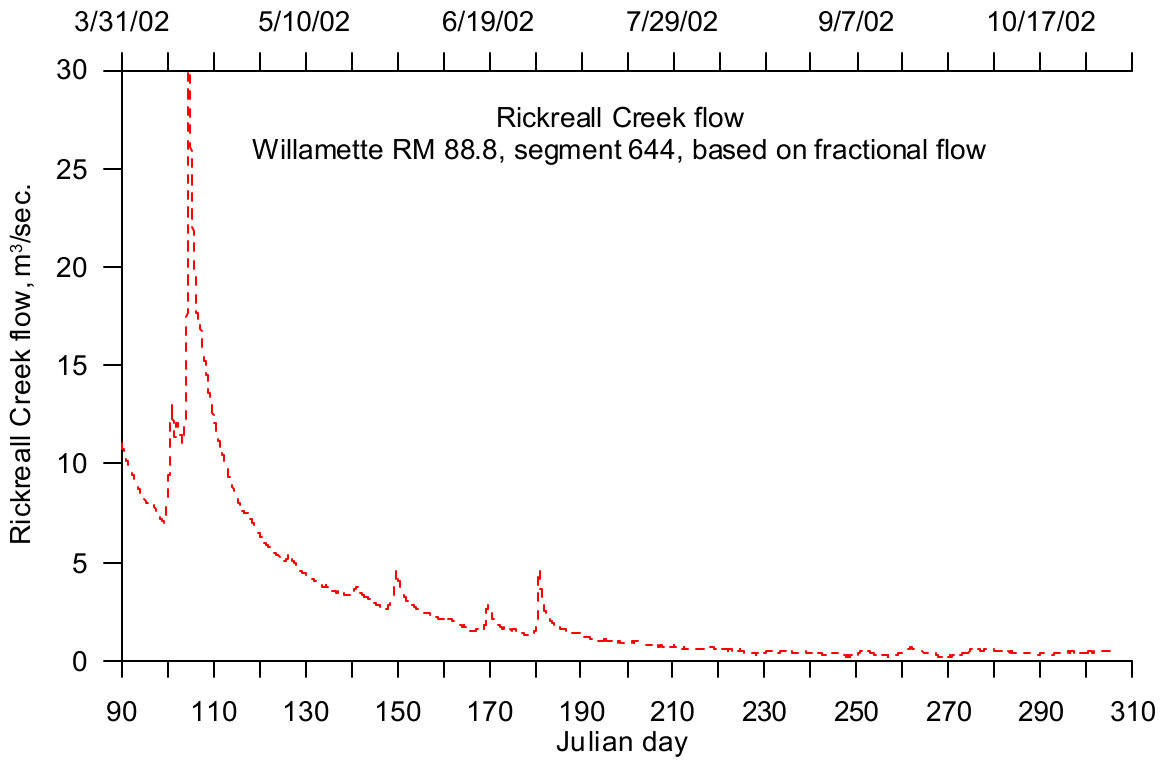


**Figure 291. Rickreall Creek flow, 2002**

## Temperature Data

Tributary temperatures were monitored by the USGS and ODEQ in 2001 and 2002. Figure 292 shows the temperature monitoring sites used in developing the tributary temperature records. The sampling frequencies were half-hourly or hourly measurements. The sites used were the same for both years except for the McKenzie River which had data from an additional gage available in 2002.

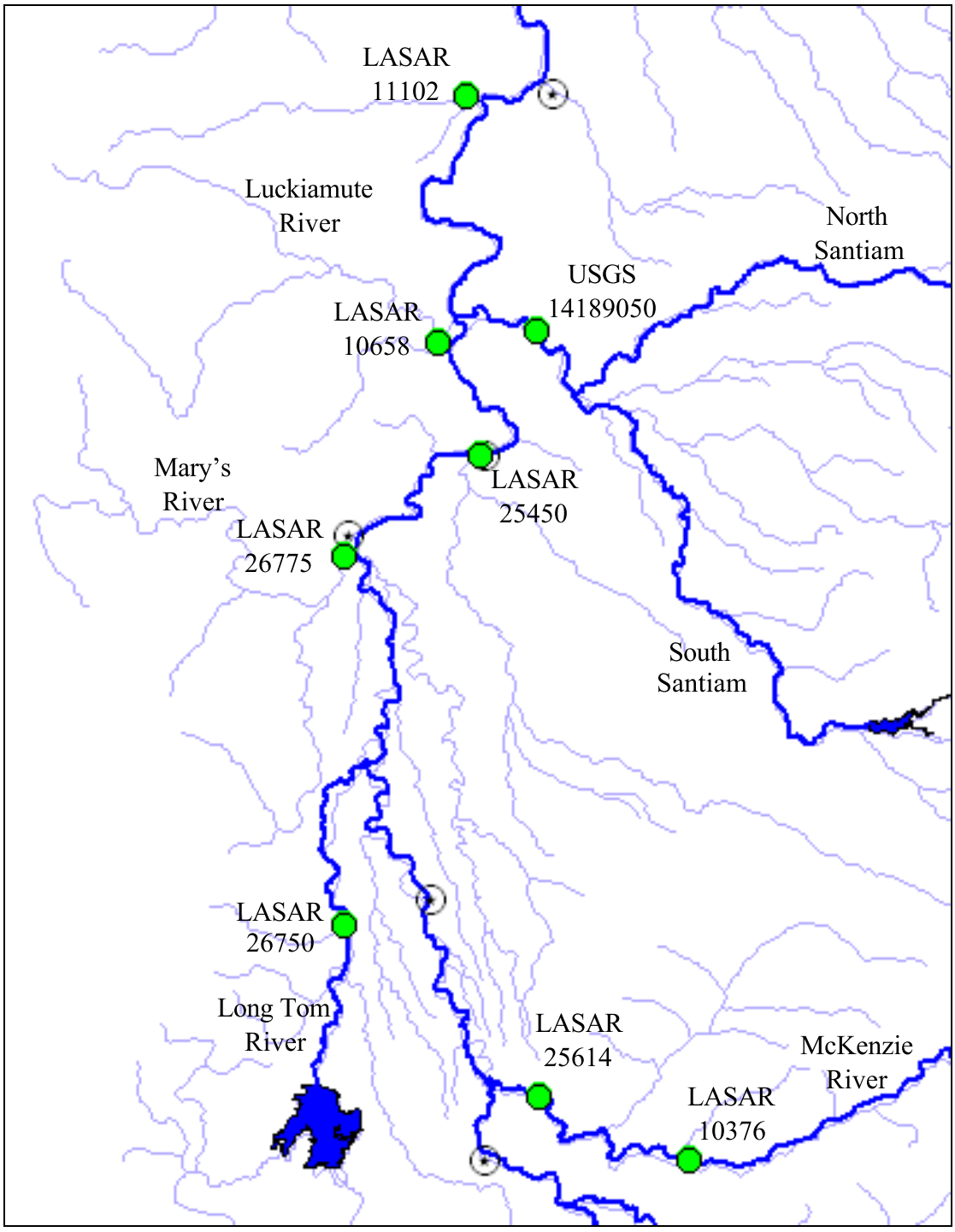


**Figure 292. Upper Willamette River model tributary temperature monitoring site locations**

## Year 2001

The sources for the 2001 tributary temperature data are shown in Table 30.

**Table 30. Upper Willamette River model tributary temperature data sources, 2001**

| Site ID | Tributary | Willamette RM | Model Segment |
|---|---|---|---|
| LASAR 25614 | McKenzie River | 175.3 | 68 |

| Site ID | Tributary | Willamette RM | Model Segment |
|---|---|---|---|
| LASAR 26750 | Long Tom River | 149.4 | 240 |
| LASAR 26775 | Mary's River | 133.4 | 343 |
| LASAR 25450 | Calapooia River | 120.2 | 432 |
| LASAR 10658 | Luckiamute River | 108.7 | 508 |
| USGS14189050 | Santiam River | 108.5 | 509 |
| LASAR 11102 | Rickreall Cr. | 88.8 | 644 |

The furthest downstream gage on the McKenzie River in 2001 was at Walterville, RM 25. The summer water temperature was expected to warm approximately 2 ºC prior to the confluence with the Willamette River. Since the McKenzie River flow was so large relative to the main stem Willamette River, an improved McKenzie River temperature estimate was developed. A correlation between the 2002 temperatures for the McKenzie River at Coburg (LASAR 10376), and the McKenzie River above Walterville (LASAR 25614), was used to generate the 2001 McKenzie River temperatures. Data from June 4, 2001 to October 1, 2002, were used to generate the correlation. The correlation and the resulting equation are shown in Figure 293. McKenzie River temperature data at LASAR 25614 were available from June 12, 2001 to October 8, 2001. The starting date in 2001 limits the calibration period. For the model scenarios, the McKenzie River tributary temperature data set was extended with temperature output from the McKenzie River model. The McKenzie River temperature is shown in Figure 294. The summer diurnal variation was approximately 4 to 6 ºC. Except in approximately July, 2001, when the temperatures were similar, the McKenzie River was 0 to 3 ºC cooler than the main stem Willamette River, with the difference being greater in the fall months.

The Long Tom River temperature data were available from June 1 to November 6, 2001. The Long Tom River temperature data are shown in Figure 295. The summer diurnal variation was approximately 2 ºC. The mean summer temperatures were approximately 1 to 3 ºC warmer than the main stem Willamette River.

The Mary's River temperature data were available from May 15, 2001 to November 1, 2001. The Mary's River temperature data are shown in Figure 296. The summer diurnal variation was approximately 2 ºC. The mean summer temperatures were approximately 0 to 2 ºC warmer than the main stem Willamette River.

The Calapooia River temperature data were available from May 30, 2001 to September 25, 2001. The data were supplemented with a correlation between the Santiam River temperature (USGS14189050) and the Calapooia River temperatures (LASAR 25450). Data from June 6, 2002 to July 19, 2002, were used to generate the correlation. The correlation and resulting equation are shown in Figure 297. Figure 298 shows the Calapooia River temperature times series including both data and calculated values. The summer diurnal variation was approximately 2 ºC. The mean summer temperatures were approximately 0 to 2 ºC cooler than the main stem Willamette River.

The Luckiamute River temperature data were available from June 4, 2001 to September 25, 2001. The data were supplemented with a correlation between the Luckiamute River temperature (LASAR 10658) and Mary's River temperatures (LASAR 26775). Data from June 11, 2001 to July 18, 2001, were used to generate the correlation. The correlation and resulting equation are shown in Figure 299. The Calapooia River temperature data are shown in Figure 300. The summer diurnal variation was approximately 2 ºC. The mean summer temperatures are approximately 0 to 2 ºC warmer than the main stem Willamette River.

Santiam River temperature data were available from May 25, 2001 to November 1, 2001. The Santiam River temperature is shown in Figure 301. The summer diurnal variation ranged from 1 to 3 ºC. The mean summer temperatures were approximately 1to 2 ºC cooler than the main stem Willamette River.

The Rickreall Creek temperature data were available from May 15, 2001 to October 31, 2001. The Rickreall Creek temperature is shown in Figure 303. The summer diurnal variation was approximately 2 ºC. The mean summer temperatures were approximately 1ºC cooler than the main stem Willamette River.

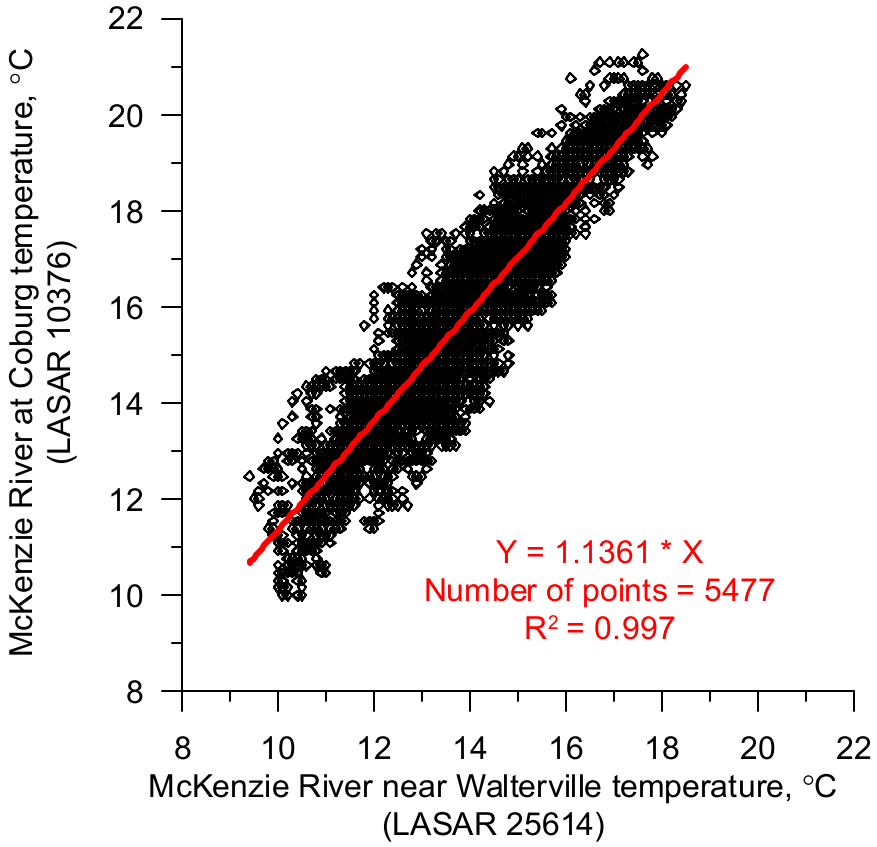


**Figure 293. McKenzie River temperature correlation.**

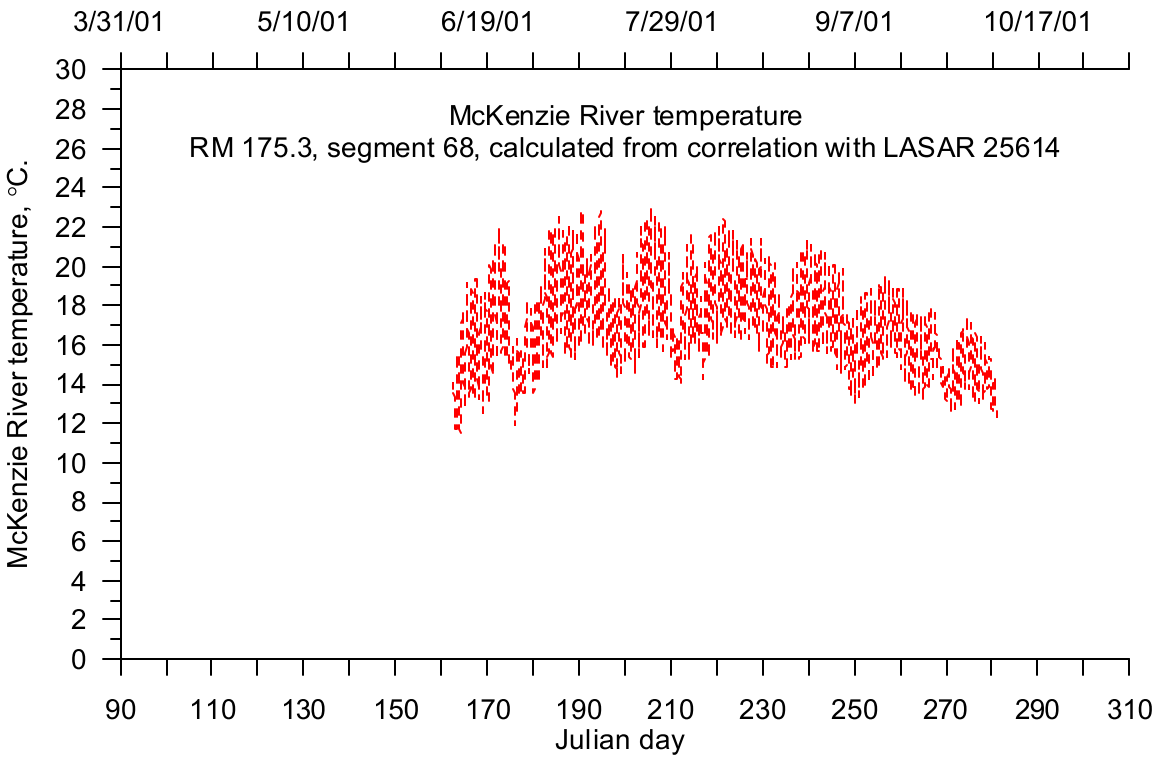


**Figure 294. McKenzie River temperature, 2001**

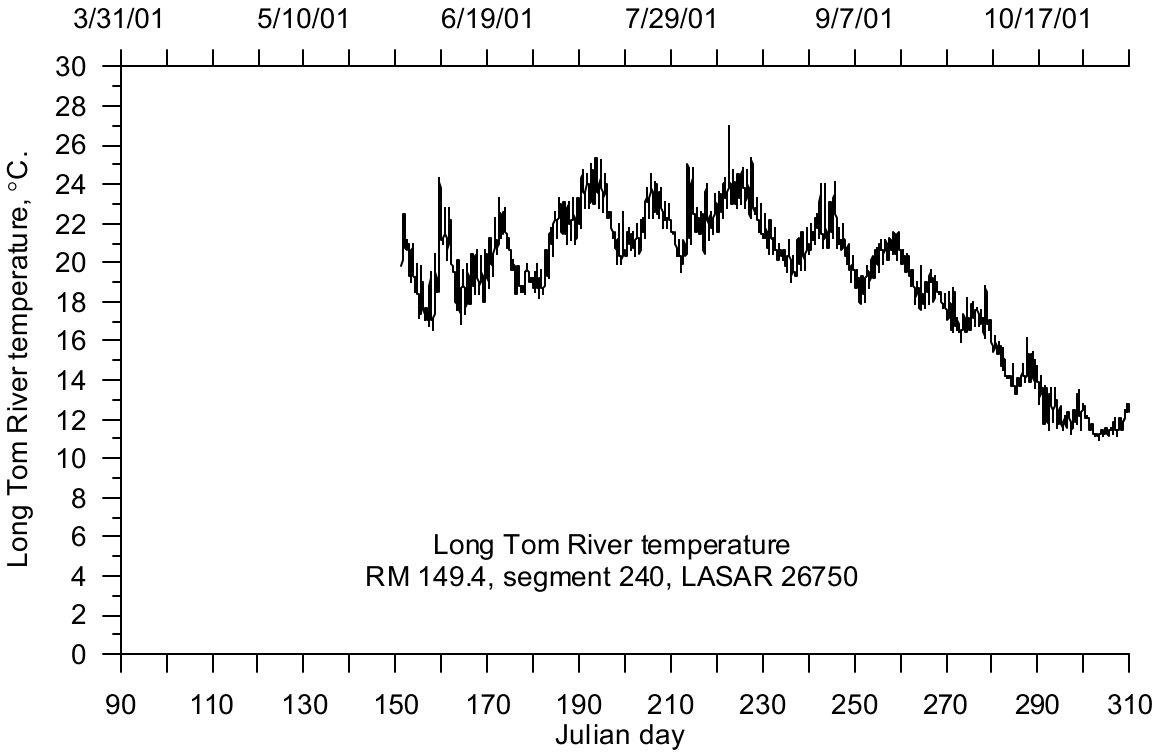


**Figure 295. Long Tom River temperature, 2001**

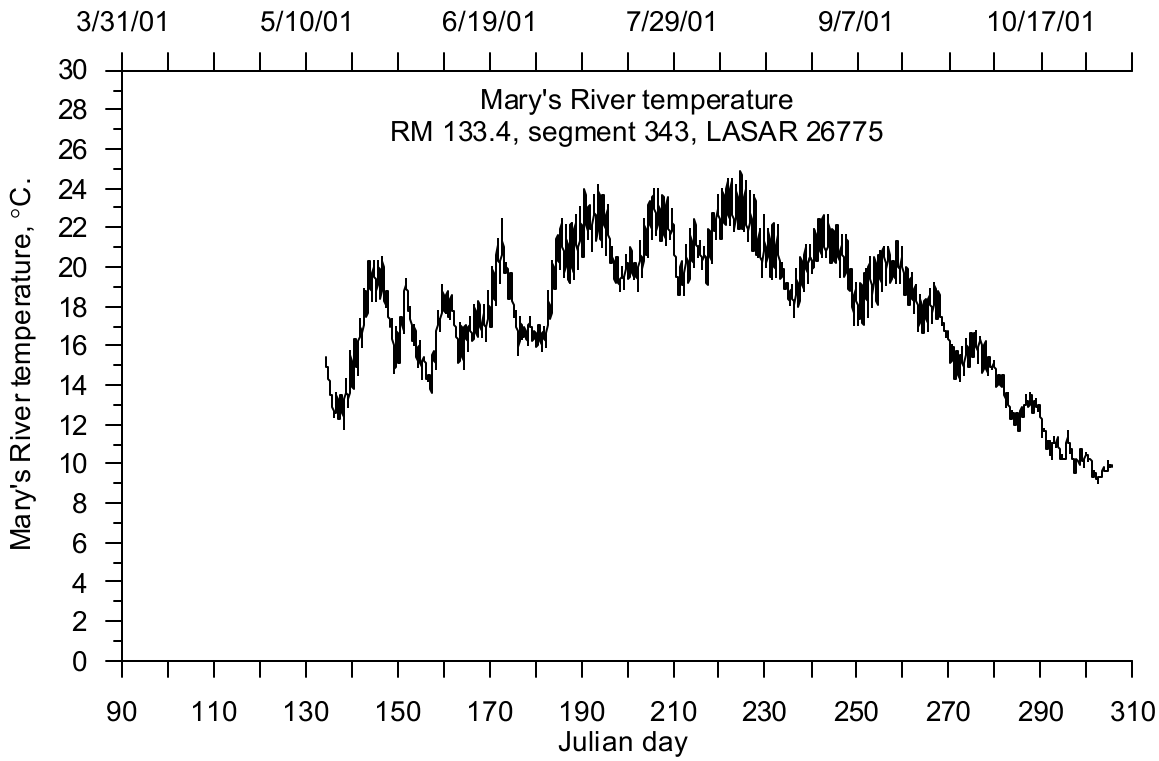


**Figure 296. Mary's River temperature, 2001**

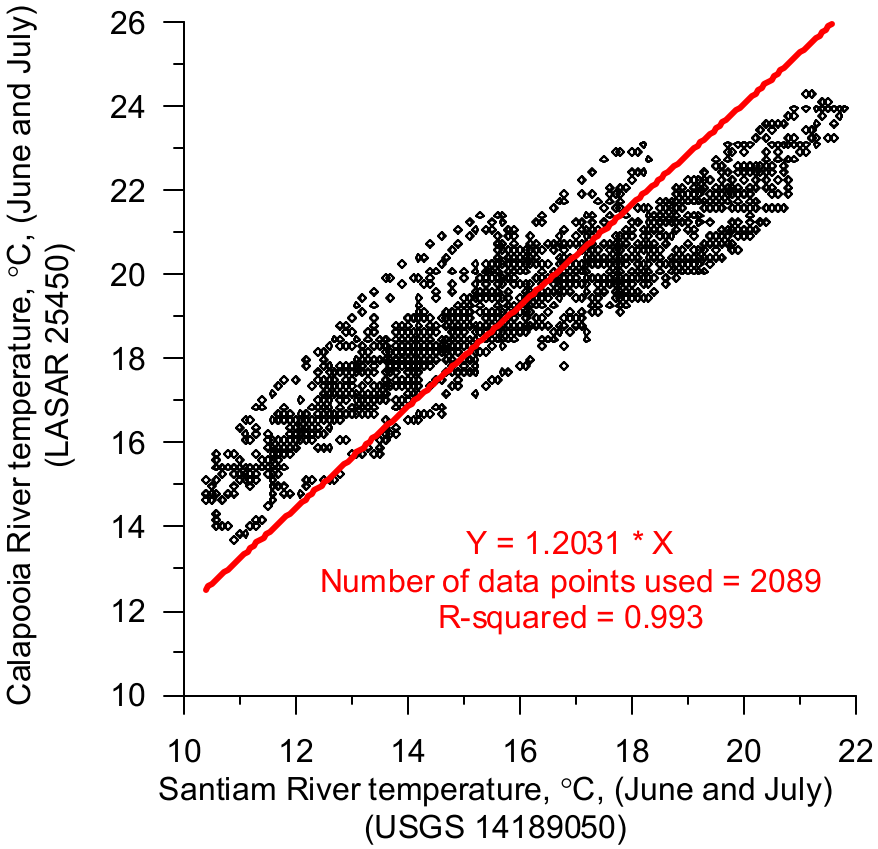


**Figure 297. Temperature correlation between Calapooia River and the Santiam River**

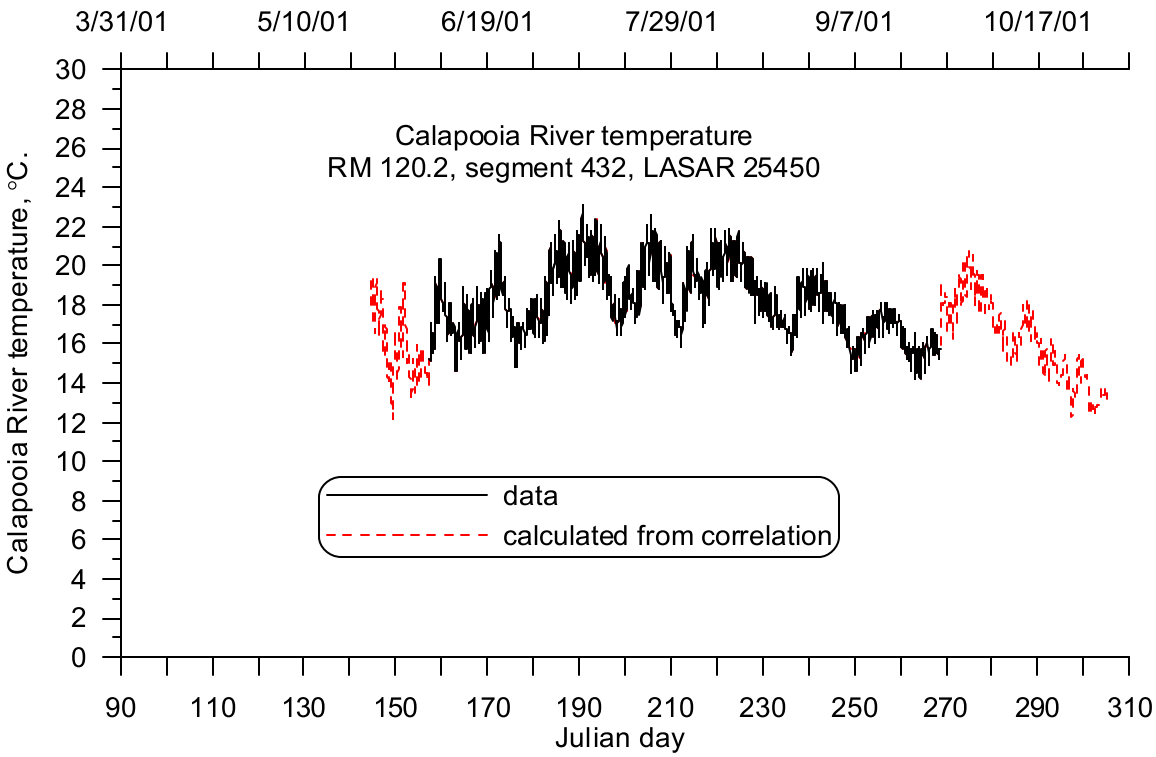


**Figure 298. Calapooia River temperature, 2001**

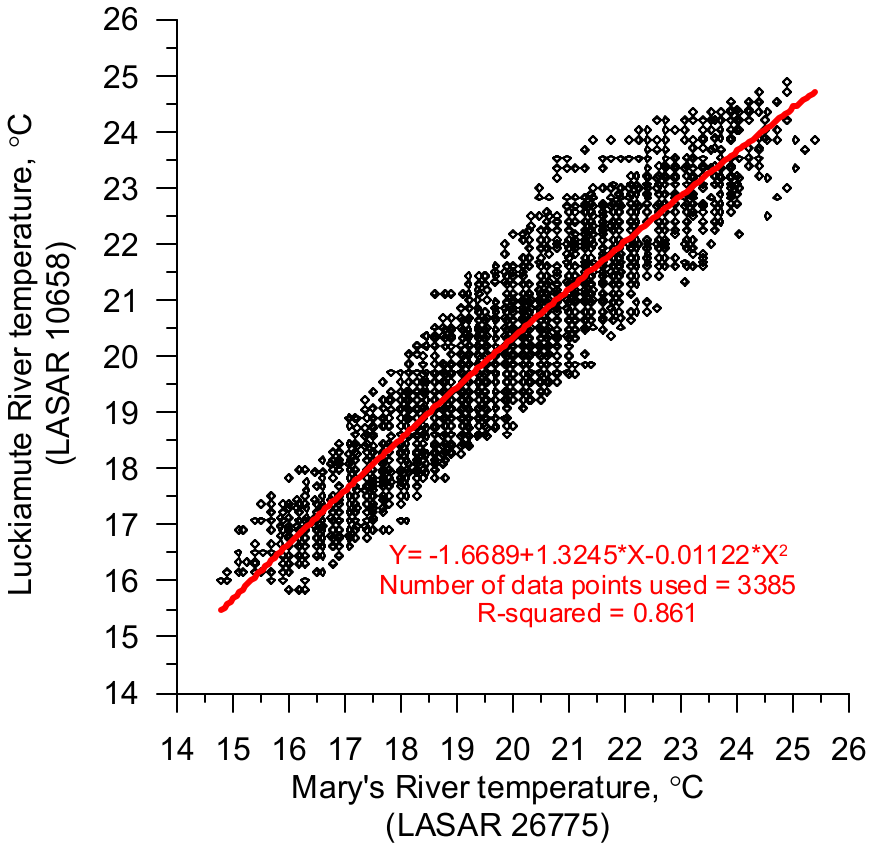


**Figure 299. Luckiamute River temperature correlation**

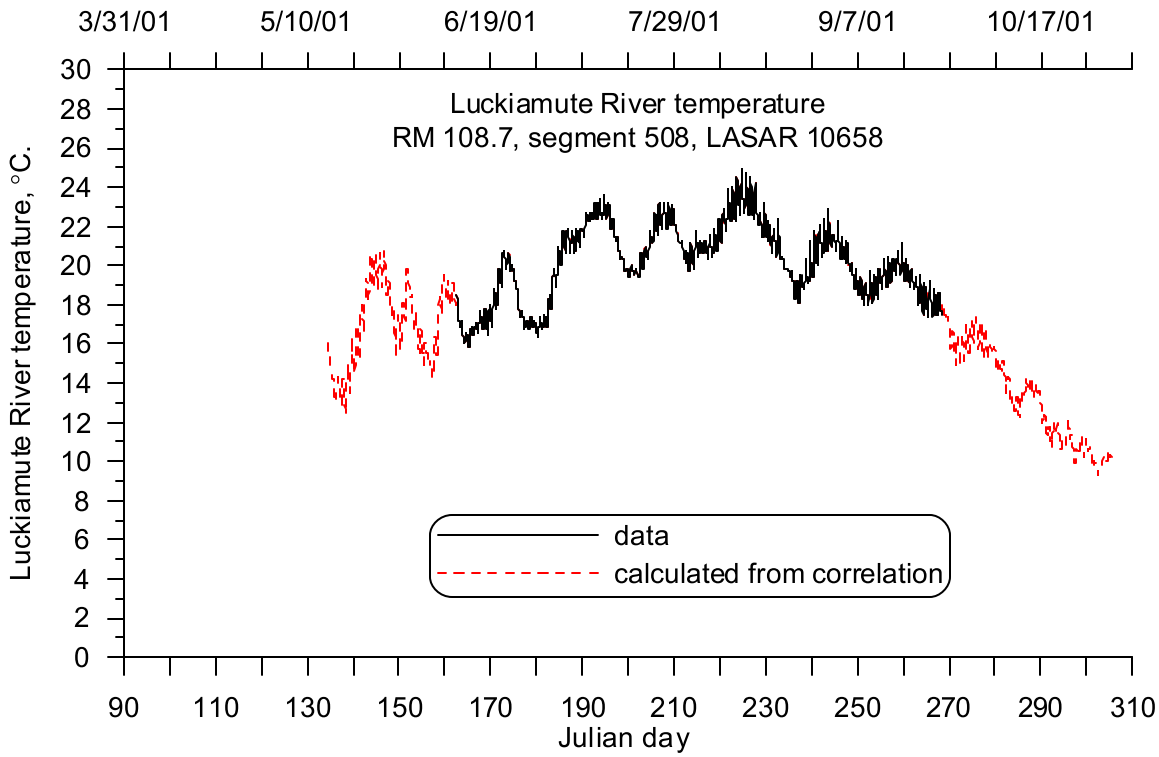


**Figure 300. Luckiamute River temperature, 2001**

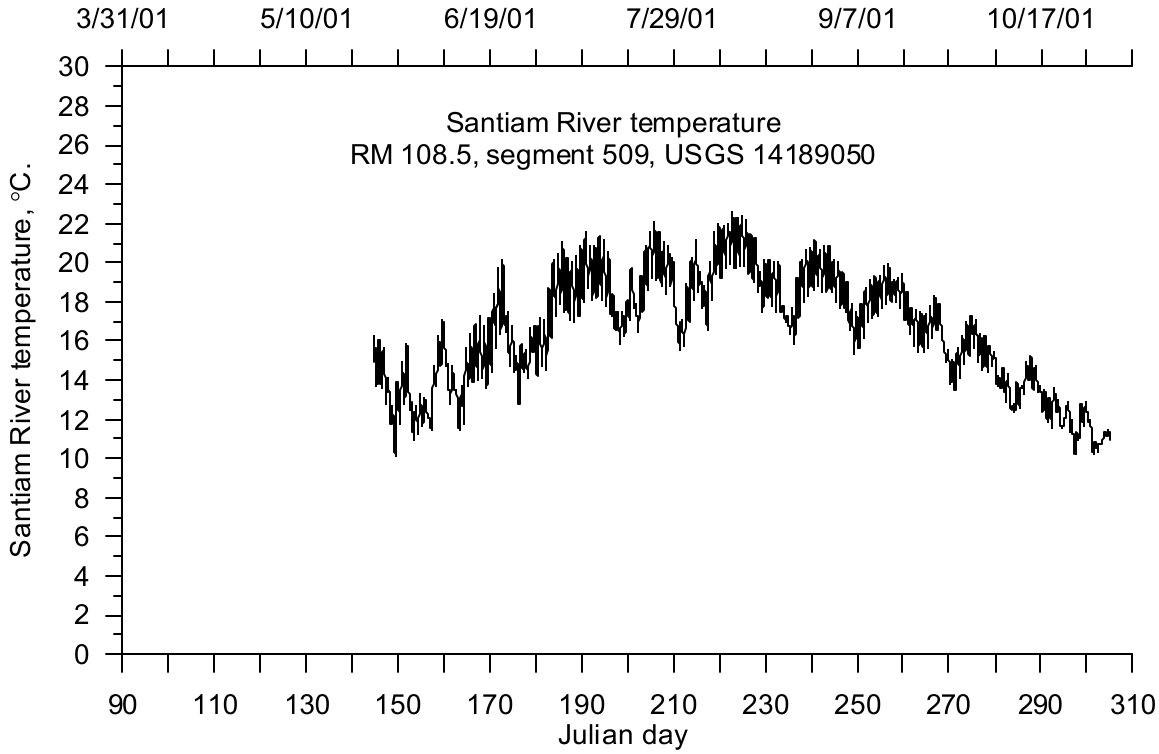


**Figure 301. Santiam River temperature, 2001**

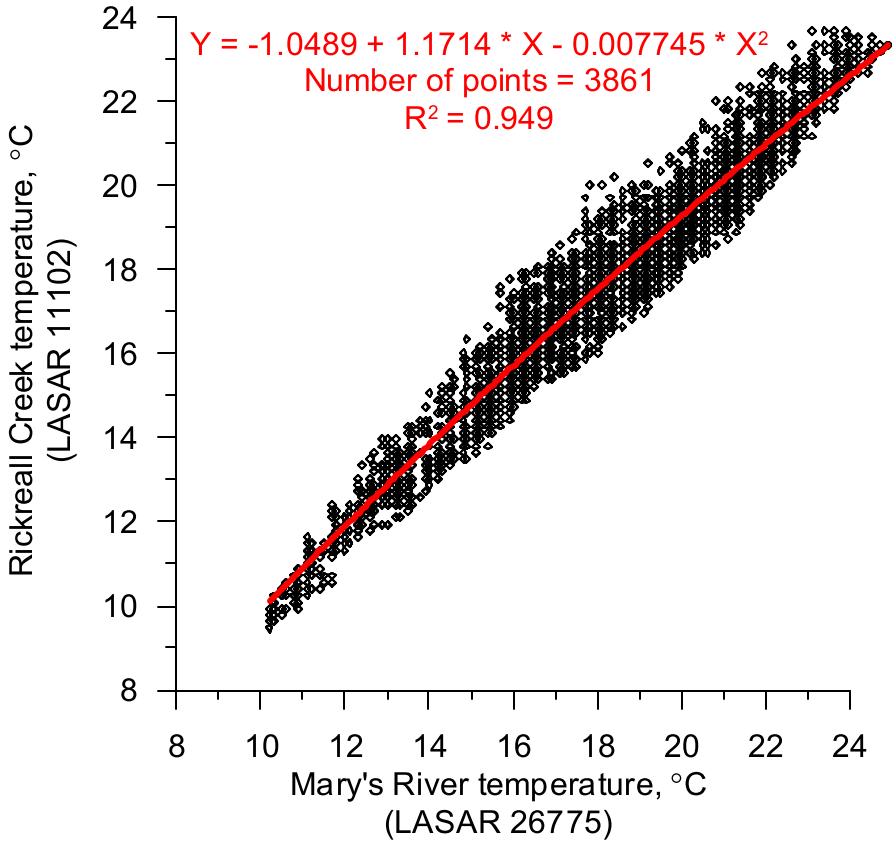


**Figure 302. Rickreall Creek temperature correlation.**

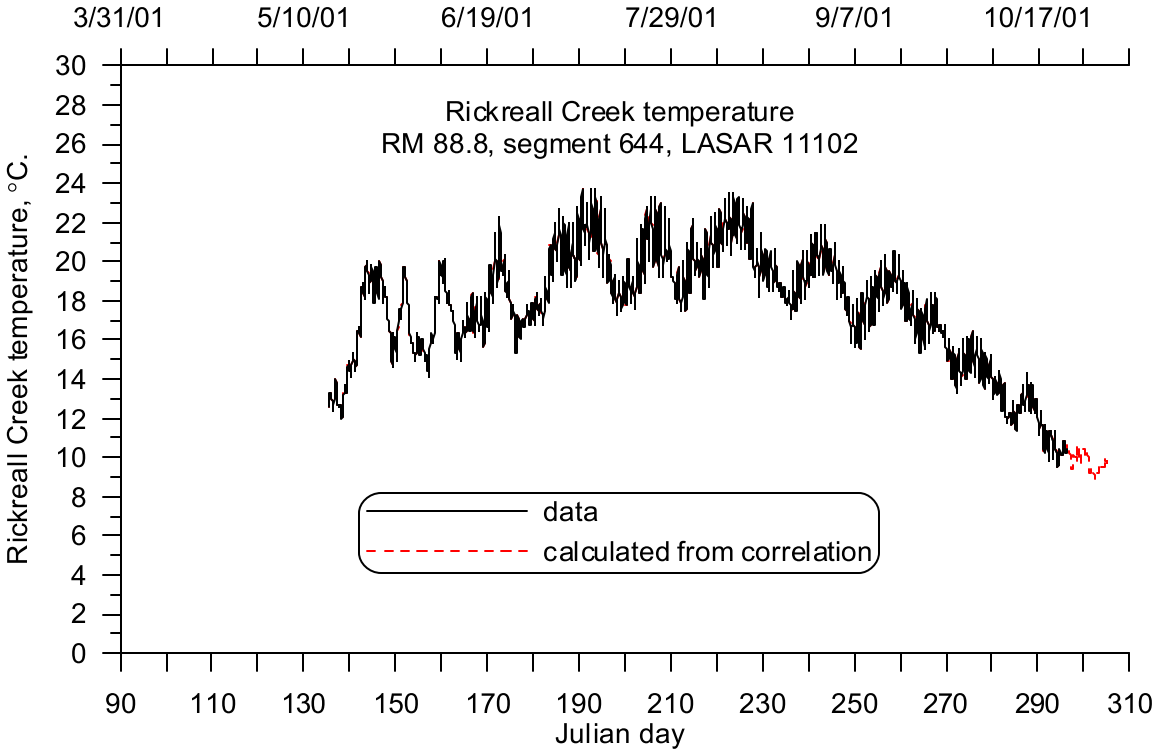


**Figure 303. Rickreall Creek temperature, 2001**

## Year 2002

The sources for the 2002 tributary temperature data are shown in Table 31.

**Table 31. Upper Willamette River model tributary temperature data sources, 2002**

| Site ID | Tributary | Willamette RM | Model Segment |
|---|---|---|---|
| LASAR 10376 | McKenzie River | 175.3 | 68 |
| LASAR 26750 | Long Tom River | 149.4 | 240 |
| LASAR 26775 | Mary's River | 133.4 | 343 |
| LASAR 25450 | Calapooia River | 120.2 | 432 |
| LASAR 10658 | Luckiamute River | 108.7 | 508 |
| USGS14189050 | Santiam River | 108.5 | 509 |
| LASAR 11102 | Rickreall Cr. | 88.8 | 644 |

McKenzie River temperature data were available from June 4, 2002 to October 1, 2002. The data were supplemented using a correlation between the temperature at Coburn (LASAR 10376) and the temperature at Walterville (LASAR 25614). Data from June 4, 2002 to October 1, 2002, were used to generate the correlation. The correlation and the resulting equation are shown in Figure 293. The McKenzie River temperature is shown in Figure 304. The summer diurnal variation was approximately 3 to 4 ºC. Except in July, 2002, when temperatures were similar, the McKenzie River was 0 to 3 ºC cooler than the main stem Willamette River with the difference being greater in the fall months.

The Long Tom River temperature data were available from May 31, 2002 to October 2, 2002. The data were supplemented using a correlation equation between the temperature at the mouth of the river (LASAR 26750) and temperature data at Monroe (USGS14170000, RM 6.8). Data from May 31, 2002 to October 2, 2002 were used to generate the correlation. The correlation and resulting equation are shown in Figure 305. The Long Tom River temperature data are shown in Figure 306. The summer diurnal variation was approximately 2 to 4 ºC. The mean summer temperatures were approximately 2 to 4 ºC warmer than the main stem Willamette River.

The Mary's River temperature data were available from May 15, 2002 to October 31, 2002. The data were supplemented with temperature data from the Willamette River at Albany (USGS 14174000). The Mary's River temperature data are shown in Figure 307. A comparison between the Willamette River temperature at Albany and Mary's River temperature is shown in Figure 308. The summer diurnal variation was approximately 1 to 2 ºC. The mean summer temperatures were approximately 2 to 4 ºC warmer than the main stem Willamette River.

Calapooia River temperature data were available from June 6, 2002 to October 9, 2002. The data were supplemented with a correlation between the Santiam River temperature (USGS 14189050), and the Calapooia River temperatures (LASAR 25450). Data from June 6, 2002 to July 19, 2002, were used to generate the correlation. The correlation and resulting equation are shown in Figure 297. The Calapooia River temperature data and calculated values are shown in Figure 309. The summer diurnal variation was approximately 2 ºC. The mean summer temperatures were approximately 0 to 1 ºC cooler than the main stem Willamette River temperatures.

The Luckiamute River temperature data were available from June 14, 2002 to July 18, 2002. The data were supplemented with a correlation between the Luckiamute River temperatures (LASAR 10658) and Mary's River temperatures (LASAR 26775). Data from June 11, 2001 to July 18, 2001, were used to

generate the correlation. The correlation and resulting equation are shown in Figure 299. The Calapooia River temperature data are shown in Figure 310. The summer diurnal variation was approximately 1 ºC. The mean summer temperatures varied within 1 ºC of the main stem Willamette River.

Santiam River temperature data were available from January 1, 2002 to October 31, 2002. The Santiam River temperature is shown in Figure 311. The summer diurnal variation was approximately 2 ºC. The mean summer temperatures were approximately 1to 2 ºC cooler than the main stem Willamette River.

The Rickreall Creek temperature data were available from March 31, 2002 to October 31, 2002. The Rickreall Creek temperature is shown in Figure 312. The summer diurnal variation was approximately 2 ºC. The mean summer temperatures varied within 1 ºC of the main stem Willamette River.

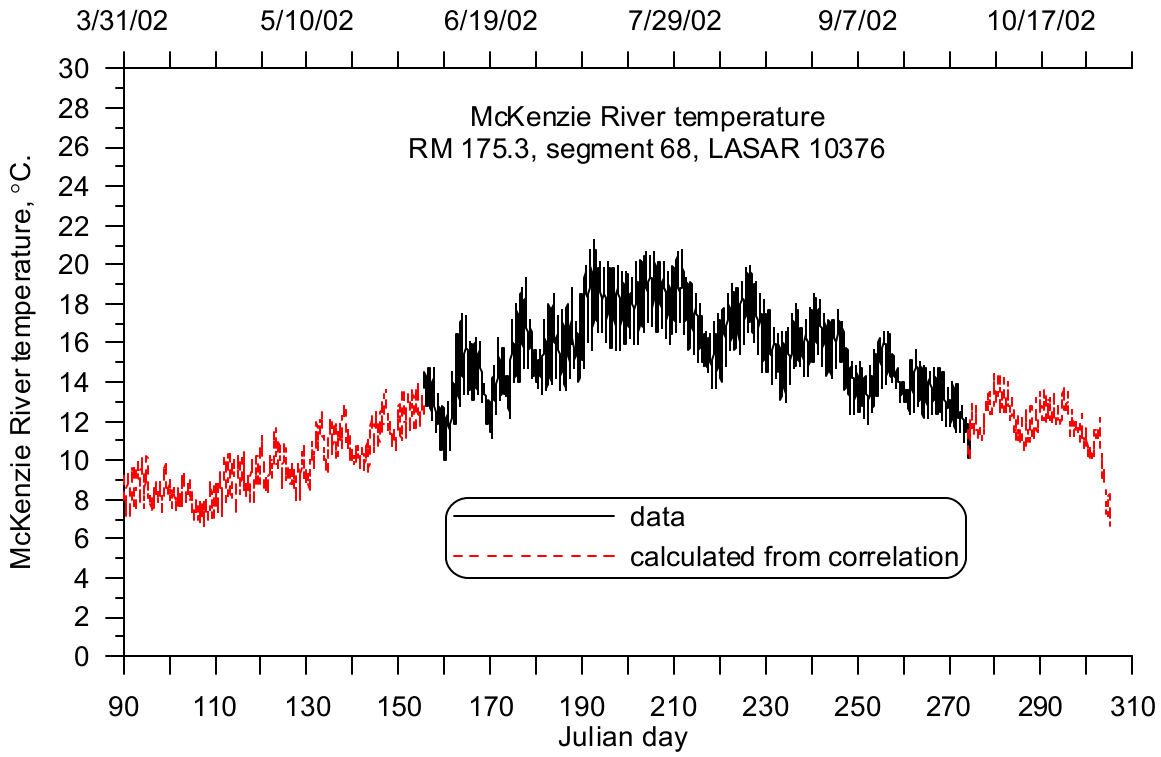


**Figure 304. McKenzie River temperature, 2002**

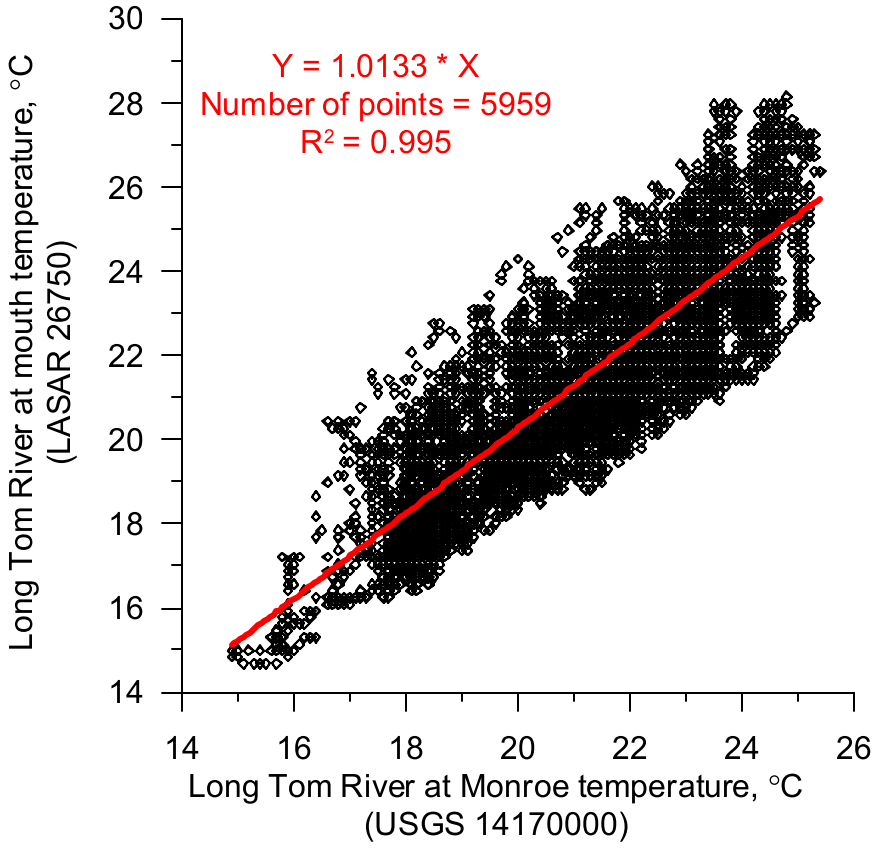


**Figure 305. Long Tom River temperature correlation.**

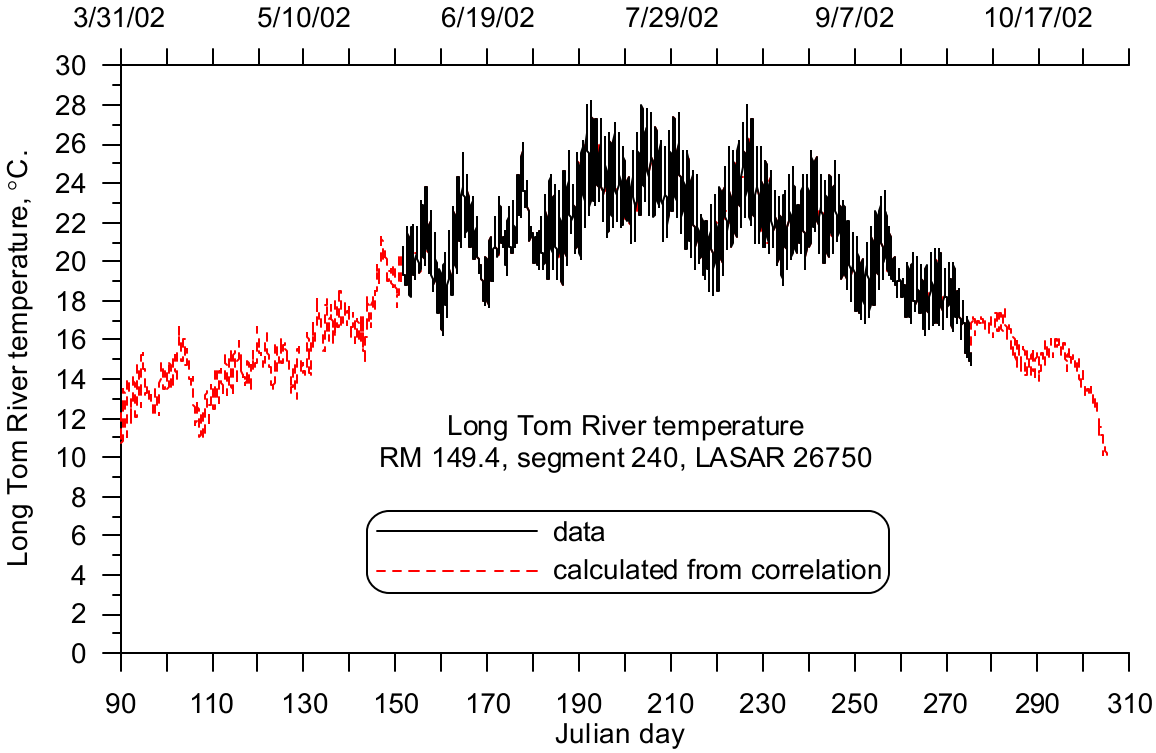


**Figure 306. Long Tom River temperature, 2002**

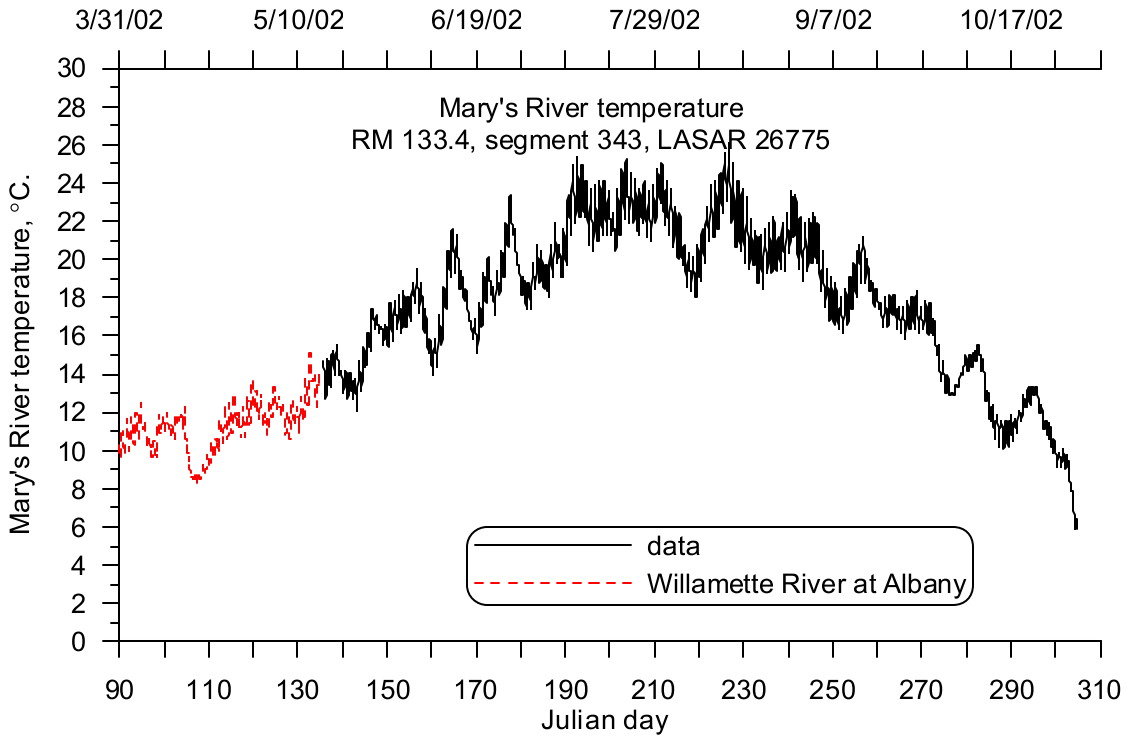


**Figure 307. Mary's River temperature, 2002**

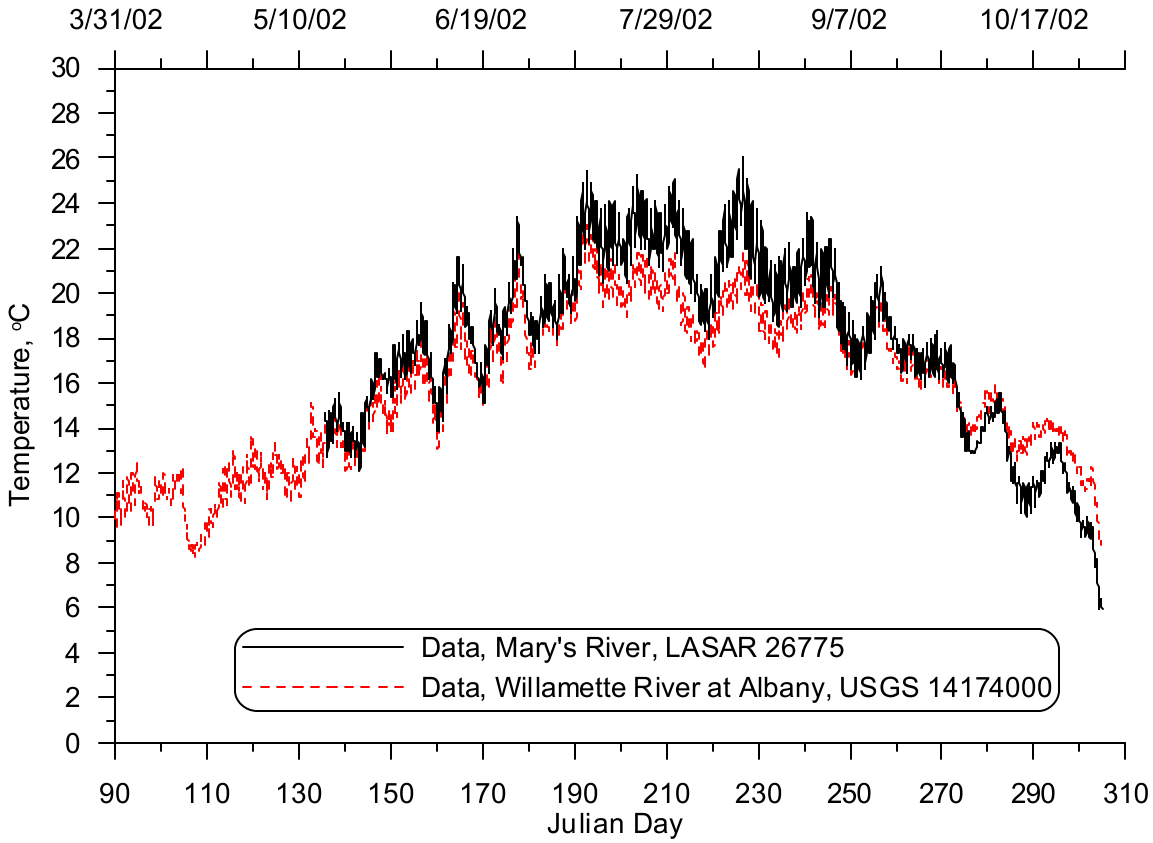


**Figure 308. Comparison of Mary's River and Willamette River at Albany temperature**

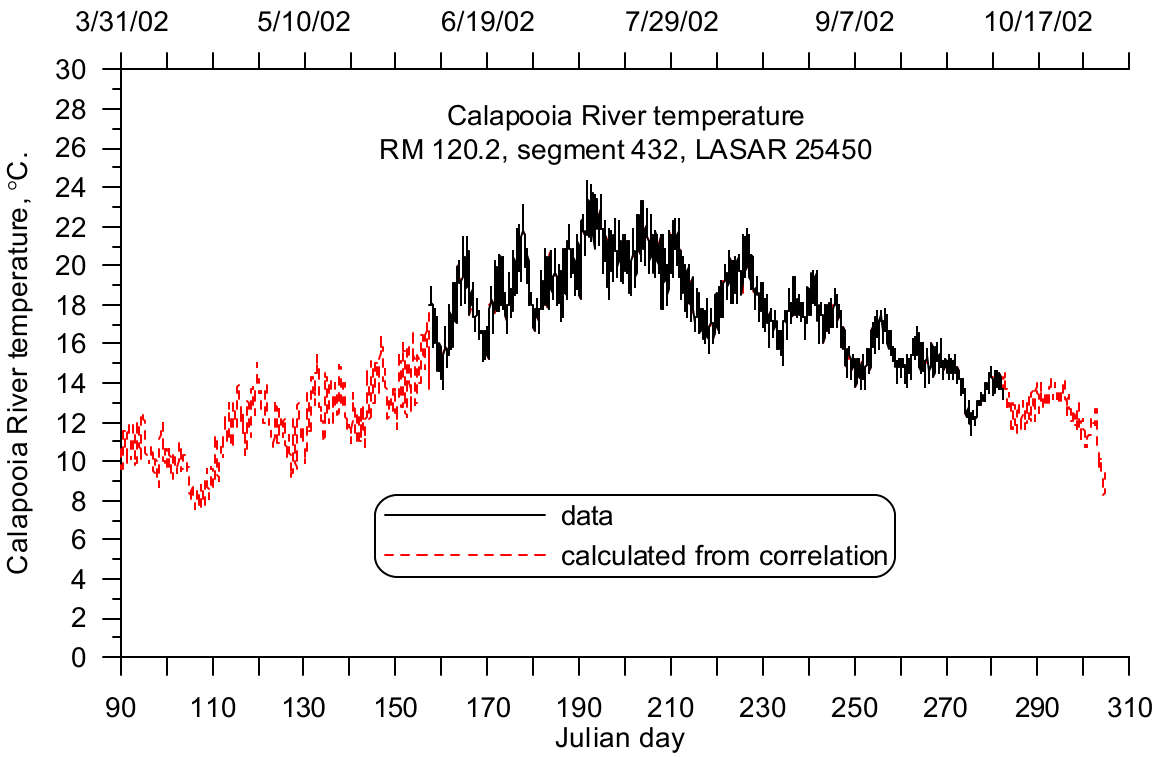


**Figure 309. Calapooia River temperature, 2002**

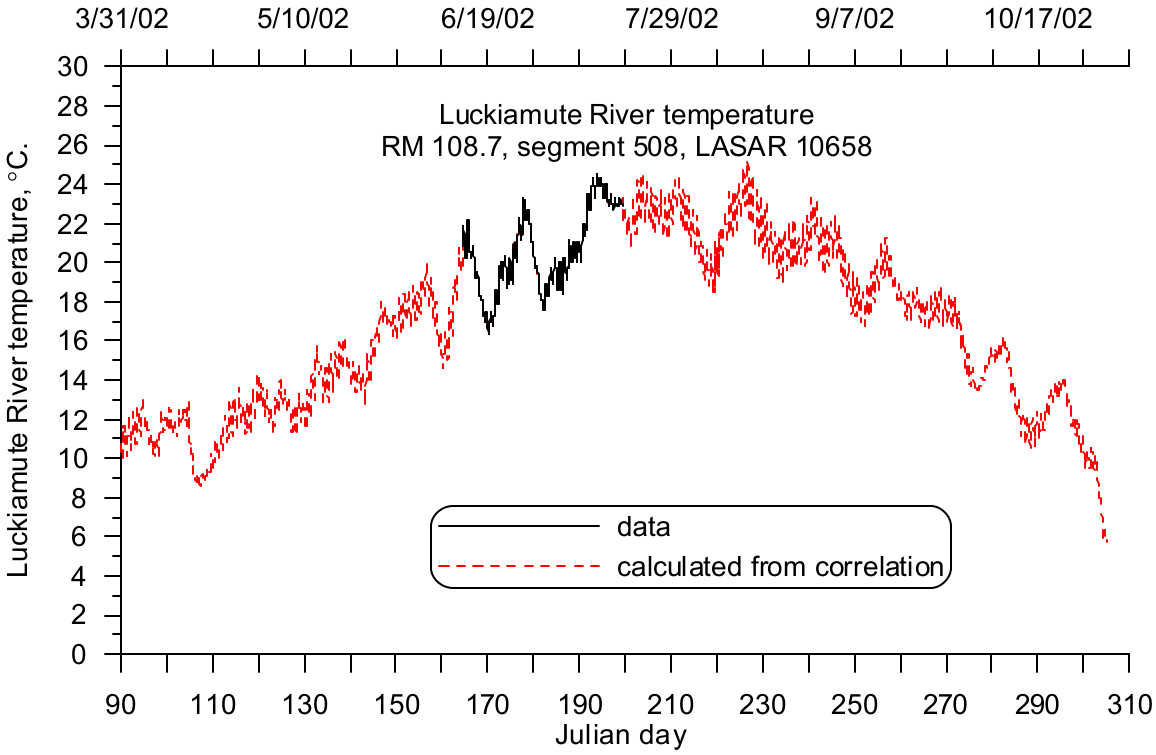


**Figure 310. Luckiamute River temperature, 2002**

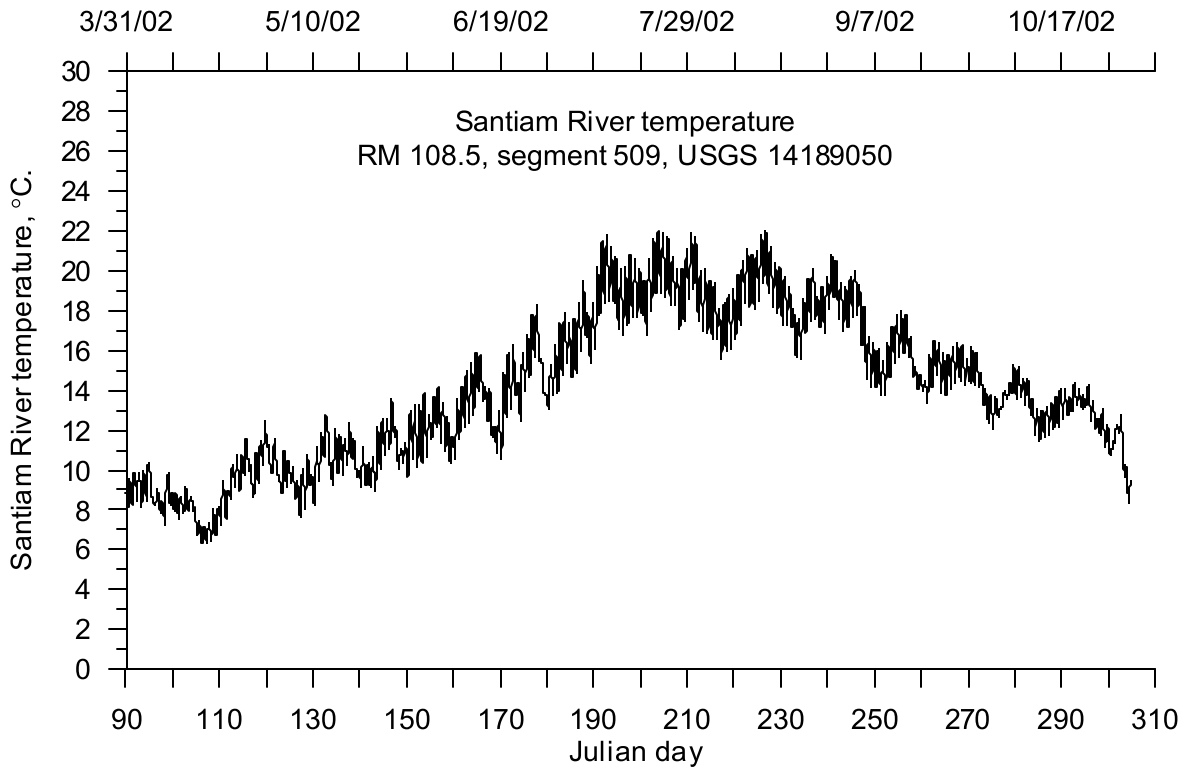


**Figure 311. Santiam River temperature, 2002**

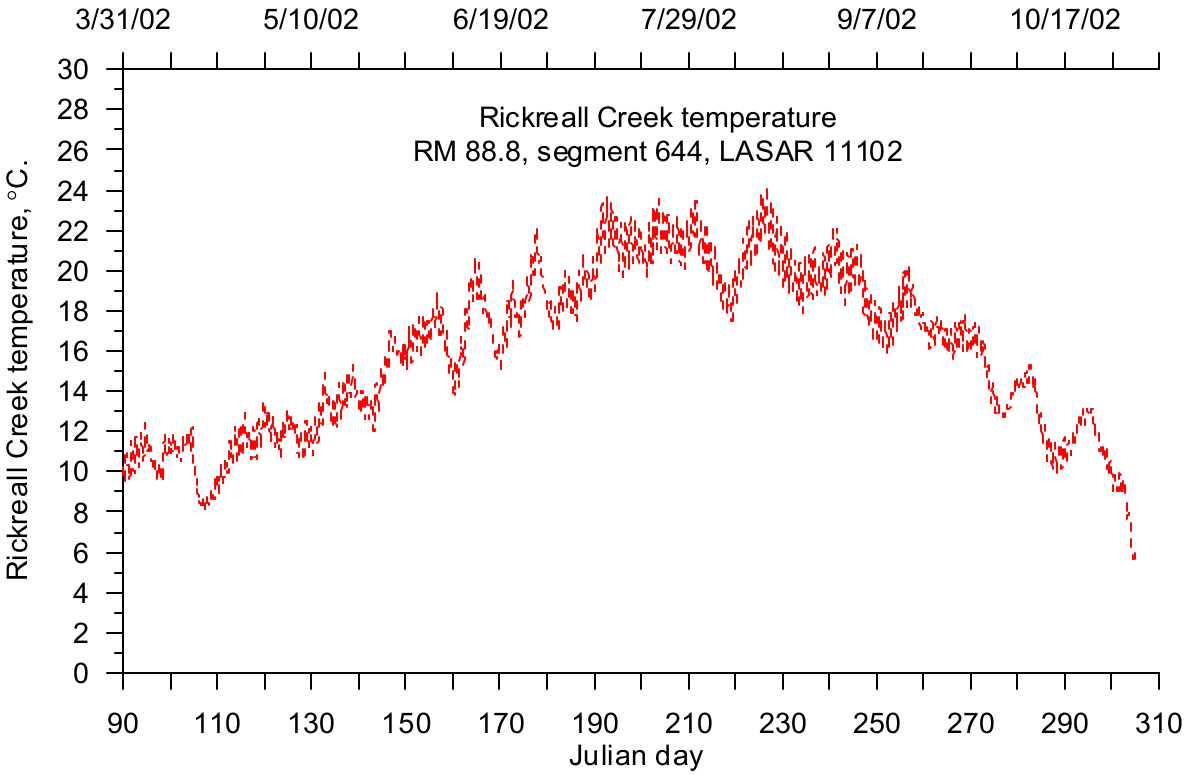


**Figure 312. Rickreall Creek temperature, correlated, 2002**

## *Distributed Tributaries*

Distributed tributary flows represent any ungaged surface runoff, groundwater exchange, or ungaged discharge and withdrawals.

### Hydrodynamic Data

Two sources of distributed inflow were identified. The first source was a groundwater inflow estimated at 4 $m^3$/sec (Laenen, 2002a) over RM 149 to 120. This flow was distributed by length over branches 7 and 8 as shown in Table 32.

**Table 32. Groundwater Inflow Distribution.**

| Branch | 7 | 8 | Start RM | End RM |
|---|---|---|---|---|
| Length, miles | 21.33 | 7.47 | 149.10 | 127.77 |
| GW inflow, $m^3$/sec | 2.96 | 1.04 | 127.77 | 120.3 |

The second source was ungaged basin inflow. Using a four-field HUC GIS coverage of the Willamette Basin, sub-basins unrepresented by any model tributary were identified. The collective area shown in Figure 313 (852.4 $km^2$) represents 4.5% of the Upper Willamette River model watershed area and 2.7% of the Willamette River watershed area. The Luckiamute River basin (815.2 $km^2$) was selected for its similar topography to generate estimated inflows based on fractional flow. Using the ratio of the basin areas, the ungaged basin inflow was estimated to be 104.6% of the Luckiamute River flow at USGS 14190500. Inflows were distributed linearly over the model length from RM 185 to RM 120 (branches 1 through 8), as shown in Table 33.

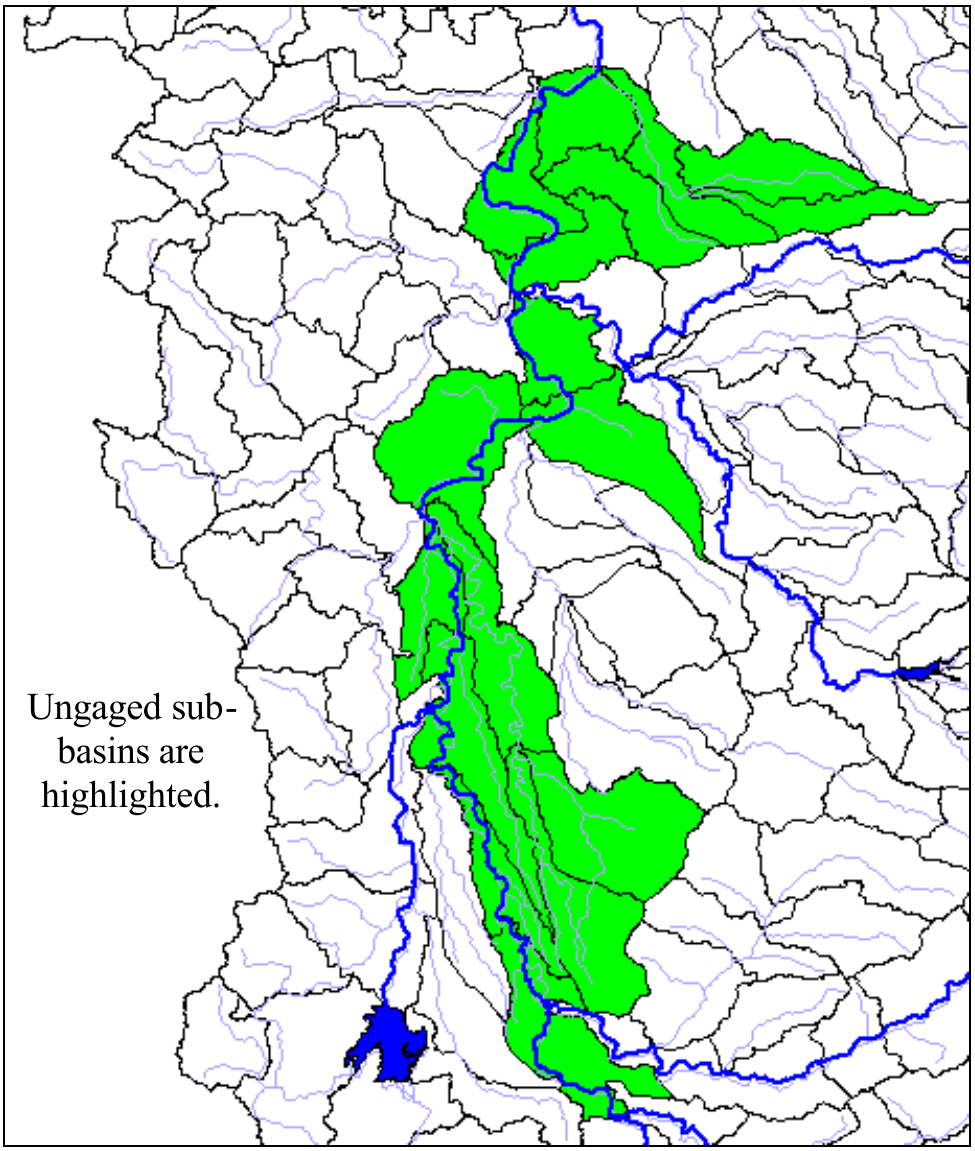


**Figure 313. Upper Willamette ungaged basins**

**Table 33. Upper Willamette River model ungaged basin distributed inflow reaches**

| Branch | Branch length, mi | Fractional Flow | Start RM | End RM |
|---|---|---|---|---|
| 1 | 2.65 | 0.0442 | 184.45 | 180.39 |
| 2 | 3.12 | 0.0520 | 180.39 | 177.27 |
| 3 | 2.34 | 0.0390 | 177.27 | 174.93 |
| 4 | 13.70 | 0.2284 | 174.93 | 161.23 |
| 5 | 6.07 | 0.1012 | 161.23 | 155.16 |
| 6 | 6.06 | 0.1010 | 155.16 | 149.10 |
| 7 | 21.33 | 0.3556 | 149.10 | 127.77 |
| 8 | 7.47 | 0.1245 | 127.77 | 120.3 |
| Total | 62.74 | 1.0460 | 184.45 | 120.3 |

## Year 2001

The ungaged basin inflows based on the 2001 Luckiamute River flows (USGS 14190500) and the 4 $m^3$/sec were used to generate the total distributed inflows over RM 185 to 120, as shown in Figure 314. No distributed inflows were applied over RM 120 to RM 85 prior to model calibration.

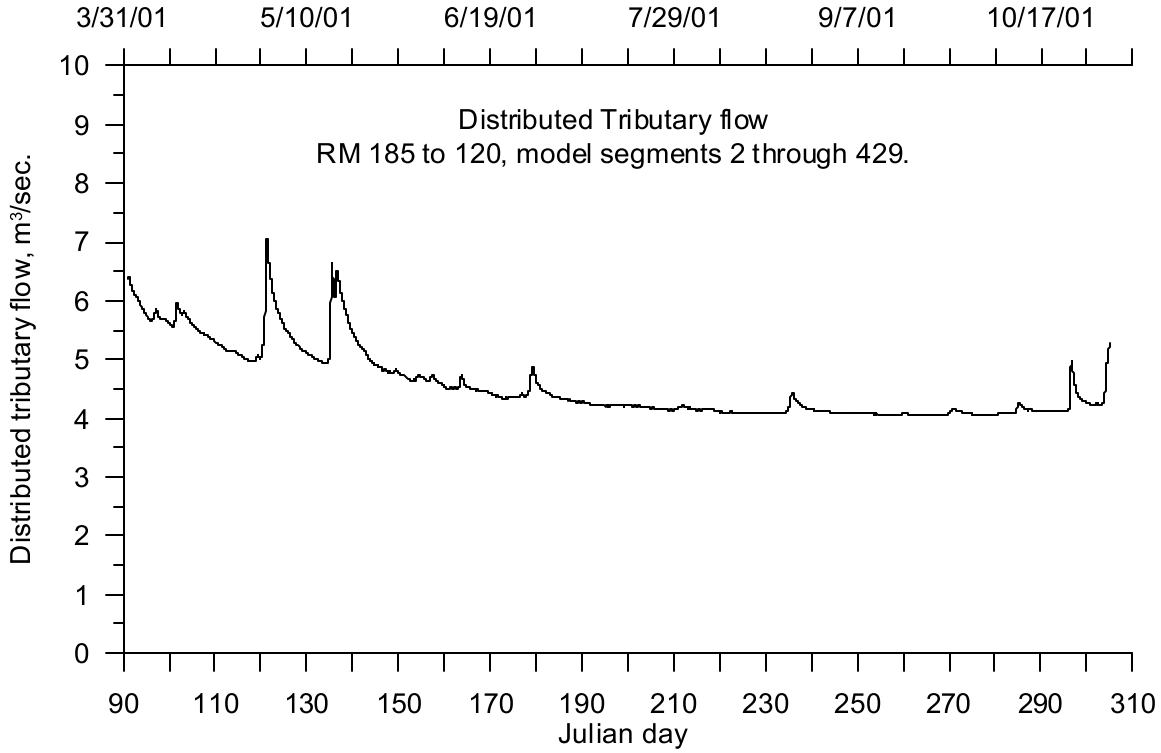


**Figure 314. Upper Willamette River model total distributed inflow from RM 185 - 120 (Branches 1 to 8), 2001**

## Year 2002

The ungaged basin inflows based on the 2002 Luckiamute River flows (USGS 14190500) and the 4 $m^3$/sec were used to generate the total distributed inflows over RM 185 to 120, as shown in Figure 315. No distributed inflows were applied over RM 120 to RM 85 prior to model calibration.

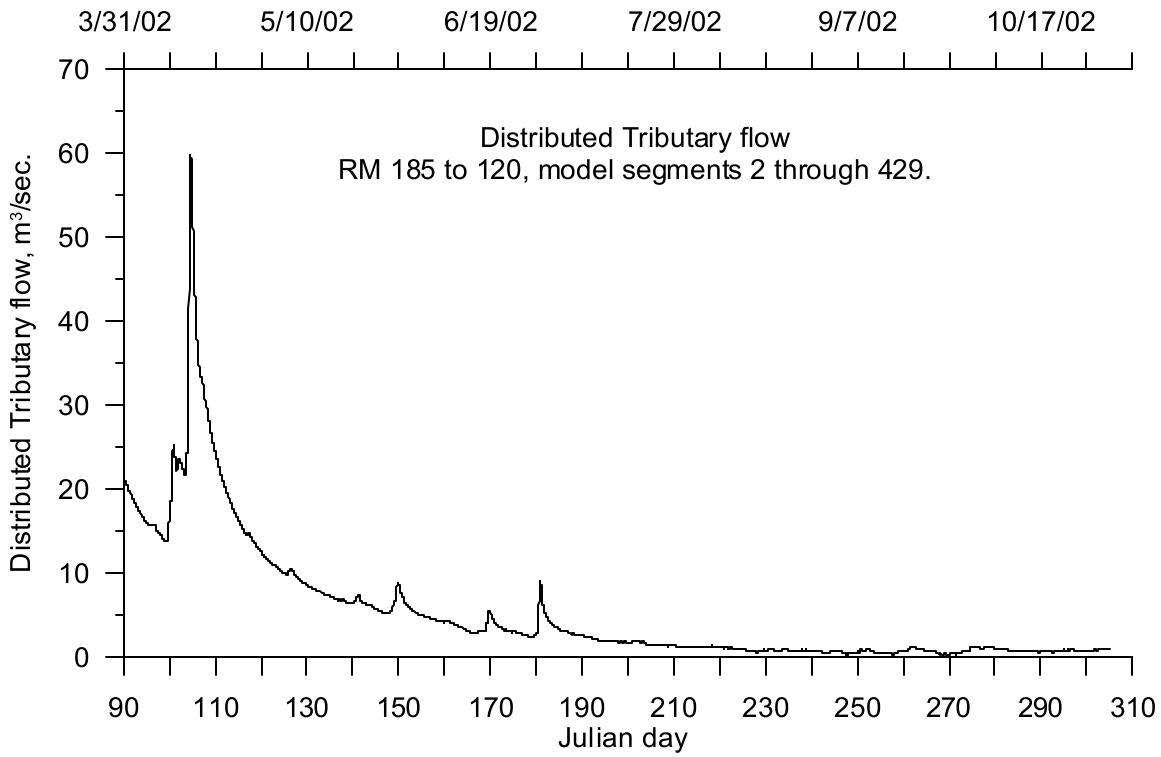


**Figure 315. Upper Willamette River model total distributed inflow from RM 185 - 120 (Branches 1 to 8), 2002**

## Temperature Data

Distributed tributary temperature values were taken to be those of the upstream tributary. Table 34 summarizes the temperature source for each branch. Temperature sources for branches 9 through 13 were included for completeness. Calibration flows utilize these temperatures.

**Table 34. Distributed tributary temperature data sources**

| Branch | Upstream RM | Upstream Model Segment | Temperature Source |
|---|---|---|---|
| 1 | 184.4 | 2 | Willamette River at Eugene |
| 2 | 181.6 | 22 | Willamette River at Eugene |
| 3 | 177.1 | 53 | Willamette River at Eugene |
| 4 | 174.8 | 71 | McKenzie River |
| 5 | 161.4 | 159 | McKenzie River |
| 6 | 155.0 | 202 | McKenzie River |
| 7 | 149.0 | 243 | Long Tom River |
| 8 | 127.6 | 382 | Mary's River |
| 9 | 120.1 | 432 | Calapooia River |
| 10 | 118.0 | 448 | Calapooia River |
| 11 | 108.2 | 514 | Santiam R |
| 12 | 102.1 | 555 | Santiam R |
| 13 | 96.2 | 595 | Rickreall Cr. |

## *Point Sources*

The Upper Willamette River model has seven point sources in the system. The discharge flow and temperature were compiled by ODEQ and consisted of data for the point sources and monthly monitoring reports. This dischargers were selected based on the magnitude of the discharge flow, and represent the larger wastewater facilities and pulp and paper mills. Figure 316 shows the point source locations along the Upper Willamette River. Table 35 lists the point source river mile and model segment location.

The point sources Halsey Fort James and Pope Talbot share an effluent pipe. These sources were incorporated into the Upper Willamette River model as separate tributaries at the same location.

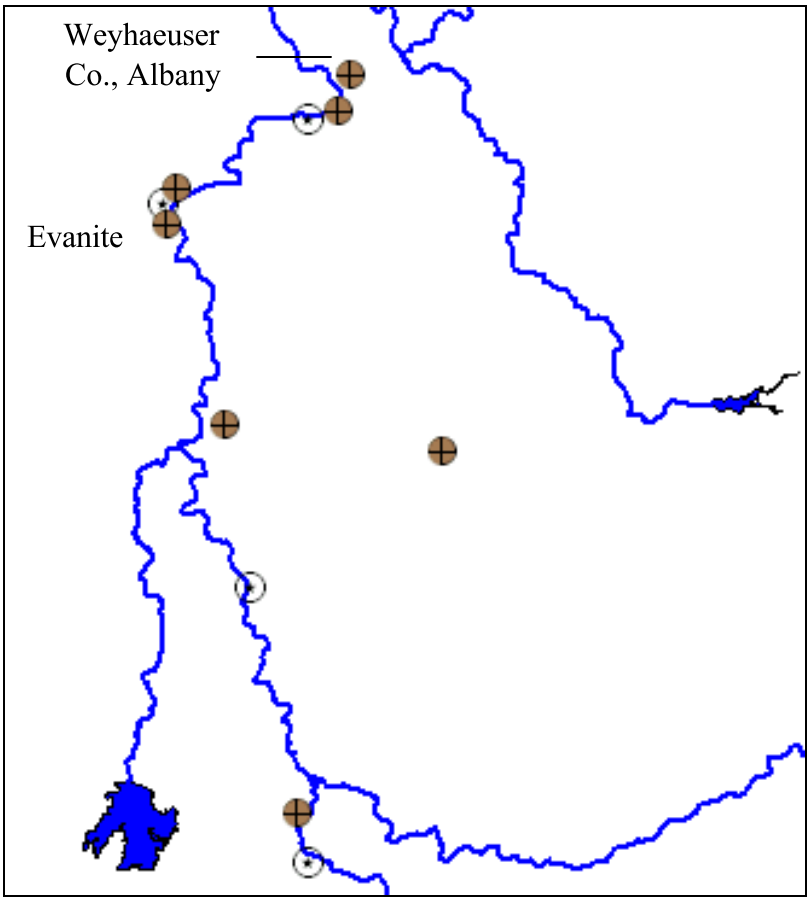


**Figure 316. Upper Willamette River point sources locations**

**Table 35. Upper Willamette point source locations**

| Point Source | Model Segment | Willamette RM |
|---|---|---|
| Eugene WWTP | 46 | 177.9 |
| Halsey Fort James | 252 | 147.6 |
| Pope Talbot | 252 | 147.6 |
| Evanite | 347 | 132.8 |
| Corvallis WWTP | 358 | 131.0 |
| Albany WWTP | 444 | 118.4 |

| Point Source | Model Segment | Willamette RM |
|---|---|---|
| Weyco Albany | 454 | 117.2 |

## Hydrodynamic Data

The discharge from the Eugene WWTP was typically around 1 $m^3$/sec and did not exceed 2.5 $m^3$/sec. Discharge from the other individual sources was less than 1 $m^3$/sec. The magnitude of the daily average discharge was largely steady, although daily variability was much higher.

### Year 2001

The dates in 2001 over which flow and temperature data were available are shown in Table 36.

**Table 36. Upper Willamette River model point sources flow data time periods, 2001**

| Point Source | Start Date | End Date |
|---|---|---|
| Eugene WWTP | 05/10/2001 | 11/02/2001 |
| Halsey Fort James | 04/01/2001 | 12/31/2001 |
| Pope Talbot | 04/01/2001 | 12/31/2001 |
| Evanite | 04/01/2001 | 11/30/2001 |
| Corvallis WWTP | 05/15/2001 | 10/31/2001 |
| Albany WWTP | 01/01/2001 | 12/31/2001 |
| Weyco Albany | 04/01/2001 | 12/31/2001 |

The Eugene WWTP discharge is shown in Figure 317. There were no data before May 10, 2001 which was prior to the calibration period.

The Halsey Fort James facility discharge for 2001 is shown in Figure 318. The 2001 flow from the Pope Talbot facility is shown in Figure 319, which discharged to the same location as the Halsey Fort James facility.

The 2001 flow from the Evanite facility is shown in Figure 320.

The City of Corvallis WWTP discharge is shown in Figure 321. There were no data before May 10, 2001.

The 2001 flow from the Albany WWTP is shown in Figure 322. The 2001 flow from the Weyhaeuser Co. Albany facility is shown in Figure 323.

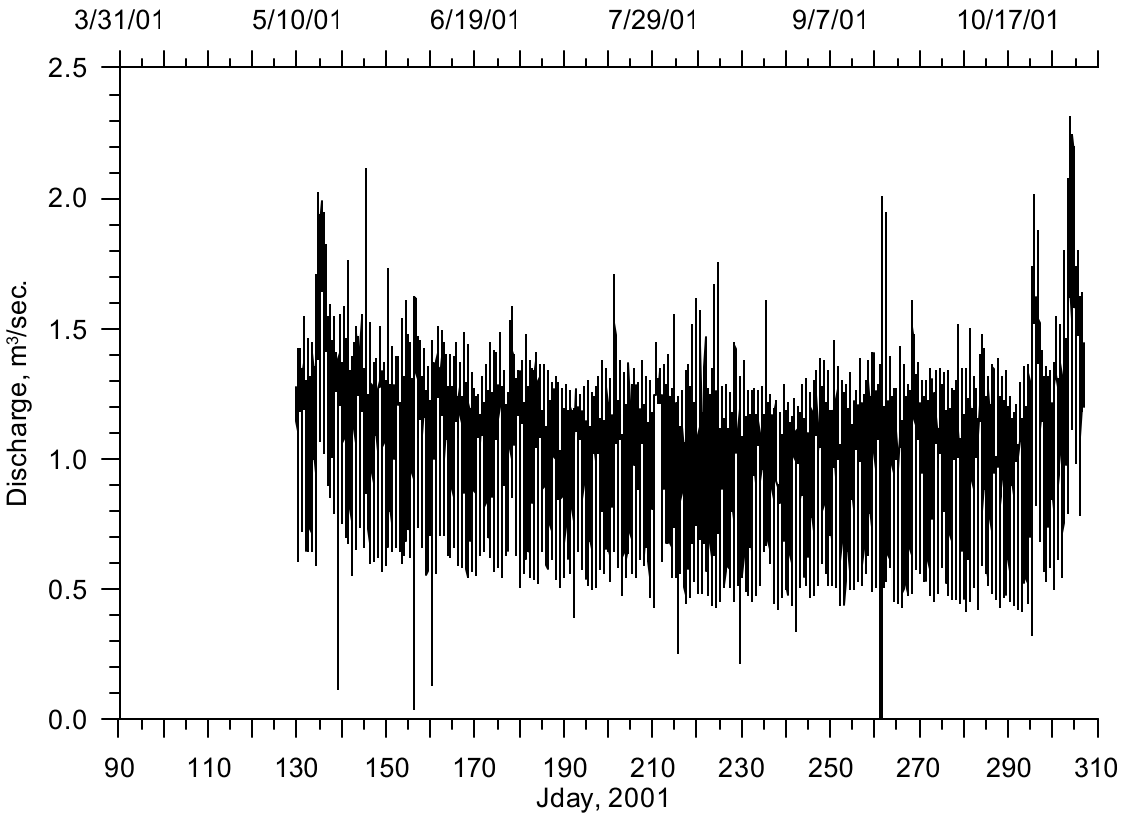


**Figure 317. Eugene WWTP discharge, 2001**

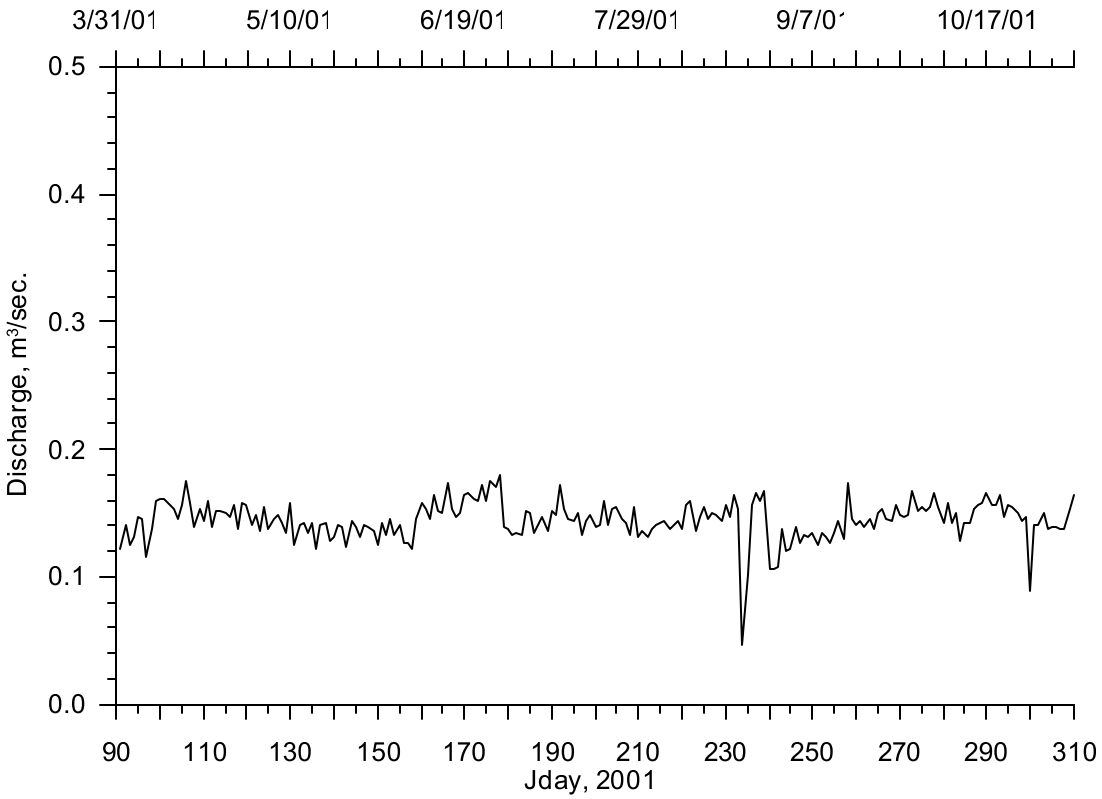


**Figure 318. Halsey Fort James discharge, 2001**

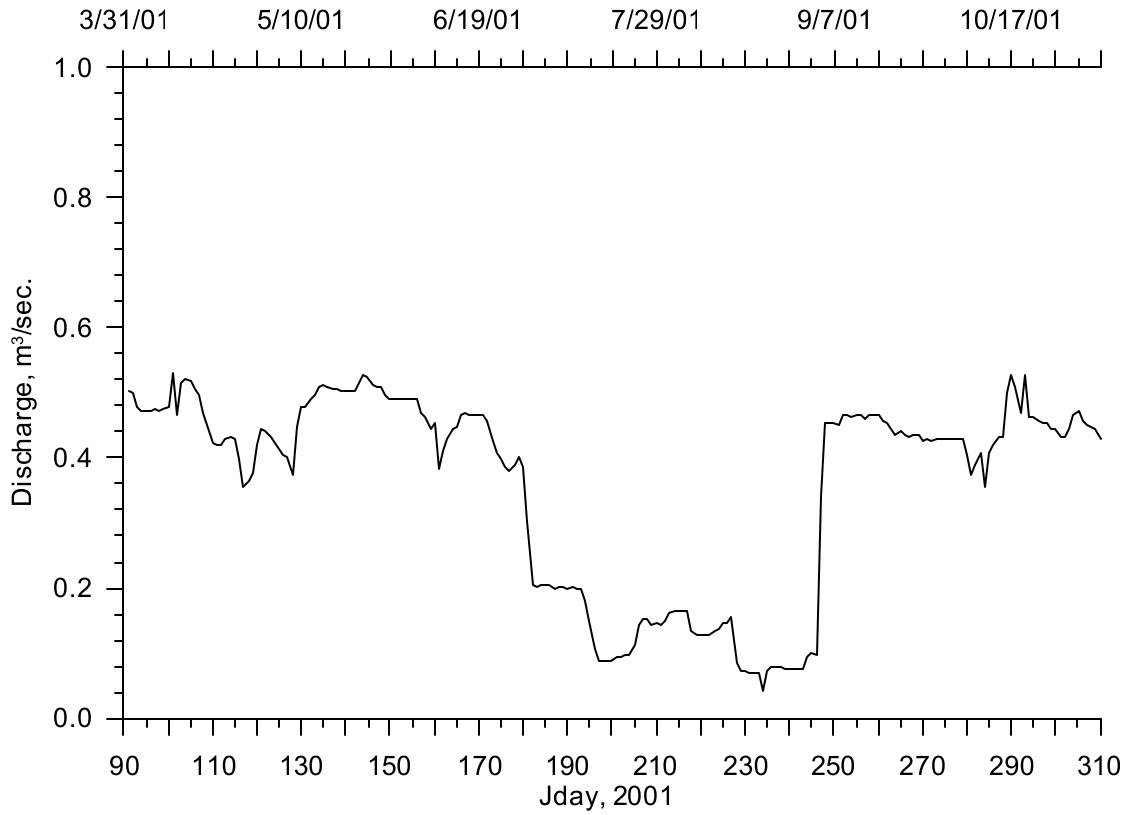


**Figure 319. Pope Talbot discharge, 2001**

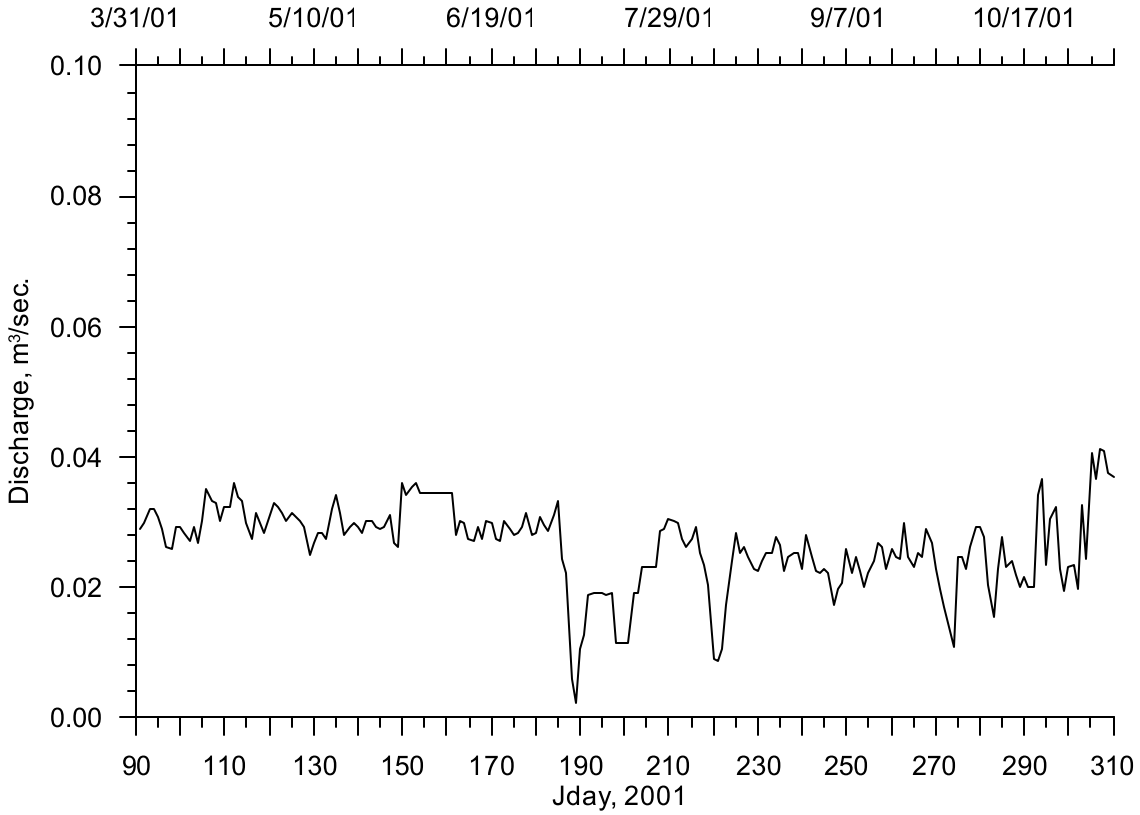


**Figure 320. Evanite discharge, 2001**

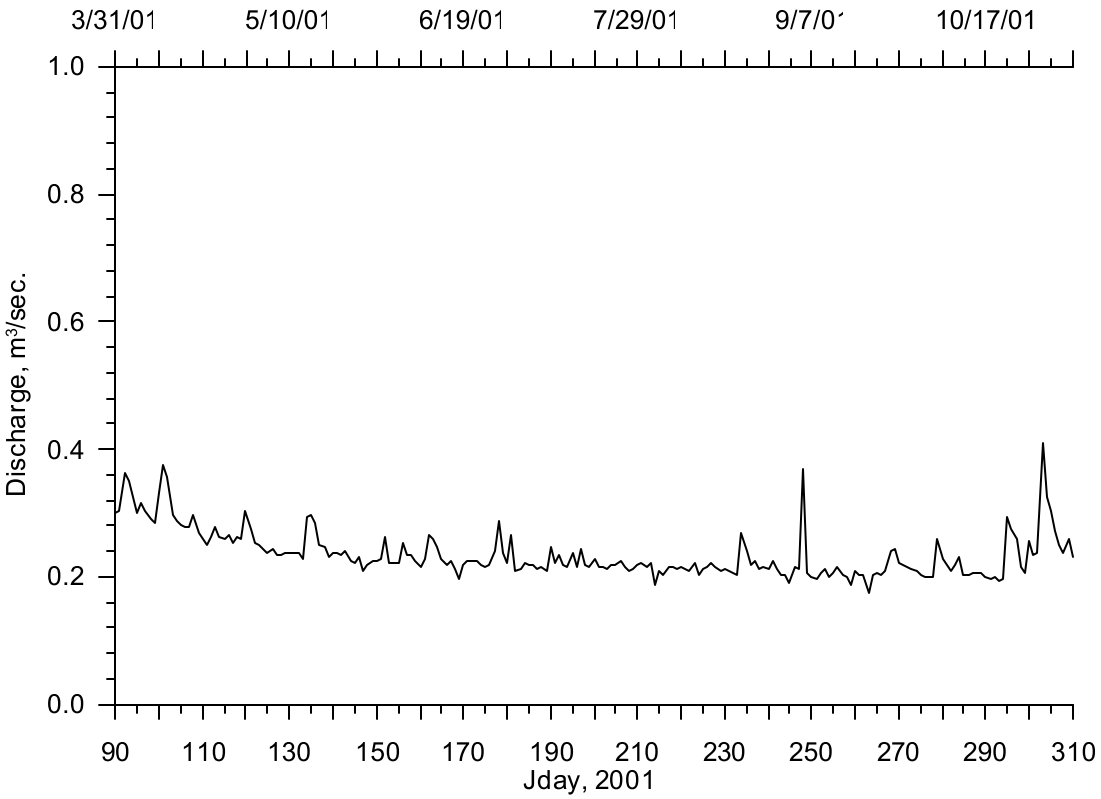


**Figure 321. Albany WWTP discharge, 2001**

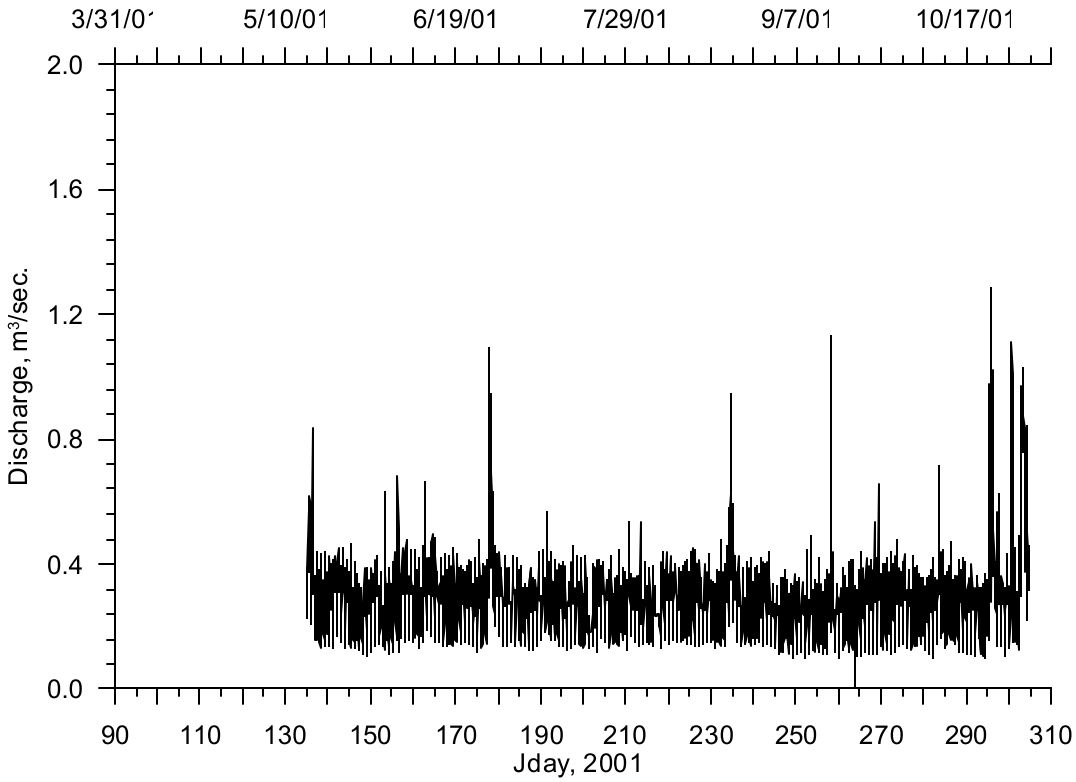


**Figure 322. Corvallis WWTP discharge, 2001**

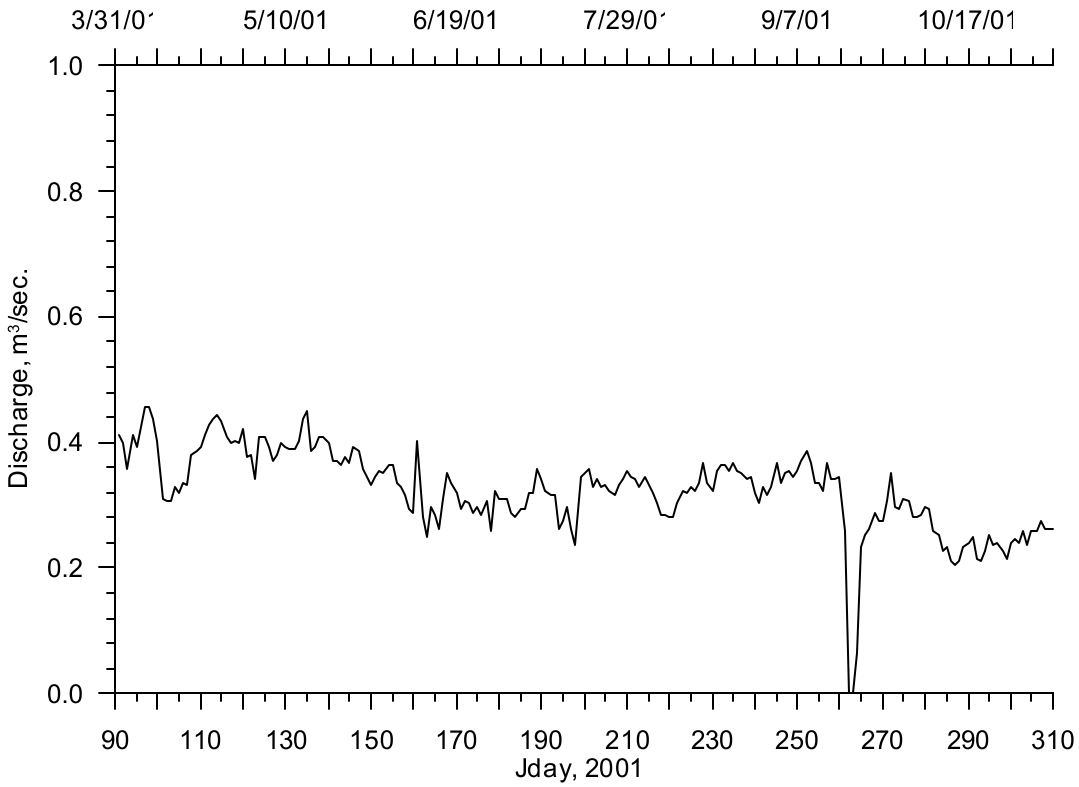


**Figure 323. Weyhaeuser Co. Albany discharge, 2001**

## Year 2002

The dates in 2002 over which flow and temperature data were available are shown in Table 37. Flow and temperature data were unavailable for the Corvallis WWTP and Albany WWTP. The 2001 data were repeated.

**Table 37. Upper Willamette River model point sources flow data time periods, 2002**

| Point Source | Start Date | End Date |
|---|---|---|
| Eugene WWTP | 05/01/2002 | 10/31/2002 |
| Halsey Fort James | 01/01/2002 | 11/30/2002 |
| Pope Talbot | 01/01/2002 | 12/31/2002 |
| Evanite | 04/01/2002 | 11/30/2002 |
| Corvallis WWTP | 05/15/2002* | 10/31/2002* |
| Albany WWTP | 01/01/2002* | 12/31/2002* |
| Weyco Albany | 01/01/2002 | 12/31/2002 |
| *There was no 2002 data so 2001 data was used. | | |

The Eugene WWTP flow for 2002 is shown in Figure 324. There were no flow data before May 1, 2002. To extend the data, all previous flow rates were set to the value of the first data point on May 1, 2002.

The 2002 flow from the Halsey Fort James facility is shown in Figure 325. The 2002 flow from the Pope Talbot facility is shown in Figure 326.

The 2002 flow from the Evanite facility is shown in Figure 327. The 2002 flow from the Weyhaeuser Co. Albany facility is shown in Figure 328.

There was no discharge data for the City of Corvallis WWTP flow for 2002 so the 2001 data set was used. The flow time series for the treatment plant is shown in Figure 322. There were no flow data before May 15, 2001. To extend the data, all previous flows were set to the value of the first data point on May 15, 2001.

Similarly there were no 2002 flow data for the City of Albany WWTP so 2001 data were used. Figure 321 shows the 2001 flow time series data used for 2002.

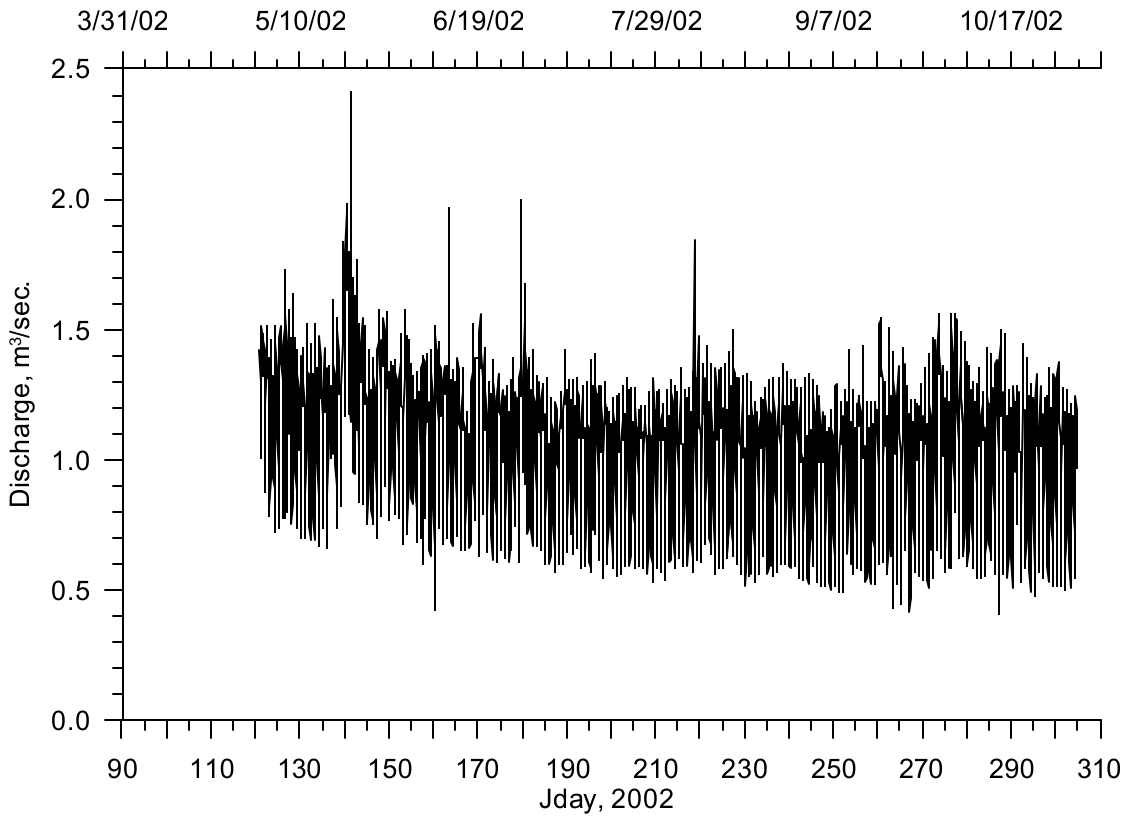


**Figure 324. Eugene WWTP discharge, 2002**

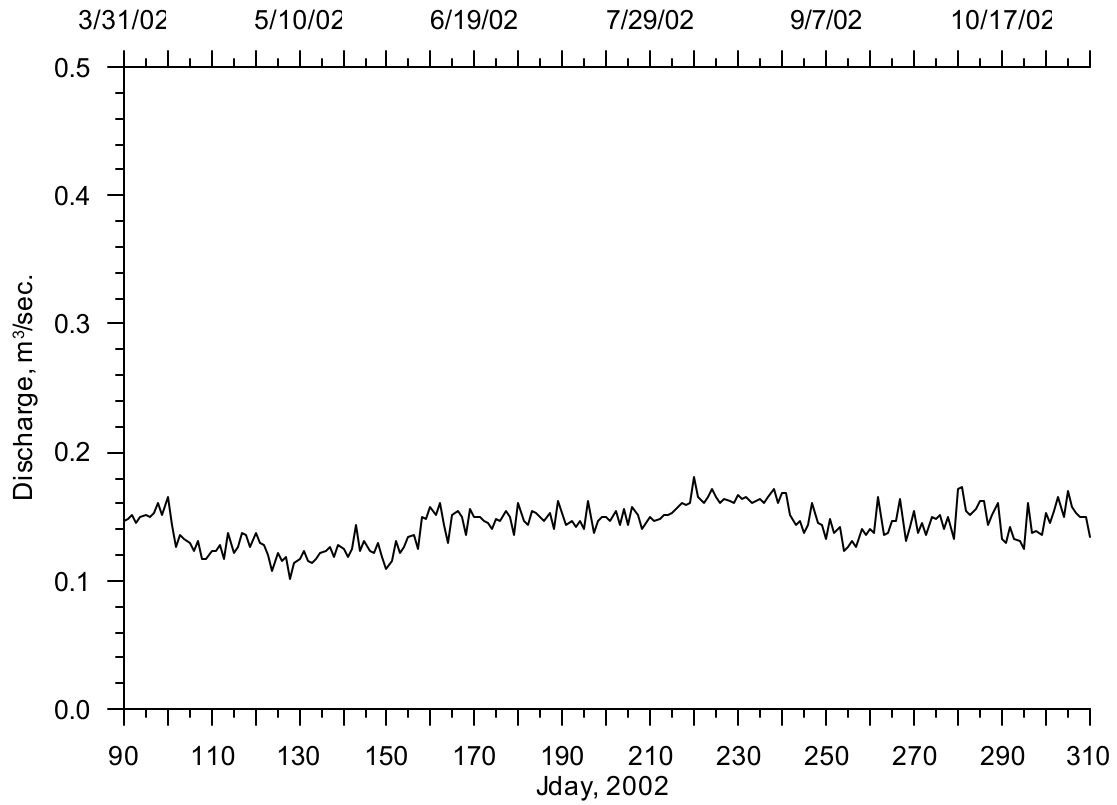


**Figure 325. Halsey Fort James discharge, 2002**

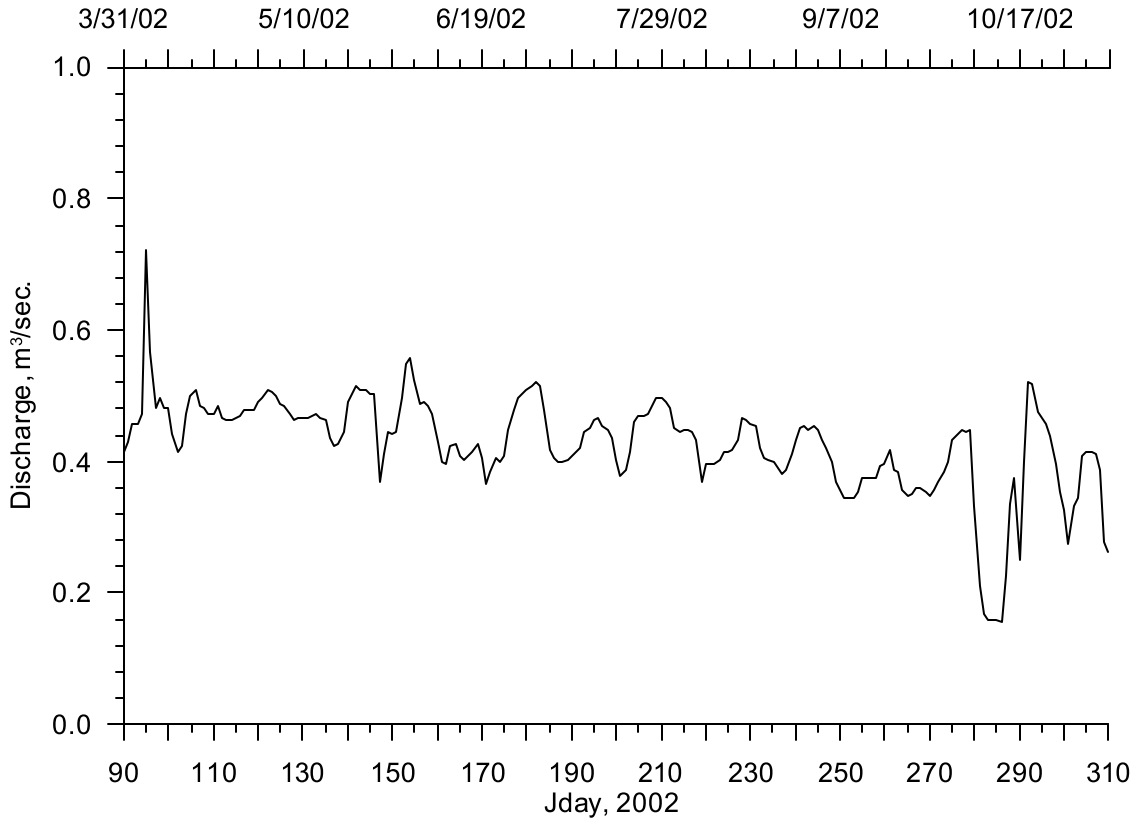


**Figure 326. Pope Talbot discharge, 2002**

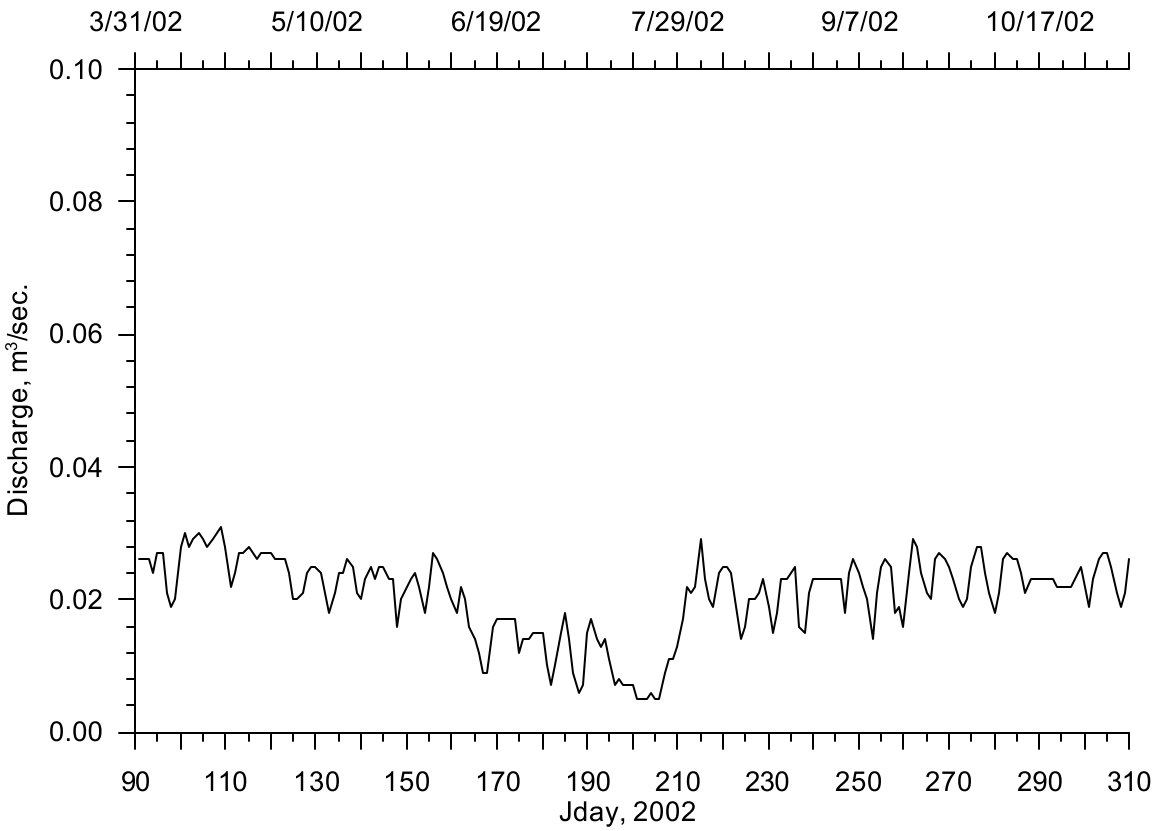


**Figure 327. Evanite discharge, 2002**

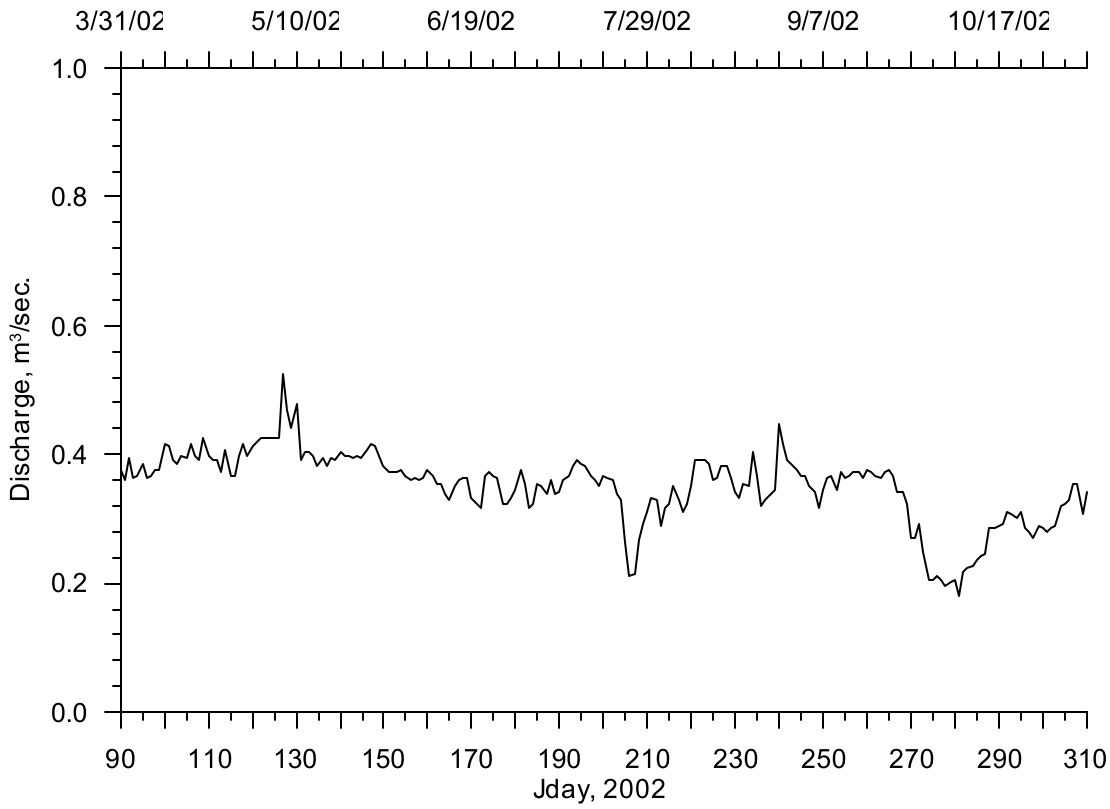


**Figure 328. Weyhaeuser Co. Albany discharge, 2002**

## Temperature Data

### Year 2001

The dates in 2001 over which flow and temperature data were available are shown in Table 38.

**Table 38. Upper Willamette River model point sources temperature data time periods, 2001**

| Point Source | Start Date | End Date |
|---|---|---|
| Eugene WWTP | 05/10/2001 | 11/02/2001 |
| Halsey Fort James | 04/01/2001 | 12/31/2001 |
| Pope Talbot | 04/01/2001 | 12/31/2001 |
| Evanite | 04/01/2001 | 11/30/2001 |
| Corvallis WWTP | 05/15/2001 | 10/31/2001 |
| Albany WWTP | 01/01/2001 | 12/31/2001 |
| Weyco Albany | 04/01/2001 | 12/31/2001 |

The City of Eugene WWTP discharge temperatures are shown in Figure 329. There were no flow data available before May 10, 2001.

The 2001 temperature data from the Halsey Fort James facility are shown in Figure 330. The 2001 temperature data from the Pope Talbot facility are shown in Figure 331. The 2001 temperature data from the Evanite facility are shown in Figure 332.

The City of Corvallis WWTP discharge temperatures are shown in Figure 334. There were no flow data before May 15, 2001.

The 2001 temperature data from the Albany WWTP are shown in Figure 333.

The 2001 temperature data from Weyhaeuser Co. Albany facility are shown in Figure 335. The discharge temperatures were warmer in the summer than the spring or fall.

In general, the summer discharge temperatures were within a couple degrees of the Willamette River temperature except for the Halsey Fort James and Weyhaeuser Co. Albany sources, which were much warmer than the river.

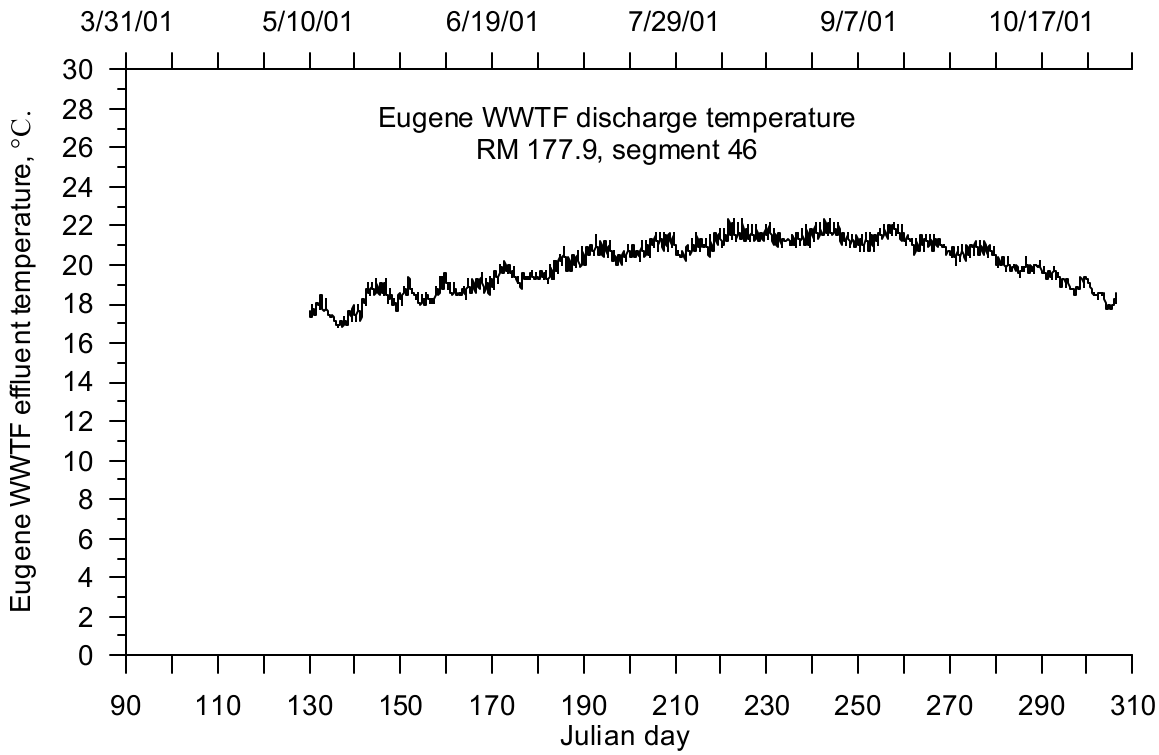


**Figure 329. Eugene WWTP effluent temperature, 2001**

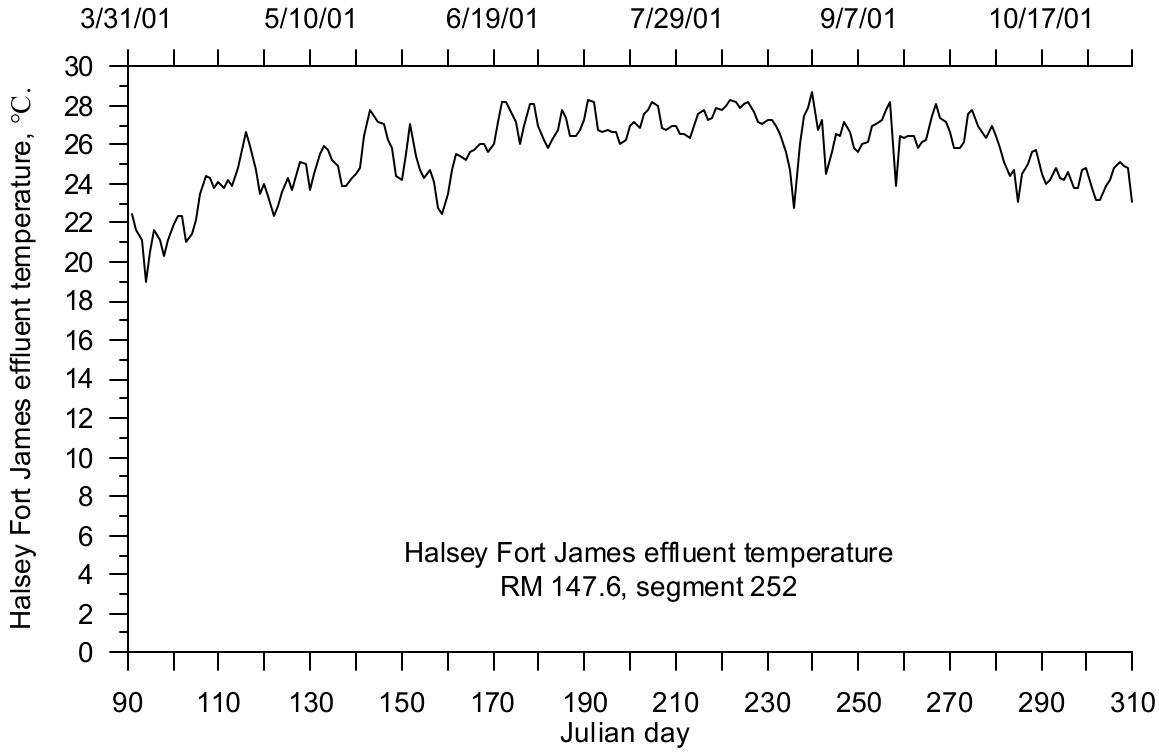


**Figure 330. Halsey Fort James effluent temperature, 2001**

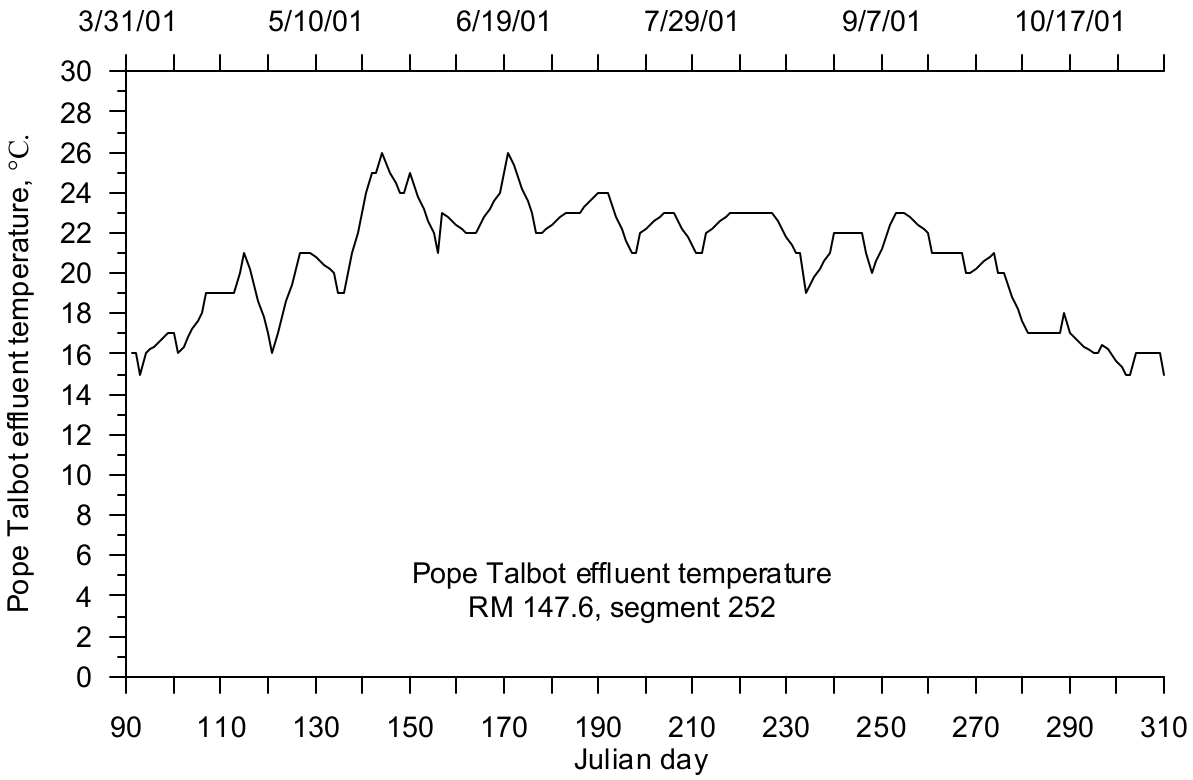


**Figure 331. Pope Talbot effluent temperature, 2001**

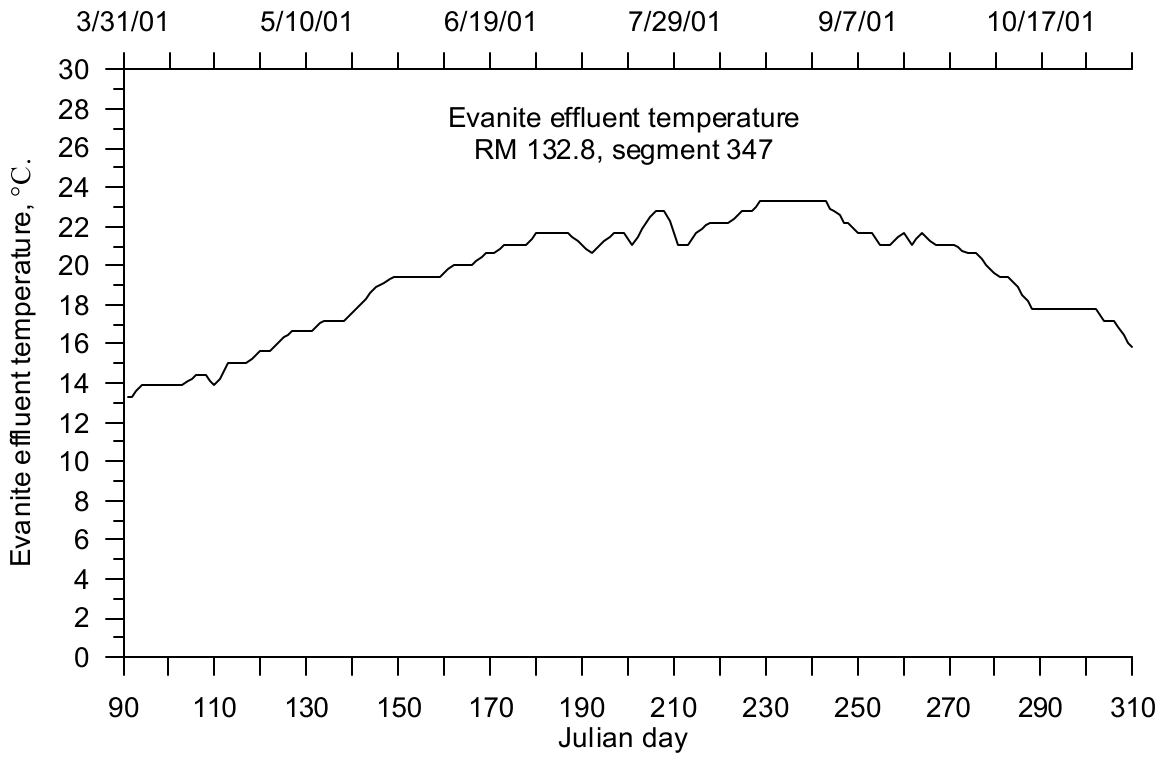


**Figure 332. Evanite effluent temperature, 2001**

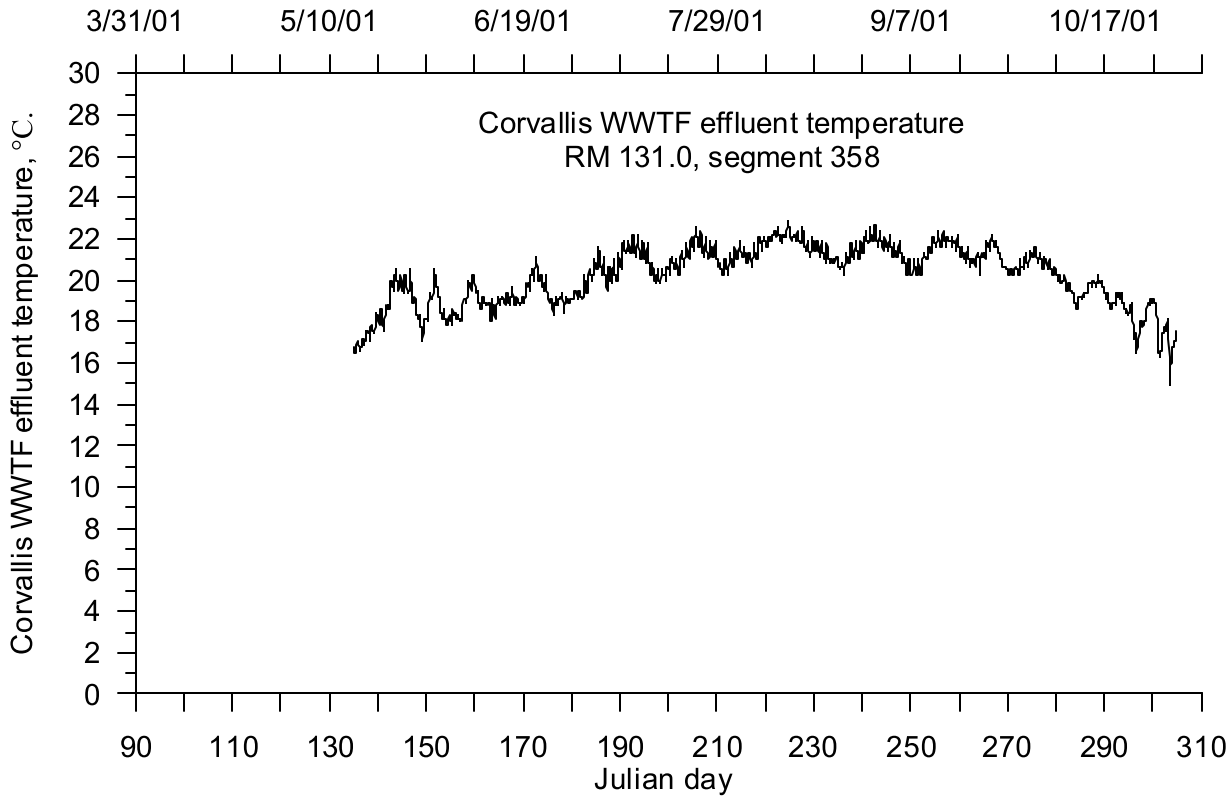


**Figure 333. Corvallis WWTP effluent temperature, 2001**

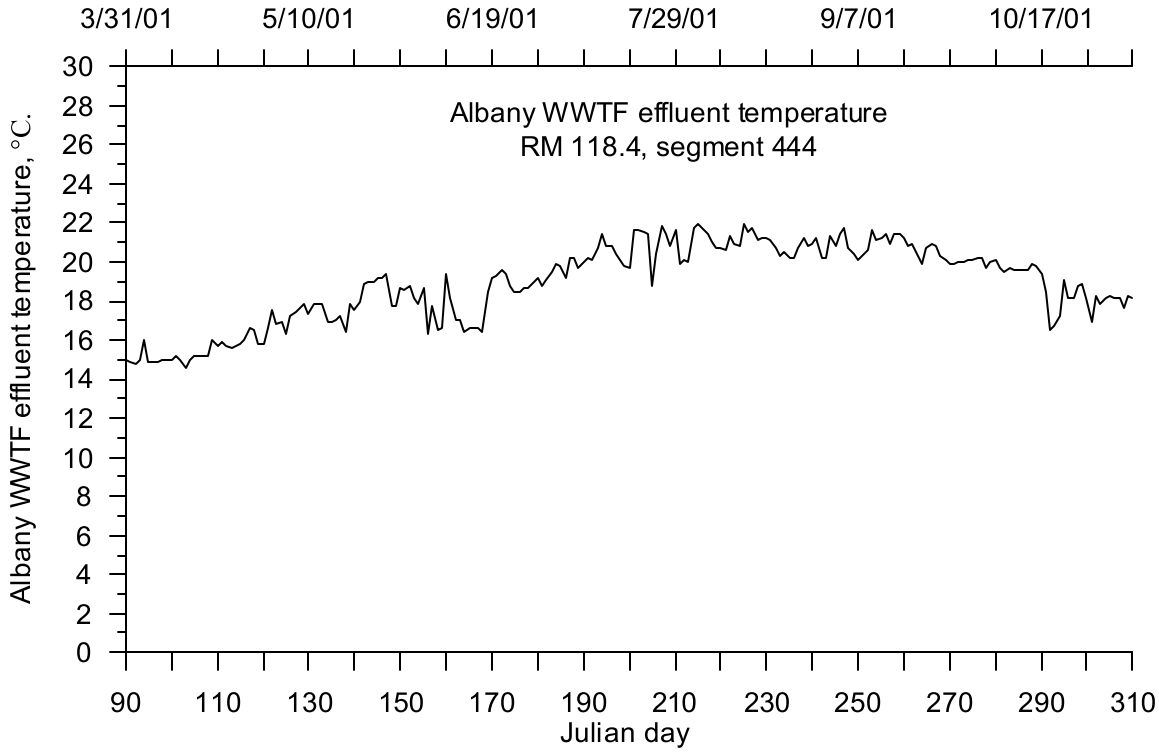


**Figure 334. Albany WWTP effluent temperature, 2001**

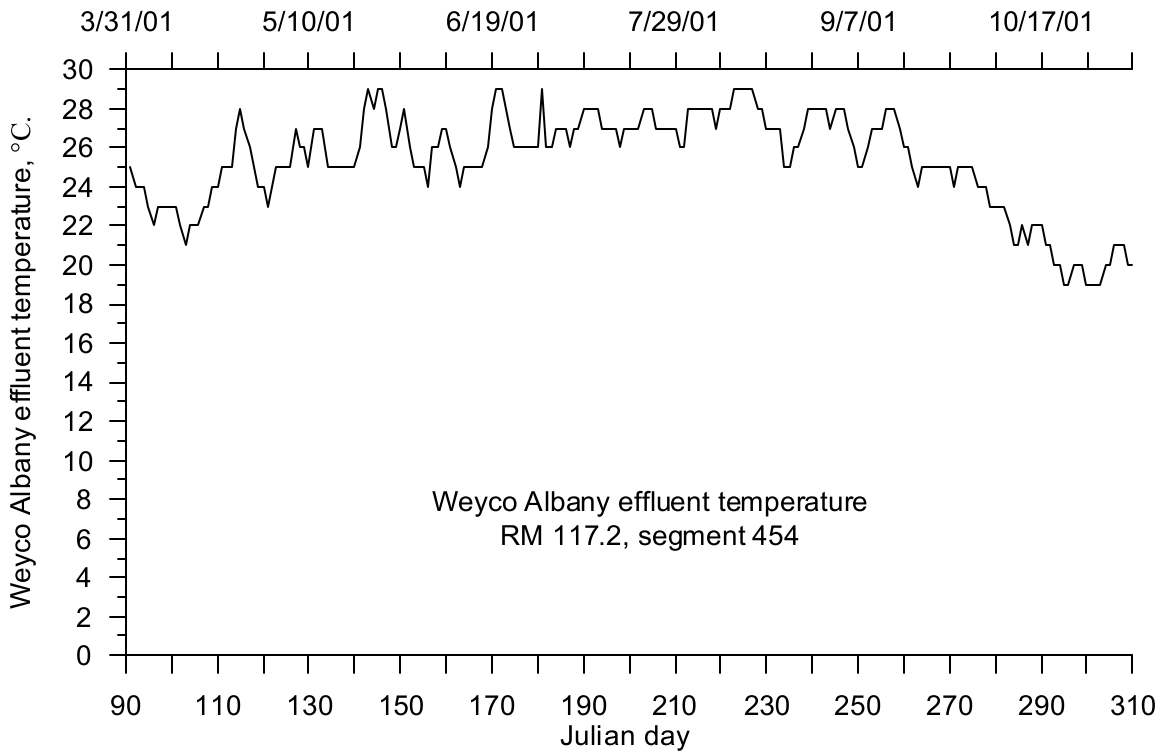


**Figure 335. Weyhaeuser Co. Albany effluent temperature, 2001**

## Year 2002

The dates in 2002 over which flow and temperature data were available are shown in Table 39. Flow and temperature data were unavailable for the Corvallis WWTP and Albany WWTP. The 2001 data were repeated.

**Table 39. Upper Willamette River model point sources temperature data time periods, 2002**

| Point Source | Start Date | End Date |
|---|---|---|
| Eugene WWTP | 05/01/2002 | 10/31/2002 |
| Halsey Fort James | 01/01/2002 | 11/30/2002 |
| Pope Talbot | 01/01/2002 | 12/31/2002 |
| Evanite | 04/01/2002 | 11/30/2002 |
| Corvallis WWTP | 05/15/2002* | 10/31/2002* |
| Albany WWTP | 01/01/2002* | 12/31/2002* |
| Weyco Albany | 01/01/2002 | 12/31/2002 |
| *2001 data was used since there was no 2002 data | | |

The City of Eugene WWTP discharge temperatures are shown in Figure 336. There were no temperature data before May 1, 2002. To extend the data, all previous temperatures were set to the value of the first data point on May 1, 2002.

The 2002 temperature data from the Halsey Fort James facility are shown in Figure 337. The 2002 temperature data from the Pope Talbot facility are shown in Figure 338. The 2002 temperature data

from the Evanite facility are shown in Figure 339. The 2002 temperature data from the Weyhaeuser Co. Albany facility are shown in Figure 340.

There were no discharge temperature data for the City of Corvallis WWTP for 2002 so the 2001 data set was used. The temperature time series for the treatment plant is shown in Figure 333.

Similarly there were no 2002 temperature data for the City of Albany WWTP so 2001 data were used. Figure 334 shows the 2001 temperature time series data used for 2002.

The discharge temperatures were warmer in the summer than the spring or fall. In general, the summer discharge temperatures were within a couple degrees of the Willamette River temperature except for the Halsey Fort James and Evanite sources, which were much warmer than the river.

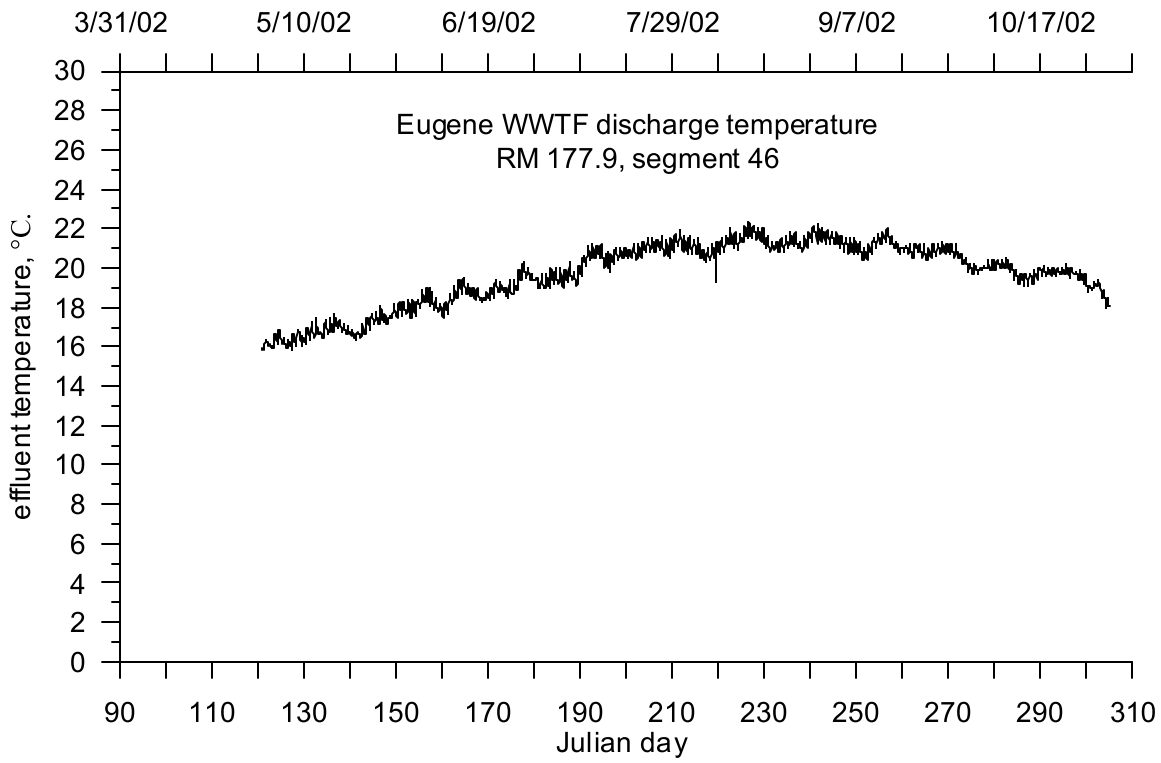


**Figure 336. Eugene WWTP effluent temperature, 2002**

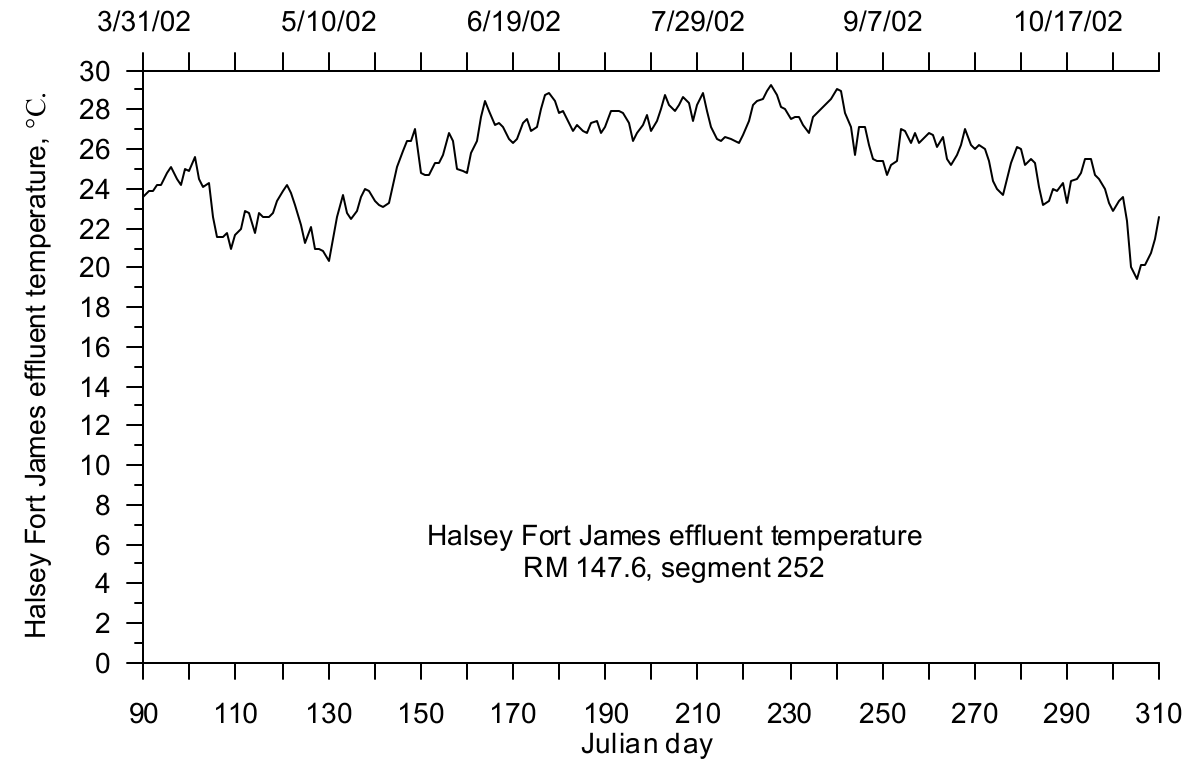


**Figure 337. Halsey Fort James effluent temperature, 2002**

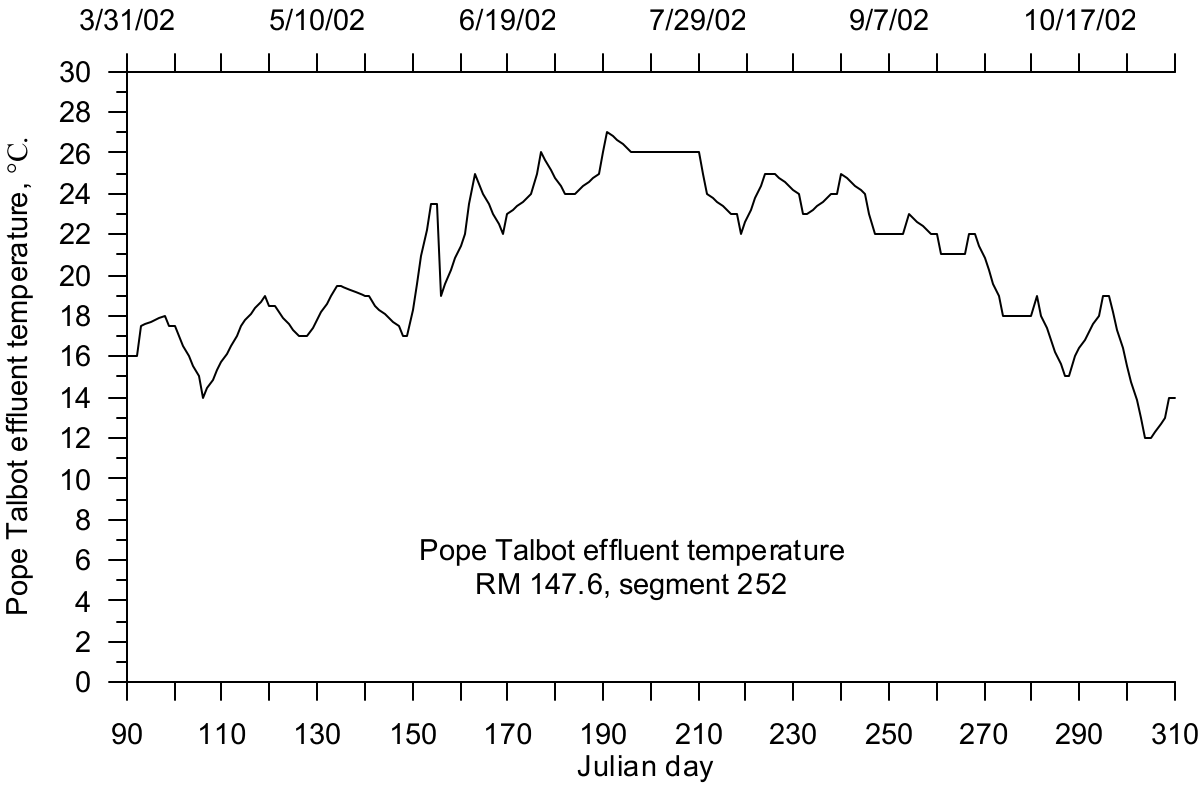


**Figure 338. Pope Talbot effluent temperature, 2002**

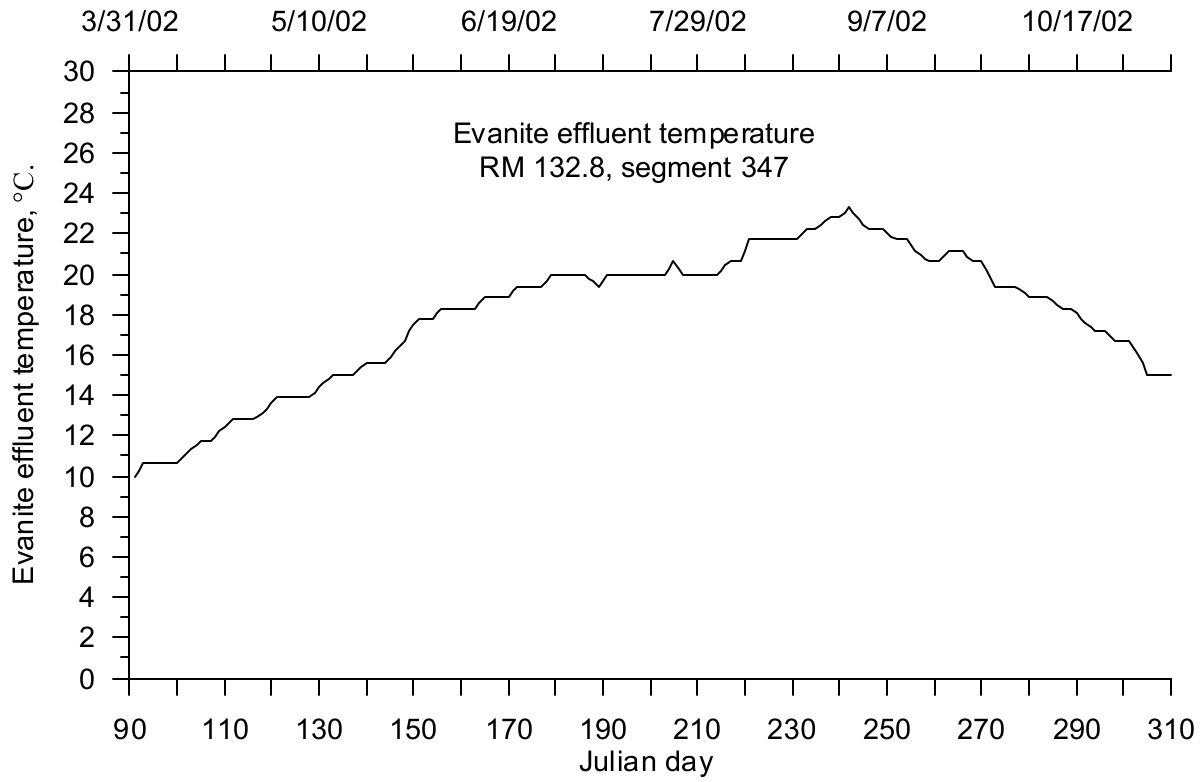


**Figure 339. Evanite effluent temperature, 2002**

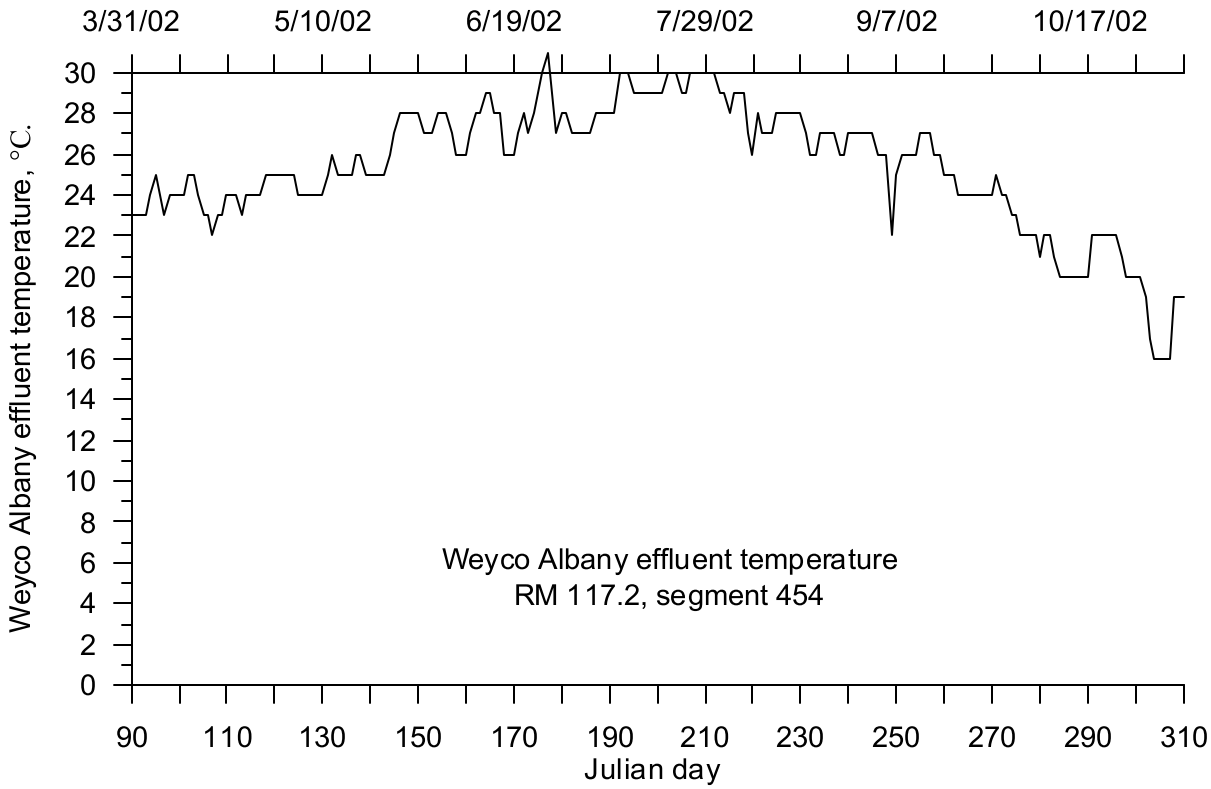


**Figure 340. Weyhaeuser Co. Albany effluent temperature, 2002**

## *Shading*

CE-QUAL-W2 incorporates both topographic and vegetative shade in the model. Topographic characteristics include the steepest inclination angle in 18 directions around a model segment. The vegetative characteristics consist of tree top elevation, distance between the river channel centerline and the controlling vegetation, and the vegetation density in summer and winter. Vegetation characteristics for both banks of the river were provided.

The vegetation and topographic characteristics for the Upper Willamette River model were developed using geographic information system (GIS) data supplied by the Oregon Department of Environmental Quality (ODEQ). The data consisted of thalweg points every 100 ft along the thalweg of the river. For each thalweg point, additional associated data were included: channel width, elevation, three topographic inclination angles, and nine vegetation compartments for each bank. Each vegetation compartment consisted of vegetation height, distance from stream bank, and density. A detailed analysis was performed to convert the ODEQ data into the shade variables for the CE-QUAL-W2 model. A detailed description of the shade analysis is shown in Appendix A.

The model employs two sets of shade reduction factors which can be used to represent summer and winter vegetation thickness. The step transition dates were April 1 for "leaf on" and October 1 for "leaf off." The tree top heights are shown for the left bank in Figure 341 and Figure 342, and for the right bank in Figure 343 and Figure 344. The tree top heights decrease moving downstream. The distance from the river centerline to the vegetative shade, also called the offset, are shown for the left bank in Figure 345 and Figure 346, and for the right bank in Figure 347 and Figure 348. The offset fairly was uniform and typically ranged from 40 to 60 m. The "leaf-on" shade reduction factors are shown for the left bank in Figure 349 and Figure 350, and for the right bank in Figure 351 and Figure 352. The shade reduction factors generally ranged from 0.5 to 0.85.

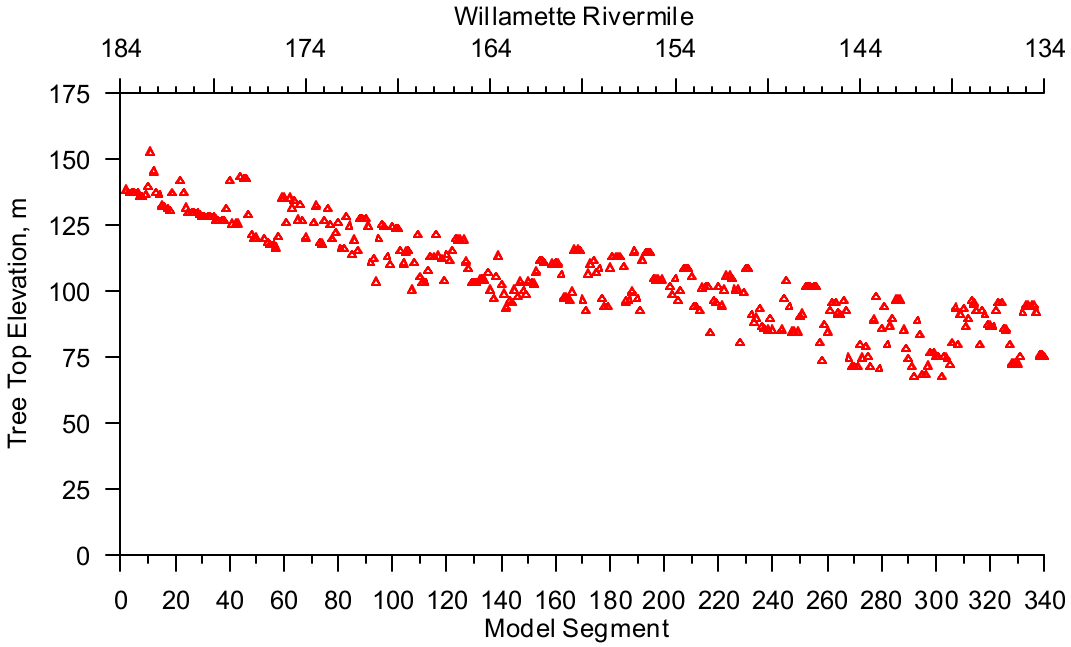


**Figure 341. Upper Willamette River Left Bank Tree Top Elevation, RM 184 to 134**

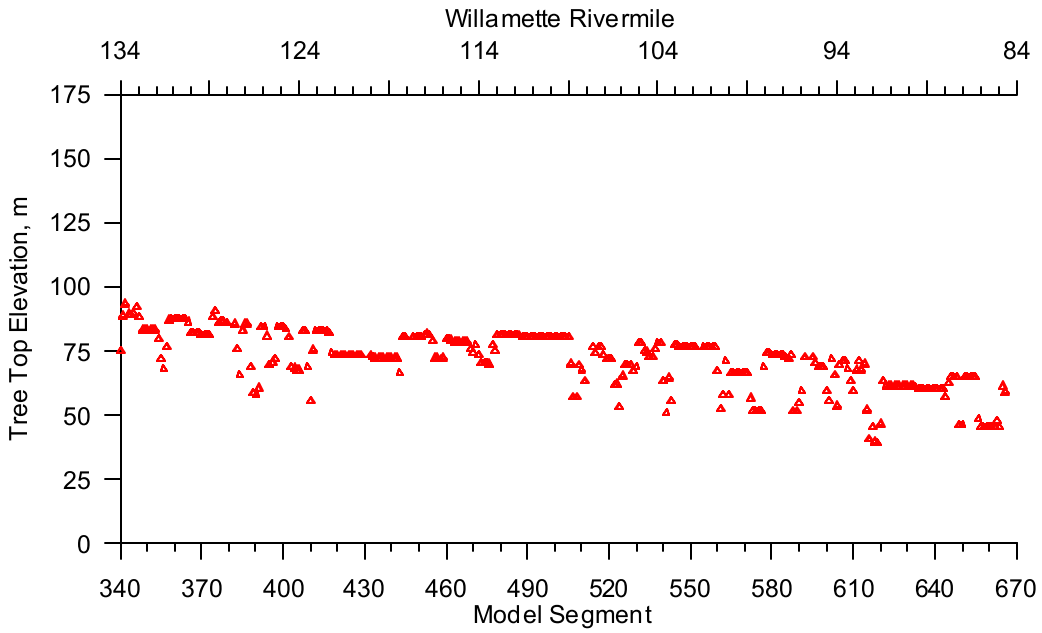


**Figure 342. Upper Willamette River Left Bank Tree Top Elevation, RM 134 to 85**

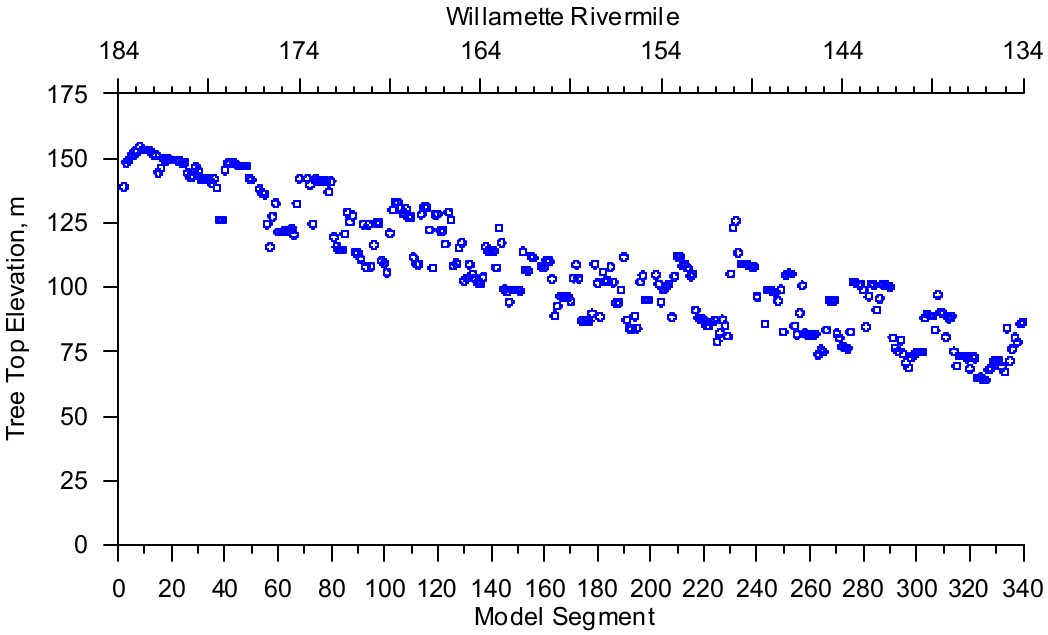


**Figure 343. Upper Willamette River Right Bank Tree Top Elevation, RM 184 to 134**

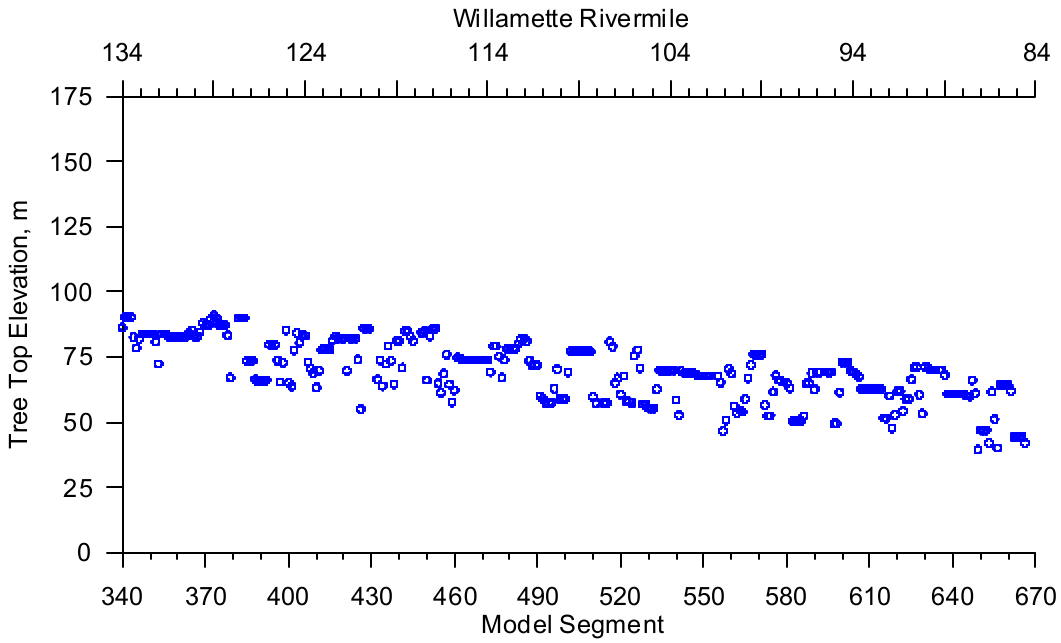


**Figure 344. Upper Willamette River Right Bank Tree Top Elevation, RM 134 to 85**

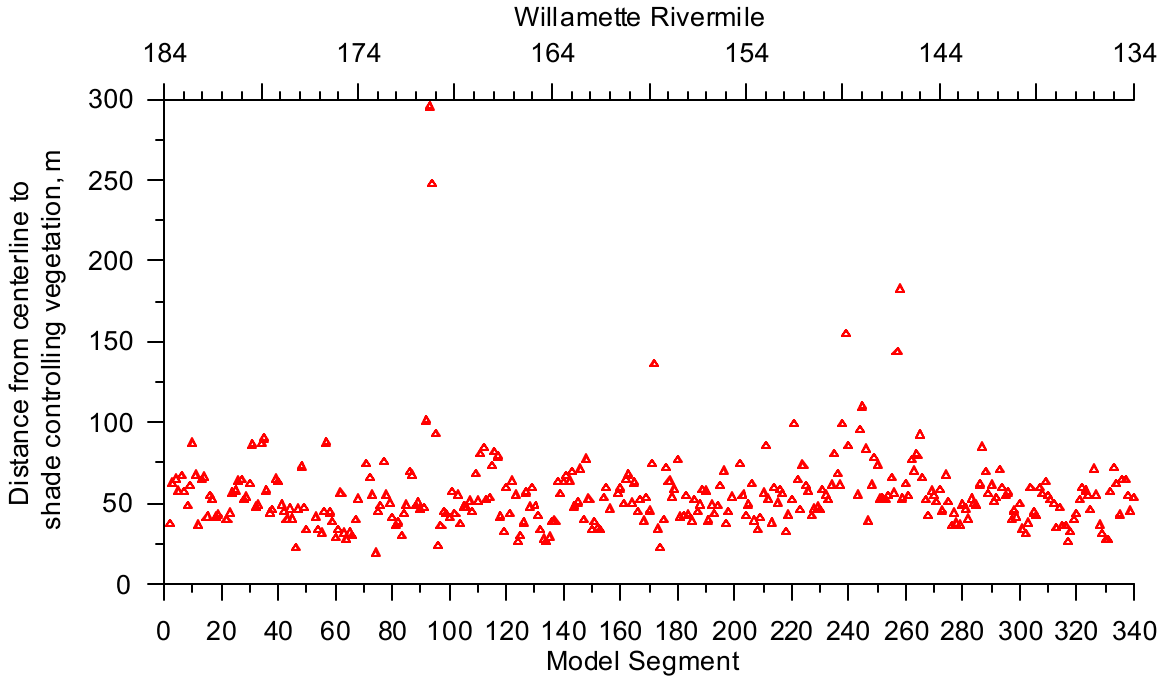


**Figure 345. Upper Willamette River Left Bank Vegetation Offset, RM 184 to 134**

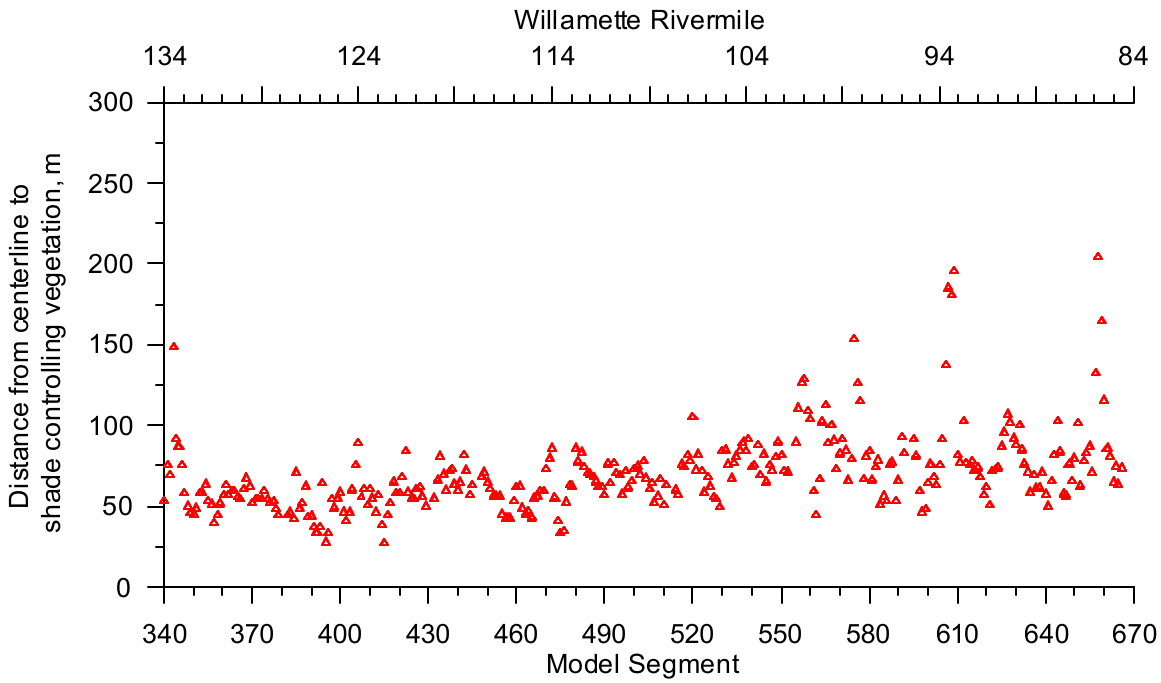


**Figure 346. Upper Willamette River Left Bank Vegetation Offset, RM 134 to 85**

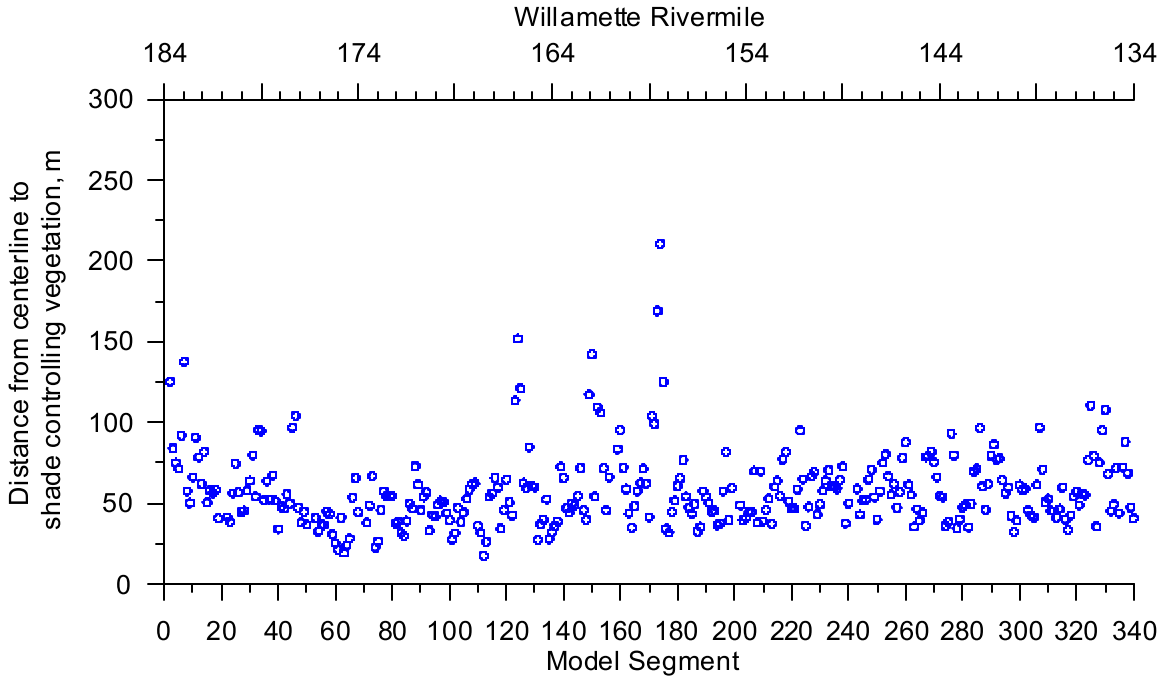


**Figure 347. Upper Willamette River Right Bank Vegetation Offset, RM 184 to 134**

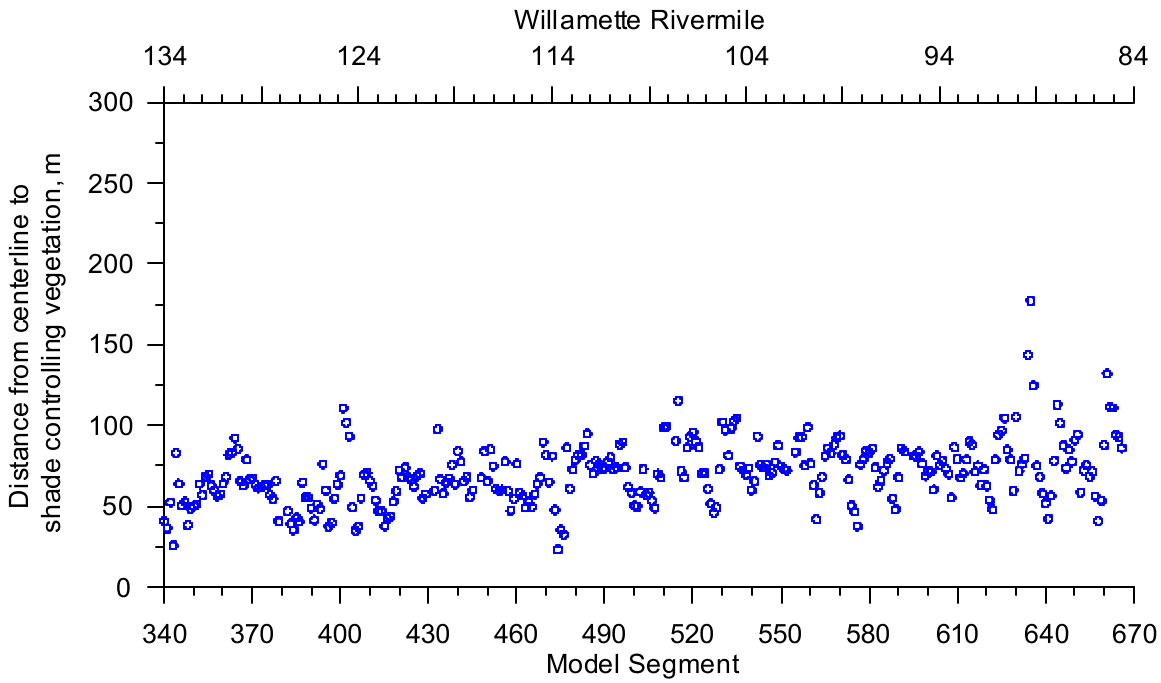


**Figure 348. Upper Willamette River Right Bank Vegetation Offset, RM 134 to 85**

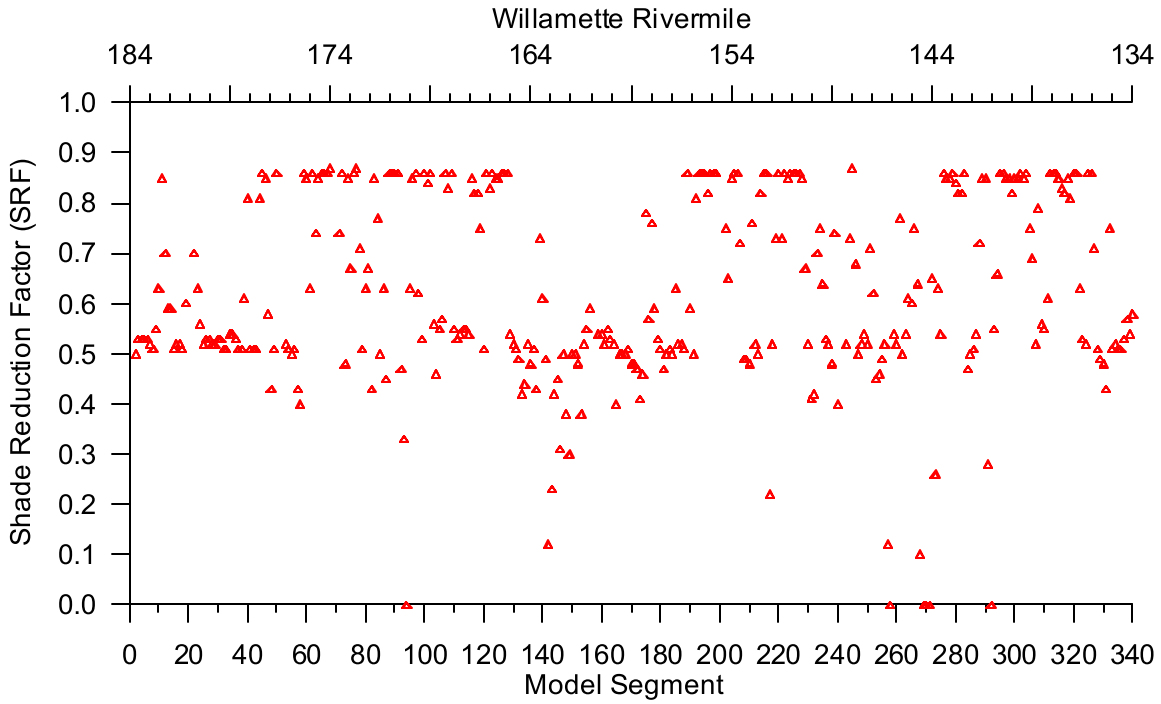


**Figure 349. Upper Willamette River Left Bank Shade Reduction Factor, RM 184 to 134**

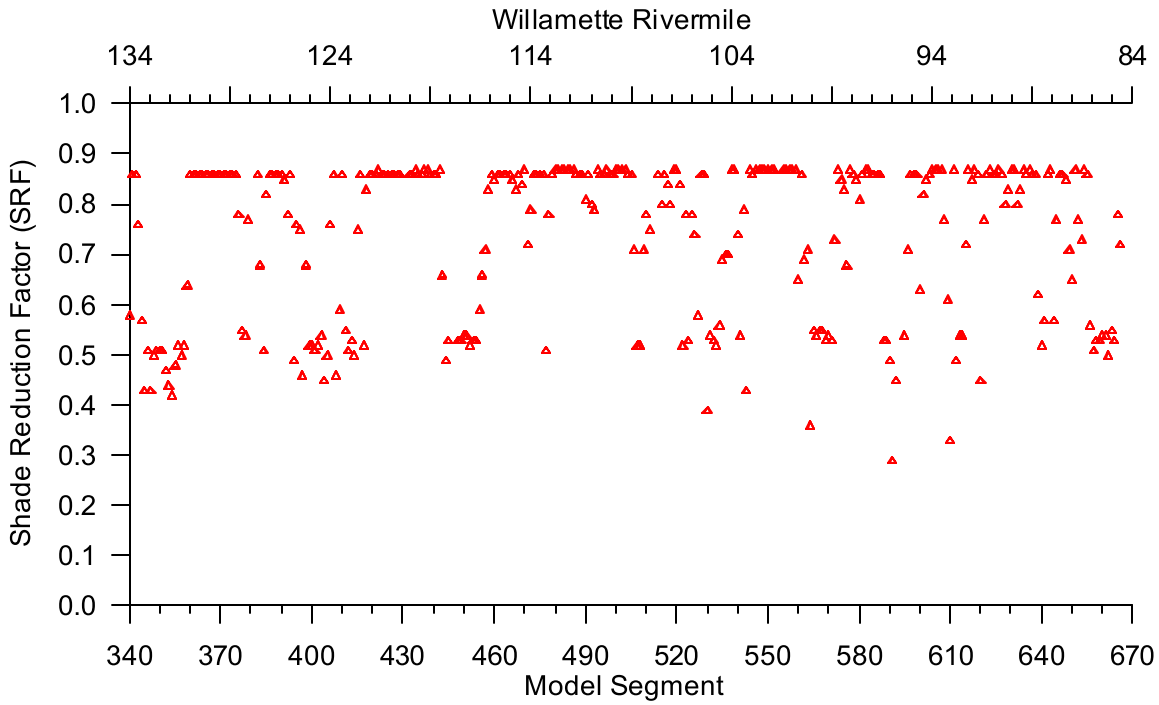


**Figure 350. Upper Willamette River Left Bank Shade Reduction Factor, RM 134 to 85**

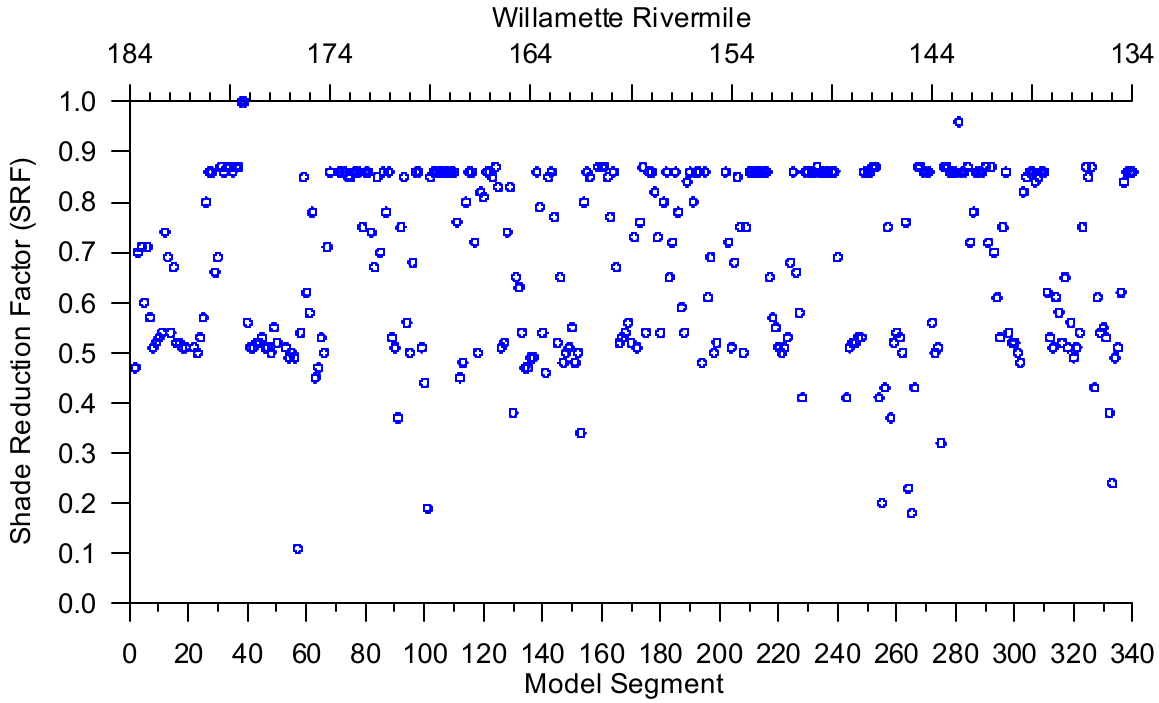


**Figure 351. Upper Willamette River Right Bank Shade Reduction Factor, RM 184 to 134**

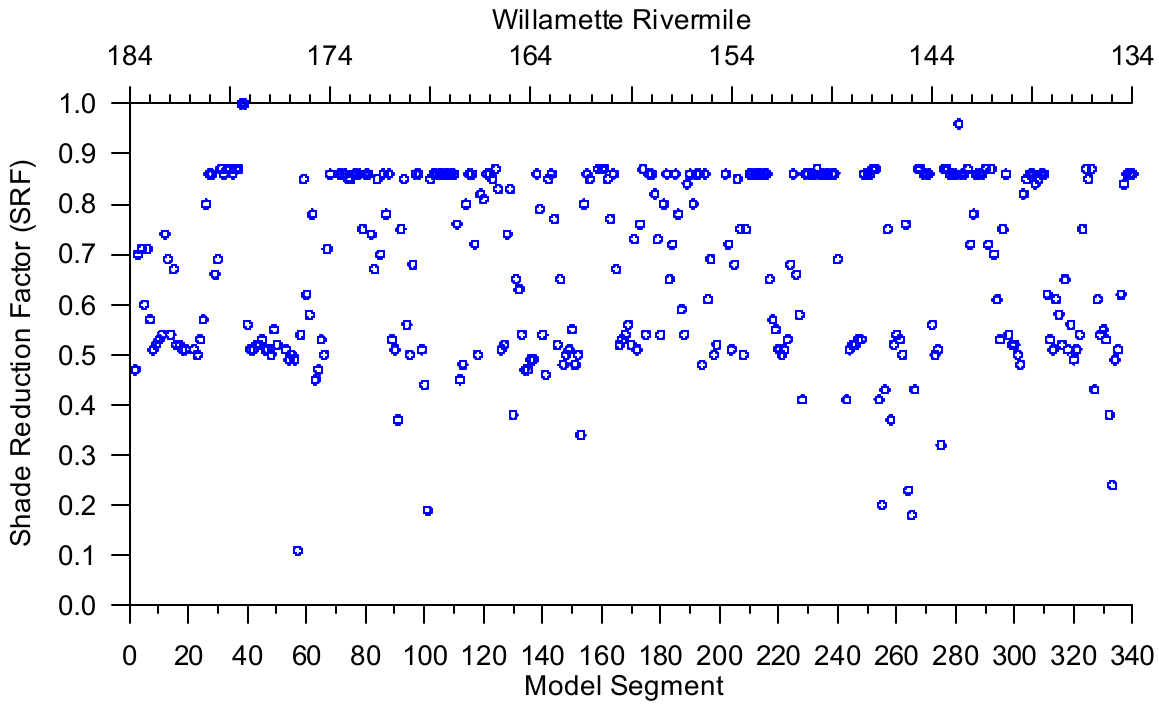


**Figure 352. Upper Willamette River Right Bank Shade Reduction Factor, RM 134 to 85**

## *Meteorology*

The Upper Willamette River model spans approximately 100 miles with an elevation change from approximately 135 to 35 m, NGVD29. Meteorological monitoring conducted by the National Weather Service, the Bureau of Reclamation, and the University of Oregon were used to develop the meteorological data for the model. The model uses these meteorological parameters: air and dew point temperature, wind speed and direction, cloud cover and solar radiation. Figure 353 shows the locations of the meteorological stations used for developing the meteorological inputs. Table 40 lists the sites and the agencies responsible for data collection. Figure 353 does not show the location of the Gladstone solar radiation monitoring site which was included in Table 40. The Gladstone monitoring site was located near the Willamette Falls.

The solar radiation data and other meteorological parameters were not collected at the same sites. Solar data from the Eugene Solar Radiation Monitoring Lab (SRML) site was joined with the Eugene airport data to form the Eugene meteorological inputs, applied to water bodies 1, and 2. Solar data from the Corvallis AGRIMET station was joined with the Corvallis Airport data to form the Corvallis meteorological inputs, applied to water bodies 3, 4, 5, and 6. Solar data from the Gladstone AGRIMET station was joined with the Salem Airport data to form the Salem meteorological inputs, applied to water bodies 7, 8, and 9. The association of the meteorological site with the model water bodies was based on proximity.

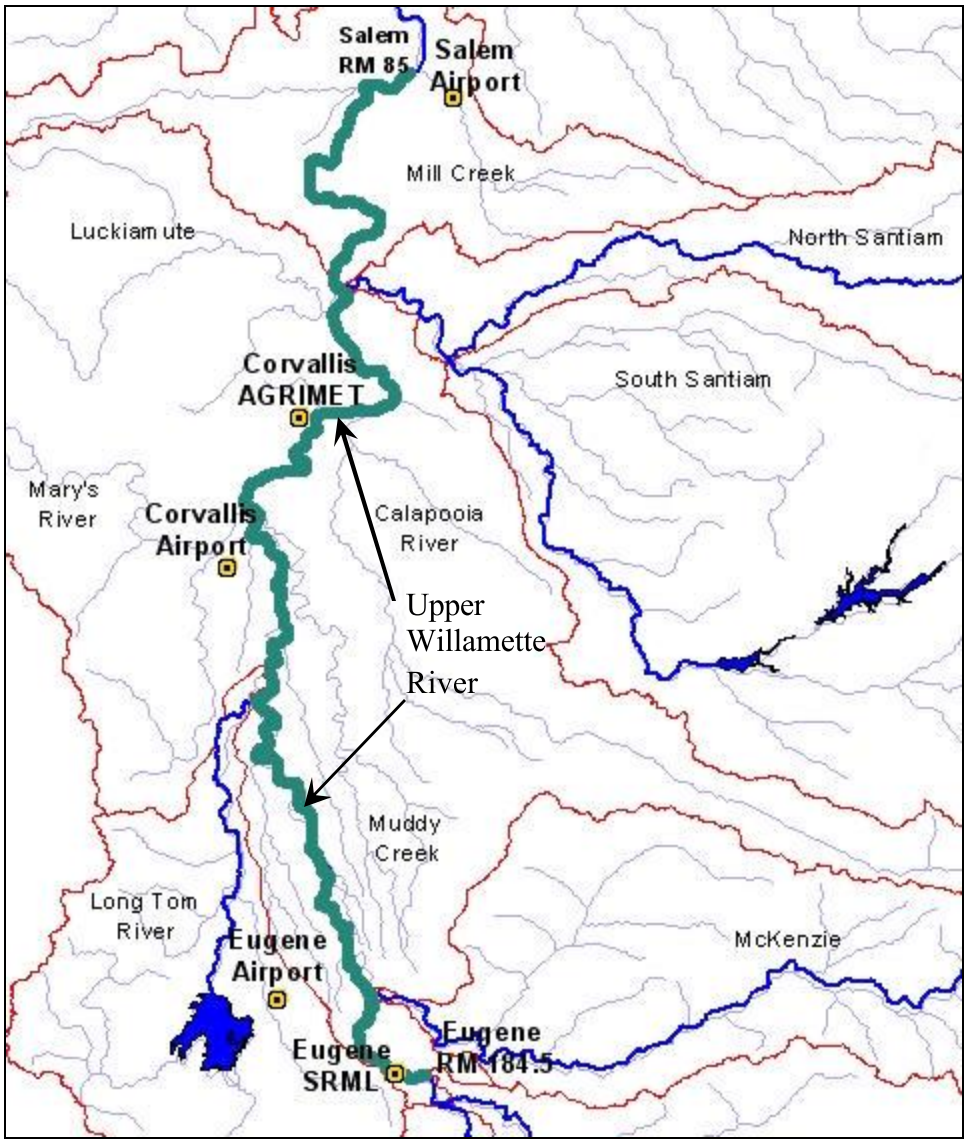


**Figure 353. Upper Willamette River model meteorological site locations**

**Table 40. Upper Willamette River model meteorological monitoring sites**

| Site | Agency (Program) | Meteorological Parameters |
|---|---|---|
| Salem Municipal Airport | National Weather Service (METAR) | Air Temperature, Dew Point Temperature, Relative Humidity, Wind Speed, Wind Direction, Cloud Cover |
| Corvallis Municipal Airport | National Weather Service (METAR) | Air Temperature, Dew Point Temperature, Relative Humidity, Wind Speed, Wind Direction, Cloud Cover |
| Eugene WSO Airport / Mahlon Sweet | National Weather Service (METAR) | Air Temperature, Dew Point Temperature, Relative Humidity, Wind Speed, Wind Direction, Cloud Cover |
| Eugene, OR | University of Oregon, | Solar Radiation |

| Site | Agency (Program) | Meteorological Parameters |
|---|---|---|
| | Solar Radiation Monitoring Lab | |
| Corvallis, OR | Bureau of Reclamation, (AGRIMET) | Solar Radiation |
| Gladstone | University of Oregon, Solar Radiation Monitoring Lab | Solar Radiation |

## Eugene Airport

### Year 2001

The Eugene WSO / Mahlon Sweet Airport records air and dew point temperature, wind speed and direction and cloud cover, but no solar radiation data. Figure 354 and Figure 355 show the air and dew point temperature respectively, over the period of April to October 2001. Figure 356 and Figure 357 show the wind speed and direction, respectively. Figure 356 indicates the minimum wind speed-recording threshold was about 1.5 m/s. The rose diagram in Figure 357 is dominated by the value of zero which is associated with wind speeds below the reading threshold. Figure 358 shows the coarseness of the cloud cover data recorded at the airport with only about five different cloud cover designations. The data points between the five values are the result of interpolations to fill data gaps in the cloud cover data. The solar radiation data collected at the SRML site is shown in Figure 359.

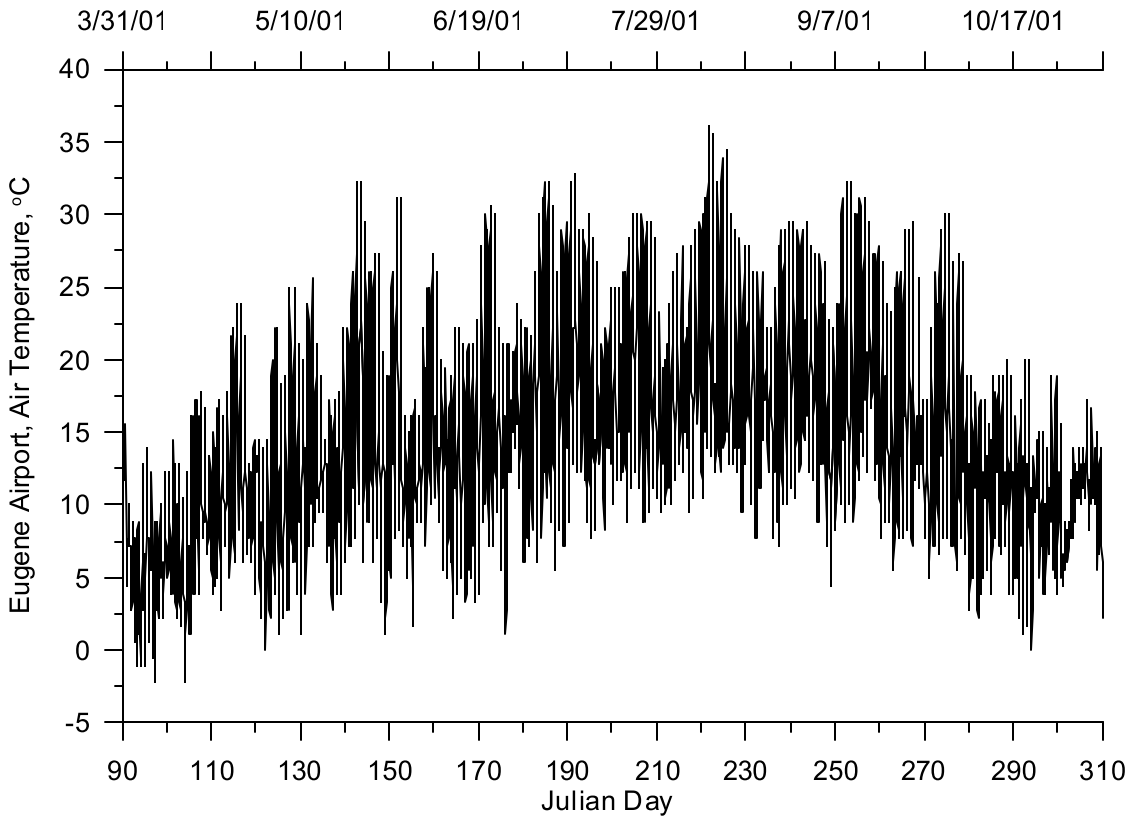


**Figure 354. Air temperature at Eugene Airport, 2001**

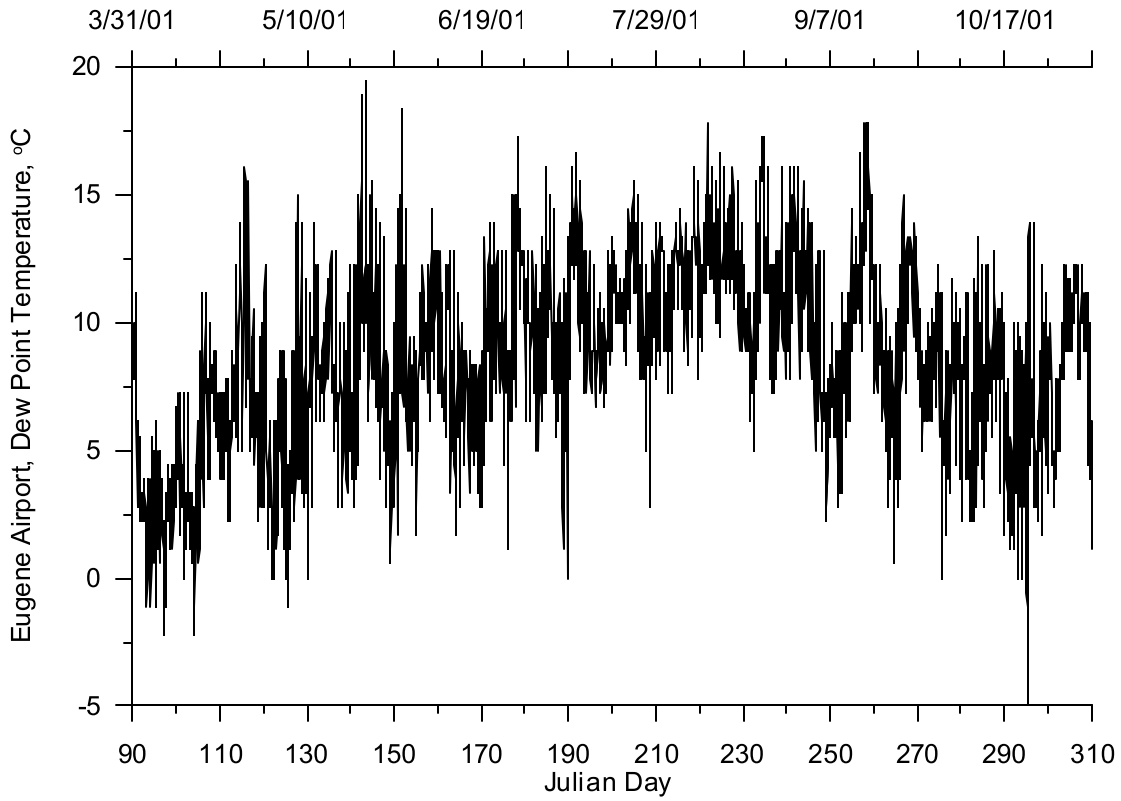


**Figure 355. Dew point temperature at Eugene Airport, 2001**

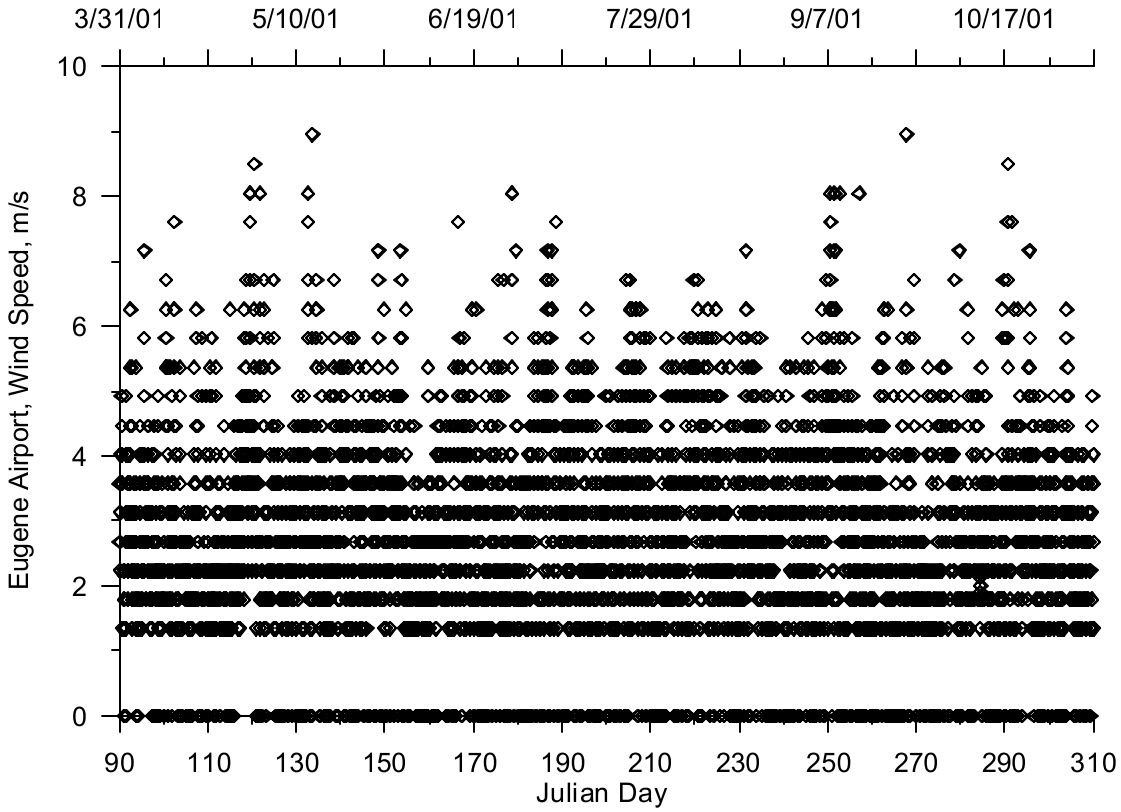


**Figure 356. Wind s peed at Eugene Airport, 2001**

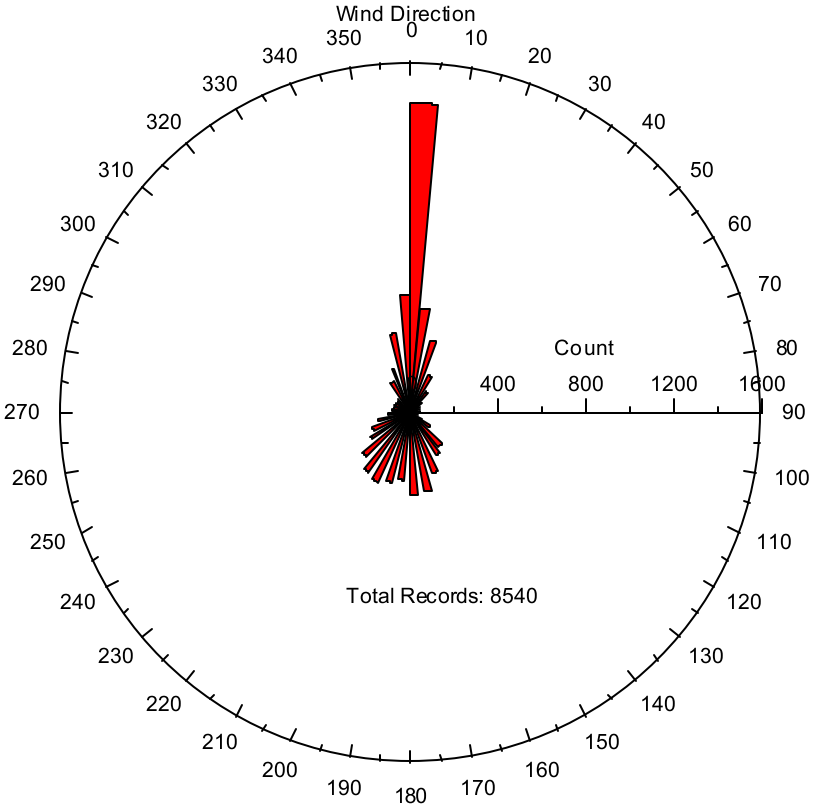


**Figure 357. Wind direction at Eugene Airport, 2001**

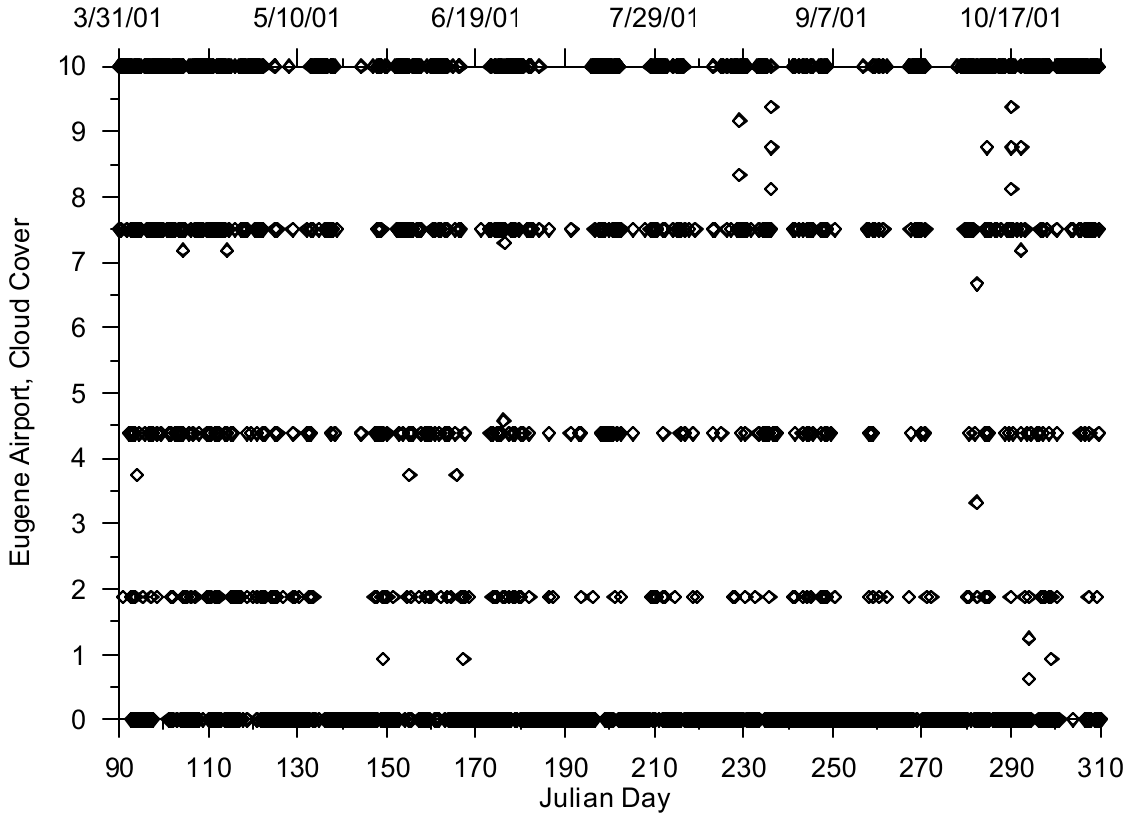


**Figure 358. Cloud cover at Eugene Airport, 2001**

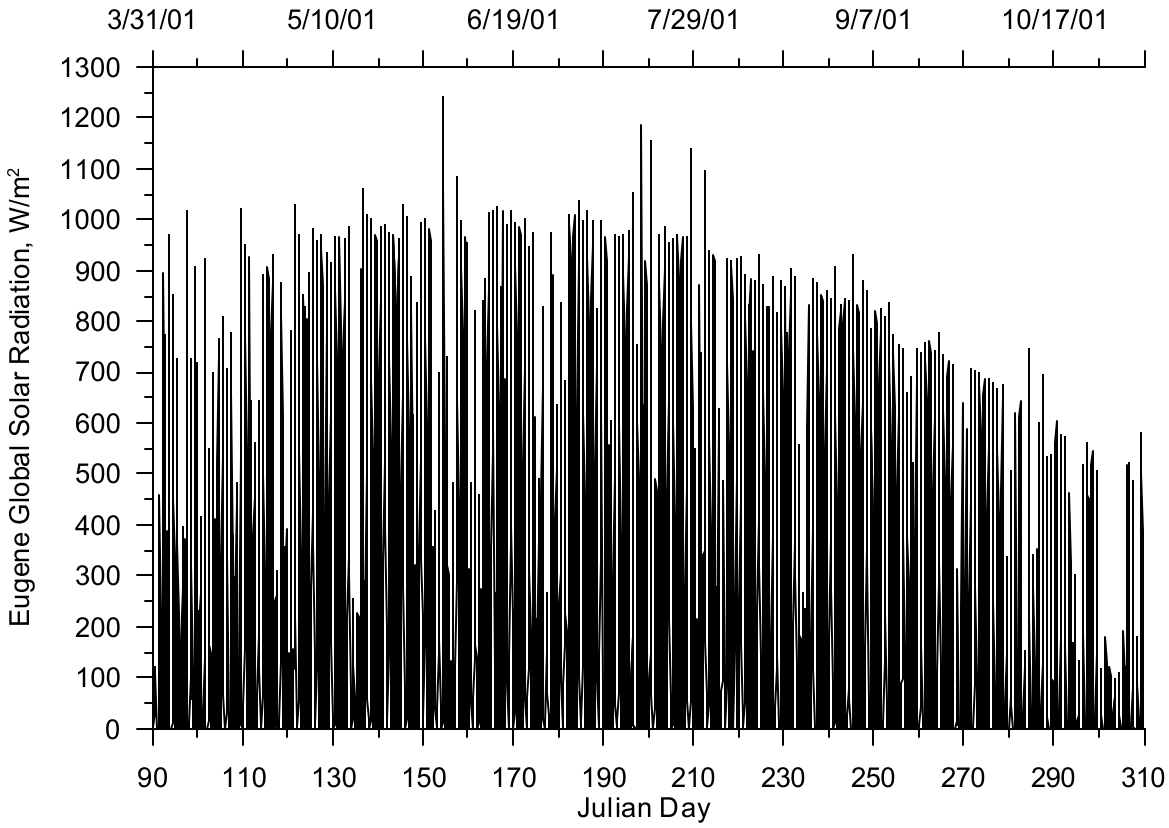


**Figure 359. Global solar radiation in Eugene, OR, 2001**

## Year 2002

The Eugene municipal airport records air and dew point temperature, wind speed and direction and cloud cover, but no solar radiation data. Figure 360 and Figure 361 show the air and dew point temperature respectively, over the period of April to October 2001. Figure 362 and Figure 363 show the wind speed and direction, respectively. Figure 362 indicates the minimum wind speed-recording threshold was about 1.5 m/s. The rose diagram in Figure 363 was dominated by the value of zero which was associated with wind speeds below the reading threshold. Figure 364 shows the coarseness of the cloud cover data recorded at the airport with only about 5 different cloud cover designations. The data points between the five values were the result of interpolations to fill data gaps in the cloud cover data. The solar radiation data collected at the SRML site is shown in Figure 365.

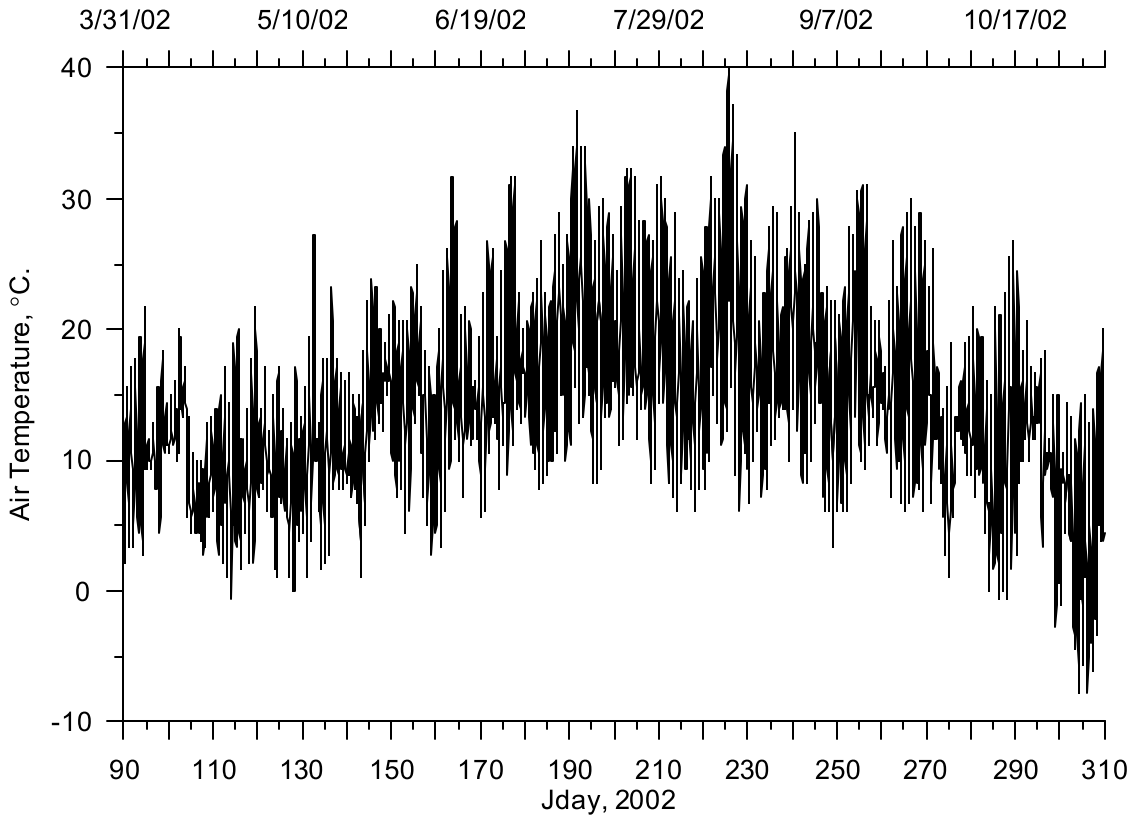


**Figure 360. Air temperature at Eugene Airport, 2002**

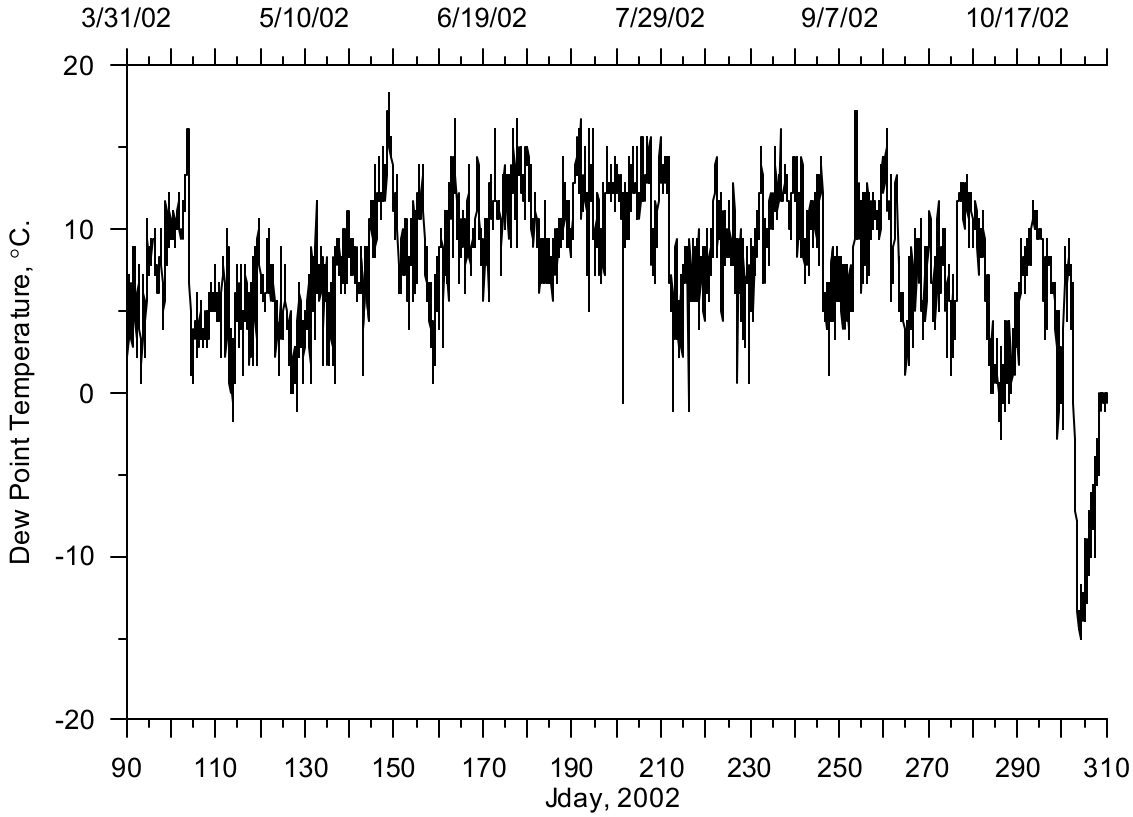


**Figure 361. Dew point temperature at Eugene Airport, 2002**

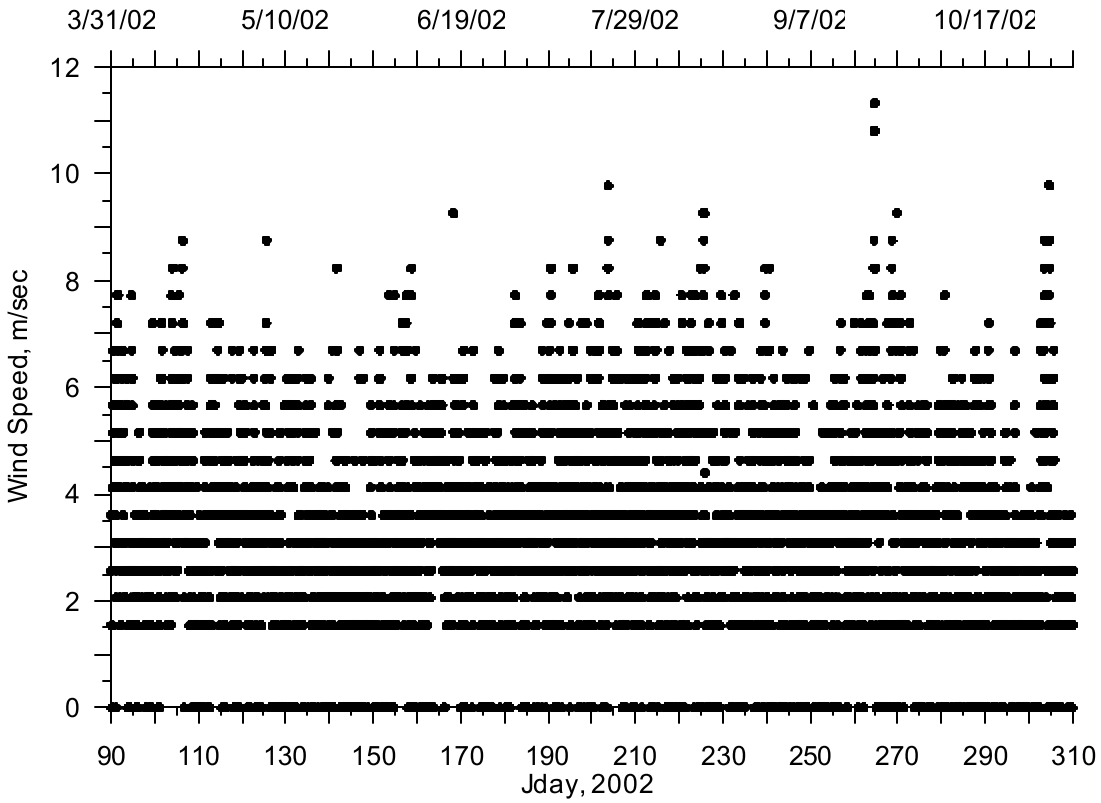


**Figure 362. Wind speed at Eugene Airport, 2002**

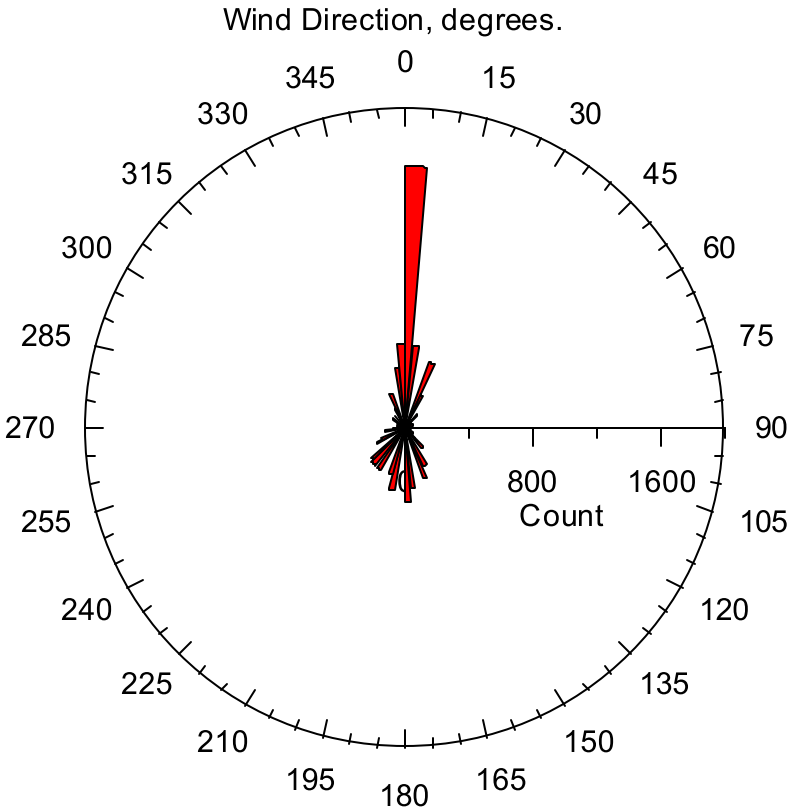


**Figure 363. Wind direction at Eugene Airport, 2002**

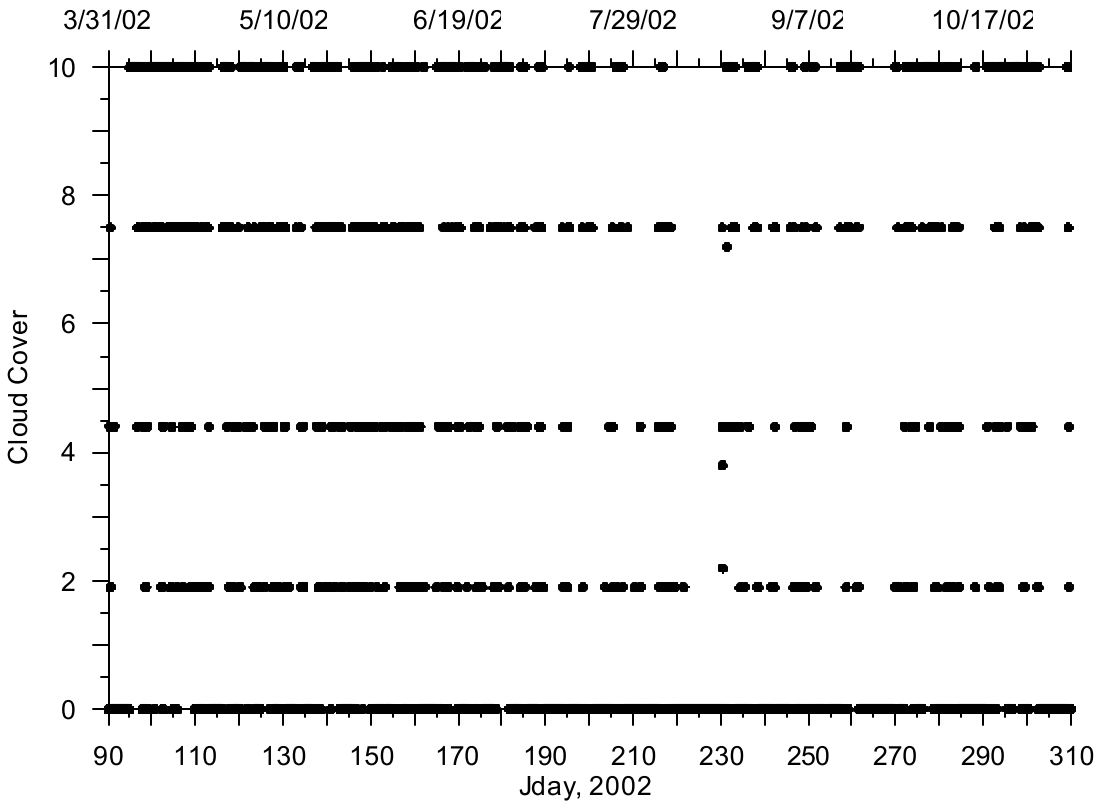


**Figure 364. Cloud cover at Eugene Airport, 2002**

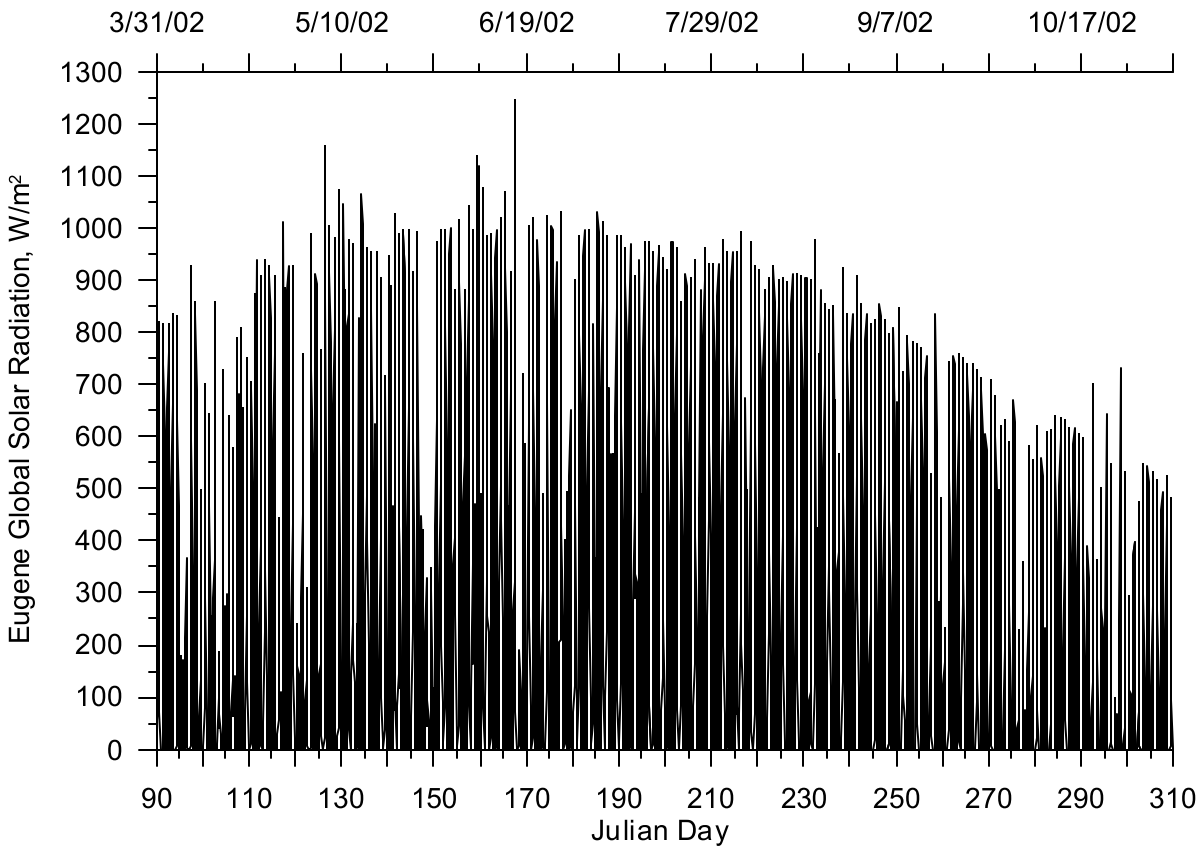


**Figure 365. Global solar radiation in Eugene, OR, 2002**

## Corvallis Municipal Airport

Year 2001

The Corvallis municipal airport records air and dew point temperature, wind speed and direction and cloud cover, but no solar radiation data. Figure 366 and Figure 367 show the air and dew point temperature respectively, over the period of April to October 2001. Figure 368 and Figure 369 show the wind speed and direction, respectively. Figure 368 indicates the minimum wind speed-recording threshold was about 1.5 m/s. The rose diagram in Figure 369 was dominated by the value of zero which was associated with wind speeds below the reading threshold. Figure 370 shows the coarseness of the cloud cover data recorded at the airport with only about five different cloud cover designations. The solar radiation data collected at the Corvallis AGRIMET site is shown in Figure 371.

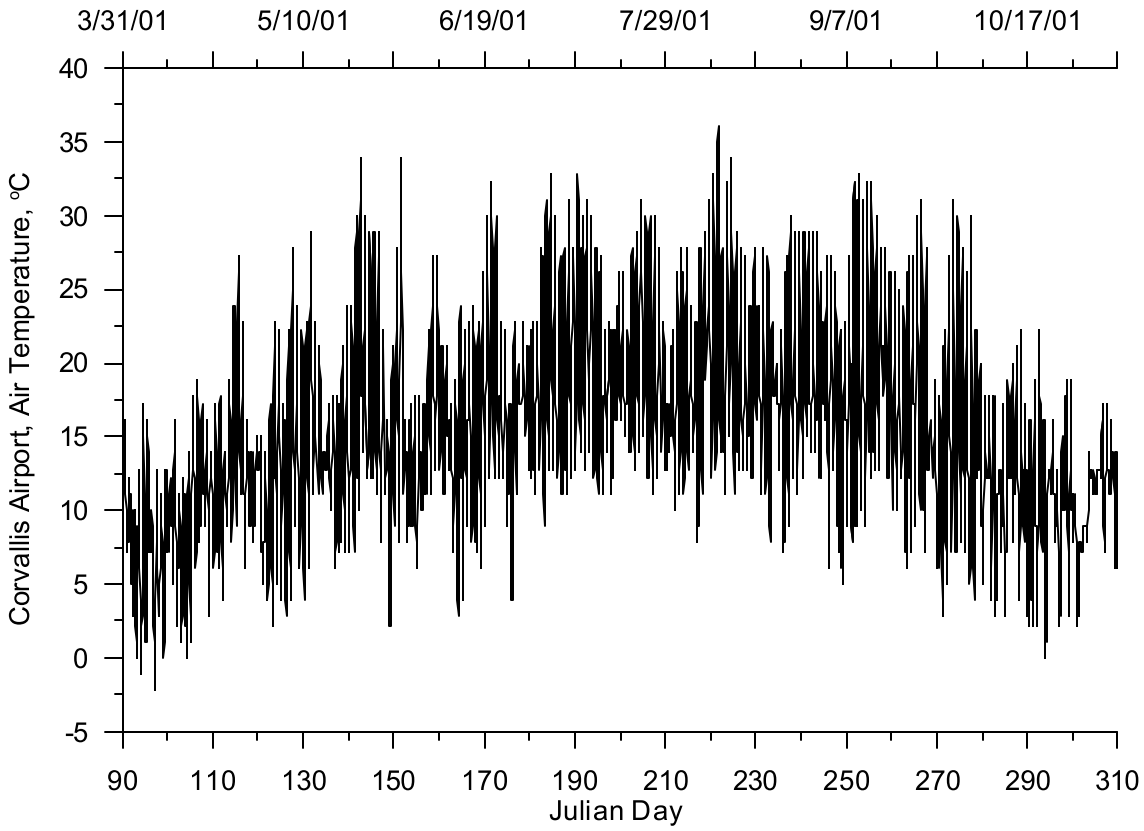


**Figure 366. Air temperature at Corvallis Municipal Airport, 2001**

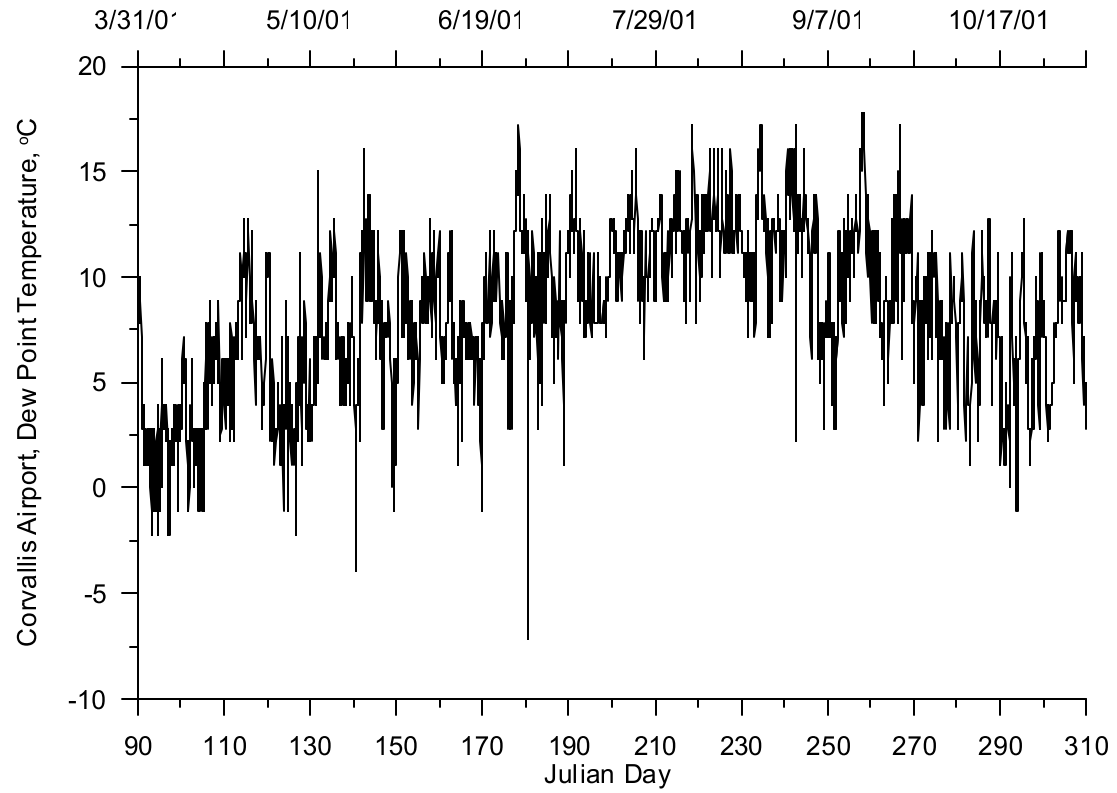


**Figure 367. Dew point temperature at Corvallis Municipal Airport, 2001**

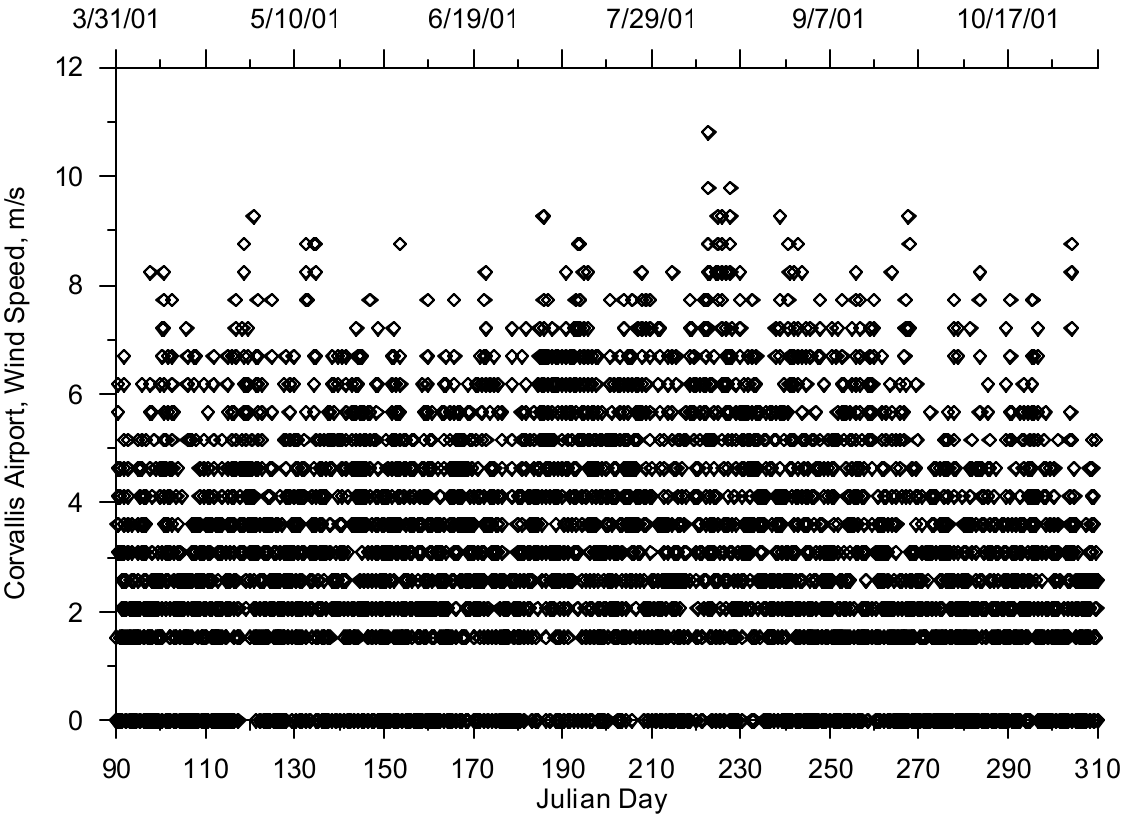


**Figure 368. Wind speed at Corvallis Municipal Airport, 2001**

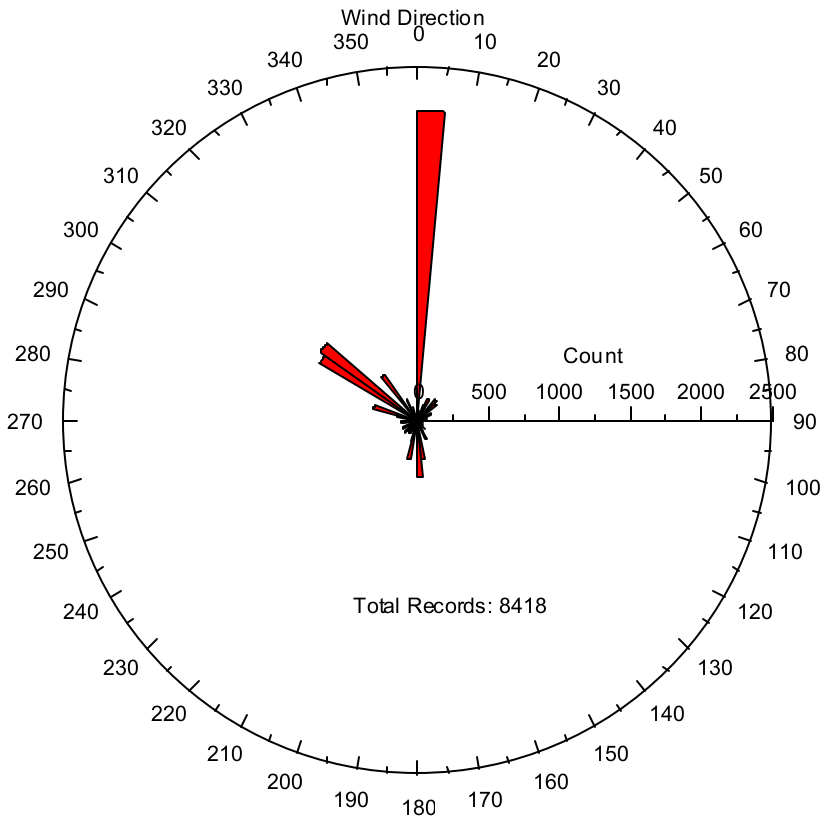


**Figure 369. Wind direction at Corvallis Municipal Airport, 2001**

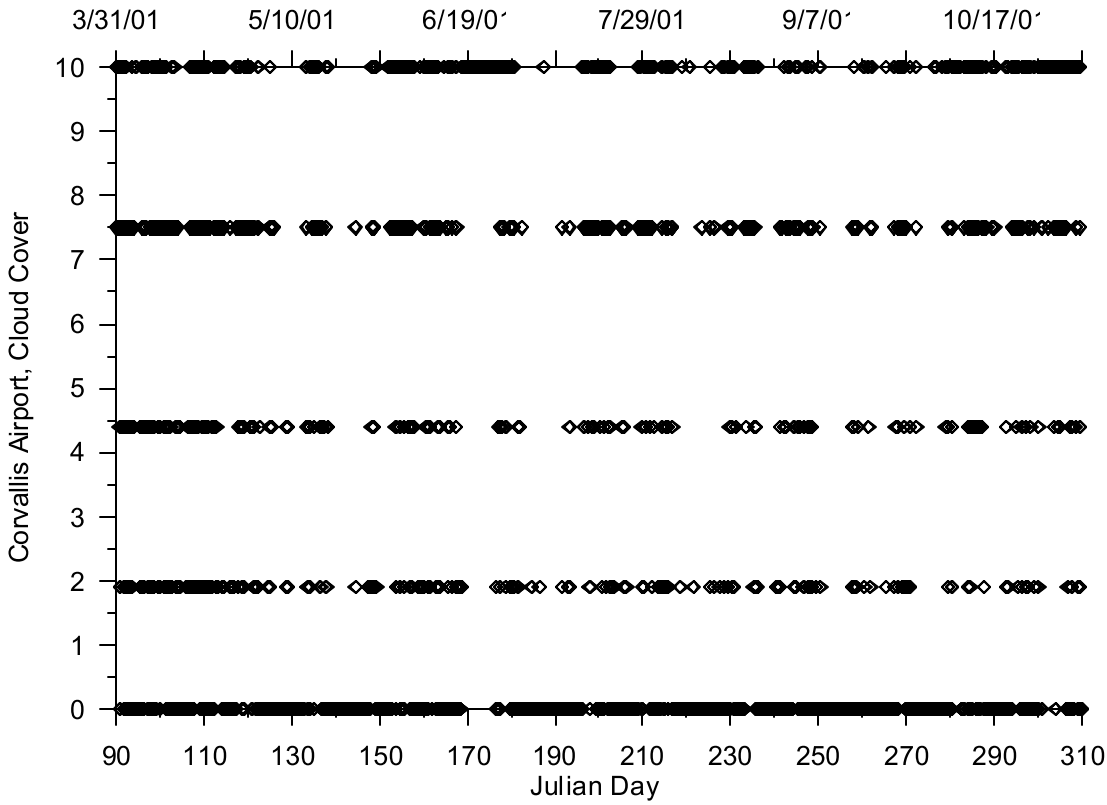


**Figure 370. Cloud cover at Corvallis Municipal Airport, 2001**

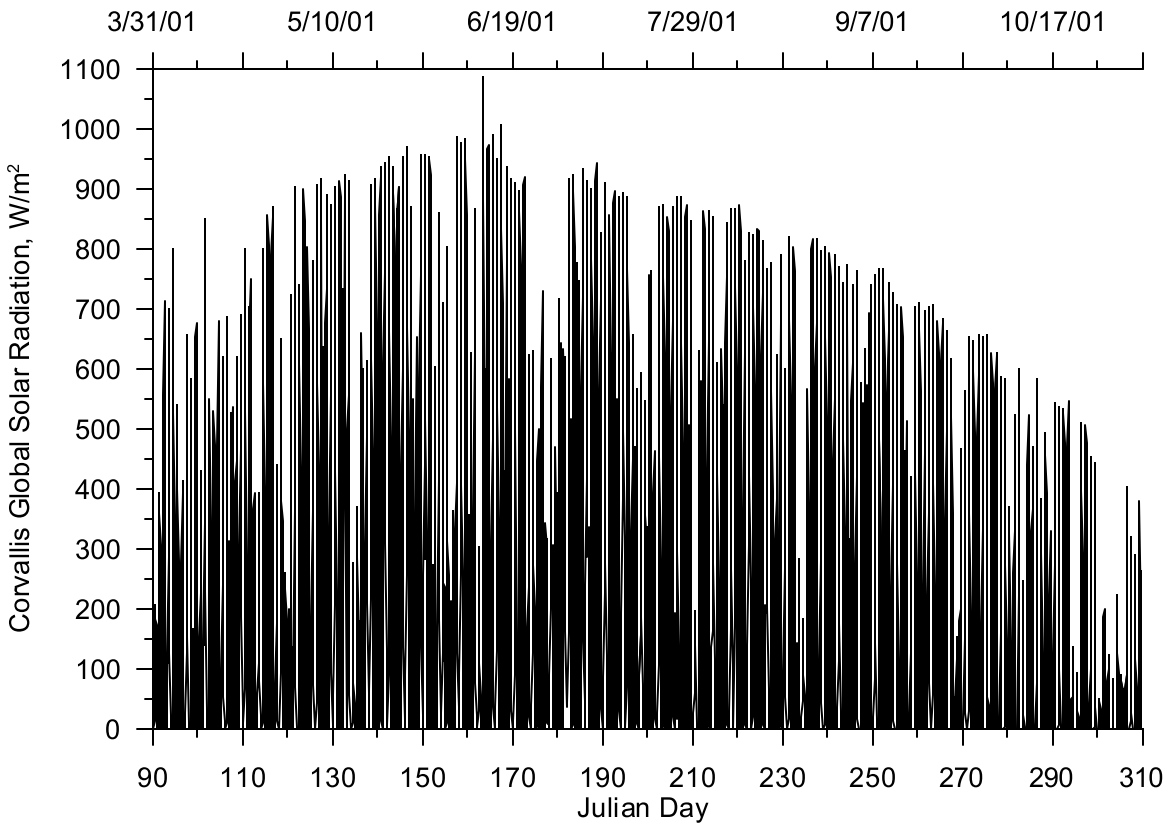


**Figure 371. Global solar radiation in Corvallis, OR, 2001**

## Year 2002

The Corvallis municipal airport records air and dew point temperature, wind speed and direction and cloud cover, but no solar radiation data. Figure 372 and Figure 373 show the air and dew point temperature, respectively. Figure 374 and Figure 375 show the wind speed and direction, respectively. Figure 374 indicates the minimum wind speed-recording threshold was about 1.5 m/s. The figure also shows several wind speed values between the minimum detection limit and zero. These values and others which fall between wind speed measurement increments represent linearly interpolated wind speeds used to fill in gaps in the data record.

The rose diagram in Figure 375 was dominated by the value of zero which is associated with wind speeds below the measurement threshold. Figure 376 shows the coarseness of the cloud cover data recorded at the airport with only about five different cloud cover designations. The cloud cover values between the five increments represent interpolated values used to fill data gaps. The solar radiation data collected at the Corvallis AGRIMET site is shown in Figure 377.

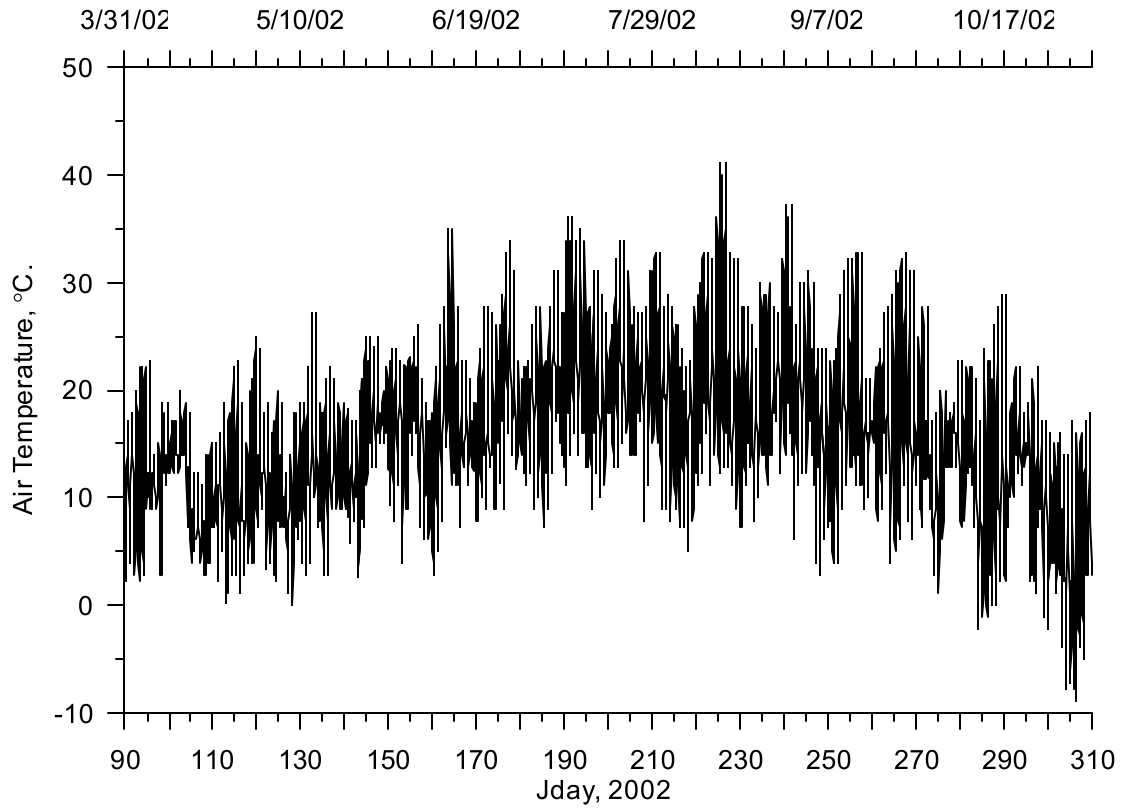


**Figure 372. Air temperature at Corvallis Municipal Airport, 2002**

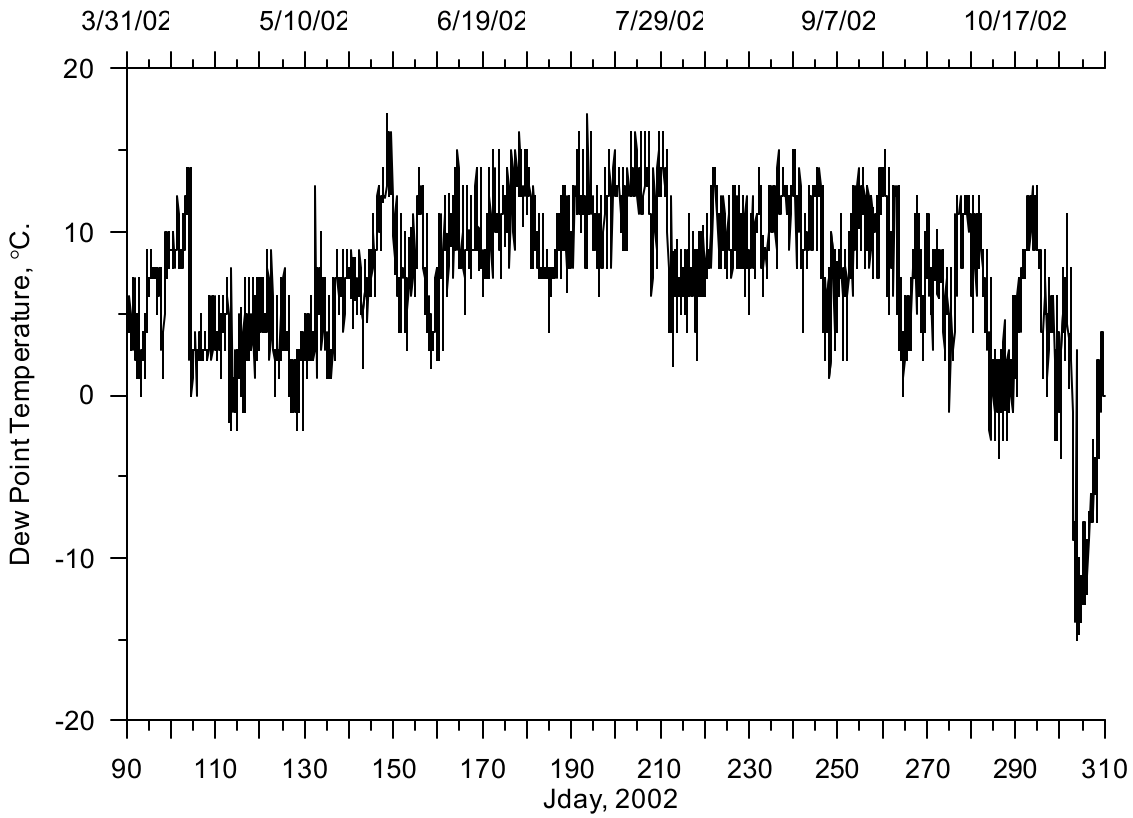


**Figure 373. Dew point temperature at Corvallis Municipal Airport, 2002**

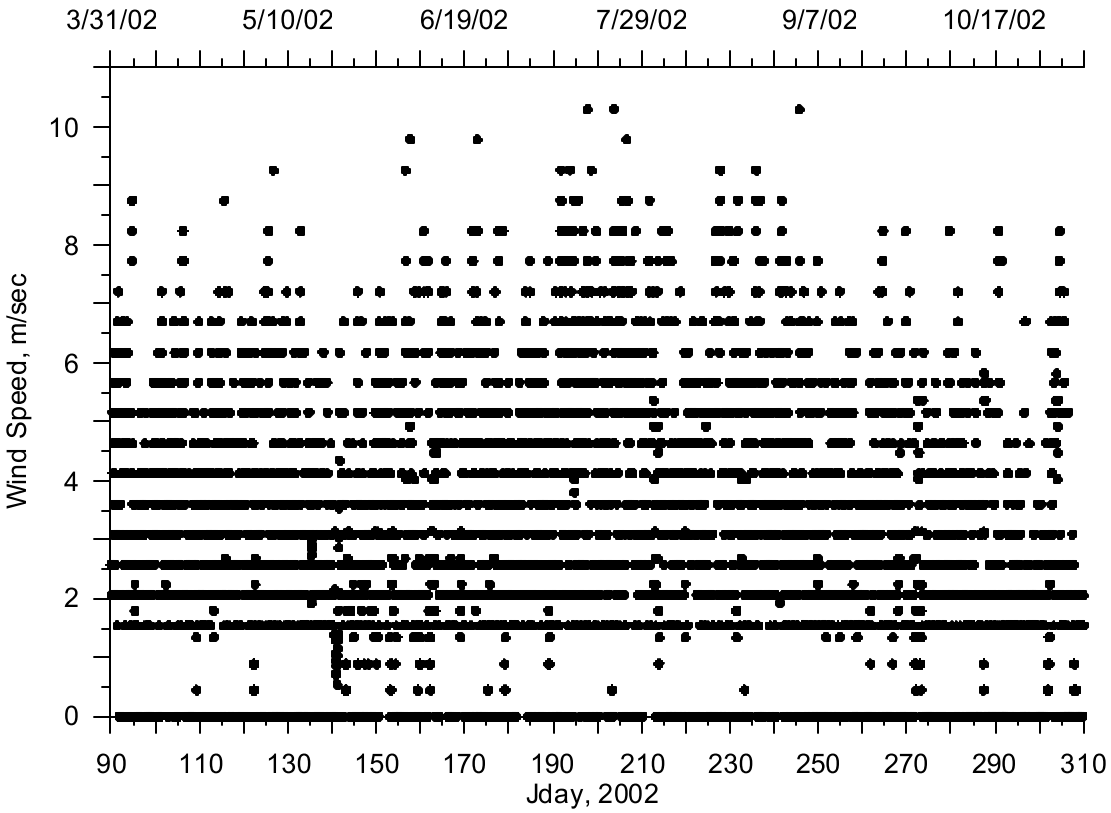


**Figure 374. Wind speed at Corvallis Municipal Airport, 2002**

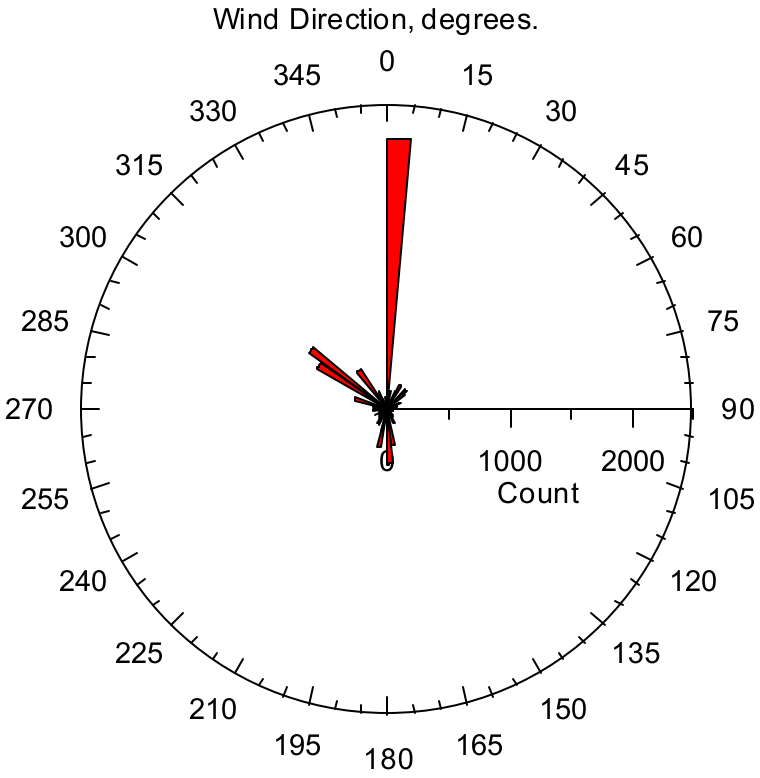


**Figure 375. Wind direction at Corvallis Municipal Airport, 2002**

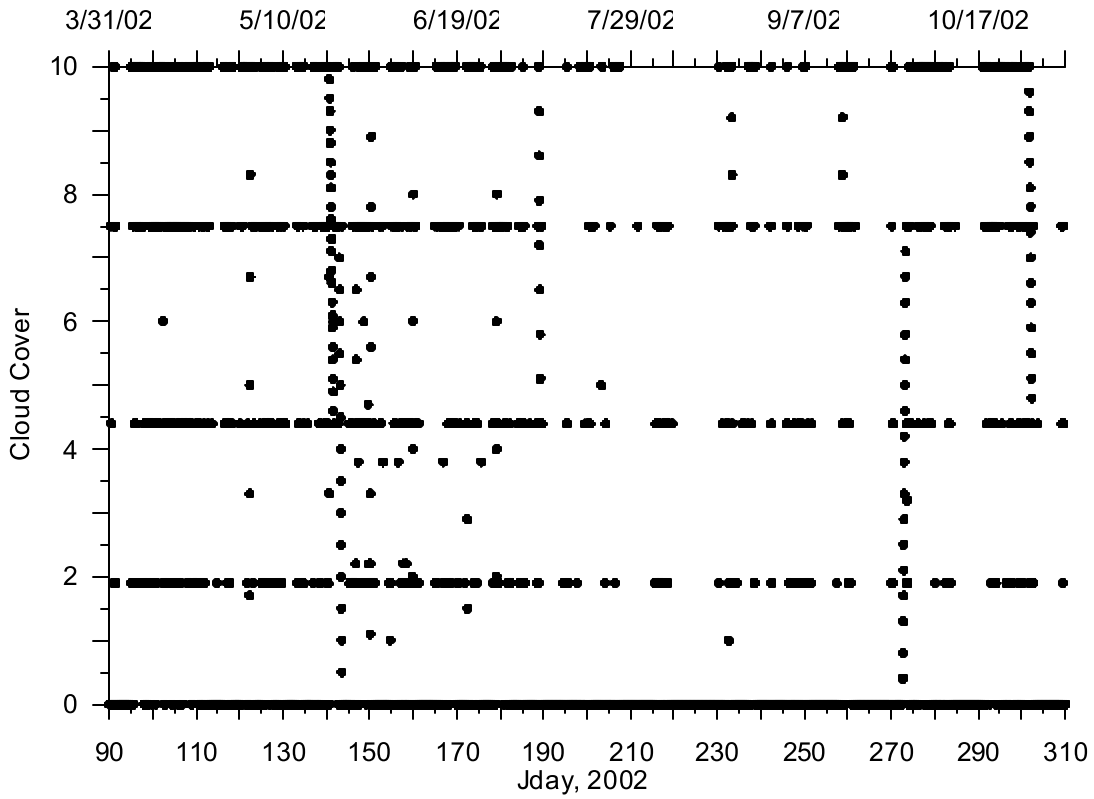


**Figure 376. Cloud cover at Corvallis Municipal Airport, 2002**

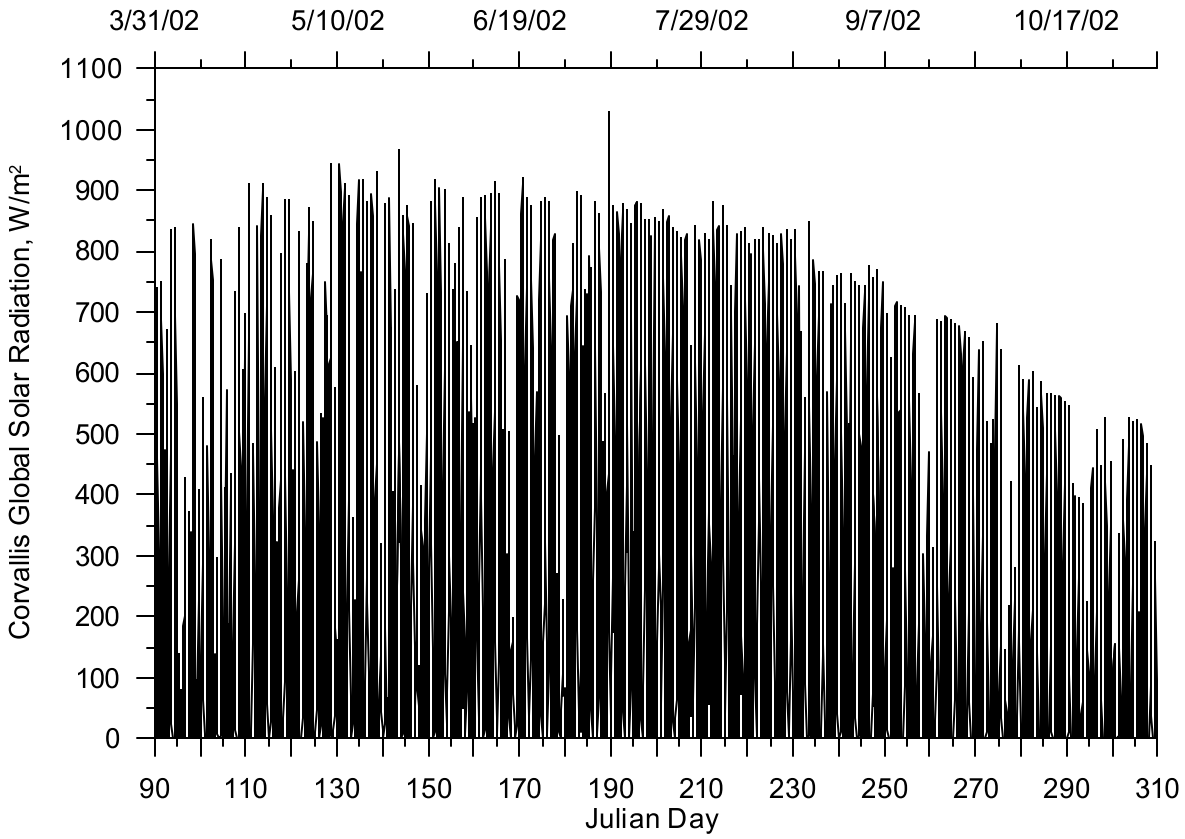


**Figure 377. Global solar radiation in Corvallis, OR, 2002**

## Salem Municipal Airport

### Year 2001

The 2001 meteorological data recorded at Salem municipal airport, which was used for the Middle Willamette River model, were also used in the lower reaches of the Upper Willamette River model. The Salem municipal airport records air and dew point temperature, wind speed and direction, and cloud cover data but no solar radiation data.

Figure 221 and Figure 222 show the air and dew point temperature, respectively. Figure 223 and Figure 224 show the wind speed and direction, respectively. Figure 223 indicates the minimum wind speed-recording threshold was about 1.5 m/s. The rose diagram in Figure 224 indicates the predominant wind direction was from the North with some periodic winds coming from other directions. When wind speeds fall below the minimum recording threshold the wind speed and direction were both set to zero resulting in wind direction from the North being over represented. Figure 225 shows the cloud cover data recorded at the airport with five different cloud cover designations. Global solar radiation data were utilized from Gladstone, OR, as shown in Figure 246.

### Year 2002

The 2002 meteorological data recorded at Salem municipal airport which was used for the Middle Willamette River model, were also used in the lower reaches of the Upper Willamette River model. The Salem municipal airport records air and dew point temperature, wind speed and direction, and cloud cover data but no solar radiation data.

Figure 226 and Figure 227 show the air and dew point temperature, respectively. Figure 228 and Figure 229 show the wind speed and direction, respectively. Figure 228 indicates the minimum wind speed-recording threshold was about 1.5 m/s. The rose diagram in Figure 229 indicates the predominant wind direction was from the North. When wind speeds fall below the minimum recording threshold the wind speed and direction were both set to zero resulting in wind direction from the North being over represented. Figure 230 shows the cloud cover data recorded at the airport with five different cloud cover designations. Global solar radiation data were utilized from Gladstone, OR, as shown in Figure 252

## Clackamas River

The Clackamas River model was developed for the Clackamas River from the Rivermill Reservoir Dam (Estacada Lake, RM 22.6) downstream to the river's confluence with the Lower Willamette River. Figure 378 shows the model region and the Clackamas River watershed. The Clackamas River watershed drained an area of approximately 2,400 $km^2$.

The model calibration periods were from April 1, 2001 to September 30, 2001, and from April 1, 2002 to October 1, 2002. The data needed to support the model consisted of three components: the river channel bathymetry, the meteorological conditions and the boundary condition inflows and temperatures.

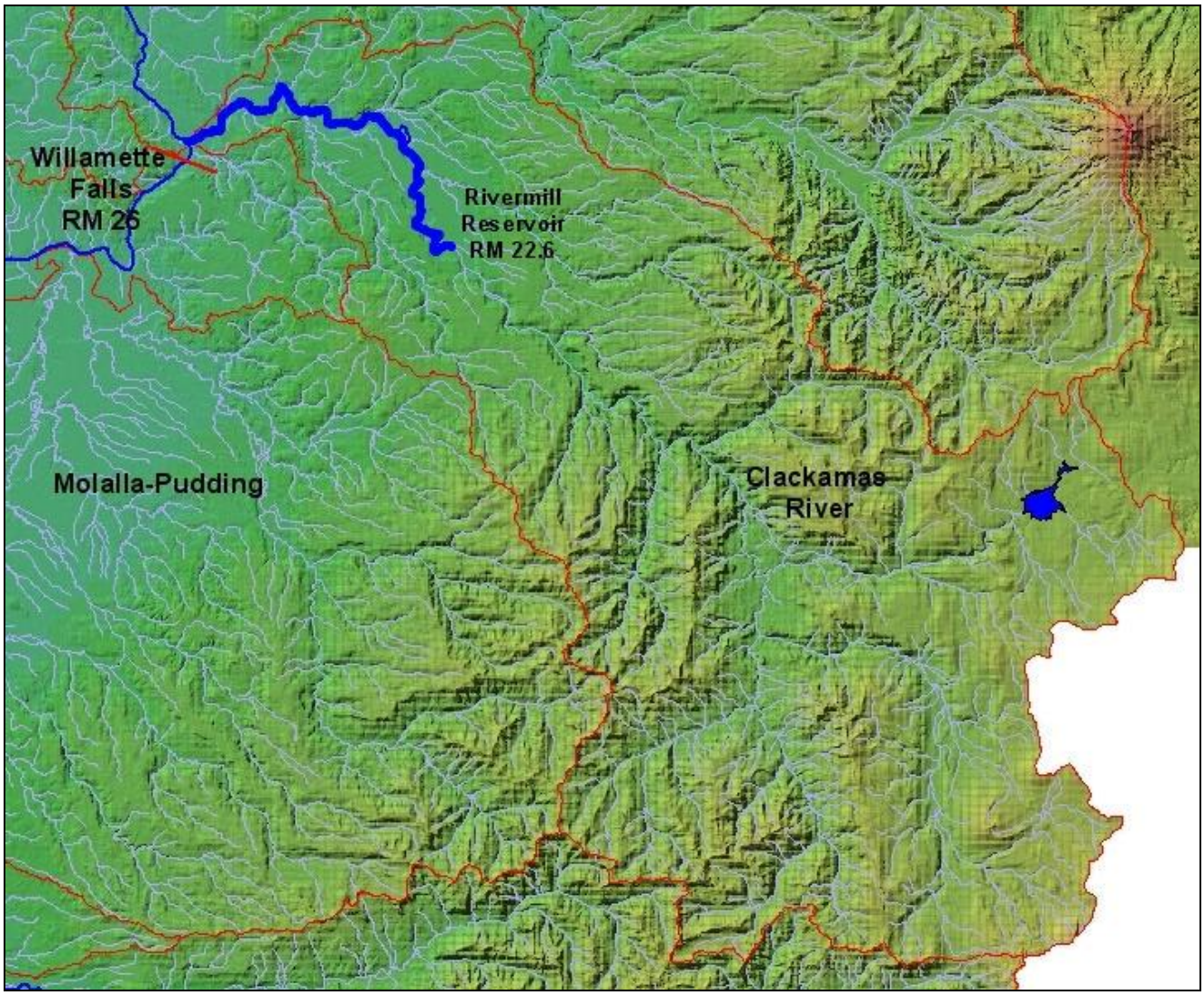


**Figure 378. Clackamas River model region**

## Bathymetry Data

The river bathymetry for the Clackamas River below River Mill Reservoir covers approximately 22.6 miles. The main source of data consisted of bathymetric river cross sections as shown in Figure 379 There were four cross sections surveyed by PGE directly below the River Mill Dam. There were also 14 cross section surveyed by DOGAMI (Oregon Department of Geology and Mineral Industries) and 52 cross sections surveyed as part of a FEMA (Federal Emergency Management Agency). As shown in Figure 379 and Figure 380, a detailed contour plot and model grid was already developed for the lower end of the of the Clackamas River up to RM 1.33 as part of a previous modeling effort (Rodriguez et al., 2001). The side channel leading to the old quarry near the river mouth (Figure 380) was not explicitly part of the model, even though the volume and area were incorporated in the river segment adjacent to the quarry.

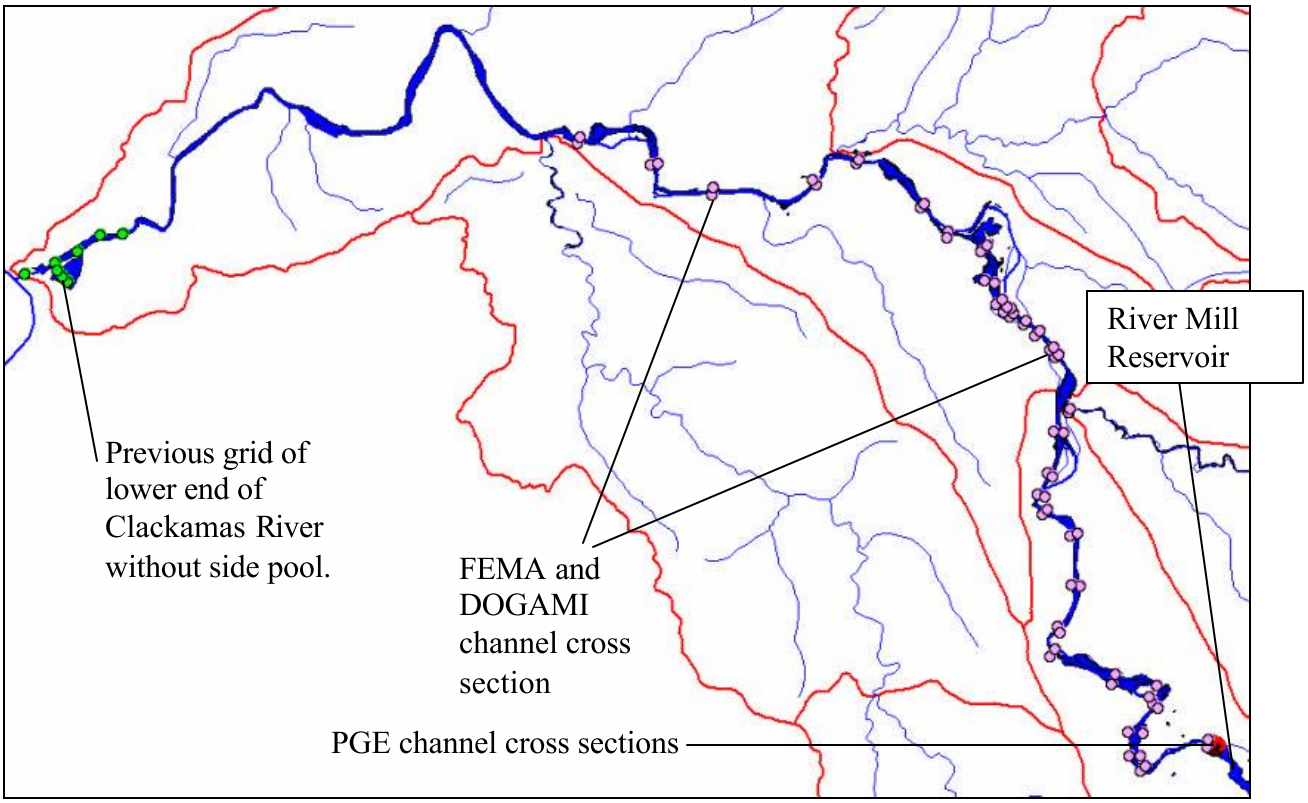


**Figure 379. Bathymetric channel cross sections below River Mill Dam**

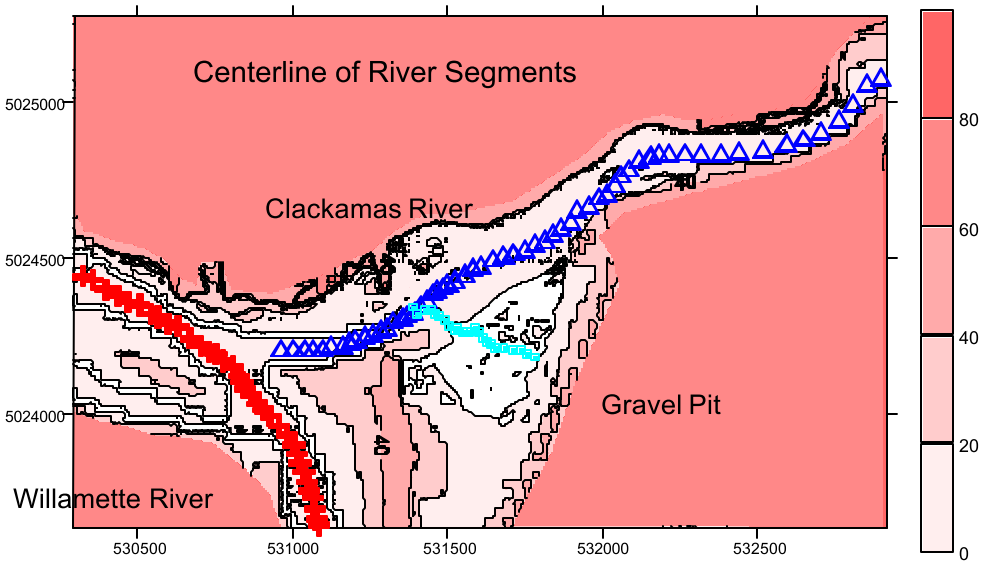


**Figure 380. Contour plot of Clackamas River confluence with the Willamette River**

## Model Grid Development

The bathymetry for the river section above the existing grid (RM 1.33) and below River Mill Dam was developed by creating a series of interpolated cross sections between the surveyed cross sections along with interpolated surveyed elevations and channel widths obtained from detailed GIS data. These GIS data were obtained from the Oregon Department of Environmental Quality. The complete set of cross sections, both surveyed and computed, were combined with topographic data for the stream banks to generate a detailed surface plot of the river channel using the contour plotting program SURFER, as shown in Figure 381. Both Figure 381 and Figure 383 reflect the complete model grid below River Mill Dam to the Willamette River.

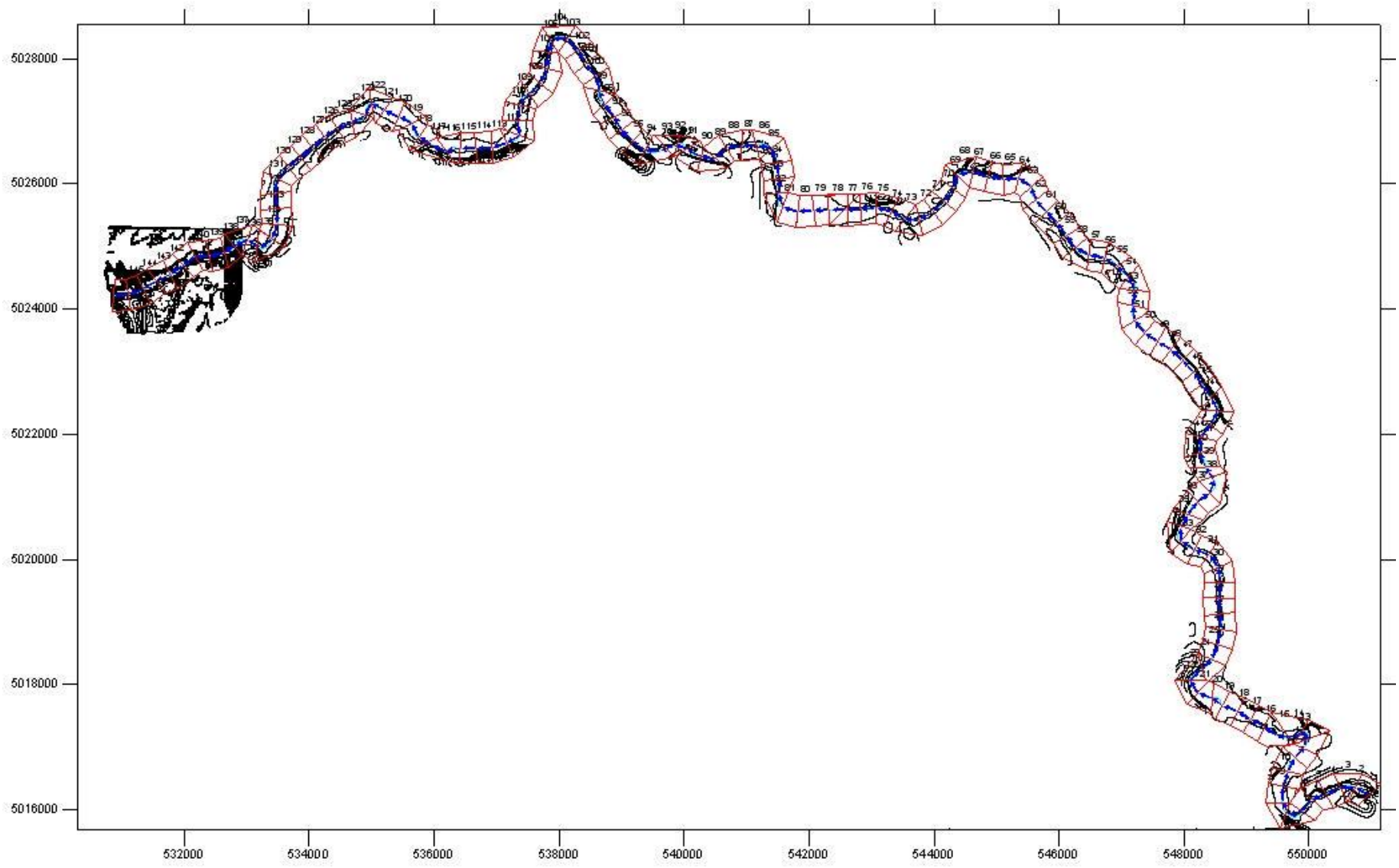


**Figure 381. Grid layout for CE-QUAL-W2 model of the Clackamas River below River Mill.**

Figure 382 shows a longitudinal profile of the channel bottom from the SURFER contour plot and the model grid channel. The model uses one water body and two branches. The branches were selected based on changes in the channel bottom slope. Table 41 lists the model grid characteristics for the Clackamas River below River Mill Reservoir and Figure 383 provides a plan view of the model grid layout and segment numbering.

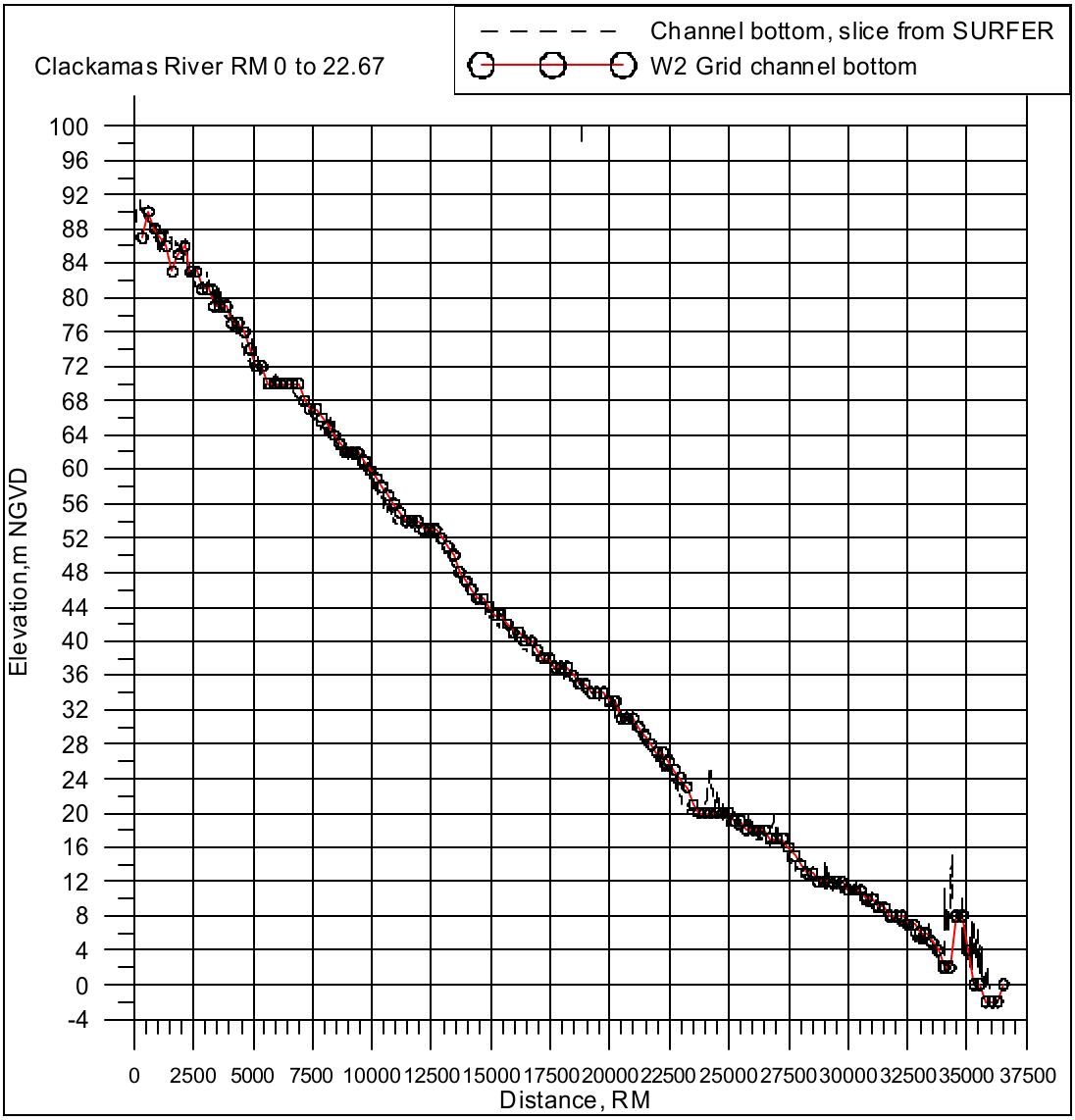


**Figure 382. Elevation differences along Clackamas River from RM 0 to RM 23, below River Mill Dam.**

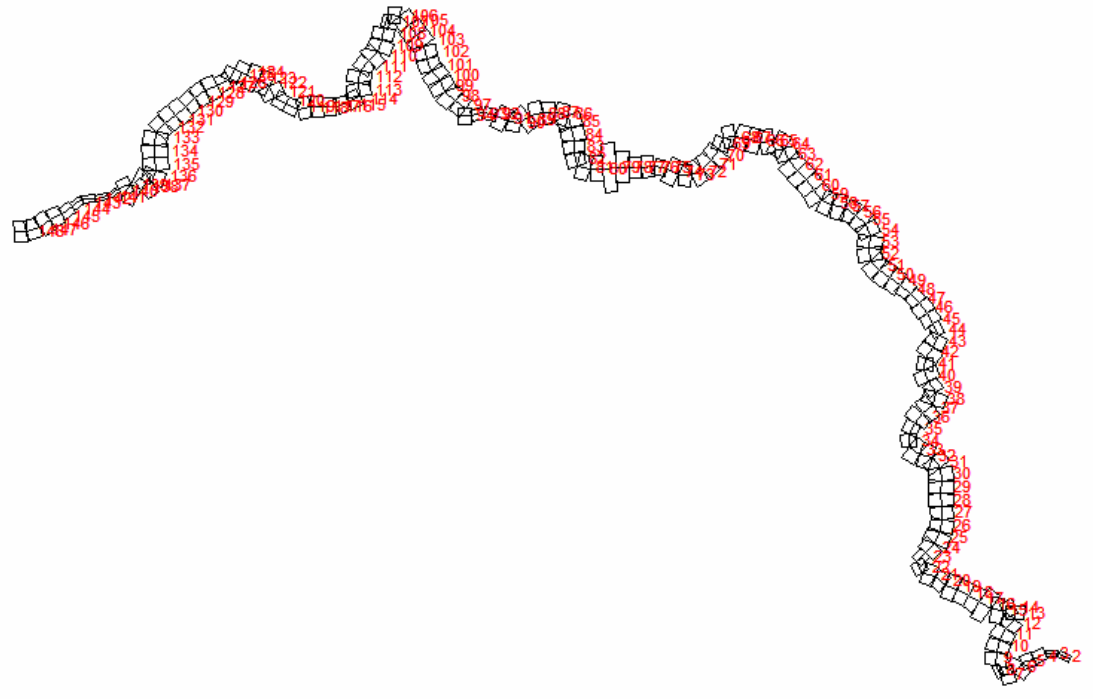

**Figure 383. Clackamas River model segment layout**

**Table 41. Clackamas River Model Grid Layout**

| Water Body | Branch | Description | Starting Segment | Ending Segment | Starting RM | Ending RM | Segment Length, m | Slope | Upstream BC | Downstream BC |
|---|---|---|---|---|---|---|---|---|---|---|
| 1 | 1 | Rivermill Reservoir to RM 8.1 | 2 | 94 | 22.5 | 8.1 | 251.06 | 0.00280 | flow | internal |
| | 2 | RM 8.1 to Willamette River confluence | 97 | 148 | 8.1 | 0.0 | 251.06 | 0.00148 | internal | internal |

## *Model Upstream & Downstream Boundary Conditions*

The upstream boundary condition for the Clackamas River model consists of flow and temperature data from the USGS gage station at Estacada, OR, (USGS 14210000) measured in 2001 and 2002. The gage station is just below the Rivermill Reservoir dam. The downstream boundary condition was an artificial spillway which discharged to the Lower Willamette River.

### Hydrodynamic Data

Figure 384 shows the upstream boundary condition gage location for the Clackamas River model. The USGS gage station (USGS 14210000) is located at RM 22.22 with flow data recorded every half-hour.

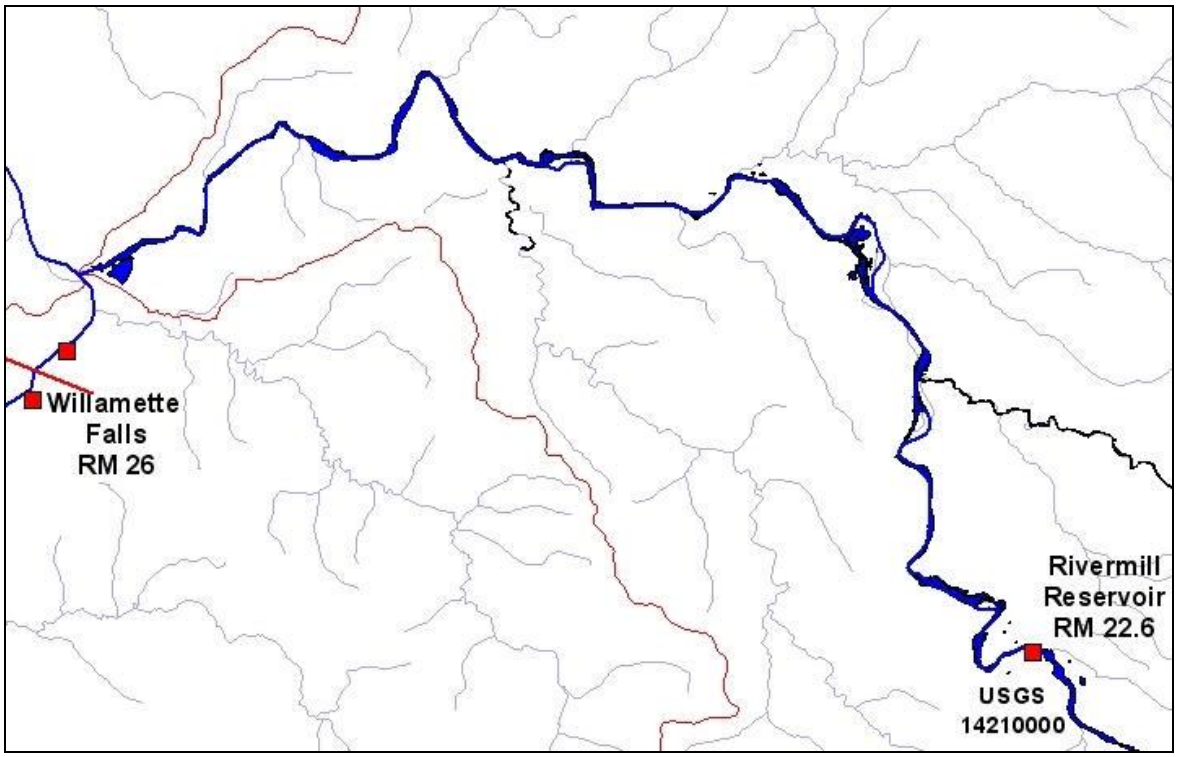


**Figure 384. Clackamas River upstream boundary condition flow gage station**

#### Year 2001

Figure 385 shows the flow data recorded at the USGS gage station at Estacada from April 1 to October 31, 2001. The figure shows a seasonal trend with higher flows in the spring and fall and decreasing flows moving into later summer.

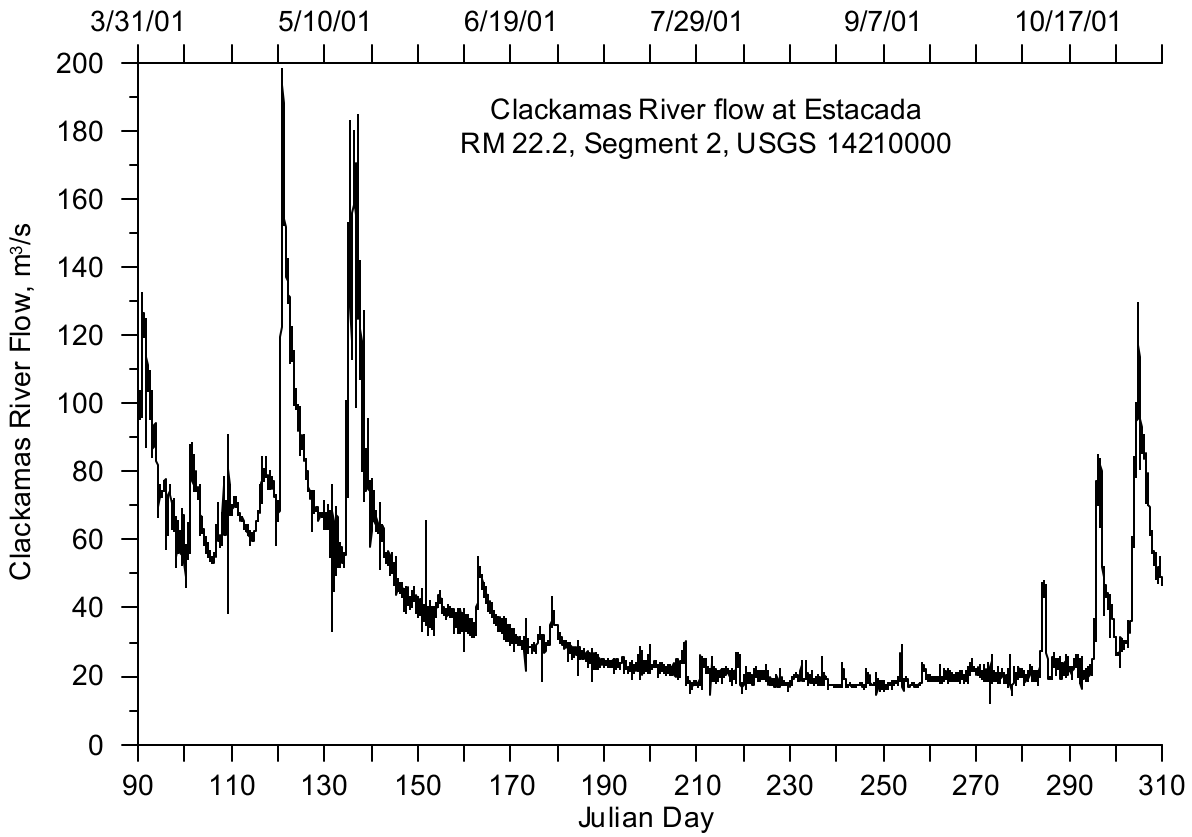


**Figure 385. Clackamas River flow below River Mill Dam, 2001**

## Year 2002

Figure 386 shows the flow data recorded at the USGS gage station at Estacada from April 1 to October 31, 2002. The figure shows a seasonal trend with higher flows in the spring and decreasing flows moving into later summer with steady flows moving into fall. The flows recorded in 2002 were larger both in the spring and throughout the summer.

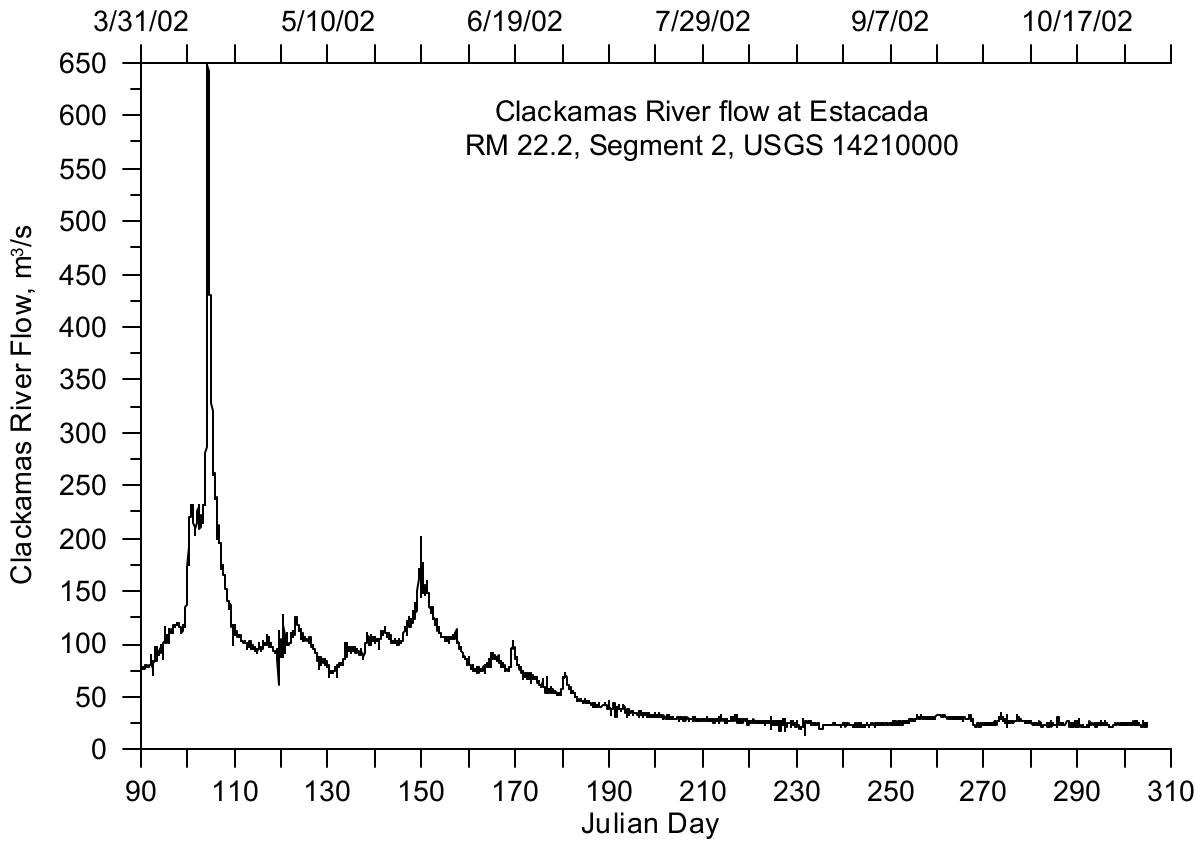


**Figure 386. Clackamas River flow below River Mill Dam, 2002**

## Temperature Data

The temperature upstream boundary condition for the Clackamas River was developed using temperature data from two monitoring sites in 2001 and one site in 2002. Figure 387 shows the temperature monitoring site locations. Table 42 lists the monitoring sites and river mile locations.

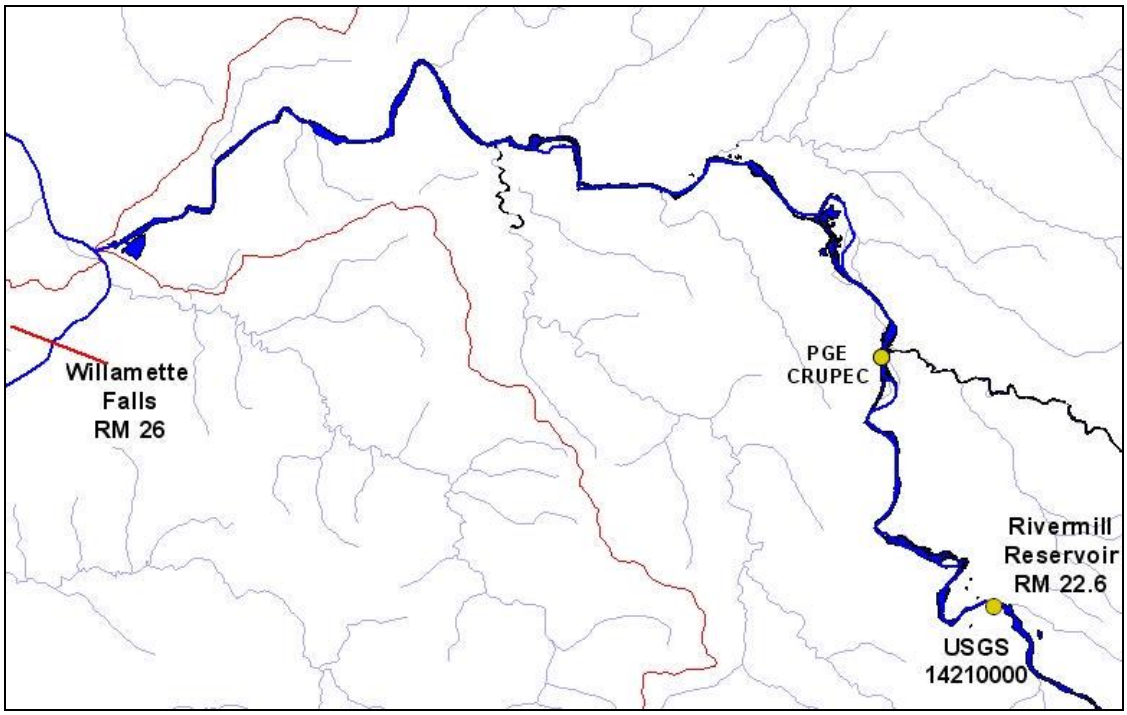


**Figure 387. Clackamas River model boundary condition temperature monitoring site locations**

**Table 42. Clackamas River model boundary condition temperature monitoring sites**

| Site Description | Site ID | RM |
|---|---|---|
| Clackamas River above Eagle Creek | PGE CRUPEC | 16.31 |
| Clackamas River at Estacada | USGS14210000 | 22.22 |

## Year 2001

The temperature upstream boundary for the Clackamas River was developed primarily from temperature data collected at the USGS gage station at Estacada below the River Mill Dam (USGS 14210000) from July 12 to November 1, 2001. The data gap from April 1 to July 12 was filled by developing a temperature correlation between the data at the USGS gage and data collected downstream by PGE at a site upstream from Eagle Creek (PGE CRUPEC). Figure 388 shows the temperature correlation between the two sites. Figure 389 shows a time series plot of the temperature data and calculated values for the Clackamas River upstream boundary condition. The calculated temperatures exhibit a larger diurnal variation (1 to 4 ºC) than the data below the dam which has a diurnal variation of less than 1 ºC. The calculated temperatures better represent the mean daily temperatures than the diurnal variation. Since the river system warms significantly moving downstream errors introduced from the diurnal swings in the calculated temperatures should dampen out moving downstream.

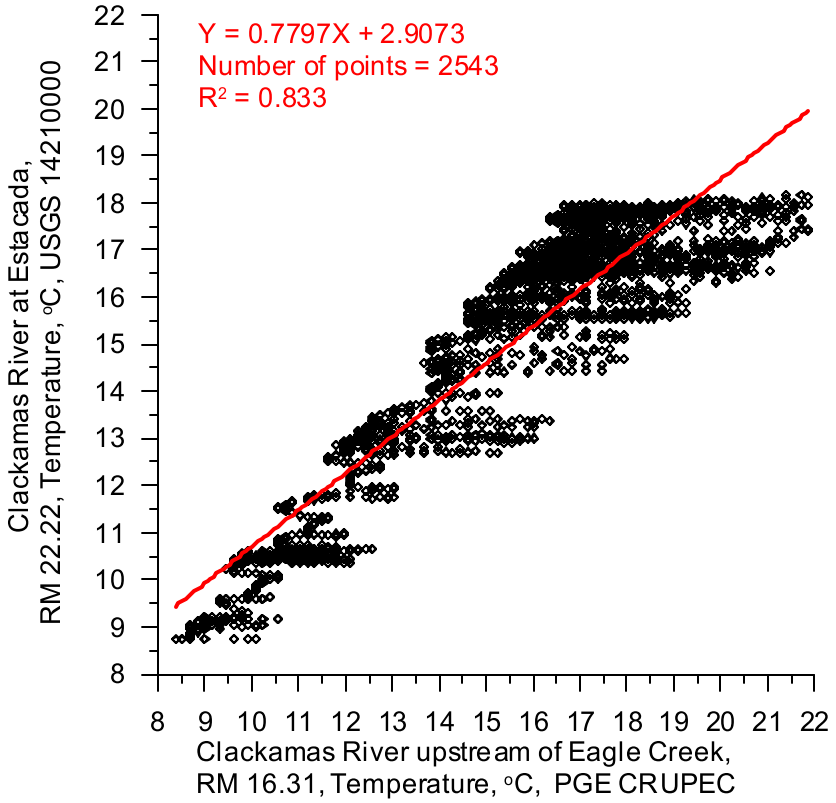


**Figure 388. Temperature correlation between Clackamas River at Estacada and upstream of Eagle Creek**

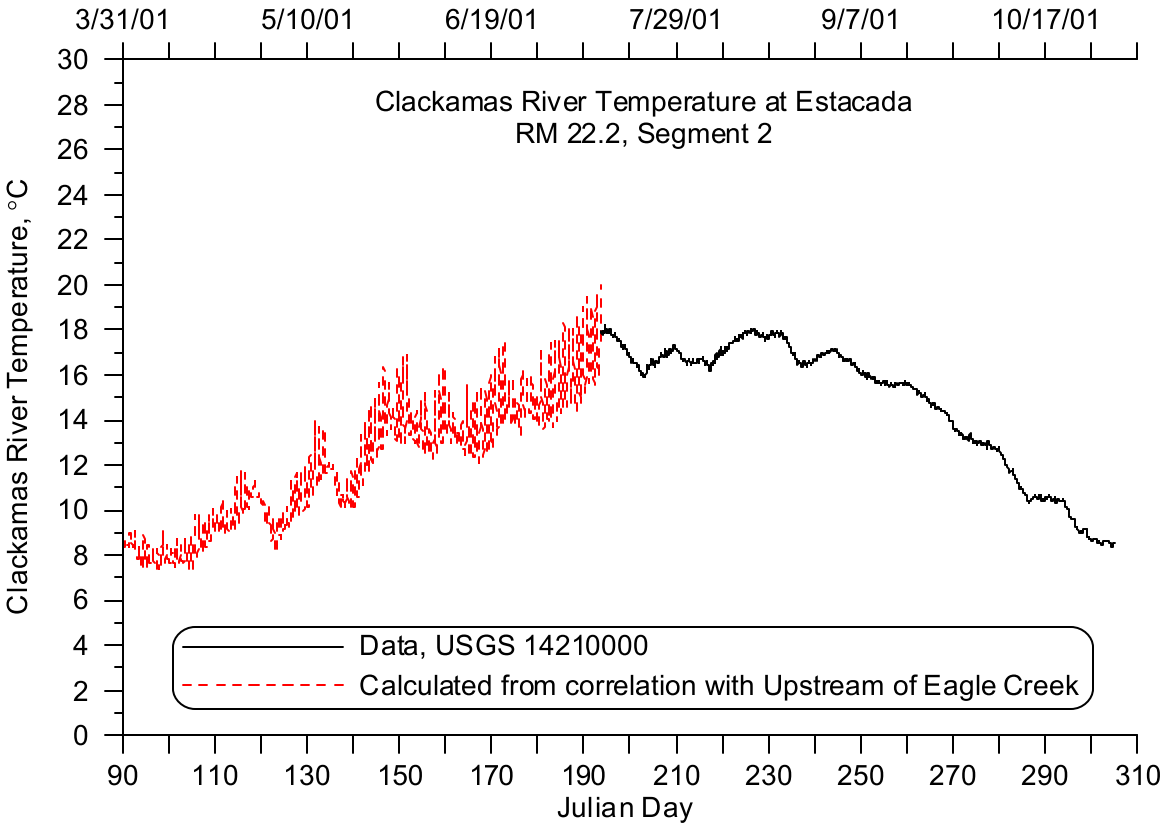


**Figure 389. Clackamas River temperature below River Mill Dam, 2001**

Year 2002

The temperature upstream boundary for the Clackamas River was developed from temperature data collected at the USGS gage station at Estacada below River Mill Dam (USGS 14210000). Figure 390 shows time series plot of the temperature data representing the model upstream boundary condition.

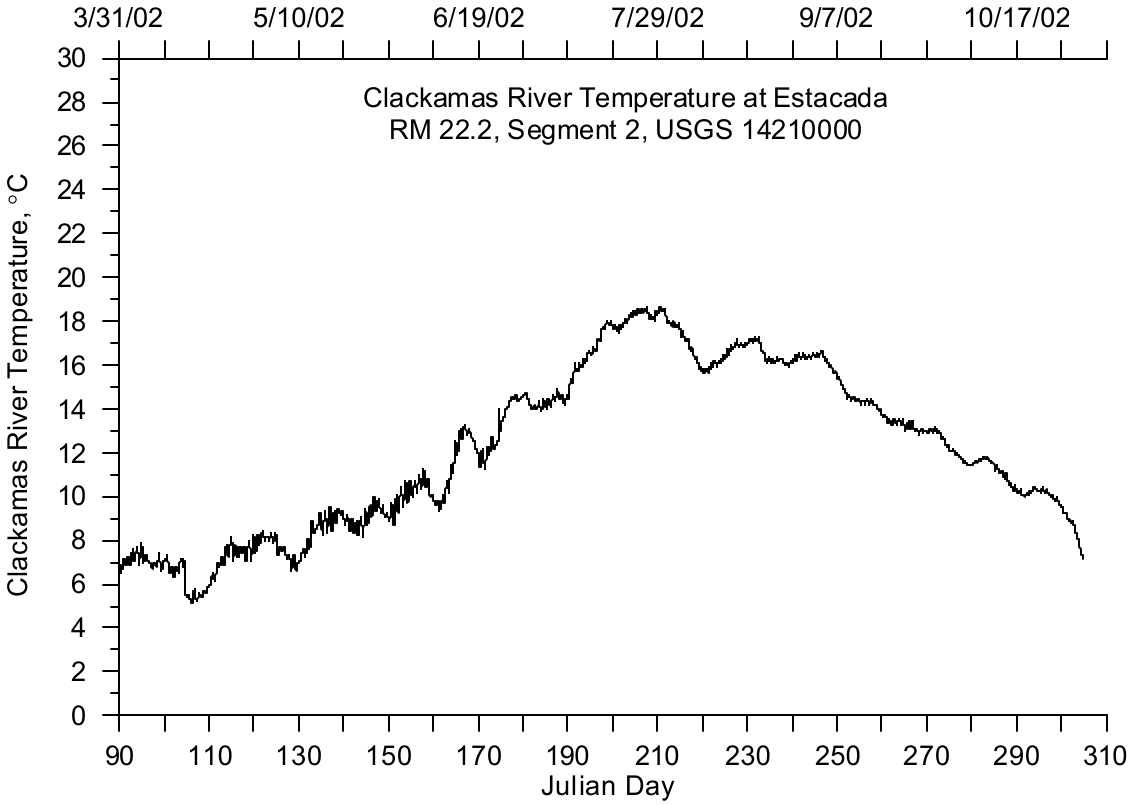


**Figure 390. Clackamas River temperature below River Mill Dam, 2002**

## *Tributaries and Distributed Tributaries*

There are four main tributaries contributing flow to the Lower Clackamas River model. Figure 391 shows the location of the tributaries along the Lower Clackamas River, and Table 43 shows the river mile and model segment location for each tributary.

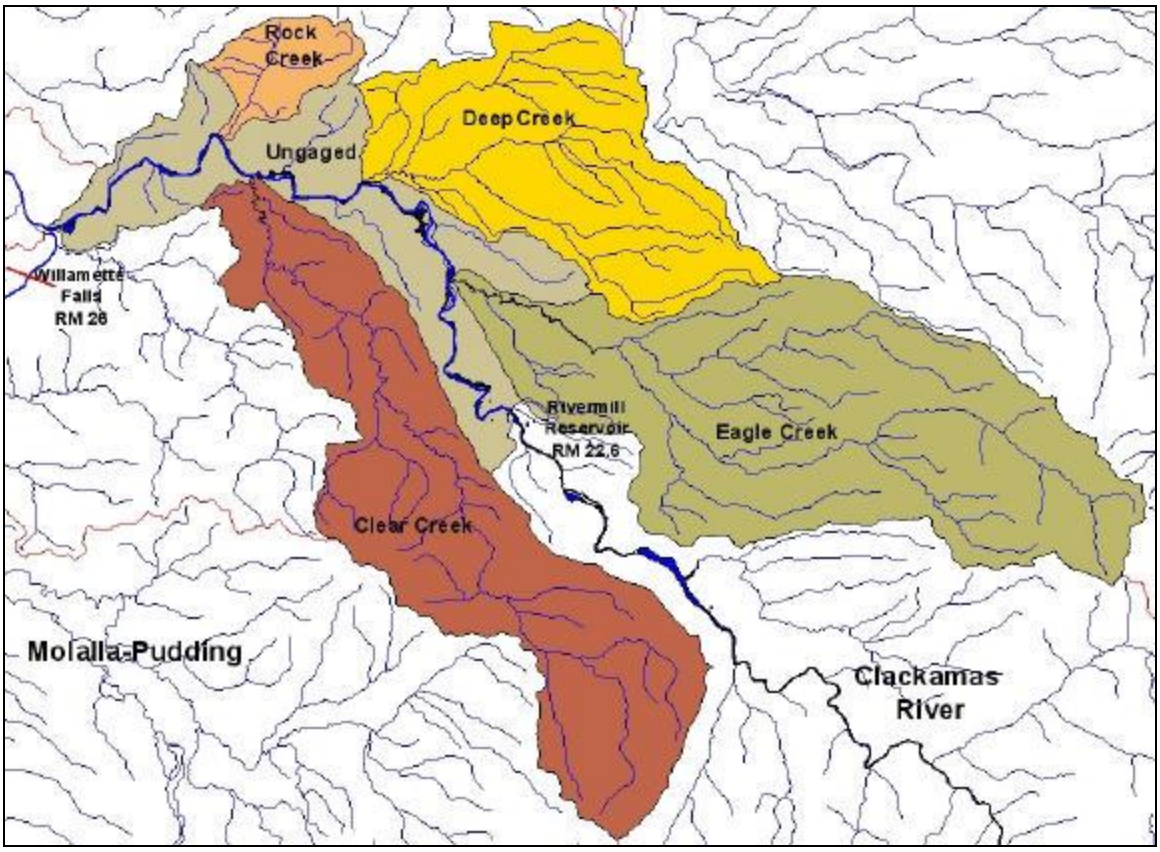


**Figure 391. Clackamas River model tributary locations**

**Table 43. Clackamas River model tributary model segments and river miles**

| Tributary | Model segment | Clackamas River Mile |
|---|---|---|
| Eagle Creek | 42 | 16.07 |
| Deep Creek | 68 | 12.15 |
| Clear Creek | 93 | 8.11 |
| Rock Creek | 105 | 6.57 |

## Hydrodynamic Data

Daily flow values were developed for Deep, Clear, and Eagle Creeks by Kent Doughty with EES, a consultant in the modeling effort for the Lower Clackamas River for Portland General Electric. The daily flow was estimated for May 1, 2000 to September 30, 2001. The daily flow estimates were then related to the daily flows at the USGS gage station at Estacada (USGS 14210000) through correlations to extend the flow information in 2001 and estimated flows for 2002.

### Year 2001

The estimated flows values for Eagle Creek were from April 1 to September 30, 2001. The gap for the month of October was filled by developing a daily flow correlation with flows at the USGS gage station at Estacada (USGS 14210000). Figure 392 shows the flow correlation between the daily flows

estimated for Eagle Creek and measured at the USGS gage station. Figure 393 shows a time series plot of the daily flow for Eagle Creek including the calculated values from the correlation. Summer flows were typically less than 2 $m^3/s$, with peak spring flows exceeding 20 $m^3/s$.

The estimated flows values for Deep Creek were from April 1 to September 30, 2001. The gap for the month of October was filled by developing a daily flow correlation with flows at the USGS gage station at Estacada (14210000). Figure 394 shows the flow correlation between the daily flows estimated for Deep Creek and measured at the USGS gage station. Figure 395 shows a time series plot of the daily flow for Deep Creek including the calculated values from the correlation. Summer flows were typically less than 1 $m^3/s$, with peak spring flows exceeding 6 $m^3/s$.

The estimated flows values for Clear Creek went from April 1 to September 30, 2001. The gap for the month of October was filled by developing a daily flow correlation with flows at the USGS gage station at Estacada (14210000). Figure 396 shows the flow correlation between the daily flows estimated for Clear Creek and measured at the USGS gage station. Figure 397 shows a time series plot of the daily flow for Clear Creek including the calculated values from the correlation. Summer flows were typically less than 2 $m^3/s$, with peak spring flows exceeding 10 $m^3/s$.

Rock Creek was ungaged and there were no daily flows estimated for the basin. The fractional flow from the Deep Creek basin was taken to estimate the flows for Rock Creek. The Deep Creek basin was selected for its proximity to the Rock Creek basin and because both basins are on the north side of the catchment and are more likely to share similar topography and rainfall patterns. The Rock Creek basin area (0.021 $km^2$) is 16.57% of the Deep Creek basin area (0.127 $km^2$). The flow for the Deep Creek basin was multiplied by the fraction of basin areas and is shown in Figure 398.

Since there were some ungaged and distributed drainage areas along the lower Clackamas River an effort was made to characterize these distributed flows. There was a USGS gage station (14211010) installed in the Clackamas River at Oregon City (RM 2.4) starting June 8, 2001. The hydrology between the two USGS gage stations at Estacada and Oregon City was analyzed using the daily estimated tributary inflows. The daily tributary flows and the daily upstream flow at Estacada were summed and then subtracted from the flow measured at Oregon City to estimate any additional inflow to the river attributable to the ungaged drainage areas. Since the methodology could be used after June 8, the data gap from April 1 to June 8 was filled by creating a flow correlation between the daily flows at Estacada (USGS 14210000) and the distributed flow that were calculated for later in the year. Figure 399 shows the flow correlation between the two sets of information. The correlation was then used to calculate the daily flow for the distributed drainage areas between April 1 and June 8. The total distributed flow was then divided in two based on the lengths of the two model branches. Model Branch 1 was 14.39 miles long and Branch 2 was 7.94 miles long of 22.33 miles. Figure 400 shows a time series plot of the estimated distributed flow for each of the two model branches.

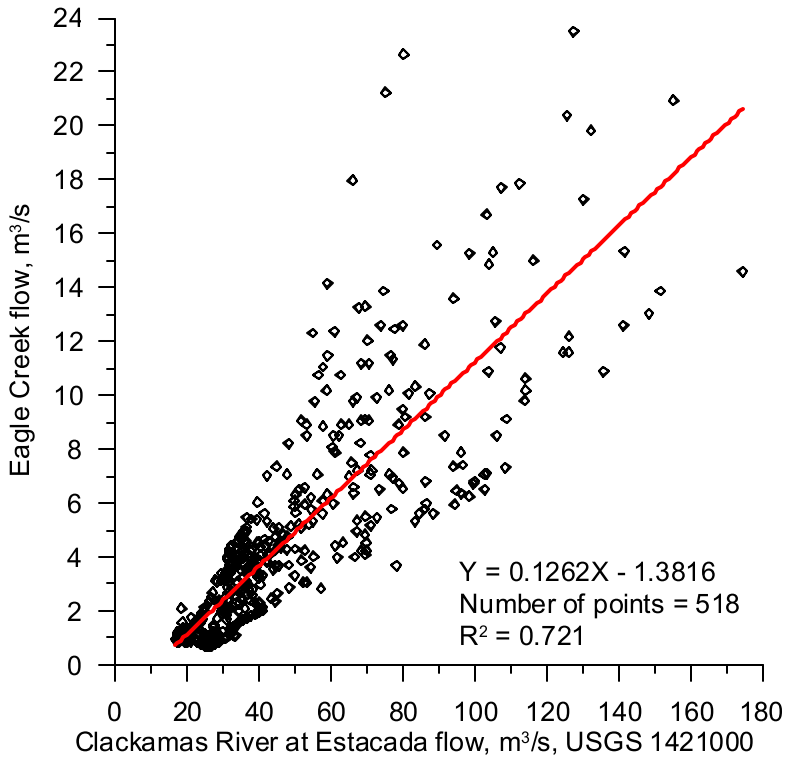


**Figure 392. Flow correlation between Eagle Creek and the Clackamas River at Estacada**

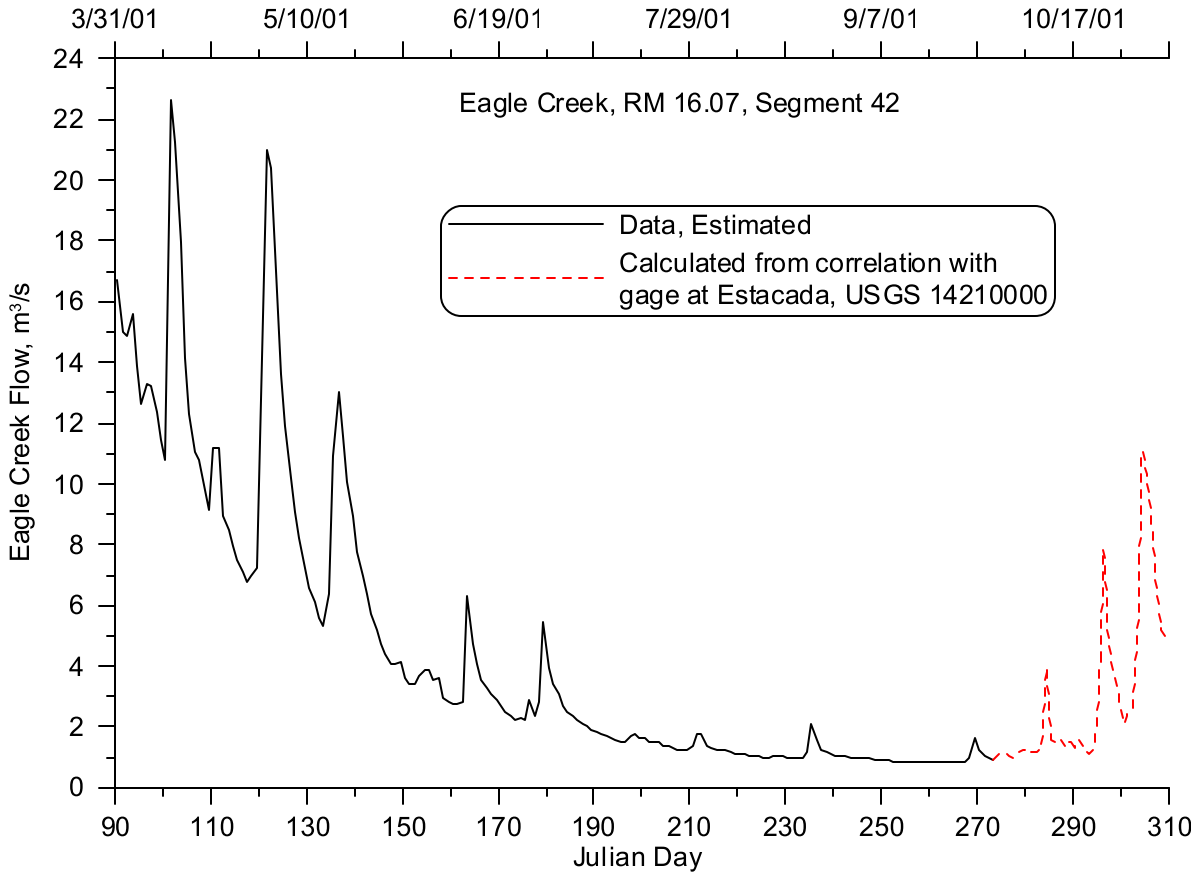


**Figure 393. Eagle Creek flow, 2001**

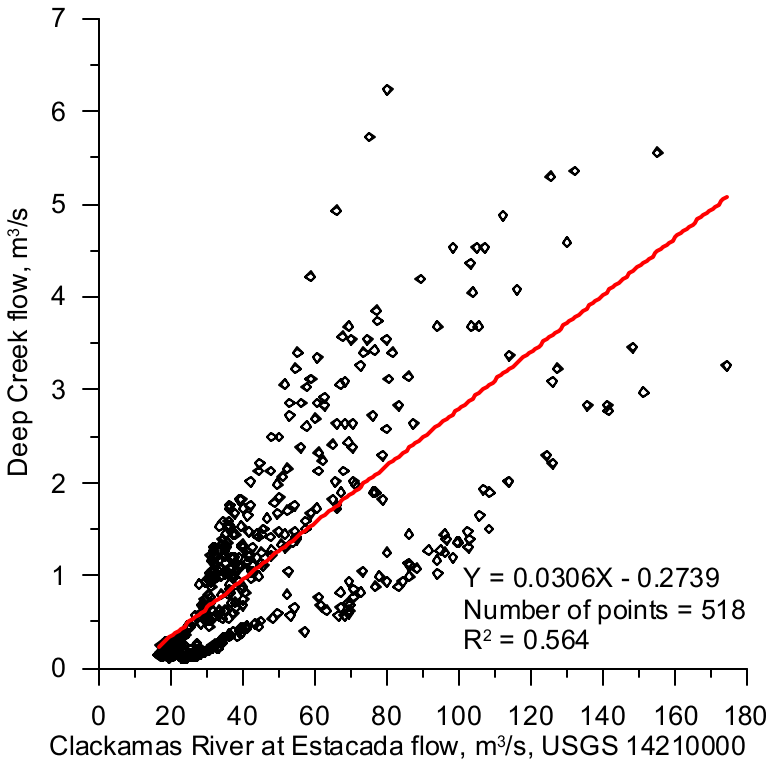


**Figure 394. Flow correlation between Deep Creek and the Clackamas River at Estacada**

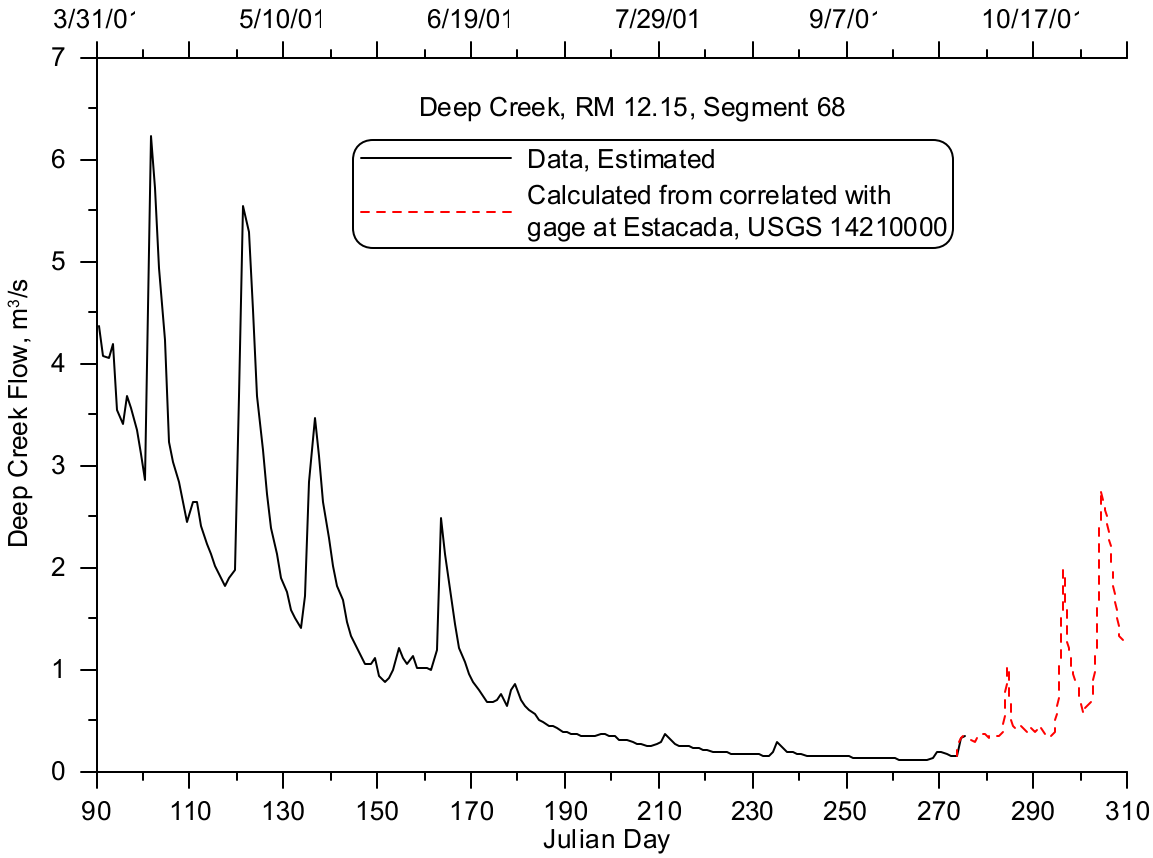


**Figure 395. Deep Creek flow, 2001**

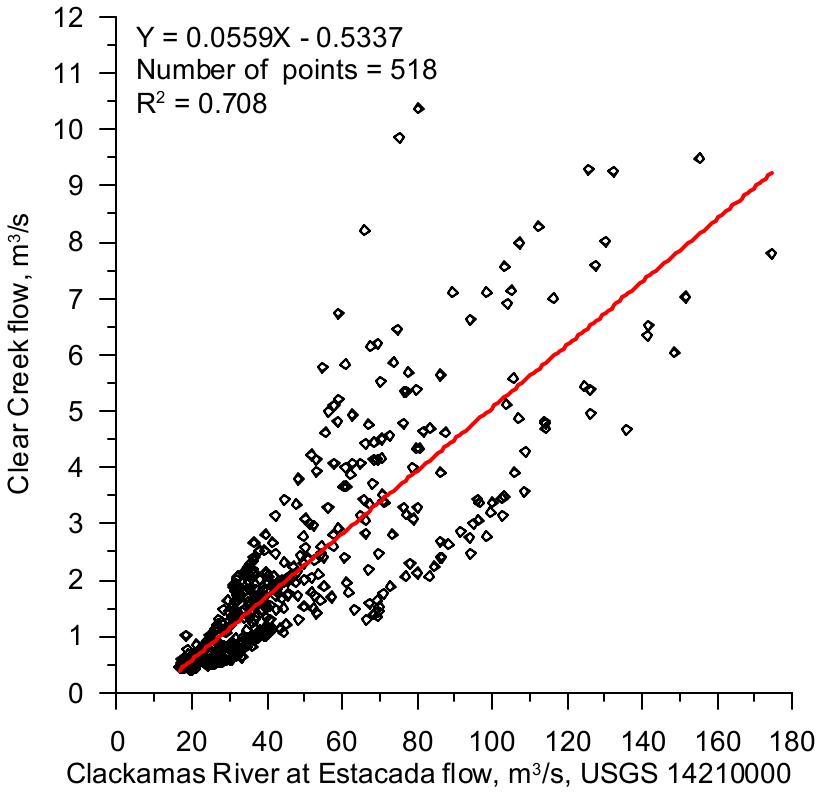


**Figure 396. Flow correlation between Clear Creek and the Clackamas River at Estacada**

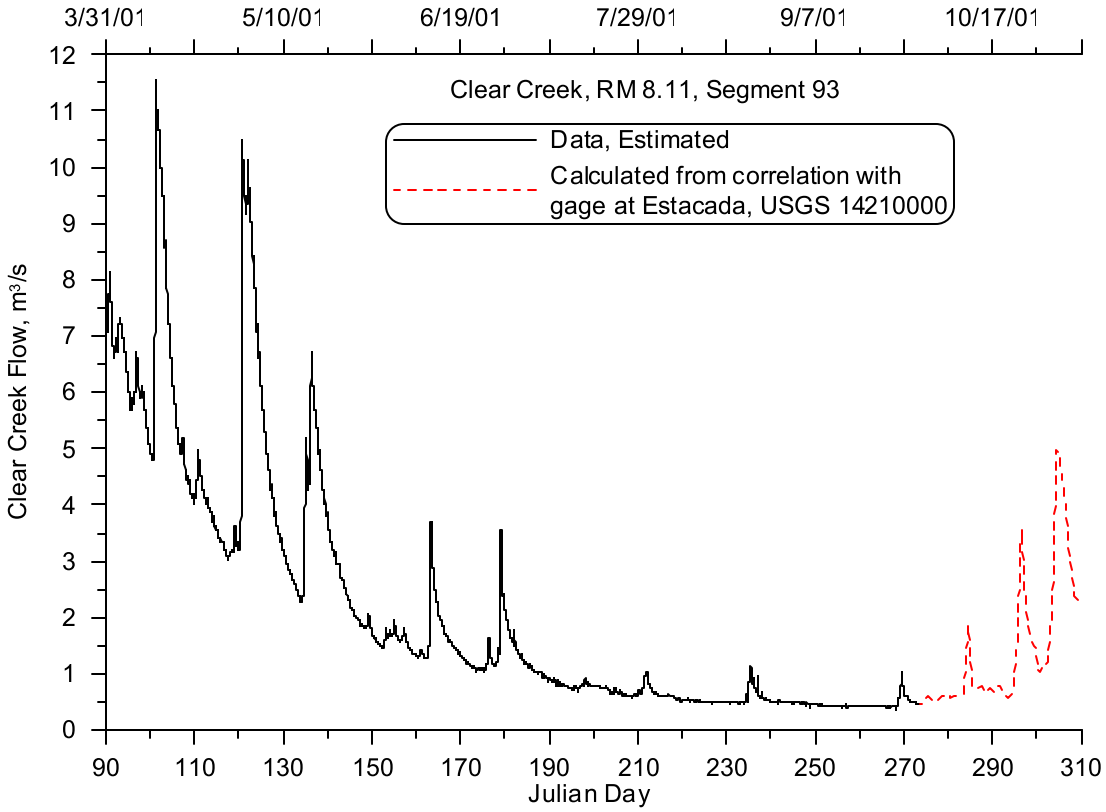


**Figure 397. Clear Creek flow, 2001**

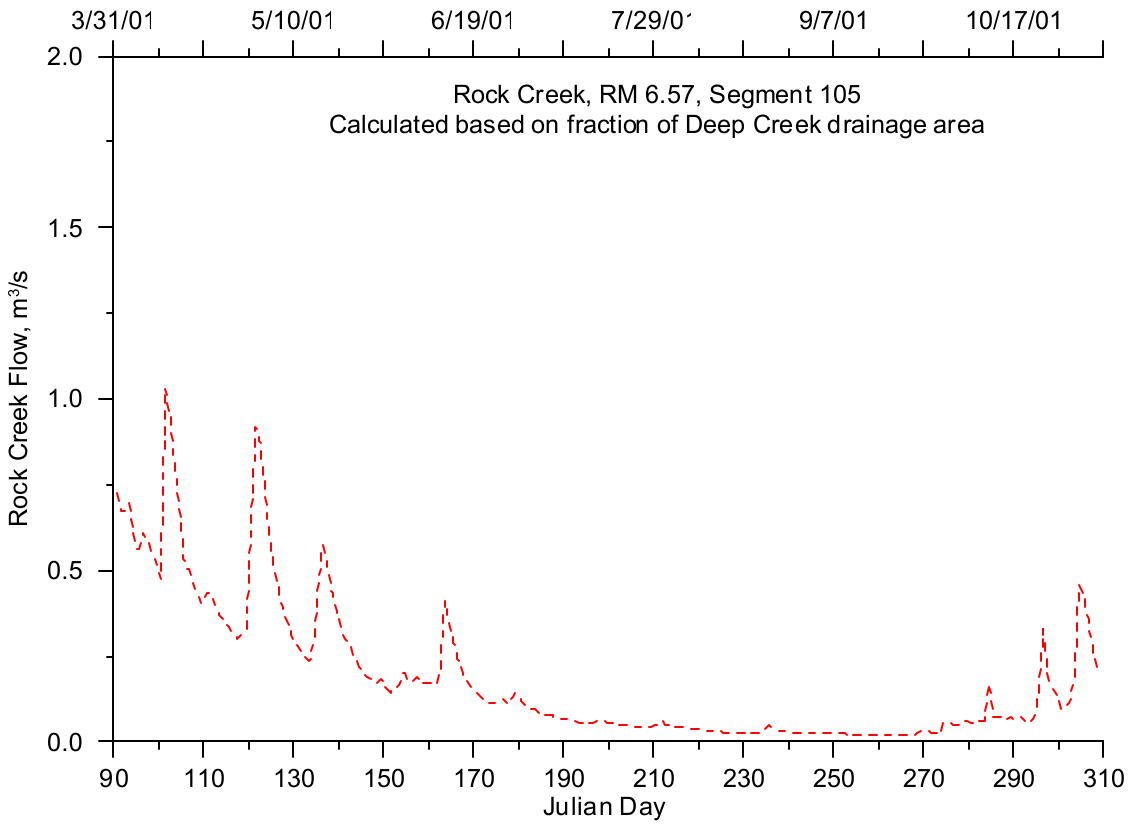


**Figure 398. Rock Creek flow, 2001**

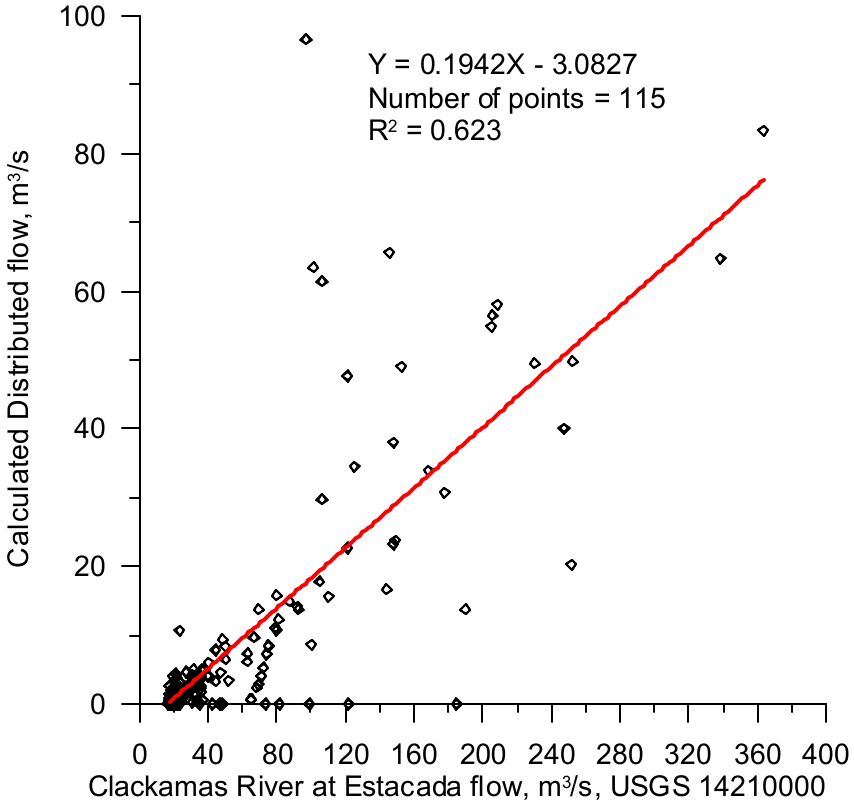


**Figure 399. Flow correlation between distributed areas (calculated) and the Clackamas River at Estacada**

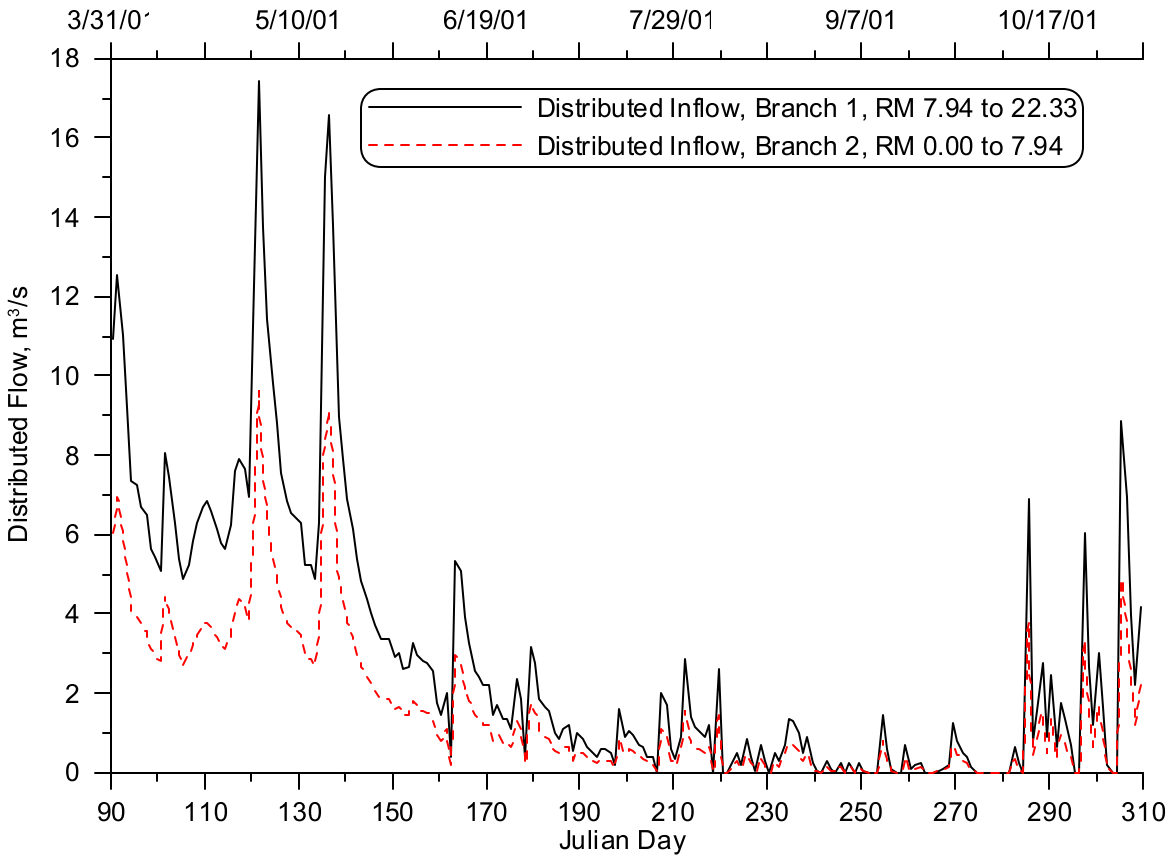


**Figure 400. Distributed flow, 2001**

## Year 2002

There were no flow estimates made for 2002 for the four large tributaries entering the Clackamas River so the flow correlations developed for the 2001 flow file development were used to develop the 2002 flow time series.

The Eagle Creek flow for 2002 was developed using the flow correlation, shown in Figure 392, and the daily flow values from the USGS gage station at Estacada (USGS 14210000). Figure 401 shows the flow time series for Eagle Creek in 2002. Typical summer flows were less than 5 $m^3/s$, with single peak spring flows exceeding 60 $m^3/s$.

Deep Creek flows for 2002 were developed using the flow correlation, shown in Figure 394, and the daily flow values from the USGS gage station at Estacada (USGS 14210000). Figure 402 shows the flow time series for Deep Creek. Typical summer flows were less than 1 $m^3/s$, with a single spring storm flow reaching 15 $m^3/s$.

Clear Creek flows for 2002 were developed using the flow correlation, shown in Figure 396, and the daily flow values from the USGS gage station at Estacada (USGS 14210000). Figure 403 shows the flow time series for Clear Creek. Summer flows were generally less than 2 $m^3/s$, with a single spring storm flow reaching 27 $m^3/s$.

Rock Creek was ungaged and there were no daily flows estimated for the basin. The fractional flow from the Deep Creek basin was taken to estimate the flows for Rock Creek. The Rock Creek basin area

(0.021 $km^2$) is 16.57% of the Deep Creek basin area (0.127 $km^2$). The flow for the Deep Creek basin was multiplied by the fraction of basin areas and is shown in Figure 404. Typical Rock Creek summer flows were less than 0.25 $m^3/s$ with spring storm flows near 2.5 $m^3/s$.

The distributed flows calculated for 2002 were based on the same methodology as introduced in estimating the 2001 flow. Since there were data collected at the Oregon City USGS gage station (USGS 14211010) for the whole year, no correlation was needed. The total distributed flow was then divided based on the lengths of the two model branches. Model Branch 1 was 14.39 miles long and Branch 2 was 7.94 miles long of a total of 22.33 miles. Figure 400 shows a time series plot of the estimated distributed flow for each of the two model branches. If the calculated flows were negative they were set to zero.

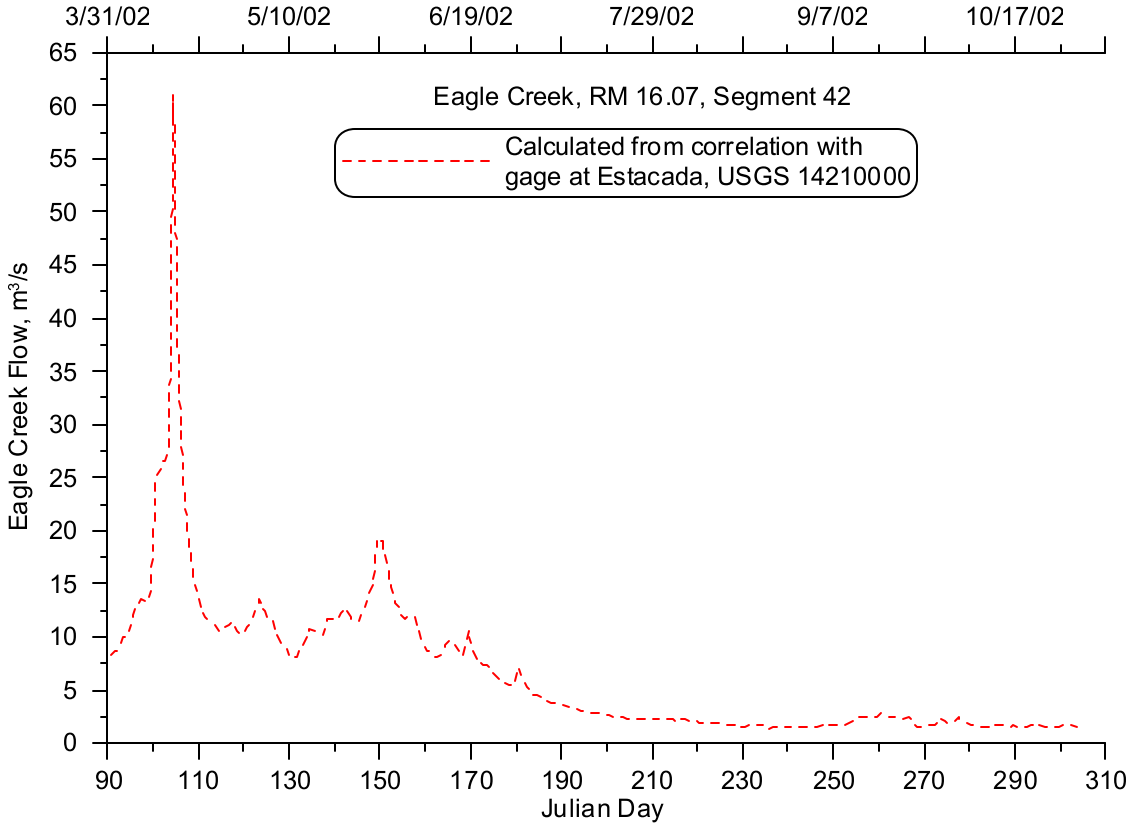


**Figure 401. Eagle Creek flow, 2002**

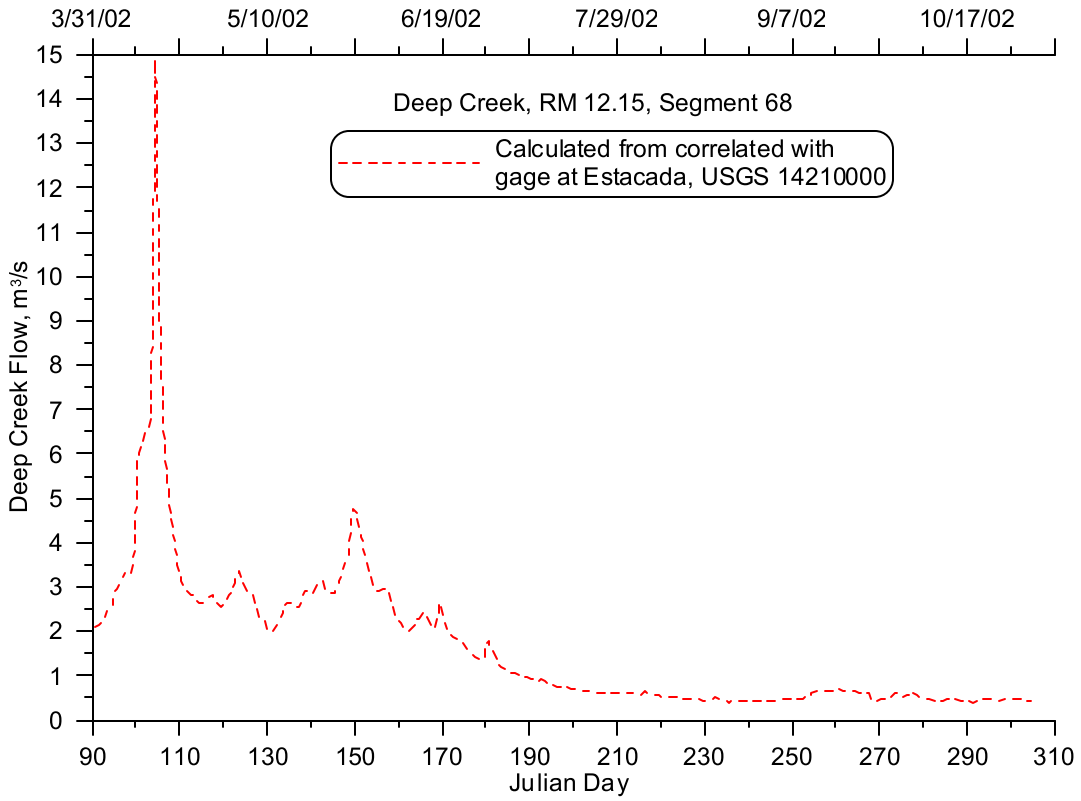


**Figure 402. Deep Creek flow, 2002**

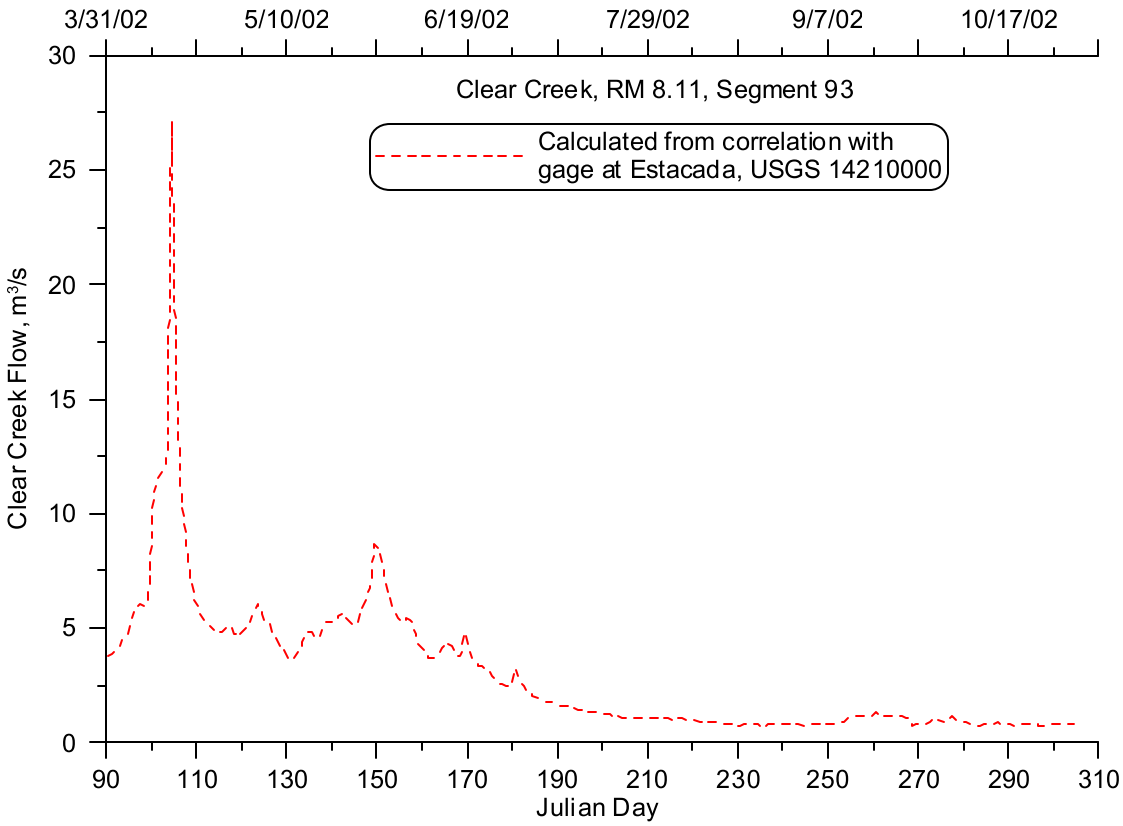


**Figure 403. Clear Creek flow, 2002**

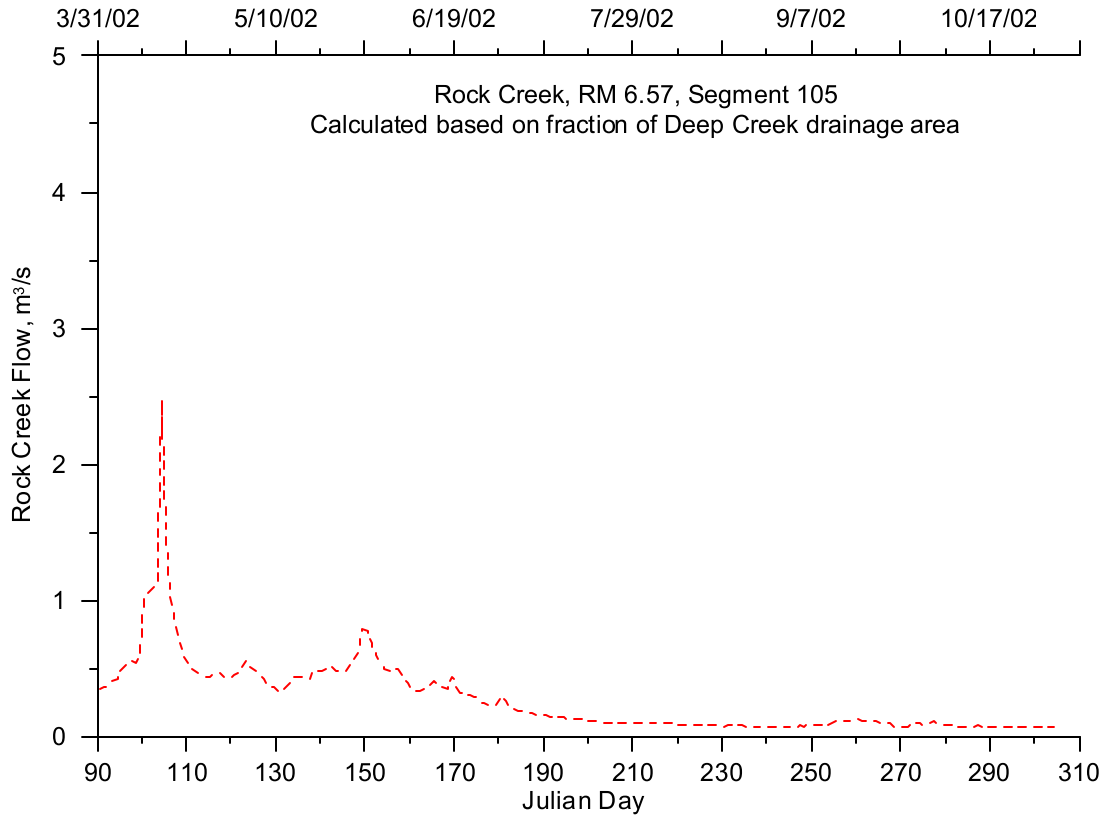


**Figure 404. Rock Creek flow, 2002**

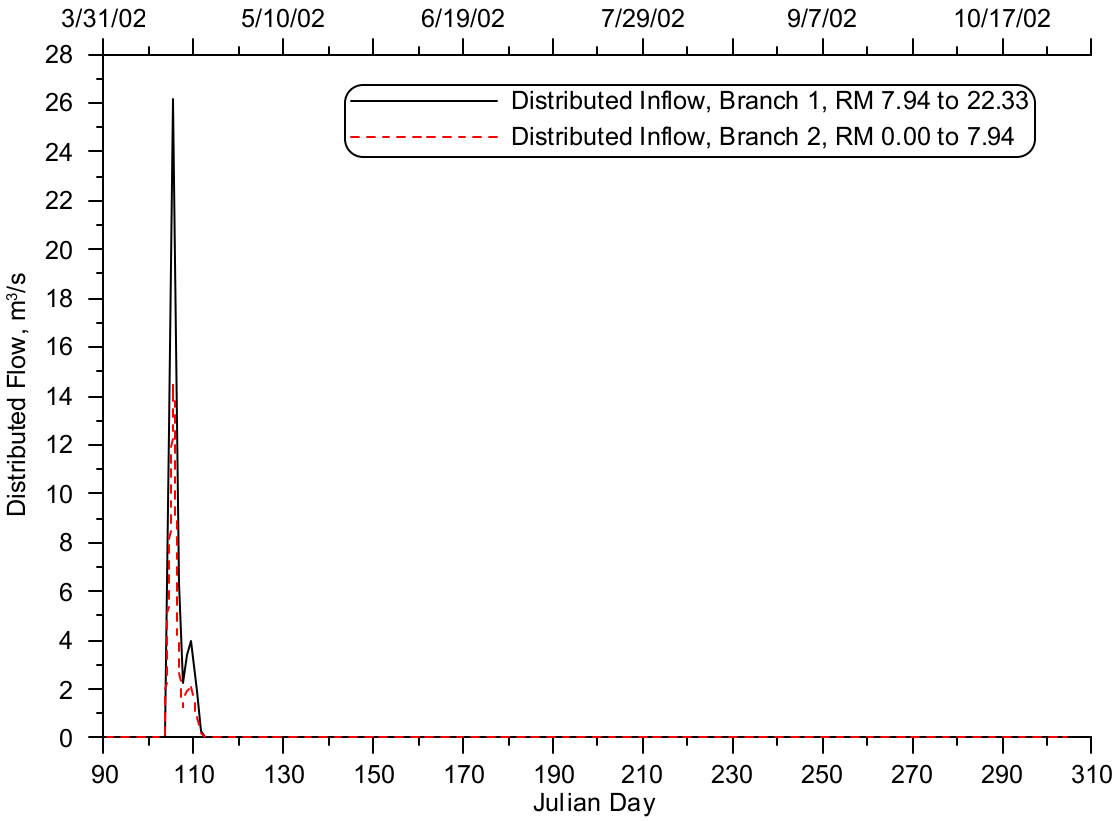


**Figure 405. Distributed flow, 2002**

## Temperature Data

Portland General Electric, as part of their hydroelectric re-licensing effort, implemented temperature monitoring in 2000 through 2002 for several tributaries along the Lower Clackamas River. Figure 406 shows the location of the PGE, USGS, and ODEQ temperature monitoring sites and Table 44 lists these sites and their locations.

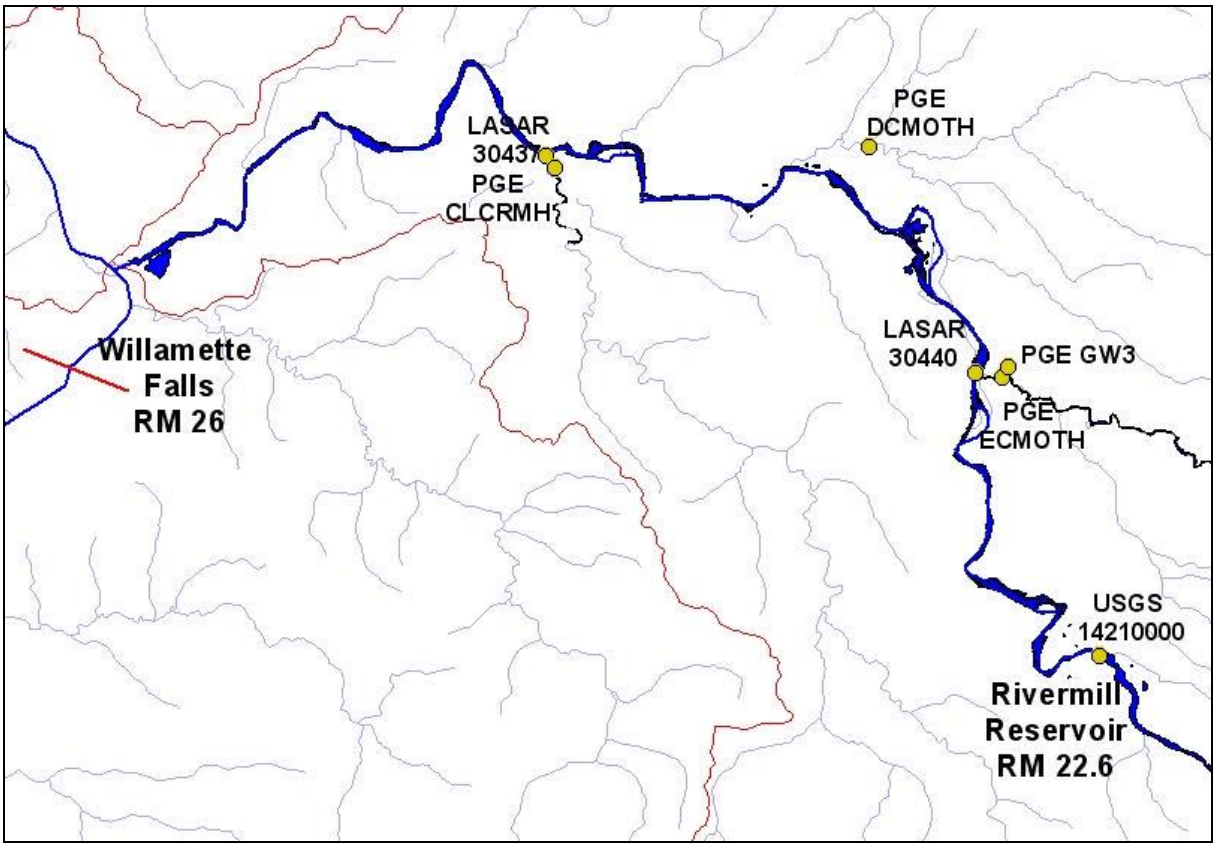


**Figure 406. Clackamas River model tributary temperature monitoring site locations**

**Table 44. Clackamas River model tributary temperature monitoring sites**

| Site ID | Tributary | RM | Model Segment |
|---|---|---|---|
| PGE ECMOTH | Eagle Creek at mouth | 16.07 | 42 |
| USGS 14210000 | Clackamas River at Estacada | 22.2 | NA |
| PGE DCMOTH | Deep Creek at mouth | 12.15 | 68 |
| PGE CLCRMH | Clear Creek at mouth | 8.11 | 93 |
| PGE GW3 | Groundwater monitoring site | 0 to 22.33 | NA |
| LASAR 30440 | Eagle Creek at mouth | 16.07 | 42 |
| LASAR 30437 | Clear Creek at mouth | 8.11 | 93 |

### Year 2001

The temperature monitoring site on Eagle Creek (PGE ECMOTH) recorded data from January 1 to October 26, 2001. The data gap from October 26 to 31, 2001, was filled by developing a temperature

correlation between the Eagle Creek site and the USGS gage on the Clackamas River at Estacada (USGS 14210000). Figure 407 shows the temperature correlation for the two sites. Figure 408 shows the temperature time series for Eagle Creek, including both the data and the calculated values based on the correlation. Stream temperatures had a diurnal variation of 1 to 4 ºC with a peak summer temperature of approximately 22 ºC.

Stream temperatures on Deep Creek were recorded from April 19 to October 26, 2001 at a monitoring site at the mouth (PGE DCMOTH). A temperature correlation was developed between Eagle Creek and Deep Creek to fill the data gap in April. Figure 409 shows the temperature correlation between the two sites. Since the Eagle temperature data were also limited to October 26 this data set could not be used to fill in the data gap for Deep Creek from October 26 to 31. A second temperature correlation was developed between Deep Creek and the Clackamas River at Estacada (USGS 14210000). Figure 410 shows the temperature correlation between these two sites. Figure 411 shows the temperature time series for Deep Creek with the data and two sets of calculated values. Temperatures had a diurnal variation of 1 to 4 ºC with a peak summer temperature of about 22 ºC.

Clear Creek temperatures were recorded from January 1 to October 26, 2001 (PGE CLCRMH). The data gap from October 26 to 31, 2001, was filled by developing a temperature correlation between the Clear Creek site and the USGS gage on the Clackamas River at Estacada (USGS 14210000). Figure 412 shows the temperature correlation for the two sites. Figure 413 shows the temperature time series for Clear Creek, including both the data and the calculated values based on the correlation. The Clear Creek water temperature had a diurnal variation of 1 to 4 ºC with a peak summer temperature of approximately 24 ºC.

Since Rock Creek was ungaged for temperature, stream temperatures from Deep Creek were used. The Deep Creek basin was selected for its proximity to the Rock Creek basin and because both basins are on the north side of the catchment and are more likely to share similar topography and rainfall patterns.

PGE had one groundwater monitoring site in the lower Clackamas River reach during 2001 (PGE GW3). This site had grab sample temperature data taken several times during the year. Since there were no other temperature data available, these data were used to represent the distributed inflow temperature for the 22.33 miles of the lower Clackamas River. Figure 414 shows a time series of the groundwater data collected. The value shown on April 1 represents a linearly interpolated value based on data collected on January 18 and August 14, 2001.

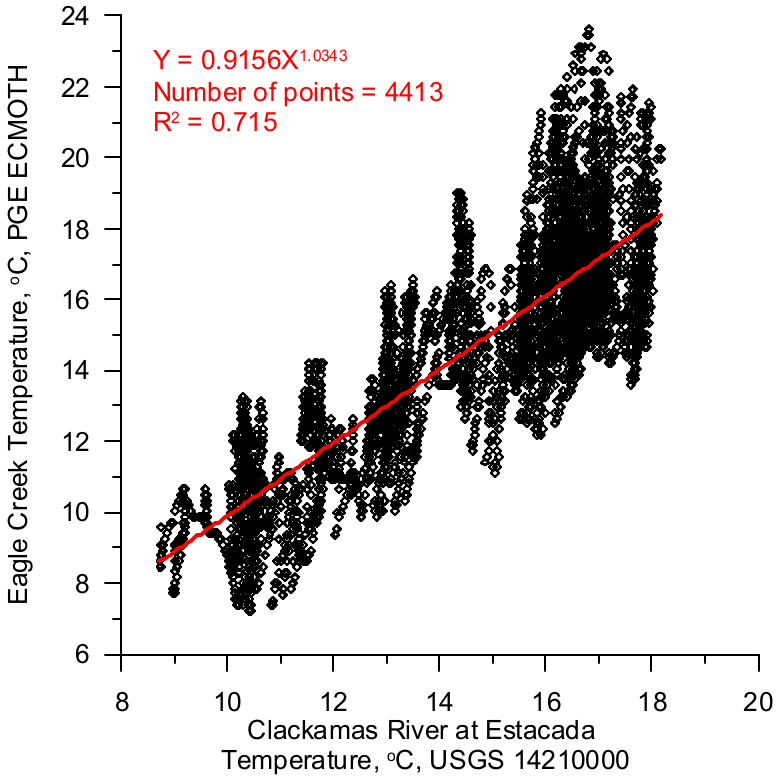


**Figure 407. Temperature correlation between Eagle Creek and the Clackamas River at Estacada**

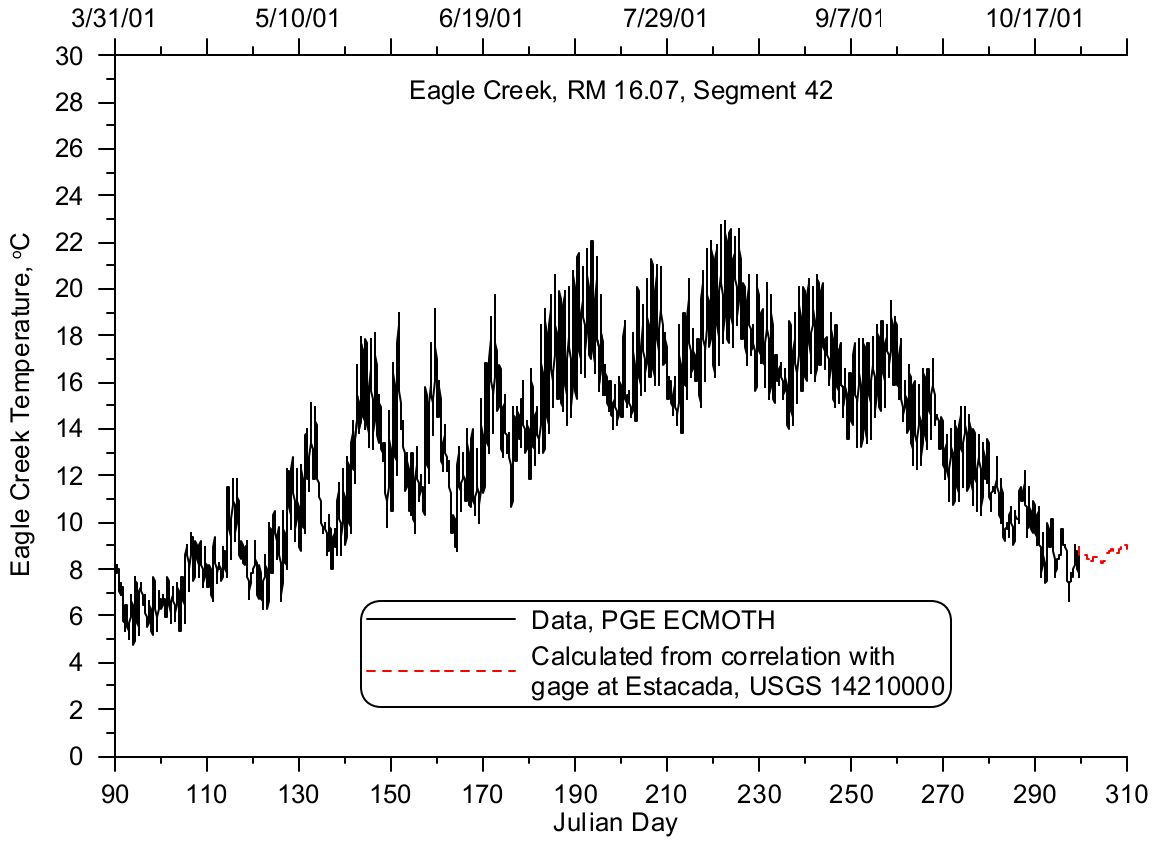


**Figure 408. Eagle Creek temperature, 2001**

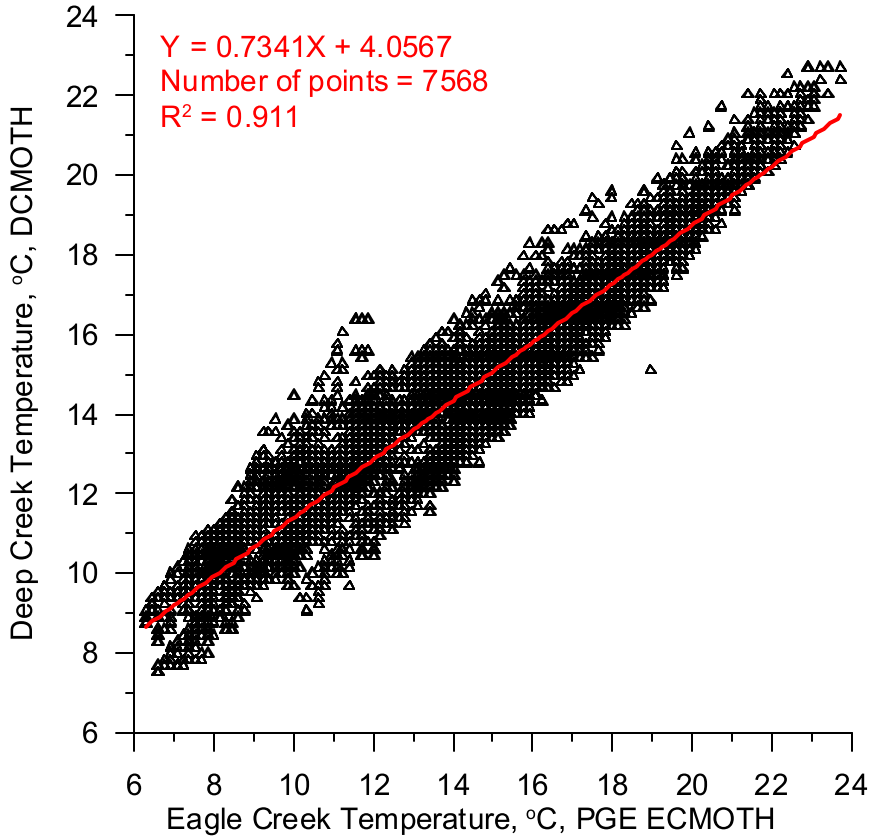


**Figure 409. Temperature correlation between Deep Creek and Eagle Creek**

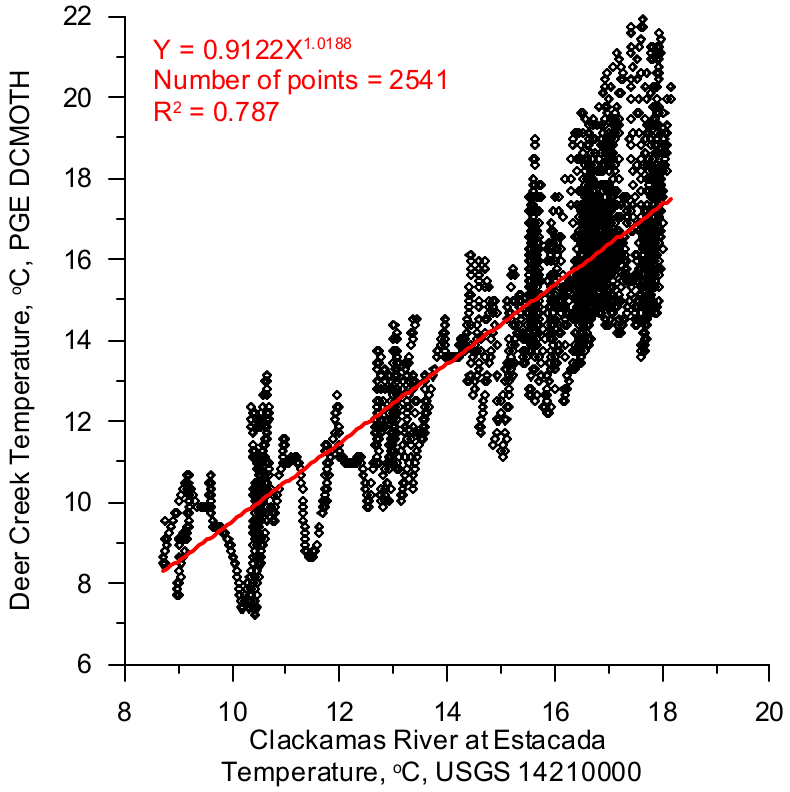


**Figure 410. Temperature correlation between Deep Creek and the Clackamas River at Estacada**

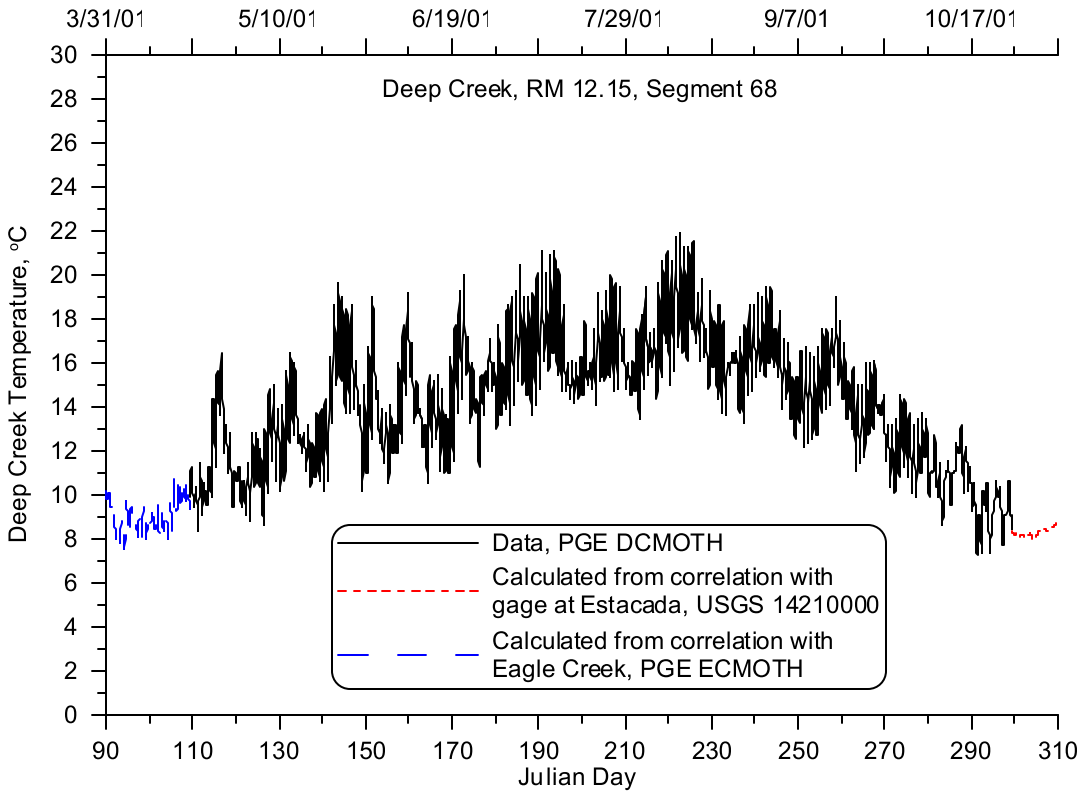


**Figure 411. Deep Creek temperature, 2001**

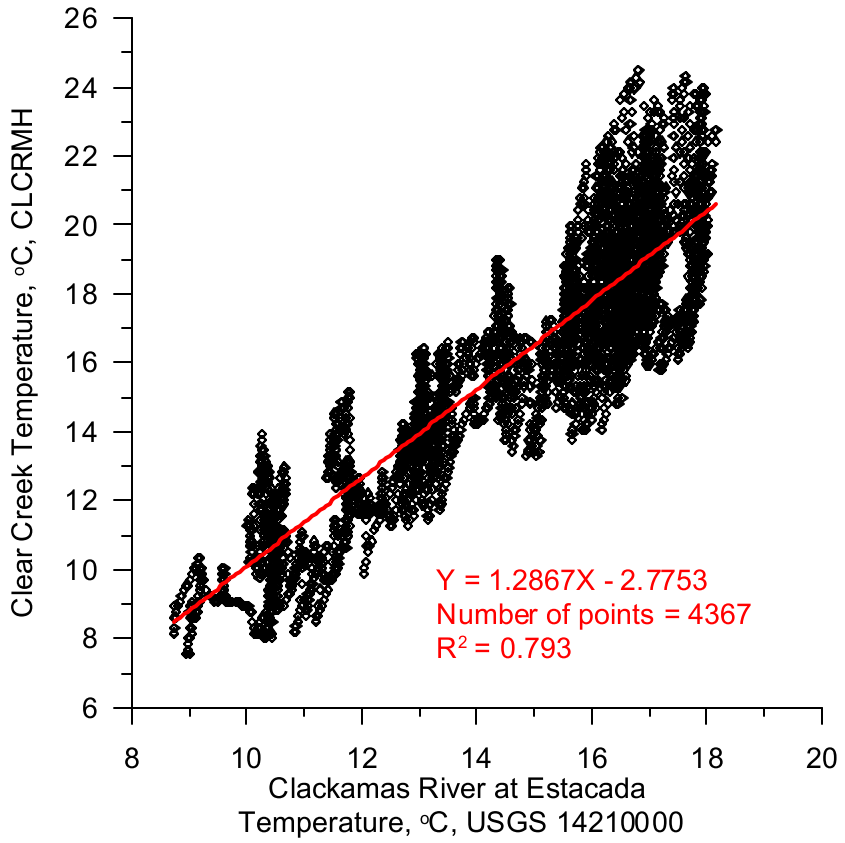


**Figure 412. Temperature correlation between Clear Creek and the Clackamas River at Estacada**

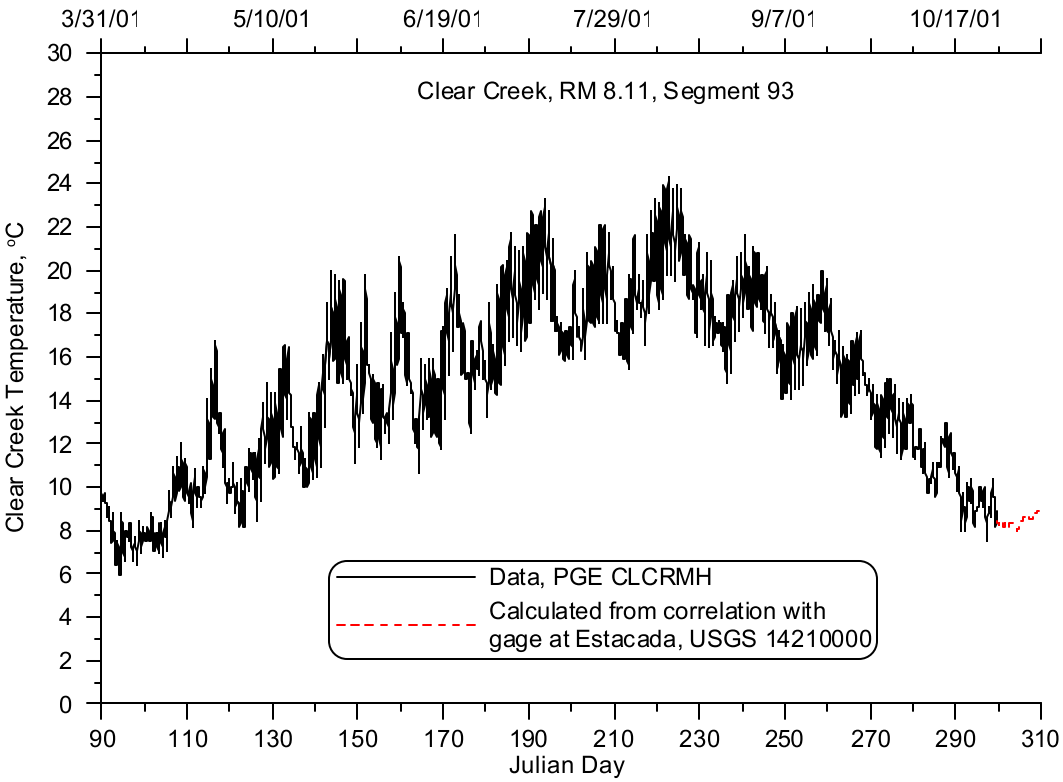


**Figure 413. Clear Creek temperature, 2001**

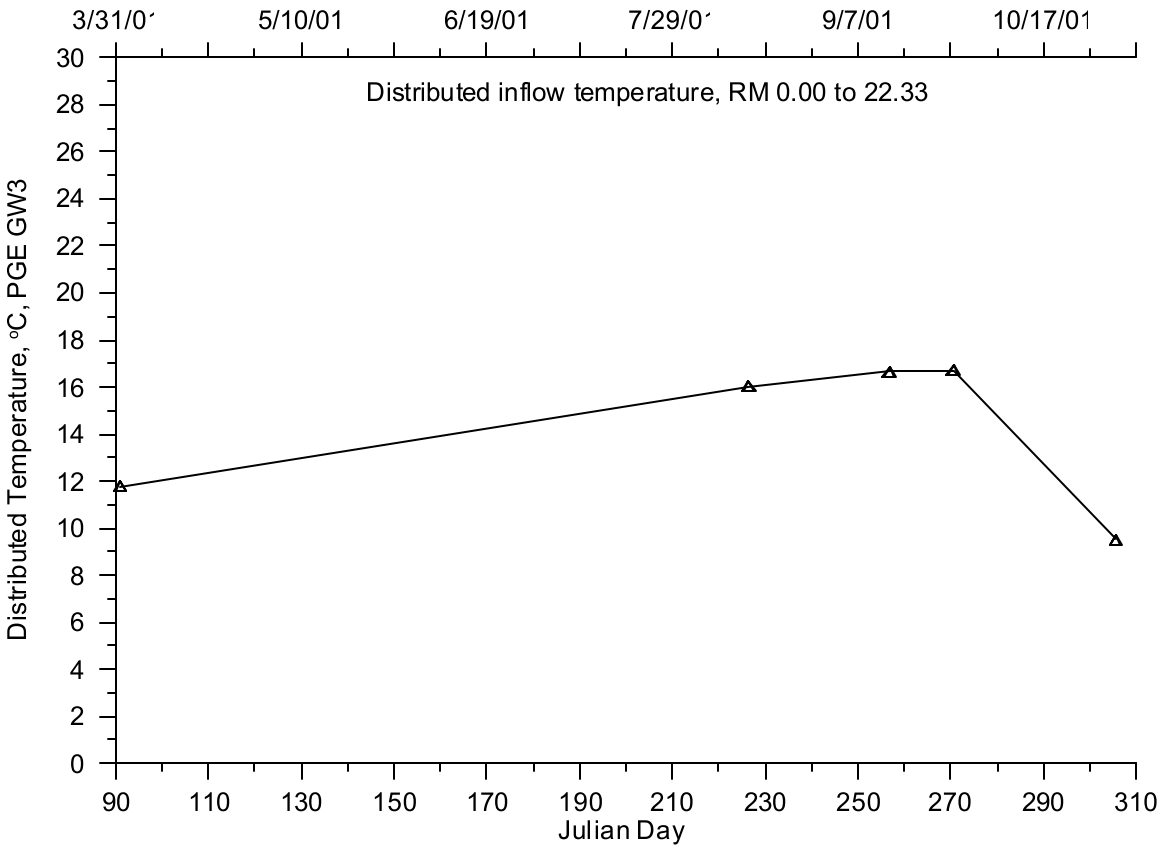


**Figure 414. Distributed inflow temperature, 2001**

## Year 2002

Eagle Creek was monitored at the mouth, as in 2001, and data were recorded from August 7 to October 24 (LASAR 30440). The data gaps from April to August and from October 24 to 31 were filled using the temperature correlation with the Clackamas River at Estacada developed for 2001, shown in Figure 407. Figure 415 shows the temperature time series for Eagle Creek including the data and calculated values. Eagle Creek water temperature had a diurnal variation of 1 to 5 ºC with a peak summer temperature of approximately 23 ºC.

Deep Creek was not monitored in 2002, so the temperature correlation developed between Deep Creek and the Clackamas River at Estacada (USGS 14210000) was used to calculate stream temperatures. Figure 416 shows a temperature time series plot for Deep Creek with the calculated values. The Deep Creek water temperature had a diurnal variation of 1 to 2 ºC with a peak summer temperature of approximately 18 ºC.

Clear Creek was monitored at the mouth, as in 2001, and data were from August 7 to October 22 (LASAR 30437). The data gaps from April to August and from October 22 to 31 were filled using the temperature correlation with the Clackamas River at Estacada (USGS 14210000), shown in Figure 412. Figure 417 shows the temperature time series for Clear Creek including the data and calculated values. Clear Creek water temperatures had a diurnal variation of 1 to 4 ºC with a peak summer temperature of approximately 24 ºC.

As in 2001, Rock Creek was ungaged for temperature, so stream temperatures from Deep Creek were used.

There were no groundwater monitoring data collected in the lower Clackamas River basin area during 2002. The temperature time series for the distributed inflow was developed by using 2000 groundwater data monitored at PGE site GW3. Figure 418 shows a time series of the groundwater data monitored in 2000 but used for the 2002 model simulation.

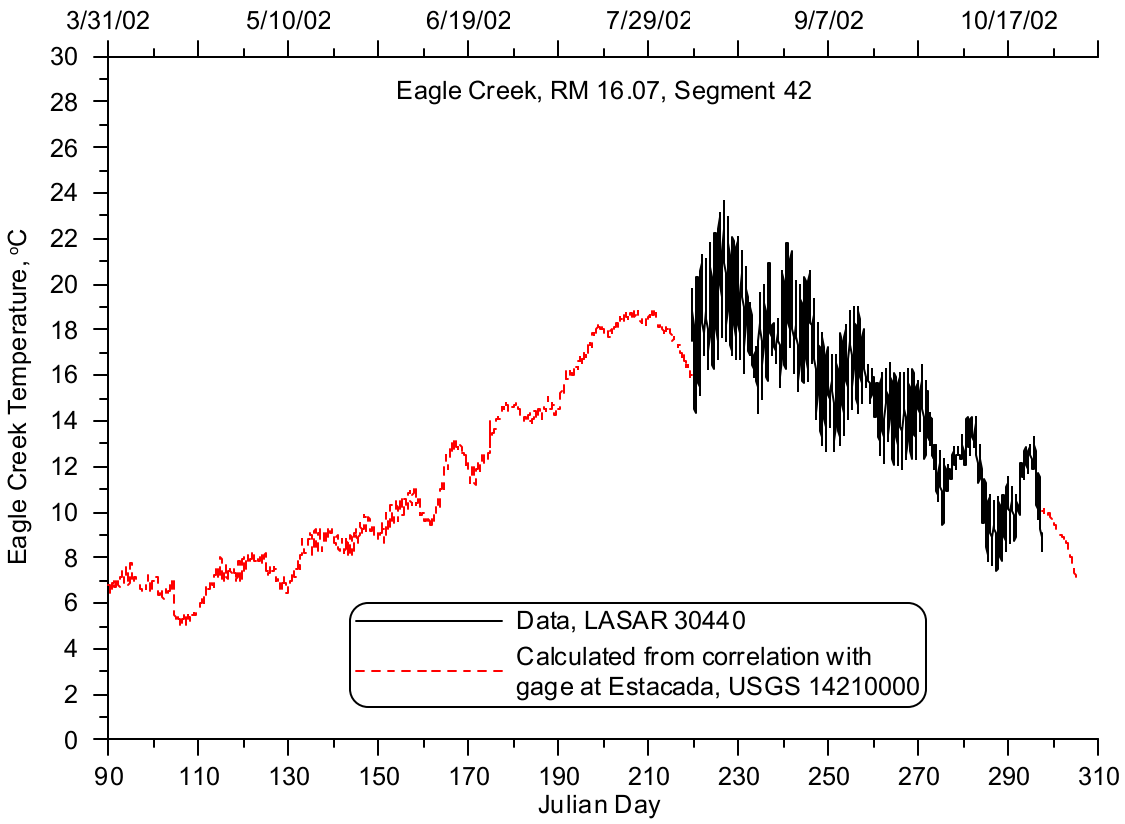


**Figure 415. Eagle Creek temperature, 2002**

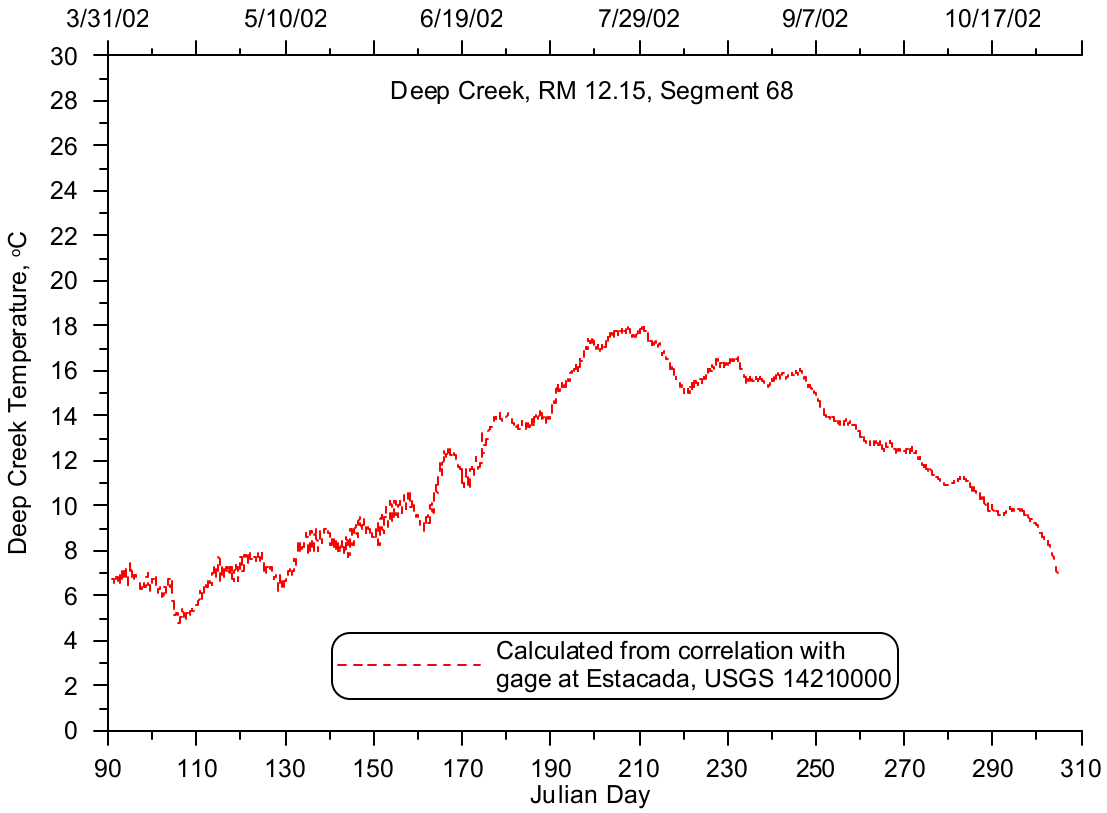


**Figure 416. Deep Creek temperature, 2002**

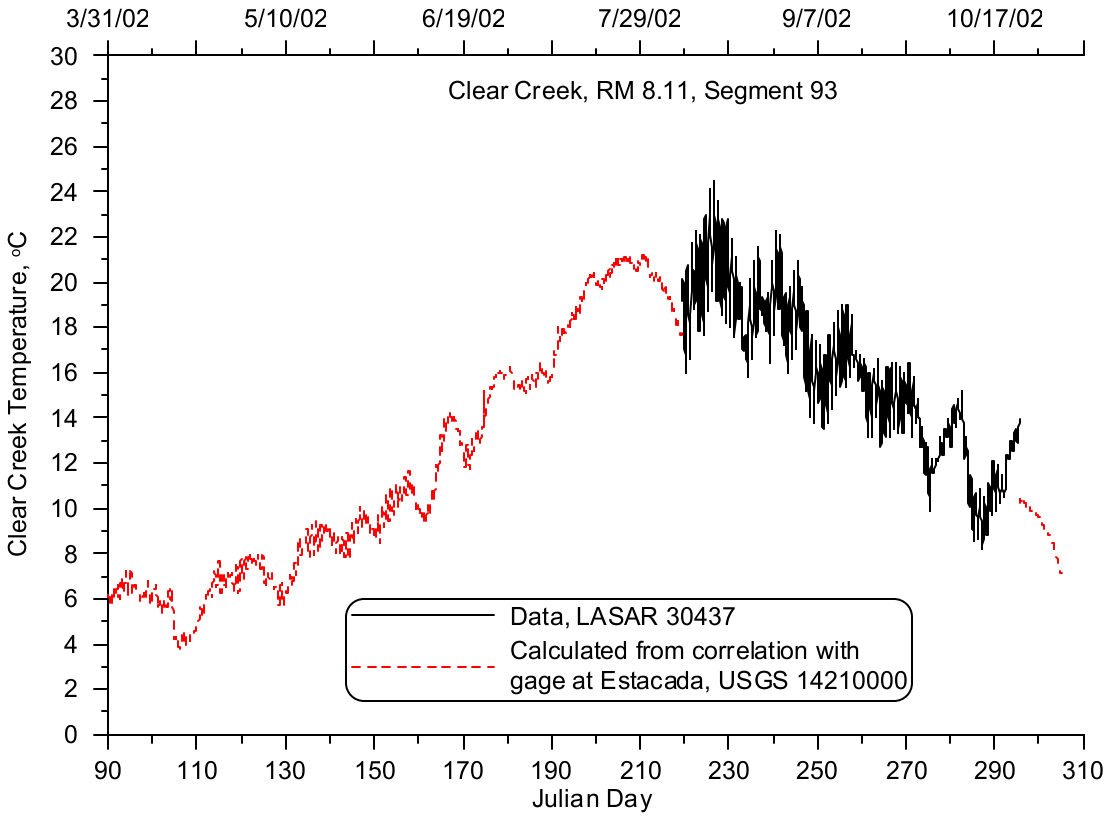


**Figure 417. Clear Creek temperature, 2002**

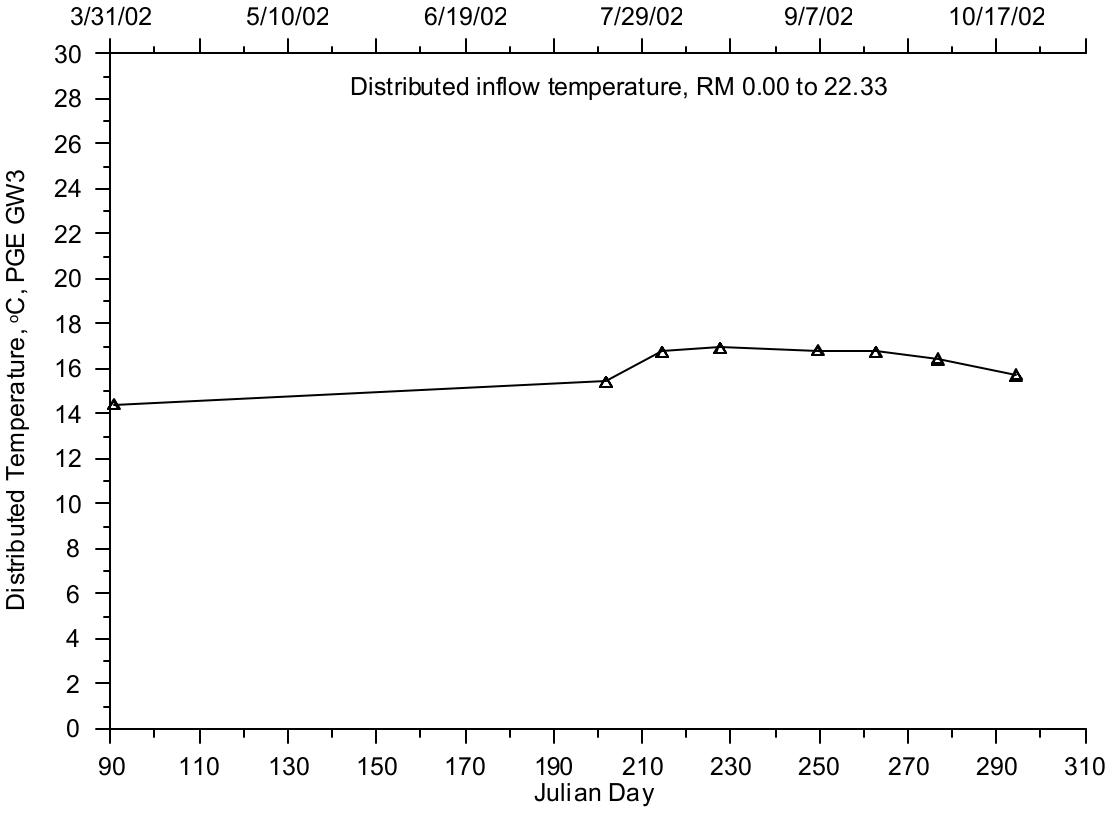


**Figure 418. Distributed inflow temperature, 2002**

## *Shading*

CE-QUAL-W2 incorporates both topographic and vegetative shade in the model. Topographic characteristics include the steepest inclination angle in 18 directions around a model segment. The vegetative characteristics consist of tree top elevation, distance between the river channel centerline and the controlling vegetation, and the vegetation density in summer and winter. The vegetation characteristics were provided for both banks of the river.

The vegetation and topographic characteristics for the Clackamas River model were developed using geographic information system (GIS) data supplied by the Oregon Department of Environmental Quality (ODEQ). The data consisted of thalweg points every 100 ft along the thalweg of the river. For each thalweg point, additional associated data included: channel width, elevation, three topographic inclination angles, and nine vegetation compartments for each bank. Each vegetation compartment consisted of vegetation height, distance from stream bank, and density. A detailed analysis was performed to convert the ODEQ data into the shade variables for the CE-QUAL-W2 model. A detailed description of the shade analysis is shown in Appendix A.

The model employs two sets of shade reduction factors which can be used to represent summer and winter vegetation thickness. The step transition dates were April 1 for "leaf on" and October 1 for "leaf off." The tree top heights are shown for the left bank in Figure 419, and for the right bank in Figure 420. The tree top heights decrease moving downstream from approximately 120 m to 20 m. The distance from the river centerline to the vegetative shade, also called the offset, are shown for the left bank in Figure 421, and for the right bank in Figure 422. The offset was fairly uniform and typically ranged from 20 to 60 m. The "leaf-on" shade reduction factors are shown for the left bank in Figure 423, and for the right bank in Figure 424. The shade reduction factors generally ranged from 0.4 to 0.85.

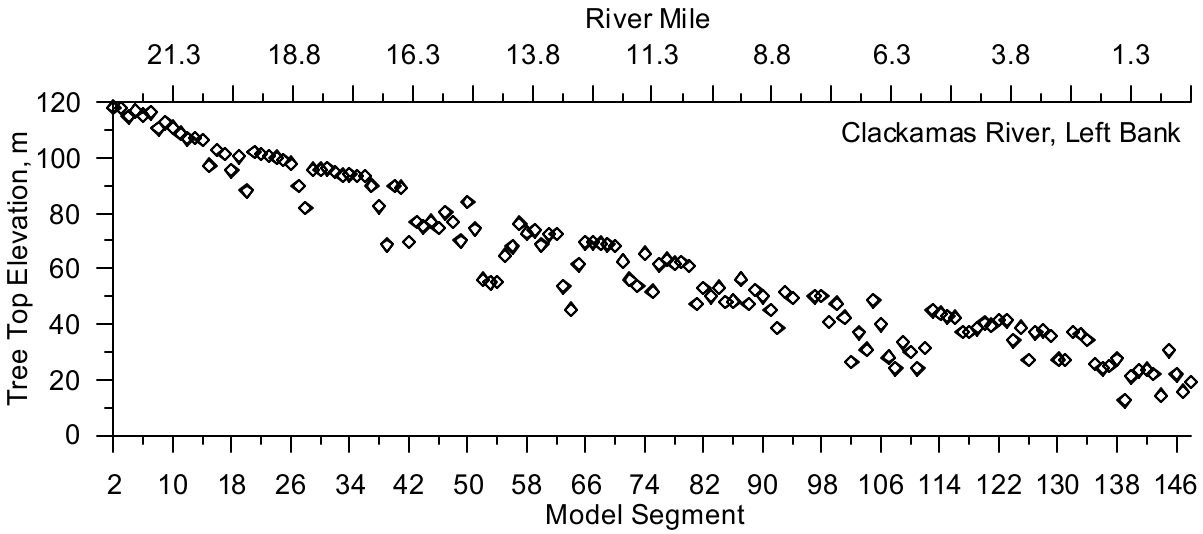


**Figure 419. Clackamas River Left Bank Tree Top Elevation**

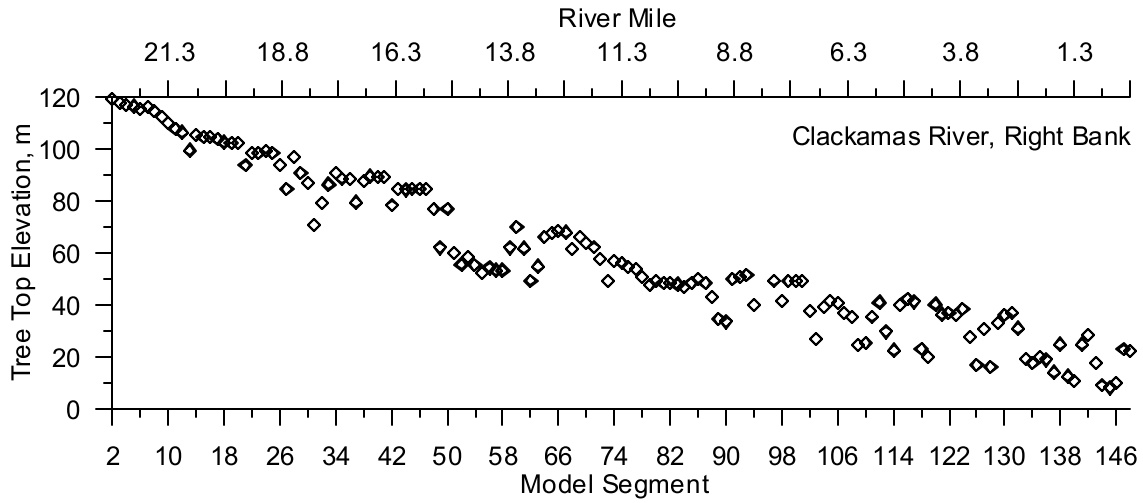


**Figure 420. Clackamas River Right Bank Tree Top Elevation**

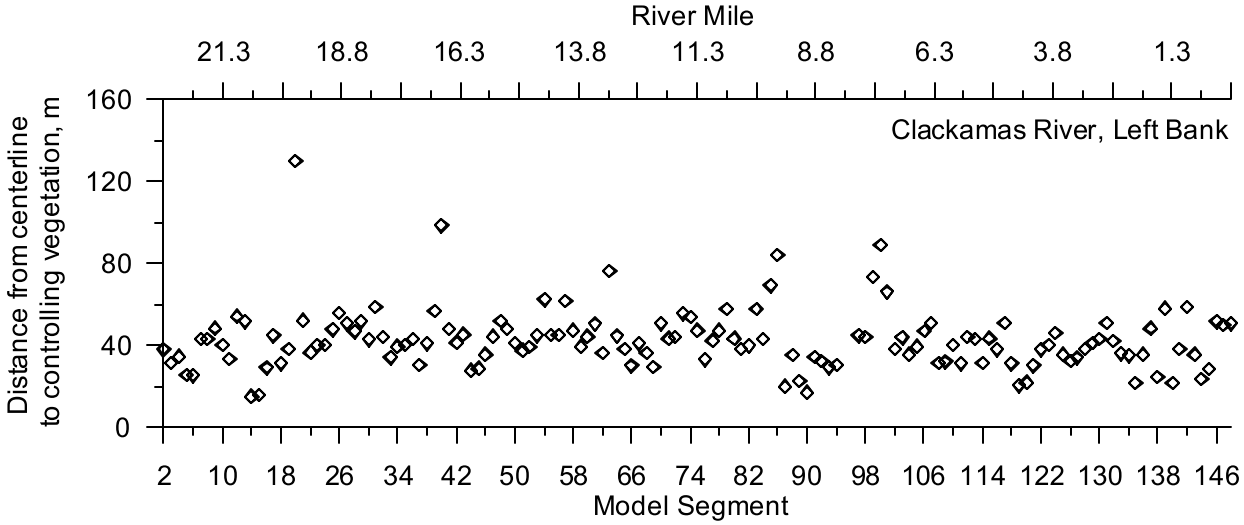


**Figure 421. Clackamas River Left Bank Distance from Centerline to Controlling Vegetation**

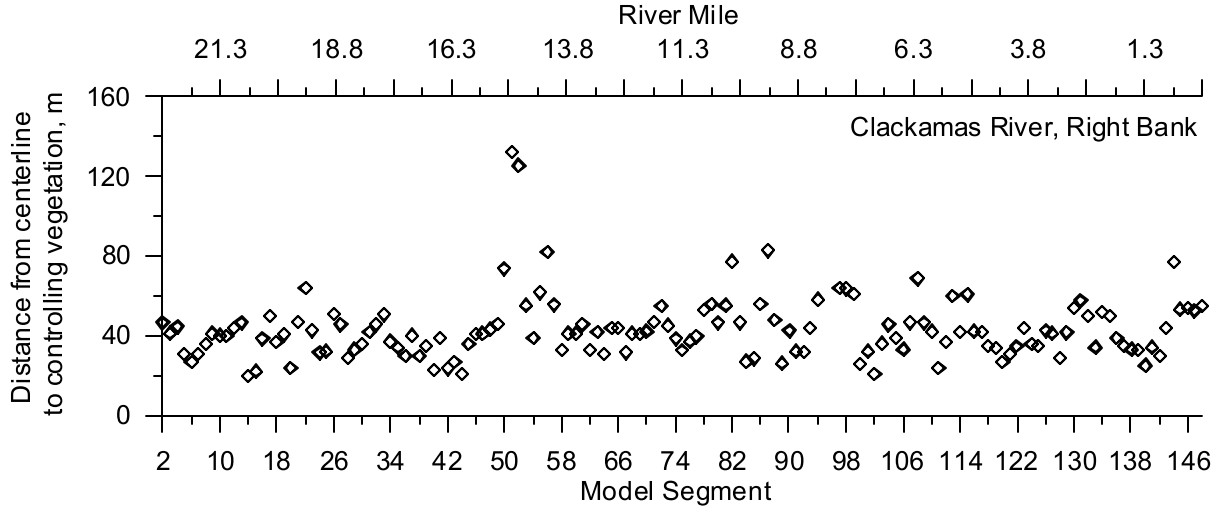


**Figure 422. Clackamas River Right Bank Distance from Centerline to Controlling Vegetation**

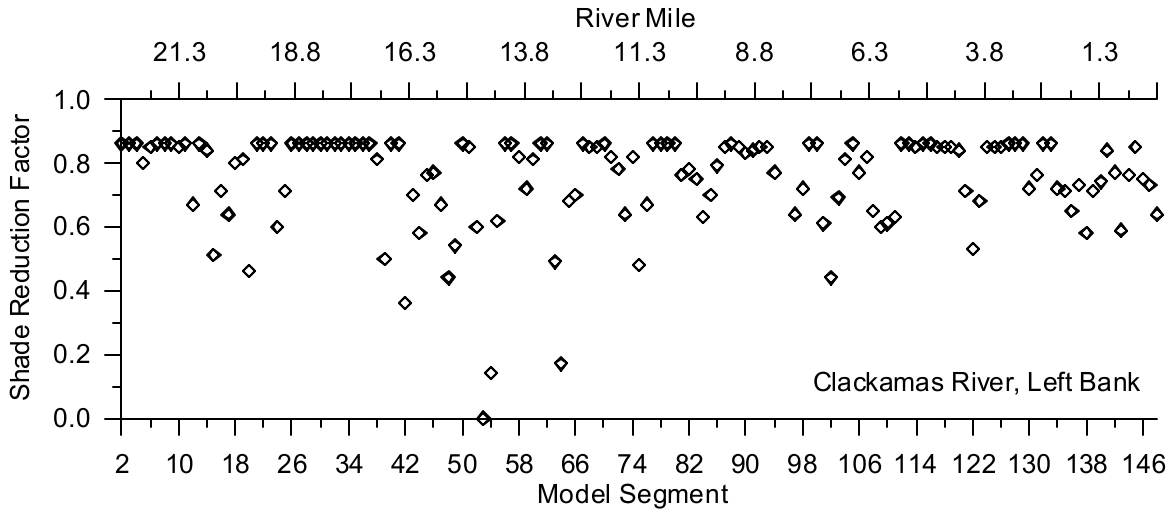


**Figure 423. Clackamas River Left Bank Shade Reduction Factor**

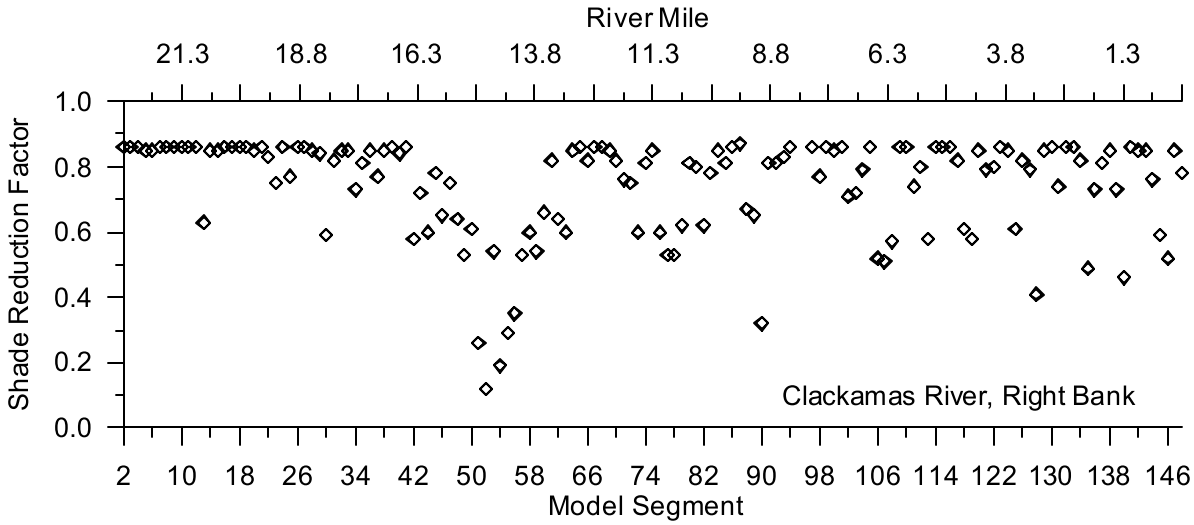


**Figure 424. Clackamas River Right Bank Shade Reduction Factor**

## *Meteorology*

The Clackamas River model includes the lower 23 miles of the river below River Mill Dam. Meteorological monitoring conducted by the National Weather Service, the Bureau of Reclamation, and the Oregon Department of Forestry were used to develop the meteorological data for the model. The model uses the meteorological parameters: air and dew point temperature, wind speed and direction, cloud cover and solar radiation. Figure 425 shows the locations of the meteorological stations used in developing the meteorological conditions. Table 45 lists the sites and the organizations responsible for data collection.

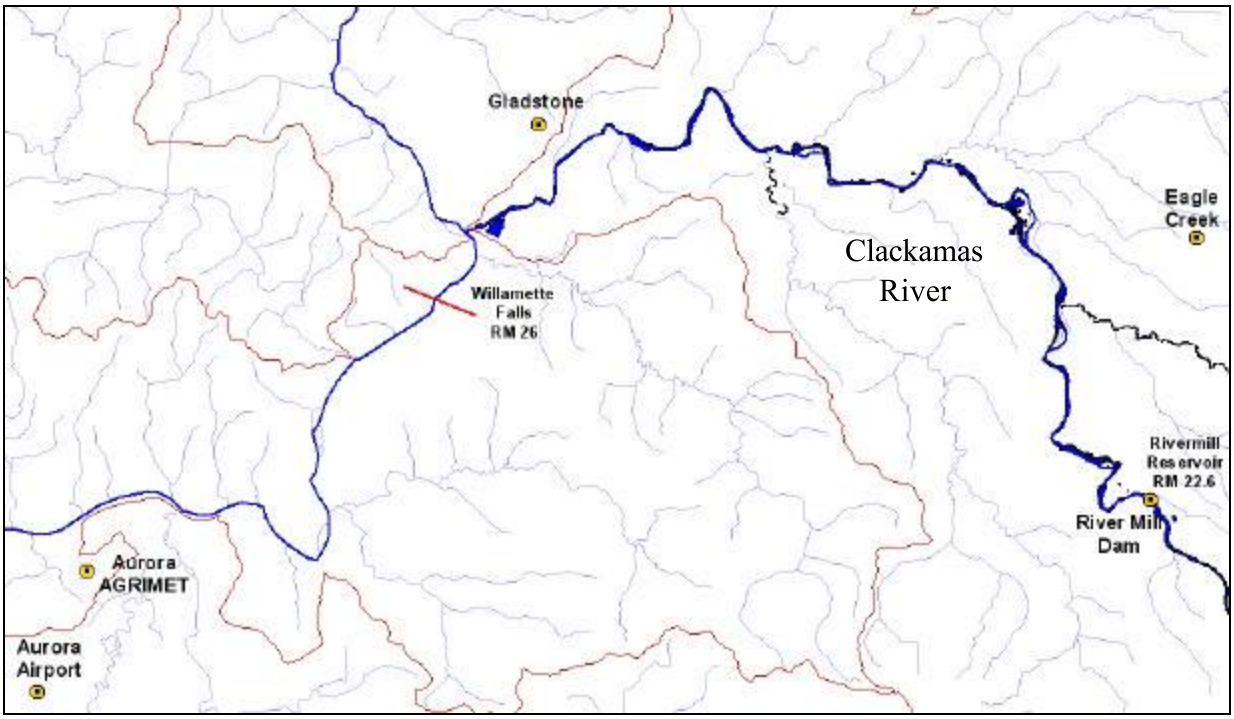


**Figure 425. Clackamas River model meteorological site locations**

**Table 45. Clackamas River model meteorological monitoring sites**

| Site | Agency (Program) | Meteorological Parameters |
|---|---|---|
| Aurora Municipal Airport | National Weather Service (METAR) | Air Temperature, Dew Point Temperature, Relative Humidity, Wind Speed, Wind Direction, Cloud Cover |
| Eagle Creek | Oregon Department of Forestry (RAWS) | Air Temperature, Relative Humidity, Wind Speed, Wind Direction |
| River Mill Dam | Portland General Electric | Air Temperature |
| Gladstone | University of Oregon, Solar Radiation Monitoring Lab | Solar Radiation |

## River Mill and Aurora Municipal Airport

### Year 2001

The meteorological data for the Clackamas River below River Mill dam were developed using meteorological data from the U.S. Forest Service Remote Automated Weather Stations (RAWS) site, Eagle Creek, and the air temperature data recorded at the River Mill Dam. The extent of the air temperature data at River Mill Dam was from April 1 to September 11, 2001. The data gap from September 11 to October 31, 2001 was filled by developing an air temperature correlation between the air temperature at River Mill Dam and the Eagle Creek site. Figure 426 shows the air temperature correlation between the two sites. Figure 427 shows the time series record of air temperature during 2001 including the data and the calculated values based on the correlation.

Only air temperature was recorded at the River Mill Dam, so the relative humidity data at Eagle Creek were used with the air temperature to calculate the dew point temperature using the equation from Singh, 1992:

$$RH = \left[ \frac{112 - 0.1T_a + T_d}{112 + 0.9T_a} \right]^8$$

Figure 428 shows the dew point temperature at Eagle Creek. Figure 429 and Figure 430 show the wind speed and direction at Eagle Creek, respectively. Figure 429 indicates the minimum wind speed-recording threshold was 0.5 m/s with wind speeds below the threshold recorded as zero. The rose diagram in Figure 430 shows a slight trend of SW to NE and NE to SW wind directions.

The cloud cover data used were from the Aurora Municipal Airport as shown in Figure 245 for the Middle Willamette River model. The global solar radiation data used were collected at Gladstone, OR, and was the same data set used for the Middle Willamette River (Figure 246).

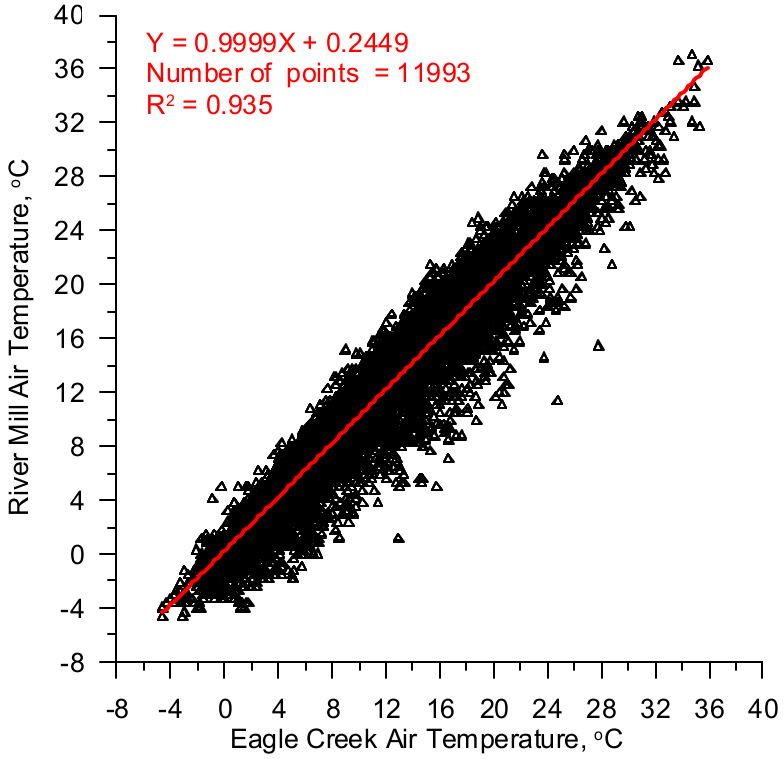


**Figure 426. Air temperature correlation between River Mill and Eagle Creek**

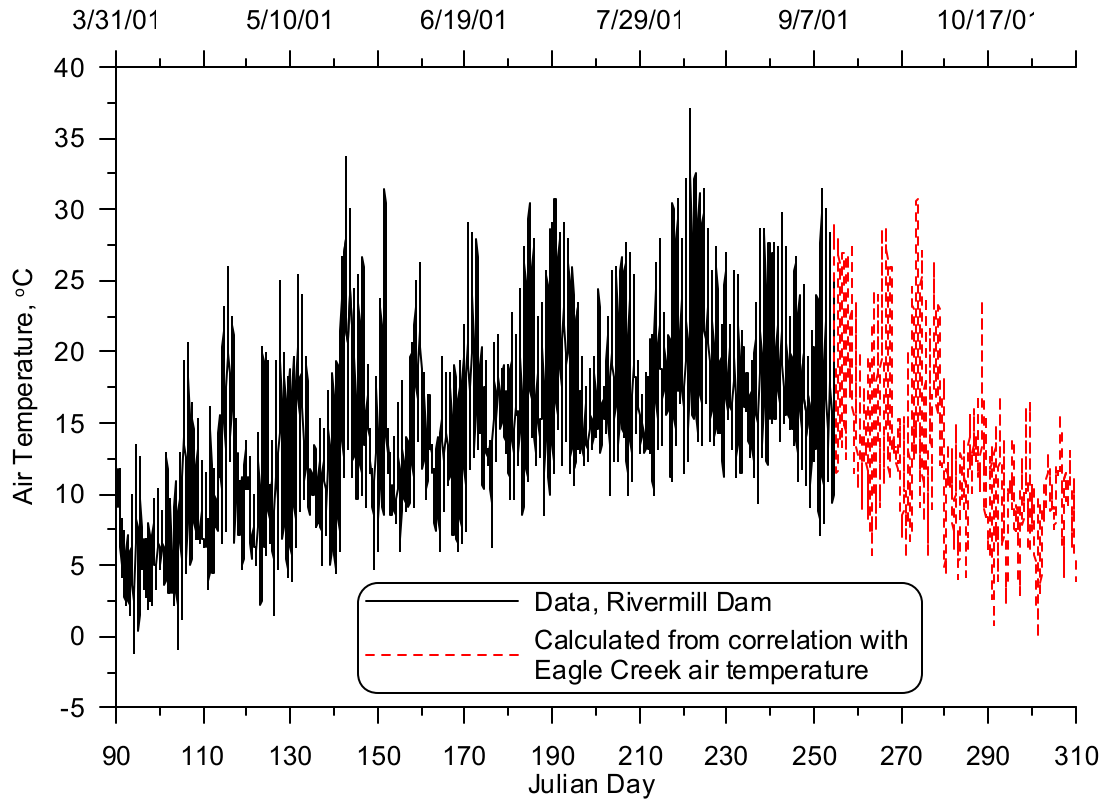


**Figure 427. Air temperature at River Mill, 2001**

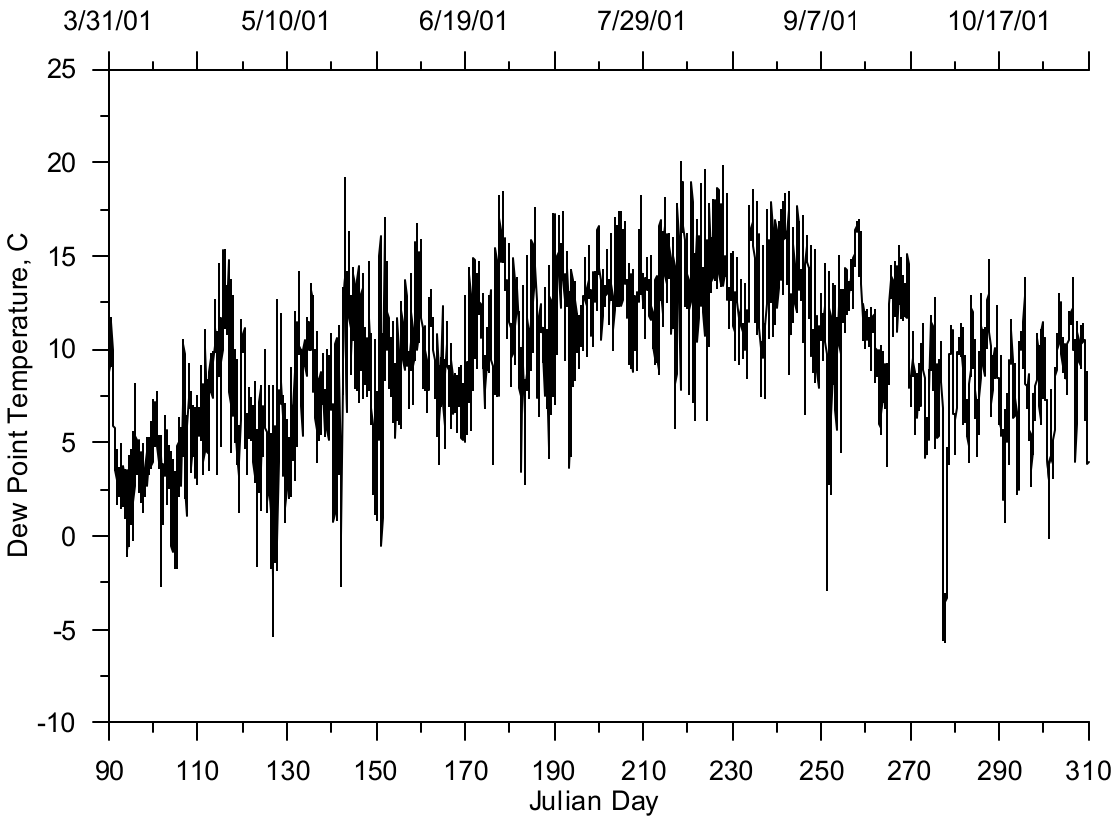


**Figure 428. Dew point temperature at Eagle Creek, 2001**

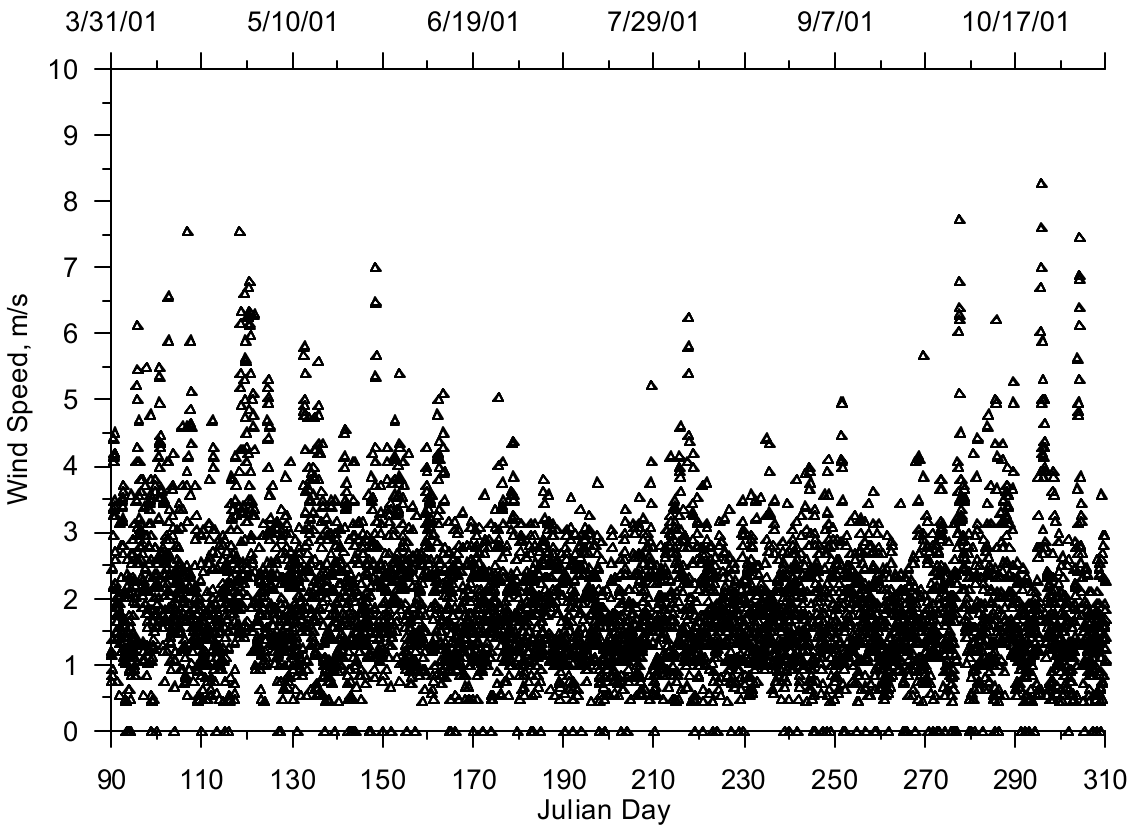


**Figure 429. Wind speed at Eagle Creek, 2001**

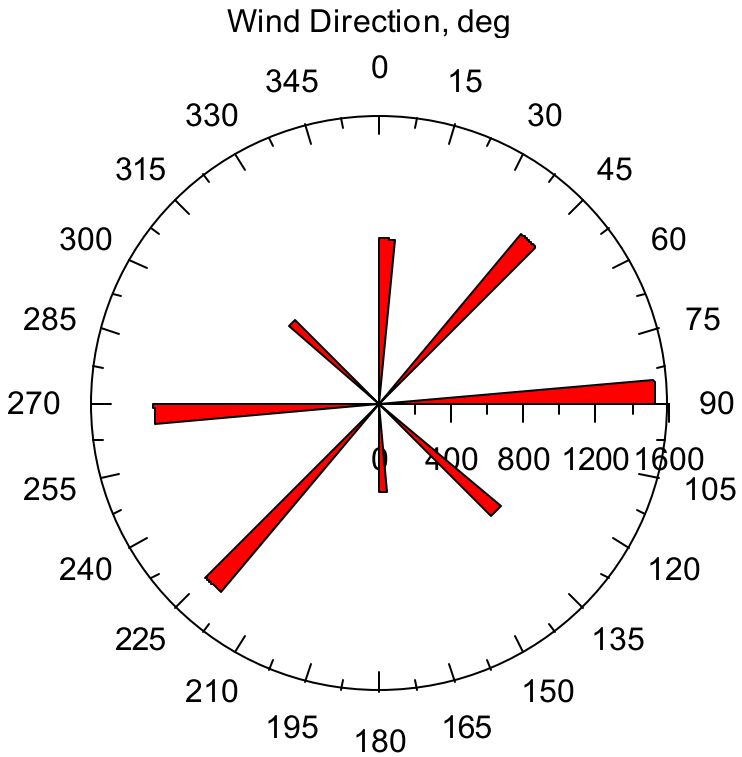


**Figure 430. Wind direction at Eagle Creek, 2001**

## Year 2002

The meteorological data recorded at the Aurora Municipal Airport which were used for the Middle Willamette River model were also used for the Clackamas River model. The Aurora Municipal Airport records air and dew point temperature, wind speed and direction, cloud cover and solar radiation data.

Figure 247 and Figure 248 show the air and dew point temperature, respectively. Figure 249 and Figure 250 show the wind speed and direction, respectively. Figure 249 indicates the minimum wind speed-recording threshold was about 1.5 m/s. The figure also shows some wind speeds below this minimum recording threshold, which represent interpolated values used to fill data gaps in the times series record. The rose diagram in Figure 250 indicates the predominant wind direction is from the North which was partly due to the wind direction being set to zero when the wind speed was below the threshold velocity. Figure 251 shows the coarseness of the cloud cover data recorded at the airport with five different cloud cover designations with some values in-between due to interpolating values to fill data gaps. Figure 252 shows the global solar radiation recorded at the Aurora Municipal Airport.

# South Santiam River

The South Santiam River model was developed from Foster Lake (reservoir) at RM 36.5 downstream to the confluence with the North Santiam River (South Santiam RM 0.0) Figure 431 shows the South Santiam River model region and the North Santiam River.

The model development and model calibration were conducted primarily by the Oregon Department of Environmental Quality (ODEQ). The model bathymetry and grid files and the shade file were developed by Portland State University.

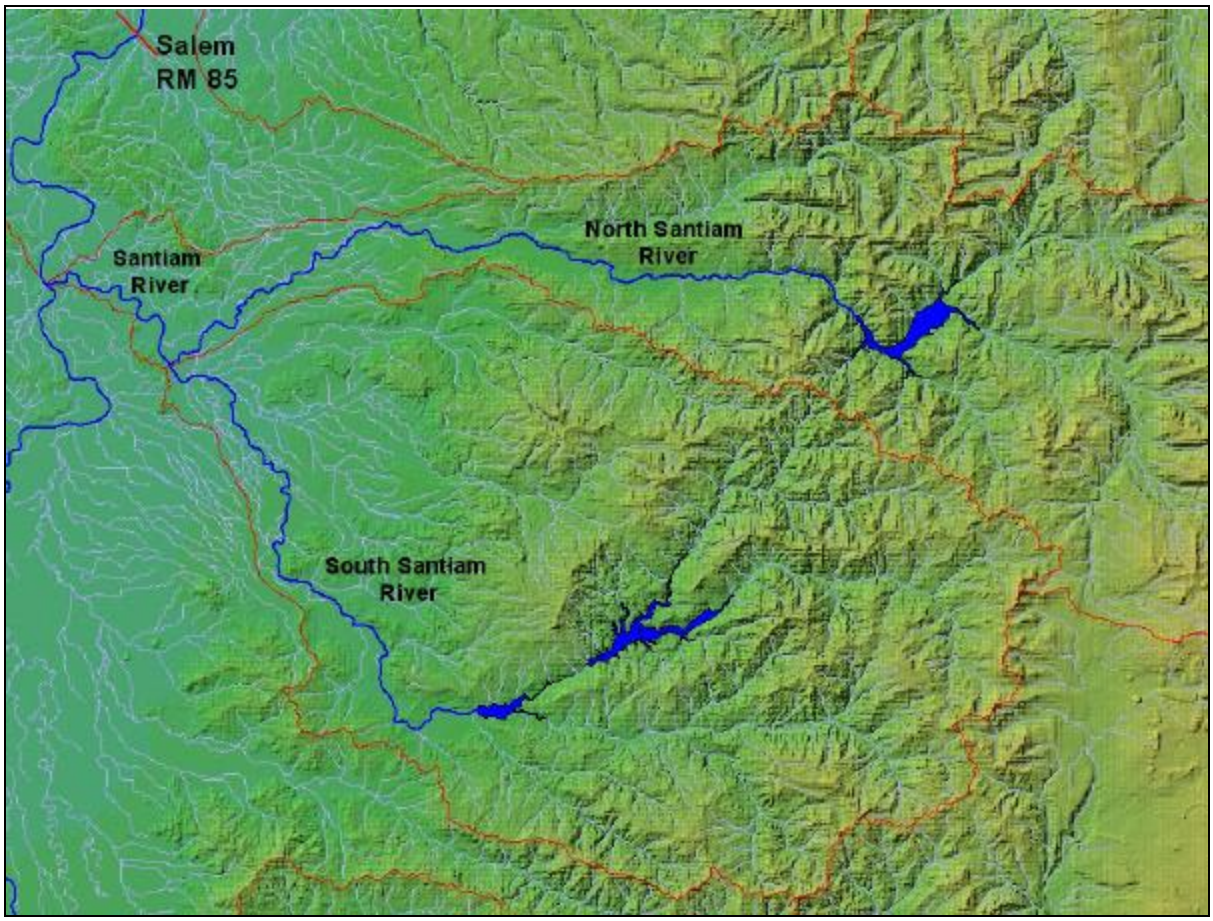


**Figure 431. South Santiam River model region**

## *Model Geometry*

### Bathymetry Data

The bathymetric data for the South Santiam River consist of HEC-2 river channel cross sections provided by ODEQ. Figure 432 shows a map of the South Santiam River, which includes the 79 HEC-2 cross section locations over 36.5 miles. Since the cross sections were taken as part of a flood study they

included the flood plain, so no elevation data from DEMs around the river channel were obtained. The river channel bathymetry between the cross sections was created by linearly interpolating between the cross sections. This process was done automatically using a FORTRAN program.

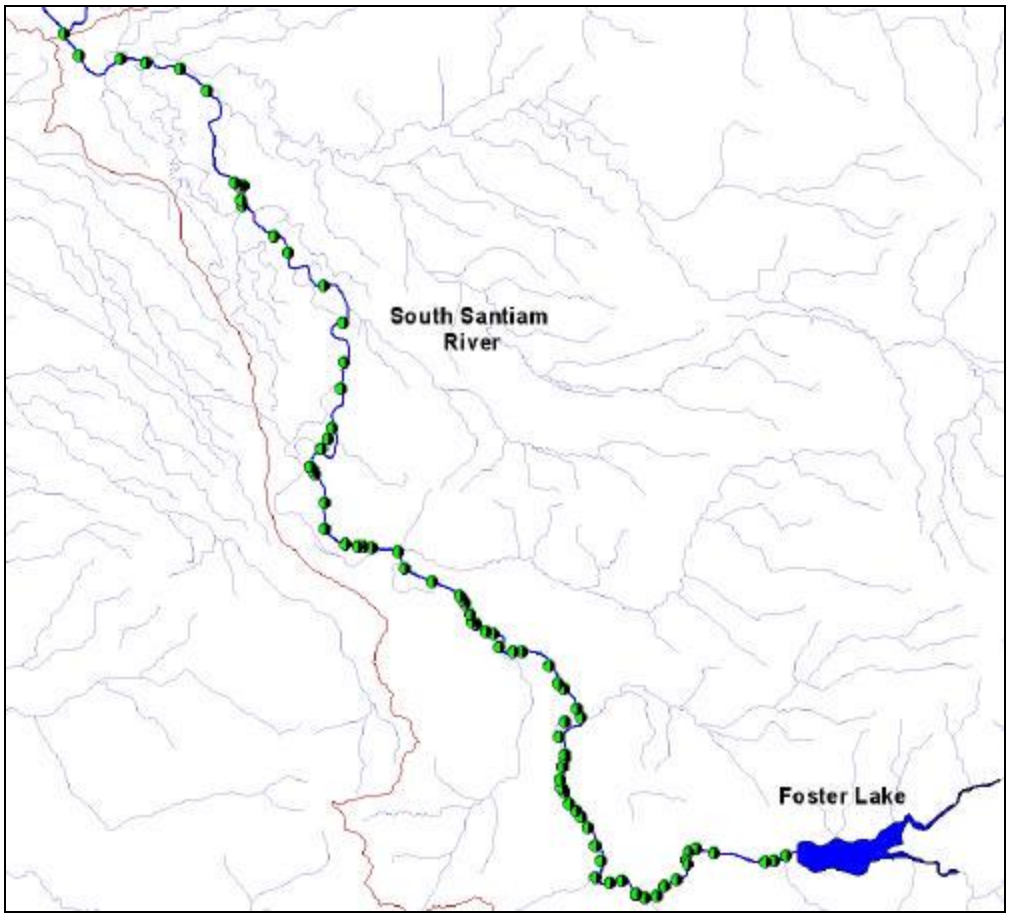


**Figure 432. South Santiam HEC-2 river channel cross section locations**

## Model Grid Development

The linearly interpolated river channel cross sections were then used to create the model grid segments for the main channel of the South Santiam River. The model grid was then modified slightly by ODEQ to incorporate two side channels. The updated model grid consisted of five water bodies and seven branches. Figure 433 shows a layout of the model grid, although the side channels are too small to be easily visible. Table 46 lists the grid characteristics.

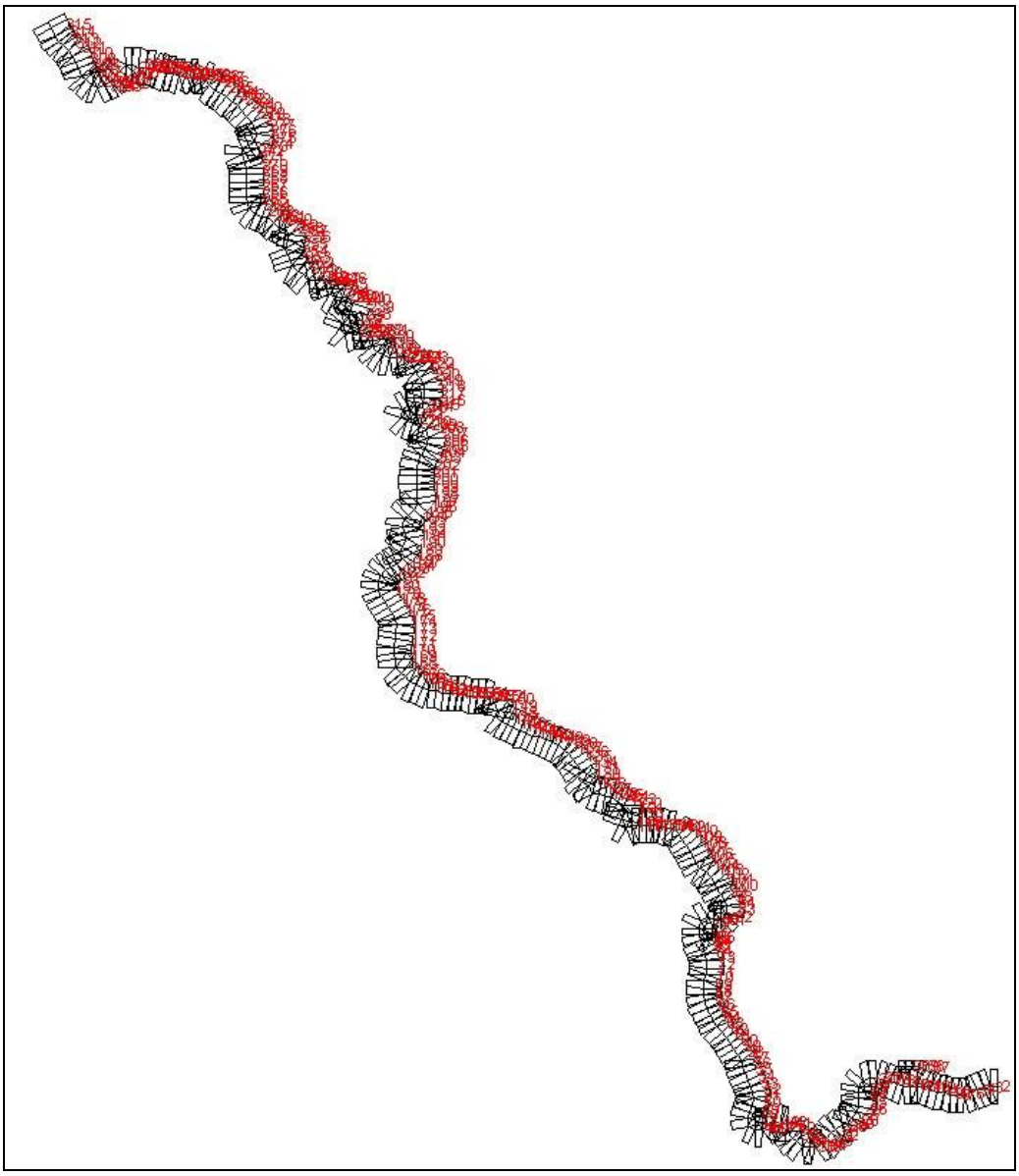

**Figure 433. South Santiam River model grid layout**

**Table 46. South Santiam River model grid characteristics**

| Water Body | Branch | Description | Starting Segment | Ending Segment | Starting RM | Ending RM | Segment Length, m | Slope | Upstream BC | Down-stream BC |
|---|---|---|---|---|---|---|---|---|---|---|
| 1 | 1 | Foster Reservoir to RM 26 | 2 | 84 | 36.50 | 26.25 | 198.80 | 0.00209 | flow | internal |
| | 2 | side channel | 87 | 90 | 35.2 | 34.6 | 198.80 | 0.00209 | internal | internal |
| | 3 | side channel | 93 | 95 | 27.3 | 26.8 | 152.50 | 0.00270 | internal | internal |
| 2 | 4 | RM 26 to RM 22 | 98 | 131 | 26.25 | 22.05 | 198.80 | 0.00182 | internal | internal |
| 3 | 5 | RM 22 to RM 19 | 134 | 155 | 22.05 | 19.33 | 198.80 | 0.00182 | internal | internal |
| 4 | 6 | RM 19 to RM 16 | 158 | 184 | 19.33 | 16.00 | 198.80 | 0.00182 | internal | internal |
| 5 | 7 | RM 16 to North Santiam River confluence | 187 | 315 | 16.00 | 0.00 | 199.55 | 0.00128 | internal | internal |

## *Shading*

CE-QUAL-W2 incorporates both topographic and vegetative shade in the model. Topographic characteristics include the steepest inclination angle in 18 directions around a model segment. The vegetative characteristics consist of tree top elevation, distance between the river channel centerline and the controlling vegetation, and the vegetation density in summer and winter. The vegetation characteristics were provided for both banks of the river.

The vegetation and topographic characteristics for the South Santiam River model were developed using geographic information system (GIS) data supplied by the Oregon Department of Environmental Quality (ODEQ). The data consists of thalweg points every 100 ft along the thalweg of the river. For each thalweg point, additional associated data included: channel width, elevation, 3 topographic inclination angles, and 9 vegetation compartments for each bank. Each vegetation compartment consisted of vegetation height, distance from stream bank, and density. A detailed analysis was performed to convert the ODEQ data into the shade variables for the CE-QUAL-W2 model. A detailed description of the shade analysis is shown in Appendix A.

Figure 434 and Figure 435 show the tree top elevation for the left and right banks of the South Santiam River. Both banks show the tree top elevation decreasing going downstream with a few reaches with vegetation heights lower than the trend line. Figure 436 and Figure 437 show the distance from the river centerline to the controlling vegetation on the left and right banks, respectively, moving downstream. The figures show that the distance to the vegetation for both banks was relatively constant until the end reach just before the confluence with the North Santiam River. Figure 438 and Figure 439 show the vegetation density for the left and right banks, respectively. The plots reveal the vegetation density for the left and right banks was highly variable.

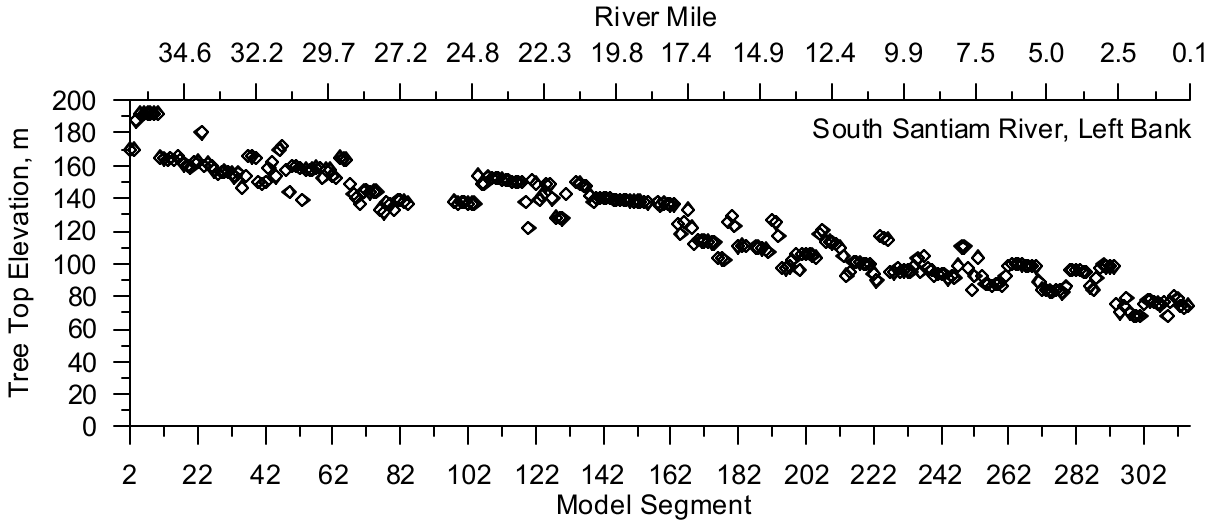


**Figure 434. South Santiam River Left Bank Tree Top Elevation**

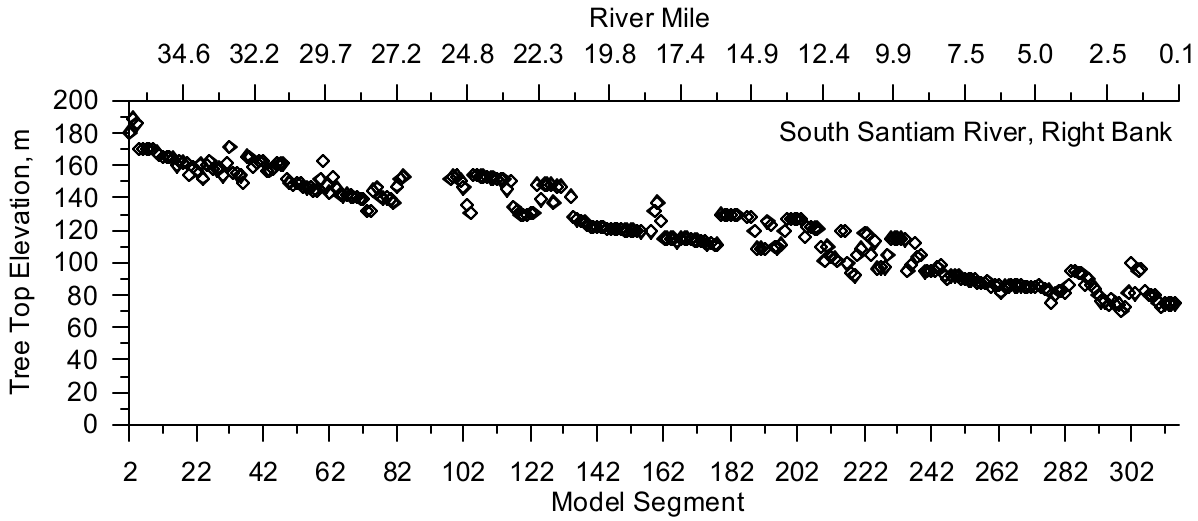


**Figure 435. South Santiam River Right Bank Tree Top Elevation**

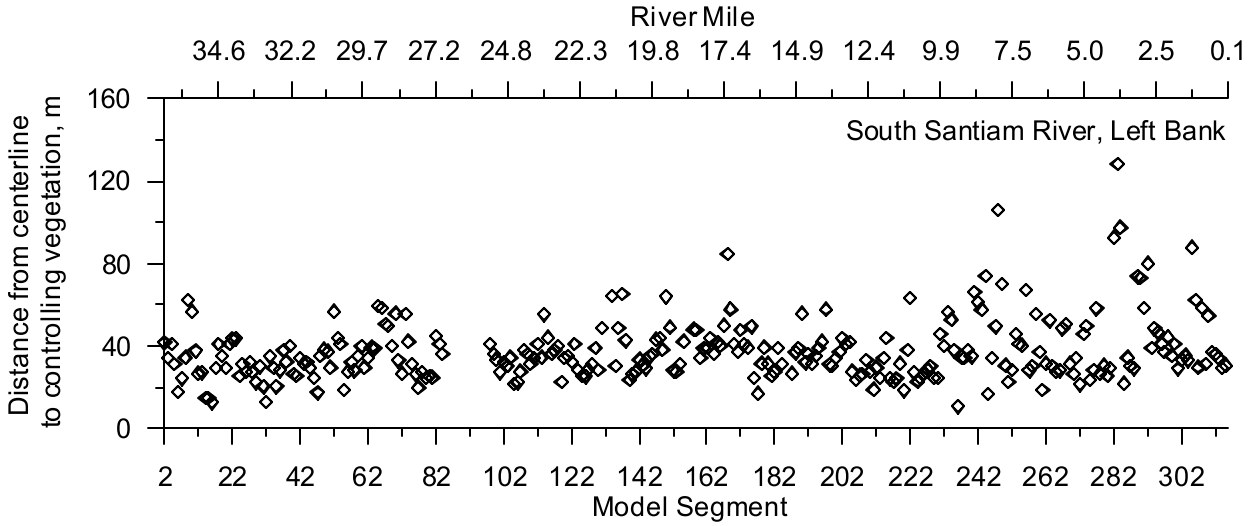


**Figure 436. South Santiam River Left Bank Distance from Centerline to Controlling Vegetation**

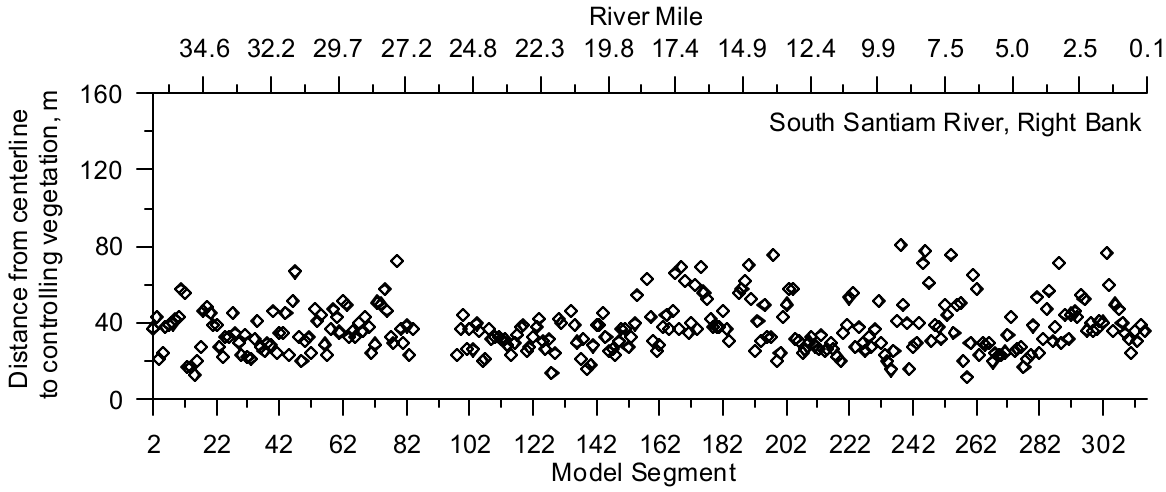


**Figure 437. South Santiam River Right Bank Distance from Centerline to Controlling Vegetation**

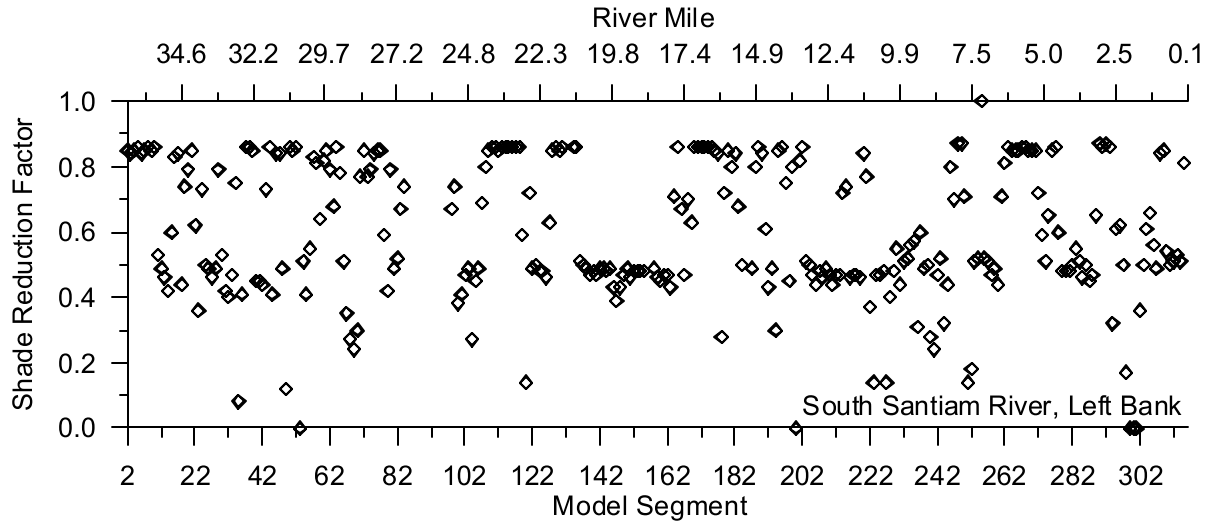


**Figure 438. South Santiam River Left Bank Shade Reduction Factor**

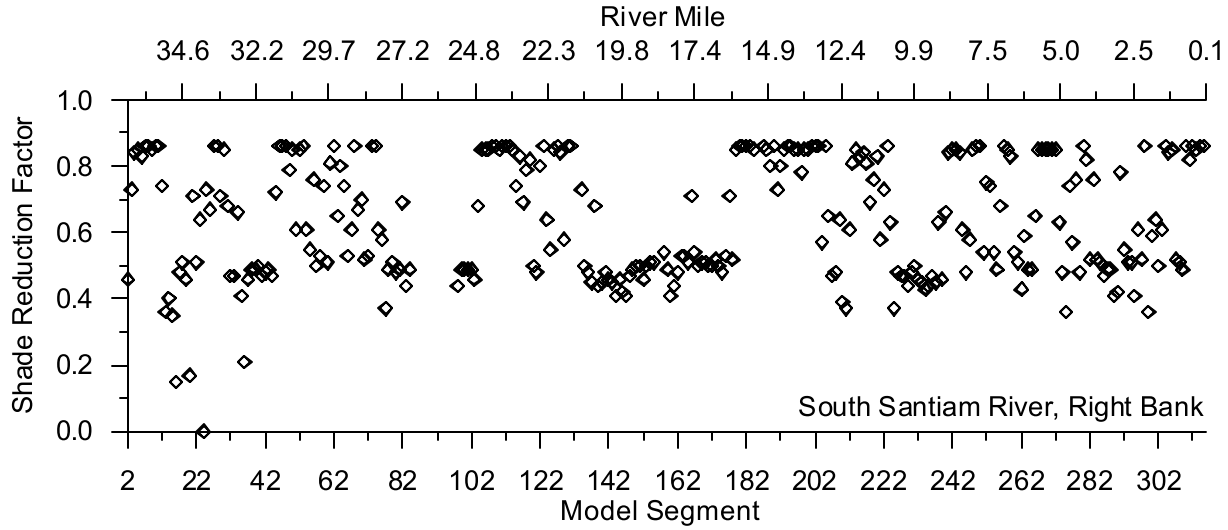


**Figure 439. South Santiam River Right Bank Shade Reduction Factor**

## Santiam River / North Santiam River

The North Santiam and Santiam River model was developed from Detroit Lake and Big Cliff Reservoir at RM 49.4 downstream to the confluence with the South Santiam River (North Fork RM 0.0, Santiam RM 12.12) and the Santiam River from the confluence of the North and South Santiam Rivers downstream to the Upper Willamette River. Figure 440 shows the North Santiam and Santiam River model region and the South Santiam River. The Santiam River basin drains an area of approximately 4700 $km^2$

The model development and model calibration was conducted primarily by the U.S. Geological Survey in Portland, Oregon (Sullivan and Rounds, 2004).

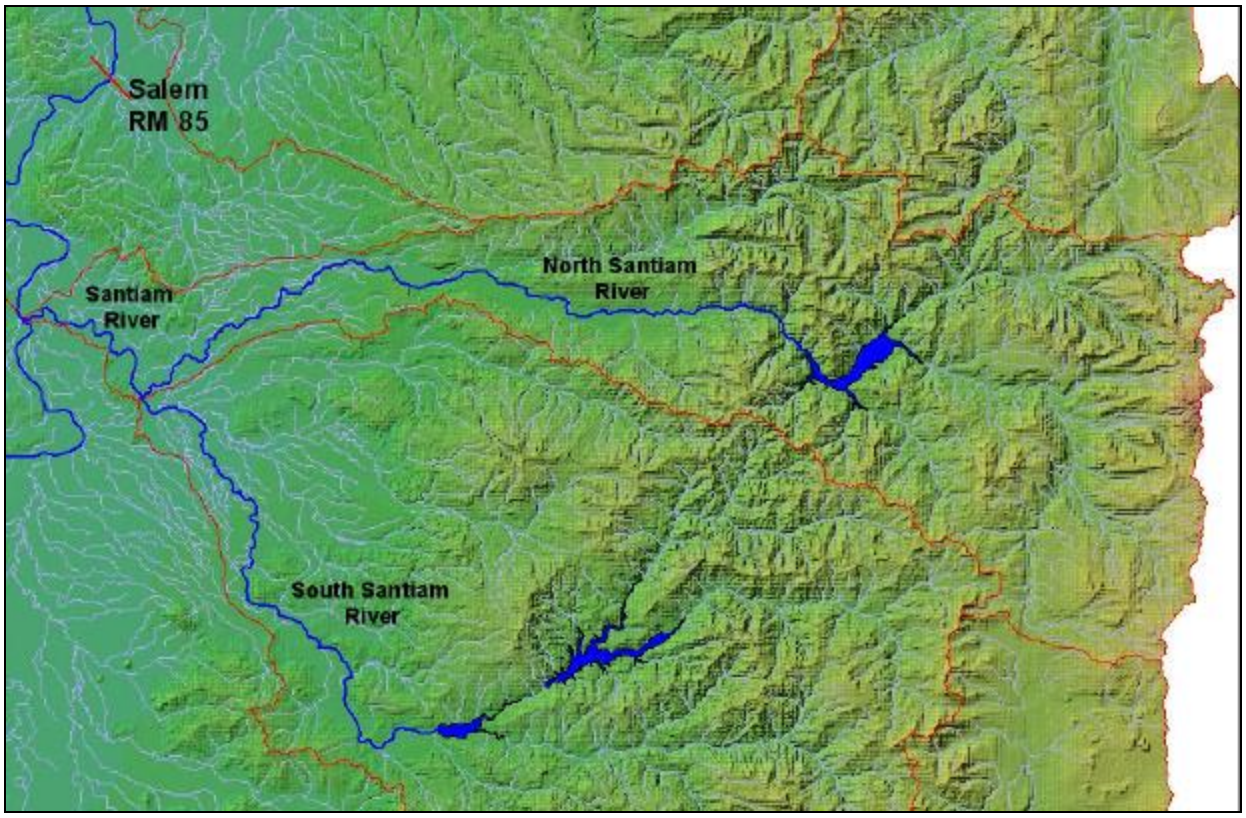


**Figure 440. North Santiam River and Santiam River model region**

# Long Tom River

The Long Tom River model started below Fern Ridge Dam at RM 23.7 and extended to its confluence with the Willamette River. There were no tributaries or withdrawals along the Long Tom River. Several weirs/dams were incorporated into the model so the flow peak timing would be accurate. Additionally, a side channel was added to the model to incorporate the travel time changes from dye releases to the river.

The model calibration periods were from May 30, 2001 to October 15, 2001, and from April 1, 2002 to October 31, 2002.

There were no tributaries or withdrawals along the Long Tom River. Several weirs/dams were incorporated into the model so the flow peak timing would be accurate. Additionally a side channel was added to the model to incorporate the travel time changes from dye releases to the river.

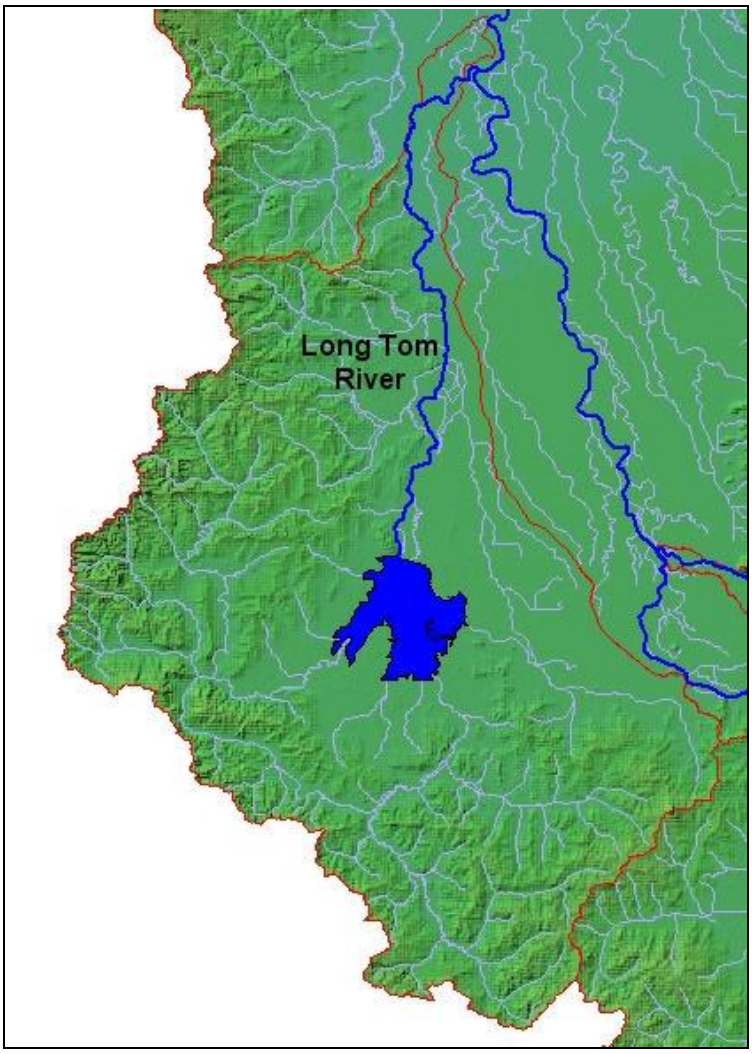


**Figure 441. Long Tom River model region**

## Bathymetry Data

The data used to generate the model bathymetry were obtained from two USGS surveyed cross sections for gage stations, Digital Elevation Maps (DEM), and GIS data sets from ODEQ. There were two USGS gage stations on the Long Tom River (14169000 and 14170000) which were regularly surveyed to ensure the gaging stations have accurate stage – flow relationship curves. Figure 442 shows the location of the two cross sections along the river, and Figure 443 shows the cross section data collected at the two gage stations.

The DEMs had a vertical resolution of 1 m, and a horizontal resolution of 10 m. Figure 444 shows a longitudinal profile of the Long Tom River from DEM data with additional elevation points estimated from USGS quadrangle maps. Using linear interpolation, additional cross sections were generated at a spacing/frequency of 100 feet for association with the river thalweg points generated from a GIS analysis conducted by ODEQ. Figure 445 shows a section of the Long Tom River with the DEM data outside the river banks and a series of interpolated cross sections along the centerline of the river.

There were no river cross sections below RM 6.86 (USGS 14170000). Additional cross sections were estimated in this reach by extending the last river cross section at RM 6.86 downstream and adjusting the width of the cross section based on the channel width from the GIS data obtained from ODEQ and by adjusting the cross section elevation based on the slope of the river from the same GIS data.

The calculated cross sections were combined with DEM data and the two surveyed cross sections into the contour mapping program, SURFER. An average volume-elevation relationship was calculated over the length of each model segment using a one meter vertical resolution. Figure 446 shows the contour plot for the Long Tom River with an enlargement of one section of the river. The contour plot and river center line were then used to slice the river into model segments.

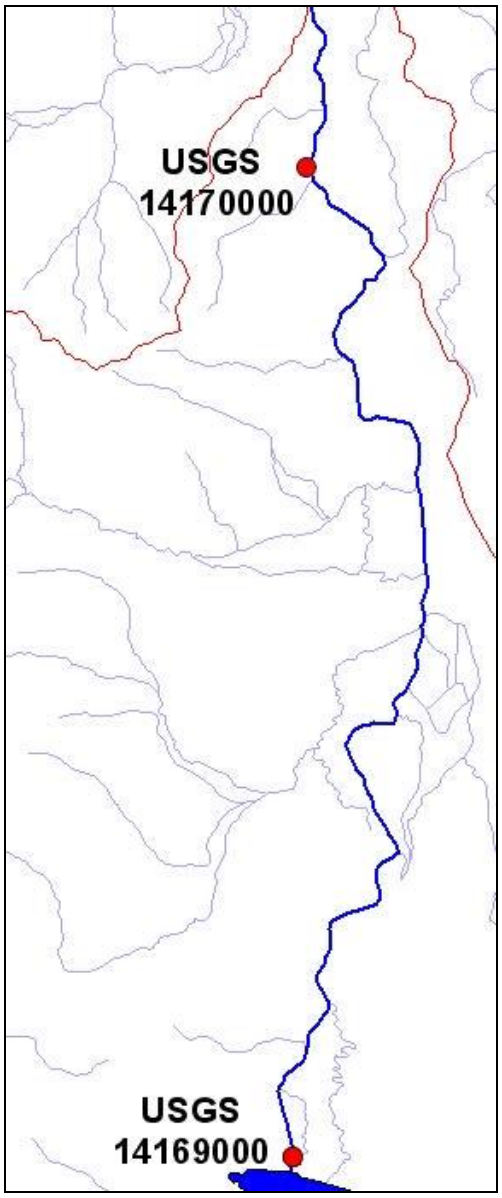


**Figure 442. Long Tom River USGS cross section locations**

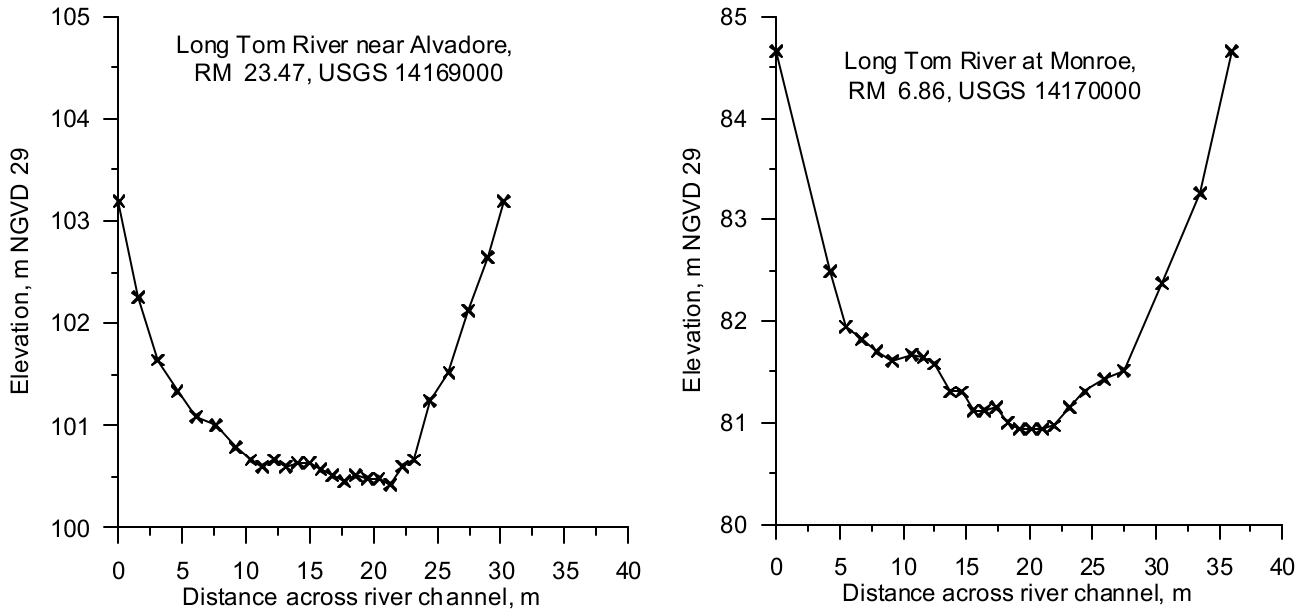


**Figure 443. Long Tom River USGS gage station cross sections**

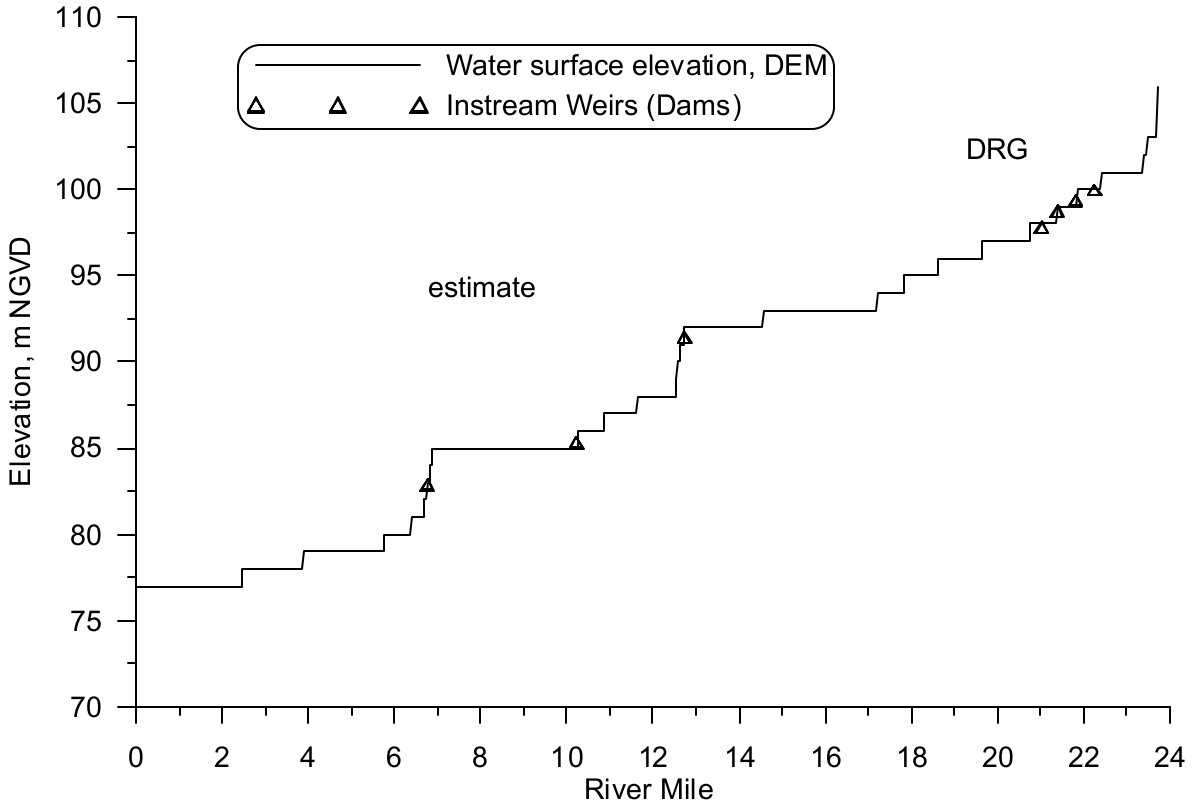


**Figure 444. Long Tom River Longitudinal Profile**

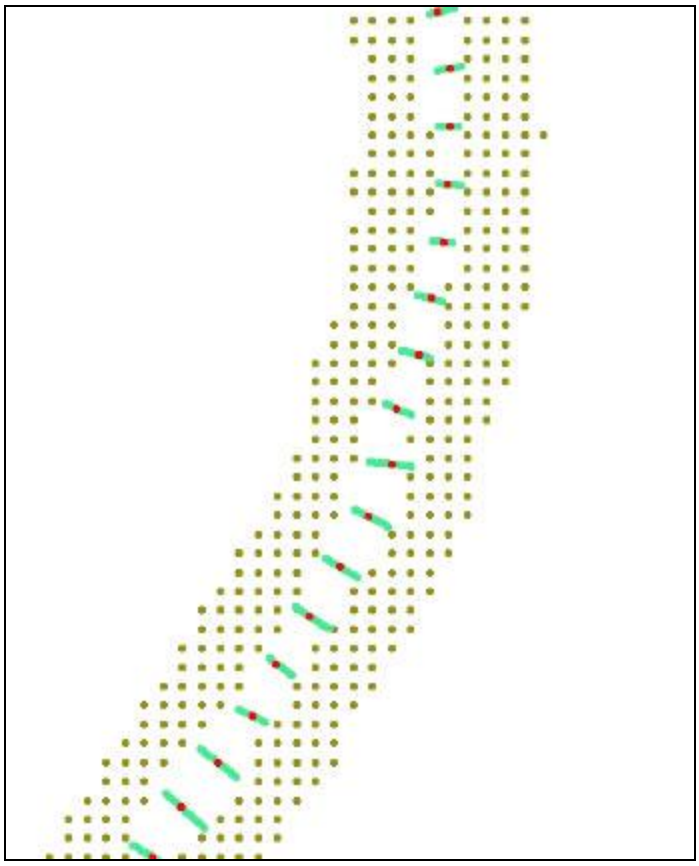

**Figure 445. Long Tom River section showing a plan view of interpolated cross section and DEM data in GIS**

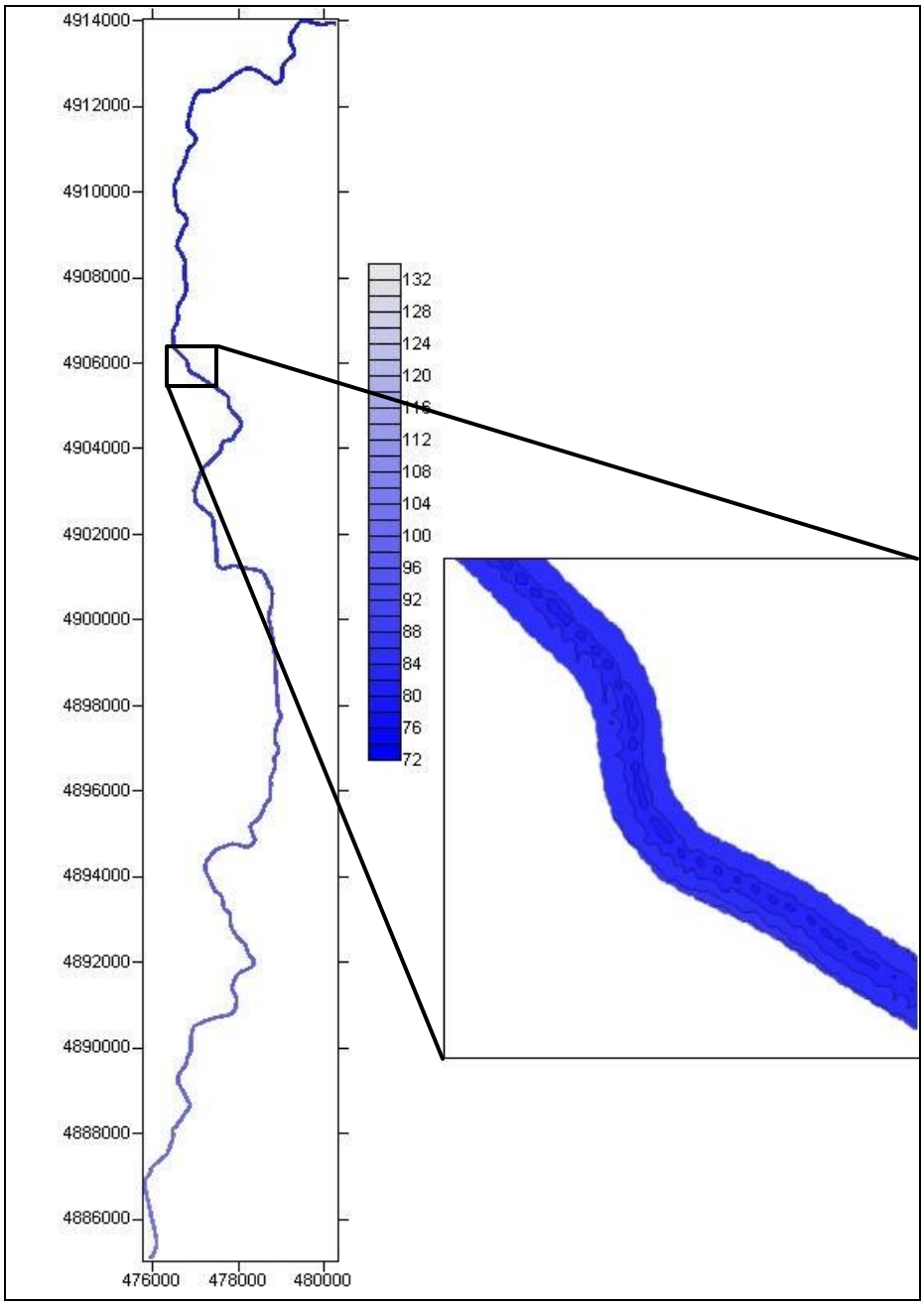


**Figure 446. Long Tom River contour plot using SURFER**

## Model Grid Development

The data were combined and used to create a contour plot of the stream channel in the contour plotting program SURFER and used to generate the model grid. The model grid consists of a single water body with 13 branches along the main river and one branch representing a side channel. Figure 447 shows a layout of the model grid, and Table 47 shows the model grid characteristics.

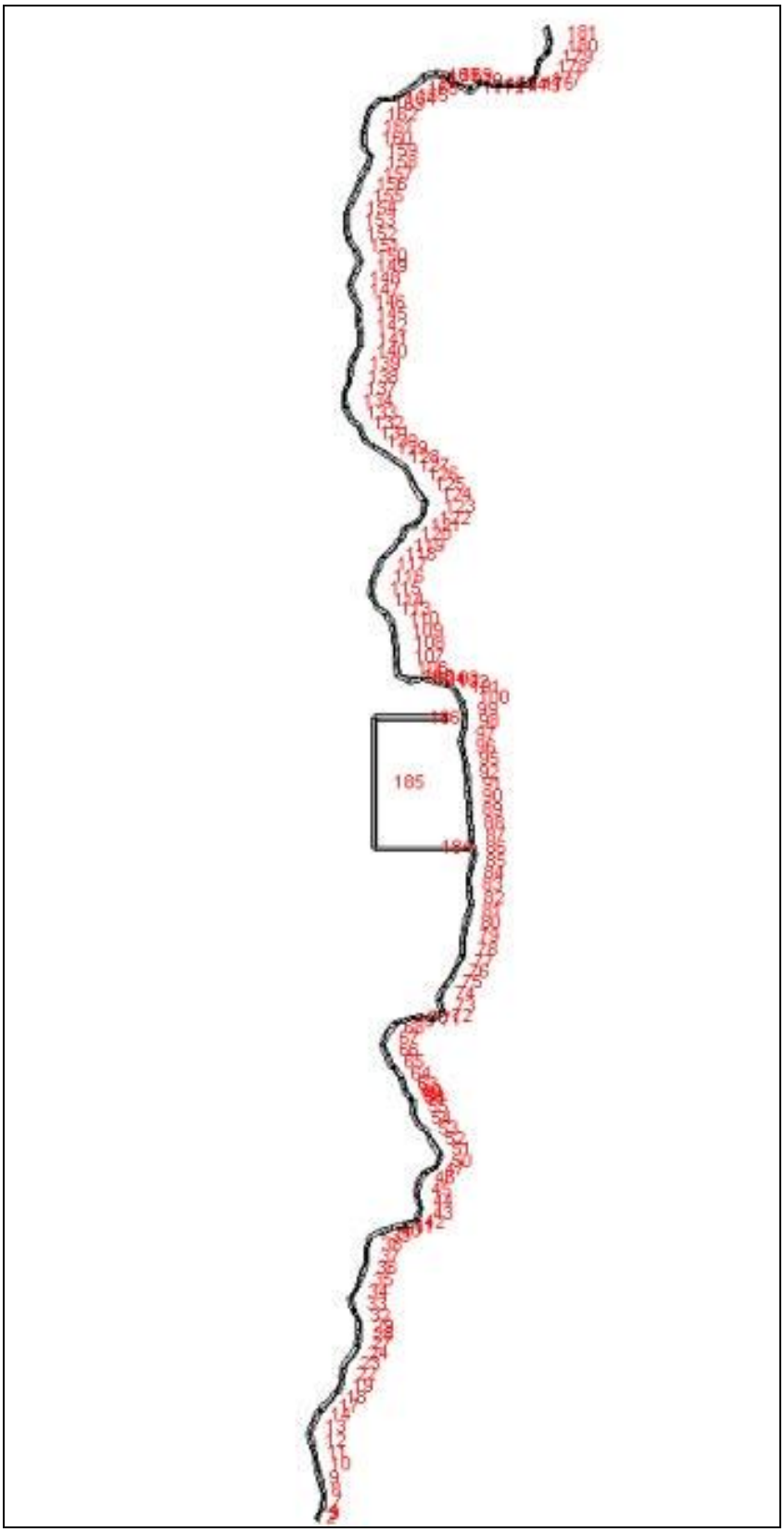


**Figure 447. Long Tom River model grid layout**

**Table 47. Long Tom River model grid characteristics**

| Water Body | Branch | Description | Starting Segment | Ending Segment | Starting RM | Ending RM | Segment Length, m | Slope | Upstream BC | Down-stream BC |
|---|---|---|---|---|---|---|---|---|---|---|
| 1 | 1 | Long Tom River | 2 | 4 | 23.7 | 23.4 | 83.88 | 0.00076 | flow | internal |
| | 2 | Long Tom River | 7 | 14 | 23.4 | 22.4 | 251.63 | 0.00076 | internal | internal |
| | 3 | Long Tom River | 17 | 19 | 22.4 | 21.7 | 251.63 | 0.00076 | internal | internal |
| | 4 | Long Tom River | 22 | 24 | 21.7 | 21.2 | 251.63 | 0.00076 | internal | internal |
| | 5 | Long Tom River | 27 | 29 | 21.2 | 20.9 | 167.75 | 0.00076 | internal | internal |
| | 6 | Long Tom River | 32 | 47 | 20.9 | 18.4 | 251.63 | 0.00076 | internal | internal |
| | 7 | Long Tom River | 50 | 55 | 18.4 | 17.5 | 251.63 | 0.00076 | internal | internal |
| | 8 | Long Tom River | 58 | 60 | 17.5 | 17.3 | 83.88 | 0.00076 | internal | internal |
| | 9 | Long Tom River | 63 | 92 | 17.3 | 12.6 | 251.63 | 0.00076 | internal | internal |
| | 10 | Long Tom River | 95 | 110 | 12.6 | 10.2 | 251.63 | 0.00076 | internal | internal |
| | 11 | Long Tom River | 113 | 134 | 10.2 | 6.7 | 251.63 | 0.00076 | internal | internal |
| | 12 | Long Tom River | 137 | 142 | 6.7 | 5.8 | 251.63 | 0.00076 | internal | internal |
| | 13 | Long Tom River | 145 | 181 | 5.8 | 0.0 | 251.63 | 0.00016 | internal | internal |
| | 14 | Side Channel | 184 | 186 | 13.7 | 12.4 | 1897, 2590, and 1427 | 0.00023 | internal | internal |

## *Model Upstream & Downstream Boundary Conditions*

### Hydrodynamic Data

The Long Tom River was 23.7 miles long and started below Fern Ridge Dam. The nearest USGS gage station was near Alvadore, OR, (USGS 14169000) at RM 23.5 and served as the model upstream boundary condition as shown in Figure 448. The model calibration period was from May 30 to October 15, 2001 due to the lack of data in the river system.

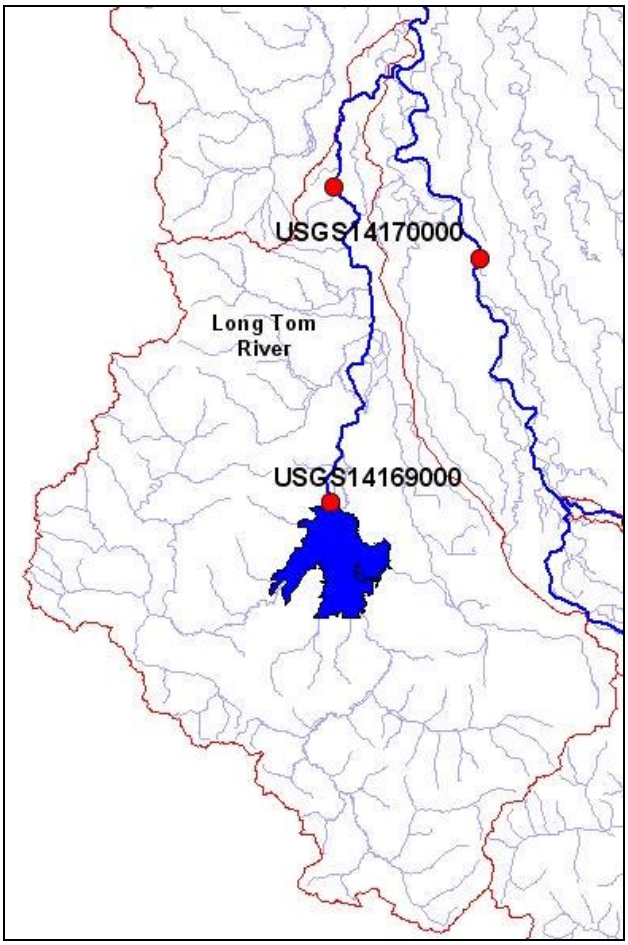


**Figure 448. Long Tom River model upstream flow boundary condition**

#### Year 2001

The upstream flow boundary for the Long Tom River model was developed from half-hourly flow data at the USGS gage 14169000. Figure 449 shows a time series plot of upstream boundary flow for the Long Tom River model. The figure showed that the 2001 summer's flows were low, with most less than 3.0 $m^3/s$. The lack of flow data after October 15 established the end of the 2001 calibration period.

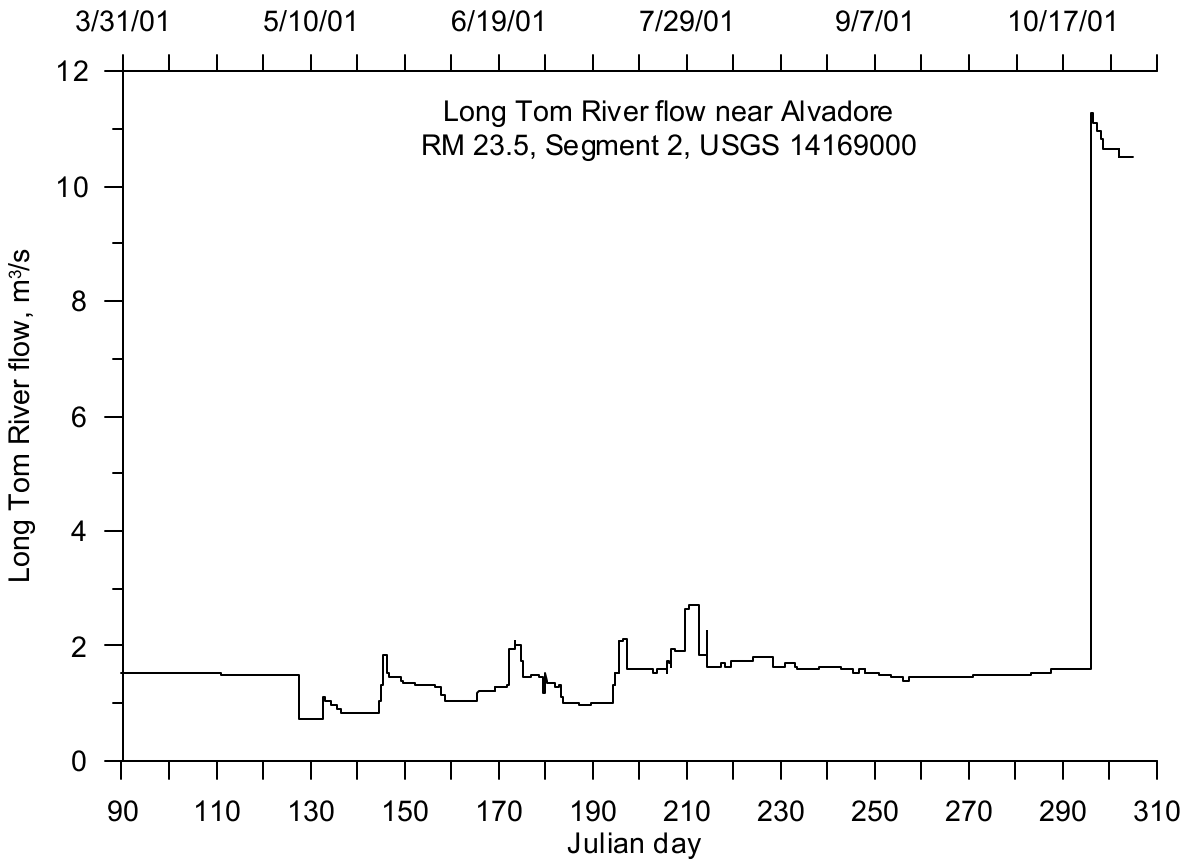


**Figure 449. Long Tom River flow below Fern Ridge Dam, 2001**

## Year 2002

The same USGS gage used to characterize the 2001 inflows to the Long Tom River model was also used for developing the upstream boundary condition for the 2002 model (USGS 14169000). Figure 450 shows a time series plot of the upstream boundary condition inflow for the Long Tom River model. Similar to 2001, the flows throughout the summer were less than 3 $m^3/s$. The lack of flow data after October 31 established the end of the 2002 calibration period. The model calibration period was from April 1, 2002 to October 31, 2002.

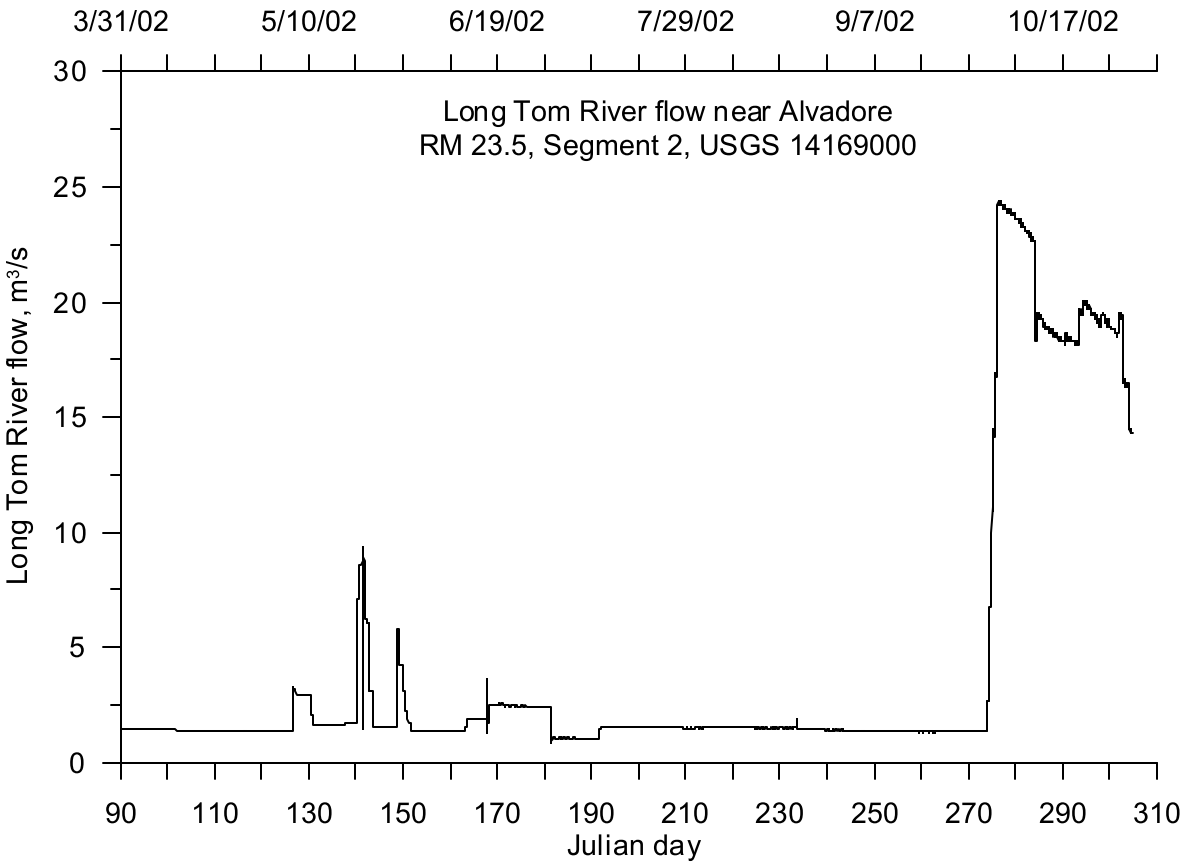


**Figure 450. Long Tom River flow below Fern Ridge Dam, 2002**

## Temperature Data

Two temperature monitoring sites were used for developing the upstream boundary condition on the Long Tom River (USGS 14169000 and LASAR 26749). Figure 451 shows the locations of the two monitoring sites.

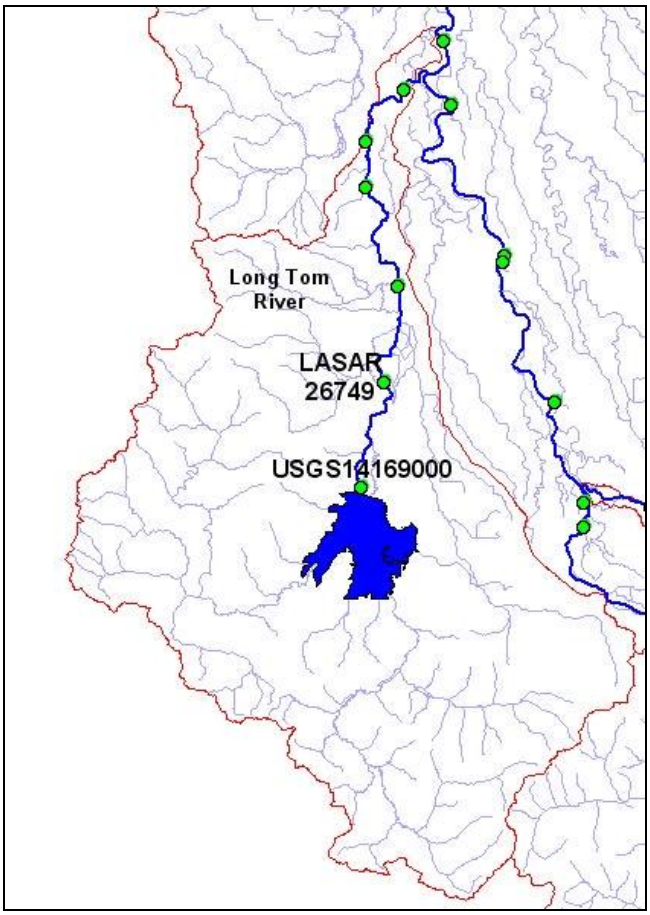


**Figure 451. Long Tom River model upstream temperature boundary condition**

## Year 2001

The upstream temperature boundary condition for the Long Tom River was monitored by the same USGS gage station as flow (14169000). The gage station did not start monitoring temperature until August 7, 2001. A temperature correlation was developed between the USGS gage station and a ODEQ LASAR site at RM 17.75 (26749). Figure 452 shows the temperature correlation between the two sites. Figure 453 shows a temperature time series for the upstream boundary condition on the Long Tom River, including the data and the calculated values. The data at LASAR 26749 were limited with data from May 30, 2001 to later in the year. This results in the temperature correlation only filled data from May 30 to August 7. There were no other data available to use in further developing the temperature upstream boundary condition, thus establishing the starting date for the 2001 model calibration period. Figure 453 shows the data has a diurnal variation of 1 to 2 ºC and the calculated temperatures have a larger diurnal variation of 1 to 4 ºC.

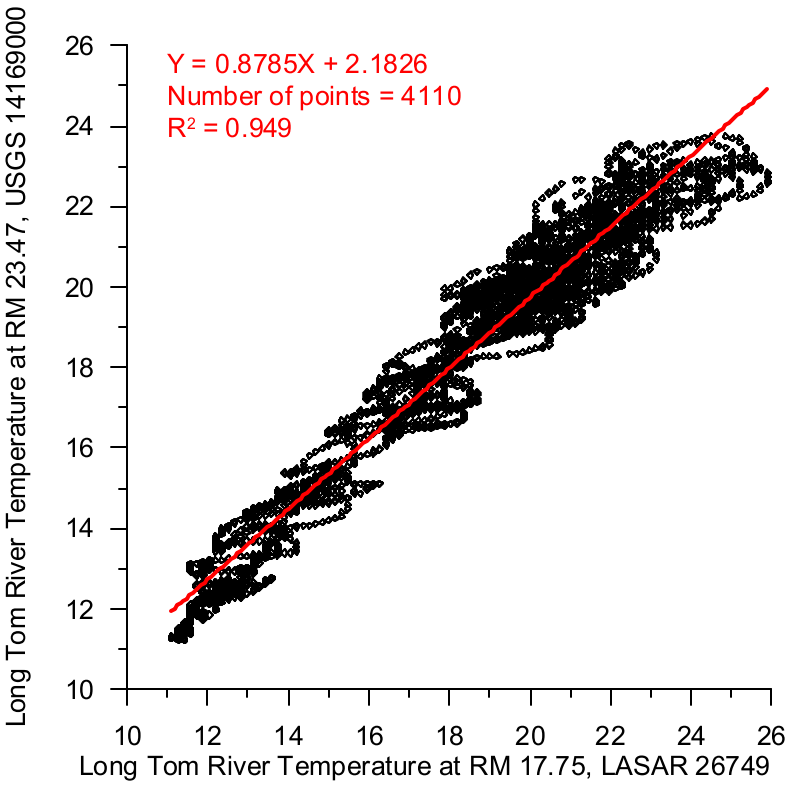


**Figure 452. Temperature correlation between two sites on the Long Tom River**

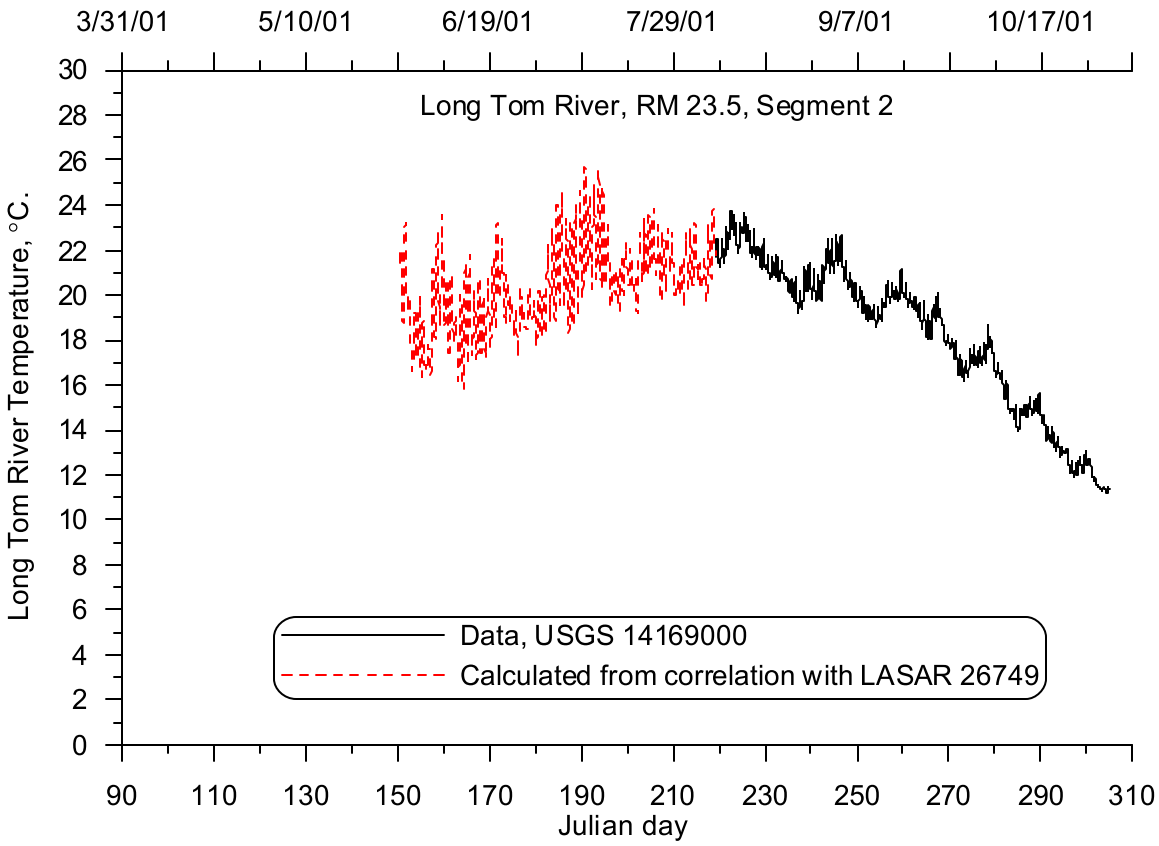


**Figure 453. Long Tom River temperature, 2001**

Year 2002

The upstream boundary of the Long Tom River was monitored for temperature continuously in 2002 at half-hour intervals at the USGS gage station 141690000. Figure 454 shows time series plot of the temperature data for 2002 illustrates the data has a diurnal variation of 1 to 2 ºC.

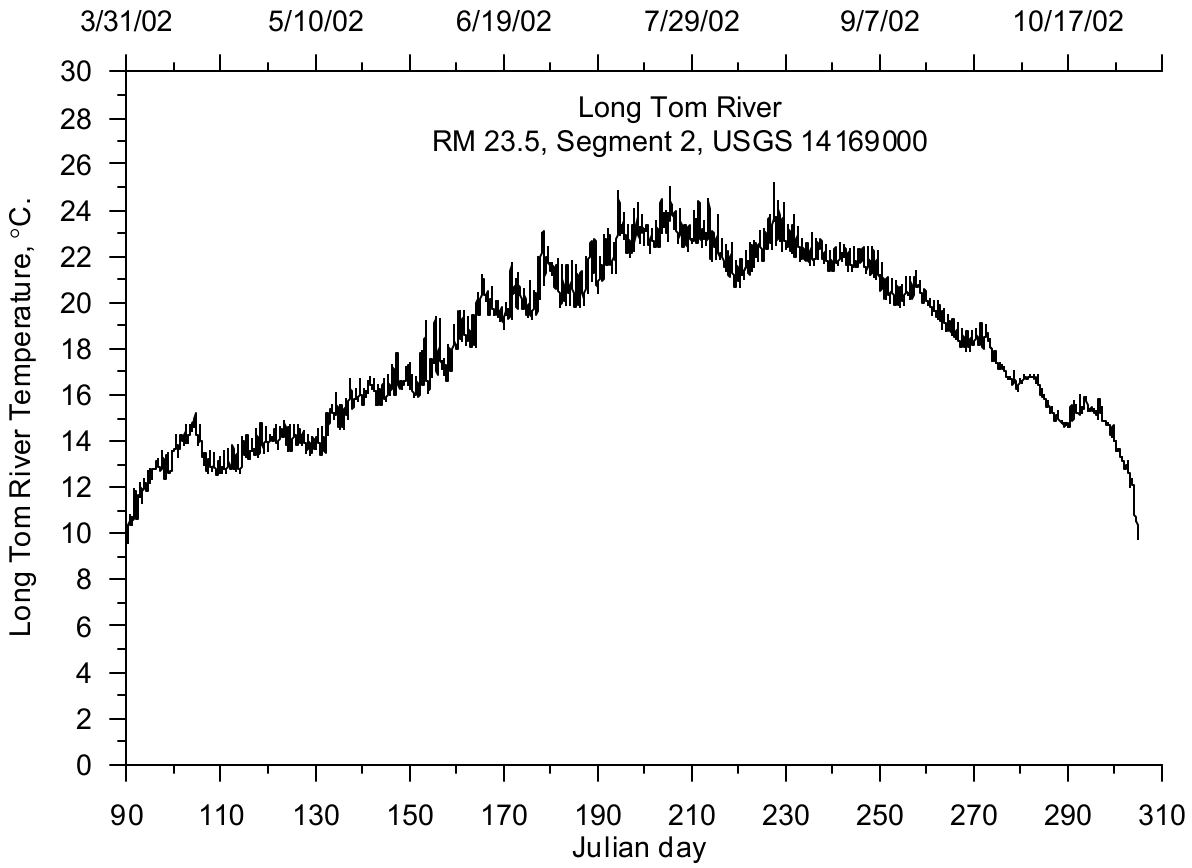


**Figure 454. Long Tom River temperature, 2002**

## *Shading*

CE-QUAL-W2 incorporates both topographic and vegetative shade in the model. Topographic characteristics include the steepest inclination angle in 18 directions around a model segment. The vegetative characteristics consist of tree top elevation, distance between the river channel centerline and the controlling vegetation, and the vegetation density in summer and winter. The vegetation characteristics were provided for both banks of the river.

The vegetation and topographic characteristics for the Long Tom River model were developed using geographic information system (GIS) data supplied by the Oregon Department of Environmental Quality (ODEQ). The data consists of thalweg points every 100 ft along the thalweg of the river. For each thalweg point, additional associated data included: channel width, elevation, three topographic inclination angles, and nine vegetation compartments for each bank. Each vegetation compartment consisted of vegetation height, distance from stream bank, and density. A detailed analysis was performed to convert the ODEQ data into the shade variables for the CE-QUAL-W2 model. A detailed description of the shade analysis is shown in Appendix A.

The model employs two sets of shade reduction factors which can be used to represent summer and winter vegetation thickness. The step transition dates were April 1 for "leaf on" and October 1 for "leaf off." The tree top heights are shown for the left bank in Figure 455, and for the right bank in Figure 456. The tree top heights decrease moving downstream from approximately 110 m to 90 m. The distance from the river centerline to the vegetative shade, also called the offset, are shown for the left bank in Figure 457, and for the right bank in Figure 458. The offset for each bank was fairly uniform, but differs between the banks. The left bank offset typically ranges from 5 to 15 m. The right bank offset typically ranges from 5 to 25 m. The "leaf-on" shade reduction factors are shown for the left bank in Figure 459, and for the right bank in Figure 460. The shade reduction factors generally range from 0.3 to 0.85.

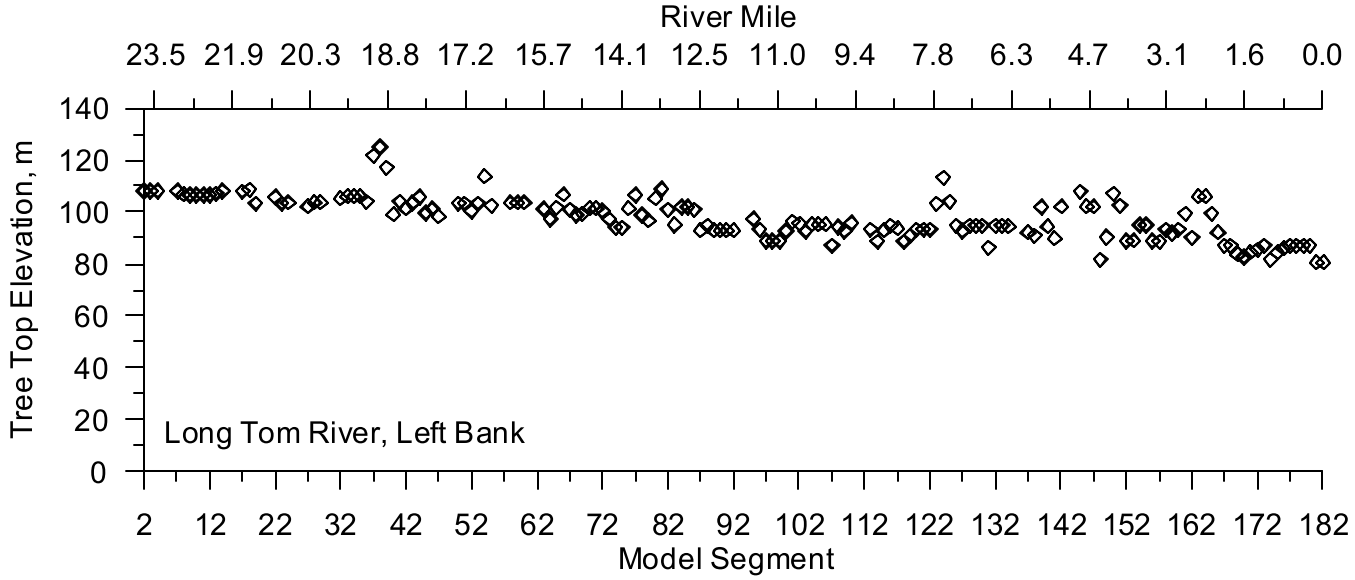


**Figure 455. Long Tom River Left Bank Tree Top Elevation**

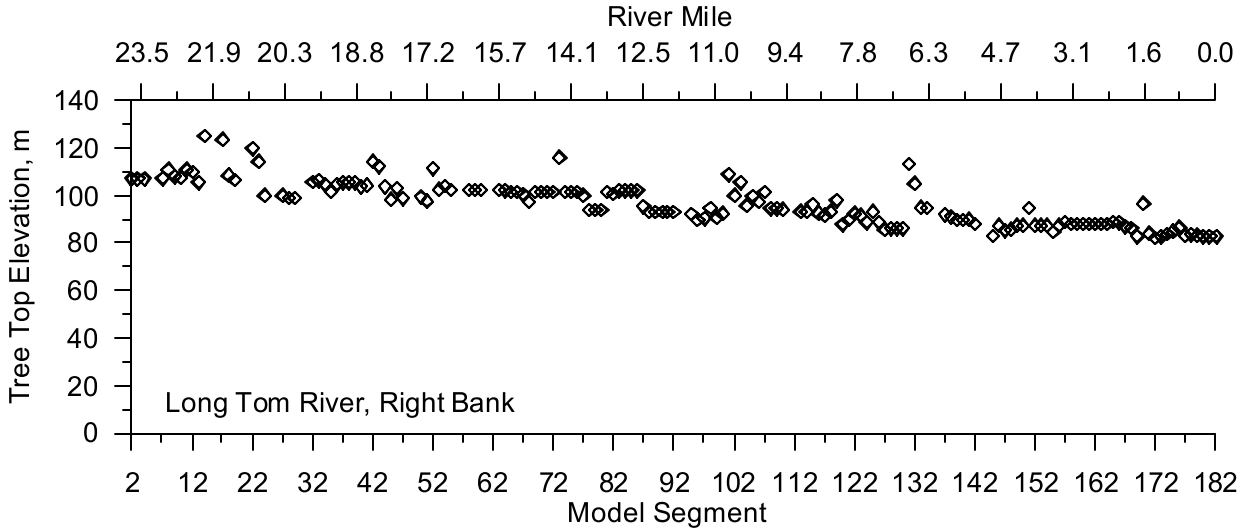


**Figure 456. Long Tom River Right Bank Tree Top Elevation**

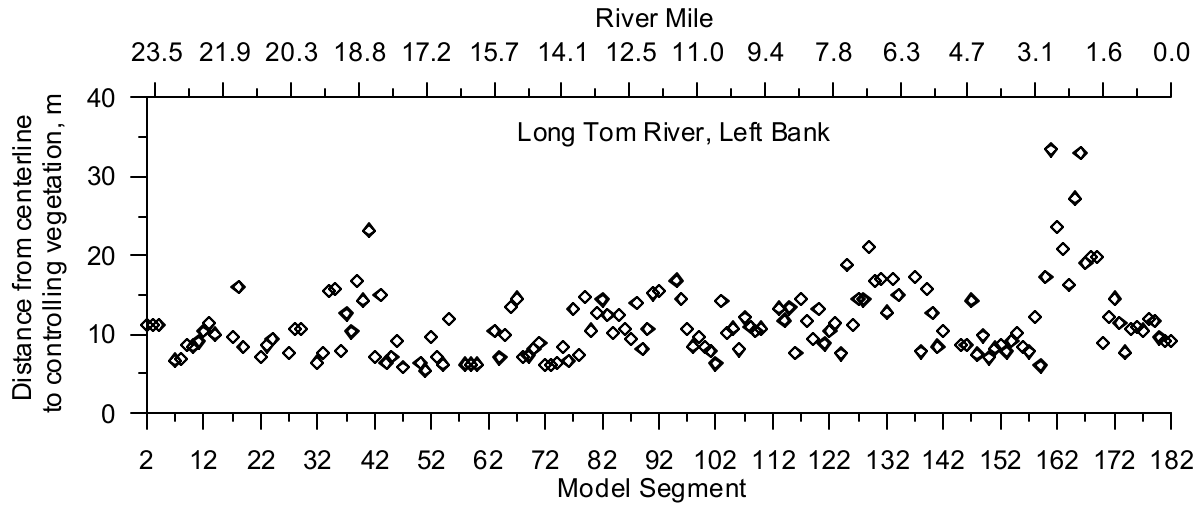


**Figure 457. Long Tom River Left Bank Distance from Centerline to Controlling Vegetation**

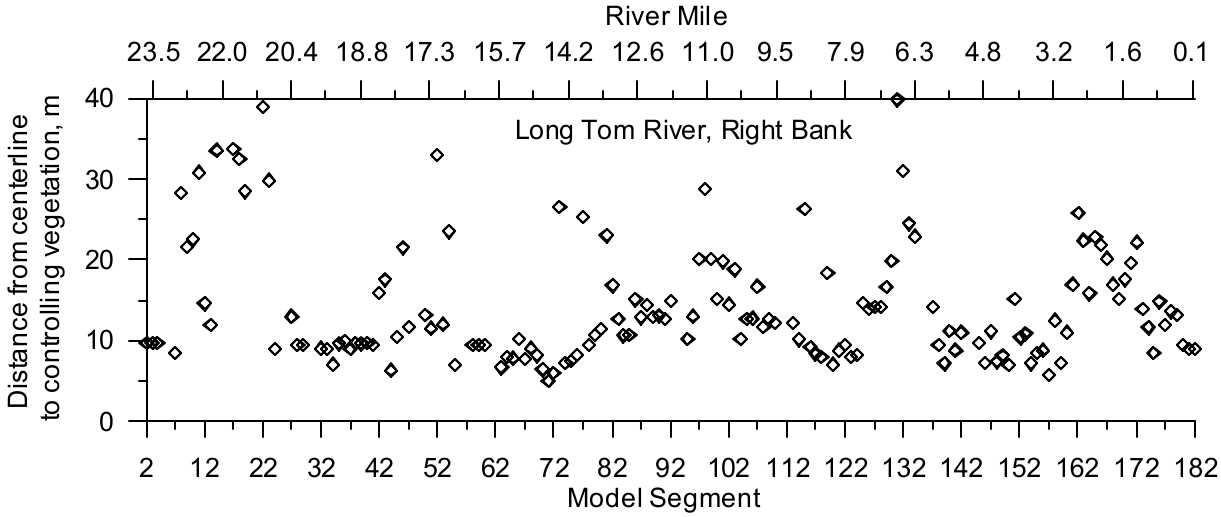


**Figure 458. Long Tom River Right Bank Distance from Centerline to Controlling Vegetation**

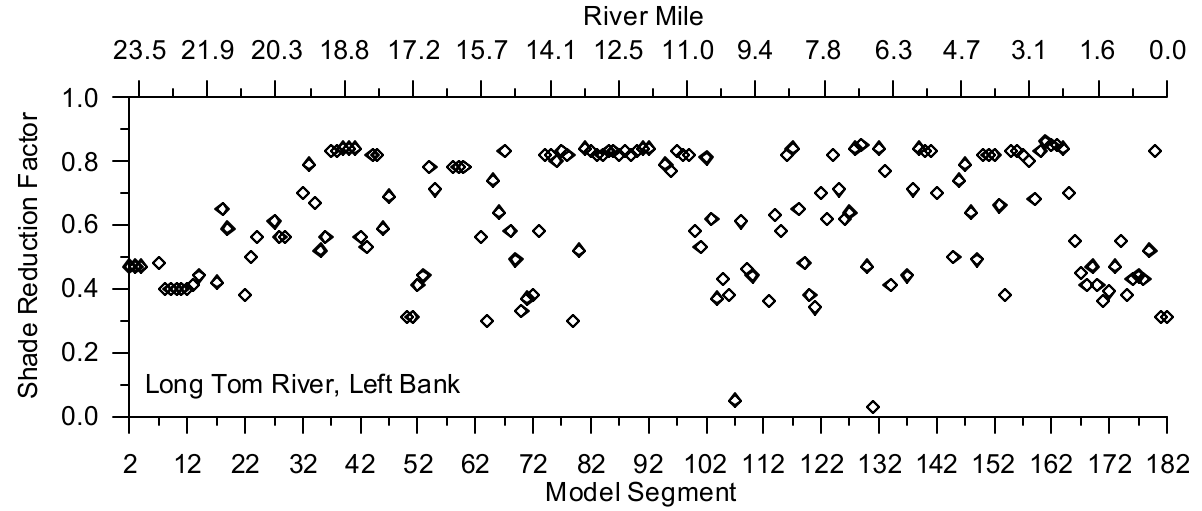


**Figure 459. Long Tom River Left Bank Shade Reduction Factor**

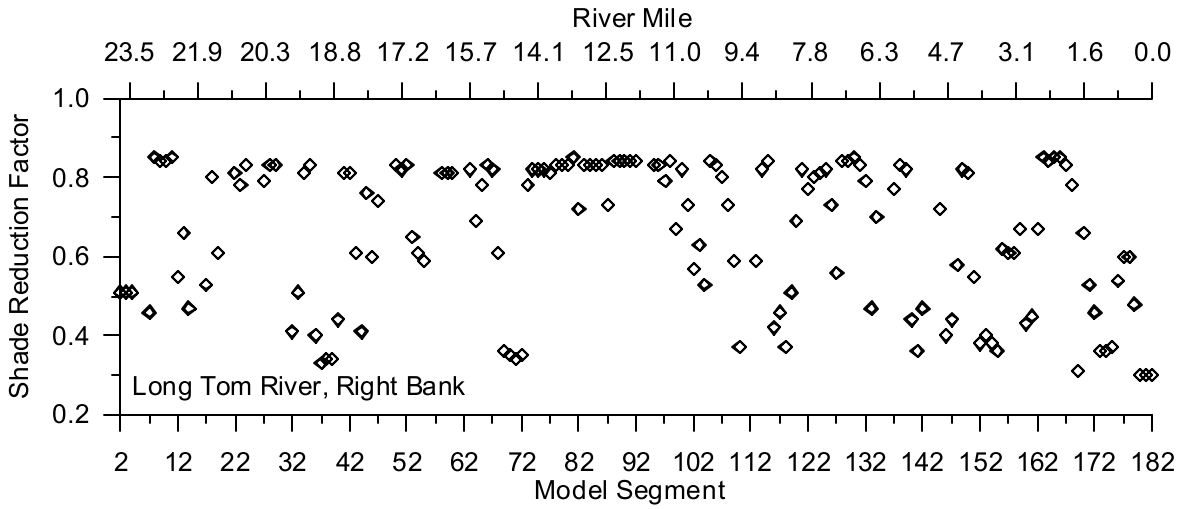


**Figure 460. Long Tom River Right Bank Shade Reduction Factor**

## *Meteorology*

The Long Tom River model utilized meteorological data from several monitoring sites in the area as shown in Figure 461. Table 48 lists the monitoring sites and the meteorological constituents monitored at each site. In 2001, meteorological data were used from the Corvallis data set and in 2002 the model utilized the Eugene data set.

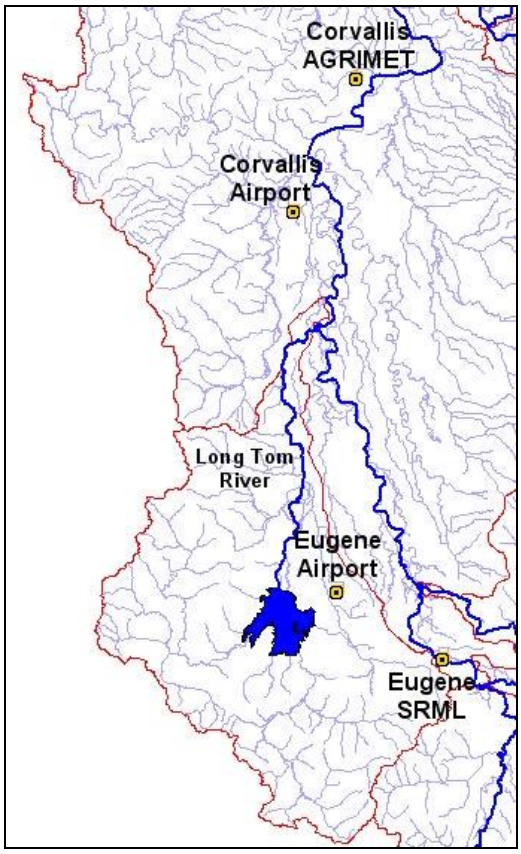


**Figure 461. Long Tom River model meteorological site locations**

**Table 48. Long Tom River model meteorological monitoring sites**

| Site | Agency (Program) | Meteorological Parameters |
|---|---|---|
| Corvallis Municipal Airport | National Weather Service (METAR) | Air Temperature, Dew Point Temperature, Relative Humidity, Wind Speed, Wind Direction, Cloud Cover |
| Eugene WSO Airport / Mahlon Sweet | National Weather Service (METAR) | Air Temperature, Dew Point Temperature, Relative Humidity, Wind Speed, Wind Direction, Cloud Cover |
| Eugene, OR | University of Oregon, Solar Radiation Monitoring Lab | Solar Radiation |
| Corvallis, OR | Bureau of Reclamation, (AGRIMET) | Solar Radiation |

## Corvallis Municipal Airport

### Year 2001

The meteorological data recorded at the Corvallis Municipal Airport which were used for the Upper Willamette River model were also used in the Long Tom River model for 2001. The Corvallis Municipal Airport records air and dew point temperature, wind speed and direction, and cloud cover data but no solar radiation data. Solar radiation data from the Corvallis AGRIMET site were added to the airport data.

Figure 366 and Figure 367 show the air and dew point temperature respectively, over the period of April to October 2001. Figure 368 and Figure 369 show the wind speed and direction, respectively. Figure 368 indicates the minimum wind speed-recording threshold was about 1.5 m/s. The rose diagram in Figure 369 was dominated by the value of zero which was associated with wind speeds below the reading threshold. Figure 370 shows the coarseness of the cloud cover data recorded at the airport with five different cloud cover designations. The solar radiation data collected at the Corvallis AGRIMET site are shown in Figure 371.

## Eugene Airport

### Year 2002

The meteorological data recorded at the Eugene Airport which were used for the Upper Willamette River model were also used in the Long Tom River model for 2002. The Eugene Airport records air and dew point temperature, wind speed and direction, and cloud cover data but no solar radiation data. Solar radiation data from the Eugene SRML site were added to the airport data.

Figure 360 and Figure 361 show the air and dew point temperature respectively, over the period of April to October 2001. Figure 362 and Figure 363 show the wind speed and direction, respectively. Figure 362 indicates the minimum wind speed-recording threshold was about 1.5 m/s. The rose diagram in Figure 363 was dominated by the value of zero which was associated with wind speeds below the

reading threshold. Figure 364 shows the coarseness of the cloud cover data recorded at the airport with only about five different cloud cover designations. The data points between the five values were the result of interpolations to fill data gaps in the cloud cover data. The solar radiation data collected at the Eugene SRML site is shown in Figure 365.

# McKenzie River

The McKenzie River model consists of 69.8 miles of the McKenzie River and the South Fork of the McKenzie River up to Cougar Reservoir. The Blue River and the Blue River Reservoir are treated as a tributary to the McKenzie River model and are not part of the model grid domain. Both the Blue River Reservoir and Cougar Reservoir are operated by the U.S. Army Corps of Engineers. The McKenzie River model also includes diversion operations to the Leaburg and Walterville canals by the Eugene Water and Electric Board (EWEB). The McKenzie River enters the Upper Willamette River at RM 175.3. The McKenzie River basin drains approximately 3500 $km^2$. Figure 462 shows a map of the McKenzie River basin and the model domain.

The model calibration periods were from May 20, 2001 to October 15, 2001 and from April 1, 2002 to October 31, 2002.

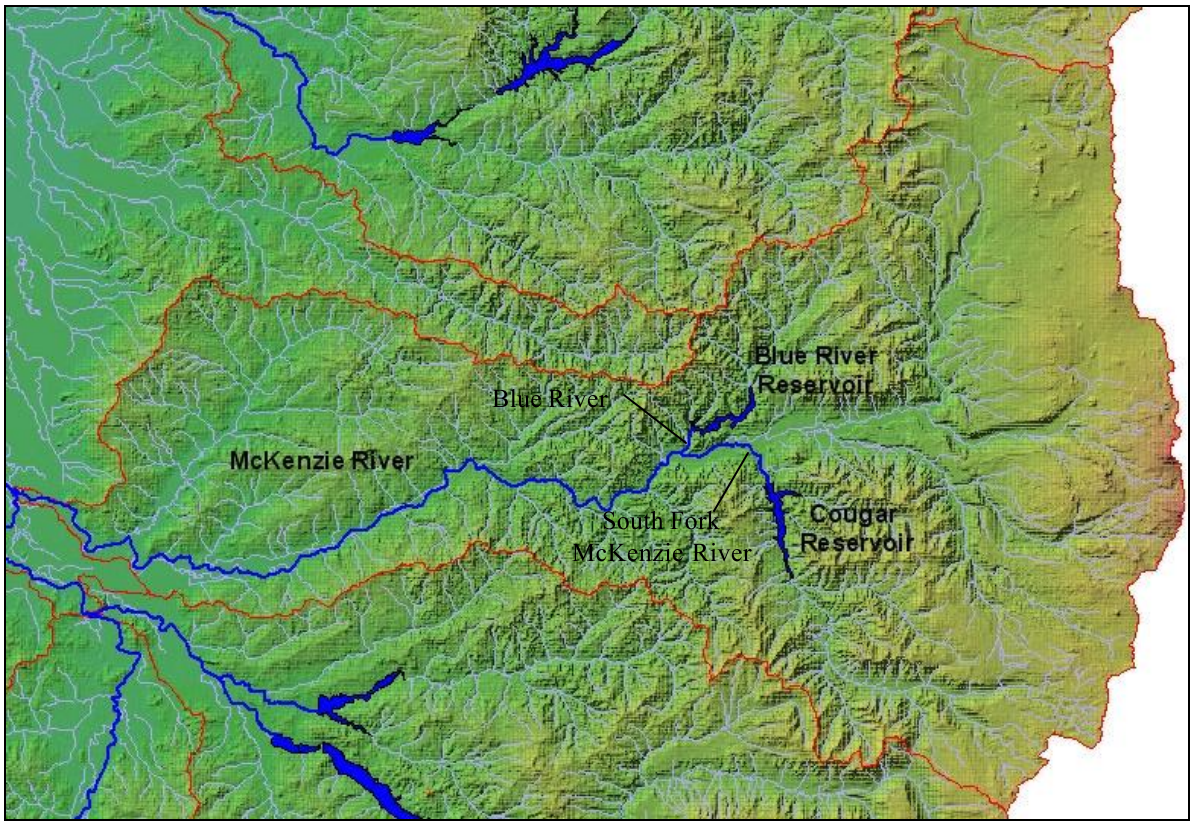


**Figure 462. McKenzie River model region**

## *Model Geometry*

### Bathymetry Data

The data used to generate the model bathymetry were obtained from two USGS surveyed cross sections for gage stations, Digital Elevation Maps (DEM), and GIS data sets from ODEQ. There were five

USGS gage stations on the McKenzie River which were surveyed to ensure the gaging stations have accurate stage – flow relationship curves. Figure 463 shows the location of the cross sections along the river. Table 49 lists the five cross sections with their river mile locations. Figure 464 shows the cross section data collected at two of the gage stations.

The DEM data had a vertical resolution of 1 m, and a horizontal resolution of 10 m. Figure 465 shows a longitudinal profile of the McKenzie River from DEM data with additional elevation points from the USGS surveyed cross sections. The figure shows the DEM data, representing water surface elevation, below the thalweg elevation data. The DEM data were representative for the specific day and time when the aerial measurements were taken. Channel morphology changes, different flow rates and reservoir operations influence the river channel bottom elevation. Using linear interpolation, additional cross sections were generated at a spacing frequency of 100 feet using the river thalweg point generated from a GIS analysis conducted by ODEQ.

There were no river cross sections taken below RM 3.26 (USGS 14165500). Additional cross sections were estimated in this reach by extending the last river cross section at RM 3.26 downstream and adjusting the cross section width based on the channel width from the ODEQ GIS data and by adjusting the cross section elevation based on the slope of the river from the same GIS data.

The calculated cross sections were combined with DEM data and the five surveyed cross sections into the contour mapping program, SURFER. An average volume-elevation relationship was calculated over the length of each model segment using a one meter vertical resolution. The longitudinal profile in Figure 465 shows the thalweg elevation profile from the SURFER contour plot. Figure 466 shows a contour plot of the McKenzie River channel. The contour plot and river center line were then used to slice the river into model segments.

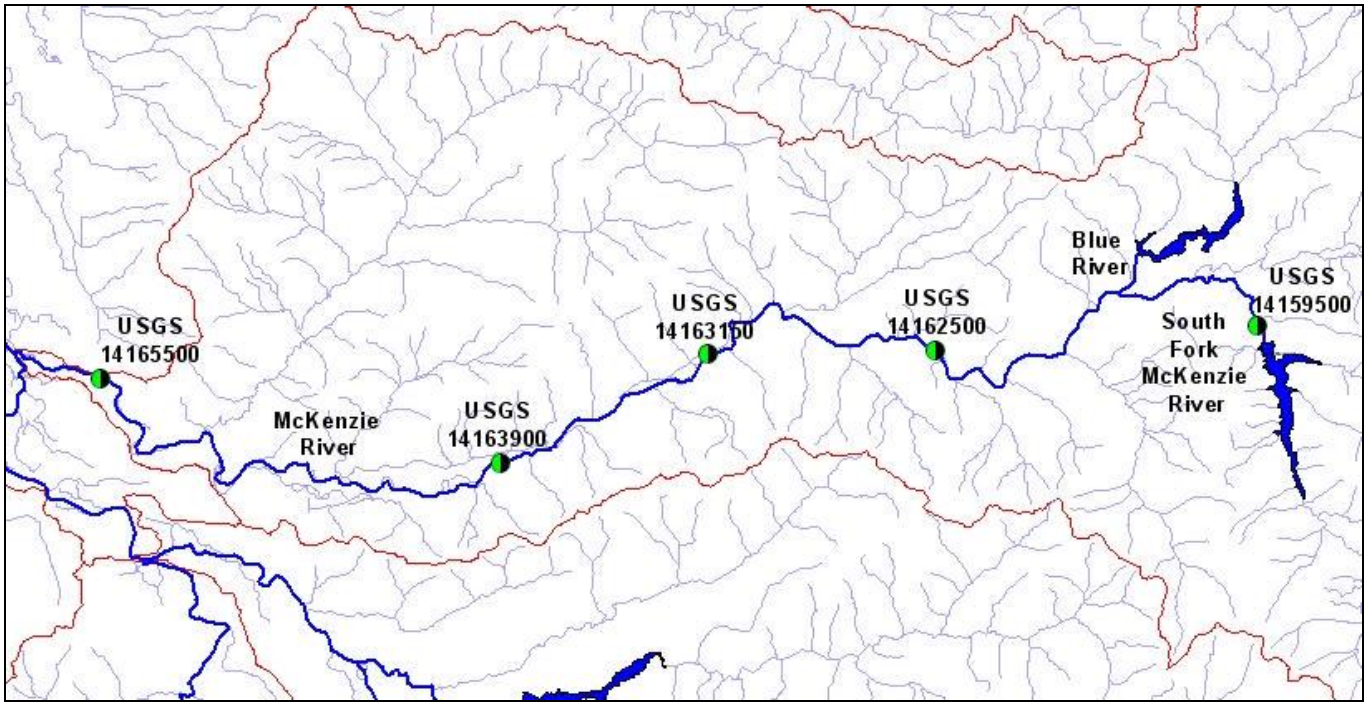


**Figure 463. McKenzie River USGS gage station cross section locations**

**Table 49. McKenzie River USGS gage station cross sections**

| Gage Station | River Mile | Description |
|---|---|---|
| USGS 14159500 | 60.39 | South Fork McKenzie River near Rainbow, OR |
| USGS 14162500 | 44.56 | McKenzie River gage station, near Vida, OR |
| USGS 14163150 | 34.11 | McKenzie River below Leaburg Dam |
| USGS 14163900 | 24.97 | McKenzie River near Walterville, OR |
| USGS 14165500 | 3.26 | McKenzie River near Coburg, OR |

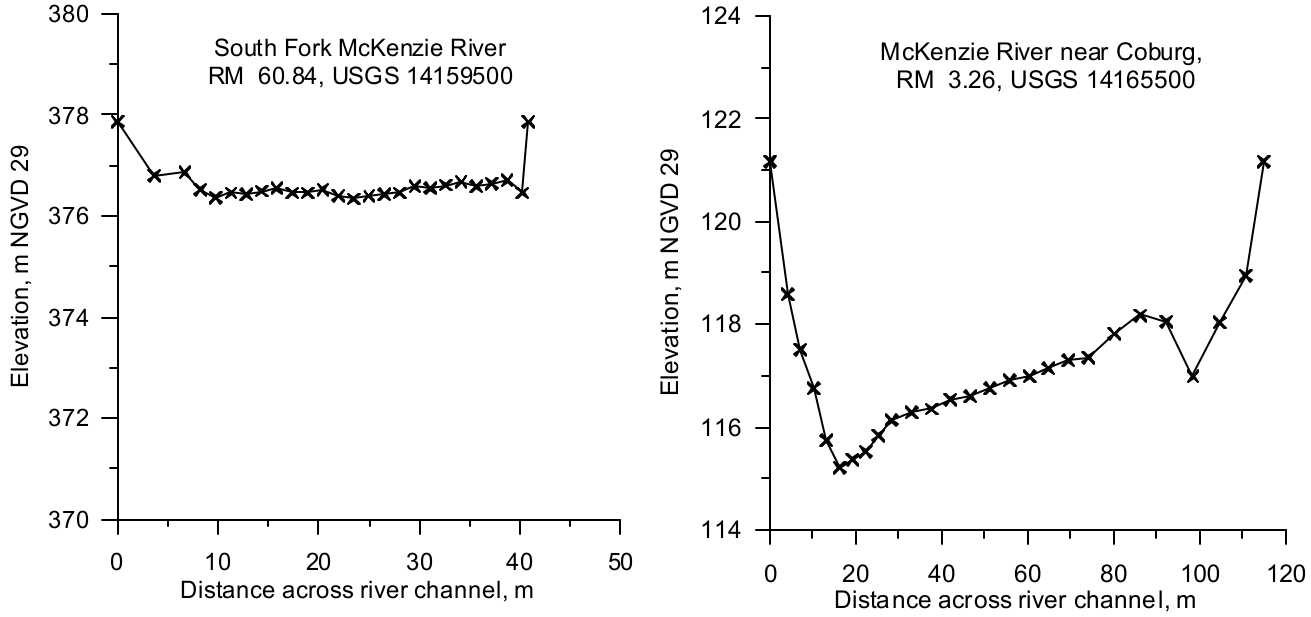


**Figure 464. McKenzie River USGS gage station cross sections**

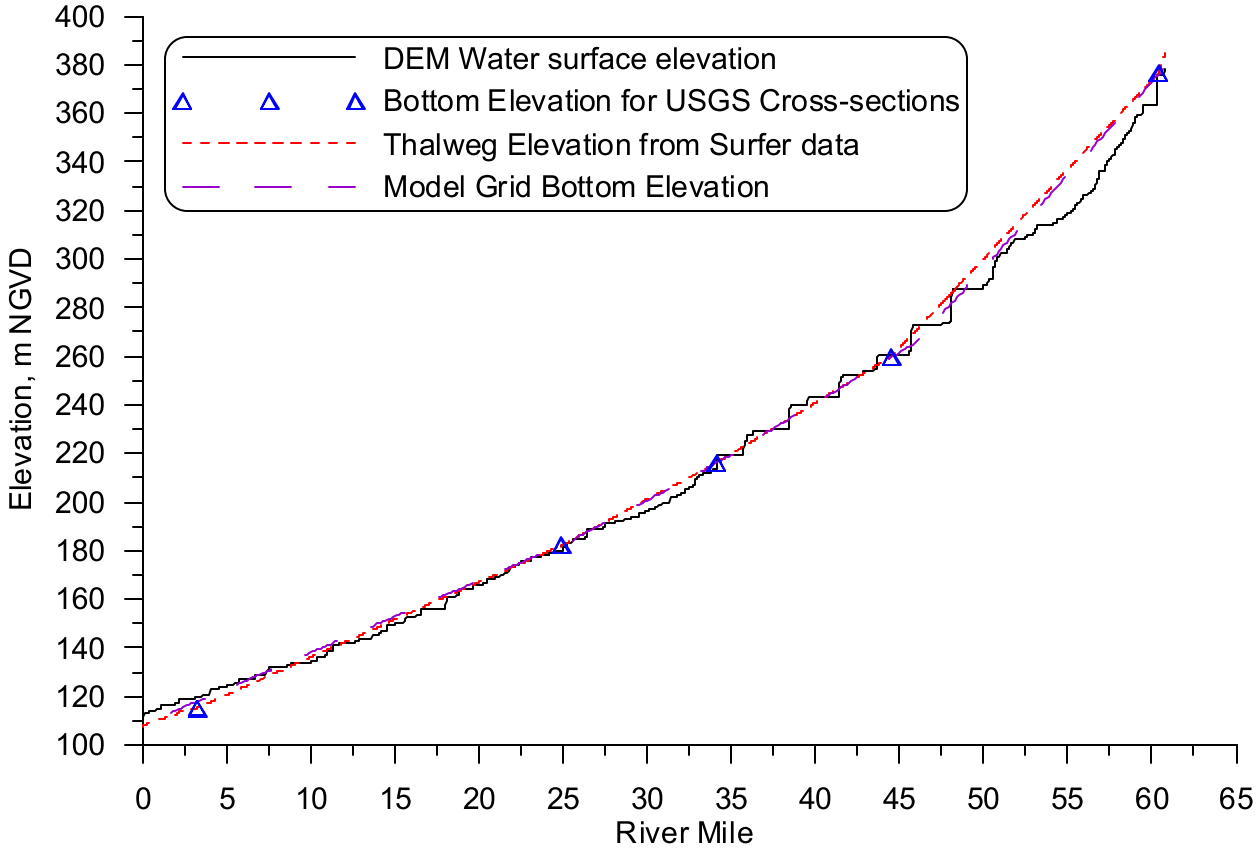


**Figure 465. McKenzie River Longitudinal Profile**

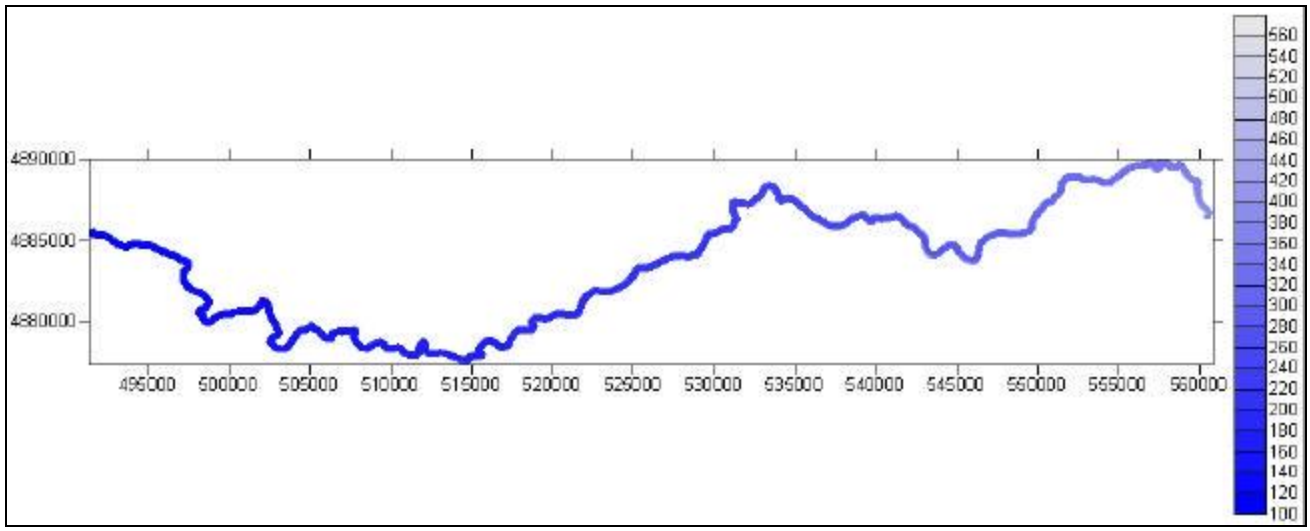


**Figure 466. McKenzie River contour plot using SURFER**

## Model Grid Development

The data were combined and the plotting program SURFER was used to create a contour plot of the stream channel. The contour plot was then used to generate the model grid. The model grid consists of

seven water bodies, each of which has a single branch. Figure 467 shows a map of the model grid layout. Table 50 lists the model grid characteristics.

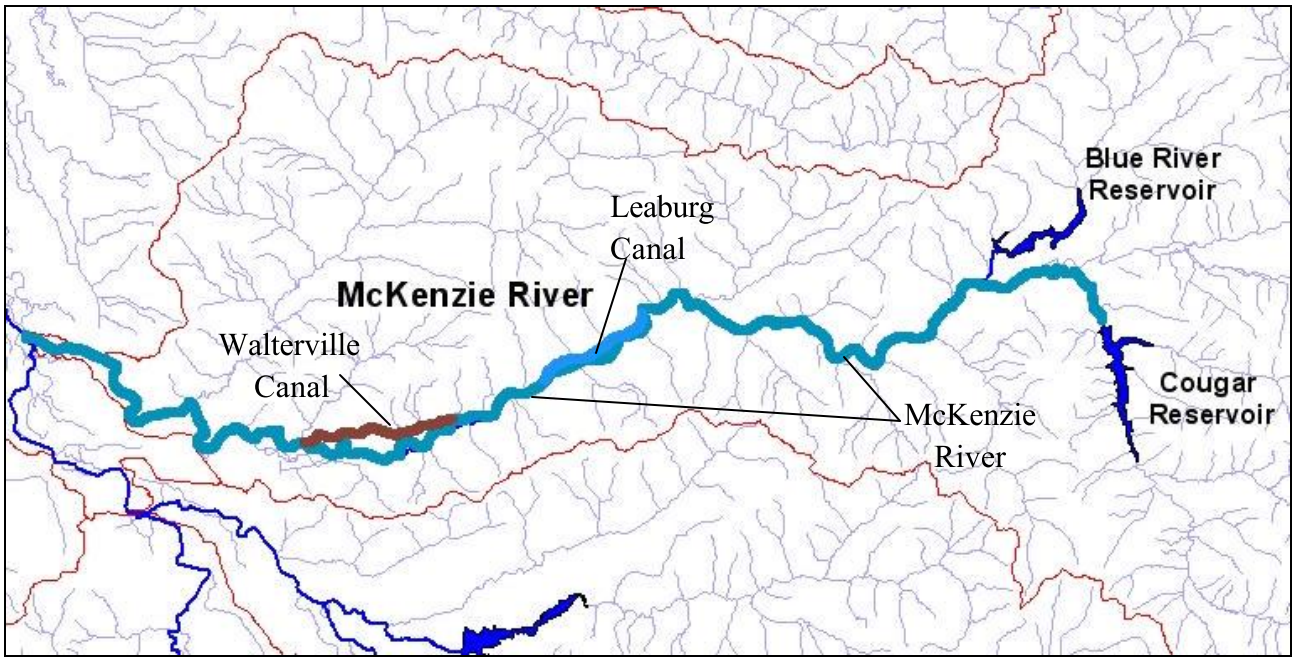


**Figure 467. McKenzie River model grid layout**

**Table 50. McKenzie River model grid layout specifications**

| Water Body | Branch | Description | Starting Segment | Ending Segment | Starting RM | Ending RM | Segment Length, m | Slope | Upstream BC | Down-stream BC |
|---|---|---|---|---|---|---|---|---|---|---|
| 1 | 1 | South Fork McKenzie River/McKenzie River | 2 | 96 | 60.8 | 46.1 | 250.55 | 0.004748 | flow | internal |
| 2 | 2 | McKenzie River | 99 | 164 | 46.1 | 35.7 | 250.55 | 0.002600 | internal | internal |
| 3 | 3 | McKenzie River | 167 | 180 | 35.7 | 33.5 | 250.55 | 0.002340 | flow | internal |
| 4 | 4 | McKenzie River | 183 | 233 | 33.5 | 25.6 | 250.55 | 0.002240 | internal | internal |
| 5 | 5 | McKenzie River | 236 | 399 | 25.6 | 0.0 | 250.55 | 0.001845 | flow | internal |
| 6 | 6 | Leaburg Canal | 402 | 431 | 25.6 | 17.4 | 265.18 | 0.000265 | flow | internal |
| 7 | 7 | Walterville Canal | 434 | 473 | 35.7 | 30.0 | 257.56 | 0.002413 | flow | internal |

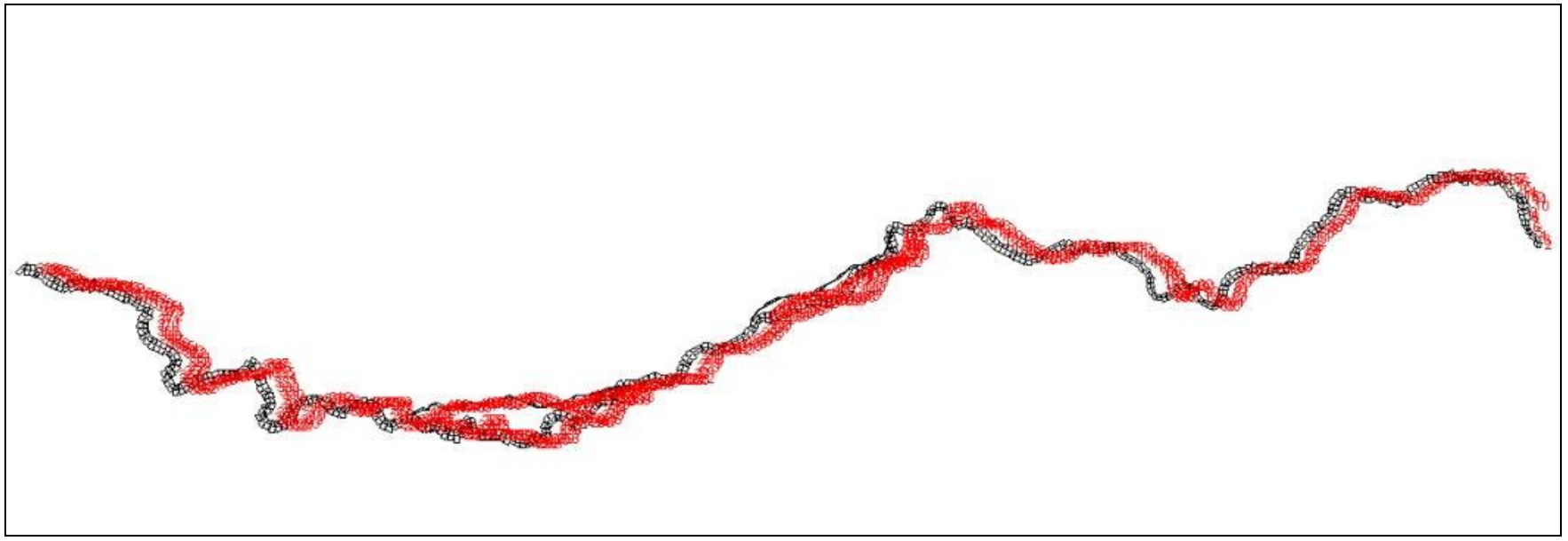

**Figure 468. McKenzie River model grid layout from preprocessor**

## *Model Upstream & Downstream Boundary Conditions*

The McKenzie River basin was modeled from the confluence of the Willamette River with the McKenzie to the South Fork of the McKenzie River and then upstream on the South Fork McKenzie to Cougar Reservoir. Figure 469 shows the upstream boundary location for the model which was represented by the USGS gage station 14159500 (South Fork McKenzie near Rainbow, OR). This gage was 724 m (0.45 mi.) downstream from the start of the model at Cougar Reservoir. Figure 469 also shows that the McKenzie River extends upstream of the South Fork McKenzie River, which will be represented as a tributary to the South Fork McKenzie River.

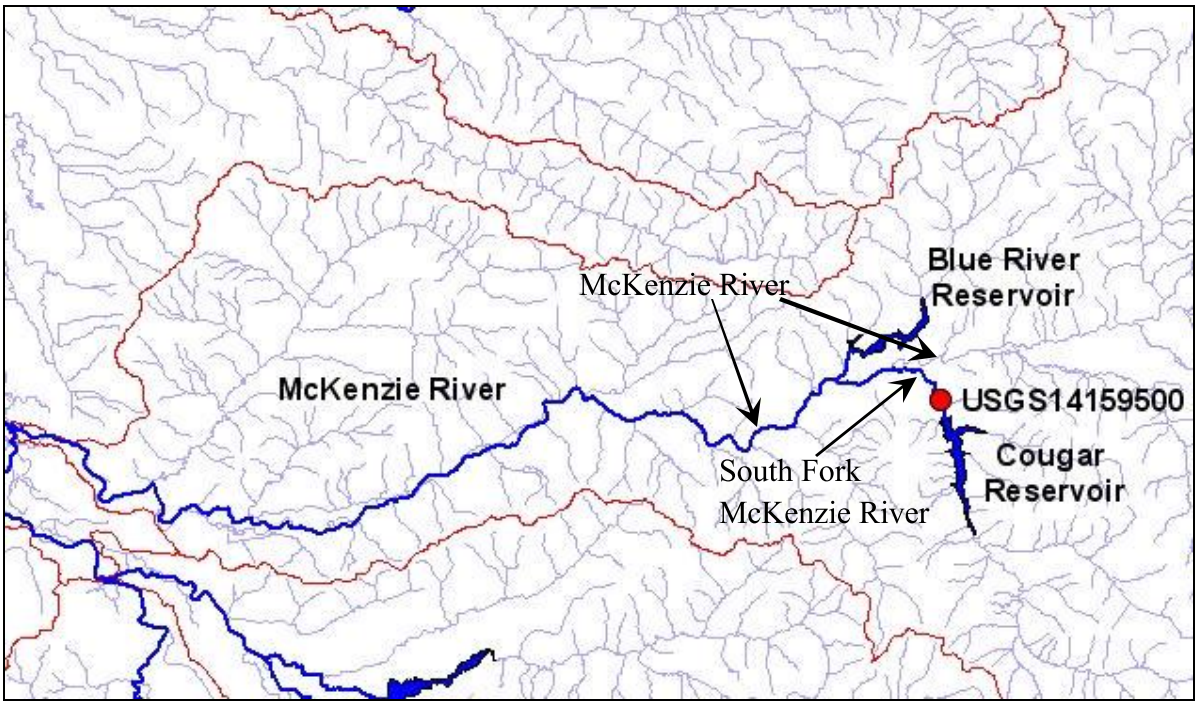


**Figure 469. McKenzie River model upstream flow and temperature boundary condition site**

### Hydrodynamic Data

#### Year 2001

The McKenzie River model was run from May 20 to October 31, 2001. The model was run for the South Fork of McKenzie River downstream to the confluence of the McKenzie River with the Willamette River. Below Cougar Dam on the South Fork of the McKenzie River, there is a USGS gage station (14159500) monitoring river flow. Figure 470 shows the time series record of the flow on the South Fork McKenzie from April 1 to October 31, 2001.

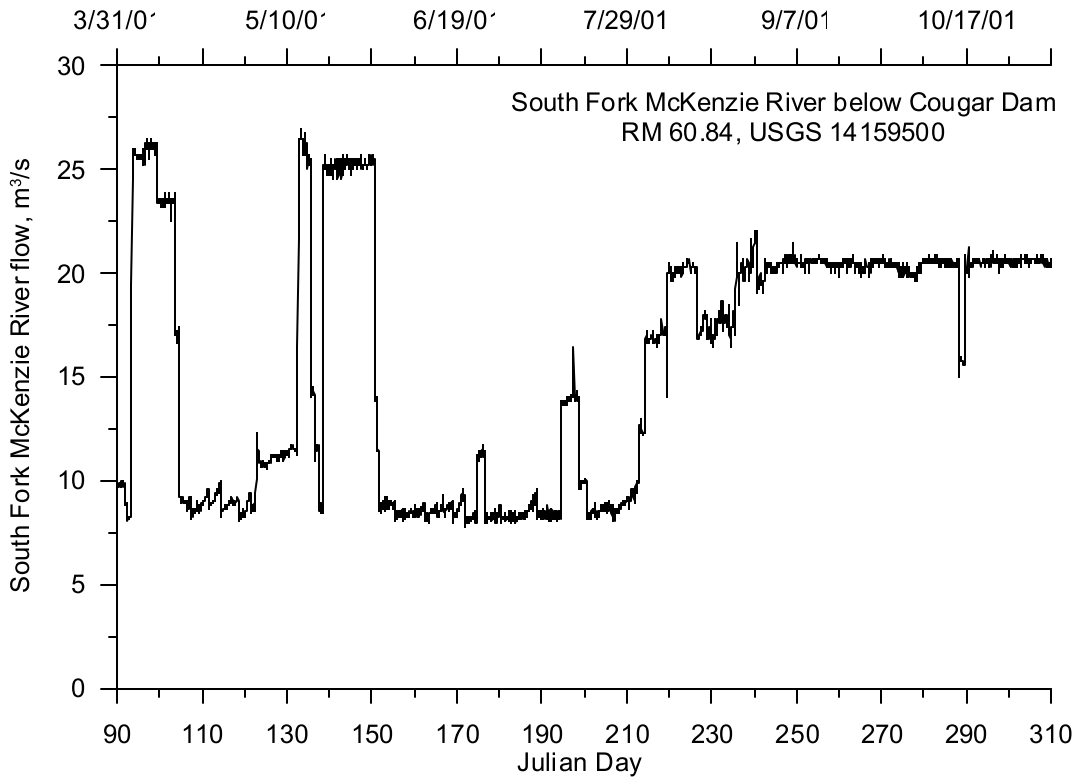


**Figure 470. South Fork McKenzie River flow, 2001**

## Year 2002

The same gage station used for characterizing the 2001 flows on the South Fork McKenzie River was also used for 2002. Figure 471 shows the flow time series for the South McKenzie River and shows that the flow in the spring of 2002 was much higher than flows in 2001.

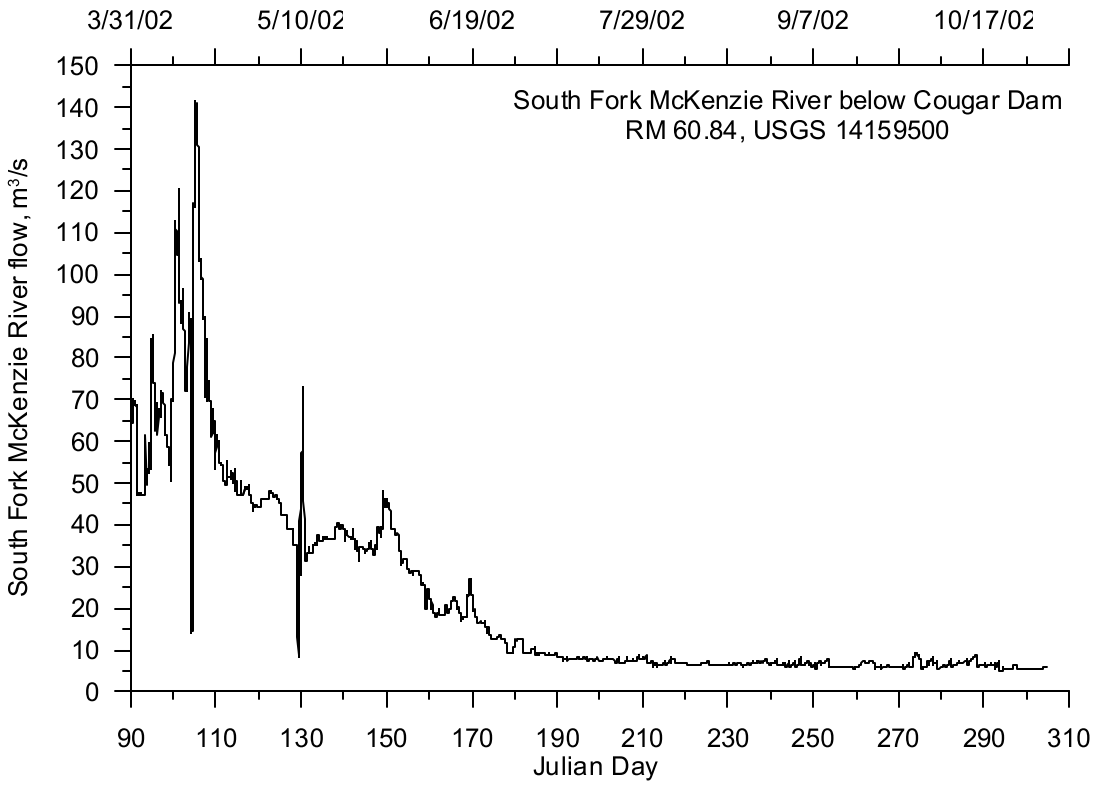


**Figure 471. South Fork McKenzie River flow, 2002**

## Temperature Data

### Year 2001

The same USGS gage station that monitored flow on the South Fork of the McKenzie River also monitored stream temperature. Figure 472 shows the temperature time series record from April to October 31, 2001. The figure illustrates the small diurnal fluctuation in the temperature data due to the reservoir operations upstream at Cougar Dam.

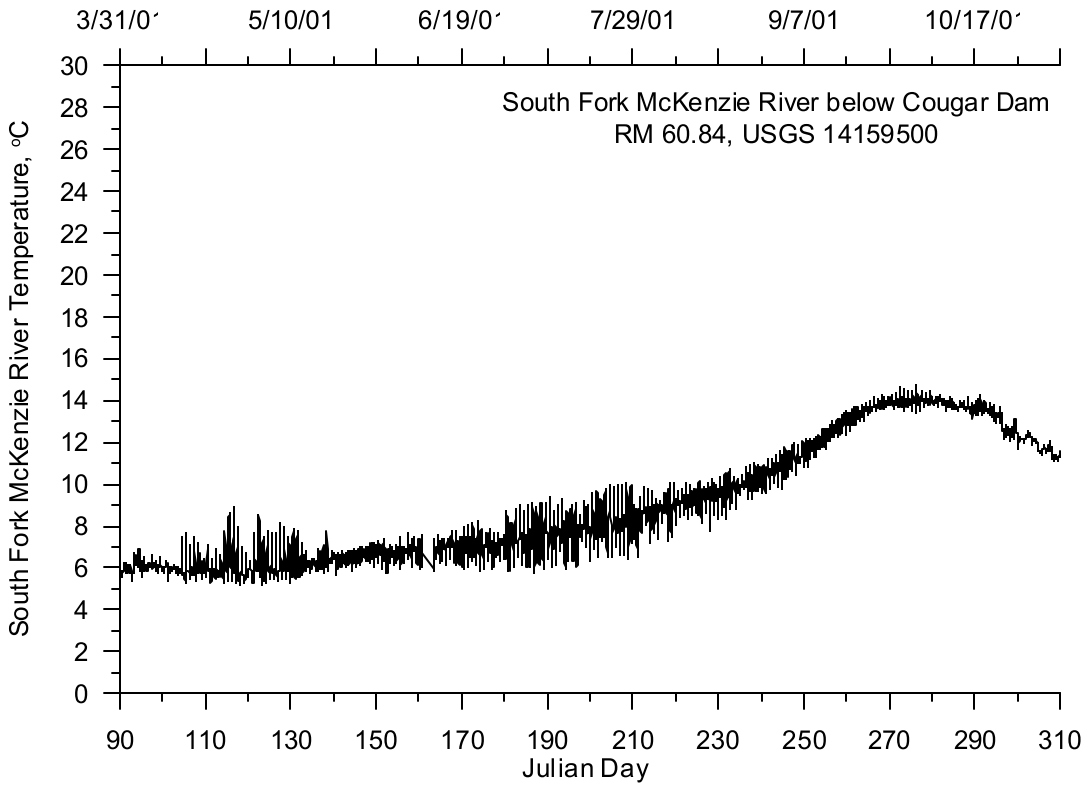


**Figure 472. South Fork McKenzie River temperature, 2001**

## Year 2002

The same USGS gage station monitoring flow on the South Fork of the McKenzie River also monitored stream temperature. Figure 473 shows the temperature time series record from April to October 31, 2002. The figure shows only a small diurnal fluctuation in the temperature due to the reservoir operations upstream at Cougar Dam. The stream temperatures recorded in 2002 were higher than in 2001 with a seasonal warming trend as expected.

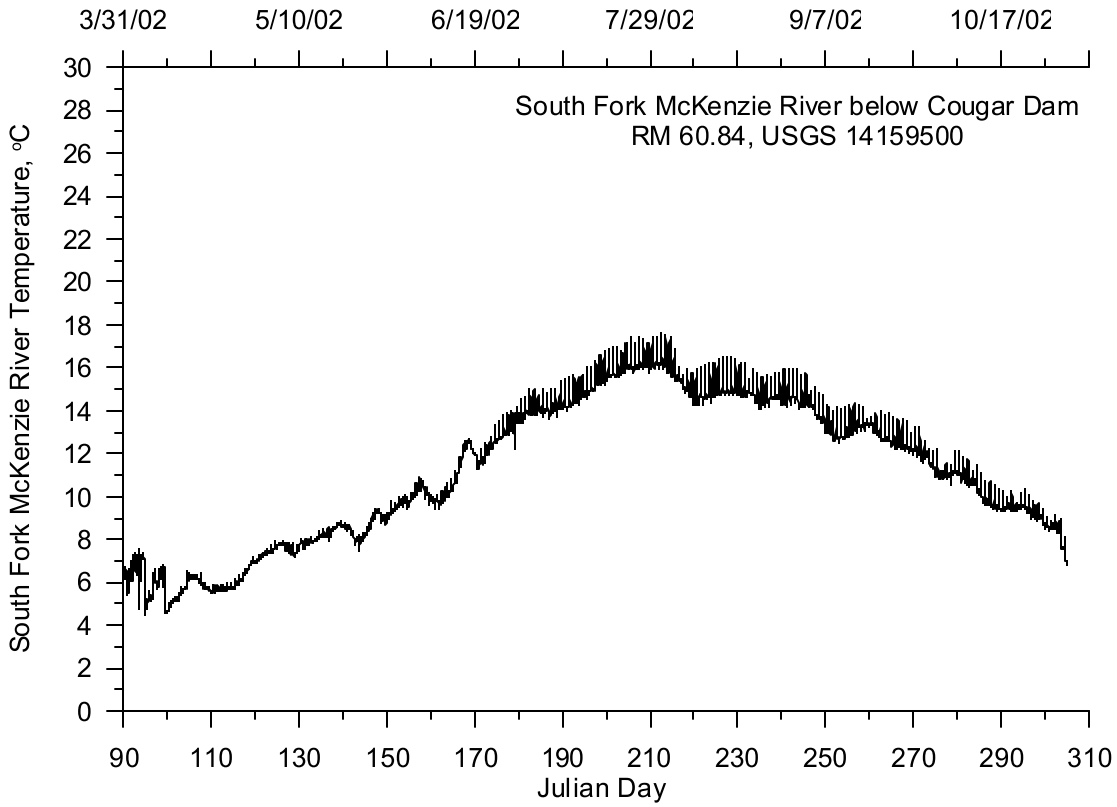


**Figure 473. South Fork McKenzie River temperature, 2002**

## *Tributaries and Distributed Tributaries*

There are nine large tributaries contributing flow to the McKenzie River. Only three of these tributaries have any flow data, one of which has only historical data. Figure 474 shows a map of the McKenzie basin illustrating the larger tributaries and distributed tributaries contributing flow. Table 51 lists the tributaries contributing flow and their river mile and corresponding model segment.

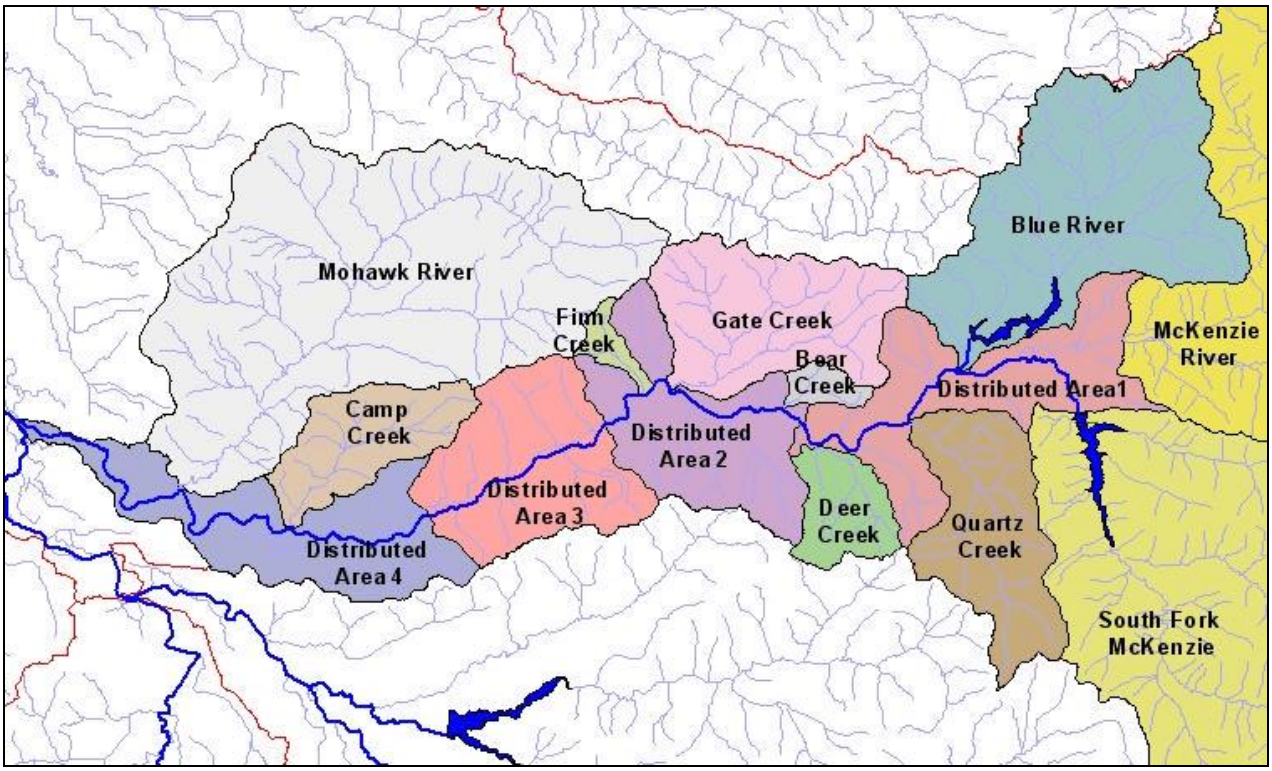


**Figure 474. McKenzie River tributary and distributed tributary sub basins**

**Table 51. McKenzie River model tributaries**

| Site ID | Tributary | McKenzie RM | Model Segment |
|---|---|---|---|
| USGS 14159000 | McKenzie River | 60.25 | 30 |
| USGS 14162200 | Blue River | 53.73 | 47 |
| ungaged | Quartz Creek | 50.70 | 67 |
| ungaged | Deer Creek | 45.76 | 100 |
| ungaged | Bear Creek | 43.66 | 114 |
| ungaged | Gate Creek | 38.13 | 149 |
| ungaged | Finn Creek | 36.55 | 159 |
| ungaged | Camp Creek | 17.33 | 288 |
| USGS 14165000 | Mohawk River | 9.66 | 338 |

## Hydrodynamic Data

### Year 2001

Since there were no flow data on the McKenzie River just upstream of the confluence with the South Fork of the McKenzie River, a correlation was developed between historical daily flow data at the discontinued USGS gage station, 14159000, and the USGS gage station downstream on the McKenzie River at RM 44.56 (14162500). Although the USGS gage station flow data at RM 44.56 reflects reservoir operations from Blue and Cougar Reservoirs, there was still a relatively strong correlation between daily flow data sets. Data used in the correlation were obtained from 1910 to 1994 with 17,074 flow measurements. Figure 475 shows the flow correlation between the two sites and the correlation

equation. The correlation equation was then used with the daily flow data recorded at the USGS gage at RM 44.56 to calculate flow for the McKenzie River upstream. The calculated flows were then adjusted to better represent the lower river flows by reducing the calculated McKenzie River flow by 10% when the downstream flow at RM 44.56 was less than 65.13 $m^3/s$ (23000 cfs). Figure 476 shows the calculated flows for the McKenzie River as a tributary to the model. The Blue River was also monitored with a USGS gage (14162200) on a half-hourly basis. Figure 477 shows the Blue River flow for 2001.

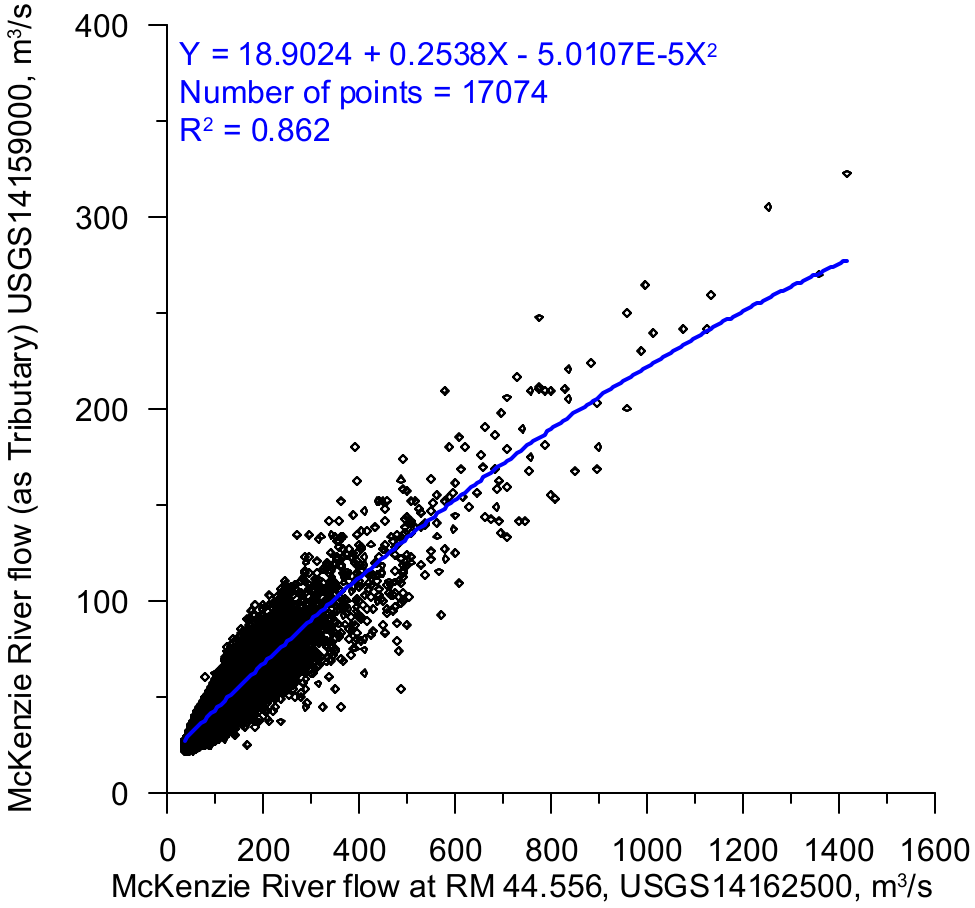


**Figure 475. McKenzie River flow correlation**

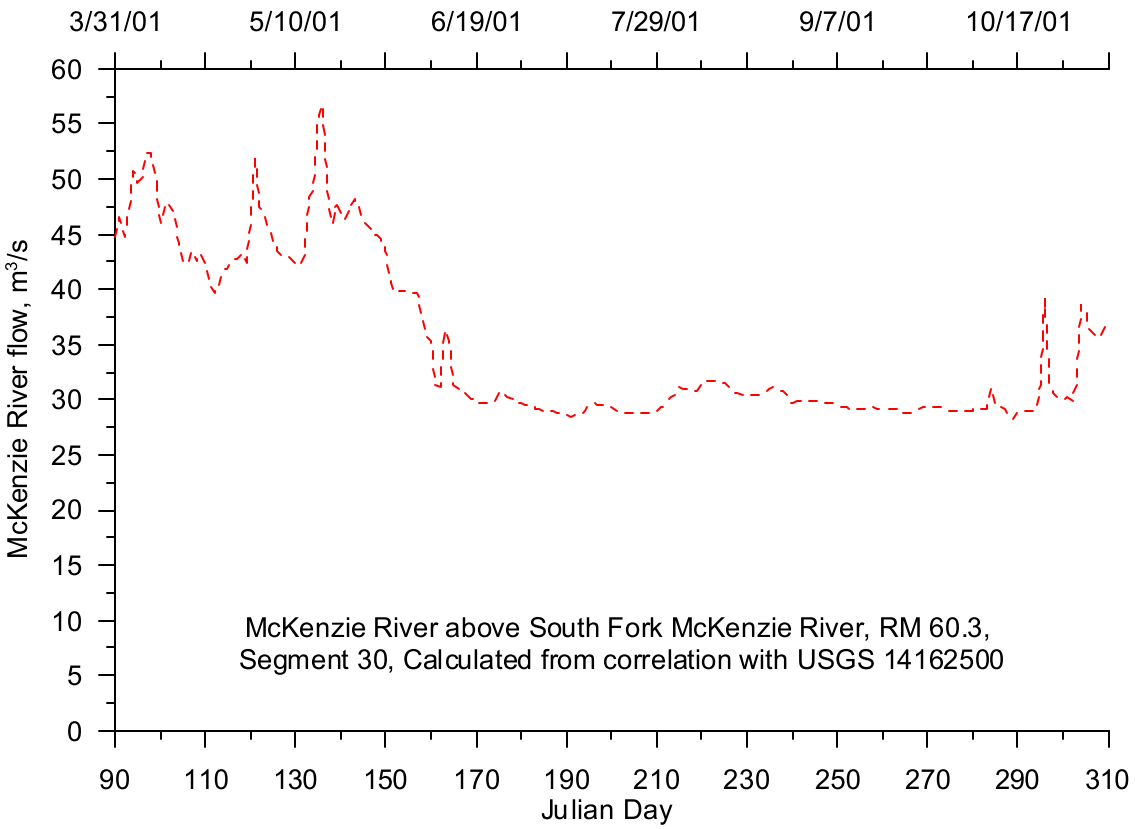


**Figure 476. McKenzie River tributary flow, 2001**

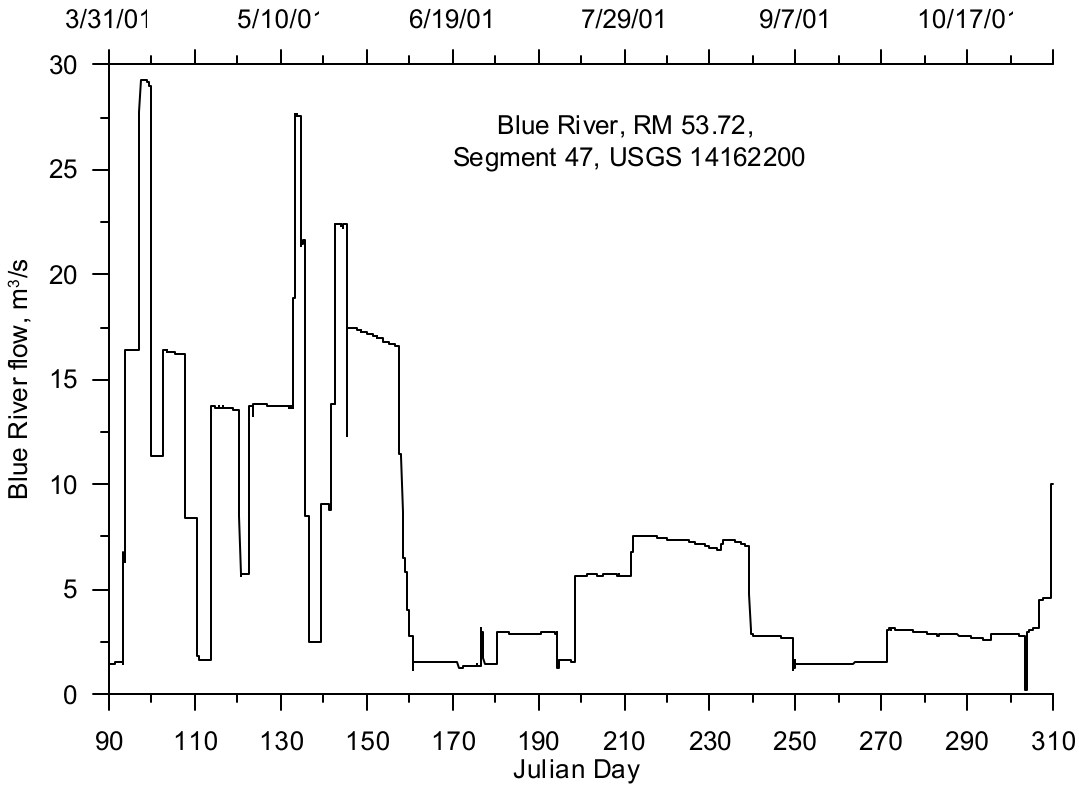


**Figure 477. Blue River flow, 2001**

The hydrology for the McKenzie River was divided into several large reaches to identify the flow contributions from several ungaged tributary basins and distributed areas along the river. The first reach is from the upstream boundary on the South Fork McKenzie River (RM 60.84, USGS 14159500) to the USGS gage at RM 44.56 (USGS 14162500). The second reach covers the McKenzie River between the gage at RM 44.56 and the USGS gage at RM 35.72 (USGS 14163150). The third reach handles the inflow between the gage at RM 35.72 and at the USGS gage at RM 24.97 (USGS 14163900).

There are no USGS gage stations below RM 24.97, and attempts to correlate historical daily flows with a retired gage at RM 3.9 were unsuccessful. There were no gage station flow data downstream of RM 24.97 so the hydrology could not be analyzed to incorporate distributed inflows, but two large tributaries were included: Camp Creek and Mohawk River. Figure 478 shows a map of the four distributed drainage areas and their corresponding river reaches defined by USGS gage locations. Table 52 summarizes the hydrological reaches. Flows used in this analysis were daily averaged flows.

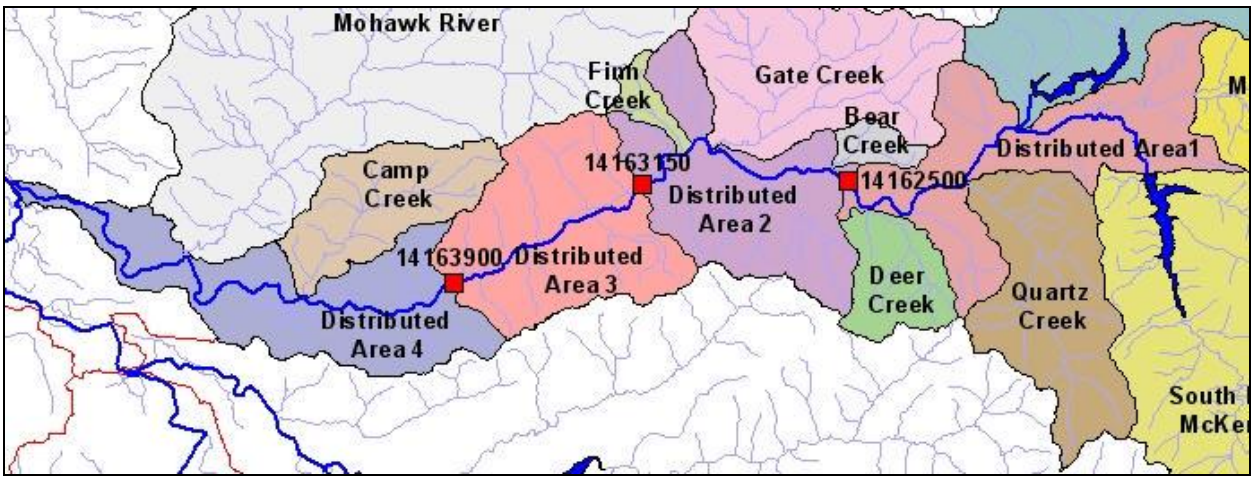


**Figure 478. McKenzie River distributed drainage areas**

**Table 52. McKenzie River hydrology analysis reaches**

| Distributed Area/ Reach | RM range | USGS Upstream gage | USGS Downstream gage | Tributaries |
|---|---|---|---|---|
| 1 | 60.84 to 44.56 | 14159500 | 14162500 | Blue and McKenzie Rivers, Quartz and Deer Creeks, and Distributed Area |
| 2 | 44.56 to 35.72 | 14162500 | 14163150 | Bear, Gate and Finn Creeks and Distributed Area |
| 3 | 35.72 to 24.97 | 14163150 | 14163900 | Distributed Area |
| 4 | 24.97 to 0.00 | 14163900 | NA | Camp Creek and Mohawk River |

Reach 1

In the first reach of the McKenzie River (RM 60.84 to 44.56), the ungaged flow was calculated by subtracting the South Fork McKenzie River, the McKenzie River and the Blue River flows from the flow monitored at RM 44.56 on the McKenzie River. The calculated ungaged flow was then divided between the two drainage basins (Deer and Quartz Creeks) and the ungaged distributed area using their fraction of the total drainage area. Table 53 shows a list of the basin areas between the two USGS gage

station for this reach, their drainage areas, and the fraction of ungaged flow attributed to each sub basin (fourth column).

**Table 53. Drainage Basin Area above McKenzie River RM 44.56**

| Basin | Area, $km^2$ | Fraction of Drainage area above RM 44.56 | Fraction of Drainage Area not gaged |
|---|---|---|---|
| Deer Creek | 32 | 1.32% | 11.72% |
| Quartz Creek | 110 | 4.59% | 40.75% |
| Ungaged Distributed | 128 | 5.35% | 47.53% |
| Blue River | 239 | 10.00% | NA |
| McKenzie River | 1345 | 56.35% | NA |
| South Fork McKenzie River | 535 | 22.39% | NA |
| Total | 2388 | 100.00% | 100.00% |

Figure 479 shows the daily flow attributed to the Quartz Creek basin for 2001. Figure 480 shows the daily flow for Deer Creek basin. Figure 481 shows the daily flows for the ungaged distributed flow for the reach between RM 60.84 and RM 44.56.

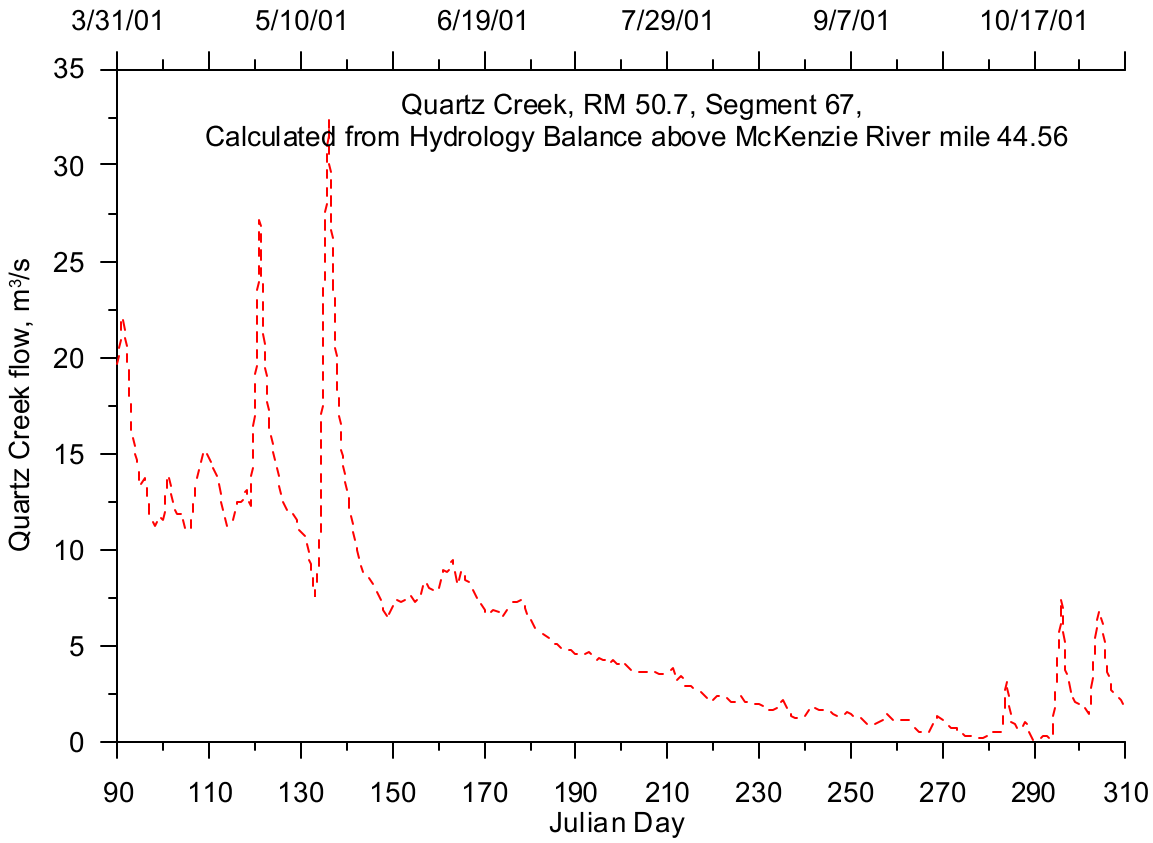


**Figure 479. Quartz Creek flow, 2001**

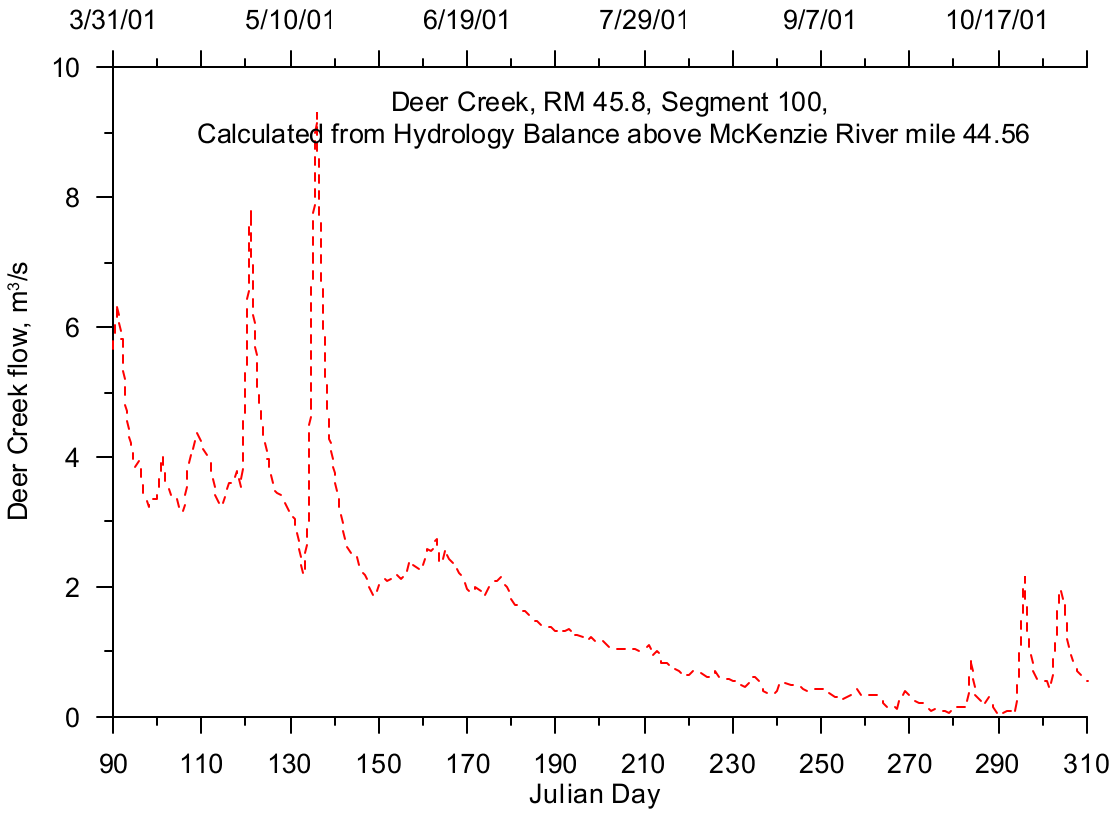


**Figure 480. Deer Creek flow, 2001**

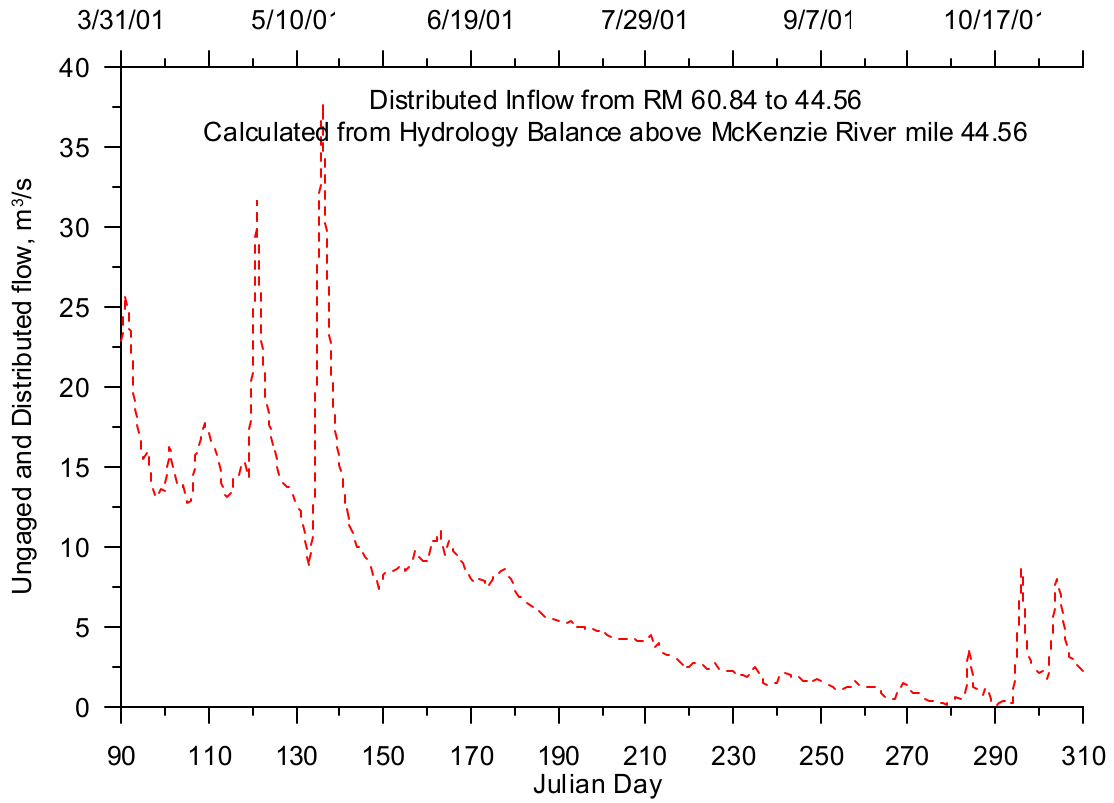


**Figure 481. Distributed flow for the McKenzie River from RM 60.84 to 44.56, 2001**

Reach 2

In the second reach of the McKenzie River (RM 44.56 to 35.72), the ungaged flows were calculated by subtracting the Leaburg Canal flow, which is diverted at RM 35.78, from the flow monitored at RM 44.56, and then subtracting this result from the flow monitored at RM 35.72. The relationship can be written:

$$UngagedInflow = USGS14163150, flow - (USGS14162500, flow - LeaburgCanalDiversion, flow)$$

The flow diversion to the Leaburg Canal was estimated using operation rules provided by the Eugene Water and Electric Board (EWEB, 2002) as discussed in the reservoir operations section below. The resulting flow was then apportioned by drainage area among the three basins and the ungaged distributed area listed in Table 54.

**Table 54. Drainage Basin Area along the McKenzie River, RM 44.56 to 35.72**

| Basin | Area, $km^2$ | Fraction of Drainage area, RM 44.56-35.72 |
|---|---|---|
| Bear Creek | 24 | 8.94% |
| Gate Creek | 125 | 47.16% |
| Finn Creek | 12 | 4.71% |
| Distributed | 104 | 39.20% |
| Total | 265 | 100.00% |

Figure 482 shows the calculated flow time series for Bear Creek in 2001. Figure 483 shows the calculated flow for Gate Creek. Figure 484 shows the calculated flow for the Finn Creek basin. Figure 485 shows the distributed flow from the ungaged drainage area between RM 44.56 and RM 35.72 along the McKenzie River.

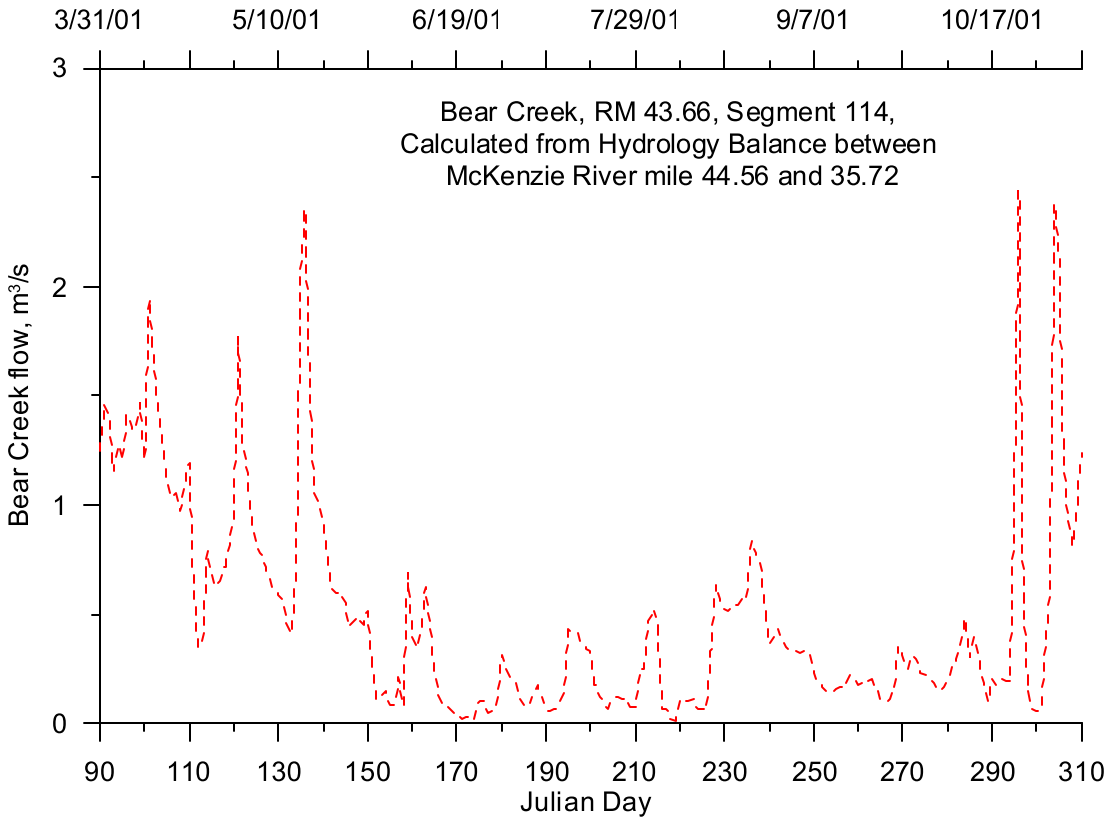


**Figure 482. Bear Creek flow, 2001**

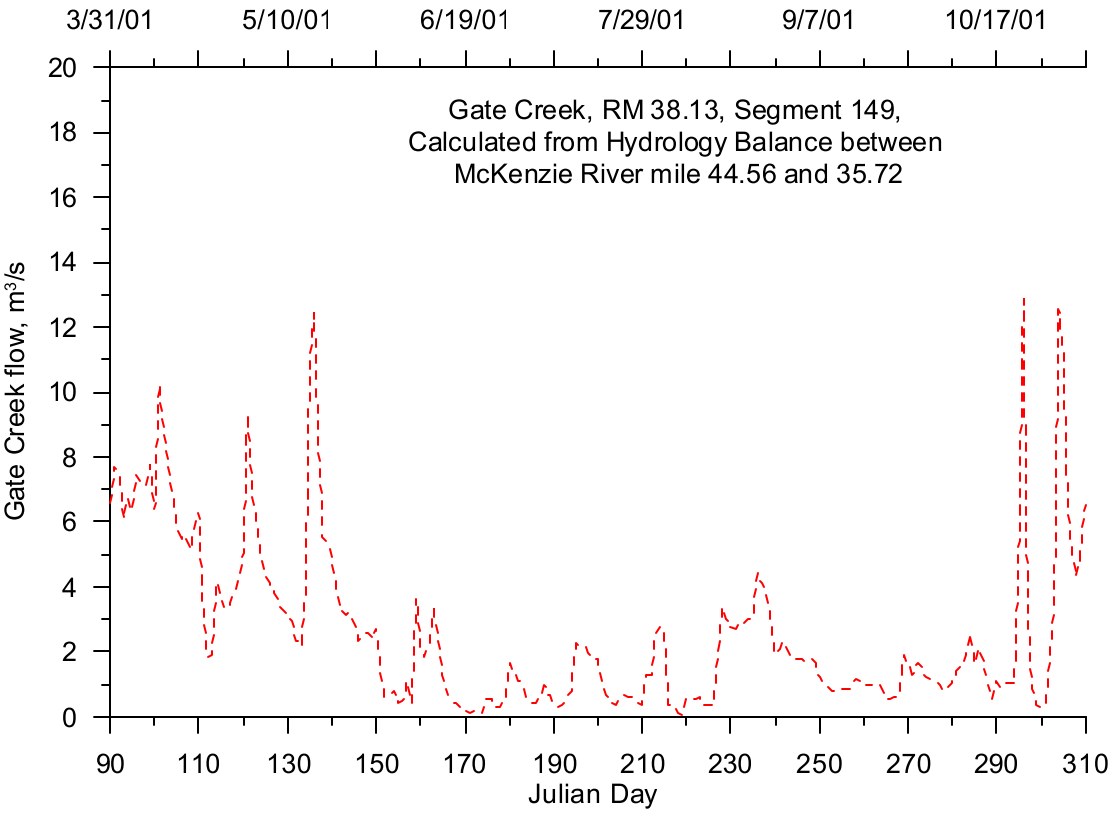


**Figure 483. Gate Creek flow, 2001**

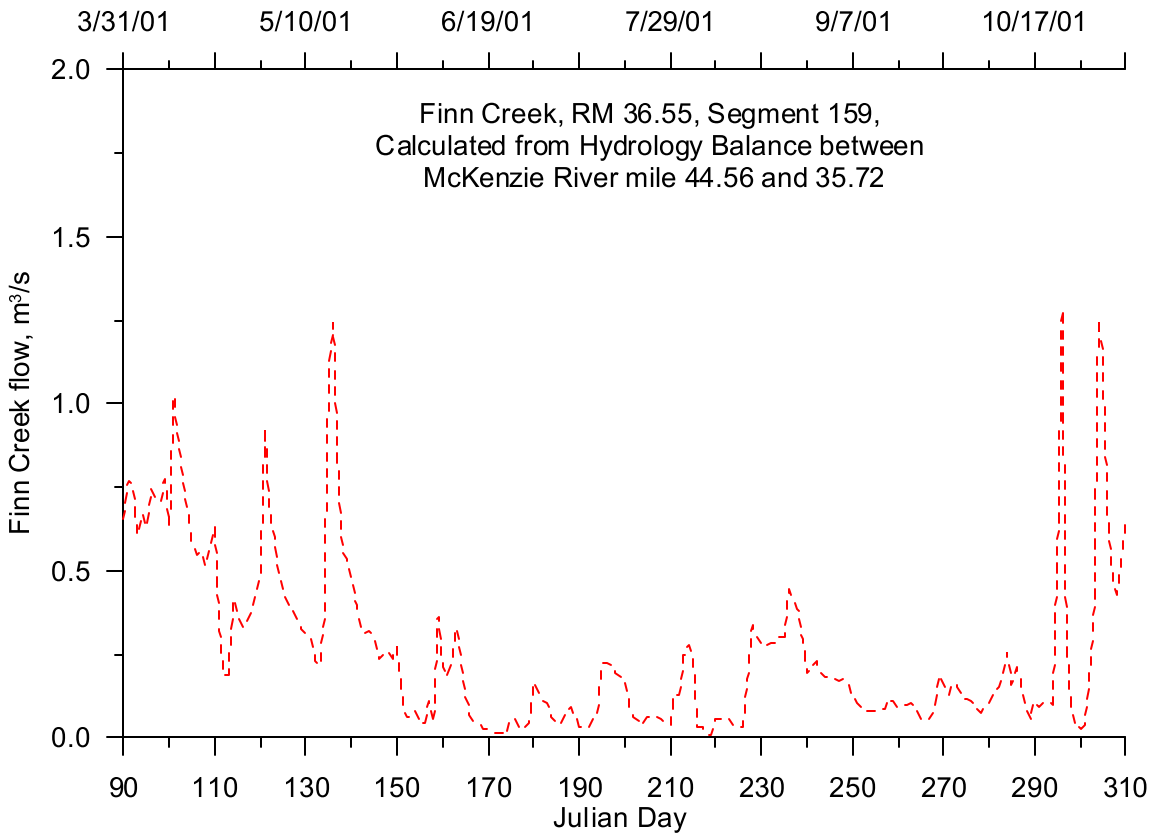


**Figure 484. Finn Creek flow, 2001**

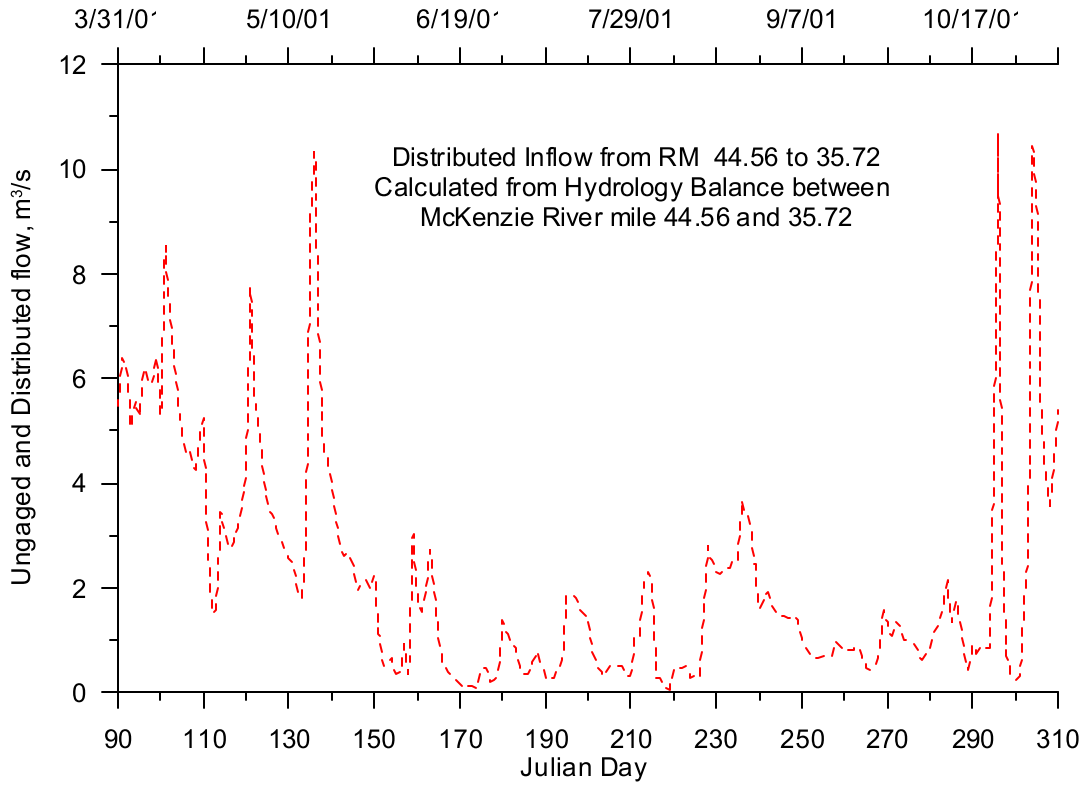


**Figure 485. Distributed flow for the McKenzie River from RM 44.56 to 35.72, 2001**

Reach 3

In the third reach of the McKenzie River (RM 35.72 to 24.97), the ungaged flow was calculated by subtracting the flows at the two gaged flows from each other and incorporating the flows from the Leaburg Canal entering at RM 30.1 and the Walterville Canal diverted at RM 25.64. The relationship can be written:

$$UngagedInflow = USGS14163900, flow - \begin{pmatrix} USGS14163150, flow + LeaburgCanalDiversion, flow - \\ WaltervilleCanalDiversion, flow \end{pmatrix}$$

The flow diverted to the Walterville Canal was estimated using operation rules provided by the Eugene Water and Electric Board (EWEB, 2002) as discussed in the reservoir operations section below. Since there were no large tributaries entering the McKenzie River in this reach, the daily calculated flow was attributed to the distributed area along the river. Figure 486 shows the distributed flows associated with the McKenzie River from RM 35.72 to 24.97.

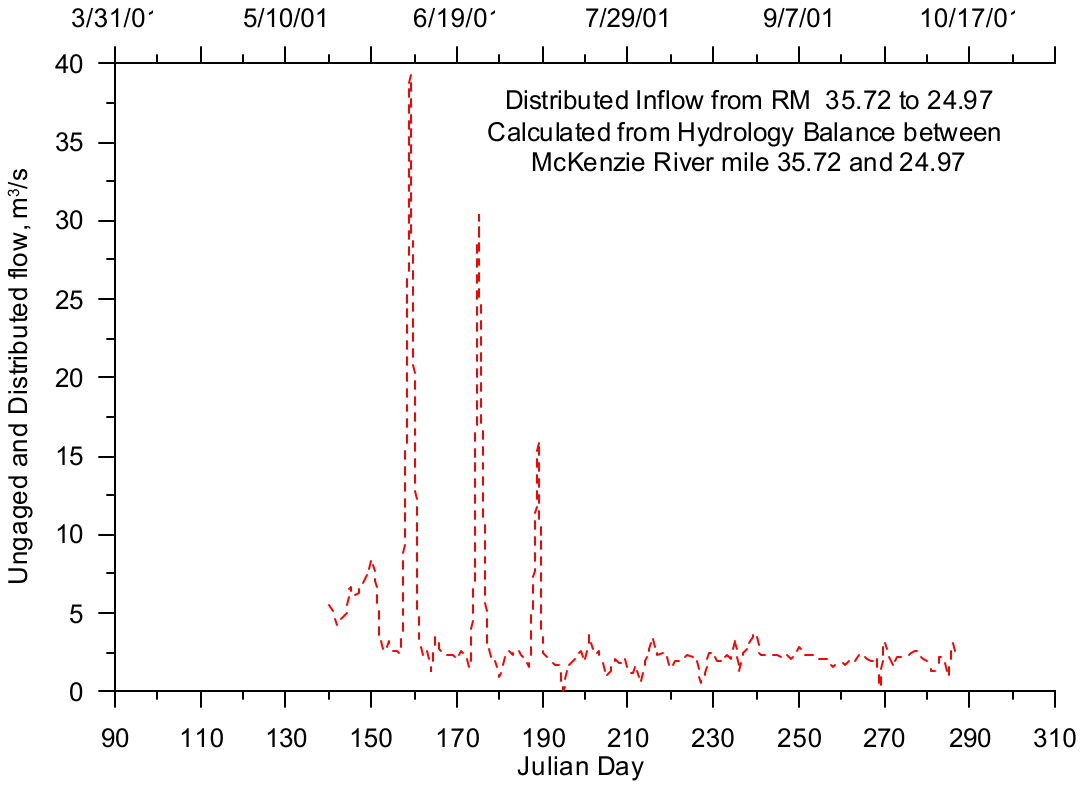


**Figure 486. Distributed flow for the McKenzie River from RM 35.72 to 24.97, 2001**

Reach 4

The furthest downstream reach of the McKenzie River (RM 23.97 to 0.00) had no downstream USGS gage to use in calculating the hydrology for this reach. Flow data for the Mohawk River were used to estimate Camp Creek flow, but no additional analysis was conducted to estimate any flows from the remaining ungaged distributed drainage area along the river. Table 55 shows a list of the basin areas between the two USGS gage station for this reach, their drainage areas, and the fraction of ungaged flow attributed to each sub basin below RM 24.97.

**Table 55. Drainage Basin Area along the McKenzie River, RM 24.97 to 0.00**

| Basin | Area, $km^2$ | Fraction of Drainage area, RM 24.97to0.00 |
|---|---|---|
| Camp Creek | 68.27 | 10.24% |
| Mohawk River | 463.61 | 69.56% |
| Distributed | 134.59 | 20.19% |
| Total | 666.46 | 100.00% |

Flows were associated with Camp Creek by taking the ratio of the Camp Creek basin area to the Mohawk River basin area and multiplying it by the flow on the Mohawk River recorded by a USGS gage (14165000). Figure 487 shows the flows calculated for Camp Creek based on flows from the nearby Mohawk River basin. Figure 488 shows the flows for the Mohawk River based on the USGS gage data.

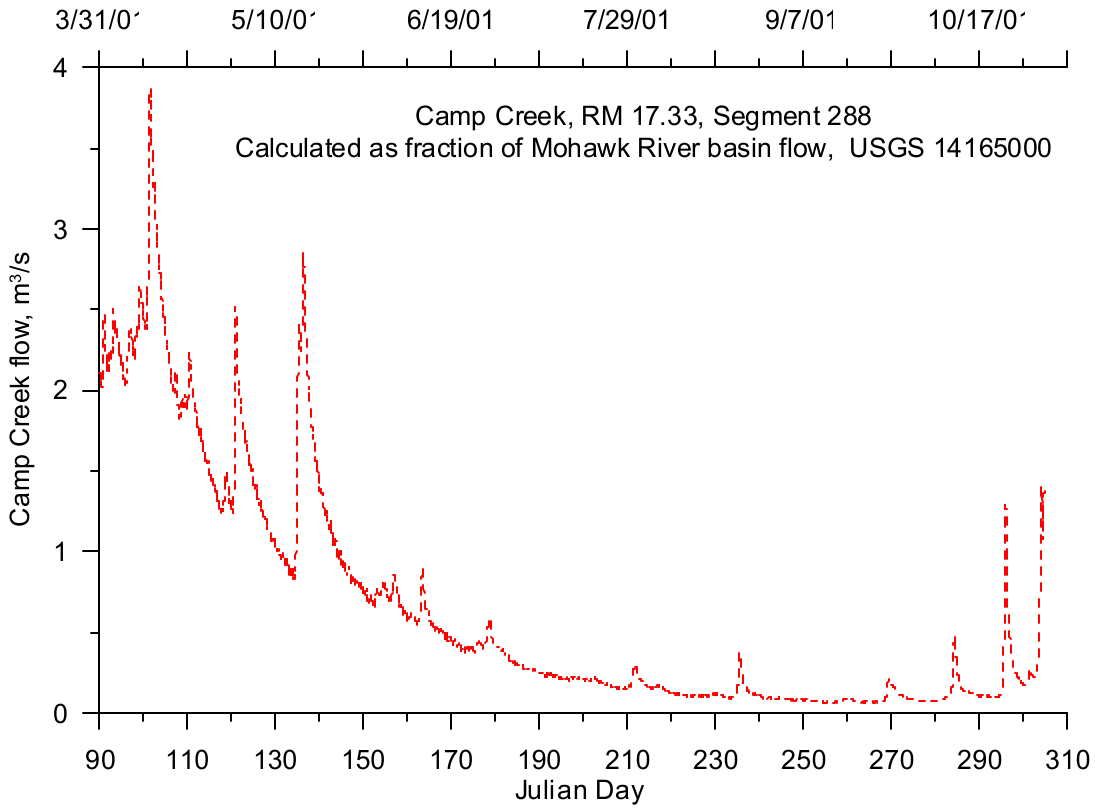


**Figure 487. Camp Creek flow, 2001**

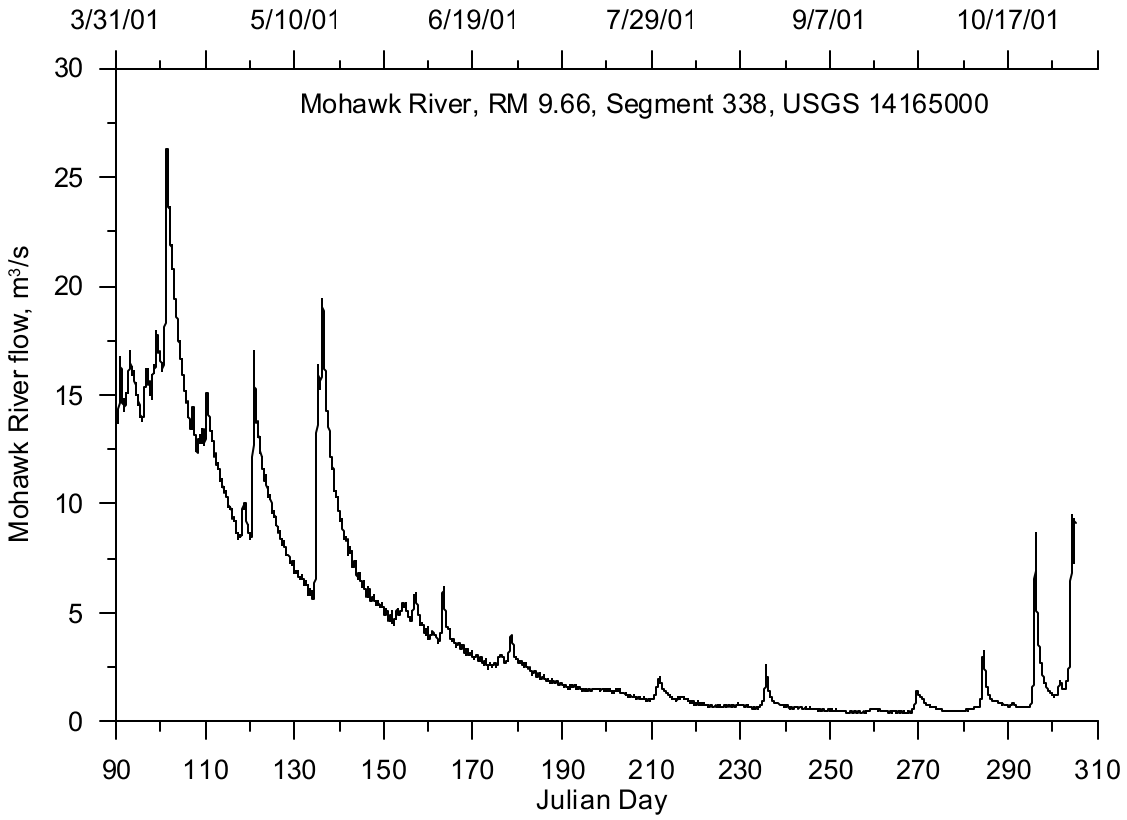


**Figure 488. Mohawk River flow, 2001**

## Year 2002

The same methodology used for developing the tributary inflow files and conducting the hydrology balances along the McKenzie River for 2001 was used for 2002. The only difference in the analysis was there was no flow in the Walterville Canal in 2002 due to the canal being shutoff for maintenance.

The same correlation used for calculating the McKenzie River tributary flow in Figure 475 was used to calculate the flow in 2002. Figure 489 shows a time series of the flow calculated for the McKenzie River. The flow for the Blue River was monitored by the USGS gage 14162200, and Figure 490 shows a time series of the flows.

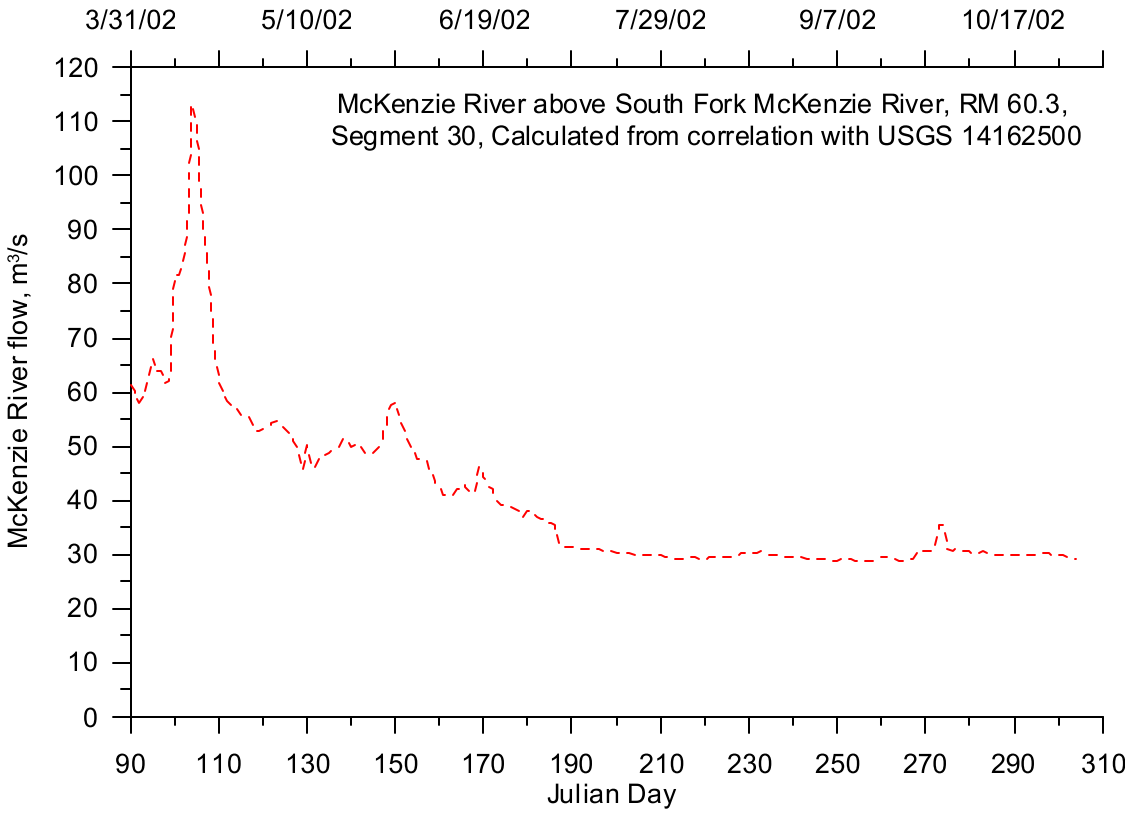


**Figure 489. McKenzie River tributary flow, 2002**

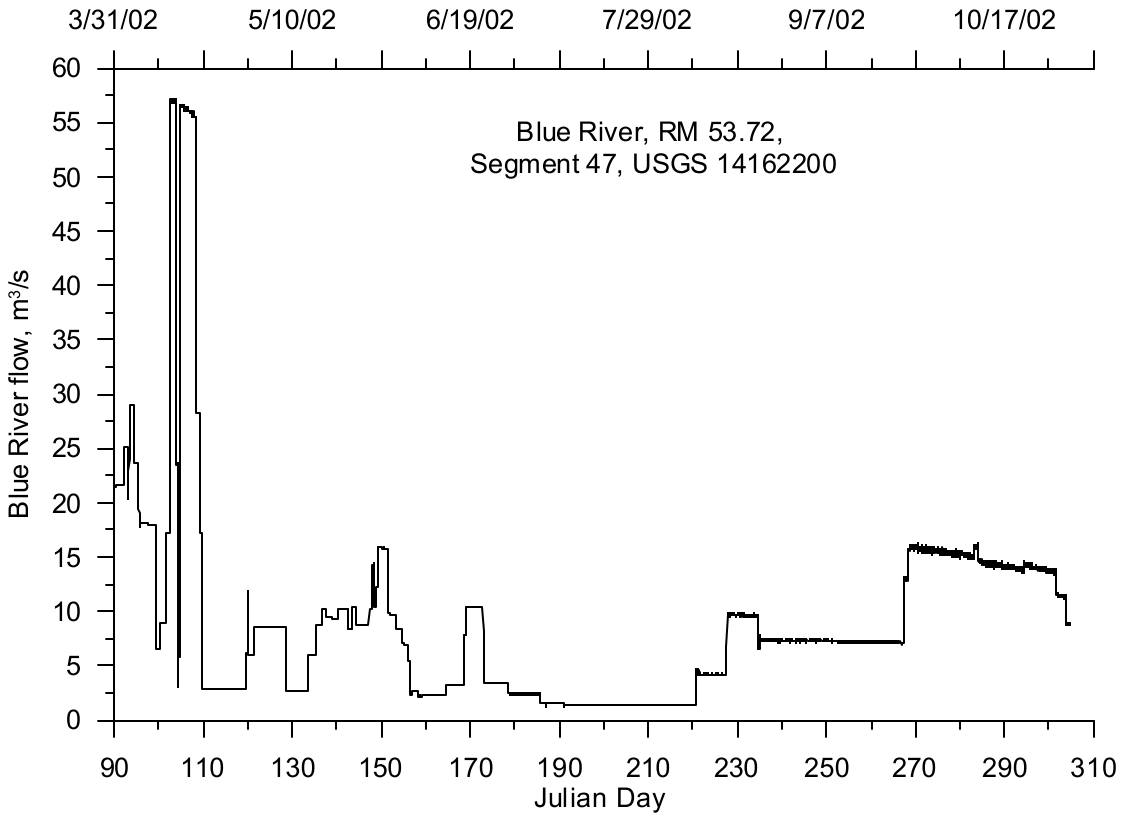


**Figure 490. Blue River flow, 2002**

Reach 1

In the first reach of the McKenzie River (RM 60.84 to 44.56) the ungaged flow was calculated by using the same method used for 2001. This resulted in daily flow estimates for Deer Creek, Quartz Creek, and the distributed ungaged drainage area along the river. Figure 491 shows a time series of the daily flows estimated for Quartz Creek. Figure 492 shows the flow estimated for Deer Creek. Figure 493 shows the daily flows estimated for the distributed drainage area between RM 60.84 and 44.56 along the river.

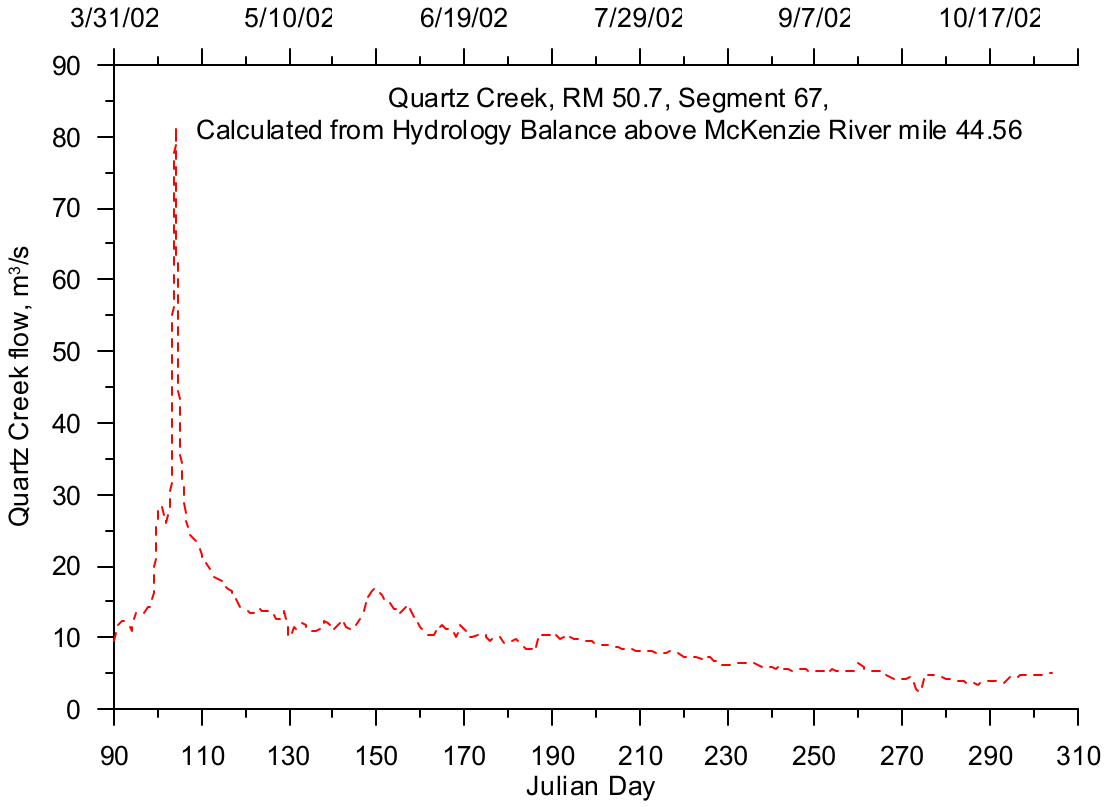


**Figure 491. Quartz Creek flow, 2002**

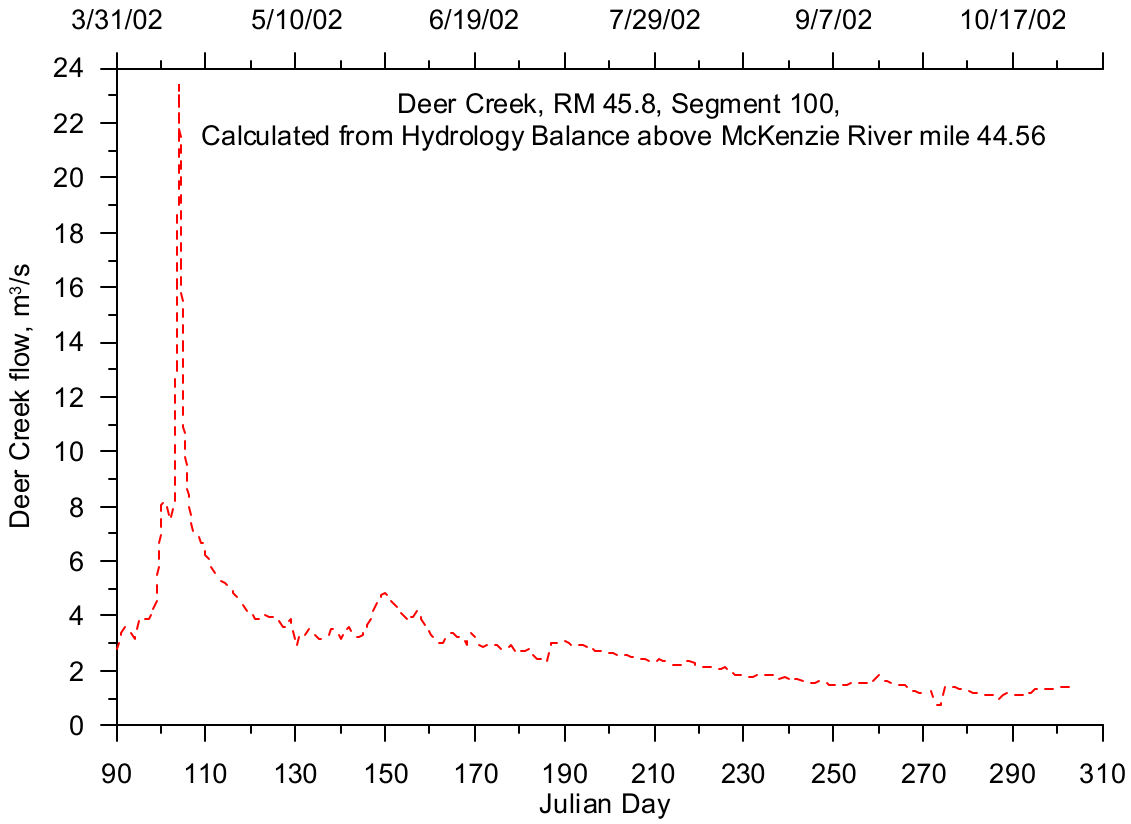


**Figure 492. Deer Creek flow, 2002**

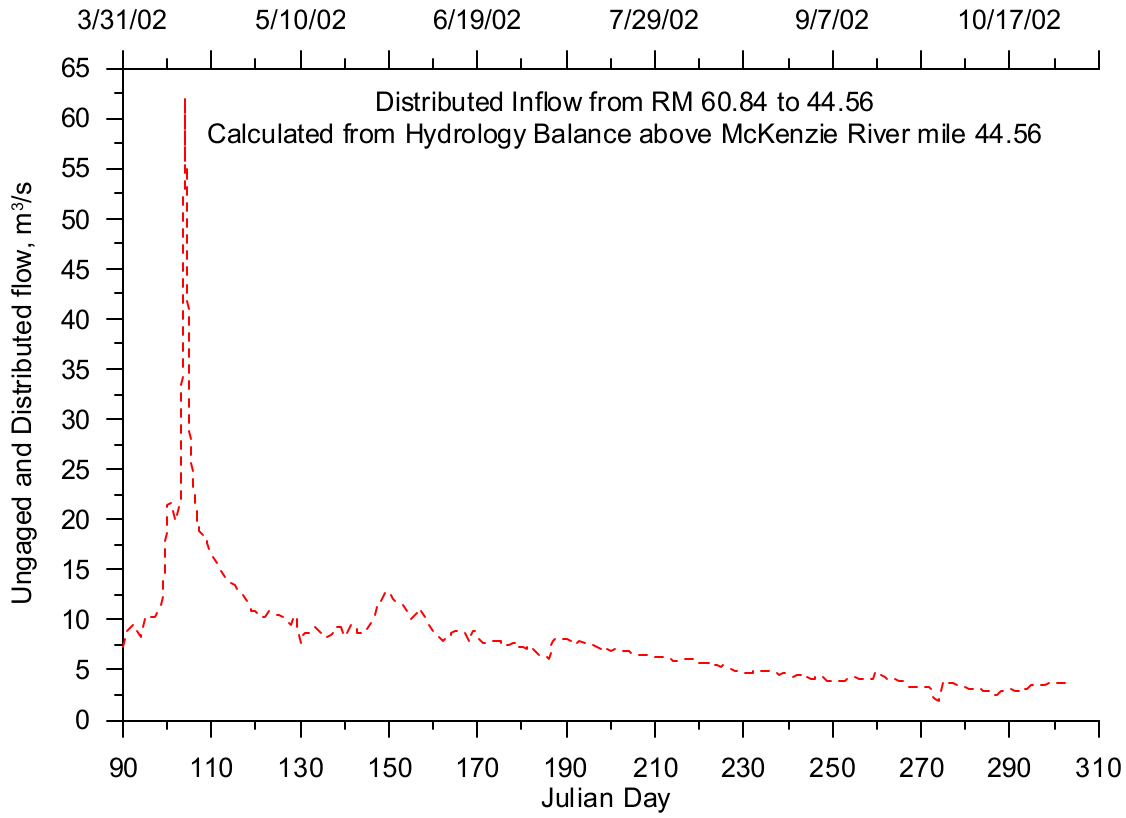


**Figure 493. Distributed flow for the McKenzie River from RM 60.84 to 44.56, 2002**

Reach 2

In the second reach of the McKenzie River (RM 44.56 to 35.72), the inflows to the river were calculated by using the same method used for 2001. This resulted in daily flow estimates for Bear, Gate and Finn Creeks. Figure 494 shows a time series of the flow for Bear Creek. Figure 495 shows a time series for Gate Creek and Figure 496 shows the estimated flows for Finn Creek. Figure 497 shows the distributed flow from the ungaged drainage area between RM 44.56 and RM 35.72 along the McKenzie River for 2002.

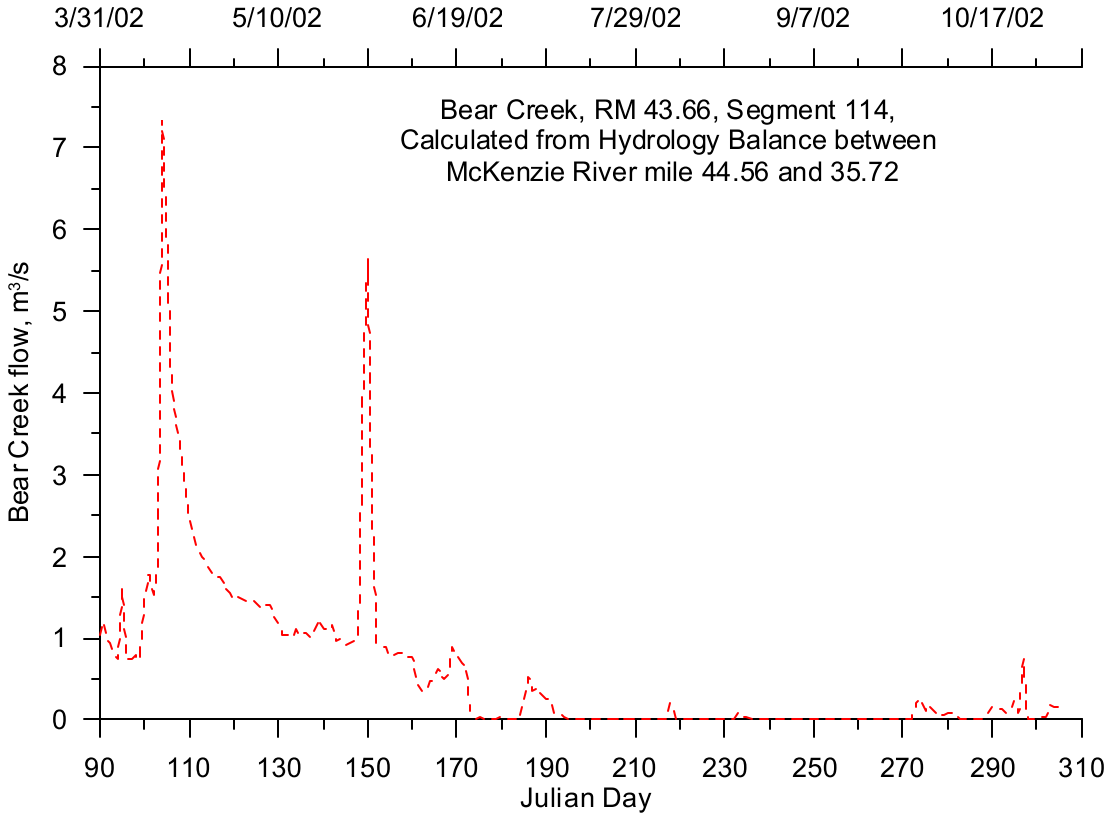


**Figure 494. Bear Creek flow, 2002**

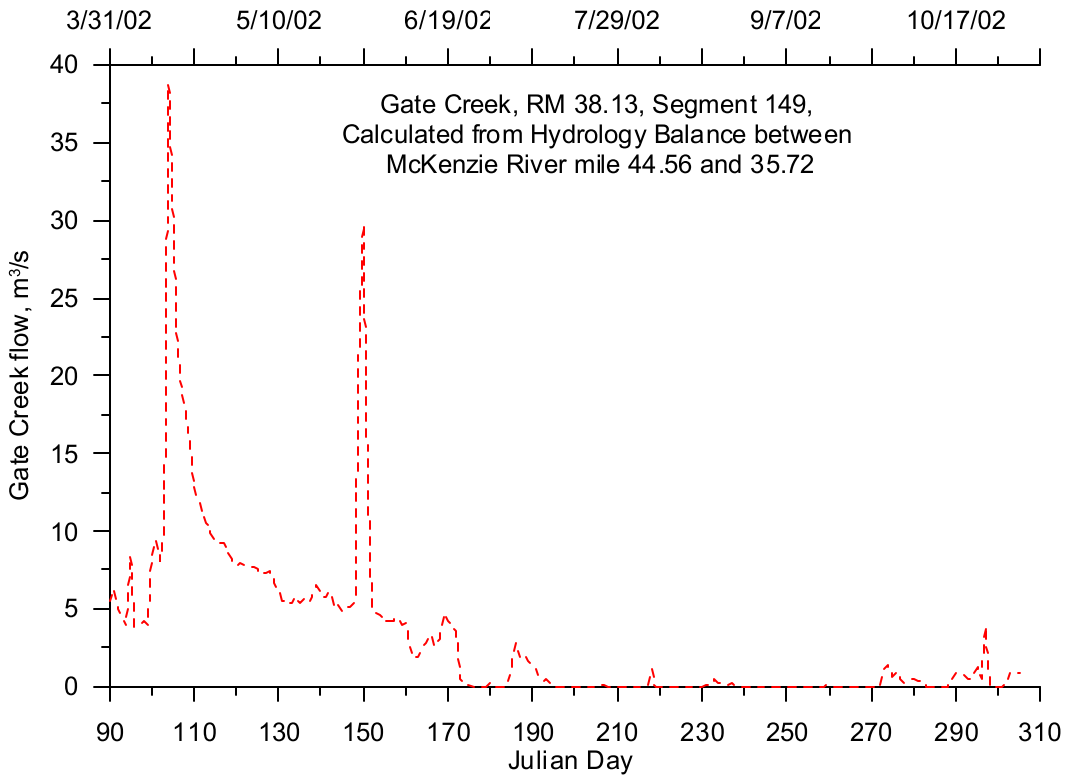


**Figure 495. Gate Creek flow, 2002**

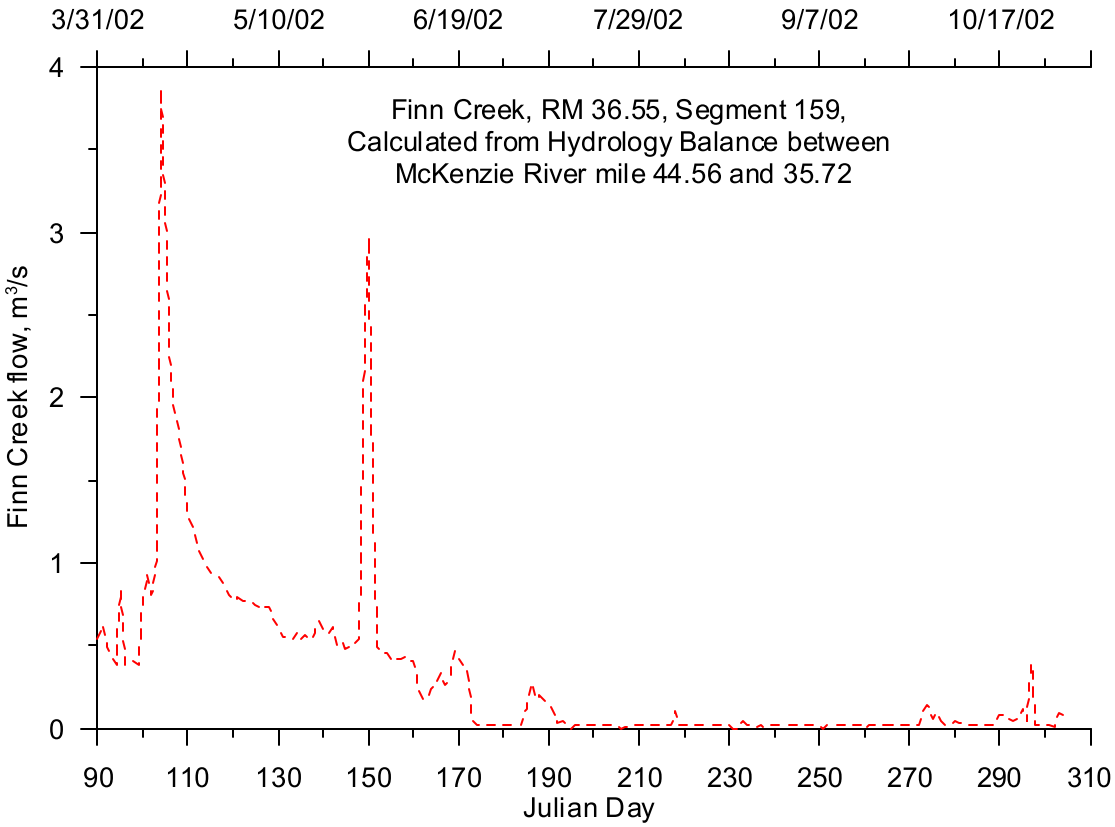


**Figure 496. Finn Creek flow, 2002**

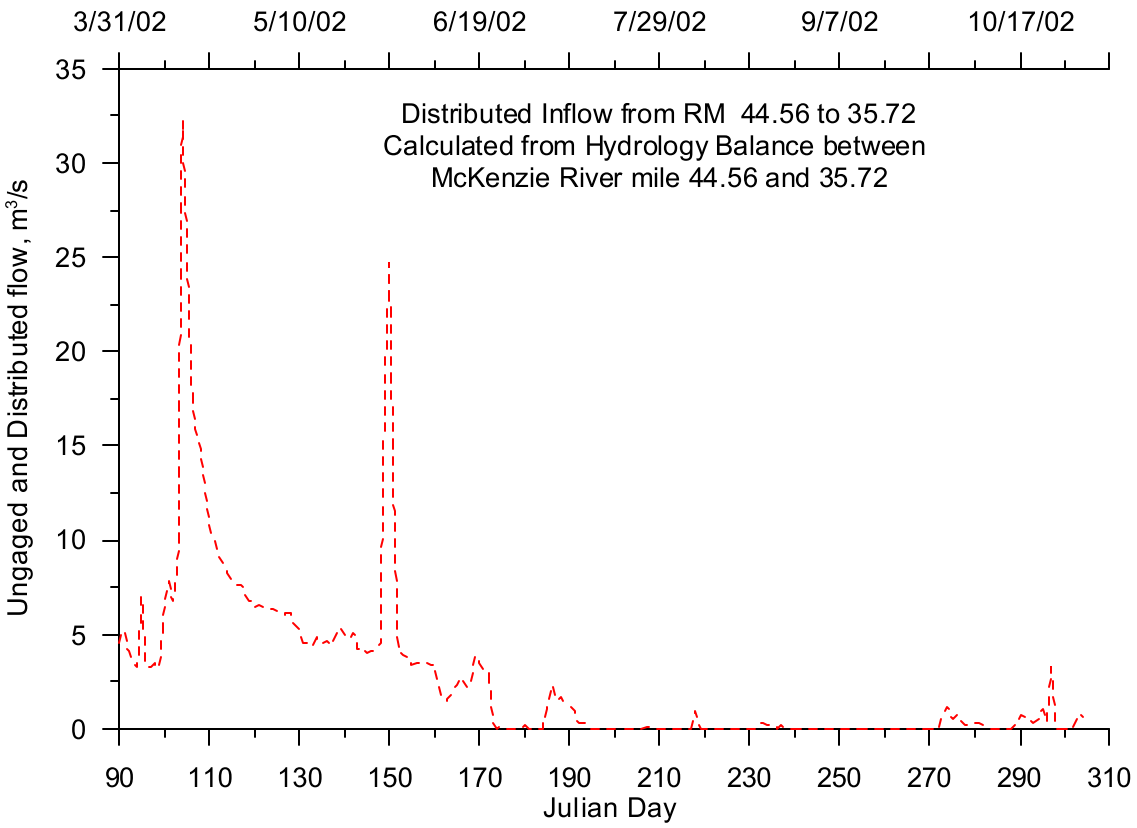


**Figure 497. Distributed flow for the McKenzie River from RM 44.56 to 35.72, 2002**

Reach 3

In the third reach of the McKenzie River (RM 35.72 to 24.97), the ungaged flow was calculated by using the same method used for 2001. This resulted in daily flow estimates for the ungaged distributed drainage area between these two river mile locations. Figure 498 shows the distributed flow from the ungaged drainage area between RM 35.72 to 24.97 along the McKenzie River for 2002. The figure shows there were considerable negative flows, losses from the river, which may be due to groundwater losses in this reach. The larger groundwater losses may be due to a higher water table along the river since the Walterville Canal was not diverting water in 2002. Additionally there may have been larger groundwater losses in 2002 than 2001 because 2001 was a dryer year.

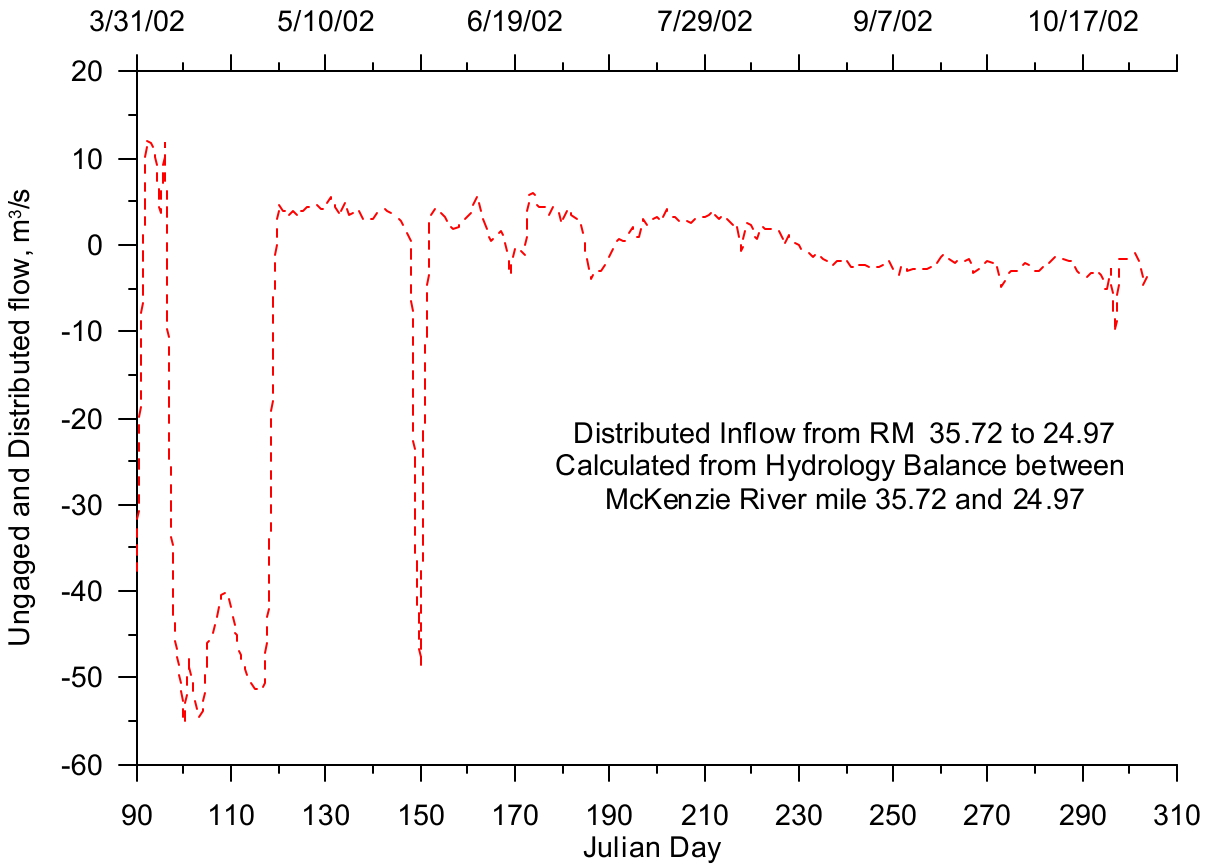


**Figure 498. Distributed flow for the McKenzie River from RM 35.72 to 24.97, 2002**

Reach 4

In the furthest downstream reach of the McKenzie River (RM 23.97 to 0.00); there was no downstream USGS gage to use in calculating the hydrology for this reach, similar to 2001. Flows were calculated for Camp Creek using the same method for 2001 using data from the Mohawk River. Figure 499 shows a time series of the calculated flow for Camp Creek. Figure 500 shows the flows for the Mohawk River based on the USGS gage data.

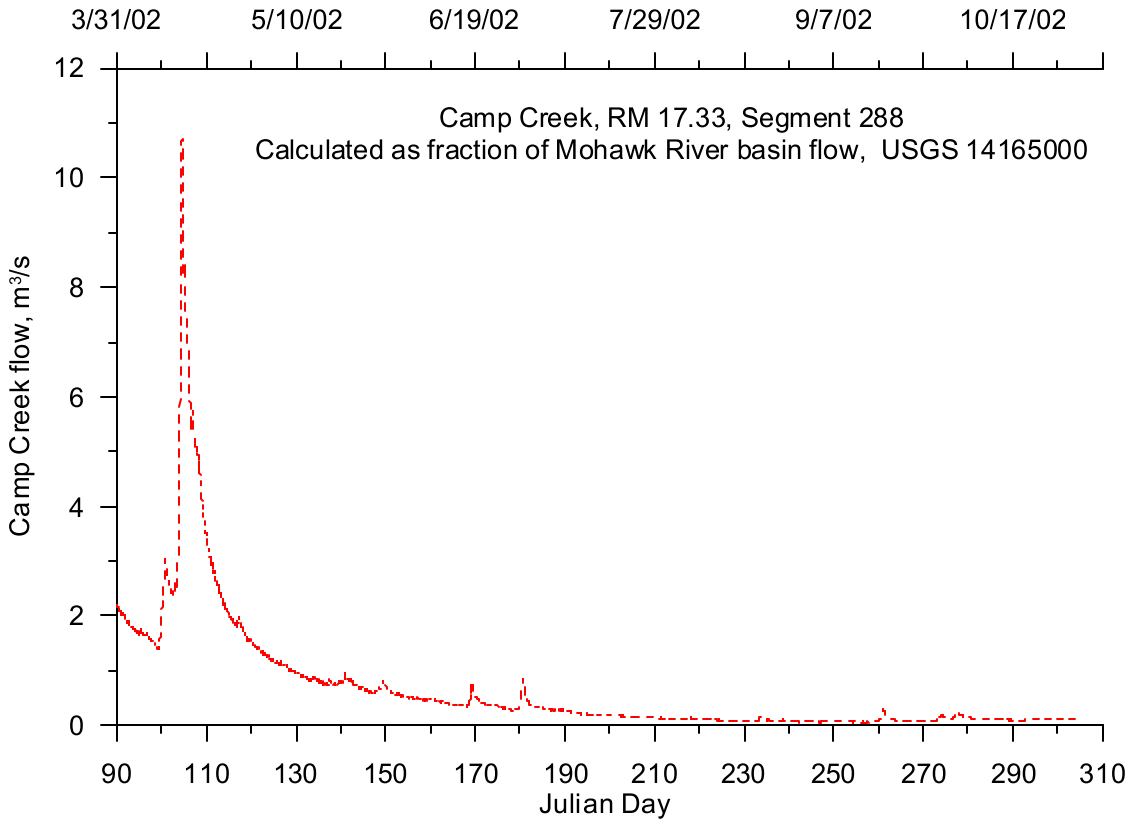


**Figure 499. Camp Creek flow, 2002**

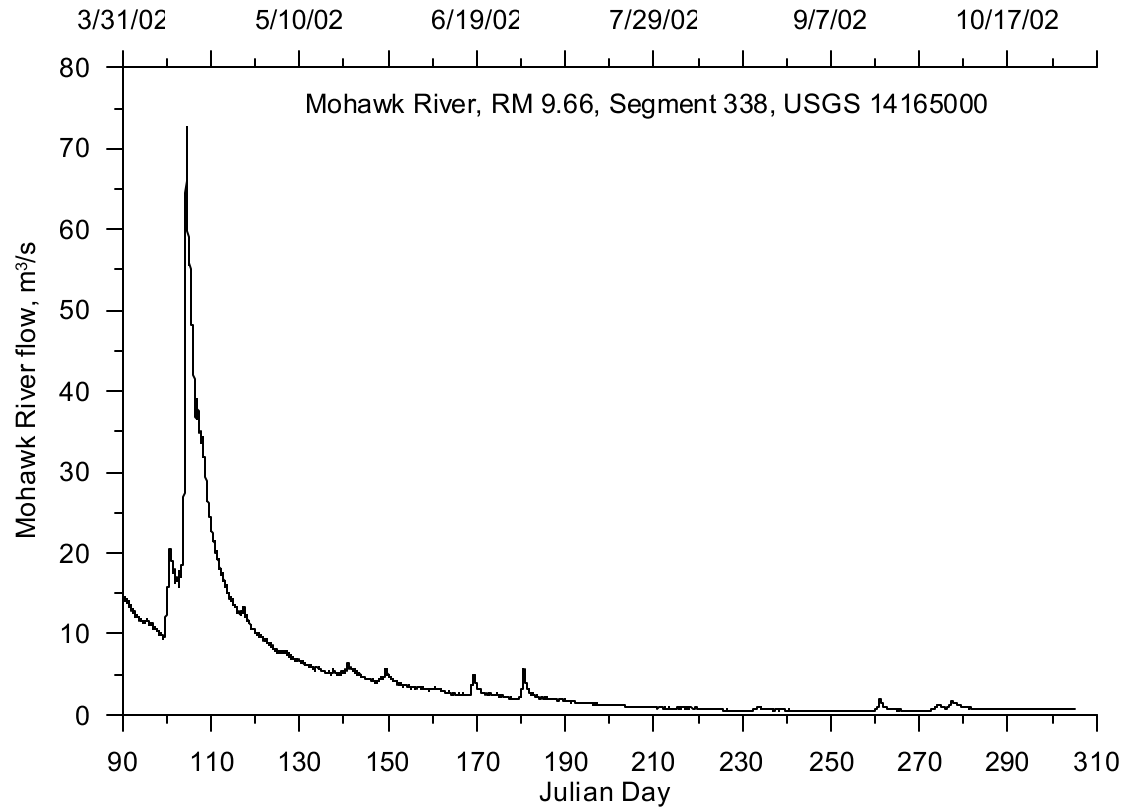


**Figure 500. Mohawk River flow, 2002**

## Temperature Data

Seven of the nine large tributaries contributing flow to the McKenzie River were monitored for temperature in 2001 and 2002. Figure 501 shows a map of the McKenzie basin with the sub basin delineations and temperature monitoring sites. Table 56 lists the tributary temperature monitoring sites, RM locations and corresponding model segments.

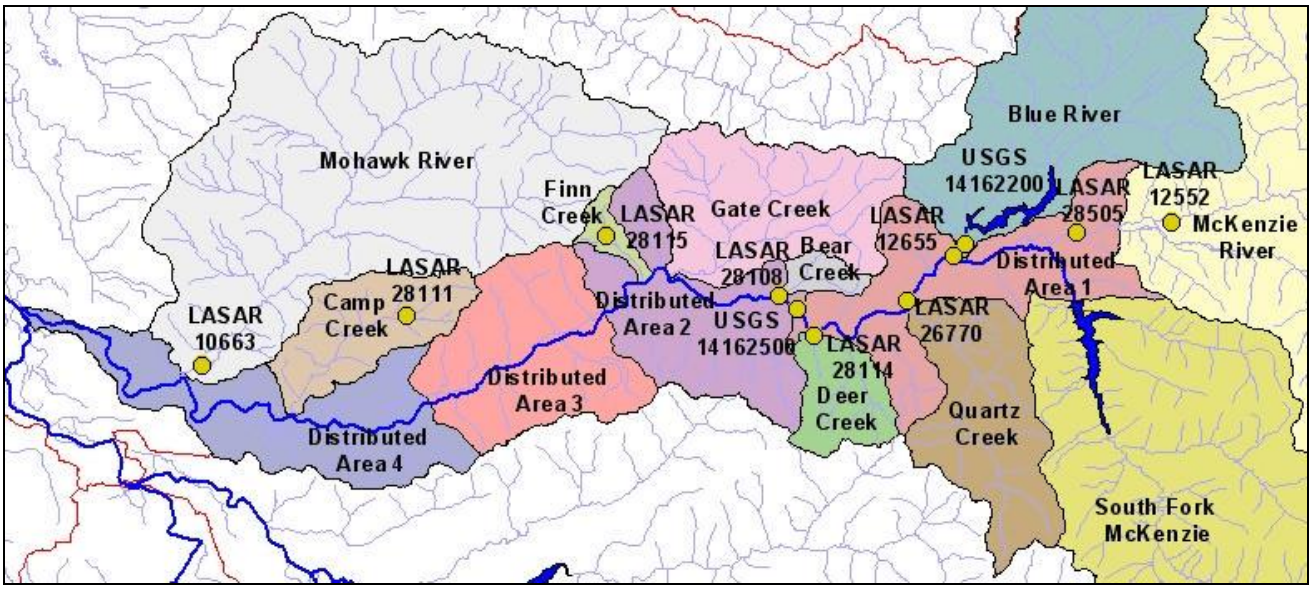


**Figure 501. McKenzie River model tributary temperature sites**

**Table 56. McKenzie River model tributary temperature sites**

| Tributary | RM | Model Segment | Data Site | Sites used in Analysis |
|---|---|---|---|---|
| McKenzie River | 60.25 | 30 | LASAR 28505 | LASAR 26770, LASAR 12552 and USGS 14162500 |
| Blue River | 53.73 | 47 | LASAR 12655 | USGS 14162200 |
| Quartz Creek | 50.70 | 67 | Deer Creek record | |
| Deer Creek | 45.76 | 100 | LASAR 28114 | LASAR 10663 and USGS 14162500 |
| Bear Creek | 43.66 | 114 | LASAR 28108 | LASAR 10663 and USGS 14162500 |
| Gate Creek | 38.13 | 149 | Bear Creek record | |
| Finn Creek | 36.55 | 159 | LASAR 28115 | LASAR 10663 and USGS 14162500 |
| Camp Creek | 17.33 | 288 | LASAR 28111 | LASAR 10663 and USGS 14162500 |
| Mohawk River | 9.66 | 338 | LASAR 10663 | USGS 14162500 |

### Year 2001

The monitoring site on the McKenzie River above its confluence with the South Fork McKenzie River was LASAR 28505 (RM 60.25). This site had data from June 21 to September 21, 2001. The data gap

from May 28 to June 21 was filled by developing a correlation between a temperature monitoring site downstream at RM 50.99 (LASAR 26770) and the RM 60.25 gage (LASAR 28505). Figure 502 shows the temperature correlation between the two data sites. Implementing the correlation was limited to May and June 2001 because of the lack of data at both sites earlier in the year. The data gaps from April 1 to May 28 and from September 21 to October 31 were filled by developing a temperature correlation between the LASAR site 28505 and the USGS gage station further downstream on the McKenzie River at RM 44.56 (USGS 14162500). Figure 503 shows the correlation equation developed and illustrates there was a strong relationship in temperature between the two sites.

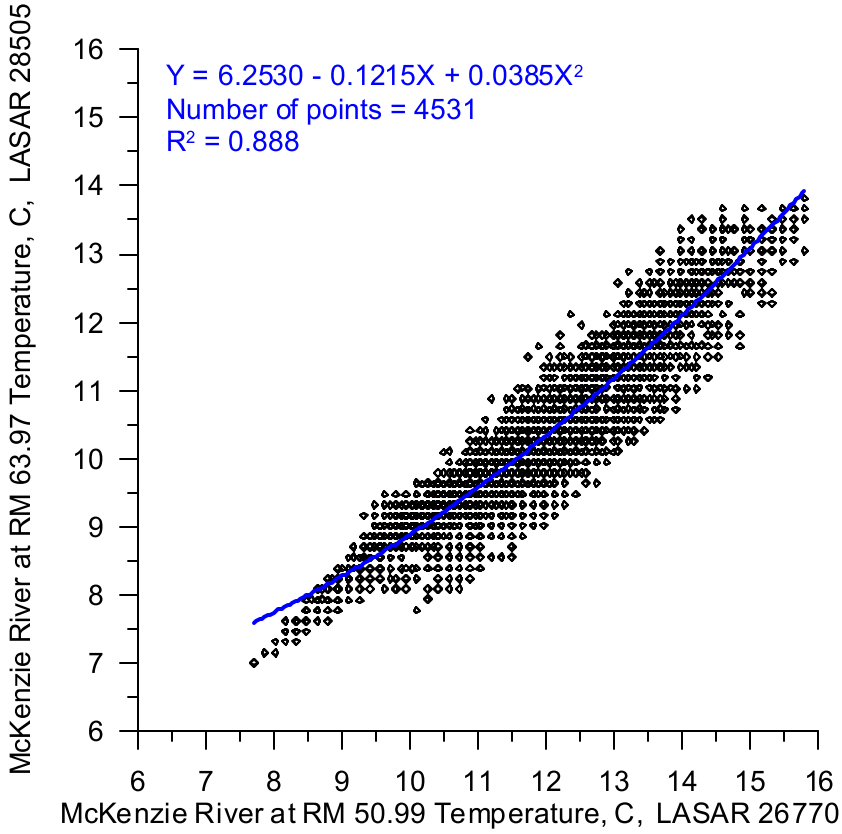


**Figure 502. McKenzie River tributary temperature correlation for May and June 2001**

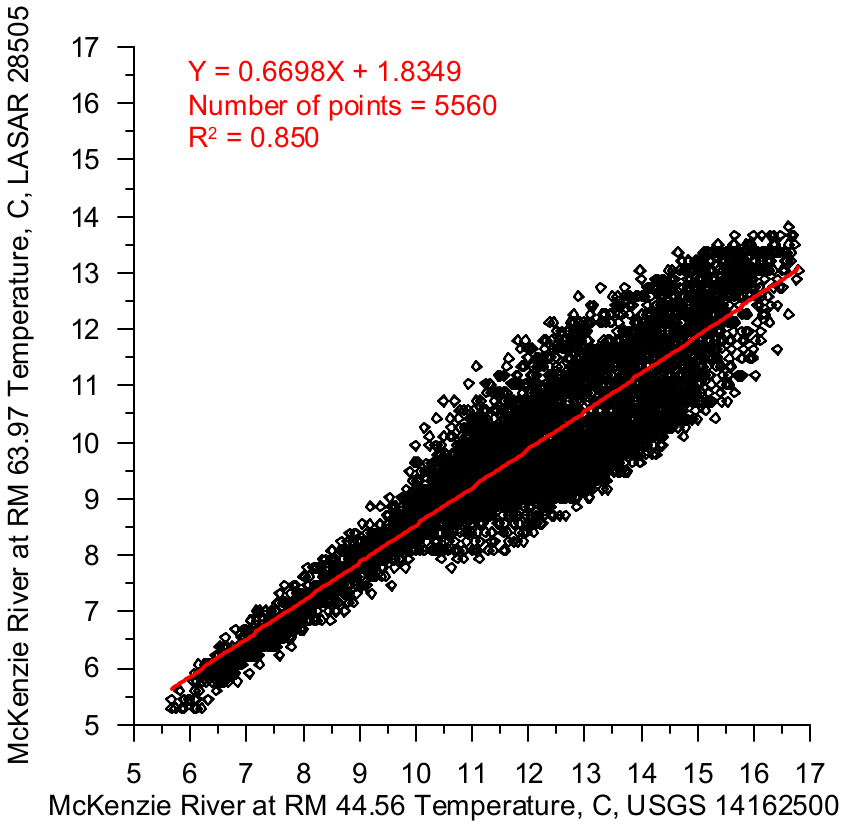


**Figure 503. McKenzie River tributary temperature correlation for spring and fall 2001**

The LASAR monitoring site for 2001 and 2002 on the McKenzie River above the South Fork McKenzie River was 3.72 miles above the confluence of the two rivers. Since the McKenzie River was unregulated and was similar to its natural condition, there was an interest in identifying is temperature increases in the last few miles of the river below the monitoring site. In 2002 there was an additional monitoring site on the McKenzie River further upstream at RM 68.794 (LASAR 12552). The 2002 data from this site and LASAR 28505 at RM 63.794 were compared by first calculating the daily maximum, minimum and average temperature at both sites. Then for the same day the difference between the sites was taken for each of the three statistics. The differences for the three statistics were then averaged over all days to get an overall average temperature difference between the two sites (0.40 $^{o}$C) as shown in Table 57. This methodology was selected to ensure the daily minimum and maximum temperature weighted similarly to the daily average temperature rather than taking the average of just the difference between daily average temperatures. Since the temperature increase between the two sites was 0.40 $^{o}$C for the 4.82 miles of river between them, and estimating that the same increase per river mile occurred below the LASAR gage at RM 63.974, then water reaching the confluence of the two rivers could be 0.31 $^{o}$C warmer as shown in Table 57. The data at LASAR 28505 and the calculated temperatures at the same site were all increased by 0.31 $^{o}$C to better represent the temperature at the river confluence with the South Fork McKenzie River. Figure 504 shows time series of the completed temperature time series for the McKenzie River.

**Table 57. McKenzie River temperature analysis**

| Site | McKenzie River RM | Distance from upstream site, mi | Overall Average Temperature Increase, 2002 |
|---|---|---|---|

| Site | McKenzie River RM | Distance from upstream site, mi | Overall Average Temperature Increase, 2002 |
|---|---|---|---|
| LASAR 12552 | 68.794 | | |
| LASAR 28505 | 63.974 | 4.82 | 0.40 °C (based on data) |
| Confluence with South Fork McKenzie | 60.254 | 3.72 | 0.31 °C (calculated based on Distance separation) |

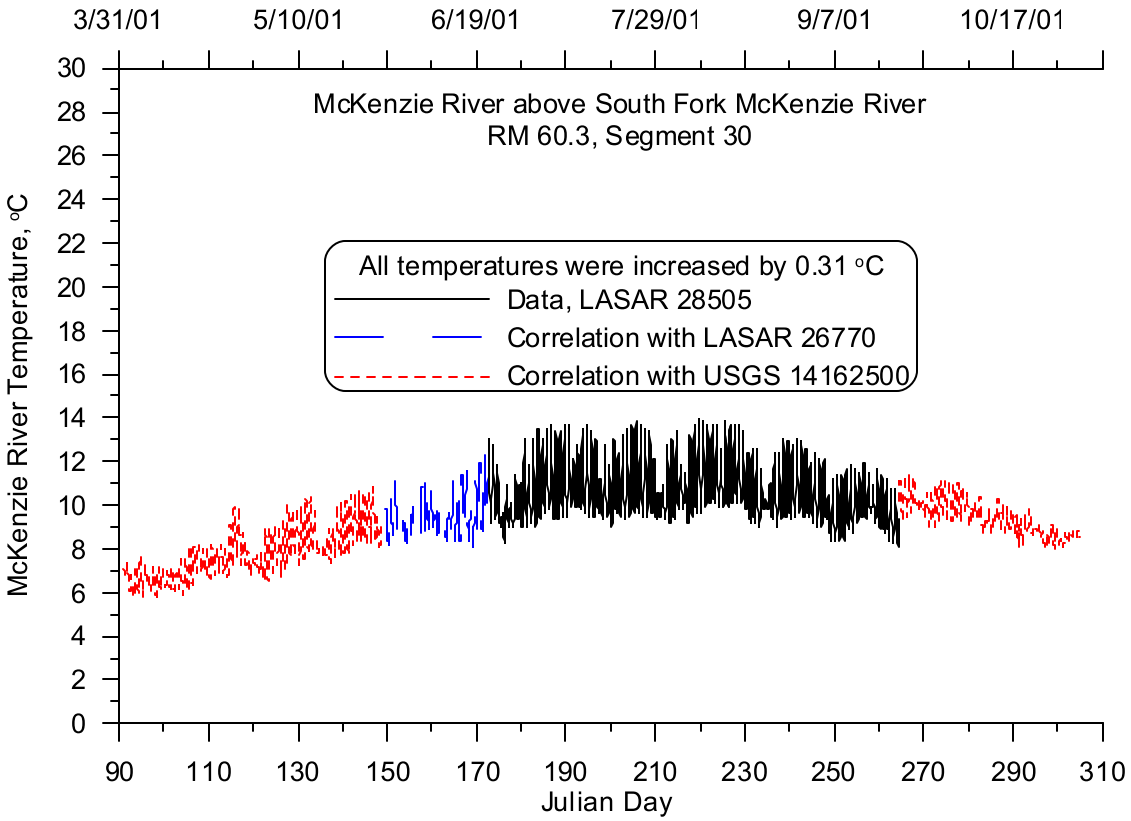


**Figure 504. McKenzie River tributary temperature, 2001**

Stream temperatures were recorded on the Blue River every half-hour from August 8 to December 31, 2001, and before that there were only five temperature grab samples at the same site (LASAR 12655). Figure 505 shows a time series of the temperature data on the Blue River for 2001. An analysis was conducted with Blue River temperature data to improve upon the linearly interpolated temperatures between the grab samples in the 2001 data. The first step was to isolate and match up in date and time the temperature data from 2002 for the same site. The difference between the data from the two years was taken and then linearly interpolated between the grab sample times for every hour half. The interpolated difference was then used to adjust the 2002 temperature data. The result was a temperature time series which matches the 2001 grab sample data but preserves some of the diurnal fluctuations from the 2002 data set. Figure 506 shows a completed time series with the 2001 half-hourly data and the 2002 data adjusted for 2001.

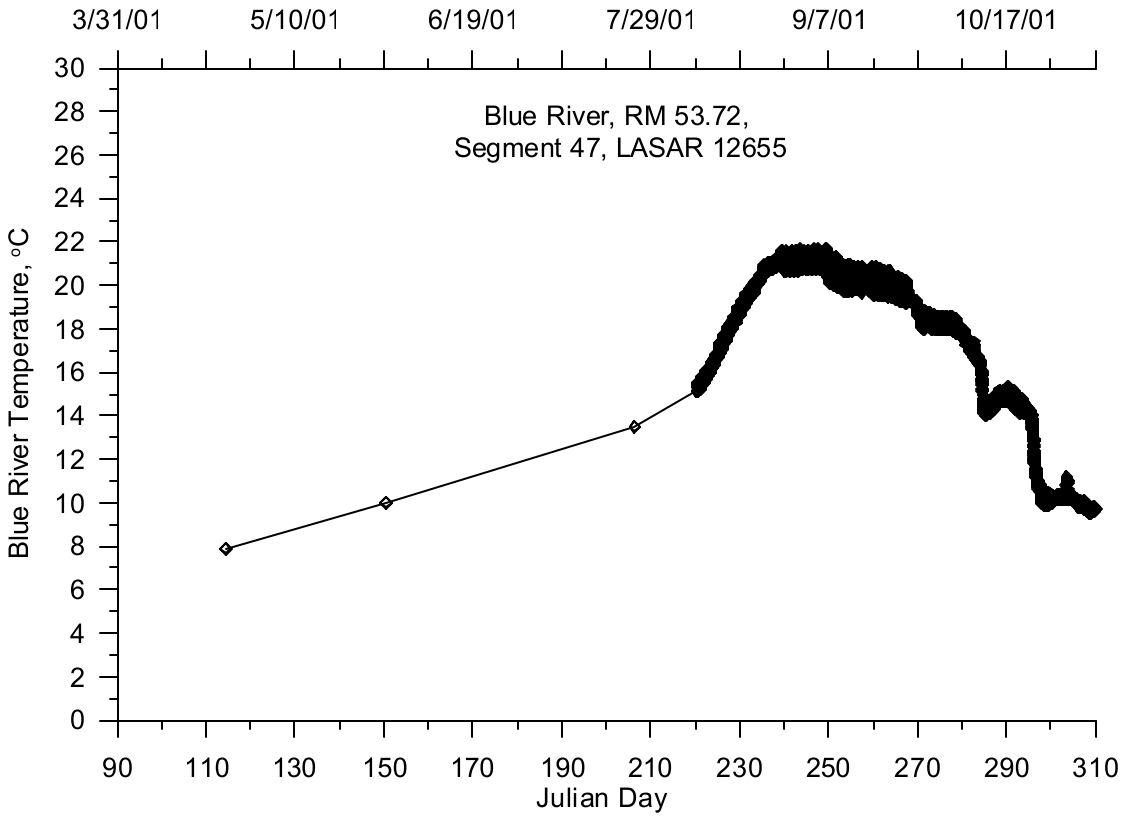


**Figure 505. Blue River 2001 temperature data for analysis**

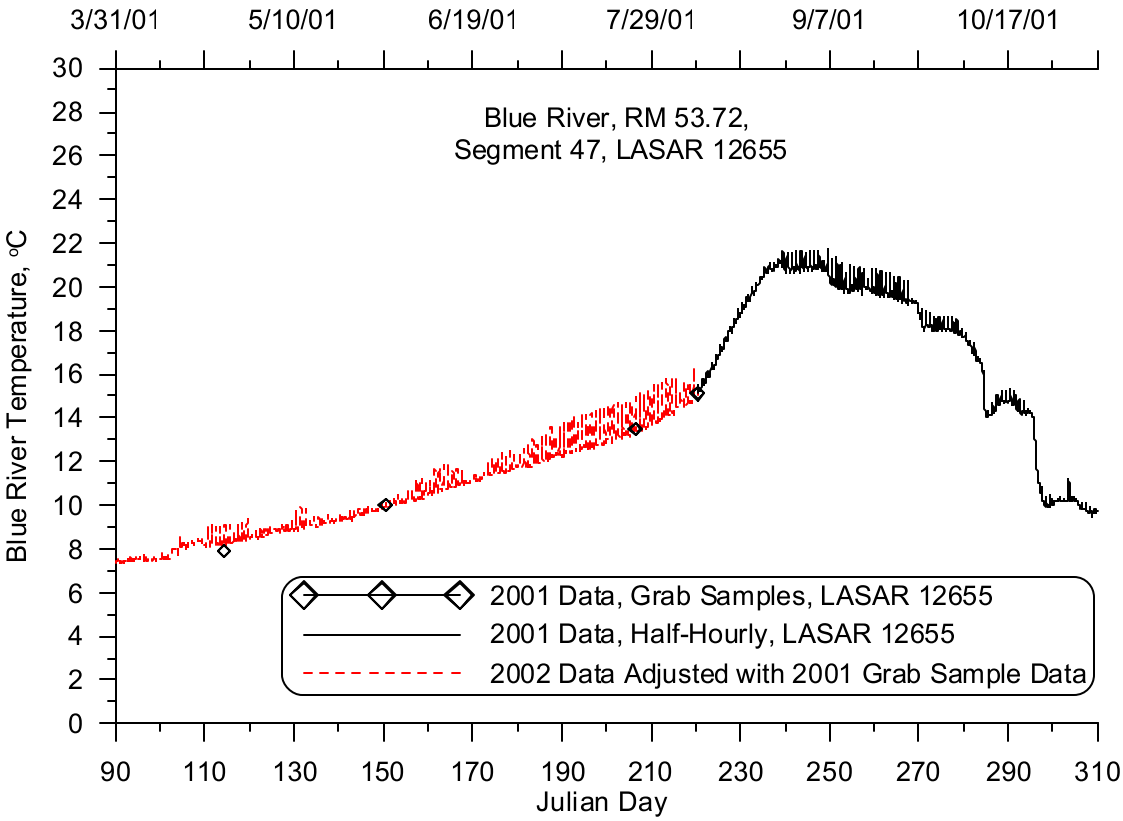


**Figure 506. Blue River temperature, 2001**

There were temperature data collected on Deer Creek from June 5 to September 13, 2001, (LASAR 28114). A temperature correlation was developed between the Deer Creek gage and data collected on the Mohawk River from LASAR 10663 to fill in a data gap from September 13 to 24. The temperature data from the Mohawk River were adjusted in time one hour earlier to address water timing issues from each basin. Figure 507 shows the temperature correlation between the two sites and the correlation equation. The data gaps from April 1 to June 5 and from September 24 to October 31 were filled using a temperature correlation developed with data collected on the McKenzie River at USGS gage 14162500. Similar to the Mohawk River, the temperature data on the McKenzie River were adjusted one hour earlier to account for different travel times. Figure 508 shows the temperature correlation between the USGS site on the McKenzie River and the site on Deer Creek. Figure 509 shows the completed temperature time series data and calculated values. There were no temperature data for Quartz Creek in 2001, so the temperature record developed for Deer Creek was used.

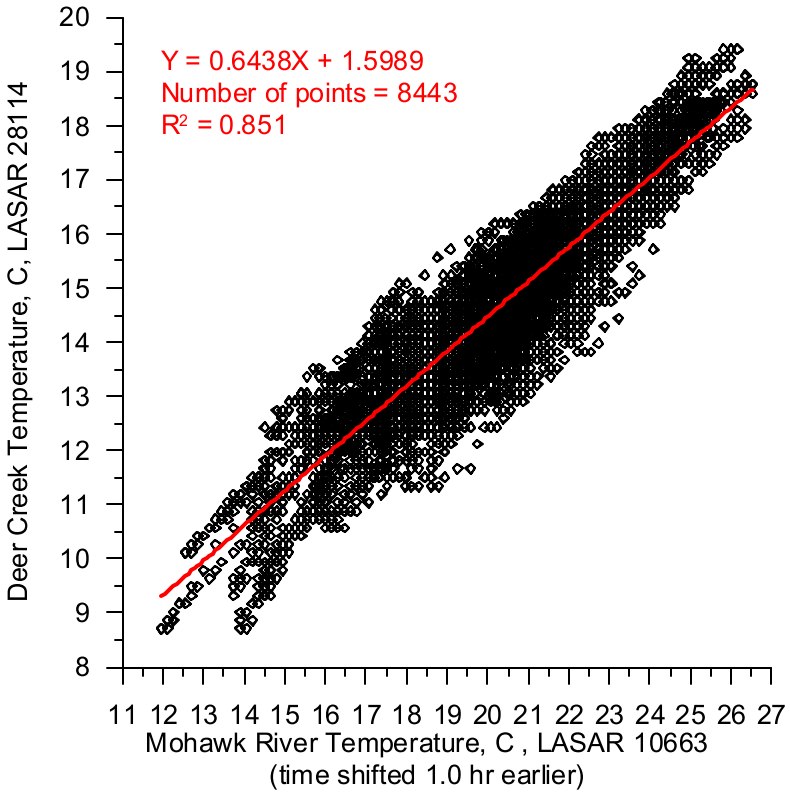


**Figure 507. Deer Creek temperature correlation for September 2001**

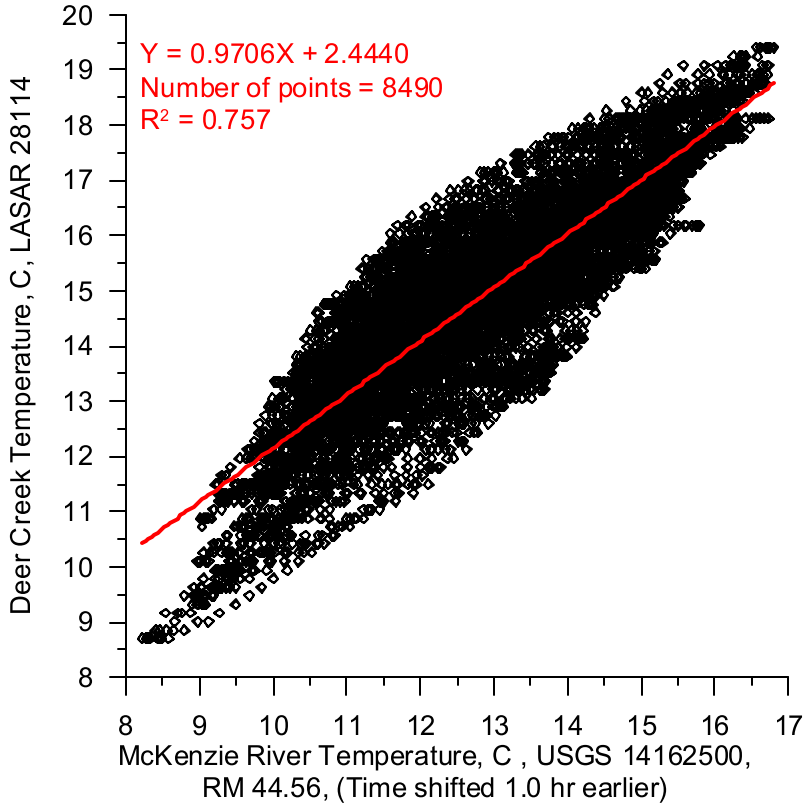


**Figure 508. Deer Creek temperature correlation for spring and fall, 2001**

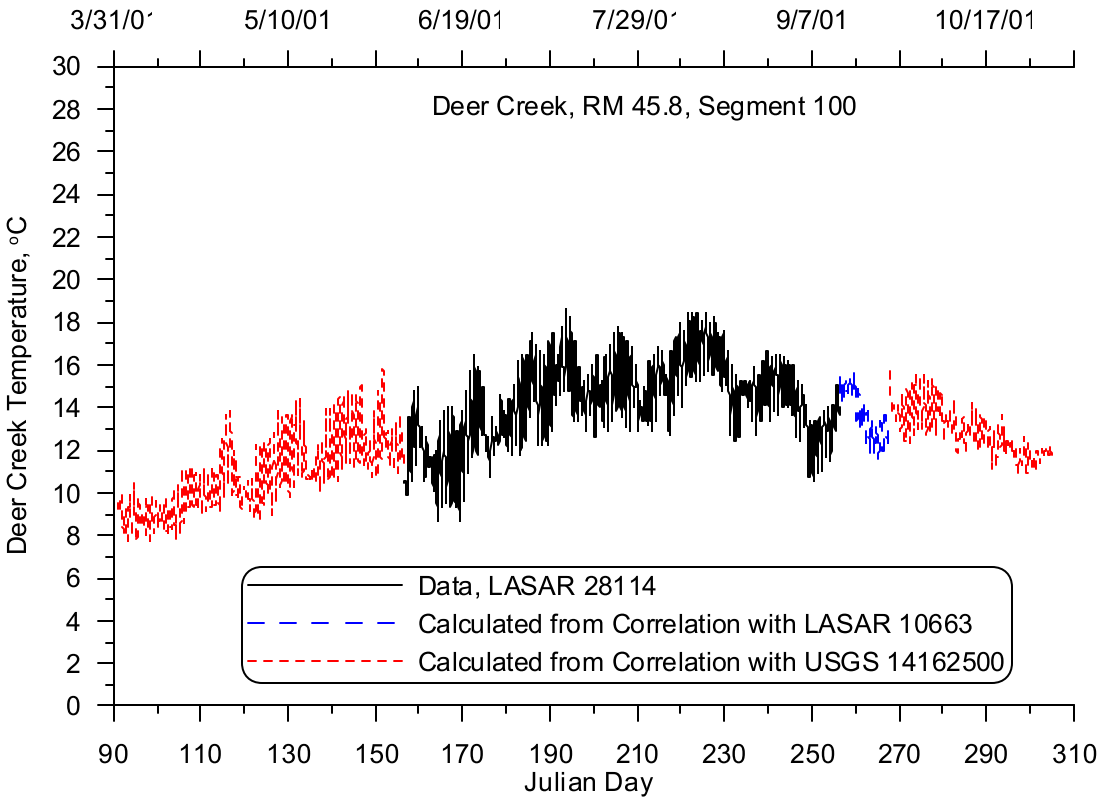


**Figure 509. Deer Creek (and Quartz Creek) temperature, 2001**

Stream temperatures were monitored on Bear Creek from June 5 to September 13, 2001, at LASAR 28108. A temperature correlation was developed with data collected on the Mohawk River from LASAR 10663 to fill in a data gap from September 13 to 24. The temperature data from the Mohawk River were adjusted in time 90 minutes earlier to address different water travel times from each basin. Figure 510 shows the temperature correlation between the two sites, including the correlation equation. The data gaps from April 1 to June 5 and from September 24 to October 21 were filled using a temperature correlation developed with data collected on the McKenzie River at USGS gage 14162500. The temperature data on the McKenzie River were adjusted one hour earlier to account for different travel times. Figure 511 shows the temperature correlation between the USGS site on the McKenzie River and the Bear Creek site. Figure 512 shows the completed time series temperature data and calculated values from the correlations. There were no temperature data collected for Gate Creek in 2001, so the temperature record developed for Bear Creek was used.

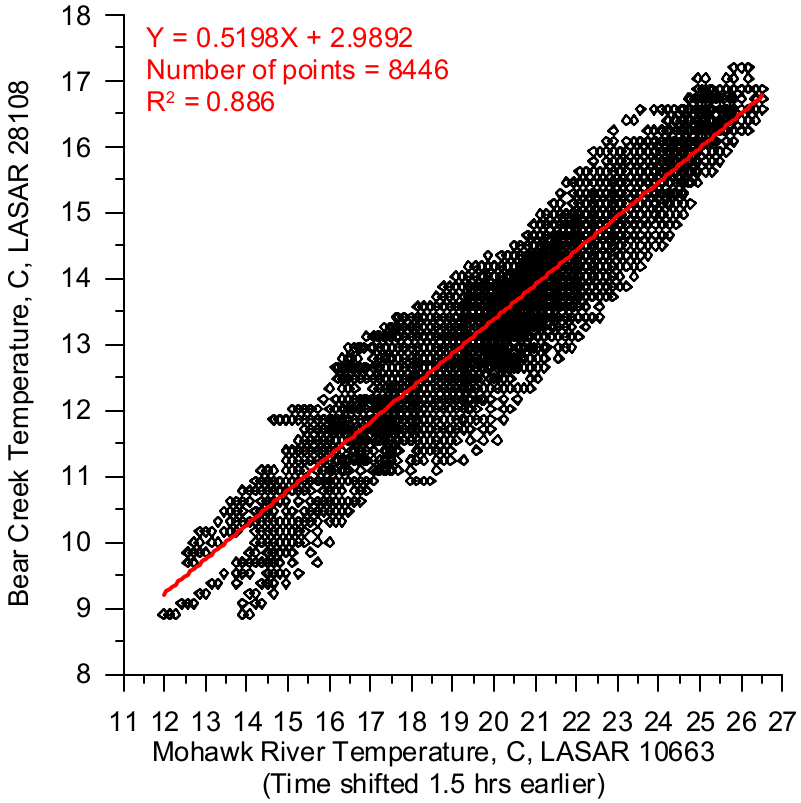


**Figure 510. Bear Creek temperature correlation for September 2001**

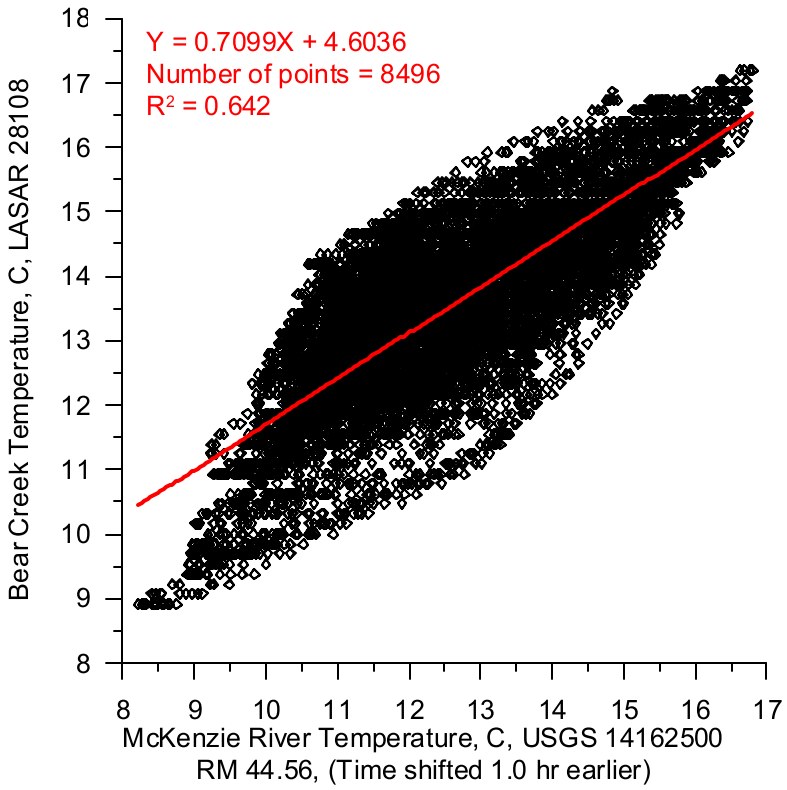


**Figure 511. Bear Creek temperature correlation for spring and fall 2001**

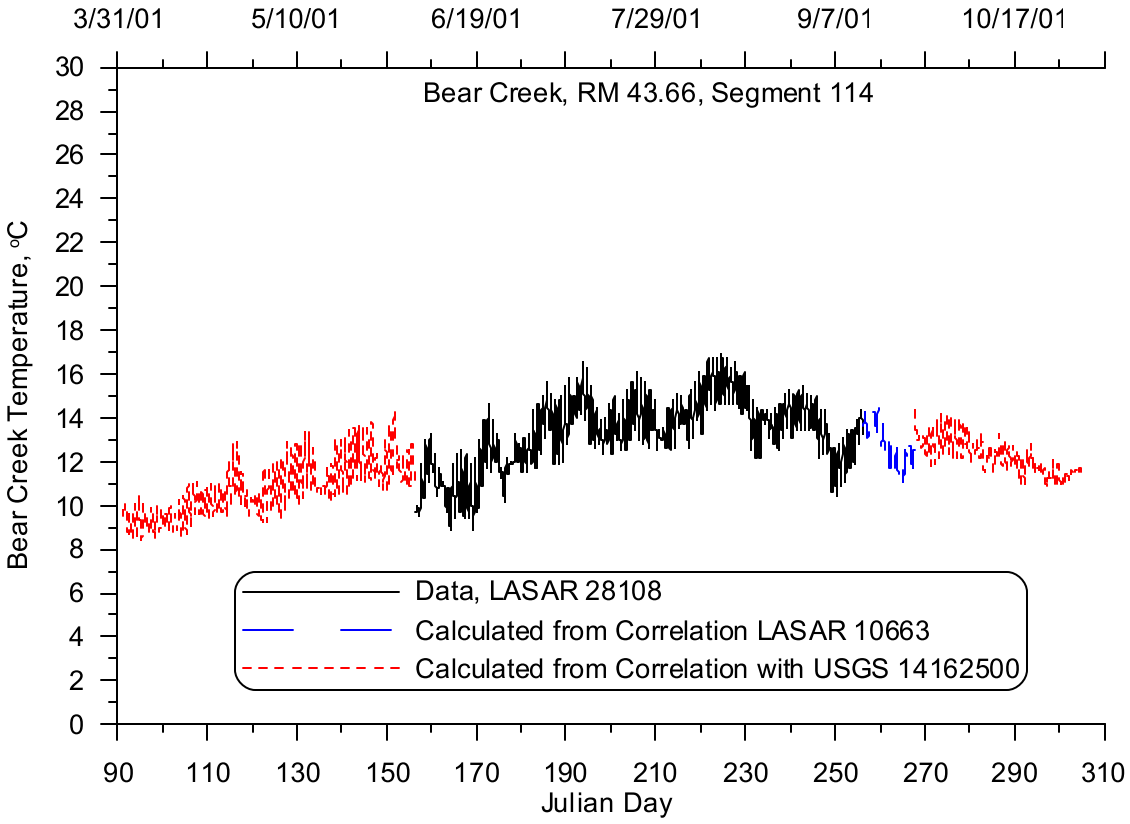


**Figure 512. Bear Creek (and Gate Creek) temperature, 2001**

There were temperature data collected on Finn Creek from June 5 to September 13, 2001, (LASAR 28115). A temperature correlation was developed between the Finn Creek data and the data collected on the Mohawk River from LASAR 10663 to fill in a data gap from September 13 to 24. The temperature data from the Mohawk River were adjusted in time one hour earlier to address water timing issues from each basin. Figure 513 shows the temperature correlation between the two sites and the correlation equation. The data gaps from April 1 to June 5 and from September 24 to October 21 were filled using a temperature correlation developed with data collected on the McKenzie River at USGS gage 14162500. The temperature data on the McKenzie River were adjusted to one hour earlier to account for different travel times. Figure 514 shows the temperature correlation between the USGS site on the McKenzie River and the site on Finn Creek. Figure 515 shows the completed time series temperature data and calculated values from the correlations.

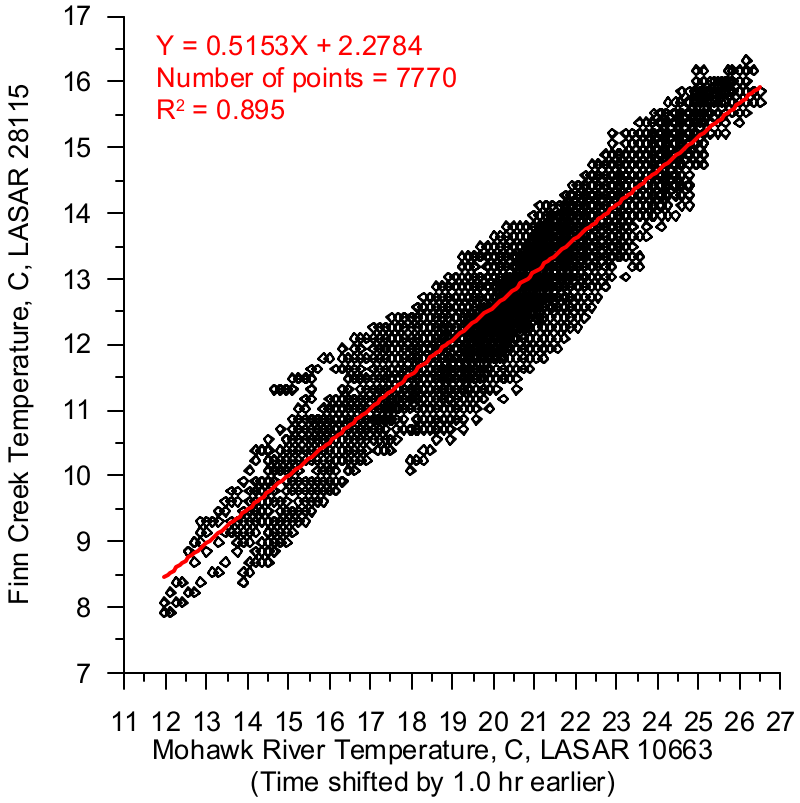


**Figure 513. Finn Creek temperature correlation for September 2001**

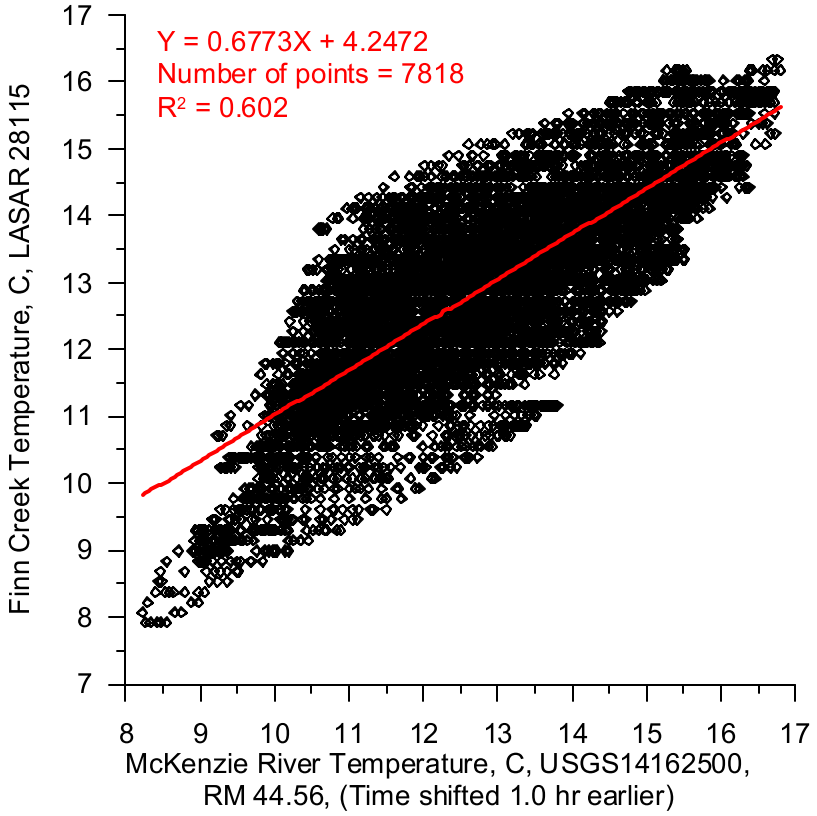


**Figure 514. Finn Creek temperature correlation for spring and fall 2001**

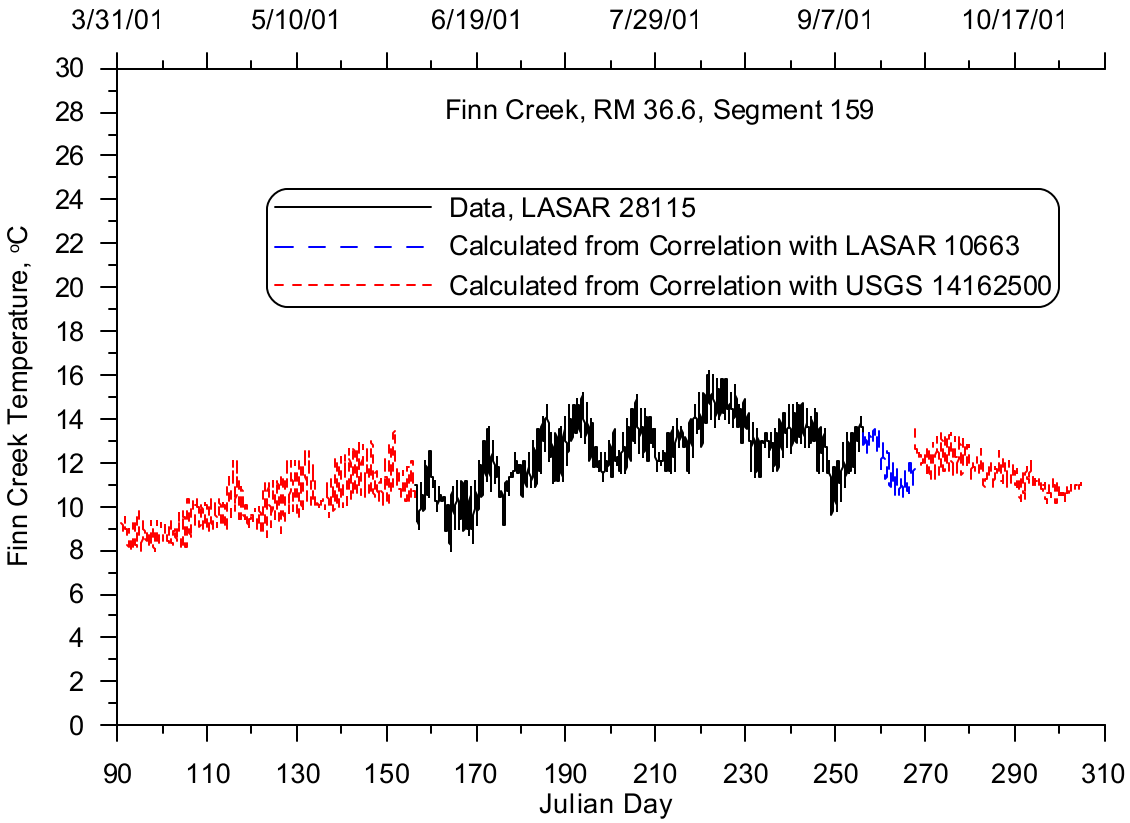


**Figure 515. Finn Creek temperature, 2001**

There were temperature data collected for Camp Creek from June 5 to September 13, 2001, (LASAR 28111). A temperature correlation was developed between the Camp Creek data and data collected on the Mohawk River from LASAR 10663 to fill in a data gap from September 13 to 24. The temperature data from the Mohawk River were adjusted in time one and half-hours earlier to address water travel times from each basin. Figure 516 shows the temperature correlation between the two sites and the correlation equation. The data gaps from April 1 to June 5 and from September 24 to October 21 were filled using a temperature correlation developed with data collected on the McKenzie River at USGS gage 14162500. The temperature data on the McKenzie River were adjusted one hour earlier to account for different travel times. Figure 517 shows the temperature correlation between the USGS site on the McKenzie River and the site on Camp Creek. Figure 518 shows the completed time series temperature data and calculated values from the correlations.

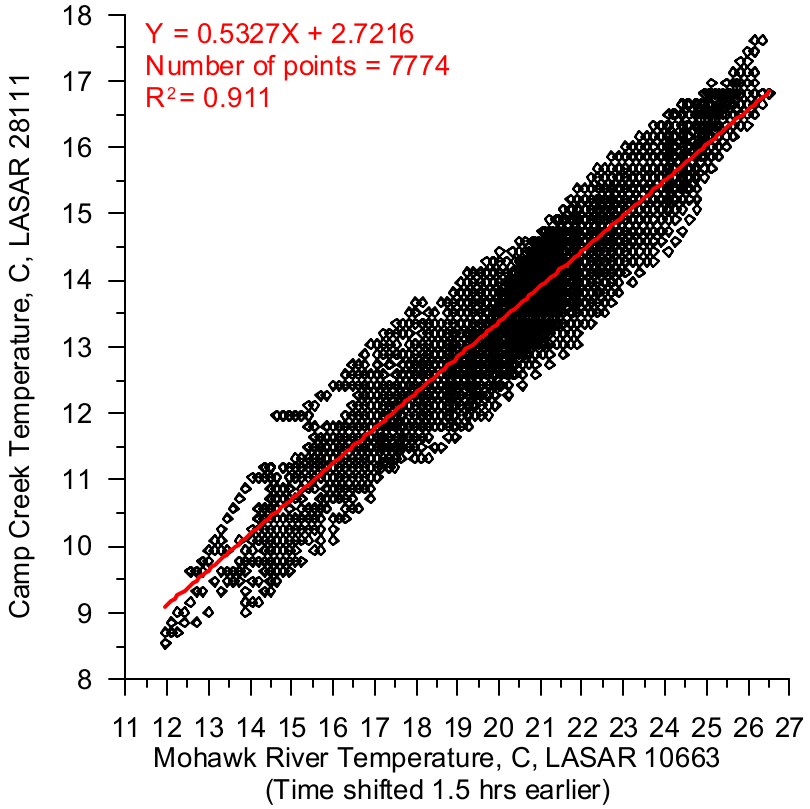


**Figure 516. Camp Creek temperature correlation for September 2001**

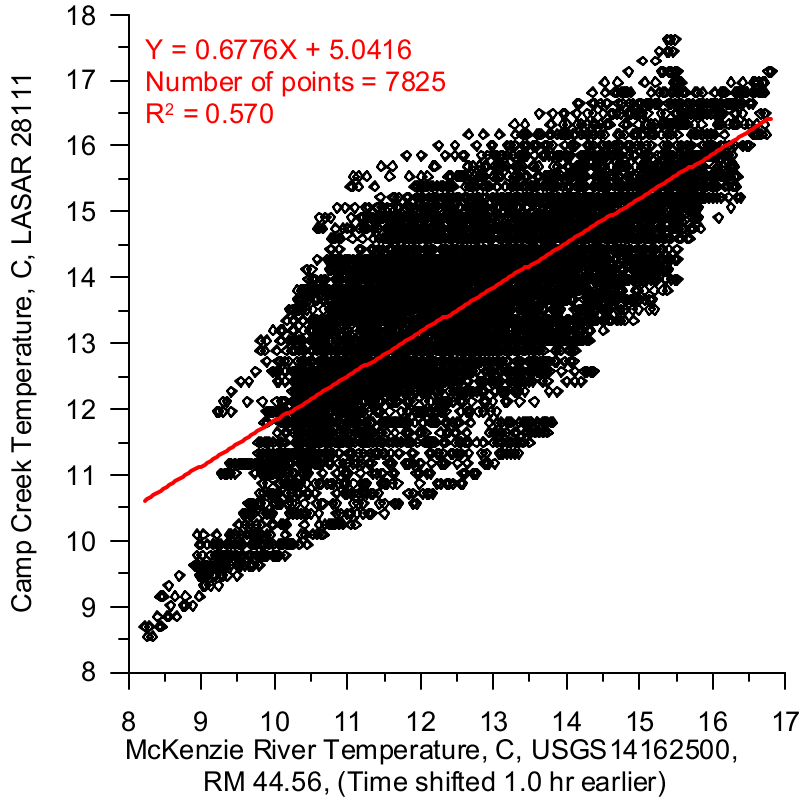


**Figure 517. Camp Creek temperature correlation for spring and fall 2001**

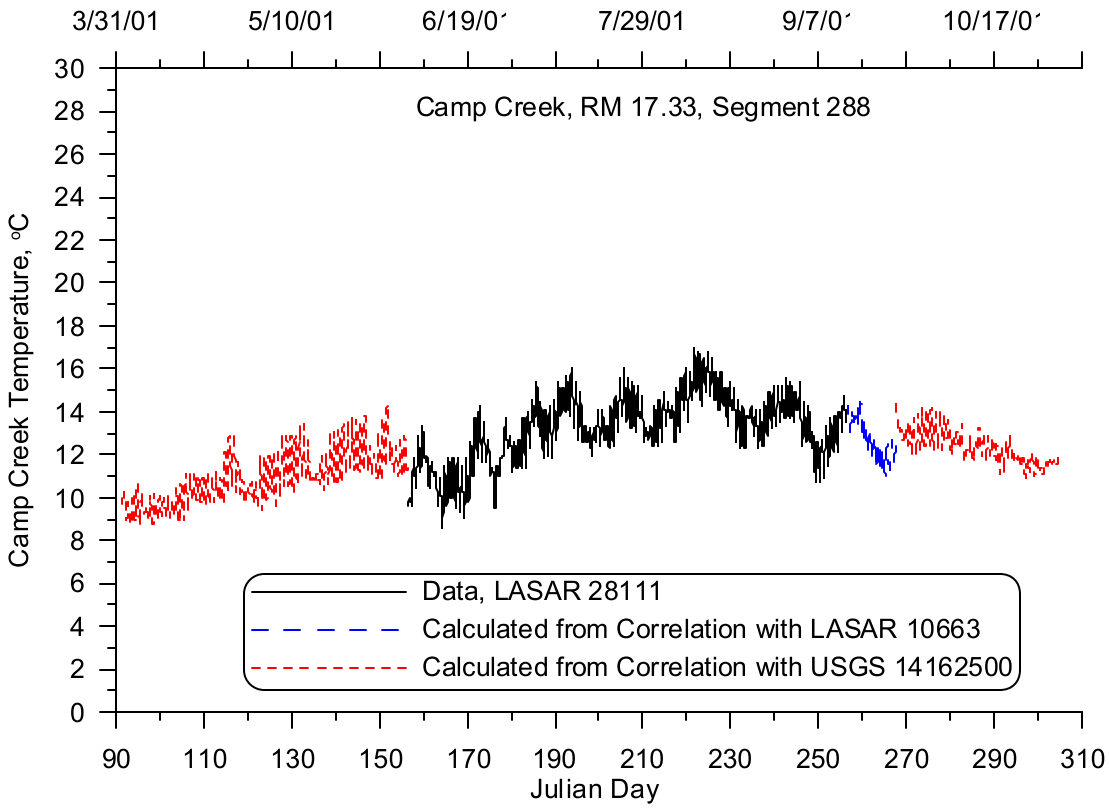


**Figure 518. Camp Creek temperature, 2001**

Stream temperatures were recorded on the Mohawk River every half-hour from June 6 to September 24, 2001, and during the year there were also nine temperature grab samples at the same site (LASAR 10663). Figure 519 shows a time series of the temperature data recorded on the Mohawk River. A temperature correlation was developed between the Mohawk River data and the temperature data collected on the McKenzie River at RM 44.56 (USGS 14162500) to fill the data gaps before June 6 and after September 24. Figure 520 shows the temperature correlation developed between the two sites. Although the correlation relationship shows some reasonable association between the two data sets when the correlation equation was used to calculate Mohawk River temperatures, the resulting time series does not agree well with the grab sample and half-hourly data collected as shown in Figure 521.

An analysis was then conducted with calculated Mohawk River temperature data to improve upon the seasonal trend shown in the grab sample data. The difference between calculated temperatures from the correlation and grab sample data for the same time were taken. The differences were then linearly interpolated between the grab sample times to fill in temperature differences for each half-hour calculated value. The interpolated differences were then used to adjust the calculated temperatures from the correlation. The result would be a calculated temperature time series which would be following the same seasonal trend as the 2001 grab sample data. Figure 522 shows a completed time series with the 2001 half-hourly data and the adjusted calculated values.

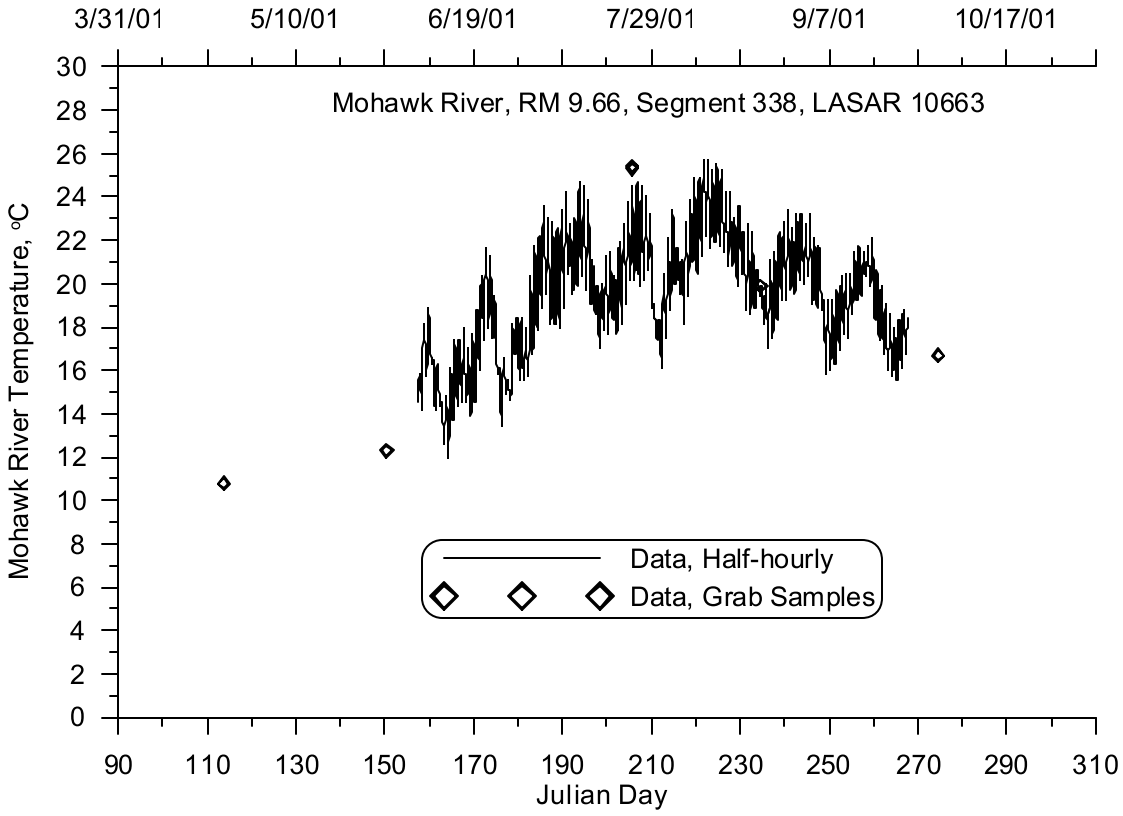


**Figure 519. Mohawk River 2001 temperature data for analysis**

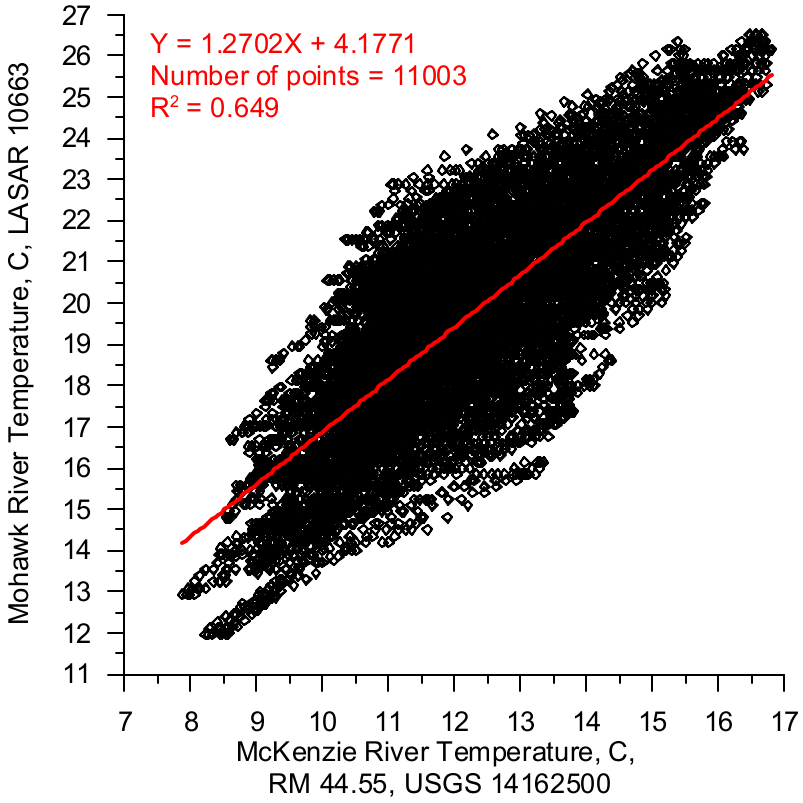


**Figure 520. Mohawk River temperature correlation**

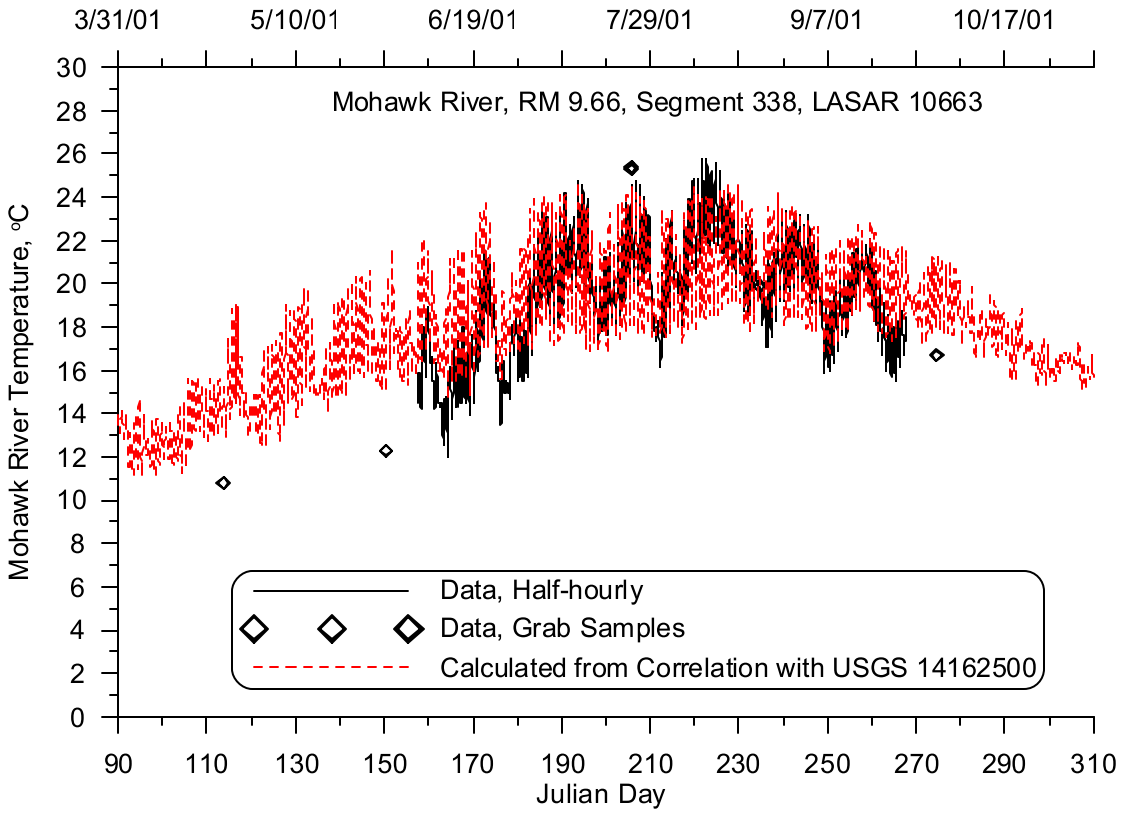


**Figure 521. Mohawk River 2001 temperature time series for analysis**

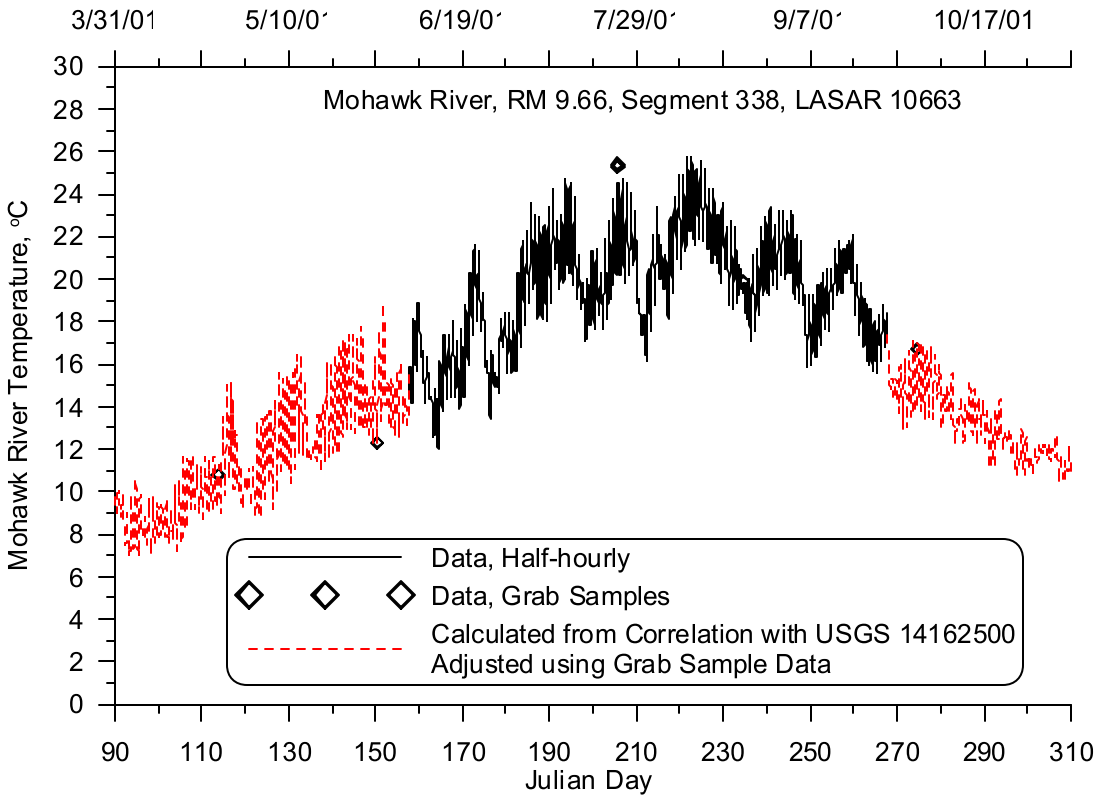


**Figure 522. Mohawk River temperature, 2001**

## Year 2002

The monitoring site on the McKenzie River above its confluence with the South Fork McKenzie River was LASAR 28505 (RM 60.25). This site had data from April 21 to September 9, 2009. The data gap from September 9 to October 3 was filled by using the correlation developed for 2001 with LASAR site LASAR 26770 as shown in Figure 502. The data at this site were limited in 2002, so it could not be implemented for a larger time window. The data gaps from April 1 to April 21 and from October 3 to 31 were filled by using the same temperature correlation developed for 2001 using the USGS gage station 14162500 as shown in Figure 503. Similar to 2001, the temperatures at this site, both data and calculated values, were increased by 0.31 °C to better represent the temperature at the river confluence with the South Fork McKenzie River. Figure 523 shows time series of the adjusted temperature data and correlated values for 2002.

Stream temperatures were recorded on the Blue River every half-hour at the USGS gage station 14162200 for the entire calendar year. Figure 524 shows the Blue River temperature time series for the model simulation period.

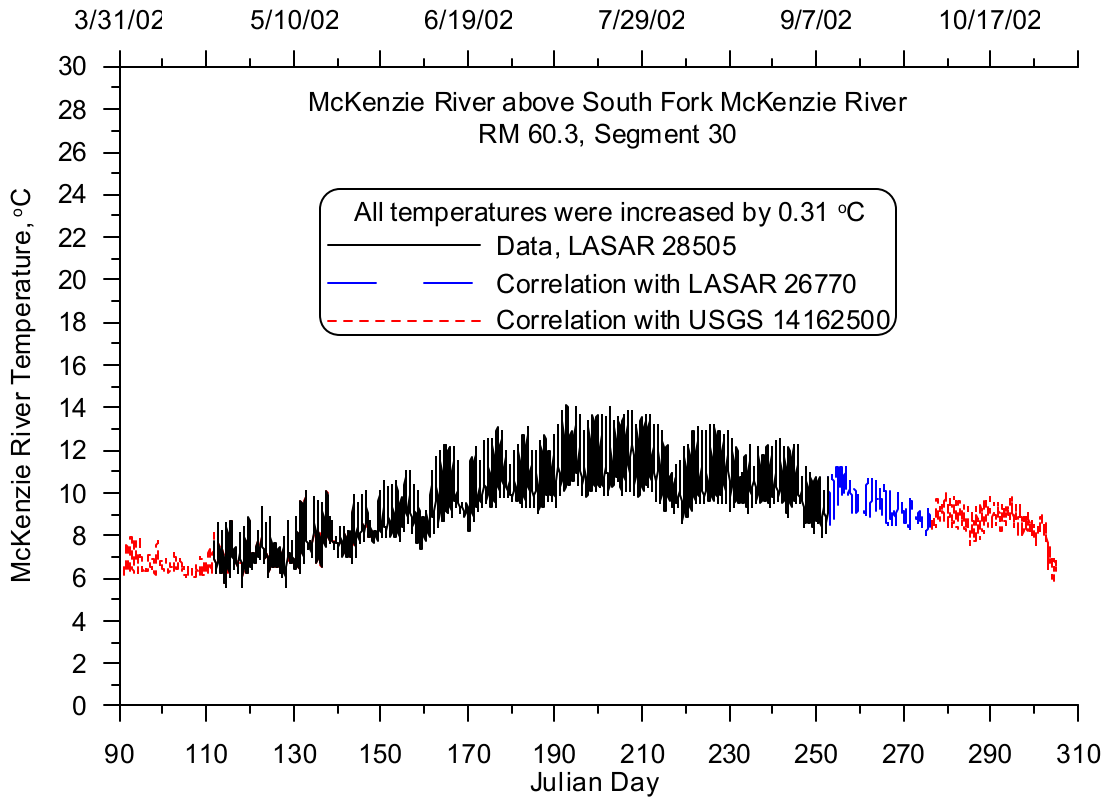


**Figure 523. McKenzie River tributary temperature, 2002**

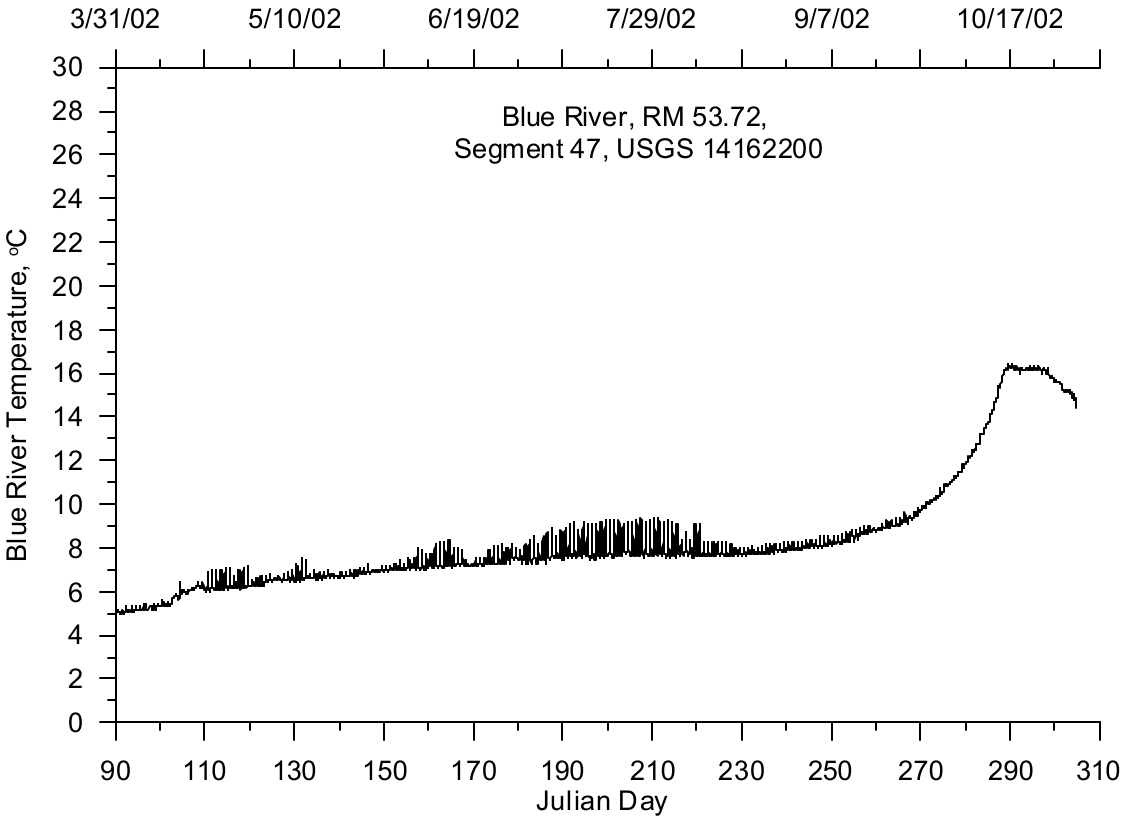


**Figure 524. Blue River temperature, 2002**

Temperature data were collected on Deer Creek from June 19 to September 4, 2002 at LASAR site 28114. The temperature correlation developed with Mohawk River data (LASAR 10663) for 2001, shown in Figure 507, was used to fill the data gaps from June 4 to 19 and from September 4 to October 1. The data gaps from April 1 to June 4 and from October 1 to 31 were filled using the same temperature correlation from 2001 using data collected on the McKenzie River at USGS gage 14162500 and shown in Figure 508. Figure 525 shows the completed temperature time series of data and calculated values for Deer Creek. There were no temperature data for Quartz Creek in 2002, so the temperature record developed for Deer Creek was used.

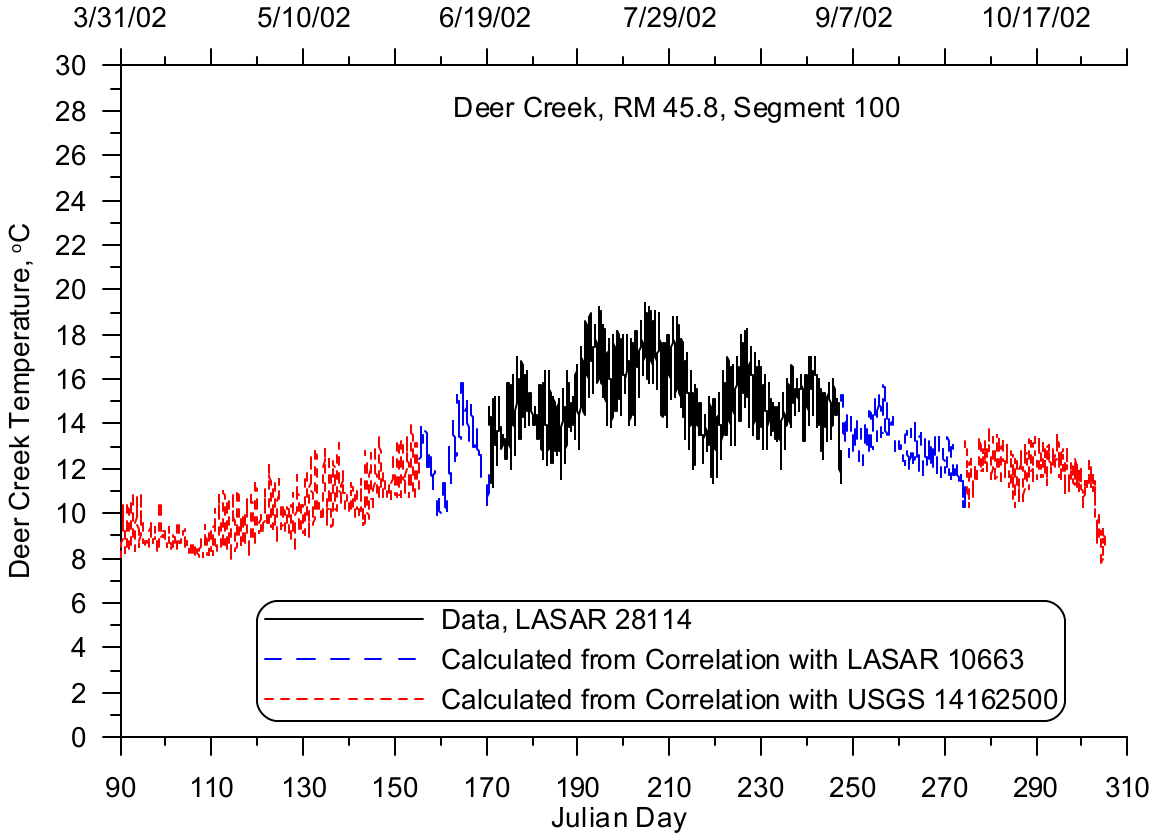


**Figure 525. Deer Creek (and Quartz Creek) temperature, 2002**

Temperature data were collected on Bear Creek from June 19 to September 4, 2002, at LASAR site 28108. The temperature correlation developed with Mohawk River data (LASAR 10663) for 2001, shown in Figure 510, was used to fill the data gaps from June 4 to 19 and from September 4 to October 1. The data gaps from April 1 to June 4 and from October 1 to 31 were filled using the same temperature correlation from 2001 using data collected on the McKenzie River at USGS gage 14162500 and shown in Figure 511. Figure 526 shows the completed temperature time series of data and calculated values for Bear Creek. There were no temperature data for Gate Creek in 2002, so the temperature record developed for Bear Creek was used.

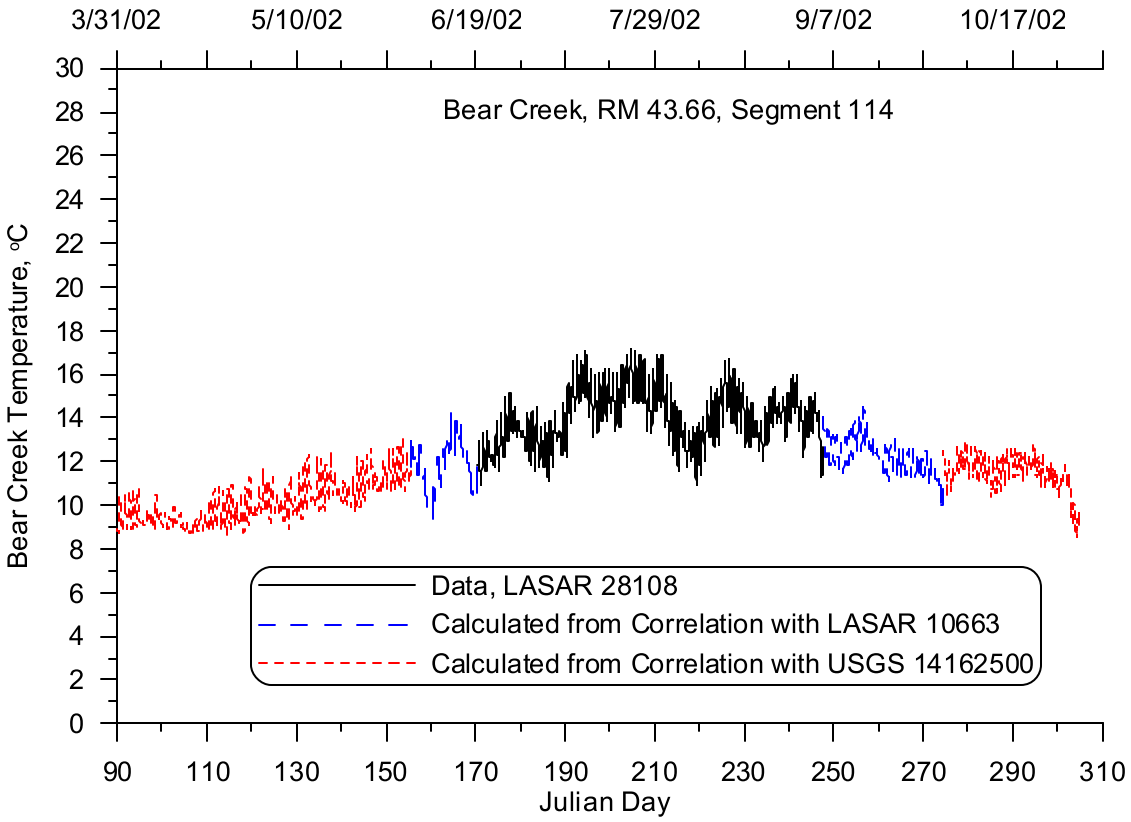


**Figure 526. Bear Creek (and Gate Creek) temperature, 2002**

Temperature data were collected on Finn Creek from July 3 to September 4, 2002 at LASAR site 28115. The temperature correlation developed with Mohawk River data (LASAR 10663) for 2001, shown in Figure 513, was used to fill the data gaps from June 4 to July 3 and from September 4 to October 1. The data gaps from April 1 to June 4 and from October 1 to 31 were filled using the same temperature correlation from 2001 using data collected on the McKenzie River at USGS gage 14162500 and shown in Figure 514. Figure 527 shows the completed temperature time series of data and calculated values for Finn Creek.

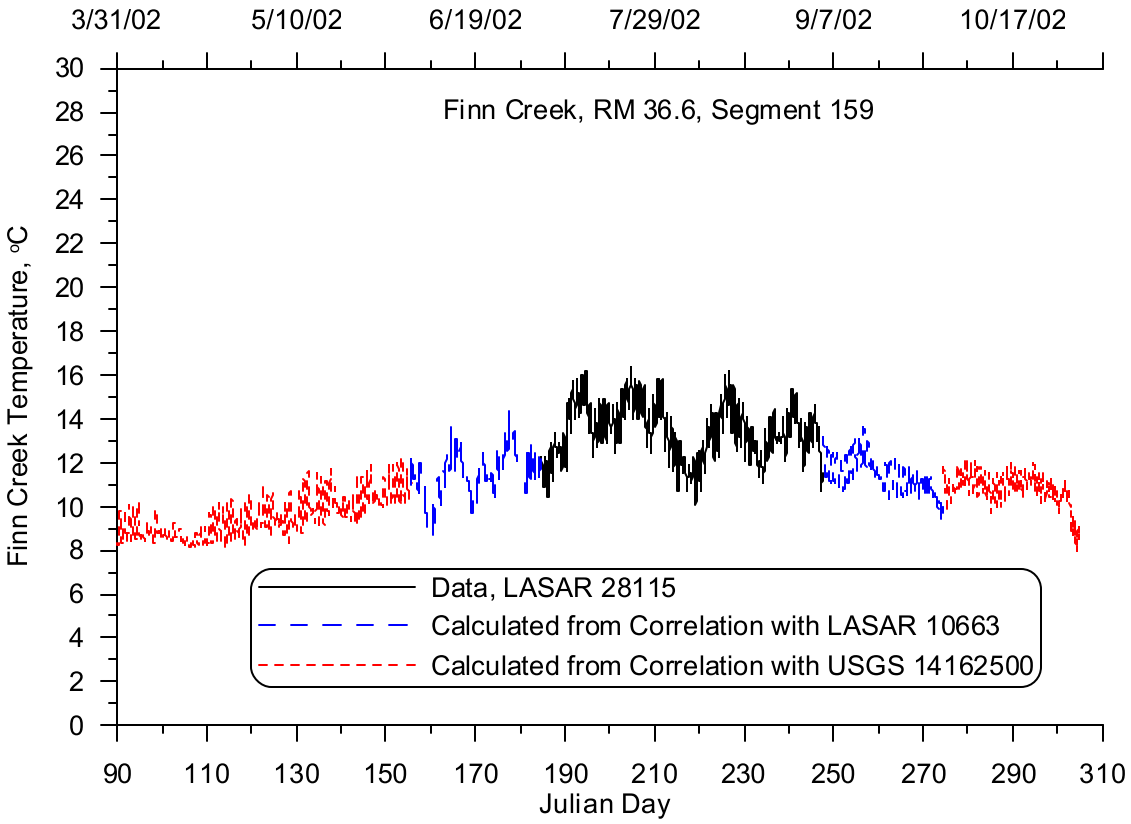


**Figure 527. Finn Creek temperature, 2002**

Temperature data were collected on Camp Creek from July 3 to September 4, 2002 at LASAR site 28111. The temperature correlation developed with Mohawk River data (LASAR 10663) for 2001, shown in Figure 516, was used to fill the data gaps from June 4 to July 3 and from September 4 to October 1. The data gaps from April 1 to June 4 and from October 1 to 31 were filled using the same temperature correlation from 2001 using data collected on the McKenzie River at USGS gage 14162500 and shown in Figure 517. Figure 528 shows the completed temperature time series of data and calculated values for Camp Creek.

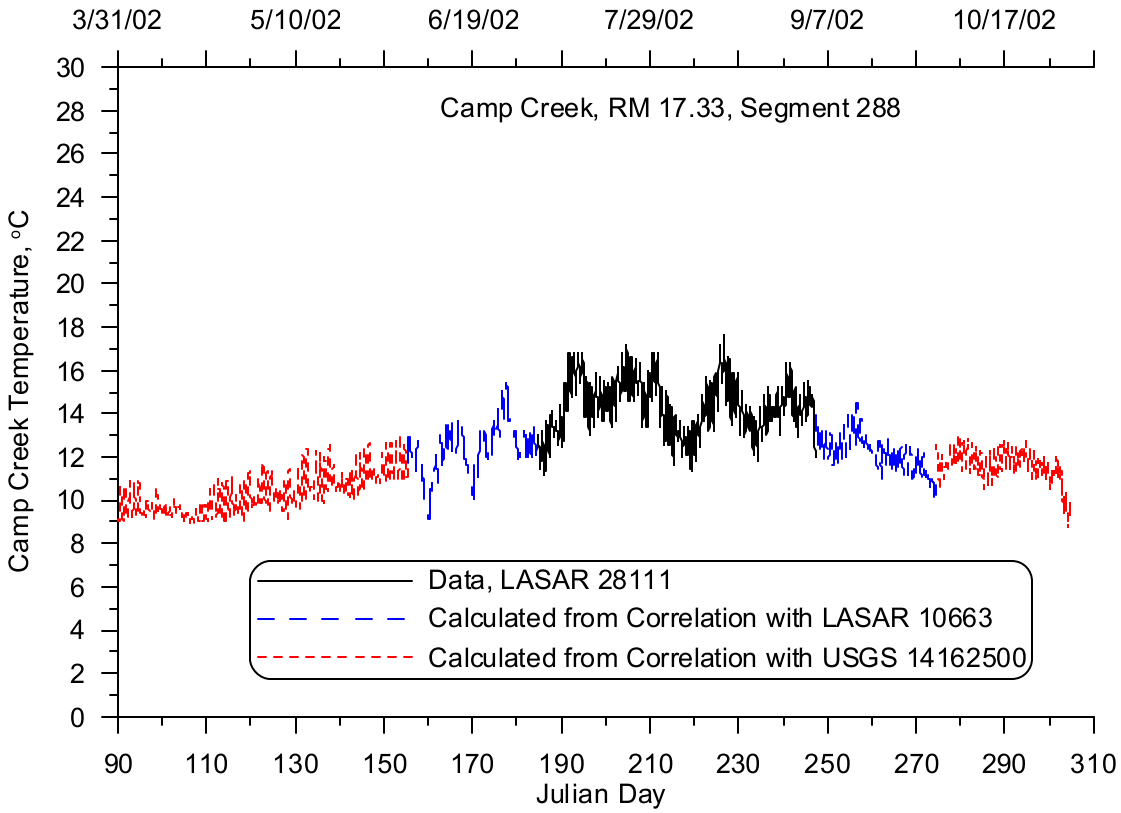


**Figure 528. Camp Creek temperature, 2002**

Stream temperatures were recorded on the Mohawk River every half-hour from June 4 to October 1, 2002, and during the year there were nine temperature grab samples at the same site (LASAR 10663). Figure 529 shows a time series of the temperature data recorded on the Mohawk River. The same temperature correlation developed with temperature data collected on the McKenzie River at RM 44.56 (USGS 14162500), as shown in Figure 520 for 2001, was used for 2002. Although this correlation relationship shows some reasonable association between the two data sets when the correlation equation was used to calculate Mohawk River temperatures, the resulting time series does not agree well with the grab sample and half-hourly data collected as shown in Figure 530.

An analysis was then conducted with calculated Mohawk River temperature data to improve upon the seasonal trend shown in the grab sample data. The difference between calculated temperatures from the correlation and grab sample data for the same time were taken. The differences were then linearly interpolated between the grab sample times to fill in temperature differences for each half-hour calculated value. The interpolated differences were then used to adjust the calculated temperatures from the correlation. The result would be a calculated temperature time series which would be following the same seasonal trend as the 2002 grab sample data. Figure 531 shows a completed time series with the 2002 half-hourly data and the adjusted calculated values.

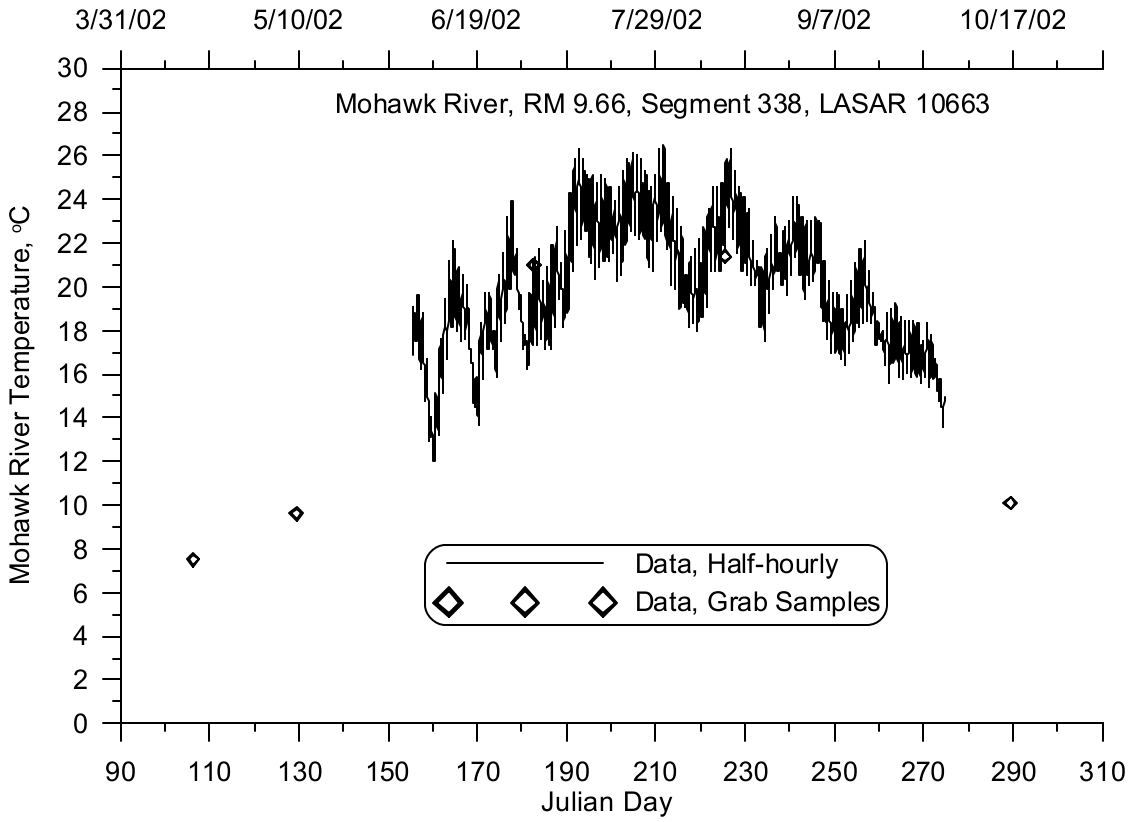


**Figure 529. Mohawk River 2002 temperature data for analysis**

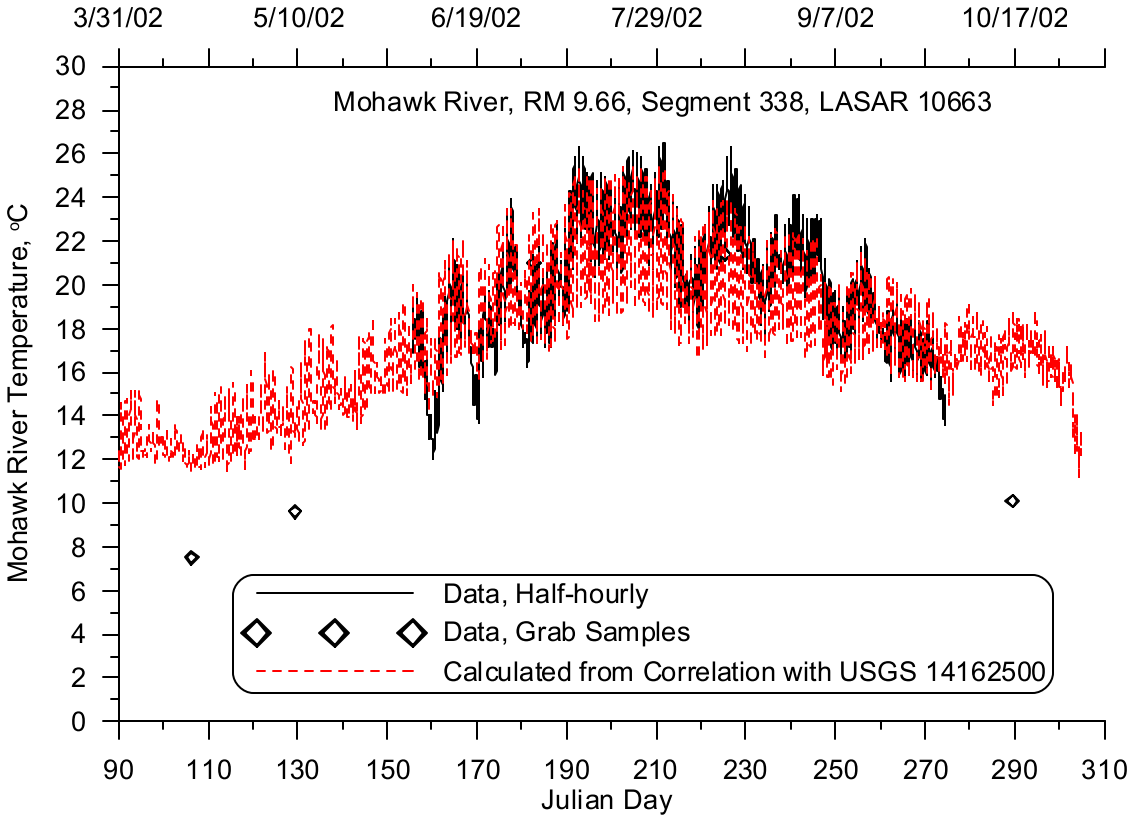


**Figure 530. Mohawk River 2002 temperature time series for analysis**

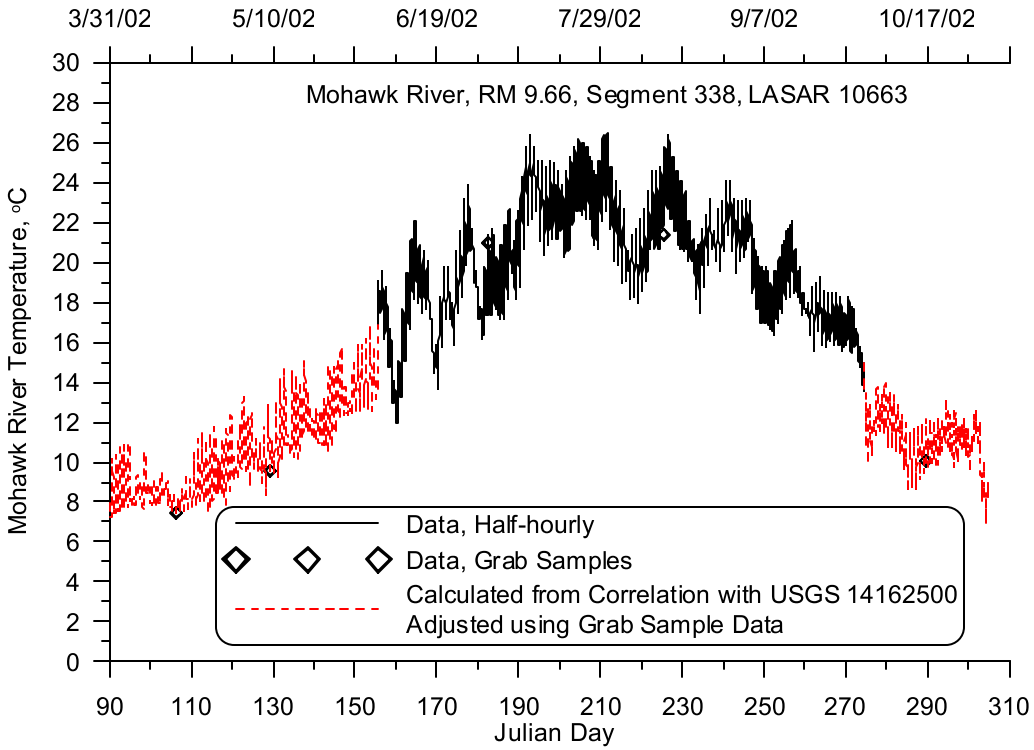


**Figure 531. Mohawk River temperature, 2002**

## *Point Sources*

ODEQ identified one major point source discharge along the McKenzie River model area on the basis of permitted discharge, the Weyerhaeuser Company. The discharge flow enters at RM 12.17 which corresponds to model segment 321. Figure 532 shows a map indicating the location of the point source discharge.

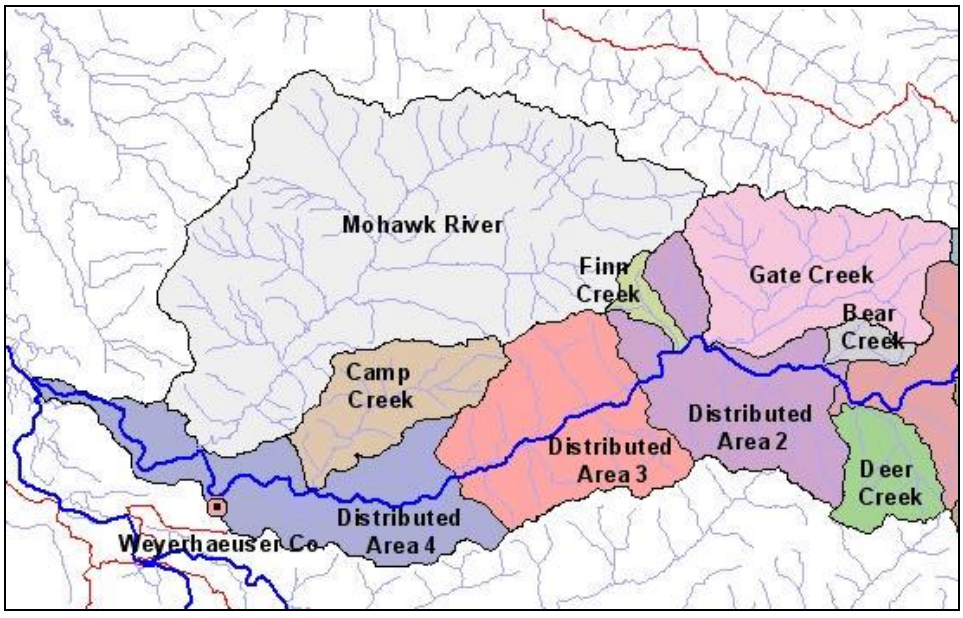


**Figure 532. McKenzie River model Point Sources**

## Hydrodynamic Data

### Year 2001

The discharge data for the Weyerhaeuser Company point source were provided to ODEQ by the Weyerhaeuser Company and consisted of daily flow measurements. Figure 533 shows a time series of the flows recorded for the Weyerhaeuser Company discharge for 2001.

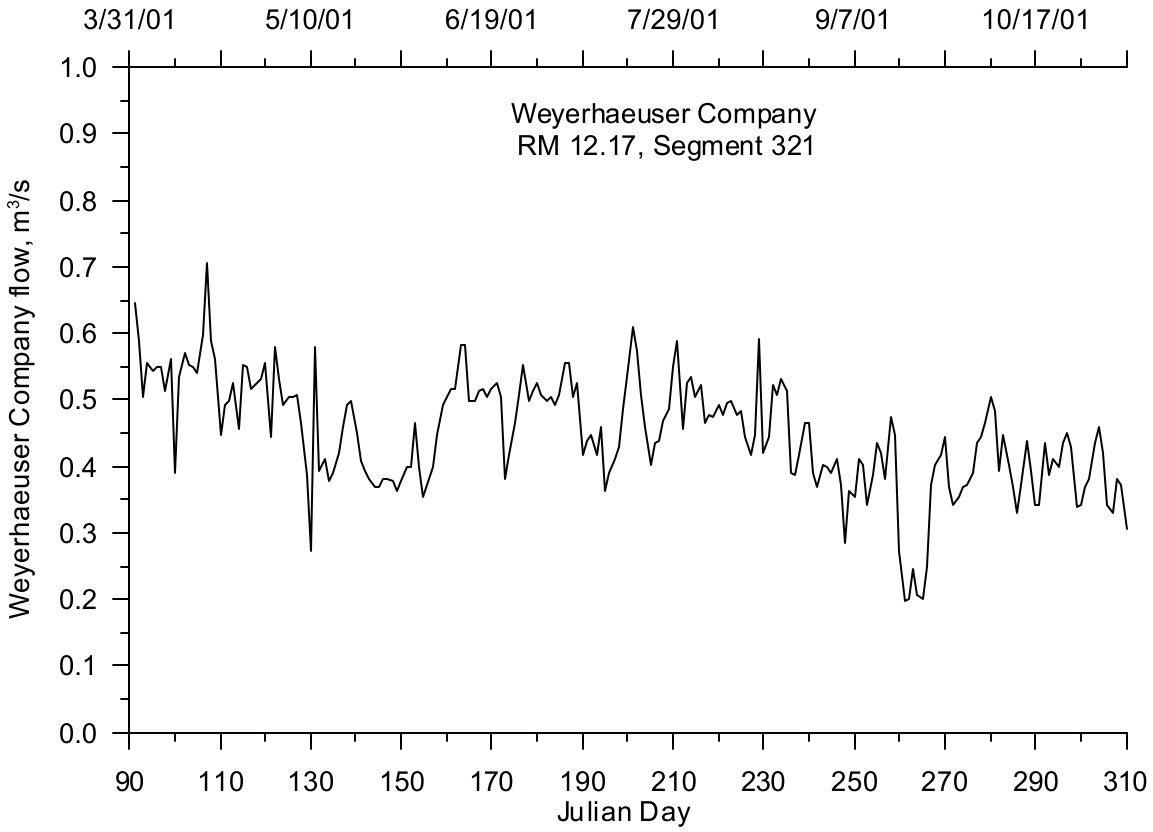


**Figure 533. Weyerhaeuser Company discharge flow, 2001**

### Year 2002

Similar to 2001, the Weyerhaeuser Company provided daily discharge flows for their effluent to ODEQ. Figure 534 shows a time series of the flows recorded for the Weyerhaeuser Company discharge for 2002. The figure shows that the flows recorded in 2002 were similar to 2001.

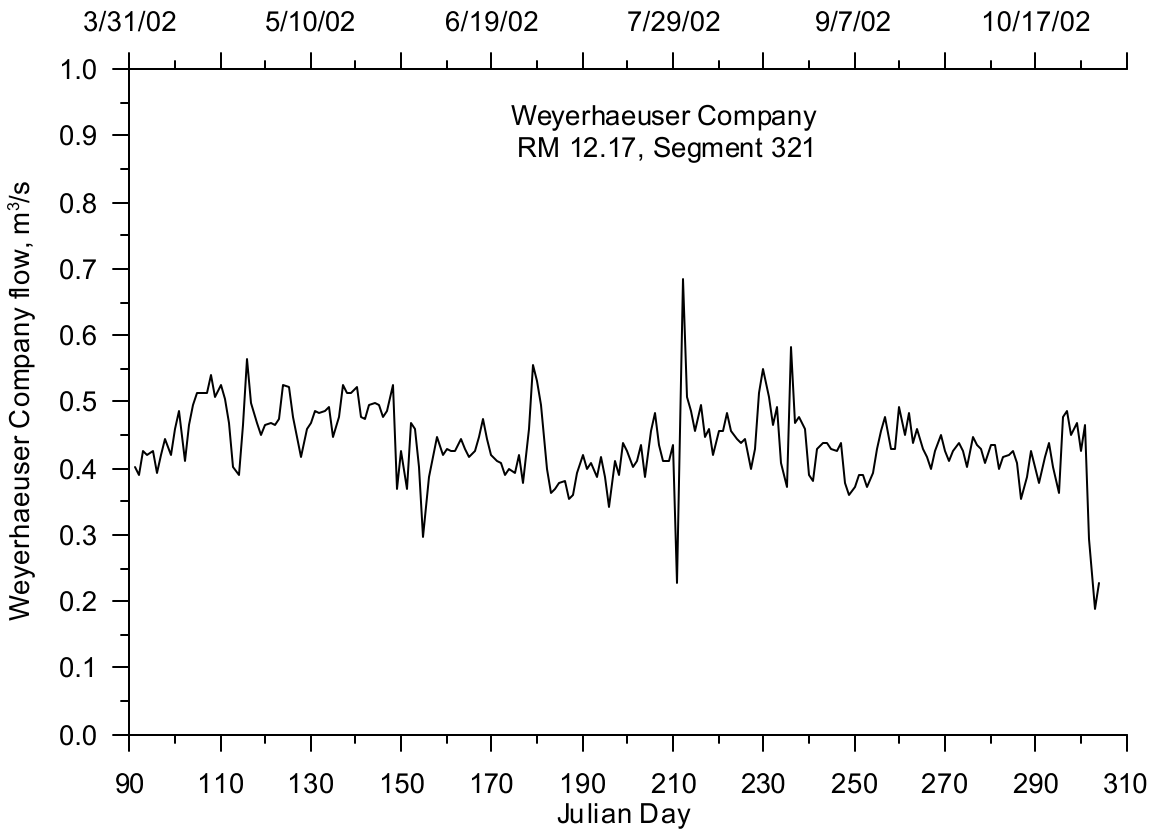


**Figure 534. Weyerhaeuser Company discharge flow, 2002**

## Temperature Data

### Year 2001

The Weyerhaeuser Company provided daily discharge temperatures for their effluent to ODEQ. The data set consisted of daily temperatures recorded every other day instead of each day during the summer. Since the values were every other day the gaps in between were estimated by interpolating between the two surroundings days. Figure 535 shows a time series of the discharge temperature data and interpolated values for the Weyerhaeuser Company discharge.

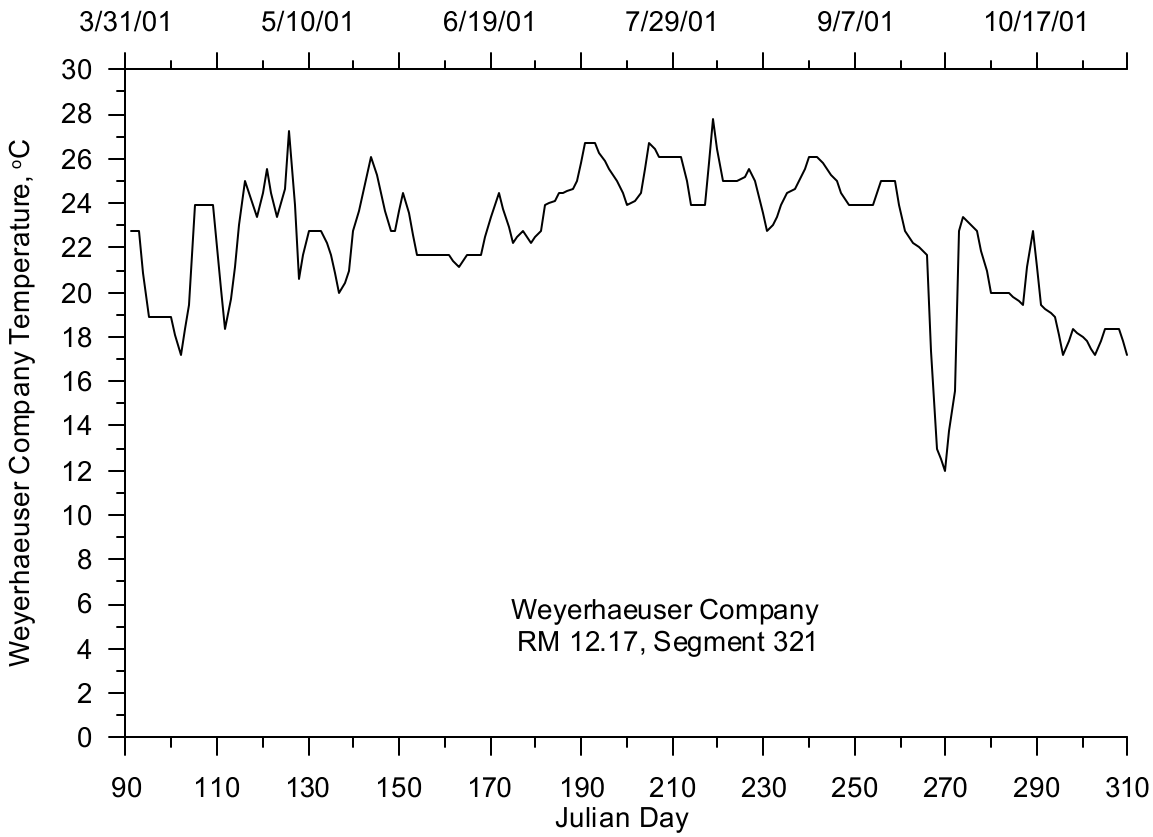


**Figure 535. Weyerhaeuser Company discharge temperature, 2001**

## Year 2002

Similar to 2001, the Weyerhaeuser Company provided daily discharge temperatures for their effluent to ODEQ. The data set consisted of daily temperatures recorded every other day instead of each day during the summer. Since the values were every other day the gaps in between were estimated by interpolating between the two surroundings days. Figure 536 shows a time series of the discharge temperature data and interpolated values for the Weyerhaeuser Company discharge.

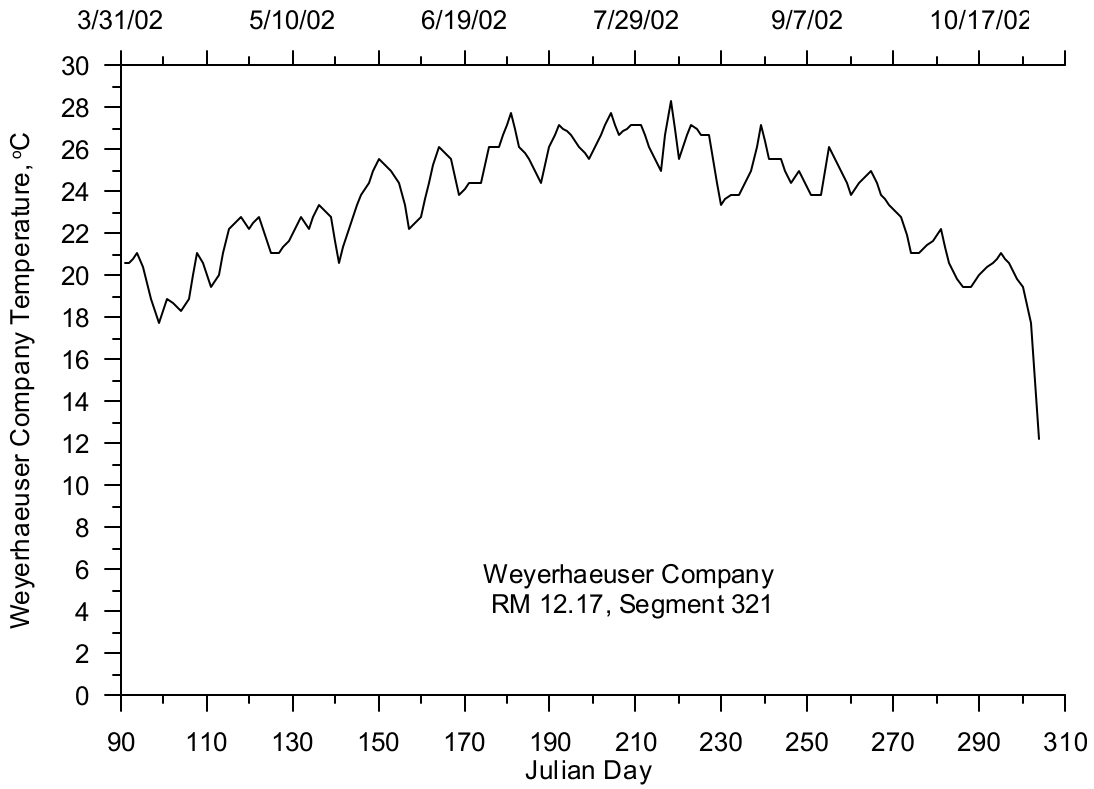


**Figure 536. Weyerhaeuser Company discharge temperature, 2002**

## *Shading*

CE-QUAL-W2 incorporates both topographic and vegetative shade in the model. Topographic characteristics include the steepest inclination angle in 18 directions around a model segment. The vegetative characteristics consist of tree top elevation, distance between the river channel centerline and the controlling vegetation, and the vegetation density in summer and winter. The vegetation characteristics were provided for both banks of the river.

The vegetation and topographic characteristics for the McKenzie River model were developed using geographic information system (GIS) data supplied by the Oregon Department of Environmental Quality (ODEQ). The data consists of thalweg points every 100 ft along the thalweg of the river. For each thalweg point, additional associated data included: width, elevation, three topographic inclination angles, and nine vegetation compartments for each bank. Each vegetation compartment consisted of vegetation height, distance from stream bank, and density. A detailed analysis was performed to convert the ODEQ data into the shade variables for the CE-QUAL-W2 model. A detailed description of the shade analysis is shown in Appendix A.

Figure 537 and Figure 538 show the tree top elevations along the McKenzie River for the left and right banks, respectively. The figures show the tree top elevations decreasing downstream, which follows the general topography of the river banks. Figure 539 and Figure 540 show the distance from the river centerline to controlling vegetation for the left and right banks, respectively. These figures show that the vegetation was relatively close to river at the upstream end and increases gradually moving downstream as the channel widens. Figure 541 and Figure 542 show the vegetation density for the left and right banks, respectively. The vegetation density plots indicate the density was higher for both banks at the

upstream end but became more variable progressing downstream with several pockets where the density decreases to zero.

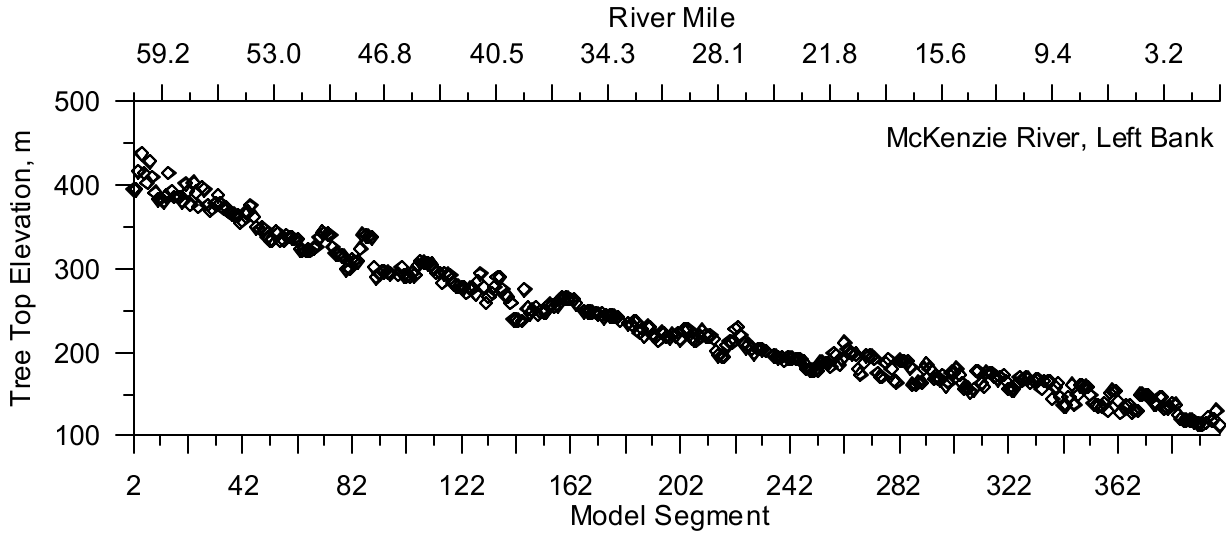


**Figure 537. McKenzie River Left Bank Tree Top Elevation**

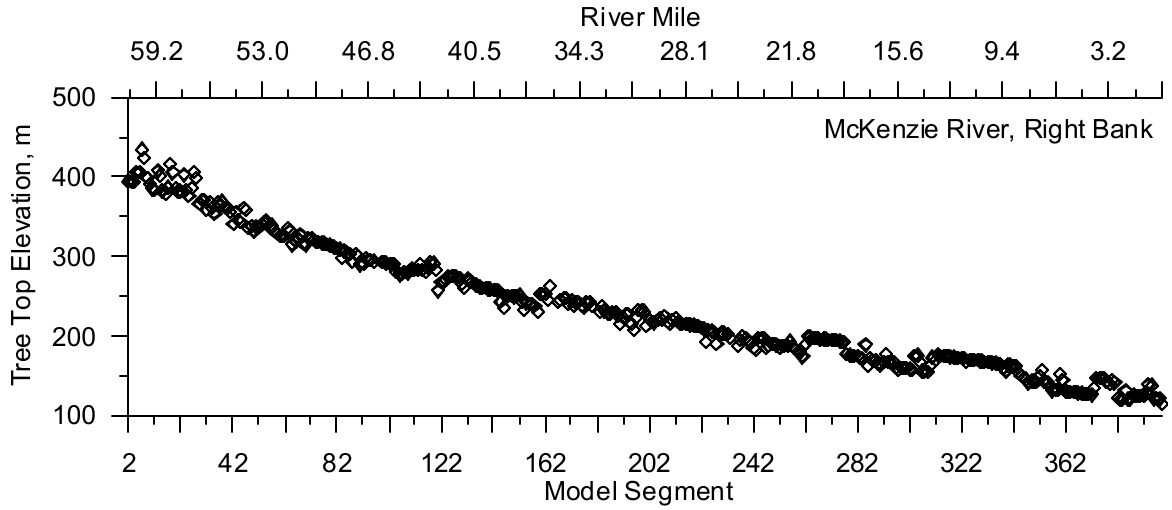


**Figure 538. McKenzie River Right Bank Tree Top Elevation**

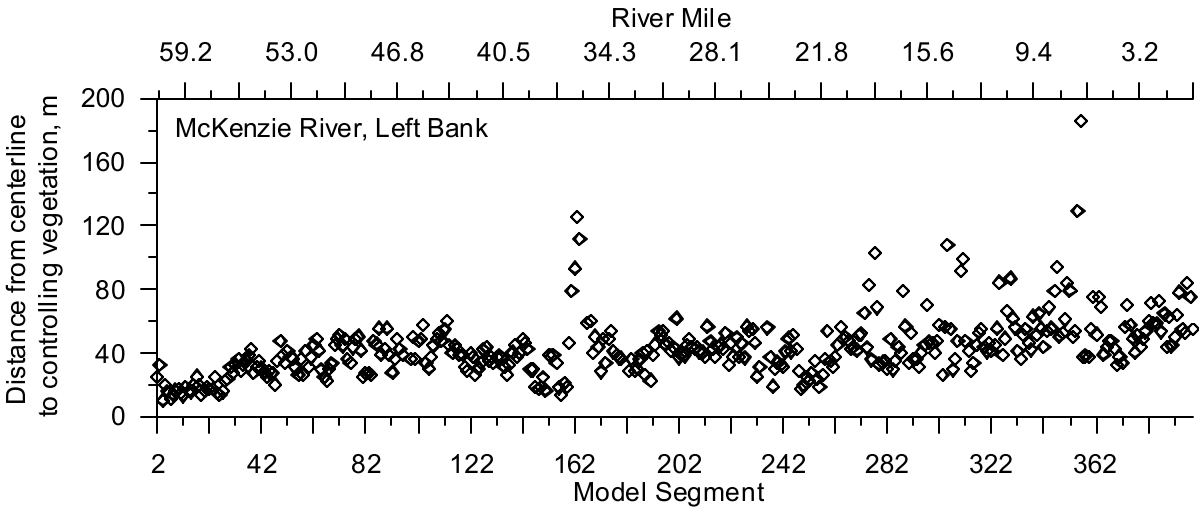


**Figure 539. McKenzie River Left Bank Distance from Centerline to Controlling Vegetation**

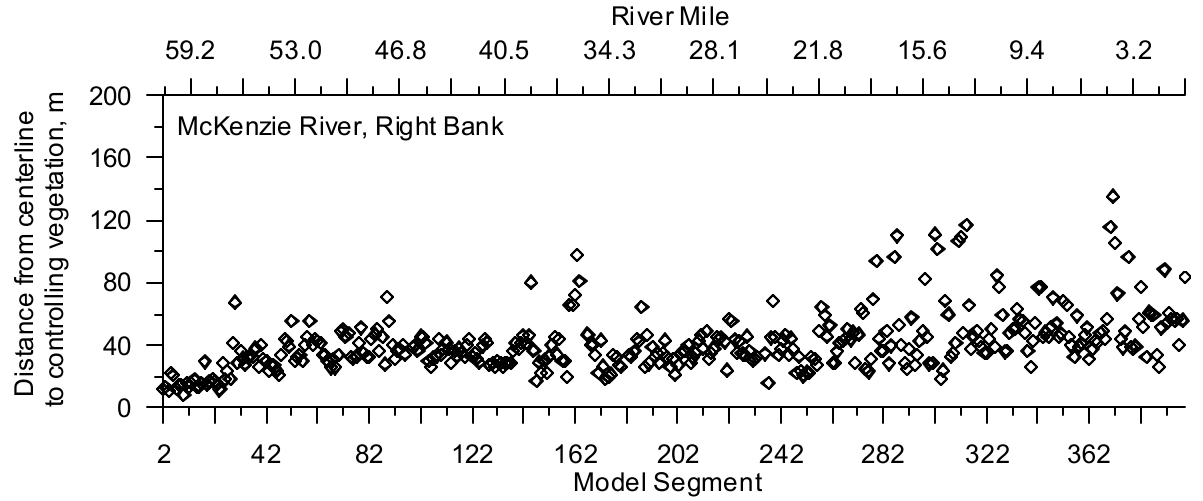


**Figure 540. McKenzie River Right Bank Distance from Centerline to Controlling Vegetation**

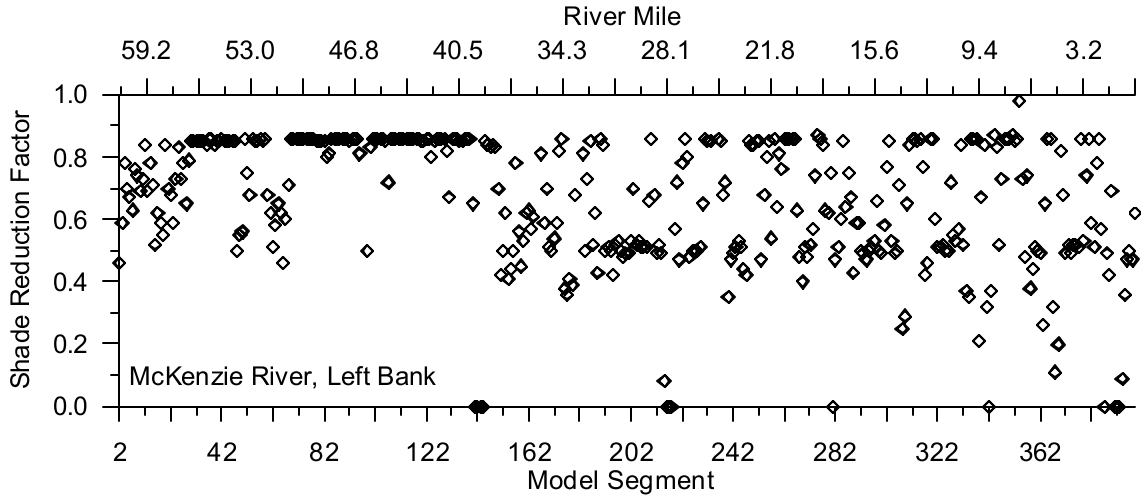


**Figure 541. McKenzie River Left Bank Shade Reduction Factor**

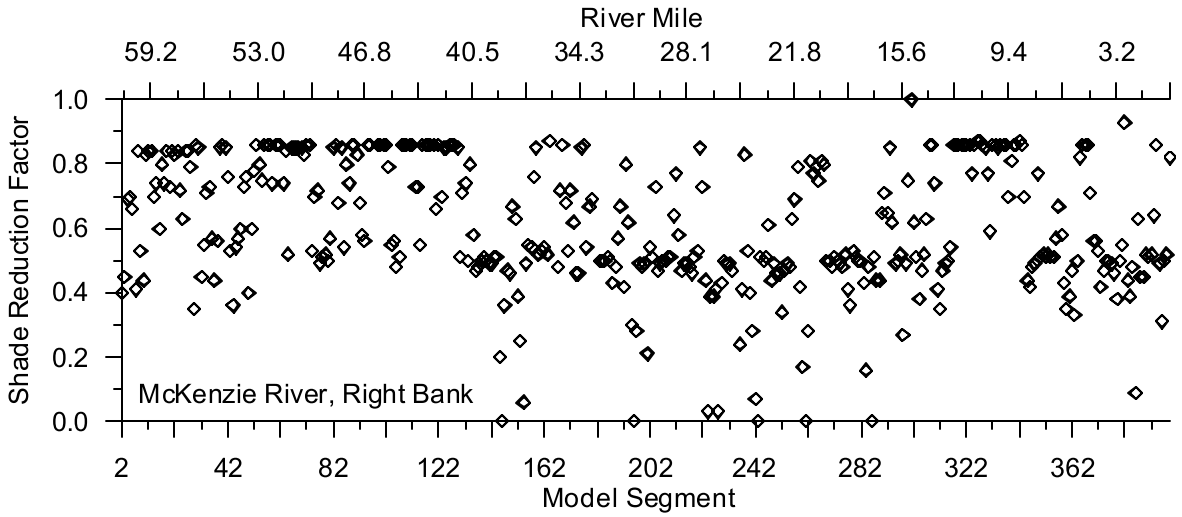


**Figure 542. McKenzie River Right Bank Shade Reduction Factor**

## *Meteorology*

The McKenzie River model utilized meteorological data from four monitoring sites from within or near the basin as shown in Figure 543. Table 58 lists the monitoring sites and the meteorological constituents monitored at each site.

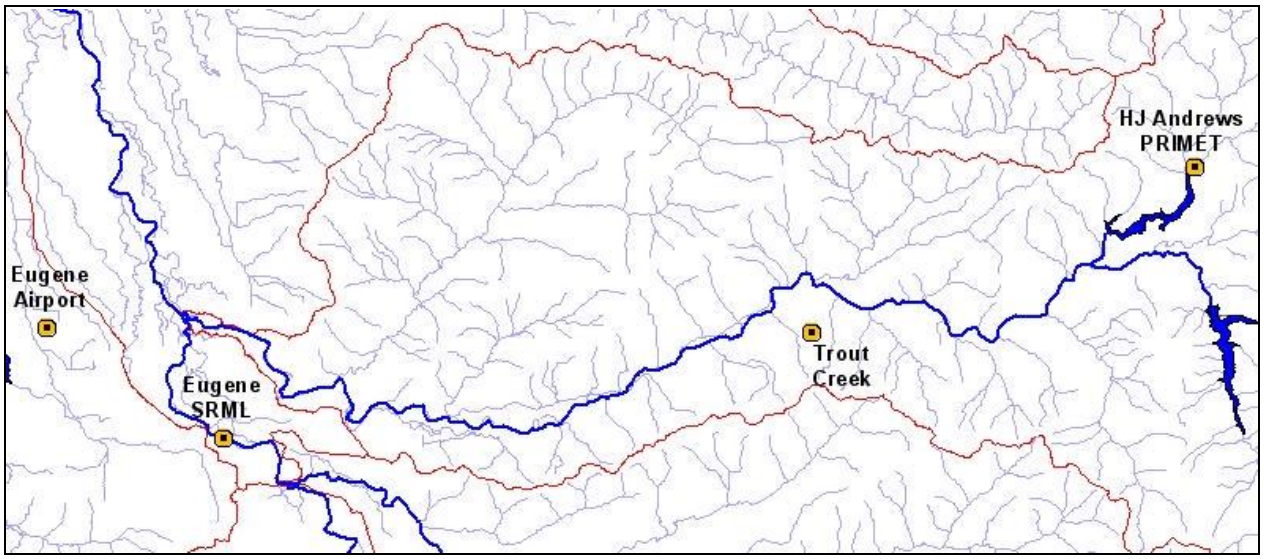


**Figure 543. McKenzie River model meteorological monitoring site locations**

**Table 58. McKenzie River model meteorological monitoring sites**

| Site | Agency (Program) | Meteorological Parameters |
|---|---|---|
| Trout Creek | Oregon Department of Forestry (RAWS) | Air Temperature, Relative Humidity, Wind Speed, Wind Direction |
| Eugene WSO Airport / Mahlon Sweet | National Weather Service (METAR) | Air Temperature, Dew Point Temperature, Relative Humidity, Wind Speed, Wind Direction, Cloud |

| Site | Agency (Program) | Meteorological Parameters |
|---|---|---|
| | | Cover |
| Eugene, OR | University of Oregon, Solar Radiation Monitoring Lab | Solar Radiation |
| H.J. Andrews Research Forest | Oregon State University | Air Temperature, Relative Humidity, Wind Speed, Wind Direction, Solar Radiation |

## H. J. Andrews Experimental Forest

The H. J. Andrews Experimental Forest is administered cooperatively by the U.S. Forest Service's Pacific Northwest Research Station, Oregon State University, and the Willamette National Forest. The forest serves as a long term ecological research forest which includes a long term meteorological station, the Primary Meteorological Station, (McKee, 2003). Meteorological data for 2001 was supplied by ODEQ and obtained from H.J. Andrews Experimental Forest's Primary Meteorological Station. Meteorological data for 2002 was obtained directly from Don Henshaw, Andrews Forest Long-Term Ecological Research Information Manager at the U.S. Forest Service Pacific Northwest Research Station. The data consists of air temperature, relative humidity, wind speed and direction and solar radiation recorded at a frequency of either 15 minutes or hourly.

### Year 2001

The long term meteorological station, Primary Meteorological Station (PRIMET) recorded air temperature as shown in Figure 544. The air temperature data were used with the relative humidity data to calculate the dew point temperature (Singh, 1992). Figure 545 shows a time series of the calculated dew point temperature. Figure 546 shows the wind speed data recorded and Figure 547 shows a rose diagram of the wind direction. The wind speed data show that the minimum wind speed measurement threshold was about 0.1 m/s. The typical wind speed recorded at the PRIMET site (0.5 to 1.0 m/s) was much lower than for many of the Willamette River Basin meteorological stations (2 to 5 m/s). The dominant wind direction was aligned along the NE/SW axis. The gage associates a value of zero with wind speed of zero, and results in the bias seen in the wind direction rose diagram. There were no cloud cover data recorded at the H. J. Andrews meteorological site, so cloud cover data were taken from the nearest site which was the Eugene Airport. Figure 358 shows the cloud cover at the Eugene Airport in 2001. Figure 548 shows the global solar radiation recorded at the Primary Meteorological Station in H. J. Andrews.

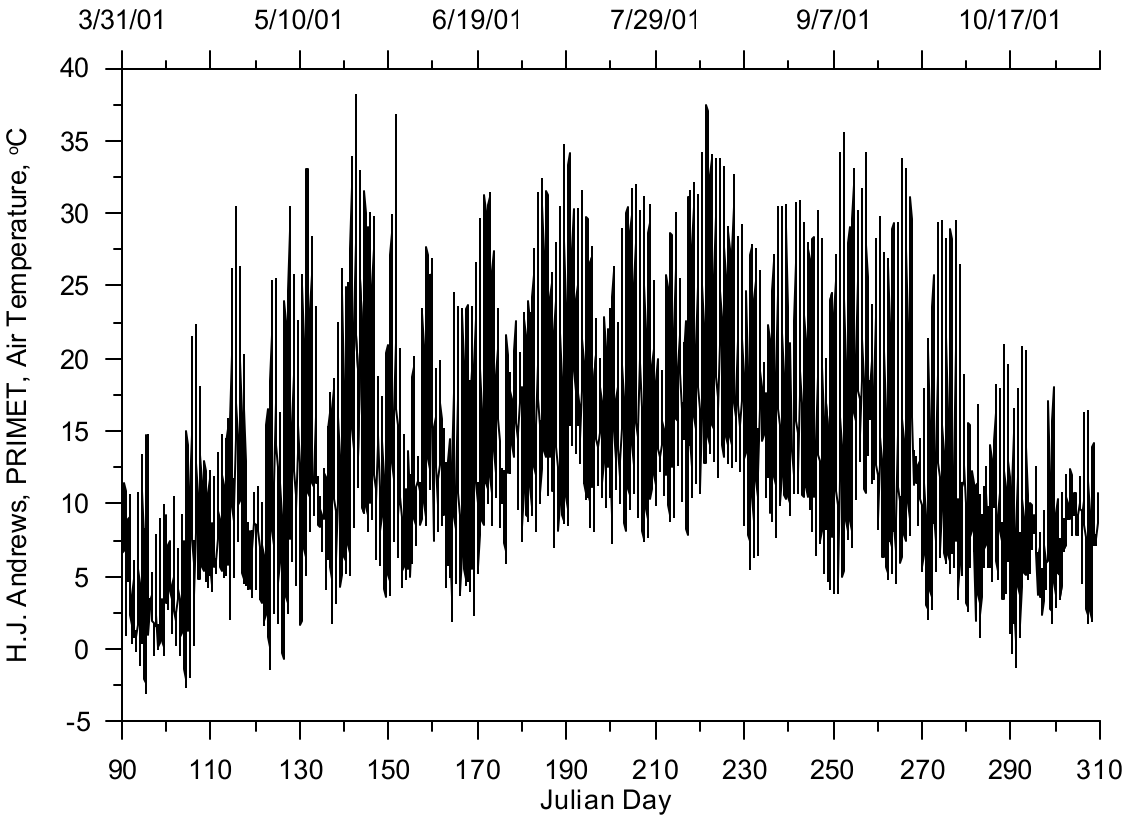


**Figure 544. Air temperature at H. J. Andrews, 2001**

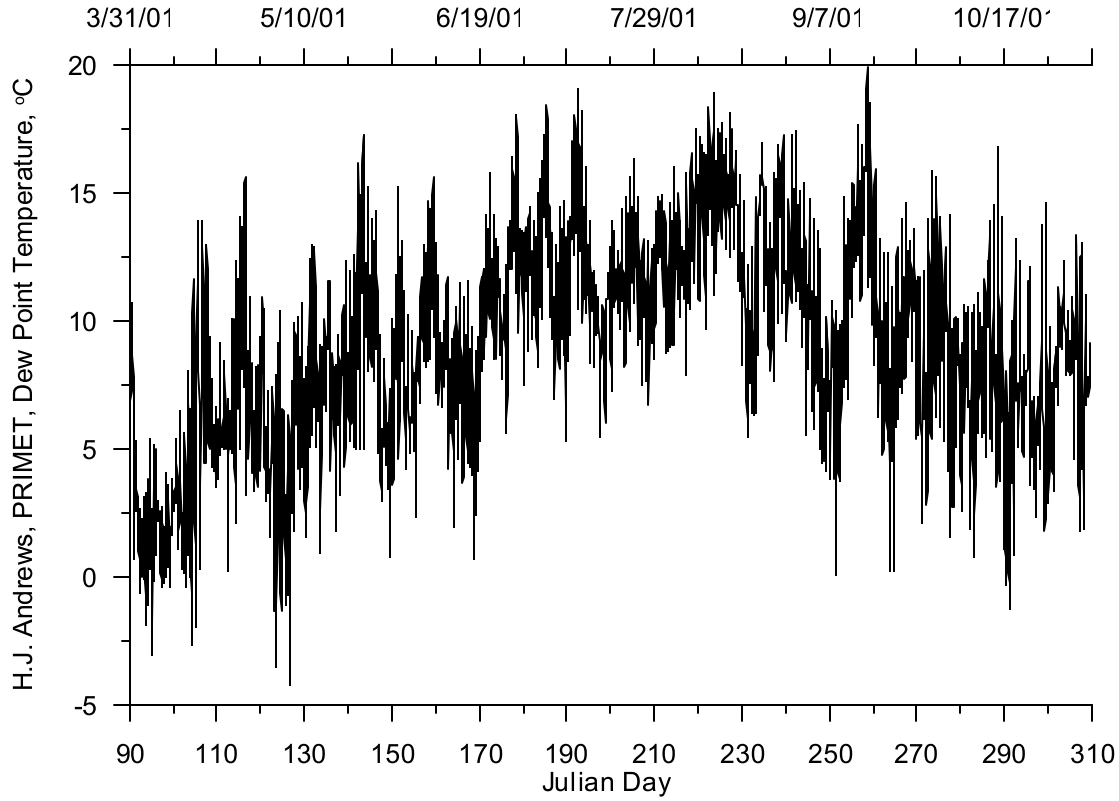


**Figure 545. Dew point temperature at H. J. Andrews, 2001**

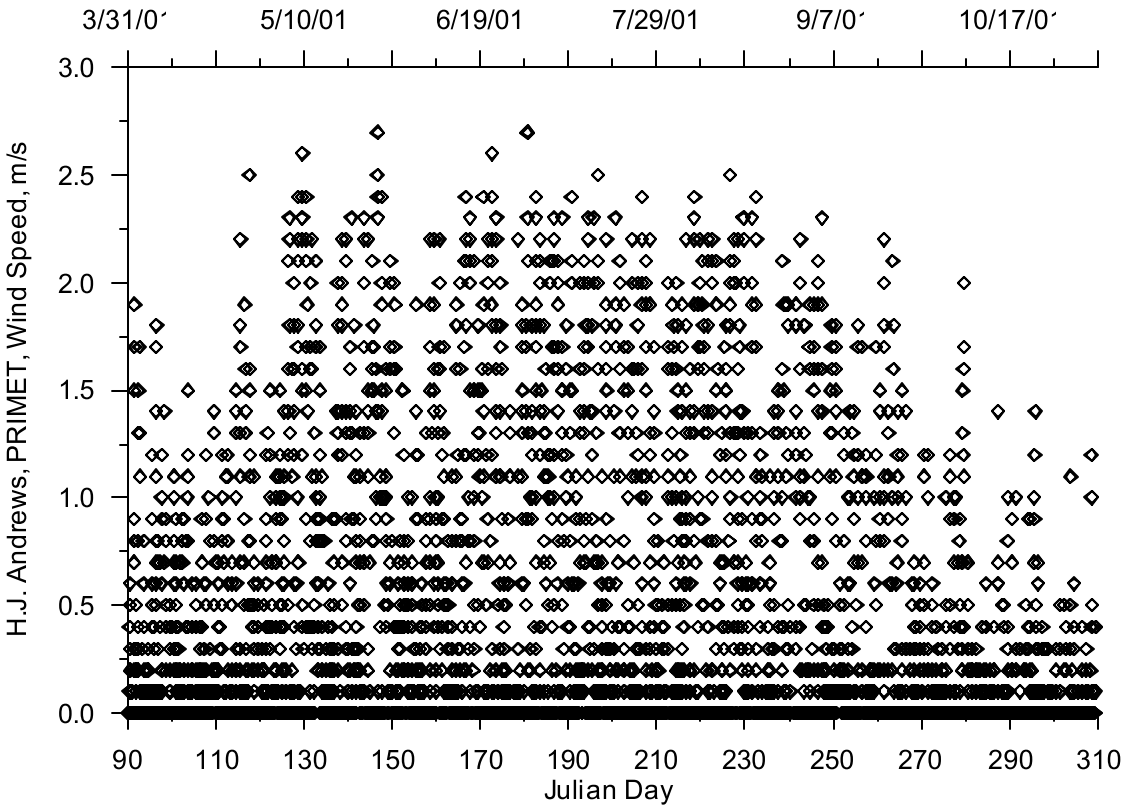


**Figure 546. Wind speed at H. J. Andrews, 2001**

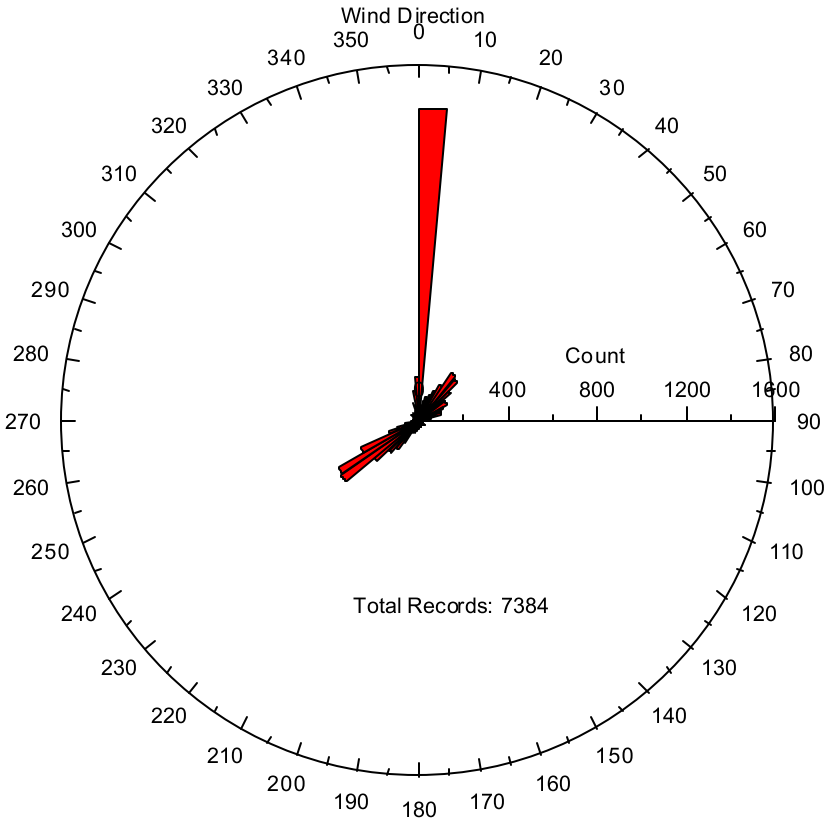


**Figure 547. Wind direction at H. J. Andrews, 2001**

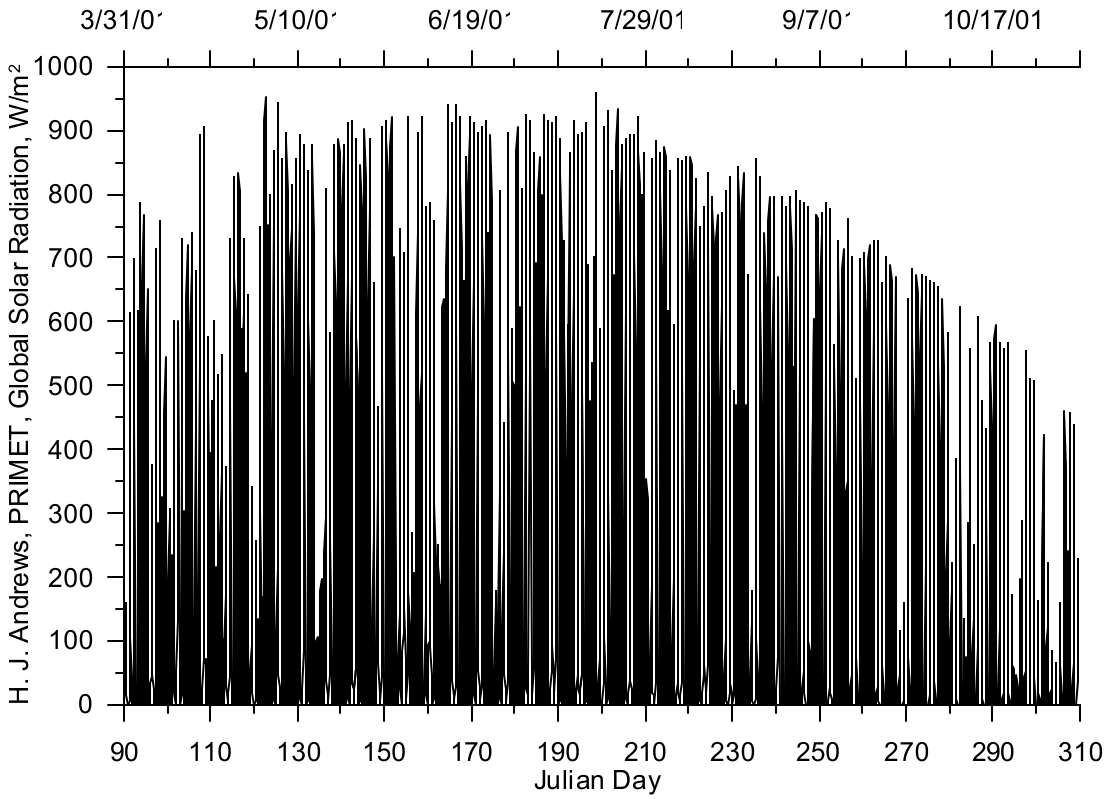


**Figure 548. Global solar radiation at H. J. Andrews, 2001**

## Year 2002

The air temperature monitored at the Primary Meteorological Station (PRIMET) is shown in Figure 549. The air temperature was used with the relative humidity data to calculate the dew point temperature using the equation Singh (1992) which was introduced earlier. Figure 550 shows a time series of the calculated dew point temperature. Figure 551 shows the wind speed data recorded and Figure 552 shows a rose diagram of the wind direction. The wind speed data show that the minimum wind speed measurement threshold was about 0.1 m/s. The typical wind speed recorded at the PRIMET site (0.5 to 1.0 m/s) was much lower than for many of the Willamette River Basin meteorological stations (2 to 5 m/s). The dominant wind direction was aligned along the NE/SW axis. The gage associates a value of zero with wind speed of zero, and results in the bias seen in the wind direction rose diagram. There were no cloud cover data recorded at the H. J. Andrews meteorological site so cloud cover data were taken from the nearest site which was the Eugene Airport. Figure 364 shows the cloud cover at the Eugene Airport in 2002. Figure 553 shows the global solar radiation recorded at the Primary Meteorological Station in H. J. Andrews.

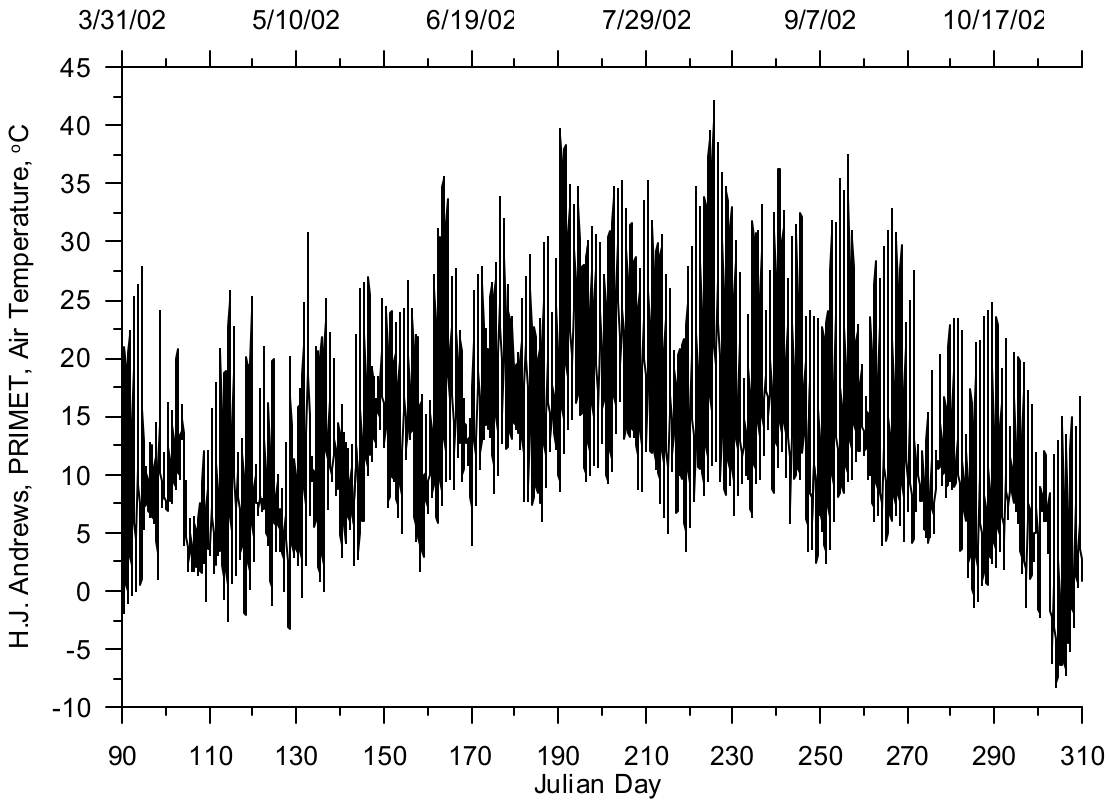


**Figure 549. Air temperature at H. J. Andrews, 2002**

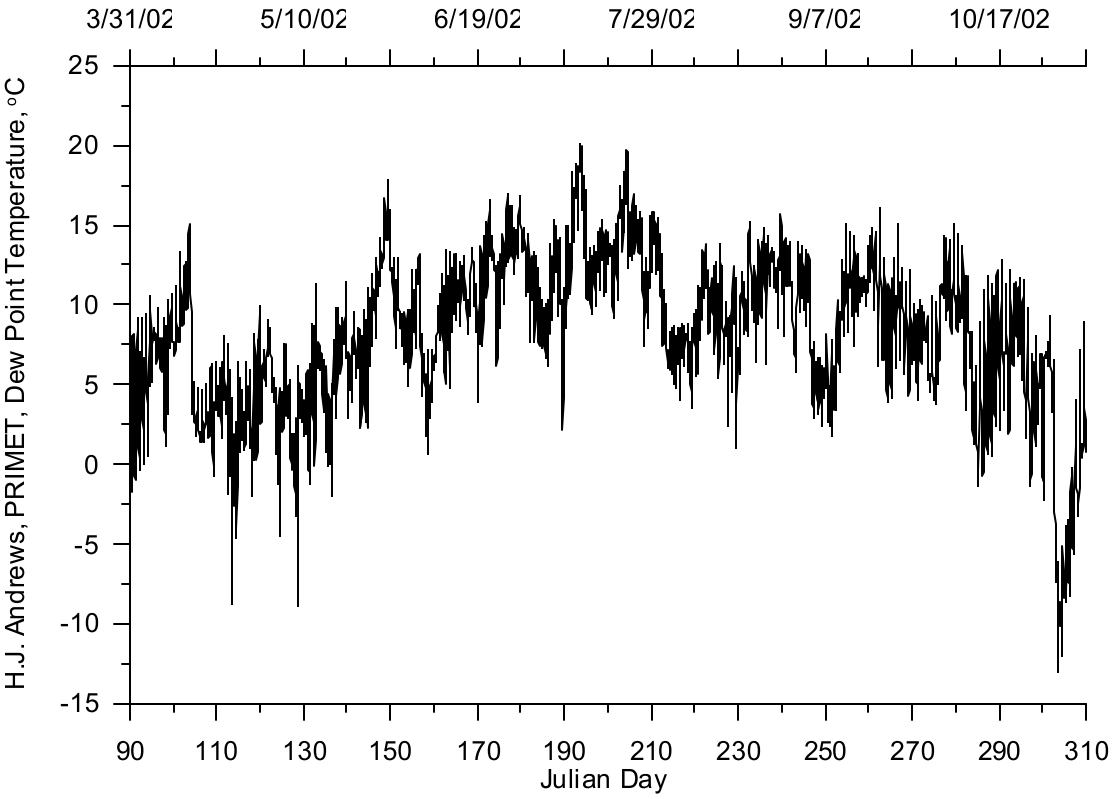


**Figure 550. Dew point temperature at H. J. Andrews, 2002**

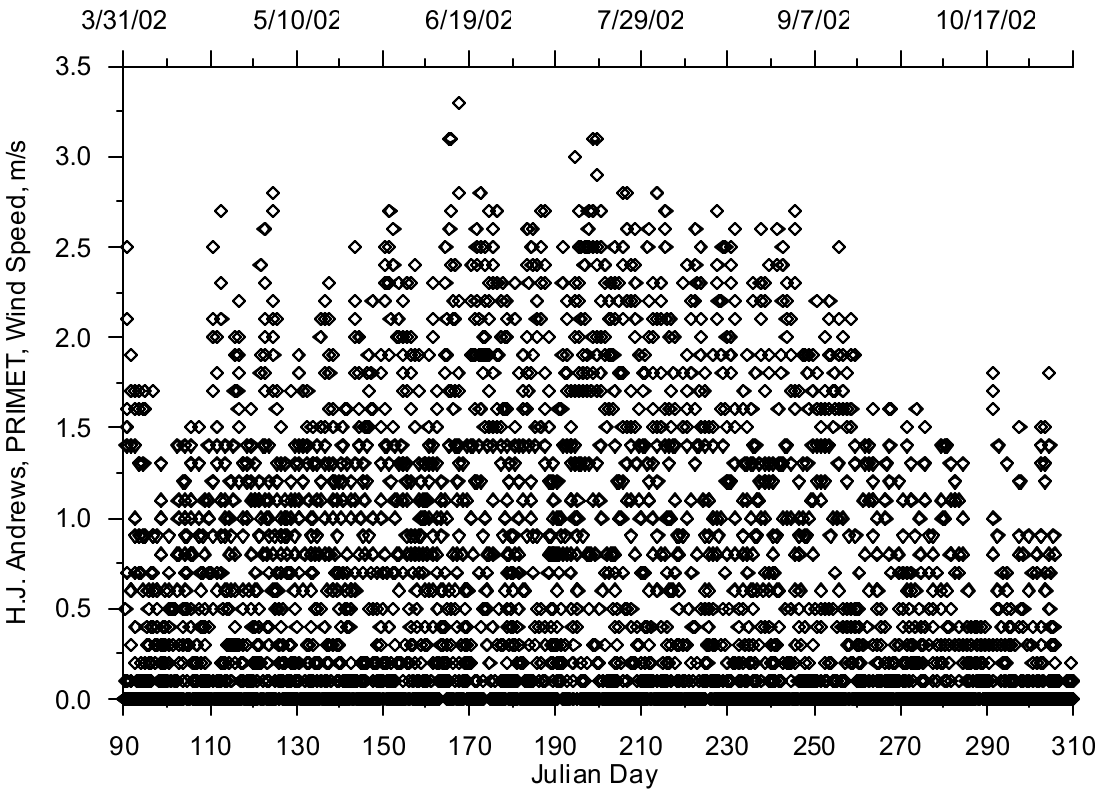


**Figure 551. Wind speed at H. J. Andrews, 2002**

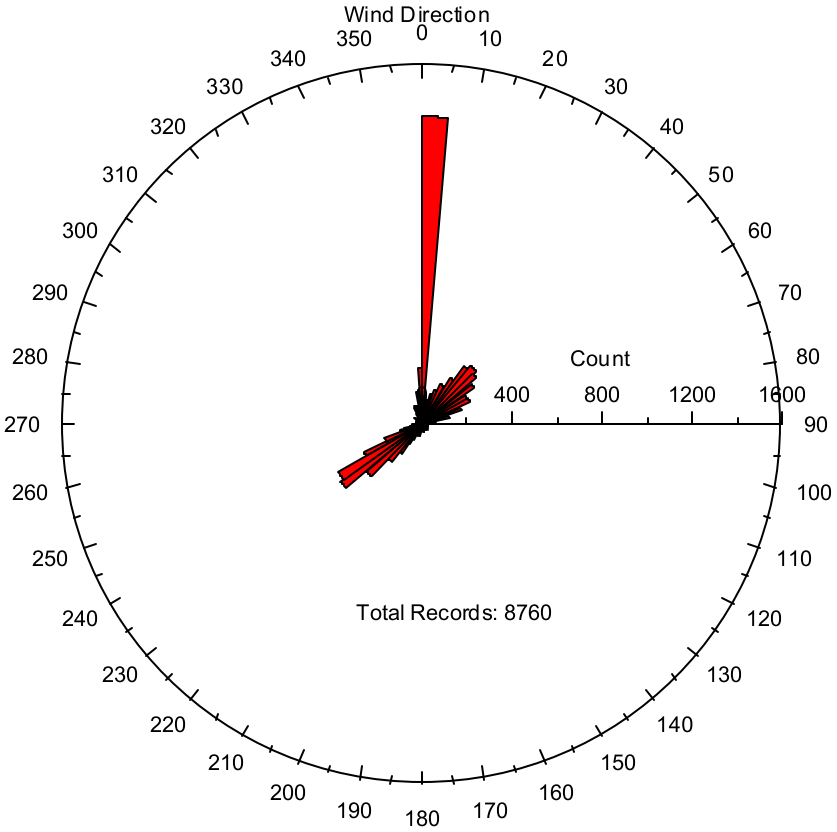


**Figure 552. Wind direction at H. J. Andrews, 2002**

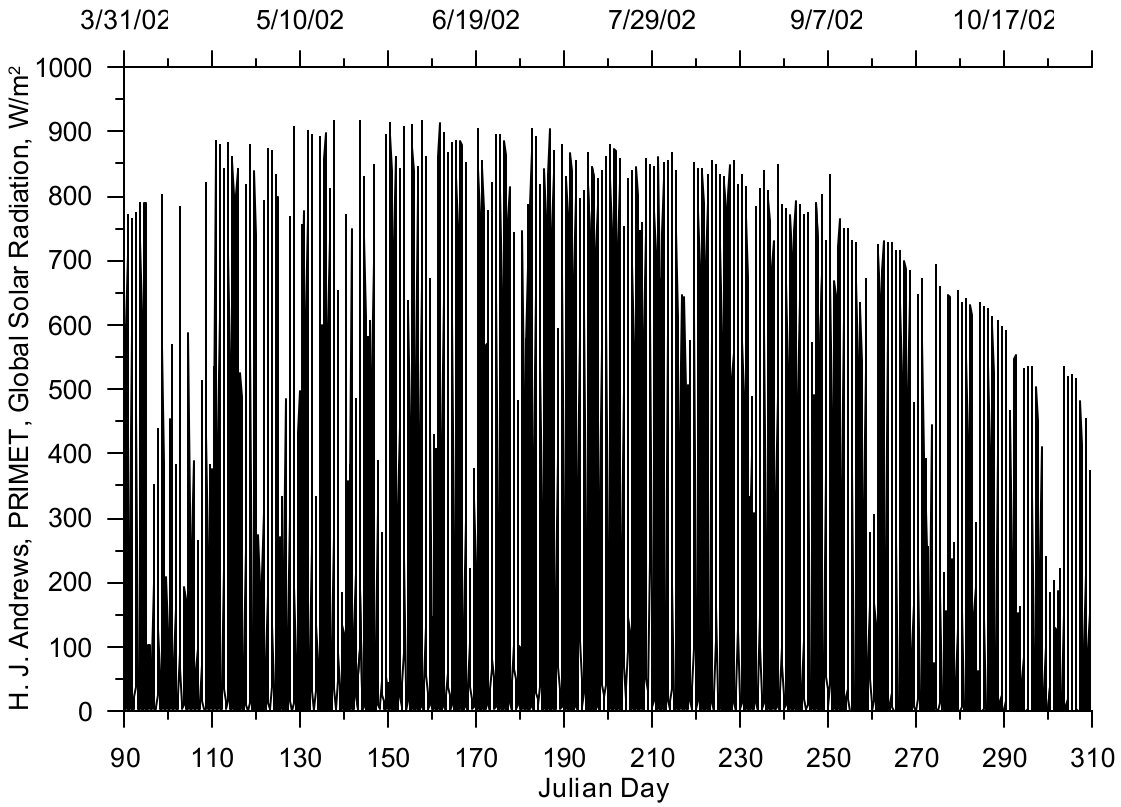


**Figure 553. Global solar radiation at H. J. Andrews, 2002**

## Trout Creek

The Trout Creek site is monitored by Oregon Department of Forestry as part of their forest fire monitoring network. The meteorological data will be used for Middle Fork Willamette River and Fall Creek. The site monitored air temperature, relative humidity, wind speed and wind direction. Cloud cover data were used from the Eugene Airport and the solar radiation data (global radiation) were obtained from the H.J. Andrews Experimental Research Forest. The air temperature and relative humidity were used to calculate the dew point temperature using the equation from Singh, 1992.

### Year 2001

The meteorological data record was complete from April 1, 2001 to October 31, 2001 with hourly values. Figure 554 shows the air temperature monitored at the Trout Creek site for 2001. Figure 555 shows the calculated dew point temperature using the air temperature and relative humidity. Figure 556 shows the wind speed data monitored during 2001. The data shows a seasonal trend with lower wind speed during the summer and higher wind speeds in the spring and fall. Figure 557 shows a wind rose diagram and reveals that the predominant wind directions are 60 to 80 degrees and 260 to 280 degrees. Figure 558 shows the cloud cover used and represents the cloud cover data monitored at the Eugene Airport since no cloud cover data were monitored at the Trout Creek site. The plot shows the coarseness of the cloud cover data recorded at the airport with only about five different cloud cover designations. The data points between the five values were the result of interpolations to fill data gaps in the cloud cover data. Figure 559 shows the global solar radiation from the H.J. Andrews Experimental Research Forest. These data were used since no solar radiation data were monitored at the Trout Creek site and better represented the solar conditions at the site over solar radiation data monitored in Eugene, OR.

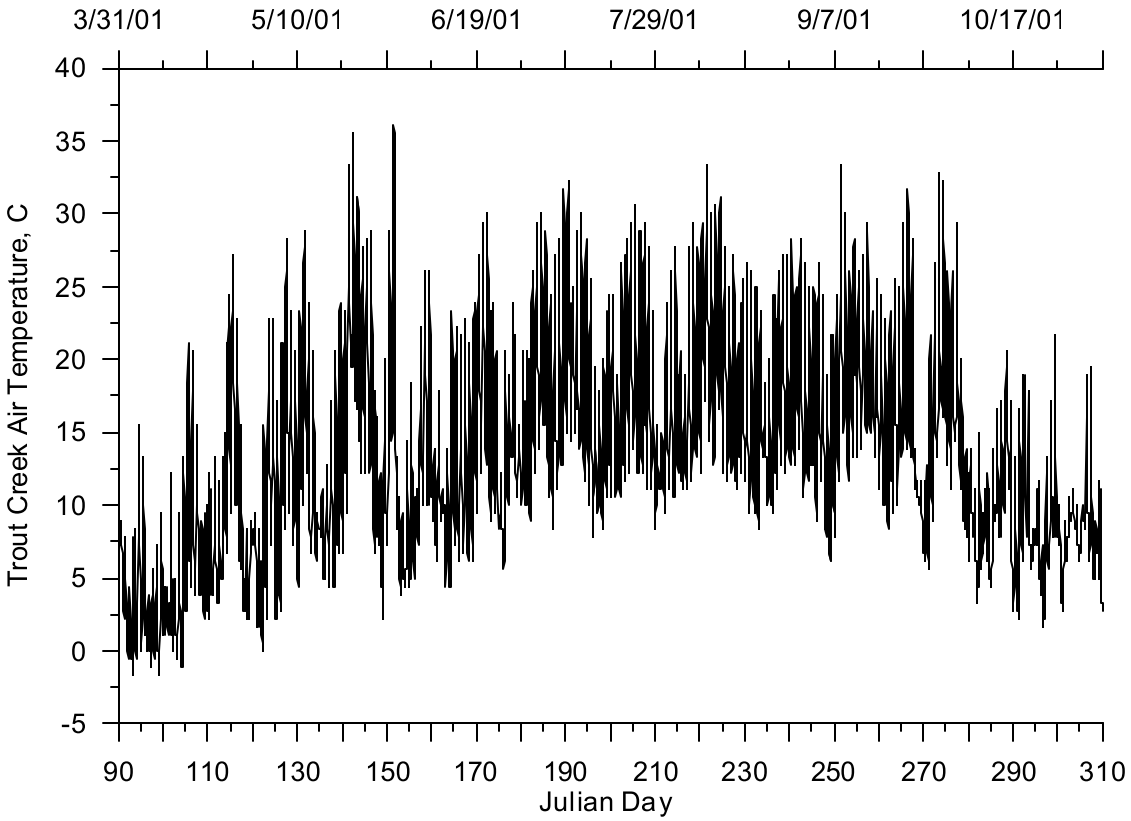


**Figure 554. Air temperature at Trout Creek, 2001**

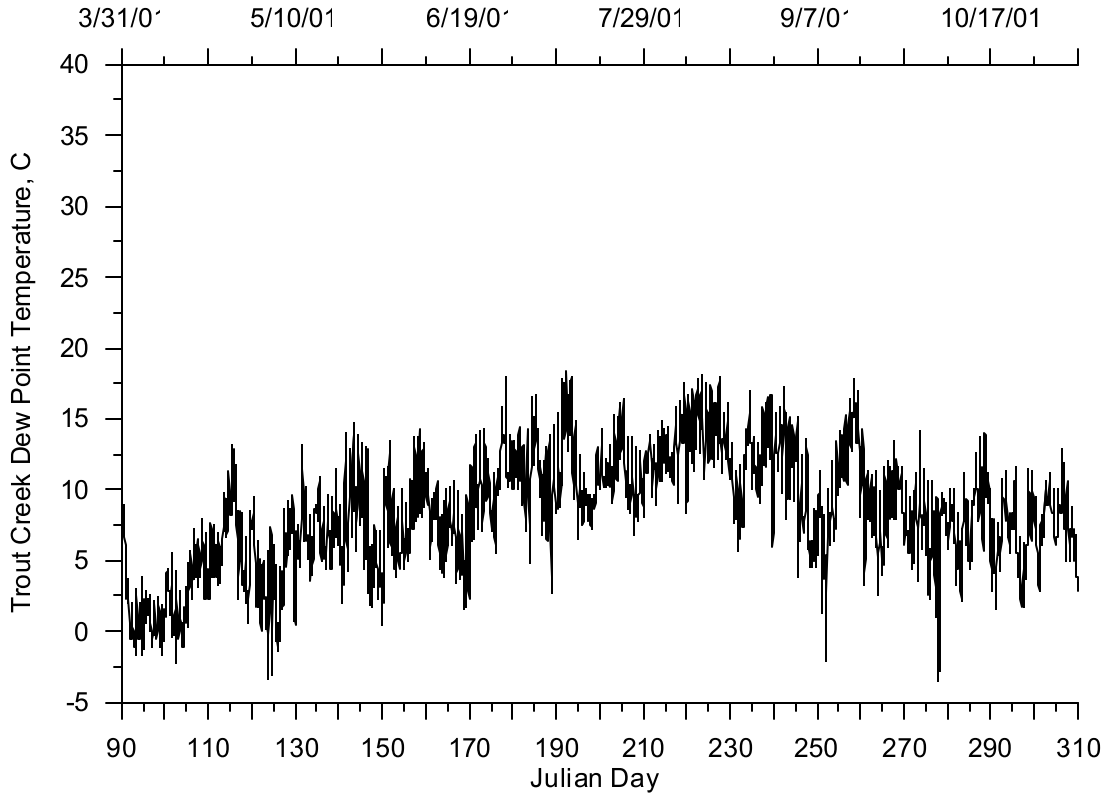


**Figure 555. Dew point temperature Trout Creek, 2001**

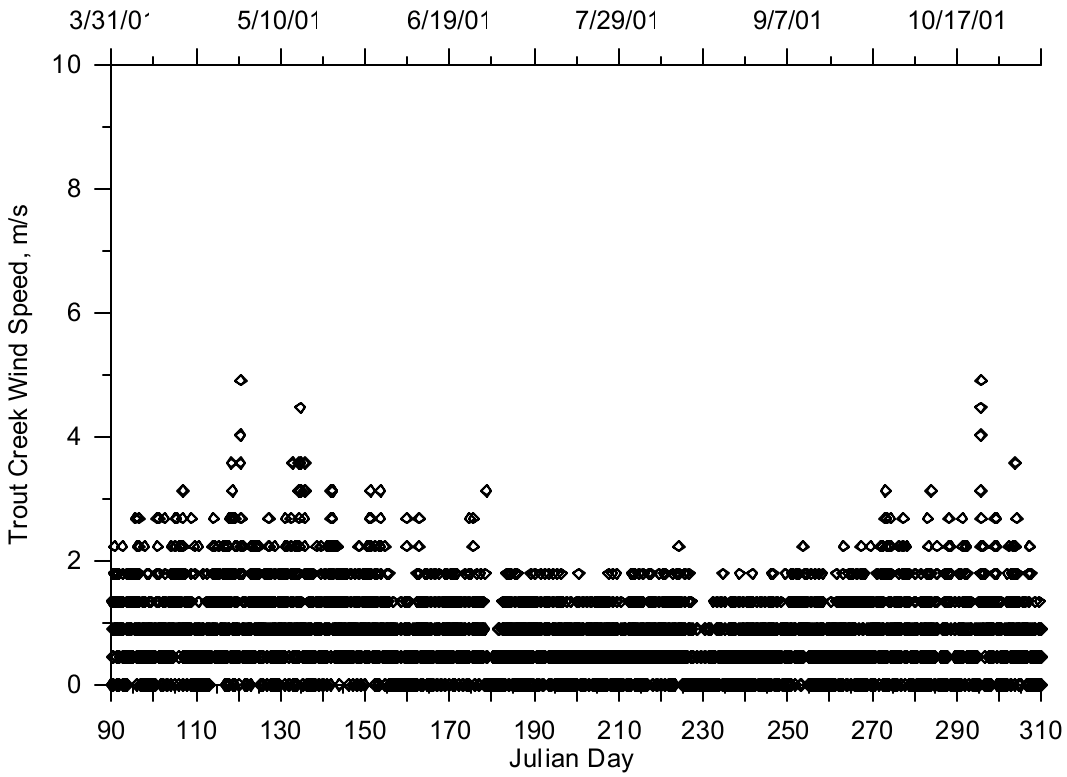


**Figure 556. Wind speed at Trout Creek, 2001**

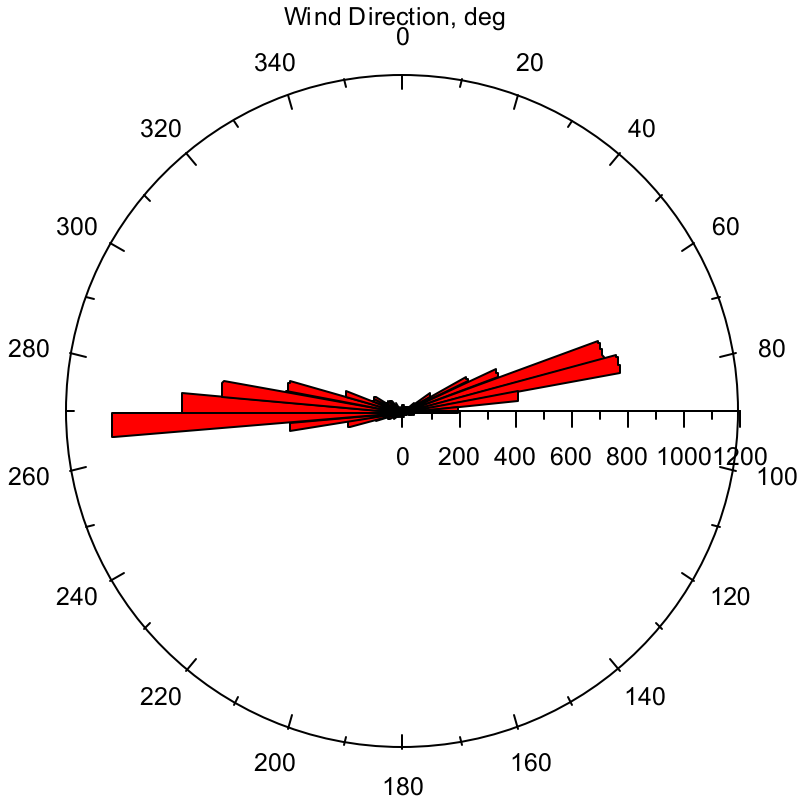


**Figure 557. Wind direction at Trout Creek, 2001**

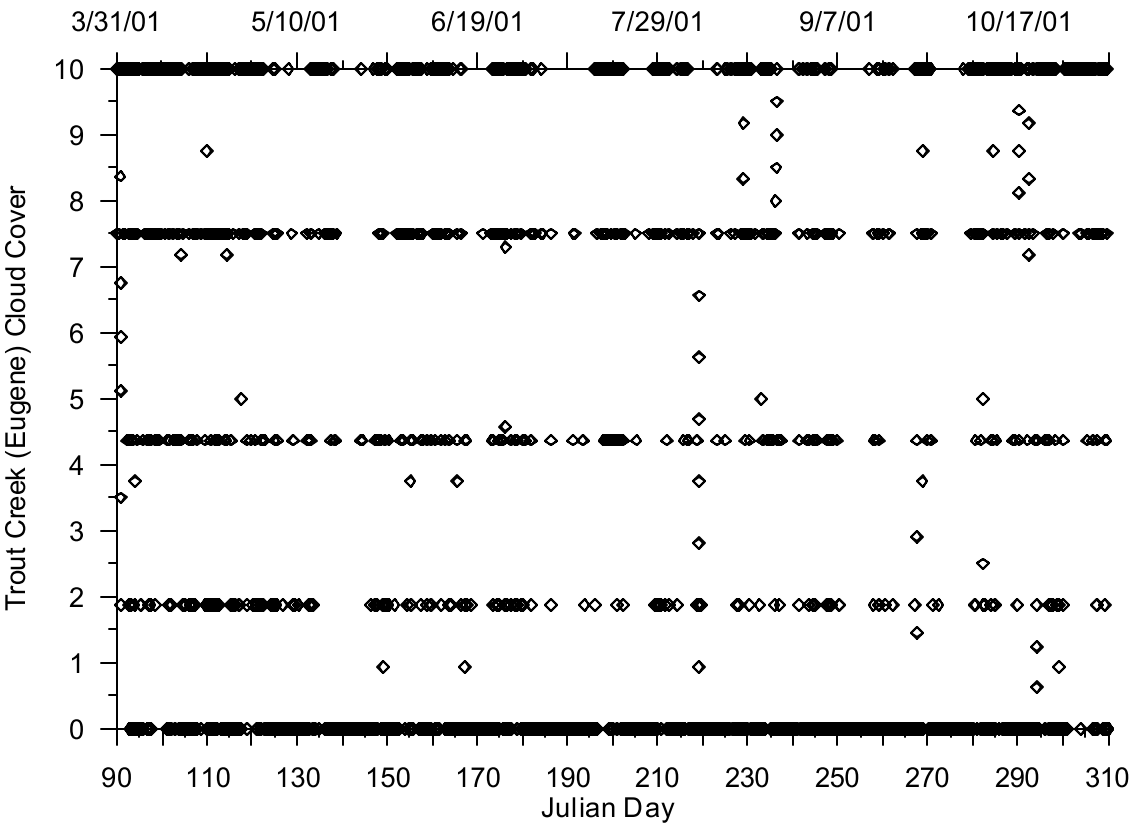


**Figure 558. Cloud cover at Eugene Airport, 2001**

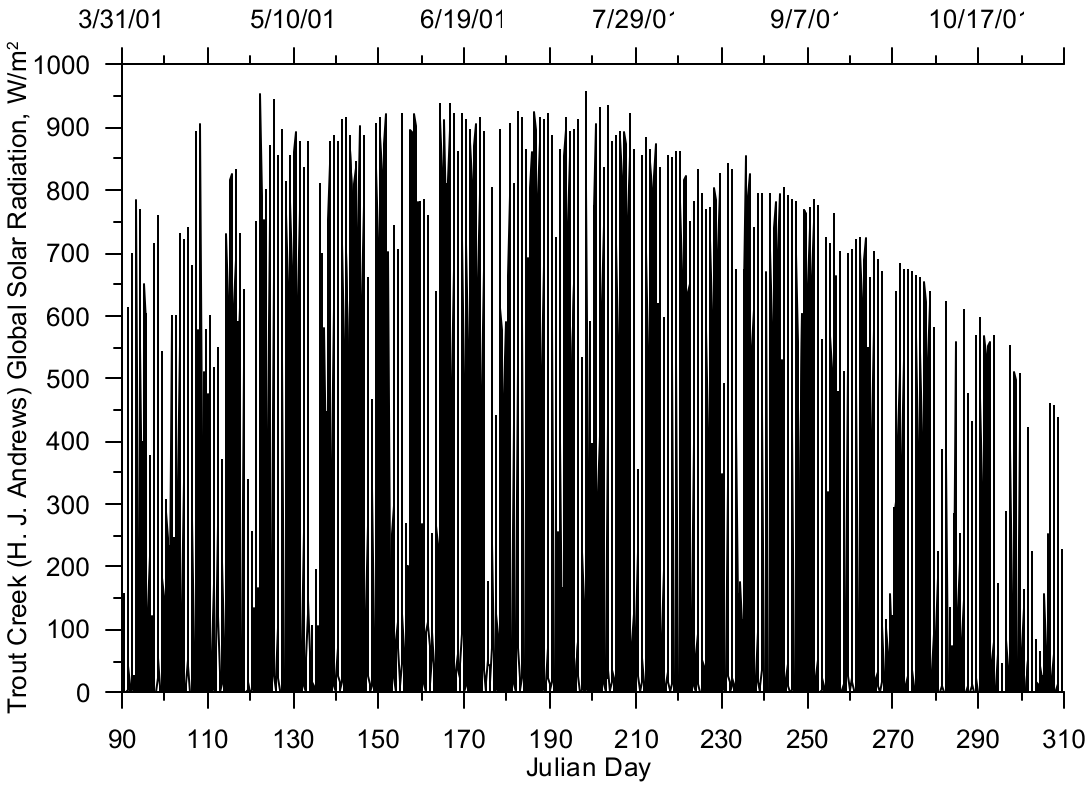


**Figure 559. Global solar radiation at H. J. Andrews, 2001**

Year 2002

The meteorological data record was complete from April 1, 2002 to October 31, 2002 with hourly values. Figure 560 shows the air temperature monitored at the Trout Creek site for 2002. Figure 561 shows the calculated dew point temperature using the air temperature and relative humidity. Figure 562 shows the wind speed data monitored during 2001. The data shows no seasonal trend in wind speeds which was different than data monitored in 2001. The values between the instrument recording values were interpolations used to fill data gaps. Figure 563 shows a rose diagram of the wind direction and reveals that the predominant wind directions were 60 to 80 degrees and 260 to 280 degrees, which was similar to the data in 2001. Figure 564 shows the cloud cover used and represents the cloud cover data monitored at the Eugene Airport since no cloud cover data were monitored at the Trout Creek site. The plot shows the coarseness of the cloud cover data recorded at the airport with only about five different cloud cover designations. The data points between the five values were the result of interpolations to fill data gaps in the cloud cover data. Figure 565 shows the global solar radiation from the H.J. Andrews Experimental Research Forest used since no solar radiation data were monitored at the Trout Creek site.

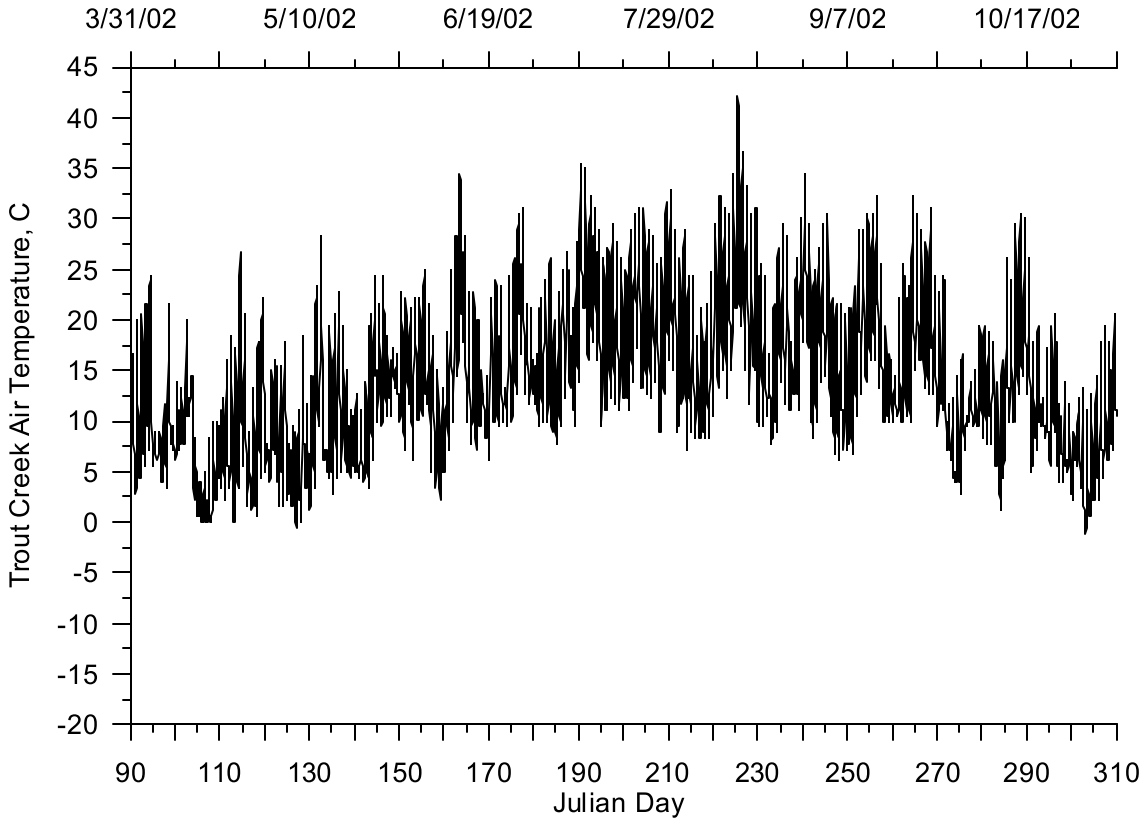


**Figure 560. Air temperature at Trout Creek, 2002**

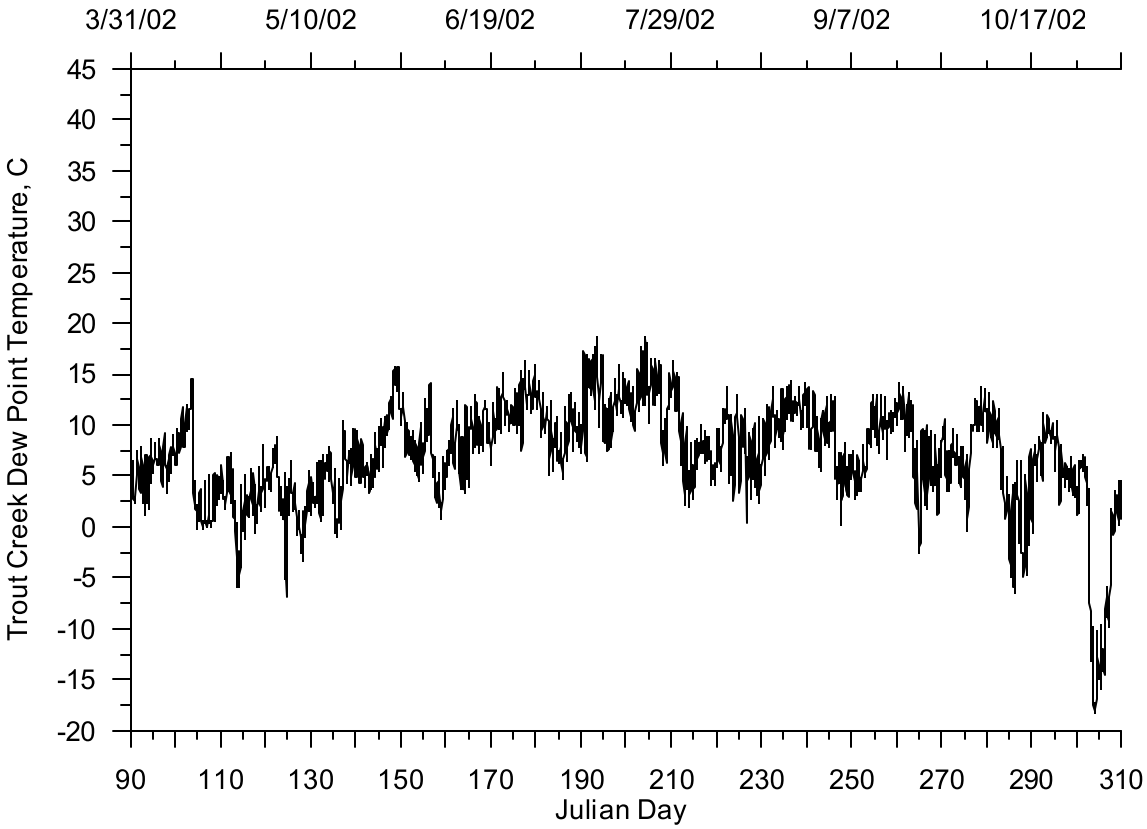


**Figure 561. Dew point temperature at Trout Creek, 2002**

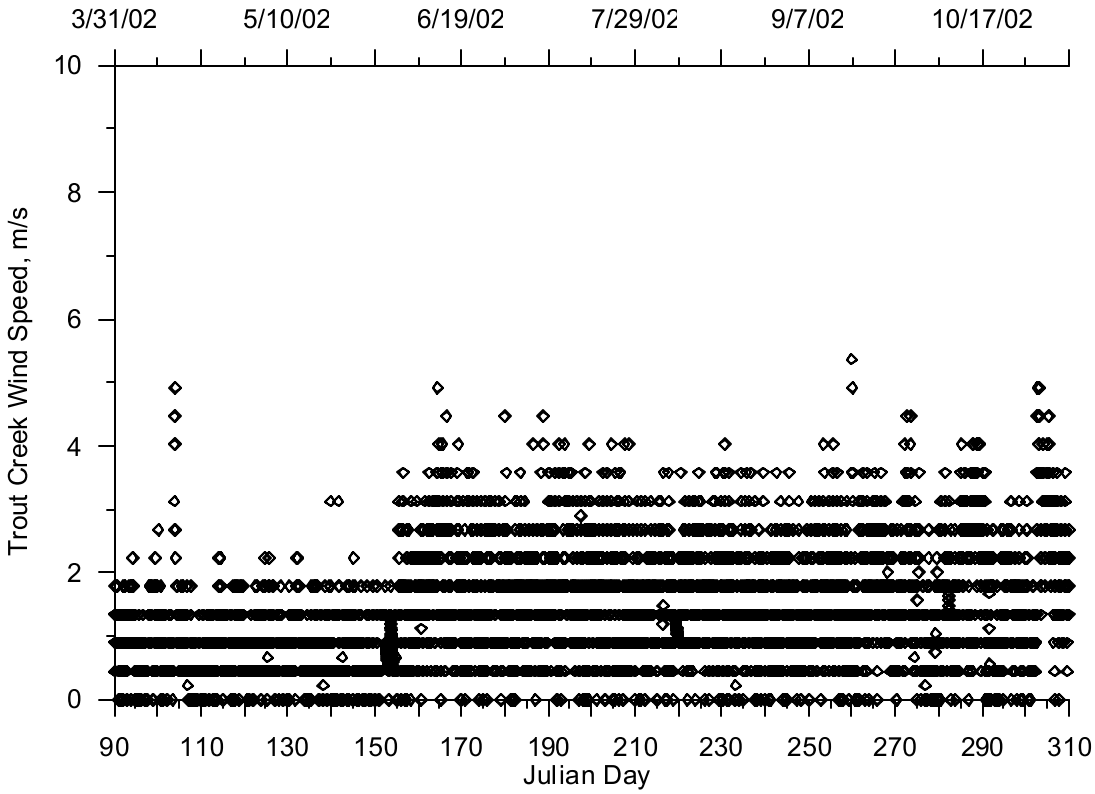


**Figure 562. Wind speed at Trout Creek, 2002**

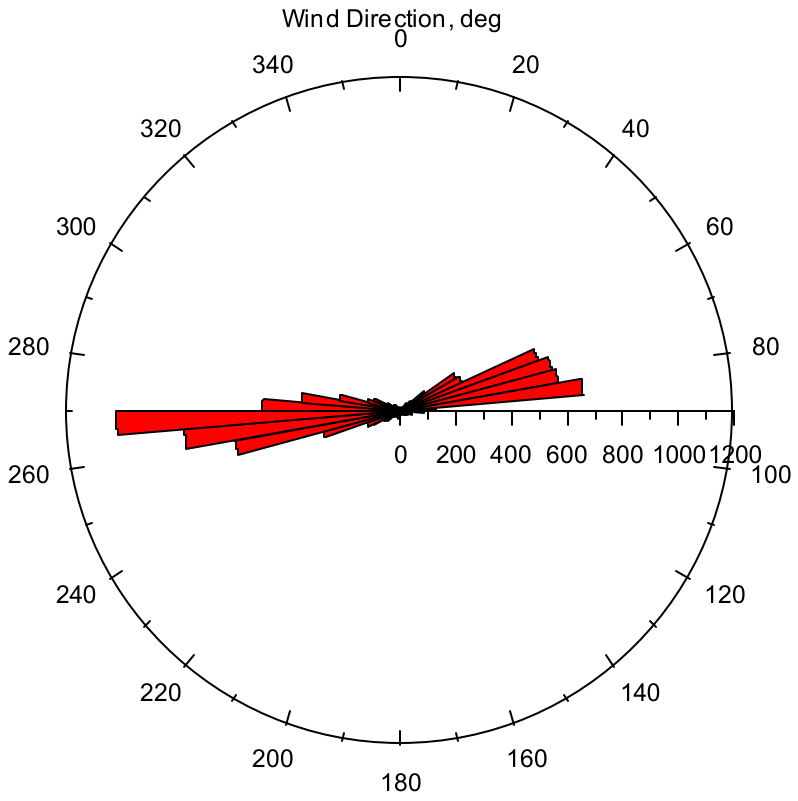


**Figure 563. Wind direction at Trout Creek, 2002**

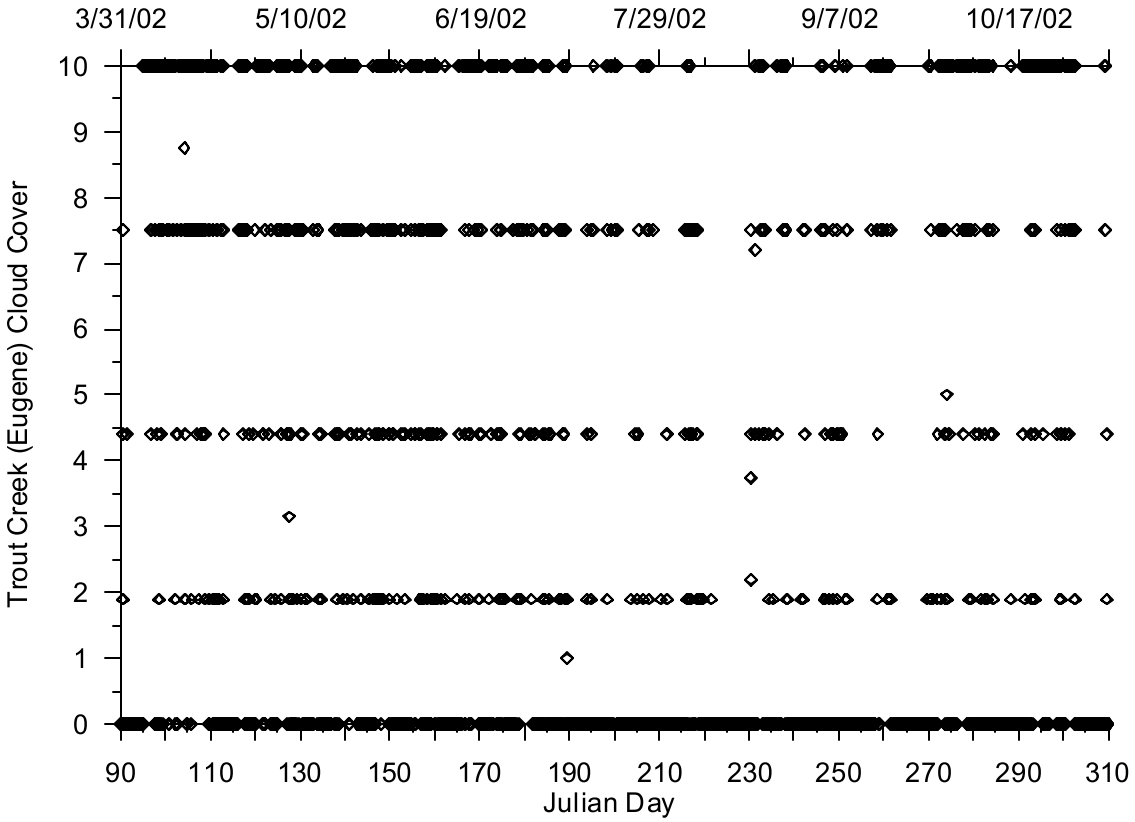


**Figure 564. Cloud cover at Eugene Airport, 2002**

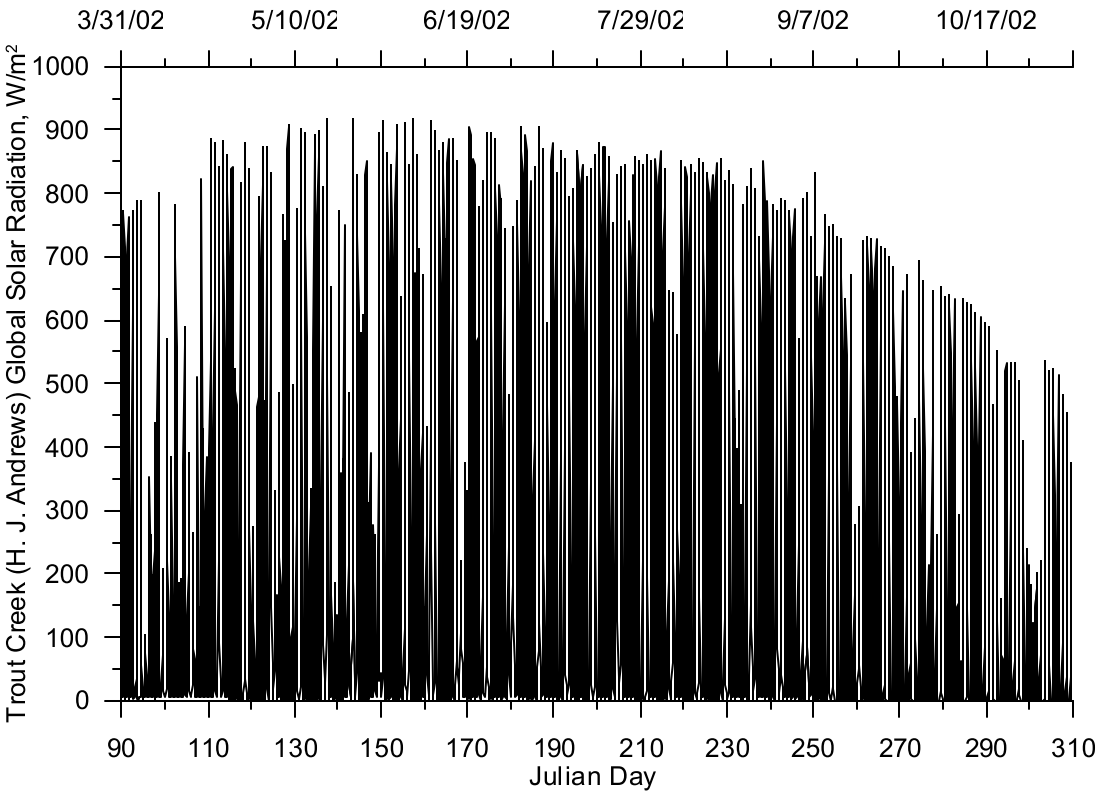


**Figure 565. Global solar radiation at H. J. Andrews, 2002**

## Eugene Airport

### Year 2001

The meteorological data recorded at the Eugene WSO / Mahlon Sweet Airport which were used for the Upper Willamette River model were also used in the lower reaches of the McKenzie River model. The Eugene Airport records air and dew point temperature, wind speed and direction, and cloud cover data but no solar radiation data.

Figure 354 and Figure 355 show the air and dew point temperature respectively, over the period of April to October 2001. Figure 356 and Figure 357 show the wind speed and direction, respectively. Figure 356 indicates the minimum wind speed-recording threshold was about 1.5 m/s. The rose diagram in Figure 357 is dominated by the value of zero which is associated with wind speeds below the reading threshold. Figure 358 shows the coarseness of the cloud cover data recorded at the airport with only about five different cloud cover designations. The data points between the five values were the result of interpolations to fill data gaps in the cloud cover data. The solar radiation data collected at the SRML site are shown in Figure 359.

### Year 2002

The meteorological data recorded at the Eugene WSO / Mahlon Sweet Airport which were used for the Upper Willamette River model were also used in the lower reaches of the McKenzie River model. The Eugene Airport recorded air and dew point temperature, wind speed and direction, and cloud cover data but no solar radiation data.

The Eugene municipal airport records air and dew point temperature, wind speed and direction and cloud cover, but no solar radiation data. Figure 360 and Figure 361 show the air and dew point temperature respectively, over the period of April to October 2001. Figure 362 and Figure 363 show the wind speed and direction, respectively. Figure 362 indicates the minimum wind speed-recording threshold was about 1.5 m/s. The rose diagram in Figure 363 was dominated by the value of zero which was associated with wind speeds below the reading threshold. Figure 364 shows the coarseness of the cloud cover data recorded at the airport with only about five different cloud cover designations. The data points between the five values were the result of interpolations to fill data gaps in the cloud cover data. The solar radiation data collected at the SRML site are shown in Figure 365.

# Coast Fork / Middle Fork Willamette River

The Coast Fork/ Middle Fork Willamette River model consisted of the Coast Fork Willamette River from RM 38.83 to 0.0, Row River, a tributary of the Coast Fork, from RM 7.54 to 0.0, the Middle Fork Willamette River from RM 16.43 to 0.0, Fall Creek, a tributary of the Middle Fork, from RM 7.03 to 0.0 and the Willamette River from the confluence of the Coast and Middle Forks to approximately the City of Springfield, OR, (RM 186.8 to RM 185.2), which is approximately two miles east of Eugene, OR. Figure 566 shows the model domain including the rivers up to the U.S. Army Corps of Engineers reservoirs.

The 2001 model simulation of the Coast and Middle Forks of the Willamette River was run from April 1 to October 31, 2001. The 2002 model simulation of the Coast and Middle Forks of the Willamette River was run from April 1 to October 31, 2002.

The Middle Fork Willamette River has a drainage area of approximately 3,500 $km^2$. The Coast Fork Willamette River has a drainage area of approximately 1700 $km^2$.

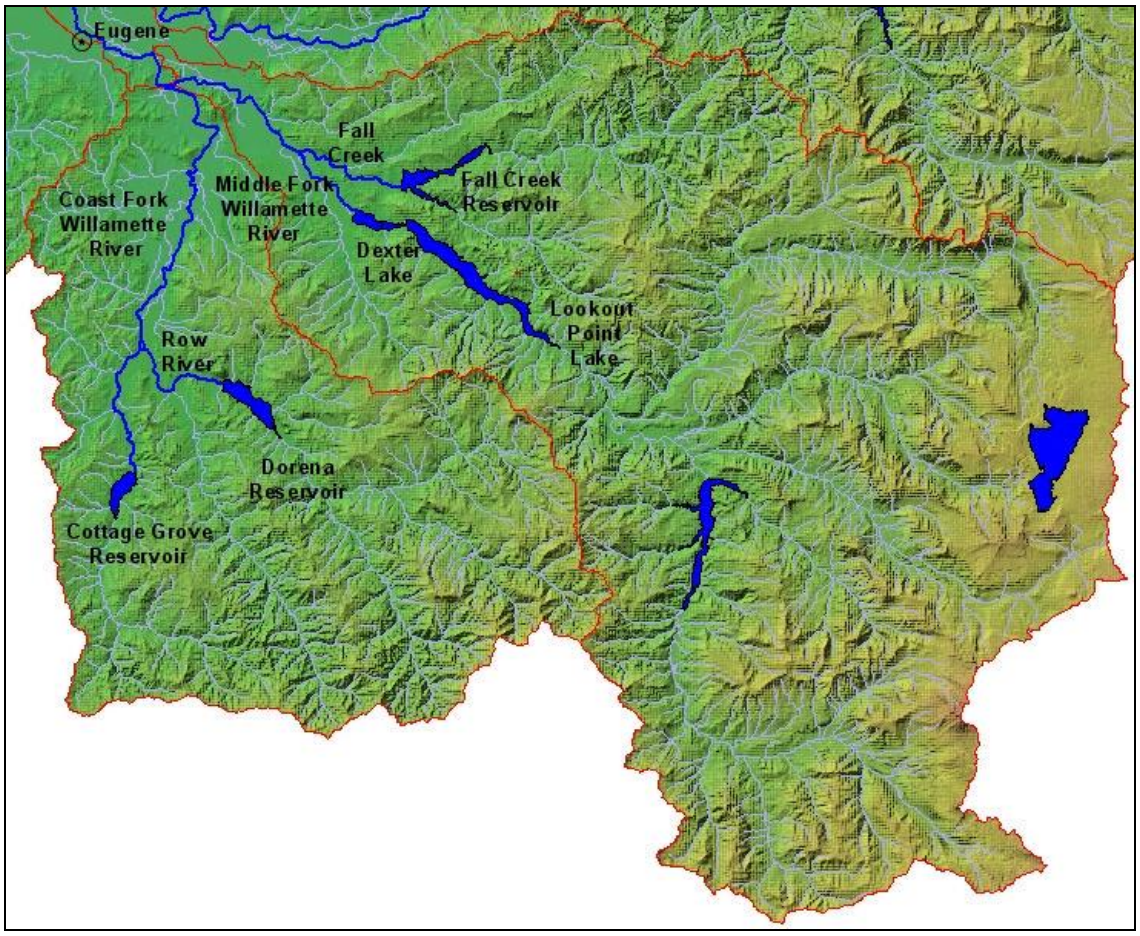


**Figure 566. Coast Fork and Middle Fork Willamette River model region**

## *Model Geometry*

### Bathymetry Data

The Coast Fork and Middle Fork Willamette River model consists of river geometry for four rivers: Coast Fork Willamette River, Middle Fork Willamette River, Row River, and Fall Creek. The data used to generate the model bathymetry were obtained from four USGS surveyed cross sections at gage stations, Digital Elevation Maps (DEM), and GIS data sets from ODEQ. There were two USGS gage stations on the Coast Fork Willamette River and two cross sections on the Middle Fork Willamette River as listed in Table 59. Figure 567 shows the location of the cross sections along the two rivers. Figure 568 shows the cross section data collected at two Coast Fork Willamette River gage stations. Figure 569 shows the cross section data collected at two Middle Fork Willamette River gage stations.

There were no river channel cross section data on Row River and Fall Creek in the Coast and Middle Fork Willamette River model. Cross sections from the Middle Fork Willamette River were used for both Fall Creek and Row River. Table 60 lists the RM locations for modified cross sections on Fall Creek and Row River.

The DEM data had a vertical resolution of 1 m, and a horizontal resolution of 10 m. Elevation data surrounding each of the four rivers were isolated to include the terrain information in the river channel bathymetry.

Additional cross sections were generated at a spacing frequency of 100 feet using the river thalweg point generated from a GIS analysis conducted by ODEQ. Channel widths for the additional cross sections were based on channel widths identified in the GIS analysis conducted by ODEQ. Elevations associated with the additional cross sections were calculated using linear interpolation between the two data cross sections from the USGS gage stations on the Coast Fork and Middle Fork Willamette River and between the two estimated cross sections on Fall Creek and Row River.

On each of the four rivers there were no cross section data upstream and downstream of the two cross sections. Additional cross sections were estimated below the cross section pair on each river by extending the downstream river cross section data downstream and adjusting the cross section width based on the channel width from the ODEQ GIS data and by adjusting the cross section elevation based on the slope of the river from the same GIS data. Additional cross sections were estimated above the cross section pair on each river by extending the upstream river cross section data further upstream. The cross section widths were adjusted based on the channel width from the ODEQ GIS data and the elevations were adjusted based on the slope of the river from the same GIS data.

The calculated cross sections on each river were combined with DEM data representing the terrain on along each river channel into four separate data sets which were analyzed separately in the contour mapping program, SURFER. An average volume-elevation relationship was calculated over the length of each model segment using a one meter vertical resolution for each river.

The bathymetry below the confluence of the Coast Fork and Middle Fork Willamette, approximately 3.0 km (1.87 mi), was originally developed for the Upper Willamette River model at transferred to this model.

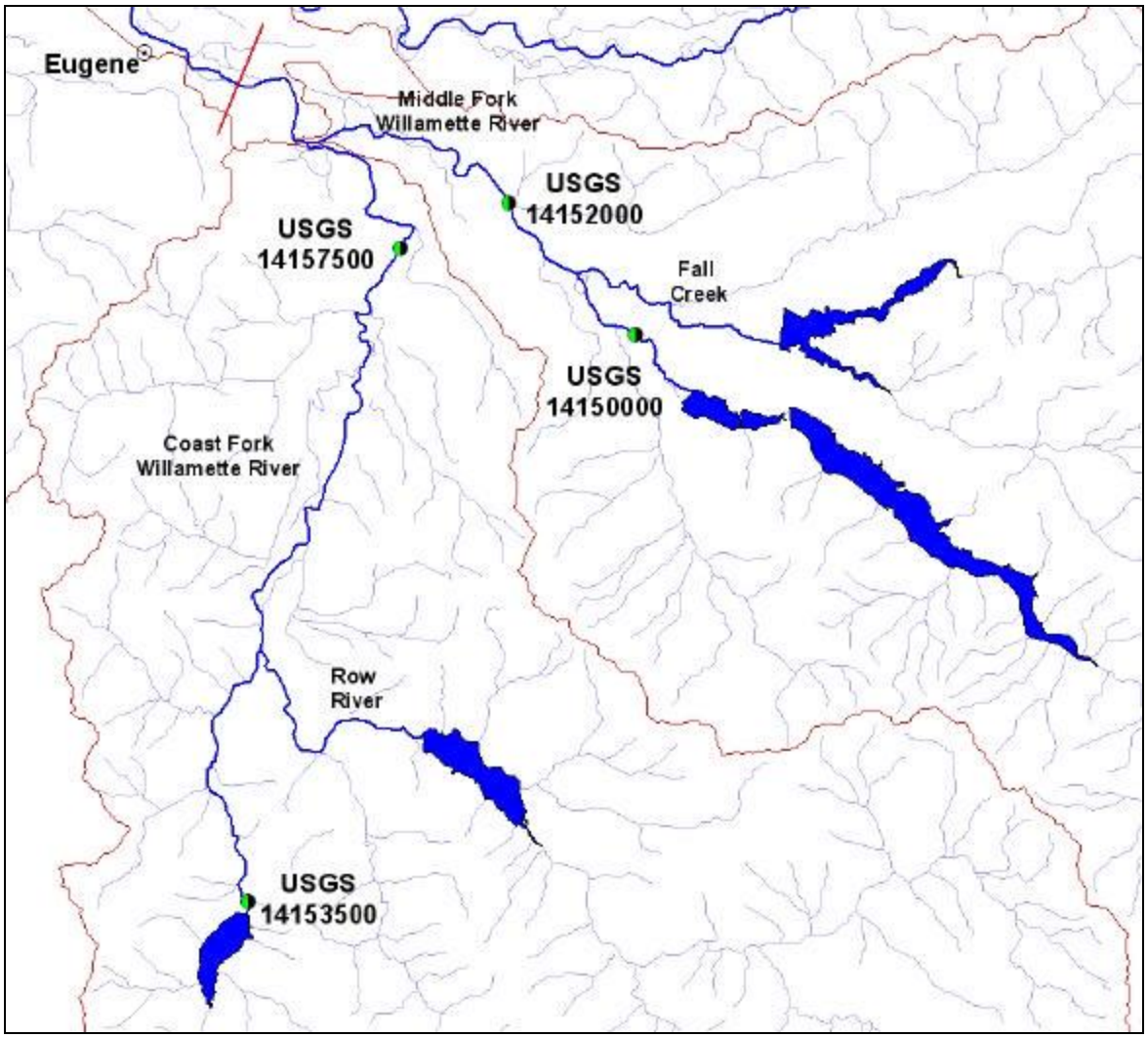


**Figure 567. Coast Fork and Middle Fork Willamette River USGS gage station cross section locations**

**Table 59. Coast Fork and Middle Fork Willamette River USGS gage station cross sections**

| Gage Station | River Mile | Description | River |
|---|---|---|---|
| USGS 14153500 | 28.69 | Coast Fork Willamette River below Cottage Grove Dam | Coast Fork WR |
| USGS 14157500 | 5.72 | Coast Fork Willamette River near Goshen, OR | Coast Fork WR |
| USGS 14150000 | 13.95 | Middle Fork Willamette River near Dexter, OR | Middle Fork WR |
| USGS 14152000 | 8.15 | Middle Fork Willamette River at Jasper, OR | Middle Fork WR |

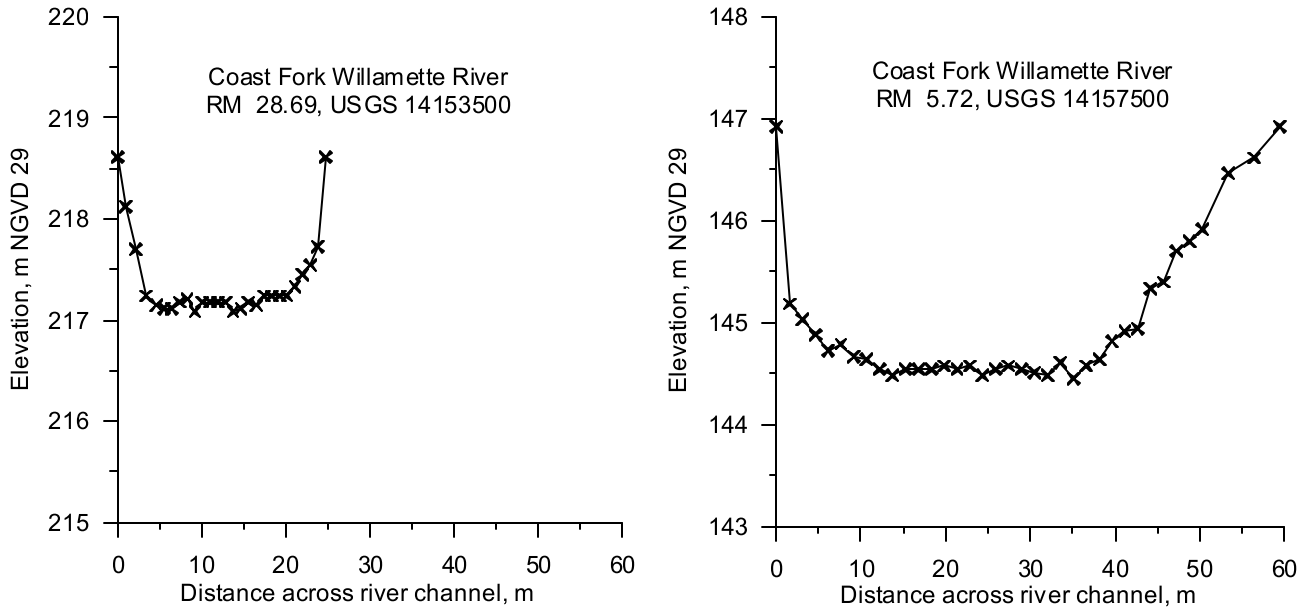


**Figure 568. Coast Fork Willamette River USGS gage station cross sections**

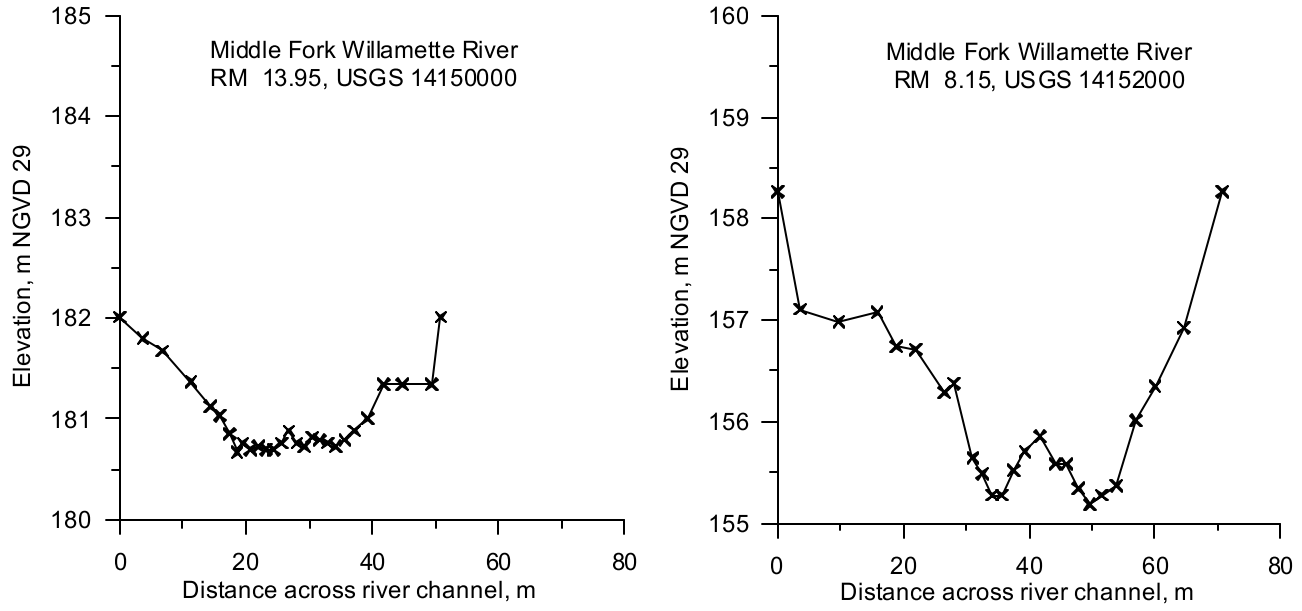


**Figure 569. Middle Fork Willamette River USGS gage station cross sections**

**Table 60. Fall Creek and Row River cross sections**

| River Mile | Description | River |
|---|---|---|
| 3.52 | Downstream cross section based on Middle Fork USGS gage 14152000 | Fall Creek |
| 6.00 | Upstream cross section based on Middle Fork USGS gage 14150000 | Fall Creek |
| 3.71 | Downstream cross section based on Middle Fork USGS gage 14152000 | Row River |
| 6.33 | Upstream cross section based on Middle Fork USGS gage 14150000 | Row River |

## Model Grid Development

The data were combined and the plotting program SURFER was used to create a contour plot of the stream channel. The contour plot was then used to generate the model grid. The model grid consists of five water bodies composed of ten branches. Figure 570 shows a map of the model grid layout. Table 61 lists the model grid characteristics. Model branch 10 (water body 5) was developed from bathymetry data analyzed as part of the Upper Willamette River model and covers the confluence of the Coast and Middle Forks of the Willamette River to the City of Springfield, OR.

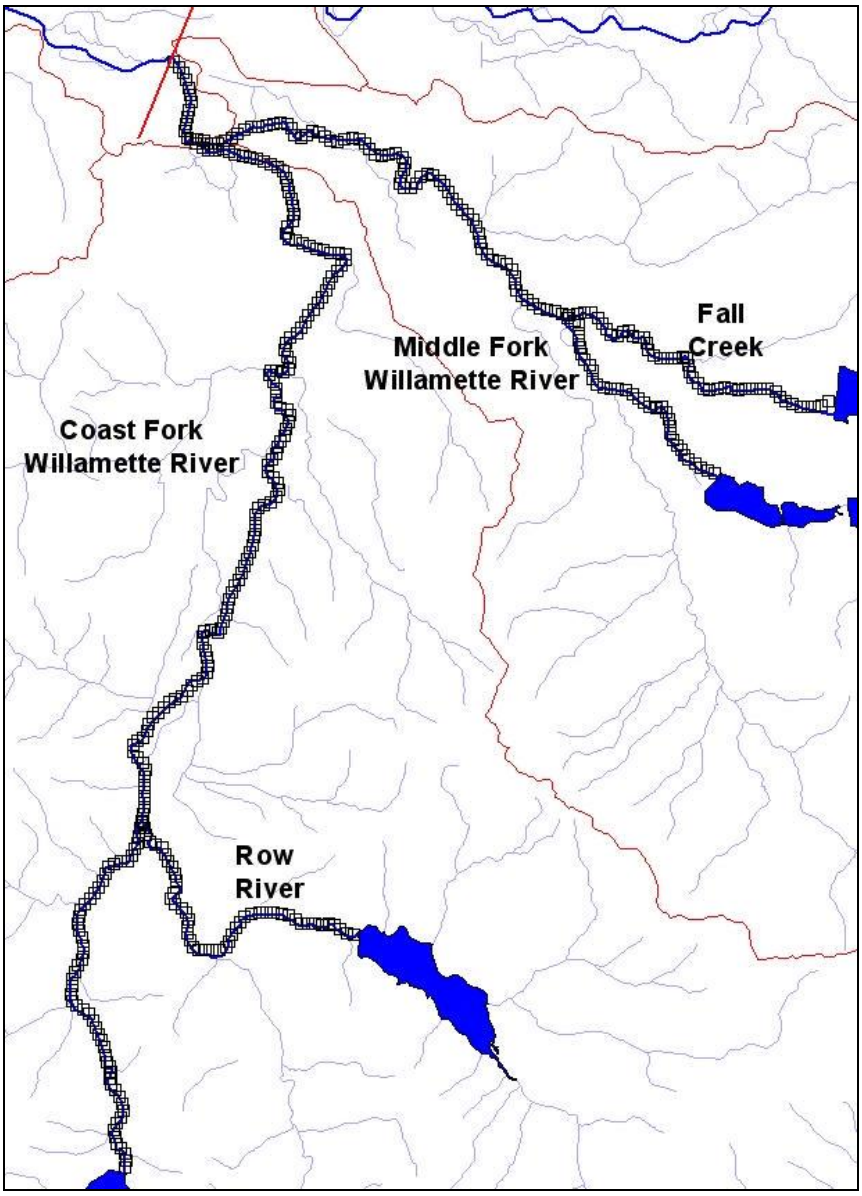


**Figure 570. Coast Fork and Middle Fork Willamette River model grid layout**

**Table 61. Coast Fork and Middle Fork Willamette River model grid layout specifications**

| Water Body | Branch | Description | Starting Segment | Ending Segment | Starting RM | Ending RM | Segment Length, m | Slope | Upstream BC | Down-stream BC |
|---|---|---|---|---|---|---|---|---|---|---|
| 1 | 1 | Coast Fork Willamette River | 2 | 114 | 22.6 | 11.3 | 250.14 | 0.001890 | flow | internal |
| | 2 | Coast Fork Willamette River | 117 | 189 | 11.3 | 0.0 | 250.14 | 0.001390 | internal | internal |
| 2 | 3 | Row River | 192 | 194 | 7.5 | 7.1 | 251.57 | 0.011500 | flow | internal |
| | 4 | Row River | 197 | 232 | 7.1 | 1.4 | 251.57 | 0.003020 | internal | internal |
| | 5 | Row River | 235 | 240 | 1.4 | 0.5 | 251.57 | 0.000001 | internal | internal |
| | 6 | Row River | 243 | 245 | 0.5 | 0.0 | 251.57 | 0.003650 | internal | internal |
| 3 | 7 | Middle Fork Willamette River | 248 | 278 | 16.5 | 11.7 | 250.59 | 0.003180 | flow | internal |
| | 8 | Middle Fork Willamette River | 281 | 355 | 11.7 | 0.0 | 250.59 | 0.002110 | internal | internal |
| 4 | 9 | Fall Creek | 358 | 402 | 7.0 | 0.0 | 254.37 | 0.002660 | flow | internal |
| 5 | 10 | Willamette River, RM 186.9 to RM 185.1 | 405 | 416 | 186.9 | 185.1 | 251.22 | 0.001070 | internal | internal |

## *Model Upstream & Downstream Boundary Conditions*

The upstream boundary conditions for the model consisted of flows from the U.S. Army Corps of Engineers reservoirs to the Coast Fork Willamette River, Row River, The Middle Fork Willamette River and Fall Creek. Flow and temperatures were monitored by USGS gages, although not always at the same gage. The downstream boundary condition was developed as flow over a spillway to pass water downstream to the Upper Willamette River model.

### Hydrodynamic Data

Figure 571 shows the nearest USGS gage station downstream of the U.S. Army Corps of Engineers reservoirs which monitor stream flow. Table 62 lists the USGS gages used for developing the model upstream boundary conditions, their actual river mile, and the river mile to which they were applied.

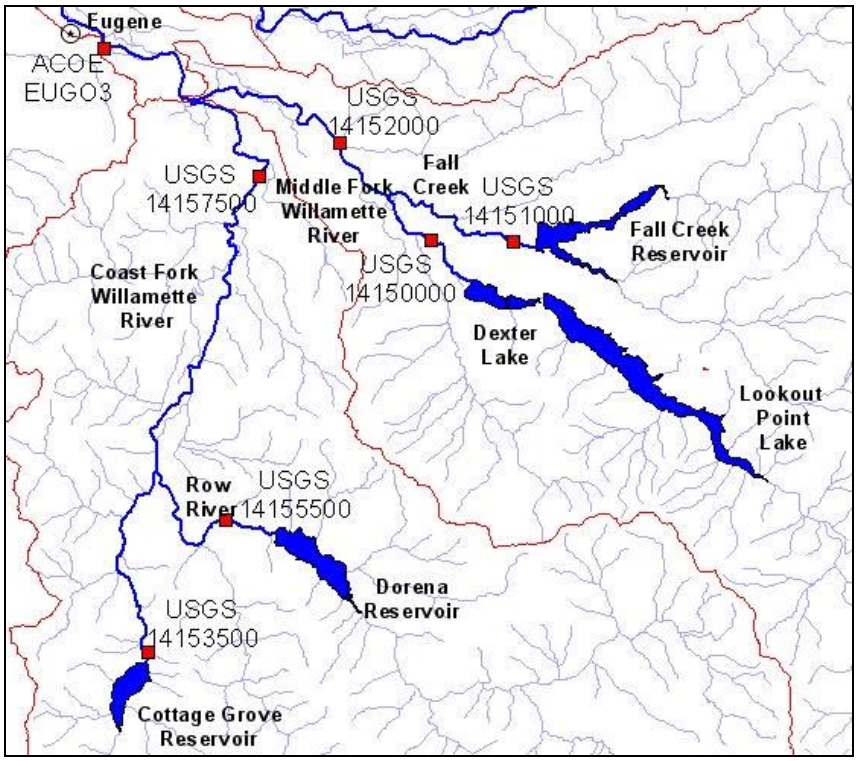


**Figure 571. Coast Fork and Middle Fork Willamette River model upstream flow boundary condition gage station locations**

**Table 62. Coast Fork and Middle Fork Willamette River model upstream flow boundary condition gage stations**

| Upstream Boundary | Flow gage | Actual RM | Boundary Condition RM |
|---|---|---|---|
| Coast Fork Willamette River | USGS 14153500 | 28.69 | 29.02 |
| Row River | USGS 14155500 | 5.51 | 7.54 |
| Middle Fork Willamette | USGS 14150000 | 13.95 | 16.53 |

| Upstream Boundary | Flow gage | Actual RM | Boundary Condition RM |
|---|---|---|---|
| River | | | |
| Fall Creek | USGS 14151000 | 6.29 | 7.14 |

## Year 2001

The four upstream boundary conditions had complete flow data records for the 2001 simulation. Figure 572 shows the inflow to the Coast Fork Willamette River from Cottage Grove Reservoir. Figure 573 show the inflow to the Row River from Dorena Reservoir. Figure 574 shows the flow in the Middle Fork Willamette River from Dexter Lake and Lookout Point Lake. Figure 575 shows the flow in Fall Creek at the USGS gage station from the Fall Creek Reservoir. All four figures show the influence of reservoir operations with large spikes in flow in the spring and fall and the steady lower flow during the summer.

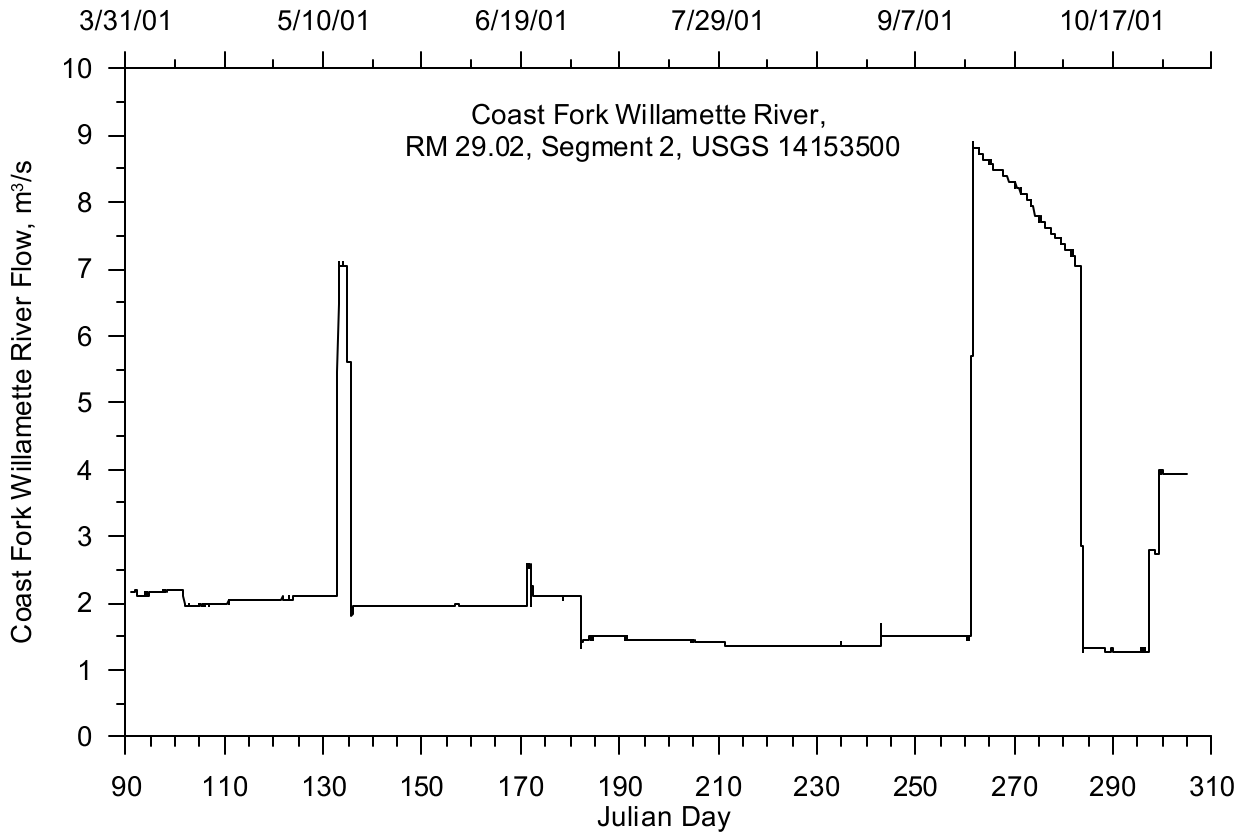


**Figure 572. Coast Fork Willamette River inflow, 2001**

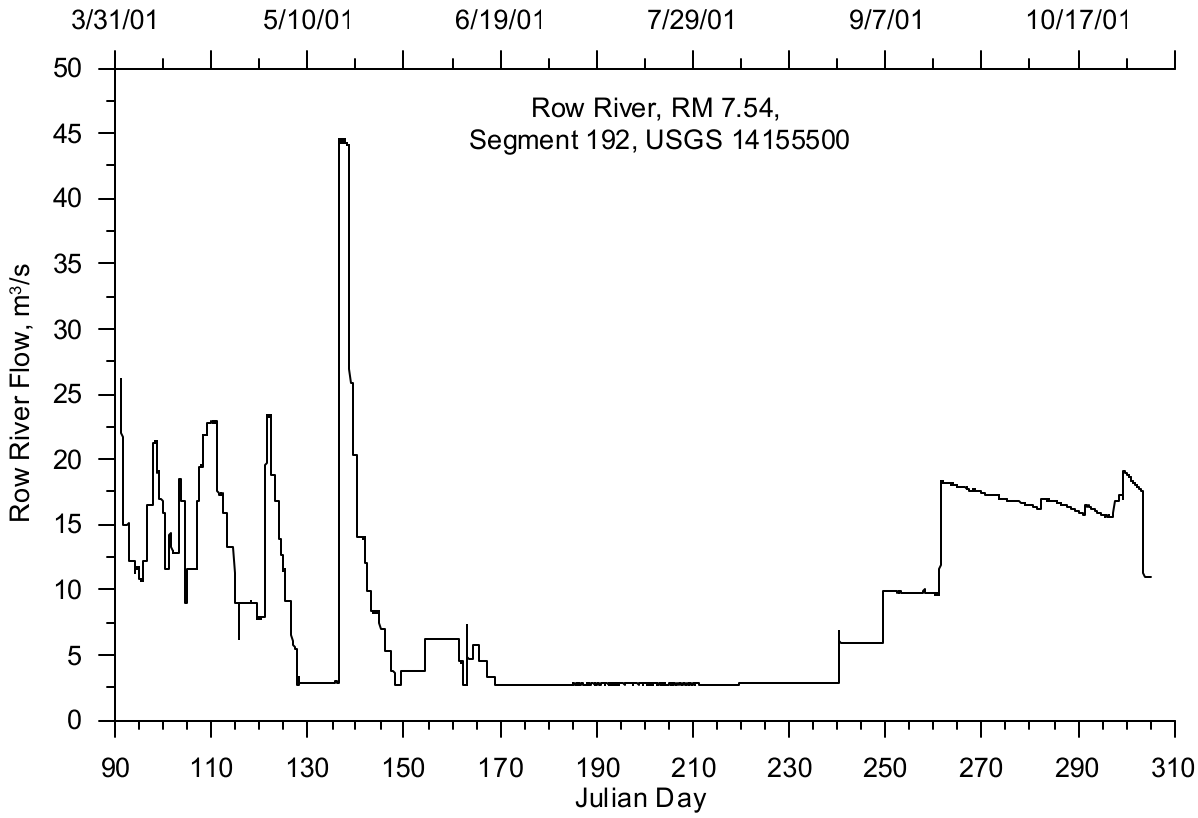


**Figure 573. Row River inflow, 2001**

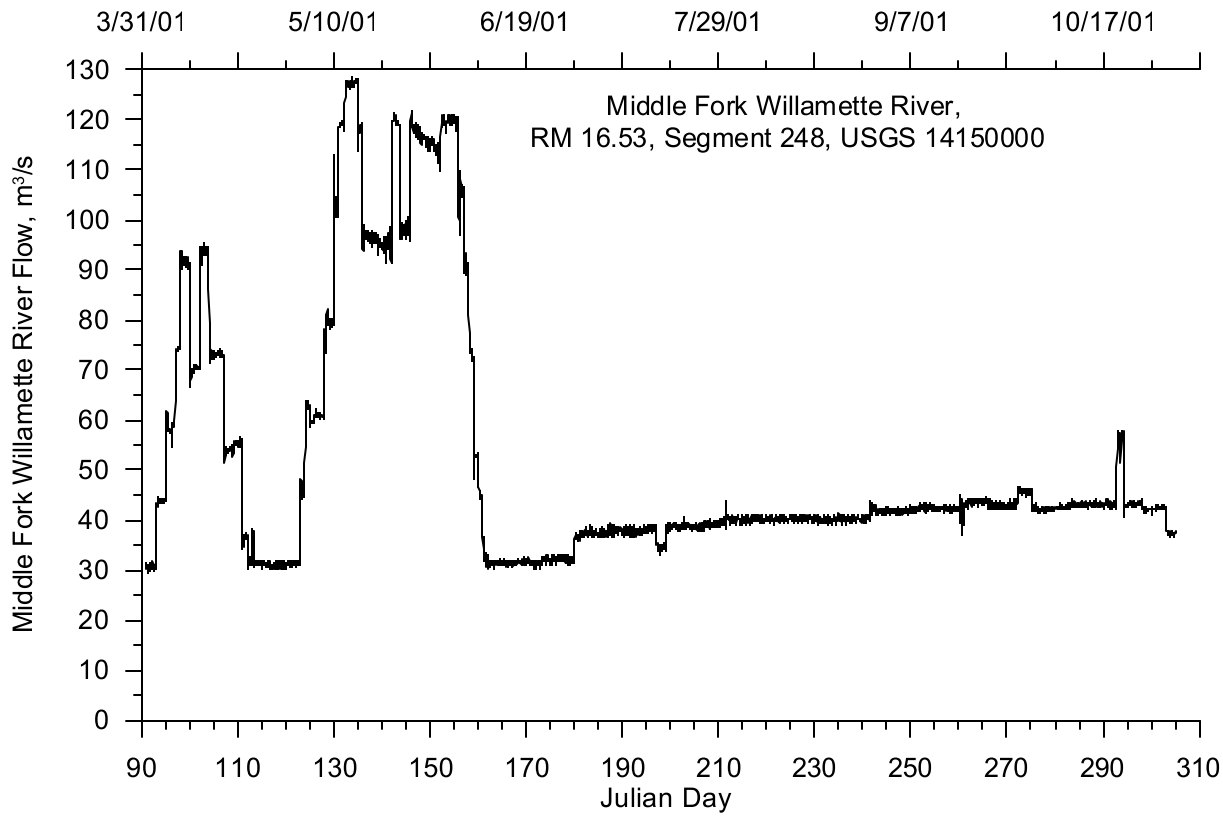


**Figure 574. Middle Fork Willamette River inflow, 2001**

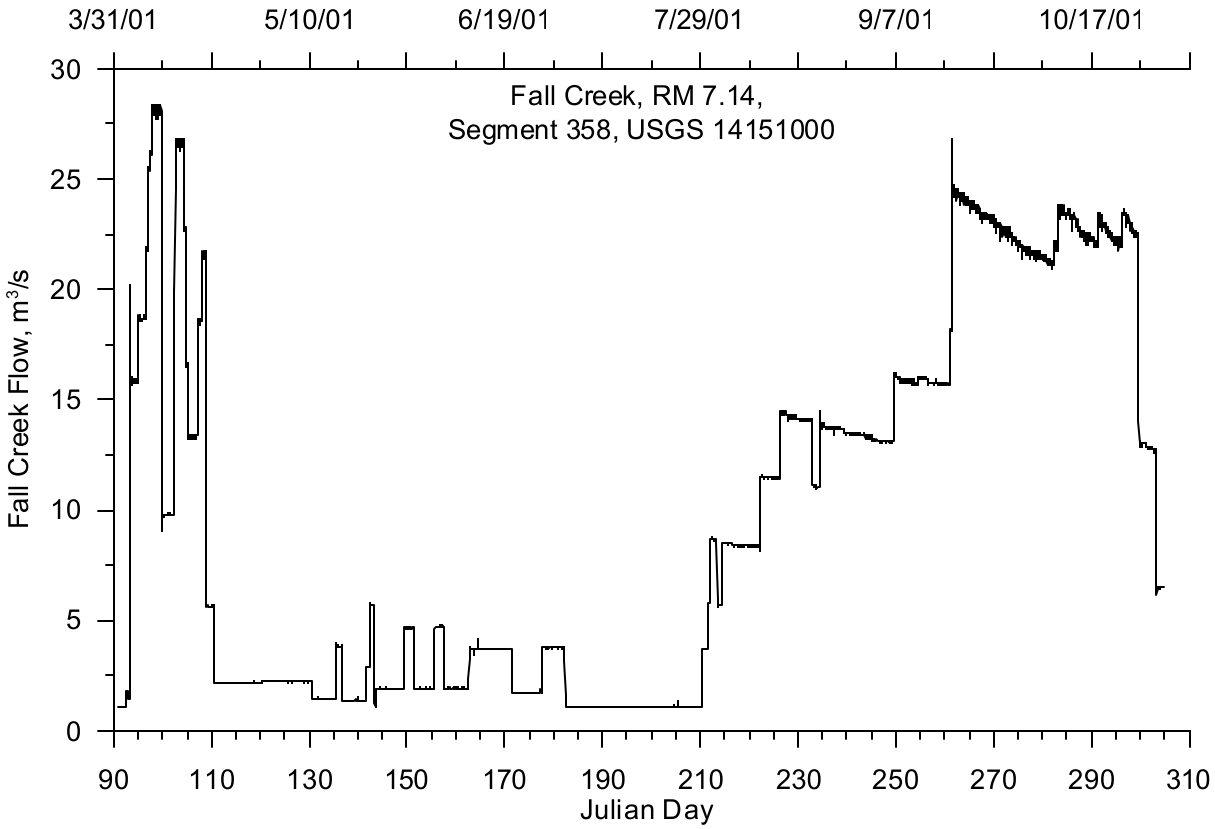


**Figure 575. Fall Creek inflow, 2001**

## Year 2002

The four upstream boundary conditions had complete flow data records for the 2002 simulation period. Figure 576 shows the inflow to the Coast Fork Willamette River from Cottage Grove Reservoir. Figure 577 show the inflow to the Row River from Dorena Reservoir. Figure 578 shows the flow in the Middle Fork Willamette River from Dexter Lake and Lookout Point Lake. Figure 579 shows the flow in Fall Creek at the USGS gage station from the Fall Creek Reservoir. Similar to 2001, the flow plots for the four rivers show the influence of reservoir operations with large spikes in flow in the spring and fall and the steady lower flow during the summer.

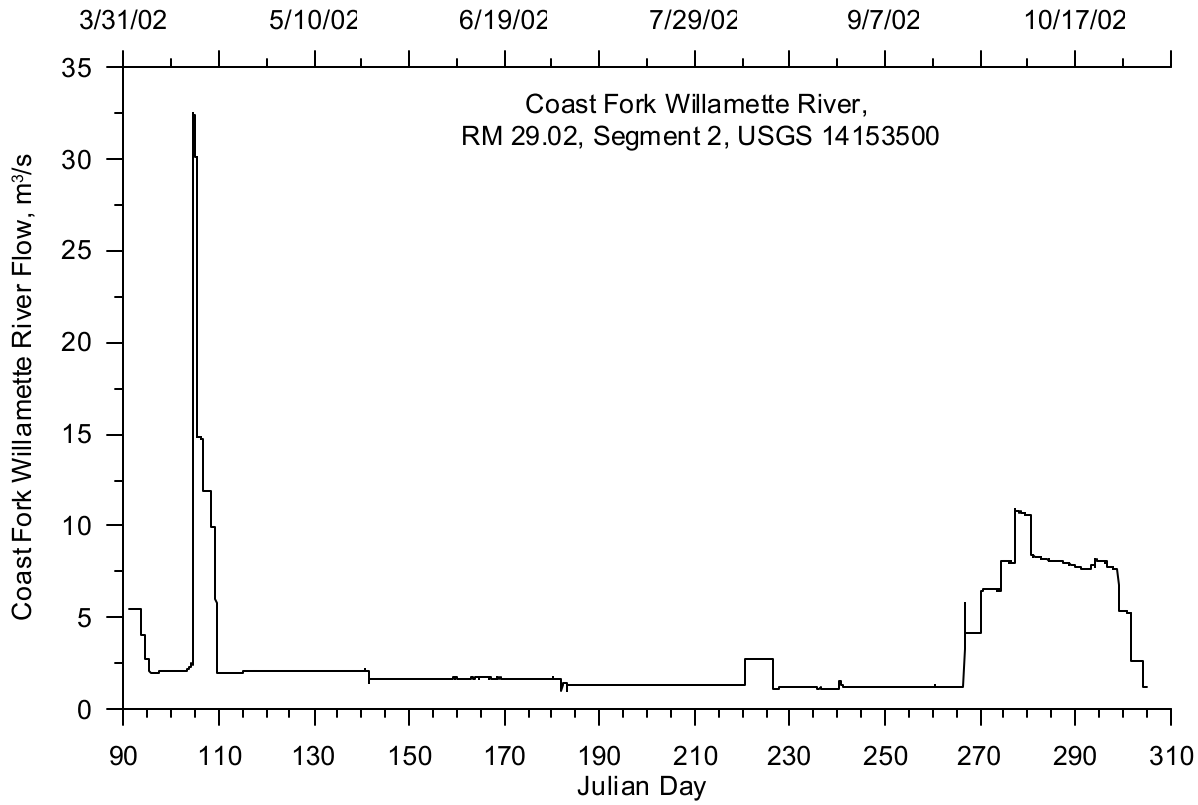


**Figure 576. Coast Fork Willamette River inflow, 2002**

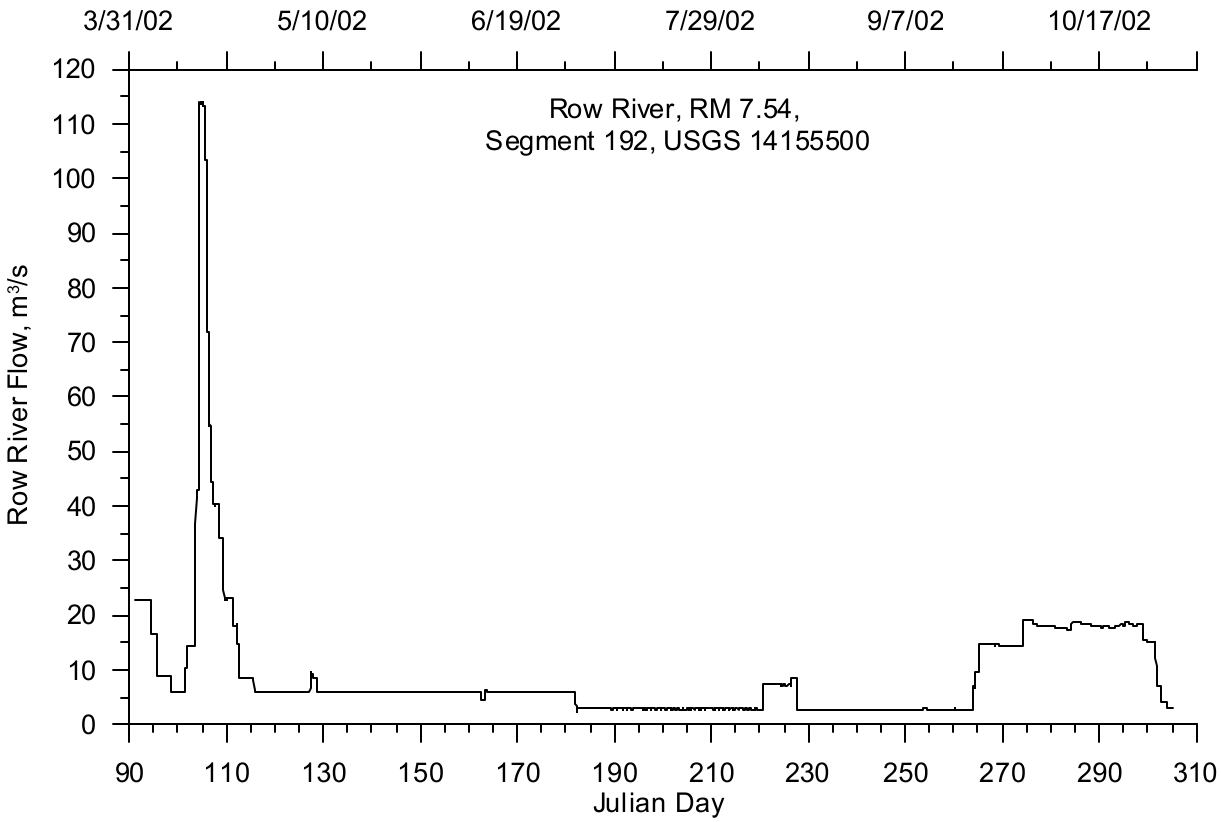


**Figure 577. Row River inflow, 2002**

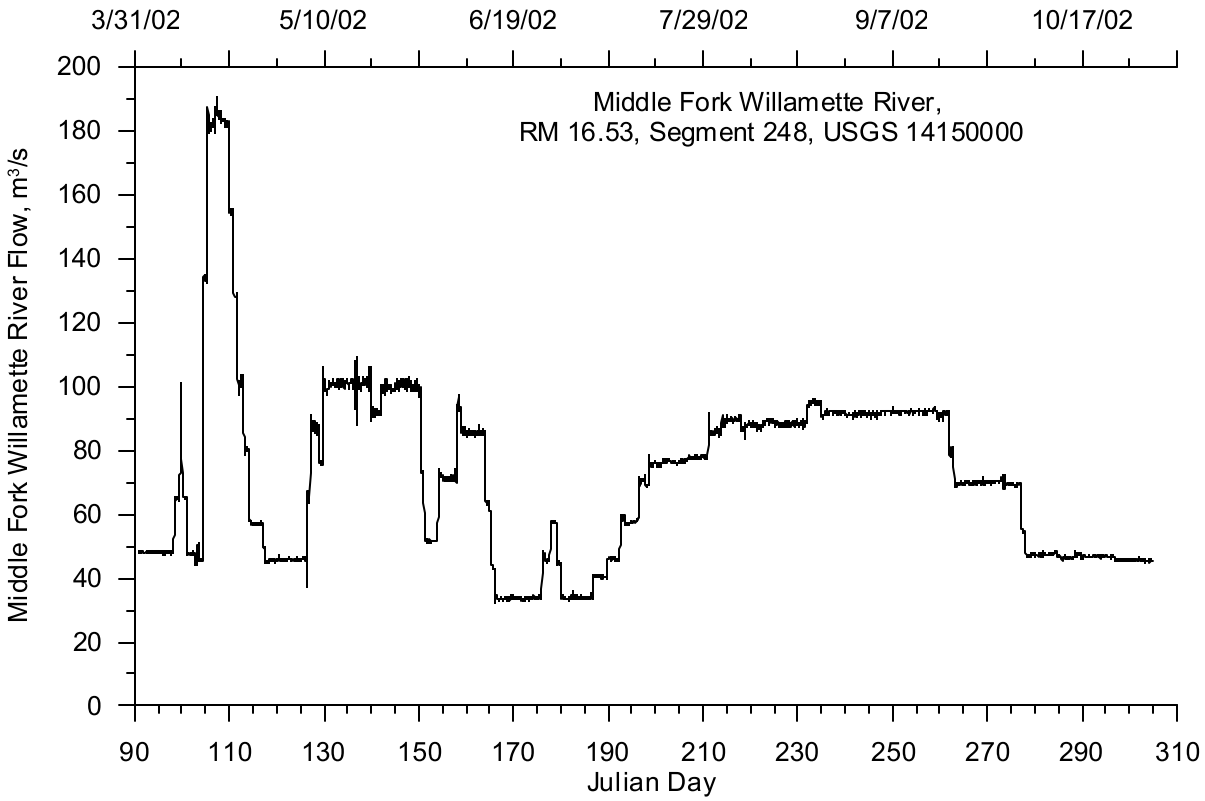


**Figure 578. Middle Fork Willamette River inflow, 2002**

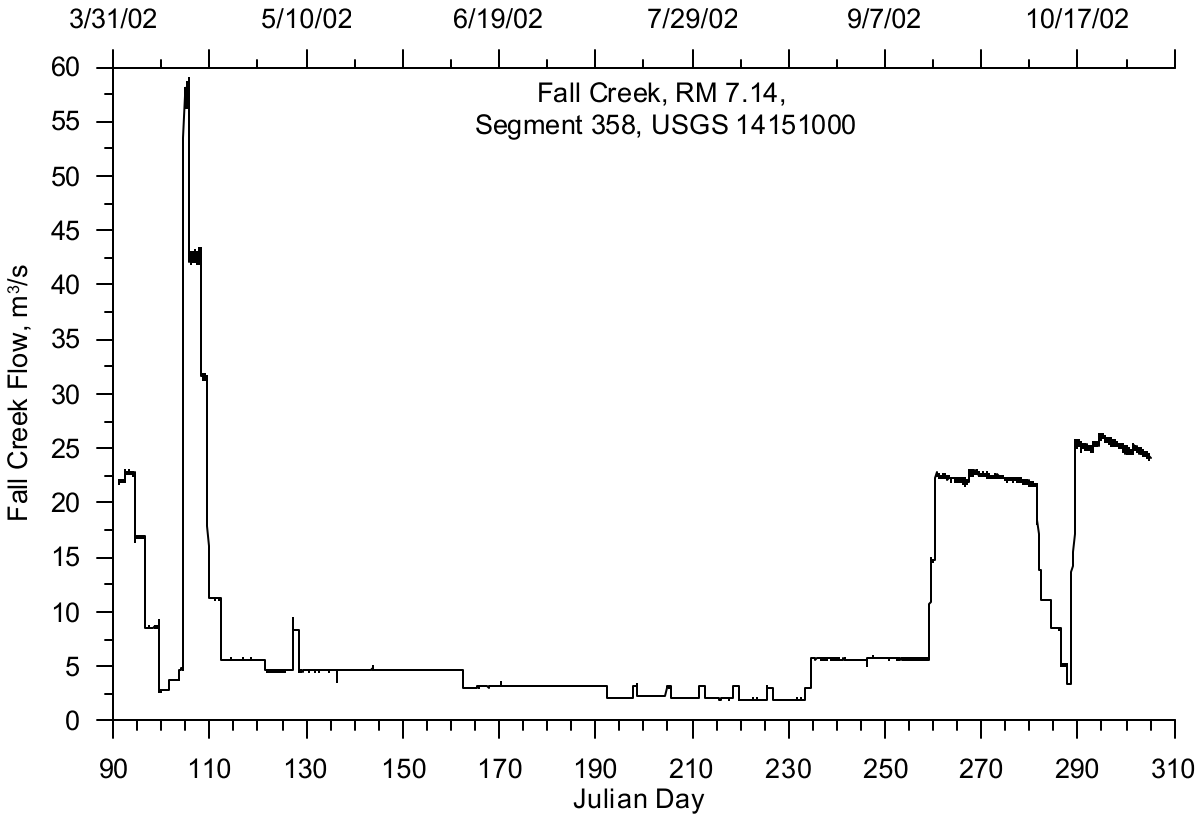


**Figure 579. Fall Creek inflow, 2002**

## Temperature Data

Several USGS gage stations recorded water temperature at either every half-hour or hour in the Coast and Middle Fork system. Figure 580 shows a map of the Coast and Middle Forks of the Willamette River and the locations of the USGS gages used for developing the temperature boundary condition. Table 63 lists the USGS gage stations used to characterize the temperature upstream boundary condition. Several of the data sets were incomplete for the model simulation periods of April 1 to October 31 for 2001 and 2002, so correlations were developed to fill data gaps.

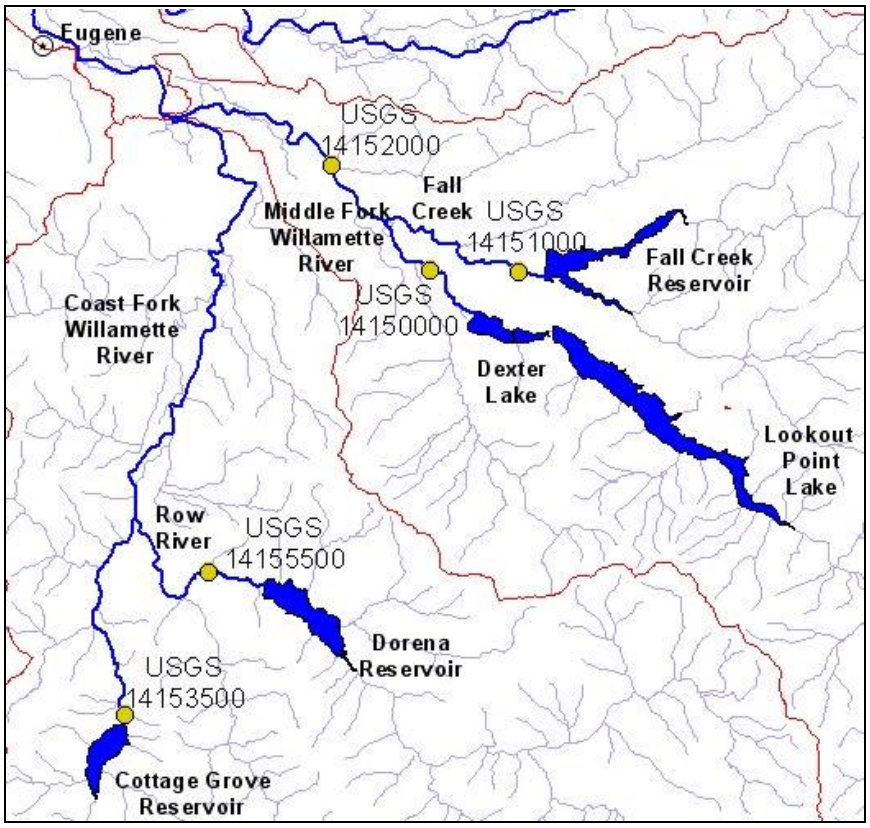


**Figure 580. Coast Fork and Middle Fork Willamette River model upstream temperature boundary condition gage station locations**

**Table 63. Coast Fork and Middle Fork Willamette River model upstream temperature boundary condition gages**

| Upstream Boundary | Temperature gage |
|---|---|
| Coast Fork Willamette River | USGS 14153500 |
| Row River | USGS 14155500 |
| Middle Fork Willamette River | USGS 14150000 and 14152000 |
| Fall Creek | USGS 14151000 and 14152000 |

### Year 2001

The upstream boundary for the Coast Fork Willamette River consists of data from a USGS gage from August 1 to October 31, 2001. In order to complete the record from April 1 to July 31, a temperature correlation was developed relating the 2002 temperature data at the USGS gage below the reservoir (14153500) with the 2001 temperature data at the same gage. This approach was selected because there

was a lack of temperature data in the Coast and Middle Fork system which could be used to develop a temperature correlation using strictly 2001 data. Figure 581 shows the temperature correlation relating the 2001 and 2002 data set at the USGS gage. Figure 582 shows the Coast Fork temperature boundary condition showing both the gage data and the calculated values. Both the correlation plot and the time series plot suggest that the calculated temperatures may have a warm bias of approximately 1 ºC.

The upstream boundary for Row River was similar to the Coast Fork Willamette River boundary condition development. Temperature data from the USGS gage was available from April 1 to July 31. A temperature correlation was developed relating the 2001 temperature data with 2002 temperature data at the same gage. Figure 583 shows the Row River temperature correlation and Figure 584 shows both the temperature data and the calculated values.

No data were available before August for the Middle Fork Willamette River and Fall Creek. No successful temperature correlation could be developed between the 2001 and 2002 gage station data sets. The data gaps for both rivers were filled with the temperature data from the downstream gage station on the Middle Fork Willamette River (USGS 14152000). Figure 585 and Figure 586 show the upstream boundary conditions for the Middle Fork Willamette River and Fall Creek, respectively.

The trend in temperatures for the Coast Fork Willamette River, Row River, and Fall Creek gages was one of increasing temperatures reaching a maximum in summer, followed by some early fall cooling, ending with a notable decrease in diurnal variation and mean temperature associated with increased fall dam releases. The Middle Fork Willamette River behaves similarly, but does not exhibit the decreased fall diurnal variations.

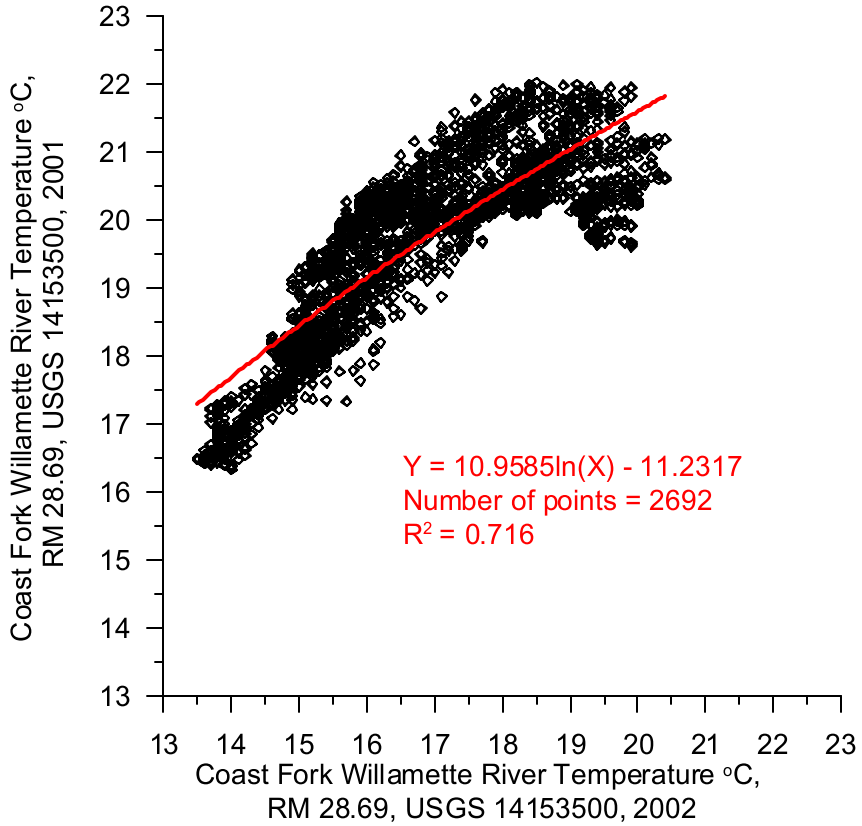


**Figure 581. Coast Fork Willamette River temperature correlation between 2001 and 2002 data.**

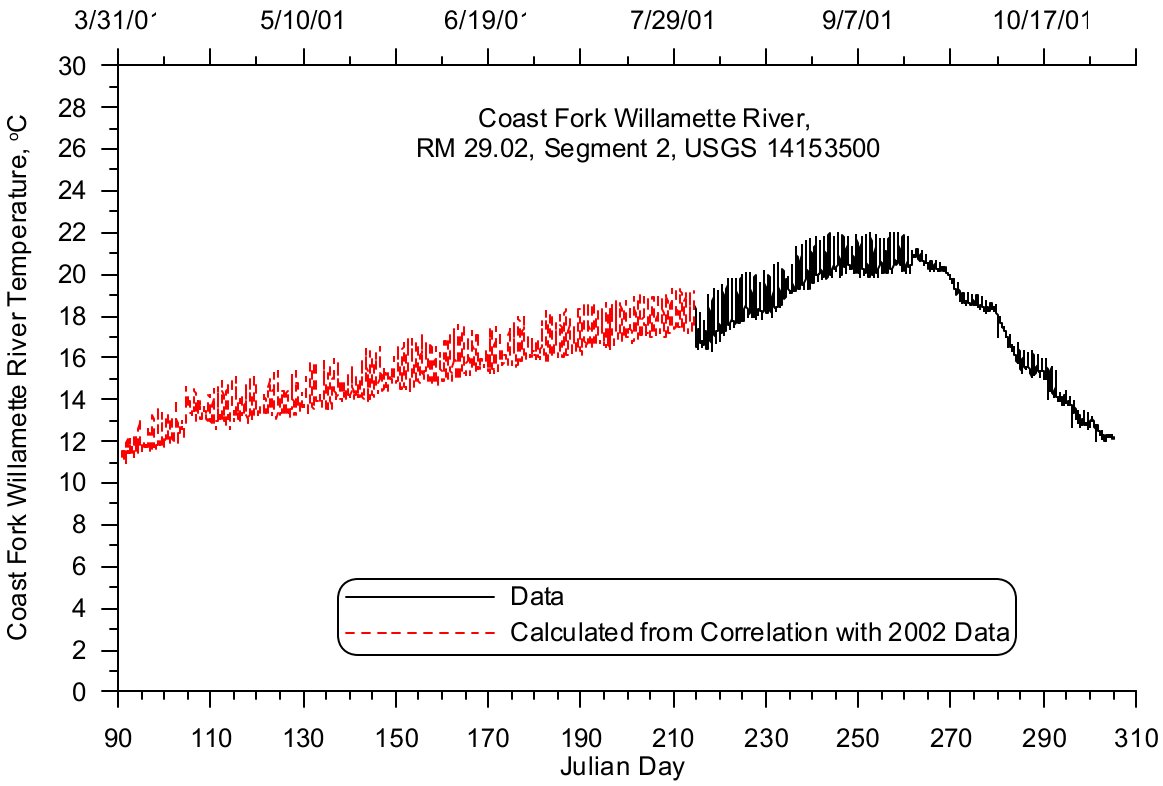


**Figure 582. Coast Fork Willamette River inflow temperature, 2001**

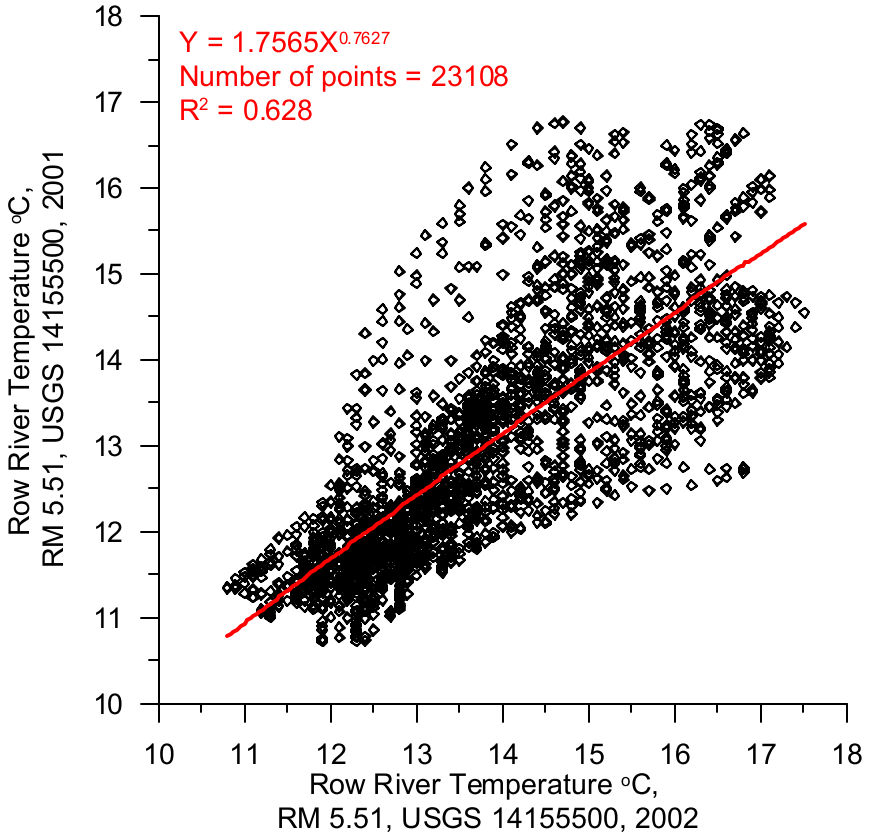


**Figure 583. Row River temperature correlation between 2001 and 2002 data.**

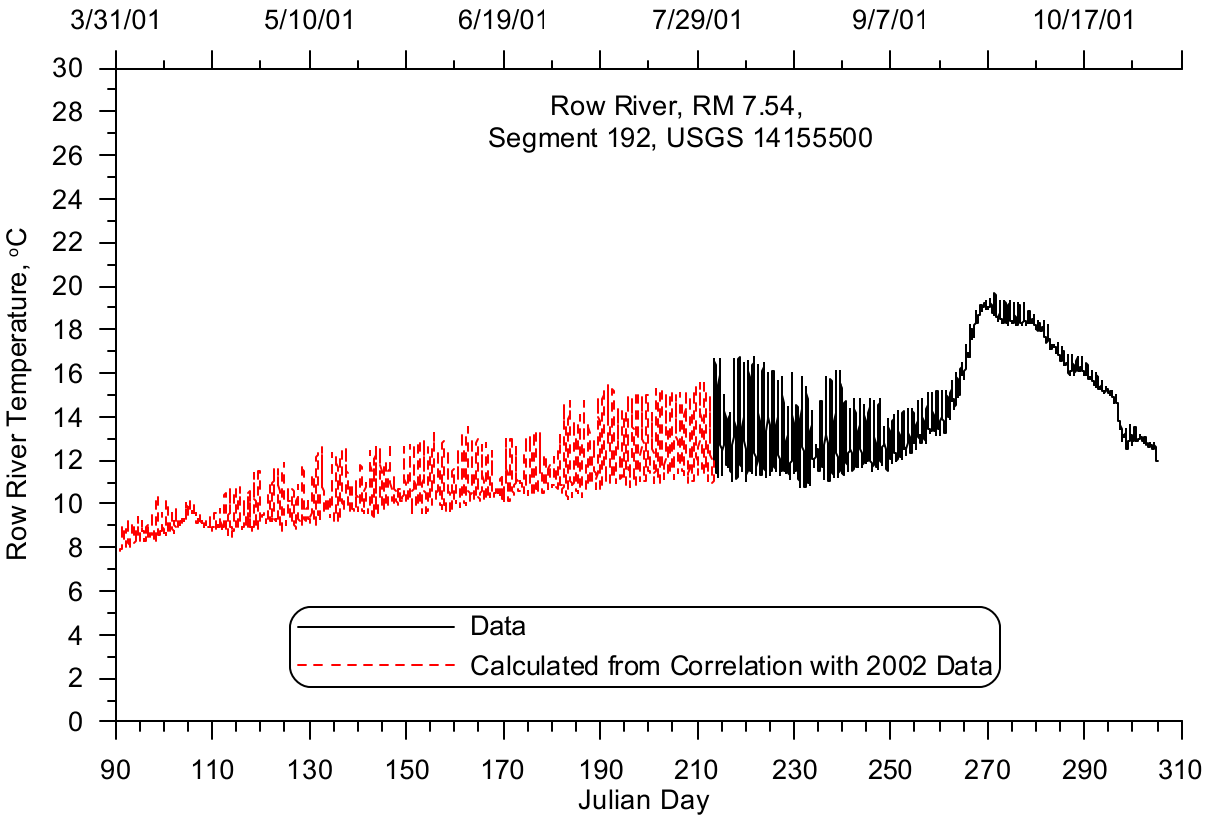


**Figure 584. Row River inflow temperature, 2001**

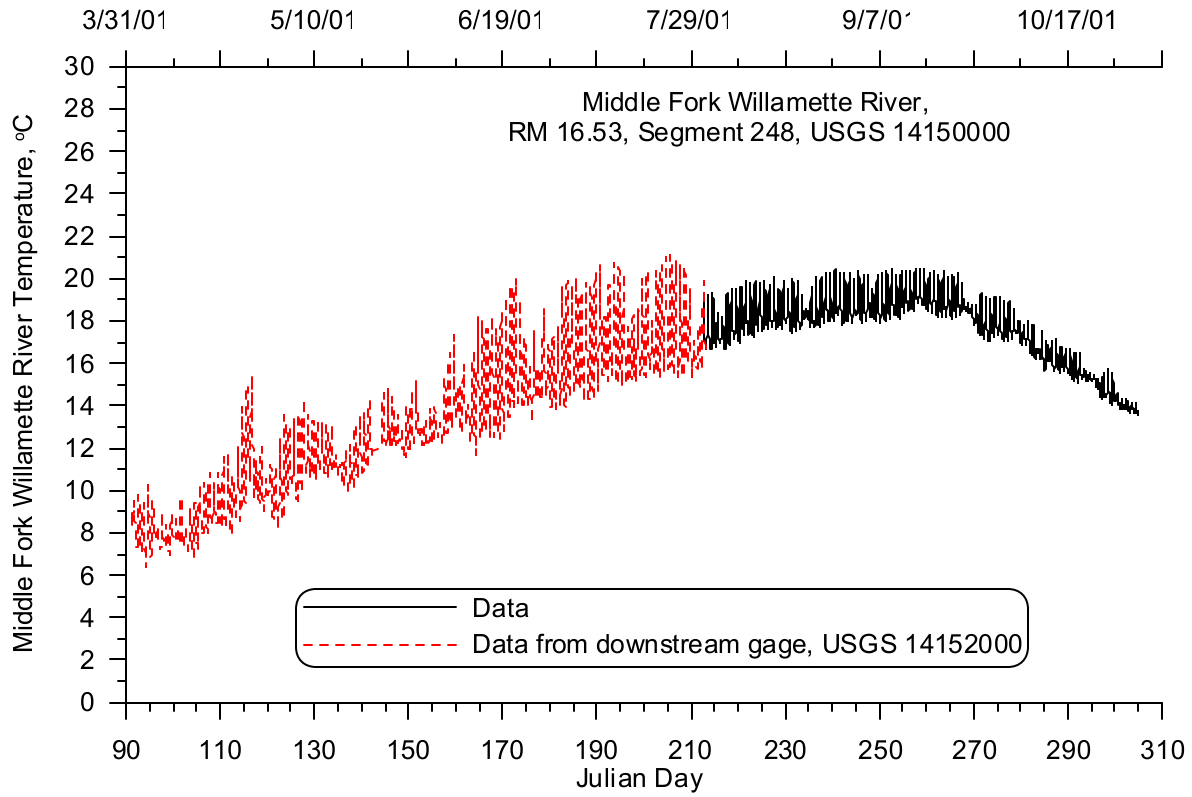


**Figure 585. Middle Fork Willamette River inflow temperature, 2001**

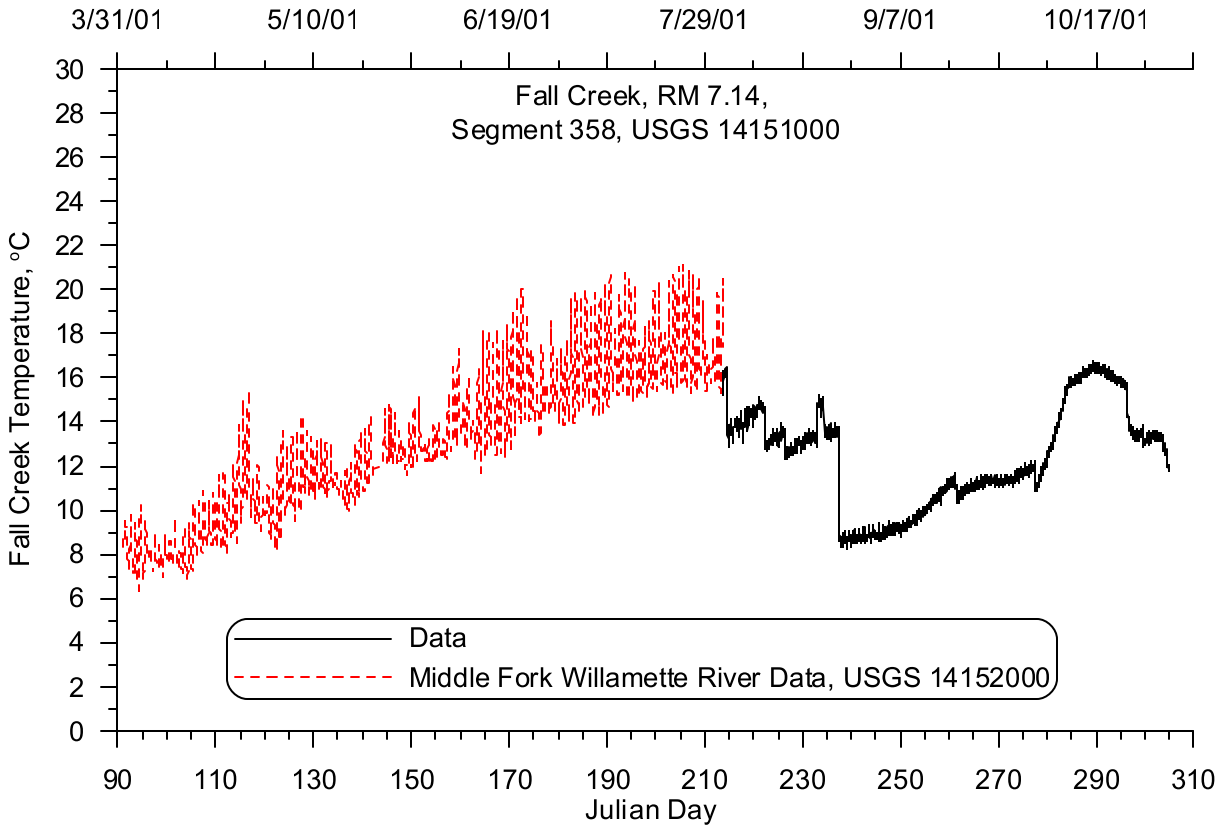


**Figure 586. Fall Creek inflow temperature, 2001**

## Year 2002

In 2002, the four USGS gage stations at the upstream ends of the river had complete data sets for the model simulation period of April 1 to October 31. The 2002 temperature trends were similar to the 2001 trends. Figure 587 shows the Coast Fork Willamette River upstream temperature boundary condition, which shows a seasonal warming trend.

Figure 588 shows the Row River upstream temperature boundary condition with the same seasonal warming trend seen in the Coast Fork Willamette River, but the diurnal temperature variations were larger. This was due to the relative proximity of the gage to the upstream dam discharge. The Coast Fork Willamette River gage was almost directly downstream of the dam and shows a reduced diurnal temperature variation typical of withdrawals at depth from a reservoir. The Row River gage was approximately two miles downstream from the reservoir, and exhibited increased diurnal temperature variation due to ambient heating and cooling. Figure 589 shows the upstream temperature boundary condition for the Middle Fork Willamette River. Figure 590 shows the Fall Creek upstream temperature boundary condition. The same seasonal warming trends seen in the Coast Fork Willamette River and Row River could also be seen in the figures for the Middle Fork Willamette River and Fall Creek. A notable difference among the temperature patterns was the steep decrease seen in the Fall Creek temperature at the beginning of September. This dramatic decrease indicated a significant change in reservoirs operations.

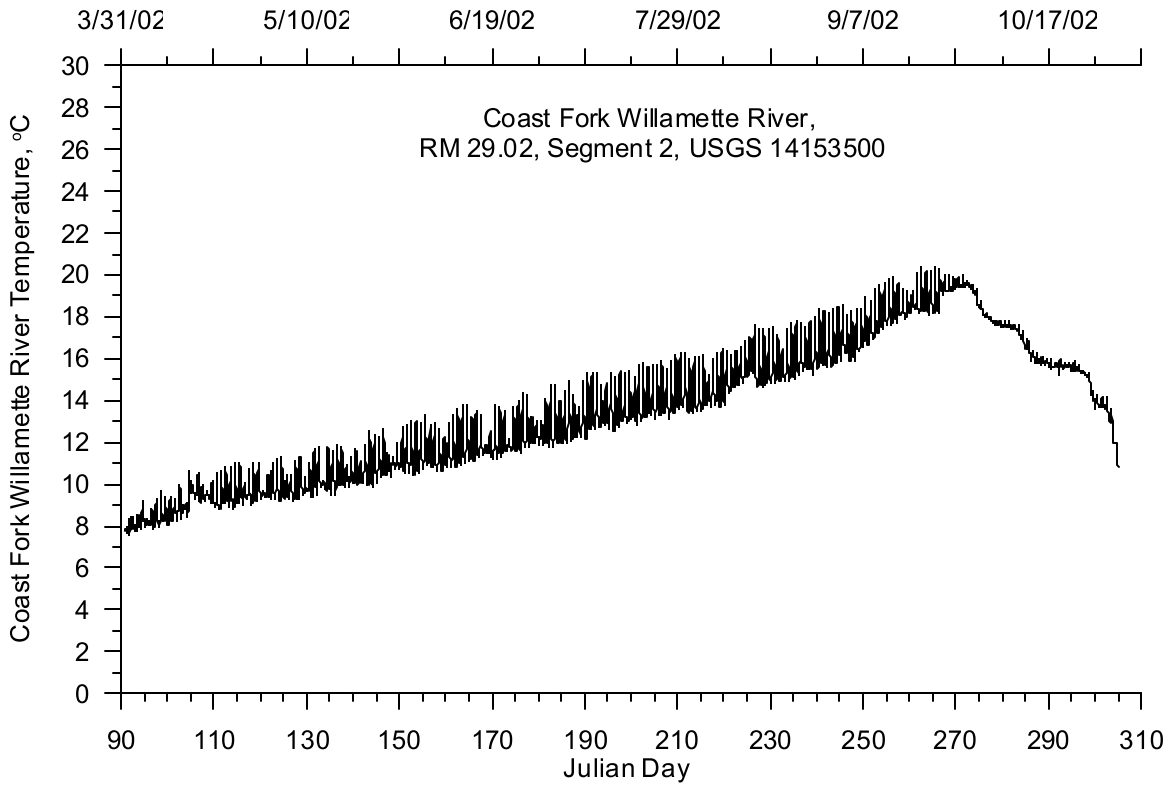


**Figure 587. Coast Fork Willamette River inflow temperature, 2002**

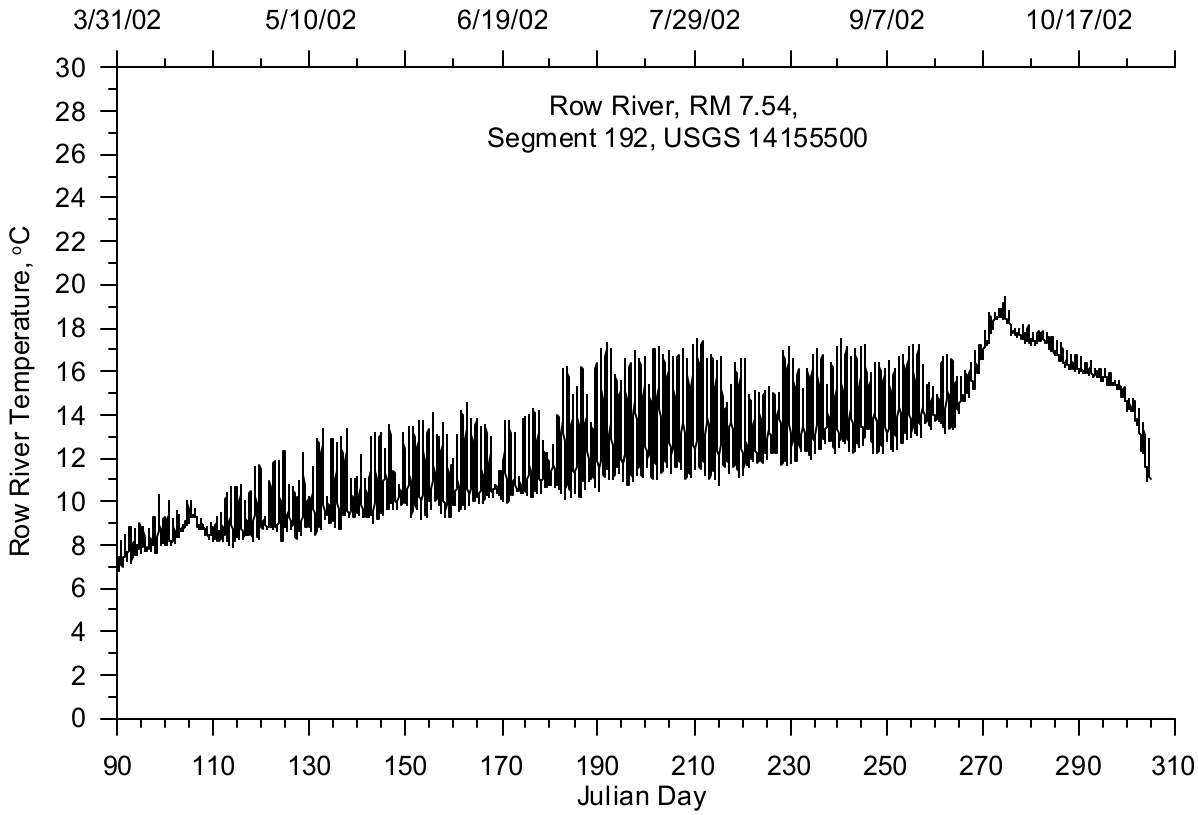


**Figure 588. Row River inflow temperature, 2002**

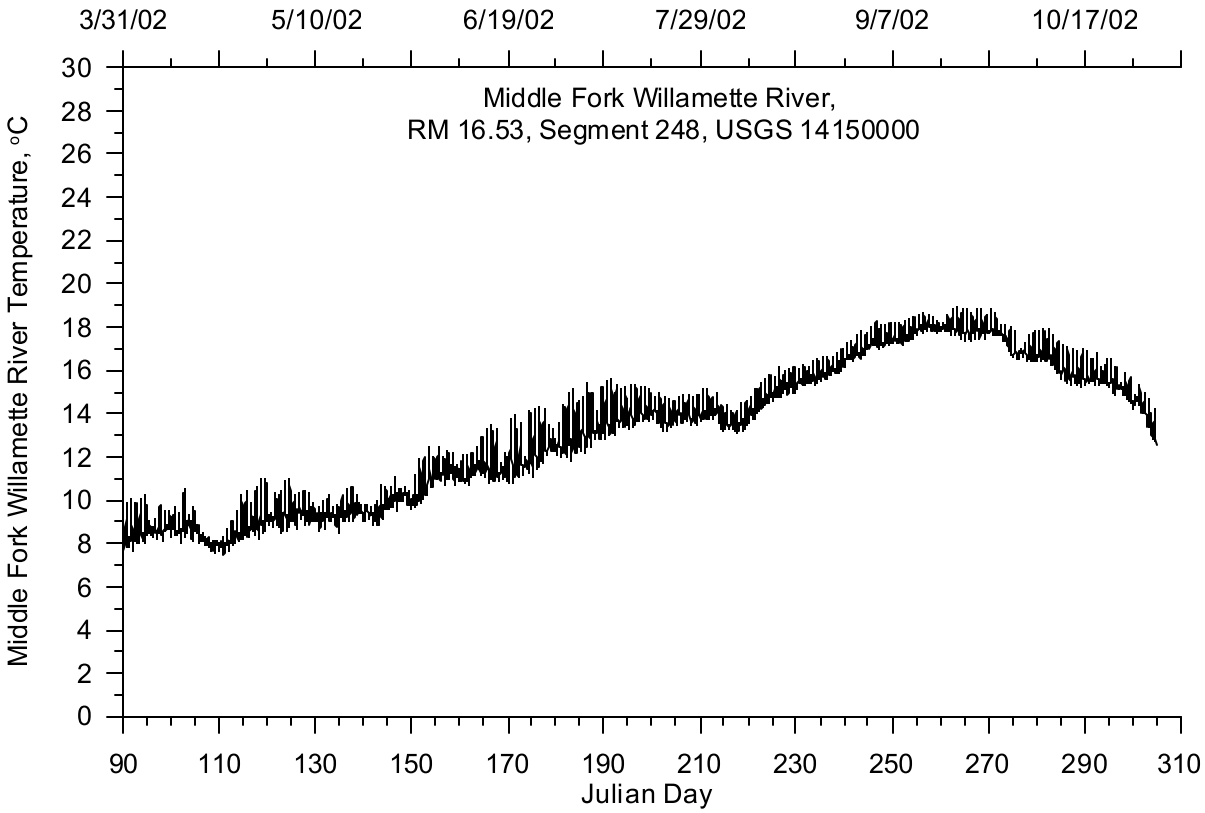


**Figure 589. Middle Fork Willamette River inflow temperature, 2002**

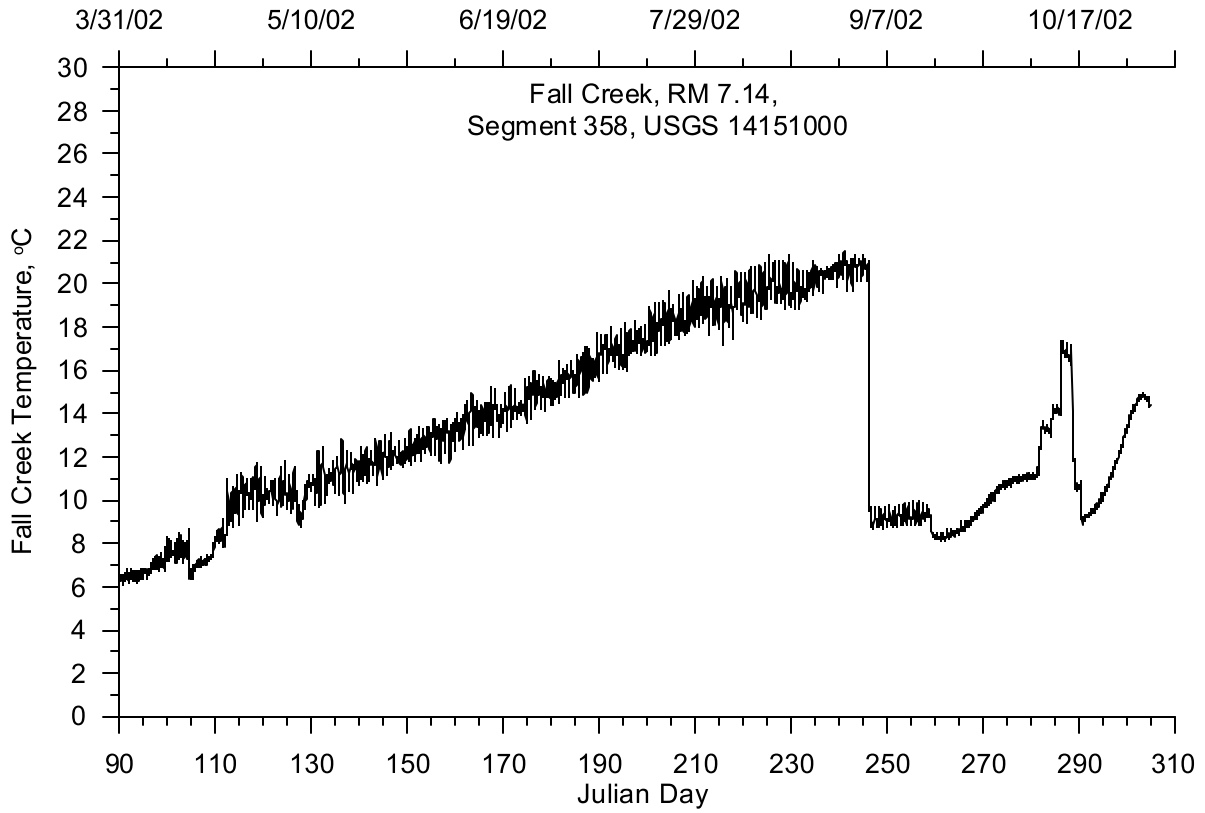


**Figure 590. Fall Creek inflow temperature, 2002**

## *Tributaries*

There was only one large tributary included in the model, Mosby Creek, which entered the Row River at RM 3.84, corresponding to model segment 217. In addition, distributed flows will be generated in the calibration process to account for other tributaries not individually included in the model, groundwater gains and losses, and other uncertainties in the model hydrodynamics.

### Hydrodynamic Data

#### Year 2001

There were no flow data for Mosby Creek for 2001. In order to develop a flow record, historical daily flow records for Row River and Mosby Creek were acquired from the USGS. A flow correlation was developed between Row River (USGS 14155500) and Mosby Creek (USGS 14156500) using data from September 1946 to October 1981. Figure 591 shows the flow correlation and the correlation equation. Figure 592 shows the daily flows calculated for Mosby Creek for 2001.

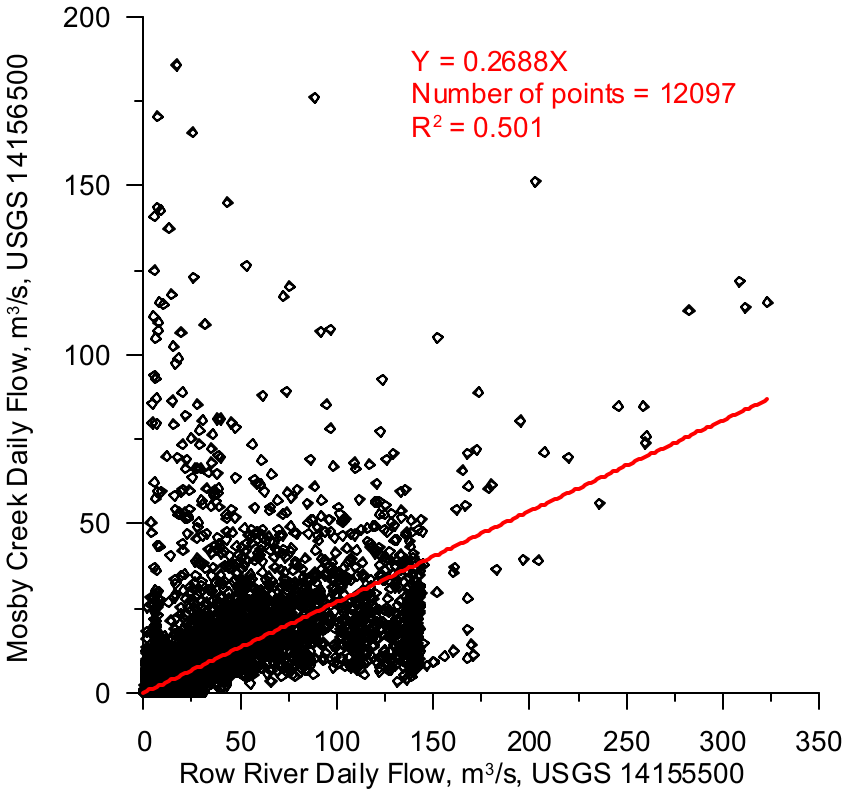


**Figure 591. Mosby Creek flow correlation with Row River**

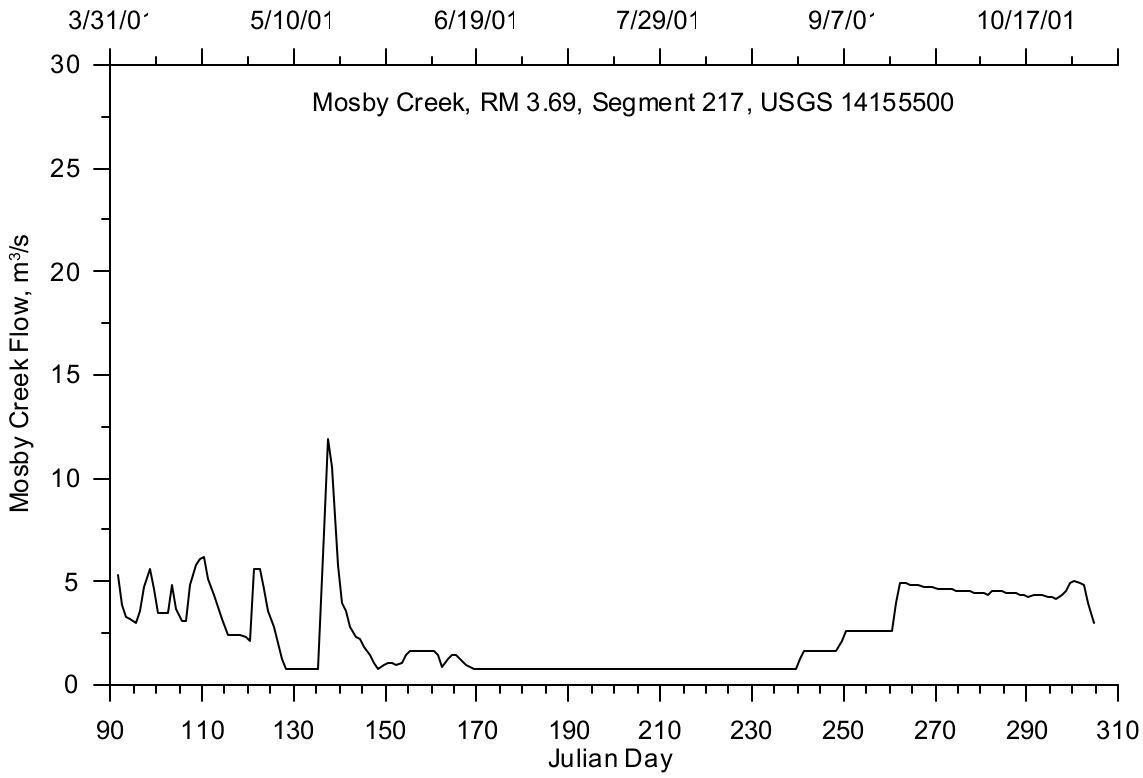


**Figure 592. Mosby Creek flow, 2001**

## Year 2002

The correlation used for developing the 2001 flows for Mosby Creek was also used to develop the Mosby Creek flows for 2002. Figure 593 shows the daily flows for Mosby Creek. The figure shows similar flow to 2001 but with a larger spring freshet dropping down to a low summer flow early in the year.

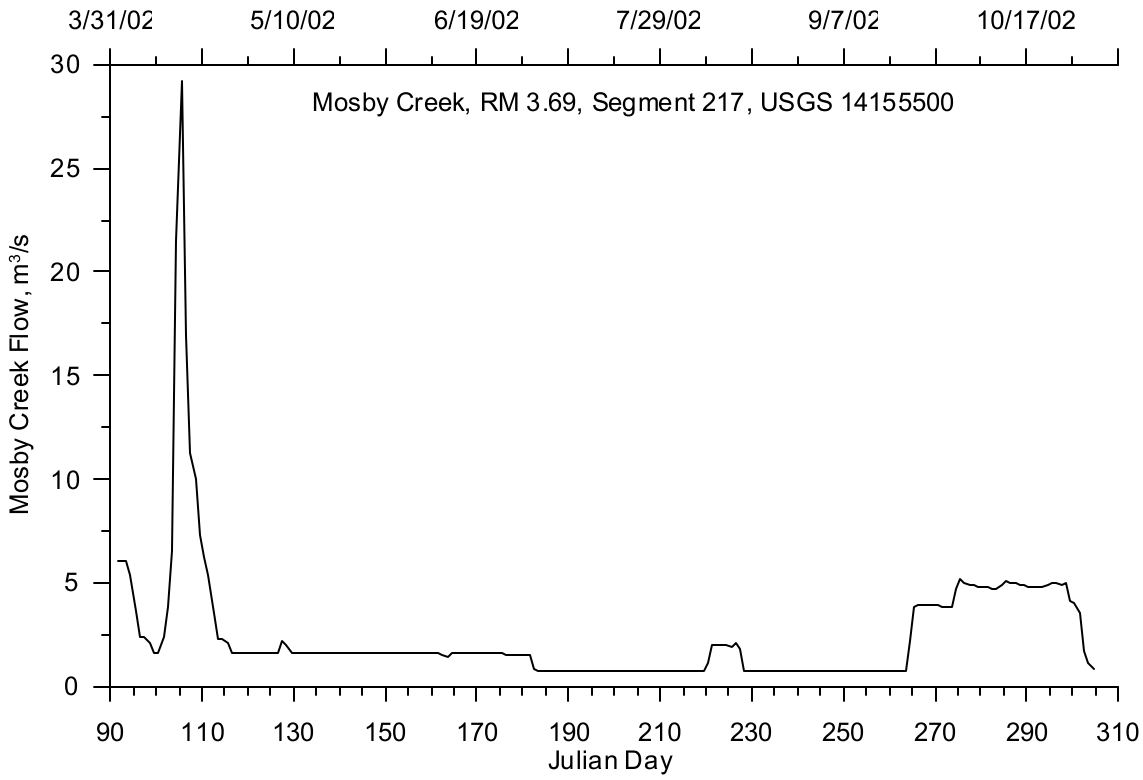


**Figure 593. Mosby Creek flow, 2002**

## Temperature Data

Mosby Creek had temperature data for both 2001 and 2002 from LASAR site 26746. The site had temperature data every half-hour, but the data set was not complete for each year, so a temperature correlation was developed to the complete data set.

### Year 2001

Mosby Creek temperature data were collected in 2001 from July 30 to later than October 31. To fill in the data gap before July 30 a temperature correlation was developed between the Mosby Creek data and water temperatures recorded on the North Fork of the Middle Fork Willamette River (LASAR 28003), which is approximately 8.4 km (5.2 mi) upstream of Lookout Point Reservoir. The site was chosen because of the completeness of data and because it was above the reservoir. Figure 594 shows the temperature correlation and equation for the 2001 data. The data from the North Fork of the Middle Fork Willamette River were only monitored as early as June 7, 2001, so the time period from April 1 to June 7 could not be filled by using the correlation. Figure 595 shows the temperature data and calculated values from the correlation for 2001.

The remaining time period from April 1 to June 7 was filled by setting the water temperature on April 1 and allowing the model to linearly interpolate between the value in April and the first one in June. This approach was taken due to the lack of data available during the spring of 2001. Since the flow of Mosby creek was not large compared to Row River and the Coast Fork Willamette River, the linear interpolation should not have much influence on the temperature calibration.

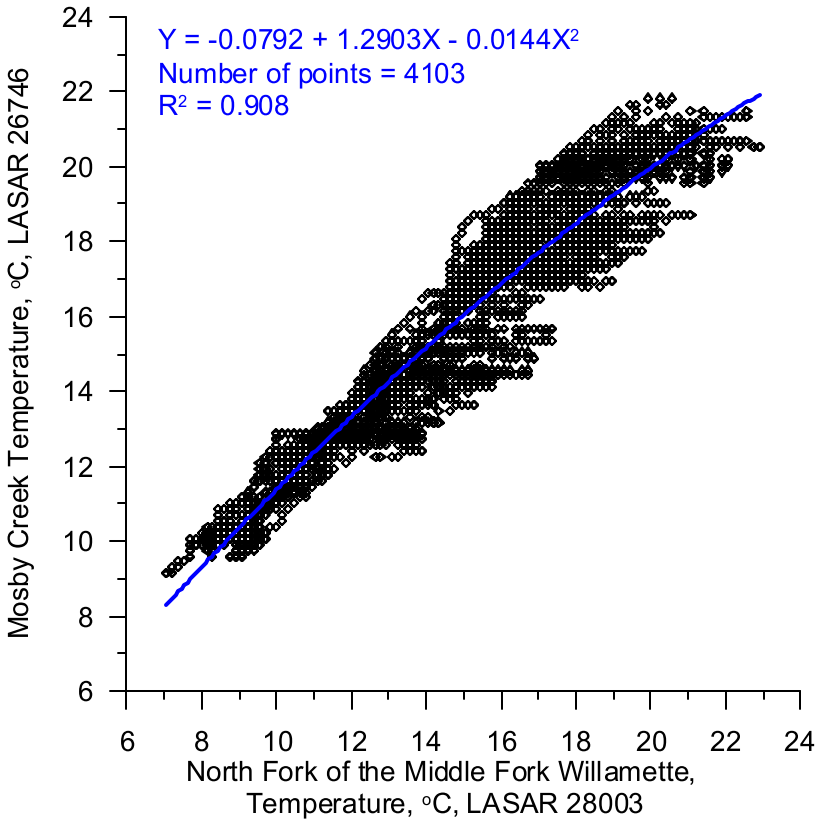


**Figure 594. Mosby Creek temperature correlation, 2001**

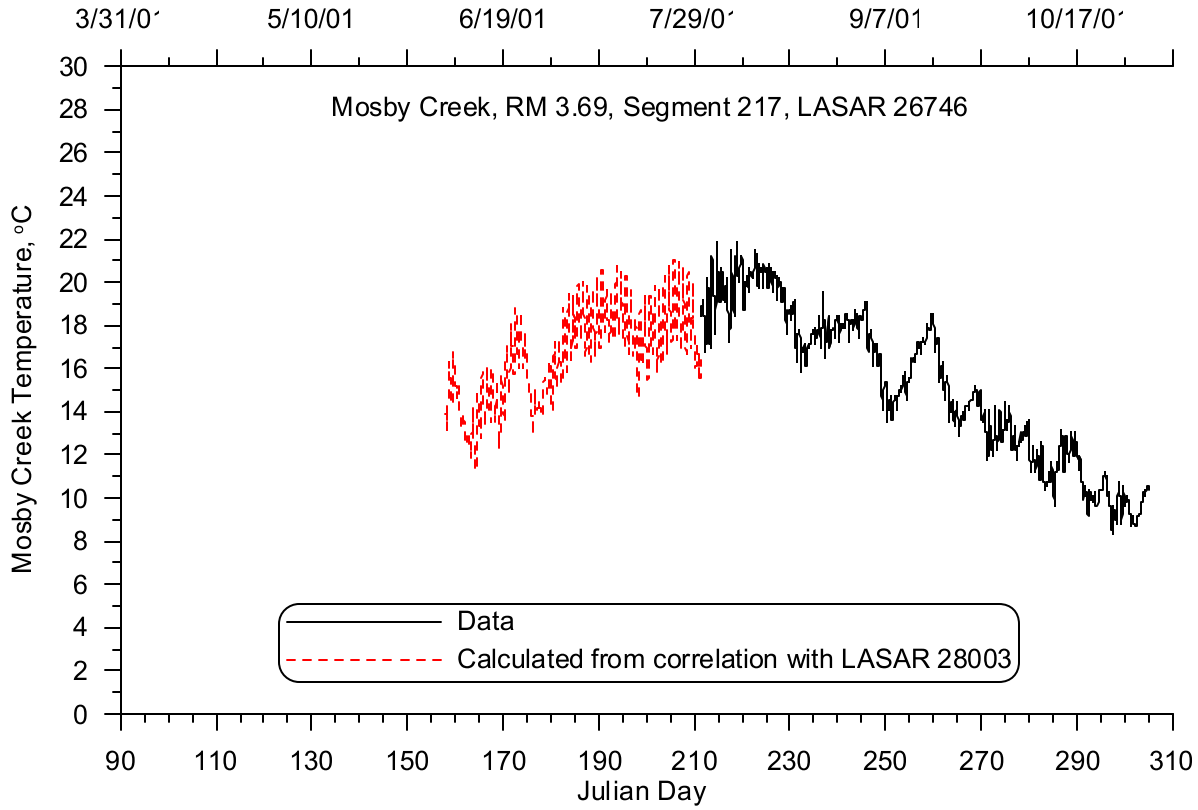


**Figure 595. Mosby Creek temperature, 2001**

Year 2002

In 2002 Mosby Creek temperature data were collected from June 20 to later than October 31. To fill in the data gap before June 20, a temperature correlation was developed between the Mosby Creek data and water temperatures recorded on the Mohawk River (LASAR 10663). There were no temperature data available for the site used for the 2001 data, North Fork of the Middle Fork Willamette River, so the Mohawk River was used. Figure 596 shows the temperature correlation and equation for the 2001 data. The data from the Mohawk River were only monitored as early as June 6, 2002, so the time period from April 1 to June 6 could not be filled by using the correlation. Figure 597 shows the temperature data and calculated values from the correlation.

The remaining time period from April 1 to June 6 was filled by setting the water temperature on April 1 and allowing the model to linearly interpolate between the values in April and June. This approach was taken due to the lack of data available during the spring of 2002 to use in a correlation. Since the Mosby Creek flow was not large compared to Row River and the Coast Fork Willamette River, the linear interpolation should not have much influence on the temperature calibration.

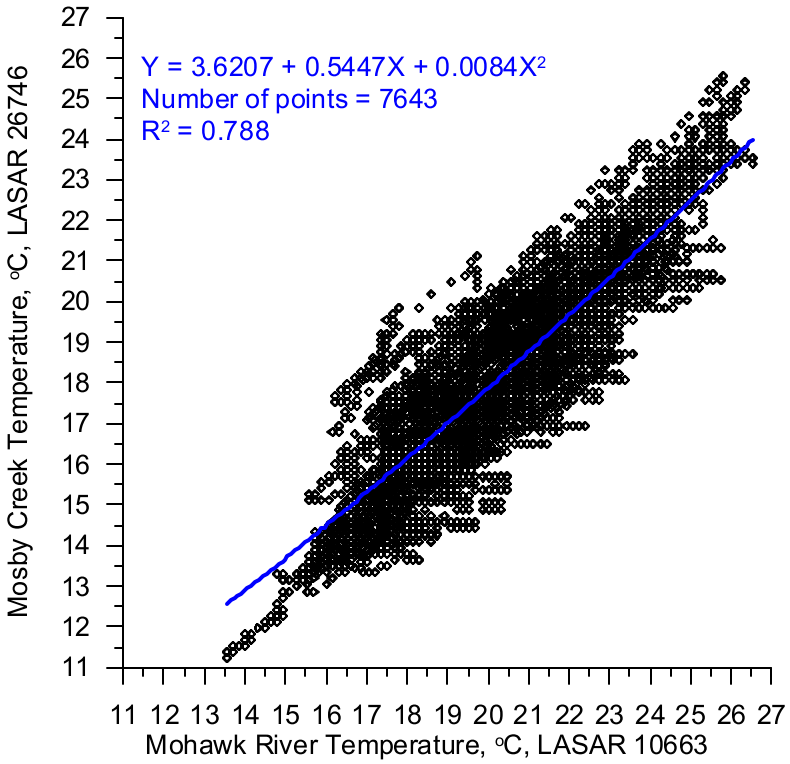


**Figure 596. Mosby Creek temperature correlation, 2002**

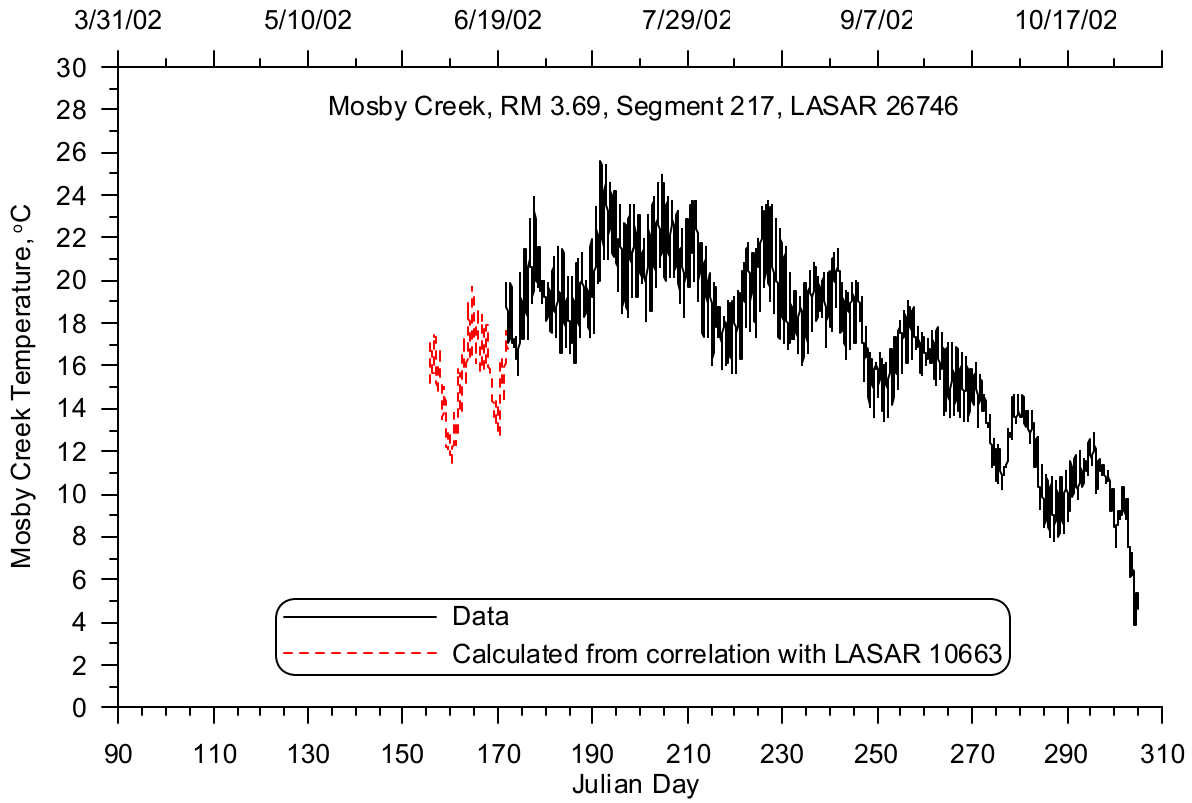


**Figure 597. Mosby Creek temperature, 2002**

## *Point Sources*

ODEQ identified a single major point source discharges over the Coast Fork & Middle Fork Willamette River model area on the basis of permitted discharge. The City of Cottage Grove discharges wastewater effluent from their wastewater treatment plant (WWTP) to the Coast Fork Willamette River at RM 21.1, which corresponds to model segment 52. The discharge flow and temperature were compiled by ODEQ and consisted from data reported by the WWTP and monthly monitoring reports. The location of the WWTP is shown in Figure 598.

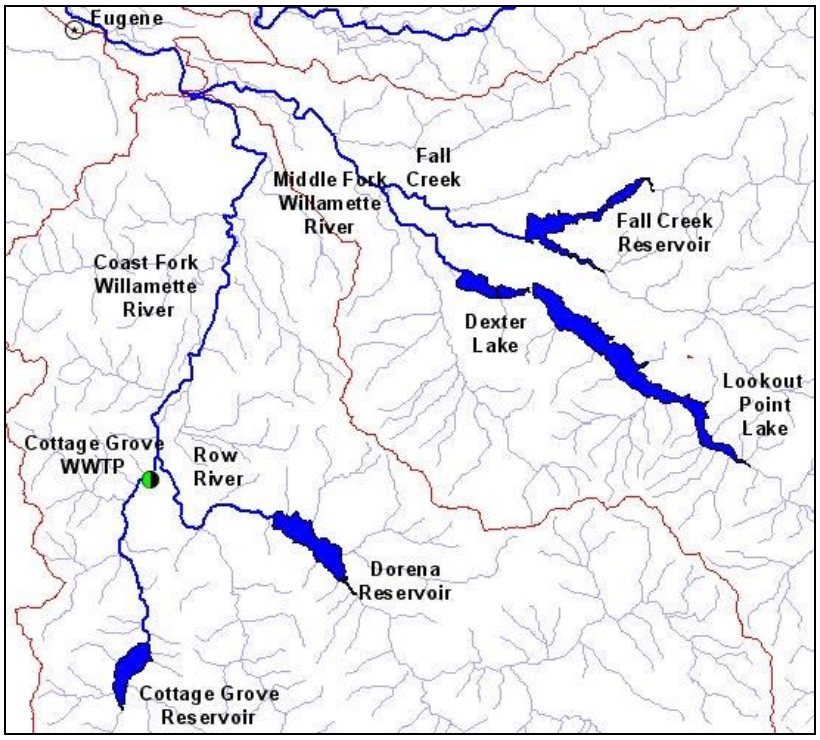


**Figure 598. Coast Fork and Middle Fork Willamette River model point sources**

## Hydrodynamic Data

### Year 2001

The Cottage Grove WWTP recorded daily discharge flows which were used to develop the model inflow file. Figure 599 shows the daily flows for 2001 and illustrates that the flow, typically under 0.1 $m^3/s$, were considerably lower than Coast Fork Willamette River flow, which was as low at 1.5 $m^3/s$. The figure also shows the flow was relatively constant throughout the summer with small increases in the spring and fall.

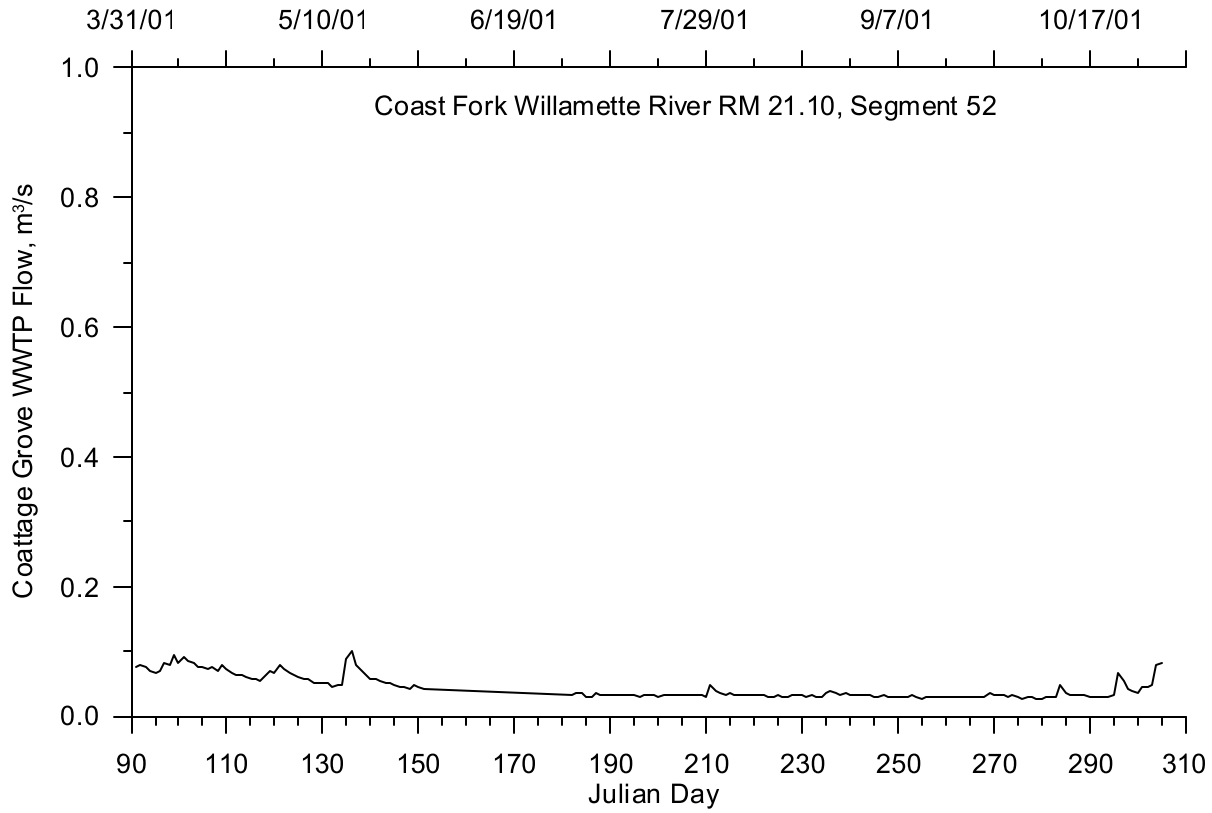


**Figure 599. Cottage Grove WWTP discharge, 2001**

### Year 2002

There was no flow data available for the Cottage WWWTP for 2002 so the flow data from 2001 were used. Figure 599 shows the daily flows for 2001.

## Temperature Data

### Year 2001

The wastewater treatment plan monitored the effluent temperature on an hourly basis from June 1 to the end of the year. Since there were no data available before June 1 to complete the record to April 1 the temperature data from 2002 were used. Figure 600 shows the effluent temperature for 2001 with data from 2002 included. The data shows some diurnal fluctuations and a general seasonal warming as seen in the upstream boundary conditions and tributary inflow. A small change occurs in the data recorded after September 7, 2001 with temperatures recorded in a more step function nature. This may due to a change in the instrument used for monitoring or its resolution.

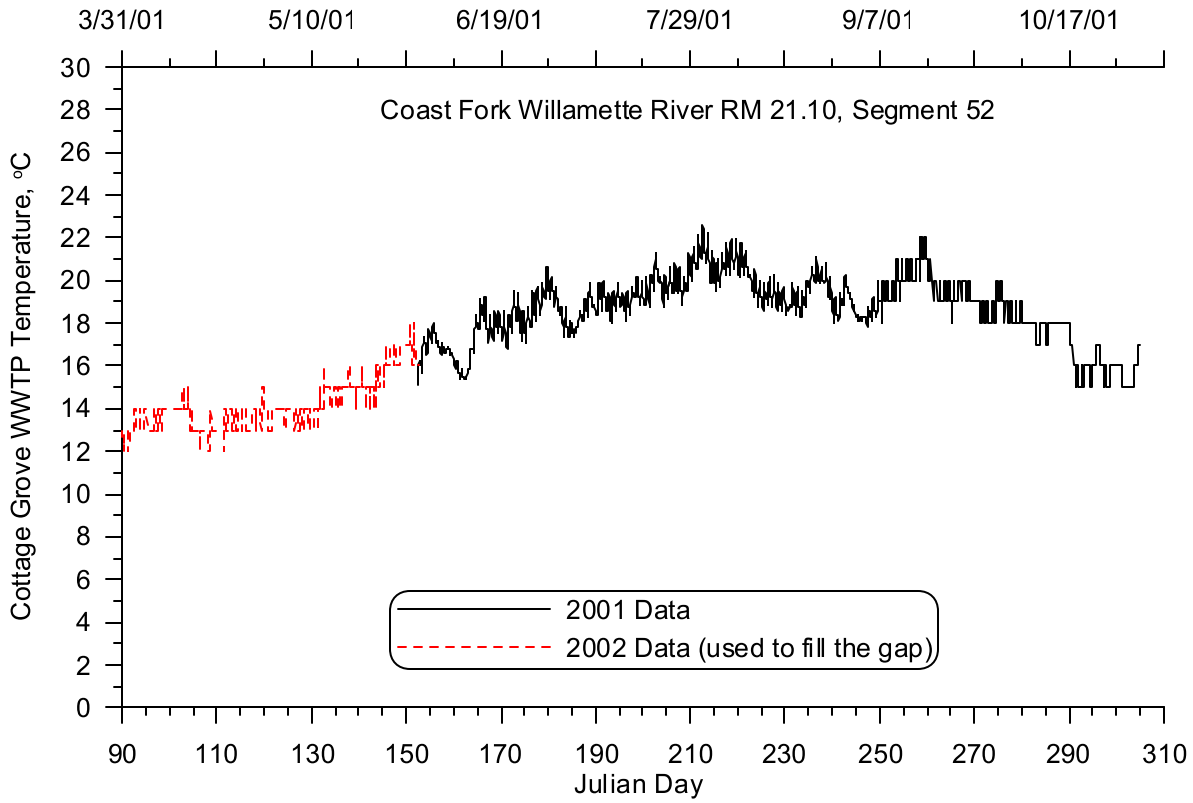


**Figure 600. Cottage Grove WWTP discharge temperature, 2001**

## Year 2002

The wastewater treatment plan monitored their effluent temperature on an hourly basis from the beginning of the year until July 3, 2002. Since there were no data available after July 1 to complete the temperature record to October 31 the temperature data from 2001 were used. Figure 601 shows the effluent temperature for 2002 with data from 2001 included. The data showed some diurnal fluctuations and a general seasonal warming over the summer.

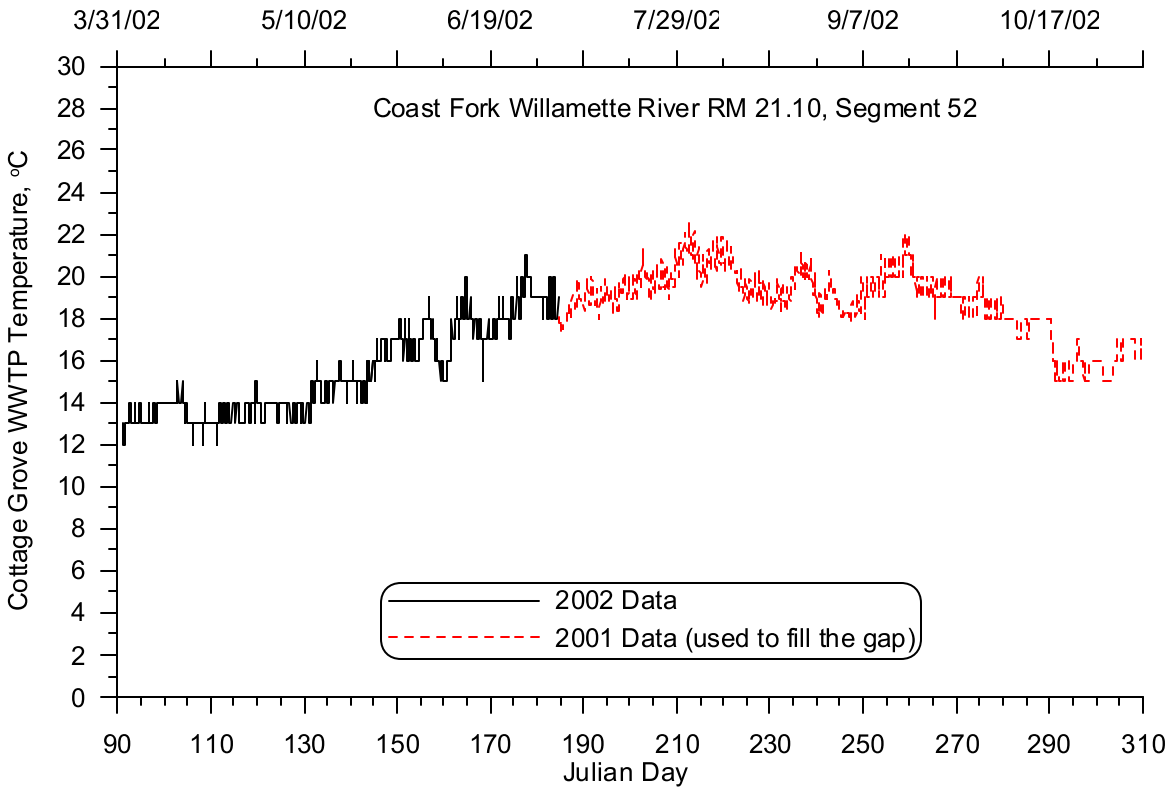


**Figure 601. Cottage Grove WWTP discharge temperature, 2002**

## *Shading*

CE-QUAL-W2 incorporates both topographic and vegetative shade in the model. Topographic characteristics include the steepest inclination angle in 18 directions around a model segment. The vegetative characteristics consist of tree top elevation, distance between the river channel centerline and the controlling vegetation, and the vegetation density in summer and winter. The vegetation characteristics were provided for both banks of the river.

The vegetation and topographic characteristics for the Middle Willamette River model were developed using geographic information system (GIS) data supplied by the Oregon Department of Environmental Quality (ODEQ). The data consists of thalweg points every 100 ft along the thalweg of the river. For each thalweg point, additional associated data included: channel width, elevation, three topographic inclination angles, and nine vegetation compartments for each bank. Each vegetation compartment consisted of vegetation height, distance from stream bank, and density. A detailed analysis was performed to convert the ODEQ data into the shade variables for the CE-QUAL-W2 model. A detailed description of the shade analysis is shown in Appendix A.

### Coast Fork Willamette River

Figure 602 and Figure 603 show the tree top elevations along the Coast Fork Willamette River for the Left and Right Banks, respectively. The figures show the tree top elevations decreasing downstream, which follows the general elevation trend of the river banks. There were several pockets where the vegetation was slightly shorter. Figure 604 and Figure 605 show the distance from the river centerline

to controlling vegetation for the left and right banks, respectively. These figures show that the vegetation was close to river at the upstream end as expected and the width away increases moving downstream as the channel widens. Figure 606 and Figure 607 show the vegetation density for the left and right banks, respectively. The vegetation density plots indicated that the density was higher for both banks at the upstream end but becomes more variable progressing downstream.

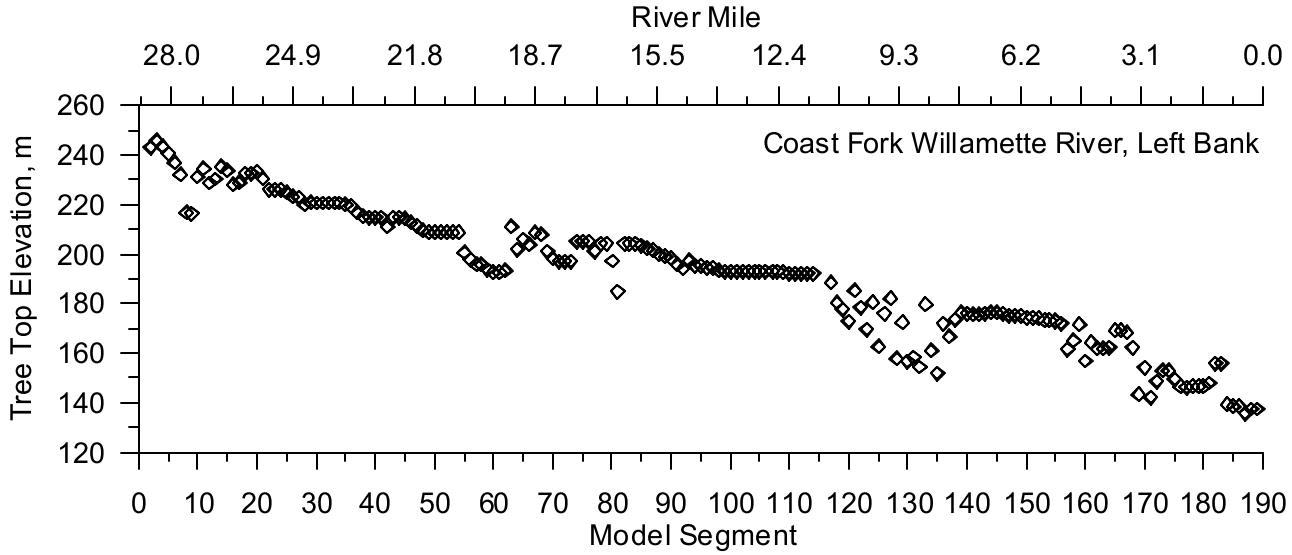


**Figure 602. Coast Fork Willamette River Left Bank Tree Top Elevation**

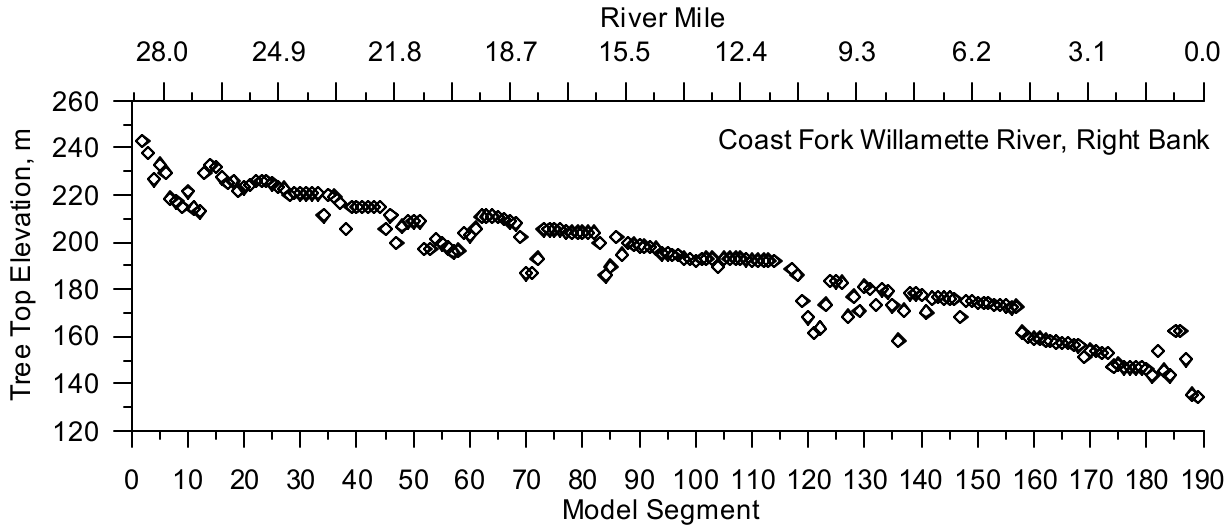


**Figure 603. Coast Fork Willamette River Right Bank Tree Top Elevation**

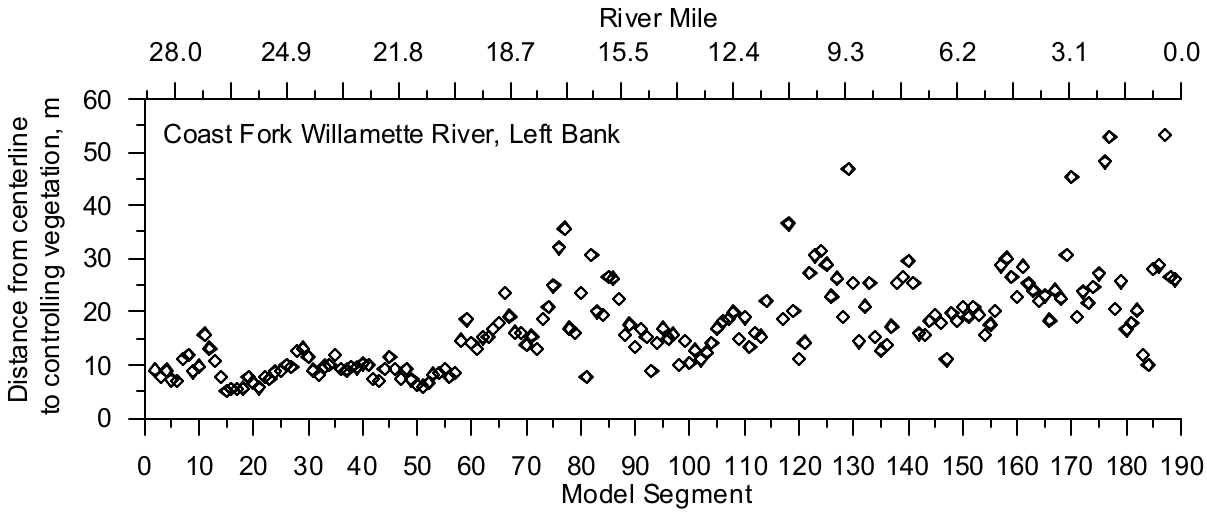


**Figure 604. Coast Fork Willamette River Left Bank Distance from Centerline to Controlling Vegetation**

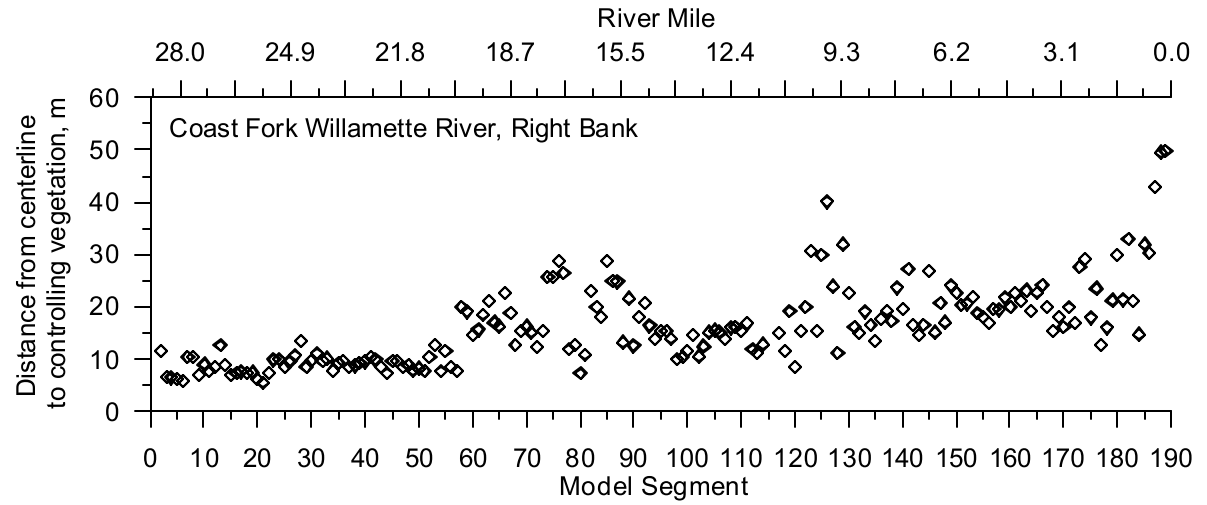


**Figure 605. Coast Fork Willamette River Right Bank Distance from Centerline to Controlling Vegetation**

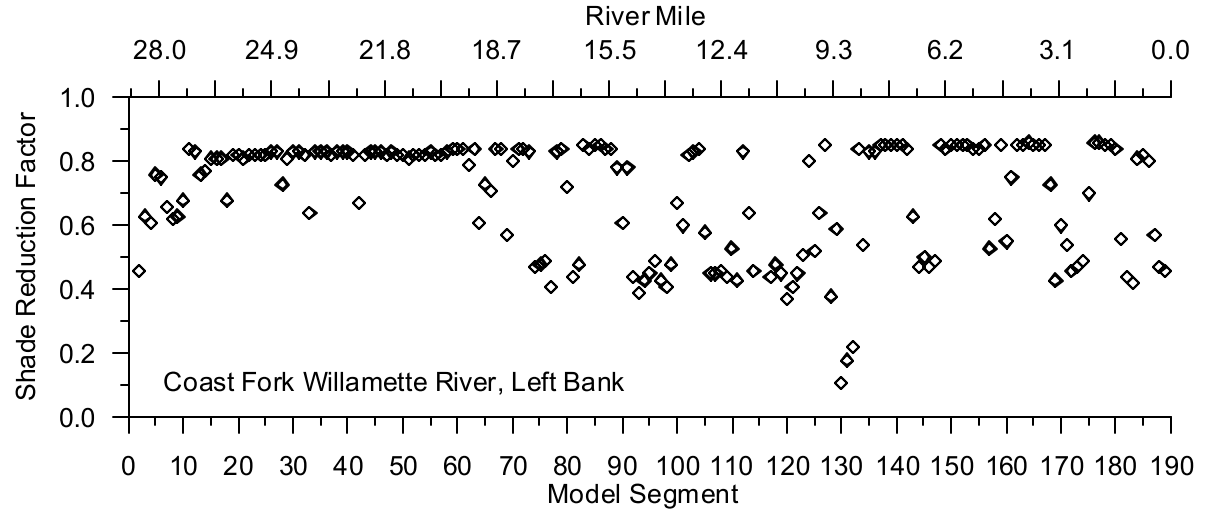


**Figure 606. Coast Fork Willamette River Left Bank Shade Reduction Factor**

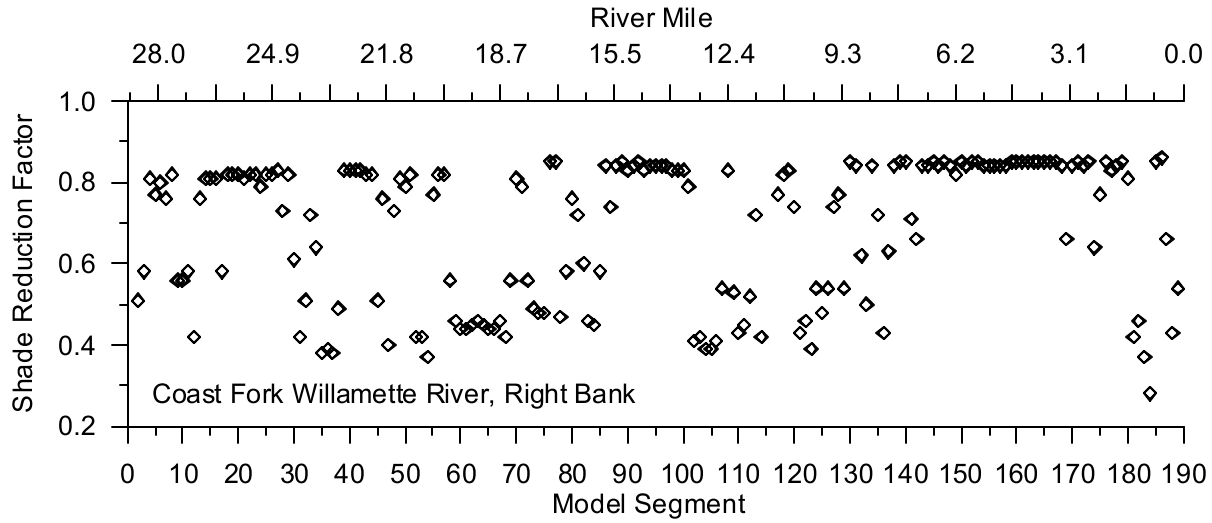


**Figure 607. Coast Fork Willamette River Right Bank Shade Reduction Factor**

## Row River

Figure 608 and Figure 609 show the tree top elevation for the left and right banks, respectively, for Row River. Both figures show the vegetation top elevation decreasing moving downstream, which follows the bank elevations. The plots also showed that the vegetation elevations were more variable at the upstream end of the river and more variable on the left bank than the right bank. Figure 610 and Figure 611 illustrate the distance from the river centerline to the controlling vegetation for the left and right banks, respectively. Figure 612 and Figure 613 show the vegetation density on each bank. The vegetation densities for both banks were highly variable moving downstream.

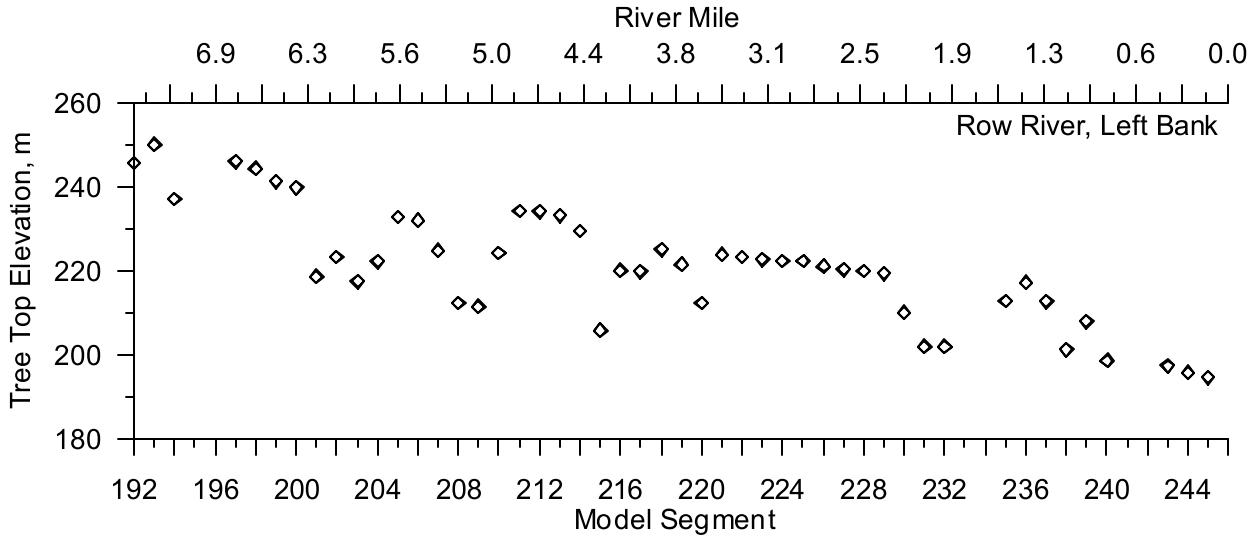


**Figure 608. Row River Left Bank Tree Top Elevation**

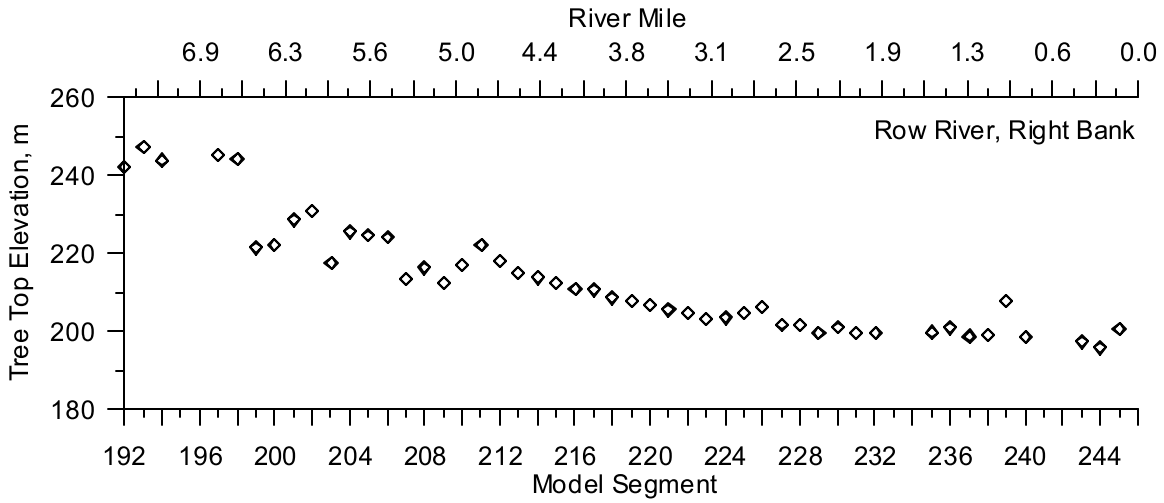


**Figure 609. Row River Right Bank Tree Top Elevation**

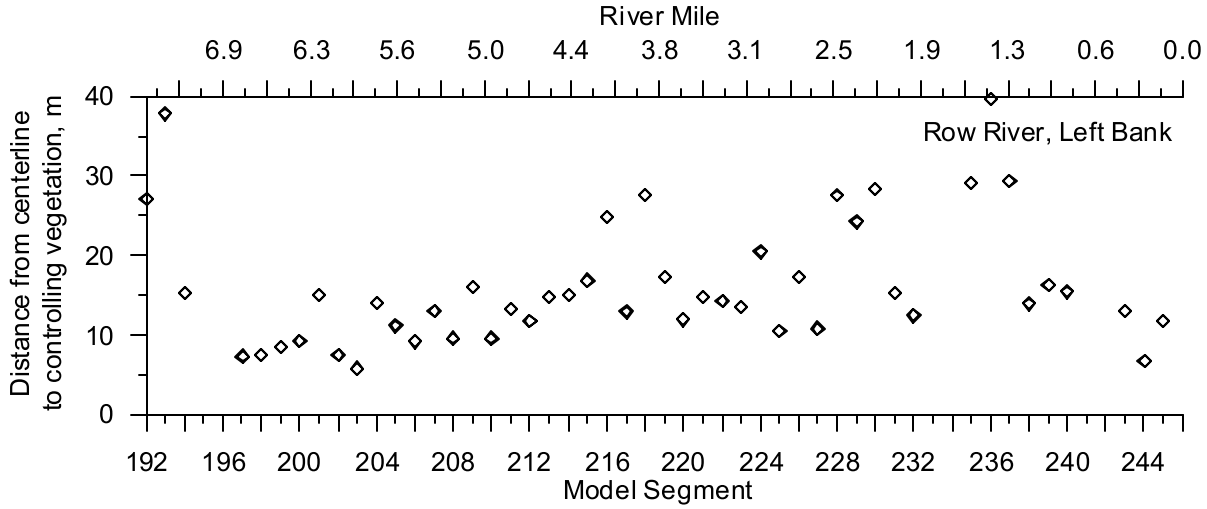


**Figure 610. Row River Left Bank Distance from Centerline to Controlling Vegetation**

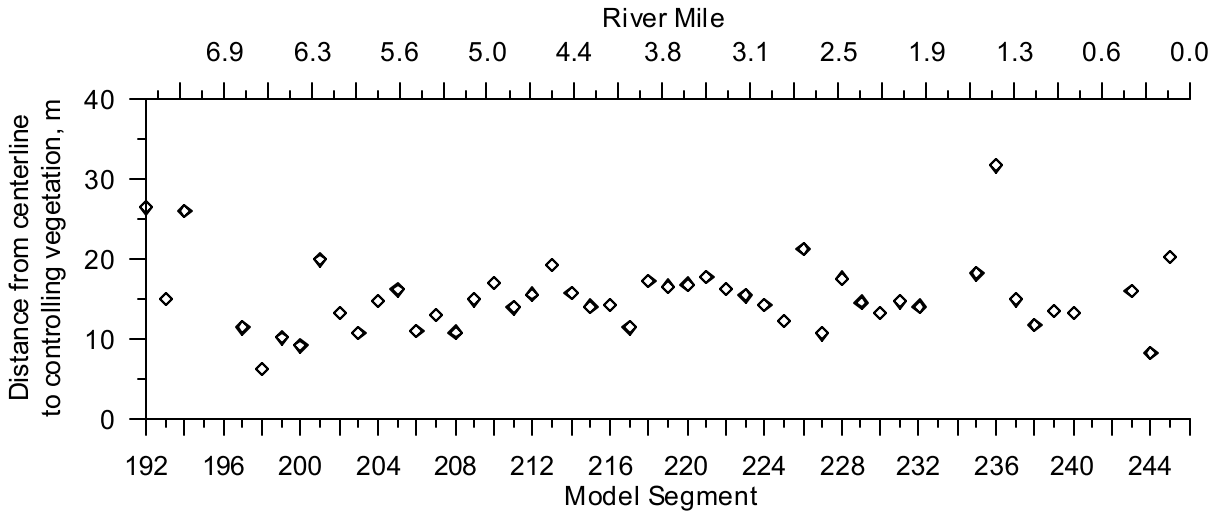


**Figure 611. Row River Right Bank Distance from Centerline to Controlling Vegetation**

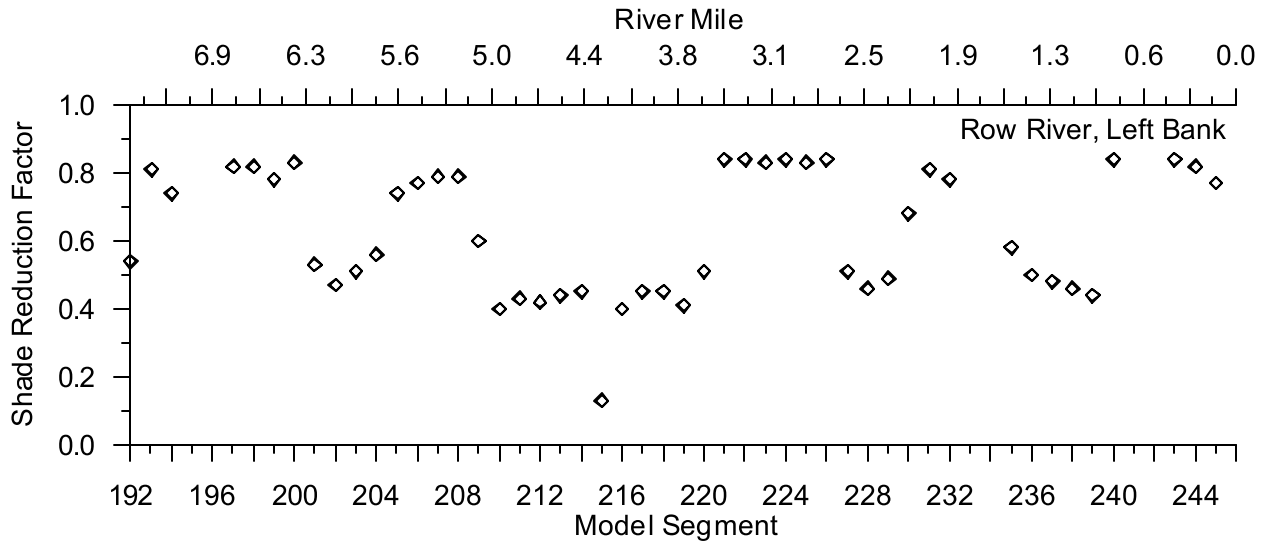


**Figure 612. Row River Left Bank Shade Reduction Factor**

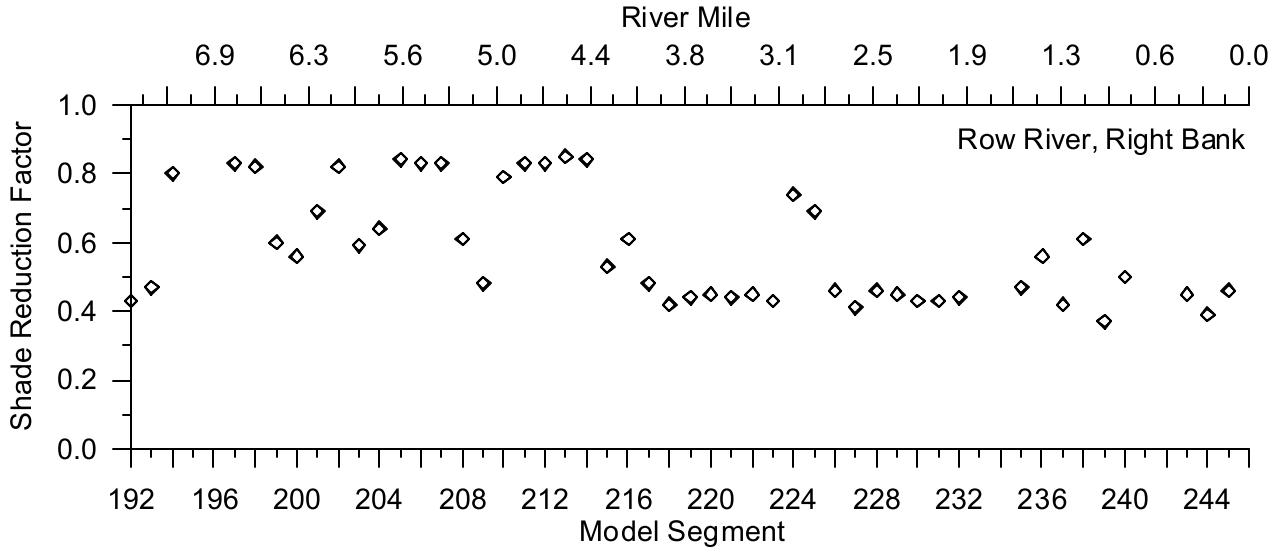


**Figure 613. Row River Right Bank Shade Reduction Factor**

## Middle Fork Willamette River

Figure 614 and Figure 615 show the tree top elevation for the left and right banks of the Middle Fork of the Willamette River. Both banks showed the tree top elevation decreasing going downstream with a few pockets of decreased vegetation height. Figure 616 and Figure 617 show the distance from the river centerline to the controlling vegetation on the left and right banks, respectively moving downstream. These figures showed that the distance to the vegetation for both banks was similar to the Coast Fork Willamette River but increases to larger than the Coast Fork moving downstream. Figure 618 and Figure 619 show the vegetation density for the left and right banks, respectively. The plots revealed that the vegetation density for the left and right banks was relatively high and higher than reaches of the Coast Fork River.

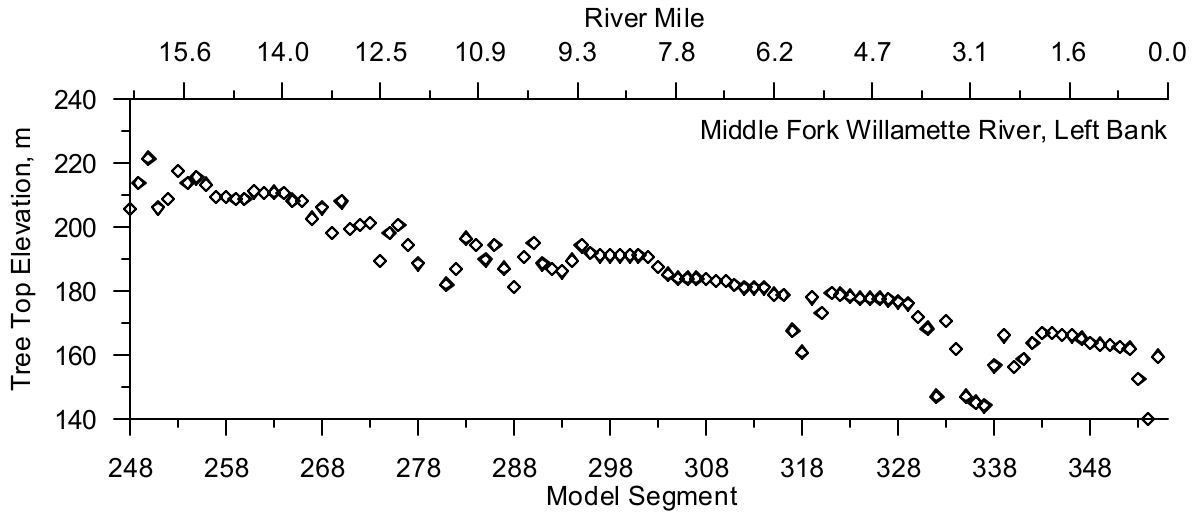


**Figure 614. Middle Fork Willamette River Left Bank Tree Top Elevation**

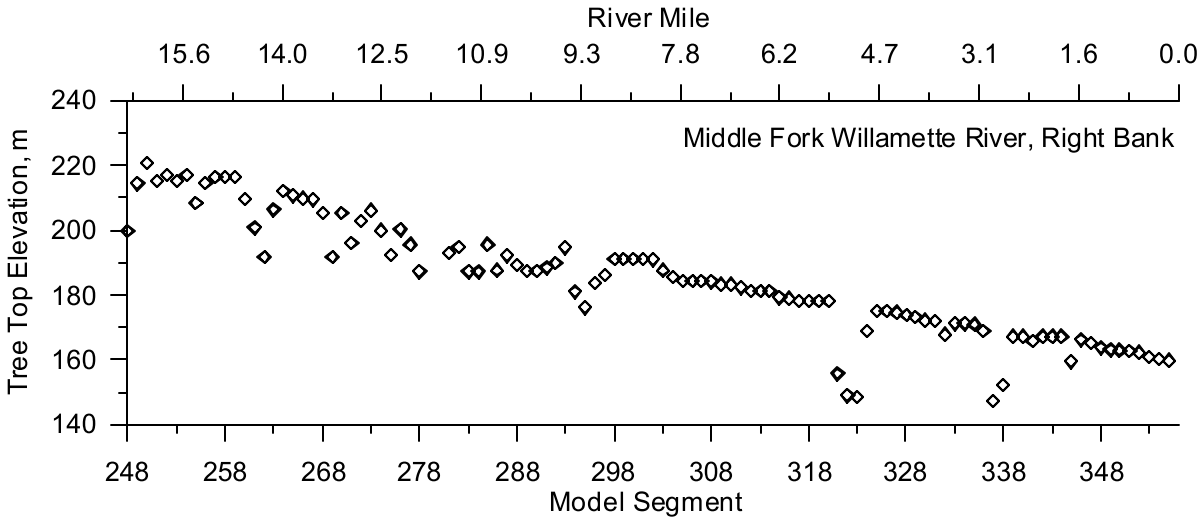


**Figure 615. Middle Fork Willamette River Right Bank Tree Top Elevation**

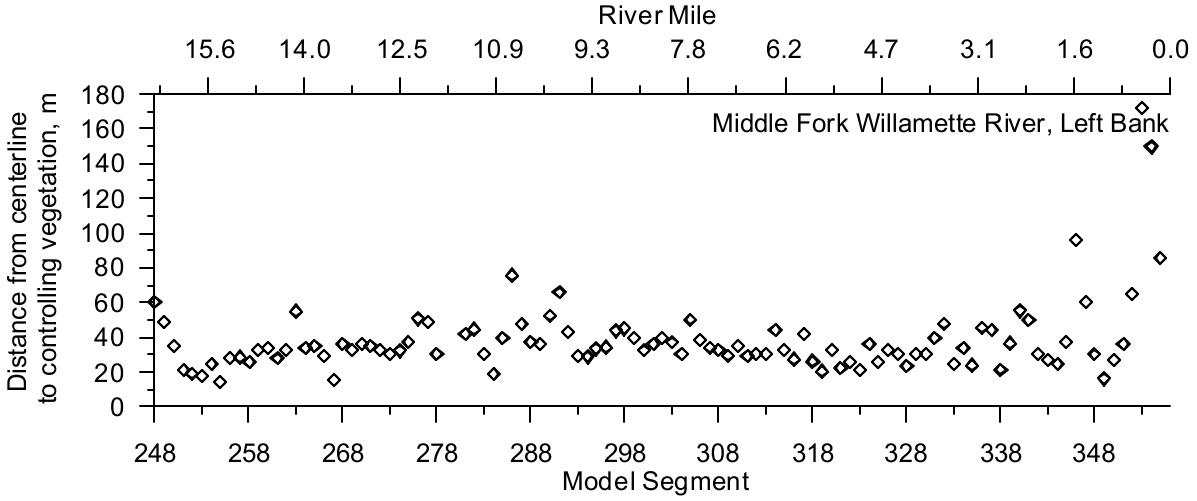


**Figure 616. Middle Fork Willamette River Left Bank Distance from Centerline to Controlling Vegetation**

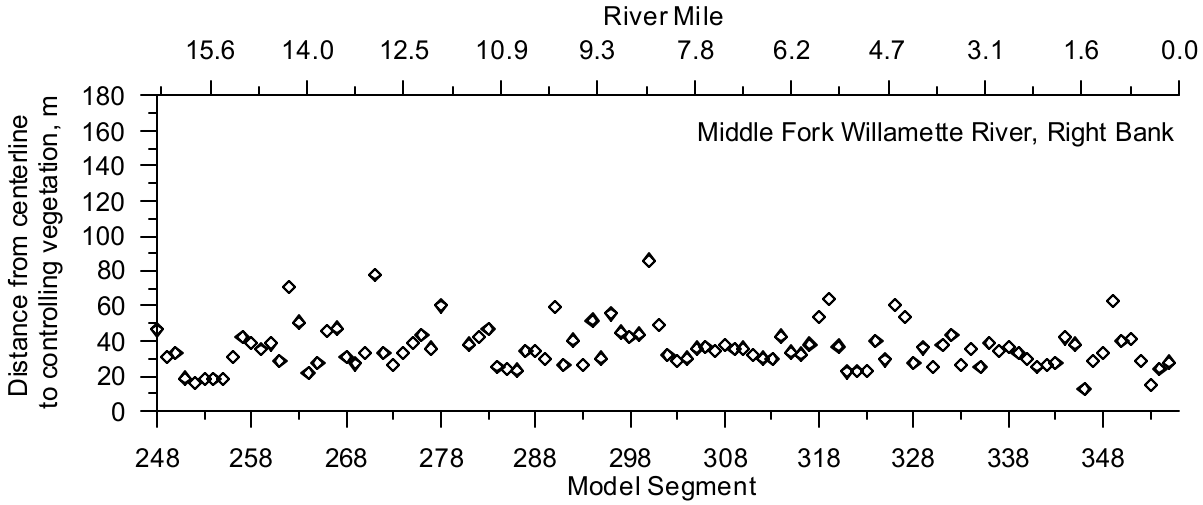


**Figure 617. Middle Fork Willamette River Right Bank Distance from Centerline to Controlling Vegetation**

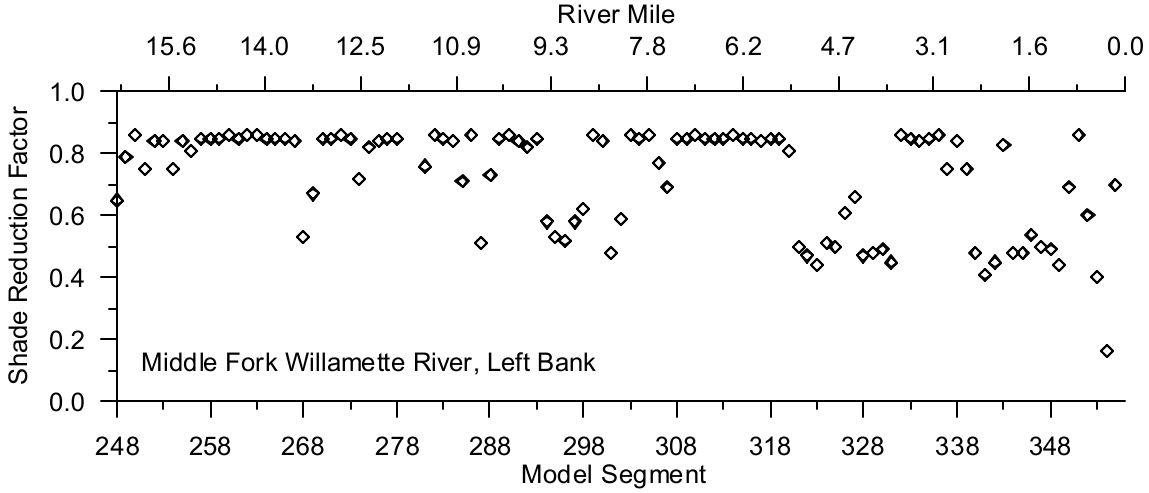


**Figure 618. Middle Fork Willamette River Left Bank Shade Reduction Factor**

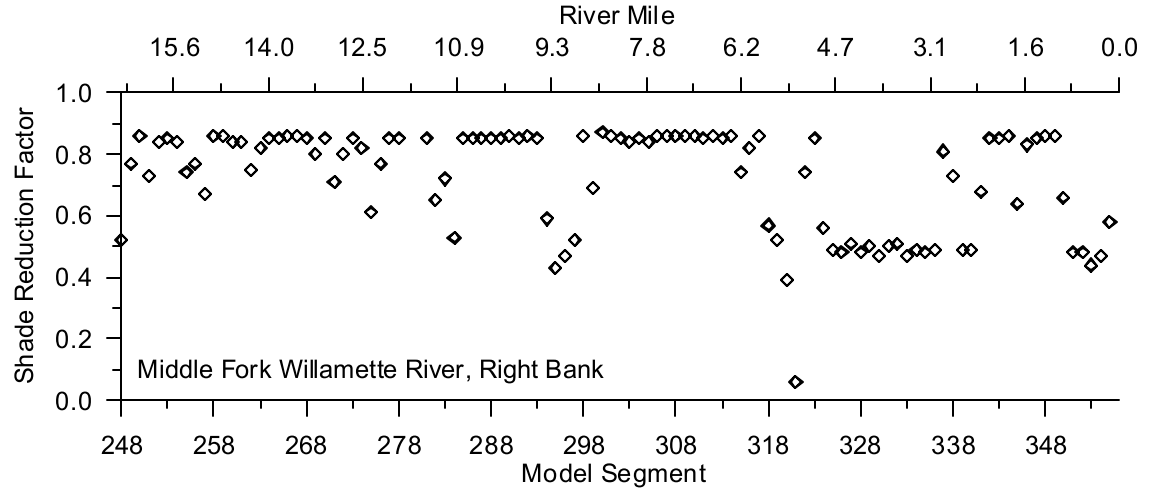


**Figure 619. Middle Fork Willamette River Right Bank Shade Reduction Factor**

## Fall Creek

Figure 620 and Figure 621 show the tree top elevation for both the left and rights banks of Fall Creek, respectively. The vegetation elevations decreased moving downstream with some variations in heights between the left and right banks. Figure 622 and Figure 623 show the distance from the river centerline to the controlling vegetation for the left and right banks, respectively. Figure 624 and Figure 625 show the vegetation density for both banks, which tends to be relatively high compared to other river reaches in the Coast Fork Middle Fork system.

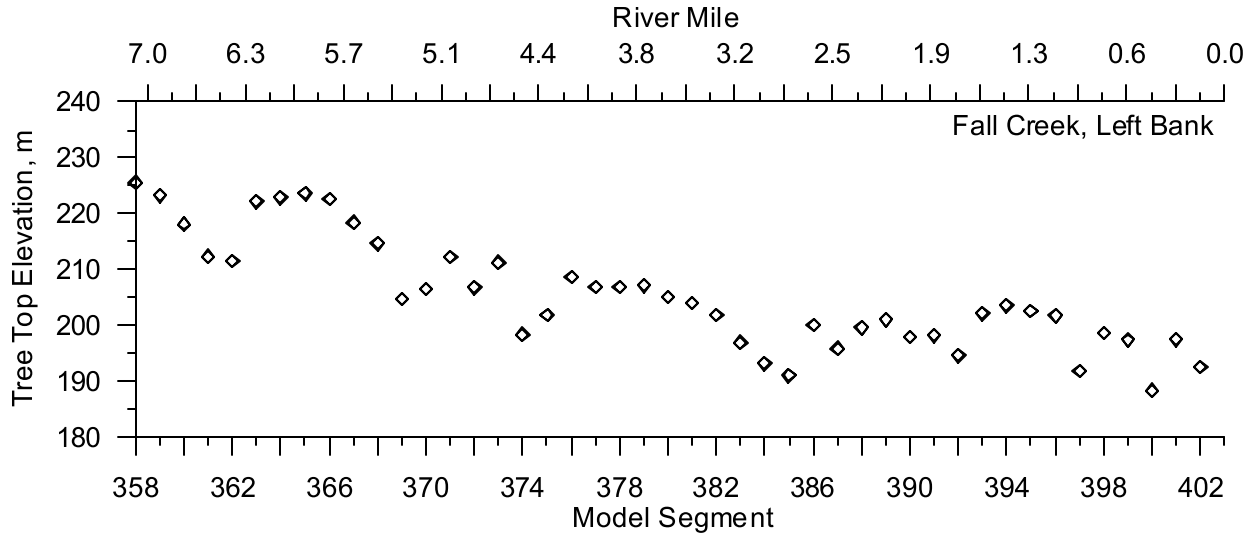


**Figure 620. Fall Creek Left Bank Tree Top Elevation**

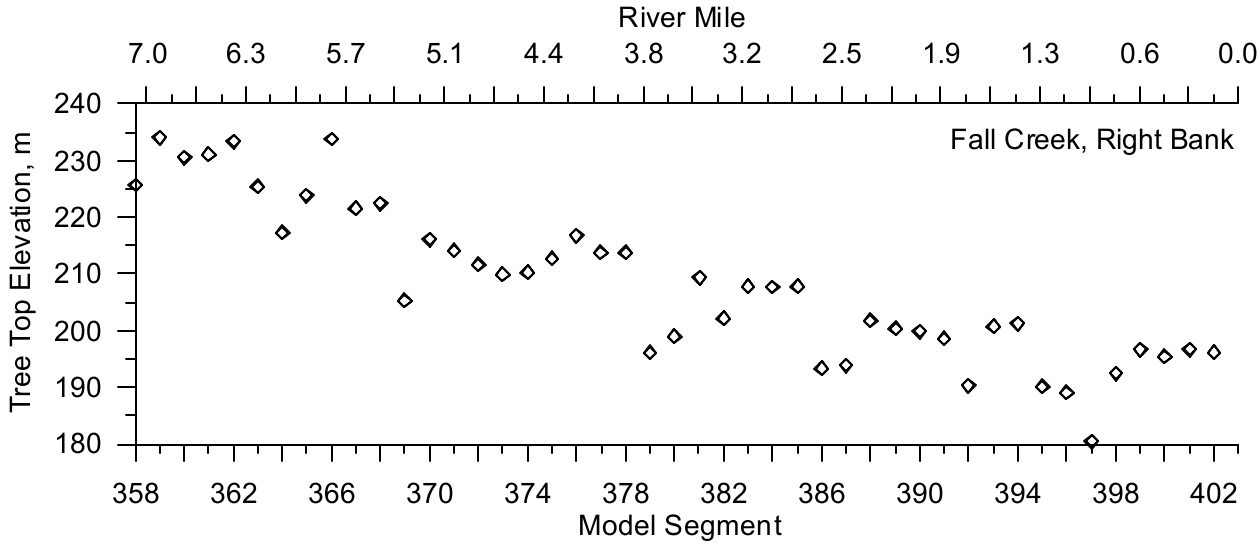


**Figure 621. Fall Creek Right Bank Tree Top Elevation**

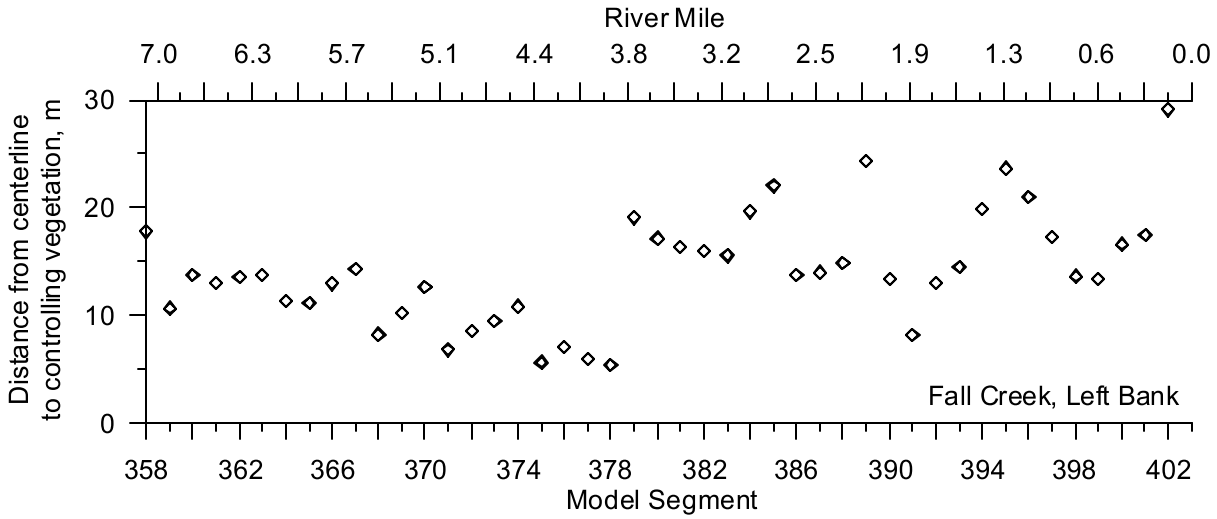


**Figure 622. Fall Creek Left Bank Distance from Centerline to Controlling Vegetation**

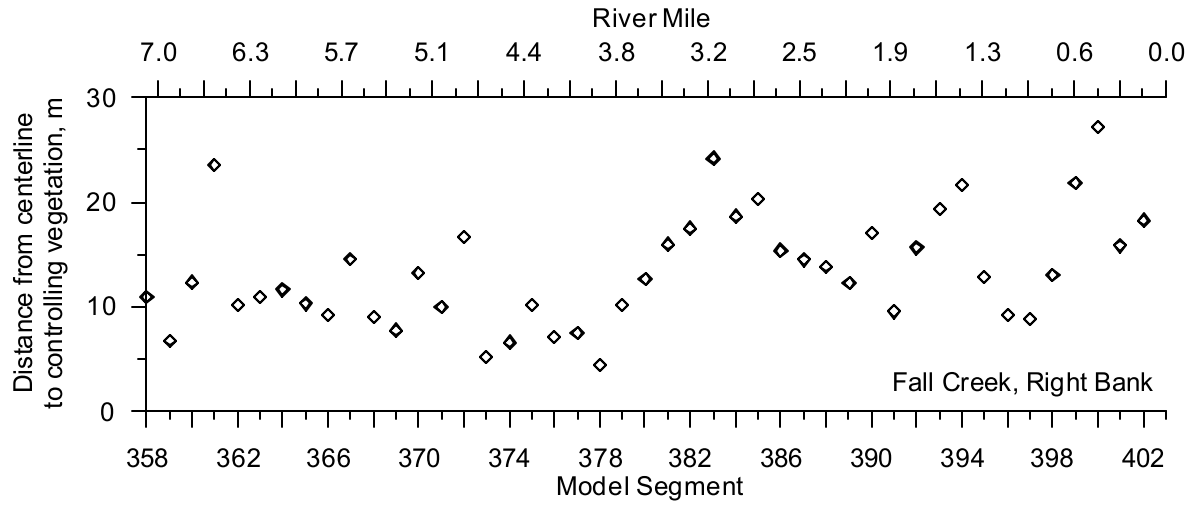


**Figure 623. Fall Creek Right Bank Distance from Centerline to Controlling Vegetation**

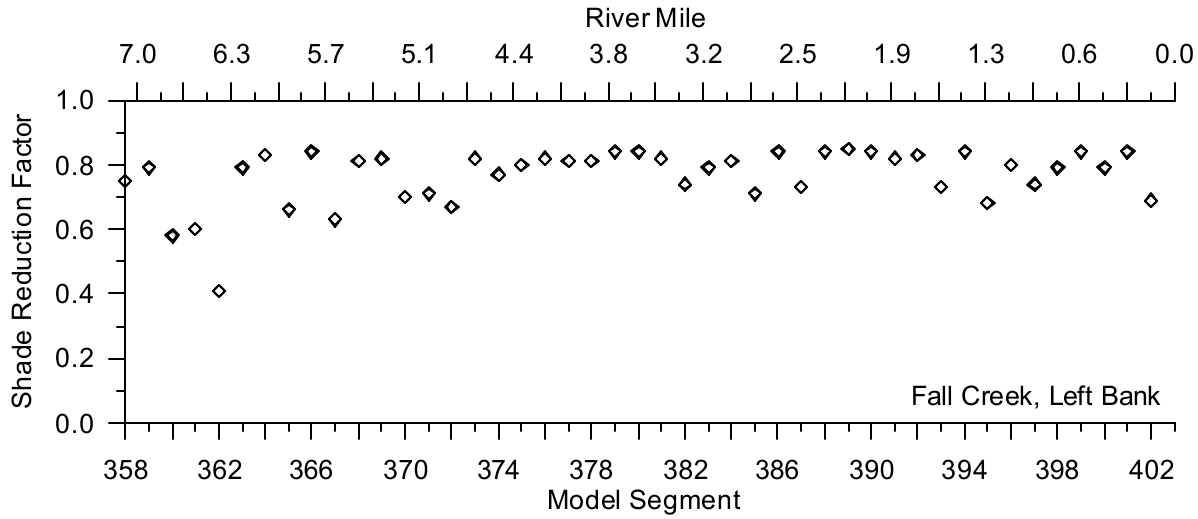


**Figure 624. Fall Creek Left Bank Shade Reduction Factor**

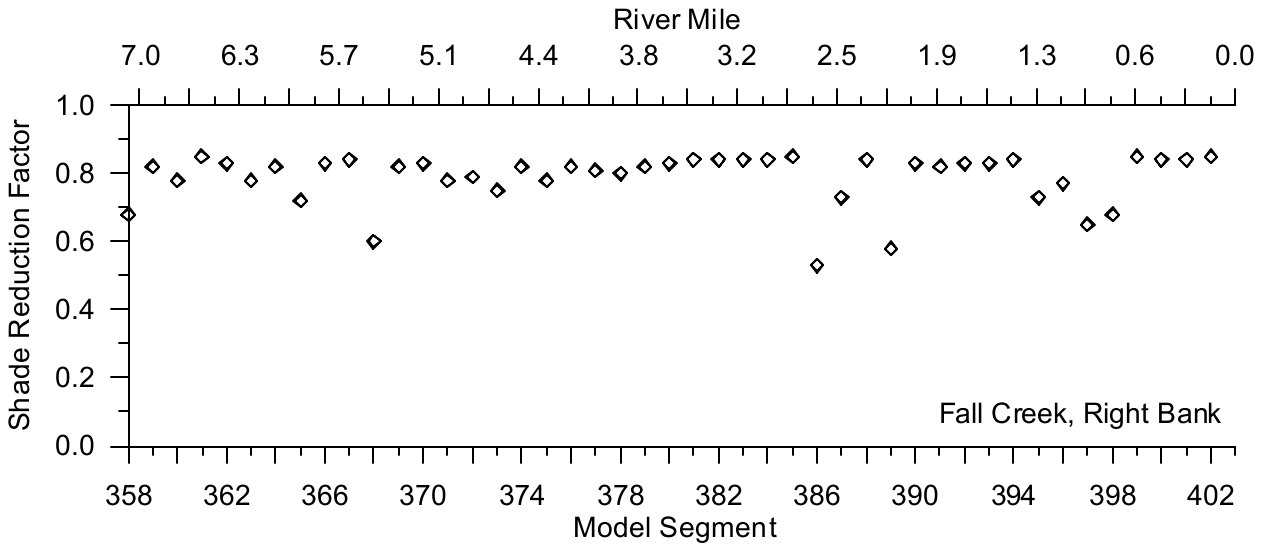


**Figure 625. Fall Creek Right Bank Shade Reduction Factor**

## Willamette River to Springfield

Figure 626 and Figure 627 show the tree top elevations for the left and rights banks of the Willamette River from the confluence of the Coast and Middle Forks to the just south of the City of Springfield. The figures show that the vegetation top elevations relatively constant on the left bank but actually increased moving downstream. Figure 628 and Figure 629 show the distance from the river centerline to the controlling vegetation for the left and right banks, respectively. The distance from the river centerline to the vegetation seems to increase slightly moving downstream for both banks. Figure 630 and Figure 631 show the vegetation density for the two river banks. The left bank vegetation remains relatively constant over the river reach but the right bank varies more and in some areas has higher vegetation density than the left bank.

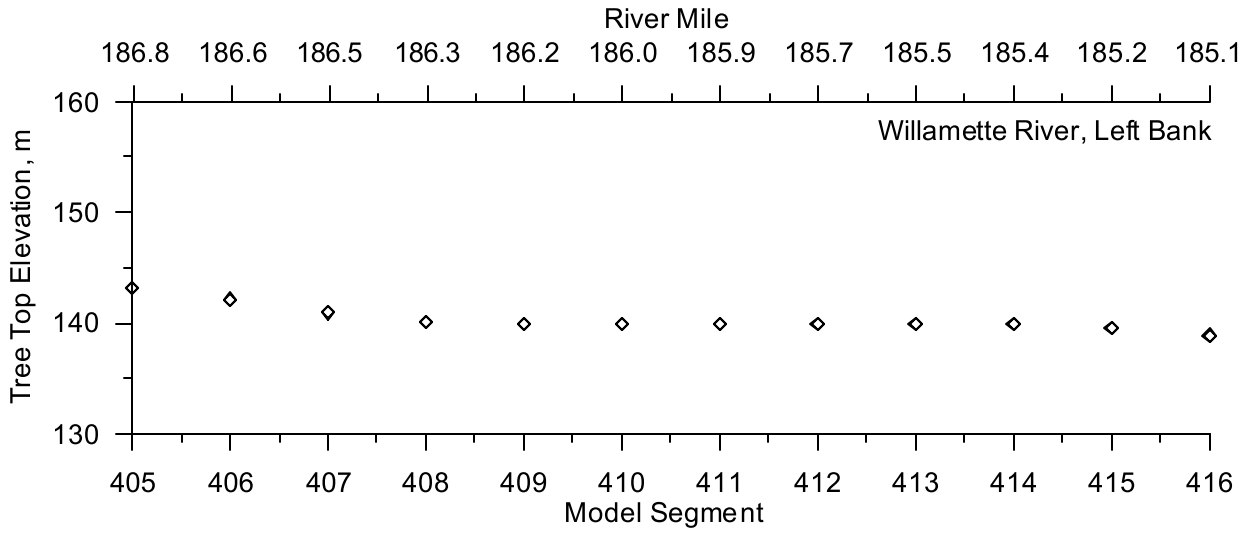


**Figure 626. Willamette River to Eugene Left Bank Tree Top Elevation**

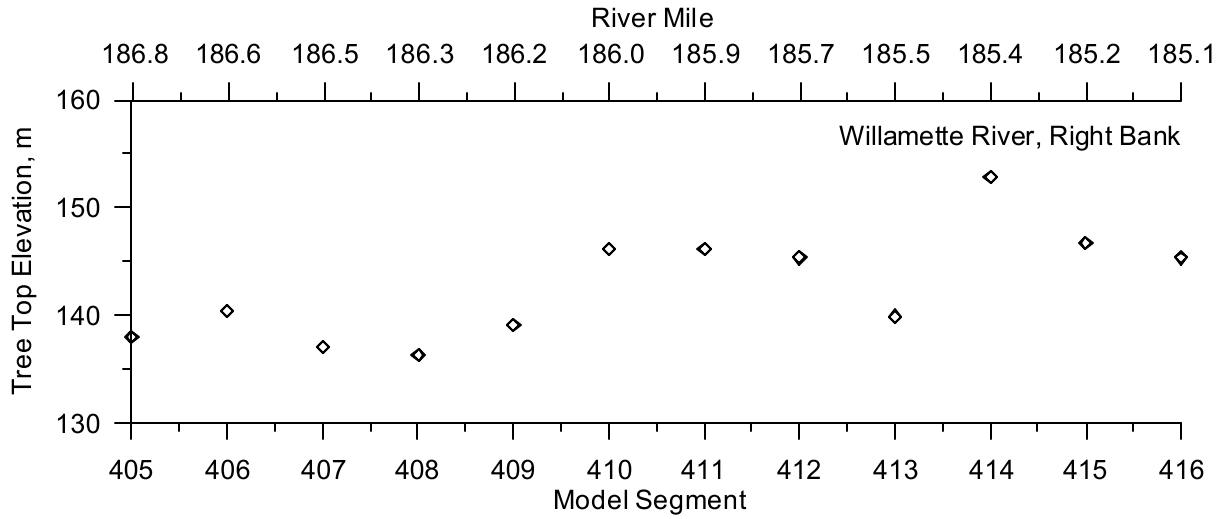


**Figure 627. Willamette River to Eugene Right Bank Tree Top Elevation**

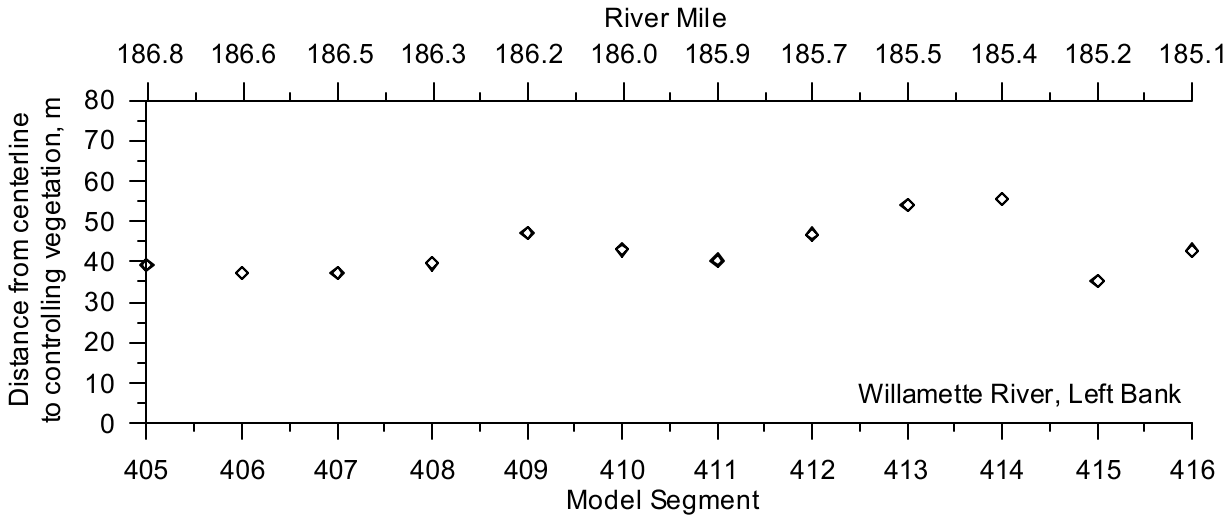


**Figure 628. Willamette River to Eugene Left Bank Distance from Centerline to Controlling Vegetation**

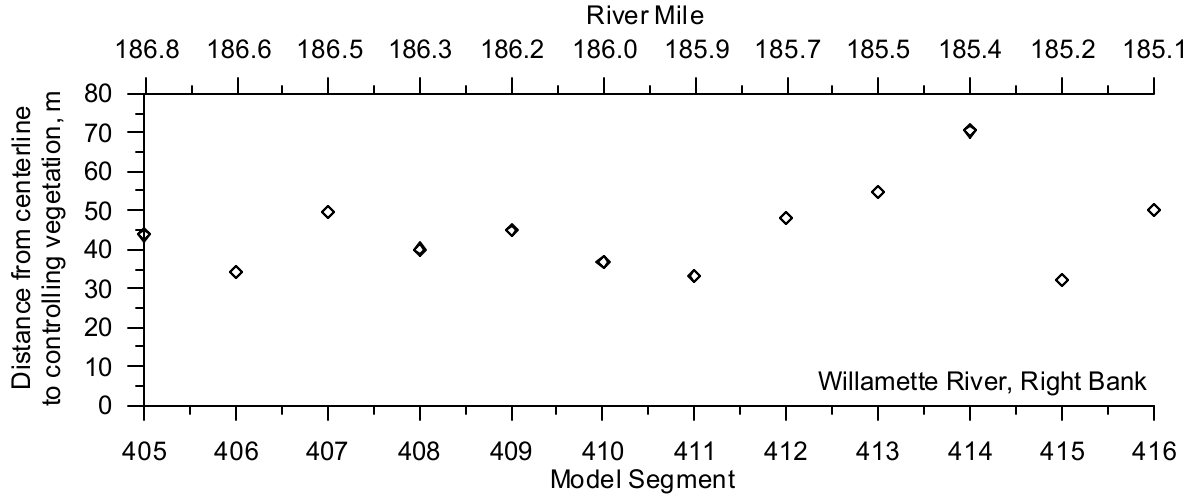


**Figure 629. Willamette River to Eugene Right Bank Distance from Centerline to Controlling Vegetation**

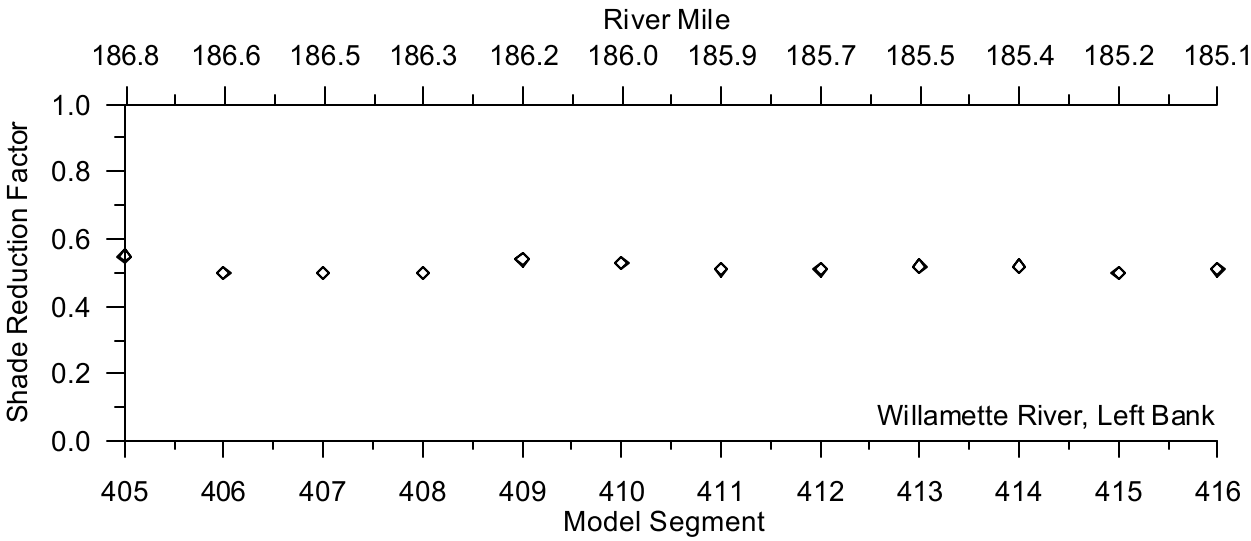


**Figure 630. Willamette River to Eugene Left Bank Shade Reduction Factor**

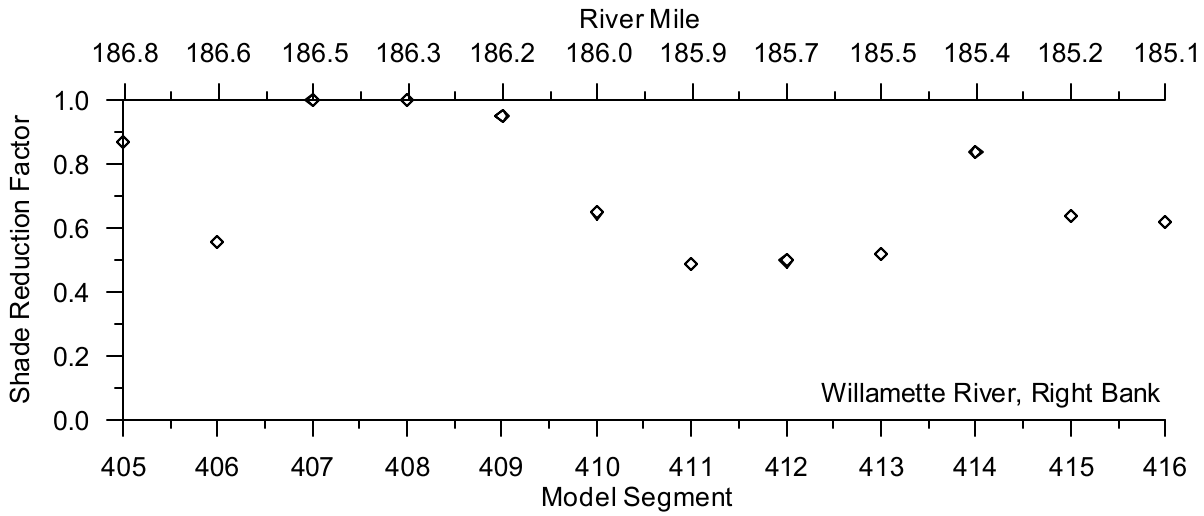


**Figure 631. Willamette River to Eugene Left Bank Shade Reduction Factor**

## *Meteorology*

The Coast Fork Middle Fork model system was relatively spread out ranging from the higher elevations in the Cascade Range down to the Willamette Valley bottom. Meteorological monitoring was conducted by several agencies, such as the National Weather Service, U.S. Forest Service and the Oregon Department of Forestry (ODF) to develop the meteorological data for the model. The model uses the meteorological parameters: air and dew point temperature, wind speed and direction, cloud cover and solar radiation. Figure 632 shows the meteorological sites used for the Coast Fork and Middle Fork Willamette River basins. Table 64 lists the sites and the agencies responsible for data collection. Meteorological data from Hawley Butte was not used because some of the meteorological data was believed to be in error. There was no information to help to determine which data records in the set were in error, so these data were not used.

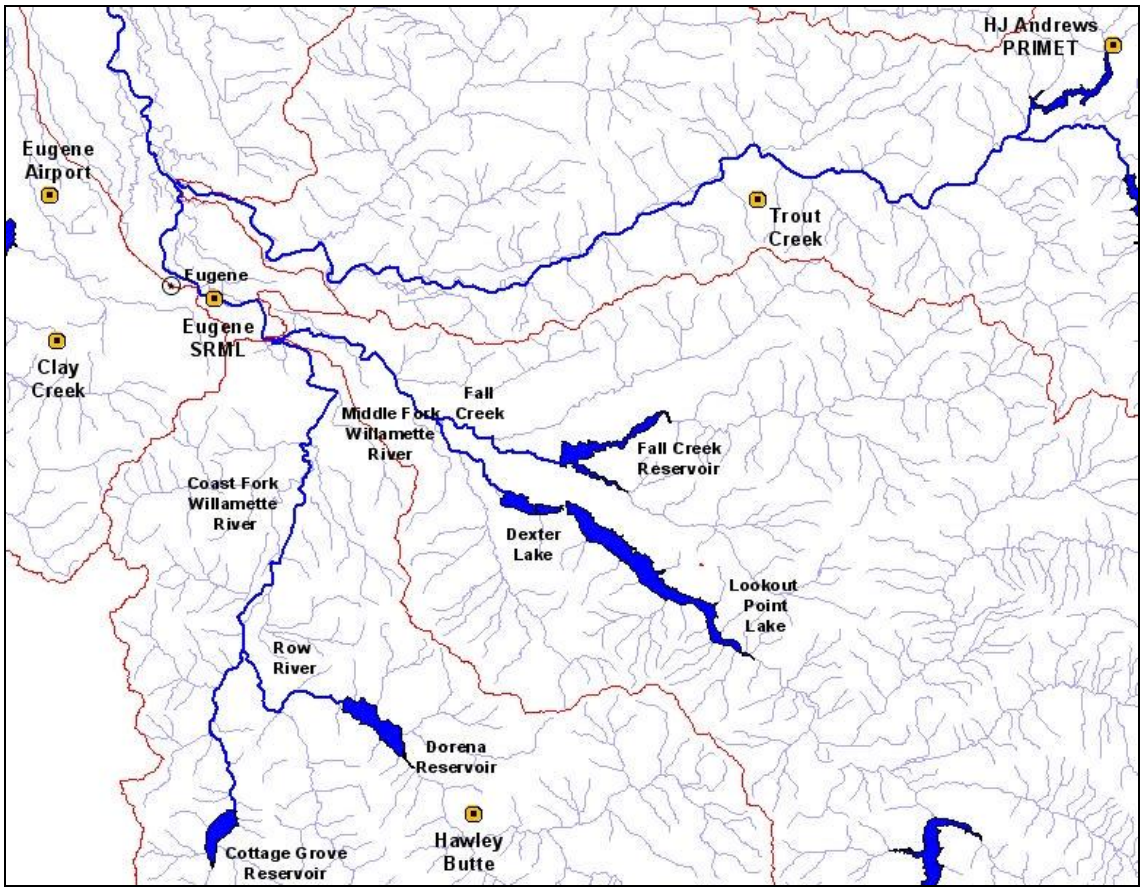


**Figure 632. Coast Fork and Middle Fork Willamette River model meteorological monitoring site locations**

**Table 64. Coast Fork and Middle Fork Willamette River model meteorological monitoring sites**

| Site | Agency (Program) | Meteorological Parameters |
|---|---|---|
| Hawley Butte | Oregon Department of Forestry (RAWS) | Air Temperature, Relative Humidity, Wind Speed, Wind Direction |
| Clay Creek | Oregon Department of Forestry (RAWS) | Air Temperature, Relative Humidity, Wind Speed, Wind Direction |
| Trout Creek | Oregon Department of Forestry (RAWS) | Air Temperature, Relative Humidity, Wind Speed, Wind Direction |
| H.J. Andrews Research Forest | Oregon State University | Air Temperature, Relative Humidity, Wind Speed, Wind Direction, Solar Radiation |
| Eugene WSO / Mahlon Sweet Airport | National Weather Service (METAR) | Air Temperature, Dew Point Temperature, Relative Humidity, Wind Speed, Wind Direction, Cloud Cover |
| Eugene | University of Oregon, Solar Radiation Monitoring Lab | Solar Radiation |

## Clay Creek

Clay Creek is monitored by the Oregon Department of Forestry as part of their forest fire monitoring network. The meteorological data gathered were applied to the Coast Fork Willamette River and the Row River. The site monitored air temperature, relative humidity, wind speed and wind direction. Cloud cover and solar radiation from the Eugene Airport were used to supplement the Clay Creek data. The solar radiation monitored represents global radiation. The air temperature and relative humidity were used to calculate the dew point temperature using an equation from Singh, 1992.

### Year 2001

Most of the meteorological data records were complete from April 1, 2001 to October 31, 2001, with an hourly recording frequency. There was a gap in the wind speed and direction data from June 5 to 22, 2001, so wind speed and wind direction data from the Eugene Airport were used. Figure 633 shows the air temperature monitored at the Clay Creek site for 2001. Figure 634 shows the calculated dew point temperature using the air temperature and relative humidity. Figure 635 shows the wind speed data monitored during 2001. The data shows that when wind speeds drop below 0.5 m/s the values were set to zero. Many of the wind speed values recorded and shown in this figure were less than the minimum value of 0.50 m/s. This may result in an under prediction of wind speeds for this location; however, low wind speeds have little influence on air-water interactions. Figure 636 shows a rose diagram of the wind direction and reveals that the wind directions were broken into 8 bins of 45 degrees. Figure 637 shows the cloud cover used and represents the cloud cover data monitored at the Eugene Airport since no cloud cover data were monitored at the Clay Creek site. The figure shows the coarseness of the cloud cover data recorded at the airport with only about five different cloud cover designations. The data points between the five values are the result of interpolations to fill data gaps in the cloud cover data. Figure 638 shows the global solar radiation from Eugene, OR, used since no solar radiation data was monitored at the Clay Creek site.

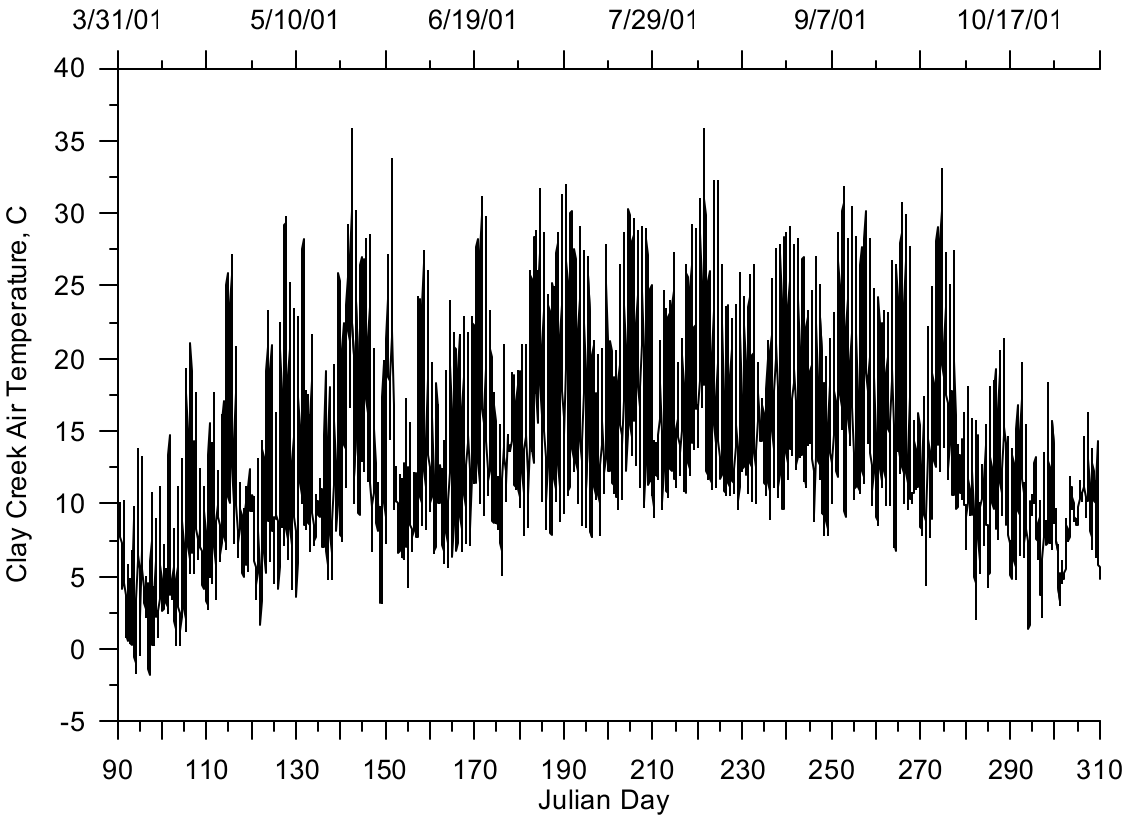


**Figure 633. Air temperature at Clay Creek, 2001**

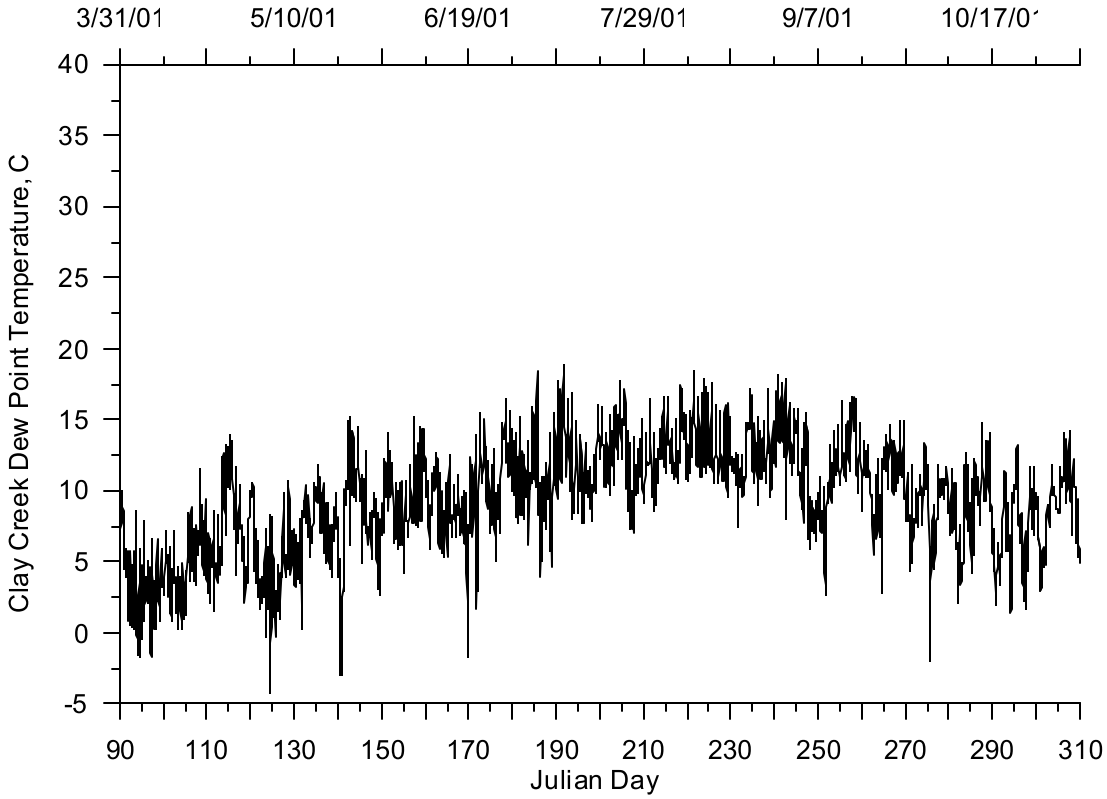


**Figure 634. Dew point temperature at Clay Creek, 2001**

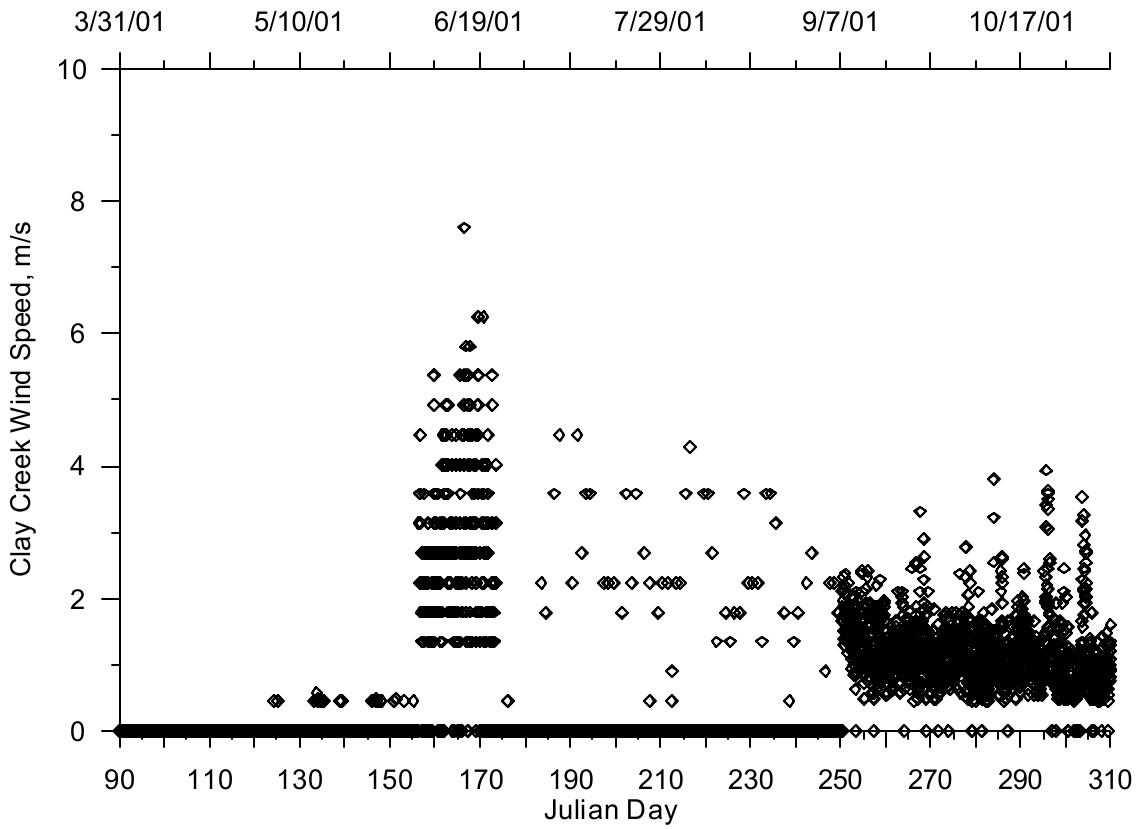


**Figure 635. Wind speed at Clay Creek, 2001**

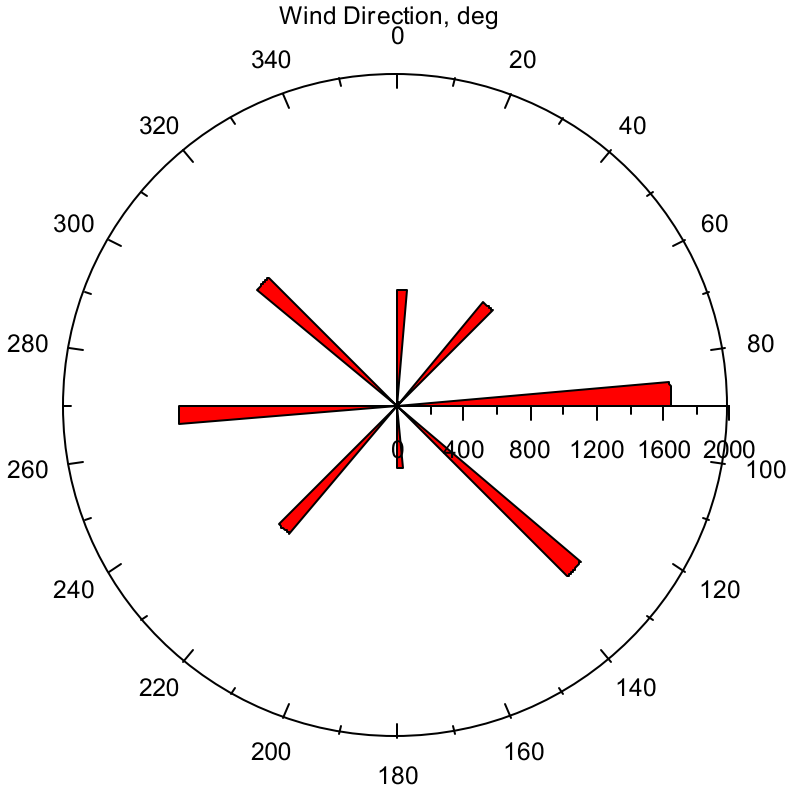


**Figure 636. Wind direction at Clay Creek, 2001**

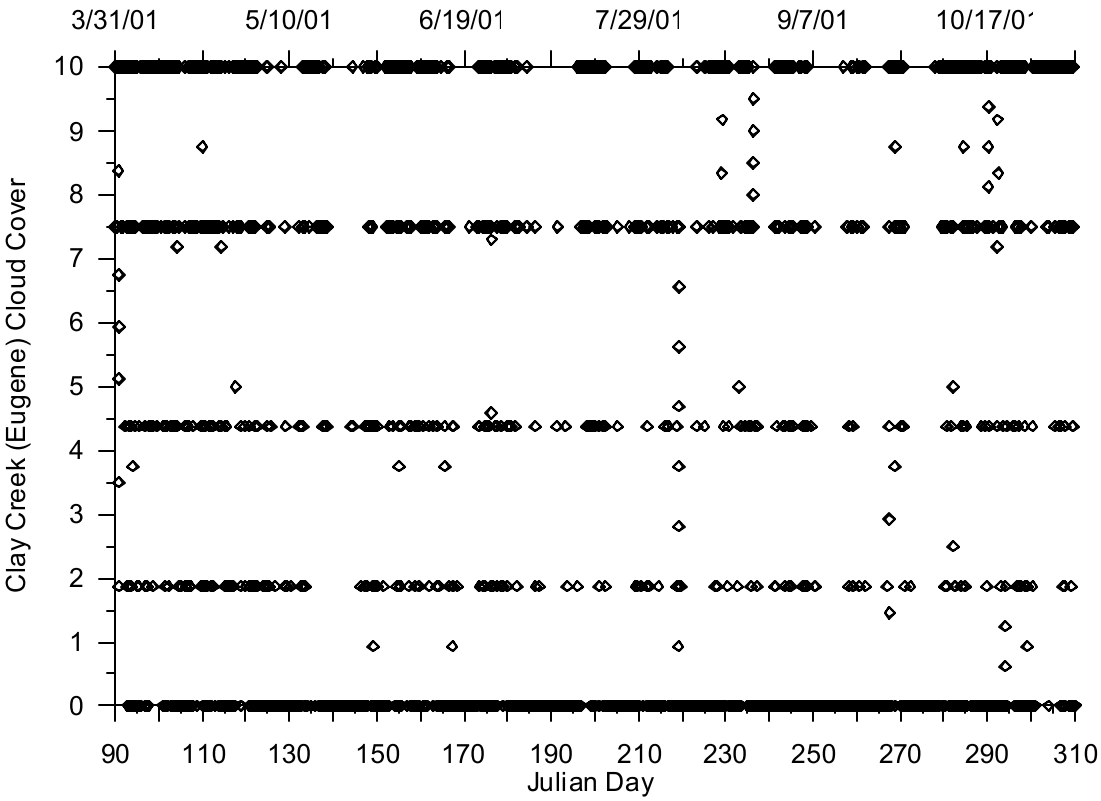


**Figure 637. Cloud cover at Eugene Airport, 2001**

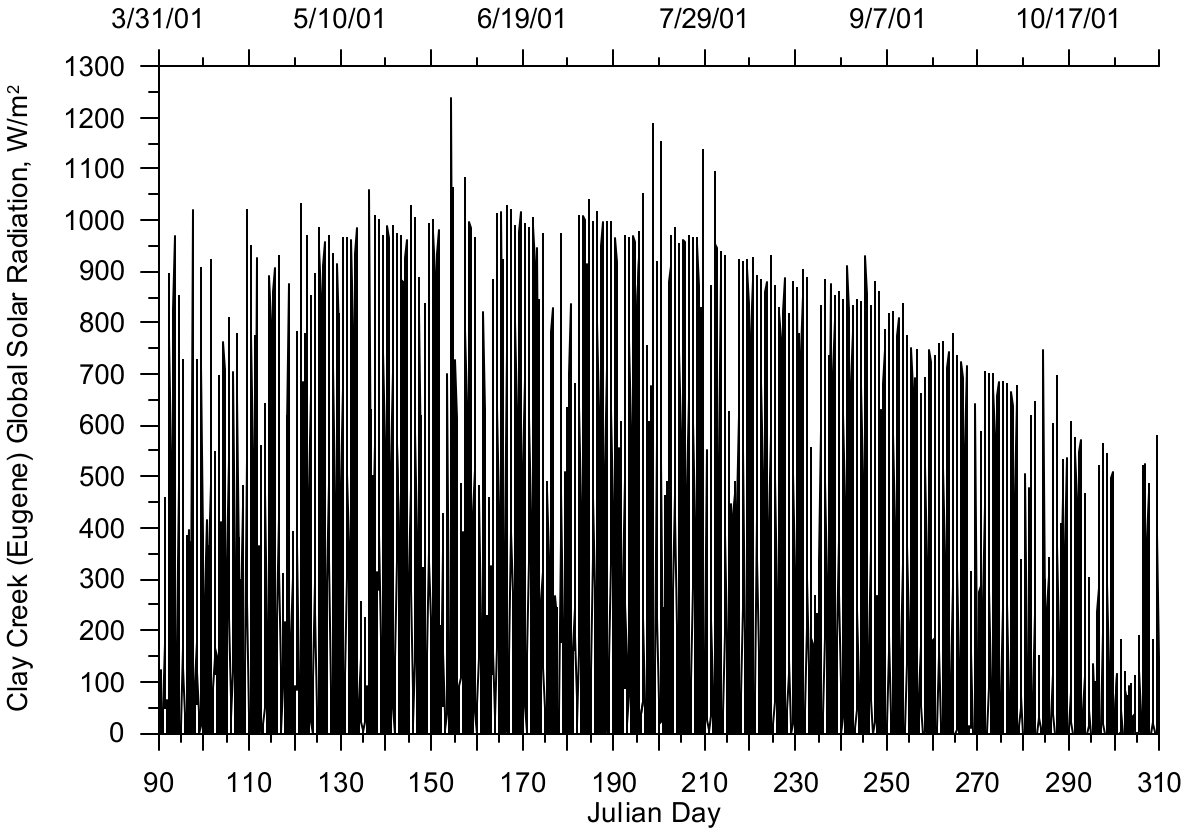


**Figure 638. Global solar radiation at Eugene Airport, 2001**

Year 2002

The meteorological data record was complete from April 1, 2002 to October 31, 2002 with an hourly recording frequency. Figure 639 shows the air temperature monitored at the Clay Creek site for 2002. Figure 640 shows the calculated dew point temperature using the air temperature and relative humidity. Figure 641 shows the wind speed data and indicates when wind speeds drops below 0.5 m/s the values were set to zero. Figure 642 shows a rose diagram of the wind direction and reveals that the wind directions were broken into 8 bins of 45 degrees, similar to the 2001 data. Figure 643 shows the cloud cover used and represents the cloud cover data monitored at the Eugene Airport since no cloud cover data were monitored at the Clay Creek site. The figure shows the coarseness of the cloud cover data recorded at the airport with only about five different cloud cover designations. The data points between the five values were the result of interpolations to fill data gaps in the cloud cover data. Figure 644 shows the global solar radiation from Eugene, OR, which was used since no solar radiation data was monitored at the Clay Creek site.

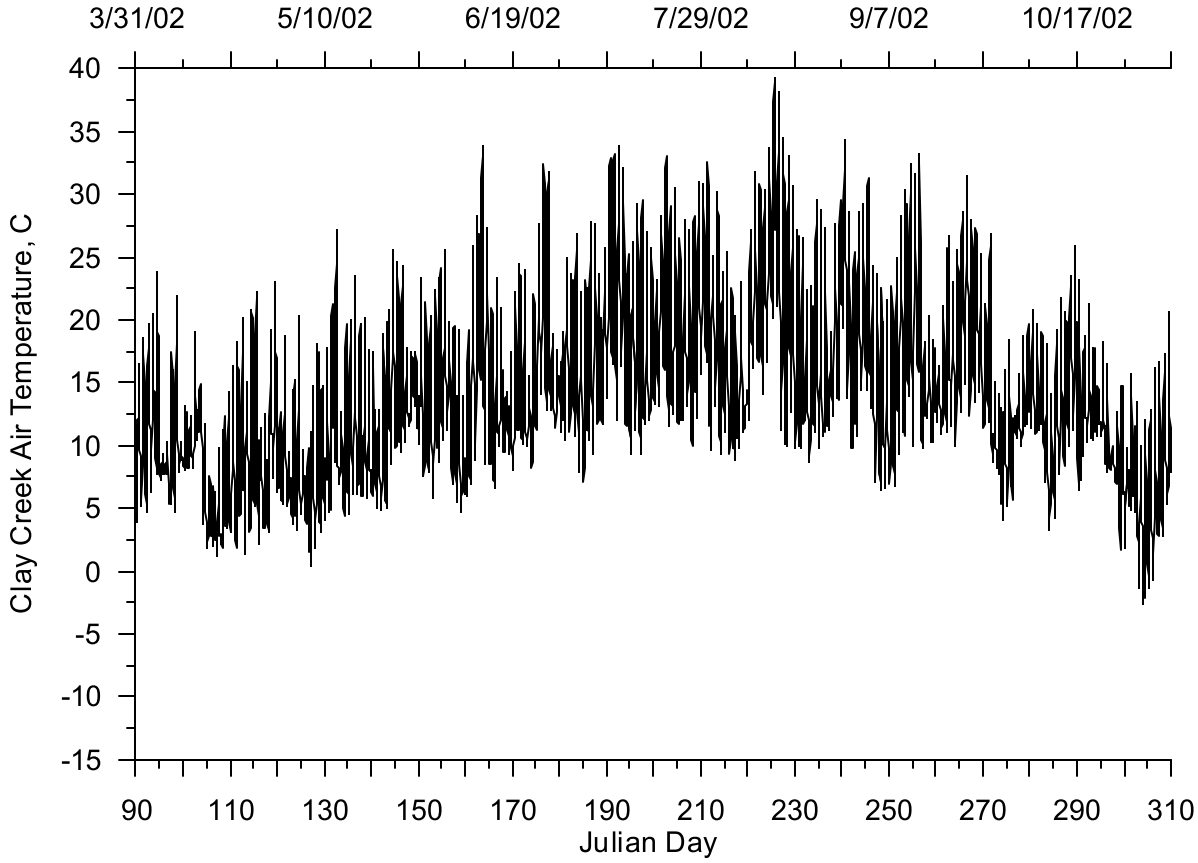


**Figure 639. Air temperature at Clay Creek, 2002**

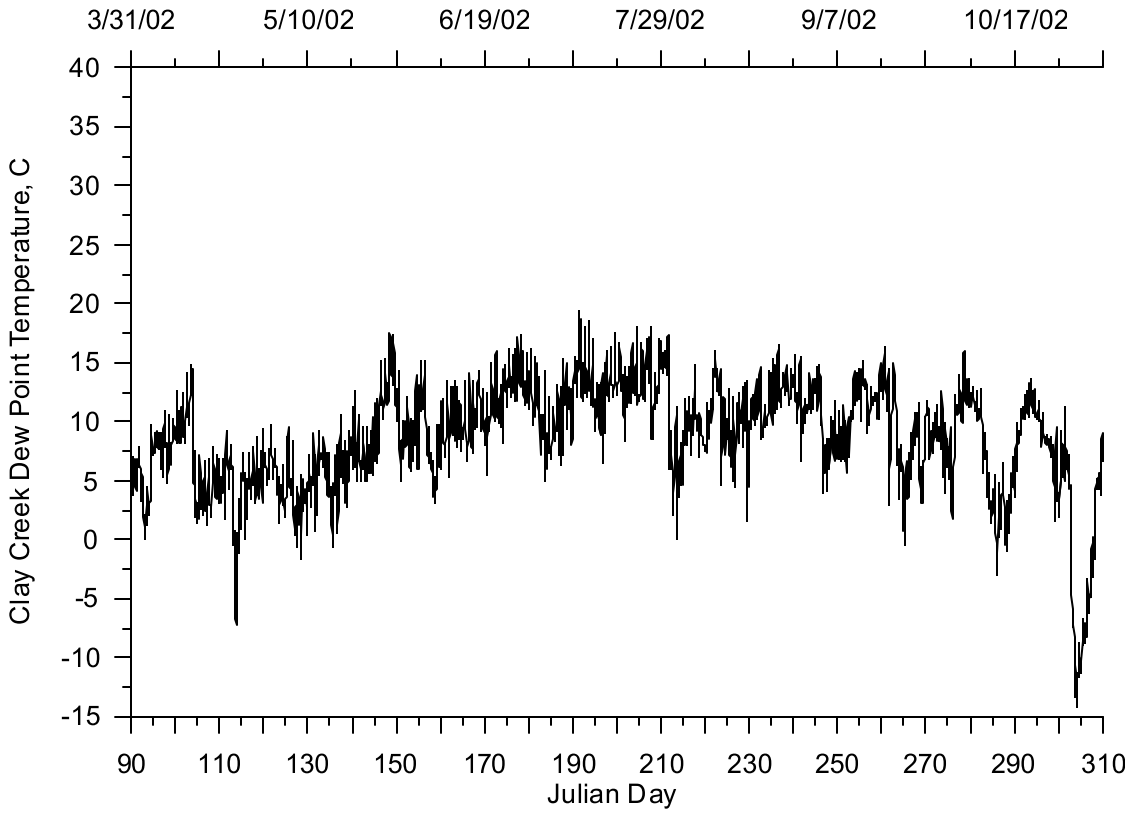


**Figure 640. Dew point temperature at Clay Creek, 2002**

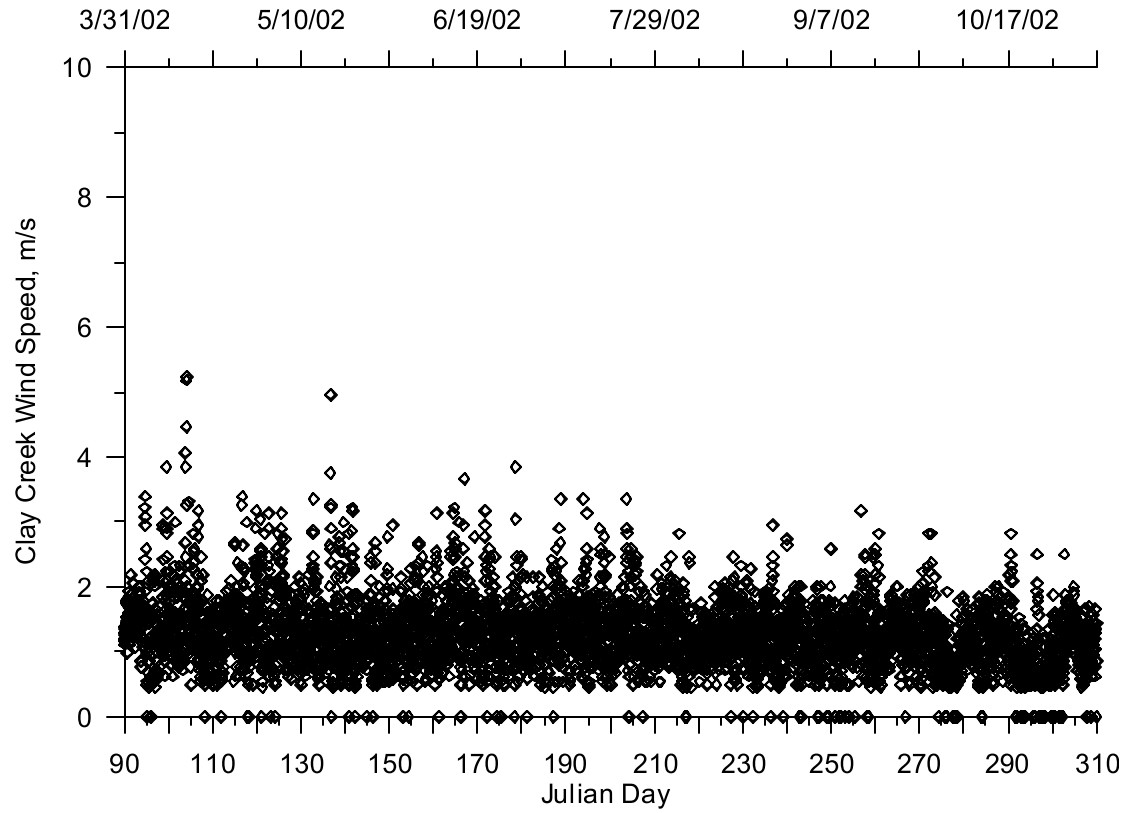


**Figure 641. Wind speed at Clay Creek, 2002**

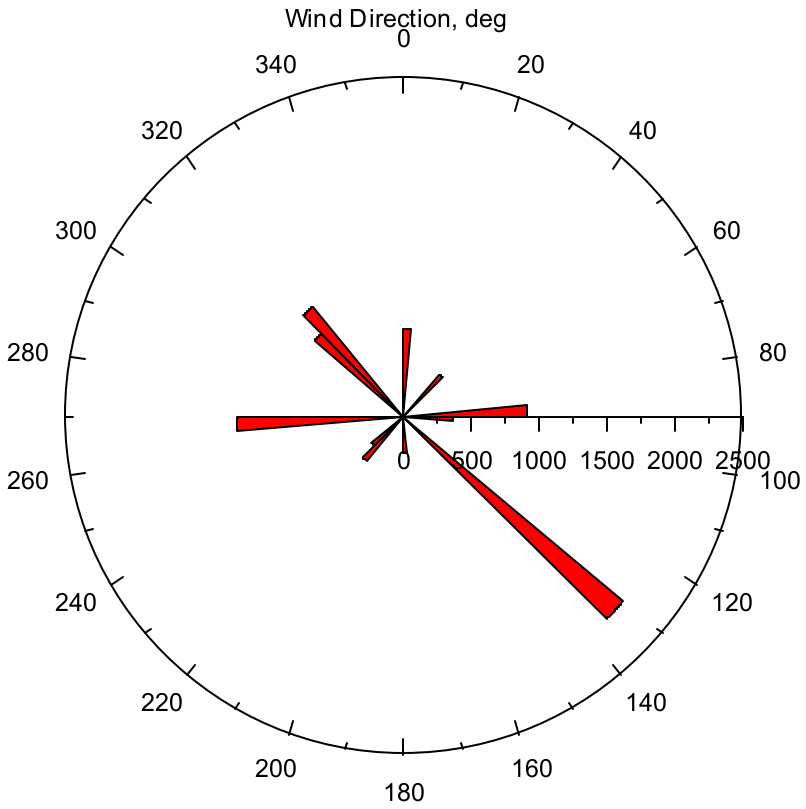


**Figure 642. Wind direction at Clay Creek, 2002**

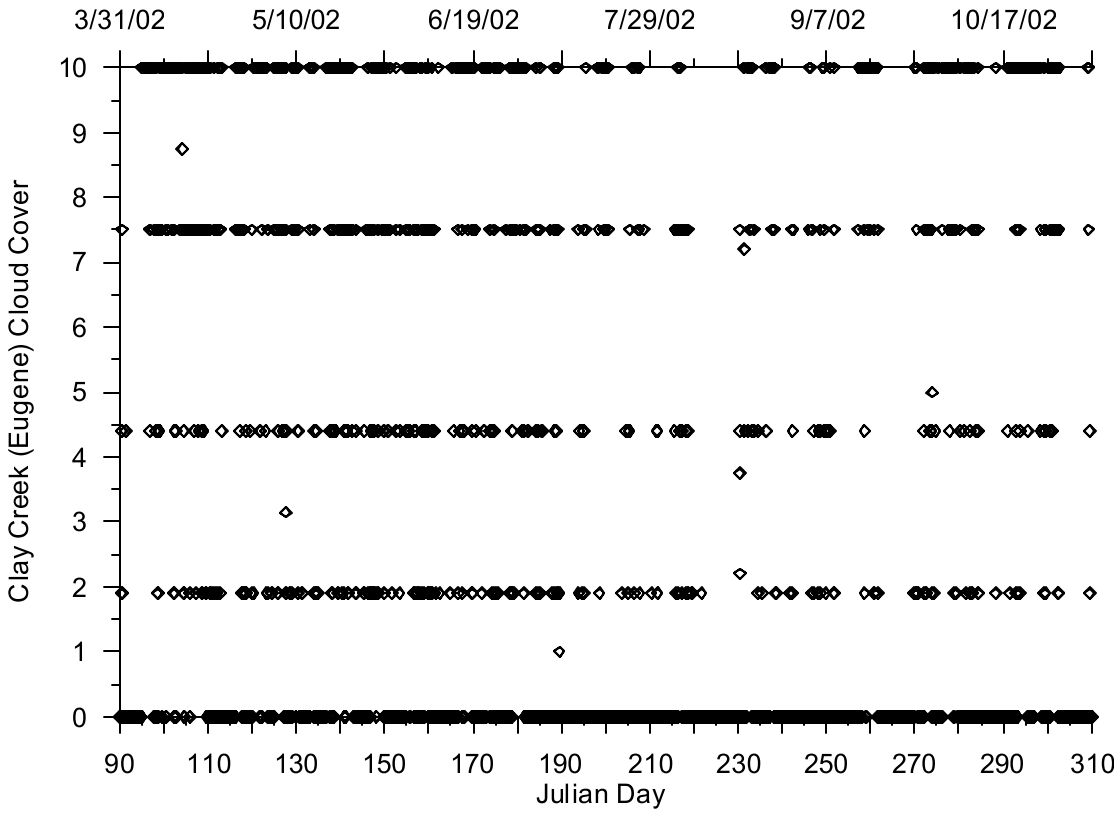


**Figure 643. Cloud cover at Eugene Airport, 2002**

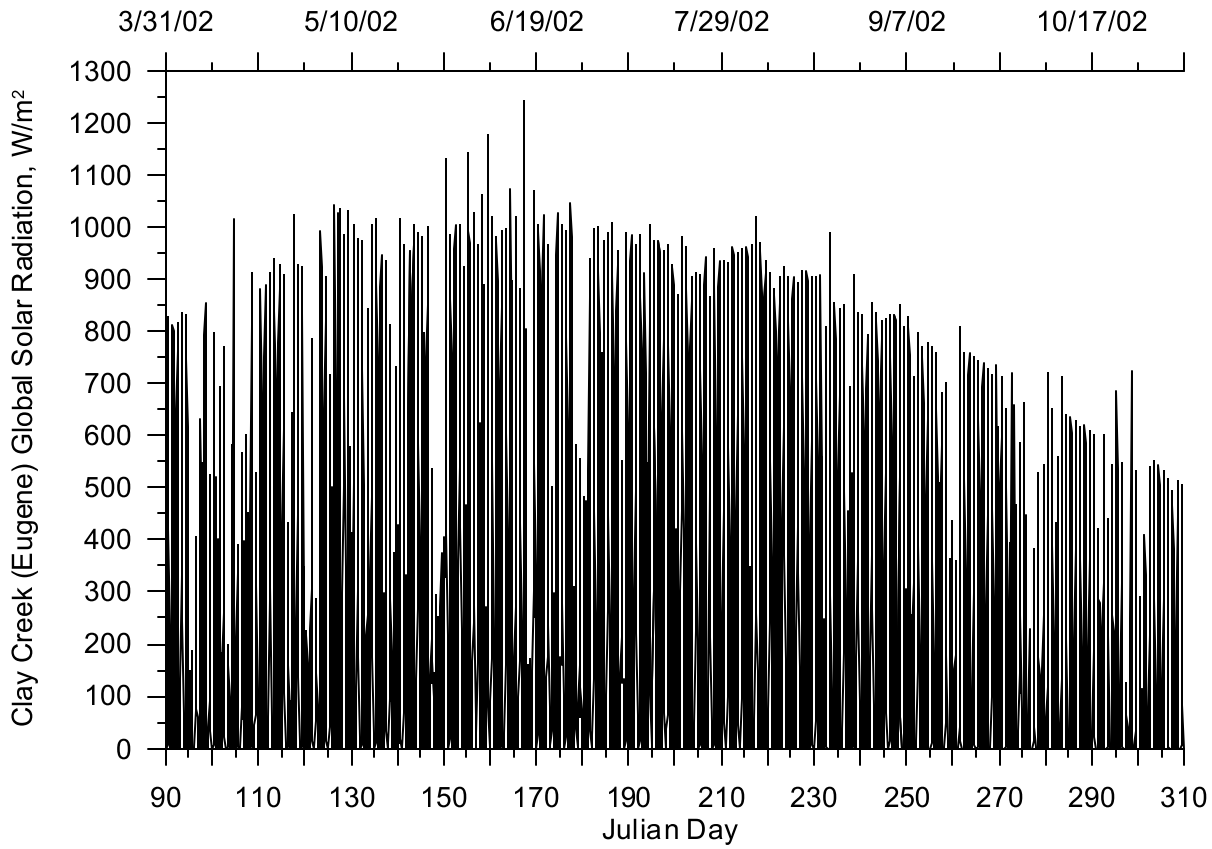


**Figure 644. Global solar radiation at Eugene Airport, 2002**

## Trout Creek

### Year 2001

The meteorological data recorded at the Trout Creek site, monitored by the Oregon Department of Forestry, were used for the McKenzie River model and were also used for Middle Fork Willamette River and Fall Creek models. The site monitors air temperature, relative humidity, wind speed, and wind direction, but no cloud cover or solar radiation data.

The meteorological data record was complete from April 1, 2001 to October 31, 2001, an hourly recording frequency. Figure 554 shows the air temperature monitored at the Trout Creek site for 2001. Figure 555 shows the calculated dew point temperature using the air temperature and relative humidity. Figure 556 shows the wind speed data monitored during 2001. The data shows a seasonal trend with lower wind speed during the summer and higher wind speeds in the spring and fall. Figure 557 shows a rose diagram of the wind direction and reveals that the predominant wind directions are 60 to 80 degrees and 260 to 280 degrees. Figure 558 shows the cloud cover used and represents the cloud cover data monitored at the Eugene Airport since no cloud cover data were monitored at the Trout Creek site. Figure 559 shows the global solar radiation from the H.J. Andrews Experimental Research Forest used since no solar radiation data were monitored at the Trout Creek site and better represents the solar conditions at the site over solar radiation data monitored in Eugene, OR.

### Year 2002

The meteorological data recorded at the Trout Creek site, monitored by the Oregon Department of Forestry, were used for the McKenzie River model and were also used for Middle Fork Willamette River and Fall Creek models. The site monitors air temperature, relative humidity, wind speed, and wind direction, but no cloud cover or solar radiation data.

The meteorological data record was complete from April 1, 2002 to October 31, 2002, an hourly recording frequency. Figure 560 shows the air temperature monitored at the Trout Creek site for 2002. Figure 561 shows the calculated dew point temperature using the air temperature and relative humidity. Figure 562 shows the wind speed data monitored during 2001. The data shows no seasonal trend in wind speeds which was different than data monitored in 2001. Figure 563 shows a rose diagram of the wind direction and reveals that the predominant wind directions were 60 to 80 degrees and 260 to 280 degrees, which was similar to the data in 2001. Figure 564 shows the cloud cover used and represents the cloud cover data monitored at the Eugene Airport since no cloud cover data was monitored at the Trout Creek site. Figure 565 shows the global solar radiation from the H.J. Andrews Experimental Research Forest used since no solar radiation data were monitored at the Trout Creek site.

## Eugene Airport

### Year 2001

The 2001 meteorological data recorded at the Eugene WSO / Mahlon Sweet Airport, which were used for the Upper Willamette River model, were also used in the lower reaches of the McKenzie River model. The Eugene Airport records air and dew point temperature, wind speed and direction, and cloud cover data, but no solar radiation data.

Figure 354 and Figure 355 show the air and dew point temperature respectively, over the period of April to October 2001. Figure 356 and Figure 357 show the wind speed and direction, respectively. Figure 356 indicates the minimum wind speed-recording threshold was about 1.5 m/s. The rose diagram in Figure 357 was dominated by the value of zero which was associated with wind speeds below the reading threshold. Figure 358 shows the coarseness of the cloud cover data recorded at the airport with only about five different cloud cover designations. The data points between the five values were the result of interpolations to fill data gaps in the cloud cover data. The solar radiation data collected at the SRML site is shown in Figure 359.

### Year 2002

The 2002 meteorological data recorded at the Eugene WSO / Mahlon Sweet Airport, which were used for the Upper Willamette River model were also used in the lower reaches of the McKenzie River model. The Eugene Airport records air and dew point temperature, wind speed and direction, and cloud cover data, but no solar radiation data.

The Eugene municipal airport records air and dew point temperature, wind speed and direction and cloud cover, but no solar radiation data. Figure 360 and Figure 361 show the air and dew point temperature respectively, over the period of April to October 2001. Figure 362 and Figure 363 show the wind speed and direction, respectively. Figure 362 indicates the minimum wind speed-recording threshold was about 1.5 m/s. The rose diagram in Figure 363 was dominated by the value of zero which

was associated with wind speeds below the reading threshold. Figure 364 shows the coarseness of the cloud cover data recorded at the airport with only about five different cloud cover designations. The data points between the five values were the result of interpolations to fill data gaps in the cloud cover data. The solar radiation data collected at the SRML site is shown in Figure 365.

## Summary

This report summarizes the foundation of all the elements of the Willamette River Basin model using CE-QUAL-W2 model. This model development includes detailed data sets:

- meteorological data
- channel bathymetry for grid development
- inflow and outflow conditions (upstream and downstream conditions)
- gaged tributary inflows
- ungaged tributary inflows used as a distributed inflow

These data were developed for the primary calibration periods of June 6 to September 25, 2001 and May16 to October 1, 2002. The use of theses data in the model of the Willamette basin including over 1000 km of river are shown in two companion reports, which describe the model calibration and application to management strategies:

- Berger, C. J., McKillip, M. L., Khan, Sher Jamal, Annear, R. L., and Wells, S. A. (2004)" Willamette River Basin Temperature TMDL Model: Model Calibration," Technical Report EWR-02-04, Department of Civil and Environmental Engineering, Portland State University, Portland, OR.– model calibration
- Annear, R L., McKillip, M. L., Khan, Sher Jamal, Berger, C. J., and Wells, S. A. (2004b)" Willamette River Basin Temperature TMDL Model: Model Scenarios," Technical Report EWR-03-04, Department of Civil and Environmental Engineering, Portland State University, Portland, OR. – application to management strategies

The USGS modeled the North Santiam and Santiam Rivers. Their work is described in Sullivan and Rounds (2004). In addition, another report is being developed by Buzzone and Wells (2004) on the impact of channel complexity on stream temperatures. This report will evaluate the historical evolution of stream channels on the upper part of the Willamette River and their impact on temperatures for fish.

# References


Ambrose, R. B.; Wool, T.; Connolly, J. P.; and Schanz, R. W. (1988) "WASP4, A Hydrodynamic and Water Quality Model: Model Theory, User's Manual, and Programmer's Guide," Envir. Res. Lab., EPA 600/3-87/039, Athens, GA.

Annear, R. L., McKillip, M. L., Khan, Sher Jamal, Berger, C. J., and Wells, S. A. (2004a)" Willamette River Basin Temperature TMDL Model: Boundary Conditions and Model Setup," Technical Report EWR-01-04, Department of Civil and Environmental Engineering, Portland State University, Portland, OR.

Annear, R. L., McKillip, M. L., Khan, Sher Jamal, Berger, C. J., and Wells, S. A. (2004b)" Willamette River Basin Temperature TMDL Model: Model Scenarios," Technical Report EWR-03-04, Department of Civil and Environmental Engineering, Portland State University, Portland, OR.

Berger, C., Annear, R. L., and Wells, S. A. (2001)"Lower Willamette River Model: Model Calibration," Technical Report EWR-2-01, Department of Civil Engineering, Portland State University, Portland, OR, 100 pp.

Berger, C. J., McKillip, M. L., Khan, Sher Jamal, Annear, R. L., and Wells, S. A. (2004)" Willamette River Basin Temperature TMDL Model: Model Calibration," Technical Report EWR-02-04, Department of Civil and Environmental Engineering, Portland State University, Portland, OR.

Bloom, J. (1997) "Hydrodynamics of the Lower Willamette River," Prepared for the Oregon Department of Environmental Quality, Portland, OR

Bloom, J. (2000) "Modeling options to address Willamette River temperature, aquatic growth, dissolved oxygen, and pH concerns," Prepared for the Oregon Department of Environmental Quality, Portland, OR

Brown, L. C. and Barnwell, T. O. (1987) "The Enhanced Stream Water Quality Models QUAL2E and QUAL2E-UNCAS: Documentation and Users Manual," EPA Environmental Research laboratory, EPA 600/3-87/007, Athens, GA.

Buzzone, J. and Wells, S. (2004) "Effect of channel complexity on stream temperatures," Technical Report EWR-04-04, Department of Civil and Environmental Engineering, Portland State University, Portland, OR.

Byrd III, Daniel., M. and Zacharewski, Tim. (1999) "Estrogenicity of Willamette River Water: Summary Report," Prepared for the Willamette Water Supply Agency (WWSA), Portland, OR

Cole, T. and Buchak, E. (1995) "CE-QUAL-W2: A Two-Dimensional, Laterally Averaged, Hydrodynamic and Water Quality Model, Version 2.0," US Army Corps of Engineers, Instruction Report EL-95-1, Waterways Experiments Station, Vicksburg, MS.

Cole, T.M., and S. A. Wells (2000). "CE-QUAL-W2: A two-dimensional, laterally averaged, Hydrodynamic and Water Quality Model, Version 3.0," Instruction Report EL-2000- , US Army Engineering and Research Development Center, Vicksburg, MS.

Cole, T.M., and S. A. Wells (2002). "CE-QUAL-W2: A two-dimensional, laterally averaged, Hydrodynamic and Water Quality Model, Version 3.1," Instruction Report EL-02-1, US Army Engineering and Research Development Center, Vicksburg, MS.

Corps of Engineers (1986) "HEC-5 Simulation of Flood Control and Conservation Systems," CPD-5Q, Hydrologic Engineering Center, Davis, CA, 1986.

Donigian, A.S., Jr., J.C. Imhoff, B.R. Bicknell and J.L. Kittle, Jr. (1984) "Application Guide for Hydrological Simulation Program Fortran (HSPF)," EPA-600/3-84-065, U.S. Envir. Prot. Agency, Athens, GA, 1984.

Edinger, J. E. and Buchak, E. M. (1978) "Reservoir Longitudinal and Vertical Implicit Hydrodynamics," Environmental Effects of Hydraulic Engineering Works, Proceedings of an International Symposium, Knoxville, TN.

Fernald, A., et al. (2001). "Transient storage and hyporheic flow along the Willamette River, Oregon: Field measurements and model estimates," Water Resources Research 37(6): 1681-1694.

Gupta, R. S. (1989). Hydrology and Hydraulic Systems, Prentice Hall, Englewood Cliff, NJ, 739 pp.

Harris, D.D. (1968). "Travel rates of water for selected streams in the Willamette River Basin, Oregon," USGS Hydrologic Investigations, Atlas HA-273.

HEC (1997) "UNET One-Dimensional Unsteady-Flow through a Full Network of Open Channels, User's Manual," US Army Corps of Engineers, Hydrologic Engineering Center, Davis, CA.

Hubbard, L., E., et al. (2000) "Water Resources Data Oregon Water Year 1999," Prepared for U.S. Geological Survey Water Resources Division, Portland, OR

Knutson, Michael. (2000) "Lower Columbia River UNET model," Prepared for the U.S Army Corps of Engineers, Portland, OR

Kyle, Theodore. (2000) "per email correspondence," Portland, OR

Laenen, A. (1995) Unpublished dye studies on the Willamette River, Oregon.

Laenen, Antonius. And Risley, John, C. (1997) "Precipitation-Runoff and Stream flow-Routing Models for the Willamette River Basin, Oregon," Prepared for the U.S. Geological Survey Water Resources Investigations, Portland, OR.

Laenen, A and K.E. Bencala. (2001). "Transient storage assessments of dye-tracer-injections in rivers of the Willamette basin, Oregon," Journal of the American Water Resources Association. 37(2): 367-377

Laenen, A. (2002a) Unpublished dye studies on the Willamette River, Oregon.

Laenen, A. (2002b) Unpublished dye studies on the Long Tom River, Oregon.

Lee, K.K. (1995). "Stream velocity and dispersion characteristics determined by dye-tracer studies on selected stream reaches in the Willamette River Basin, Oregon," USGS Water Resources Investigations Report 95-4078.

Limno-Tech, Inc. (1997) "Willamette River CSO Predesign project: Willamette River Hydraulics Characterization," Prepared for the City of Portland Bureau of Environmental Services, Portland, OR

Masters, G. M. (1997). "Introduction to Environmental Engineering and Science, 2nd ed," Prentice Hall, Upper Saddle River, New Jersey.

McKee, W. 2003. Meteorological data at the Andrews Experimental Forest: Benchmark and secondary meteorological stations: Long-Term Ecological Research. Corvallis, OR: Forest Science Data Bank: MS001. [Database]. http://www.fsl.orst.edu/lter/data/abstract.cfm?dbcode=MS001. (29 December 2003)

Montgomery Watson. (1997) "Willamette River Raw Water Monitoring Program Annual Report 1994-1996," Prepared for the Tualatin Valley Water District, Tualatin, OR

Montgomery Watson. (1999) "Willamette River Raw Water Monitoring Program Annual Report 1998-1999," Prepared for the City of Tigard, Tigard, OR

Normandeau Associates, Inc. (2000) "Study Plan to Assess Effects of Dam and Flashboards and Project Operations on Water Quality with Respect to Temperature, Dissolved Oxygen, and Gas Saturation," Prepared for Willamette Falls Project Fisheries, Aquatics, Terrestrial Workgroup, Portland, OR

Portland General Electric Company. (1998) "Willamette Falls Hydroelectric Project," Prepared for the Portland General Electric Smurfit Newsprint Corporation, Portland, OR

Ryel, R., (2002) "per email correspondence," Portland, OR

Richmond, M., C., et al. (2000) "Dissolved Gas Abatement Study (DGAS)," prepared for the U.S Army Corps of Engineers, Battelle Pacific Northwest Division, Richland, WA

Rodriguez, H. G., Annear, R. L., Wells, S. A., and Berger, C. (2001) "Lower Willamette River Model: Boundary Conditions and Model Setup," Technical Report EWR-1-01, Department of Civil Engineering, Portland State University, Portland, Oregon, 134 pages.

Rounds, Stewart (2002) Bathymetric data collected by U.S. Geological Survey in support of model construction for Willamette basin temperature TMDLS: centerline and cross sectional data

Savage, Greg. (2000) "per email correspondence," Portland, OR

Sinclair, Kirk, A. and Pitz, Charles, F. (1999) "Estimated Baseflow Characteristics of Selected Washington Rivers and Streams," Prepared for the Washington State Department of Ecology Environmental Assessment Program, Olympia, WA

Singh, V. (1992) Elementary Hydrology, Prentice Hall, NY.

Smith, D. J. (1978) "Water Quality for River Reservoir Systems, Generalized computer program for River-Reservoir systems," U.S. Army Corps of Engineers, Hydrologic Engineering Center, Davis, Ca.

Sullivan, A.B. and Rounds, S.A. (2004) "Modeling streamflow and water temperature in the North Santiam and Santiam Rivers, Oregon," U.S. Geological Survey Scientific Investigations Report 2004-5001.

Tetra tech, Inc. (1995) "Willamette River Basin Water Quality Study – Final Report: Summary and Synthesis of Study Findings," prepared for the Oregon Department of Environmental Quality, Portland, OR

Tetra tech, Inc. (1995) "Willamette River Basin Water Quality Study – Phase II: Steady-State Model Refinement Component," prepared for the Oregon Department of Environmental Quality, Portland, OR

USGS website: (http://waterdata.usgs.gov/nwis/sw)

Wells, S. A. (1997) "Theoretical Basis for the CE-QUAL-W2 River Basin Model," Technical Report EWR-6-97, Department of Civil Engineering, Portland State University, Portland, Oregon, 62 pp.

Wells, S. A. (1998) "Code Development and Testing of the CE-QUAL-W2 River Basin Model," Technical Report EWR-4-98, Department of Civil Engineering, Portland State University, Portland, Oregon, 85 pp.

Wells, S. A. (1999) "River Basin Modeling Using CE-QUAL-W2 Version 3," Proc. ASCE Inter. Water Res. Engr. Conf., Seattle, WA, 1999.

Wells, S. A. (2000) Modeling the Lower Willamette: Model Selection, Technical Report, Department of Civil Engineering, Portland State University, Portland, OR

Wells, S. and Berger, C. (1998) "The Lower Snake River Model," prepared for HDR Engineering, Boise, ID.

Wentz, Dennis, et al. (1998) "Water Quality in the Willamette Basin, Oregon, 1991-95," Portland, OR

# Appendix A: Shade methodology

CE-QUAL-W2 incorporates both topographic and vegetative shade in the model. Topographic characteristics include the steepest inclination angle in 18 directions around a model segment. The vegetative characteristics consist of tree top elevation, distance between the river channel centerline and the controlling vegetation, and the vegetation density in summer and winter. The vegetation characteristics are provided for both banks of the river. The model also employs two sets of shade reduction factors which can be used to represent summer and winter vegetation thickness. The step transition dates were set at April 1 for "leaf on" and October 1 for "leaf off." Table 65 shows a list of the topographic and vegetative shade characteristics incorporated in the model.

**Table 65. CE-QUAL-W2 shade file characteristics**

| Variable | Variable Description |
|---|---|
| SEG | Segment Number |
| DYNSH | Dynamic shading or static shading |
| VEL | Vegetative elevation left bank, m |
| VER | Vegetative elevation right bank, m |
| DL | Distance to vegetation left bank, m |
| DR | Distance to vegetation right bank, m |
| SRFL#1 | Shade reduction factor #1, left bank, summer |
| SRFL#2 | Shade reduction factor #2, left bank, winter |
| SRFR#1 | Shade reduction factor #1, right bank, summer |
| SRFR#2 | Shade reduction factor #2, right bank, winter |
| TOPO1 | Topographic angle #01 at $0^o$, radians |
| TOPO2 | Topographic angle #02 at $20^o$, radians |
| TOPO3 | Topographic angle #03 at $40^o$, radians |
| TOPO4 | Topographic angle #04 at $60^o$, radians |
| TOPO5 | Topographic angle #05 at $80^o$, radians |
| TOPO6 | Topographic angle #06 at $100^o$, radians |
| TOPO7 | Topographic angle #07 at $120^o$, radians |
| TOPO8 | Topographic angle #08 at $140^o$, radians |
| TOPO9 | Topographic angle #09 at $160^o$, radians |
| TOPO10 | Topographic angle #10 at $180^o$, radians |
| TOPO11 | Topographic angle #11 at $200^o$, radians |
| TOPO12 | Topographic angle #12 at $220^o$, radians |
| TOPO13 | Topographic angle #13 at $240^o$, radians |
| TOPO14 | Topographic angle #14 at $260^o$, radians |
| TOPO15 | Topographic angle #15 at $280^o$, radians |
| TOPO16 | Topographic angle #16 at $300^o$, radians |
| TOPO17 | Topographic angle #17 at $320^o$, radians |
| TOPO18 | Topographic angle #18 at $340^o$, radians |
| JDSRF1 | Starting date for SRF#1, Julian day, switch vegetation density to summer |
| JDSRF2 | Starting date for SRF#2, Julian day, switch vegetation density to winter |

The vegetation and topographic characteristics for each model piece were developed using geographic information system (GIS) data supplied by the Oregon Department of Environmental Quality (ODEQ).

The GIS data were the same data used in their shade and Heat Source models. The data consists of thalweg points every 100 ft (30.48 m) along the centerline of the river. Figure 645 shows an example of these points along the McKenzie River around RM 40.0. For each thalweg point, additional associated data included: channel width, land surface elevation, three topographic inclination angles, and nine vegetation compartments for each bank. Each vegetation compartment consists of vegetation height, distance from stream bank, and density.

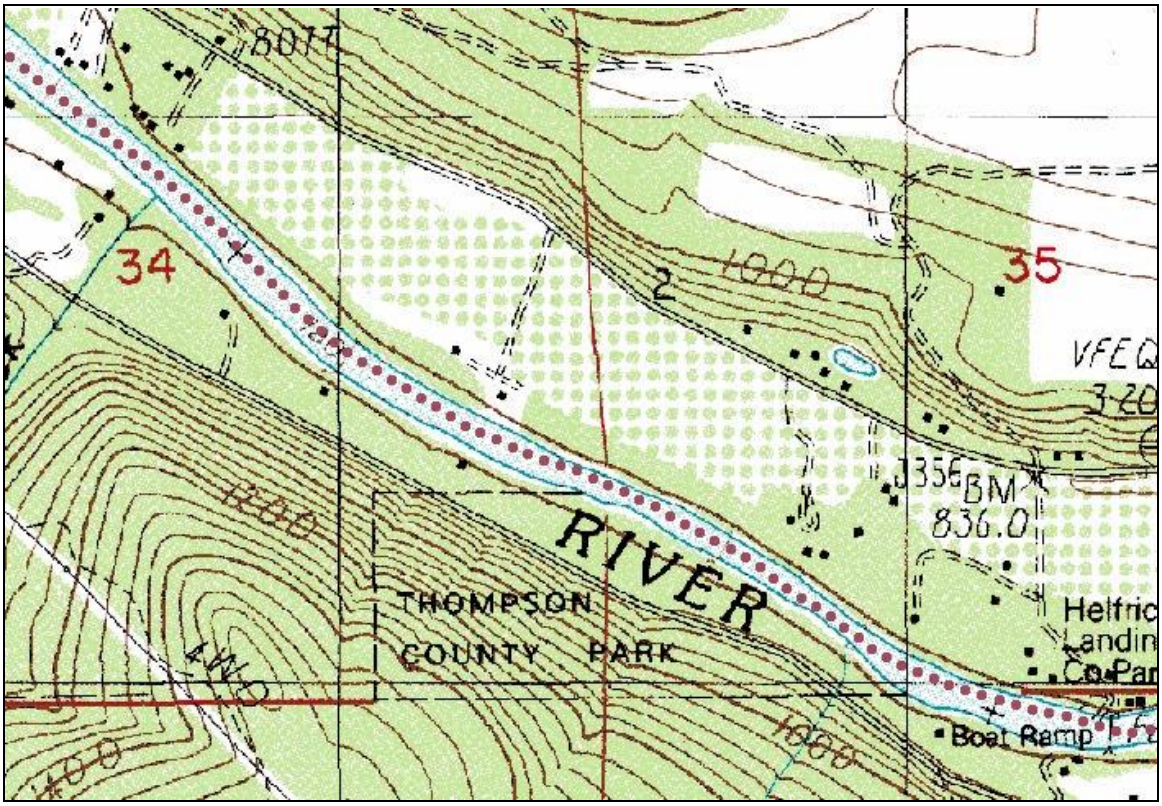


**Figure 645. McKenzie River thalweg points created by ODEQ**

Each thalweg point was also associated with a RM along the river section analyzed based on the calculating the cumulative distance from the furthest downstream point to the furthest upstream point. The river miles calculated using this method often did not agree with river miles specified on USGS topographic maps due to finer resolution of the thalweg points following the meanders of the river than the topographic maps. The thalweg points used for characterizing the vegetation and topography through a GIS analysis by ODEQ were the same points used in the bathymetry analysis and model grid development for each model piece. The result was that the RM designation used for the shade characteristics corresponded to the RM designation for the model grid development.

The GIS data supplied by the ODEQ were first used to calculate the CE-QUAL-W2 shade file characteristics at the same resolution as the original data (100ft, 30.48 m). The nine vegetation compartments for each bank were reduced to the set of controlling vegetation for each bank. First the distance from each vegetation compartment to the river centerline was calculated by adding the distance from the thalweg point to the river bank with the distances from each vegetation compartment to the river bank. The controlling vegetation for each bank was then calculated by taking the ratio of the vegetation height to the distance from the river centerline to each compartment and then isolating the compartment resulting in the highest ratio. The highest ratio represents the tallest vegetation relative to distance from the river, which would control the stream side shading. The vegetation height from the

controlling vegetation was then combined with the land surface elevation to get the elevation of the top of the vegetation. The distance from the vegetation to the river centerline and the vegetation density from the controlling vegetation compartment were also isolated for each bank. To ensure the vegetation density was not underrepresented by only using the vegetation density from only the controlling vegetation compartment the cumulative vegetation density was calculated for all nine vegetation compartments. Since the cumulative density may over-represent the vegetation density influencing shade the vegetation density from the vegetation compartment identified as controlling shade and the cumulative shade density from the nine compartments were averaged and then associated with the other controlling vegetation characteristics

The three topographic inclination angles (East, South, and West) provided with the vegetation characteristics were used to create the eighteen topographic inclination angles for the CE-QUAL-W2 model. Linear interpolation was used with the three topographic inclination angles to create the eighteen inclination angles ($20^{o}$ increments) surrounding each model segment. No inclination angle was provided for the direction "North" of each thalweg point, so inclination angles from the West and East were used to interpolate around "North" of each point. Although the topography could change considerably over the 180 degrees of interpolation, the approach was considered reasonable since the inclination angles towards the North are less important since the sun will be below the horizon.

The result of this first stage of the analysis was a set of CE-QUAL-W2 shade characteristics consisting of vegetation top elevation, density, and distance from the river thalweg for both the left and right river banks and eighteen topographic inclination angles surrounding each thalweg point. The resolution of the information was every 100 ft along the river. The model grid resolution was variable across the Willamette River system and in some cases within each model piece.

The next step was to convert the vegetation and topographic information from 100 ft resolution to the model grid resolution. First, the furthest upstream river mile for each model piece was identified and used with the model bathymetry files to calculate the river mile range for each model segment. Table 66 lists the upstream river mile for each model piece. If a segment length was longer than the thalweg point resolution (100ft, 30.48 m), then the thalweg points which were in the river mile range of the segment were used to take the average vegetation and topographic characteristics for that segment. If a model segment length was less than the thalweg point resolution, the nearest thalweg points upstream and downstream were identified by RM and linear interpolation was used to estimate the vegetation and topographic characteristics for that segment. The result of this analysis was set of vegetation characteristics and topographic inclination angles for each model segment.

**Table 66. Willamette River model piece upstream river mile locations**

| Model Piece | Model grid upstream RM |
|---|---|
| Clackamas River | 22.62 |
| Lower Willamette River | 26.64 |
| Middle Willamette River | 85.50 |
| Upper Willamette River | 186.87 |
| Fall Creek | 7.11 |
| Row River | 7.50 |
| Coast Fork Willamette River | 28.91 |
| Middle Fork Willamette River | 16.50 |
| South Santiam River | 36.50 |

| | |
|---|---|
| McKenzie River | 60.84 |
| Long Tom River | 23.71 |

The vegetation and topographic data analysis was conducted for each model piece separately. In addition, each side channel to the river included in the model, i.e., each modeled bifurcation, and was also analyzed separately since the RM designations for each side channel would be different than the river.

# Appendix B: Willamette Basin Dye Studies

Several existing Willamette basin dye studies were available to calibrate the hydrodynamics of the CE-QUAL-W2 model. The studies available were listed in Table 67. A study exists for most reaches of the rivers in the study area. The more recent dye study reaches are shown in Figure 646. The comprehensive 1962-63 USGS dye study reaches are shown in Figure 647. The studies prior to the 1995-1996 floods were subject to scrutiny due to the potential changes in channel bathymetry. Studies more recent than the 1968 were not available for the McKenzie River, the Middle and Coast Forks of the Willamette, and the North and South Santiam Rivers.

**Table 67. Willamette basin dye studies available.**

| Study year | Rivers | Data source |
|---|---|---|
| 1962-3 | Coast Fork Willamette<br>Middle Fork Willamette<br>Willamette<br>McKenzie<br>North Santiam<br>Middle Santiam (above Foster Reservoir)<br>South Santiam<br>Santiam | Harris, D.D. (1968). *Travel rates of water for selected streams in the Willamette River Basin, Oregon.* USGS Hydrologic Investigations, Atlas HA-273. |
| 1992 | (Upper) Willamette<br>Clackamas | Lee, K.K. (1995). *Stream velocity and dispersion characteristics determined by dye-tracer studies on selected stream reaches in the Willamette River Basin, Oregon.* USGS Water Resources Investigations Report 95-4078. |
| 1995 | Santiam | Laenen, A and K.E. Bencala. (2001). Transient *storage assessments of dye-tracer-injections in rivers of the Willamette basin, Oregon.* Journal of the American Water Resources Association. 37(2): 367-377. |
| 1998 | (Upper) Willamette | Fernald, A., et al. (2001). *Transient storage and hyporheic flow along the Willamette River, Oregon: Field measurements and model estimates.* Water Resources Research 37(6): 1681-1694. Part of the USGS's National Water-Quality Assessment (NAWQA) Program. |
| 2002 | Willamette | Laenen, A. (2002a) Unpublished dye studies on the Willamette River, Oregon. |
| 2002 | Long Tom | Laenen, A. (2002b) Unpublished dye studies on the Long Tom River, Oregon. |

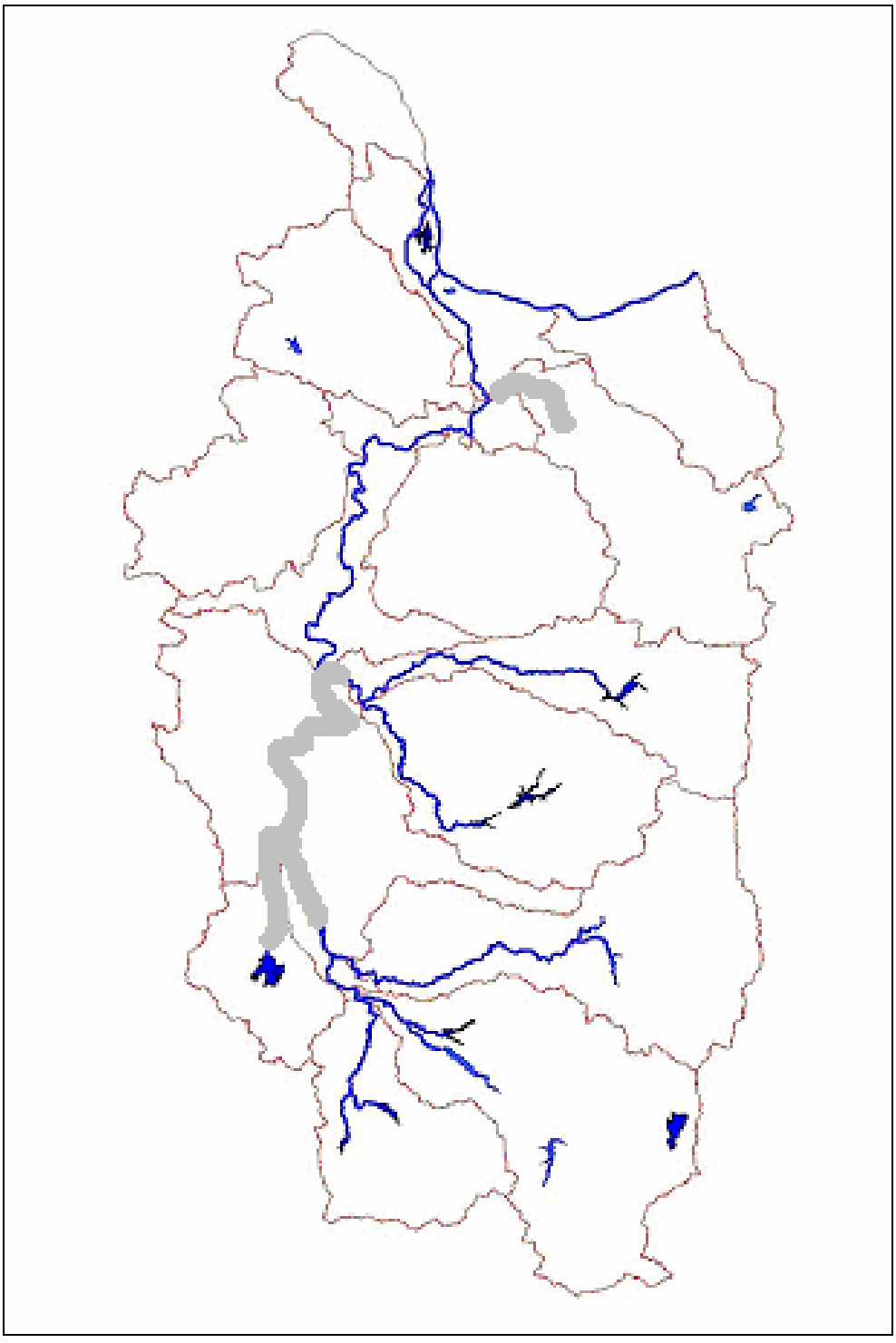

**Figure 646: Willamette River dye studies, 1992-2002**

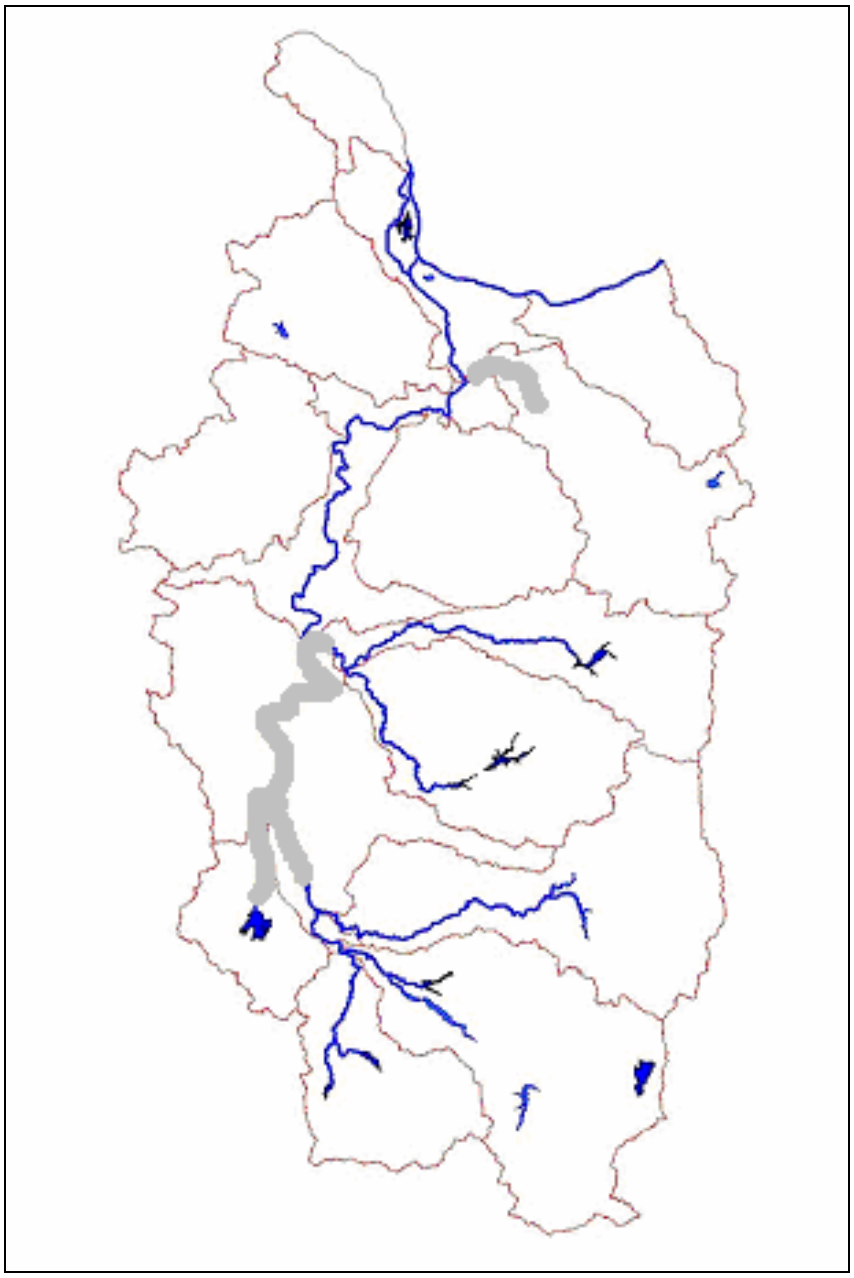

**Figure 647. Willamette River USGS dye study reaches, 1962-63**

## *1962-1963 USGS dye studies*

The USGS conducted numerous dye studies in the Willamette basin for the purpose of determining travel times of selected waterways. Results were reported in the USGS Hydrologic Atlas HA-273 by Harris in 1968. These studies reported travel rate and time as a function of discharge graphically. For most reaches, travel rate data were available at three discharges: a minimum anticipated flow, an average historical flow, and a high flow selected as the median 30-day annual high flow. The median 30-day annual high flow was defined as "the annual values of highest mean discharge for 30 consecutive days for the period of record." Table 68 shows the rivers and reaches reported. The tabular data for these reaches were included in the appendix.

Later studies on the Willamette (q.v. 1995, 2002 studies) indicated that the travel times were generally slightly longer (i.e., slower velocities) than the values reported in 1968 by approximately 8-12 percent.

**Table 68. River reaches in the 1962-1963 USGS dye studies.**

| River | Upstream RM | Downstream RM |
|---|---|---|
| Middle Fork Willamette & Willamette | 203.7 | 26.6 |
| Coast Fork Willamette | 23.9 | 0.0 |
| McKenzie | 81.5 | 3.6 |
| North Santiam | 45.6 | 0.0 |
| Santiam | 11.7 | 0.0 |
| Middle Santiam (above Foster Reservoir) | 5.7 | 0.0 |
| South Santiam | 40.0 | 0.0 |

## *1995 Santiam River*

Laenen and Bencala (2001) reported a dye study conducted June 8, 1995, on the lower Santiam River, RM 5.1 to 0.0 (Figure 648). The purpose of the investigation was to conduct a transient storage assessment. 3600 ml of tracer was injected at river mile 5.1 at 10:40 a.m. An average discharge of 93.4 $m^3/s$ was reported for all sampling stations over the study time period. As seen in Table 69, 108% mass recovery was determined at the first sampling station, suggesting the dye may not be well-mixed.

The low dye recovery at RM 2.0 was the result of transient storage. Notable hyporheic linkages exist over sub-sections of the Santiam. In the lower 10 km of the Santiam River, a groundwater exchange of up to ~5 $m^3/s$, perhaps 10 to 20% of the total discharge, exists under the low, summer flows (35 to 50 $m^3/s$). Higher summer flow (~100 $m^3/sec$) exhibits a groundwater exchange of up to 10 $m^3/s$. Characteristic of pool-and-riffle streams, the exchange alternates between groundwater influx and out flux. The patterns of surface-subsurface exchange were highly variable with time and space. Under high flows, the channel controls the river hydraulics. Under low flows, where riffles control the flow, Laenen and Bencala (2001) found that adjusting the convective dispersion and dye decay rate did not adequately characterize the recession response of the observed dye concentrations. A transient storage model was found to yield improved results.

**Table 69. 1995 USGS Santiam River dye study discharge and mass recovery**

| **Injection at RM 5.1 on June 8, 1995.** | | | |
|---|---|---|---|
| River Mile | Q, cfs | Q, $m^3/s$ | Mass Recovery, % |
| 3.0 | 3300 | 93.4 | 107.9 |
| 2.5 | " | " | 99.3 |
| 2.0 | " | " | 67.7 |
| 1.5 | " | " | 90.1 |
| 1.0 | " | " | 88.7 |
| 0.0 | " | " | 85.1 |

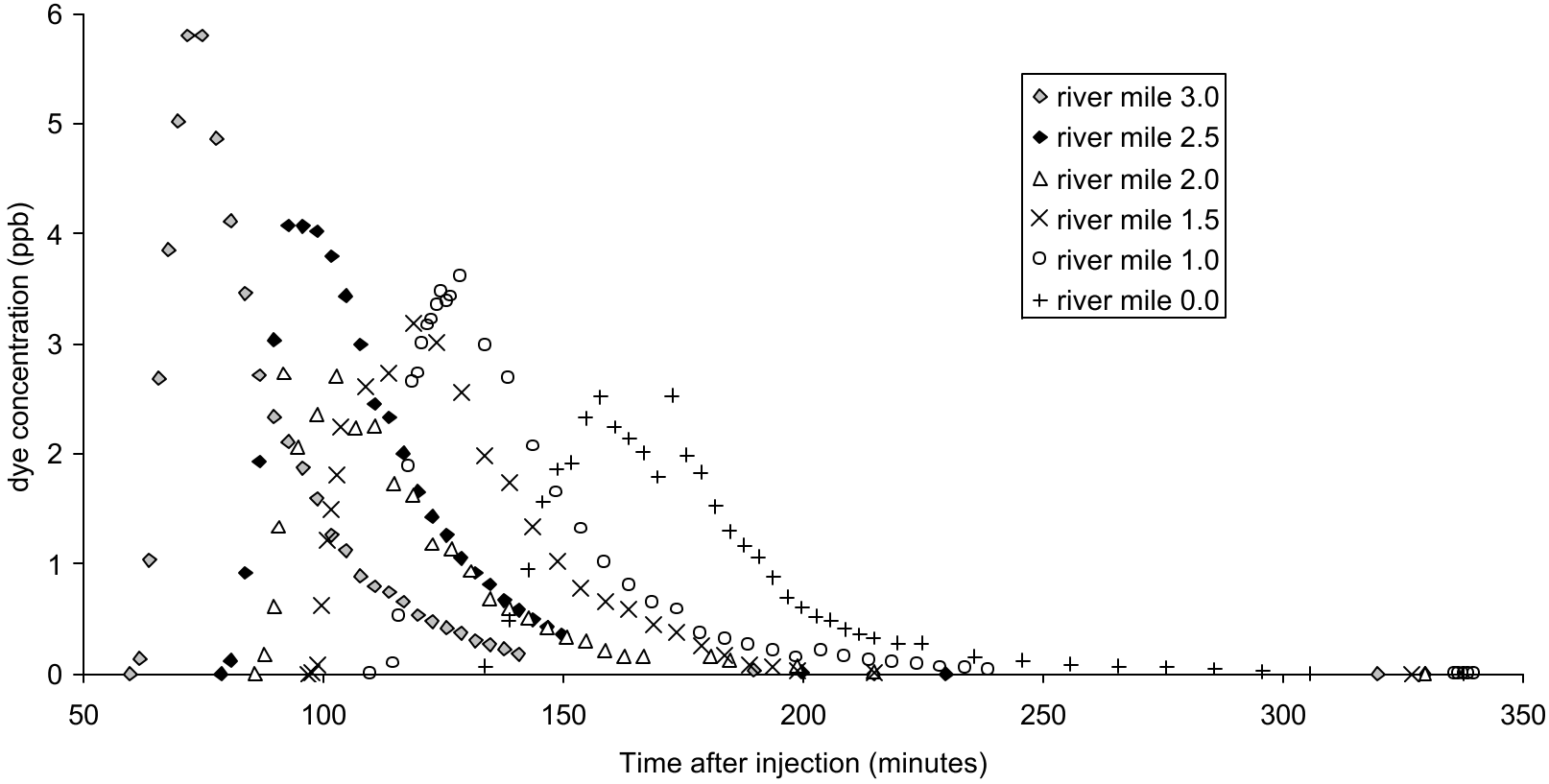


**Figure 648. 1995 USGS Santiam River dye study. Injected at RM 5.1. The dye may not be mixed laterally at river mile 3.0 as 108% of the dye was recovered.**

## *1992 Clackamas River*

Five 1992 dye studies conducted on the Clackamas River were reported in USGS Water Resources Investigations Report 95-4078. (Lee, 1995). Two injection points, RM 22.8 and RM 13.3, were used and studies were conducted at a high flow (37 to 39 $m^3/s$) and a low flow (17 to 21 $m^3/s$) condition. The high flow studies are shown in Figure 649 (RM 13.3) and Figure 650 (RM 22.8). 3.0 Liters of 20% dye injected at 0900, May 14, at RM 13.3 and sampled at six downstream stations. 2.8 Liters of 20% dye injected at 0825, May 15, 1992 at RM 22.8 and sampled at four downstream stations. Equipment problems caused the loss of data at two stations for the May 15 study. Recorded discharge is shown in Table 70.

**Table 70. 1992 USGS Clackamas River dye studies discharge under high flow conditions**

| River mile | Q, cfs | Q, $m^3/s$ |
|---|---|---|
| **May 14, 1992 at RM 13.3** | | |
| 11.0 | 1310 | 37.1 |
| 9.5 | 1310 | 37.1 |
| 8.0 | 1370 | 38.8 |
| 4.8 | 1370 | 38.8 |
| 1.7 | 1370 | 38.8 |
| 0.5 | 1370 | 38.8 |
| **May 15, 1992 at RM 22.8** | | |
| 19.7 | 1350 | 38.2 |
| 17.0 | 1320 | 37.4 |
| 13.9 | 1290 | 36.5 |
| 11.0 | 1290 | 36.5 |

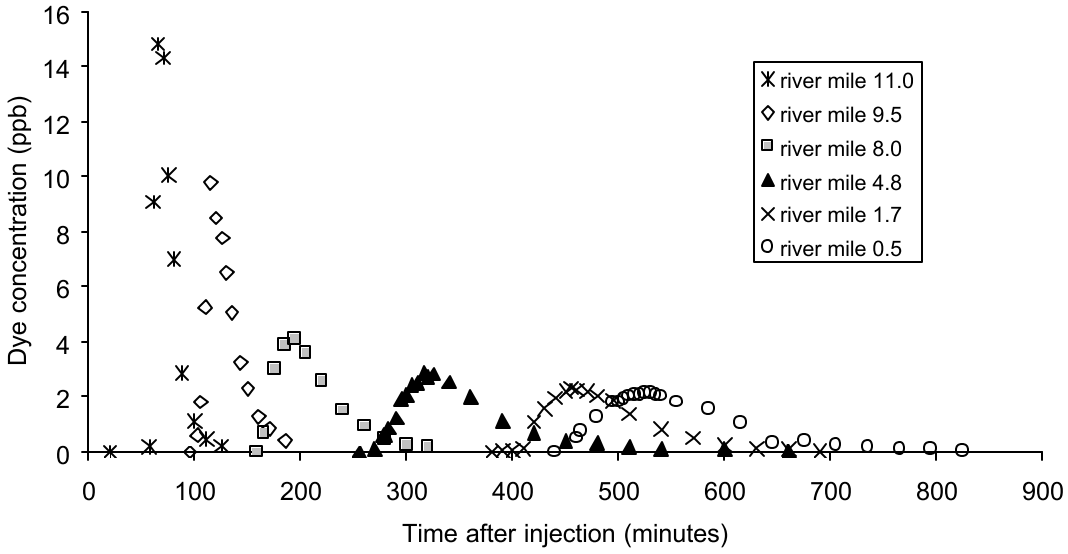


**Figure 649. 1992 USGS Clackamas River dye study. Injected at RM 13.3**

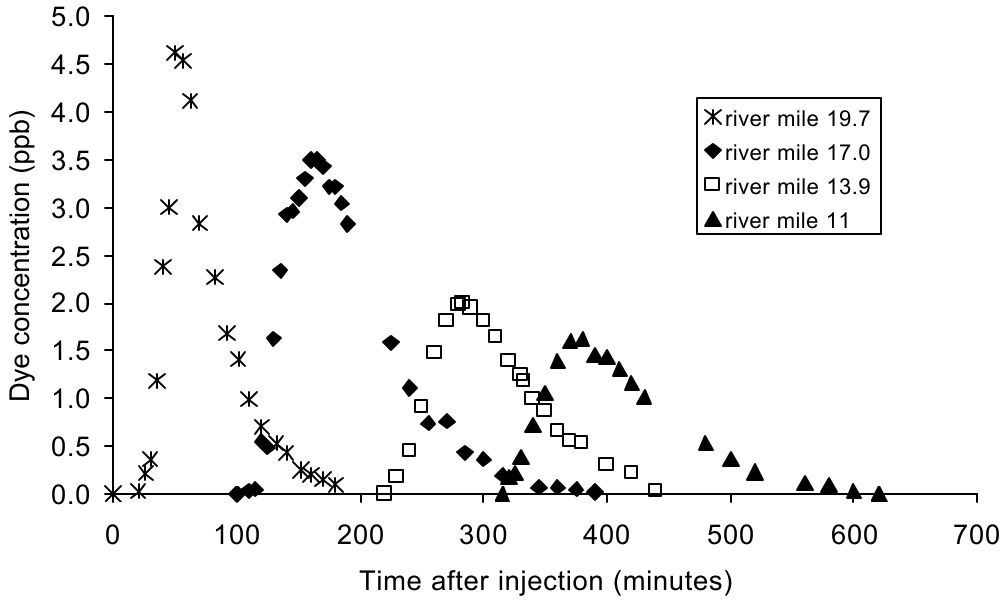


**Figure 650. 1992 USGS Clackamas River dye study. Injected at RM 22.8**

The low flow studies are shown in Figure 651 (RM 13.3) and Figure 652 (RM 22.8). 3.0 Liters of 20% dye were injected at 0847, July 22, 1992 at RM 13.3 and sampled at five downstream stations. 1.5 Liters of 20% dye injected at 0832, July 23, 1992 at RM 22.8 and usable data was taken at three downstream stations. Background sampling was conducted to ensure no residual dye concentration was present. Because of the missing data at RM 4.8, and additional study was conducted July 24, 1992, using 0.3 Liters of 20% dye injected at RM 8.0 and sampled at RM 4.8. The data are shown in Figure 653. Discharges are reported in Table 71.

**Table 71. 1992 USGS Clackamas River dye studies discharge under low flow conditions.**

| Reach | Discharge | |
|---|---|---|
| | (cfs) | ($m^3$/sec) |
| RM 13.3-0.5 | 600 | 17.0 |
| RM 22.8-13.9 | 750 | 21.2 |
| RM 8.0-4.8 | 650 | 18.4 |

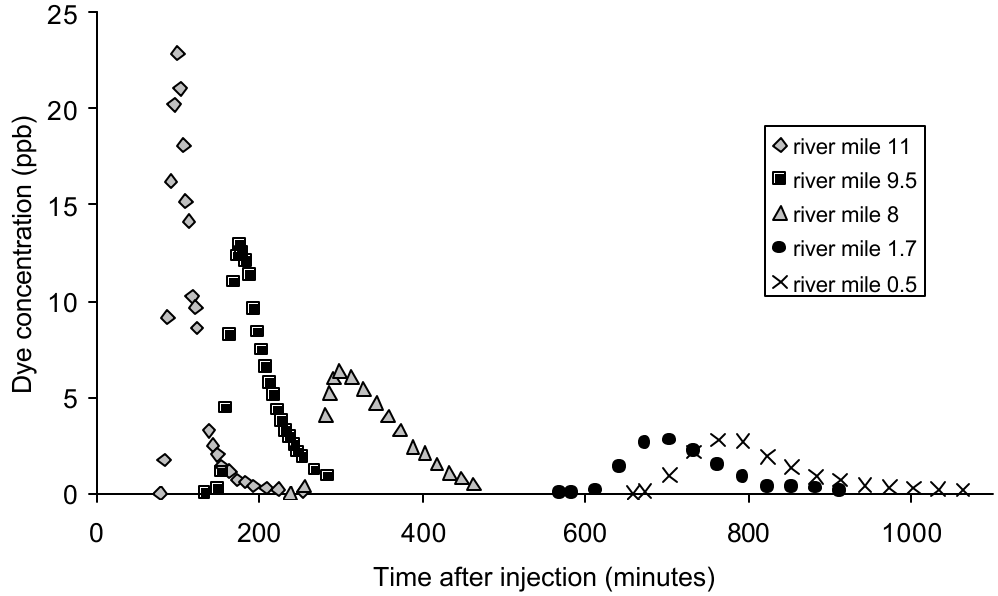


**Figure 651. 1992 USGS Clackamas River dye study. Injected at RM 13.3**

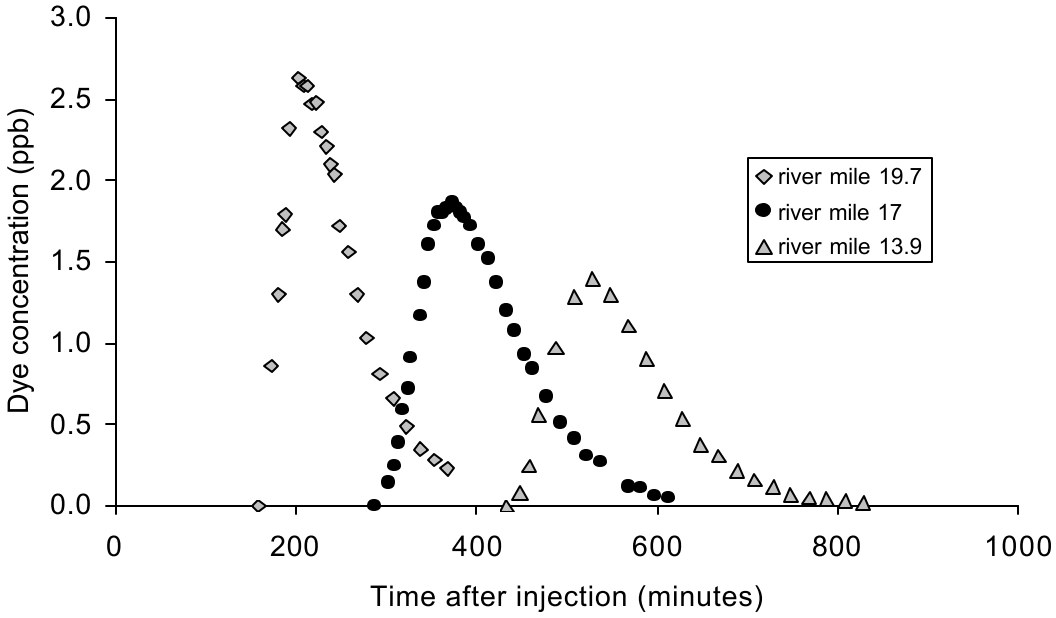


**Figure 652. 1992 USGS Clackamas River dye study. Injected at RM 22.8.**

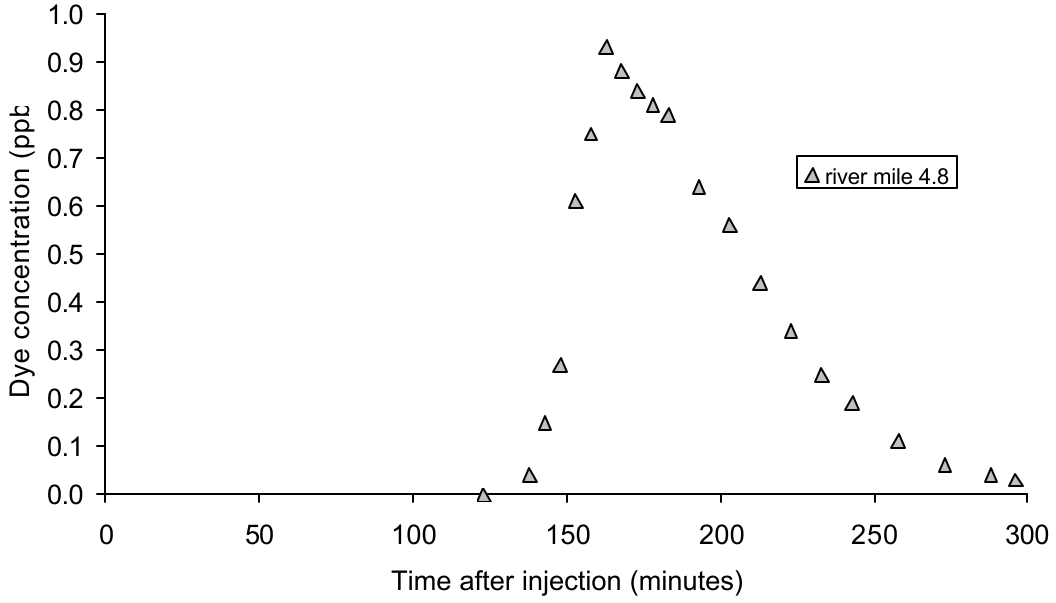


**Figure 653. 1992 USGS Clackamas River dye study. Injected at RM 8.0.**

## *1992 Willamette River*

In 1992, the USGS conducted two dye studies on the Willamette River main stem. The results were reported in USGS Water Resources Investigations Report 95-4078. (Lee, 1995). The first study was conducted June 9, 1992, as shown in Figure 654. 5.0 liters of 20% concentration fluorescent dye were injected at 12:50 p.m. at RM 150.9. Concentrations were measured downstream at four locations: RM 147.3, 144.8, 141.2, 138.3. Recorded discharges at RM 147.3, 144.8, and 138.3 were 100.1, 98.6, and 96.1 $m^3$/sec, respectively. These were very low summer flows for this reach. More typical average low flows are in the range of 110 to 170 $m^3$/s.

The second dye study was conducted on June 10, 1992, as shown in Figure 655. 7.0 liters of 20% concentration dye was injected at 9:40 a.m. at RM 161.2. Concentrations and discharges were measured at four downstream locations: RM 156.5, 154.0, 150.9, and 141.2, with recorded discharges of 97.7, 100.8, 101.9, and 96.0 $m^3$/sec, respectively. Table 72 summarizes the recorded discharge for both the low and high flow dye studies.

**Table 72. 1992 USGS Willamette River dye studies discharge.**

| River mile | Discharge | |
|---|---|---|
| | (cfs) | ($m^3$/sec) |
| **June 9, 1992 at RM 150.9.** | | |
| 147.3 | 3530 | 100.1 |
| 144.8 | 3480 | 98.6 |
| 138.3 | 3390 | 96.1 |
| **June 10, 1992 at RM 161.2** | | |
| 156.5 | 3450 | 97.7 |
| 154.0 | 3560 | 100.8 |

| | | |
|---|---|---|
| 150.9 | 3600 | 101.9 |
| 141.2 | 3390 | 96.0 |

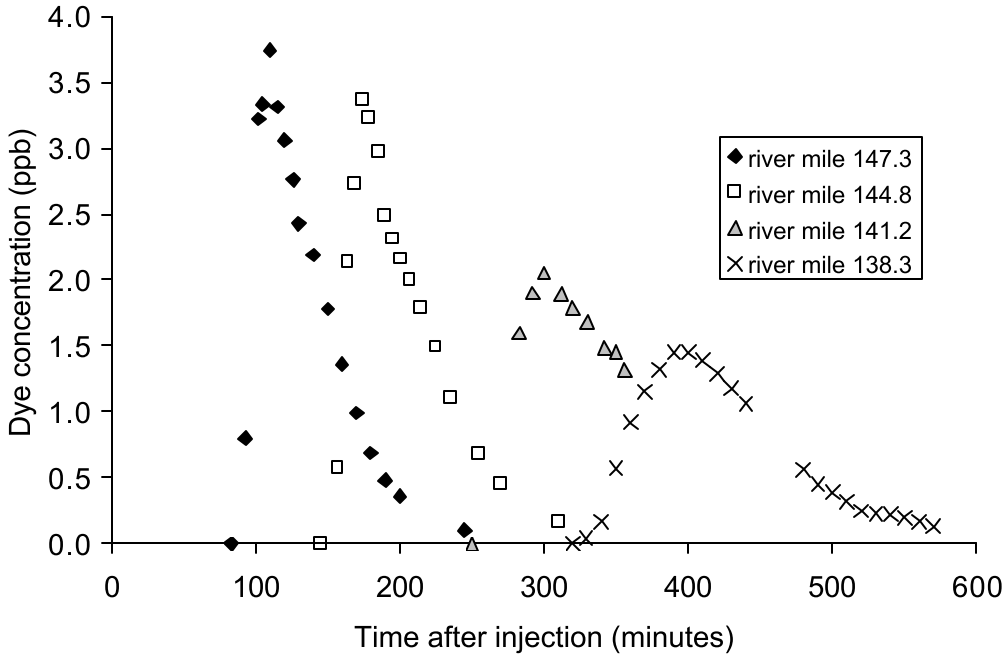


**Figure 654. 1992 USGS Willamette River dye study. Injected at RM 150.9.**

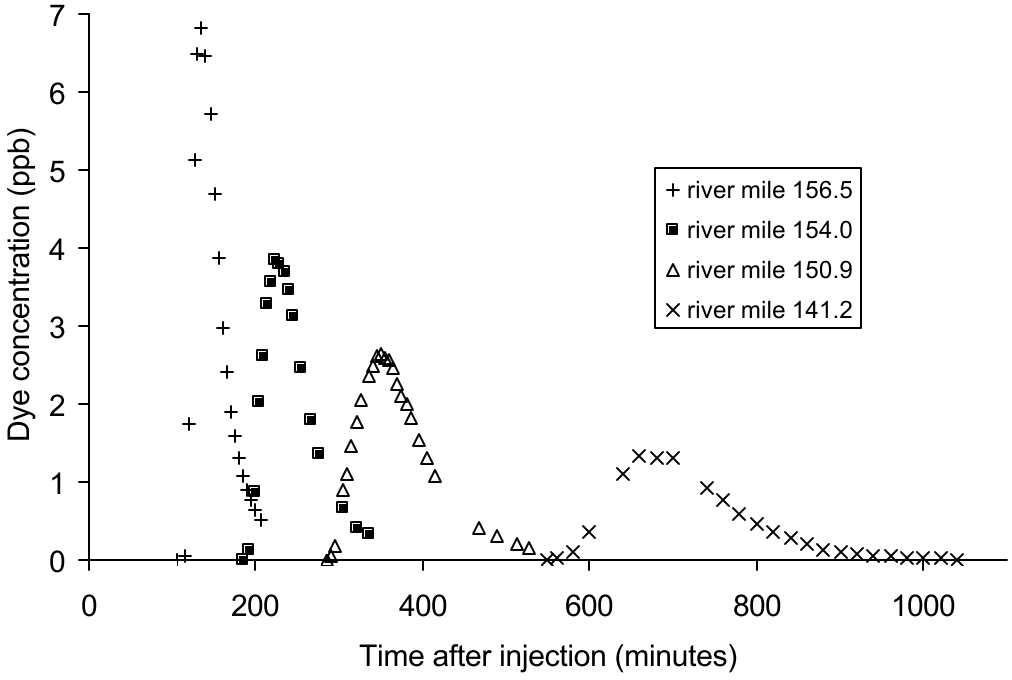


**Figure 655. 1992 USGS Willamette River dye study. Injected at RM 161.2**

## *1998 Upper Willamette River*

A 1998 dye study reported by Fernald, et al. (2001), investigated hyporheic flow over a reach of the upper Willamette River, RM 153 to 169. Three injections over three contiguous reaches were made in the summer of 1998. Each reach was subdivided into three sub-reaches. Results are shown in Figure 656, Figure 657, and Figure 658. 3.0 Liters of dye were injected July 2, 1998, at RM 169.5. 4.1 Liters of dye were injected June 29, 1998, RM 166.2. 5.0 Liters of dye were injected June 25, 1998, RM 158.6. Each study used 20% Rhodamine WT dye tracer.

The average discharge during the dye study, measured at each sampling stations, was reported in Table 73. The average discharge over the full reaches of the July 2, June 29, and June 25, 1998, were 170, 175, and 186 $m^3$/sec, respectively.

A dozen riffle complexes, which exhibit hyporheic flow, were identified in the study area. At one complex, it was estimated that a 6% flow loss occurred and later reemerged downstream. Fernald, et al., suggest that perhaps 70-75% of the low flow river volume could flow through hyporheic pathways over the study area.

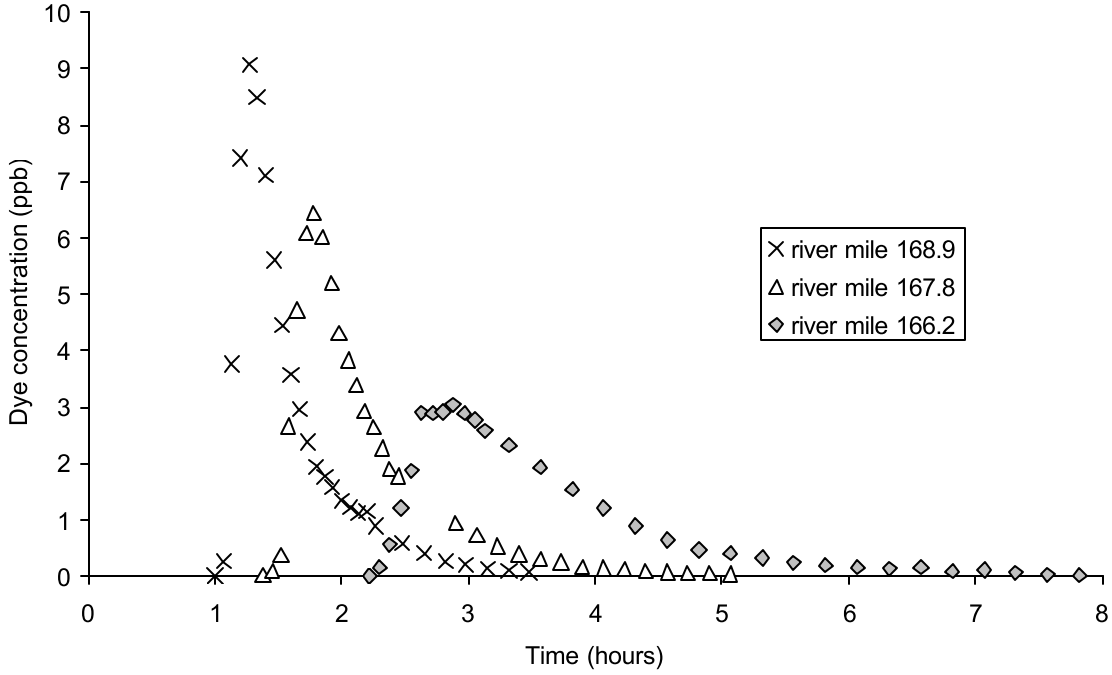


**Figure 656. 1998 USGS Willamette River dye study. Injected at RM 169.5.**

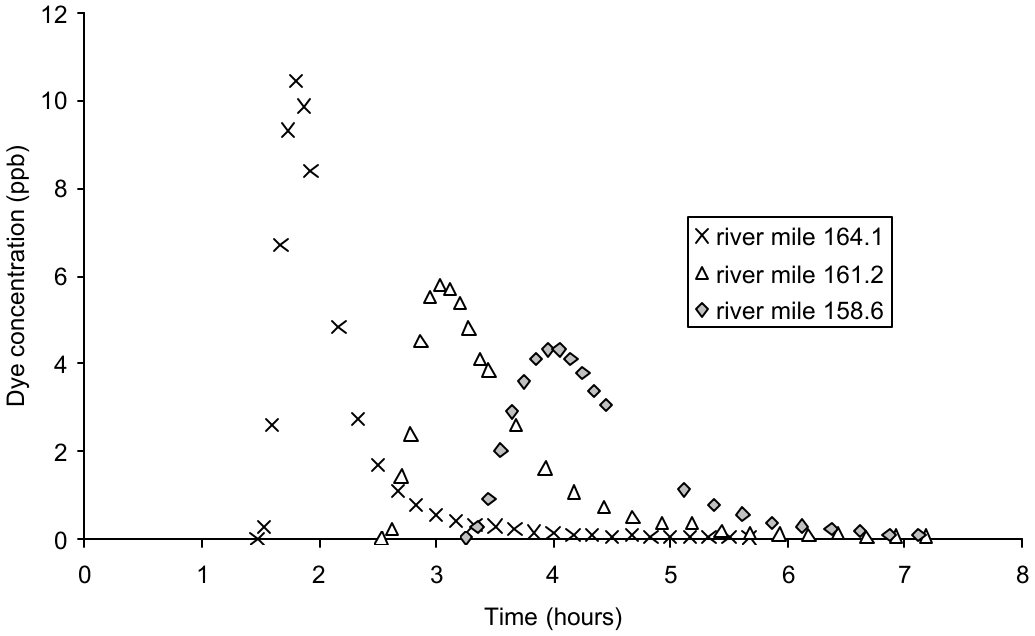


**Figure 657. 1998 USGS Willamette River dye study. Injected at RM 166.2.**

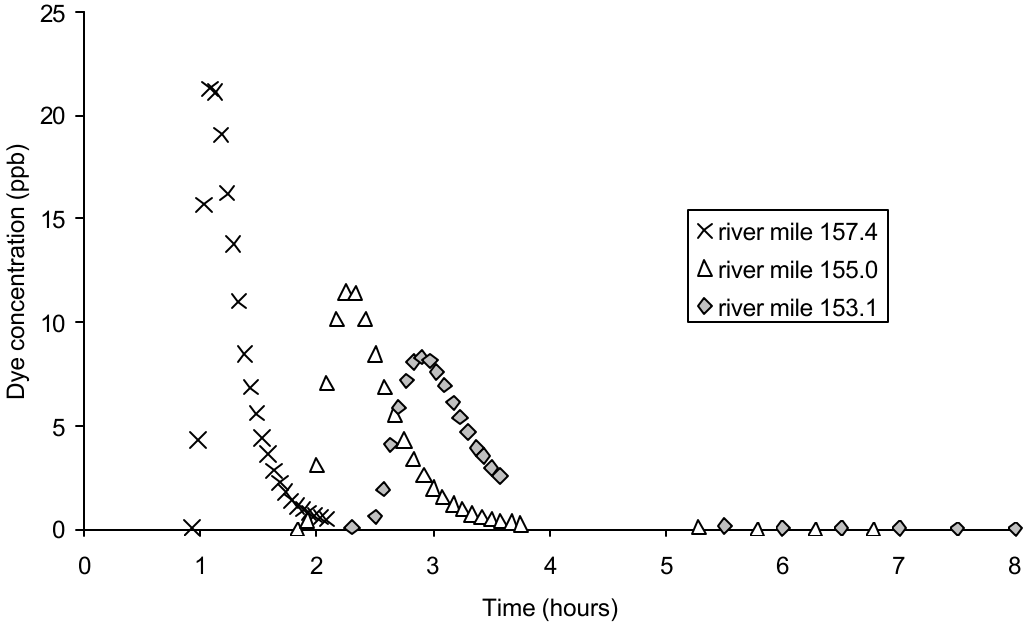


**Figure 658. 1998 USGS Willamette River dye study. Injected at RM 158.6.**

**Table 73. 1998 USGS Willamette River dye studies discharge**

| River mile | Discharge | |
|---|---|---|
| | (cfs) | ($m^3$/sec) |
| **July 2, 1998 at RM 169.5.** | | |
| 169.5 | 6183 | 175.1 |
| 168.9 | 5830 | 165.1 |

| | | |
|---|---|---|
| 167.8 | 5982 | 169.4 |
| 166.2 | 6070 | 171.9 |
| **June 29, 1998 at RM 166.2.** | | |
| 166.2 | 6172 | 174.8 |
| 164.1 | 6158 | 174.4 |
| 161.2 | 6180 | 175.0 |
| 158.6 | 6190 | 175.3 |
| **June 25, 1998 at RM 158.6.** | | |
| 158.6 | 6596 | 186.8 |
| 157.4 | 6603 | 187.0 |
| 155.0 | 6459 | 182.9 |
| 153.1 | 6614 | 187.3 |

## *2002 Willamette River*

In 2002, the USGS conducted three dye studies on the Willamette River between approximately Salem (RM 85) and Peoria, Oregon (RM 141.4).

Over June 11 to13, 2002, the USGS conducted two dye studies on the upper Willamette. The June 11th study encompassed Adair, Oregon, (RM 121.9) to RM 108. The June 12-13th study covered Peoria (RM 141.4) to RM 127.6. 12.0 L and 14.0 L of 20% Rhodamine WT dye were injected, respectively. A failure with the dye boat prevented the accumulation of data at RM 121.9 during the second study. Flows were recorded at the Albany gaging station (USGS 14174000) and show a decrease in discharge with time from 7280 to 6970 cfs over the study time period.

From a water balance of gaged inflows and outflows, Laenen (2002a) estimates a linear groundwater inflow of 150 cfs between RM 142.1 and RM 122. This was consistent with two previous 1992-93 gain-loss measurements of 200-400 cfs, respectively. (q.v., Laenen (1995)).

**Table 74. June 2002 USGS Willamette River dye studies sampling locations and discharge**

| Geographic landmark | River mile | Discharge | |
|---|---|---|---|
| | | (cfs) | ($m^3$/sec) |
| **June 11, 2002, at RM 121.9.** | | | |
| below WTP intake (injection) | 121.9 | 7280 to 7140 | 212 to 206 |
| Albany bridge | 119.4 | | |
| | 115.0 | | |
| | 111.0 | | |
| confluence with Santiam | 108.0 | | |
| **June 12, 2002, at RM 141.4.** | | | |
| Peoria boat ramp (injection) | 141.4 | 7020 to 6970 | 199 to 197 |
| | 137.1 | | |
| Corvallis WTP intake | 134.1 | | |
| Corvallis bridge | 131.4 | | |
| | 127.6 | | |

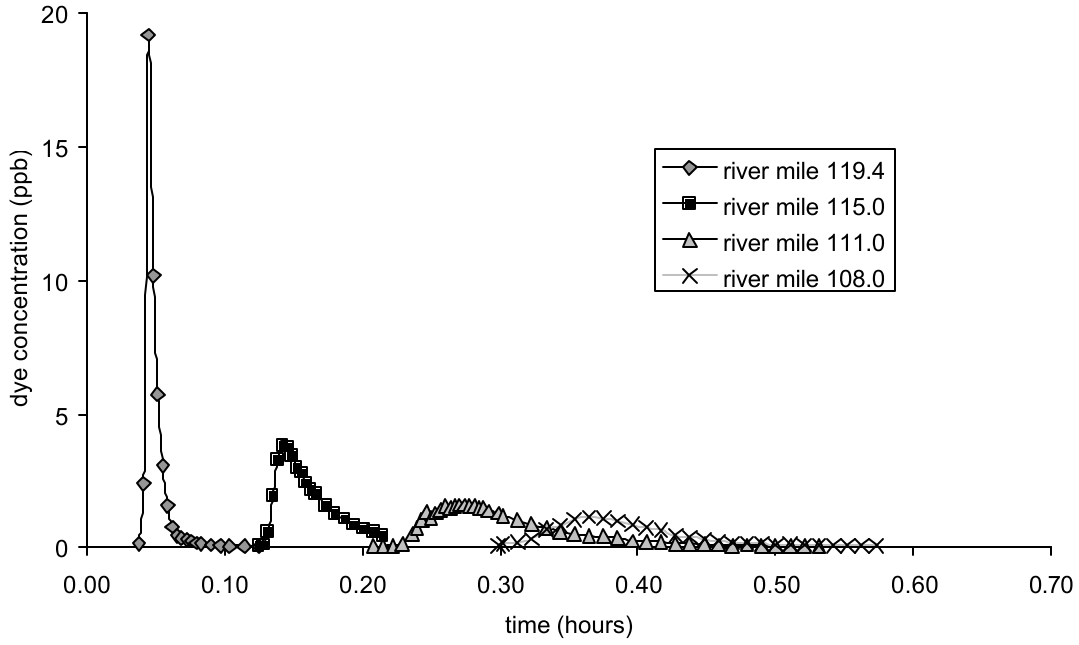


**Figure 659. 2002 USGS Willamette River dye study: Injected at RM 121.9.**

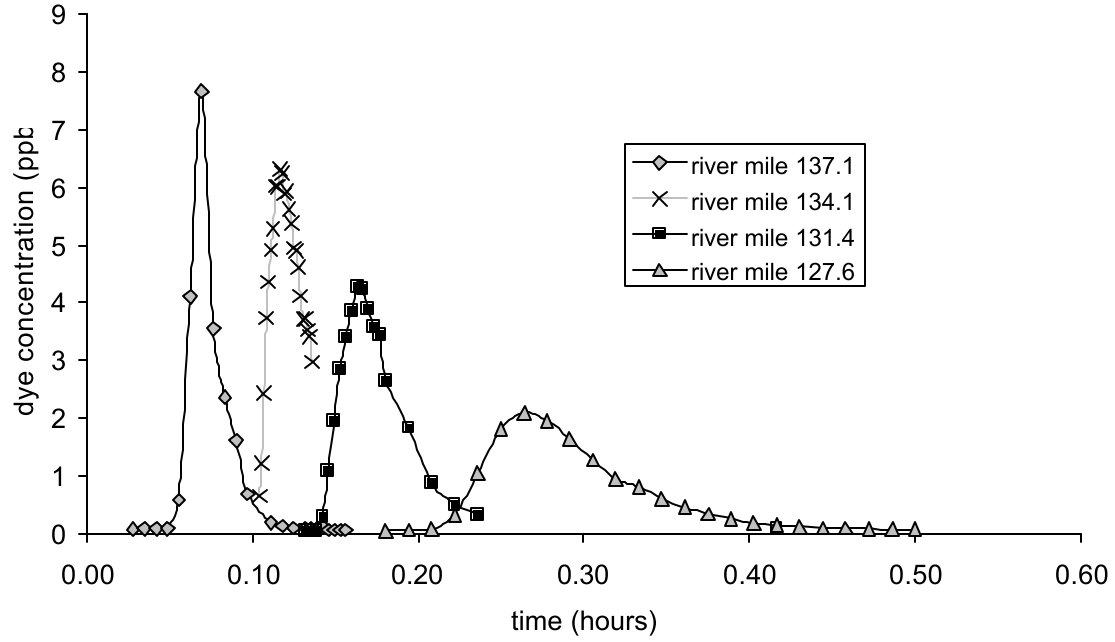


**Figure 660. 2002 USGS Willamette River dye study. Injected at RM 141.4.**

On September 24, 2002, the USGS conducted a dye study on the upper Willamette from Corvallis (RM 131) to Independence Bridge (RM 96). 19.0 L of 20% Rhodamine WT dye were injected at 8:00 a.m. at the Corvallis Bridge, and sampled at six locations. Steady-flow was indicated for the period of the study by the Albany stream gage (USGS 14174000) where the investigators measured a flow of 5580 cfs. This value was 3% higher than the discharge reported at the Albany stream gage for the same period.

The flows varied spatially from 5290 cfs at Corvallis to 7810 cfs at Independence Bridge, which was 14 miles below the confluence with the Santiam River. A linear groundwater inflow of 560 cfs was estimated between RM 131-96. This inflow was consistent with work done in 1992-3.

A comparison of the travel rates generated by these studies and the 1992 Lee study to the Harris study (1962-63), reveals a slower travel rate for the more recent studies. The 2002 and the 1992 studies show travel rates of the peak to be ~7 and ~3 percent slower, respectively, than the older 1962-63 dye studies. This increases to ~8 percent slower if the leading edge travel rates were included in the calculation. This could be indicative of an increase in the effective channel cross sectional area.

**Table 75. September 2002 USGS Willamette River dye studies sampling locations and discharge.**

| Geographic landmark | River mile | Discharge | |
|---|---|---|---|
| | | (cfs) | ($m^3$/sec) |
| **September 24, 2002, at RM 131.25.** | | | |
| Corvallis bridge (injection) | 131.25 | 5580 | 158 |
| | 126.0 | | |
| Adair WTP intake | 122.1 | | |
| | 115.0 | | |
| above Santiam confluence | 108.3 | | |
| Buena Vista Ferry | 106.4 | | |
| Independence bridge | 96.1 | | |

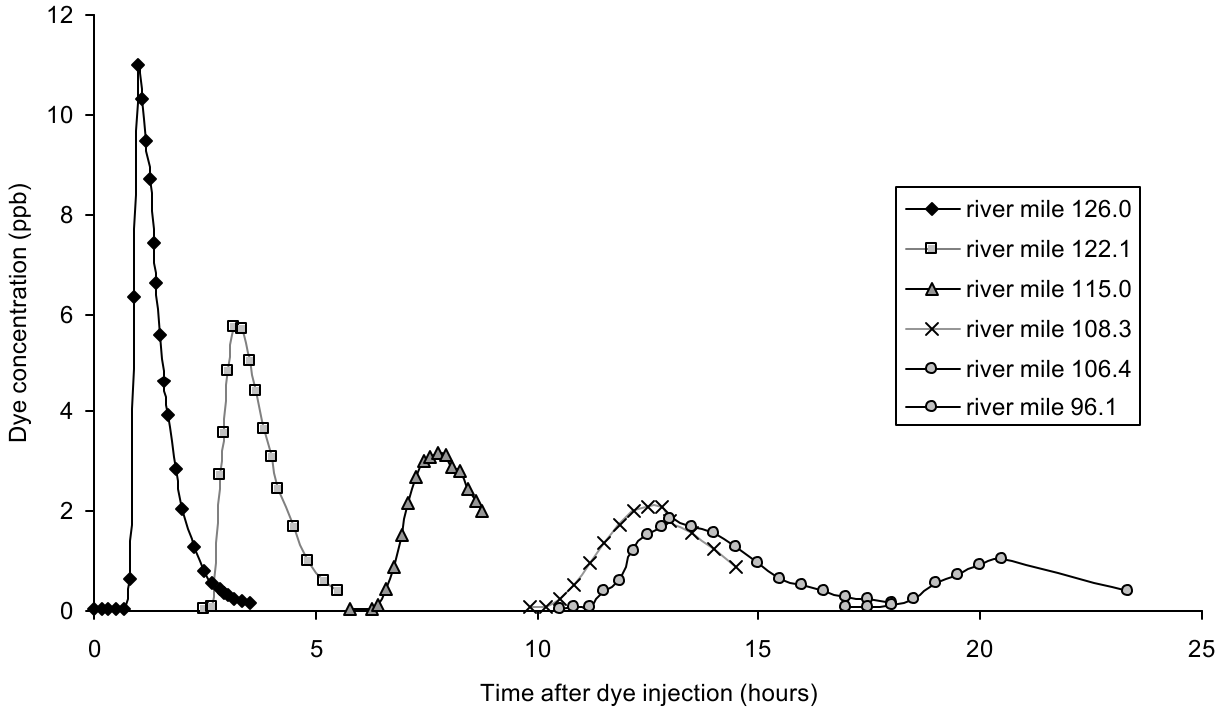


**Figure 661. USGS Willamette River dye study. Injected at RM 131.25.**

## *2002 Long Tom River*

The USGS conducted a high-flow and a low-flow set of dye studies on the Long Tom River in May and August 2002, respectively. The reported discharges in both sets of studies were a combination of gaged flows and predicted tributaries and groundwater inflows, as estimated by Laenen, et al. (1997).

In May 2002, the USGS conducted two dye studies on the Long Tom River. On May 7th, 1.5 L of 20% Rhodamine WT dye were injected at Alvadore, Oregon, (RM 23.1) and sampled at four downstream sites as reported in Table 76. The last site, the apron below Ferguson Dam (RM 12.05), became the injection point for the May 8th study (1.0 L of dye) which was also sampled at four downstream locations, the furthest downstream site, Bundy Bridge, was 0.9 river miles from the confluence with the Willamette River.

While steady discharge from Fern Ridge Reservoir was achieved for the duration of both May studies, the first reach (RM 23.1 to 12.05) has several inflows: Coyote Creek, Bear Creek, Amazon Creek, and groundwater seepage from the dam near the stream gage at Alvadore (USGS#14169000). These inflows were 8, 18.8, 15.3, and 5 cfs, respectively, as estimated by Laenen (2002b). The Ferguson Diversion at RM 13.05 drew 80 cfs from the main channel discharge of 156 cfs. The diversion is the pre-channelized Long Tom River which joins with Ferguson Creek approximately a mile before returning to the main Long Tom River channel just downstream of Ferguson Dam. The length of the separation from the main channel is 4.4 miles. Ferguson Creek had a discharge of 13.9 cfs. There was an additional diversion at Ferguson Dam of a net estimate of 4 cfs to water fields to the east.

The second study was timed so as to also capture the dye peaks from the day before. This can be seen in Figure 663, especially at RM 9.25. The last peak to occur was the dye which had moved down the main stem of the Long Tom (i.e., crested the dam) from the previous day. Hidden within the first peak is a spike from the portion of the flow which passed through the diversion at Ferguson dam. It was expected to arrive approximately 5 hours ahead of the main-stem peak. Analysis of the dye volumes shows that this did occur. There may not be sufficient separation of the peaks to calculate accurate leading edge travel times for the second study, but a mass recovery shows the superposition of two peaks.

The stream gage at Monroe (~RM 6.3) was taken to be the discharge over the lower reach. The diversion for the dam just downstream of the stream gage has an estimated flow of 1 cfs.

**Table 76. May 2002 USGS Long Tom River dye studies sampling locations and discharges.**

| Geographic landmark | River mile | Discharge | |
|---|---|---|---|
| | | (cfs) | ($m^3$/sec) |
| **May 7, 2002, at RM 23.1.** | | | |
| Franklin Bridge | 20.5 | 114 | 3.22 |
| Cheshire Bridge | 17.15 | 122 | 3.45 |
| Cox Butte Road | 13.0 | 141 | 3.99 |
| Ferguson Dam (below apron) | 12.05 | 72 | 2.04 |
| **May 8, 2002, at RM 12.05.** | | | |
| Stroda Ford | 9.25 | 166 | 4.70 |
| Monroe Dam | 6.2 | 166 | 4.70 |
| Bellfountain Road Bridge | 2.8 | 166 | 4.70 |
| Bundy Bridge | 0.9 | 166 | 4.70 |

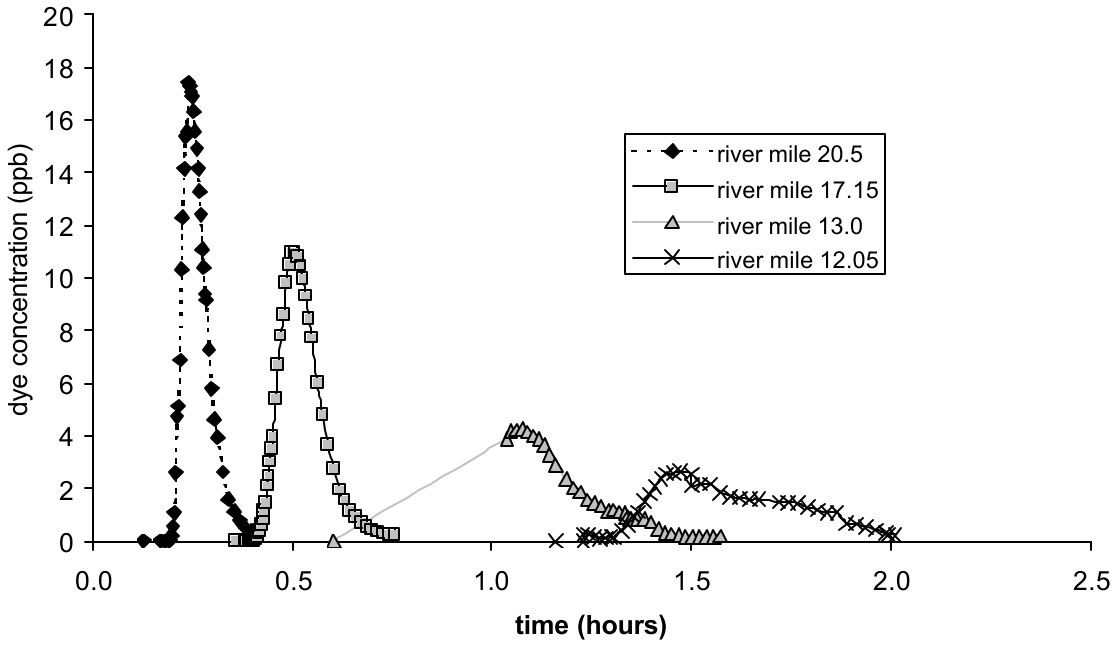


**Figure 662. May 2002 USGS Long Tom River dye study. Injected at RM 23.1.**

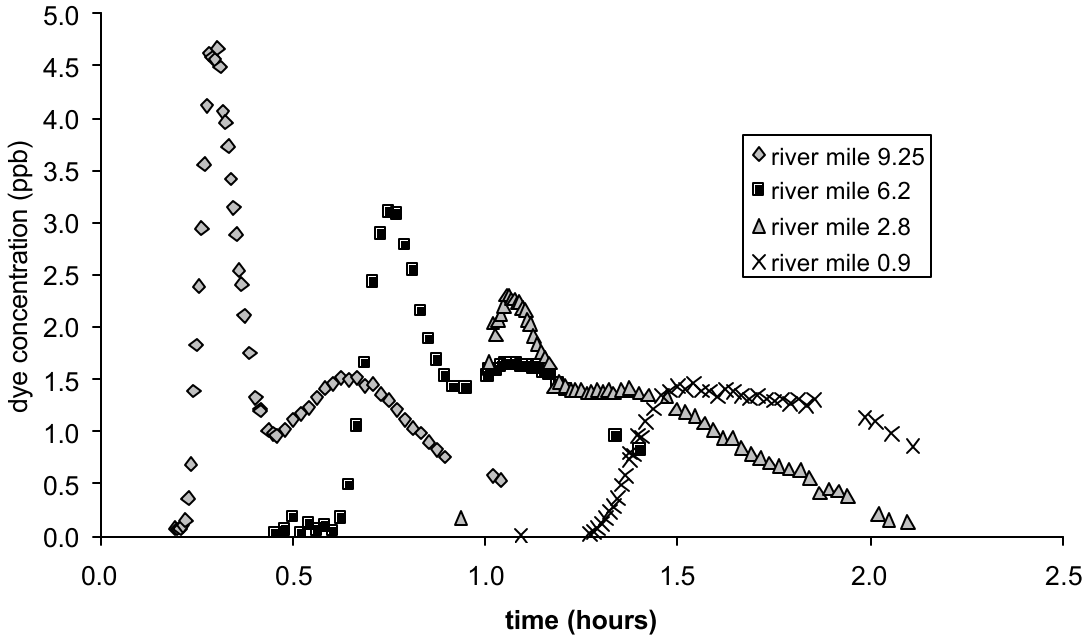


**Figure 663. May 2002 USGS Long Tom River dye study. Injected at RM 12.05.**

In August 2002, two dye-tracer studies were conducted along similar reaches. For the lower reach study conducted on August 19, the injection of 1.0 L of dye was moved downstream to Stroda Ford (RM 0.25) and an additional sampling station was placed at RM 4.35. Flows over this reach were 35.3 cfs, as compared to the 166 cfs of the May study.

For the upper reach, RM 23.1 to Stroda Ford (RM 9.75), the 1.0 L of dye injected on August 20 was additionally measured after the confluence with Ferguson Creek at RM 11.95 and at Stroda Ford (RM 9.25). The incomplete data at Ferguson Dam is due to a vandalized dye boat.

The inflows over the August study period include the Coyote Creek, Bear Creek, Amazon Creek, and Ferguson Creek at 3.1, 0.4, 1.6, and 28.3 cfs, respectively. A miscellaneous diversion loss of 2 cfs between RM 23.1 and RM 20.5 replaced the groundwater inflows seen in May. The diversions at Ferguson and Monroe Dams were estimated to be net losses of 34 and 0.8 cfs, respectively. This large withdrawal at Ferguson dam resulted in only 8 cfs of flow over the dam crest. Consequently, flow through the Ferguson Diversion was much faster than through the main channel. This estimated 8 hour lag resulted in the second peak not being sampled due to time constraints.

**Table 77. August 2002 USGS Long Tom River dye studies sampling locations and discharges.**

| Geographic landmark | River mile | Discharge | |
|---|---|---|---|
| | | (cfs) | ($m^3$/sec) |
| **August 19, 2002, at RM 9.25.** | | | |
| Monroe Dam | 6.2 | 35.3 | 1.00 |
| Stow Pitt Road Bridge | 4.35 | 35.3 | 1.00 |
| Bellfountain Road Bridge | 2.8 | 35.3 | 1.00 |
| Bundy Bridge | 0.9 | 35.3 | 1.00 |
| August 20, 2002, at RM 23.1. | | | |
| Alvadore-(injection) | 23.1 | 53.8 | 1.52 |
| Franklin Bridge | 20.5 | 51.8 | 1.47 |
| Cheshire Bridge | 17.15 | -- | -- |
| Cox Butte Road | 13.0 | 56.9 | 1.61 |
| Ferguson Dam (below apron) | 12.05 | 8.2 | 0.23 |
| Stroda Ford | 9.25 | 36.5 | 1.03 |
| Ferguson Creek Diversion (alternate route) | 11.95 | 36.5 | 1.03 |

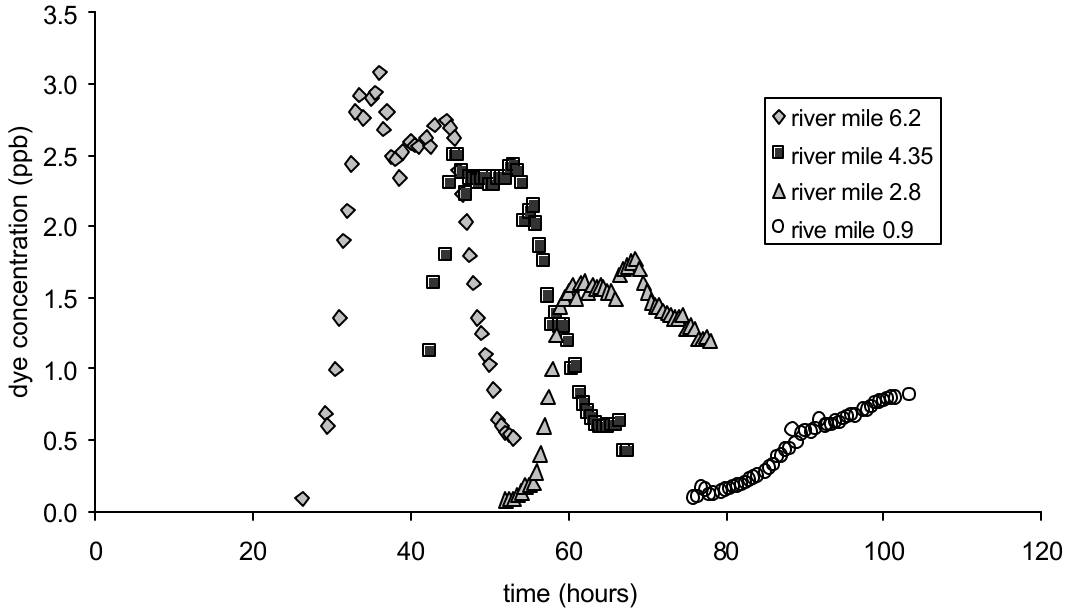


**Figure 664. August 2002 USGS Long Tom River dye study. Injected at RM 9.25.**

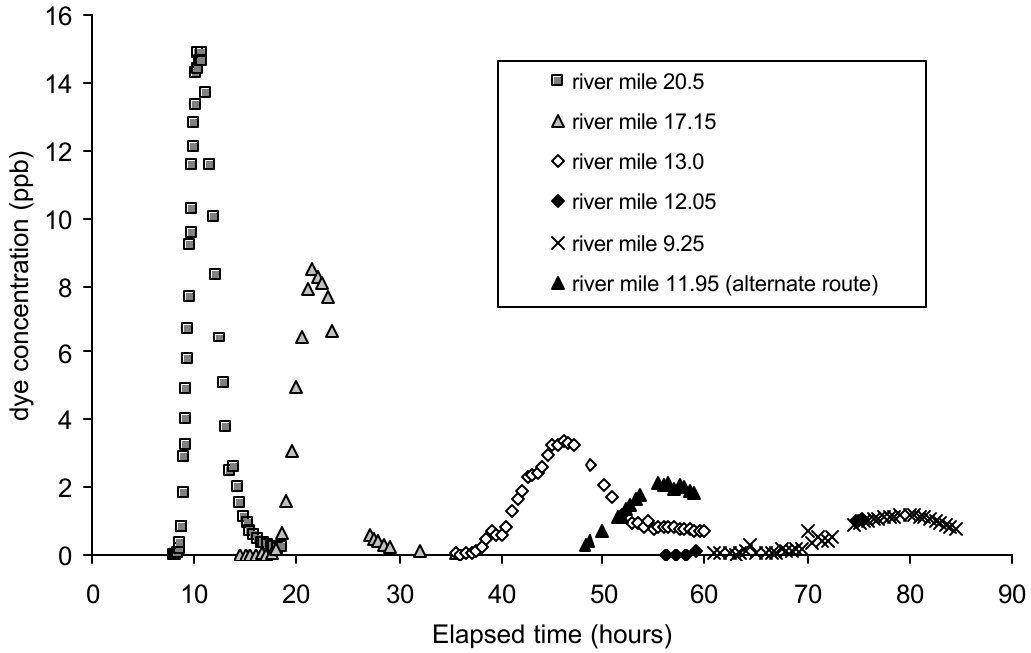


**Figure 665. August 2002 USGS Long Tom River dye study. Injected at RM 23.1. The sampling at RM 11.95 is along a diversion downstream of the point of injection.**

**Table 78: Summary of groundwater exchanges.**

| River reach | River discharge, m3/s | Hyporheic exchange | | Net gain (inflow) | Net loss (outflow) | Source |
|---|---|---|---|---|---|---|
| Santiam River | | | | | | |
| RM 5 to RM 0 | 35 to 50 | 5 | or | -- | -- | Laenen and |

| | | | | | | |
|---|---|---|---|---|---|---|
| | ~100 | m3/s<br>10<br>m3/s | 10%<br>of<br>flow | | | Bencala, (2001) |
| Willamette River | | | | | | |
| RM 169 to 153 | 170 to 190 | 6% of flow | | -- | -- | Fernald, et. al., (1998) |
| RM 142 to 122 | ~200 | -- | | 4 to 11 m3/s | -- | Laenen (2002a), unpublished |
| RM 131 to 96 | ~160 | -- | | 16 m3/s | -- | Laenen (2002a), unpublished |
| RM 161 to 118 | 100<br>200 | 0 to 10 % of flow | | -- | -- | Laenen and Bencala, (2001) |
| Long Tom | | | | | | |
| RM 23.1 to 12.05<br>RM 23.1 to 12.05 | 3 to 5 (May)<br>1 to 2 (August) | -- | | 5 cfs<br><br>-- | 2 cfs (diversion losses) | Laenen (2002b), unpublished |

# Appendix C: South Santiam River Meteorological Analysis

This analysis was designed to explore the best method of utilizing available meteorological data to simulate the meteorological conditions for the South Santiam River model, as shown in Figure 666. The general approach of this analysis was to utilize the stations surrounding the Stayton station to predict the meteorological data at Stayton. Since the Stayton site was used to predict meteorological inputs for the South Santiam River model.

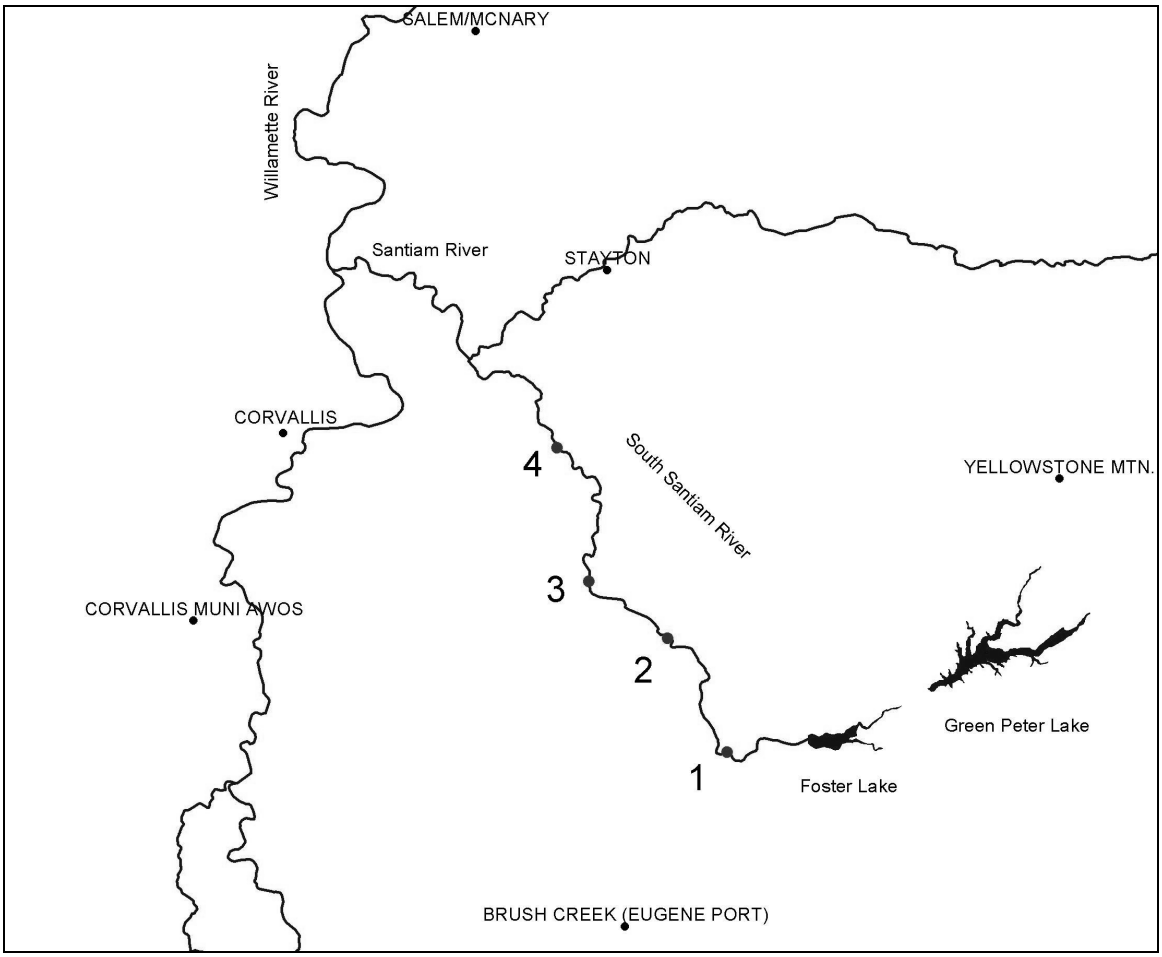


**Figure 666. Meteorological station data available. The points labeled 1, 2, 3, and 4 are model water body center points. The points labeled in capitals are meteorological stations.**

## *Data summary*

Six meteorological stations in reasonable proximity to the model region had data: Salem/McNary, Stayton, Yellowstone Mountain, Corvallis and Corvallis Municipal AWOS. Station information was reported in Table 79. The Corvallis site contains solar data, but not wind or temperature data. The stations furthest apart are 68.5 km east to west and 70.7 km north to south. The Yellowstone Mountain and Brush Creek stations are located in the mountainous region in the southwest of the Santiam basin; the remaining stations are in the lower-lying valley floor. The data examined includes hourly temperature, wind speed, wind direction, and relative humidity for the period of January 1, 2001 through

December 31, 2001. Data were not always available at all sites for a given day and hour. Approximately 15% of the total possible data for 2001 was missing. Approximately one-third of the missing data were composed of entire missing days from January 1 through 4 and after December 15. The remaining missing data were distributed within the data set, with a greater frequency of data lost in November and December. The data are shown in Figure 667, Figure 668, Figure 669, Figure 670, Figure 671, Figure 672, and Figure 673. Descriptive statistics for the data sets are shown in Table 80.

The stations utilize different measuring equipment and were operated by three different agencies. Consequently, some differences between the data sets were due to sampling frequency and averaging periods, as well as equipment sensitivity. The Stayton site recorded wind speed in 10 minute intervals, whereas the Corvallis MUNI site recorded wind speed in 20 minute intervals. As seen in Figure 670 and Figure 671, there are consequently more wind speed measurement values of zero. The mean wind speed at the Stayton station was expected to be less than the mean value for the remaining stations. Additionally, the wind gages at Salem and Corvallis MUNI appear to have a higher minimum wind speed threshold as evidenced by the lack of any data points between 0 and 1.54 m/sec. (see Figure 670).

An examination of the descriptive statistics reveals that the wind behavior at Stayton was not similar to Brush Creek, Corvallis MUNI, and Salem, which were more similar. All the stations will be poor predictors of the wind speed at Stayton due to the fundamentally different wind speed measurements. The wind direction at Stayton was recorded discretely in bins of 45 degrees (i.e., either 0, 45, 90, 135...315). The other stations recorded wind direction as a continuum, with a precision better than 5 degrees.

The Salem and Corvallis MUNI sites record temperature with less precision (0.1 ºC) than the Brush Creek, Stayton, and Yellowstone Mountain sites. Relative humidity data are shown in Figure 672 and Figure 673.

**Table 79. Locations of Santiam basin meteorological stations.**

| Site name | Northing*, m | Easting*, m | Station elevation, NGVD29 units, m | Distance to Stayton, m | Station type |
|---|---|---|---|---|---|
| Brush Creek (Eugene Port) | 4903137 | 511969.1 | 701 | 51853 | RAWS |
| Corvallis (solar radiation data) | 4942113 | 484929.7 | 70 | 28650 | AGRIMET |
| Corvallis MUNI AWOS | 4927247 | 477835.9 | 75 | 42868 | METAR |
| Salem-McNary Field | 4973863 | 500094.8 | 61 | 21584 | METAR |
| Stayton | 4954971 | 510532.7 | 155 | -- | RAWS |
| Yellowstone Mountain | 4938466 | 546295.7 | 939 | 39388 | RAWS |
| *Coordinates are in UTM zone 10, NAD 27. | | | | | |

**Table 80. Meteorological data descriptive statistics.**

| Temperature (ºC) | Brush Cr | Corvallis MUNI | Salem | Yellowstone | Stayton | Dist Method |
|---|---|---|---|---|---|---|
| Mean | 10.77 | 12.65 | 12.09 | 9.89 | 11.74 | 11.39 |
| Standard Error | 0.08 | 0.08 | 0.08 | 0.09 | 0.08 | 0.08 |
| Median | 10 | 12.2 | 11.1 | 8.89 | 11 | 10.49 |

| | | | | | | |
|---|---|---|---|---|---|---|
| Standard Deviation | 7.08 | 7.22 | 6.91 | 7.77 | 6.82 | 6.95 |
| Sample Variance | 50.09 | 52.19 | 47.75 | 60.42 | 46.51 | 48.27 |
| Skewness | 0.49 | 0.41 | 0.46 | 0.49 | 0.51 | 0.52 |
| Range | 38.32 | 38.9 | 41.1 | 39.45 | 39.94 | 38.1 |
| Minimum | -3.88 | -2.8 | -5 | -5.56 | -5.22 | -3.9 |
| Maximum | 34.44 | 36.1 | 36.1 | 33.89 | 34.72 | 34.2 |
| Count | 7706 | 7706 | 7706 | 7706 | 7706 | 7706 |
| Wind speed (m/s) | Brush Cr | Corvallis MUNI | Salem | Yellowstone | Stayton | Dist Method |
| Mean | 2.7 | 2.72 | 2.73 | 1.68 | 0.78 | 2.46 |
| Standard Error | 0.02 | 0.03 | 0.02 | 0.01 | 0.02 | 0.02 |
| Median | 2.68 | 2.57 | 2.57 | 1.34 | 0 | 2.24 |
| Standard Deviation | 1.39 | 2.22 | 2.15 | 1.2 | 1.52 | 1.35 |
| Sample Variance | 1.94 | 4.94 | 4.61 | 1.43 | 2.3 | 1.83 |
| Skewness | 0.97 | 0.57 | 0.93 | 1.46 | 2.31 | 1.22 |
| Range | 11.18 | 11.32 | 14.41 | 10.28 | 11.4 | 9.18 |
| Minimum | 0 | 0 | 0 | 0 | 0 | 0.1 |
| Maximum | 11.18 | 11.32 | 14.41 | 10.28 | 11.4 | 9.28 |
| Count | 7705 | 7705 | 7705 | 7705 | 7705 | 7705 |
| Wind direction (degrees) | Brush Cr | Corvallis MUNI | Salem | Yellowstone | Stayton | Dist Method |
| Mean | 221.12 | 172.28 | 164.37 | 152.59 | 145.89 | 175.97 |
| Standard Error | 1.31 | 1.52 | 1.48 | 1.18 | 1.23 | 0.83 |
| Median | 201 | 190.22 | 179.91 | 193 | 135 | 181.68 |
| Standard Deviation | 111.74 | 129.58 | 125.88 | 100.24 | 105.08 | 70.83 |
| Sample Variance | 12485.51 | 16791.91 | 15845.38 | 10048.25 | 11041.3 | 5017.08 |
| Skewness | -0.52 | -0.23 | -0.03 | 0.06 | 0.12 | -0.08 |
| Range | 359 | 359.82 | 359.82 | 359 | 315 | 346.69 |
| Minimum | 0 | 0 | 0 | 0 | 0 | 0.97 |
| Maximum | 359 | 359.82 | 359.82 | 359 | 315 | 347.66 |
| Count | 7268 | 7268 | 7268 | 7268 | 7268 | 7268 |
| Relative humidity (%) | Brush Cr | Corvallis MUNI | Salem | Yellowstone | Stayton | Dist Method |
| Mean | 74.74 | 70.77 | 76.75 | 75.61 | 80.59 | 74.57 |
| Standard Error | 0.24 | 0.21 | 0.22 | 0.28 | 0.22 | 0.21 |
| Median | 78 | 76.05 | 80.81 | 81.81 | 86.87 | 78.41 |
| Standard Deviation | 20.79 | 18.28 | 19.18 | 24.58 | 19.53 | 17.98 |
| Sample Variance | 432.37 | 334.17 | 367.76 | 604.23 | 381.51 | 323.42 |
| Skewness | -0.45 | -0.67 | -0.64 | -0.55 | -0.97 | -0.62 |
| Range | 86 | 86.66 | 82.35 | 91.02 | 84.91 | 80.23 |
| Minimum | 13 | 13.34 | 17.65 | 8.98 | 15.09 | 19.54 |
| Maximum | 99 | 100 | 100 | 100 | 100 | 99.78 |
| Count | 7694 | 7694 | 7694 | 7694 | 7694 | 7694 |

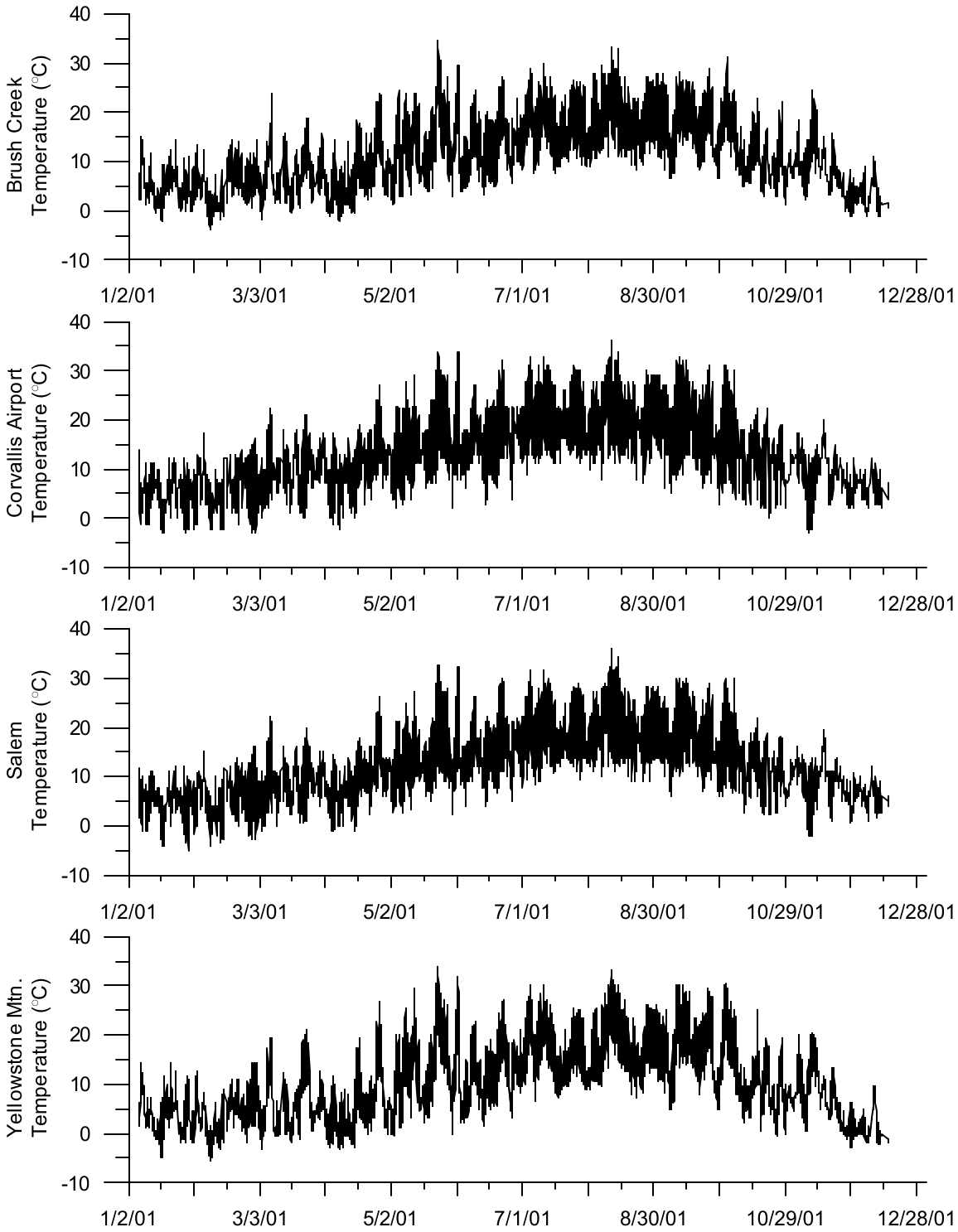


**Figure 667. Air temperature data for Brush Cr., Corvallis MUNI, Salem, and Yellowstone Mountain**

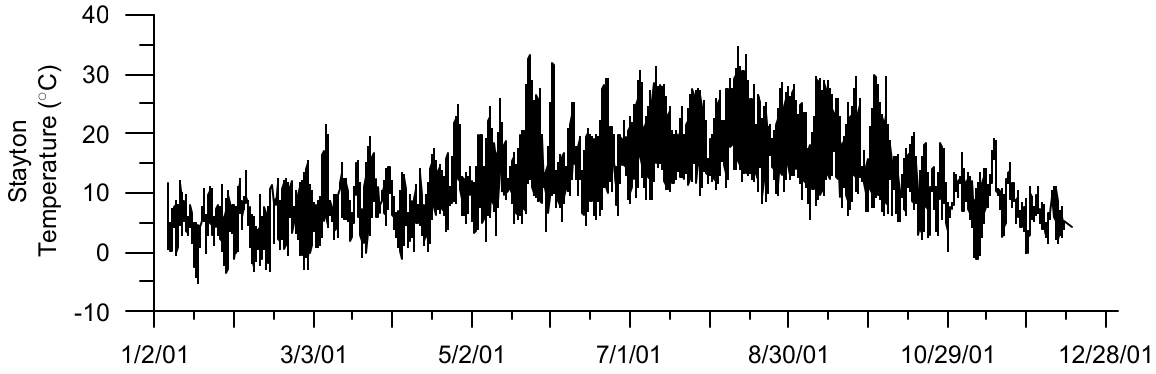


**Figure 668. Air temperature at Stayton.**

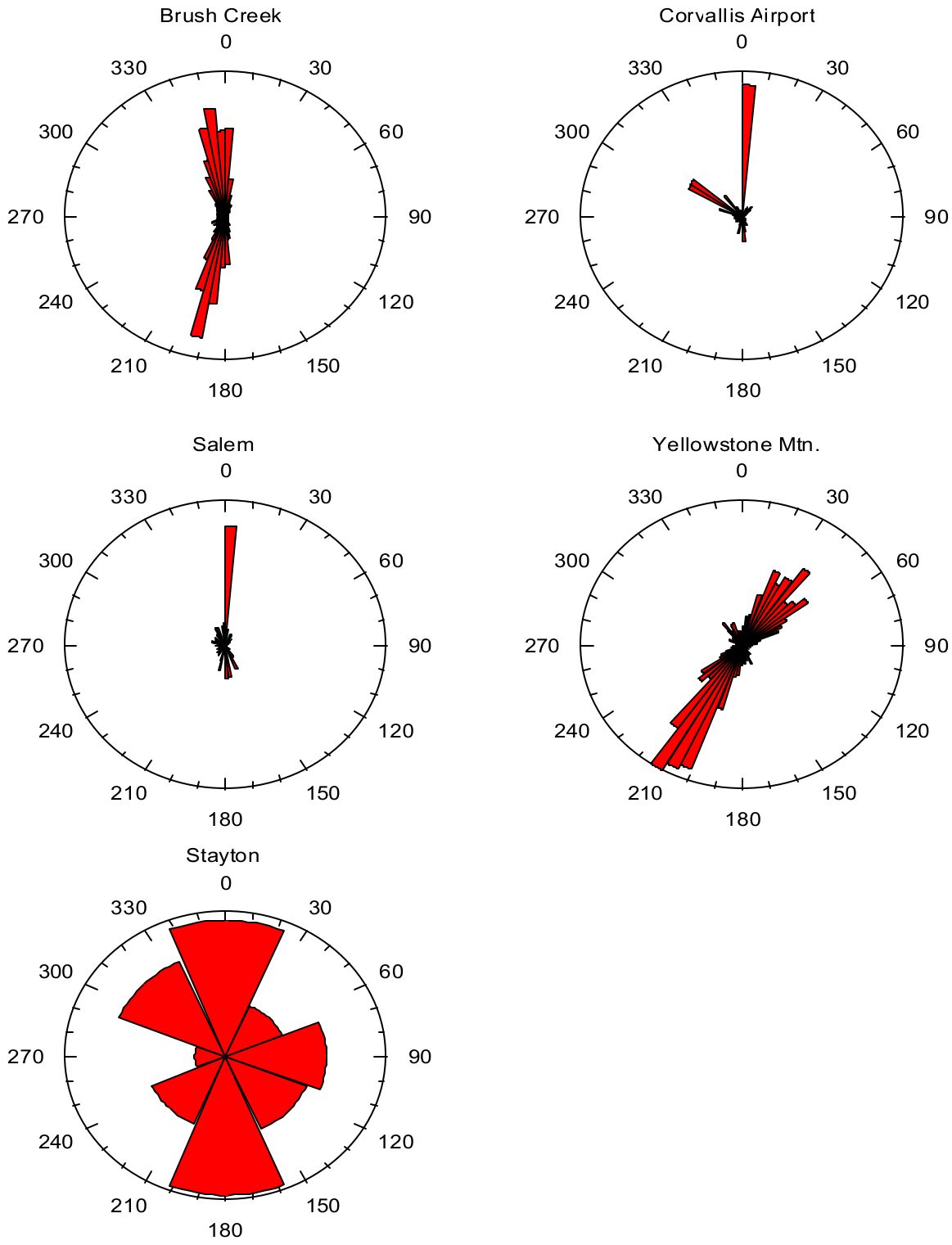


**Figure 669. Rose plots of wind direction data. The data at Stayton is measured in discrete 45 degree bins. The other sites measure wind direction as a continuum.**

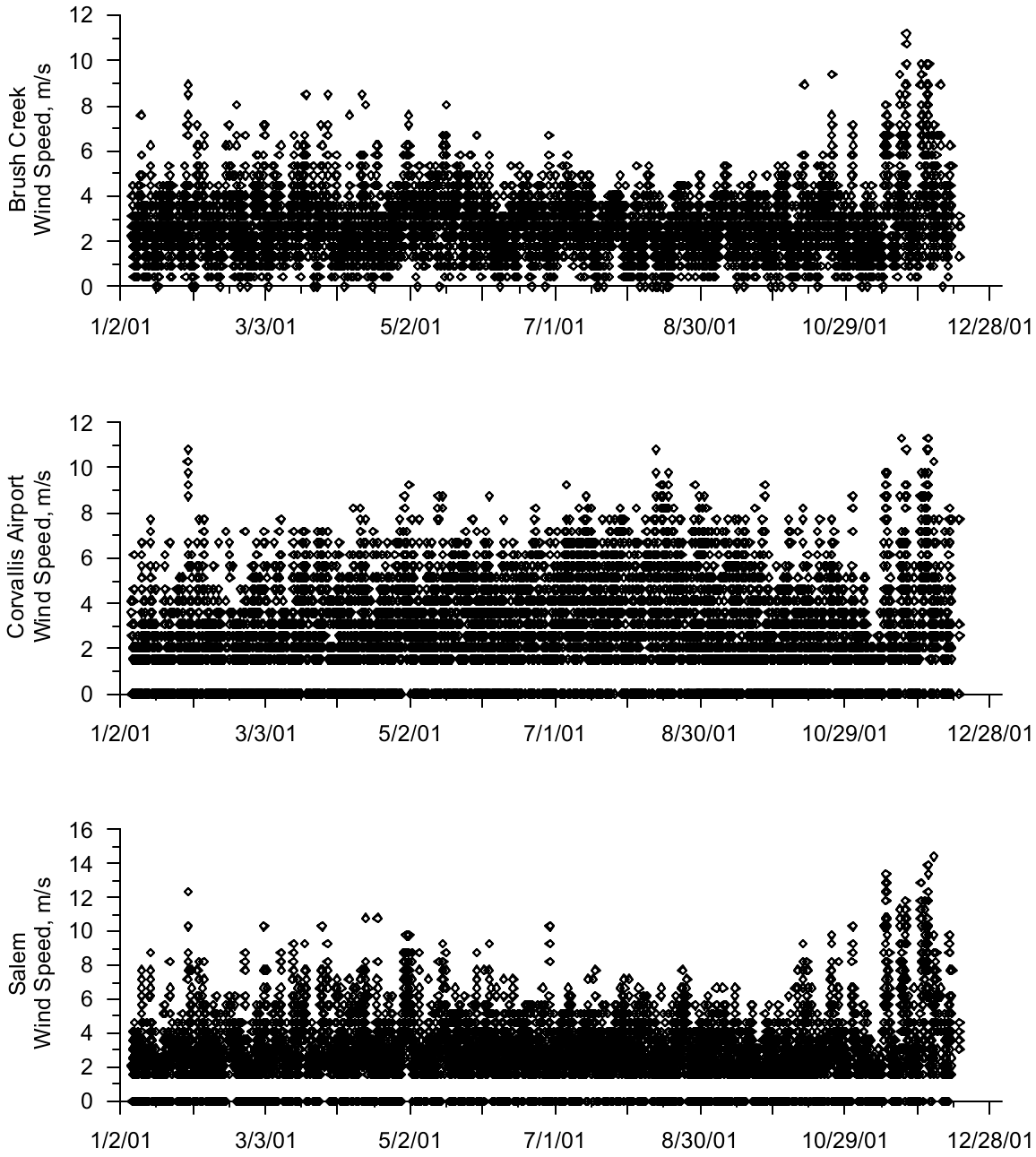


**Figure 670. Wind speed data for Brush Cr., Corvallis MUNI, and Salem. N.b., the Corvallis MUNI and Salem meteorological stations have a minimum measurement threshold of ~1.5 m/sec.**

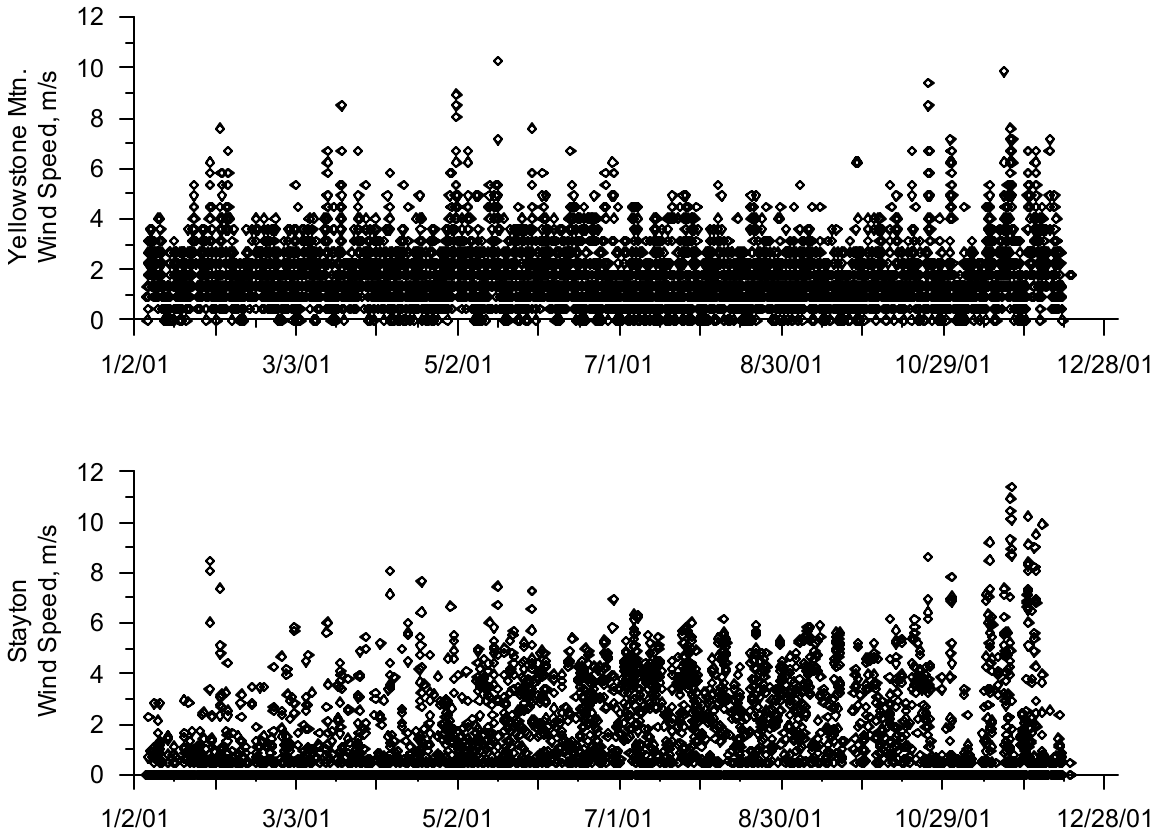


**Figure 671. Wind speed data for Yellowstone Mountain and Stayton. The greater frequency of "zero" wind speed at Stayton is a result of the stations smaller averaging period, i.e., greater sampling frequency.**

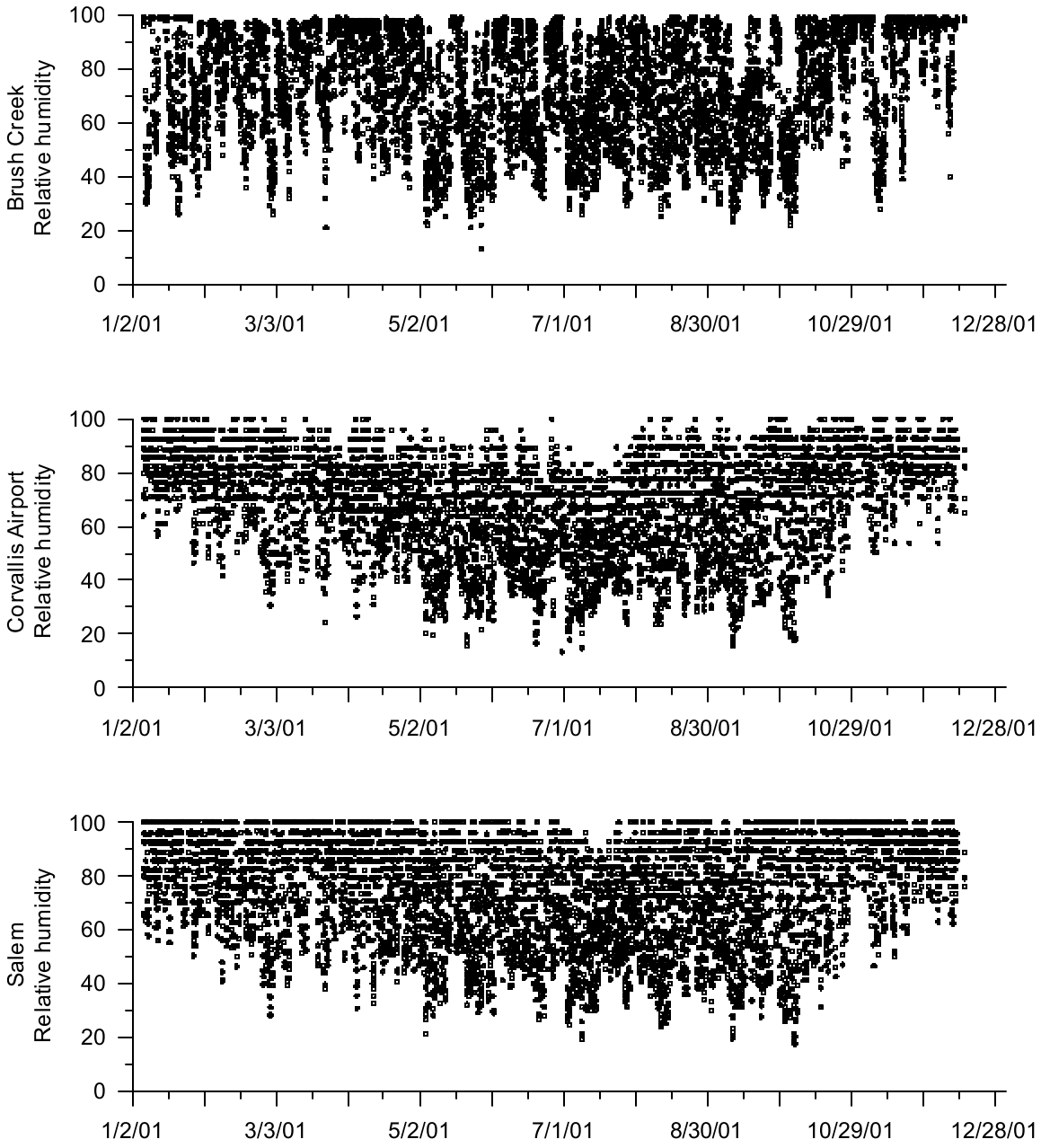


**Figure 672. Relative humidity data for Brush Cr., Corvallis MUNI, and Salem.**

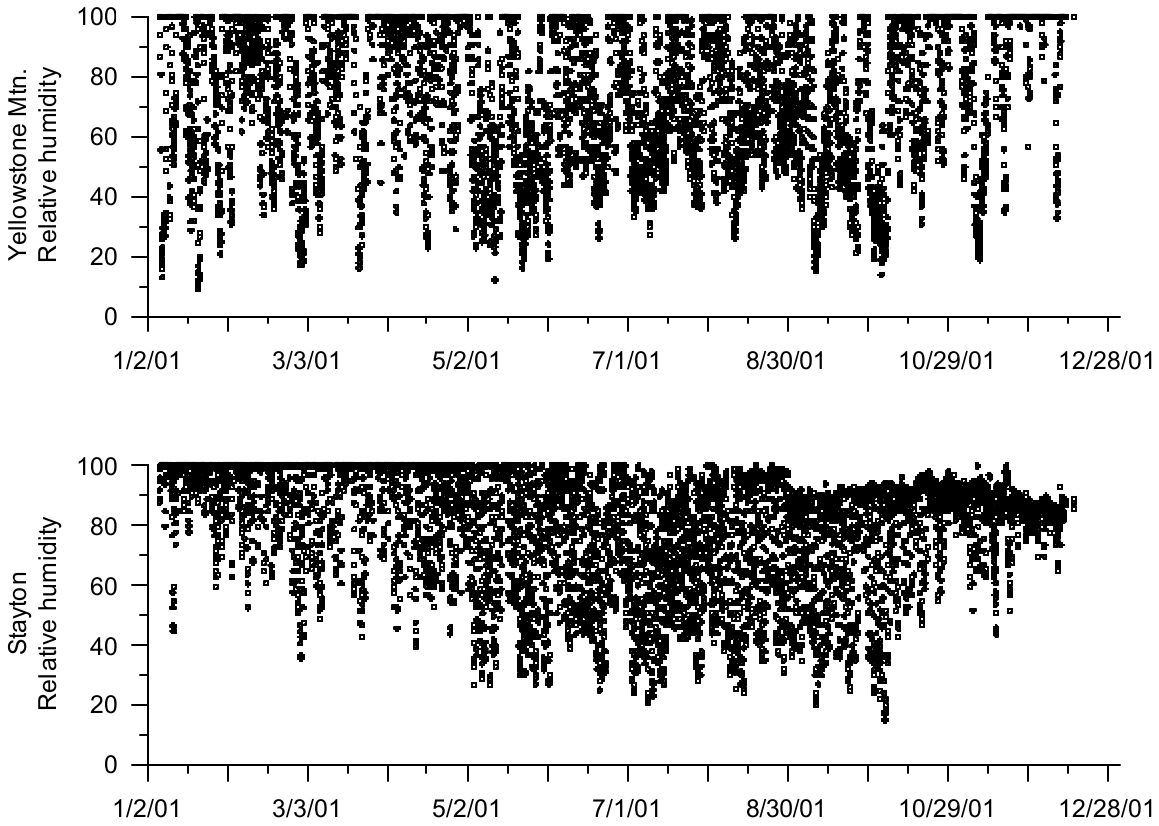


**Figure 673. Relative humidity for Stayton and Yellowstone Mountain**

## *Analysis approach and methodology*

Four meteorological variables were independently examined: temperature, wind speed, wind direction, and relative humidity. For all variables, each site (Salem, Corvallis MUNI, Brush Creek, and Yellowstone Mountain) was directly compared to Stayton; an inverse distance approach for reproducing the Stayton values was examined; and a stepwise statistical regression was performed. Temperature was additionally examined to account for elevation effects using a moisture lapse rate. A summary of these approaches follows.

### Inverse distance weighting approach:

The distances between the four stations (Salem, Corvallis MUNI, Brush Creek, and Yellowstone Mountain) and the Stayton station were calculated.

The weighting factor for each station was computed as the sum of the distances of the other stations to Stayton divided by the sum of the distance between each station to Stayton. E.g.,

For station, A, the weighting factor was $\frac{B+C+D}{A+B+C+D}$ where each letter represents the distance from a station to Stayton.

The predicted value was then the sum of the product of the individual site data values and the individual weighting factors divided by the sum of the weighting factors, as shown below. The utilized weighting factors were reported in Table 81.

$$value@\,Stayton = \frac{0.667 * Brush + 0.725 * Corv + 0.861 * Salem + 0.747 * Yellow}{0.667 + 0.725 + 0.861 + 0.747}$$

## Temperature correction due to elevation effects:

Due to the higher elevations of both the Yellowstone Mountain and Brush Creek stations and the observed cooler temperatures compared to Stayton, a general atmospheric conditions moist adiabatic lapse rate of 6 ºC/km (Masters, 1997) was applied to correct the measured temperatures for elevation effects. The temperature corrections used were reported in Table 81.

**Table 81. Distance weighting factors and temperature correction factors used.**

| Site name | Distance weighting factor | Temperature correction °C |
|---|---|---|
| Brush Creek | 0.667 | +3.28 |
| Corvallis MUNI | 0.725 | -0.48 |
| Salem-McNary Field | 0.861 | -0.56 |
| Yellowstone Mountain | 0.747 | +4.71 |

**Table 82. Statistical analysis results of data and predicted values to observed values at Stayton. The bold type denotes the most favorable values.**

| **Temperature (degrees Celsius)** | | | | | |
|---|---|---|---|---|---|
| | **ME** | **AME** | **RMS** | **$R^2$** | **Notes:** |
| Brush Creek | -0.970 | 2.75 | 3.31 | 0.897 | 7706 records |
| Corvallis MUNI | 0.914 | 1.57 | 1.92 | 0.973 | |
| Salem-McNary Field | **0.350** | **0.87** | **1.15** | **0.987** | |
| Yellowstone Mountain | -1.850 | 3.94 | 4.53 | 0.847 | |
| Distance weighted average | -0.354 | 1.53 | 1.85 | 0.965 | |
| **Temperature (elevation corrected: 6 deg. C per km lapse rate)** | | | | | |
| Brush Creek | 2.309 | 2.83 | 3.91 | 0.897 | **1ºC/km lapse rate |
| Corvallis MUNI | 0.404 | 4.70 | 1.73 | 0.973 | |
| Salem-McNary Field | -0.209 | **0.83** | **1.11** | **0.987** | |
| Yellowstone Mountain | 2.859 | 3.58 | 5.03 | 0.847 | |
| Distance weighted average | 2.290 | 2.37 | 2.92 | 0.965 | |
| Distance weighted average** | **0.086** | 1.45 | 1.81 | 0.965 | |
| **Temperature (arithmetic shift for zero-bias correction)** | | | | | |
| Brush Creek | 0.0 | 2.50 | 3.16 | 0.897 | |
| Corvallis MUNI | 0.0 | 1.31 | 1.69 | 0.973 | |
| Salem-McNary Field | 0.0 | **0.81** | **1.09** | **0.987** | |
| Yellowstone Mountain | 0.0 | 3.37 | 4.13 | 0.847 | |
| Distance weighted average | 0.0 | 1.46 | 1.81 | 0.965 | |

| | | | | | |
|---|---|---|---|---|---|
| **Wind speed (m/sec)** | | | | | |
| Brush Creek | 1.925 | 2.18 | 2.52 | 0.135 | 7705 records |
| Corvallis MUNI | 1.940 | 2.18 | 2.89 | 0.149 | |
| Salem-McNary Field | 1.948 | 2.11 | 2.76 | 0.220 | |
| Yellowstone Mountain | **0.903** | **1.44** | **1.78** | 0.143 | |
| Distance weighted average | 1.680 | 1.87 | 2.18 | **0.283** | |
| **Wind direction (radians)** | | | | | |
| Brush Creek | 1.228 | 2.18 | 2.94 | 0.0031 | 7269 records |
| Corvallis MUNI | 0.430 | 2.24 | 2.85 | 0.00002 | |
| Salem-McNary Field | 0.301 | 1.80 | 2.56 | 0.0242 | |
| Yellowstone Mountain | **0.109** | **1.58** | 2.13 | **0.0608** | |
| Distance weighted average | 0.491 | **1.58** | **2.05** | 0.0196 | |
| **Relative humidity (percent)** | | | | | |
| Brush Creek | -5.851 | 12.0 | 17.19 | 0.456 | 7694 records |
| Corvallis MUNI | -9.821 | 11.7 | 14.18 | 0.726 | |
| Salem-McNary Field | **-3.840** | **7.4** | **10.04** | **0.780** | |
| Yellowstone Mountain | -4.979 | 15.5 | 21.90 | 0.298 | |
| Distance weighted average | -6.016 | 9.3 | 12.23 | 0.704 | |

### Arithmetic temperature shift of zero-bias:

The data sets for Brush Creek, Corvallis MUNI, Salem, and Yellowstone Mountain were adjusted via an arithmetic constant to match the mean temperature value of the Stayton data set. Graphically, this was a vertical shift to align the mean values of the data sets. The data sets were then compared. The resulting error in prediction reflects the variability of the data sets. The statistical results of this diagnostic are shown in
Table 82.

## *Analysis results*

Descriptive statistics of the data sets were displayed in Table 80. Statistical results of the weighted average prediction versus the observations at Stayton are shown in
Table 82. Temperature, wind speed, and relative humidity were strongly correlated between Stayton and the other stations, as well as between the distance-method prediction and Stayton. For wind direction, only the Corvallis MUNI station was not correlated with the Stayton data. A one-tailed significance level of 95% was assumed. ($r_{crit}$ ~0.05)

In general, for each meteorological variable, the inverse distance weighting approach did not perform as well as the best individual station, but did perform better than some stations.

Temperature at Stayton was predicted with minimal bias and error by the Salem station. Attempts to correct for the bias of the higher elevation stations, Brush Creek and Yellowstone Mountain, did not meet with any success (Figure 674). The lapse rate was examined as a calibration parameter. A 1ºC/km lapse rate resulted in the best statistical fit. While the bias was low, the amount of error was greater than the individual Corvallis MUNI or the Salem data, as seen in

Table 82. This indicates that more than an arithmetic shift of the data were needed to increase the quality of the temperature prediction. The zero-bias arithmetic shift diagnostic showed that the amount of error in the Salem and distance method predictions was largely unaffected by the bias shift. This suggests that the bulk of the error was due to nonlinearities and variations of the data, and not a bias of the mean values.

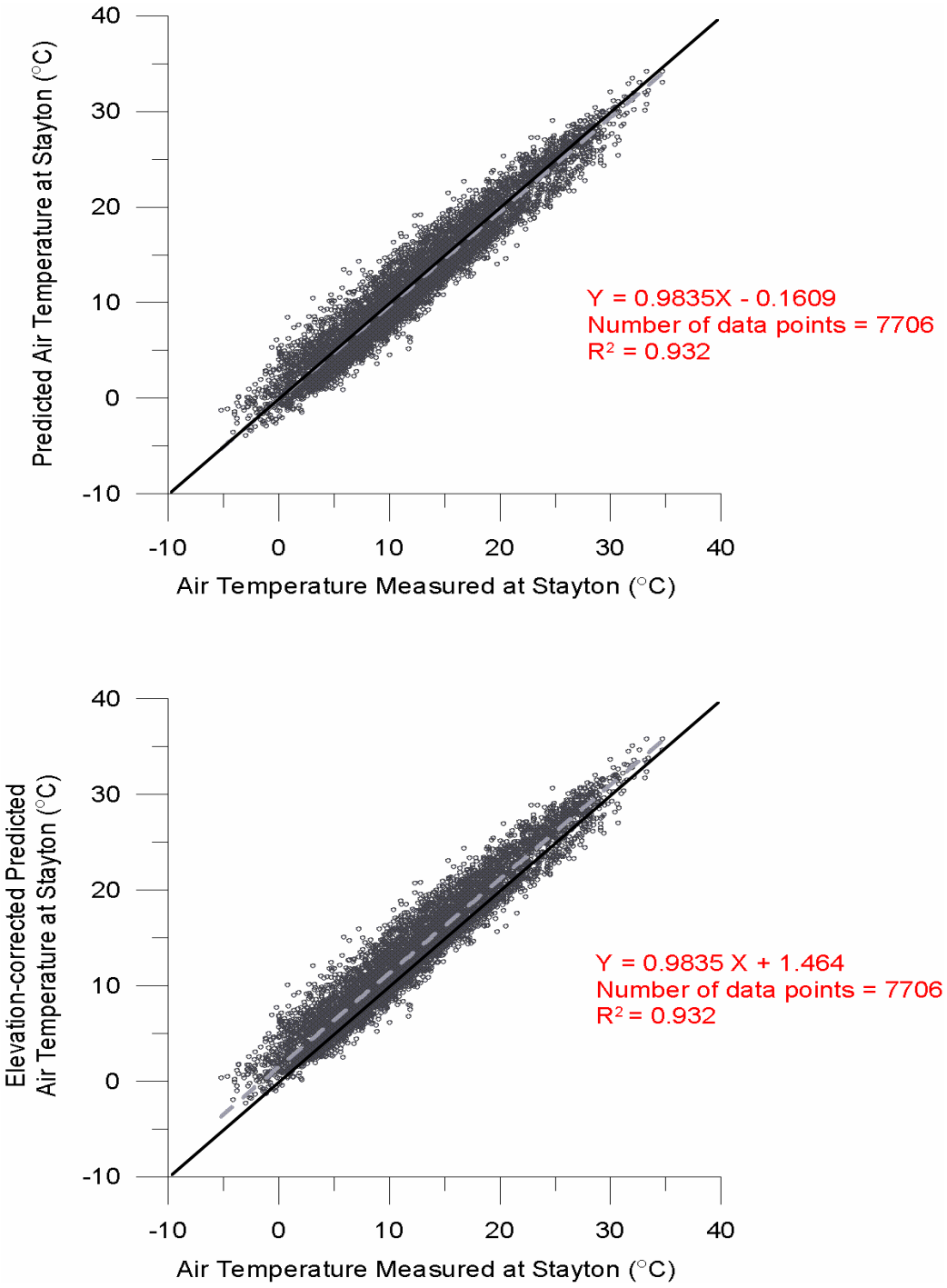


**Figure 674. Comparison of observed and predicted temperatures at Stayton. The dashed line is the regression line for the reported equation. The solid line denotes an ideal relationship.**

Weighted average predicted wind speed and wind direction are shown in Figure 675 and Figure 676, respectively. Wind speed and wind direction were predicted with the least error and bias by the Yellowstone Mountain station. However, the data at Stayton were not similar to the other data sets. All stations and the inverse distance method over predicted wind speed at Stayton. The over prediction was in part due to the sampling method of the Stayton wind gage. An examination of the graphical data, Figure 670 and Figure 671, shows the distribution of wind speed was approximately similar between the stations except for the frequency of no measured wind, which was more frequent at Stayton and much less common at the higher elevation Brush Creek and Yellowstone Mountain stations. By examining the tabular data, the frequency of the no wind condition at Salem and Corvallis MUNI was approximately one to two days, and the duration is on the scale of hours. Over half the data points for Stayton have a value of zero. The annual mean wind speed at Stayton was approximately one-fourth the mean of the Brush Creek, Corvallis MUNI, and Salem stations.

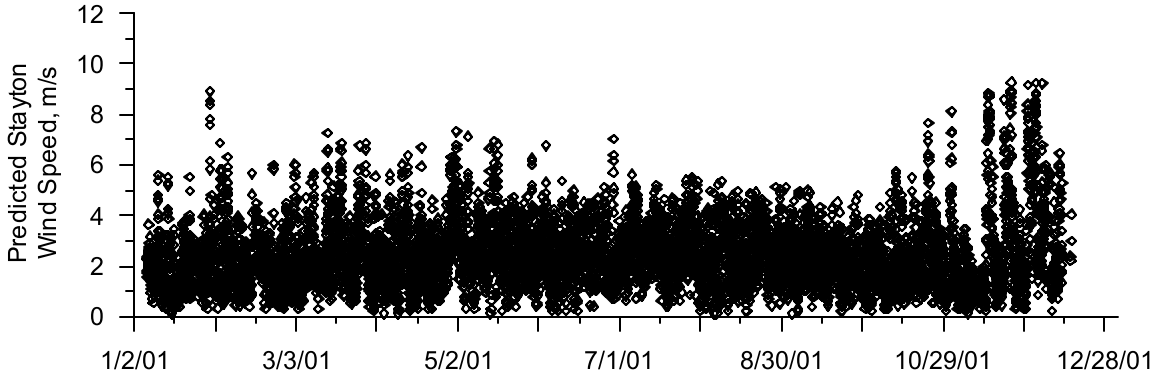


**Figure 675. Weighted average predicted wind speeds at Stayton.**

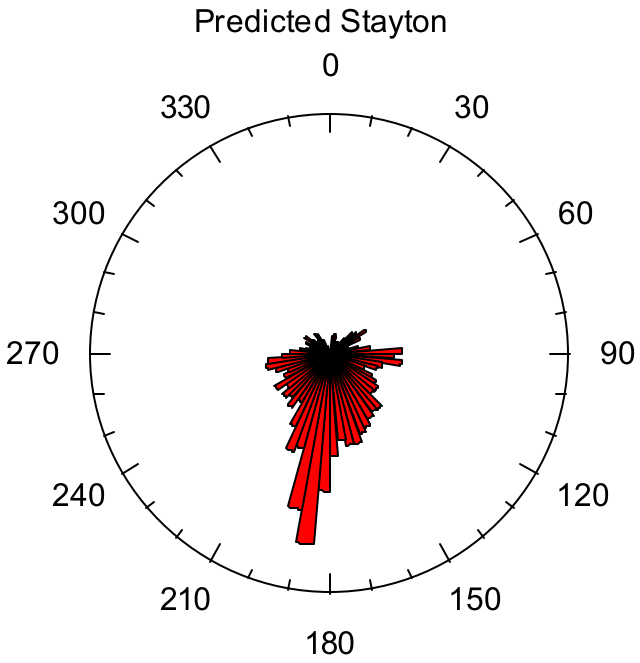


**Figure 676. Weighted average predicted wind direction at Stayton.**

A statistical approach for reproducing the Stayton wind speed data set was examined. The results of the stepwise linear regression are shown in Table 83. The low regression coefficient of 0.33 for the first

step, which only used the Salem data, shows that wind speed at Stayton was much less than the wind speed at Salem.

**Table 83. Stepwise linear regression results.**

| Variable | Step | Linear regression constant | Stepwise regression coefficient | | | | $R^2$ |
|---|---|---|---|---|---|---|---|
| | | | Brush Cr | Corvallis | Salem | Yellowstone Mountain | |
| Temperature | 1 | 0.505 | -- | -- | 0.974 | -- | 0.9747 |
| | 2 | 0.434 | -- | 0.176 | 0.795 | -- | 0.9763 |
| | 3 | 0.206 | 0.0651 | 0.180 | 0.731 | -- | 0.9772 |
| | 4 | 0.198 | 0.0955 | 0.178 | 0.730 | -0.0268 | 0.9773 |
| Temperature (with elevation correction) | 1 | 0.505 | -- | -- | 0.974 | -- | 0.9747 |
| | 2 | 0.434 | -- | 0.176 | 0.795 | -- | 0.9763 |
| | 3 | 0.206 | 0.0651 | 0.180 | 0.731 | -- | 0.9772 |
| | 4 | 0.198 | 0.0955 | 0.178 | 0.730 | -0.0268 | 0.9773 |
| Wind speed | 1 | -0.124 | -- | -- | 0.331 | -- | 0.2199 |
| | 2 | -0.394 | -- | -- | 0.265 | 0.268 | 0.2557 |
| | 3 | -0.530 | -- | 0.122 | 0.200 | 0.256 | 0.2785 |
| | 4 | -0.730 | 0.134 | 0.109 | 0.176 | 0.221 | 0.2893 |
| Wind direction | 1 | 1.86 | -- | -- | -- | 0.258 | 0.0606 |
| | 2 | 1.65 | -- | -- | 0.0945 | 0.236 | 0.0729 |
| | 3 | 1.93 | -0.081 | -- | 0.0983 | 0.244 | 0.0801 |
| | 4 | 1.97 | -0.075 | -0.0278 | 0.104 | 0.245 | 0.0811 |
| Relative humidity | 1 | 11.53 | -- | -- | 0.8998 | (did not | 0.7804 |
| | 2 | 9.98 | -- | 0.318 | 0.6268 | improve | 0.7970 |
| | 3 | 7.64 | 0.129 | 0.311 | 0.5384 | regression) | 0.8073 |

The weighted average predicted relative humidity is shown in Figure 677. Relative humidity was approximately 5 percent higher at Stayton than the other stations, except Corvallis MUNI, where it was approximately 10 percent higher. The relative humidity at Stayton was best correlated with Corvallis MUNI and Salem.

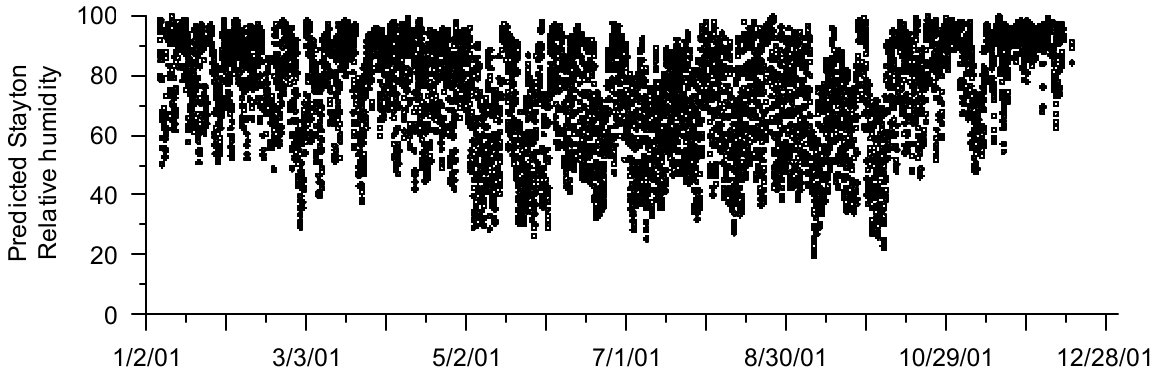


**Figure 677. Weighted average predicted relative humidity at Stayton.**

## *Discussion*

The biggest weakness in generating the meteorological input data will be the lack of data from directly at the model site. The available 2001 data were generally complete, but some concerns about accuracy and precision exist. The greatest concern, shared by Jim Trost from the Oregon Department of Forestry, rests with the accuracy of the anemometer at the Stayton station. The wind speed data at Stayton were

characteristically different from the nearby Corvallis MUNI and Salem wind speed data in mean value, frequency of data points with a value of zero, and distribution shape. The histograms in Figure 678 illustrate the difference in the data. Without additional information, it was suggested that the wind speed data at Stayton not be utilized. Additional analyses could be conducted using data from additional years to develop better statistical correlations.

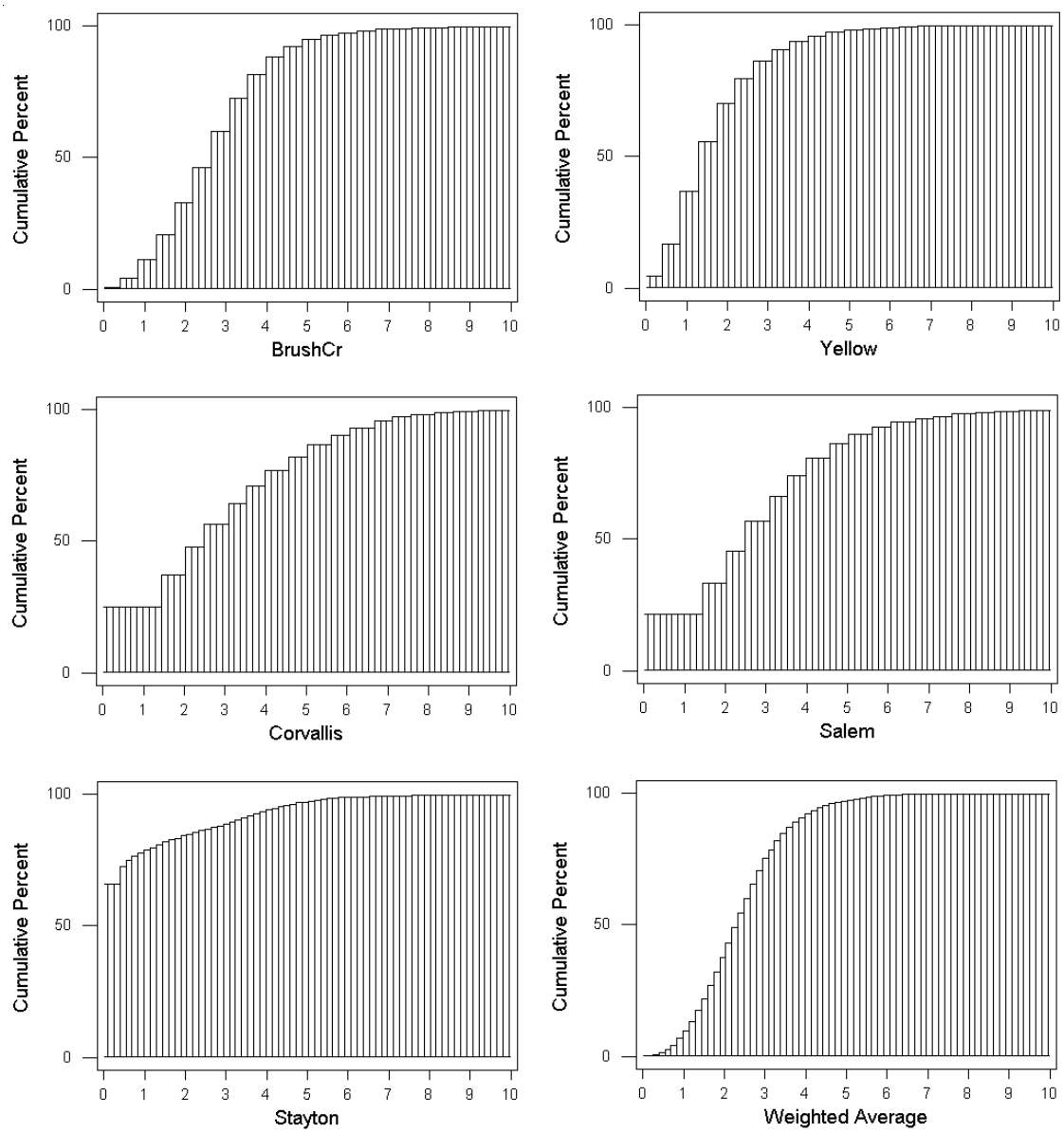


**Figure 678. Cumulative wind speed histograms. The horizontal axis is wind speed (m/sec).**

The wind speed data at Yellowstone Mountain and Brush Creek are complete and reasonable. However, these stations were located in mountainous areas, and the distribution of the wind speed was notably different. Generally, there was less variability of wind speed for the higher elevation station data sets.

The wind speed data at Salem and Corvallis MUNI was similar, but both gages were high speed gages and have a minimum wind speed threshold of 1.54 m/sec. These data can be edited to complete the distribution of wind speeds by replacing all values of zero with 0.77 m/sec. A more accurate distribution method was possible, but since the model system was a river, the most important aspect of

the wind will be in evaporation and heat flux. Any inaccuracies at low wind speeds will introduce very small if not negligible error to the results. The wind gages at Salem and Corvallis MUNI record the wind direction for wind speeds below the minimum threshold as zeros. This results in a large percentage of the wind direction data having a value of zero, as seen in Figure 669. While efforts can be made to address this inaccuracy, the effect of wind direction on a moderately fast flowing river model is negligible.

The Salem or Corvallis MUNI wind direction and wind speed data were reasonably accurate and representative model input data. The Salem data shows a larger range than the Corvallis MUNI data, but was otherwise very similar. The Brush Creek wind data were complete and accurate, but may not be representative of the less mountainous model area.

Relative humidity influences the model evaporation rate. N.b., the CE-QUAL-W2 model employs the related variable, dew point temperature. Examining Figure 672 and Figure 673, the behavior of the data from the Corvallis MUNI, Salem, and Stayton sites were quite different, despite their relative proximity. Stayton shows the highest annual mean value (80%), and Corvallis MUNI the lowest (71%). The sites show a different frequency of data points with a value of 100%: Corvallis MUNI (1.4%), Salem (12.8%), and Stayton (22.2%). While the effect of latent heat transfer upon the model can be significant, the difference between the potential input data sets will probably be subtle. The drier values will result in less warming of the river in the warmer months. A couple considerations exist to help chose an input data set. 1) Examine the physical environment of the stations. E.g., the drier Corvallis MUNI values could reflect being situated in a drier environment, such as a tarmac, as opposed to a grass field or forest. 2) Use each data set in the model and compare their performance. The month of September, 2001, shows a difference in behavior between Salem or Corvallis MUNI and the Stayton site; the Stayton site appears to have a lower maximum diel value. This data difference could be used to evaluate model sensitivity to relative humidity inputs.

The higher elevation Brush Creek and Yellowstone Mountain relative humidity data appears to fluctuate with a different pattern. E.g., the higher elevation sites show less seasonal variability (see Figure 672 and Figure 673). There was little to suggest that these sites would be better predictors of the model area's relative humidity.

Attempts to generate a temperature prediction for the model area using a weighted average or statistical approach were only marginally successful, and would be difficult to validate. Such an approach has some additional drawbacks. The approaches are labor and data intensive. The results did not perform significantly better than the nearby Salem site chosen by simple principles. An averaging approach runs the risk of mitigating the extreme in the data set. Since the atypical conditions are of great interest for model calibration and management scenarios, accuracy of the data were extremely important.

The elevation of the model water bodies, approximately 80 to 145 meters, was similar to the lower lying stations elevations, 61 to 155 m (Table 79). Any effect solely due to elevation on temperature would be near 0.5 ºC or less. 0.9 ºC and 0.3 ºC mean difference exists between the data from Stayton and the data from the Corvallis MUNI and Salem sites, respectively. A time-series plot of the differences showed no large trend in the distribution of the differences apart from the bias; i.e. the bias was homoscedastic. As commented upon earlier, the warmer values at Corvallis MUNI may be the result of the station surroundings as much as any elevation difference with the Stayton site.

The higher elevation sites, Brush Creek and Yellowstone Mountain, show a notably lower temperature (1 to 2 ºC) than the other sites. Despite Brush Creek being the closest site to water body number 4, the

temperature data may be unrepresentative. Table 80 shows that all the temperature data sets appear to have a similar distribution about the mean value. Thus, the selection of the station for temperature input data was in more a selection of the mean value than the shape of the distribution.

Given the relationship between relative humidity, or dew point temperature, and air temperature, it was preferable to utilize the same station for both input sets.

# Appendix D: Tabular Summary of USGS Atlas HA-273

USGS Hydrologic Investigations, Atlas HA-273: TRAVEL RATES OF WATER FOR SELECTED STREAMS IN THE WILLAMETTE RIVER BASIN, OREGON. 1968.

Subreach discharge for Middle Fork Willamette (1-2) and Willamette Rivers (3-30)

| Reach # | Start description | River mile start | End description | River mile end | Total reach length (m) | Discharge ($m^3/s$) | Travel rate (m/s) | Travel time (hrs) |
|---|---|---|---|---|---|---|---|---|
| 1 | Dexter Dam | 203.7 | Coast Fork Willamette River | 187.0 | 26876 | 73.6 | 1.028 | 7.26 |
| 1 | Dexter Dam | 203.7 | Coast Fork Willamette River | 187.0 | 26876 | 135.9 | 1.341 | 5.57 |
| 1 | Dexter Dam | 203.7 | Coast Fork Willamette River | 187.0 | 26876 | 424.8 | 2.235 | 3.34 |
| 2 | Coast Fork Willamette River | 187.0 | Springfield Bridge | 185.3 | 2736 | 79.3 | 0.492 | 1.55 |
| 2 | Coast Fork Willamette River | 187.0 | Springfield Bridge | 185.3 | 2736 | 138.8 | 0.983 | 0.77 |
| 2 | Coast Fork Willamette River | 187.0 | Springfield Bridge | 185.3 | 2736 | 623.0 | 2.414 | 0.31 |
| 3 | Springfield Bridge | 185.3 | Ferry Street Bridge, Eugene | 182.2 | 4989 | 62.3 | 0.536 | 2.58 |
| 3 | Springfield Bridge | 185.3 | Ferry Street Bridge, Eugene | 182.2 | 4989 | 141.6 | 0.894 | 1.55 |
| 3 | Springfield Bridge | 185.3 | Ferry Street Bridge, Eugene | 182.2 | 4989 | 651.3 | 1.833 | 0.76 |
| 4 | Ferry Street Bridge, Eugene | 182.2 | McKenzie River | 174.8 | 11909 | 34.0 | 0.581 | 5.69 |
| 4 | Ferry Street Bridge, Eugene | 182.2 | McKenzie River | 174.8 | 11909 | 113.3 | 0.849 | 3.89 |
| 4 | Ferry Street Bridge, Eugene | 182.2 | McKenzie River | 174.8 | 11909 | 679.6 | 1.922 | 1.72 |
| 5 | McKenzie River | 174.8 | Harrisburg bridge | 161.2 | 21887 | 96.3 | 1.207 | 5.04 |
| 5 | McKenzie River | 174.8 | Harrisburg bridge | 161.2 | 21887 | 212.4 | 1.296 | 4.69 |
| 5 | McKenzie River | 174.8 | Harrisburg bridge | 161.2 | 21887 | 1161.0 | 1.833 | 3.32 |
| 6 | Harrisburg bridge | 161.2 | Irish Bend | 151.0 | 16415 | 138.8 | 0.939 | 4.86 |
| 6 | Harrisburg bridge | 161.2 | Irish Bend | 151.0 | 16415 | 229.4 | 1.162 | 3.92 |
| 6 | Harrisburg bridge | 161.2 | Irish Bend | 151.0 | 16415 | 679.6 | 1.788 | 2.55 |
| 7 | Irish Bend | 151.0 | Long Tom River | 145.9 | 8208 | 118.9 | 0.983 | 2.32 |
| 7 | Irish Bend | 151.0 | Long Tom River | 145.9 | 8208 | 232.2 | 1.252 | 1.82 |
| 7 | Irish Bend | 151.0 | Long Tom River | 145.9 | 8208 | 736.2 | 1.431 | 1.59 |
| 8 | Long Tom River | 145.9 | Peoria | 141.4 | 7242 | 152.9 | 0.671 | 3.00 |
| 8 | Long Tom River | 145.9 | Peoria | 141.4 | 7242 | 237.9 | 1.341 | 1.50 |
| 8 | Long Tom River | 145.9 | Peoria | 141.4 | 7242 | 906.1 | 2.772 | 0.73 |
| 9 | Peoria | 141.4 | Corvallis filtration plane | 133.9 | 12070 | 158.6 | 0.983 | 3.41 |
| 9 | Peoria | 141.4 | Corvallis filtration plane | 133.9 | 12070 | 229.4 | 1.028 | 3.26 |
| 9 | Peoria | 141.4 | Corvallis | 133.9 | 12070 | 962.8 | 1.609 | 2.08 |

| | | | | | | | | |
|---|---|---|---|---|---|---|---|---|
| | | | filtration plane | | | | | |
| 10 | Corvallis filtration plane | 133.9 | Camp Adair water intake | 122.1 | 18990 | 167.1 | 0.849 | 6.21 |
| 10 | Corvallis filtration plane | 133.9 | Camp Adair water intake | 122.1 | 18990 | 257.7 | 1.028 | 5.13 |
| 10 | Corvallis filtration plane | 133.9 | Camp Adair water intake | 122.1 | 18990 | 1132.7 | 1.565 | 3.37 |
| 11 | Camp Adair water intake | 122.1 | Albany bridge | 119.3 | 4506 | 169.9 | 1.028 | 1.22 |
| 11 | Camp Adair water intake | 122.1 | Albany bridge | 119.3 | 4506 | 260.5 | 1.296 | 0.97 |
| 11 | Camp Adair water intake | 122.1 | Albany bridge | 119.3 | 4506 | 453.1 | 1.609 | 0.78 |
| 12 | Albany bridge | 119.3 | Santiam River | 108.0 | 18186 | 169.9 | 0.626 | 8.07 |
| 12 | Albany bridge | 119.3 | Santiam River | 108.0 | 18186 | 283.2 | 0.805 | 6.28 |
| 12 | Albany bridge | 119.3 | Santiam River | 108.0 | 18186 | 1444.2 | 1.788 | 2.83 |
| 13 | Santiam River | 108.0 | Buena Vis ta Ferry | 106.4 | 2575 | 198.2 | 1.028 | 0.70 |
| 13 | Santiam River | 108.0 | Buena Vista Ferry | 106.4 | 2575 | 396.4 | 1.252 | 0.57 |
| 13 | Santiam River | 108.0 | Buena Vista Ferry | 106.4 | 2575 | 2123.8 | 2.146 | 0.33 |
| 14 | Buena Vista Ferry | 106.4 | Independence bridge | 96.1 | 16576 | 198.2 | 0.983 | 4.68 |
| 14 | Buena Vista Ferry | 106.4 | Independence bridge | 96.1 | 16576 | 424.8 | 1.252 | 3.68 |
| 14 | Buena Vista Ferry | 106.4 | Independence bridge | 96.1 | 16576 | 2435.2 | 1.967 | 2.34 |
| 15 | Independence bridge | 96.1 | Rickreall Creek | 88.1 | 12875 | 198.2 | 0.894 | 4.00 |
| 15 | Independence bridge | 96.1 | Rickreall Creek | 88.1 | 12875 | 396.4 | 1.386 | 2.58 |
| 15 | Independence bridge | 96.1 | Rickreall Creek | 88.1 | 12875 | 1529.1 | 1.788 | 2.00 |
| 16 | Rickreall Creek | 88.1 | Southern Pacific Railroad bridge, Salem | 83.9 | 6759 | 192.6 | 0.805 | 2.33 |
| 16 | Rickreall Creek | 88.1 | Southern Pacific Railroad bridge, Salem | 83.9 | 6759 | 424.8 | 1.118 | 1.68 |
| 16 | Rickreall Creek | 88.1 | Southern Pacific Railroad bridge, Salem | 83.9 | 6759 | 1585.7 | 2.280 | 0.82 |
| 17 | Southern Pacific Railroad bridge, Salem | 83.9 | Wheatland Ferry | 71.9 | 19312 | 184.1 | 0.939 | 5.71 |
| 17 | Southern Pacific Railroad bridge, Salem | 83.9 | Wheatland Ferry | 71.9 | 19312 | 396.4 | 1.162 | 4.62 |
| 17 | Southern Pacific Railroad bridge, Salem | 83.9 | Wheatland Ferry | 71.9 | 19312 | 1557.4 | 1.743 | 3.08 |
| 18 | Wheatland Ferry | 71.9 | Weston Landing | 60.2 | 18829 | 181.2 | 0.894 | 5.85 |
| 18 | Wheatland Ferry | 71.9 | Weston Landing | 60.2 | 18829 | 481.4 | 1.296 | 4.03 |
| 18 | Wheatland Ferry | 71.9 | Weston Landing | 60.2 | 18829 | 962.8 | 1.431 | 3.66 |
| 19 | Weston Landing | 60.2 | Yamhill River | 54.9 | 8530 | 195.4 | 1.431 | 1.66 |
| 19 | Weston Landing | 60.2 | Yamhill River | 54.9 | 8530 | 481.4 | 1.520 | 1.56 |
| 19 | Weston Landing | 60.2 | Yamhill River | 54.9 | 8530 | 991.1 | 1.609 | 1.47 |
| 20 | Yamhill River | 54.9 | Newburg pulp mill outflow | 50.0 | 7886 | 181.2 | 0.447 | 4.90 |
| 20 | Yamhill River | 54.9 | Newburg pulp | 50.0 | 7886 | 509.7 | 0.760 | 2.88 |

| | | | mill outflow | | | | | |
|---|---|---|---|---|---|---|---|---|
| 20 | Yamhill River | 54.9 | Newburg pulp mill outflow | 50.0 | 7886 | 1047.7 | 0.939 | 2.33 |
| 21 | Newburg pulp mill outflow | 50.0 | Highway 219 bridge | 48.6 | 2253 | 181.2 | 0.197 | 3.18 |
| 21 | Newburg pulp mill outflow | 50.0 | Highway 219 bridge | 48.6 | 2253 | 509.7 | 0.402 | 1.56 |
| 21 | Newburg pulp mill outflow | 50.0 | Highway 219 bridge | 48.6 | 2253 | 2265.3 | 1.699 | 0.37 |
| 22 | Highway 219 bridge | 48.6 | Champoeg State Park | 46.0 | 4184 | 178.4 | 0.264 | 4.41 |
| 22 | Highway 219 bridge | 48.6 | Champoeg State Park | 46.0 | 4184 | 509.7 | 0.536 | 2.17 |
| 22 | Highway 219 bridge | 48.6 | Champoeg State Park | 46.0 | 4184 | 2265.3 | 1.520 | 0.76 |
| 23 | Champoeg State Park | 46.0 | Butteville | 43.0 | 4828 | 178.4 | 0.179 | 7.50 |
| 23 | Champoeg State Park | 46.0 | Butteville | 43.0 | 4828 | 509.7 | 0.393 | 3.41 |
| 23 | Champoeg State Park | 46.0 | Butteville | 43.0 | 4828 | 2265.3 | 1.028 | 1.30 |
| 24 | Butteville | 43.0 | Corral Creek | 39.8 | 5150 | 184.1 | 0.183 | 7.80 |
| 24 | Butteville | 43.0 | Corral Creek | 39.8 | 5150 | 509.7 | 0.358 | 4.00 |
| 24 | Butteville | 43.0 | Corral Creek | 39.8 | 5150 | 2208.7 | 1.073 | 1.33 |
| 25 | Corral Creek | 39.8 | Old Wilsonville Ferry | 38.8 | 1609 | 178.4 | 0.215 | 2.08 |
| 25 | Corral Creek | 39.8 | Old Wilsonville Ferry | 38.8 | 1609 | 538.0 | 0.492 | 0.91 |
| 25 | Corra1 Creek | 39.8 | Old Wilsonville Ferry | 38.8 | 1609 | 877.8 | 0.671 | 0.67 |
| 26 | Old Wilsonville Ferry | 38.8 | Molalla River | 35.7 | 4989 | 181.2 | 0.156 | 8.86 |
| 26 | Old Wilsonville Ferry | 38.8 | Molalla River | 35.7 | 4989 | 566.3 | 0.371 | 3.73 |
| 26 | Old Wilsonville Ferry | 38.8 | Molalla River | 35.7 | 4989 | 906.1 | 0.536 | 2.58 |
| 27 | Molalla River | 35.7 | Canby Ferry | 34.4 | 2092 | 135.9 | 0.161 | 3.61 |
| 27 | Molalla River | 35.7 | Canby Ferry | 34.4 | 2092 | 594.7 | 0.492 | 1.18 |
| 27 | Molalla River | 35.7 | Canby Ferry | 34.4 | 2092 | 934.5 | 0.805 | 0.72 |
| 28 | Canby Ferry | 34.4 | New Era | 31.4 | 4828 | 184.1 | 0.219 | 6.12 |
| 28 | Canby Ferry | 34.4 | New Era | 31.4 | 4828 | 594.7 | 0.492 | 2.73 |
| 28 | Canby Ferry | 34.4 | New Era | 31.4 | 4828 | 962.8 | 0.805 | 1.67 |
| 29 | New Era | 31.4 | Tualatin River | 28.4 | 4828 | 186.9 | 0.161 | 8.33 |
| 29 | New Era | 31.4 | Tualatin River | 28.4 | 4828 | 594.7 | 0.447 | 3.00 |
| 29 | New Era | 31.4 | Tualatin River | 28.4 | 4828 | 934.5 | 0.492 | 2.73 |
| 30 | Tualatin River | 28.4 | Willamette Falls | 26.6 | 2897 | 623.0 | 0.317 | 2.54 |
| 30 | Tualatin River | 28.4 | Willamette Falls | 26.6 | 2897 | 962.8 | 0.420 | 1.91 |

Subreach discharge for Coast Fork Willamette River (31-36)

| Reach # | Start description | River mile start | End description | River mile end | Total reach length (m) | Discharge ($m^3/s$) | Travel rate (m/s) | Travel time (hrs) |
|---|---|---|---|---|---|---|---|---|
| 31 | Gaging Station 1535 | 29.4 | Highway 231 bridge | 23.9 | 8851 | 2.10 | 0.215 | 11.46 |
| 31 | Gaging Station 1535 | 29.4 | Highway 231 bridge | 23.9 | 8851 | 90.61 | 1.699 | 1.45 |
| 32 | Highway | 23.9 | Row River | 20.7 | 5150 | 2.27 | 0.228 | 6.27 |

| | | | | | | | | |
|---|---|---|---|---|---|---|---|---|
| | 231 bridge | | | | | | | |
| 32 | Highway 231 bridge | 23.9 | Row River | 20.7 | 5150 | 90.61 | 1.431 | 1.00 |
| 33 | Row River | 20.7 | Interstate 5 bridge | 15.7 | 8047 | 11.33 | 0.313 | 7.14 |
| 33 | Row River | 20.7 | Interstate 5 bridge | 15.7 | 8047 | 22.09 | 0.367 | 6.10 |
| 33 | Row River | 20.7 | Interstate 5 bridge | 15.7 | 8047 | 260.52 | 1.475 | 1.52 |
| 34 | Interstate 5 bridge | 15.7 | Cloverdale bridge | 12.8 | 4667 | 12.18 | 0.492 | 2.64 |
| 34 | Interstate 5 bridge | 15.7 | Cloverdale bridge | 12.8 | 4667 | 22.09 | 0.715 | 1.81 |
| 34 | Interstate 5 bridge | 15.7 | Cloverdale bridge | 12.8 | 4667 | 283.17 | 2.235 | 0.58 |
| 35 | Cloverdale bridge | 12.8 | Highway 58 bridge | 6.4 | 10300 | 13.03 | 0.416 | 6.88 |
| 35 | Cloverdale bridge | 12.8 | Highway 58 bridge | 6.4 | 10300 | 22.09 | 0.536 | 5.33 |
| 35 | Cloverdale bridge | 12.8 | Highway 58 bridge | 6.4 | 10300 | 283.17 | 1.788 | 1.60 |
| 36 | Highway 58 bridge | 6.4 | mouth | 0 | 10300 | 22.65 | 0.380 | 7.53 |
| 36 | Highway 58 bridge | 6.4 | mouth | 0 | 10300 | 311.49 | 1.609 | 1.78 |

Subreach discharge for McKenzie River (37-51)

| Reach # | Start description | River mile start | End description | River mile end | Total reach length (m) | Discharge ($m^3/s$) | Travel rate (m/s) | Travel time (hrs) |
|---|---|---|---|---|---|---|---|---|
| 37 | Gaging station 1588.5 | 81.5 | Belknap Springs | 74.6 | 11104 | 23.79 | 1.073 | 2.88 |
| 37 | Gaging station 1588.5 | 81.5 | Belknap Springs | 74.6 | 11104 | 45.31 | 1.296 | 2.38 |
| 38 | Belknap Springs | 74.6 | McKenzie Bridge | 68.2 | 10300 | 31.15 | 1.073 | 2.67 |
| 38 | Belknap Springs | 74.6 | McKenzie Bridge | 68.2 | 10300 | 55.22 | 1.341 | 2.13 |
| 39 | McKenzie Bridge | 68.2 | South Fork McKenzie River | 59.7 | 13679 | 67.96 | 1.341 | 2.83 |
| 40 | South Fork McKenzie River | 59.7 | Blue River | 57.0 | 4345 | 65.13 | 0.760 | 1.59 |
| 40 | South Fork McKenzie River | 59.7 | Blue River | 57.0 | 4345 | 84.95 | 1.073 | 1.13 |
| 40 | South Fork McKenzie River | 59.7 | Blue River | 57.0 | 4345 | 181.23 | 1.922 | 0.63 |
| 41 | Blue River | 57.0 | Finn Rock bridge | 54.2 | 4506 | 67.96 | 1.162 | 1.08 |
| 41 | Blue River | 57.0 | Finn Rock bridge | 54.2 | 4506 | 93.45 | 1.654 | 0.76 |

| | | | | | | | | |
|---|---|---|---|---|---|---|---|---|
| 41 | Blue River | 57.0 | Finn Rock bridge | 54.2 | 4506 | 198.22 | 2.593 | 0.48 |
| 42 | Finn Rock bridge | 54.2 | Goodpasture bridge | 40.6 | 21887 | 67.96 | 0.939 | 6.48 |
| 42 | Finn Rock bridge | 54.2 | Goodpasture bridge | 40.6 | 21887 | 110.44 | 1.162 | 5.23 |
| 42 | Finn Rock bridge | 54.2 | Goodpasture bridge | 40.6 | 21887 | 237.86 | 1.788 | 3.40 |
| 43 | Goodpasture bridge | 40.6 | Leaburg Dam | 38.8 | 2897 | 67.96 | 0.331 | 2.43 |
| 43 | Goodpasture bridge | 40.6 | Leaburg Dam | 38.8 | 2897 | 113.27 | 0.443 | 1.82 |
| 43 | Goodpasture bridge | 40.6 | Leaburg Dam | 38.8 | 2897 | 263.35 | 1.073 | 0.75 |
| 44 | Leaburg Dam | 38.8 | Deerhorn Park bridge | 31.5 | 11748 | 67.96 | 0.358 | 9.13 |
| 44 | Leaburg Dam | 38.8 | Deerhorn Park bridge | 31.5 | 11748 | 118.93 | 0.626 | 5.21 |
| 44 | Leaburg Dam | 38.8 | Deerhorn Park bridge | 31.5 | 11748 | 274.67 | 1.520 | 2.15 |
| 45 | Deerhorn Park bridge | 31.5 | Walterville Canal intake | 28.5 | 4828 | 121.76 | 0.983 | 1.36 |
| 45 | Deerhorn Park bridge | 31.5 | Walterville Canal intake | 28.5 | 4828 | 283.17 | 1.565 | 0.86 |
| 46 | Walterville Canal intake | 28.5 | Hendricks Bridge | 24.0 | 7242 | 16.99 | 0.367 | 5.49 |
| 46 | Walterville Canal intake | 28.5 | Hendricks Bridge | 24.0 | 7242 | 84.95 | 0.983 | 2.05 |
| 46 | Walterville Canal intake | 28.5 | Hendricks Bridge | 24.0 | 7242 | 254.85 | 1.565 | 1.29 |
| 47 | Hendricks Bridge | 24.0 | Walterville Canal return | 20.9 | 4989 | 23.79 | 0.536 | 2.58 |
| 47 | Hendricks Bridge | 24.0 | Walterville Canal return | 20.9 | 4989 | 84.95 | 0.983 | 1.41 |
| 47 | Hendricks Bridge | 24.0 | Walterville Canal return | 20.9 | 4989 | 260.52 | 1.475 | 0.94 |
| 48 | Walterville Canal return | 20.9 | Hayden Bridge | 14.8 | 9817 | 67.96 | 0.983 | 2.77 |
| 48 | Walterville Canal return | 20.9 | Hayden Bridge | 14.8 | 9817 | 127.43 | 1.028 | 2.65 |
| 48 | Walterville Canal return | 20.9 | Hayden Bridge | 14.8 | 9817 | 325.64 | 1.431 | 1.91 |
| 49 | Hayden Bridge | 14.8 | Mohawk River | 13.9 | 1448 | 67.96 | 0.492 | 0.82 |
| 49 | Hayden Bridge | 14.8 | Mohawk River | 13.9 | 1448 | 138.75 | 0.849 | 0.47 |
| 49 | Hayden Bridge | 14.8 | Mohawk River | 13.9 | 1448 | 424.75 | 1.431 | 0.28 |
| 50 | Mohawk River | 13.9 | Coburg bridge | 7.3 | 10622 | 70.79 | 0.715 | 4.13 |
| 50 | Mohawk River | 13.9 | Coburg bridge | 7.3 | 10622 | 141.58 | 0.983 | 3.00 |
| 50 | Mohawk River | 13.9 | Coburg bridge | 7.3 | 10622 | 538.02 | 1.878 | 1.57 |
| 51 | Coburg bridge | 7.3 | alternate mouth | 3.6 | 5955 | 67.96 | 0.805 | 2.06 |
| 51 | Coburg bridge | 7.3 | alternate mouth | 3.6 | 5955 | 144.42 | 0.894 | 1.85 |

| | | | | | | | | |
|---|---|---|---|---|---|---|---|---|
| 51 | Coburg bridge | 7.3 | alternate mouth | 3.6 | 5955 | 538.02 | 1.922 | 0.86 |

Subreach discharge for North Santiam River (52-59) and Santiam River (60-62)

| Reach # | Start description | River mile start | End description | River mile end | Total reach length (m) | Discharge ($m^3/s$) | Travel rate (m/s) | Travel time (hrs) |
|---|---|---|---|---|---|---|---|---|
| 52 | Gaging station 1815 | 45.6 | Gates bridge | 39.3 | 10139 | 84.95 | 1.028 | 2.74 |
| 52 | Gaging station 1815 | 45.6 | Gates bridge | 39.3 | 10139 | 135.92 | 1.475 | 1.91 |
| 53 | Gates bridge | 39.3 | Mill City bridge | 35.4 | 6276 | 84.95 | 1.341 | 1.30 |
| 53 | Gates bridge | 39.3 | Mill City bridge | 35.4 | 6276 | 135.92 | 1.565 | 1.11 |
| 54 | Mill City bridge | 35.4 | Mehama bridge | 27.0 | 13518 | 84.95 | 1.296 | 2.90 |
| 54 | Mill City bridge | 35.4 | Mehama bridge | 27.0 | 13518 | 135.92 | 1.654 | 2.27 |
| 55 | Mehama bridge | 27.0 | Salem water supply diversion | 19.7 | 11748 | 79.29 | 1.207 | 2.70 |
| 55 | Mehama bridge | 27.0 | Salem water supply diversion | 19.7 | 11748 | 124.59 | 1.431 | 2.28 |
| 56 | Salem water supply diversion | 19.7 | Stayton bridge | 16.7 | 4828 | 79.29 | 0.894 | 1.50 |
| 56 | Salem water supply diversion | 19.7 | Stayton bridge | 16.7 | 4828 | 130.26 | 1.252 | 1.07 |
| 57 | Stayton bridge | 16.7 | Southern Pacific Railroad spur bridge | 11.1 | 9012 | 79.29 | 1.073 | 2.33 |
| 57 | Stayton bridge | 16.7 | Southern Pacific Railroad spur bridge | 11.1 | 9012 | 124.59 | 1.565 | 1.60 |
| 58 | Southern Pacific Railroad spur bridge | 11.1 | Greens Bridge | 2.9 | 13197 | 76.46 | 0.715 | 5.13 |
| 58 | Southern Pacific Railroad spur bridge | 11.1 | Greens Bridge | 2.9 | 13197 | 124.59 | 1.341 | 2.73 |
| 59 | Greens Bridge | 2.9 | confluence with South | 0 | 4667 | 67.96 | 1.028 | 1.26 |

| | | | | | | | | |
|---|---|---|---|---|---|---|---|---|
| | | | Santiam River | | | | | |
| 59 | Greens Bridge | 2.9 | confluence with South Santiam River | 0 | 4667 | 135.92 | 1.207 | 1.07 |
| 60 | Confluence of North and South Santiam Rivers | 11.7 | Jefferson bridge | 9.6 | 3380 | 82.12 | 0.849 | 1.11 |
| 60 | Confluence of North and South Santiam Rivers | 11.7 | Jefferson bridge | 9.6 | 3380 | 127.43 | 1.162 | 0.81 |
| 60 | Confluence of North and South Santiam Rivers | 11.7 | Jefferson bridge | 9.6 | 3380 | 707.92 | 2.235 | 0.42 |
| 61 | Jefferson bridge | 9.6 | Interstate 5 bridge | 6.4 | 5150 | 82.12 | 0.536 | 2.67 |
| 61 | Jefferson bridge | 9.6 | Interstate 5 bridge | 6.4 | 5150 | 127.43 | 0.715 | 2.00 |
| 61 | Jefferson bridge | 9.6 | Interstate 5 bridge | 6.4 | 5150 | 707.92 | 1.788 | 0.80 |
| 62 | Interstate 5 bridge | 6.4 | Santiam River mouth | 0 | 10300 | 82.12 | 0.715 | 4.00 |
| 62 | Interstate 5 bridge | 6.4 | Santiam River mouth | 0 | 10300 | 127.43 | 0.849 | 3.37 |
| 62 | Interstate 5 bridge | 6.4 | Santiam River mouth | 0 | 10300 | 707.92 | 1.788 | 1.60 |

Subreach discharge for Middle Santiam River (63-64) and South Santiam River (65-72)

| Reach # | Start description | River mile start | End description | River mile end | Total reach length (m) | Discharge ($m^3/s$) | Travel rate (m/s) | Travel time (hrs) |
|---|---|---|---|---|---|---|---|---|
| 63 | Green Peter Dam | 5.7 | Hufford Bridge | 0.9 | 7725 | 4.247 | 0.188 | 11.43 |
| 63 | Green Peter Dam | 5.7 | Hufford Bridge | 0.9 | 7725 | 33.976 | 0.894 | 2.40 |
| 63 | Green Peter Dam | 5.7 | Hufford Bridge | 0.9 | 7725 | 82.110 | 1.386 | 1.55 |
| 64 | Hufford Bridge | 0.9 | mouth | 0 | 1448 | 4.530 | 0.112 | 3.60 |
| 64 | Hufford Bridge | 0.9 | mouth | 0 | 1448 | 33.976 | 0.626 | 0.64 |
| 64 | Hufford Bridge | 0.9 | mouth | 0 | 1448 | 84.941 | 1.341 | 0.30 |
| 65 | Mouth of Middle Santiam River | 40.0 | Foster bridge | 37.7 | 3701 | 6.795 | 0.367 | 2.80 |

| | | | | | | | | |
|---|---|---|---|---|---|---|---|---|
| 65 | Mouth of Middle Santiam River | 40.0 | Foster bridge | 37.7 | 3701 | 50.965 | 0.805 | 1.28 |
| 65 | Mouth of Middle Santiam River | 40.0 | Foster bridge | 37.7 | 3701 | 124.580 | 1.386 | 0.74 |
| 66 | Foster bridge | 37.7 | Sweet Home water plant | 33.6 | 6598 | 6.795 | 0.286 | 6.41 |
| 66 | Foster bridge | 37.7 | Sweet Home water plant | 33.6 | 6598 | 56.627 | 0.715 | 2.56 |
| 66 | Foster bridge | 37.7 | Sweet Home water plant | 33.6 | 6598 | 155.725 | 1.296 | 1.41 |
| 67 | Sweet Home water plant | 33.6 | McDowell Creek | 27.7 | 9495 | 5.663 | 0.179 | 14.75 |
| 67 | Sweet Home water plant | 33.6 | McDowell Creek | 27.7 | 9495 | 56.627 | 0.671 | 3.93 |
| 67 | Sweet Home water plant | 33.6 | McDowell Creek | 27.7 | 9495 | 203.858 | 1.252 | 2.11 |
| 68 | McDowell Creek | 27.7 | Waterloo bridge | 23.4 | 6920 | 7.078 | 0.170 | 11.32 |
| 68 | McDowell Creek | 27.7 | Waterloo bridge | 23.4 | 6920 | 59.459 | 0.626 | 3.07 |
| 68 | McDowell Creek | 27.7 | Waterloo bridge | 23.4 | 6920 | 198.196 | 1.252 | 1.54 |
| 69 | Waterloo bridge | 23.4 | Lebanon diversion dam | 20.8 | 4184 | 7.078 | 0.143 | 8.13 |
| 69 | Waterloo bridge | 23.4 | Lebanon diversion dam | 20.8 | 4184 | 70.784 | 0.760 | 1.53 |
| 69 | Waterloo bridge | 23.4 | Lebanon diversion dam | 20.8 | 4184 | 220.847 | 1.520 | 0.76 |
| 70 | Lebanon diversion dam | 20.8 | Lebanon bridge | 18.3 | 4023 | 7.362 | 0.192 | 5.81 |
| 70 | Lebanon diversion dam | 20.8 | Lebanon bridge | 18.3 | 4023 | 62.290 | 0.715 | 1.56 |
| 70 | Lebanon diversion dam | 20.8 | Lebanon bridge | 18.3 | 4023 | 251.992 | 1.878 | 0.60 |
| 71 | Lebanon bridge | 18.3 | Sanderson Bridge | 7.6 | 17220 | 7.928 | 0.125 | 38.21 |
| 71 | Lebanon bridge | 18.3 | Sanderson Bridge | 7.6 | 17220 | 65.121 | 0.805 | 5.94 |
| 71 | Lebanon bridge | 18.3 | Sanderson Bridge | 7.6 | 17220 | 260.486 | 1.699 | 2.82 |
| 72 | Sanderson Bridge | 7.6 | confluence with N. | 0 | 12231 | 8.211 | 0.210 | 16.17 |

| | | | | | | | | |
|---|---|---|---|---|---|---|---|---|
| | | | Santiam | | | | | |
| 72 | Sanderson Bridge | 7.6 | confluence with N. Santiam | 0 | 12231 | 76.447 | 0.849 | 4.00 |
| 72 | Sanderson Bridge | 7.6 | confluence with N. Santiam | 0 | 12231 | 339.764 | 1.833 | 1.85 |